Climate Change Modeling, Mitigation, and Adaptation

EDITED BY

Rao Y. Surampalli,
Tian C. Zhang, C.S.P. Ojha,
B.R. Gurjar, R.D. Tyagi,
and C.M. Kao

ASCE

EWRI
ASCE
ENVIRONMENTAL &
WATER RESOURCES
INSTITUTE

Climate Change Modeling, Mitigation, and Adaptation

EDITED BY

Rao Y. Surampalli
Tian C. Zhang
C. S. P. Ojha
B. Gurjar
R. D. Tyagi
C. M. Kao

SPONSORED BY

Environmental Council
Environmental and Water Resources Institute (EWRI)
of the American Society of Civil Engineers

Published by the American Society of Civil Engineers

Cataloging-in-Publication Data on file with the Library of Congress.

Published by American Society of Civil Engineers
1801 Alexander Bell Drive
Reston, Virginia, 20191-4400
www.asce.org/pubs

ISBN 978-0-7844-1271-8 (paper)
ISBN 978-0-7844-7772-4 (PDF)
Manufactured in the United States of America.

Contents

This page intentionally left blank

Preface

Intensified economic activities are very much responsible for rapid consumption of fossil fuels, thereby leading to a rise in Green House Gas (GHG) emissions. These GHGs interact with energy flows in the atmosphere and influence the earth's climate. Climate change–the phenomenon of great concern to everyone–is going to influence human life and ecosystem in the near future if GHG emissions continue to grow without abatement. The primary socio-economic concerns pertaining to global climate change are economic, health and safety, food production, and security-related activities of human society. It is necessary to take serious actions to reduce the build-up of GHGs so as to lower the magnitude and the rate of climate change. Many policies and programs have been framed to reduce GHGs, mitigate climate change and develop adaptation-related strategies. Accordingly, this publication is an attempt to compile, edit and disseminate the most relevant information about GHGs and climate change.

The Environmental Council, Environmental and Water Resources Institute (EWRI) of ASCE, has identified GHG Emissions and Climate Change as the globally preeminent issue. This is why the ASCE-EWRI has made an effort to work with the contributors to put this book together in the context of a) basic science and vulnerability assessment (see Chapters 2–7); b) modeling/predicting (see Chapters 8–17); and 3) reducing and adapting (Chapters 18–25). This structure reflects the fact that thousands of studies related to GHGs and Climate Change are focused on these issues.

This book is intended to be of interest to students, scientists, engineers, government officers, policy makers and researchers. This book provides state-of-the-art reviews and research/technology developments with respect to basic scientific approaches, the past and current status of GHG emissions and climate change, mitigation measures and corresponding challenges and opportunities.

We gratefully appreciate the hard work and patience of all contributing authors of this book. We thank Pralhad Walvekar for his help in preparation of this book. The views and opinions expressed in each chapter of this book are those of the authors and should not be interpreted as opinions of their affiliated organizations.

– RYS, TCZ, CSPO, BRG, RDT, CMK

This page intentionally left blank

About the Editors

Dr. Rao Y. Surampalli, P.E., Dist.M.ASCE, received his M.S. and Ph.D. degrees in Environmental Engineering from Oklahoma State University and Iowa State University, respectively. He is a Registered Professional Engineer in the branches of Civil and Environmental Engineering, and also a Board Certified Environmental Engineer (BCEE) of the American Academy of Environmental Engineers (AAEE) and Diplomate of the American Academy of Water Resources Engineers (DWRE). He is an Adjunct Professor in seven universities and honorary professor in four universities. Currently, he serves, or has served, on 55 national and international committees, review panels, or advisory boards including the ASCE National Committee on Energy, Environment and Water Policy. He is a Distinguished Engineering Alumnus of both the Oklahoma State and Iowa State Universities, and is an elected Fellow of the American Association for the Advancement of Science, an elected Member of the European Academy of Sciences and Arts, an elected Member of the Russian Academy of Engineering, an elected Fellow of the Water Environment Federation and International Water Association, and a Distinguished Member of the American Society of Civil Engineers. He also is Editor-in-Chief of the ASCE Journal of Hazardous, Toxic and Radioactive Waste. He has authored over 500 technical publications in journals and conference proceedings, including 12 patents, 12 books and 64 book chapters.

Dr. Tian C. Zhang, P.E., M.ASCE is a Professor in the department of Civil Engineering at the University of Nebraska-Lincoln (UNL). He received his Ph.D. in environmental engineering from the University of Cincinnati in 1994; after being a post-doctor for a few months, he joined the UNL faculty in August 1994. Professor Zhang teaches water/wastewater treatment, biological wastes treatment, senior design, remediation of hazardous wastes, among others. Professor Zhang has over 70 peer-reviewed journal publications since 1994. His research involves water, wastewater, and stormwater treatment and management, remediation of contaminated environments, and detection and control of emerging contaminants in aquatic environments. Professor Zhang is a member of the following professional organizations: American Society of Civil Engineers; American Water Works Association; the Water Environmental Federation; Association of Environmental Engineering and Science Professors; and the International Water Association. He has been the Associate Editor of *Journal of Environmental Engineering* (since 2007), *Journal of Hazardous, Toxic, and Radioactive Waste* (since 2006), and *Water Environment Research* (since 2008). He has been a registered professional engineer in Nebraska since 2000.

Dr. C.S.P. Ojha is a Professor in Civil Engineering Department of Indian Institute of Technology, Roorkee. He holds a Ph.D. in Civil Engineering from Imperial College of Science, Technology and Medicine, London, U.K. He has published more than 150 research papers in peer-reviewed journals and supervised/co-supervised 34 PhD theses and 85 M.Tech. dissertations. His research interests include modeling of water resources and environmental engineering systems with a focus on Food and water security related problems. He has worked as Editor for Journal of Indian Water Resources Society and also as guest editor for couple of special issues. Dr. Ojha has been a Commonwealth Research Scholar at Imperial College of Science, Technology and Medicine, London, U.K. (Oct. 1990-Sept. 1993); Visiting Scholar at Louisiana State University, USA. (April-July 2000); Alexander Von Humboldt Fellow at Water Technology Center, Karlsruhe, Germany (Dec. 2001-July, 2002); Guest AvH Fellow, Institute for Hydromechanics, University of Karlsruhe, Germany (Jan. 2002-July, 2002); and Visiting Professor, Civil Engineering, AIT Bangkok (Aug. 2004-Nov. 2004). He has coordinated/co-coordinated several international research projects involving EU, Germany, France, Canada, U.K. and USA. He was conferred BCEEM by American Academy of Environmental Engineers in 2011 and E.M. Curtis Visiting Professorship by Purdue University in 2012.

Dr. B. R. Gurjar is on the faculty of Environmental Engineering in the Civil Engineering department of Indian Institute of Technology – IIT Roorkee. He is also Core Faculty in IIT Roorkee's Centre for Transportation Systems, and Centre of Excellence in Disaster Mitigation & Management, and heading Max Planck Partner Group for Megacities and Global Change. He holds a PhD in Environmental Risk Analysis from IIT Delhi. He is fellow and life member of several professional bodies and organizations and Honorary Secretary of Roorkee Local Centre of The Institution of Engineers (India). He is co-author/co-editor of six books and a number of research papers. He has received several awards and fellowships including the prestigious Advanced Postdoctoral Research Fellowship of the Max Planck Society (Germany) to support his research tenure (2002-2005) at the Max Planck Institute for Chemistry (MPIC) in Mainz, Germany. The Scientific Steering Committee of the global change System for Analysis, Research and Training (START), Washington, D.C., U.S.A., honored him with the 2004 START Young Scientist Award. He is also co-recipient of The Nawab Zain Yar Jung Bahadur Memorial Medal (best research paper award) from Environmental Engineering Division of The Institution of Engineers (India), Kolkata, for the year 1995-96. The Institution of Engineers (India)'s National Design and Research Forum (NDRF) has recently awarded him the National Design Award for Environmental Engineering 2011.

Dr. R. D. Tyagi is an internationally recognized Professor with 'Institut national de la recherche scientifique – Eau, terre, et environment', (INRS-ETE), University of Québec, Canada. He holds Canada Research Chair on, 'Bioconversion of wastewater and wastewater sludge to value added products.' He conducts research on hazardous/solids waste management, water/wastewater treatment, sludge treatment/ disposal, and bioconversion of wastewater and wastewater sludge into value added products. He has developed the novel technologies of simultaneous sewage sludge digestion and metal leaching, bioconversion of wastewater sludge (biosolids) into Bacillus thuringiensis based biopesticides, bioplastics, biofertilisers and biocontrol agents. He is a recipient of the ASCE State-of-the Art of Civil Engineering Award, ASCE Rudolph Hering Medal, ASCE Wesley Horner Medal and ASCE Best Practice Oriented Paper Award. He also received 2010

Global Honor Award (Applied Research) of International Water Association, 2010 Grand Prize (University research) of American Academy of Environmental Engineers, and Excellence Award of Natural Sciences and Engineering Research Council of Canada for Industry-University collaborative research. Dr. Tyagi has published/presented over 500 papers in refereed journals, conferences proceedings and is the author of nine books, fifty book chapters, ten research reports and nine patents.

Dr. C.M. Kao, P.E, F.ASCE is a distinguished professor with the Institute of Environmental Engineering at National Sun Yat-Sen University, Taiwan. He received his MS and Ph.D. degrees in Environmental Engineering from North Carolina State University. Prof. Kao is a Fellow of the American Society of Civil Engineers and American Association for the Advancement of Science, and a Diplomate of the American Academy of Environmental Engineers and American Academy of Water Resources Engineers. He is also the Associate Editor of the ASCE journal Hazardous, Toxic, and Radioactive Waste and WEF journal, Water Environment Research. He serves as the executive committee and program chair of the Taiwan Association of Soil and Groundwater Environmental Protection and Taiwan Environmental Engineering Association. Dr. Kao has published more than 120 refereed journal articles including 15 patents, 4 books and numerous book chapters.

This page intentionally left blank

Contributors

Adebayo J. Adeloye, *Heriot-Watt University, Riccarton Edinburgh, UK*

C.M. Ajila, *INRS, Universite du Quebec, Quebec, QC, Canada*

Aavudai Anandhi, *Indian Institute of Science, Bangalore, India*

Timothy J. Bellerby, *University of Hull, Hull, UK*

Satinder K. Brar, *INRS, Universite du Quebec, Quebec, QC, Canada*

Donald H. Burn, *University of Waterloo, Ontario, Canada*

A. Chandran, *INRS, Universite du Quebec, Quebec, QC, Canada*

S. F. Cheng, *National Sun Yat-Sen University, Kaohsiung, Taiwan*

Ioan M. Ciumasu, *Alexandru Loan Cuza University of Lasi, Lasi, Romania*

Mihai Costica, *Alexandru Loan Cuza University of Lasi, Lasi, Romania*

Dilek Demirbas, *Northumbria University, Newcastle upon Tyne, UK*

Safa Demirbas, *Ministry of Custom Duty and Trade, Bakır Han, İstanbul, Turkey*

Gurpreet S. Dhillon, *INRS, Universite du Quebec, Quebec, QC, Canada*

S. Ghosh, *Indian Institute of Technology, Bombay, India*

M.K. Goyal, *Nanyang Technological University, Singapore*

B.R. Gurjar, *Indian Institute of Technology Roorkee, India*

J. Patrick A. Hettiaratchi, *University of Calgary, Calgary, Canada*

Fiona Johnson, *The University Of New South Wales, Sydney, Australia*

C.M. Kao, *National Sun Yat-Sen University, Kaohsiung, Taiwan*

Surinder Kaur, *INRS, Universite du Quebec, Quebec, QC, Canada*

D. Nagesh Kumar, *Indian Institute of Science, Bangalore, India*

Rakesh Kumar, *National Institute of Hydrology, Roorkee, India*

Amitabh Kundu, *Jawaharlal Nehru University, New Delhi, India*

L. M. Lye, *Memorial University of Newfoundland, Canada*

Rajeshwar Mehrotra, *The University Of New South Wales, Sydney, Australia*

P. P. Mujumdar, *Indian Institute of Science, Bangalore, India*

Najmur R. Nawaz, *University of Leeds, Leeds, UK*

Koji Nishiyama, *Kyushu University, Japan*

CSP Ojha, *Indian Institute of Technology Roorkee, India*

R.P. Pandey, *National Institute of Hydrology, Roorkee, India*

R. K. Rai, *DHI, New Delhi, India*

D. Raje, *Indian Institute of Technology, Bombay, India*

V.U. M. Rao, *Central Research Institute for Dryland Agriculture, Hyderabad*, *India*

Lopamudra Ray Saraswati, *Jawaharlal Nehru University, New Delhi, India*

Cristian V. Secu, *Alexandru Loan Cuza University of Lasi, Lasi, Romania*

Ashish Sharma, *The University Of New South Wales, Sydney, Australia*

R.D. Singh, *National Institute of Hydrology, Roorkee, India*

V.V. Srinivas, *Indian Institute of Science, Bangalore, India*

Uriel Mancebo del Castillo Sternenfels, *University of Calgary, Calgary, Canada*

Rao Y. Surampalli, *University of Nebraska-Lincoln, USA*

T. T. Tsai, *National Sun Yat-Sen University, Kaohsiung, Taiwan*

R.D. Tyagi, *INRS, Universite du Quebec, Quebec, QC, Canada*

V. Tyagi, *Indian Institute of Technology Roorkee, India*

Y. T. Tu, *National Sun Yat-Sen University, Kaohsiung, Taiwan*

Alka Upadhyay, *DHI, New Delhi, India*

B. Venkateswarlu, *Central Research Institute for Dryland Agriculture, Hyderabad*, *India*

Mausam Verma, *INRS, Universite du Quebec, Quebec, QC, Canada*

P.P. Walvekar, *Indian Institute of Technology Roorkee, India*

Song Yan, *INRS, Universite du Quebec, Quebec, QC, Canada*

Tian Zhang, *University of Nebraska-Lincoln, USA*

Xiaolei Zhang, *INRS, Universite du Quebec, Quebec, QC, Canada*

CHAPTER 1

Introduction

R.Y. Surampalli, B.R. Gurjar, T.C. Zhang and C.S.P. Ojha

The present book deals with one of the most important challenges of our times, i.e., Greenhouse Gas (GHG) Emissions and Climate Change. The book is divided in three parts. The first part deals with the basic science and vulnerability assessment related to GHG emissions and climate change. The second part focuses on the application of various techniques in climate change studies. It also covers the impact of climate change in certain spheres of life. The last part of the book deals with approaches to mitigate the impact of climate change. An outline of different chapters is given below.

To start with GHG emissions and climate change, chapter 2, by Gurjar et al., presents an overview of GHG emissions and climate change. The chapter explains GHGs, their global trends and possible roles in climate change. This chapter also discusses the challenges and opportunities in GHG emission control and climate change mitigation along with the policies and programs to reduce GHG emissions. Since the emissions of GHGs can be understood fairly within the broader socioeconomic context, this aspect of GHG emissions and climate change has been addressed in this chapter.

Chapter 3, by Dhillon et al., looks into the contribution of GHGs to climate change. This chapter deals with a detailed description of the GHGs, their current scenario and factors (both natural and anthropogenic) responsible for increasing concentrations. The authors also shed light on causes, effects and impacts of climate change. Various government initiatives such as The Montreal Protocol (1987, Canada), The Kyoto Protocol (1997, Japan), the Underwater Meeting of Maldives Cabinet and Climate Change Summit Copenhagen, Denmark (December 2009) have also been discussed. The chapter also put forth the challenges of Limiting Global Warming to 2^{o}C. To address the challenge of climate change destabilization, it is necessary to decrease dependence on fossil fuel consumption, which needs government initiatives and mass movements for the reduction of GHGs in the environment in order to maintain the inhabitable nature of the planet.

The decision makers need to know clearly the GHGs emission picture so as to put in place the emission control policies. In chapter 4 by Gurjar et al., contributions of various sources of direct and indirect GHGs emissions are presented. Authors provide an overall picture of GHG emissions and trends from various sources like energy, industries, other product use, agriculture, forestry, other land use, transportation, and residential areas. The role of each sector in GHGs emissions can be understood through this chapter.

Next, chapter 5, by Zhang and Surampalli, focuses principally on the impact of GHGs emissions and climate change. Each of the impacts is studied in detail such as higher temperatures, changing landscapes, rising seas, increased risks of natural disasters, threats to human health, biodiversity and wildlife at risk, and social/economic impacts. A framework has been suggested so as to combat climate change with the efforts of the entire society.

GHG emissions and corresponding concentrations need to be reduced and/or stabilized so as to mitigate the climate change. Chapter 6, by Demirbas and Demirbas, sheds light on GHG emissions, concentrations and economics of their stabilization. The authors of this chapter show that future stabilization pathways are dependent on assumptions about energy intensity. It is also stated that in case insufficient action is taken now to reduce emissions, stabilization will become more difficult in the longer term due to the speed of the transition required and the consequent costs of mitigation. Stabilization of GHG concentrations will require deep emission cuts of at least 25% by 2050, and ultimately less than one-fifth of today's levels.

Chapter 7, by Kundu and Saraswati, overviews the indices that have been proposed in recent years to measure different aspects of climate change including the causal factors like GHG emissions and their impact on vulnerability within the framework of human development. Thus, it addresses the critical issues pertaining to the assessment of the impact of climate linked factors on socio-spatial development and vice versa. The chapter is also helpful in evolving a methodology for environmental accounting and computation of green income, often used as the basis for restructuring growth strategies for mitigating depletion of non-renewable resources and ensuring their use without compromising sustainability of development. The chapter mainly focuses on conceptual issues underlying the tools of measurement, examination of their implications for the empirical realities of the region and proposing modifications for better capturing the ground situation.

Impacts of climate change on hydrology have been widely studied in recent literature. Of large relevance in hydrology is the quantification of uncertainties involved in hydrologic projections. It is also acknowledged that hydrologic analyses and designs using assumptions of stationarity are no longer valid because of non-stationarities introduced by climate change. In chapter 8, by Raje et al., a broad overview of uncertainty modeling and methodologies for uncertainty quantification in assessment of hydrologic impacts of climate change is provided. Various sources of uncertainties arising in the impact assessment process are presented. Case studies of quantification, combination and propagation of uncertainty in impact assessment are discussed.

Chapter 9, by Goyal et al., looks into statistical downscaling which has become a powerful means of utilizing outputs on the basis of General Circulation Models (GCMs) to locally observed hydrologic and meteorological variables. The work uses some simplified approaches, such as regression and Artificial Neural Networks (ANN) to establish the linkage between GCM based outputs to locally available variables, such as temperature, precipitation and evaporation. Many a time, input variables to the model may be also correlated, and a rational approach under these situations is to derive another set of variables, also known as principal components. Using these principal components, one can also fit in various models for downscaling. While developing relationships for precipitation, it was observed that use of principal components as variables did not lead to any distinct improvement over the use of raw GCM variables.

Global climate change is one of the key factors that affects the hydrological cycle. In Chapter 10, Pandey et al. aims at presenting the current level of comprehension on relevance of climate change with floods and droughts in different climatic regions; they also enhance understanding and the ability to cope with adverse impacts of floods and droughts on the society. This chapter deals with evidences of increase in extreme events and the complete methodology to estimate flood frequency and the impact of climate change. Two case studies are also included in the chapter to know about the evaluation of impact of climate change on floods of various return periods and probable maximum flood. In the end, authors strongly recommend that the relations presented in this Chapter can be used as a sensible tool for prediction of regional drought characteristics and the planning of appropriate drought management strategies for different climatic regions.

Despite the immense progress in impacts modeling, the range of uncertainties inherent in assessments continues to cause divisions among practitioners deciding how best to incorporate future climate change in the planning process. In chapter 11, by Adeloye et al., through a series of case studies, the major challenges facing the water planner responsible for providing protection against the threat of flooding and drought are discussed along with details on the future implications for planners of continued progress in climate science understanding. In particular, authors focus on the implications of very high resolution climate modeling and probabilistic climate change scenarios.

Chapter 12, by Anandhi et al., deals with Malaprabha River Basin in India. In this chapter, the Support Vector Machine based methodology is suggested for downscaling precipitation and temperature in the river basin. Possible consequences on hydrology of the river basin are also discussed. Furthermore, some of the conceptual and philosophical issues concerning the use of downscaling models are provided in the chapter.

Chapter 13, by Sharma et al., presents an application of a methodology to simulate daily rainfall at 45 locations near Sydney, Australia, using future simulations for three emission scenarios from the CSIRO Mk3.0 Climate Model. Significant improvements are noted in the downscaled rainfall sequences compared to the case where simpler downscaling formulations are used, especially with respect to the ability to simulate sustained droughts and periods of heavy rain.

Chapter 14, by Rai et al., looks into time series modeling of hydro-climatic variables. Authors deal with various statistical tests and demonstrate their approach with data from Yamuna River basin. The chapter uncovers various statistical methods of short- and long-term dependence, trend analysis and periodicity in detail. The application of the methodology for dependence, trend and periodicity is demonstrated using the hydro-climatic data of the Yamuna River basin. The authors conclude that short term dependence is very important for small water resources projects, which requires a shorter period of hydrologic data. Similar to the short term dependence, when a water resources project is planned based on the longer series it is required to test the long term dependence or persistence. Once the persistence test is over, the series is subject to trend analysis.

As developing countries like India are more vulnerable in view of the high population depending on agriculture and excessive pressure on natural resources, Venkateswarlu and Rao have discussed climate change and its impact specifically on Indian agriculture in chapter 15. This chapter covers various trends in key weather parameters, roles of GHGs and their emissions from specific Indian agriculture. Authors have described the impact of climate change on agriculture, livestock, poultry, fisheries, crop water requirements and water resources. Although research on adaptation and mitigation is at the nascent stage in India, authors did not forget to mention the crop based and resource management based strategies. Along with socio-economic and policy issues, this chapter also sheds light on India's first National Action Plan (NAP) on climate change released on June 30, 2008. According to Venkateswarlu and Rao, state agricultural universities and regional research centers will have to play a major role in adaptation research which is more region and location specific while national level efforts are required to come up with cost effective mitigation options, new policy initiatives and global cooperation.

The relationship between agriculture and climatic change is an important issue because the food production resources are under pressure due to a rapid increase in population. Keeping this as a key research area into mind, Kao et al. explained various crop models like EPCI model, ORYZA2000, ORYZA1, SIMRIW and CERES-Rice in chapter 16. The modeling aspects of various crops (e.g., rice, wheat, potatoes, maize, barley, sugarcane and soybean) have been detailed in this chapter. Authors highlighted that the multi-ensembles approach, with varying climate models, emissions scenarios, crop models, and downscaling techniques would enable a move towards a more complete sampling of uncertainty in crop yield projections.

Through an illustration of the application of Self Organizing Map (SOM) analysis to meteorological studies, chapter 17, by Nishiyama, explains 1) the pattern recognition of high-dimensional weather situations using the SOM, 2) the construction of visualized relationships on the two-dimensional SOM space between formed patterns and independent local variable (heavy rainfall frequency in the example) observed in a specific target area, and 3) the features of the local variable frequency identified for each synoptic pattern. For the last decade, unlike the EOF linear conventional analysis, non-linear pattern recognition technique called a self-organizing map (SOM) has also been applied to meteorological studies. This is a kind of unsupervised ANNs technique that provides useful information for visually interpreting high-dimensional complicated climate and weather data. This chapter also recommends some other usages of the SOM methodology.

Chapter 18, by Ciumasu et al., is a limited introduction to the complex issue of climate change and its varying effects of various scales. This deals with particularly those aspects that require distinct, albeit related, understanding of climate changes and elaboration of appropriate policies at local, national, continental and global scales. Authors present the details of techniques and people's perceptions for mitigating climate change, education, training and outreach change and also related challenges and controversies. The chapter ends with the conclusion that the next technological-economic cycle of development will probably be tailored according to the type and degree of success in achieving eco-innovation: capacity to both mitigate and adapt to environmental impacts of past human activities.

Recent climate changes are likely to accelerate as human activities continue to perturb the climate system, and many reviews have made predictions of serious consequences for ecosystems and for supplies and security. As plants take carbon from the atmosphere and store it in their biomass and in soils, land use and land management are important tools in mitigating climate change. With this as a key subject area, Kao et al. in chapter 19, magnifies on enhancing verdurization for mitigating climate change. From the basics of plant biology and photosynthesis, the authors discussed the impact of climate change on plant growth, biodiversity and plant diseases as well as also presented how to mitigate climate change by verdurizing forests and wetland systems.

While there are options like increasing energy efficiency or switching to less carbon-intensive sources of energy, chapter 20 focuses on Carbon Capture and Storage (CCS) because the CCS option is very compatible with the large energy production and delivery infrastructure being in place. To provide the background for CCS, Zhang and Surampalli have described and discussed issues related to carbon cycle, sources of CO_2 and targeted CO_2 sources for CCS and historical evaluation of CCS. Carbon capture technologies, transport of CO_2 and long-term storage means of CO_2 such as geological, mineral and ocean storage are explained in detail in this chapter. The authors also discussed major concerns, constraints and future perspectives of CCS. Accordingly, it is imperative to overcome the technical, regulatory, financial and social barriers of CCS.

Zhang et al. presented the estimation of GHGs emissions during wastewater treatment processes. The strategies of the emission reduction are discussed in chapter 21. Sludge management, including treatment and disposal, is a significant contributor of GHG emissions in wastewater treatment; hence, the emissions are described followed by discussions on reduction and key control strategies. A case study assessing the impacts of changes in treatment technology on energy production and GHG emissions is presented. The authors strongly believe that the adoption of key strategies for reducing GHG emissions in wastewater treatment could significantly reduce the average carbon footprint of citizens and prevent adverse climate change before it affects future generations.

In chapter 22, Hettiaratchi et al. provide a brief review of literature related to landfill methane generation and methods available to quantify bio gas generation within landfills. A short description is followed then after of innovative landfill technologies available to minimize GHG escape, concentrating primarily on landfill bioreactor technology. There is also a detailed description of soil methanotrophy and the technologies that utilize methanotrophy to mitigate GHG emissions from landfills.

With a short description about causes, impacts and overall mitigation options for climate change, Chandran et al. highlighted recycling as an effective option for mitigating climate change in chapter 23. As waste recycling is a growing field of activity, recycling can reduce the use of virgin raw materials and energy, and thus the GHG emissions as well. Chandran et al. clearly mentioned recycling of paper wastes, plastic, textile wastes and organic wastes as an effective strategy for reduction of GHGs. However, authors also make us aware that there are challenges to increasing material recycling, such as market demand of the recycled products, and processes for achieving high quality recycled materials.

Chapter 24, by Dhillon et al., discusses the use of different energy sources in a world scenario as green energy sources to combat growing greenhouse gases emissions. Various climate change mitigation initiates are presented in this chapter, starting with The Montreal Protocol in 1987 to the Climate change summit at Copenhagen, Denmark held in 2009. The authors explained in detail the emerging developments in renewable as well as various international bodies involved in promoting ocean energy, e.g., The European Commission, The International Energy Agency (IEA) and The European Marine Energy Centre (EMEC). Thus, development of green fuels is an important step towards reduction of GHGs emissions and mitigates climate change.

As natural systems pronounce a great amount of GHGs emissions, which is around 4800 Tg CO_2 equivalent per year, Zhang et al., in chapter 25, describe the mechanisms of GHG emissions from natural systems including wetlands, oceans, freshwaters, and so on, and additionally, discuss the strategies to control the emissions. Natural systems that cause GHG emissions include wetlands, oceans and freshwaters, permafrost, termites, ruminant animals, geologic emissions, and wildfires. The biggest GHG emission contributor is wetlands, followed by oceans and freshwaters, permafrost, and geologic emissions, while termites, ruminant animals, and wildfires give a very small amount of emissions. Authors in the end ensures the reduction of global GHG emissions provided current life styles should be changed;

education on consequences of GHG emissions should be popularized; and regulation on limitation of fossil fuel waste should be set.

As briefly described above, the book presents a comprehensive treatise on GHG emissions and climate change incorporating all aspects from causes through processes, impacts and mitigation strategies.

This page intentionally left blank

PART 1

Basic Science and Vulnerability Assessment

CHAPTER 2

Greenhouse Gas Emissions and Climate Change: An Overview

B.R. Gurjar, C.S.P. Ojha, R.Y. Surampalli, P.P. Walvekar, and V. Tyagi

2.1 Introduction

Although initially it was not accepted by many that climate change is real, attention of the world was urgently drawn towards climate change in 1990 when the First Assessment Report of Intergovernmental Panel on Climate Change (IPCC) was published (Prabhakar and Shaw 2008). The IPCC is the leading scientific body for the assessment of climate change, established by the United Nations Environment Programme (UNEP) and the World Meteorological Organization (WMO) to provide the world with a clear scientific view on the current state of climate change and its potential environmental and socio-economic consequences. IPCC reviews and assesses the most recent scientific, technical and socio-economic information produced worldwide and relevant to the understanding of climate change. Thousands of scientists all over the world contribute to the work of IPCC on a voluntary basis as authors, contributors and reviewers. In its report in 2007, IPCC asserted that quite significant climate changes are about to happen, which are linked to increasing concentration of greenhouse gases (GHGs) in the atmosphere. (IPCC 2007a, b).

The increasing GHG emissions from the consumption of fossil fuels are linked to the economic development of a country. The economic activities are further intensified because of globalization and liberalization policies of governments (Ramachandra and Shwetmala 2009).If present GHG emissions are controlled and associated climate risks are coped up better, then there is a possibility of reducing impacts of future climate change (Thomalla et al. 2006). So, it is essential to know about GHG emissions and climate change thoroughly.

2.1.1 Greenhouse Gases

There exists a balanced natural system, known as greenhouse effect that regulates temperature on the earth. The anthropogenic activities can upset this balanced natural system by releasing heat trapping GHGs in the atmosphere.

Thehuman induced enhanced greenhouse effect causes environmental concern in terms of global warming and climate change (IPCC 2007a).

The energy balance of the climate system is significantly altered because of change in atmospheric concentrations of GHGs (IPCC 2007a). The major sources of these gases include industrial processes, fossil fuel combustion for power generation, transportation, burning of the forests, agricultural activities, changes in land use, etc. All forms of burning results into ultimate emission of carbon dioxide (CO_2) gas, which has a high potential GHG. The partial combustion of burning also emits certain gases such as, oxides of nitrogen (NO_x) and carbon monoxide (CO) which can react with other gases in atmosphere to form ozone–another GHG. Water vapor, CO_2, methane (CH_4),nitrous oxide (N_2O)and ozone are considered to be direct GHGs while CO, Fluorocarbons (CFCs, HFCs, SF_6 etc.),oxides of sulphur (SO_x), hydrocarbons and NO_x as indirect GHGs (IPCC 2007b).Although water vapor is the most important GHG, its concentration is not influenced extensively by direct anthropogenic emissions. However, water vapor intensifies warming of the atmosphere as atmosphere holds more water vapor while warming (Smith 1993). But, water vapor is of natural origin and human activities do not affect its concentrations directly.

CO_2contributes the highest proportion of greenhouse effect mainly because of its higher concentration in the atmosphere. Followed by CO_2, Chlorofluorocarbons (CFCs), although present in low concentrations, are very strong greenhouse gases. Anthropogenic emissions of CO_2, CH_4, CFCs and N_2O are the key contributors to the enhanced greenhouse effect. When complex photochemical reactions occur among several pollutants, it leads to formation of tropospheric ozone, which may be a significant GHG, but not quantified globally at present. These GHGs also have direct negative impacts on human health and the ecosystem. The increase in CO_2 concentration in the atmosphere has a major share (over half) of the enhanced greenhouse effect. The rest of the share is contributed mainly by increase in concentrations of halocarbons and CH_4 (Smith 1993). Annual emissions of CO_2 have grown from 21 to 38 GT during 1970 to 2004 (Figure 2.1). It represents 77% of total anthropogenic GHG emissions in 2004. As indicated in Figure 2.1, the rate of growth of CO_2 equivalent emissions was much higher in the recent decade of 1995–2004 than the previous period of 1970–1994. The contribution of non-CO_2 gases to total emissions can be estimated by expressing the emissions of all the gases in CO_2-equivalent units. Most of the observed increase in global average temperatures since the mid-20th century is very likely due to the observed increase in anthropogenic GHG concentrations (IPCC 2007b). Anthropogenic warming over the last three decades has likely had a discernible influence at the global scale on observed changes in many physical and biological systems (IEA 2006).

2.1.2 Role of GHGs in Climate Change

The entire climate system, atmospheric chemistry and life on earth are driven mainly by incident solar radiation. While 30% solar radiation reflected back to the space, the remaining 70% is absorbed by the surface atmosphere system which leads to heating effect of the atmosphere. When the surface and atmosphere become warm, the infrared radiation is emitted. It is also called as long wave radiation. The process of net incoming solar energy (i.e., downward solar energy less the reflected) and outgoing heat radiation from the warmer planet which escapes to space will continue until the two energy components are in balance. This energy balance of radiation provides a strong constraint on the global average temperature of the planet. GHGs absorb and emit long wave radiation, while aerosols absorb and scatter solar radiation. Large size aerosols also absorb and emit long wave radiation, but this process is not significant for the smaller human induced aerosols.

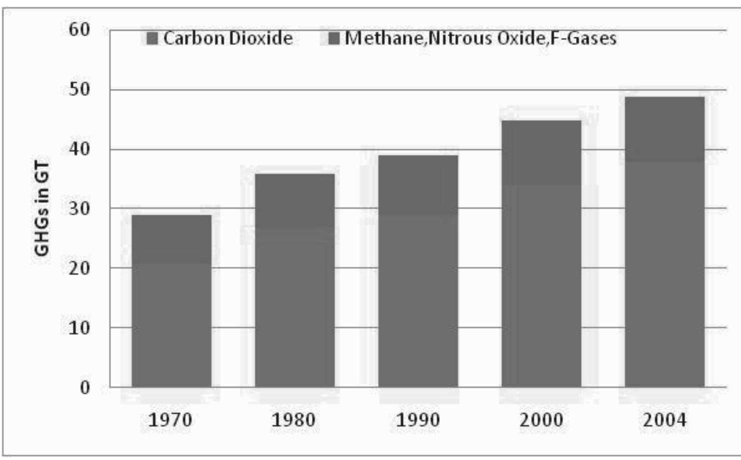

Figure 2.1. Global anthropogenic GHG emissions (Adapted from IPCC 2007b)

As shown in Figure 2.2, trapping of long wave radiation can be explained well by principles of quantum mechanics (Ramanathan and Feng 2009). The oxygen atoms vibrate with carbon atom in centre. The frequency of this vibration matches with some of the long wave radiations from the earth surface and the atmosphere, resulting in absorption of radiation by GHGs. These gases colloid with other air molecules and trapped radiation is converted into heat which is given back to the Earth's surface. As the concentration of GHGs increases in the atmosphere, the infrared layer also becomes thicker resulting in an accumulation of excess energy on the planet. The planetary system gets rid of this excess energy by warming and emitting excess infrared radiations until the surface atmosphere system is in balance.

When variations in components of the climatic system take place, it results in climate change (Smith 1993). The climatic system has five components coupled with each other, namely, atmosphere, land, ocean, ice and biosphere. Atmospheric processes strongly interact with other components of the climate system giving rise to climate change. Particularly, energy from the Sun is the driving force in the climatic system. Greenhouse effect causes significant changes in other components of the climatic system, resulting in climate change. Accordingly, climate change refers to the undermining impact on climate and weather patterns. Increased severe weather conditions like draughts, storms, floods, change in the ecosystem, loss of animal and plant species, stresses to human health, and alterations in regional agricultural productivity are accompanied with very small changes in average atmospheric temperatures (PLANYC 2007). Hence, it is very important to establish a good link between GHGs and climate change to make value judgements for limiting the effects.

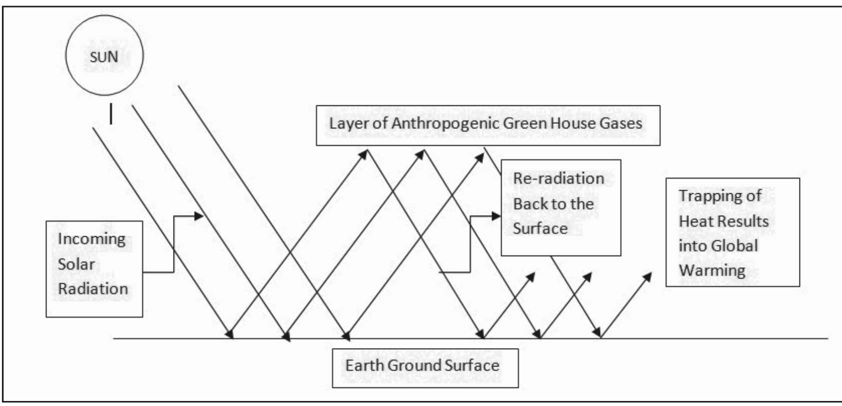

Figure 2.2. GHGs and climate change through global warming

2.2 Trends of GHG Emissions (Change in Climatic Parameters)

The global trend in total GHG emissions is dominated by fossil-fuels emissions. Between 1970 and 2004, global anthropogenic CH_4 emissions increased by almost 40%, N_2O by 50% and the F-gases by almost 400%. F-gas emissions doubled in the 1990–2004 period. If weighted by their Global Warming Potential (GWP), total emissions of all GHGs increased by over 75% since 1970 (IEA 2006).

As illustrated in Figure 2.3, the concentrations of gases such as CO_2, N_2O, and CH_4 are presently increasing in the atmosphere. The stagnation phase was observed of CH_4 a few years ago, but it is now increasing again. The production of CFC-11 ($CFCl_3$) and CFC-12 (CF_2Cl_2) have been completely stopped and banned for use because these are the two main culprits for ozone depletion. While the atmospheric CFCs and other greenhouse gases are showing a slow decreasing trend, they will remain in the atmosphere for the next few decades due to their long lifetimes (Lal 2010).

The details of mixing ratios of some of the GHGs in ppm by volume or ppb by volume during pre-industrial time, present time, annual increase rates and GWP of these gases are shown in Table 2.1. GWP is a measure of a given mass of GHG that is estimated to contribute to global warming. It is a relative scale which compares a particular gas to that of the same mass of CO_2 whose GWP is 1. A GWP is calculated over a specific time interval as the lifetimes of these gases differ considerably.

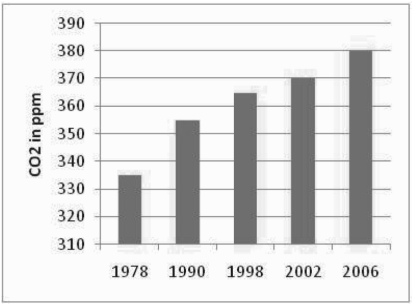

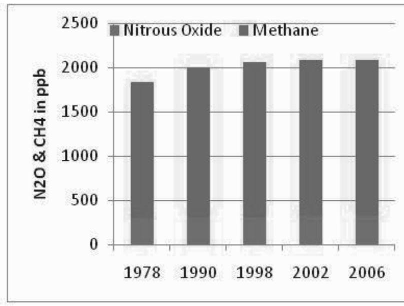

Figure 2.3. Average concentrations of GHGs for the last three decades (Adapted from Lal, 2010)

Table 2.1. Mixing ratios of some of the GHGs during pre-industrial time and present day along with other parameters (adapted from IPCC 2001; Lal 2010)

GHG	Concentration (Pre-industrial time)	Concentration (Present day)	Annual increase rate	Lifetime	GWP (100 yrs horizon)
CO_2	280 ppmv	387 ppmv	1.8 ppmv	5–200 yrs*	1
CH_4	700 ppbv	1.74 ppmv	1.7ppbv	12 yrs	25
N_2O	270 ppbv	320 ppbv	0.7 ppbv	150 yrs	298
Tropospheric ozone	10–20 ppbv	35–50 ppbv	0.12 ppbv	Few days to months	1200–2000

*No single lifetime can be defined for CO_2 because of the different rates of uptake by different removal processes.

Global warming will be increased if GHG emissions are continued at or above current rates, causing significant changes in the global climate system during the 21st century. These changes will very likely be larger than those observed during the 20th century (IPCC 2007b). Emissions of the GHGs covered by the Kyoto Protocol increased by about 70% from1970–2004 (by 24% from 1990–2004), with CO_2 being the largest source, having grown by about 80%. The largest growth in CO_2 emissions has come from power generation and road transport. CH_4 emissions rose by about 40% from 1970, with an 85% increase from the combustion and use of fossil fuels. Agriculture, however, is the largest source of CH_4 emissions. N_2O emissions grew by about 50%, due mainly to increased use of fertilizer and the growth of agriculture. Atmospheric CO_2 concentrations have increased by almost100 ppm since their pre-industrial level, reaching 379 ppm in2005, with mean annual growth rates during 2000–2005 higher than in the 1990s. The total CO_2-equivalent (CO_2-eq) concentration of all long-lived GHGs is now about 455 ppmCO_2-eq.incorporating the cooling effect of aerosols, other air pollutants and gases released from land-use change into the equivalent concentration, leads to an effective 311–435 ppm CO_2-eq concentration.

The global GHGs will continue to grow over next few decades if there is no significant change in current climate change mitigation policies and related sustainable development practices (IPCC 2007b).For 2030, projections of total GHG emissions consistently show an increase of 25–90% compared with 2000,with more recent projections higher than earlier ones (IPCC 2007c).

2.3 Impacts of Climate Change at Different Scales

The rising emissions of GHGs and the greenhouse effect are responsible for the overall warming of the Earth's climate, leading to global warming, although the condition varies with the regions, as either cooling or wetter weather can be experienced at various regions; while on average the temperature of the planet is rising. There are so many evidences of increases in global average air and ocean temperatures, widespread snow and ice melting and rise in global average sea level. These observations prove that climate change is now an indisputable matter. Climate change has widespread impacts on ecosystems, biodiversity, human health, hydrology, and water resources. It may even give rise to certain extreme events disturbing the balance in the components of the climatic system. Based on respective sensitivity, adaptive capacity and vulnerability, different regions and sectors are impacted by climate change. The adverse impacts of climate change are beard by less developed and poor societies. Many developing countries have not even tuned their policies to the existing climate variability. These countries are more vulnerable to climate change impacts such as high damage to assets and life as compared to developed countries (Shukla et al. 2003).

A study in the US suggests that a warming climate could increase the severity of summertime pollution episodes in the north-eastern and mid-western United States. The decrease in frequency of surface cyclones tracking across southern Canada is the cause of concern for the increased severity of summer time pollution episodes in north-eastern and mid-western United States (Mickley et al. 2004).With reference to conditions in central Europe, it is estimated based on model calculations that there will be an increase in heat load days in summer; on the contrary, the number of days with cold load in winter will decrease. The power consumption will probably fall in cities where the winter is the determining factor (Kuttler 2001).

The World Health Organisation estimates that the warming and precipitation trends due to anthropogenic climate change of the past 30 years claim more than 150,000 lives per year (WHO 2002). Many prevalent human diseases are correlated to climate fluctuations, such as cardiovascular mortality, respiratory illnesses due to heat waves, altered transmission of infectious diseases and undernourishment from crop failures. Potentially vulnerable regions include the temperate latitudes, which are projected to warm disproportionately. The regions around the Pacific and Indian oceans are currently subjected to large rainfall variations due to expansive cities where the urban heat island effect could intensify extreme climatic events.

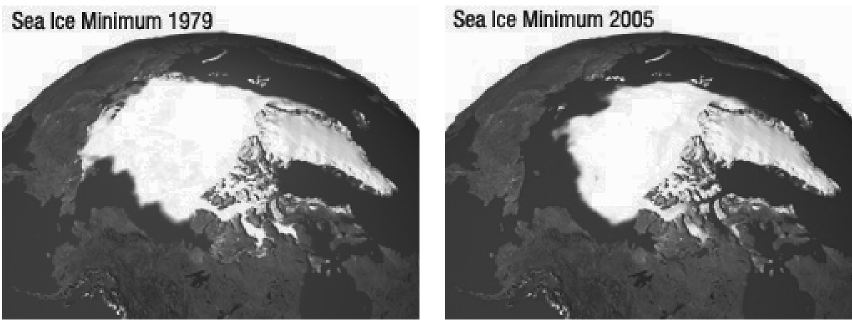

Figure 2.4. Summer Arctic Sea ice decline (Source: NASA 2005)

The rates of warming and sea level rise accelerated during the 20^{th} century and more intense precipitation, drought and, to some extent, tropical cyclones occurred. Eleven of the last twelve years rank among the twelve hottest years on record. Mountain glaciers and snow cover have declined, on the whole, in both the northern and southern hemispheres. Average Arctic sea extent ice has shrunk by 20% at its summer-time minimum since satellite observations began in 1978 (Figure 2.4). The understanding of anthropogenic warming and cooling influences on climate has improved now, leading to very high confidence that the globally averaged net effect of human activities, since 1750, has been one of warming (IPCC 2007a).

IPCC observed relative differential change in observed average surface temperature, sea level and northern hemisphere snow cover. The 100year linear trend (1906–2005) of 0.74 °C is larger than the corresponding trend of 0.6 °C (1901–2000). A widespread temperature increase is observed all over the world while it is greater at higher northern latitudes. The rise in sea level observed is also consistent with global warming. The average rate of sea level rise since 1961 is 1.8mm/yr and 3.1 mm/yr since 1993 because of the contributions from thermal expansion, melting glaciers and ice caps and polar ice sheets. The decrease in snow and ice extent is also consistent with warming. Eastern parts of North and South America, northern Europe, northern and central Asia have experienced increased precipitation from 1990 to 2005 differentiating with Sahel, the Mediterranean, southern Africa and parts of southern Asia where precipitation is decreased. The increase in draught affected area is observed all over the world since the 1970s. More frequent cold days, cold nights and frosts are likely to be replaced nowadays by frequent hot days and hot nights (IPCC 2007b).

It is believed that most of the ecosystems can sustain global temperature change of 0.1^{0}C per decade at the most before experiencing adverse ecological stresses which may lead, in some cases, to species extinction (Buchdahl 2002). The response of individual species to new conditions will be changed by the composition and geographic distribution of ecosystems which are not managed properly. The combination of climate change, deforestation and other environmental stresses may lead to degradation and fragmentation of the habitats simultaneously. The habitats exposed to first impact, experiencing severe effects and not having adequate adaptive capacity are considered as most vulnerable ecosystems, like tropical forests, deserts, low lying areas, arctic regions, wetlands, mountain systems, coral reefs and coastal marshy areas. These vulnerable ecosystems are influenced by changes in climatic components such as temperature, rainfall, sunlight radiation, cloud cover and other extreme events. It is predicted that tropical forests and grasslands will be nowhere by the 2080s, if GHG emissions are not mitigated especially in South America and central southern Africa. This loss will be substantially reduced even before the 2230s, if CO_2 emissions are reduced to 550 ppm (Buchdahl 2002).

Climate change leads to biodiversity menace. The tropics, particularly tropical forests have a high degree of biodiversity. It is estimated that extinction of species occurs at a rate of 1–11% per decade in tropical forests (Buchdahl 2002). Climate change through global warming also gives rise to human health problems related to cardiovascular, respiratory, and other diseases. Greater intensity heat waves for longer durations, floods, storms and other extreme climatic events may result in major or minor injuries, psychological disorders and even deaths. However, cold related deaths should be reduced by warmer temperatures in cold climates. But negative effects are not at all balanced by such positive effects. Instead, indirect effects are more important in longer term.

2.4 GHGs Emission Reduction and Climate Change Mitigation

Climate change mitigation is the action taken to decrease the intensity of radiative forcing so as to reduce the potential effects of global warming. The reduction of greenhouse gas emissions by reducing waste energy and switching to cleaner energy sources is the key solution for climate change mitigation. There are various energy conservation methods available such as increasing the fuel efficiency of vehicles, change in lifestyle and change in business practices. The climate change mitigation focuses mainly on use of renewable energy sources such as solar, wind, tidal, geothermal, and biomass power. Scientists prepared a plan to power 100% of the world's energy with wind, hydroelectric, and solar power by the year 2030 (Jacobson and Delucchi 2009). GHGs mitigation can be achieved by adopting newly developed and currently available technologies including renewable energy and nuclear power which is more controversially nowadays. The use of carbon sinks, carbon credits, and taxation are also aimed to achieve precise GHGs mitigation.

More essential proposals which may be grouped with mitigation include bio sequestration of atmospheric CO_2 and geo-engineering techniques ranging from carbon sequestration projects including CO_2 capture, transport and storage. Such measures are quite effective mostly for countries with ever-increasing global population and the planned growth of national GDPs.

A program is proposed by Pacala and Socolowso as to reduce CO_2 emissions by 1 billion metric tons per year or 25 billion tons over the 50year period (Pacala and Socolow 2004). The programs proposed to achieve this target are:

1. more efficient vehicles−increase fuel economy from 30 to 60 mpg (7.8 to 3.9 L/100 km) for 2 billion vehicles;
2. reduce use of vehicles−improve urban design to reduce miles driven from 10,000 to 5,000 miles (16,000 to 8,000 km) per year for 2 billion vehicles;
3. efficient buildings−reduce energy consumption by 25%;
4. improve efficiency of coal plants from 40% to 60%;
5. replace 1,400 GW (gigawatt) of coal power plants with natural gas;
6. capture and store carbon emitted from 800 GW of new coal plants;
7. capture and store carbon from coal to syn fuels conversion at 30 million barrels per day (4,800,000 m^3/d);
8. displace 700 GW of coal power with nuclear;
9. add 2 million 1 MW wind turbines (50 times current capacity);
10. displace 700 GW of coal with 2,000 GW (peak) solar power (700 times current capacity);
11. produce hydrogen fuel from 4 million 1 MW wind turbines;
12. use biomass to make fuel to displace oil (100 times current capacity);
13. stop de-forestation and re-establish 300 million hectares of new tree plantations; and
14. Conservation tillage−apply to all crop land (10 times current usage).

If these proposed programs are implemented properly, climate change mitigation can be expected–provided challenges against these are overcome successfully.

2.4.1 Challenges and Opportunities

The climate change mitigation measures differ from region to region because of differential nature of economic development needs, resource endowments, adaptive and mitigative capacities across regions. There is as such no common approach which fits in all conditions to the climate change problem. The solutions to this problem will differ regionally according to various socioeconomic conditions and also geographical differences to a lesser extent. The adoption of suitable policy approach is the key factor in climate change mitigation. The most promising policy approaches are those which make the advantage of natural synergies between developmental priorities and climate protection so that both will advance simultaneously (IPCC 2007c).

Worldwide several challenges and threats are experienced while solving climate change problem by various countries. These challenges are generally classified as economic, psychological, and informational, and institutional. The present world economic system including its price structure presents a serious threat. Growing market failures and price distortions continue to produce inequitable results which will weaken international agreements and compliance. Initiatives must be introduced to improve on pricing systems and overcome the serious market failures that still persist. The attitudes of several countries towards accepting responsibility will weaken international agreements and hence affect national decisions (Davidson 1995). Develop countries must accept the concept of "natural debt", the accumulation of historical GHG in the atmosphere and therefore should be central in solving the problem. Developing countries must be prepared to adopt low-GHG emission strategy to contribute towards the solution of the climate problem.

Data limitations and poor access to information are major threats to the solution of the climate problem. This more true for analysis and technological development. If this area is not improved, significant large number of countries will find it hard to be involved in solving the climate problem. Significantly large number of countries in the world lack adequate institutions to cope with climate change analysis and this will present serious problems in developing national plans and actions. The need for institutions and appropriate organizational arrangements is crucial to mitigation analysis in any country (Davidson 1995).

The integrated scientific retort is required to understand clearly the causes and impacts of climate change because of its inherent complexity. There is also a need for a scientific policy interface which helps to generate new forms of engagement among scientists, policy makers and stakeholders. These engagements may contribute to more informative climate policy and practice (Martens et al. 2009).

Adaptation of climate change can take many forms such as upgradation of buildings and critical infrastructure, change in agricultural practices and development of new methodologies to keep cool during a heat wave. The knowledge of risks associated with climate change, likely impacts of it, and also the capacity and ability to act based on that knowledge is required for effective adaptation of climate change (The Action Plan, 2010). Few other barriers which come across adaptation of climate change specifically related to Asian coastal megacities are given by Fuchs, such as lack of awareness about the magnitude of risks and rapidly increasing vulnerability due to climate change and urban growth, need to handle the problems of housing, transportation and poverty. The budgetary constraints, lack of institutional mechanism to coordinate relevant activities, territorial jurisdiction and also lack of technical, scientific and managerial capacity are considered to be the major constraints which should be overcome first (Fuchs 2010).

The assessment of effectiveness of GHG mitigation measures will be quite difficult in future because of the vast changing conditions. The implementation of agricultural GHG mitigation will be limited to less than 35% of total biophysical potential by 2030 because of economic constraints. It will be limited further by various constraints (Smith et al. 2007).

2.4.2 Global Policies and Programs to Reduce GHG Emissions

The magnitude and rate of climate change will be lowered if serious actions are taken right now to reduce the significant built-up of GHGs (Abraham 2007). The

United Nations Framework Convention on Climate Change (UNFCCC) plays a crucial role for promoting international responses to climate change. There are various policies and programs conducted globally to put down the GHG emissions. The first addition to the treaty, the Kyoto Protocol was initially adopted on 11 December 1997 in Kyoto, Japan and entered into force on 16 February 2005. As of February 2007, 168 states and the European Economic Community have ratified the Protocol. According to Article 3.1 of Kyoto Protocol, Annex I Parties in aggregate agreed to reduce their overall GHG emissions to at least 5% below 1990 levels (IPCC 2007c). This is considered to be the first step towards achieving the GHGs reduction targets. Its full implementation by all the Protocol signatories, however, would still be far from reversing overall global GHG-emission trends.

Other voluntary international initiatives to develop and implement new technologies to reduce GHG emissions include: Carbon Sequestration Leadership Forum which promotes CO_2 capture and storage; the Hydrogen partnership; the $CH_4$to Markets Partnership, and the Asia-Pacific Partnership for Clean Development and Climate, which includes Australia, USA, Japan, China, India and South-Korea. In the meeting in Gleneagles, Scotland in2005 of G8, Climate change has also been considered as an important growing concern. A plan of action was developed and the task is given to the International Energy Agency, the World Bank and the Renewable Energy and Energy Efficiency Partnership (IPCC 2007c). The meeting leads to the development of a dialog process about a Clean Energy, Climate Change and Sustainable Development for the largest emitters.

The Japanese government proposed that a sectoral approach would be effective for reducing GHG emissions, on both national and international levels. The proposal integrates sector-based or bottom-up approaches to determine the reduction targets for national emissions and presents flexible emission reduction targets which are practical in nature for developing countries, including intensity improvement targets by sector. It also indicates that environmental issues like climate change must be considered globally, but these should be acted upon locally (Akimoto et al. 2010).

Currently, the policies are evaluated based on Concept of global warming potential of each GHG relative to that of CO_2, integrated over different time horizons. However, this process is quite complicated because of indirect effects from unquantifiable chemical reactions and by uncertainties associated with the effective residence time of CO_2 in the atmosphere (Smith 1993).

2.5 Socio-economic and Political Implications

GHG emissions can only be understood appropriately within the broader socioeconomic context. This context is not only in respect of emissions, but the degree to which countries have the financial and institutional capacity to address the causes and consequences of climate change. Evidences prove that the poorest people are not only often more exposed to specific climate change impacts, but are also more vulnerable to those impacts. Climate change will widen existing inequalities, globally and locally, unless social impacts are actively addressed across the range of adaptation and mitigation measures (SNIFFER 2009).

A striking aspect of the major GHG-emitting countries is their disparities in development levels, as measured by income per capita and other economic and human development indicators. Although in terms of percentage, per capita income is growing faster in developing countries than in industrialized countries, in absolute terms, the income gap is actually widening. In 2002, annual per capita income among the top emitting countries ranged from over $34,000in the United States (4th globally) to under $2,000in Pakistan (138thglobally). Other significant measures of acountry's capacity to address climate change or other complex social challenges include life expectancy, educational achievement, and quality of governance(for example, political stability, level of corruption).

The major four GHG emitters have significant electricity access deficits, with India alone accounting for almost 600 million people. About half of the developing world—2.4 billion people—rely on traditional forms of biomass for cooking and heating. It follows that, without commercial energy services, modern conveniences like refrigeration are often unobtainable (Baumert et al. 2005).

A study was carried out to evaluate the economic impacts of climate change on agriculture and fishing sector of Namibia, as both constitute important economic sectors in the Namibian economy (approximately 5% of GDP each). The study revealed that the climate change impacts on the total GDP could range between losses of N$ 500 and 1000 million if only the agricultural impacts are considered. These figures correspond to about 1.5% and 3.5% of GDP. If production losses within the fishing industry are included, the total losses could be up to N$ 2000 million in a worst case scenario, implying 6.5% of the total GDP (Reid et al. 2007).

Chen et al. (1999) examined the economic damages in the agricultural sector arising from a potential climate change induced shift in El Niño Southern Oscillation (ENSO) event frequency and strength. The damage estimates reported here are in the context of the global agricultural system. Annual damages in context of global agricultural system in the $3–400 million U.S. dollar range are found if only the frequency of ENSO events changes. However, annual damages rise to over $1 billion if the events also intensify in strength. Event anticipation and crop mix adaption on the part of farmers can help offset the damages but cannot fully alleviate them.

According to a study by Kumar et al. (2008) the estimated economic losses due to the impact of climate change in Mumbai are described in Table 2.2. It includes the impact of temperature rise on rains and floods, and their consequent effects on health. Other consequences like increase in deaths due to vector-borne diseases, dislocation due to floods and sea-level rise have been shown as projected economic losses for the years 2025 and 2050.

Both climate change and policies to minimize its effects have enormous environmental and economic implications. The costs of climate change will vary widely from country to country. Developed countries are responsible for over two thirds of past emissions and some 75% of current emissions, but they are best positioned to protect themselves from damage. Developing countries have low per capita emissions and are in great need of economic development and are more vulnerable to climate-change impacts (Earth Summit+5 1997).

Table 2.2. Estimate economic losses due to climate change impact in Mumbai (Adapted from Kumar et al. 2008)

Type of impact	Cost in Rupees (crores)
Dislocation due to extreme events of flooding till 2050	407.6
Material damage till 2050	6413
Mortality costs till 2050	3050
Disability adjusted life years lost due to diseases like, malaria, diarrhoea and leptospirosis	3153
Building-foundation damages due to sea-level rise	15,01725
Tourism loss: less number of tourists visiting Mumbai	19,63,500

The political issue in the climate change debate is whether the developed countries, which emit much of the GHGs in the atmosphere, should bear much more responsibility with regard to climate change. The Southern countries insist on the principle of 'common but differentiated responsibilities' with regard to climate change. This is the basic issue in the climate change debate since the Kyoto Protocol, which has been systematically challenged by lobby of developed countries during the recent Copenhagen summit to push the agenda of reduction in GHG emissions by both the 'North' and the 'South', and to regard 'global warming' as a common concern of both the developed and developing countries (Lahiry 2010). Since the GHG emission reduction policies and programs directly influence the economic growth of a country, it is yet to be seen how developing countries and emerging economies respond in the post-Copenhagen era.

2.6 References

Akimoto, K., Sano, F., Homma, T., Oda, J., Nagashima, M., and Kii, M. (2010). "Estimates of GHG emission reduction potential by country, sector, and cost."*Energy Policy*, 38, 3384–3393.

Abraham, M. (2007). "Global Climate Change:Corporate and Personal Action." Published online 7 March 2007 in Wiley InterScience <www.interscience.wiley.com>. DOI 10.1002/ep.10196.

Baumert, K. A., Herzog, T.,and Pershing, J. (2005). “Navigating the Numbers: Greenhouse Gas Data andInternational Climate Policy.” World Resource Institute. ISBN: 1-56973-599-9.

Buchdahl, J. (2002). “Climate Change: Fact Sheet Series forKey Stage 4 and A-Level.”*ACE* (Atmosphere Climate and Environment) *Information Programme*, aric, Manchester Metropolitan University, Chester Street, Manchester M1 5GD.

Chen, C. -C., McCarl, B. A., and Adams, R. M. (1999). “Economic implications of potential climate change induced ENSO frequency and strength shifts.” Available at <www.usgcrp.gov/usgcrp/nacc/agriculture/chen3> (accessed Oct. 2011).

Davidson, O. R. (1995). “Strategies to mitigate climate change in a sustainable development framework.” In: *International Conference on National Action to Mitigate Global Climate Change at Copenhagen*, *UNEP Collaborating Centre on Energy and Environment*, Riso National Laboratory, Denmark, June 1995.

Earth Summit+5 (1997). “Special session of the general assembly to review and appraise the implementation of Agenda 21.” available at <http://www.un.org/ecosocdev/geninfo/sustdev/climate.htm> (accessed Oct. 2011).

Fuchs, R. J. (2010). “Cities at risk: Asia’s coastal cities in an age of climate change.”*Asia-Pacific Issues*, Analysis from the East-West Center No. 96, July 2010.

Grover, R. C. (2008). “CDM Projects–How companies can benefit from it?” Available at <http://aidaindia.org/its08/images/date%2021-3-08/.../R.C%20 Grover.ppt> (accessed Oct. 2011).

International Energy Agency (IEA) (2006). *Part III: Greenhouse Gas Emissions.*CO_2 *Emissions from Fuel Combustion* (2006 Edition).*International Energy Agency (IEA)*, published on 13 November 2006.

IPCC (2001). *Climate Change (2001): The Science Basis, Summary for Policy Makers*. Contribution of Working Group I. Cambridge University Press, Cambridge.

IPCC (2007a). *Climate Change (2007): The Physical Science Basis*. Contribution of Working Group I to the Fourth Assessment Report of the Intergovernmental Panel on Climate Change [Solomon, S., D. Qin, M. Manning, Z. Chen, M. Marquis, K.B. Averyt, M. Tignor and H.L. Miller (eds.)]. Cambridge University Press, Cambridge, United Kingdom and New York, NY, USA, 996 pp.

IPCC (2007b). *Climate Change (2007): Synthesis Report*. Contribution of Working Groups I, II and III to the Fourth Assessment Report of the Intergovernmental Panel on Climate Change [Core Writing Team, Pachauri, R.K and Reisinger, A. (eds.)]. *IPCC*, Geneva, Switzerland, 104 pp.

IPCC (2007c). *Climate Change 2007: Mitigation*. Contribution of Working Group III to the Fourth Assessment Report of the IntergovernmentalPanel on Climate Change [B. Metz, O.R. Davidson, P.R. Bosch, R. Dave, and L.A. Meyer (eds)], *IPCC*, Cambridge University Press, Cambridge, United Kingdom and New York, NY, USA.

Jacobson, M.Z., and Delucchi, M.A. (2009). "A plan to power 100 percent of the planet with renewables (originally published as "A path to sustainable energy by 2030")." *Scientific American,* 301(5), 58–65.

Kumar, R., Jawale, P., and Tandon, S. (2008). "Economic impact of climate change on Mumbai, India."*Regional Health Forum*, 12(1), 38–42.

Kuttler, W. (2001). "Urban climate and global climate change." In *Climate of the 21st Century: Changes and Risks Scientific Facts*, Edited by Lozan, J. L., Grabl, H., and Hupfer, P., WissenschaftlicheAuswertungenHamburg, 2001.

Lahiry, S. (2010). "Climate change: socio-political implications."*Mainstream*, Volume XLVIII, No 29, July 10, 2010. Available at <http://www.mainstreamweekly.net/article2188.html> (accessed 9/10/2010).

Lal, S. (2010). "India and global climate change." In: *Science in India Achievements and Aspirations: 75 Years of the Academy*, H.Y. Mohan Ram and P.N. Tandon (eds.), *Indian National Science Academy,*Bahadur Shah ZafarMarg, New Delhi.

Martens, P., McEvoy, D., and Chang, C. (2009). "The climate change challenge: linkingvulnerability, adaptation,and mitigation."*Current Opinion in Environmental Sustainability*, 1(1), 14–18.

Mickley, L.J., Jacob, D. J., Field, B.D., and Rind, D. (2004). "Effects of future climate change on regional air pollution episodes in the United States."*Geophysical Research Letters*, 31, L24103, doi:10.1029/2004 GL021216.

NASA (2005). "Arctic sea ice continues to decline, arctic temperatures continue to rise in 2005." News on NASA website. Available at <http://www.nasa.gov/centers/goddard/news/topstory/2005/arcticice_decline.hhth> (accessed May, 2011).

Pacala, S., and Socolow, R. (2004). "Stabilization wedges: Solving the climate problem for next 50 years with current technologies." *Science*, 305, 968–971.

PLANYC (2007). "Inventory of New York City, greenhouse gas emissions - April 2007." Mayor's Office of Operations, Office of Long-Term Planning and Sustainability, 253 Broadway, 10th floor New York, NY 10007.

Prabhakar, S. V. R. K., and Shaw, R. (2008). "Climate change adaptation implications for drought risk mitigation: a perspective for India."*Climatic Change*, 88, 113–130.

Ramachandra, T., V., and Shwetmala (2009). "Emissions from India's transport sector: Statewise synthesis."*Atmospheric Environment*, 43, 5510–5517.

Ramanathan, V., and Feng, Y. (2009). "Air pollution, greenhouse gases and climate change: Global and regional perspectives."*Atmospheric Environment,* 43, 37–50.

Reid, H.,Sahlen, L.,MacGregor, J., and Stage, J. (2007). "The economic impact of climate change in Namibia: How climate change will affect the contribution of Namibia's natural resources to its economy?" Environmental Economics Programme Discussion Paper 07-02.International Institute for Environment and Development, London.

Shukla, P. R., Sharma, S. K., Ravindranath, N.H., Garg, A., and Bhattacharya, S. (2003). *Climate Change and India: Vulnerability Assessment and Adaptation*.

ISBN 8173714711, Universities Press (India) Private Limited, 3-5-819, Hyderguda, Hyderabad, 500029.

Smith, I.M. (1993). "CO_2 and climate change: An overview of the science."*Energy Conversion Management*, 34(9–11), 729–735.

Smith, P., Martino, D., Cai, Z., Gwary, D., Janzen, H., Kumar, P., McCarl, B., Ogle, S., O'Mara, F., Rice, C., Scholes, B., Sirotenko, O., Howden, M., McAllister, T., Pan, G., Romanenkov, V., Schneider, U., andTowprayoon, S. (2007). "Policy and technological constraints to implementation ofgreenhouse gas mitigation options in agriculture."*Agriculture, Ecosystems and Environment*, 118, 6–28.

SNIFFER (Scotland and Northern Ireland Forum for Environmental Research), 2009. *DifferentialSocial Impacts of Climate Change in the UK*. January, 2009. Project UKCC22.

The Action Plan (2010). *Taking Action for Victoria's Future: Victorian Climate change White Paper–The Action Plan.Victorian Government Department of Premier and Cabinet*, Melbourne, Australia, July 2010. Available at:<www.premier.vic.gov.au.> (accessed April 2011).

Thomalla, F.,Downing, T., Spanger-Siegried, E.,Han, G., and Rockstrom, J. (2006)."Reducing hazard vulnerability: Towardsa common approach between disaster riskreduction and climate adaptation." *Disasters*, 30(1), 39–48.

WHO (World Health Organisation) (2002). *The World Health Report 2002: Reducing Risks, Promoting Healthy Life.WHO*, Geneva 27, Switzerland.

CHAPTER 3

Greenhouse Gas Contribution on Climate Change

Gurpreet S. Dhillon, Ajila C. M, Surinder Kaur, Satinder K. Brar,
Mausam Verma, R.D. Tyagi, and Rao Y. Surampalli

3.1 Introduction

Earth is made inhabitable by a layer of greenhouse gases (GHGs) present in the atmosphere which reflect sun radiations back to the Earth's surface. GHGs, such as carbon dioxide, water vapor, methane, nitrous oxide, ozone and fluorocarbons act as natural temperature regulators. In the past century, the GHGs layer has become thicker, and it has resulted in continuous increase in temperature i.e. global warming. Due to human activities in the recent years, the concentration of GHGs is increasing at very fast pace. The increase in concentration of GHGs has an alarming impact on the environment. Global warming results in melting of the glaciers/ice caps and causes rise in sea levels, droughts, hurricanes, floods, forest fires with greater rage, which are threatening fragile eco-systems and affecting migration of species. The increasing anthropogenic concentration of carbon dioxide in the atmosphere has resulted in ocean acidification threatening marine ecosystems (Buseck and Posfai 1999).

GHGs act as Earth's natural shield which helps to maintain the temperature needed for survival of life, i.e., 53^{o}F (15^{o}C), which is 33^{o}C warmer than with an atmosphere without GHGs. The greenhouse effect is defined as the rise in temperature level of the Earth due to the presence of GHGs in the atmosphere, such as water vapor, CO_2, N_2O, O_3, fluorocarbons and CH_4 which have the ability to trap solar energy.Climate is primarily influenced by Earth's energy budget, which depends on radiation received from the sun and energy radiated back to the atmosphere. Incoming solar radiations are basically in the visible range, whereas the exiting radiations are in the infrared (IR) region. GHGs, such as H_2O, CO_2, CH_4, and N_2O absorb IR and radiate it back to the Earth's surface as shown in Figure 3.1.

In addition to GHGs, aerosol particles (suspensions of solid or liquid particles in air), such as volcanic mineral emissions, desert dust, re-entrained road dust, sea salt, sulfates, carbonaceous materials, organic compounds, among others, also exert an important influence on global climate. The aerosol particles are ubiquitous in troposphere, and they can locally intensify or moderate the effects of GHGs through the scattering or absorption of both incoming solar radiation and thermal radiation emitted from the Earth's surface as well as by acting as cloud condensation nuclei (CCN) and modify the radiative properties of clouds. However, the influence of aerosol particles on Earth's radiation balance is less widely realized; the role of air-borne minerals has be identified only quite recently (Buseck and Posfai 1999).

According to the effectiveness of absorbing long wave radiations, the different GHGs are placed in the following order (IPCC 2007a): a) water vapor: 36–70%; b) carbon dioxide: 9–26%; c) methane: 4–9%; and d) ozone: 3–7%.

GHGs do not have any effect on the incoming solar radiation (shortwave radiation). The sunlight is absorbed by the Earth's environment. Heat from the Earth's surface radiates up to the atmosphere in the infrared energy form (long wave radiation), which is absorbed by the GHGs. Therefore, GHGs act as a shield and protect these long wave radiations to pass through. In the absence of GHGs, heat would escape back into space, and Earth's average temperature would be about 60ºF (-18^{o}C) colder which will not be suitable for the living beings. From the last few decades, the concentration of these GHGs is rising alarmingly at enormous rates which pose negative effects on climate. The increasing Earth's temperature leads to the phenomenon known as global warming. Due to global warming, our planet is coping with adverse consequences, such as severe floods and droughts, rising sea levels, high prevalence of insects, changes in Earth`s precipitation. These environmental changes have several catastrophic effects on society, such as health problems and decreasing economic development. In recent years, various organizations have been concerned with rising GHGs concentrations. After the 1997 Kyoto Protocol, different strategies have been devised for reduction of GHGs emissions in the environment.

In the given context, this chapter discusses in detail about the GHGs and their impact on climate change, factors responsible for increasing concentrations of GHGs/global warming and various causes of climate changes. This chapter also covers impact of climate change on environment, human health and on Marine Eco-Systems. Finally, the government initiatives on climate change and challenge of limiting global warming to 2 ^{o}C are discussed in detail.

3.2 Greenhouse Gases

Gases, such as carbon dioxide are known as long-lived gases, remaining semi-permanently in the atmospheres that do not respond chemically or physically to changes in temperature. These gases are described as ''forcing'' climate whereas other gases, such as water vapour which respond chemically/physically to changes in temperature are termed as ''feedbacks.'' Therefore, the increasing GHGs concentration in the environment has impact on the climate and thus affects various organisms. Figure 3.2 shows the distribution of GHGs in the Earth's environment. Different GHGs are described as follows.

3.2.1 Water Vapor (H_2O)

Water vapour is not considered as the major component to have effect on long-term climate change. It is the most abundant GHGs. It is naturally cycled into and out of the atmosphere on a relatively short time period. As the Earth's atmosphere warms, water vapour increases but so does the likelihood of clouds and precipitation. The water vapour is considered as the most important ''feedback'' mechanism to the greenhouse effect.

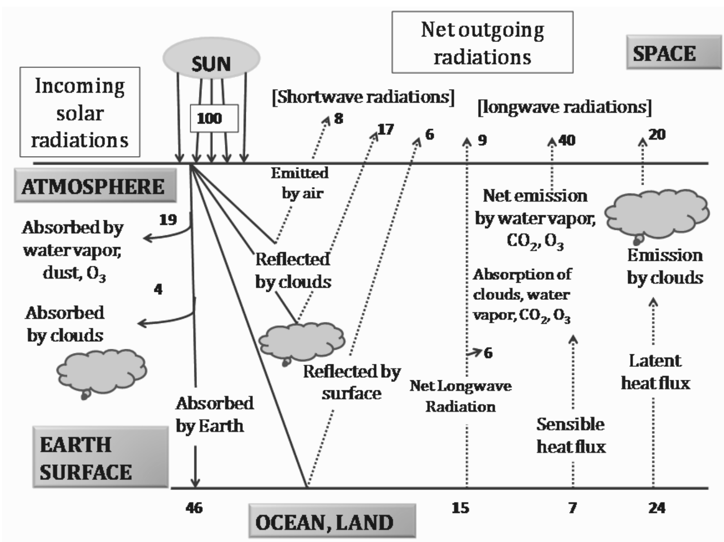

Figure 3.1. The energy balance in the atmosphere (modified from http://zebu.uoregon. edu/1998/es202/l13.html.). The digits donate energy absorbed or emitted in %

3.2.2 Carbon Dioxide (CO_2)

CO_2 is one of the most prominent among all GHGs. Burning of fossil fuels, respiration, volcanic eruptions and deforestation are the major causes of rising CO_2 concentration in the Earth's environment. According to World Energy Council, the worldwide carbon dioxide emissions from burning fossil fuels increased by 12% from 1990 to 1995 (Prax, 2011). Due to human activities, 30 billion tons of CO_2 is emitted in the atmosphere which is 30% more than in 1750 (Envirolink 1998). The carbon dioxide emissions increased by 2.8% worldwide in 1996. The U.S. was leading with 25% of total emissions and reported an increase of 3.3% in 1996. Developing countries were responsible for 3 times more carbon dioxide emissions than developed countries. During 1990–95, carbon dioxide emissions from burning fossil fuels increased 35%, Africa increased by 12% and Eastern Europe increased by 75%. CO_2 is the most important long-lived ''forcing'' of climate change. The industrial activities of worldwide large stationary CO_2 sources with emissions of more than 0.1 $MtCO_2$ per year are given in Table 3.1.

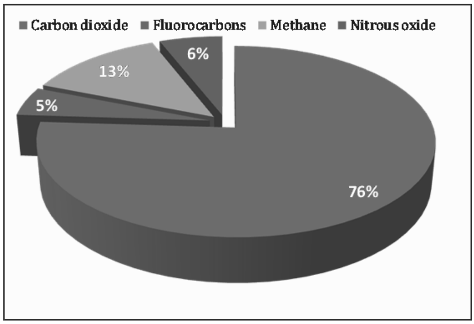

Figure 3.2. Distribution of GHGs in Earth's atmosphere (modified from http://www.abcnews.com)

Table 3.1. Summary by process or industrial activity of worldwide large stationary CO_2 sources with emissions of more than 0.1 $MtCO_2$ per year

Process	Number of sources	Emissions ($MtCO_2$ yr^{-1})
Fossil fuels		
Power	4,942	10,539
Cement production	1,175	932
Refineries	638	798
Iron and steel industry	269	646
Petrochemical industry	470	379
Oil and gas processing	N/A	50
Other sources	90	33
Biomass		
Bioethanol and bioenergy	303	91
Total	7,887	13,466

Citation source: IPCC (2005)

3.2.3 Methane

Methane is 25 times more potent as a GHG than carbon dioxide. Methane is mainly released from landfills resulting from dumping of municipal solid waste (MSW) and other industrial wastes. Each year, approximately hundreds of millions of tons of municipal solid waste (MSW) is produced, e.g., 254 million tons of MSW was generated in 2007 in the U.S. (USEPA 2008), with a similar amount of industrial wastes around the world. Globally, landfills are the 3rd largest anthropogenic (human-induced) emission source accounting for nearly 12% of global methane emissions or about 750 million metric tons of CO_2 equivalents ($MMTCO_2E$), (USEPA 2006). Methane makes up about 25% or even more of the anthropogenic contribution to global warming (IPCC 1992). Moreover, methane oxidation (45 g/m^2-d) to CO_2 has been observed in a soil-covering landfill in the presence of methanogenic bacteria (Whalen et al. 1990). Landfill gas (LFG) also contains volatile organic compounds (VOCs) that can contribute to the formation of photochemical smog. The typical composition of raw landfill gas is given in Table 3.2.

Table 3.2. Typical composition of raw landfill gas (composition by volume unless otherwise stated)

Component	**Content**
Methane (CH_4)	40–60%
Carbon dioxide (CO_2)	20–40%
Nitrogen (N_2)	2–20%
Hydrogen sulphide (H_2S)	40–100
Heavier hydrocarbons (C_nH_{2n+2})	< 1%
Oxygen (O_2)	< 1%
Ammonia (NH_3)	0.1–1%
Complex organics	1000–2000 ppm
Siloxane, chlorinated organics	at ppb level

Methane emissions from municipal landfills represent 3% of the total US GHG emissions that contribute to climate change. In 1994, the US Environmental Protection Agency (USEPA) created the Landfill Methane Outreach Program (LMOP), with the objective of reducing landfill GHGs emissions by promoting the development of landfill-gas-to-energy projects (Jaramillo and Matthews 2005).

Landfill gas (LFG) results from the biological decomposition of organic matter of municipal solid waste and is a flammable and odorous gaseous mixture, consisting mostly of methane (CH_4) and carbon dioxide (CO_2) together with a few parts per million (ppm) of hydrogen sulphide (H_2S), nitrogen (N_2) and volatile organic compounds (VOCs) (Qin et al. 2001; Liamsanguan and Gheewala 2008). Harvesting LFG to generate energy not only encourages more efficient collection thereby reducing GHGs emissions into the atmosphere but also generates revenues for economic development.

Bacteria inhabiting livestock, such as cows, buffaloes, sheep, goats and camels produce methane naturally. Every year 350–500 million ton of methane is added to the environment mainly by raising livestock, rice fields, landfill gases, coal mining and drilling for oil and natural gases (WBE 1982; USEPA 2006). Methane has a half-life of only 12 years, but it traps 20 times more heat than CO_2. The concentration of methane has doubled since 1750 and is expected to be doubled again by 2050 as given in Table 3.2.

3.2.4 Nitrous Oxide

Nitrous oxide is a GHG released from oceans and by bacteria in soils. N_2O has increased by 15% since 1750, and 7–13 million tons of N_2O is added into the atmosphere, mainly by using nitrogen based fertilizers, disposing of human and animal waste and automobiles exhaust, nitric oxide production, biomass burning and various other sources. The half-life of N_2O is 114 years, which makes it necessary to cut-off the N_2O emissions (Blasing 2009).

3.2.5 Fluorocarbons

Fluorocarbons are a group of synthetic organic compounds which contains fluorine and carbon, such as chlorofluorocarbons (CFCs). CFCs possesses an inherent property of phase change, i.e., they can be easily converted from gas to liquid or liquid to gas phase due to which they can be used in aerosol cans, refrigerators and air conditioners. There is well established fact that CFCs, when released into the environment, breakdown molecules in the Earth's ozone layer (WBE 1982b) and are thus responsible for the widening of the ozone hole in the atmosphere. Due to this reason, the production of CFCs is banned in United States and the use of CFCs has significantly decreased since then. Nevertheless, other countries also have to follow suit and impose such norms. Hydrofluorocarbons (HFCs) have replaced the CFCs. HFCs do not breakdown the ozone molecules but still are laden with some problems which affect the climate. They trap the heat in the atmosphere aiding in global warming. HFCs are used as coolant in the refrigerators and air conditioners. The coolant should be recycled; leaks should be properly sealed; the coolant should be recovered during dumping of the both devices, which is the only way to strategically reduce emission of this GHGs.

3.3 Current Scenario of Greenhouse Gases

Effects of GHGs on climate are clearly evident from observation reported by Ruddiman (2001). According to him, within last 100,000 years the concentrations of carbon dioxide have cycled between low (190 ppm) and high (300 ppm) values. The high levels of CO_2 occur in warmer periods and low CO_2 occurs in cooler periods. Recent GHGs concentrations present in the atmosphere are given in Table 3.3.

Table 3.3. Trends in recent GHG concentrations (IPCC 2007a; Blasing 2009)

Greenhouse gas	Pre-1750 tropospheric concentration	Current tropospheric concentration	Atmospheric lifetime (years)	Increased Radiative forcing (W/m^2)
Carbon dioxide (CO_2) (ppm)	280	384.8	100	1.66
Methane (CH_4) (ppb)	700	1865	12	0.48
Nitrous oxide (N_2O) (ppb)	270	322	114	0.16
Ozone (O_3) (ppb)	25	34	Hours-days	0.35
Fluorocarbons (ppt)				
CFC-11 (CCl_3F)	0	244	45	0.063
CFC-12 (CCl_2F_2)	0	538	100	0.17
CF-113 (CCl_2FFClF_2)	0	77	85	0.024
HCFC-22 ($CHClF_2$)	0	206	12	0.033
HCFC-141b (CH_3CClF)		21	9.3	0.0025
HCFC-142b (CH_3CClF_2)	0	21	17.9	0.0031
Halon ($CBrClF_2$)	0	4.4	16	0.001
Halon ($CBrClF_3$)	0	3.3	65	0.001
HFC-134a (CH_2FCF_3)	0	54	14	0.0055
Carbon tetrachloride (CCl_4)	0	89	26	0.012
Methyl chloroform (CH_3CCl_3)	0	10.5	5	0.0011
Sulphur hexafluoride (SF_6)	0	6.7	3200	0.0029

Abbreviations: ppm = parts per million; ppb = parts per billion; ppt = parts per trillion; and W/m^2 = Watts per square meter

During the past 20,000 years, Earth's climate has been dominated by a cyclic development of long glacial periods intermittently followed by short warmer interglacial periods. The climate was also influenced by natural climate fluctuations on shorter time-scales (Bonan 2002). The current interglacial period, which has seen an expansion of human beings and civilization all over the Earth, is named the Holocene (Roberts 1998). At the end of December 2008, researchers measured an additional 16.2 billion tons of CO_2 and 12.2 million tons of CH_4 in the atmosphere. Total global CO_2 concentrations were the highest with 386 ppm, compared to 280 ppm before the industrial revolution began in the 1800s (Science Daily 2009).

Radiative forcing is a measure of how the energy balance of the Earth-atmosphere system is influenced when climate affecting factors, such as GHGs are altered. According to IPCC (2007a), the radiative forcing of climate from 1750 to 2005 with the net forcing due to human activities has been found to be positive i.e. with respect to global warming as given in Fig 3.3.

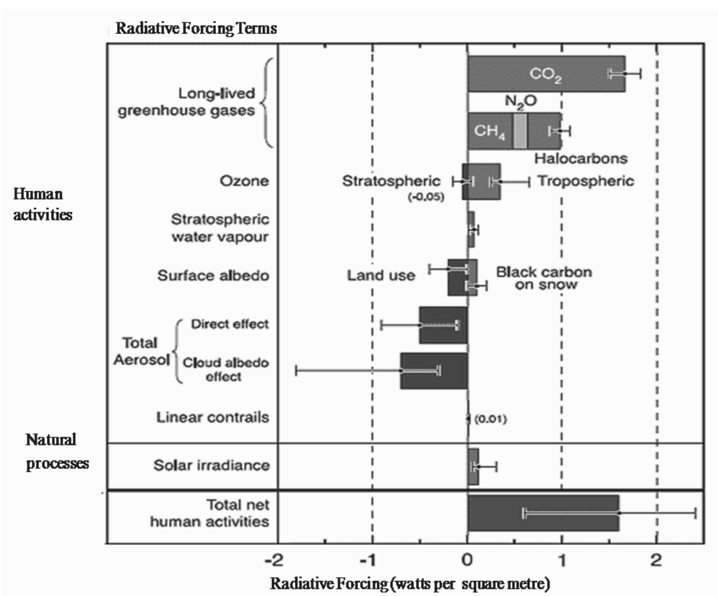

Figure 3.3. Radiative forcing of climate between 1750 and 2005 (IPCC 2007a)

3.4 Factors Responsible for Increasing Concentrations of Greenhouse Gases/Global Warming

Several theories have emerged to explain the phenomenon of global warming. Among all these theories, anthropogenic global warming (AGW) is considered as the foremost theory which holds human beings responsible for most of the slight warming trend seen since the little ice age. According to the scientific report issued by the IPCC (2007a), the burning of fossil fuels and other human endeavour are causing global warming. Till date, human activity has been altered between a third and a half of Earth's land surface by different activities, especially farming, pasture, forestry and urbanization (Vitousek et al. 1997). These human activities have consequences on key biogeochemistry cycles, changing the composition of atmosphere resulting in considerable alterations of ecosystems (Foley et al. 2005). Land-use changes result in biogeochemical climatic effects through alteration of the vegetation and soil carbon pools (Houghton and Goodale 2004), as well as modification of the hydrological cycle (Gordon et al. 2005). These changes influence atmospheric greenhouse gas levels and the global climate (Foley et al. 2003). Human activities, such as land clearing, industrial emissions and transportation emissions increase GHGs and aerosols.

Since pre-industrial times, CO_2 growth has increased by more than 2% each year. Ever since 1800, the growth rate of CO_2 concentrations has been doubling after every 31 years. At the same pace, the CO_2 concentrations will be expected to reach 560 ppm, almost double than the pre-industrial revolution values by the year 2050 (Hofman et al. 2009). The humans are responsible for 2 ppm rise in CO_2 per year at a rate that is 2,000 times more than the natural rate over the past thousands of years. This sudden increase in atmospheric CO_2 concentrations is the reason behind the climate change since 1970s. The concentration of GHGs from year 0 to 2005 is provided in Fig. 3.4.

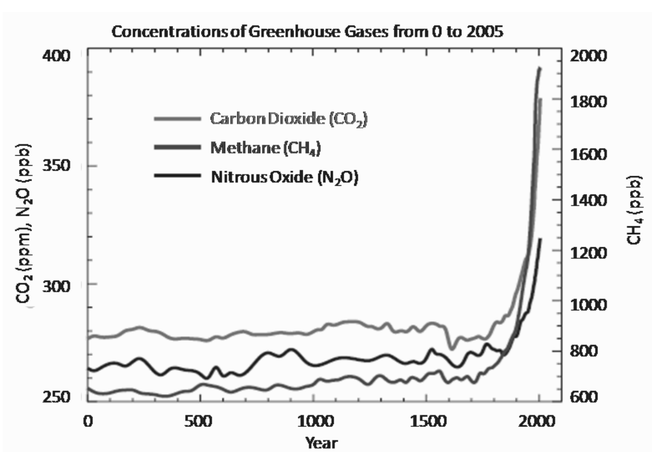

Figure 3.4. Concentrations of greenhouse gases from year 0 to 2005 (IPCC 2007a)

The large volcanic eruptions of Mountain Agung during 1963 in Indonesia and Mountain Pinatubo during 1991 in Philippines, each slowed CO_2 accumulation for several years (Science Daily 2009). Volcanic emissions cooled the lower atmosphere and scattered sunlight which in turn reduced plant respiration, a process that releases carbon dioxide, and boost photosynthesis, removing carbon dioxide from the air. According to Hofman et al. (2009), the atmospheric CO_2 emission rate is best reflected by the world population trend. Over the past century, the two are increasing at the same pace. A break in the close relation between population growth and CO_2 growth would be sought to limit atmospheric CO_2 concentrations.

Deforestation affects the global climate by releasing the carbon stored in the living trees and soils and by changing the physical properties of the planetary surface. Deforestation exerts a warming influence by: 1) adding CO_2 in the atmosphere; 2) eliminating the possible increased carbon storage in plants as a future CO_2 assimilation, and; and 3) decreasing evapotranspiration, particularly in the tropics (Snyder et al. 2004; Bala et al. 2007). Deforestation for agriculture and pasture is a major driver of the accelerating land transformation and for rising concentration of carbon dioxide in the environment (Williams 2000). Domestic fuel need, logging wood for different purposes, widening of residential areas, shipbuilding and charcoal consumption, metal melting are additional driving forces behind the increased forest clearing over the centuries. An increasing human population and a civilization with technology advances within agriculture, forestry, mining and trade have caused substantial changes in forest vegetation (Williams 2000). Estimated loss of natural forest/woodland areas as a result of human activity was 6% by 1700, 14% by 1850 and 34% by 1990 of the natural land cover (Klein-Goldewijk 2001). Forests act as natural carbon sinks and help to alleviate carbon dioxide from the environment. As the area under forest declines, recycling of carbon dioxide is less. Forest fires and burning of wood and agricultural wastes in the fields are directly and indirectly responsible for high levels of carbon dioxide.

Fossil fuels are the most important factors responsible for increased concentration of GHGs in the atmosphere. The fossil fuels, such as coal, petroleum and natural gas emit GHGs in the environment, when burned. The fossil fuels supply most of the world's energy whereas renewable sources contribute only a small portion. During the last 250 years, about 1,200 billion tons of CO_2 have been released into the atmosphere mainly from fossil fuel emissions. Ironically, half of these emissions have occurred only since the mid-1970s (Romm 2007). The utilization of energy from renewable sources is an attractive alternative to reduce GHGs resulting from the use of fossil fuels. The renewable sources are likely to provide 40% of the required energy by 2050, which would help to alleviate global warming and air pollution (www.www.doc.mmu.ac.uk/ aric/gcc/cell.html#pos6).

In recent years, bioethanol is gaining momentum as a biofuel across the globe due to its sustainable production from renewable biomass. Ethanol directly or in blends has a great impact on the environment as it helps in reducing emissions due to their clean burning characteristics and thus can be thought about as an alternative energy source (Lynd et al. 1991). Ethanol can easily be blended with gasoline at different levels. Various blends of ethanol and gasoline are currently used in various countries, such as from E5 (ethanol 5%) to E100 (ethanol 100%) (http://en.wikipedia.org/wiki/Common_ ethanol_fuel_mixtures). Such blends have proven to be effective in reducing the octane number, thereby improving the engine efficiency. Thus, bioethanol can serve as a good and clean aviation fuel. Ethanol can reduce the dependency on petroleum across the globe and thus help to alleviate greenhouse effect.

3.5 Causes of Climate Changes

The effect of climate change has a great impact on the planet, and various life forms that inhabit it. Climatic changes have been speeded up because of uncontrolled human activities. The causes of climatic changes should be identified first for the better understanding of climate change. The causes of climate change can be divided into two categories mainly human and natural causes, and are discussed below. Manifests

3.5.1 Natural Causes of Climate Change

The earth climate is influenced and changed through many natural causes like ocean currents, volcanic eruptions, earth's orbital changes, solar variations; some of the main causes are discussed here (Figure 3.5).

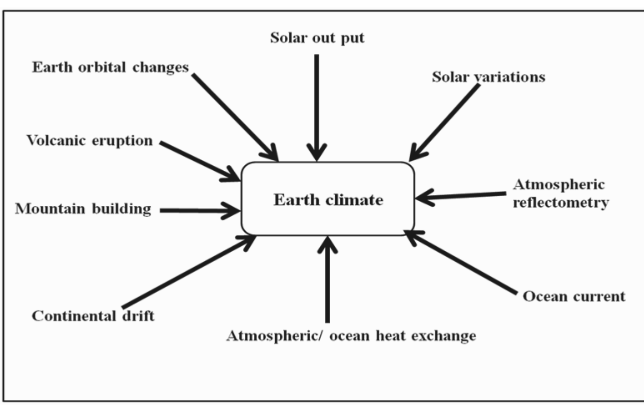

Figure 3.5. Natural causes for climate changes

Volcanic Eruptions. During volcanic eruption, material from the Earth's core and mantle is brought to the surface, as a result of the heat and pressure generated inside the earth. Volcanic eruptions and geysers release particulates into the Earth's atmosphere, that affect climate. Volcanic eruption is one of the major causes for climatic change. Climatologist have noticed a connection between large explosive volcanic eruptions and during volcanic eruptions, large volumes of sulfur dioxide (SO_2), water vapor, dust and ash throws out into the atmosphere. This gases and ash can have effects for years by increasing planetary reflectivity causing atmospheric cooling. Tiny particles, aerosols which are produced by volcanoes reflect solar energy back into space and create cooling effect on the world. Volcanic eruptions produce ash and sulphate gas into the atmosphere. The sulphate may combine with water to produce tiny aerosols of sulphuric acid, which reflects back sunlight into space. During volcanic eruption, greenhouse gas, small amount carbon dioxide also produced which is less compared to the GHGs produced by human activity. Climatologists have noticed a connection between large explosive volcanic eruption and short term climatic change. It was reported that most of the major volcanic eruption showed a pattern of cooler global temperatures lasting 1-3 years after their eruption (Kelly et al. 1996).

Earth Orbital Changes. Earth is tilted at an angle of 23.5 °C to the perpendicular plane of its orbital path, and it makes one full orbit around the sun each year. The changes in the tilt of the earth create small but climatically important changes in the strength of the seasons (Kelly and Wigley 1992). More tilt creates warmer summers and colder winters, and less tilt creates cooler summer and milder winters. The minor changes in the earth's orbit can be climatically important changes in the strength of the season over tens of thousands of years, thereby producing ice ages (Foukal et al. 2006). Earth's orbit oscillates very slightly between nearly circular and more elongated every 100,000 years, and this cycle is evident in the glacial and interglacial cycles of roughly the same period. There is also a slow wobble in the earth's spin axis, which causes the peak of winter to occur at different points along the earth's elliptical orbital path. This change in the seasons occurs on an approximately 23, 000 year cycle.

Ocean Current. Ocean currents transfer vast amounts of heat across the planet. The atmospheric circulation (winds) and ocean currents carry heat from the tropics towards the poles. Changes in deep Ocean produce longer lived climate variations that endure for decades to centuries. Phenomena's, such as El-Nino are mainly due to the interaction between the ocean and atmosphere. Oceans play an important role in determining the atmospheric concentration of CO_2. Changes in ocean circulation may affect the climate through the movement of CO_2 into or out of the atmosphere. Oceans have an important role in determining the concentration of CO_2. Changes in ocean circulation, chemistry and biology have shifted the balance of CO_2 gas in the atmosphere and CO_2 dissolved in the ocean surface. These changes may affect climate by slowly moving CO_2 into or out of the atmosphere.

Solar Variations: The changes in sun's energy to earth over an extended period of time can lead to climate changes. It was reported that a warming in the half of the 20th century was due to an increase in the output of solar energy. Scientific studies demonstrate that solar variations have performed a role in past climate changes. The decrease in solar energy triggered the little ice age between 1650 and 1850. Greenland was largely cut off by ice from 1410 to the 1720s and glaciers advanced in the Alps.

3.5.2 Human Causes for Climate Changes

Anthropogenic factors are human activities that change the environment. The effect of human influence on the climate is direct and unambiguous in some cases and in other instances it is less clear. The increase in global average temperatures over the past several decades mainly is due to the anthropogenic activities. The anthropogenic factors affecting the climate are mainly variation in the level of CO_2 and other GHGs, land use, ozone depletion, agriculture, deforestation, etc. (Figure 3.6).

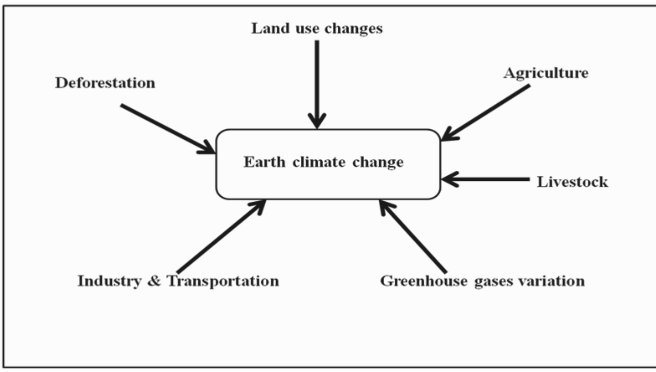

Figure 3.6. Human causes for climate changes

CO_2 and Other Greenhouse Gas Variations. The greenhouse effect is a natural warming process. CO_2 and certain other gases are always present in the atmosphere. These gases create a warming effect that has some similarity to the warming inside a greenhouse, hence the name “greenhouse effect.” The major GHGs are carbon dioxide (CO_2), methane (CH_4), nitrous oxide (N_2O) and chlorofluorocarbons (CFCs). The increasing atmospheric CO_2 concentration is likely the most significant cause of global warming resulting increased climate variability (increased variance in weather patterns and incidence of extreme events) and climate change (long-terms change and shifts). A naturally occurring shield of “GHGs” (primarily water vapor, carbon dioxide, methane, and, nitrous oxide), comprising 1 to 2 percent of the Earth’s atmosphere, absorbs some of the solar radiation that would otherwise be radiated to space and helps warm the planet to a comfortable temperature range. The earth temperature would be approximately -2 degrees rather than the current without this natural “greenhouse effect,” the average temperature on Earth would be approximately -2 degrees Fahrenheit, rather than the normal temperature. Many natural and human-made gases contribute to the greenhouse effect that warms the Earth's surface. Increasing the amount of greenhouse gas intensifies the greenhouse effect. Higher concentrations of CO_2 and other GHGs trap more infrared energy in the atmosphere and cause additional warm up in the atmosphere and earth’s surface. The increasing atmospheric CO_2 concentration is one of the major causes of the current global warming. The greenhouses gases are increasing day by day because of different type of human activities (Fig. 3.6). CO_2 is a by-product of burning of fossil fuels. Reducing CO_2 emissions rapidly is difficult because to do so means major restructuring to the way that the industrial world operates. Other GHGs such as CFCs also play a major role in industrial processes such as air conditioning.

Table 3.4. The main greenhouse gases and its global warming potential

Greenhouse gas	Pre-industrial concentration (ppmv*)	Concentration in 1998 (ppmv)	Main human activity source	Global warming potential (GWP)
H_2O	1-3	1-3	-	-
CO_2	280	365	Fossil fuels, cement production, land use	1
CH_4	0.7	1.75	Fossil fuels, waste dumps, livestock	23
N_2O	0.27	0.31	Fertilizers, combustion	296
CHF_3	0	0.000014	Electronics, refrigerants	12000
CF_3CH_2F	0	0.0000075	Refrigerants	1300
CH_3CHF_2	0	0.0000005	Industrial processes	120
Perfluoro-methane	0	0.00008	Aluminium production	5700
Perfluoro-ethane	0.00004	0.000003	Aluminium production	11900
Sulphur hexafluoride	0	0.0000042	Dielectric fluid	22200

*Parts per million in volume (United Nations Environmental Programme)

The greenhouse effect is caused by a range of different gases in the earth's atmosphere. Water vapor makes the most significant contribution to the greenhouse effect, followed by CO_2 (Table 3.4). At present the concentration of CO_2 in the atmosphere is about 385 ppm (parts per million). Before industrialization it was about 280 ppm. It was reported that earth's average temperature has risen by 0.74 degrees in the period from 1906 to 2005.

CO_2 contributes more to the recent increase in greenhouse warming than any other gas. CO_2 persists in the atmosphere longer and longer as concentrations continue to rise. Other gases such as methane, nitrous oxide, and halocarbons produced by different activities also contribute to the global greenhouse effect. A number of additional chemicals related to urban pollution, such as low-level (tropospheric) ozone and black soot, can have a strong regional and perhaps global warming effect. Sulfate aerosols may also have a greenhouse gas effect.

Carbon dioxide is produced from the burning of fossil fuels (oil, natural gas, and coal), solid waste, trees and wood products, and also as a result of other chemical reactions (e.g., manufacture of cement). Methane is emitted during the production and transport of coal, natural gas, and oil and also from livestock and other agricultural practices and by the decay of organic waste in municipal solid waste landfills. Nitrous oxide is released during agricultural and industrial activities, as well as during combustion of fossil fuels and solid waste. Fluorinated gases, such as hydrofluorocarbons, perfluorocarbons, and sulfur hexafluoride are synthetic, powerful greenhouse gases that are emitted from a variety of industrial processes.

Land Use Changes. The regional climate system changes when humans transform land from forests to seasonal crops or from natural to urban environments. Changing the use of the land is also associated with changes in the usage and availability of water as well as the production of GHGs. Urban environment creates islands of heat from industry, buildings, automobiles and the absorption of energy by dark colored surfaces. Another major source of emission from land use change is through the degradation and harvesting of peat bogs. There are about 4 trillion m^3 of peat in the world covering a total of around 2% of global land mass. About 7% of total peat lands have been used for fuel, agriculture and forestry (http://www.climate-leaders.org/climate-change-resources/climate-change/causes-of-climate-change). At 106 g CO_2/MJ, the carbon dioxide emissions released through burning peat are higher than those of coal (at 94.6 g CO_2/MJ) and natural gas (56.1 g CO_2/MJ).

Changes in land use and land cover are linked in complex and interactive ways to global climate changes. Changes in greenhouse gas emissions and surface roughness are the primary mechanisms by which land-use and land cover change affect climate. Generally water cycle depends heavily on vegetation, surface characteristics, soil properties and water resources development by humans such as dams, irrigation, channeling and drainage of wetlands, which in turn affects water availability and quality. Land use and land cover change, climate variability and change, soil degradation and other environmental changes all interact to affect natural resources through their effects on ecosystem structure and functioning.

Agriculture and Livestock. According to the Intergovernmental Panel on Climate Change, the three main causes of the increase in GHGs observed over the past 250 years have been fossil fuels, land use, and agriculture. Agriculture has been shown to produce significant effects on climate change, primarily through the production and release of GHGs such as carbon dioxide, methane, and nitrous oxide. Agriculture alters the earth's land cover, which can change its ability to absorb or reflect heat and light. Land use change such as deforestation and desertification, together with use of fossil fuels, are the major anthropogenic sources of carbon dioxide.

Methane is second most significant GHG and cause of climate change and 21 times more damaging than CO_2. Livestock and specifically cattle are major source of methane and produce by digesting grass and exhale it through their breath. Methane is also a by-product from rice and paddy dumps. Other GHGs emissions resulting from agriculture include N_2O which is released as a by-product of the application of fertilizers.

Deforestation. Deforestation is one of the major causes for climatic change. Rain forests play an important role in the ecosystem. They form part of a delicate ecosystem that has taken millions of years for evolution. Rainforests every year help to absorb almost 20% of manmade CO_2 since trees are known absorb CO_2. The United Nations Conference on Environment and Development (UNCED) in 1992 defines deforestation as "land degradation in arid, semi-arid, and sub-humid areas resulting from various factors including climatic variations and human activities." The effects of deforestation can be categorized in three ways, i.e., environmental effects, local social effects, and global social effects. Many of the environmental effects contribute to the severity of the social problems. That is why it is important to understand the environmental effects of deforestation and how they contribute to the social effects of deforestation. Deforestation by cutting down and burning the forests and starting of agriculture and industry produces more CO_2. Deforestation results in production of extra 17% of GHGs. Most of the forests have given way to agriculture fields, pastures and industry. Deforestation accounts for 20–25% of global greenhouse gas emissions which is the major source of emissions in developing countries. Deforestation also has significant impact on soil quality, biodiversity, local livelihoods and indigenous communities. Deforestation in various geographical regions is destroying the unique environments. Most of the animals and plant animals are facing the specter of extinction because of the climate change. The extinction of the plants and animals leads to diminished gene pool. The lack of biodiversity and a reduced planetary gene pool could have many unforeseen ramifications, some of which could be fatal to the future of humanity. In addition, there are ethical, aesthetic and philosophical question regarding mankind's responsibility for other life.

3.6 Effect of Greenhouse Gases on Climate

Due to the increasing concentration of GHGs in the atmosphere, the greenhouse effect will be significantly devastating, and it will raise the temperature of Earth day by day. We are experiencing climate change through erratic weather patterns, forest fires and glacier melting. Day by day increasing GHGs emissions is likely to increase the severity and frequency of severe weather events. According to the director of National Oceanic and Atmospheric Administration's (NOAA), the net effect of increasing GHGs is the rise in temperature by 1 degree Fahrenheit in the last 100 years (www.abcnew.com/sections/ us/global106.html). According to Hansen et al. (2006), global surface temperature has increased by approximately 0.2 ^{o}C per decade in the last 30 years. Warming is intensive in the Western Equatorial pacific than in the Eastern Equatorial pacific over the past century. Hansen et al. (2006) suggested that the difference in West-East temperature gradient may have increased the likelihood of strong El Niños (El Niño is defined by prolonged differences in Pacific-Ocean surface temperatures when compared with the average value. El Niño is best-known for its association with floods, droughts and other weather disturbances in many regions of the world) similar to those of 1983 and 1998. They concluded that global warming of more than 1^{o}C, relative to 2000, will represent dangerous climate change as evident from likely effects on sea level and extinction of species.

The human activities are having a significant impact on global warming. The Intergovernmental Panel on climate change (IPCC), the world's leading authority on global warming, has concluded by consensus about the discernible human influence on global change in climate. They have warned about the severe impacts of global warming on human health, natural ecosystems, agriculture and coastal communities (www.toowarm.org./factsheets/basfact.html). All these facts support the common principle that global warming results due to the increased emission of GHGs, such as carbon dioxide, nitrous oxide, methane and HFCs in the environment. According to Archer (2005), global warming could result in the release of large amounts of GHGs, such as from melting permafrost or destabilized methane clathrates on continental shelves. Such release of GHGs may be associated with the largest warming in the Earth's history and mass extinctions (Benton 2003; Archer 2005). Even though such devastating GHGs releases may require many centuries, still it demands caution in estimating requirements to avoid dangerous anthropogenic interference (DAI) due to unawareness of GHGs climate feedbacks. The United Nations framework Convention on Climate change (UNFCC) has the objective ''to achieve stabilization of GHGs concentrations'' at a level preventing DAI (Danny Harvey 2007). In one of the study published in *Proceedings of National Academy of Sciences*, Hansen et al. (2006) suggested the global temperature as a useful measure to access propinquity to DAI as the knowledge of Earth's history, global temperature can be related to key dangers that the Earth faces.

Since the pre-industrial era, the increase in the concentration of GHGs has most likely committed the Earth to a warming of 2.4 ^{o}C (1.4 ^{o}C to 4.3 ^{o}C) above the pre-industrial surface temperatures (Ramanathan and Feng 2008). This rise in surface temperature is clearly inferred from the recent IPCC estimates of the greenhouse forcing and climate sensitivity (Parry et al. 2007; Rogner et al. 2007). According to Ramanathan and Feng (2008), the estimated rise of 2.4 ^{o}C in temperature is the equilibrium warming above pre-industrial temperatures that the world will detect even if GHGs concentrations are held fixed at their 2005 concentration levels but without the effect of any anthrogenic forces, such as the cooling effect of aerosols.

Various scientists have worked on modelling the impacts of increased emissions of GHGs in the atmosphere relative to pre-industrial levels. According to Hadley Center (2012), climate change models that have studied the impacts of GHGs emissions from pre-industrial levels are given in Table 3.5. They warned that by the 2090, nearly one-fifth of the world's population will be exposed to ozone levels well above the safe-health level recommended by World Health Organization (WHO).

Table 3.5. Likely effects of four different GHGs emission reduction models

Mode of Action		Increase/decrease in GHGs emissions	Rise in global temperature by 2100 as compared to pre-industrial levels
1.	No action taken	132% increase in emissions by 2050	5.5–7.1^{o}C
2.	Action starts in 2030- Late and slow decline	76% increase in emissions by 2050	4–5.2^{o}C
3.	Action starts in 2010- Early but slow decline	Emissions return to 1990 levels by 2050	2.9–3.8^{o}C
4.	Action starts in 2010- Early and rapid decline	47% decrease in emissions by 2050	2.1–2.8^{o}C

In case no action is taken regarding the reduction of GHGs emission, the projected temperature level of 5.5^{o}C would likely lead to the mid-to-high-range of currently projected sea level rise of 5 feet or more by 2100, followed by 10-20 inches per decade for centuries (Romm 2008).

Due to global warming, the oceans are expanding, promoting a rise in sea level, and more land would be covered by water. The Maldives Islands (nation of 1190 islands) in the Indian Ocean and densely populated Bangladesh is facing the problem of increasing land under water. The sea level in Maldives Islands is on average height of 1.5 meters above sea level, which would force many people to abandon their homes. A sea level rise by 1 meter by 2100 would be a sheer catastrophe for the Earth, and it would flood 17% of Bangladesh, abandoning millions of people (http://yosemite.epa.gov). Southern Louisiana and South Florida would certainly be abandoned. Effects of rising sea levels will be more pronounced by salt water infiltration (Ferguson and Gleeson, 2012).

In 2007, according to an IPCC report, it was warned that as global average temperature increase exceeds by 3.5 ^{o}C relative to 1980–99 levels, the model projections suggest significant extinction of species to the tune of approximately 40–70% around the globe IPCC 2007b). A study published in *Nature Geosciences* warned that global warming may create ''dead zones'' in the ocean that would be devoid of fish and sea food and last for up to 2 millennia. Today, nearly 2% of the total sea resembles a 'dead zone', with naturally uninhabited oxygen-starved regions where higher life forms cannot survive due to lack of food or breathing. According to a computer simulation carried out to 100,000 years in the future, these zones would engulf one-fifth of the seas within a few millennia if the carbon dioxide emissions could not be reduced in future with immediate effect. Oxygen deficiency in sea waters (dead zones) is due to the fact that water loses its ability to dissolve oxygen as it warms, so hotter oceans mean larger dead zones. The ocean circulation will also slow down due to heating of oceans and could deplete oxygen content by up to 54 percent worldwide by the year around 5000 (Reilly 2009).

Increases in CO_2 can make marine animals more susceptible to low concentrations of oxygen, and thus aggravate the effects of low-oxygen "dead zones" in the ocean. The partial pressure of dissolved carbon dioxide gas (pCO_2) in low-oxygen zones will rise much higher which could have significant consequences for marine life in these zones. High concentrations of CO_2 in seawater will make it difficult for marine animals to take out oxygen from seawater. High concentration of CO_2 and low oxygen concentration in sea water makes it harder for these animals to find food, avoid predators and reproduce. Presently, deep-sea life is endangered by a combination of increasing CO_2 and decreasing oxygen concentrations. The amount of dissolved CO_2 is increasing because the oceans are absorbing more and more CO_2 from the atmosphere. At the same time, ocean surface waters are warming and becoming more stable, which allows less oxygen to be carried from the surface down into the depth. In an attempt to quantify the impacts of this high CO_2 and decreasing oxygen concentration on marine organisms, Brewer and Peltzer (2009) came up with a "respiration index" which is based on the ratio of oxygen and CO_2 gas in a given sample of seawater. The lower the respiration index, the harder it is for marine organisms to respire. The respiration index will be helpful for providing a more accurate and quantitative way for oceanographers to identify such areas. Marine biologists would be able to predict which ocean waters are at risk of becoming dead zones in the future by tracking changes in the respiration index (Reilly 2009).

In an attempt to estimate such devastating effects in the open ocean, the Monterey Bay Aquarium Research Institute (MBARI) researchers calculated the respiration index at various ocean depths, for several forecasted concentrations of atmospheric CO_2. The study established that the harshest effects would take place in "oxygen minimum zones," typically 300 to 1,000 meters below the surface, where oxygen concentrations are already quite low in many parts of the world's oceans. Earlier marine biologists have assumed that the effects of increasing CO_2 in the oceans would be greatest at the sea surface, where most of the CO_2 is absorbed by the ocean. Such studies have expected a doubling of pCO_2 (from about 280 to 560 micro-atmospheres) at the sea surface over the next 100 years. However, Brewer and Peltzer's (2009) respiration index calculations implied that the partial pressure of CO_2 will increase even faster in the deep oxygen minimum zones, with pCO_2 increasing by 2.5 times, from 1,000 to about 2,500 micro-atmospheres. This will result in a huge expansion of the oceanic dead zones. They suggested that both oxygen and CO_2 in the oceans should be taken care of, rather than just one or the other. The impact of these chemical changes may be smaller in well-oxygenated ocean areas.

The global warming could persist far into the future as natural processes require hundreds of thousands of years to remove CO_2 from the atmosphere resulting from the fossil fuel burning (Archer 2005). In 2009, a study published in *Nature Geosciences* established that expanding global warming may have large global impacts, such as ocean oxygen depletion and associated unfavourable effects on marine life, such as more frequent mortality events (Shaffer et al. 2009). In this study, they estimated the projected global change over the next 100,000 years using a low-resolution Earth system model and expected severe, long-term oxygen depletion and expansion of ocean oxygen-minimum zones for scenarios of high emissions and climate sensitivity (Shaffer et al. 2008, 2009).

Marine oxygen depletion leading to anoxia is believed to have played a role in the major mass extinctions in the past, such as The Great Dying, that occurred at the end of the Permian, 250 million years ago, which wiped out 95% of all marine life. Areas of low oxygen exist in today in shallow areas next to the coast, where runoff from agricultural fertilizer causes a multiplication of oxygen-gobbling algae producing the dead zones. However, some coastal dead zones could be recovered by reduction of fertilizer utilization; expanded low-oxygen areas caused by global warming will remain for thousands of years, adversely affecting fisheries and ocean ecosystems far into the future.

According to one study, a large amount of nitrous oxide is produced by bacteria in the oxygen poor parts of the ocean using nitrites. Bacteria that produce nitrous oxide thrive well at a depth of around 130 metres where an oxygen minimum zone prevails (Codispoti 2010). Gas produced at this depth could escape to the atmosphere. Nitrous oxide is a potent GHG, nearly 300 times stronger than CO_2; it also attacks the ozone layer and causes acid rain. Albeit present in low concentrations, nitrous oxide is becoming a key factor in stratospheric ozone destruction. As dissolved oxygen levels decreased, N_2O production increased. Under well-oxygenated conditions, microbes produce N_2O at low rates. When oxygen concentration decreased to hypoxic levels, the increased production of N_2O occurs. In suboxic waters (oxygen essentially absent) at depths of less than 300 feet, heights favourable for denitrification can cause N_2O production rates to be 10,000 times higher than the average for the open ocean. The future of marine N_2O production depends critically on what will happen to ~10% of the ocean volume that is hypoxic and suboxic (Codispoti 2010). The increasing CO_2 could cause an expansion of the oxygen minimum zones in the world, triggering greater emissions of N_2O exerting more pronounced effects on climate (Matear and Hirst 2003; Stramma et al. 2008).

3.7 Impact of Climate Change

Three major impacts of climate change are discussed below.

Impact on the Environment. Increasing concentrations of GHGs in the environment do augment the greenhouse effect which results in many environmental problems. This is evident from the melting glaciers and polar ice caps, increased temperature on land and ocean surface, increased water vapour in the air, rising sea levels (average between 4–10 inches by 2100), severe floods and droughts (Leggett 2009). The profound effects of rising sea level can result in increased salinity of fresh waters throughout the world and coastal lands to be washed under the ocean. Tropical cyclones can occur by warmer waters and increased humidity. Finally, changing wave patterns could produce more tidal waves which would be responsible for increased erosion on the coasts.

Studies suggest that global warming will significantly increase the intensity of the most extreme storms worldwide. The stronger tropical storms are getting much stronger, with the most notable increases in the North Atlantic and northern Indian oceans (Schiermeier 2008). Since 1981, the maximum wind speeds of the strongest tropical cyclones have increased significantly. They estimated that 1°C increase in sea-surface temperatures would lead to 31% increase in the global frequency of category 4 and 5 storms per year. The tropical oceans have warmed by an average of 0.5°C since 1970.Computer models suggested that the temperature will raise by 2°C by 2100 considering old emission scenarios. However, according to current emission scenarios, key parts of the tropical oceans are expected to warm considerably by more than 2°C by the end of 2100.

In 2010, the powerful cyclone ‘‘Laila’’ caused widespread havoc across the South Indian state of Andhra Pradesh. It is the worst storm to hit this region in last 14 years. Laila's stroke also brought destruction in Sri Lanka. The indirect impact of the cyclone was compounded as heavy pre-monsoonal showers set in over parts of the country. In May 2008, Cyclone called ‘‘Nargis’’ killed more than 100,000 people in southern Myanmar. Hurricane ‘‘Gustav’’, the second most destructive hurricane of the 2008 Atlantic hurricane season, caused serious damage and casualties in Haiti, the Dominican Republic, Jamaica, the Cayman Islands, Cuba and the United States. Hurricane ‘‘Katrina’’ wrought havoc in 2005 in New Orleans, devastating lives and levelling homes. It was one of the five deadliest hurricanes, in the history of the United States (Knabb et al. 2005).

Since 1960, the number of reported weather-related natural disasters has been occurring at more than tripled frequency worldwide resulting in over 60,000 deaths mainly in developing countries. Rising seawater levels and increasingly harsh weather events will demolish houses, medical facilities and other fundamental services. More than 60% of the world's population is inhabited within 60 km of the sea. Due to severe floods, people may be forced to move, which in turn heightens the risk of a series of health effects, from communicable diseases to mental disorders. Increasingly erratic rainfall patterns are likely to affect the supply of safe drinking water, compromising hygiene and increased risk of diarrhoeal diseases, which kills more than 2.2 million people every year. In some extreme cases, water shortage leads to drought and food crisis. According to Arnel (2004), climate change is likely to broaden the area affected by drought, twice the frequency of severe droughts and increasing their average duration by six times. Increasing frequency and intensity of floods is alarming. Floods contaminate fresh water supplies; heighten the risk of water-borne diseases and create breeding grounds for disease carrying insects, such as mosquitoes. Floods are also responsible for mortality due to drowning and physical injuries, damage houses and interrupt the supply of medical and health services. Escalating temperatures and inconsistent precipitation are likely to decrease the production of staple foods in many regions by up to 50% by 2020 in some African countries (Climate change 2007). Finally, it also results in increased prevalence of malnutrition and under-nutrition which currently causes 3.5 deaths every year.

Impact on Human Health. According to IPCC, climate change due to global warming is likely to have adverse and long lasting impacts on human health, jeopardizing the life. Increasing concentrations of GHGs in the environment and global warming would lead to more heath concerns. Although global warming has some localized benefits, such as lower mortality rate in temperate climates and increased food production in certain areas but the overall health effects of a varying climate are likely to be devastating. Climate change affects the fundamental requirements for health, such as clean air, safe drinking water, sufficient food and secure shelter. Severe high air temperatures contribute directly to the deaths from cardiovascular and respiratory diseases, preferably among elders (World health organization, Geneva 2009). The incidences of heat stroke, heart attacks and other ailments will be more aggravated among people directly due to direct effect of heat and other effects as seen in Fig 3.7. A heat wave in Chicago killed more than 700 people in a few days (Kaiser et al., 2007). Similarly, according to a report from the Earth Policy Institute more than 52,000 deaths were recorded in Europe in the heat wave of summer 2003 (Larson, 2006). High temperatures also increase the level of ozone and other pollutants in the air that aggravate cardiovascular and respiratory disease. It is estimated that urban pollution causes about 1.2 million deaths every year. High atmospheric temperature favours smoke particles and noxious gases to linger in the air and this result in the formation of other pollutants through chemical reactions. This will lead to an increased incidence of respiratory diseases, such as bronchitis and asthma. During extreme heat, the level of pollens and other aeroallergens is also higher which triggers asthma affecting around 300 million people. According to World health organization (WHO) assessment, taking into consideration only a subset of possible health impacts of climate change, it was concluded that the modest increase in temperature that has occurred since the 1970s has already caused more than 140,000 extra deaths annually by the year 2004 (World health organization 2009).

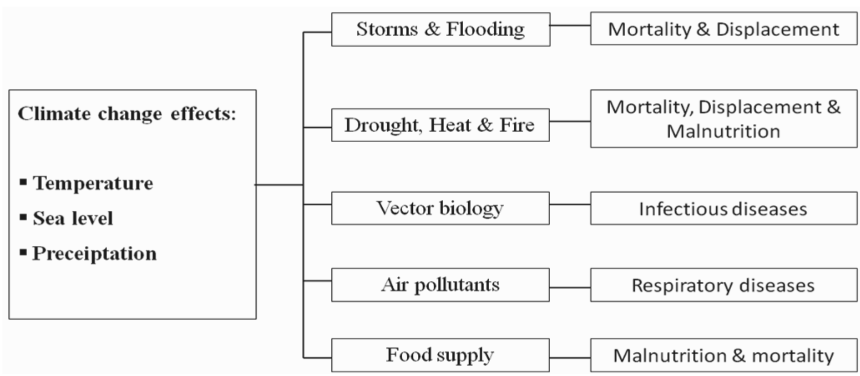

Figure 3.7. Impacts of climate change in human health

Climatic conditions strongly affect water-borne diseases and diseases transmitted through insects, snails and other cold blooded animals. Climate changes are likely to increase the transmission seasons of important vector-borne diseases and to alter their geographic range (e.g., the snail-borne disease schistosomiasis affected area is projected to widen due to climate change in China (Zhou et al. 2008).

The increase in temperature towards the poles could results in migration of insects and other pests towards Earth's poles. The insects and pests could carry diseases, such as dengue fever, malaria, plague, among many others. Thus, due to global warming the population of insects and pests carrying diseases is likely to increase towards the poles which could be responsible for 50-80 million more cases of malaria annually according to the American Association for the advancement of Science (Haley 2002). Climate change is a determining factor in terms of spreading of malaria, dengue and cholera (. Transmitted by female Anopheles mosquito, malaria kills nearly 1 million people every year; especially African children fewer than five years age are more vulnerable. The Aedes mosquito vector of dengue is also extremely sensitive to changing climate conditions. According to studies, the climate change could expose an additional 2 billion people to dengue transmission by the end of 2080 (Hales et al. 2002). Growth of toxic algae is also promoted due to the warming of oceans which can increase the risk of cholera.

Impact on Marine Eco-Systems. Concentrations of CO_2 are increasing rapidly in the Earth's atmosphere, mainly because of human activities. About one third of the CO_2 that humans produce by burning fossil fuels is being absorbed by the world's oceans, gradually causing seawater to become more acidic. Ocean acidification resulting from rising atmospheric CO_2 concentrations has an unexpected impact on marine eco-systems putting sea life at risk (The Royal Society 2005; Kleypas et al. 2006; Hoegh-Guldberg et al. 2007; Fabry et al. 2008; Munday et al. 2009). According to The Royal Society (2005) and Fabry et al (2008), in the past 200 years, approximately 30% of the anthropogenic CO_2 released into the environment has been absorbed by the oceans. As a result, the ocean pH declined at a rate of 100 times faster than that in the last 650,000 years. Worldwide ocean pH has been found to decrease by 0.1 units since preindustrial times and is expected to fall another 0.3–0.4 units by 2100, due to increasing CO_2 emissions at a faster pace imposed by human activities. These changes will produce irreversible ecological regime shifts in marine habitats, such as massive reduction in coral reef habitats and their associated biodiversity as well as reduced availability of carbonate ions for calcifying species.

Elevated levels of CO_2 and acidic seawater pH can dramatically affect the behavioural decisions of marine organisms during a critical life history stage. Research published by Munday et al. (2009) in *Proceedings of the National Academy of Sciences* has shown that ocean acidification disrupts the olfactory sense of clownfish larvae making it difficult for the fish to find their natural reef habitat. The persistence of most of the coastal marine species depends on the capability of larvae to locate suitable habitat at the end of pelagic stage that can last for weeks/months. Coral reef fish larvae use the reef sound, olfactory cues and smell of water to distinguish their native reefs from others (Gerlach et al. 2007; Munday et al. 2009). Loss of larval olfactory ability in marine organisms due to acidification could have significant impact on marine biodiversity.

Ocean acidification also represents negative consequences for survival, growth and reproduction of corals reefs, calcifying algae and diverse range of other organisms by reducing the calcification rate as demonstrated in Figure 3.8. Moreover, the acidification is also affecting the symbiotic relationship between coral reefs, dinoflagellates and the productivity of their association (Anthony et al. 2008). High CO_2 concentrations act as a bleaching agent for corals and crustose coralline algae (CCA) under high irradiance, acting synergistically with warmer to lower thermal bleaching thresholds. It is well established that reduced carbonate-ion saturation states accompanying lower seawater pH can affect the ability of marine calcifers to form shells and skeletons. Increased oceanic acidity reduces carbonate, the mineral used to form the shells and skeletons of many shellfish and corals. The effect is related to osteoporosis, slowing growth and making shells weaker. If pH levels drop enough, the shells will literally dissolve. These findings foretell a bleak upcoming future for the giant coral reef ecosystem as well as calcifying marine organisms around the globe.

According to Mcneil and Matear (2008), Southern ocean acidification is detrimental to multiple calcifying plankton species. Absorption of anthropogenic CO_2 by oceans has lowered the pH and concentration of carbonate ions (CO_3^{2-}) since preindustrial times to levels where calcium carbonate (aragonite and calcite) shells begin to dissolve. These changes in carbonate ion levels strongly vary between ocean basins. The carbonate ion levels over most of the surface ocean are expected to remain supersaturated with respect to aragonite, the more soluble form of calcium carbonate (Caldeira and Wikett 2003; Orr et al. 2005; Macneil and Matear 2007). Despite this fact, the studies have established that calcifying organisms depend on variations in aragonite saturation state which allows marine organisms to adequately secrete and accumulate this carbonate mineral during growth and development (Feely et al. 2004; Orr et al. 2005; Raven 2005). However, the Southern Ocean is expected to begin to experience aragonite under-saturation by the year 2050, assuming surface ocean CO_2 equilibrium with the atmosphere. The aragonite under-saturation will augment the dissolution of aragonite and reduce formation of aragonite shells of marine organisms (Raven 2005; Iglesias-Rodriguez et al. 2008).

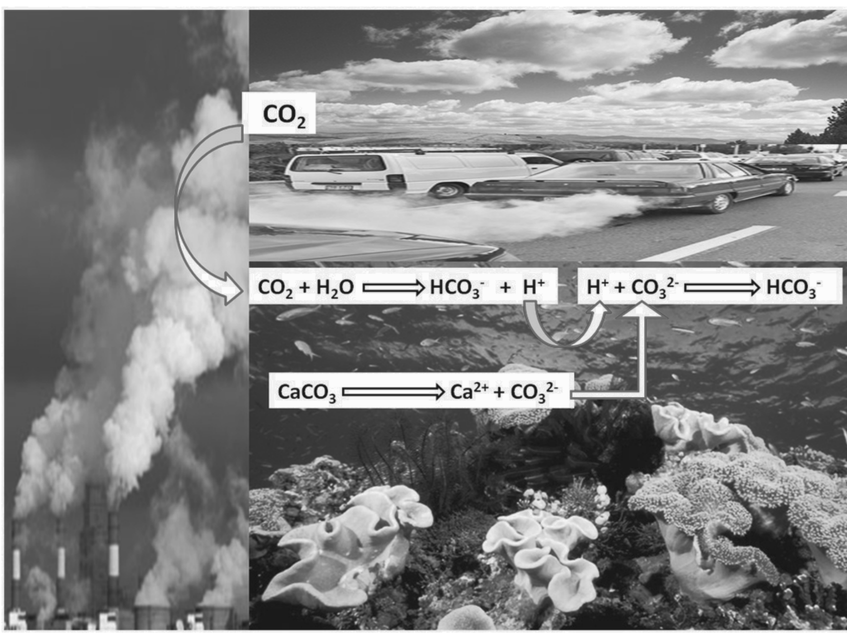

Figure 3.8. Relationship between accumulated atmospheric CO_2 and slowing of coral reef calcification due to ocean acidification. Approximately 25% of the CO_2 emitted due to human activity during the period 2000–2006 was taken up by the ocean (Canadell et al. 2007) where it combined with H_2O to produce carbonic acid, which releases a proton that combines with a carbonate ion. This decreases the concentration of carbonate, making it unavailable to marine calcifying organisms, such as corals

The new chemical composition of oceans is expected to endanger a wide range of ocean life. The resulting disruption to the ocean ecosystem could have a widespread effect on marine ecosystems worldwide. A more acidic ocean could wipe out species; disrupt the food web and impact marine life, tourism and any other human endeavour that relies on the sea. In a recent study, it has been shown that elevated levels of dissolved CO_2 and acidic seawater pH also affect development, metabolic and behavioural processes of some marine species, including non-calcifying species, such as fishes. During laboratory and field-based experiments, altered behaviour of larval fish was detected at 700 ppm CO_2. Many individuals were becoming attracted to the smell of predators. Meanwhile with further increase in the CO_2 concentration to 850 ppm, the ability of larvae to sense predators was fully impaired (Munday et al. 2010). According to one study published in 2010 in Nature Geoscience, oceans are acidifying at ten times the rate that preceded the mass marine species extinction 55 million years ago (Ridgwell and Schmidt 2010)

CO_2 induced acidification is also affecting lower salinity estuaries and temperate coastal ecosystems. Coastal and estuarine biomes are among the most biologically productive and maintain some of the most extensive and measurable ecosystem services, such as commercial and recreational fisheries, fish and invertebrate nursery grounds, water purification, flood and storm surge protection, and human recreation. Estuarine and coastal habitats being shallower, less saline and lower alkalinity are more susceptible to changes in pH than the open ocean. Estuaries are also more prone to substantial enrichment in CO_2, produced by the respiration of both natural and anthropogenic carbon. Although many estuaries already have high and variable pCO_2, more CO_2 enrichment from atmosphere will move the value even higher. For these reasons, these habitats are likely to experience more acute impacts from elevated levels of CO_2 in future (Wong 1979; Cai et al. 1998; Langdon 2002; Carpenter et al. 2008; Miller, et al. 2009).

3.8 Government Initiatives on Climate Change

3.8.1 The Montreal Protocol (1987, Canada)

The 1987 Montreal Protocol on substances that deplete ozone layer, such as chlorofluorocarbons (CFCs) and other ozone depleting substances (ODS) is a milestone agreement that has successfully reduced the worldwide production, consumption and emissions of ODS (WMO, 1995, 1999, 2003, 2007; Intergovernmental Panel on Climate Change 2005; Velders et al. 2007). CFCs and ODSs are now recognized as responsible for the observed depletion of ozone layer. The potential for CFCs to deplete stratospheric ozone layer was first accounted by Molina and Rowland (1974). A decade later, the ozone hole over Antarctica was discovered resulting from ODSs (Farman et al. 1985; Solomon et al. 1986; WMO, 1988). The Montreal Protocol approved effective and significant decreases in the production, utilization, emissions, and observed atmospheric concentrations of CFC-11, CFC-113, methyl chloroform and various other ODSs (Solomon 2004; Rowland 2006; WMO, 2007). According to WMO, (2007), there is emerging evidence about the recovery of stratospheric ozone.

CFCs and ODSs are also GHGs and contribute to the radiative forcing (RF) of climate. Earlier studies have established that continued growth in ODS emissions would lead to significant increase in direct RF or climate warming (Wigley 1988; Fisher et al. 1990; Solomon et al. 1986), although ozone depletion by ODSs would counteract some of the RF (Intergovernmental Panel on Climate Change 2001). Reduction in atmospheric ODSs concentrations serves dual purpose: a) it protects ozone and; b) it serves to protect climate due to reduction of GHGs in the atmosphere. The objective of Montreal protocol to reduce ODSs emissions in the atmosphere and absence of formal climate considerations paves the way to consider other GHGs emissions in the atmosphere. In this context, Kyoto Protocol 1997 treaty of *United Nations Framework Convention on Climate Change* (UNFCCC) came into force in February 2005, to reduce the emissions of CO_2, the leading GHGs among five other gases except ODSs.

3.8.2 The Kyoto Protocol (1997, Japan)

The Kyoto Protocol is an international agreement linked to the United Nations Framework Convention on Climate Change (UNFCCC), signed by about 180 countries. The Kyoto Protocol was adopted in Kyoto, Japan, on 11 December 1997 and entered into force on 16 February 2005. The detailed rules for the implementation of the Protocol were adopted at Conference of parties 7 (COP 7) in Marrakesh in 2001, and are called the "*Marrakesh Accords*." The major feature of the Kyoto protocol is that it commits 38 industrialized nations and European community for reducing their emissions of GHGs, specifically, CO_2, CH_4, N_2O, SF_6, HFC, and PFCs levels over a five-year period 2008 and 2012 to levels that are 5.2% lower than 1990 levels. GHGs cause a steady increase in the levels of carbon and other pollutants in the atmosphere, in turn leading to a significant warming of the earth over time. Global warming could cost the world about US $5 trillion, with developing countries being hardest hit by disastrous environmental changes, such as violent storms, melting ice caps and rising sea levels.

The major difference between the Protocol and the Convention is that while the Convention encourages industrialized countries to stabilize GHGs emissions, the Protocol commits them to do so. The Kyoto Protocol, as the Convention, is also designed to assist countries in adapting to the adverse effects of climate change. It facilitates the development and deployment of techniques that can help increase resilience to the impacts of climate change. The 'Adaptation Fund' was also established by the committee to finance adaptation projects and programmes in developing countries that are members of the Kyoto Protocol. The compliance to the Montreal protocol and Kyoto protocol have protected climate in the past and can add to climate protection in future.

3.8.3 Underwater Meeting of Maldives Cabinet

The government of Maldives, one of the Indian Ocean nations held underwater cabinet meeting on October 2009 to call for global action on climate change. Maldives, the lowest-lying nation on the Earth with islands averaging only 7 feet above sea level has a particularly dire stake in the battle to avert global warming.

Due to its low-lying topography, Maldives is struggling with the very likely possibility that it willbe engulfed by rising sea levels within the next few decades. The United Nations ‘‘Intergovernmental Panel on Climate Change’’ has forecast a rise in sea levels of at least 7.1 inches (18 cm) by the end of the century. In this global awareness campaign, the Maldives Government held the meeting underwater to sign a document calling on all nations to cut their carbon emissions. Researchers predicted that rising sea levels caused by melting glaciers and polar ice caps are likely to swamp this Indian Ocean archipelago within a century unless the world takes strong action to curtail carbon dioxide emissions. The Maldives Government had pledged to become the world's first carbon-neutral nation within a decade. According to the statement of Maldives President, the Maldives is a frontline state but this is not merely an issue for the Maldives but for the whole world. At the meeting, the Cabinet signed a declaration calling for global cuts in CO_2 emissions and presented it before a U.N. climate summit which was held in Copenhagen, Denmark (December 2009).

The underwater meeting held in Maldives was part of a wider campaign by international environmental Non-Governmental Organization (NGO). This NGO called on political leaders to commit to deep cuts in greenhouse gas emissions at Copenhagen, 2009. James Hansen, world’s top climatologist of the NASA/Goddard Institute, cautioned that atmospheric levels of carbon dioxide must return to the safe threshold of 350 ppm from current levels of 385 ppm if catastrophic global warming was to be avoided.

3.8.4 Climate Change Summit Copenhagen, Denmark (Dec. 2009)

The climate conference was held in Copenhagen, Denmark to discuss the things that can be done across the globe to slowdown or reverse the effects of climate change on Earth. The conference in Copenhagen was the 15th conference of parties (COP15) in the Framework Convention on Climate Change. At the conference in Copenhagen2009, the parties of the *United Nations Framework Convention on Climate Change* (UNFCCC) met for the last time on government level. The Kyoto Protocol aiming to prevent climate changes and global warming will expire in 2012. To keep the process in the line, there is an urgent need to renew or set up a new climate protocol.

According to the reports issued by UNFCCC, the heads of countries and delegations at the Copenhagen, 2009, stated in accord that climate change is one of the greatest challenges of our time. They emphasized to urgently combat climate change in accordance with the principle of common but differentiated responsibilities and respective capabilities. To achieve the ultimate objective of the Convention to stabilize greenhouse gas concentration in the atmosphere at a level that would prevent dangerous anthropogenic interference with the climate system, they recognized that the increase in global temperature should be below $2^{o}C$, to enhance the long-term cooperative action to combat climate change. They also recognized the critical impacts of climate change and the potential impacts of response measures on countries particularly vulnerable to its adverse effects and stressed the need to establish a comprehensive adaptation programme including international support. They agreed that deep cuts in global emissions are required, as documented by the IPCC Fourth Assessment Report with a view to reduce global emissions so as to hold the increase in global temperature below 2^{o}C. They urged to cooperate in achieving the peaking of global and national emissions as soon as possible, recognizing that the time frame for peaking will be longer in developing countries and bearing in mind that social and economic development and poverty eradication are the first and prevailing priorities of developing countries and at the same time low-emission development strategy is crucial to sustainable development.

They mentioned that adaptation to the unfavourable effects of climate change and the potential impacts of response measures is a challenge faced by all countries. Enhanced action and international cooperation on adaptation is urgently sought to ensure the implementation of the Convention by enabling and supporting the implementation of adaptation actions aimed at reducing vulnerability and building pliability in developing countries, especially in those that are particularly vulnerable, such as least developed countries, such as Small Island developing States and Africa. They agreed that developed countries shall provide adequate, predictable and sustainable financial resources, technology and capacity-building to support the implementation of adaptation action in developing countries (The United Nations Climate Change Conference 2009).

3.9 Challenge of Limiting Global Warming to 2 ^{o}C

In the 1980s, an advisory group formed by the *World Meteorological Organization* (WMO), *The International Council of Scientific Union* and *United Nations Environment Programme* recommended 2 ^{o}C global mean Earth's temperature from the industrial levels as the threshold for dangerous anthropogenic interference (DAI). Till now, this recommendation has been accepted by the *European Council*, *German Advisory Council on Climate Change*, among other national and international bodies (Ramanathan and Feng 2008). According to Council of the European Union (2006) and Pachauri and Reisinger (2007), more than 100 countries have adopted global warming limit of 2 ^{o}C or below as a guiding principal for mitigation efforts to reduce climate change hazards. Recently, Hansen et al. (2007) have adopted a similar approach and recommended 1 ^{o}C above the global mean temperature of the year 2000 as the DAI threshold value.

However, predicting probabilistic climate change for future GHGs emission scenarios is challenging due to uncertainties in carbon cycle, radiative forcing and climate response. According to Hansen et al. (2006), global surface temperature is a popular measure for predicting state of climate change. In an effort to unveil the relation between GHGs emissions corresponding to specified maximum warming, Meinshausen et al. (2009) provide a comprehensive probabilistic analysis for quantifying GHGs emission budget for the 2000–50 periods that would limit global warming throughout the 21st century to below 2^{o}C target, based on a combination of published distributions of climate system properties and observational constraints. They showed that for the chosen class of emission scenarios, both cumulative emissions up to 2050 and emission levels in 2050 are strong indicators of the probability that global warming will not exceed to 2^oC in 21^{st} century relative to pre-industrial temperatures. There is a 25% probability that warming will exceed 2^oC if cumulative CO_2 emissions are limited to 1,000 Gt and a limit of 1,440 Gt CO_2 yields a 50% probability–given a representative estimate of the distribution of climate system properties. As evident, in 2000–06 CO_2 emissions were ~234 Gt CO_2 (Canadell 2007). Considering this emission rate, achieving a target of global warming limit of 2^oC or below is not impossible. Recently, G8 (2008) summit predict halved global GHGs emissions by 2050, which estimated the means with 12–45% probability of exceeding 2^oC by assuming 1990 as the emission base year and a range of published climate sensitivity distributions (Meinshausen et al. 2009).

3.10 Conclusion and Future Outlook

GHGs have become the dominant climate force in recent decades. Climate stabilization can be achieved by reducing net emission of GHGs. This target can be achieved by decreasing dependence on fossil fuel consumption or alternatively by enhancing sequestration of carbon dioxide. The avoidance of deforestation and supporting afforestation is another strategy to slow down global warming.

Increasing GHGs concentrations have direct consequences on flora and fauna including humans. GHGs concentrations in the environment should be curtailed on priority in order to avoid disease epidemics. Reduction in concentrations of GHGs in the environment will also help to reduce the impacts of natural disasters. Ocean acidification is a direct consequence of increasing atmospheric CO_2 levels. To avoid substantial damage to ocean ecosystems in future, deep and immediate reductions in global CO_2 emissions are required. Reduction of greenhouse gas emissions due to fossil fuel burning is required over the next generations to limit ongoing ocean oxygen depletion and acidification to overcome their long-term adverse inputs. Government initiatives and mass movements are required for the reduction of GHGs in the environment in order to maintain the inhabitable nature of the planet.

3.11 Acknowledgements

The authors are sincerely thankful to the Natural Sciences and Engineering Research Council of Canada (Discovery Grant 355254), FQRNT (ENC 125216) and MAPAQ (No. 809051) for financial support. The views or opinions expressed in this article are those of the authors.

3.12 Abbreviations

CFCs = Chlorofluorocarbons; COP = Conference of parties; DAI = dangerous anthropogenic interference; GHGs = greenhouse gases; HFCs = hydrofluorocarbons; IPCC = The Intergovernmental Panel on climate change; NGO = Non Governmental Organization; ODSs = ozone depleting substances; RF = radiative forcing; UNEP = United Nations Environment Programme; UNFCCC = United Nations Framework Convention on Climate Change; WMO = World Meteorological Organization

3.13 References

Anthony, K. R. N., Kline, D. I., Diaz-Pulido, G., Dove, S., and Hoegh-Guldberg, O. (2008).‘‘Ocean acidification causes bleaching and productivity loss in coral reef builders.’’*PNAS*, 105(45).17442–17446.

Archer, D. (2005). ‘‘Fate of fossil fuel CO_2 in geologic time.’’*Journal Geophysics Research*, 110, C09S05.

Arnell, N. W. (2004). ‘‘Climate change and global water resources: SRES emissions and socio-economic scenarios. Global environmental change-Human and policy dimensions, 14, 31–52.

Bala, G., Caldeira, K., Wickett, M., Phillips, T. J., Lobell, D. B., Delire, C., And Mirin, A. (2007). ‘‘Combined climate and carbon-cycle effects of large-scale deforestation.’’ *PNAS*, 104(16), 6550–6555.

Benton, M. J. (2003). *When life nearly died*. Thames and Hudson, London.

Bärring, L. (1993). ‘‘Climate - change or variation?’’ *Climatic Change,* 25, 1–13.

Bindoff, N. L., Willebrand, J., Artale, V., Cazenave, A., Gregory, J., Gulev, S., Hanawa, K., Le Quéré, C., Levitus, S., Nojiri, Y., Shum, C. K., Talley, L. D., and Unnikrishnan, A. (2007). “Observations: Oceanic climate change and sea level.” In: *Climate Change 2007: The Physical Science Basis.* Contribution of Working Group I to the Fourth Assessment Report of the Intergovernmental Panel on Climate Change [Solomon, S., Qin, D., Manning, M., Chen, Z., Marquis, M., Averyt, K. B., Tignor, M., and Miller, H. (eds.)]. Cambridge University Press, Cambridge, United Kingdom and New York, NY, USA.

Blasing, T. J. (2009). ‘‘Recent greenhouse gas concentrations.’’ The carbon dioxide information analysis center. <http://cdiac.ornl.gov/pns/current_GHGs.html> (accessed March 2012). DOI: 10.3334/CDIAC/atg.032

Bonan, G. (2002). *Ecological Climatology: Concepts and Applications*. Cambridge University Press, Cambridge

Brewer, P. G., and Peltzer, E. T. (2009). “Limits to marine life**.’’** *Science,* 324 (5925), 347–348.

Buseck, P. R., and Posfai, M. (1999). “Airborne minerals and related aerosol particles: Effects on climate and the environment.’’ *Proceedings of the National Academy of Science,* 96, 3372–3379.

Cai, W-J., and Wang, Y. (1998). ‘‘The chemistry, fluxes, and sources of carbon dioxide in the estuarine waters of the Satilla and althamaha rivers, Georgia.’’ *Limnology Oceanography*, 43, 657–668.

Caldeira, K., and Wickett, M. E. (2003). ‘‘Anthropogenic carbon and ocean pH.’’*Nature,* 425, 365–365.

Canadell, J. G., Quéré, C. L., Raupach, M. R., Fielde, C. B., Buitenhuis, E. T., Ciais, P., Conway, T. J., Gillett, N. P., Houghton, R. A., and Marland, G. (2007). ‘‘Contributions to accelerating atmospheric CO_2 growth from economic activity, carbon intensity and efficiency of natural sinks.’’*PNAS*, 104, 18866–18870.

Carpenter, K. E., Abrar, M, Aeby, G., Aronson, R. B., Banks, S., Bruckner, A., Chiriboga, A., Cortés, J., Delbeek, J. C., DeVantier, L., Edgar, G. J., Edwards, A. J., Fenner, D., Guzmán, H. M., Hoeksema, B. W., Hodgson, G., Johan, O., Licuanan, W. Y., Livingstone, S. R., Lovell, E. R., Moore, J.A., Obura, D.O., Ochavillo, D., Polidoro, B. A., Precht, W. F., Quibilan, M. C., Reboton, C., Richards, Z. T., Rogers, A. D., Sanciangco, J., Sheppard, A., Sheppard, C., Smith, J., Stuart, S., Turak, E., Veron, J. E. N., Wallace, C., Weil, E., and Wood, W. (2008). “One-third of reef-buildings corals face elevated extinction risk from climate change and local impacts.” *Science,* 321, 560–563.

Climate change (2007). *Impacts, adaptation and vulnerability*. Geneva, Intergovernmental Panel on Climate Change, 2007. Contribution of working group II to the fourth assessment report of the Intergovernmental Panel on Climate Change.

Codispoti, L. A. (2010). ‘‘Interesting times for marine N_2O.’’ *Science*, DOI: 10.1126/science.1184945.

Confalonieri, U., Menne, B., Akhtar, R., Ebi, K. L., Hauengue, M., Kovats, R. S., Revich, B., and Woodward, A. (2007). “Wind, storms and floods.” Section 8.2.2 in book chapter: Human health. In: *Climate Change 2007: Impacts, Adaptation and Vulnerability*. Contribution of Working Group II to the Fourth Assessment Report of the Intergovernmental Panel on Climate Change (Parry, M. L., Canziani, O. F., Palutikof, J. P., van der Linden, P. J., and Hanson, C. E., Eds.). Print version: Cambridge University Press, Cambridge, UK.

Council of the European Union (2006). *Presidency conclusions*, European commission, Brussels. 23/24 March 2006. 7775/06, pp 1–36.

Danny Harvey L. D. (2007). ‘‘Dangerous anthropogenic interference, dangerous climatic change, and harmful climatic change: non-trivial distinctions with significant policy implications’’. Climatic Change, 82, 1–25.

Envirolink (1998) "Global warming is happening." *Envirolink,* March 8, 1998. <http://www.envirolink.org/prgs/edf/sitemap.html>

Fabry, V. J., Seibel, B. A., Feely, R. A., and Orr, J. C. (2008). ‘‘Impacts of ocean acidification on marinefauna and ecosystem processes.’’ *ICES Journal Marine Science,* 65, 414–432.

Feely, R. A., Sabine, C., Lee, K., Hernandez-Ayon, J. M., and Ianson, D. (2004).‘‘Impact of anthropogenic CO_2 on the $CaCO_3$ system in the oceans.’’ *Science*, 305, 362–66.

Farman, J. C., Gardiner, B. G., and Shanklin, J. D. (1985). ‘‘Large losses of total ozone in Antarctica reveal seasonal ClXNOX interaction.’’ *Nature,* 315, 207–210.

Ferguson, G., and Gleeson, T. (2012). "Vulnerability of coastal aquifers to groundwater use and climate change." *Nature Climate Change,* 2, 342–345.

Fisher, D. A., Hales, C. H., Wang, W. C., Ko, M. K. W., and Sze, N. D. (1990). ''Model calculations of the relative effects of CFCs and their replacements on global warming.'' *Nature*, 344, 513–516.

Foley, J. A., Costa, M. H., Delire, C., Ramankutty, N., and Snyder, P. (2003). ''Green surprise? How terrestrial ecosystems could affect earth's climate.'' *Frontiers in Ecology and the Environment,* 1, 38–44.

Foley, J. A, DeFries, R., Asner, G. P., Barford, C., Bonan, G., Carpenter, S. R, Chapin, F. S., Coe, M. T., Daily, G. C., Gibbs, H. K., Helkowski, J. H., Holloway, T., Howard, E. A., Kucharik, C. J., Monfreda, C., Patz, J. A., Prentice, I. C., Ramankutty, N., and Snyder, P. K. (2005).''Global consequences of land use.'' *Science,* 309, 570–574.

Foukal, P., Frohlich, C., Spruit, H., and Wigley, T. M. L. (2006).''Variations in solar luminosity and their effect on the Earth's climate.'' *Nature*, 443, 161–166

Frame, D. J., and Allen, M. R. (2009). ''Greenhouse-gas emission targets for limiting global warming to 2°C.'' *Nature Letters*. DOI: 10.1038/nature08017.

G8 (2008). "Hokkaido Tokyo Summit Leaders Declaration." <http://www.mofa.go.jp/policy/economy/summit/2008/doc/doc080714_en.html>.

Gerlach, G., Atema, J., Kingsford,M. J., Black, K. P., and Miller-Sims, V. (2007). ''Smelling home canprevent dispersal of reef fish larvae.'' *Proceedings of the National Academy of Science,* 104, 858–863.

Gille, S. T. (2002). "Warming of the southern ocean since the 1950s." *Science*, 295 (5558), 1275–1277.

Gordon, L. J., Steffen, W., Jönsson, B. F., Folke, C., Falkenmark, M., and Johannessen, Å. (2005). ''Human modification of global water vapor flows from the land surface.'' *Proceedings of the National Academy of Science,* 102, 7612–7617

Hadley Center (2012). ''Catastrophic 5–7 °C warming by 2100 on current emissions path." Available at <http://climateprogress.org/208/12/21/hadley-study-warns-of-catastrophic-5%c2%b0c-warming-by-2100-on-current-emissions-path/> (accessed Feb. 2012).

Hales, S., Wet, N. D., Maindonald, J., and Woodward, A. (2002). ''Potential effect of population and climate changes on global distribution of dengue fever: An empirical model.'' *The Lancet*, 360, 830–834.

Haley, J. (2002). *Global warming: Opposing viewpoints series*. Greenhaven Press, Inc., San Diego, California. ISBN 0-7377-0908-1, pp 1–224.

Hansen, J., Sato, M., Ruedy, R., Lo, K., Lea, D. W., and Medina-Elizade, M. (2006). "Global temperature change." *PNAS,* 103 (39), 14288–14293.

Hansen, J., Sato, M., Ruedy, R., Kharecha, P., Lacis, A., Miller, R., Nazarenko, L., Lo, K., Schmidt, G. A., Russell, G., Aleinov, I., Bauer, S., Baum, E., Cairns, B., Canuto, V., Chandler, M., Cheng, Y., Cohen, A., Del Genio, A., Faluvegi, G., Fleming, E., Friend, A., Hall, T., Jackman, C., Jonas, J., Kelley, M., Kiang, N. Y., Koch, D., Labow, G., Lerner, J., Menon, S., Novakov, T., Oinas, V., Perlwitz, J, Perlwitz, Ja., Rind, D., Romanou, A., Schmunk, R., Shindell, D., Stone, P., Sun, S., Streets, D., Tausnev, D., Yao, M., and Zhang,

S. (2007). ''Dangerous human-made interference with climate.A GISS modelE study.'' *Atmospheric Chemistry and Physics*, 7, 2287–2312.

Hoegh-Guldberg, O., Mumby, P. J., Hooten, A. J., Steneck, R. S., Greenfield, P., Gomez, E., Harvell, C. D., Sale, P. F., Edwards, A. J., Caldeira, K., Knowlton, N., Eakin, C. M., Iglesias-Prieto, R., Muthiga, N., Bradbury R. H., Dubi A., and Hatziolos, M. E. (2007). ''Coral reefs under rapid climate change and ocean acidification.'' *Science,* 318, 1737–1742.

Hofman, D., Butler, J., and Tans, P. (2009). ''A new look at atmospheric carbon dioxide.'' *Atmospheric Environment,* 43, 2084–2086.

Houghton, R. A., and Goodale, C. L. (2004). ''Effects of land-use change on the carbon balance of terrestrial ecosystems.'' In: DeFries, R., Asner, G., and Houghton, R. (eds.) *Ecosystems and Land Use Change*. *Geophysical Monograph Series* 153, American Geophysical Union, Washington DC.

Iglesias-Rodriguez, M. D., Halloran, P. R., Rickaby, R. E. M., Hall, I. R., and Colmenero-Hidalgo, E., Gittins J. R., Green D. R. H., Tyrrell T., Gibbs S. J., von Dassow P., Rehm E., Armbrust E. V., and Boessenkool K. P (2008). ''Phytoplankton calcification in a high-CO_2 world.''*Science,* 320, 336–40.

Intergovernmental Panel on Climate Change/Technology and Economic Assessment Panel (2005). *Special Report: Safeguarding the Ozone Layer and theGlobal Climate System: Issues Related to Hydrofluorocarbons and Perfluorocarbons*. Cambridge Univ. Press, New York.

IPCC (Intergovernmental Panel on Climate Change) 1992. *Climate Change. The IPPC Scientific Assessment*. Houghton, E. J. T., Jenkins, G. J., and Ephramus, J. L. (eds.). Cambridge University Press, Cambridge.

IPCC (2005). *IPCC Special Report on Carbon Dioxide Capture and Storage.* IPCC Working Group III. Cambridge Univ. Press, Dec., 19, 2005, pp. 431.

IPCC (2007a). *Climate change 2007: The physical science basis*. Contribution of working group 1 to the fourth Assessment Report of Intergovernmental Panel on Climate Change (Solomon, S., D. Qin, M. Manning, Z. Chen, M, Marquis, K. B. Averyt, M. Tignor and H. L Miller (eds.). Cambridge University press, Cambridge United kingdom and New York, USA. pp. 996.

IPCC (2007b). *Climate change 2007. Synthesis report.* An Assessment of the Intergovernmental Panel on Climate Change. Fourth Assessment Report (AR4). *1-22.*

Jaramillo, P., and Matthews, H. S. (2005). "Landfill-gas-to-energy projects: analysis of net private and social benefits." *Environ. Sci. Technol.*, 39(19), 7365–7373.

Kaiser R., Le Tertre, A., Schwartz, J., Gotway, C., Daley, W., and Rubin, C. (2007). "The effects of the 1995 heat wave in Chicago on all-cause and cause-specific mortality." *Am. J. Public Health*, 97(Suppl 1), 58–62.

Kelly, P. M., and Wigley, T. M. L. (1992). "Solar cycle length variations, greenhouse forcing and global climate." *Nature,* 360, 328–330

Kelly, P. M., Jones, P. D., and Pengqun, J. (1996). ''The spatial response of the climate system to explosive volcanic eruptions.'' *International Journal of Climatology,* 16, 537–550.

Klein-Goldewijk, K. (2001). ''Estimating global land use change over the past 300 years: The HYDE database.'' *Global Biogeochemical Cycles,* 15, 417–433.

Kleypas, J. A., Feely, R. A., Fabry, V. J., Langdon, C., Sabine, C. L., and Robbins, L. L. (2006). *Impacts of Ocean acidification on Coral Reefs and OtherMarine Calcifiers: A Guide for Future Research* (NOAA/Pacific Marine Environmental Laboratory, Seattle).

Knabb, R. D., Rhome, J. R., and Brown, D. P. (2005). *Tropical Cyclone Report, Hurricane Katrina*. National Hurricane Center.

Kyoto Protocol to the United Nations Framework Convention on Climate Change (1998). http://unfccc.int/resource/docs/convkp/kpeng.pdf.

Langdon, C. (2002). ‘‘Review of experimental evidence for effects of CO_2 on calcification of reef builders.’’ *Proceedings of the 9th international coral reef symposium*, 2, 1091–1098.

Larson, J. (2006). Setting the record straight. Eco-Economy Updates, Earth Policy Institute, www.earth-policy.org.

Leggett, J. A. (2009). *Climate Change: Science Highlights*. CRS report for congress. RL34266. 1–24.

Liamsanguan, C., and Gheewala, S. H. (2008). “The holistic impact of integrated solid waste management on greenhouse gas emissions in Phuket.” *Journal of Cleaner Production*, 16, 1865–1871.

Lynd, L. R., Cushman, J. H., Nichlos, R. J., and Wyman, C. E. (1991). ‘‘Fuel ethanol from cellulosic biomass.’’ *Science,* 251, 34 –40.

Matear, R. J., and Hirst, A. C. (2003). “Long term changes in dissolved oxygen concentrations in the ocean caused by protracted global warming.” *Global Biogeochem Cycles*, 17, 1125.

Mcneil, B. I., and Matear, R. J. (2007). ‘‘Climate change feedback on future oceanic acidification.’’ TellusSer59B. *Chemical Physical Meteorology*, 59, 191–198.

Mcneil, B. I., and Matear, R. J. (2008). ‘‘Southern Ocean acidification: A tipping point at 450-ppm atmospheric CO_2.’’ *Proceedings of the National Academy of Sciences*, 105, 18860–18864.

Meinshausen, M., Meinshausen, N., Hare, W., Raper, S. C. B., Frieler, K., Knutti, R., Frame, D. J., and Allen, M. R. (2009). ‘‘Greenhouse-gas emission targets for limiting global warming to 2^{o}C.’’ *Nature Letters*, 458, doi:10.1038/nature08017.

Mitchell, J. M. Jr., Dzerdzeevskii, B., Flohn, H., Hofmeyr, W. L., Lamb, H. H., Rao, K. N., and Wallén, C. C. (1966). *Climatic Change*. WMO Technical Note No 79, World Meteorological Organization, Geneva, 79 pp.

Miller, A. W., Reynolds, A. C., Sobrino, C., and Riedel, G. F. (2009). ‘‘Shell fish face uncertain future in high CO_2 world: Influence of acidification on oyster larvae calcification and growth in estuaries.’’ *Plos one*, 4(5), 1–8.

Molina, M. J., and Rowland, F. S. (1974). ‘‘Stratospheric sink for chlorofluoromethanes: Chlorine ion catalyzed destruction of ozone.’’ *Nature,* 249, 810–812.

Molina, M., Zaelke, D., Sarmac, K. M., Andersen, S. O., Ramanathane, V., and Kaniaruf, D. (2009). ‘‘Tipping elements in earth systems special feature: Reducing abrupt climate change risk using the Montreal Protocol and other regulatory actions to complement cuts in CO_2 emissions’’. *PNAS*, 106, 20616.

Munday, P. L., Dixson, D. L., McCormick, M. I., Meekan, M., Ferrari, M. C. O., and Chivers, D. P. (2010). ‘‘Replenishment of fish populations is threatened by ocean acidification.’’ *PNAS*, DOI/10.1073/pnas.1004519107.

Munday, P. L., Dixson, D. L., Donelsona, J. M., Jonesa, G. P., Pratchett, M. S., Devitsinac, G. V., and Døving, K. B. (2009). ‘‘Ocean acidification impairs olfactory discrimination and homing ability of a marine fish.’’*PNAS,* 106(6), 1848–1852.

Olofsson, J., and Hickler, T. (2008). “Effects of human land-use on the global carbon cycle during the last 6000 years.” *Veget. Hist. Archaeobot*. 17, 605–615.

Orr, J. C., Fabry, V. J., Aumont, O., Bopp, L., Doney, S. C., Feely, R. A., Gnanadesikan, A., Gruber, N., Ishida, A., Joos, F., Key, R. M., Lindsay, K., Maier-Reimer, E., Matear, R., Monfray, P., Mouchet, A., Najjar, R. G., Plattner, G-K., Rodgers, K. B., Sabine, C. L., Sarmiento, J. L., Schlitzer, R., Slater, R. D., Totterdell, I. J., Weirig, M-F., Yamanaka, Y., and Yool, A. (2005). ‘‘Anthropogenic ocean acidification over the twenty first century and its impact on calcifying organisms.’’ *Nature,* 437, 681–86.

Pachauri, R. K., and Reisinger, A. (eds) (2007). *Climate change, synthesis report*. Intergovernmental Panel on Climate Change, Cambridge, UK, 2007.

Parry, M. L., Canziani, O. F., Palutikof, J. P., van der Linden, P. J., and Hanson, C. E. (2007). *Technical summary, Climate Change 2007: Impacts, Adaptation and Vulnerability*. Contribution of Working Group II to the Fourth Assessment Report of the Intergovernmental Panel on Climate Change. eds. *Cambridge Univ. Press,* Cambridge, UK, 23–78 .

Pielke, R. Jr. (2004). ‘‘What is climate change?’’ *Issues in Science and Technology* Summer, 1–4.

Prax V. (2011). “What are greenhouse gases? Do they impact the environment?” <http://suite101.com/article/what-are-greenhouse-gases-do-they-impact-the-environment-a330750> (accessed Jan. 2012).

Qin, W., Egolfopoulos, F. N., and Tsotsis, T. T. (2001). “Fundamental and environmental aspects of landfill gas utilization for power generation.” *Chemical Engineering Journal*, 82, 157–172.

Ramanathan, V., and Feng, Y. (2008). “On avoiding dangerous anthropogenic interference with the climate system: Formidable challenges ahead.’’ *PNAS*, 115(38), 14245–14250.

Raven, J. (2005). “Ocean acidification due to increasing atmospheric carbon dioxide.’’ *Royal Society London*. Policy document 12/05, ISBN 0 85403 617 2, 1–68.

Reilly, M. (2009). “Ocean dead zones could approach mass extinction levels.” Available at <http://dsc.discovery.com/news/2009/01/26/ocean-dead-zones.html> (accessed Feb. 2012).

Riebesell, U., Zondervan, I., Rost, B., Tortell, P. D., Zeebe, R. E., and Morel, F. M. M. (2000). ‘‘Reduced calcification of marine plankton in response to increased atmospheric CO_2.” *Nature,* 407(6802), 364–367.

Roberts, N. (1998). *The Holocene: An Environmental History*. Blackwell, Oxford.

Robine, J. M., Cheung, S. L., Leroy, S., Van-Oyen, H., Griffiths, C., Michel, J. P., and Hermann, F. R. (2008). "Death toll exceeded 70,000 in Europe during the summer of 2003.'' *Comptes Rendus Biologies*, 331(2), 171–78.

Rogner, H. H., Bradley, R.,Crabbé P., Edenhofer, O., Hare, B., Kuijpers, L., and Yamaguchi, M. (2007). *Introduction, Climate Change 2007: Mitigation.* Contribution of Working Group III to the Fourth Assessment Report of the Intergovernmental Panel on Climate Change, Metz, B., Davidson, O. R., Bosch, P. R., Dave, R., and Meyer, L. A. (eds.), Cambridge Univ. Press, Cambridge, UK, pp. 95–116.

Romm, J. (2007). *Hell and high water. Global Warming–the Solution and the Politics–and What We Should Do?* New York: William Morrow. ISBN 0-06-117212-X, pp 292.

Romm, J. (5 Sep. 2008). ''Stunning new sea level rise research: Most likely 0.8 to 2.0 meters by 2100.'' http://thinkprogress.org/climate/2008/09/05/203057/stunning-new-sea-level-rise-research-part-1-most-likely-08-to-20-meters-by-2100/.

Rowland, F. S. (2006). "Stratospheric ozone depletion." *Philosophical Transactions of the Royal Society London B Biological Sciences*, 361, 769–790.

Ruddiman, W. F. (2001). *Earth's Climate–Past and Future*. W. H. Freeman and Company, New York.

Schiermeier, Q. (2008). "Hurricanes are getting fiercer.'' *Nature*, DOI:10.1038 /news.2008.1079.

Ridgwell, A., and Schmidt, D. N. (2010). "Past constraints on the vulnerability of marine calcifiers to massive carbon dioxide release." *Nature Geoscience,* 3, 196–200.

Science Daily (2009). "Greenhouse gases continue to climb despite economic slump.'' http://www.sciencedaily.com/releases/2009/04/090424195920.html> (accessed Nov. 2011).

Shaffer, G., Olsen, S. M., and Pedersen, J. O. P. (2008). "Presentation, calibration and validation of the low-order, DCESS Earth System model.'' *Geoscientific Model Development,* 1, 17–51.

Shaffer, G., Olsen, S. M., and Pedersen, J. O. P. (2009). "Long-term ocean oxygen depletion in response to carbon dioxide emissions from fossil fuels.'' *Nature Geoscience*, DOI: 10.1038/NGEO420.

Solomon, S., Garcia, R. R., Rowland, F. S., and Wuebbles, D. J. (1986). "On the depletion of Antarctic zone.'' *Nature,* 321,755–758.

Solomon, S. (2004). ''The hole truth.'' *Nature,* 427, 289–291.

Solomon, S., and Daniel, J. S. (1996). "Impact of the montreal protocol and its amendments on the rate of change of global radiative forcing.'' *Climatic Change*, 32, 7–17.

Snyder, P. K., Foley, J. A., Hitchman, M. H., and Delire, C. (2004). "Analyzing the effects of complete tropical forest removal on the regional climate using a detailed three-dimensional energy budget: A application to Africa.'' *Journal Geophysics Research*, 109, D21102, DOI: 10.1029/2003JD004462.

Stramma, L., Johnson, G. C., Sprintall, J., and Mohrholz, V. (2008) "Expanding oxygen-minimum zones in the tropical oceans." Science. 320, 655–658.

The Royal Society (2005). *Ocean Acidification Due to Increasing Atmospheric Carbon Dioxide*. The Royal Society, London. Policy document 12/05, ISBN 0 85403 617 2, 1–68.

The United Nations Climate Change Conference (2009). *The United Nations framework on Climate Change*. Copenhagen, Denmark, Dec. 2009.

USEPA (2006). *Global Anthropogenic Emissions of Non-CO_2 Greenhouse Gases: 1990 -2020.* USEPA Report 430-R-06-003.

USEPA (2008). *Municipal Solid Waste Generation, Recycling, and Disposal in the United States: Facts and Figures for 2007.* EPA-530-F-08-018, Solid Waste and Emergency Response (5306P), Washington, DC 20460, Nov. 2008.

Velders, G. J. M., Andersen, S. O., Daniel, J. S., Fahey, D. W., and McFarland, M. (2007). "The importance of the Montreal Protocol in protecting climate.'' *PNAS*, 104(12), 4814–4819.

Vitousek, P. M., Mooney, H. A., Lubchenco, J., and Melillo, J. M. (1997). "Human domination of Earth's ecosystems.'' *Science,* 277, 494–499

Whalen, S. C., Reeburgh, W. S., and Sandbeck, K. A. (1990). "Rapid methane oxidation in a landfill cover soil." *Appl. Environ. Microb.*, 56(11), 3405–3411.

Wigley, T. M. L. (1988). "Future CFC concentration changes under the Montreal Protocol and their greenhouse effect implications.'' *Nature,* 335, 333–335

Williams, M. (2000). "Dark ages and dark areas: global deforestation in the deep past.'' *Journal of Historical Geography,* 26, 28–46.

Wong, G. T. (1979). "Alkalinity and pH in the southern Chesapeake Bay and the James River estuary.'' *Limnology Oceanography*, 24, 970–977.

World Health Organization (2009). "Global health risks: mortality and burden of disease attribute to selected major risks.'' Geneva, ISBN 978 92 4 156387 1, pp 1–7.

WMO (World Meteorological Organization) (1988). *Report of the International Ozone Trends Panel.* WMO, Geneva, Report 18.

WMO (1995). *Scientific Assessment of Ozone Depletion: 1994.* WMO, Geneva, Report 37.

WMO (1999). *Scientific Assessment of Ozone Depletion: 1998.* WMO, Geneva, Report 44.

WMO (2003). *Scientific Assessment of Ozone Depletion: 2002.* WMO, Geneva, Report 47.

WMO (2007). *Scientific Assessment of Ozone Depletion: 2006.* WMO, Geneva, Report 50.

WBE (World Book Encyclopaedia) (1982a). Methane, *WBE*, Vol. 7, p. 270.

WBE (1982b). Fluorocarbons, *WBE*, Vol. 13, Hatch, p. 358.

Zhou, X. N., Yang, G. J., Yang, K., Wang, X. H., Hong, Q. B., Sun, L. P., Malone, J. B., Kristensen, T. K., Bergquist, N. R., and Utzinger, J. (2008). "Potential impact of climate change on schistosomiasis transmission in China.'' *American Journal of Tropical Medicine and Hygiene*, 78, 188–194.

CHAPTER 4

Greenhouse Gas Emissions from Different Sources

B. R. Gurjar, C. S. P. Ojha, R. Y. Surampalli, and V. Tyagi

4.1 Introduction

Anthropogenic sources of air pollution emissions include a number of sectors and activities e.g., fossil fuel and biofuel combustion in industrial and residential areas, transportation (road, rail, air and ships), waste disposal, industrial processes, agricultural activities, solvent production and usage. Emissions of greenhouse gases (GHGs), such as Carbon dioxide (CO_2), methane (CH_4) and nitrous oxide (N_2O) are a major concern from climate change perspective. This because they obstruct the escape of infrared (heat) energy to outer space by absorbing them and leading to increase in earth's temperature along with other climatic changes (Bond et al. 2004). Anthropogenic activities annually attribute to an estimated 3%, 64%, and 24% of global emissions of CO_2, CH_4 and N_2O, respectively (Duxbury 1994). Megacities contribute a major portion in these global emissions. As reported by Butler et al. (2008) megacities account for approximately between 9% and 12% of the global emissions of CO, NO_x, and NMVOC.

Satellite based observations elucidate that emissions from any part of the world can get transported from one region to another into trans-oceanic and trans-continental plumes within a week (Olivier et al. 1998; Ramanathan and Feng 2009). Hence, not only in the atmosphere over major continents, a major increase in the concentration of radiatively active gases (CO_2, CH_4 and N_2O) has also been observed in the air trapped in Antarctica and Greenland ice with the commencement of industrial revolution (US EPA 1994). During the past 100 years, increases in CO_2 and aerosols concentrations in the atmosphere have led to an augmentation in the earth's surface temperature by 0.7 degrees centigrade (Srinivasan 2008). During the year 1990, atmospheric concentration of CO_2 was 25% higher in comparison to the preindustrial (1750–1800) time, mostly due to human induced emissions. In the year 1980, CO_2 increased by about 0.5% annually due to fossil fuel burning, and 0.6–2.5 Pg (Petagram) due to deforestation. The global atmospheric CO_2 concentration (Fig. 4.1) increased from a value of approximately 280 ppm during the pre-industrial time to 379 ppm in 2005 (IPCC 2007a). Main anthropogenic sources responsible for high CO_2 emissions are fossil fuels (coal, oil and gas) and biomass combustion, land use changes, and minor contribution from industries (Kram et al. 2000). In the past 150 years, collective CO_2 emissions linked with land clearance for agriculture are analogous to fossil fuel combustion, although currently fossil fuel is the key CO_2 source and is further expected to become more dominant (Duxbury 1994). In 2008, around 30,377 Tg (Teragram) CO_2 was released to the atmosphere globally due to fossil fuels combustion (US EPA 2010).

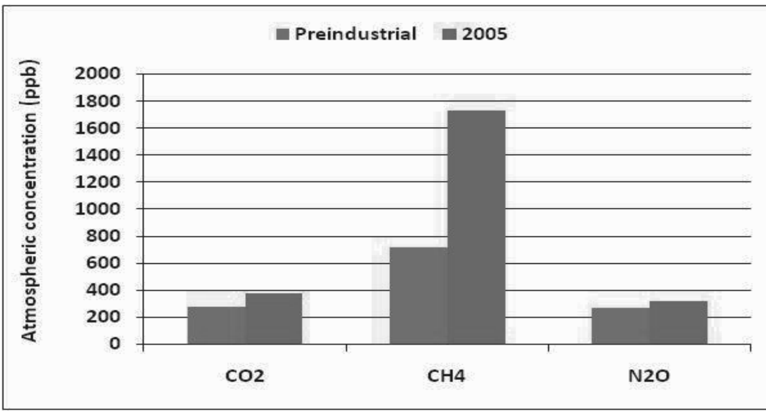

Figure 4.1. Changes in atmospheric concentration of GHGs since preindustrial era (1750–1800) and 2005

CH_4 being 20 times more radiatively active in comparison to CO_2, strongly influences the photochemistry of the atmosphere (Cao et al. 1996). In the past two hundred years, the atmospheric CH_4 concentration has increased above twofold, while the terrestrial CH_4 emissions showed 49% growth from 1940 (280 Tg) to 1980 (420 Tg) (Cao et al. 1996). The global atmospheric concentration of CH_4 has increased from a value of about 715 ppb during the pre-industrial time to 1732 ppb in the early 1990, and 1774 ppb in 2005 (IPCC 2007b). According to Prather et al. (2001) natural sources account for 20–40% CH_4, anthropogenic fossil fuel related sources for 20% and the remaining 40–60% comes from other anthropogenic sources (El-Fadel and Massoud 2001). During 1990, around 70% of the worldwide CH_4 emissions were from the combined anthropogenic sources (US EPA 2001).

N_2O is not only a GHG with high global warming potential but also a key source of nitrogen oxides to the stratosphere and acts as a catalyst in ozone destruction. As depicted in Fig. 4.1, atmospheric N_2O concentrations increased to 319 ppb during the year 2005, from 270 ppb during the pre-industrial time (IPCC 2007b). Global N_2O emissions in 1991 were estimated to be 15 Tg, in which 3.2 Tg (20%) was from the anthropogenic sources, mainly emitted from agriculture and land use related sources (Olivier et al. 1998). Around 60% of the total global N_2O emissions are from the natural sources including undisturbed soil, ocean water and probably atmospheric formation. Once emitted, N_2O remains in the atmosphere for approximately 114 years before removal (IPCC 2007b).

Apart from the GHGs there are other gases which do not have a direct global warming impact, but play a circuitous role by disturbing the terrestrial and/or solar radiation absorption and affect the formation/destruction of GHGs, including tropospheric and stratospheric ozone (O_3) (US EPA 2010). Most of these pollutants are product of incomplete combustion and are called indirect GHGs: carbon monoxide (CO), nitrogen oxides (NO_x) and non methane volatile organic carbon (NMVOC). These pollutants react with other gaseous species present in the atmosphere, leading to the formation of a secondary pollutant (Ramanathan and Feng 2009). Anthropogenic emissions of CH_4 and NO_x increase the concentration of O_3 in the troposphere and lower stratosphere, where O_3 acts as a GHG (US EPA 1994). NO_x released mainly from fossil fuel combustion, leads to acidification and O_3 formation in the troposphere, hence affecting the oxidant balance of troposphere and human health (Olivier et al. 1998). NO_x is a short-lived gas with a lifetime of 1–10 days and leads to the formation of nitric acid, removed as acid rain, in the atmosphere (Olivier et al. 1998). Various anthropogenic sources responsible for the emissions of NO_x and N_2O are fossil fuel combustion, biomass burning, industrial processes, waste treatment and microbiological emissions from natural and agricultural soils (Olivier et al. 1998). A major portion of the NO_x emissions comes from the transportation sector and accounts for approximately 5% of the global NO_x emission from fossil fuel (Parashar et al. 1998). According to Zhang et al. (2003) on reducing NO_x emissions from fossil fuel, air pollution can be reduced in urban areas, due to lesser quantity of ozone precursors.

Photochemical oxidations of NMVOCs lead to formation of CO_2, ozone (O_3) and organic acid. Oxidation of atmospheric VOCs leads to the formation of organic peroxy radicals which facilitate cycling of NO to NO_2, a process directly responsible for ozone formation. Major anthropogenic sources of NMVOCs include fossil fuel combustion, direct release from industry, industrial processing of chemicals, and waste. The lifetimes of NMVOCs range from a few minutes to a few months. CO has a lifetime of around two months, and is a significant compound as, by reacting with OH radicals, it affects the oxidizing capacity of the troposphere (Olivier et al. 1999). Major anthropogenic sources emitting CO include fossil fuel combustion in vehicles, industrial processes, non-transportation fuel combustion, oxidation of CH_4, and oxidation of non-methane hydrocarbons (Bradely et al. 1999). In cities, automobile exhaust account for around 95% of all CO emissions (US EPA 2010).

The following sections discuss these GHG emissions sector wise, whereas indirect GHG emissions on a general basis.

4.2 Overview of Sector Emissions and Trends

4.2.1 Energy

The energy sector includes GHG emissions from fuels used in stationary and mobile energy activities. According to the World Energy Outlook (2008), aggregate demand in final-use sectors (industry, transport, residential, services, agriculture and non-energy use) is projected to grow by 1.4% per year from 2006 to 2030 (see Table 4.1). The largest source of global anthropogenic GHG emissions is energy consumption (Edwards et al. 2003). Approximately 73% of the GHG emissions were from total energy use during 1990–2005. CO_2 is responsible for approximately 95% of the emissions from the energy sector, with CH_4 and N_2O responsible for the balance (IPCC 2006). In 1990, the energy sector accounted for 1931 $TgCO_2$ eq. of non-CO_2 GHG emissions. Fugitive emissions from natural gas and oil systems were the largest source of the emissions of CH_4 and N_2O from the energy sector, accounting for 51 and 63% of energy related emissions in 1990 and 2020, respectively (US EPA 2006b). Major factors responsible for the emissions from the energy sector were: economic restructuring in Eastern Europe and Former Soviet Union (FSU); shift from coal to natural gas as an energy source in many regions; restructuring in several key coal mining countries and expansive growth in energy consumption in less developed regions. Fossil fuel combustion and cement production have contributed to approximately 270 (+30) Pg of CO_2 in the atmosphere from 1850 to 1998 (IPCC 2000).

Table 4.1. Global energy consumption sector wise (Tgoe) (adapted from: World Energy Outlook 2008)

Sectors	2000	2006	2015	2030	2006–2030*
Industry	1879	2181	2735	3322	1.8
Coal	405	550	713	838	1.8
Oil	325	329	366	385	0.7
Gas	422	434	508	604	1.4
Electricity & Other	727	867	1148	1496	4.2
Transport	1936	2227	2637	3171	1.5
Oil	1844	2105	2450	2915	1.4
Biofuel	10	24	74	118	6.8
Other	82	98	113	137	1.4
Residential, services and agriculture	2635	2937	3310	3918	1.2
Coal	108	114	118	100	-0.5
Oil	462	472	493	560	0.7
Gas	542	592	660	791	1.2
Electricity & Other	1523	1759	2040	2466	2.9
Non energy use	598	740	876	994	1.2
Total	7048	8086	9560	11405	1.4

*average annual growth rate

Anthropogenic emissions from energy use contribute approximately 60% of the additional global warming annually (Hippel et al. 1993). CO_2 emissions increase from 1990–95 was 27% (633 Tg) globally. Electricity and heat production (7.7 Pg) was the highest CO_2 emitting sector during the year 1995, followed by industry (5 Pg), transport (4.5 Pg) and 'other' (3.4 Pg) with considerable variations between countries and regions (Ellis and Treanton 1998). From 14.3 Pg in 1971, CO_2 emissions from fossil fuel combustion increased to 21.4 Pg in 1990 and 22.1 Pg in 1995. The total global CO_2 emissions from energy consumption were 27 Pg in 2004 (Wallington et al. 2008). Global energy related CO_2 emissions (Fig. 4.2) are expected to increase by 43% in 2035 from that of 2007, with 29.7 Pg in 2007 to 33.8 Pg in 2020 and 42.4 Pg in 2035 (EIA 2010). Globally 45.4 Pg of GHGs (CO_2 eq.) were emitted in 2005, in which approximately 59% (27 Pg) CO_2 eq. were emitted due to the combustion of fossil fuel (OECD 2010). EDGAR 4.0 data (IEA 2009b) estimated global GHG emissions in 2005 to be less at 42.4 Pg CO_2 eq. with 27.1 Pg CO_2 (64%) from energy.

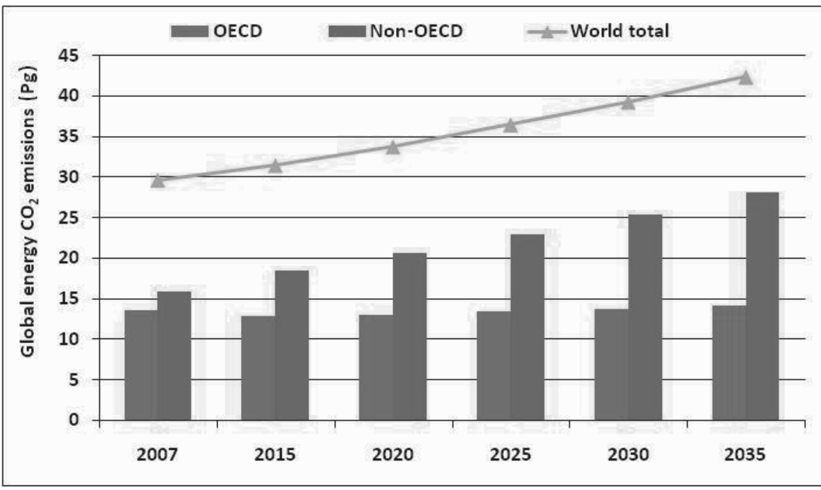

Figure 4.2. Global energy-related CO_2 emissions, 2007–2035 (Pg) (adapted from EIA 2010)

From total anthropogenic emissions of 263 Tg CH_4 during 1990, 30% were from the energy sector (Cofala et al. 2007). Global CH_4 emissions from natural gas and oil system have increased since 1990 (47 Tg) to 2010 (64 Tg) and are expected to reach 87 Tg in 2020 (US EPA 2006b). Total CH_4 emissions of developed (Annex I countries under the UNFCCC) countries from natural gas and oil systems are estimated to be 32 Tg in 1990 and 33 Tg in 2010, with major contributory countries being Russia and the U.S. (US EPA 2001). CH_4 is the major component of natural gas (95%) and is emitted from production, transmission, distribution and processing operations of natural gas (US EPA 2001). More than 56% of coal mining CH_4 emissions during the year 2000 were from China, the U.S, India, and Australia (US EPA 2006a). US EPA (2006a) projected that CH_4 emissions will grow by 20% from 2000 to 2020, with China increasing its share of global emissions from 31 to 42% due to rapid economic growth and expected doubled coal consumption (US EPA 2006a). Global GHG emissions from the energy sector were 23408 Tg for CO_2, 1646 TgCO_2 eq. of CH_4 and 237 Tg CO_2 eq. of N_2O for the year 2000 (US EPA 2006a). Non-CO_2 emissions from the energy sector are projected to rise considerably (927 Tg CO_2 eq.) during 1990–2020. Noteworthy rise is expected from natural gas and oil systems (84%) and stationary and mobile combustion (42%); and decline in coal mines by 13% through 2020. Global CH_4 emissions from coal mines were expected to 24 Tg in

1990 and are projected to decline to 21 Tg in 2020. Stationary and mobile combustion accounted for 3 Tg CH_4 and 0.5 Tg N_2O in 1990 and projected to be 3.7 Tg and 0.8 Tg respectively in 2020 (US EPA 2006b).

In developed countries, estimated emissions of N_2O from stationary sources (fuels used in large power plants and boilers) in 1990 were 0.20 Tg and increased in 2010 (0.24 Tg), because of increased energy demand (US EPA 2001). N_2O from mobile sources (automobiles and airplanes) of developed countries was 0.26 Tg in 1990 and 0.47 Tg in 2010, due to strong economic growth. GHG emissions from the energy sector in Annex I countries during 1990–2007 was observed in the transport sector (17.9%) and energy industries (5.6%) (UNFCCC 2009). In the U.S. about 37% of CH_4 and 13% of N_2O emissions in 2008, came from energy-related activities (US EPA 2010). During the past 20 years, combined fossil fuel CO_2 emissions from Asia and China more than tripled, and were 9.9% and 13.6% respectively in the year 1995, of the world energy related CO_2 emissions (Ellis and Treanton 1998). CO_2, CH_4 and N_2O emissions from the energy sector of India during 2007 were 992 Tg, 4.3 Tg and 0.057 Tg respectively (INCCA 2010).

Transportation. The transport sector is one of the fastest growing consumers of energy and source of GHGs. Emissions from the global transport sector have increased by around 27% since 1990 (Ribeiro et al. 2007). The transport sector comprises road vehicles, trains, ships and aircraft, in which road transport accounts for between 55% and 99% of GHGs, and two-third of this are attributable to the private car, primarily in the form of CO_2. According to EIA (2010) transportation uses around 30% of the world's total delivered energy, majority in the form of liquid fuels. Almost 95% of the transport energy is derived from oil-based fuels, mainly diesel (23.6 EJ, or about 31% of total energy) and gasoline (36.4 EJ, 47%). The transport sector used a total of 77 EJ of energy (Table 4.2), with road transport accounting for more than three-quarters, with light-duty vehicles and freight trucks having the highest share (Ribeiro et al. 2007).

Table 4.2. Use of energy in global transport sector by mode during 2000 (adapted from: Ribeiro et al. 2007)

Mode	Energy use (EJ)	Share (%)
Light duty vehicles (LDVs) & 2-wheelers	35.4	46.1
Heavy freight trucks	12.48	16.2
Medium freight trucks	6.77	8.8
Buses	4.76	6.2
Rail	1.19	1.5
Air & Shipping	16.27	21.1
Total	76.87	100

The transport sector was responsible for approximately 25% of energy use in 1990; and 22% of the global CO_2 emissions during 1990 and 24% during 1995 (IPCC 1996 a). ITF (2005) estimated that global CO_2 emissions from various transportation modes were 4614 Tg in 1990 and 6337 Tg in 2005. CO_2 emissions from road transport were the major contributory mode of transportation with 3306 Tg in 1990 and 4648 Tg in 2005 (Figure 4.3). The transport sector was responsible for 13% of the global GHG emissions in 2004 and 14.5% in 2007. In the year 2004, global CO_2 emissions from transportation were 6202 Tg, which was 23% of global energy related CO_2 emissions. Road transportation accounted for 74% of the total CO_2 emissions from transportation (Ribeiro et al. 2007). Percent share of CH_4 and N_2O from the transport sector were between 0.1–0.3% and 2.0–2.8%, respectively of the total transport GHG emissions (based on the US, Japan and EU data only). The transportation share of world total liquids consumption is projected to rise from 53% in 2007 to 61% in 2035 (IPCC 1996a).

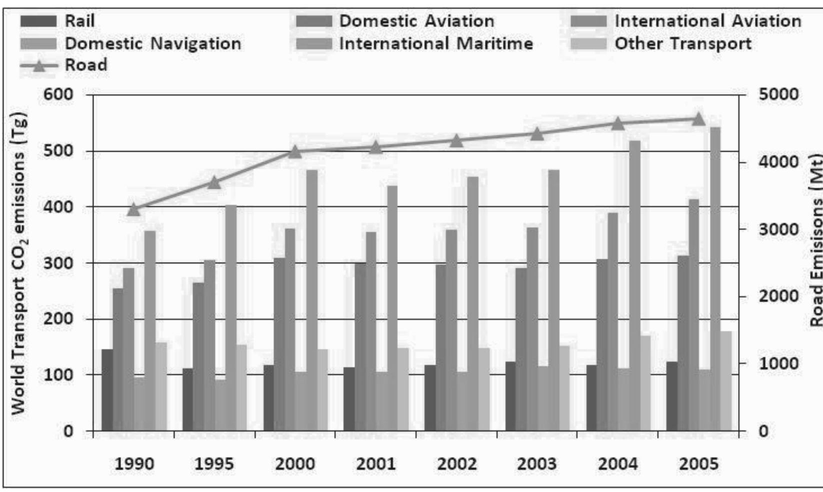

Figure 4.3. World CO_2 emissions from various transportation modes (adapted from: ITF 2005)

Non Annexure I countries (developing and newly industrialized countries) use less energy for transport in comparison to Annexure I countries due to low level of vehicle ownerships, but the trend is expected to rise over the next two decades (OECD 2002). Around 60% of the CO_2 emissions in road transport are from automobiles and light trucks, though in low and middle-income developing countries, freight trucks (and in some cases, even buses) are responsible for the aforesaid light-duty vehicles (Schipper et al. 2009). Around 20.7 Pg and 22.8 Pg of CO_2 were emitted from the global transport sector in 1990 and 1999 (OECD 2002). During the year 1995, world total CO_2 emissions from transport increased to 20% from that of 19.3% (Ellis and Treanton 1998). The transport sector accounts for 24% of the total U.S. CO_2 emissions (Borgwardt 1992). Collectively, CH_4 and N_2O emissions corresponded to 13% of all U.S. GHGs in 2003, but accounted for only 2% of the transportation total. CO_2 emissions from transportation sources increased by 22% (319 Tg rise from 1990 emissions) and emitted 1781 Tg in 2003 (US EPA 2006c). CO_2 emissions from passenger transport in U.S. during 1992 were 968 Tg, almost three times of all combined European countries (Scholl 1992). CO_2 emissions share from the transport sector was approximately 25% and 27% in OECD countries, and around two-third of the global CO_2 emissions from transport are from OECD countries. Global transport CO_2 emissions have increased by 45% between 1990 and 2007, led by road sector emissions in terms of volume and by shipping and aviation in terms of highest growth rates (OECD 2010). About 7 Pg of CO_2 was emitted in 2005, which is expected to reach 18 Pg by 2050 from the global transport sector (Vinot and Coussy 2009). Though China and India are responsible for 80% of the total CO_2 emissions in Asia, still their contribution in the transport sector is less and more in power sector, which leads to the reduced share of the transport sector (10%) in Asia's total CO_2 emissions during 1980-2005 (Timilsina and Shrestha 2009). Road transport in France contributes to major portion of 85% to the CO_2 emissions from the transport sector; followed next by aviation, with a mere 14%., similar situation to that of world (Vinot and Coussy 2009).

Total CO_2 emissions from fossil fuels increased from 20.9 Pg in 1990 to 28.8 Pg in 2007, in which transport was responsible for 4.58 Pg in 1990 and 6.63 Pg in 2007, representing approximately 45% increase (OECD 2010). Passenger vehicles (cars and light duty trucks) accounted for around 4.4% and 2.9% of global fossil fuel CO_2 emissions in US and EU-15 during the year 2004. Light duty vehicles were responsible for approximately 3 Pg on a global scale in 2004, which was 11% of the total fossil fuel (27 Pg) CO_2 emissions (Wallington et al. 2008). Cumulative emissions of CO_2 from the transport sector in Asia more than tripled from 210 Tg in 1980 to 745 Tg in 2005 with an average annual growth rate of 5.2% (Timilsina and Shrestha 2009). With a compounded annual growth rate (CAGR) of 7%, CO_2 emissions from the road transport sector have increased by approximately 400% from 27 Tg in 1980 to 105 Tg in 2000 in India (Singh et al. 2008). According to INCCA, (2010) total emissions from the transport sector (road, aviation, railways and navigation are considered) were 139, 0.023 and 0.008 Tg of CO_2, CH_4 and N_2O, respectively during the year 2007. Of the total CO_2 equivalent GHG emissions from the transport sector, road transport emitted 87%, aviation sector 7%, railways and navigation sectors emitted 5% and 1%, respectively.

In Australia, the transport sector contributed 76.2 Tg CO_2 eq., which is about 13.5% of Australia's net emissions. Passenger cars were the major contributor of transport emissions, contributing 41.7 Tg CO_2 eq., increasing by 18% between 1990 and 2004 (Hensher 2008). In UK, with 53.9 Tg C in 2004, 18% growth took place in CO_2 emissions from transportation in comparison to that of 1990. Out of 53.9 Tg CO_2 emissions from the transport sector, road transport was responsible for 33 Tg, around 10% more emissions from that of 1990 and expected to be 36.2 Tg by 2020. A growth of 8% and 25% was observed in Car and heavy goods vehicles (HGV) in UK from 1990–2004 (EAC 2006). IEA estimates that CO_2 emissions from the global transport sector will increase by 92% between 1990 and 2020. The share of the transport sector emissions is expected to be highest in Latin America followed by North America during 1990–2020. According to IEA, global CO_2 emissions are projected to rise strongly with a total of approximately 30 Pg by 2010 and 36 Pg by 2020 (OECD 2002). IEA projects that the transport sector emissions globally will rise by around

75% over the period of 1997–2020. The proportion of CO_2 emissions from the transport sector in OECD countries is projected to rise from 23 to 33% during 1990–2020 (Gorhum 2002). In Europe around 40% increase in CO_2 emissions from transportation sector can be expected between 1995 and 2010 if existing trends continue (Stead 1999). Transport related CO_2 emissions in China and India are projected to be 4 Pg and 1.5 Pg by 2050 in comparison to 0.332 Pg and 0.1 Pg of 2005 (Vinot and Coussy 2009).

Residential. Globally, about one third of all end-use energy is consumed in the household sector (Isaac and Vuuren 2009). Household-level combustion of biomass and coal are estimated to account for about 10% of global energy use and 13% of direct carbon emissions. Werf et al. (2006) estimated that the average emissions for the eight year study period of 1997–2004 were 8903 Tg CO_2/yr, 433 Tg CO/yr, and 21 Tg CH_4/yr.

According to the International Transport Forum (ITF), CO_2 emissions in the year 1990 were 1899 Tg, declined in 2007 to 1877 Tg, but are projected to rise in 2020 to 2031 Tg and 2198 Tg in 2030. Biomass is used as fuel for cooking, lighting and heating in the developing countries (non Annex I countries). Emissions of CH_4 and N_2O from the combustion of biomass in the developing countries were 7666 Gg, 84 Gg in 1990, 8869 Gg and 102 Gg in 2005 and are projected to be 10137 Gg and 118 Gg in 2020 respectively. Combined regions of South and East Asia, China and Africa approximately contributed over 90 and 84% of CH_4 and N_2O emissions, respectively (US EPA 2006b). In the U.S. CO_2 emissions were 339 Tg in 1991 and 342 Tg in 2008 from the residential sector and accounted for 21% of CO_2 emissions from fossil fuel combustion in 2008 (US EPA 2010). The combined CO_2 emissions from both heating and cooling are projected to rise from 0.8 Pg in 2000 to 2.2 Pg in 2100, i.e. about 12% of total CO_2 emissions from energy use, with the highest increase in Asia (Isaac and Vuuren 2009). Residential sector accounted for 5% of the total GHG emissions in U.S. during the year 2007. During the year 1995, on a global level 17.5 Gg of N_2O was emitted from the fossil fuel use and 52 Gg from biofuel combustion in residential sector (Olivier et al. 1998). GHG emissions from residential sector of India were 79 Tg of CO_2 eq. in 1994 and 138 Tg CO_2 eq. in 2007. The sector emitted 69 Tg of CO_2, 2.7 Tg of CH_4 and 0.036 Tg of N_2O in 2007. Biomass comprises of the largest portion of the total fuel mix use in the residential sector of India (INCCA 2010). CO_2 emissions from the residential sector of United Kingdom declined by 5% during 2006 and 2007, due to reduced gas and oil consumption in the sector (Prime et al. 2008). Estimated emissions of N_2O from residential sector of Taiwan were 0.040 Gg in 2000 and reduced to 0.035 Gg in 2003 (Tsai and Chyan 2006). In South Asia, combustion of biofuel in residential sector is responsible for relatively a large part of the trace pollutant emissions, ranging from 7.5% of CO_2. Biofuel burning is responsible for relatively a major portion of the trace pollutant emissions in South Asia (ranging from 7.5% for CO_2 to nearly 65% for CO), compared to a much smaller contribution from biofuel burning in North Asia, North America and Europe (Fig. 4.4), or in the world as a whole (for which the BFB source ranges from about 2–25% of the total emissions) (Lawrence and Lelieveld 2010).

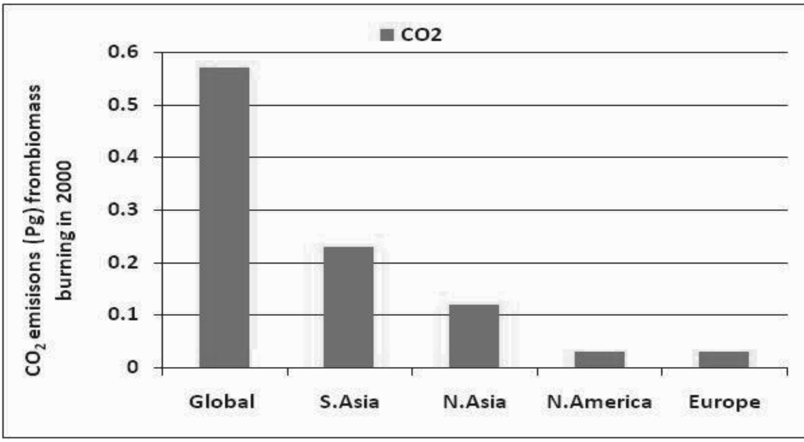

Figure 4.4. CO_2 emissions (Pg) from biomass burning in the year 2000 (adapted from Lawrence and Lelieveld 2010)

Electricity Generation. In the past thirty years, an average annual growth of 4% was observed in the world electricity consumption (Can and Price 2008). During 1990–2004, the growth rate of CO_2 emissions from power sector was 3.5% at the global level (Shrestha et al. 2009). Electricity and heat production accounted for 35% in 1995 compared to 31.6% during the year 1990 of global CO_2 emissions from fuel combustion (Ellis and Treanton 1998). Around 36% of the total CO_2 emissions in the world were from power sector in 2004, with more than half of the total CO_2 emissions from Australia, China, India and Singapore. The main fuel used for power generation was coal in Australia, China and India; natural gas in Bangladesh, New Zealand and Pakistan (Shrestha et al. 2009). CO_2 emissions from electricity generation in the U.S. were 1820 Tg in 1990 and 2363 Tg in 2008, and emitted 42% of CO_2 from fossil fuel combustion in 2008 (US EPA 2010). Among most of the Asian countries, Sri Lanka accounted for a very low share of CO_2 emissions from power (8% in 1985 and 28% in 2005) sector in comparison to the transport (55% in 1980 and 45% in 2005) and industrial (22% in 1980 and 16% in 2005) sectors. The reason behind the low share of power sector during 1980s was the use of renewable sources like hydro- power for electricity generation, though after 1996 the shifts towards fossil fuel lead to increased share of CO_2 from power generation (Timilsina and Shrestha 2009). The total emissions of CO_2, CH_4 and N_2O from electricity generation in India were 716 Tg, 0.008 Tg and 0.011 Tg in 2007 (INCCA 2010). Though, electricity consumption increased by 24% in United Kingdom between 1990 and 2007, CO_2 emissions from the power sector decreased by 11%. A reduction of 2% in CO_2 emissions was observed in 2007 compared to 2006, which was due to more use of gas in place of coal and oil to generate electricity (Prime et al. 2008). Electricity generation in Taiwan emitted 0.19 Gg of N_2O during 2000 and decreased to 0.13 Gg in 2003 (Tsai and Chyan 2006).

4.2.2 Emissions from Industrial and Other Products Use

EIA (2010) states that on a global scale approximately 50% of the world's total delivered energy is consumed in the industrial sector, which is more than any other end-use sector. The industrial sector broadly comprises of energy-intensive industries (e.g., iron and steel, chemicals, petroleum refining, cement, aluminum, pulp, and paper) and light industries (e.g., food processing, textiles, wood products, printing and publishing, and metal processing). In the industrial sector consumption of primary energy grew from 89 EJ in 1971 to 140 EJ in 2000 (Can and Price 2008). According to the World Energy Council, with 1425 Tg of CO_2 emission during year 1990, about 12% of the world energy consumption was from iron and steel sector. During 1990, CO_2 emissions were 319 Tg with 20% from China, 20% from former Soviet Union and Eastern Europe together, 15% from EU, 11% from Japan, 10% from India, and 7% from the US (Hidalgo et al. 2005). As depicted in Fig. 4.5 global emissions of CO_2 from industrial processes was 0.83 Pg during 2000, with major contribution of 0.38 Pg from North Asian countries (densely-populated regions of North Asia include: Northeast China, Szechuan Basin, Pearl River Delta (including Hong Kong), Korea, and Japan) followed by Europe (Lawrence and Lelieveld 2010). According to Ellis and Treanton (1998), globally manufacturing industries and construction were the second most important source of fossil fuel CO_2 emissions from energy, with 24% in 1990 and 22.5% during 1995.

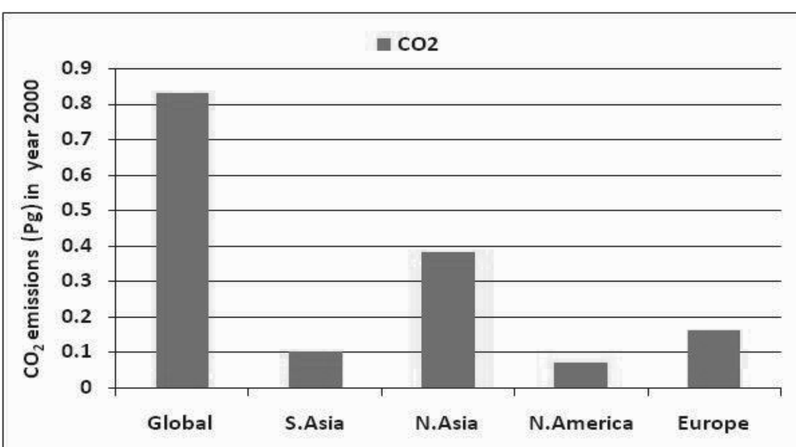

Figure 4.5. CO_2 emissions from industrial processes (Pg/yr) during 2000 (adapted from Lawrence and Lelieveld 2010)

According to Hu et al. (2006) approximately 6 to 7% of the total anthropogenic CO_2 emissions are from the steel industry. Global N_2O emissions from the industrial processes were 0.3 Tg in 1990 (Olivier et al. 1998). GHG emissions from the industrial sector for the year 2000 were 829 Tg of CO_2, 155 Tg CO_2 eq. of

N_2O and 6 Tg CO_2 eq. of CH_4 (US EPA 2006a). According to the US EPA (2006a), around 5% of the total global N_2O emissions in 2000 were from nitric and adipic acid production. N_2O emissions were 721 Gg in 1990 and are projected to be 570 Gg in 2020 (US EPA 2006b). Total 79% of N_2O emissions of industrial production were from Eastern Europe, the U.S., China, and European Union (EU-15). Developed countries account for 606 Gg of N_2O in 1990, 342 Gg in 2000 and 372 Gg in 2010 from industrial processes (US EPA 2001). EDGAR 4.0 data (IEA 2009b), estimated that out of the total global GHG emissions (42 Pg CO_2 eq.) in 2005, 1.3 Pg CO_2 (3%) came from the industrial.

Hidalgo et al. (2005) estimated that global CO_2 emissions from the iron and steel sector will decrease by 15% in 2030 (1248 Tg) from that of 1990 (1461 Tg), due to a shift of integrated steelworks to mini-mills. According to the projections made by Szabo et al. (2006) in business as usual scenario, CO_2 emissions from the cement industry will be 2100 Tg, increasing by more than 50% by the year 2030 at global level. A growth of 13% is expected from 2005 and 2020, in global N_2O emissions from industrial production sources (US EPA 2006a). CO_2 emissions from industrial sector of U.S. were 845 tg in 1990 and decreased to 819 Tg in 2008, and accounted for 27% of CO_2 from fossil fuel combustion in 2008 (US EPA 2010). In India, Petroleum refining and solid fuel (coke & briquettes) manufacturing industries emitted 34 Tg of CO_2 eq. in 2007. About 412 Tg of CO_2 eq. of GHG in India was emitted from the industrial activities during the year 2007. Industrial activities included emissions from manufacturing of minerals, metals, chemicals, other specific industries, and from non energy product use. Approximately 32% of the total CO_2 eq. emissions during 2007 from the industry sector came from the cement industry (130 Tg of CO_2 eq.) of India (INCCA 2010). Manufacturing industries were responsible for 0.5 Gg in 2000 and 0.7 Gg in 2003 (Tsai and Chyan 2006). In the U.S. N_2O emissions from product uses, accounted for about 0.1 % of total U.S. anthropogenic GHG emissions in 2008. Industrial emission in United Kingdom showed a decline of 15% in 2007 compared to 1990 levels (Prime et al. 2008).

4.2.3 Agriculture, Forestry and Other Land Use

Agricultural emissions contain anthropogenic emissions from agricultural activities including: livestock enteric fermentation, livestock manure management, rice cultivation, agricultural soil management and field burning of agricultural residues. From 1990–2005, agriculture contributed 16% of the global GHG emissions. Agricultural activities were responsible for around 25%, 65% and 90% of global total anthropogenic emissions of CO_2, CH_4 and N_2O, respectively (Duxbury 1994). Cofala et al. (2007) estimated that out of 263 Tg of total anthropogenic CH_4 emissions during the year 1990, around one third were due to livestock farming. Anthropogenic sources emitted around 15 million of N_2O during the year 1990, with fertilized arable land, animal excreta, soil under natural vegetation, oceans, and biomass burning as main contributory sources, in which 30% was from food production (Olivier et al. 1998). Global emissions of CH_4 during the year 1990 were 80 Tg from livestock, with cattle's as the largest source (almost 75% of the total livestock emissions) and 65 Tg from rice cultivation (US EPA 1994). Approximately 50% of the total livestock CH_4 emissions were from: India (13%), former Soviet Union (11%), Brazil (9%), China (8%) and United States (7%). Around 3.15 Tg of N_2O was emitted during 1995, from the cropland system of the world (Snyder et al. 2009). Global N_2O emissions were 13000 Gg, with India accounting for 158-443 Gg of the emissions (Parashar et al. 1998). Approximately 50% of the global atmospheric CH_4 and 75% of global N_2O emissions during the year 2000 were estimated to be from agriculture related activities (Rose and Lee 2008). According to US EPA, (2006b) worldwide emissions of CH_4 from enteric fermentation were 84388 Gg (1772 $TgCO_2$ eq.) in 1990, 91851 Gg (1929 $TgCO_2$ eq.) in 2005, and are expected to be 111633 Gg (2344 $TgCO_2$ eq.) in 2020 (Fig. 4.6). The top five CH_4 emitting countries (from enteric fermentation) were China, Brazil, India, the U.S. and Russia in 1990, with total of 43% (761 $TgCO_2$ eq.). In 2020, the top five are expected to be China, Brazil, India, the U.S. and Pakistan.

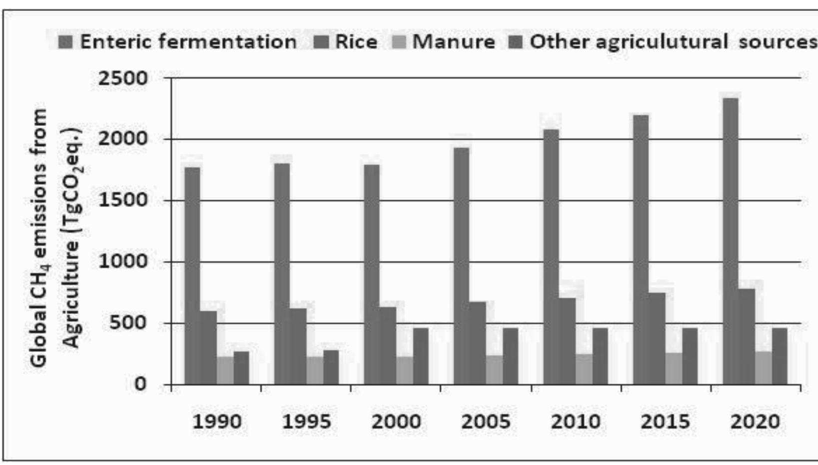

Figure 4.6. Global emissions of CH_4 ($TgCO_2$ eq.) from Agricultural sector (adapted from US EPA 2006b)

Global emissions from the agriculture sector in the year 2000 were 7631 Tg of CO_2, 3113 Tg CO_2 eq. of CH_4 and 2616 Tg CO_2 eq. of N_2O (US EPA 2006b). According to US EPA, (2001) approximately 24% of CH_4 emissions in the developed countries during the year 2000 were from livestock enteric fermentation, with 27500 Gg in 1990 and 26300 Gg in 2010, approximately 4% lower in 2010 than in 1990. Agricultural emissions of CH_4 and N_2O were responsible for almost 13.5% of global GHG emissions during the year 2004 (IPCC 2007b; Vermont and Cara 2010). Major sources of CH_4 and N_2O from agricultural activities are ruminant livestock production, paddy rice cultivation biomass burning. Along with the above, N_2O sources also include nitrogen applications to crops (synthetic and organic) and pasture lands (organic) (Golub et al. 2009). In the U.S., approximately 78% of the total N_2O emissions are released due to application of nitrogenous fertilizer and cropping practices. It was anticipated that in the European Union, CH_4 and N_2O are responsible for about 10% of GHG emissions, in which 49 and 63%, respectively, have been attributed to agriculture (Johnson et al. 2007). In India the agriculture sector emitted 14 Tg of CH_4 and 0.15 Tg of N_2O in 2007. Livestock enteric fermentation emitted 10 Tg of CH_4, manure management- 0.12 Tg of CH_4, 0.07 Gg of N_2O and rice cultivation was responsible for 3 Tg of CH_4 during 2007 (INCCA 2010). Olivier et al. (1998) stated that agriculture sector (approximately 50%) is the largest contributor to the global emission of nitrogen.

According to IPCC (1992), rice paddies are a significant CH_4 contributor, with 20% of the total CH_4 atmospheric emissions and 1% from U.S. (Cao et al. 1996). Total global CH_4 emissions from rice cultivation were 28628 Gg in 1990, 31995 Gg in 2005 and are projected to rise to 36958 Gg in 2020 (US EPA 2006b). China and South East Asian regions are the largest contributors to CH_4 emissions from rice cultivation, accounting for nearly 90% of the emissions for this source in 1990. The projected increase in CH_4 emissions from 1990 to 2020 is primarily attributed to increased rice consumption due to expected population growth in rice consuming countries. Aselmann and Crutzen (1989) estimated that rice paddies accounted for 36 Tg/yr of global CH_4 emissions. Highest CH_4 emitting countries were India (14.4 Tg), China (12.3 Tg), Indonesia (4.7 Tg), Bangladesh (4.0 Tg), and Thailand (2.9 Tg). Estimated emissions of CH_4 in Asia were higher in comparison to other countries, as most of the rice is grown under intensive cultivation, in high-temperature regions and seasons. CH_4 emissions were 1.3 Tg from America, 1.8 Tg from Africa, 0.5 Tg from Europe, 0.8 Tg from the U.S.A. and 0.5 Tg from Brazil (Cao et al. 1996). Prather et al. (2001) stated that out of the total anthropogenic emissions cattle production, paddy rice and biomass burning account for 22%, 15%, and 10%, respectively of CH_4. On a global level, irrigated rice is responsible for 70–80% of the total CH_4 produced from rice, rainfed rice accounts for 15% and deepwater rice for about 10% of the CH_4 (Johnson et al. 2007).

Out of the total CH_4 emissions from anthropogenic activities enteric fermentation and manure management represented 25% and 8% of CH_4 emissions in U.S. during the year 2008 (US EPA 2010). US EPA, (2006b) estimated that from manure management global CH_4 emissions were 10596 Gg, 11170 Gg and 12832 Gg, while N_2O emissions were 631 Gg, 11170 Gg and 818 Gg during 1990 2005 and 2020. Around 71% of N_2O emissions from manure management in 1990 were from China, Russia, the U.S., Japan, Ukraine, Poland, France, Brazil, Thailand, and Germany. CH_4 emissions from manure management in developed countries were 4840 Gg in 1990, 4930 Gg in 2000 and 5210 Gg in 2010, with 5% rise during 1990 and 2010. The growth is due to animal population growth expected to meet demand for milk and meat and increased use of liquid manure management systems (US EPA 2001). In Taiwan, during the year 2000, about 7 Gg of N_2O was emitted from manure management, which decreased to 6 Gg in 2003 and is projected to be 5 Gg in 2020 (Tsai and Chyan 2006).

The US EPA (2006a) projects that by 2020, N_2O emissions from agricultural soil are projected to increase by 37%, with enteric livestock CH_4 emissions being 30%, manure CH_4 and N_2O being 24%, and rice CH_4 being 22% of that compared with 2000 levels. N_2O emissions from global agricultural soil were 6455 Gg in 1990, 7418 Gg in 2005 and projected to reach 9474 Gg in 2020. In 1990, OECD, China, Latin America, and Africa were the four regions accounting for more than 80% of N_2O emissions from agricultural soils (US EPA 2006b). US EPA, (2001) estimated N_2O emissions in developed countries from manure management to be 302 Gg in 1990, 277 Gg in 2000 and again 302 Gg in 2010. In Russia and Eastern Europe, the economic decline lead to less demand for livestock products and hence decrement in livestock populations and thus lower emissions. N_2O emissions in developed countries from agricultural soil were 2120 Gg in 1990, 2060 Gg in 2000 and 2260 Gg in 2010 (US EPA 2001). The reduction in fertilizer use in EU countries between 1990 and 1995 led to a significant decrease in emissions. Non CO_2 GHG emissions (Fig. 4.7) between 1990 and 2020 are projected to raise more than 2,000 Tg CO_2 eq. from agricultural sources. Global emissions of CH_4 and N_2O from other agricultural activities are projected to raise to 21698 Gg and 885 Gg respectively in 2020 from 12745 Gg and 526 Gg in 1990 (US EPA 2006b). According to the US EPA (2001) developed countries contributed 1390 Gg in 1990 and 1440 Gg in 2010 from other agricultural sources.

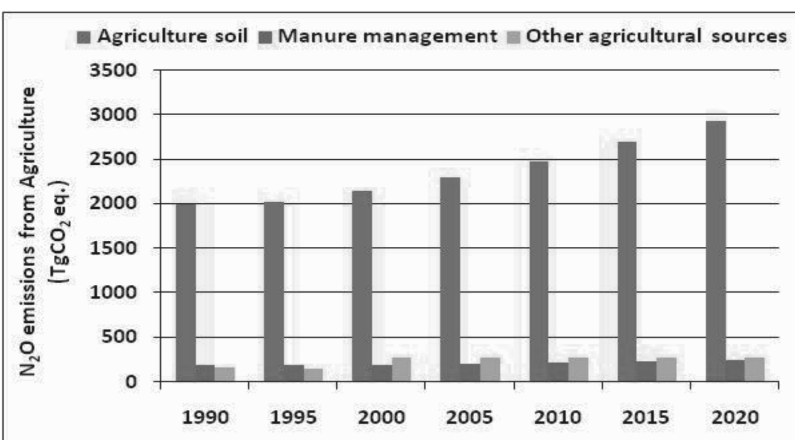

Figure 4.7. N_2O emissions (Tg CO_2 eq.) from the Agricultural sector (adapted from US EPA 2006b)

Land use, Land-use change, and forestry include emissions of CH_4 and N_2O, and CO_2 emissions and removal. During 1850, approximately one third of the total CO_2 emissions into the atmosphere were from land use change and the remainder from fossil-fuel (Golub et al. 2009). Total CO_2 release in the atmosphere during 1850 to 1985 was expected to be approximately 115 Pg due to land use changes, mainly deforestation. IPCC (2000) stated that approximately 136 (+ 55) Pg CO_2 has been emitted from land-use change, predominantly from forest ecosystems from 1850–1998. Net GHG removals by land use change and forestry, in Annexure I countries increased by 12.7% from 1990–2007, and decreased by 4.3% between 2006 and 2007 (UNFCCC 2009). EDGAR 4.0 data (IEA 2009b), estimated that from the global GHG emissions in 2005 (42 Pg CO_2 eq.), 3.8 Pg CO_2 (9%) was emitted from Land use change and forestry (OECD 2010).

4.2.4 Waste

The waste sector includes GHG emissions from waste management activities. GHG emissions are produced on anaerobic decomposition of municipal and industrial wastewater and their sludge residue (El-Fadel and Massoud 2001). Average global CH_4 emissions from municipal and industrial wastewater management were 2.3 and 33 Tg/yr during the year 1990 (El-Fadel and Massoud 2001). Industrial wastewater treatment accounts for around 76% of the global CH_4 emissions in developed countries and 24% in developing countries (US EPA 1994). From 263 Tg of total anthropogenic CH_4 emissions during 1990, 23% came from waste treatment and disposal (Cofala et al. 2007). With 22% of the total CH_4 emissions in the year 2008, landfills were the major contributor from waste sector in U.S, followed by waste water (4%) treatment (US EPA 2010). During the year 2000, GHG emissions from the waste sector were 1255 Tg CO_2 eq. of CH_4 and 106 Tg CO_2 eq. of N_2O. Around 42% of the world's CH_4 emissions from landfills come combined from United States, Africa, Eastern Europe, and China (US EPA 2006a).

According to the US EPA (2006b) CH_4 emissions from landfill were 36257 Gg in 1990 (Fig. 4.8) and are predicted to rise to 38898 Gg in 2020. Areas showing high growth in CH_4 emissions during 1990 and 2020 were Africa (77%), South and East Asia (34%), Latin America (52%). US EPA, (2006a) estimated that global emissions of CH_4 will grow by 9% between 2005 and 2020, with decrease in industrialized countries and increase in developing countries. In developed countries CH_4 emissions were 23900 Gg in 1990 and 23600 Gg in 2010 from landfilling of solid waste (US EPA 2001). The minor decline is due to collecting and flaring of or use of landfill CH_4. Global CH_4 emissions from wastewater are expected to grow by approximately 20% between 2005 and 2020 (US EPA 2006a). The US EPA (2006b) estimated that global CH_4 emissions from wastewater were 21 Tg (446 Tg CO_2 eq.) in 1990, 28 Tg (594 Tg CO_2 eq.) in 2010 and are projected to be 31 Tg (665 Tg CO_2 eq.) in 2020 (Fig. 4.8).

The largest CH_4 emitters were China (21%), India (18%), the U.S. (6%), and Indonesia (4%) in 1990, and South and East Asia (56%) in 2020. The estimated share of developed countries in CH_4 emissions from wastewater was 1770 Gg in 1990, 1740 Gg in 2000 and 1800 Gg in 2010 (US EPA 2001). Most of the developed countries rely on centralized aerobic wastewater treatment to handle their municipal wastewater; hence the emissions of CH_4 are small and incidental. N_2O emissions (Fig. 4.9) from municipal wastewater (sewage) accounted for approximately 260 Gg (81 Tg CO_2 eq.) in 1991, 293 Gg (91 Tg CO_2 eq.) in 2000 and are projected to be 346 Gg

(107 Tg CO_2 eq.). Indonesia, U.S., India, and China were responsible for approximately 50% of total N_2O emissions from domestic wastewater in 2000 (US EPA 2006a). In India, about 2.5 Tg of CH_4 and 0.016 Tg of N_2O were emitted from the waste sector. In the total emissions from waste sector, municipal solid waste generation and disposal was responsible for 0.6 Tg of CH_4; whereas domestic and industrial wastewater emitted 0.86 Tg and 1 Tg of CH_4 respectively (INCCA 2010). N_2O emissions from the waste sector of Taiwan were 1.3 Gg in 2000 and projected to be 1.4 Gg during 2020 (Tsai and Chyan 2006).

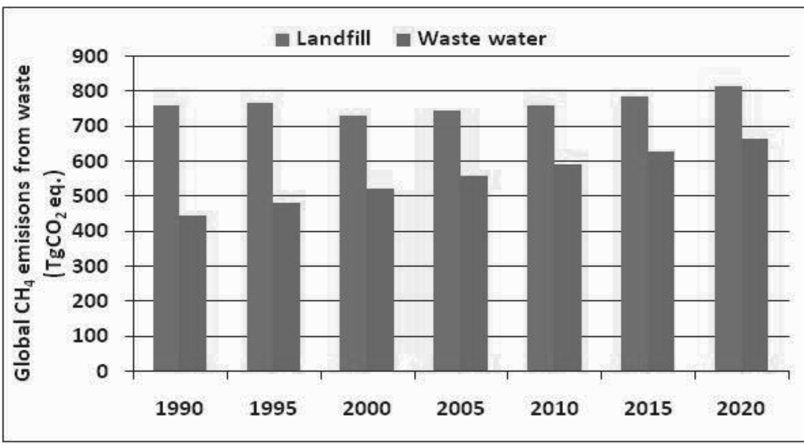

Figure 4.8. Global emissions of CH_4 (Tg CO_2 eq.) from the waste sector (adapted from: US EPA 2006b)

4.3 Indirect GHGs

4.3.1 NO_x (Oxides of Nitrogen)

According to the World Resource Institute, global emissions of NO_x were 99 Tg in 1990, and 126 Tg in 2000. As reported by Lawrence and Lelieveld. (2010) NO_x emissions were 43 Tg during the year 2000 (Fig. 4.10), which is quite less in comparison to those estimated by WRI. North America with 8.2 Tg accounted for major emissions among South and North Asia, North America and Europe. The highest NO_x emissions were from the combustion of fossil fuels (Fig. 4.10) among all the regions. During the year 1990, estimated global anthropogenic NOx emissions were 31 Tg, with major sources including fossil fuel combustion in transport (31%) and power plants (20%), biomass burning (20%) and 5% each from industrial processes and biofuel use (Olivier et al. 1998). Approximately 25% of the global emissions were from North America, and 10% contributions were from Western Europe, former USSR, Latin America, Africa and China (Olivier et al. 1998). In 2000, road transportation accounted for major anthropogenic NO_x emissions (41%), followed by power plants (21%), industry (16%) and non-road (13%) vehicles (Cofala et al. 2007). Global emissions of NO_x were 40000 Gg, and 1470–2550 Gg of the emissions were from India (Parashar et al. 1998). On the whole, the transport sector accounts for about 3342 Gg NO_x, which is approximately 5% of the global fossil fuel (19.9 Tg) emissions (Parashar et al. 1998). Gurjar et al. (2004) estimates that in Delhi itself, about 6% of the NO_x emissions were from the power sector. Anthropogenic sources responsible for emissions of NO_x include vehicular exhaust, coal combustion and biomass burning, with vehicles being the dominant source. In the year 2000, global emissions of NO_x were 84 Tg (declined from 83 Tg in 1990 according to the study carried by Cofala et al. (2007) and 90 Tg according to EDGAR. According to both Cofala et al., (2007) and EDGAR, maximum contribution of NO_x emissions was from OECD countries with 37 Tg and 34 Tg respectively. In Europe the NO_x emissions have reduced considerably during 1980 to 1990 by 32%, which was due to decline in the energy use related to socioeconomic situation in different parts of Europe owing to fuel switches and to technological measures implementation. A small decline (26%) in NO_x emissions also occurred in North America from 1990. But on a global scale the decline was only 1% by year 2000, as in other world regions, control measures and environmental policies are not state of the art (Monks et al. 2009).

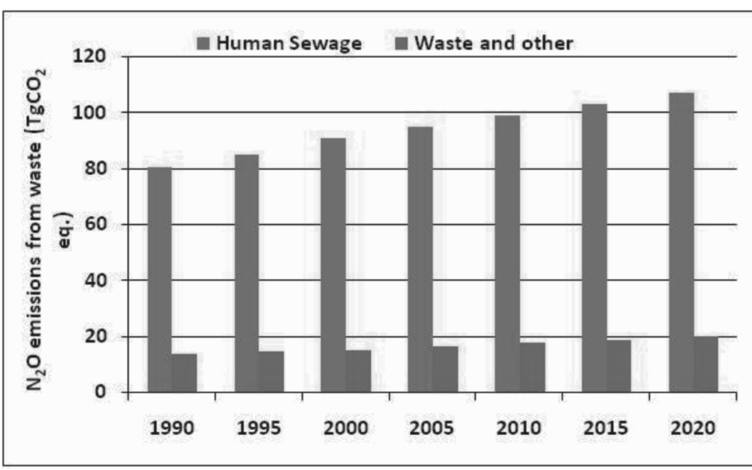

Figure 4.9. N_2O emissions ($TgCO_2$ eq.) from waste sector (adapted from US EPA 2006b)

Butler et al. (2008) have compared emissions of NO_x and NMVOC from three different global inventories: EDGAR; IPCC-AR4; and RETRO (REanalysis of the TROpospheric chemical composition) for the year 2000 for the world and megacities. In EDGAR inventory, globally maximum percent contribution to NO_x emissions was from the industrial (45.6%) sector followed by traditional (44%) and domestic sector contributed only 10% of the emissions, similar trend of emissions was in the megacities with 52%, 40% and 7% respectively. On the other hand, globally the emissions from IPCC-AR4 and RETRO showed different proportions with 58% and 48% from transport, 37% and 40% from industries and 5 and 3% from residential sector. NO_x emissions were 30.3 Tg for EDGAR, 28 Tg for IPCC-AR4 and 27 Tg for RETRO inventory. Worldwide emissions of NO_x were 32 Tg/yr, in which 21 Tg were from fossil fuel combustion, and U.S. contributed 7.3 Tg/yr (33%) of NO_x (Zhang et al. 2003). According to Monks et al. (2009), the transport sector accounted for highest emissions of NO_x with 34%, followed by 22% from power plants and 14% from industrial sector. In China, NO_x emissions were 9.5 Tg in 1990 and increased to 12 Tg in 1995, with major increase from the transportation sector (62%), followed by industrial (26%), domestic (21%) and power sector (20%), respectively (Streets et al. 2000). The largest NO_x emission contributor in China was the industrial sector (5 Tg), followed by power (4.1 Tg), transport (1.4 Tg), domestic fossil fuel use (0.9 Tg) and biofuels use (0.5 Tg) respectively. NO_x emissions from road transport of India were found to increase from 0.3 Gg in 1980 to 1.1 Gg in 2000 (Singh et al. 2008). Major portion (84%) of NO_x emissions from road transportation were from the diesel powered vehicles, as all the passenger and freight transport vehicles have been using it as fuel in India during 1980 to 2000. According to the estimations of Parashar et al. (1998) agricultural biomass burning with 109 Gg and agricultural soils with 230 Gg of NO_x emissions contributes to a minute fraction annually. This is based on the India's contribution of 12% to global biomass burning (Parashar et al. 1998). Streets et al. (2000) projected that NO_x emissions in China will be in the range 26–30 Tg by 2020.

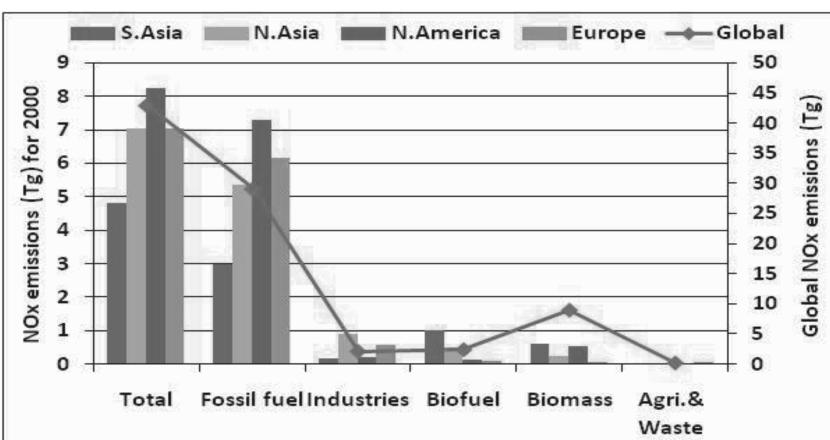

Figure 4.10. Global emissions of NO_x during the year 2000 (adapted from Lawrence and Lelieveld 2010)

4.3.2 CO (Carbon Monoxide)

During the year 1990, CO emissions from anthropogenic sources were estimated to be 996 Tg according to IPCC; while Olivier et al. (1999) estimated the emissions to be 974 Tg. According to Olivier et al. (1999) key anthropogenic sources responsible for CO emissions during the year 1990 included: large-scale biomass burning (50%, of which 21% is from agricultural waste burning; 18% from savanna burning and 11% from deforestation), fossil fuel combustion (27%, predominantly road transport at 22%) and biofuel use (19%). Approximately one fourth of the total global anthropogenic emissions were from Africa and 15% from Latin America, while 10% of the emissions were from China, India and the U.S. each. According to the World Resource Institute, global emissions of CO were 841 Tg in 1990, 852 Tg in 1995 and 1076 Tg in 2000. As depicted in Fig. 4.11, almost similar emissions (983 Tg) were reported by Lawrence and Lelieveld (2010) for the year 2000. Globally, biomass burning was responsible for major portion of emissions with 435 Tg. Agricultural activities are responsible for approximately 50% of CO emissions (Duxbury 1994). Anthropogenic CO emissions were 523 Tg during the year 1990, with one half of them from residential and one-third from road transport, 8% from industry and 6% from non-road vehicles (Cofala et al. 2007). In 2000, according to Cofala et al. (2007) CO emissions increased to 542 Tg, while 531 Tg were estimated by EDGAR. Global emissions of CO for the year 2000 were 531 Tg in EDGAR, 471 Tg- IPCC-AR4 and 477 Tg for RETRO (Butler et al. 2008). Residential sector (50%, 51% and 59%) was responsible for the highest share, followed by transport (37%, 41% and 40%) and industries (12%, 8% and 0.9%) with the least share among the three sectors from EDGAR, IPCC-AR4 and RETRO inventories. According to Monks et al. (2009) in the REAS inventory, the key contributory sources were domestic fuel use (48%), followed by industrial activities and transportation.

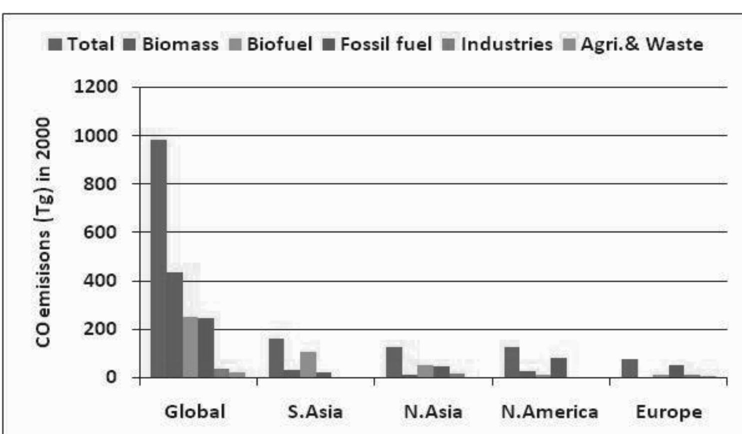

Figure 4.11. Global emissions of CO (Tg) from various sectors in 2000 (adapted from Lawrence and Lelieveld 2010)

During 1994–95, CO emissions in East Asia were estimated to be 94 Tg, with more than half of them from residential biomass burning (Tonooka et al. 2001). CO emissions were 99 Tg in 1990 and are projected to decline from 115 Tg in 1995 to 97 Tg in 2020 in China, due to more efficient combustion techniques, particularly in the transportation sector; in case these measures are not realized emissions could increase to 130 Tg by 2020. The major contributors to CO emissions in China during 1990–1995 were domestic (75–64%) and transportation (14–22%) sectors (Streets et al. 2000). In the year 2001, total CO emissions over India were estimated to be about 69 Tg, with 34 Tg from biofuel sources, which is almost 50% of total Indian CO emissions, being the most significant CO contributor over the Indian region. Coal combustion in thermal power plants and iron and cement industries contributed to 16 Tg of CO emissions (Dalvi et al. 2006). From automobiles, global CO emissions were 213 Tg in the year 1991 and 177 Tg in 1995. The U.S. was responsible for around 17% of the global CO emissions from motor vehicles in 1991, but it decreased to 12% (22 Tg) of the global (177 Tg) emissions in 1995 (Bradely et al. 1999). CO emissions in India from road transportation were found to increase from 0.9 Gg in 1980 to 2 Gg in 1990 and 3.5 Gg in 2000 (Singh et al. 2008). Gasoline powered vehicles accounted for approximately 65% of the total CO emissions in India. According to Bradely et al. (1999) CO concentrations are higher in the northern hemisphere, particularly in the urban industrial areas, in comparison to the southern hemisphere, where the number of vehicles is comparatively less. Butler et al. (2008) stated that global emissions of CO were more from the residential sector in comparison to the transport sector.

4.3.3 NMVOC (Non Methane Volatile Organic Compounds)

According to the World Resource Institute (WRI), NMVOC emissions were 153 Tg in 1990, 159 Tg in 1995 and 186 Tg in 2000. Emissions reported by Lawrence and Lelieveld (2010) for 2000 were less with 129 Tg (Fig. 4.12) in comparison to those reported by WRI. A major portion of the total global emissions of CO and NMVOC are contributed from the South Asian region, approximately 1.5 times as large as its relative contribution to the total global CO_2 and NO_x emissions. Also among the south and north Asian countries, emissions are dominated by India and China, respectively, with the two countries accounting for 60%, 64%, and 54% of the total Asian emissions of NO_x, CO and NMVOC, respectively (Lawrence and Lelieveld 2010). NMVOC emissions in China during the year 1990 were 5.5 Tg. NMVOC emissions estimated by Tonooka et al. (2001) for East Asia during 1994–95 were 17.7 Tg. Key contributory sources responsible for NMVOC emissions in East Asia, mainly China are small coal boilers and residential biomass use. Approximately 40% of VOCs are released from the transportation sector (Stead 1999). In India NMVOC emissions from road transport were estimated to increase by more than three times, with 0.2 Gg in 1980 and 0.7 Gg in 2000 (Singh et al. 2008). NMVOC emissions from China, Japan, South Korea and Taiwan during 1990 were 17.7 Tg, in which China shared 78% of the emissions (Tonooka et al. 2001).

NMVOC emissions were 136 Tg for EDGAR, 116 Tg for IPCC-AR4 and 152 Tg for RETRO. Industrial sectors shared the highest emissions with 51% and 66% for EDGAR and RETRO, while it was the transport sector in IPCC-AR4 (Butler et al. 2008). NMVOC emissions in China were 11.1 Tg in 1990 and 13.1 Tg in 1995, principally from the combustion of biofuels and coal in small combustors. Emissions of NMVOC in China are projected to grow from 15.6 Tg in 2000 to 17.2 Tg in 2010, and 18.2 Tg in 2020. In spite of controls on motor vehicles and a decline in the emissions from stationary combustion in China, NMVOC emissions are projected to increase by approximately 64% by 2020 compared to that of 1990, mainly due to rapid growth in the use of personal transport and solvents in China (Klimont et al. 2002). Solvents and other products are significant for GHGs and other emission inventories, as they are a noteworthy contributor to NMVOC emissions. Of the total NMVOC emissions, solvent use represents 31% emissions from both Italy and Denmark, 25% from Netherland and 24% from both Finland and the U.S. and only 3% in Nigeria. Approximately 11% of total NMVOC emissions are from total global NMVOC release from solvent use (IPCC 1996b).

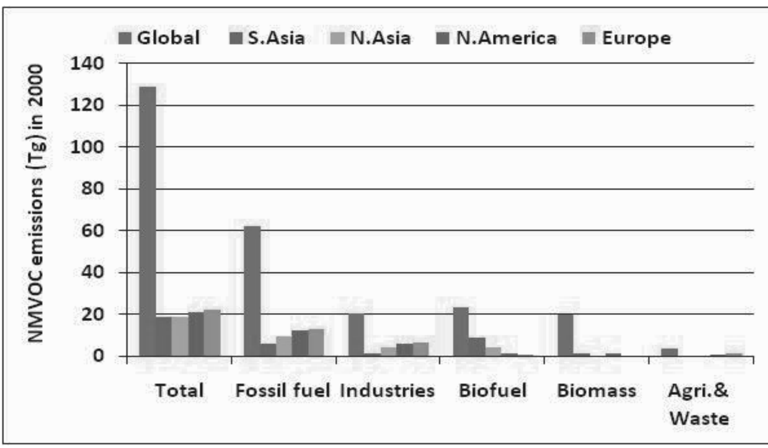

Figre 4.12. Global emissions of NMVOC from 1990- 2000 (adapted from Lawrence and Lelieveld 2010)

4.4 Summary

The global atmospheric concentration of CO_2 has increased approximately from 280 ppm during the pre-industrial time to 379 ppm in 2005 (IPCC 2007a). CH_4 increased from about 715 ppb during the pre-industrial time to 1774 ppb in 2005 (IPCC 2007b). Atmospheric N_2O concentrations increased to 319 ppb during the year 2005, from 270 ppb during the pre-industrial time (IPCC 2007b).

Among global GHG emissions, approximately 3% CO_2, 64% CH_4, and 24% of N_2O come from the anthropogenic activities (Duxbury 1994). Megacities, a major concern, account for CO, NO_x, and NMVOC emissions, approximately between 9% and 12% of the global emissions (Butler et al. 2008).

When we consider GHG emissions from different sectors or sources, anthropogenic emissions from energy use contribute approximately 60% of the additional global warming annually (Hippel et al. 1993). During 1990–2005, total energy use accounted for approximately 73% of the GHG emissions. Largest source of CH_4 and N_2O emissions were the fugitive emissions from natural gas and oil systems from the energy sector, accounting for 51% and 63% of energy related emissions in 1990 and 2020, respectively (US EPA 2006b). The total global CO_2 emissions from energy consumption were 27 Pg in 2004 (Wallington et al. 2008).

The transport sector uses approximately 30% of the world's total delivered energy, majority in the form of liquid fuels (EIA 2010). The transport sector was responsible for 13% of the global GHG emissions in 2004 and 14.5% in 2007. Global CO_2 emissions from various transportation modes were 4614 Tg in 1990 and 6337 Tg in 2005 (ITF 2005). From transportation 74% of total CO_2 emissions were from road transportation (Ribeiro et al. 2007).

Household-level combustion of biomass and coal are estimated to account for about 10% of global energy use and 13% of direct carbon emissions. Average emissions for 1997–2004 were 8903 Tg CO_2/yr, 433 Tg CO/yr, and 21 Tg CH_4/yr (Werf et al. 2006). CO_2 emissions in the year 1990 were 1899 Tg, declined in 2007 to 1877 Tg, but are projected to rise in 2020 to 2031 Tg and 2198 Tg in 2030 (International Transport Forum). In the residential sector, globally, 17.5 Gg of N_2O was emitted during 1995, from combustion of fossil fuel and 52 Gg from biofuel (Olivier et al. 1998).

Electricity and heat production accounted for 35% in 1995 compared to 31.6% during 1990 of global CO_2 emissions from fuel combustion (Ellis and Treanton 1998). CO_2 emissions from electricity generation in the U.S. were 1820 Tg in 1990 and 2363 Tg in 2008, and emitted 42% of CO_2 from fossil fuel combustion in 2008 (US EPA 2010). In the Asian countries, Sri Lanka shared very less CO_2 emissions from power sector (8% in 1985 and 28% in 2005), as during 1980s the renewable sources like hydro-power were used for electricity generation, though after 1996 the shifts towards fossil fuel lead to increased share of CO_2 from power generation (Timilsina and Shrestha 2009).

On a global scale, the industrial sector consumes around 50% of the total delivered energy (EIA 2010). Global emissions of CO_2 from industrial processes were 0.83 Pg during 2000, with the major contribution of 0.38 Pg from North Asian countries [densely-populated regions of North Asia include: Northeast China, Szechuan Basin, Pearl River Delta (including Hong Kong), Korea, and Japan] followed by Europe (Lawrence and Lelieveld 2010).

During 1990–2005, agriculture contributed 16% of the global GHG emissions and was responsible for around 25%, 65% and 90% of global total anthropogenic emissions of CO_2, CH_4 and N_2O respectively (Duxbury 1994). Out of 263 Tg of total anthropogenic CH_4 emissions during 1990, around one third were from livestock farming (Cofala et al. 2007). Global CH_4 emissions are expected to grow by approximately 20% from wastewater between 2005 and 2020 (US EPA 2006a). N_2O

emissions from wastewater were approximately 81 Tg CO_2 eq. in 1991, 91 Tg CO_2 eq. in 2000 and are projected to be 107 Tg CO_2 eq.

Global anthropogenic NO_x emissions were 31 Tg during 1990, with major sources including fossil fuel combustion in transport (31%) and power plants (20%), biomass burning (20%) and 5% each from industrial processes and biofuel use (Olivier et al. 1998). NO_x emissions were 43 Tg during the year 2000. Among South and North Asia, North America and Europe, major emissions were from North America (8.2 Tg) (Lawrence and Lelieveld 2010).

CO emissions from anthropogenic sources during 1990 were 996 Tg (IPCC); while 974 Tg were estimated by Olivier et al. (1999). Key anthropogenic sources responsible for CO emissions included: large-scale biomass burning (50%, of which 21% is from agricultural waste burning; 18% from savanna burning and 11% from deforestation), fossil fuel combustion (27%, predominantly road transport at 22%) and biofuel use (19%). Globally, 435 Tg of CO emissions were from biomass burning. CO emissions for 2000 were 129 Tg (Lawrence and Lelieveld 2010). A major portion of the total global emissions of CO and NMVOC are contributed from the South Asian region, approximately 1.5 times as large as its relative contribution to the total global CO_2 and NO_x emissions. Also among the south and north Asian countries, emissions are dominated by India and China, respectively, with the two countries accounting for 60%, 64%, and 54% of the total Asian emissions of NO_x, CO and NMVOC, respectively (Lawrence and Lelieveld 2010). NMVOC emissions were 136 Tg for EDGAR, 116 Tg for IPCC-AR4 and 152 Tg fro RETRO. The industrial sector shared the highest emissions with 51% and 66% for EDGAR and RETRO, while it was the transport sector in IPCC-AR4 (Butler et al. 2008). Approximately 11% of total NMVOC emissions are from total global NMVOC release from solvent use (IPCC 1996b).

4.5 References

Aselmann I., and Crutzen P. J. (1989). "Global distribution of natural freshwater wetlands and rice paddies, their net primary productivity, seasonality and possible methane emissions." *Journal of Atmospheric Chemistry*, 8, 307–358.

Bond, T., Venkataraman, C., and Masera, O. (2004). "Global atmospheric impacts of residential fuels." *Energy for Sustainable Development*, VIII No. 3.

Borgwardt R. H. (1992). "A technology for reduction of CO_2 emissions from the transportation sector." *Energy Conversion and Management*, 33(5–8), 443–449.

Bradely, K. S., Stedman, D. H., and Bishop, G. A. (1999). "A global inventory of carbon monoxide emissions from motor vehicles." *Chemosphere:Global Change Science*, 1, 65–72.

Butler, T. M., Lawrence, M. G., Gurjar, B. R., Aardenne, J. van., Schultz, M., and Lelieveld, J. (2008). "The representation of emissions from megacities in global emission inventories." *Atmospheric Environment*, 42, 703–719.

Can, S de Ia Rue du., and Price, L. (2008). "Sectoral trends in global energy use and greenhouse gas emissions." *Energy Policy*, 36, 1386–1403.

Cao, M., Gregson, K., Marshall, S., Dent, J. B., and Heal, O. W. (1996). "Global methane emissions from rice paddies." *Chemosphere*, 33(5), 879–897.

Cofala, J., Amann, M., Klimont, Z., Kupiainen, K., and Isaksson, L. H. (2007). "Scenarios of global anthropogenic emissions of air pollutants and methane until 2030." *Atmospheric Environment*, 41, 8486–8499.

Dalvi, M., Beig, G., Patil, U., Kaginalkar, A., Sharma, C., and Mitra, A. P. (2006). "A GIS based methodology for gridding of large-scale emission inventories: Application to carbon-monoxide emissions over Indian region." *Atmospheric Environment*, 40, 2995–3007.

Duxbury J.M. (1994). "The significance of agricultural sources of Greenhouse gases." *Fertilizer Research*, 38, 151–163.

Environmental Audit Committee (EAC) (2006). *Reducing Carbon Emissions from Transport*, Ninth Report of Session 2005–06. Volume I Report, together with formal minutes: Ordered by The House of Commons, Environmental Audit Committee.

Edwards, R. D., Smith, K. R., Zhang, J., and Ma, Y. (2003). "Models to predict emissions of health-damaging pollutants and global warming contributions of residential fuel/stove combinations in China." *Chemosphere*, 50, 201–215.

Energy Information Administration (EIA) (2010). *International Energy Outlook 2010–Highlights*. Report: DOE/EIA-0484(2010). Full report available July 2010. Available at: <http://www.eia.doe.gov/oiaf/ieo/highlights.html> (Retrieved on: July 14, 2010).

El-Fadel, M., and Massoud, M. (2001). "Methane emissions from wastewater management." *Environmental Pollution*, 114, 177–185.

Ellis, J., and Treanton, K. (1998). "Recent trends in energy-related CO_2 emissions." *Energy Policy*, 26(3), 159–166.

Golub, A., Hertel, T., Lee, H. L., Rose, S., and Sohngen, B. (2009). "The opportunity cost of land use and the global potential for greenhouse gas mitigation in agriculture and forestry." *Resource and Energy Economics*, 31, 299–319.

Gorhum, R. (2002). *Air pollution from ground transportation: An assessment of causes, strategies and tactics, and proposed actions for the international community*. The Global Initiative on Transport Emissions. A Partnership of the United Nations and the World Bank. Division for Sustainable Development, Department of Economic and Social Affairs. United Nations.

Gurjar, B. R., van Aardenne, J. A., Lelieveld, J., and Mohan, M., (2004). "Emission estimates and trends (1990–2000) for megacity Delhi and implications." *Atmos. Environ.*, 38, 5663–5681.

Hensher D. A. (2008). "Climate change, enhanced greenhouse gas emissions and passenger transport –What can we do to make a difference?" *Transportation Research Part D*, 13, 95–111.

Hidalgo, I., Szabo, L., Ciscar, J. C., and Soria, A. (2005). "Technological prospects and CO_2 emission trading analyses in the iron and steel industry: A global model." *Energy*, 30, 583–610.

Hippel, D. V., Raskin, P., Subak S., and Stavisky, D. (1993). "Estimating greenhouse gas emissions from fossil fuel consumption: Two approaches compared." *Energy Policy*, 691–702.

Hu, C. Q., Chen, L. Y., Zhang, C. X., Qi, Y. H., and Yin, R. Y. (2006). "Emission mitigation of CO_2 in steel industry: Current status and future scenarios." *Journal of Iron and Steel Research International*, 13(6), 38–42, 52.

Indian Network for Climate Change Assessment (INCCA) (2010). *India: Greenhouse Gas Emissions 2007: Executive Summary.* Ministry of Environment and Forests, Government of India, May 2010.

Intergovernmental Panel on Climate Change (IPCC) (1992). *Climate change 1992, the supplementary report to the IPCC Scientific Assessment*. Intergovernmental Panel on Climate Change. Cambridge University Press, Cambridge, UK.

Intergovernmental Panel on Climate Change (IPCC) (1996a). *Impacts, Adaptation and Mitigation Options.* IPCC Working Group II. Cambridge University Press, Cambridge, UK.

Intergovernmental Panel on Climate Change (IPCC) (1996b). *Revised 1996 IPCC Guidelines for National Greenhouse Gas Inventories*. Houghton, J. T., Filho, L. G. M., Lim, B., Treanton, K., Mamaty, I., Bonduki, Y., Griggs, D. J., Callender, B. A. (eds.), IPCC/OECD/IEA. UK Meteorological Office, Bracknell.

Intergovernmental Panel on Climate Change (IPCC) (2000). *Summary for Policymakers: Land Use, Land-Use Change, and Forestry.* A Special Report of the Intergovernmental Panel on Climate Change.

Intergovernmental Panel on Climate Change (IPCC) (2006). *IPCC Guidelines for National Greenhouse Gas Inventories.* Prepared by the National Greenhouse Gas Inventories Programme, Eggleston H. S., Buendia L., Miwa K., Ngara T. and Tanabe K. (eds.). Published: IGES, Japan. ISBN 4-88788-032-4.

Intergovernmental Panel on Climate Change (IPCC) (2007a). *Climate Change 2007, Fourth Assessment Report. Synthesis Report.* Intergovernmental Panel on Climate Change. Cambridge University Press, Cambridge, UK.

Intergovernmental Panel on Climate Change (IPCC) (2007b). *Climate Change 2007: The Physical Science Basis*. Contribution of Working Group I to the Fourth Assessment Report of the Intergovernmental Panel on Climate Change. Cambridge University Press, Cambridge, UK.

Isaac, M., and Vuuren, D. P. V. (2009). "Modeling global residential sector energy demand for heating and air conditioning in the context of climate change." *Energy Policy*, 37, 507–521.

International Transport Forum (ITF) (2005). International Transport Forum-Transport CO_2 emissions. World, Total CO_2 from Fuel Combustion including International Air and Maritime. Available at: <http://www.internationaltransportforum.org/Topics/c02emissions.html> (Retrieved on July 15, 2010).

Johnson, J. M. F., Franzluebbers, A. J., Weyers, S. L., and Reicosky, D. C. (2007). "Agricultural opportunities to mitigate greenhouse gas emissions." *Environmental Pollution*, 150, 107–124.

Klimont, Z., Streets, D. G., Gupta, S., Cofala, J., Lixin, F., and Ichikaw, Y. (2002). "Anthropogenic emissions of non-methane volatile organic compounds in China." *Atmospheric Environment*, 36, 1309–1322.

Kram, T., Morita, T., Riahi, K., Roehrl, R. A., Rooijen, S. V., Sankovski, A., and De Vries, B. (2000). "Global and regional greenhouse gas emissions scenarios." *Technological Forecasting and Social Change*, 63, 335–371.

Lawrence, M. G., and Lelieveld, J. (2010). "Atmospheric pollutant outflow from southern Asia: a review." *Atmospheric Chemistry and Physics Discussion*, 10, 9463–9646.

Monks, P. S., Granier, C., Fuzzi, S., Stohl, A., Williams, M. L., Akimoto, H., Amanni, M., Baklanov, A., Baltensperger, U., Bey, I., Blake, N., Blake, R. S., Carslawn, K., Cooper, O. R., Dentener, F., Fowler, D., Fragkou, E., Frost, G. J., Generoso, S., Ginoux, P., Grewet, V., Guenther, A., Hansson, H. C., Hennew, S., Hjorth, J., Hofzumahaus, A., Huntrieser, H., Isaksen, I. S. A., Jenkin, M. E., Kaiser, J., Kanakidou, M., Klimont, Z., Kulmala, M., Laj, P., Lawrence, M. G., Lee, J. D., Liousse, C., Maione, M., McFiggans, G., Metzger, A., Mieville, A., Moussiopoulos, N., Orlando, J. J., O'Dowd, C. D., Palmer, P. I., Parrish, D. D., Petzold, A., Platt, U., Poschl, U., Prevot, A. S. H., Reeves, C. E., Reimann, S., Rudich, Y., Sellegri, K., Steinbrecher, R., Simpson, D., ten Brink, H., Theloke, J., van der Werf, G. R., Vautard, R., Vestreng, V., Vlachokostas, Ch., and von Glasow, R. (2009). "Atmospheric composition change–global and regional air quality." *Atmospheric Environment*, 43, 5268–5350.

OECD (2002). *Strategies to Reduce Greenhouse Gas Emissions from Road Transport: Analytical Methods*. Head of Publications Service, OECD Publications Service, 2, rue André-Pascal, 75775 Paris Cedex 16, France.

OECD, 2010. *Reducing Transport Greenhouse Gas Emissions: Trends & Data*. International Transport Forum, OECD/ITF 2010.

Olivier, J. G. J., Bouwman, A. F., van der Hock, K. W., and Berdowski, J. J. M. (1998). "Global air emission inventories for anthropogenic sources of NO_x, NH_3, and N_2O in 1990." *Environmental Pollution*, 102, 135–148.

Olivier, J. G. J., Bloos, J. P. J., Berdowski, J. J. M., Visschedijk A. J. H., and Bouwman, A. F. (1999). "A 1990 global emission inventory of anthropogenic sources of carbon monoxide on 1° x 1° developed in the framework of EDGAR/GEIA." *Chemosphere: Global Change Science*, 1, 1–17.

Parashar, D. C., Kulshrestha, U. C., and Sharma, C. (1998). "Anthropogenic emissions of NO_x, NH_3 and N_2O in India." *Nutrient Cycling in Agroecosystems*, 52, 255–259.

Prather, M., and Ehhalt, D. (2001). "Atmospheric chemistry and Greenhouse Gases." Pages 239–287 in J. T. Houghton, Y. Ding, D. J. Griggs, M. Noguer, P. J. van der Linden, X. Dai, K. Maskell, and C. A. Johnson (editors). *Climate Change 2001: the scientific basis.* Contribution of Working Group I to the Third Assessment Report of the Intergovernmental Panel on Climate Change. Cambridge University Press, Cambridge, United Kingdom and New York, New York, USA.

Prime, J., Knight, J., and Evans, H. (2008). "Carbon dioxide emissions and energy consumption in the UK." Special feature–Carbon dioxide emissions. Available at: <www.berr.gov.uk/files/file50671.pdf> (Retrieved on July 19, 2010).

Ramanathan, V., and Feng, Y. (2009). "Air pollution, greenhouse gases and climate change: Global and regional perspectives." *Atmospheric Environment*, 43, 37–50.

Ribeiro, S. K., Kobayashi, S., Beuthe, M., Gasca, J., Greene, D., Lee, D. S., Muromachi, Y., Newton, P. J., Plotkin, S., Sperling, D., Wit, R., and Zhou, P. J. (2007). "Transport and its infrastructure." In *Climate Change 2007: Mitigation*. Contribution of Working Group III to the Fourth Assessment Report of the Intergovernmental Panel on Climate Change. Cambridge University Press, Cambridge, United Kingdom and New York, NY, USA.

Rose, S. K., and Lee, H. L. (2008). "Non-CO_2 greenhouse gas emissions data for climate change economic analysis." GTAP Working Paper No. 43.

Schipper, L., Fabian, H., and Leather, J. (2009). "Transport and carbon dioxide emissions: Forecasts, options analysis, and evaluation." ADB Sustainable Development Working Paper Series. No. 9, December 2009.

Scholl, L., Schipper L., and Kiang N. (1992). "CO_2 emissions from passenger transport: A comparison of international trends from 1973 to 1992." *Energy Policy*, 24(1), 17–30.

Shrestha, R. M., Anandarajah, G., and Liyanage, M. H. (2009). "Factors affecting CO_2 emission from the power sector of selected countries in Asia and the Pacific." *Energy Policy*, 37, 2375–2384.

Singh A., Gangopadhyay, S., Nanda, P. K., Bhattacharya, S., Sharma, C., and Bhan, C. (2008). "Trends of greenhouse gas emissions from the road transport sector in India." *Science of the total environment*, 390, 124 – 131.

Snyder, C. S., Bruulsema, T. W., Jensen, T. L., and Fixen, P. E. (2009). "Review of greenhouse gas emissions from crop production systems and fertilizer management effects." *Agriculture, Ecosystems and Environment*, 133, 247–266.

Srinivasan, J. (2008). "Climate change, greenhouse gases and aerosols." *Resonance*, 1146–1155.

Stead, D. (1999). "Relationships between transport emissions and travel patterns in Britain." *Transport Policy*, 6, 247–258.

Streets, D. G., and Waldhoff, S. T. (2000). "Present and future emissions of air pollutants in China: SO_2, NO_x, and CO." *Atmospheric Environment*, 34, 363–374.

Szabo, L., Hidalgo, I., Ciscar, J. C., and Soria, A. (2006). "CO_2 emission trading within the European Union and Annex B countries: The cement industry case." *Energy Policy*, 34, 72–87.

Timilsina, G. R., and Shrestha A. (2009). "Transport sector CO_2 emissions growth in Asia: Underlying factors and policy options." *Energy Policy*, 37, 4523–4539.

Tonooka, Y., Kannari, A., Higashino, H., and Murano, K. (2001). "NMVOCs and CO emission inventory in East Asia." *Water, Air, and Soil Pollution*, 130, 199–204.

Tsai, W. T., and Chyan, J. M. (2006). "Estimation and projection of nitrous oxide (N_2O) emissions from anthropogenic sources in Taiwan." *Chemosphere*, 63, 22–30.

United Nations Framework Convention on Climate Change (UNFCCC) (2009). *National greenhouse gas inventory data for the period 1990–2007*. Subsidiary Body for Implementation, Thirty-first session, Copenhagen. 7–18 December 2009.

United States Environment Protection Agency (US EPA) (1994). *International anthropogenic methane emissions: estimates for 1990.* EPA/230-R-93-010. U.S. Environmental Protection Agency, Office of Research and Development, Washington, U.S.A.

United States Environment Protection Agency (US EPA) (2001). *Non-CO_2 Greenhouse Gas Emissions from Developed Countries: 1990–2010*. December 2001. EPA 430-R-01-007. U.S. Environmental Protection Agency, 1200 Pennsylvania Ave., NW Washington, U.S.A.

United States Environment Protection Agency (US EPA) (2006a). *Global Mitigation of Non-CO_2 Greenhouse Gases*. EPA 430-R-06-005. U.S. Environmental Protection Agency, Office of Atmospheric Programs, Washington, U.S.A.

United States Environment Protection Agency (US EPA) (2006b). *Global anthropogenic non-CO_2 greenhouse gas emissions: 1990–2020.* Office of Atmospheric Programs, Climate Change Division. U.S. Environmental Protection Agency, 1200 Pennsylvania Avenue, NW, Washington, U.S.A.

United States Environment Protection Agency (US EPA) (2006c). *Greenhouse Gas Emissions from the U.S. Transportation Sector, 1990–2003.* EPA 420-R-06-003. U.S. Environmental Protection Agency, Office of Transportation and Air Quality, U.S.A.

United States Environment Protection Agency (US EPA) (2010). *Inventory of U.S. GHG Emissions and Sinks: 1990– 2008.* April 15, 2010. EPA 430-R-10-006. U.S. Environmental Protection Agency, 1200 Pennsylvania Ave., N.W. Washington, U.S.A.

Vermont, B., and Cara, S. D. (2010). "How costly is mitigation of non-CO_2 greenhouse gas emissions from agriculture? A meta-analysis." *Ecological Economics*, 69, 1373–1386.

Vinot, S., and Coussy P. (2009). IFPEN, 2009. "Greenhouse gas emissions and the transport sector." Panorama. Available at: <http://www.ifp.com/information-publications/notes-de-synthese-panorama/ panorama-2009> (Retrieved on: July 16, 2010).

Wallington, T. J., Sullivan J. L., and Hurley M. D. (2008). "Emissions of CO_2, CO, NO_x, HC, PM, HFC-134a, N_2O and CH_4 from the global light duty vehicle fleet." *Meteorologische Zeitschrift*, 17(2), 109–116.

Werf, G. R. V., Randerson, J. T., Giglio, L., Collatz, G. J., Kasibhatla, P. S., and Arellano, A. F. (2006. "Interannual variability in global biomass burning emissions from 1997 to 2004." *Atmospheric Chemistry and Physics*, 6, 3423–3441.

World Energy Oultook (WEO) (2008). OECD/IEA (International Energy Agency). <www.iea.org/weo/docs/weo2008/WEO2008_es_English.pdf> (accessed Jan. 2012).

Zhang, R., Tie, X., and Bond, D. W. (2003). "Impacts of anthropogenic and natural NO_x sources over the U.S. on tropospheric chemistry." *PNAS*, 100(4), 1505–1509.

CHAPTER 5

Impact of Greenhouse Gas Emissions and Climate Change

Tian C. Zhang and Rao Y. Surampalli

5.1 Introduction

Nowadays, the term 'climate change' is often used interchangeably with the term 'global warming.' However, these two terms have different meanings. In general, global warming is an average increase in the temperature of the atmosphere near the Earth's surface and in the troposphere. While it can occur from a variety of causes, global warming often refers to the warming due to the increase in emissions of greenhouse gases (GHG) from human activities. As usual, global warming may contribute to changes in global climate patterns. Climate change refers to any significant change in measures of climate (e.g., temperature, precipitation, or wind) lasting for an extended period (decades or longer) (USEPA 2011). Climate change may result from (USEPA 2011): a) natural factors (e.g., solar cycle variation, volcanic eruptions, or slow changes in the Earth's orbit around the sun); b) natural processes within the climate system (e.g. changes in ocean circulation); and c) human activities that change radiative forcing due to changes in atmosphere's composition (e.g. through burning fossil fuels) and the land surface (e.g. deforestation, reforestation, urbanization, desertification, etc.). For example, it is well known that the speed up of GHG emissions since 1750 is closely related to human activities. Currently, the phrase climate change is growing in preferred use to global warming because it helps convey that there are other changes in addition to rising temperatures (NAP 2011).

Nonetheless, our initial understanding about climate change starts from GHG emissions and global warming. There was a 70% increase in emissions of greenhouse gases worldwide between 1970 and 2004. In the energy supply sector, the increase was 145%. The growth from transport was 120% and from industry 65%. There was a 40% increase from the reduced capacity of forests to 'trap' carbon dioxide emissions, and as a result of changes in land use (EC 2007). Since it is very likely that it was caused primarily by human activities, climate change becomes a reality and poses significant risks to humans and the environment. Weather becomes more and more strange and unpredictable in various parts of the world; there are days when extreme weather is becoming more and more frequent with extended periods of time.

On the one hand, in some parts of the planet or the same places but different seasons, one sees stronger storms and increased floods or storm damage; on the other hand, one see increased risk of drought and fire in the other parts of the planet or the same places but different seasons. It seems that seasons are shifting; temperatures are climbing; and sea levels are rising. Climate change has been transforming life on Earth: more heat-related illness and disease are occurring; the landscape is changing; and wildlife is at risk. For example, with rapid climate change, one-fourth of the Earth's species could be headed for extinction by 2050 (TNC 2011). In this chapter, some of the most dangerous threats and impacts of GHG emissions and climate change are discussed. Understanding these threats and impacts would better prepare humans for future actions.

5.2 Major Impacts

The major impacts of GHG emissions and climate changes are listed in Table 5.1. This section will discuss the major facts and related issues of these major impacts.

Table 5.1. Major impacts of GHG emissions and climate changes

Impact	Brief description
Higher temperatures	The five hottest years on record have all occurred since 1997. About 93.4% of global warming goes into the ocean.
Changing landscapes	Climate change is causing vegetation shifts and conservation challenges.
Rising seas	Sea level rises from climate change could displace tens of millions of people, causing a huge negative environmental impact.
Increased risks of natural disasters	Global warming is speeding up the cycling of water between the ocean, atmosphere and land, making natural disasters more frequent and severe.
More threats of human health	Climate change brings more health risks associated with heat-related morbidity/mortality, disease, and worse air quality.
Biodiversity and wildlife at risk	Through a complex interaction of species and their habitats, climate change impacts biodiversity via changes in habitats and their ecological functions.
Social/economic impacts	Climate change also contributes to social disruption, economic decline and displacement of regional populations.

5.2.1 Higher Temperatures

The cycles of the Earth's orbit around the sun vary slowly (over tens of thousands of years), and at present, are in an overall cooling trend, presumably leading towards an ice age. However, GHG emitted by power plants, automobiles, deforestation and other sources are changing the composition of the atmosphere and warming up the planet. According to NASA (2010) data, the Earth's average surface temperature has increased by about 1.2 to 1.4 ºF in the last 100 years. The eight warmest years on record (since 1850) have all occurred since 1997, including the warmest years on record (2005 and 2010). If greenhouse gases continue to increase, climate models predict that the average temperature at the Earth's surface could increase from 3.2 to 7.2 ºF above 1990 levels by the end of this century (NAP 2011).

Global warming not only has been observed via modern instruments but also predicted by climate models. Usually, a computer-based climate model represents five components of the climate system: atmosphere, hydrosphere, cryosphere, land surface, and biosphere (IPCC 2007). These models have been used for a) the causes of recent climate change; and b) predication of whether global warming or cooling will occur. By comparing the observed changes to those projected by the models from either natural or human-derived causes, the models indicate that the warming since 1970 is dominated by man-made greenhouse gas emissions (IPCC 2007). However, the models do not unambiguously attribute the warming that occurred from approximately 1910 to 1945 to either natural variation or human effects (Wikipedia 2011). Currently, the results of these models match the observations of global temperature changes over the last century. However, all aspects of climate are not simulated by these models. For example, observed Arctic shrinkage has been faster than predicted (Stroeve et al. 2007); increase in precipitation is significantly faster than predicted (Wentz et al. 2007; Liepert and Previdi 2009).

Currently, there are uncertainty, concern, and controversy about global warming due to our imperfect understanding of the nature of and factors related to global warming. The disputed issues include whether a) the global warming trend is unprecedented or within normal climatic variations, b) human being has contributed significantly to it, and c) the increase is wholly or partially an artifact of poor measurements. Particularly, our understanding of global warming related feedbacks is very limited. Feedback is a process in which changing A may change B, and the change in B in turn changes A. One important feedback is the additional GHG emissions emanated from melted and decomposing permafrost. Even based on three very conservative assumptions, melted and decomposing permafrost can release as much as 190 ± 64 Gt C of permafrost carbon, about 1/2 of all carbon released from fossil fuel burning since the dawn of the Industrial Age (Schaefer et al. 2011). It is highly possible that IPCC 2007's temperature projections underestimate the expected climate change because IPCC models did not account the permafrost carbon emissions. Many other feedbacks (e.g., water vapor, clouds formation, radiative cooling, increased methane emissions) need to be considered in these models.

It should be pointed out that the majority of global warming goes into the ocean (93.4%), followed by atmosphere (2.3%), continents (2.1%), arctic sea ice (0.8%), Greenland Ice Sheet (0.2%), and Antarctice Ice Sheet (0.2%) (Cook 2011). A global study that assesses the temperature change in ocean currents has made two findings: a) as the Earth's temperature rises, so does the temperatures in a collection of major ocean currents; and b) those currents are warming faster than the average warming of the ocean and the globe as a whole. The average warming of the currents over a century has been around 1.2°C, while the global mean rise in temperatures is 0.62°C for the same period (Chirgwin 2012). Actually, climate change and GHG emissions has been driving the ocean system toward conditions not seen for millions of years, which could cause fundamental and irreversible transformation of our ecosystems.

5.2.2 Changing Landscapes

Climate change will significantly affect all types of land use and ecosystem services, as well as the quality of life for societies; these changes in turn, may accelerate GHG emission. For example, since 1900, the seasonally frozen ground in the Northern Hemisphere has shrunken by some 7%. This has freed large amounts of methane, a greenhouse gas far more potent than carbon dioxide. Most of the pattern-process interactions will be affected by climate change. In the past, however, climate change has received little attention from landscape ecologists. For example, between 1990 and 2008, only four papers with climate change in the title were published in the journal Landscape Ecology (1991, 1993, 2004, 2007), and only two in Landscape and Urban Planning (2007, 2008). Nevertheless, many studies have explored the global distribution of potential arable land, in terms of biophysical circumstances, under current and future climate conditions. Zhang and Cai (2011) concluded that, although the magnitudes of the projected changes vary by scenario, the increasing or decreasing trends in arable land area are regionally consistent due to the difference in climate change and population growth patterns around the world.

It is well known that climate change results in changes in patterns of wind, rain, snow, river and streams flow, and ocean circulation, etc., which cause short-term and long-term effects on landscapes. One example of short-term effects caused by the wind can be the dust bowl, which was caused by farmers tilling over the native grasses that held the dirt in place, when they were gone the wind simply picked up the ground. The long-term effects can be wind erosion–it changes the landscape by blowing over or on the landscape. The wind wears away rocks and mountains–like sandpaper does to wood; in time, it grinds them to dust and then picks up the dust and moves it around, which further erodes the landscape. Therefore, the wind is a contributing factor in making such sandy deserts, and causes sand storms around many different places (a famous one is in northern China). The landscape changes can have significant results. For example, in many places of Africa, water holes that should be filling for the animals are just thick dry mud; in many other places, this applies to humans as well.

The long-term effects of rising temperatures and changing patterns of rain and snow are that trees and plants around the world are forced to move toward Polar Regions and up mountain slopes. Climate affects erosion mainly by the transition from a period of climate stability, in which landscapes had attained equilibrium configurations, to a time of frequent and abrupt changes in temperature, precipitation and vegetation, which prevented fluvial and glacial systems from establishing equilibrium states (Zhang et al. 2001). In the tundra, thawing permafrost will allow shrubs and trees to take root. In the Great Plains of the US, grasslands will likely become forests. New England’s fiery fall foliage will eventually fade as maple and beech forests shift north toward cooler temperatures. Glaciers can turn low-lying hills into deep valleys as they move along slowly over the years. Glaciers often "pick up" rocks as they move along, and this is from their "cutting' through the landscape. As plant communities try to adjust to the changing climate by moving toward cooler areas, the animals that depend on them will be forced to move. Development and other barriers may block the migration of both plants and animals. Some species and communities such as polar bears and alpine meadows may be left without any remaining viable habitat, putting much of our treasured wildlife at risk. This long-term impact is very significant to human beings as it will affect both crop yield and the land area that are suitable for agriculture.

Zhang and Cai (2011) reported a spatially explicit estimate of the impact of climate change on worldwide agricultural land availability, considering uncertainty in climate change projections and ambiguity with regard to land classification. It is found that regions characterized by relatively high latitudes such as Russia, China and the US may expect an increase of total arable land by 37–67%, 22–36% and 4–17%, respectively, while tropical and sub-tropical regions may suffer different levels of lost arable land. For example, South America may lose 1–21% of its arable land area, Africa 1–18%, Europe 11–17%, and India 2–4% (Zhang and Cai 2011).

It is important to know that, in many developing countries, the changing primitive processes for normal cultivation that totally relies on climate could be even slower than changes in landscapes due to long-term climate change. As a result, in these countries poverty-prone farmers have to face more devastating situation. On the other hand, even though more land in the U.S. is predicted to be conducive for agricultural uses, a mix of global economics, politics and population changes will dictate how much of that land actually gets developed.

It is interesting to know that when we are preparing to offer solutions for dealing with impacts of climate change, the two most viable strategies are all linked with landscapes. The first strategy is to reduce the GHG emissions by enhancing biological (e.g., fostering) carbon sequestration. The second strategy is to adapt the use and structure of landscapes to changing climate conditions. There are a range of landscape architecture-based mitigation strategies that, if employed at mass scale, can help reduce GHG emissions by 50-85 percent by 2050 and limit temperature rise to 2 ^{o}C, targets that the U.N. recommends (ASLA 2012). Given the effects of climate change are already being felt in many communities, landscape architecture-based adaptation measures are also now being planned and implemented across cities and countries. One example of adaptation is development and maintenance of migration corridors. Corridors 1,200 feet wide, to include aquatic, riparian and upland habitat, are generally sufficient for most species, based on research studies. Besides habitat being restored or preserved, invasive species and water pollution have to be controlled enough for the plants, animal, and fungi to migrate. One of the most successful approaches is to save an area before it is sold to developers (Imlay 2011).

In preparation of anticipated changes, landscape architects are already working with policymakers and other design professionals to create "climate resilient communities." However, it is a great challenge to build a knowledge basis for making landscapes resilient to the increased dynamics caused by climate change and for managing and adapting landscapes to maintain multiple ecosystem services in response to climate change. These challenges transcend political and jurisdictional boundaries and require a more networked approach to ensure the sustainability of land, water, wildlife and cultural resources.

5.2.3 Rising Seas

As the Earth heats up, sea levels rise because warmer water takes up more room than colder water, a process known as thermal expansion. Melting glaciers compound the problem by dumping even more fresh water into the oceans. Sea levels have risen between four and eight inches in the past 100 years. Current projections suggest that sea levels could continue to rise between 4 inches and 36 inches over the next 100 years (NAP 2011; IPCC 2007).

The environmental impacts of rising seas are that rising seas will increase coastal erosion, pollution, storm damage and flooding; contaminate groundwater and threaten landfills and hazardous waste sites due to intruding salt water; and threaten coastal roads, bridges, jetties, etc.; and destroy ecosystems such as mangroves, wetlands and estuaries that protect coasts against storms and floods and filter many dangerous pollutants. The impacts of rising seas to human society are that rising seas will threaten to inundate low-lying areas and islands, threaten dense coastal populations, erode shorelines, and damage property. In the US, nearly 75 percent of Americans live on or within 50 miles of the coast. A 36-inch increase in sea levels would swamp every city on the East Coast of the United States, from Miami to Boston. Worldwide, approximately 100 million people live within three feet of sea level. Sea level rise associated with climate change could displace tens of millions of people in low-lying areas–especially in developing countries. Inhabitants of some small island countries that rest barely above the existing sea level are already abandoning their islands, some of the world’s first climate change refugees. Some Pacific Ocean island nations, such as Tuvalu, Kiribati, and the Maldives, are considering an eventual evacuation as flood defense may cost too much. Tuvalu already has an ad hoc agreement with New Zealand to allow phased relocation.

5.2.4 Increased Risks of Natural Disasters

Climate change is making floods, fires and droughts more frequent and severe and is causing storms, hurricanes and tropical storms to become more intense. Climate change is intensifying the circulation of water on, above and below the surface of the Earth–causing drought and floods to be more frequent, severe and widespread. Overall, global warming will result in increased world rainfall. Higher temperatures increase the amount of moisture that evaporates from land and water, leading to drought in many areas. Along with drought in some areas, flooding and erosion will increase in others. Lands affected by drought are more vulnerable to flooding once rain falls. As temperatures rise globally, droughts will become more frequent and more severe, with potentially devastating consequences for agriculture, water supply and human health. The United Nations estimates that an area of fertile soil the size of Ukraine is lost every year because of drought, deforestation, and climate instability (Smith and Edwards 2008). For example, in some parts of Asia and Africa, droughts have become longer and more intense. The lengthy period of drought is a key trigger for mass migration and other humanitarian crises in the Horn of Africa and the Sahel. Approximately 2.4 billion people living in the drainage basin of the Himalayan rivers (in India, China, Pakistan, Bangladesh, Nepal and Myanmar) could experience floods followed by droughts in coming decades. Since water is a powerful landscaper, it can weather and erode rock over many years to create new structures or wear them down, which in turn significantly change the landscapes and the associated biodiversity.

Climate warming will affect forests by first stimulating forests growth and then changing the disturbance regimes. Increase in forest growth is due to the increased photosynthesis rate caused by warmer temperatures, increased carbon dioxide, and more precipitation. Changing the disturbance regimes involves changes in the long-term patterns of fire, drought, insects, and diseases that are basic to forest development. In the conifer forests of the western US, earlier snowmelts, longer summers and an increase in spring and summer temperatures have increased fire frequency by 400 percent and have increased the amount of land burned by 650 percent since 1970 (TNC 2011). Large fires associated with climate patterns include the 1910 Idaho fires, 1988 Yellowstone fires, and 2002 Biscuit Fire in southwest Oregon (Rapp 2004). Results of computer modeling indicate that the western US gets wetter winters and warmer summers throughout the 21st century (as compared to current climate), with expanded woody growth across the West and thus, increased fire risk. The accuracy of 2002 and 2003 forecasts has validated the model's approach, suggesting it can eventually be a useful planning tool for fire managers. Lindner et al. (2010) reported that, in Europe, the increasing atmospheric CO_2 content and warmer temperatures are expected to result in positive effects on forest growth and wood production, at least in the short–medium term. On the other hand, increasing drought and disturbance risks will cause adverse effects. These negative impacts are very likely to outweigh positive trends in Southern and Eastern Europe. From west to east, the drought risk increases. In the Mediterranean regions productivity is expected to decline due to strongly increased droughts and fire risks.

Scientific research indicates that climate change will cause hurricanes and tropical storms to become more intense–lasting longer, unleashing stronger winds, and causing more damage to coastal ecosystems and communities. The main culprit is higher ocean temperatures as hurricanes and tropical storms get their energy from warm water. As sea surface temperatures rise, developing storms will contain more energy. US Climate Change Science Program (CCSP) reported that the annual numbers of tropical storms, hurricanes, and major hurricanes in the North Atlantic have increased over the past 100 years, a time in which Atlantic sea surface temperatures also increased. It is very likely that the human-induced increase in GHGs has contributed to the increase in sea surface temperatures in the hurricane formation regions. Hurricane/typhoon wind speeds and core rainfall rates will increase in response to human-caused warming. Analyses of model simulations suggest that for each 1°C increase in tropical sea surface temperatures, hurricane surface wind speeds will increase by 1 to 8% and core rainfall rates by 6 to 18% (CCSP 2008 a). Research has been conducted to evaluate the impacts of climate change on transportation systems and infrastructure in the Gulf Coast; it has been found that the intensity of major storms may increase 5–20%. This indicates that Category 3 storms and higher may return more frequently to the central Gulf Coast and thus cause more disruptions of transportation services (CCSP 2008 b). At the same time, other factors such as rising sea levels, disappearing wetlands, and increased coastal development threaten to intensify the damage caused by hurricanes and tropical storms.

5.2.5 More Threats to Human Health

Climate change brings more health risks associated with heat-related morbidity/mortality, disease, and worse air quality.

Elevated temperatures during summer months are associated with excess morbidity and mortality. In 1995, Chicago suffered a heat wave that killed more than 700 people. Chicagoans could experience that kind of relentless heat up to three times a year by 2100 (EDF 2012). Exposure to extreme and prolonged heat is associated with heat cramps, heat syncope (fainting), heat exhaustion, and heatstroke (McGeehin and Mirabelli 2001). Conservative estimates are that, on average, 240 heat-related deaths occur annually in the United States, while in a 1980 heat wave, there were 1,700 deaths (CFDCP 1995). The World Health Organization believes that even the modest increases in average temperature that have occurred since the 1970s are responsible for at least 150,000 extra deaths a year–a figure that will double by 2030, according to WHO's conservative estimate. In 2003, for example, extreme heat waves caused more than 20,000 deaths in Europe and more than 1,500 deaths in India. Scientists have linked the deadly heat waves to climate change and warn of more to come (TNC 2011).

Major risk factors for heat-related morbidity and mortality include urban living, age, and socioeconomic factors, as well as preventive behaviors (McGeehin and Mirabelli 2001). Models were used to evaluate the weather–mortality relationships, and it was found that populations in northeastern and midwestern U.S. cities are likely to experience the greatest number of illnesses and deaths in response to changes in summer temperature. Physiologic and behavioral adaptations may reduce morbidity and mortality. Within heat-sensitive regions, urban populations are the most vulnerable to adverse heat-related health outcomes. The elderly, young children, the poor, and people who are bedridden or are on certain medications are at particular risk. Heat related illnesses and deaths are largely preventable through behavioral adaptations, including the use of air conditioning and increased fluid intake (McGeehin and Mirabelli 2001). However, more information is needed about which weather parameters are important in the relationship between weather and health. In addition, our understanding of the importance of urban design to heat is very limited.

Climate change may increase the spread of infectious diseases. In 2008 the World Conservation Society identified a ‘Deadly Dozen,’ 12 animal-borne diseases that may more likely to spread due to climate change. The list includes bird flu, tuberculosis, Ebola, cholera, babesiosis, parasites, Lyme disease, plague, Rift Valley fever, sleeping sickness, yellow fever and red tides (algal blooms) (Hasham 2011).There are several ways this could happen (Farino 2012; Hasham 2011): 1) changing weather patterns (e.g., increase in temperature, rainfall patterns) will provide an opportunity for the insects and animals that transmit infectious diseases to change their geographic range. Diseases and pests that were once limited to the tropics–such as mosquitoes that carry malaria–may find hospitable conditions in new areas that were once too cold to support them. Examples include dengue fever, tick-borne encephalitis (which causes brain inflammation), Leishmaniasis (carried by the sand fly); 2) climate change can also amplify the prevalence of a disease in places where it already exists. Warmer weather and longer, frost-free seasons can expand both the sheer number of individual disease carriers, as well as the time period during which people are vulnerable to bites; and 3) warmer weather may help the pathogens within infected carriers multiply more quickly, or warmer weather stimulates evolution of carriers of “vector-borne” diseases. For example, warming temperatures helped enable the West Nile virus to evolve a new strain to displace the original strain. The new strain replicates faster inside mosquitoes than the older strain, increasing the likelihood that mosquitoes will transmit the disease to humans; it can also reproduce more easily at even higher temperatures. Thus, it could lead to an increase in the number of cases of West Nile, especially in the northern parts of the US. Detailed information is described by Patz et al. (2001).

Climate change can impact human health in many other ways, such as via flooding, compromised water and food security and hygiene that are compromised during extreme weather events. The impacts of climate change upon the dietary health of indigenous people may include increases in diabetes and hypertension, and increased obesity caused by the replacement of traditional food with processed food. Moreover, climate change is expected to contribute to some air quality problems (IPCC 2007). Respiratory disorders may be exacerbated by warming-induced increases in the frequency of smog (ground-level ozone) events and particulate air pollution. The number of Americans with asthma has more than doubled over the past two decades to 20 million. Continued warming will only worsen the problem. In principle, more hot days mean ripe conditions for ground-level ozone, or smog, which forms when pollutants from tailpipes and smokestacks mix in sunny, stagnant conditions. Sunlight and high temperatures, combined with other pollutants such as nitrogen oxides and volatile organic compounds, can cause ground-level ozone to increase. Smog triggers asthma attacks and worsens other breathing problems. Ground-level ozone can damage lung tissue, and is especially harmful for those with asthma and other chronic lung diseases. In addition, climate change may indirectly affect particulate matter (PM) pollution in the air by affecting natural or "biogenic" sources of PM such as wildfires and dust from dry soils. PM is a complex mixture of extremely small particles and liquid droplets. When breathed in, these particles can reach the deepest regions of the lungs. Exposure to particle pollution is linked to a variety of significant health problems. Particle pollution also is the main cause of visibility impairment (haze) in the nation's cities and national parks (USEPA 2012).

5.2.6 Biodiversity and Wildlife at Risk

Climate change impacts biodiversity through a complex interaction of species and their habitats by changing both the structure of habitats and their ecological functions. The direct impacts on populations include: a) distribution changes (due to habitat loss); b) range changes (either contraction and expansion, relating to their dispersal ability); c) phenological changes (changes in timing of life stages); and d) ecological changes (mismatching of species life-cycle events and food sources, decoupled predator–prey relationships, new invasions and the spread of already established invasive alien species) (EEA 2010). It is evidenced that many species are already feeling the heat; some examples are as follows (Shah 2011; TNC 2011; EEA 2010):

- In 1999, the death of the last Golden Toad in Central America marked the first documented species extinction driven by climate change.
- Due to melting ice in the Arctic, polar bears may be gone from the planet in as little as 100 years.
- In the tropics, increased sea temperatures are causing more coral reefs to "bleach," as the heat kills colorful algae necessary to coral health and survival.
- Several U.S. states may even lose their official birds as they head for cooler climates–including the Baltimore oriole of Maryland, black-capped chickadee of Massachusetts, and the American goldfinch of Iowa.
- Climate change could wipe out 20% of the world's lizard species by 2080.
- Phytoplankton may eventually run out of nutrients due to ocean stratification.
- In the past 20 years, three-quarters of the bird populations (122 common species) in European (18 countries) declined whereas one-quarter benefitted.
- In 2008, the polar bear became the first animal to be added to the Endangered Species Act list of threatened species due to global warming. Two-thirds of the polar bear could be lost by mid-century as sea ice continues to retreat.
- The Rocky Mountains in Canada and the US have seen nearly 70,000 square miles of forest die since 2000 due to outbreaks of tree-killing insects.
- It is possible in the future we won't see the zebra, elephants, giraffes, wildebeest, impala, etc. as we see them now.

Rising temperatures are changing weather and vegetation patterns across the globe, forcing animal species to migrate to new, cooler areas in order to survive (Parmesan and Yohe 2003). For example, European studies indicated that 19-50% of habitats (e.g., bogs, mires, and fens) have been negatively affected (EEA 2010).

Migration patterns for animals as diverse as whales and butterflies are being disrupted. Moreover, the Arctic, Antarctic and high latitudes have had the highest rates of warming, and this trend will continue. Satellite images show that the extent of Arctic summer sea ice has decreased by almost 9% per decade since 1979; the Arctic summer could be ice-free by mid-century. A 2005 survey of 442 glaciers from the World Glacier Monitoring Service found that 90% of the world's glaciers are shrinking as the planet warms. During the 20th century, the overall volume of glaciers in Switzerland decreased by two-thirds, Arctic ice thickness in late summer and early autumn decreased by about 40%, and Mount Kenya lost 92% of its ice mass while Mount Kilimanjaro lost 82% (CBD 2007). The extent of sea ice, and its thickness and age are reduced, resulting in more rapid melting, which may cause the loss of an entire biome (SCBD 2010) and speed up the warming of oceans. GHG emissions and climate change will result in a) increasing ocean acidification due to more CO_2 absorption (the current rate of ocean acidification is the fastest in 65 million years); b) increasing ocean stratification; and c) increasing oceanic dead zones (too little O_2 in the sea to support life). All of these can cause fundamental changes far beyond death, extinctions, and habitat loss: fundamental processes are being altered, community assemblages are being reorganized and ecological surprises are likely (Shah 2011).

However, it is not clear whether the rapid nature of climate change is likely to exceed the ability of many species to migrate or adjust. It is hard to imagine climate change as a major cause of extinctions in the near future simply because of an increase in temperature by ~3 ^{o}C even though the Earth will be set to be warmer than at any period in the past 1–40 Myr (Thomas et al. 2004). Using climate-envelope modeling, Thomas et al. (2004) reported that, on the basis of mid-range climate-warming scenarios for 2050, 15–37% of species in their sample of regions (covering some 20% of the Earth's terrestrial surface) and taxa will be 'committed to extinction.' However, recent studies have demonstrated significant variability in species-climate envelope models to project species extinction risk under climate change scenarios. There remains a pressing need to validate models and to reduce uncertainties. Using observed distribution shifts among 116 British breeding-bird species over the past 20 years, Araújo et al. (2005) provided the first independent validation of four envelope modelling techniques under climate change. They reported that implementations of species-climate envelope models for testing hypotheses and predicting future events may prove wrong, while being potentially useful if put into appropriate context. Therefore, caution is required in interpreting results from these models. At least, topography or "microclimatic buffering" needs to be captured, along with considerations of the full acclimation capacity of plants and animals (Willis and Bhagwat 2009). In addition, Parmesan (2005) reported that there is strong evidence that climate extremes play a dominant role in many impact processes. Therefore, it seems that more attention should be paid on the potential for biodiversity changes in the magnitude and frequency of extreme weather events.

5.2.7 *Social and Economic Impacts*

Climate change also contributes to social disruption, economic decline, and displacement of regional populations due to a) its impact on agricultural production, already-scarce water resources, and extreme weather events and b) our mitigation methods (e.g., shifting to biofuel) to combat GHG emissions. The impacts of climate change can be evaluated in terms of sensitivity and vulnerability. "Sensitivity" is the degree to which a particular system or sector might be affected, positively or negatively, by climate change and/or climate variability. "Vulnerability" is the degree to which a particular system or sector might be adversely affected by climate change (IPCC 2007).

The sensitivity of human society to climate change varies. Sectors sensitive to climate change include water resources, coastal zones, human settlements, and human health. Industries sensitive to climate change include agriculture, fisheries, forestry, energy, construction, insurance, financial services, tourism, and recreation (IPCC 2007). Here, impacts on food supply/security, biofuel production and associated water consumption as well as population migration will be described briefly.

Food supply will be negatively affected by climate change. For about a 1–3 °C increase in global mean temperature (by the years 2090-2100, relative to temperature in the years 1990–2000), there would be productivity decreases for some cereals in low latitudes, and productivity increases in high latitudes (IPCC 2007). Climate change will increase the number of people at risk of hunger (i.e., food security being jeopardized).

Another major impact is the transformation to a clean, diverse, and energy-independent economy in order to combat climate change. For instance, through the American Recovery and Reinvestment Act (ARRA), the US allocated over $90 billion for clean energy technologies (USDOS 2010). The US is targeting to produce 7.5 billion gallons of ethanol by 2012, and the existing and under construction ethanol refineries will affect nearly half of the U.S. The EU aims to have a share of 20 % renewable energy by 2020, which can only be achieved by increasing biomass production by 70%. Large-scale production of biomass will significantly impact the landscapes, associated functions of our society, and water consumption. Gerbens-Leenes et al. (2009) reported that the water footprint (WF) of the average bioenergy carriers, although varied, is much larger than that of fossil energy. The WF of average bio-energy carriers grown in the Netherlands is 24 m^3/GJ, in the US 58 m^3/GJ, in Brazil 61 m^3/GJ, and in Zimbabwe 143 m^3/GJ. For the fossil energy carriers, the WF increases in the following order: uranium (0.1 m^3/GJ), natural gas (0.1 m^3/GJ), coal (0.2 m^3/GJ), and finally crude oil (1.1 m^3/GJ). The WF of biomass is 70 to 400 times larger than the WF of the other primary energy carriers (excluding hydropower). The production of palm oil in Sri Lanka for instance consumes about 3500 liter of water per 1 liter of oil. This causes competition with other claims, such as water for food. Therefore, it is imperative to conduct comprehensive life cycle analyses (LCA) by including all effects on the environment to capture landscape changes and to consider also social aspects to determine the real greenhouse gas balance and environmental costs.

Climate change causes displacement of people in several ways: a) the increased number and severity of natural disasters destroy homes and habitats and force people to migrate to other places; b) slow changes (e.g., desertification and rising sea levels) gradually erode livelihoods and force people to move (e.g., in areas of Africa's Sahel, the semi-arid belt); and c) deteriorating environments and deleting natural resources that in turn displace people (this is different to prove as the decision to migrate is taken at the household level). In addition, climate change has the potential to exacerbate existing tensions or create new ones–serving as a threat multiplier or a catalyst for violent conflict and a threat to international security (Wikipedia 2012).

Vulnerabilities to climate change are often related to a) climate phenomena that exceed thresholds for adaptation (i.e., extreme weather events and/or abrupt climate change), and (b) limited access to resources (financial, technical, human, institutional) to cope. For these reasons, the impacts of climate change are not distributed uniformly within society and geographically. Individual and social factors such as gender, age, education, ethnicity, geography and language will lead to differential vulnerability and capacity to adapt to the effects of climate change. The poor, who make up half of the world's population, usually cannot afford adaptation mechanisms (e.g., air conditioning or insurance) to climate change. In developing countries, > 90% of the deaths related to natural disasters occur. Climate change effects such as hunger, poverty and diseases like diarrhea and malaria, disproportionately impact children (i.e. about 90 percent of malaria and diarrhea deaths are among young children). The combined effects of climate change may have particularly harsh effects on people and countries without the resources to mitigate those effects.

It should be pointed out that the cost of combating climate change will be limited, much less than the cost of the damage climate change will cause if we take no action. For example, if developed countries agree to cut their collective emissions by 30% by 2020, annual economic growth would be trimmed by less than 0.2% (EC 2007). This would be a small price to pay to avoid the potential long-term costs of climate change. In addition, the economic costs of emission reduction are likely to be more than offset by several benefits such as reduced air pollution, security of energy supply at predictable prices, improved competitiveness through innovation, and achievement of priorities of jobs, growth, and sustainable development.

5.3 Summary and Future Perspectives

Climate change not only affects the ecosystems via changing weather patterns (e.g., more intense and frequent extreme events) and the environment, but also impacts our daily life by changes in water, air, food quality and quantity, ecosystems, agriculture, and economy. Many experts believe that global warming must be limited to no more than 2°C above the preindustrial temperature if we are to prevent climate change from having irreversible impacts (EC 2007). However, the world's average temperature could rise by as much as 6°C above today's levels in this century if no further action is taken. While there are significant uncertainties on how the climate system will respond a century or more from now, it is important to realize that climate change is a manageable risk, not an existential crisis. To combat climate change, it is important to combine efforts of the entire society (i.e., including central and local governments, private entities, people in different communities and countries) to complete the following framework:

- Understanding current circumstances [e.g., identify the population, geographic, climate, economic profiles; understand energy reserves/production/consumption, transportation systems, industry (e.g., agriculture), waste management, urban/rural structure, landscapes (forests, grazing)].
- Investigating GHG inventory (direct/indirect GHG emissions by sectors, their trends (per capita and per dollar of gross domestic product, and sinks).
- Initiating policies and establishing measures for projecting future GHG emissions, reducing GHG emissions and carbon footprint, and developing clean energy technologies.
- Assessing climate change impacts in terms of sensitivity, vulnerability and adaptation measures.
- Establishing framework and mechanisms to secure financial resources and technology transfer associated with vulnerability and adaptation programs.
- Stimulating multilateral research/collaboration, and implementation of systematic observation.
- Enhancing education, training and outreach efforts to engaging the entire society on climate change.
- Enhancing international collaboration, establishing a new global agreement on climate change, and mobilizing companies and business leaders across the world to contribute knowledge, resources and leadership to combating climate change.

The threat from climate change is serious, it is urgent, and it is growing. Our generation's response to this challenge will be judged by history, for if we fail to meet it–boldly, swiftly, and together—we risk consigning future generations to an irreversible catastrophe (Obama 2009).

5.4 References

Araújo, M., Pearson, R. G., Thuiller, W., and Erhard, M. (2005). "Validation of species-climate impact models under climate change." *Global Change Biology*, 11, 1–10.

ASLA (American Society of Landscape Architects) (2012). "Combating climate change with landscape architecture." Available at <http://www.asla.org> (accessed Feb. 2012).

CBD (Convention on Biological Diversity) (2007). "Biodiversity and climate change." Available at <http://www.cbd.int> (accessed Feb. 2012).

CCSP (US Climate Change Science Program) (2008a). *Weather and Climate Extremes in a Changing Climate*. *Regions of Focus: North America, Hawaii, Caribbean, and U.S. Pacific Islands.* A report by the U.S. Climate Change Science Program and the Subcommittee on Global Change Research. [Thomas R. Karl, Gerald A. Meehl, Christopher D. Miller, Susan J. Hassol, Anne M. Waple, and William L. Murray (eds.)]. Department of Commerce, NOAA's National Climatic Data Center, Washington, D.C., USA, 164 pp.

CCSP (US Climate Change Science Program) (2008b). *Impacts of Climate Change and Variability on Transportation Systems and Infrastructure: Gulf Coast Study, Phase I.* A report by the U.S. CCSP and the Subcommittee on Global Change Research [Savonis, M. J., V. R. Burkett, and J. R. Potter (eds.)]. Department of Transportation, Washington, DC, USA, 445 pp.

CFDCP (Centers for Disease Control and Prevention) (1995). "Heat-related illnesses and deaths–United States, 1994–1995." *Mor Mortal Wkly Rep* 44, 465–468.

Chirgwin, R. (2012). "Ocean currents emerge as climate change hot-spots." *The Register*, available at <http://www.theregister.co.uk> (accessed Feb. 2012).

Cook, J. (2011). "Infographic on where global warming is going." Available at <http://www.skepticalscience.com> (accessed Feb. 2012).

EC (European Commission) (2007). *Combating climate change: The EU leads the way.* EC, Directorate-General for Communication, Publications B-1049, Brussels.

EDF (Environmental Defense Fund) (2012). "Climate change impacts: The effects of warming on our world can be seen today." Available at <http://www.edf.org> (accessed Feb. 2012).

EEA (European Environment Agency) (2010). "10 messages for 2010 climate change and biodiversity." Available at <http://www.eea.europa.eu> (accessed Feb. 2012).

Farino, L. (2012). "Climate change and the spread of infectious diseases." Available at <http://health.msn.com> (accessed Feb. 2012).

Gerbens-Leenes, P. W., Hoekstra, A. Y., and van der Meer, Th. (2009). "The water footprint of energy from biomass: a quantitative assessment and consequences of an increasing share of bio-energy in energy supply." *Ecological Economics*, 68, 1052–1060.

Hasham, A. (2011). "Climate change spreads infectious diseases worldwide." *International New services.com*, Jan. 25, 2011. Available at <http://www.Internationalnewservices.com> (accessed Feb. 2012).

Imlay, M., (2011). "Wildlife migration corridors could help plants and naimals cope with climate change." *Chesapeake*, available at <http://maryland.sierraclub.org> (accessed Feb. 2012).

IPCC (Intergovernmental Panel on Climate Change) (2007). *Climate Change 2007: Synthesis Report.* The Fourth Assessment Report (AR4). Contribution of

Working Groups I, II and III to the Fourth Assessment Report of IPCC. ISBN 92-9169-122-4.

Liepert, B. G., and Previdi, M. (2009). "Do models and observations disagree on the rainfall response to global warming?" *J. Climate*, 22(11), 3156–3166.

Lindner, M., Maroschek, M., Netherer, S., Kremer, A., Barbati, A.,Garcia-Gonzal, J., Seidl, R., Delzon, S., Corona, P., Kolstro, M., Lexer, M. J., and Marchetti, M. (2010). "Climate change impacts, adaptive capacity, and vulnerability of European forest ecosystems." *Forest Ecology and Management*. 259, 698–709.

McGeehin, M. A., and Mirabelli, M. (2001). "The potential impacts of climate variability and change on temperature-related morbidity and mortality in the United States." *Environ. Health Persp*., 109, 185–189.

NASA (2010). "2009 Ends Warmest Decade on Record." NASA Earth Observatory Image of the Day, 22 January 2010. Available at <http://earthobservatory. nasa.gov/ IOTD/view.php?id=43292> (assessed Oct. 2011).

NAP (The National Academies Press) (2011). *America's Climate Choices*. The National Academies Press, Washington, D.C.

Obama, B. (2009). Speech delivered at United Nations Summit on Climate Change. In USDOS (United States Department of State) (2010). *U.S. Climate Action Report 2010.* 5th ed., Washington: Global Publishing Services, January 2010.

Parmesan, C. (2005). "Biotic response: range and abundance changes." In Lovejoy, T.E. and L. Hannah (eds.) *Climate Change and Biodiversity*. Yale University Press. New Haven, Conn.

Parmesan, C., and Yohe, G. (2003). "A globally coherent fingerprint of climate change impacts across natural system." *Nature*, 421, 37–42.

Patz, J. A., Githeko, A. K., McCarty, J. P., Hussein, S., Confalonieri, U., and de Wet, N. (2001) "Climate change and infectious diseases." Chapter 6, pp. 103–132, in *Climate Change and Human Health: Risks and Responses*, ed. by A. J. McMichael, D. H. Campbell-Lendrum , C. F. Corvalan, K. L. Ebi, A. Githeko, J. D. Scheraga, and A. Woodward, World Health Organization, Geneva.

Rapp, V. (2004). "Western forests, fire risk, and climate change." *Science Update*, 6, 1–11. Available at <http://www.fs.fed.us/pnw> (accessed Feb. 2012).

SCBD (Secretariat of the Convention on Biological Diversity) (2010). *Global Biodiversity Outlook 3*. Montréal, 94 pp.

Schaefer, K., Zhang, T., Bruhwiler, L., and Barrett, A. P. (2011). "Amount and timing of permafrost carbon release in response to climate warming." *Tellus B*, 63, 165–180, doi: 10.1111/j.1600-0889.2011.00527.x.

Shah, A. (2011). "Climate change affects biodiversity." Available at <http://www. globalissues.com> (accessed Feb. 2012).

Smith, K., and Edwards, R. (2008). "2008: the year of global food crisis." *Heraldscotland*, March 8, 2008.

Stroeve, J., Holland, M. M., Meier, W., Scambos, T., and Serreze, M. (2007). "Arctic see ice decline: Faster than forecast." *Geophysical Res. Letters*, 34(9), L09501, 5 pp.

Thomas, C. D., Cameron1, A., Green, R. E., Bakkenes, M., Beaumont, L. J., Collingham,Y. C., Erasmus, B. F. N., de Siqueira, M. F., Grainger, A., Hannah, L., Hughes, L., Huntley, B., van Jaarsveld, A. S., Midgley, G. F., Miles, L., Ortega-Huerta1, M. A., Peterson, A. T., Phillips, O. L., and Williams, S. E. (2004). "Extinction risk from climate change." *Nature*, 427, 145–148.

TNC (The Nature Conservancy) (2011). "Climate change: Threats and impacts." Available at <http://www.nature.org> (accessed Oct. 2011).

USDOS (United States Department of State) (2010). *U.S. Climate Action Report 2010*. 5th ed., Washington: Global Publishing Services, January 2010.

USEPA (U.S. Environmental Protection Agency) (2011). "Climate change." Available at <http://epa.gov/climatechange/> (accessed Nov. 2011).

USEPA (U.S. Environmental Protection Agency) (2012). "Climate change–health and environmental effects." Available at <http://epa.gov> (accessed Feb. 2012).

Wentz, F. J., Ricciardulli, L., Hilburn, K., and Mears, C. (2007). "How much more rain will global warming bring?" *Science*, 317 (5853), 233–235.

Wikipedia (2011). "Global warming." Available at <http://en.wikipedia.org/wiki/Global_ warming> (accessed Oct. 2011).

Wikipedia (2012). "Effects of climate change on humans." Available at <http://en.wikipedia.org> (accessed Feb. 2012).

Willis, K. J., and Bhagwat, S. A. (2009). "Biodiversity and climate change." *Science*, 325(5954), 806–807.

Zhang, P., Molnar, P., and Downs, W. R. (2001). "Increased sedimentation rates and grain sizes 2-4 Myr ago due to the influence of climate change on erosion rates." *Nature*. 401, 891–897.

Zhang, X., and Cai, X. (2011). "Climate change impacts on global agricultural and availability." *Environ. Res. Letter*, 6(1), 014014 (8 pp).

CHAPTER 6

Greenhouse Gas Emissions (GHG) and Economics of Stabilisation

Dilek Demirbas and Safa Demirbas

6.1 Introduction

A Dictionary of Earth Sciences (2008) defined the term of green house as 'composed of molecules that absorb and reradiate infrared electromagnetic radiation in the atmosphere, and consists of water vapour, carbon dioxide, methane, N_2O, ozone, and certain halocarbon compounds.' In order to detect the absorptive capacity of the principal GHGs (Green House Gasses), a new concept was developed which is called as global warming potential (GWP), the atmospheric warming effect of each compared with that of carbon dioxide (a value = 1). The values take account of the wavelengths at which each gas absorbs radiation and its atmospheric residence time. On this scale, for example, the GWP of methane is 11, N_2O 270, CFC-11 4000, and CFC-12 8500. That makes it possible to measure the effect of GHGs onto climate.

The Earth's climate system is changing at greater rates, and these patterns are beyond the characteristics of natural variation. In recent studies, Breecker et al. (2010) and Solomon et al. (2007) found that the concentration of carbon dioxide (CO_2) in the atmosphere today, the most prevalent anthropogenic GHG, far exceeds the natural range of 180–300 ppm, and more scarcity the present concentration is the highest during the last 800,000 years, probably during the last 20 million years (Le Quéré et al. 2009).

The primary source of the increased concentration of CO_2 is unequivocally due to the burning of fossil fuels such as coal, oil, and natural gas (Solomon et al. 2007a). Annual fossil fuel CO_2 emissions have increased year on year from an average of 23.4 $GtCO_2$ per year in the 1990s to 30 $GtCO_2$ per year today (2012). To put this in perspective, the increase in annual emissions over the past 20 years is almost double the total emissions produced by EU27 nations each year (European Environment Agency 2009). Changes in land use have also contributed significantly to increasing rates of CO_2 emissions, contributing around 5.5 $GtCO_2$ per year to the atmosphere (NEF 2010).

Numerous scientific papers were published by revealing that climate change is far more serious even than reported in the most recent reviews of the science (Engelhaupt 2007; Rosenzweig et al. 2008; Richardson et al. 2009). As this global temperature rise caused by increased concentration of CO_2 during the last decade it is more likely expected to have a large impact on rainfall patterns and intensity, ocean salinity, wind patterns and aspects of extreme weather including droughts, heavy precipitation, heat waves and the intensity of tropical cyclones (Swanson and Tsonis 2009, Knight et al. 2009, Richardson et al. 2009). Such changes to the biophysical world are already having harmful impacts on society, which will worsen with time (Heffernan 2009; Rahmstorf 2009).

In order to stop this trend, there were some serious attempts in the past. One of them is Kyoto Protocol. In 1992, the UNFCCC was established with the ultimate objective to achieve stabilization of GHG concentrations in the atmosphere at a level that would prevent dangerous anthropogenic interference with the climate system. In October 1998, 176 countries had signed the convention on the way to stabilize the GHG concentration in the atmosphere. However, the convention does not specify either GHG concentration targets or emission reduction levels. With the intention to set more specific targets, countres organised conferences in Geneva in 1996, in Kyoto in 1997, in Buenos Aires in 1998, and in Bonn in 1999. In particular at the Kyoto conference in 1997, a first specific agreement was reached to move forward, and thirty-eight countries, mainly developed nations in North America, Europe, Asia, and Australia, jointly agreed to reduce emissions of six GHGs [carbon dioxide (CO_2), CH_4 (mathane), nitrous oxide (N_2O), hydro-fluorocarbons (HFCs), perfluorocarbons (PFCs), and sulphur hexafluoride (SF_6)] to five to eight percent below 1990 levels. Nevertheless, U.S. negotiators only agreed to reduce emissions by seven percent. The resultant, commonly called Kyoto protocol, requires each participating party to "have made demonstrable progress in its commitments by 2005 and to achieve the emission reductions within the period of 2008–2012. In addition to emission reductions, the treaty approves offsets through enhancement of sinks which absorb GHGs (McCarl and Scheneider 2001). After Kyoto protocol countries met again in Copenhagen in 2009 to progress further and made some challenging developments.

One of the most comprehensive studies on climate change, the Stern Review, was published in 2006 to assess the impacts of GHGs on our climate. According to Stern Review (Stern 2006), despite the higher GWP of other GHGs over a 100-year horizon, 'carbon dioxide' constitutes around three-quarter of the total GWP of emissions. This is because the vast majority of emissions, by weight, are carbon dioxide. Hydrofluorocarbons (HFCs) and Perfluoracarbon (PFCs) include many individual gases; the data shown are appropriate ranges across these gases. The characteristics of GHGs can be seen much clearer in Table 6.1.

According to the above characteristics (Table 6.1) CH_4 is removed from the atmosphere much more rapidly than carbon dioxide, and its short term effect is even greater than is suggested by its 100-year GWP. However, overreliance on abatement of gasses with strong warming effects but short lifetimes could lock in long term impacts from the build up of carbon dioxide. Some gasses like SF_6 have both a stronger warming effect and longer lifetime than CO_2, therefore abating their emissions is very important in the long term (Stern, 2007).

Table 6.1. Characteristics of basic GHGs

GAS	Pre-1750 tropospheric concentration	Recent tropospheric concentration	GWP (100-yr time horizon)	Atmospheric lifetime (years)	Increased radiative forcing (W/m^2)
CO_2	280 ppm	386.3 ppm	1	~ 100	1.66
CH_4	700 ppb	1866/1742 ppb	25	12	0.48
N_2O	270 ppb	323/321 ppb	298	114	0.16
Tropospheric ozone (O_3)	25 ppb	34 ppb	NA	Hours-day	0.35
CCl_2F_2	zero	537/535 ppt	10,900	100	0.17
SF_6	zero	6.84/6.44 ppt	22,800	3,200	0.0029

Source: CDIAC (2010).

There have been many reasons for different researchers to study climate change; the most important one has been driven by economic development. Economists claim that the primary source of climate change has been driven by economic development and CO_2 emissions per head have been strongly correlated with GDP per head across time and countries. North America and Europe have produced around 70% of CO_2 emissions from energy production since 1750, while developing countries under Kyoto Protocol account for less than one quarter of cumulative emissions. At the moment GHG emission levels are around 386 ppm CO_2 and it is rising every day. The only way to eliminate this environmental problem is to stabilise the pollution and the risks of the worst impacts of climate change can be substantially reduced if greenhouse gas levels in the atmosphere can be stabilised between 450 and 550 ppm CO_2 equivalent (CO_2e). The current level is around 430 ppm CO_2e today, and it is alarmingly worrying to know that it is rising at more than 2 ppm each year. Therefore, stabilisation would require emissions to be at least 25% below current levels by 2050. Ultimately, stabilisation–at whatever level–requires that annual emissions be brought down to more than 80% below current levels. Central estimates of the annual costs of achieving stabilisation between 500 and 550 ppm CO_2e are around 1% of global GDP and this is seen as a major challenge by all countries. On the same line, IPCC (2007a) also reports that in the space of just 250 years, as a result of the Industrial Revolution and changes to land use, such as the growth of cities and the felling of forests, we have released cumulatively more than 1800 giga tonnes (Gt) of CO_2 into the atmosphere. Global atmospheric concentrations of CO_2 are a record around 400 ppm, almost 40 percent higher than that at the beginning of the Industrial Revolution.

In this chapter we will examine GHG effect and economics of stabilisation of GHG emission and concentration, first in general, and then in different countries. Our intention is to evaluate GHG effect in the context of economics of stabilisation, which will provide a review of the recent literature and will reemphasize the importance of stabilisation of GHG emission despite its high economic cost. This chapter is structured as follows: Section 6.2 provides the basic background of GHG effect and climate change. In this section GHGs, their sectoral distribution, and global warming will be discussed. Section 6.3 discusses GHG emission/concentration and economics of stabilisation. Section 6.4 presents global strategies and actions around the world as well as the practical implications of these global strategies, such as Kyoto Protocol in the USA, Europe, and developing countries. Then, Kyoto protocol and future global strategies will be discussed in Section 6.5, and final words will be summarised in Section 6.6.

6.2 GHG Effect and Climate Change

GHGs are crucial to life on earth, as they are fundamental to maintaining the planet's temperature within limits supportive of life, and they are made of different gasses, present in the atmosphere, that are produced in part by natural sources. There are four important GHGs: water vapour (H_2O), CO_2, N_2O and CH_4 (Hendry 2010). Among them, CH_4, (mathane), CO_2 (carbon dioxide) and N_2O (nitrous oxide) are the most important Green House Gasses, and these gasses prevent heat emitted by the Earth from escaping to space. Gases are measured in parts per million (ppm), parts per billion (ppb) or parts per trillion (ppt) by volume. The natural greenhouse effect is necessary to life, and vital to maintain the Earth's surface temperature at an average of 15ºC, 33ºC warmer than it would be otherwise (NOAA 2007).

All of these GHGs are presently increasing at different rates, and are likely to alter their relative impacts in the future. As GHGs can absorb infrared radiation, changes in their atmospheric concentrations can alter the energy balance of the climate system. For scientists the atmosphere is considered a reservoir, where each of these gases resides for a specific lifetime. Other reservoirs include oceans and soils. Material can be transferred from one reservoir to another–a process described as a flux. Fluxes into a reservoir such as the atmosphere are known as sources, while fluxes out are called sinks. Each reservoir also has an overall budget, which represents the balance sheet of all sources and sinks. Long-lived GHGs such as CO_2, CH_4 and N_2O are chemically stable and persist in the atmosphere over time scales of a decade in the case of CH_4 to centuries or longer for N_2O (USEPA 2010). According to Nordhaus (2007), GHGs accumulate in the atmosphere and have a very long residence time, in the order of 100 years. Higher concentrations of GHGs lead to surface warming of the land and oceans. Over the longer run, this produces profound changes in many earth systems and consequently to biological and human activities that are sensitive to the climate.

Because sources of CO_2, CH_4 and N_2O to the atmosphere are essentially processes that release gases into the air, other term for this is called as "emissions," which describe the actual movement of these gases into the atmosphere. As mentioned above, emissions of these gases have a long-term effect on climate. These gases become diffused throughout the atmosphere and are not very easily removed (Solomon et al. 2007a). Scientists have detected that the emissions and atmospheric concentrations of GHGs are rising, and there are signs of rapidly increasing average surface temperatures. Scientists have detected diagnostic signals–such as greater high-latitude warming. Increases in GHG concentrations in the atmosphere produce a net increase in the absorption of energy by the Earth, leading to climate change such as a warming of the Earth's surface (USEPA 2007). Figure 6.1 shows the climate process drivers and presents the emission of these GHGs.

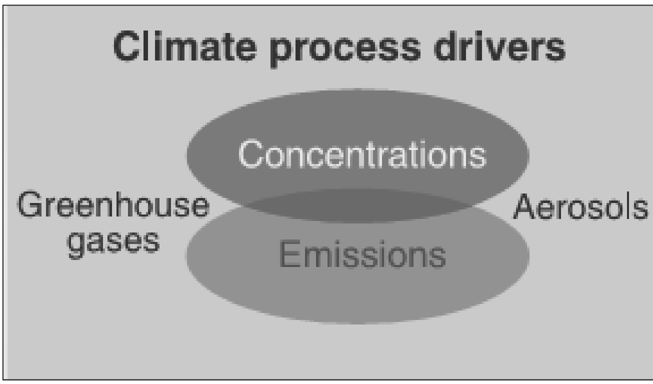

Figure 6.1. GHGs and climate process drivers (IPCC 2007)

In 2008, global emissions of CO_2 mainly from fossil fuels and cement were estimated to be around 8.7 billion tons of carbon. From these emissions, 45% of these emissions went to atmostphere 29% to land sinks and 26% to oceans. Recent evidence and model predictions suggest that the increase in atmostpheric CO_2 raised the global temprature and ocean acidity (Nordhaus 2010), and August 2010 was the third warmest August on record since 1880. It was also estimated that atmospheric CO_2 for September 2010 was 388.80 ppm. Changes in the atmospheric concentrations of GHGs and aerosols, land cover and solar radiation alter the energy balance of the climate system and are drivers of climate change.

GHGs affect the absorption, scattering and emission of radiation within the atmosphere and at the Earth's surface. The resulting positive or negative changes in energy balance due to these factors are expressed as radiative forcing, which is used to compare warming or cooling influences on global climate.

CO_2 is an odourless, colourless gas, which is faintly acidic and non-flammable. Although CO_2 is mainly in the gaseous form, it also has a solid and liquid form. CO_2-equivalent emission (CO_2e) is the amount of CO_2 emission that would cause the same time-integrated radiative forcing, over a given time horizon. The equivalent CO_2 emission is obtained by multiplying the emission of a GHG by its GWP for the given time horizon. For a mix of GHGs, it is obtained by summing the equivalent CO_2 emissions of each gas (Solomon et al. 2007a). Equivalent CO_2 emission is a standard and useful metric for comparing emissions of different GHGs but does not imply the same climate change responses, which is also the concentration of CO_2 that would cause the same amount of radiative forcing as a given mixture of CO_2 and other forcing components.

N_2O is a long-lived GHG, responsible for increased radioactive forcing on the climate system. N_2O has an atmospheric lifetime of about 114 years, and over a 100-year period, each molecule of N_2O has a direct global warming potential 298 times that of a single molecule of CO_2 (Solomon et al. 2007b). Ice core data for N_2O have been reported extending back more than 2,000 years from the present. These data show relatively little change in mixing ratios over the first 1,800 years of this record. Since the beginning of the industrial revolution, however, N_2O levels exhibit a relatively rapid rise. Since 1998, atmospheric N_2O levels have steadily risen, reaching 319 ± 0.12 ppb in 2005 (Forster et al. 2006; USEPA 2010).

Similarly, CH_4 is the most abundant organic molecule in the Earth's atmosphere and plays important roles in both the planet's radioactive energy budget and global atmospheric chemistry. CH_4 is one of the most important GHGs and has a GWP 25 times that of CO_2 on a 100-year timescale (Forster et al. 2007). Its removal is estimated at 9.6 years (Folland et al. 2001). Once emitted, however, CH_4 actually remains in the atmosphere for what is known as a "perturbation lifetime" of approximately 12 years before removal (Solomon et al. 2007b). The longer perturbation lifetime of CH_4 is primarily a result of feedbacks between CH_4, OH, and its by product CO_2, which is also removed by reactions with OH. Minor removal processes include reaction with chlorine in the marine boundary layer, a soil sink, and stratospheric reactions. Increasing emissions of CH_4 reduce the concentration of OH, a feedback that may increase the atmospheric lifetime of CH_4 (Solomon et al. 2007b).

Major agricultural impacts of increased GHG emission may include changes of the species composition in a given area, changes in crop yields, changes in irrigation water requirements and supply, and changes in cost of production. Many scientists believe the risks of negative impacts across society outweigh potential benefits (Bruce et al. 1996) and suggest that society reduce net GHG emissions (GHGE) to insure that future problems do not arise (McCarl and Scheneider 2001). Agriculture's global share of anthropogenic emissions has been estimated to be about fifty percent of CH_4, seventy percent of N_2O, and twenty percent of carbon dioxide (Cole et al. 1994; Isermann 1994). Contributions across countries vary with large differences existing between developing and developed countries. Agriculture based emissions in developing countries largely arise from deforestation and land degradation. While, agriculture based emissions in developed countries are largely caused by fossil fuel based emissions through energy use; reductions in soil carbon through intensive tillage; N_2O emissions through fertilizer applications, livestock feeding, residue management, and tillage (Watson et al. 1996 2009); CH_4 emissions from livestock raising and rice production. Within livestock production about two thirds of CH_4 emissions stem from enteric fermentation of ruminant animals, mainly cattle with the rest from animal waste. Costs of agricultural GHGE reduction strategies have been examined by a number of authors (Watson et al. 1996, 2009; McCarl and Scheneider 2001).

Since 1960, atmospheric concentrations of CO_2, the chief heat-trapping GHG, have risen 35 percent, from about to 390 ppm. Figure 6.2 shows global atmospheric

CO_2 concentration between 1960 and 2010, and demonstrates the sharp atmospheric concentration rate of CO_2 over the years.

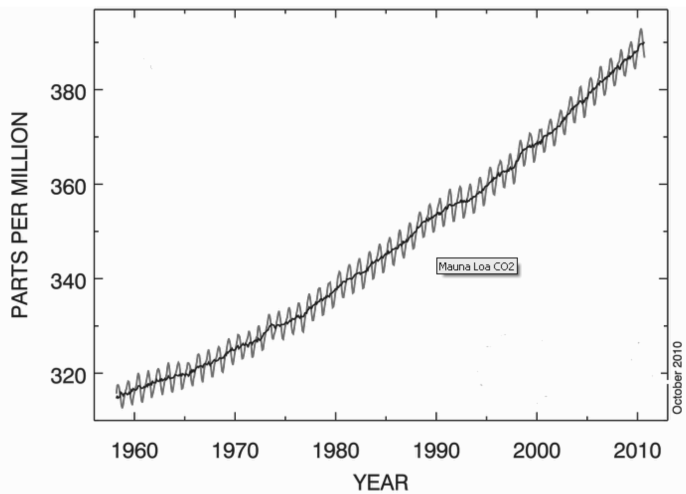

Figure 6.2. Atmospheric CO_2 concentrations in 1960–2010 (NOAA Research at Mauno Loa 2010)

On the side of climate damages, for most of the timespan of human civilizations, global climatic patterns have stayed within a very narrow range,varying at most a few tenths of a degree Centigrade (°C) from century to century. Human settlements, along with their ecosystems and pests, have generally adapted to the climates and geophysical features they have grown up with. However, global temperature changed during the 20th century. According to latest IPCC report (IPCC 2010), leading climate scientists are now 90 percent sure that human activity is heating up the planet since Industrial Revolution. Now, close as 700 scientists 2,500 reviewers and countless government officials agree that global warming is a reality and "very likely" human-induced. Economic studies suggest that those activities will more likely continue to affect climate over the next century (Nordhaus 2007).

Figure 6.3 shows atmospheric concentrations of CO_2, CH_4 and N_2O over the last 10,000 years (large panels) and since 1750 (inset panels) (IPCC 2007). Measurements are shown from ice cores (symbols with different colours for different studies) and atmospheric samples (red lines). The corresponding radiative forcings relative to 1750 are shown on the right hand axes of the large panels. As can be seen from the Figure all three gases have the tendency to increase over the centuries, but in particular over the last 100 years this increase has doubled.

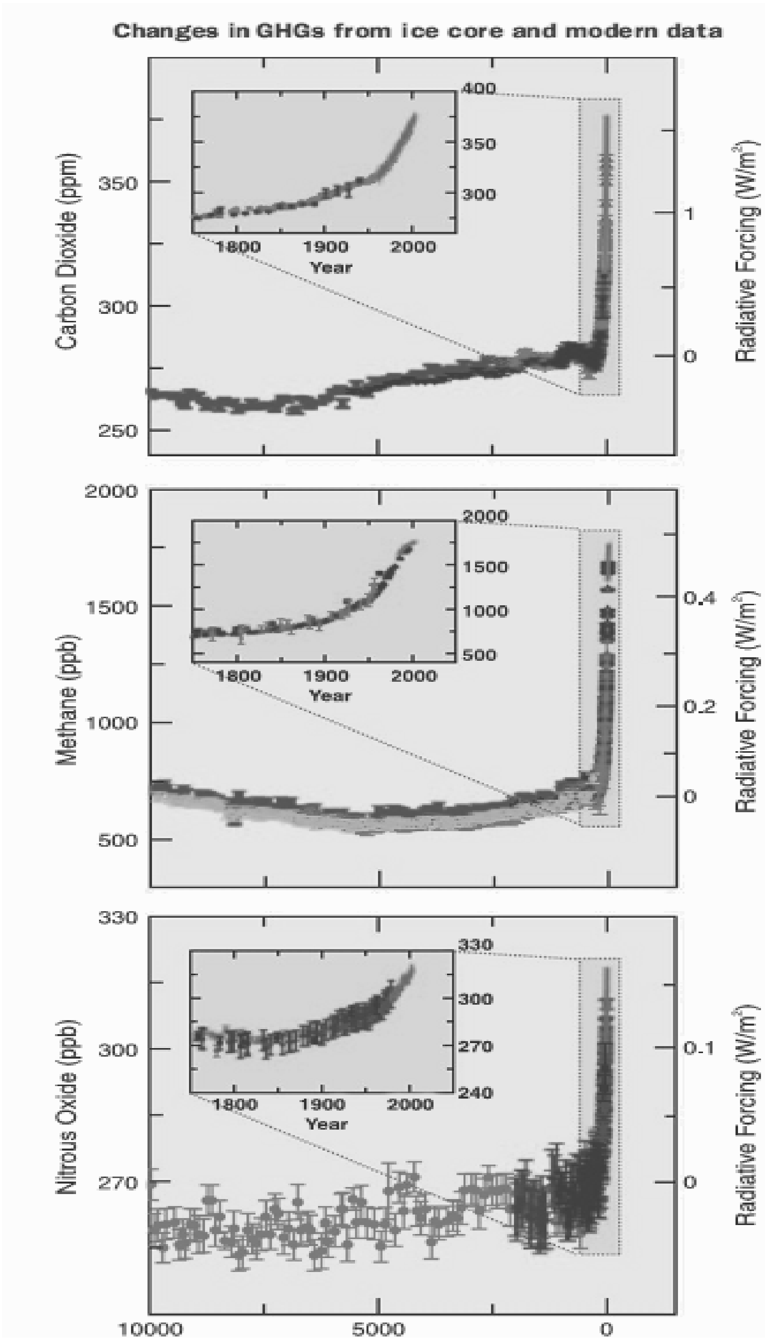

Figure 6.3. Changes in GHGs (CO_2, CH_4 and N_2O) (IPCC 2007a)

GHGs in our atmosphere have mainly increased due to the consumption of fossil fuels, new forms of land use, and agriculture. For scientists, sources of GHG emissions in 2009 comprised: i) fossil-fuel combustion for energy purposes in the power, transport, buildings and industry sectors amounted to 26.1 $GtCO_2$. Combustion of coal, oil and gas in electricity and heat plants accounted for most of these emissions, followed by transport (of which three quarters is road transport), manufacturing and construction and buildings; ii) land-use change such as deforestation releases stores of CO_2 into the atmosphere; and iii) CH_4, N_2O and F-gases are produced by agriculture, waste and industrial processes. Industrial processes such as the production of cement and chemicals involve chemical reactions that releases CO_2 and non- CO_2 emissions. Also, the process of extracting fossil fuels and making them ready for use generates CO_2 and non-CO_2 emissions (so-called fugitive emissions). Of all the human activities that contribute to these increases, fossil fuel combustion is by far the largest, accounting for almost 60% of the greenhouse warming resulting from anthropogenic sources in recent years. 57% of emissions are from burning fossil fuels in power, transport, buildings and industry; agriculture and changes in land use (particularly deforestation) produce 41% of emissions (Stern, 2006).

While atmospheric pollution has had a cooling effect during the last centuries, the massive increase in GHGs has lead to a rise of average temperatures by 0.74^{o}C since 1901. Scientists are 90 percent sure that the last half of the 20th century has been the hottest period in the Northern Hemisphere since 500 years (IPCC 2010). Findings also show that the atmosphere now holds more water vapor, one of the driving forces of tropical storms and floods. Since 1960, Westerly winds have gained in strength all over the planet. The Atlantic was particularly affected by more frequent and severe tropical cyclones, a phenomenon in line with rising surface water temperatures. The report says that there is a chance of six out of ten that recent severe storms were boosted by global warming. Arctic temperatures have increased twice as fast as global average temperatures. Summer ice in the Arctic Ocean is decreasing by 7.4 percent per decade. By the end of the century, the Arctic might well be ice-free in summer. Meanwhile permafrost is on the retreat. Since 1900, the seasonally frozen ground in the Northern Hemisphere has shrunken by some 7 percent. This has freed large amounts of CH_4, another potent GHG. To which extent such side-effects amplify ongoing global warming is not yet properly understood.

Figure 6.4 shows the warming effect of GHGs (the 'radiative forcing') in terms of CO_2e since 1850. The blue line shows the value for CO_2 only. The red line is the value for the six Kyoto GHGs (CO_2, CH_4, N_2O, PFCs, HFCs and SF_6) and the grey line includes CFCs (regulated under the Montreal Protocol). The uncertainty on each of these is up to 10%. The rate of annual increase in GHG levels is variable year-on-year, but is increasing.

Currently, many countries are considering policy actions regarding net GHGE reduction, and trying to find different ways to please different segments of the societies. One way to reduce net emissions is to increase absorption of GHG into the ecosystem through use of, for example, the soil or forests as a sink. This strategy is also commonly called carbon sequestration. Reducing GHGs, particularly deep reductions, will require primarily taking costly steps to reduce CO_2. Some steps involve reducing the use of fossil fuels. Others involve using different production techniques or different fuels or energy sources. Societies have considerable experience in employing different approaches to changing energy production and use patterns. Economic history and analysis indicate that it will be most effective to use market signals, primarily higher prices of carbon fuels, to give signals and provide incentives for consumers and firms to change their energy use and reduce their carbon emissions. In the longer run, higher carbon prices will provide incentives for firms to develop new technologies to ease the transition to a low-carbon future.

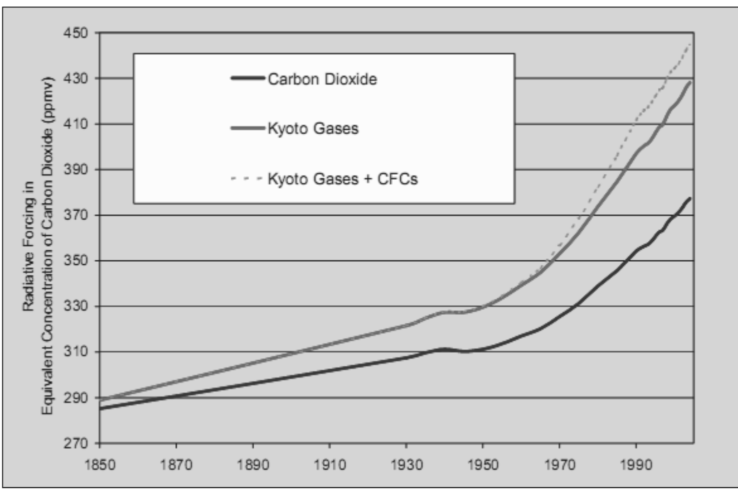

Figure 6.4. Rising levels of GHGs (Gohar and Shine 2007; reproduced with permission from Wiley)

Even though we all know very well that if we do not take urgent policy action it will be too late, we still do not tact the way we should. In August 2008, NEF (2010) calculated that 100 months from 1 August 2008, atmospheric concentrations of GHGs will begin to exceed a point whereby it is no longer *likely* we will be able to avert potentially irreversible climate change. It means that at a particular level of GHG concentration, there is only a 66–90% chance of global average surface temperatures stabilising at 2°C above pre-industrial levels. In December 2007, the likely CO_2e concentration is estimated to be just under 377 ppm, based on a CO_2 concentration of 383 ppm, but this figure increased to 386.80 ppm in September 2010. If stabilisation occurs at 400 ppm, there is a 10–34 percent chance of overshooting a 2°C warming. Beyond this point, the probability of stabilising global surface temperatures at less than 2°C decreases. It would seem that if policy-makers are at all serious about avoiding dangerous climate change at a threshold of 2°C or less, emissions need to be reduced significantly and immediately.

6.3 Emissions/Concentrations of GHGs and Economics of Stabilisation

According to European Environment Agency (2009), we as a human being release just over 1000 tonnes of CO_2 into the Earth's atmosphere every second. Annual EU-27 CO_2 only emissions are currently 4.114 billion tonnes. In 2007, the best estimation of the temperature change over the coming century was at the range from 1.8 to 4.0°C. While this seems like a small change, it is much more rapid than any changes that have occurred for more than 10,000 years (Nordhaus 2007). The IPCC's fourth report (IPCC 2007b) also stated that if fossil fuels continued to be burnt at the current rate, global average surface temperatures could rise by 4°C by the end of the century. The 'committed' level of warming by the end of the century is 2.4°C if atmospheric concentrations of GHGs are held at 2005 levels; this value is based on past emissions and includes the warming already observed of 0.76°C plus 1.6°C of additional warming which is yet to occur due to the thermal inertia of the climate system and the 'masking' by cooling aerosols (Ramanathan and Feng 2008).

From IPCC (2010), scientists have refined their simulations and now have a fairly good idea of the effects of CO_2 emissions. A doubling of CO_2 levels in the atmosphere, relates to a surface warming of some $3^oC \pm 1^oC$. Even if we manage to reduce carbon emissions to year 2000 levels, such a doubling of CO_2 is unpreventable. Meanwhile glaciers all over the world are declining, an effect that is also perceivable at the fringes of the vast Antarctica ice shield. Scientists say that sea levels have already risen 17 centimeters during the 20^{th} century, most of it due to the simple fact that warm water has a larger volume than cold water. With the melting of icecaps and glaciers, the annual rise has nearly doubled since 1993 to a rate of about 3.1 mm. Even if CO_2 emissions can be stabilized, sea levels will keep on rising for centuries until the temperature gain will reach the deep oceans.

6.3.1. GHG Emission and Concentration

In 2006, Stern Review projected that the growth of GHG emission has been driven by economic development, and CO_2 emissions per head have been strongly correlated with GDP per head across time and countries (Stern 2006). In particular, developed countries, such as Europe and North America have produced around 70% of CO_2 emissions from energy production since 1850, while developing countries account for less than one quarter of cumulative emissions. Nevertheless, it is suprising to know that most future emissions growth will come from today's developing countries, because of more rapid population and GDP growth than developed countries, and an increasing share of energy-intensive industries.

In addition, for Stern Review, 'the global emissions of CO_2, which accounts for the largest share of GHGs, grew at an average annual rate of around 2½% between 1950 and 2000. In particular, in 2000, emissions of all GHGs were around 42Gt CO_2e, increasing concentrations at a rate of about 2.7ppm CO_2e per year (Stern'

2006). Human activities result in emissions of four long-lived GHGs: CO_2, CH_4, N_2O and halocarbons (a group of gases containing fluorine, chlorine or bromine) and they are still in rise. Atmospheric concentrations of GHGs increase when emissions are larger than removal processes (IPCC 2007?). Even if annual GHG emissions remained at the current level of 42 $GtCO_2e$ each year, the world would experience major climate change. These emission rates would be sufficient to take GHG concentrations to over 650 ppm CO_2e by the end of this century, likely to result eventually in a rise in the global mean temperature of at least 3°C from its pre-industrial level' (Stern' 2006).

In 2007, GHG concentrations in the atmosphere standed at around 400 ppm CO_2e, compared with only 280 ppm before the Industrial Revolution and its key economic activities. The global atmospheric concentration of CO_2 increased from a pre-industrial value of about 280 ppm to 386.80 ppm in 2010. It is depressing to know that without action to combat climate change, atmospheric concentrations of GHGs will continue to rise. In a plausible 'business as usual' scenario, they will reach 550 ppm CO_2e by 2035, then increasing at 4½ppm per year and still accelerating with China alone accounting for over one third of the increase in energy-related CO_2 emissions between 2004 and 2030, according to the International Energy Agency (2007).

The causal link between GHGs concentrations and global temperatures is well established by scientists even in the nineteenth century. The greenhouse effect is a natural process that keeps the Earth's surface around 15–25°C warmer than it would be otherwise. Without this effect, the Earth would be too cold to support life (Pearce 2003; Pierrehumbert 2004).

Global increases in CO_2 concentrations are due primarily to fossil fuel use, with land-use change providing another significant but smaller contribution. The annual CO_2 concentration growth rate was larger during the last 10 years (1995–2005 average: 1.9ppm per year) than it has been since the beginning of continuous direct atmospheric measurements (1960–2005 average: 1.4ppm per year), although there is year-to-year variability in growth rates. It is very likely that the observed increase in CH_4 concentration is predominantly due to agriculture and fossil fuel use. The CO_2 radioactive forcing increased by 20% from 1995 to 2005, the largest change for any decade in at least the last 200 years. The global atmospheric concentration of CH_4 has increased from pre-industrial value of about 715 ppb to 1732 ppb in the early 1990s, and was 1774 ppb in 2005. The increase in N_2O concentration is primarily due to agriculture. The global atmospheric N_2O concentration increased from a preindustrial value of about 270 ppb to 319 ppb in 2005. The combined radioactive forcing due to increases in CO_2, CH_4 and N_2O is +2.3 [+2.1 to +2.5] W/m^2, and its rate of increase during the industrial era is very likely to have been unprecedented in more than 10,000 years. In 2000, total GHG emissions were 42 Gt CO_2e of which 77% were CO_2, 14% CH_4, 8% N_2O and 1% so-called F-gases such as perfluorocarbon and sulphur hexafluoride (IPCC 2007b).

Current and Projected Global GHG Emission by Sector. In 2000, sources of GHG emissions comprised 57% of emissions from burning fossil fuels in power, transport, buildings and industry; 41% of emissions from agriculture and changes in land use (particularly deforestation). By focusing on energy-related CO_2 emissions from the combustion of fossil fuel, which have been more thoroughly investigated than emissions from land use, agriculture and waste, annual emissions projected to increase under 'business-as-usual' can be better understood.

Figure 6.5 shows sources of GHG emissions by sector in 2005 from several countries. Since nearly three quarters of China's GHG emissions result from the combustion of fossil fuels for energy (with around 5,000 mmt), new Chinese energy policies will have a profound impact on China's contribution to global warming. While China has traditionally avoided policies that explicitly target GHG emissions, its energy and forestry programs have provided the framework for its National Climate Change Program. United States' GHG emissions also result from the combustion of fossil fuels for energy with around 6,000MMT, while EU-27's emissions reach 4,000MMT from the energy related emission.

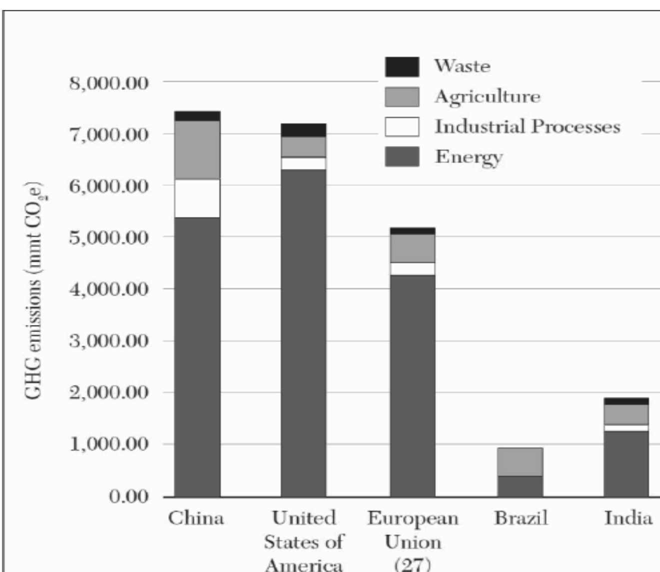

Figure 6.5. International comparison of GHG emission by sector in 2005 (World Resources Institute 2009a; reproduced with permission from WRI)

Figure 6.5 also gives us the chance to compare developed countries' GHG emissions with developing countries. According to latest findings, large developing countries such as India and Brazil are on the way to catch up the developed countries' GHG emission in the next few decades. That is also a bigger danger to increase global GHG emissions stabilisation policies.

Total global emissions grew 12.7% between 2000 and 2005, an average of 2.4% a year. However, individual sectors grew at rates between 40% and near zero percent, and there are substantial differences in sectoral growth rates between developed and developing countries. The higest CO_2 emission in both 2000 and 2005 is in electricity and heat sector. While the US has the higest emission in electricity and heat in developed countries, China fills this place in the category of developing countries in both 2000 and 2005. Following electricity and heat sector, transportation and industry are the sectors which have the highest emission amount. Total global CO_2 emission growth by sector is shown in Figure 6.6. Figure 6.6 indicates that electricity and heat consumption composes the highest emissions growth by sector from 2000 to 2005. Within this sector China and United States have the biggest shares. It also shows that in 2005 global CO_2 emission from electricity and heat increased 21% relative to 2000. Transportation and industry sectors are the sectors that follow electricity and heat sector with a respective growth rate of 12% and 21%.

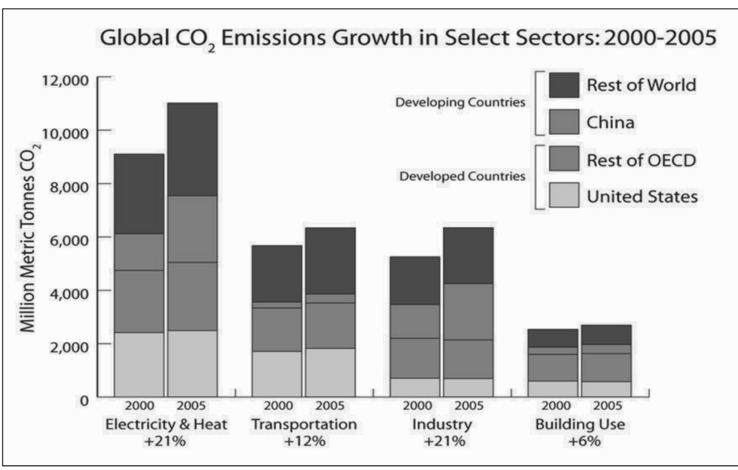

Figure 6.6. Total global emission by sector from 2000 to 2005 (World Resources Institute 2006; reproduced with permission from WRI))

It is predicted that even if the annual flow of emissions did not increase beyond today's rate, the stock of GHGs in the atmosphere would reach double pre-industrial levels by 2050 (i.e., 550 ppm CO_2e) and would continue growing thereafter. But the annual flow of emissions is accelerating, as fast-growing economies invest in high-carbon infrastructure and as the demand for energy and transport increases around the world. The level of 550 ppm CO_2e could be reached as early as 2035. At this level there is at least a 77% chance–and perhaps up to a 99% chance, depending on the climate model used–of a global average temperature rise exceeding 2°C. Figure 6.7 shows the historical and projected global emissions from 1990 to 2050 in much more detailed sectors and illustrates the increasing trend of GHG emissions from 1990 to 2050.

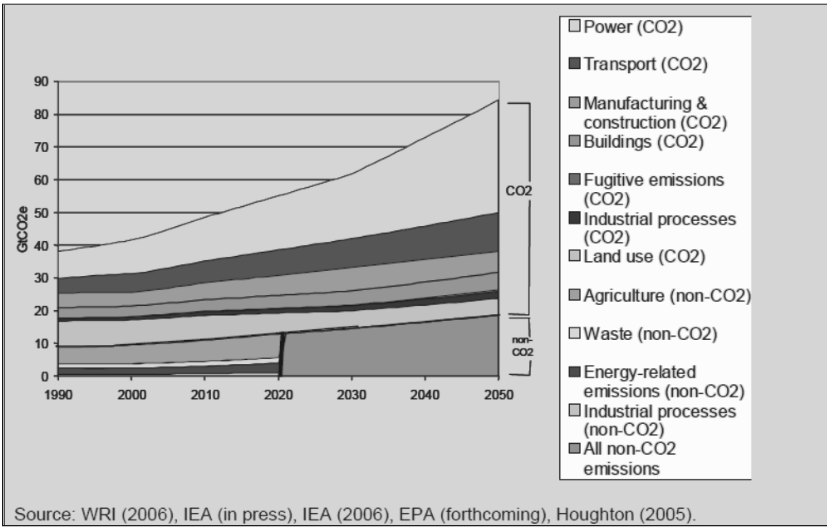

Figure 6.7. Historical and projected GHG emission by sector in 1990–2050 (World Resources Institute 2006; reproduced with permission from WRI)**)**

Projections of long-term GHG emissions growth depend heavily on assumptions about critical factors such as economic and population trends and the rate of technology development and diffusion. Projections at the national level can be highly uncertain, and the uncertainties are especially acute in developing country economies, which tend to be more volatile and vulnerable to external shocks. The range in projections reflects both differing assumptions, for instance, with respect to future policy choices and substantial uncertainties, particularly regarding economic forecasts. Among the most widely cited emissions projections are those developed by the Energy Information Administration (EIA) of the U.S. Department of Energy. Under EIA's mid-range or "reference case" scenario, global emissions of CO_2 from the consumption of fossil fuels are projected to rise 30 percent over the period from 2006–2025 as shown in Figure 6.8.

The reduction of global carbon emissions is now widely regarded as paramount if the world is to avoid major negative consequences throughout the course of the next century. Current levels at around 400 ppm, represent both a record high and an unprecedentedly rapid rise (by 30 ppm in just 17 years). To avoid adverse consequences and possible catastrophe, experts believe that urgent action must be taken now to limit peak CO_2 to 450 ppm (Stern 2006).

Kaya Identity and CO_2 emission growth. One indicator was developed during the last twenty years to measure the emission at country or global level, which is called as Kaya Identity. The Kaya identity is an equation relating factors that determine the level of human impact on climate, in the form of emissions of GHG

CO_2. The Kaya Identity, developed by the Japanese energy economist Yoichi Kaya in 1990, represents key drivers of CO_2 emissions growth. It breaks down into different components and shows that total (anthropogenic) emission levels depend on the product of four variables: population, Gross Domestic Product (GDP) per capita, energy use per unit of GDP (energy intensity) and emissions per unit of energy consumed (carbon intensity of energy). The Kaya Identity was adapted to take into account natural carbon sinks and is shown in Eq. 6.1 (NEF 2010):

$$NetF = P\left(\frac{G}{P}\right)\left(\frac{E}{G}\right)\left(\frac{F}{E}\right) - S = Pgef - S \qquad \text{(Eq. 6.1)}$$

where Net F is the magnitude of net carbon emissions; F is global CO_2 emissions from human sources; P is global population; G is world GDP and g (= G/P) is global per capita GDP; E is global primary energy consumption and e (= E/G) is the energy intensity of world GDP; f (= F/E) is the carbon intensity of energy; and S is the natural (or induced) carbon sink.

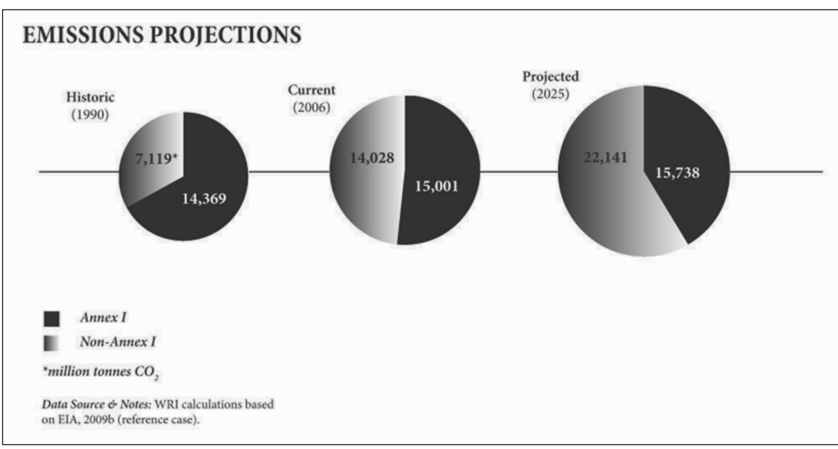

Figure 6.8. Global emission projections over the period 2006–2025 (World Resources Institute 2009a; reproduced with permission from WRI))

Carbon intensity (f) of energy relates to improvements in efficiency of carbon-based energy supply and decarbonisation of the energy supply through diffusion of renewable energy technology (wind, hydro, solar, geothermal and biomass) and nuclear fission (NEF 2010). Trends in each of these components can then be considered in turn. In particular, it can immediately be seen that increases in world GDP will tend to increase global emissions, unless income growth stimulates an offsetting reduction in the carbon intensity of energy use or the energy intensity of GDP (Stern 2006).

Historically, global carbon intensity of energy from Kaya Identity has declined at an average rate of around 1.3 percent per year since the mid-1800s. However, disaggregating these data over the past 40 years gives a much more detailed picture (see Table 6.2). Table 6.2 presents average rate of change (negative numbers imply a fall, positive numbers imply a rise) (NEF 2010).

Table 6.2. Change in global carbon intensity in 1970–2007

Time period	Carbon intensity of the economy (F/GDP)	Energy intensity of the economy (E/GDP)	Carbon intensity of energy (F/E)	Total carbon emissions
1970–1980	-0.79%	-0.65%	-0.16%	2.25%
1980–1990	-1.32%	-0.83%	-0.41%	1.11%
1990–2000	-1.44%	-1.17%	0.18%	0.89%
2000–2007	-0.03%	-0.40%	0.37%	3%

Source: IEA (2009) in NEF (2010).

Table 6.3 arranges the list of countries by their ratio of GDP (nominal and by purchasing power parities) to CO_2 emissions. GDP data is for the year 2006 produced by the International Monetary Fund. CO_2 emissions data is for 2006, provided by the CDIAC for United Nations from the impact of population size and focuses on emissions per head, which are equal to the product of income per head, carbon intensity of energy and energy intensity. These are reported for the world and various countries and groupings within it. Table 6.3 illustrates the wide variation in emissions in selected countries, and how this variation is driven primarily by variations in income per head and, to a lesser extent, by variations in energy intensity. It also illustrates the similarity in the carbon intensity of energy across countries.

Table 6.3. Key ratios for CO_2 emissions in selected countries in 2006

Country	Annual CO_2 emissions (in 10^3 metric tons)	GDP (current, in billions of US dollars)	GDP/Emissions (in US dollars/ ton)	GDP (PPP, in billions of current international dollars	PPP GDP/Emissions (in international dollars/ton)
USA	5,752,289	13,178.35	2,291	13,178.35	2,291
UK	568,520	2,435.70	4,284	2,048.99	3,604
Switzerland	41,826	388.68	9,293	283.84	6,786
France	383,148	2,271.28	5,928	1,974.39	5,153
Japan	1,293,409	4,363.63	3,374	4,079.14	3,154
India	1,510,351	874.77	579	2,672.66	1,770
China	6,103,493	2,657.84	435	6,122.24	1,003

Source: IMF (2006); United Nations Statistic Division (2008).

Some of the factors determining these ratios change only very slowly over time. Geographers have drawn attention to the empirical importance of a country's endowments of fossil fuels and availability of renewable energy sources (Neumayer 2004), which appear to affect both the carbon intensity of energy use and energy use itself.

'The rate fell back somewhat in the three decades after 1970, but was still 1.7% on average between 1971 and 2002 (compared with an average rate of increase in energy demand of 2.0% per year). The slowdown appears to have been associated with the temporary real increases in the price of oil in the 1970s and 1980s, the sharp reduction in emissions in Eastern Europe and the former Soviet Union due to the abrupt changes in economic systems in the 1990s, and increases in energy efficiency in China following economic reforms' (Stern 2006).

IPCC Special Report on Emissions Scenarios (2000). Global GHG emissions will continue to grow over the next few decades. Baseline emissions scenarios are comparable in range to those presented in SRES. 'The SRES scenarios project an increase of baseline global GHG emissions by a range of 9.7 to 36.7 Gt CO_2e (25 to 90%) between 2000 and 2030. In these scenarios, 'fossil fuels are projected to maintain their dominant position in the global energy mix to 2030 and beyond. Hence CO2 emissions from energy use between 2000 and 2030 are projected to grow 40 to 110% over that period'(IPCC 2007a).

SRES (Special Report on Emisions Scenarios) refers to the scenarios described in the IPCC Special Report on Emissions Scenarios (SRES 2000). The SRES scenarios are grouped into four scenario families (A1, A2, B1 and B2) that explore alternative development pathways, covering a wide range of demographic, economic and technological driving forces and resulting GHG emissions. The SRES scenarios do not include additional climate policies above current ones. The emissions projections are widely used in the assessments of future climate change, and their underlying assumptions with respect to socio-economic, demographic and technological change serve as inputs to many recent climate change vulnerability and impact assessments.

Figure 6.9 provides an illustraion of IPCC's SRES projections to 2100. As can be seen there are different secenarios, such as A1, A1T, B2, etc. The A1 storyline assumes a world of very rapid economic growth, a global population that peaks in mid-century and rapid introduction of new and more efficient technologies. A1 is divided into three groups that describe alternative directions of technological change: fossil intensive (A1FI), non-fossil energy resources (A1T) and a balance across all sources (A1B). B1 describes a convergent world, with the same global population as A1, but with more rapid changes in economic structures toward a service and information economy. B2 describes a world with intermediate population and economic growth, emphasising local solutions to economic, social, and environmental sustainability. A2 describes a very heterogeneous world with high population growth, slow economic development and slow technological change. No likelihood has been attached to any of the SRES scenarios.

Figure 6.9 also demonstrates global GHG emissions (in $GtCO_2e/yr$) in the absence of additional climate policies: six illustrative SRES marker scenarios (coloured lines) and 80^{th} percentile range of recent scenarios published since SRES (post-SRES) (gray shaded area). Dashed lines show the full range of post-SRES scenarios. The emissions include CO_2, CH_4, N_2O and F-gases.

Studies published since SRES (i.e. post-SRES scenarios) have used lower values for some drivers for emissions, notably population projections. However, for those studies incorporating these new population projections, changes in other drivers, such as economic growth, result in little change in overall emission levels. Economic growth projections for Africa, Latin America and the Middle East to 2030 in post-SRES baseline scenarios are lower than in SRES, but this has only minor effects on global economic growth and overall emissions. Aerosols have a net cooling effect and the representation of aerosol and aerosol precursor emissions, including sulphur dioxide, black carbon and organic carbon, has improved in the post-SRES scenarios. Generally, these emissions are projected to be lower than reported in SRES (IPCC 2000).

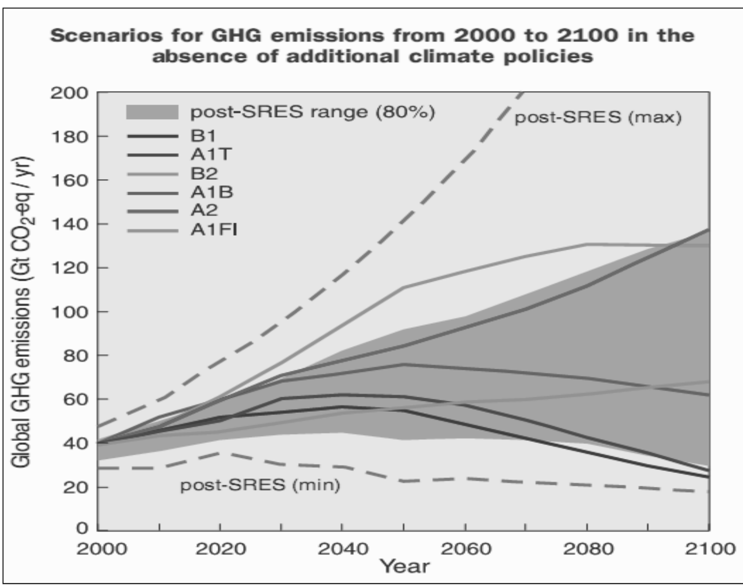

Figure 6.9. Emissions Scenarios in 2000–2100 (IPCC 2007a)

6.3.2 Economics of Stabilisation

In the literature, the relationship between emission and income growth is examined by Environmental Kuznet Curve (EKC) coined by World Bank in 1992 in their environment report. EKC hypothesizes that the relationship between per capita income and the use of natural resources and/or the emission of wastes has an inverted U-shape (see Figure 6.10). According to this specification, at relatively low levels of income the use of natural resources and/or the emission of wastes increase with income. Beyond some turning point, the use of the natural resources and/or the emission of wastes decline with income. Reasons for this inverted U-shaped relationship are hypothesized to include income-driven changes in: 1) the composition of production and/or consumption; 2) the preference for environmental quality; 3) institutions that are needed to internalize externalities; and/or 4) increasing returns to scale associated with pollution abatement (Richmond 2007).

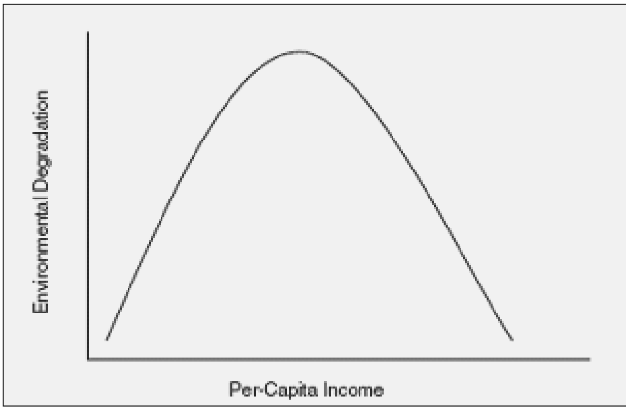

Figure 6.10. Environmental Kuznets Curve.

Subsequent statistical analysis, however, showed that while the relationship may hold in a few cases, it could not be generalized across a wide range of resources and pollutants. In particular, on the skecptical side, Stern (1996 2004) claims that in the case of climate change, the EKC hypothesis is not very convincing, for three reasons. First, at a global level, there has been little evidence of large voluntary reductions in emissions as a result of consumers desire to reduce emissions as they become richer. That may change as people's understanding of climate-change risks improves, but the global nature of the externality means that the incentive for uncoordinated individual action is very low. Second, the pattern partly reflects the relocation of manufacturing activity to developing countries. So, at the global level, the structural shift within richer countries has less impact on total emissions. Third, demand for some carbon-intensive goods and services–such as air transport–has a high income elasticity, and will continue to grow as incomes rise. Demand for car transport in many developing countries, for example, is likely to continue to increase rapidly. For these reasons, 'at the global level, in the absence of policy interventions, the long-run positive relationship between income growth and emissions per head is likely to persist. Breaking the link requires significant changes in preferences, relative prices of carbon-intensive goods and services and/or breaks in technological trends' (Stern 2006). The best policy we can adopt seems to stabilise the emission at a realistic level even if we cannot immediately reduce it.

'Business as usual' emissions will take GHG concentrations and global temperatures way beyond the range of human experience. In the absence of action, the stock of GHGs in the atmosphere could more than triple by the end of the century. Stabilisation of concentrations will require deep emissions cuts of at least 25% by 2050, and ultimately to less than one-fifth of today's levels. The costs of achieving this will depend on a number of factors, particularly progress in bringing down the costs of technologies. Overall costs are estimated at around 1% of GDP for stabilisation levels between 500–550 ppm CO_2e. The costs will not be evenly felt–some carbon-intensive sectors will suffer, while for others, climate change policy will create opportunities. Climate change policies may also have wider benefits where they can be designed in a way that also meets other goals. Comparing the costs and benefits of action clearly shows that the benefits of strong, early action on climate change outweigh the costs. The current evidence suggests aiming for stabilisation somewhere within the range 450–550 ppm CO_2e. Ignoring climate change will eventually damage economic growth; tackling climate change is the pro-growth strategy (Stern 2006).

Slowly reducing emissions of GHGs that cause climate change is likely to entail some costs. Costs include the expense of developing and deploying low-emission and high-efficiency technologies and the cost to consumers of switching spending from emissions-intensive to low-emission goods and services. Fossil fuel emissions can be cut in several ways; reducing demand for carbon-intensive products, increasing energy efficiency, and switching to low-carbon technologies. Non-fossil fuel emissions are also an important source of emission savings. Costs will differ considerably depending on which methods and techniques are used.

Stabilising at or below 550 ppm CO_2e (around 440–500 ppm CO_2 only) would require global emissions to peak in the next 10–20 years, and then fall at a rate of at least 1–3% per year. By 2050, global emissions would need to be around 25% below current levels. These cuts will have to be made in the context of a world economy in 2050 that may be three to four times larger than today – so emissions per unit of GDP would need to be just one quarter of current levels by 2050. Delaying the peak in global emissions from 2020 to 2030 would almost double the rate of reduction needed to stabilise at 550 ppm CO_2e. A further ten-year delay could make stabilisation at 550 ppm CO_2e impractical, unless early actions were taken to dramatically slow the growth in emissions prior to the peak.

To stabilise at 450 ppm CO_2e, without overshooting, global emissions would need to peak in the next 10 years and then fall at more than 5% per year, reaching 70% below current levels by 2050. This is likely to be unachievable with current and foreseeable technologies. If carbon absorption were to weaken, future emissions would need to be cut even more rapidly to hit any given stabilisation target for atmospheric concentration. Overshooting paths involve greater risks to the climate than if the stabilisation level were approached from below, as the world would experience at least a century of temperatures, and therefore impacts, close to those expected for the peak level of emissions. Some of these impacts might be irreversible. In addition, overshooting paths require that emissions be reduced to extremely low levels, below the level of natural absorption, which may not be feasible. Energy systems are subject to very significant inertia. It is important to avoid getting 'locked into' long-lived high carbon technologies, and to invest early in low carbon alternatives (Stern 2006). Reducing annual emissions below the rate of natural absorption would lead to a fall in concentration. However such a recovery would be very slow process even if very low emissions were achieved, conentration would fall by a few ppm per year.

This rate would be further reduced if carbon absorption were to weaken as projected. Figure 6.11 gives illustrative results from one study that shows the level of cumulative emissions between 2000 and 2300 for a range of stabilisation levels (CO_2 only). For the green bars, natural carbon absorption is not affected by the climate. The grey bars include the feedbacks between the climate and the carbon cycle.

Assuming that climate does not affect carbon absorption, a recent study projects that stabilising CO_2 concentrations at 450 ppm would allow cumulative *emissions* of close to 2100 Gt CO_2 between 2000 and 2100 (assuming no climate-carbon feedback as shown in Figure 6.9) (equivalent to roughly 60 years of emissions at today's rate). This means that approximately 75% of emissions would have been absorbed. Stabilising at 550 ppm CO_2 would allow roughly 3700 $GtCO_2$.

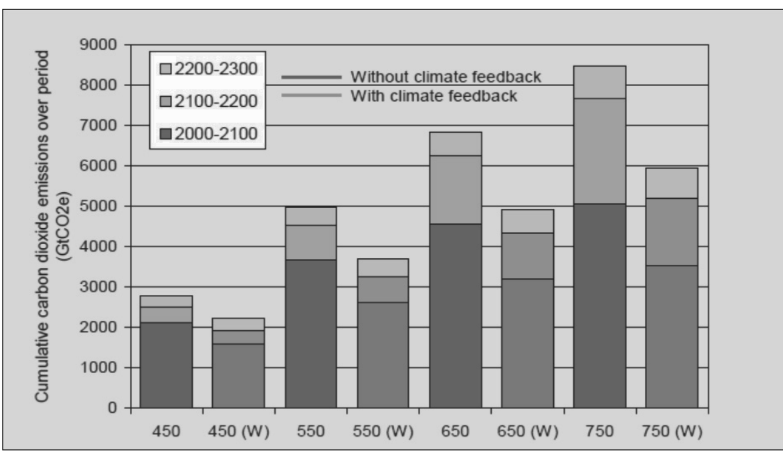

Figure 6.11. Cumulative emissions of CO_2 at stabilisation (Stern 2006; under Crown Copyright)

Hendry (2010) briefly considers three mechanisms (i.e., markets, permits and auctions) that might help create the correct incentives for mitigation. 'Designing market mechanisms in general, and creating schemes to mitigate GHG emissions in particular, are both large literatures: see (e.g.) Roth (2002) for the former and Klemperer (2009) for the latter.

Figure 6.12 below illustrates the types of impacts that could be experienced as the world comes into equilibrium with more GHGs. The top panel shows the range of temperatures projected at stabilisation levels between 400 ppm and 750 ppm CO_2 e at equilibrium. The solid horizontal lines indicate the 5–95% range based on climate sensitivity estimates from the IPCC 2012 and a recent Hadley Centre ensemble study. The vertical line indicates the mean of the 50^{th} percentile point. The dashed lines show the 5–95% range based on eleven recent studies. The bottom panel illustrates the range of impacts expected at different levels of warming. The relationship between global average temperature changes and regional climate changes is very uncertain, especially with regard to changes in precipitation. Figure 6.12 shows potential changes based on current scientific literature.

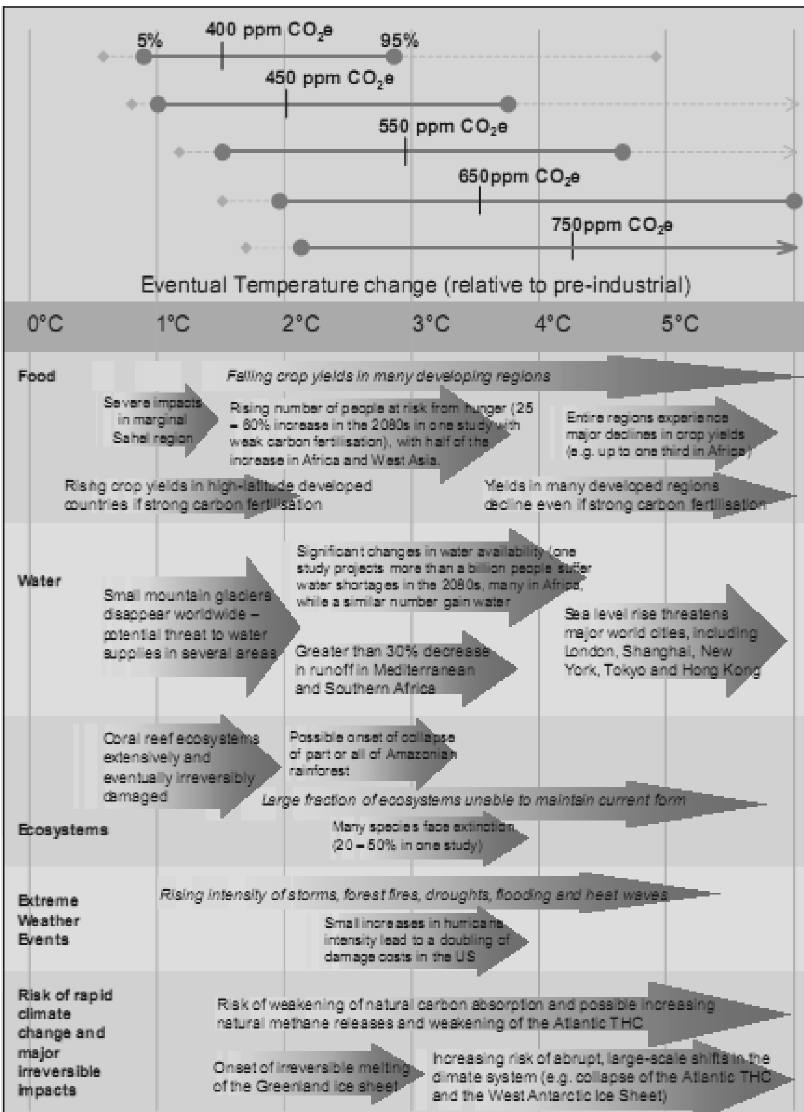

Figure 6.12. Stabilisation levels and probability ranges for temperature increases (Stern 2006; under Crown Copyright)

Careful analyses are essential to ensure that incentives to reduce pollution are correctly aligned, are relatively accurately costed, do not create a 'substitution' to the least regulated or cheapest areas, nor undermine living standards, and yet protect the poorest sections of society. These are demanding, but not infeasible, requirements.

As the world economy emerges from the financial-crisis induced sharpest downturn since the Great Depression, there is a potential role for modern finance theory in designing options and *permit trading*, despite their reputation as 'weapons of financial mass destruction'. Given a long-run emissions target, say, McKibbin and Wilcoxen (2002) propose that a fixed number of long-term permits be issued, designed to rise in value as carbon prices rise, and so could create balance sheet value to offset current increased abatement costs.

The Theory of Auctions also has an important role to play in the design of effective carbon trading schemes (see e.g., Milgrom 2004). As shown by Klemperer (2002) and Binmore and Klemperer (2002) for the various different G3 telecom auctions, auction design can have a huge impact on the realized outcomes.

Costs of Mitigation and Long-term Stabilisation Targets. The macro-economic costs of mitigation generally rise with the stringency of the stabilisation target and are relatively higher when derived from baseline scenarios characterised by high emission levels. There is high agreement and medium evidence that in 2050 global average macro-economic costs for multi-gas mitigation towards stabilisation between 710 and 445 ppm CO_2e are between 1% gain to 5.5% decrease of global GDP (Table 6. 4). This corresponds to slowing average annual global GDP growth by less than 0.12 percentage points. Estimated GDP losses by 2030 are on average lower and show a smaller spread compared to 2050 (Table 6.4). For specific countries and sectors, costs vary considerably from the global average (IPCC 2007b).

Table 6.4. Estimated global macroeconomic costs in 2030 and 2050[a]

Stabilisation levels (ppm CO_2e)	Median GDP	Reduction (%)	Range of GDP	Reduction (%)	Reduction of GDP growth	Average annual rates
	2030	2050	2030	2050	2030	2050
445–535	NA	NA	<3	<5.5	<0.12	<0.12
535–590	0.6	1.3	0.2 to 2.5	Slightly negative to 4	<0.1	<0.1
590–710	0.2	0.5	-0.6 to 1.2	-1 to 2	<0.06	<0.05

[a]Source: IPCC (2007b). [b] NA = not available. Notes: Values given in this table correspond to the full literature across all baselines and mitigation scenarios that provide GDP numbers. a) Global GDP based on market exchange rates. b) The 10^{th} and 90^{th} percentile range of the analysed data are given where applicable. Negative values indicate GDP gain. The first row (445–535ppm CO_2e) gives the upper bound estimate of the literature only. c) The calculation of the reduction of the annual growth rate is based on the average reduction during the assessed period that would result in the indicated GDP decrease by 2030 and 2050 respectively. d) The number of studies is relatively small, and they generally use low baselines. High emissions baselines generally lead to higher costs. e) The values correspond to the highest estimate for GDP reduction shown in column three.

In order to calculate the costs of emission, Dasgupta (2007) critically compared Stern Review's calculation method with Nordhaus' method and came to calculation that there are differences between Page Model (Stern 2006) and DICE Model (Nordhaus, 2007). For Dasgupta (2007), the Review takes it that the trade off among the well-being between the present US and the future THEMs should be, roughly speaking, one-to-one, or in other words, that we should not discount future generations' well-beings simply because those generations will appear only in the future. The Review assumes that delta ought to be set equal to 0.1% per year, which is a very low figure if we are to compare it with the values advocated by other climate economists (see below). This is to adopt a very egalitarian attitude across the *time* dimension. But curiously, the Review adopts a very *in* egalitarian attitude with regard to the distribution of wellbeing across people when futurity is not the issue–for example, when comparing the well-beings of the poor and rich in the contemporary world. 'The Review's central case is based on the assumption that eta ought to be unity, which, as I show below, reflects a fairly indifferent attitude toward equity over the distribution of well-being among people. The distinction between the two parameters is crucial. As the numerical figures that are assumed for them influence estimates of the economic costs and benefits of controlling carbon emissions, enlarging sequestration possibilities, and investing in alternative energy technologies, delta and eta are hugely significant parameters' (Dasgupta 2007).

Nordhaus and others have used a considerably higher figure for delta (point (1) above). In contrast to the Review's figure of 0.1% per year, Nordhaus (2007) in recent years has used a starting value of 3% a year for delta, declining to about 1% a year in 300 years' time. Interestingly, Nordhaus also takes eta (point (2) above) to be unity. He further reports that the first-period social price of carbon (which is a measure of the social damage a marginal unit of carbon emitted today inflicts on humanity) is about $13 per ton, whereas the figure reached in the Review's central case is about $310 per ton. But if the Review's figure for delta is put to work on DICE, the first-period social price of carbon becomes about $150 per ton. This is about 'half the figure offered by the Review, but it's enough to suggest that the drivers behind the Review's findings are very low values of the two ethical parameters, delta and eta. Indeed, modifying DICE slightly, so as to take a more alarming view for the worst case scenario under business as usual raises the figure for the social price of carbon to $400 per ton, in excess of the figure recommended in the Review (Nordhaus 2007).

Endogenous technical changes due to learning and increased R&D efforts responding to carbon prices and emission reduction policies tend to reduce long-term costs. To switch to technologies which produce fewer emissions and lower the carbon intensity of production includes some more detail on which technologies can be used to cut emissions in each sector, and the associated costs.

The array of abatement opportunities can be assessed in terms of their cost per unit of GHG reduction ($/t CO_2e), both at present and through time. In theory, abatement opportunities can be ranked along a continuum of the kind shown in

Figure 6.13. This shows that some measures (such as improving energy efficiency and reducing deforestation) can be very cheap, and may even save money. Other measures, such as introducing hydrogen vehicles, may be a very expensive way to achieve emission reductions in the near term, until experience brings costs down. The precise ranking of measures differs by country and sector. It may also change over time (represented in Figure 6.13 by arrows going from right to left). For example, research and development of hydrogen technology may bring the costs down in the future (illustrated by the downward shift in the abatement curve over time).

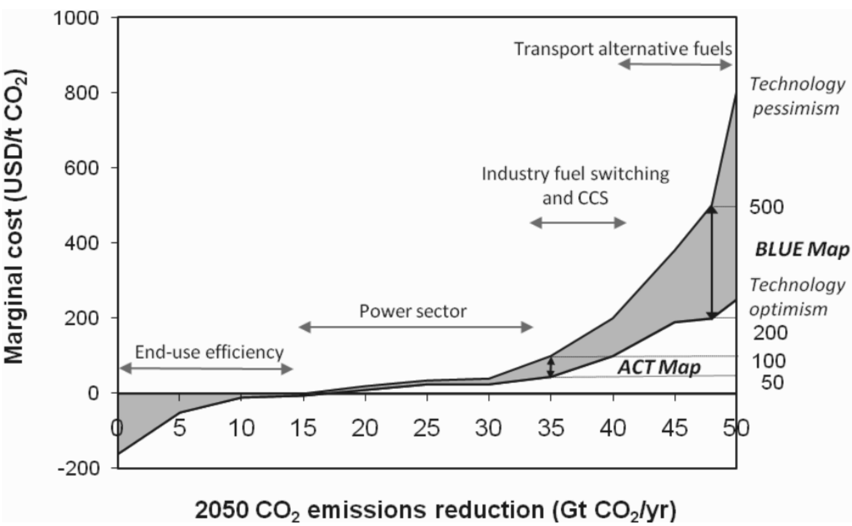

Figure 6.13. Marginal abatement cost curve by 2050 (IEA 2008, 2010)

The abatement curve, consisting of hundreds of options conveys two important messages. First, costs are relatively flat up to the ACT Map scenario objective to stabilise emissions at 2005 levels in 2050. But they rise quickly as the additional emissions reduction technologies implicit in the BLUE Map scenario are required. Second, although there is a high degree of uncertainty about the cost of the cheapest reduction measures, they are clearly negative. There is less uncertainty about the cost of technologies needed to achieve the ACT Map target. But costs become more uncertain again as the measures needed to achieve the BLUE Map scenario emission reduction objectives come into play. Nonetheless, *ETP 2008* makes it clear that on the right-hand side of the picture mostly representing abatement in the transport sector; the lower end of the range of [marginal costs] has a much higher likelihood than the upper end.

In fact, reducing demand for emissions-intensive goods and services is part of the solution. If prices start to reflect the full costs of production, including the GHG externality, consumers and firms will react by shifting to relatively cheaper low-carbon products. Increasing awareness of climate change is also likely to influence demand. But demand-side factors alone are unlikely to achieve all the emissions reductions required. In addition, efficiency gains offer opportunities both to save money and to reduce emissions, but require the removal of barriers to the uptake of more efficient technologies and methods.

As a matter of fact, a range of low-carbon technologies is already available, although many are currently more expensive than fossil-fuel equivalents. Cleaner and more efficient power, heat and transport technologies are needed to make radical emission cuts in the medium to long term. Their future costs are uncertain, but experience with other technologies has helped to develop an understanding of the key risks. The evidence indicates that efficiency is likely to increase and average costs to fall with scale and experience.

Reducing non-fossil fuel emissions will also yield important emission savings. The cost of reducing emissions from deforestation, in particular, may be relatively low, if appropriate institutional and incentive structures are put in place and the countries facing this challenge receive adequate assistance. Emissions cuts will be more challenging to achieve in agriculture, the other main non-energy source.

Calculating the Costs of Cutting GHG Emissions. An estimate of resource costs suggests that the annual cost of cutting total GHG to about three quarters of current levels by 2050, consistent with a 550 ppm CO_2e stabilisation level, will be in the range –1.0 to +3.5% of GDP, with an average estimate of approximately 1%. This depends on steady reductions in the cost of low-carbon technologies, relative to the cost of the technologies currently deployed, and improvements in energy efficiency. The range is wide because of the uncertainties as to future rates of innovation and fossil-fuel extraction costs. The better the policy, the lower the cost. Mitigation costs will vary according to how and when emissions are cut. Without early, well-planned action, the costs of mitigating emissions will be greater (Stern 2006).

A simple first approximation to the cost of reducing emissions can be obtained by considering the probable cost of a simple set of technological and output changes that are likely to achieve those reductions. One can measure the extra resources required to meet projected energy demand with known low-carbon technologies and assess a measures of the opportunity costs, for example, from forgone agricultural output in reducing deforestation. If the costs were less than the benefits that the emissions reductions bring, it would be better to take the set of mitigation measures considered than do nothing. But there may be still better measures available. The formal economics of marginal policy changes or reforms have been studied in a general equilibrium framework that includes market imperfections. A reform, such as reducing GHG emissions by using extra resources, can be assessed in terms of the direct benefits of a marginal reform on consumers (the emission reduction and the reduced spending on fossil fuels), less the cost at shadow prices of the extra resources.

The formal economics draws attention to two issues that are important in the case of climate-change policies. *First*, the policies need to bring about a large, or non-marginal, change. The marginal abatement cost (MAC) – the cost of reducing emissions by one unit – is an appropriate measuring device only in the case of small changes. For big changes, the marginal cost may change substantially with increased scale. Using the MAC that initially applies, when new technologies are first being deployed, would lead to an under-estimate of costs where marginal costs rise rapidly with the scale of emissions. This could happen, for example, if initially cheap supplies of raw materials start to run short. But it may over-estimate costs where abatement leads to reductions in marginal costs – for example, through induced technological improvements. These issues will be discussed in more detail below, in the context of empirical estimates, where average and total costs of mitigation are examined as along with marginal costs (Stern 2006). It is important to keep the distinction between marginal and average costs in mind throughout, because they are likely to diverge over time. On the one hand, the marginal abatement cost should rise over time to remain equal to the social cost of carbon, which itself rises with the stock of GHGs in the atmosphere). The average cost of abatement will be influenced not only by the increasing size of emissions reductions, but also by the pace at which technological progress brings down the total costs of any given level of abatement.

Second, as formal economics has shown, shadow prices and the market prices faced by producers are equal in a fairly broad range of circumstances, so market prices can generally be used in the calculations in this chapter. But an important example where they diverge is in the case of fossil fuels. Hydrocarbons are exhaustible natural resources, the supply of which is also affected by the market power of some of their owners, such as OPEC. As a result, the market prices of fossil fuels reflect not only the marginal costs of extracting the fuels from the ground but also elements of scarcity and monopoly rents, which are income transfers, not resource costs to the world as a whole. When calculating the offset to the global costs of climate-change policy from lower spending on fossil fuels, these rents should not be included.

6.4 Global Strategies and Practical Implications of Global Strategies with Kyoto Protocol

What is the best strategy to encourage research and development on new energy technologies in a market economy? What steps can ensure a rapid and efficient transition to an economy that has much lower net carbon emissions?

This states that, under limited conditions, a necessary and sufficient condition for an appropriate innovational environment is a universal, credible, and durable price on carbon emissions. The carbon price would be one that balances the marginal costs and marginal damages from carbon emissions; it should not contain a correction factor for inducing technological change. Price fundamentalism for innovation applies principally to the market-oriented part of research and innovation. There are qualifications to this result regarding the efficacy of intellectual property protection, the proper level of carbon prices, and the application to market sectors. But this basic theorem should be kept in mind when encouraging the emergence of technologies to combat global warming.

Green innovations, such as those embodied in low-carbon technologies or energy conservation measures, not only improve productive efficiency but do so in a way that reduces the carbon intensity of production (or, more generally, reduce the emissions of some harmful byproducts per unit of output). We can contrast green innovations with "normal" innovations, which increase efficiency but are environmentally neutral. That is, a normal innovation is one that increases output per unit of input but does not change the ratio of pollution to output (Nordhaus 2010). The economic theory and history show that innovations will be introduced by the private sector if they are profitable at market prices, that is, if they lower costs or provide new or improved goods or services that can be sold profitably in the marketplace. The theory of induced innovation suggests that factor-biased technological change (as in green innovations) will occur primarily if the factor prices of the biased factor (here pollution) increase relative to other factors. If market prices do not fully correct for pollution and other externalities, there is no economic reason why innovations should be green rather than normal (Nordhaus 2010).

Literature shows that historically, economic development has been associated with increased energy consumption and hence energy-related CO_2 emissions per head. Across 163 countries, from 1960 to 1999, the correlation between CO_2 emissions per head and GDP per head (expressed as natural logarithms) was nearly 0.9 (Neumayer 2004). Similarly, one study for the United States estimated that, over the long term, a 1% rise in GDP per head leads to a 0.9% increase in emissions per head, holding other explanatory factors constant (Huntington 2005). In Huntington's study GDP per head is itself a function of many other variables, and emissions projections should in principle be based upon explicit modelling of the sources of growth; for example, the consequences for emissions will be different if growth is driven by innovations in energy technology rather than capital accumulation.

Consistent with this, emissions per head are highest in developed countries and much lower in developing countries–although developing countries are likely to be closing the gap, because of their more rapid collective growth and their increasing share of more energy-intensive industries (Hovi and Holtsmark 2006). McKitrick and Strazicich (2005) have pointed out that global emissions per head have behaved as a stationary series subject to structural breaks. But this does not preclude increases in global emissions per head in future, either because of structural changes within economies or changes in the distribution of emissions across fast and slow-growing economies, leading to further structural breaks.

There are large uncertainties concerning the future contribution of different technologies. However, all assessed stabilisation scenarios concur that 60 to 80% of the reductions over the course of the century would come from energy supply and use and industrial processes. Including non-CO_2 and CO_2 land-use and forestry mitigation options provides greater flexibility and cost-effectiveness. Energy efficiency plays a key role across many scenarios for most regions and time scales. For lower stabilisation levels, scenarios put more emphasis on the use of low-carbon energy sources, such as renewable energy, nuclear power and the use of CO_2 capture and storage (CCS).

Structural changes in economies will have a significant impact on their emissions. In some rich countries, the shift towards a service-based economy has helped to slow down, or even reverse, the growth in national emissions. Indeed, emissions per head have fallen in some countries over some periods (e.g. they peaked in the United Kingdom in 1973 and fell around 20% between then and 1984).

GHGE constitute a global production externality which is likely to adversely affect climate. The United Nations Framework Convention on Climate Change (UNFCCC) was established to negotiate net GHGE reduction. Actions under that convention yielded the Kyoto Protocol which represents the first significant international agreement towards GHGE reduction (McCarl and Scheneider 2001).

Kyoto Protocol in 1997. The reduction of GHGs has been discussed in a number of international conventions. In particular, the third Conference of Parties to the United Nations Framework Convention on Climate Change (COP3) held in Kyoto (Ishikiwa and Kiyono 2006). In December 1997, 160 nations reached agreement on a historic step to control GHG emissions in Kyoto, Japan. This legally binding protocol, the so-called Kyoto Protocol, set differentiated GHG-reduction targets for key industrial powers in 38 developed countries ranging from 6% to 8% below baseline levels (1990 and 1995, depending on the gas). The time frame set for countries (which consist of the OECD members and the countries in the former USSR and Eastern Europe) meeting the agreement's goals was to reduce emission 5.2% below 1990 levels between 2008 and 2012 (Ishikiwa and Kiyono 2006).

The US agreed to a 7% reduction. However, when various accounting rules for the set of six gases are factored in, and when offsets for activities that absorb CO_2 are considered, the level of effort required from the US is at most a 3% real reduction below 1990 levels by 2008–2012. Meeting such a goal is going to require a major national effort. Over the time frame of the goals (1990–2012), the US forecasts to increase its CO_2 emissions by more than 30%, and energy prices are expected to rise only slightly. Within this context, a "full court press" will be needed to improve the performance of low-carbon and efficient technologies, and various incentives, codes, standards, and information programs will be needed to instill in Americans a stronger desire to purchase them (Brown et al. 1998).

Copenhagen Summit in 2009. United Nations Climate Change Conference, commonly known as the Copenhagen Summit, was held in Copenhagen, Denmark, between 7 December and 18 December in 2009. The conference covered 193 countries, including parties to the United Nations Framework Conventions on Climate Change and parties to the Kyoto Protocol.

A US-led initiative called the Copenhagen Accord has formed the centre-piece of a deal at UN climate talks in Copenhagen, despite some countries' opposition. The Accord, reached between the US, China, India, Brazil and South Africa, contains no reference to a legally binding agreement, as some developing countries and climate activists wanted (BBC, 2009). The text recognises the need to limit global temperatures rising no more than 2^{o}C (3.6^{o}F) above pre-industrial levels. The language in the text shows that 2C is not a formal target, just that the group "recognises the scientific view that" the temperature increase should be held below this figure. The deal promises to deliver $30bn (£18.5bn) of aid for developing nations over the next three years. It outlines a goal of providing $100bn a year by 2020 to help poor countries cope with the impacts of climate change. The Accord says the rich countries will jointly mobilise the $100bn, drawing on a variety of sources: "public and private, bilateral and multilateral, including alternative sources of finance." A green climate fund will also be established under the deal. It will support projects in developing countries related to mitigation, adaptation, "capacity building" and technology transfer.

The pledges of rich countries will come under "rigorous, robust and transparent" scrutiny under the UN Framework Convention on Climate Change (UNFCCC). In the Accord, developing countries will submit national reports on their emissions pledges under a method "that will ensure that national sovereignty is respected." Pledges on climate mitigation measures seeking international support will be recorded in a registry.

The implementation of the Copenhagen Accord will be reviewed by 2015. This will take place about a year-and-a-half after the next scientific assessment of the global climate by the Intergovernmental Panel on Climate Change (IPCC). However, if, in 2015, delegates wanted to adopt a new, lower target on global average temperature, such as 1.5C rather than 2C, it would be too late. On transparency: Emerging nations monitor own efforts and report to UN every two years. No detailed framework on carbon markets-"various approaches" will be pursued.

6.4.1 In the USA

The impacts of global warmng in the USA is projected as:

- Warming in western mountains is projected to cause decreased snowpack, more winter flooding and reduced summer flows, exacerbating competition for over-allocated water resources.
- In the early decades of the century, moderate climate change is projected to increase aggregate yields of rain-fed agriculture by 5 to 20%, but with important variability among regions. Major challenges are projected for crops

that are near the warm end of their suitable range or which depend on highly utilised water resources.
- Cities that currently experience heat waves are expected to be further challenged by an increased number, intensity and duration of heat waves during the course of the century, with potential for adverse health impacts.
- Coastal communities and habitats will be increasingly stressed by climate change impacts interacting with development and pollution (IPCC 2007)

Up to now, most nations have set a low bar in their climate change policies, and indeed the bar for the US has been at ground level. However, new U.S. legislative initiatives in 2010 would, if enacted, set a daunting challenge for the nation's energy system. The size of that challenge can be seen by measuring the implied technological transformation necessary under legislation proposed by the House Committee on Energy and Commerce. That legislation would impose reductions in emissions of CO_2 of 3 percent of 2005 emissions by 2012, 17 percent by 2020, 42 percent by 2030, and 83 percent by 2050. Breaks in the relationship between emissions per head and GDP per head have taken place, as seen in Figure 6.14 for the USA, at income levels around $6,000 per head, $12,000 per head and $22,000 per head (Stern 2006).

The UN climate change negotiations have shown that unless the United States commits to the reductions in GHG emissions needed in order to limit global warming, other nations will not do so. Without this international cooperation, all will face escalating damages and risks from climate change. Yet, some US interest groups nonetheless claim that the economic costs of reducing emissions would be unacceptably high. Such claims are baseless. All economic studies of the issue conclude that even with currently available technologies, GHG emissions can be reduced by 80 percent by 2050 without substantially affecting economic growth (Repetto 2010).

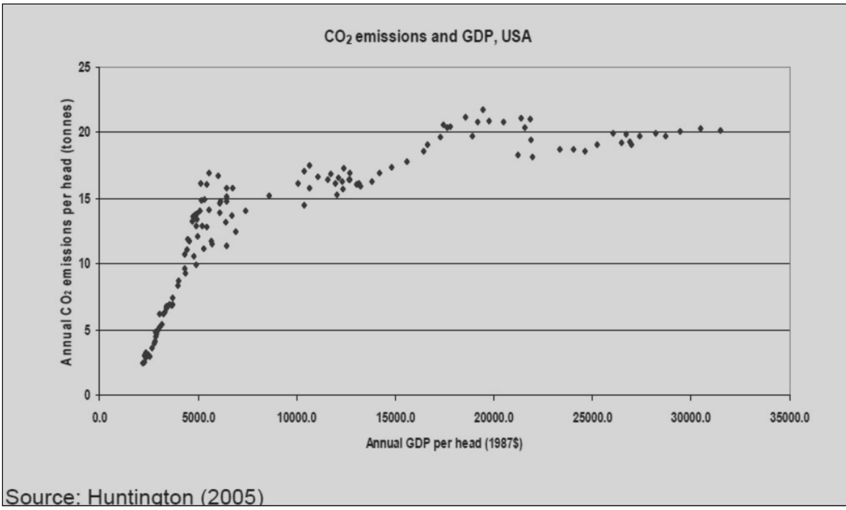

Figure 6.14. Annual emissions of CO_2 per head vs. GDP per head, USA (Huntington 2005; reproduced with permission from Elsevier)

Other nations will not make comparable efforts without committed action by the United States. International cooperation is essential: no nation or bloc of nations can achieve climate stabilization without cooperation from all major emitters. If international efforts fall short, the United States and other countries will face escalating risks of a wide range of climate change damages, including more frequent extreme weather, disruption of water supplies, frequent fire, disease and pest outbreaks, crop losses, ocean acidification and sea level rise, among other effects. These changes may become irreversible. Despite these risks, the question is whether the US economy can withstand the transition from fossil to low-carbon fuels without unacceptable costs and economic disruption (Repetto 2010).

Figure 6.15 shows the annual rate of change in the ratio of CO_2 emissions to real GDP for the historical period (left light-blue bars) and that required under current climate change legislative proposals in the United States (right light-red bars). (Nordhaus 2010). Over the last half-century, the carbon intensity of the U.S. economy has declined by an average of 1.7 percent per year (the first six left light-blue bars). That is, energy-sector CO_2 emissions have grown at a rate that is 1.7 percent per year slower than growth of real GDP. The four bars on the right in the figure show the rates of further decarbonization that the proposed legislation would require (assuming all reductions are domestic). Decarbonization would need to accelerate sharply during the coming decades, to rates of between 5 percent and a little more than 8 percent in 2018–2050.

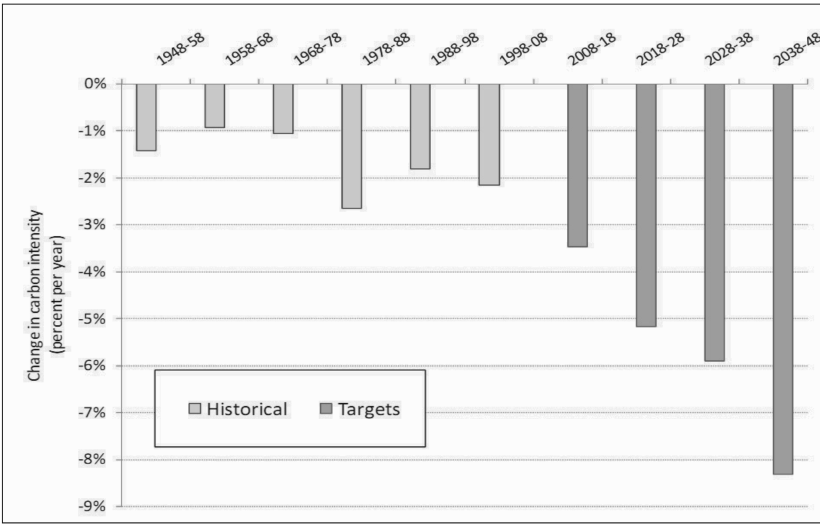

Figure 6.15. Historical and required future changes in U.S. carbon intensity (Nordhaus 2010; reproduced with permission from Elsevier)

Reducing US GHG emissions by more than 80 percent by 2050, as current Congressional bills propose, will require a far-reaching transformation of the economy. Fossil fuels will have to be largely replaced by low-carbon energy sources, and the economy must become far more energy-efficient. Failure to enact legislation to accomplish this transition will undermine efforts to build international cooperation to stabilize the global climate (Ropetto 2010). Achieving such a large decline in the CO_2-GDP ratio implies an enormous technological transition. We can get a rough idea of how enormous this would be by comparing these rates of change with the rates of technological change actually achieved in various industry groups over 1987–2006. The idea is that to achieve such a large decline in the CO_2-GDP ratio, carbon-free technologies must have differential technological change that is large relative to the rest of the economy (Nordhaus 2010).

The fundamental importance of the price of carbon in stimulating innovation for global warming. The major condition that must be met to ensure that climate-friendly innovation occurs is that the price of carbon be sufficiently high. It is difficult to see how technological change to combat global warming can be achieved unless carbon prices are at a level that internalizes the climate externality. Under very limited conditions, setting carbon prices to reflect the damages from carbon emissions is also a sufficient condition for the appropriate innovation to be undertaken in market-oriented sectors. The conclusion about price fundamentalism must be qualified if the price is wrong, for those parts of research that are not profit-driven (particularly basic research), and when energy investments have particular burdens such as networking or large scale (Nordhaus 2010).

6.4.2 In EU

Impact of climate change in Europe:

- Climate change is expected to magnify regional differences in Europe's natural resources and assets. Negative impacts will include increased risk of inland flash floods and more frequent coastal flooding and increased erosion (due to storminess and sea level rise).
- Mountainous areas will face glacier retreat, reduced snow cover and winter tourism, and extensive species losses (in some areas up to 60% under high emissions scenarios by 2080).
- In southern Europe, climate change is projected to worsen conditions (high temperatures and drought) in a region already vulnerable to climate variability, and to reduce water availability, hydropower potential, summer tourism and, in general, crop productivity.
- Climate change is also projected to increase the health risks due to heat waves and the frequency of wildfires (IPCC 2007b).

According to European Environment Agency (2009), GHG emissions in the EU-27 by gas and sector in 2007 are illustrated in Figure 6.16.

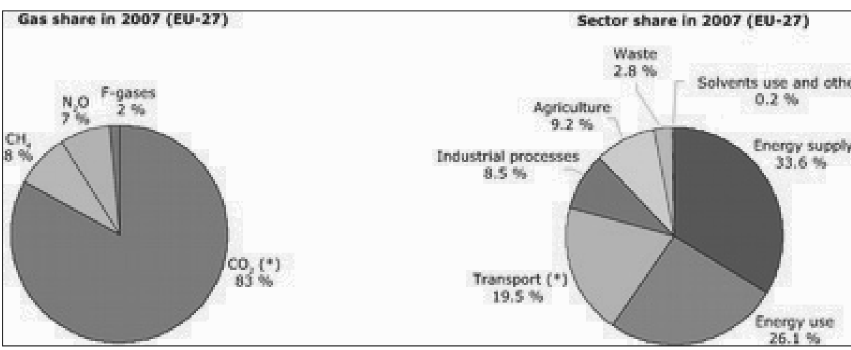

Figure 6.16. GHG emissions in the EU-27 by gas and sector in 2007 (European Environment Agency 2009)

6.4.3 In UK

Emission intensity in the manufacturing sector decreased 1.2 percent in 2008 with emissions falling at a faster rate than economic output due to lower fossil fuel consumption. The continuing switch away from coal to natural gas for electricity generation meant emissions per unit of output also fell by 2.1 percent in the electricity, gas and water supply sector. Emissions intensity fell by 3.3 percent in transport and communications, whilst increased by 0.5 per cent in agriculture as output decreased at a faster rate than emissions. These four industry sectors accounted for over 80 percent of the emissions of GHGs by the UK economy (excluding households) in 2008 and represented just over one fifth of economic output.

The first signs of the economic downturn were seen in 2008 but the decrease in emissions intensity indicates that the overall fall in greenhouse emissions was not wholly driven by reduced economic growth. Emissions intensity has continued to improve across the non-household sector and GHG emissions per unit of output in 2008 were 43.9 percent below those in 1990. According to Guardian Newspaper (2010b), UK GHG emissions of the main GHG, CO_2, fell 9.8% in 2009, while overall output of a group of six GHGs fell 8.6%. Figure 6.17 shows GHG emisions by end use between 1990 and 2008 in the UK.

According to the Department for Energy and Climate Change the estimated decrease in CO_2, from 533m tones in 2008 to 481m tones in 2009, was mainly caused by a significant fall in energy consumption as the economy contracted. A switch from coal to nuclear for electricity generation also helped, the department said.

Joan Ruddock, energy and climate change minister, said: "The significant reduction in emissions would no doubt have been impacted by the recent economic circumstances. However, we should still recognize the good progress we are making towards meeting our [climate change] targets, and should not underestimate the effort made so far by government, industry, business and homeowners alike. We are determined to continue to strengthen and sustain the momentum behind the low-carbon transition in the UK."

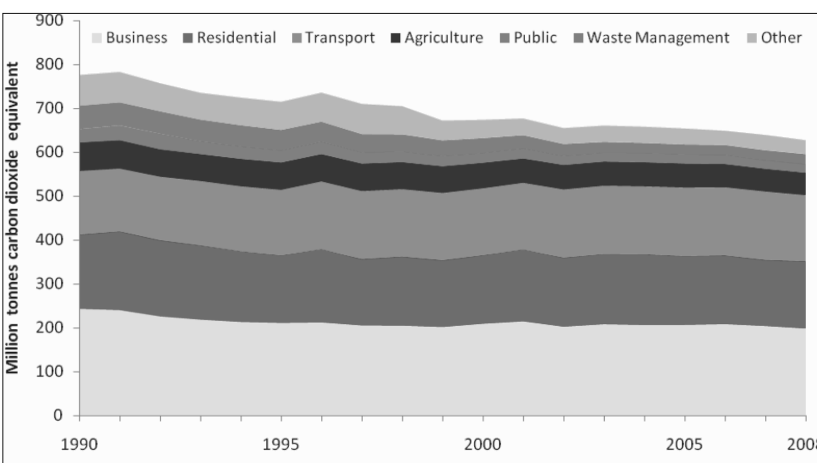

Figure 6.17. UK GHG emissions by end-user in 1990–2008 (Department of Climate Change 2010)

David Symons, director at environment consultants WSP Environment and Energy, said: "The recession forecast to reduce emission by 3 to 7% last year. That the UK actually achieved a reduction of 8.6% in GHG emissions in 2009 is very encouraging." But Andy Atkins, head of Friends of the Earth, said: "These figures suggest that UK emissions have fallen more in one year than in all the other years of the Labor government put together, but it's taken a major recession to make this happen." Department for Energy and Climate Change said the biggest falls in emissions in 2009 came from businesses and industrial processes, while a drop in domestic consumption of fossil fuels for space heating–because last year was slightly warmer than 2008–led to a drop in domestic emissions of 5%. Public sector emissions fell by just 0.1%, while transport emissions, not including international flights and shipping, fell 7% because of lower fuel consumption in the face of the recession and greater use of biofuels, Department for Energy and Climate Change said. Figure 6.18 illustrates UK CO_2 emissions by end user between 1998 and 2008.

The UK is on track to exceed its Kyoto protocol target for the period 2008–2012, which is a 12.5% cut in GHG emissions below 1990 levels. But environmental campaigners point out this has been achieved in part by the increasing use of gas to generate electricity and the export of manufacturing to other countries, rather than specific emissions reduction policies (Guardian 2010b).

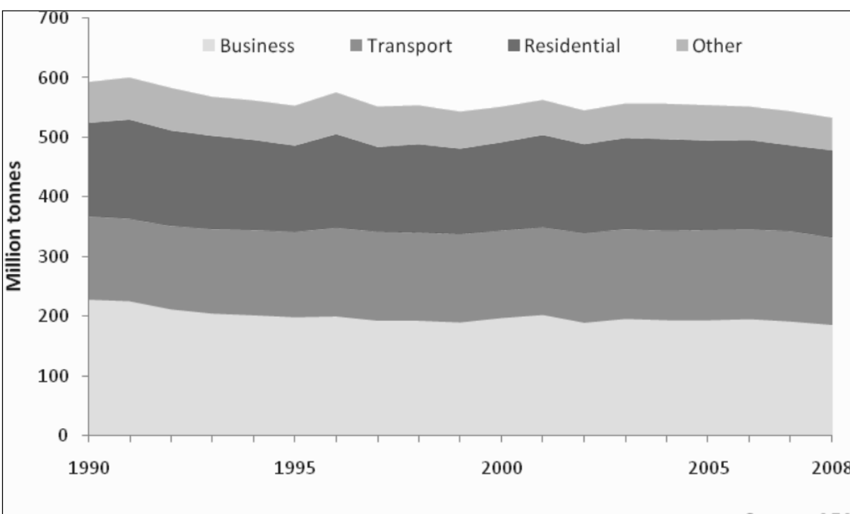

Figure 6.18. UK CO_2 emissions by end-user in 1990–2008 (Department of Climate Change 2010)

6.4.4 In Developing Countries

Impact of clımate change in Africa:

- By 2020, between 75 and 250 million of people are projected to be exposed to increased water stress due to climate change.
- By 2020, in some countries, yields from rain-fed agriculture could be reduced by up to 50%. Agricultural production, including access to food, in many African countries is projected to be severely compromised. This would further adversely affect food security and exacerbate malnutrition.
- Towards the end of the 21st century, projected sea level rise will affect low-lying coastal areas with large populations. The cost of adaptation could amount to at least 5 to 10% of GDP.
- By 2080, an increase of 5 to 8% of arid and semi-arid land in Africa is projected under a range of climate scenarios (high confidence) (IPCC 2007b)

Impact of clımate change in Asia:

- By the 2050s, freshwater availability in Central, South, East and South-East Asia, particularly in large river basins, is projected to decrease.
- Coastal areas, especially heavily populated megadelta regions in South, East and South-East Asia, will be at greatest risk due to increased flooding from the sea and, in some megadeltas, flooding from the rivers.
- Climate change is projected to compound the pressures on natural resources and the environment associated with rapid urbanisation, industrialisation and economic development.
- Endemic morbidity and mortality due to diarrhoeal disease primarily associated with floods and droughts are expected to rise in East, South and South-East Asia due to projected changes in the hydrological cycle (IPCC 2007b)

Take India as an example, impact of climate change would be:

- India’s GHG emissions rose by 58 per cent between 1994 and 2007 with the energy sector contributing over half of the emissions, a new government report said.
- But India's emissions per unit national wealth (or gross domestic product), a measure of GHG intensity, declined by 30 per cent during this period, the report showed
- India released its last emissions estimate in 1994. Minister for environment and forests Jairam Ramesh, who released the new report yesterday, said India was the first developing country to release 'updated' estimates.
- India's emissions are up from 1.2 billion tones in 1994 to 1.7 billion tones of CO_2 equivalent in 2007.

The country now ranks fifth globally in total GHG emissions, behind the United States, China, the European Union and Russia in 2007. The emissions of the United States and China are four times that of India in 2007.

India's energy sector contributed 58 percent of emissions followed by industry with 22 percent and 17 percent by agriculture. In November 2009, ahead of the international climate summit in Copenhagen, India announced it would reduce its 'GHG emission intensity'–the amount of gases released per unit growth in national wealth–by 20–25 percent between 2005 and 2020. Ramesh said India would continue to improve its methods for emission estimates, bridge data gaps and develop country-specific GHG emission estimate models. In October 2009, India announced setting up a new climate research centre and building climate satellites to improve data collection (Guardian, 2010a).

6.5 Post Kyoto and Future Policies

Continued GHG emissions at or above current rates would cause further warming and induce many changes in the global climate system during the 21st century that would very likely be larger than those observed during the 20th century. For the next two decades a warming of about 0.2°C per decade is projected for a range of SRES emissions scenarios. Even if the concentrations of all GHGs and aerosols had been kept constant at year 2000 levels, a further warming of about 0.1°C per decade would be expected. Afterwards, temperature projections increasingly depend on specific emissions scenarios (IPCC 2007a).

There is high confidence that neither adaptation nor mitigation alone can avoid all climate change impacts. Adaptation is necessary both in the short term and longer term to address impacts resulting from the warming that would ocur even for the lowest stabilisation scenarios assessed. There are barriers, limits and costs that are not fully understood. Adaptation and mitigation can complement each other and together can significantly reduce the risks of climate change. Adaptation will be ineffective for some cases such as natural ecosystems the disappearance of mountain glaciers that play vital roles in water storage and supply, or adaptation to sea level rise of several metres. It will be less feasible or very costly in many cases for the projected climate change beyond the next several decades (such as deltaic regions and estuaries). There is high confidence that the ability of many ecosystems to adapt naturally will be exceeded this century. Even under worst-case assumptions built into models, as GHG emissions fall by 80 percent by 2050, economic impacts are mild, and economic growth will continue robustly despite higher delivered energy prices. Under worst-case assumptions gross domestic product and household consumption might be 1 to 3 percent lower by 2030 than in the baseline scenario because of higher energy prices. This implies a marginally slower rate of economic growth over two decades, from about 2.71 percent per year to 2.68 percent per year. This predicted difference in growth rates is much smaller than the error such models make in forecasting economic growth over these lengths of time (Repetto 2010). In addition, multiple barriers and constraints to effective adaptation exist in human systems Unmitigated climate change would, in the long term, be likely to exceed the capacity of natural, managed and human systems to adapt. Reliance on adaptation alone could eventually lead to a magnitude of climate change to which effective adaptation is not possible, or will only be available at very high social, environmental and economic costs (IPCC 2007b).

The availability of technological options significantly affects costs. If the expansion of nuclear power is limited, if carbon capture and storage from coal and gas-fired power plants proves infeasible or prohibitively expensive, or if the expansion of wind, solar and geothermal power is restricted by a lack of transmission facilities, then the costs of achieving the reduction in emissions will be much higher. The analyses also find that policy choices are important: good policy choices can substantially reduce costs. The most cost-effective way of implementing a large, long-term reduction in GHG emissions is to create an economy-wide price on carbon through a comprehensive cap-and-trade system. "What, where and when" flexibility lowers costs compared to command-and-control approaches. A comprehensive approach lowers costs by including all sources of emissions. If some sources are left uncontrolled, some low-cost mitigation options may be sacrificed, and there must be tighter controls on the remaining ones, leading to inefficiencies, higher abatement costs and higher energy prices (Repetto 2010, page 6).

The role of technology and efficiency in breaking the link between growth and emissions. The relationship between economic development and CO_2 emissions growth is not immutable. Historically, there have been a number of pervasive changes in energy systems, such as the decline in steam power, the spread of the internal combustion engine and electrification. The adoption of successive technologies changed the physical relationship between energy use and emissions. The ability of energy technologies to reduce GHG emissions extends beyond energy efficiency. In particular, technologies and fuels that produce energy with lower CO_2 emissions are crucial if such emissions are to be reduced (Brown et al. 1998).

A number of authors have identified in several countries structural breaks in the observed relationship that are likely to have been the result of such switches (Lanne and Liski 2004; Huntington 2005). Using US data, Huntington (2005) found that, after allowing for these technology shifts, the positive relationship between emissions per head and income per head has remained unchanged, casting some doubt on the scope for changes in the structure of demand to reduce emissions in the absence of deliberate policy. Also, an MIT study suggests that, since 1980, changes in US industrial structure have had little effect on energy intensity (Sue-Wing and Eckaus 2004). Shifts usually entailed switching from relatively low-energy-density fuels (e.g. wood, coal) to higher-energy density ones (e.g. oil), and were driven primarily by technological developments, not income growth (although cause and effect are difficult to disentangle, and changes in the pattern of demand for goods and services may also have played a role). The energy innovations and their diffusion were largely driven by their advantages in terms of costs, convenience and suitability for powering new products. As the discussion of technology below suggests given the current state of knowledge, alternative technologies do not appear, on balance, to have the inherent advantages over fossil-fuel technologies (e.g. in costs, energy density or suitability for use in transport) necessary if decarbonisation were to be brought about purely by private commercial decisions. Strong policy will therefore be needed to provide the necessary incentives.

Technical progress in the energy sector and increased energy efficiency are also likely to moderate emissions growth. For instance, illustrates that the efficiency with which energy inputs are converted into useful energy services in the United States has increased seven-fold in the past century. One study has found that innovations embodied in information technology and electrical equipment capital stocks have played a key part in reducing energy intensity over the long term (Sue-Wing and Eckaus 2004). But, in the absence of appropriate policy, incremental improvements in efficiency alone will not overwhelm the income effect. For example, a review of projections for China carried out for the Stern (2006) suggests that energy demand is very likely to increase substantially in 'business as usual' scenarios, despite major reductions in energy intensity. In the USA, emissions per head are projected to rise whenever income per head grows at more than 1.8% per year (Huntington 2005). But the scale of potential cost-effective energy efficiency improvements, which will be explored elsewhere in this Review, indicates that energy efficiency and reductions in energy intensity constitute an important and powerful part of a wider strategy. Figure 6.19 illustrates efficiency gains from technological improvements to cut CO_2 emission successfully by 2050. According to Figure 6.19, baseline emissions of 57 Gt can be reduced to Blue Map emissions of 14 Gt by 2050 throughout gaining 38% efficiency in end-use fuel and electricity, 15% efficiency from end-use fuel switching, 5% efficiency from power generation and fuel switching, 6% efficiency from nuclear, 17% efficiency from renewable and 19% efficiency from CCS.

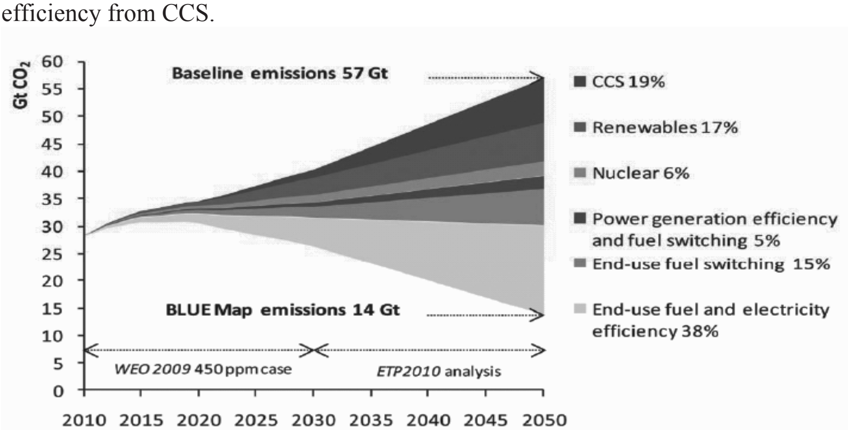

Figure 6.19. Technology and CO_2 emission cut (IEA Energy Technology Perspective 2010)

Efforts to mitigate GHG emissions to reduce the rate and magnitude of climate change need to account for inertia in the climate and socio-economic systems. After GHG concentrations are stabilised, the rate at which the global average temperature increases is expected to slow within a few decades. Small increases in global average temperature could still be expected for several centuries. Sea level rise from thermal expansion would continue for many centuries at a rate that eventually decreases from that reached before stabilisation, due to ongoing heat uptake by oceans. Delayed emission reductions significantly constrain the opportunities to achieve lower stabilisation levels and increase the risk of more severe climate change impacts. Even though benefits of mitigation measures in terms of avoided climate change would take several decades to materialise, mitigation actions begun in the short term would avoid locking in both long-lived carbon intensive infrastructure and development pathways, reduce the rate of climate change and reduce the adaptation needs associated with higher levels of warming (IPCC 2007b).

Figure 6.20 illustrates, in gray lines at the top, the projected business-as-usual emissions from 2000 to 2050 in six of these leading models. All projections are referenced to the latest available Annual Energy Outlook produced by the Department of Energy's Energy Information Agency in 2005, and take into account the most recent available energy legislation and economic forecasts. Nonetheless, it is obvious that different models predict widely different growth rates of emissions in future years under business-as-usual assumptions. In the most optimistic, emissions grow from about 7 to about 8 billion tons over 50 years; in the least optimistic, they increase to about 11 billion tons, a percentage increase more than three times as rapid. The lines in red at the bottom of the Figure 6.20 represent the mitigation trajectories that all analysts used as a basis for comparing model results. The steepest decline represents approximately an 80 percent reduction from emissions in 2005.

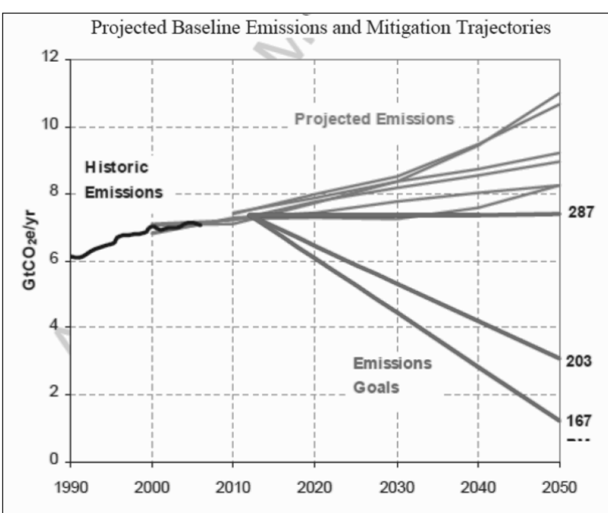

Figure 6.20. Projected baseline emissions and mitigation (Annual Energy Outlook 2005)

There is high agreement and much evidence that all stabilisation levels assessed can be achieved by deployment of a portfolio of technologies that are either currently available or expected to be commercialised in coming decades, assuming appropriate and effective incentives are in place for development, acquisition, deployment and diffusion of technologies and addressing related barriers. Worldwide deployment of low-GHG emission technologies as well as technology improvements through public and private RD&D would be required for achieving stabilisation targets as well as cost reduction (IPCC 2007b).

Figure 6.21 gives illustrative examples of the contribution of the portfolio of mitigation options. The contribution of different technologies varies over time and region and depends on the baseline development path, available technologies and relative costs, and the analysed stabilisation levels. Stabilisation at the lower of the assessed levels (490 to 540 ppm CO_2e) requires early investments and substantially more rapid diffusion and commercialisation of advanced low-emissions technologies over the next decades (2000–2030) and higher contributions across abatement options in the long term (2000–2100). This requires that barriers to development, acquisition, deployment and diffusion of technologies are effectively addressed with appropriate incentives. Without sustained investment flows and effective technology transfer, it may be difficult to achieve emission reduction at a significant scale. Mobilising financing of incremental costs of low-carbon technologies is important.

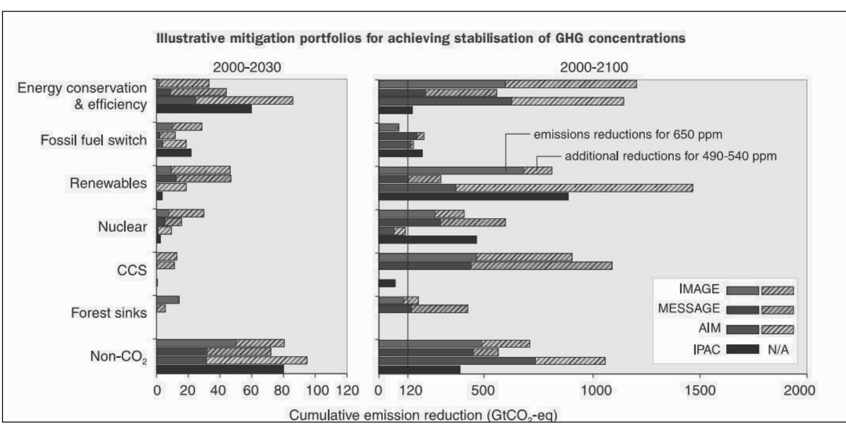

Figure 6.21. Mitigation portfolios (IPCC 2007b)

There are large uncertainties concerning the future contribution of different technologies. However, all assessed stabilisation scenarios concur that 60 to 80% of the reductions over the course of the century would come from energy supply and use and industrial processes. Including non-CO_2 and CO_2 land-use and forestry mitigation options provides greater flexibility and cost-effectiveness. Energy efficiency plays a key role across many scenarios for most regions and time scales. For lower stabilisation levels, scenarios put more emphasis on the use of low-carbon energy sources, such as renewable energy, nuclear power and the use of CO_2 capture and storage (CCS) (Figure 6.21).

Figure 6.21 illustrates cumulative emissions reductions for alternative mitigation measures for 2000–2030 (left-hand panel) and for 2000–2100 (right-hand panel). The figure shows 'illustrative scenarios from four models aiming at the stabilisation at low (490 to 540 ppm CO_2e) and intermediate levels (650 ppm CO_2e) respectively. Dark bars denote reductions for a target of 650 ppm CO_2e and light bars denote the additional reductions to achieve 490 to 540 ppm CO_2e. Note that some models do not consider mitigation through forest sink enhancement and that the share of low-carbon energy options in total energy supply is also determined by inclusion of these options in the baseline. CCS includes CO_2 capture and storage from biomass. Forest sinks include reducing emissions from deforestation. The figure shows emissions reductions from baseline scenarios with cumulative emissions between 6000 to 7000 Gt CO_2e (2000–2100) (IPCC 2007b).

6.6 Conclusions

Stabilising the stock of GHGs requires urgent, substantial action to reduce emissions, firstly to ensure that emissions peak in the next few decades and secondly, to make the rate of decline in emissions as low as possible. Based on research we have shown that future stabilisation pathways are dependent on assumptions about energy intensity and, therefore, energy efficiency throughout technological changes and government alternative plans. If insufficient action is taken now to reduce emissions, stabilisation will become more difficult in the longer term, in terms of the speed of the transition required and the consequent costs of mitigation.

It is very likely that hot extremes, heat waves and heavy precipitation events will become more frequent and it is more likely that future tropical cyclones (typhoons and hurricanes) will become more intense, with larger peak wind speeds and more heavy precipitation associated with ongoing increases of tropical sea-surface temperatures. There is less confidence in projections of a global decrease in numbers of intense storms since 1970 in some regions is much larger than simulated by current models for that period (IPCC 2007b). 'Anthropogenic warming and sea level rise would continue for centuries due to the time scales associated with climate processes and feedbacks, even if GHG concentrations were to be stabilised. If radiative forcing were to be stabilised, model experiments show that a further increase in global average temperature of about 0.5°C would still be expected by 2200. In addition, thermal expansion alone would lead to 0.3 to 0.8m of sea level rise by 2300 (relative to 1980–1999). Thermal expansion would continue for many centuries, due to the time required to transport heat into the deep ocean' (IPCC 2007a).

The cost of mitigation is huge, and there are many other barriers we face. Removing of these barriers to the uptake of more efficient technologies and methods can be a good starting point. According to the report of New Economic Foundation (2010), barriers for energy efficiency improvements are as follows:

- **Technical barriers:** Options may not yet be available, or actors may consider options not sufficiently proven to adopt them.
- **Knowledge/information barriers:** Actors may not be informed about possibilities for energy-efficiency improvement. Or they know certain technologies, but they are not aware to what extent the technology might be applicable to them.
- **Economic barriers:** The standard economic barrier is that a certain technology does not satisfy the profitability criteria set by firms. Another barrier can be the lack of capital for investment. Also the fact that the old equipment is not yet depreciated can be considered as an economic barrier.
- **Institutional barriers:** Especially in energy-extensive companies there is no well-defined structure to decide upon and carry out energy-efficiency investments.
- **The investor-user or landlord-tenant barrier:** This barrier is a representative of a group of barriers that relate to the fact that the one carrying out an investment in energy efficiency improvement (e.g., the owner of an office building) may not be the one who has the financial benefits (in this example the user of the office building who pays the energy bill).
- **Lack of interest in energy-efficiency improvement:** May be considered as an umbrella barrier. For the vast majority of actors, the costs of energy are so small compared to their total (production or consumption) costs that energy-efficiency improvement is even not taken into consideration. Furthermore, there is a tendency that companies, organisations and households focus on their core activities only.

In particular, costs include the expense of developing and deploying low-emission, high-efficiency technologies and the cost to consumers of switching spending from emissions-intensive to low-emission goods and services are the most important ones among many other. But we can still stabilise emissions in several ways: reducing demand for carbon-intensive products, increasing energy efficiency, switching to low-carbon technologies and adopting a better government policy. According to Stern Review an estimate of resource costs suggests that the annual cost of cutting total GHG to about three quarters of current levels by 2050, consistent with a 550 ppm CO_2e stabilisation level, will be in the range –1.0 to +3.5% of GDP, with an average estimate of approximately 1%. By employing low-carbon technologies, supporting the improvements in energy efficiency and adapting the most appropriate government policies we can save both money and reduce emission at the same time. Otherwise, without early, well planned actions the costs of mitigations will be greater, more damaging and irreversible.

6.7 References

Allaby, M. (2008). *A Dictionary of Earth Sciences*. Oxford University Press, USA.

Binmore, K., and Klemperer, P. (2002). "The biggest auction ever: the sale of the British 3G telecom licenses." *Economic Journal*, 112, 74–96.

Breecker, D., Sharp, Z., and McFadden, L. (2010). "Atmospheric CO_2 concentrations during ancient greenhouse climates were similar to those predicted for A.D. 2100." *Proceedings of the National Academy of Sciences,* 107, 576–580.

Brown, S., Lim, B., and Schlamadinger, B. (1998). *Evaluating Approaches to Estimating Net Emissions of Carbon Dioxide from Forest Harvesting and Wood Products*. IPCC/OECD/IEA Programme on National Greenhouse Gas Inventories.

Bruce, J., Lee, H., and Haites, E. (1996). *Climate Change 1995–Economic and Social Dimensions of Climate Change*. Contribution of Working Group III to the Second Assessment Report of the Intergovernmental Panel on Climate Change. *Cambridge University Press*, Cambridge.

CDIAC (Carbon Dioxide Information Analysis Center). (2010). "Recent Greenhouse Gas Concentrations." DOI: 10.3334/CDIAC/atg.032, <http://cdiac.ornl.gov/pns/current_ghg.html> (Retrieved on September 2010).

Cole, J. J., Caraco, N. F., Kling, G. W., and Kratz, T. K. (1994). "Carbon dioxide supersaturation in the surface waters of lakes." *Science* 265, 1568–1570.

Dasgupta, P. (2007). "Comments on the Stern Review's Economics of Climate Change." *University of Cambridge*. November 11 2006. (Revised: December 12).

Department of Climate Change (DECC) (2010). *2008 Greenhouse Gas Emıssıons, Fınal Fıgures By End-User*. <http://www.decc.gov.uk/assets/decc/statistics/climate_change/1_20100414165435_e_@@_ghgnatstatsrelease140410rev1.pdf > (Retrieved on July 2010).

Engelhaupt, E. (2007). "Models underestimate global warming impacts." *Environmental Science and Technology*, 41, 4488–4489.

European Environment Agency (2009). "Greenhouse gas CO_2" Total GHG emissions in EU, 1990–2007. <dataservice.eea.europa.eu/PivotApp/pivot.aspx?pivoted =475> [Retrieved on July 2010).

Folland, C. K., Rayner, N. A., Brown, S. J., Smith, T. M., Shen, S. S. P., Parker, D. E., Macadam, I., Jones, P. D., Jones, R. N., Nicholls, N. and Sexton, D. M. H. (2001). "Global temperature change and its uncertainties since 1861." *Geophysical Research Letters 2*8 2621–2624.

Forster, P., Ramaswamy, V., Artaxo, P., Berntsen, T., Betts, R., Fahey, D. W., Haywood, J., Lean, J., Lowe, D. C., Myhre, G., Nganga, J., Prinn, R., Raga, G., Schulz, M., and Van Dorland, R. (2007). *Changes in atmospheric constituents and in radioactive forcing.* Fourth Assessment Report of Working Group I of the Intergovernmental Panel on Climate Change. In: *Climate Change*. *CambridgeUniversity Press*, UK.

Forster, P. M., Shine, K. P., and Stuber, N. (2006). "Correction to it is premature to include non-CO_2 effects of aviation in emission trading schemes." *Atmospheric Environment*, 40, 1117–1121.

Gohar, L. K., and Shine, K. P. (2007). “Equivalent CO_2 and its use in understanding the climate effects of increased greenhouse gas concentrations.” *Weather*, 62, 307–311.

Guardian (2010a). “India's greenhouse gas emissions rise by 58%.” <http://www.guardian.co.uk/environment/2010/may/12/india-greenhouse-gas-emissions-rise> (12 May 2010).

Guardian (2010b). “UK greenhouse gas emissions drop by 8.6%.” <http://www.guardian.co.uk/environment/2010/mar/25/uk-greenhouse-gas-emissions-drop> (25 March 2010).

Heffernan, O. (2009). “Copenhagen summit urges immediate action on climate change.” *Nature News* (March12).

Hendry, D. (2010). “Climate change: Lessons for our future from the distant past.” Department of Economics Discussion Paper Series, No. 485, May 2010. University of Oxford.

Holtsmark, B. (2006). ‘Are Global Per Capita CO2 Emissions Likely to Remain Stable? *Energy and Environment*, 17(2), March.

Hovi, J., and Holtsmark, B. (2006). “Cap-and-trade or carbon taxes? The feasibility of enforcement and the effects of non-compliance.” İn *International Environmental Agreements: Politics, Law and Economics*, *Springer*, 6(2), 137–155.

Huntington, T. G. (2005). “Evidence for intensification of the global water cycle: review and synthesis.” *Journal of Hydrology*, 319, 83–95.

International Energy Agency (IEA) (2007). *Tracking Industrial Energy Efficiency and CO_2 Emissions*, Paris, France.

International Energy Agency (IEA) (2008). “Price caps and price floors in climate policy: A quantitative assessment.” By Cédric Philibert, International Energy Agency, December 2008, IEA Information Paper <http://www.iea.org/papers/2008/price_caps_floors_web.pdf> (accessed Aug. 2011).

International Energy Agency (IEA) (2009). “CO_2 emissions from fuel combustion: Beyond 2020 documentation.” <http://wds.iea.org/wds/pdf/documentation_co2_2009.pdf> (accessed Aug. 2011).

International Energy Agency (IEA). “Energy technology perspective (2010).” Implementation through Multilateral Co-operation. <http://www.iea.org/papers/2010/technology_initiatives.pdf> (accessed Aug. 2011).

International Energy Agency (IEA) (2010). “Energy technology perspective (2010).” <http://www.iea.org/Textbase/npsum/ETP2010SUM.pdf> (accessed 08/2011).

International Monetary Fund (IMF) (2007). *International Monetary Fund, World Economic Outlook Database*, <http://www.imf.org/external/pubs/ft /weo/2006/01/pdf/weo0406.pdf> (Retrieved on June 2010).

Intergovermental Panel on Climate Change (IPCC) (2000). *IPCC Special Report on Emissions Scenarios (SRES)*, UNEP, WMO, Hague.

Intergovermental Panel on Climate Change (IPCC) (2007a). *Climate change 2007: Synthesis Repor*t. Contribution of Working Group I, II and III to the Fourth Assessment Report of the Intergovernmental Panel on Climate Change (Geneva, Switzerland: IPCC).

Intergovermental Panel on Climate Change (IPCC) (2007b). *Towards New Scenarios for Analysis of Emissions, Climate Change, Impacts, and Response Strategies: Technical Summary* (Noordwijkerhout, the Netherlands: IPCC).

Intergovermental Panel on Climate Change (IPCC) (2010). *Climate change 2007: Synthesis Report*. Contribution of Working Group I, II and III to the Fourth Assessment Report of the Intergovernmental Panel on Climate Change (Geneva, Switzerland: IPCC).

Intergovermental Panel on Climate Change (IPCC) (2010). *The UN Global Warming Report Facts and Predictions* (Geneva, Switzerland: IPCC).

Isermann, K. (1994). "Agriculture's share in the emission of trace gases affecting the climate and some cause-oriented proposals for sufficiently reducing this share." *Environmnetal Polution*, 83 (1–2), 95–111.

Ishikawa, J., and Kiyono, K. (2006). "Greenhouse-gas emission controls in an open economy international." *Economic Review,* 47(2), 431–450.

Jones, M. D., Roberts, C. N., Leng, M. J., and Turkes, M. (2006). "A high-resolution late Holocene lake isotope record from Turkey and links to North Atlantic and monsoon climate." *Geology*, 34, 361–364.

Kaya, Y. (1990). "Impact of carbon dioxide emission control on GNP growth: Interpretation of proposed scenarios." Paper presented to the IPCC Energy and Industry Subgroup, Response Strategies Working Group, Paris.

Klemperer, P. (2002). "What really matters in auction design." *The Journal of Economic Perspectives*, 16, 169–189.

Klemperer, P. (2009). "What is the top priority on climate change?" In Schellnhuber, H.-J., Molina, M., Stern, N., Huber, V., and Kadner, S. (eds.), *Global Sustainability–A Nobel Cause* 231–240: Lavoisier, France.

Knight, J., Kennedy, J., Folland, C., Harris, G., Jones, G, Palmer, M., Parker, D., Scaife, A., and Stott, P. (2009). "Do global temperature trends over the last decade falsify climate predictions?" *Bulletin of the American Meteorological Society*, 90, S22–S23.

Lanne, M., and Liski, M. (2004). "trends and breaks in per-capita carbon dioxide emissions, 1870–2028." *The Energy Journal*, *International Association for Energy Economics* 25(4), 41–66.

Le Quéré, C., Raupach, M., Canadell, J., Marland, G., Bopp, L., Ciais, P., Conway, T., Doney, S., Feely, R., Foster, P., Friedlingstein, P., Gurney, K., Houghton, R., House, J., Huntingford, C., Levy, P., Lomas, M., Majkut, J., Metzl, N., Ometto, J. P., Peters, P., Prentice, C., Randerson, J., Running, S., Sarmiento, J., Schuster, U., Sitch, S., Takahashi, T., Viovy, N., van der Werf, G., and Woodward, F. (2009). "Trends in the sources and sinks of carbon dioxide." *Nature Geosciences 2*, 831–836.

McCarl, B. A., and Scheneider, U. S. (2001). "Clımate change: Greenhouse gas mitigation in U.S. agriculture and forestry." *Science*, 294 (5551) 2481–2482.

McKibbin, W. J., and Wilcoxen, P. J. (2002). "Climate change after Kyoto: Blueprint for a realistic approach." Monograph, The Brookings Institution, Washington.

McKitrick, R., and Strazicich, M.C. (2005). "Stationarity of global per capita carbon dioxide emissions: Implications for global warming scenarios." Working Papers 0503, University of Guelph, Department of Economics.

Milgrom, P. (2004). *Putting Auction Theory to Work*. Cambridge: Cambridge University Press.

National Oceans and Atmospheric Adminstration (NOAA) (2007). 2007 a Top Ten Warm Year for U.S. and Globe. United States Department of Commerce.

National Oceanic and Atmostpheric Administration (NOAA) (2010). United States Department of Commerce. <http://www.esrl.noaa.gov/gmd/ccgg/trends/> (Retrieved on June 2010)

National Oceans and Atmospheric Adminstration (NOAA) (2010). Trends in Atmospheric Carbon Dioxide-Full Mouna Loa CO_2 records 1960–2010. National Oceanic and Atmospheric Administration

Neumayer, E. (2004). "National carbon dioxide emissions: Geography matters.''*Area*, 36 (1), 33–40.

New Economic Foundation (NEF) (2010). "Growth isn't possible: Why we need a new economic direction." By A. Simms, V. Johnson, and P. Chowla, *New Economic Foundation*: *London*, <http://www.neweconomics.org/sites/neweconomics.org/files/Growth_Isnt_Possible.pdf> (Retrieved on June 2010).

Nordhaus, W. (2007). "The Stern Review on the economics of climate change." Yale University, USA. <http://nordhaus.econ.yale.edu/stern_050307.pdf.> (accessed April 2012).

Nordhaus, W. (2010). "Designing a friendly space for technological change to slow global warming" at the two Snowmass Conferences on Technologies to Combat Global Warming in 2008 and 2009.

Pearce, D. (2003). "The social cost of carbon and its policy implications." *Oxford Review of Economic Policy*, 19(3), 362–384.

Peterson, T., and Baringer, M. (2009). "State of the climate in 2008." *Bulletin of the American Meteorological Society*, 90, S1–S196.

Pierrehumbert, R. T. (2004). "High levels of atmospheric carbon dioxide necessary for the termination of global glaciation." *Nature,* 429, 646–649.

Quah, D. (1996). "The invisible hand and the weightless economy." CEP occasional paper; 12. Centre for Economic Performance, London School of Economics and Political Science, London.

Ramanathan, V., and Feng, Y. (2008). "On avoiding dangerous anthropogenic interference with the climate system: Formidable challenges ahead." *Proceedings of the National Academy of Sciences*, 105, 14245–14250.

Repetto, R. (2010). *Economic Impacts of Reducing Greenhouse Gas Emissions*. United Nations Foundation.

Richardson, K., Steffen, W., Schellnhuber, H., Alcamo, J., Barker, T., Kammen, D., Leemans, R., Liverman, D., Munasinghe, M., Osman-Elasha, B., Stern, N., and Wæver, O. (2009). *Synthesis report from "Climate change: Global risks, challenges and decisions*. Copenhagen: University, Copenhagen.

Richmond, A. (2007). *Environmnetal Kuznets Curve*. Encyclopedia of Earth, C. J. Cleveland (ed.) (Washington, D.C: Environmental Information Coalition, National Council for Science and the Environment).

Rosenzweig, C., Karoly, D., Vicarelli, M., Neofotis, P., Casassa, Q., Menzel, A., Root, T., Estrella, N., Seguin, B., Tryjanowski, P., Liu, C., Rawlins, S., and

Imeson, A. (2008). “Attributing physical and biological impacts to anthropogenic climate change.” *Nature*, 453, 353–357.

Roth, A. E. (2002). “The economist as engineer: Game theory, experimentation, and computation as tools for design economics.” *Econometrica*, 70, 1341–1378.

Stern, D. I. (1996). “Economic growth and environmental degradation: The environmental Kuznets curve and sustainable development.” *World Development* 24(7), 1151–1160.

Stern, D. I. (2004). “The rise and fall of the environmental Kuznets curve.” *World Development*, 32(8), 1419–1439.

Stern, N. (2006). *The Economics of Climate Change: The Stern Review*. Cambridge, UK: Cambridge University Press 2007. online at <http://www.hm-treasury.gov.uk/independent_reviews/stern_review_economics_climate_change/sternreview_index.cfm> (accessed April 2011).

Solomon, S., Qin, D., Manning, M., Marquis, M., Averyt, K., Tignor, M., Miller, H., and Chen, Z. (2007a). *Climate Change 2007: The Physical Science Basis*. Contribution of Working Group I to the Four Assessment Report of the Intergovernmental Panel on Climate Change, Cambridge University Press, Cambridge.

Solomon, S., Rosenlof, K. H., Portmann, R. W., Daniel, J. S., Davis, S. M., Sanford, T. J., and Plattner, G. K. (2007b). “Contributions of stratospheric water vapor to decadal changes in the rate of global warming.” *Science*, 327 (5970), 1219 – 1223.

Sue-Wing, I., and Eckaus, R. S. (2004). *Explaining Long-Run Changes in the Energy Intensity of the U.S. Economy*. MIT Joint Program on the Science and Policy of Global Change Report, vol. 116.

Swanson, K., and Tsonis, A. (2009). “Has the climate recently shifted?” *Geophysical Research Letters*, 36, L06711.

USEPA (United States Environment Protection Agency). (2007). Climate Leaders Fact Sheet, December 2007.

United Nations Statistic Division (2008). List of countries by carbon dioxide emissions. United Nations Millennium Development Goals Indicators. New York City. <http://mdgs.un.org/unsd/mdg/SeriesDetail.aspx?srid=749&crid=/> (Retrieved on June 2010).

Watson, R. T., Zinyowera, M. C., Moss, R. H., and Dokken, D. J. (1996). *Climate Change 1995–Impacts, Adaptations and Mitigation of Climate Change: Scientific-Technical Analyses*. Contribution of Working Group II to the Second Assessment Report of the Intergovernmental Panel on Climate Change. Cambridge University Press, Cambridge.

Watson, A. J., Bakker, D. C. E., Boyd, P. W., Ridgwell, A. J., and Law, C. S. (2000). “Effect of iron supply on Southern Ocean CO_2 uptake and implications for glacial atmospheric CO_2”. *Nature,* 407, 730–733.

Watson, A. J., Schuster, U., Bakker, D. C. E., Bates, N., Corbiere, A., Gonzalez-Davila M., Friedrich, T., Hauck, J., Heinze C., Johannessen T., Kortzinger A., Metz N., Olaffson, J., Oschlies, A., Pfeil, B., Olsen A., Oschlies, A., Santano-Casiano, J. M., Steinhoff T., Telszewski M., Rios, A., Wallace, D. W. R., and

Wanninkhof, R. (2009). “Tracking the variable North Atlantic sink for atmospheric CO_2.” *Science*, 326 (5958), 1391–1393.

World Resources Institute (2006). *Target: Intensity. An Analysis of Greenhouse Gas Intensity Targets*. Washington, DC.

World Resources Institute (2009a). Climate Analysis Indicator Tools, Washington, DC. Available at <http://earthtrendsdelivered.org/international_comparison_of _ghg_ emissions_by_sector_2005> (accessed April 2012).

World Resources Institute (2009b). World Greenhouse Gas Emissions in 2005. Available at <http://www.wri.org/publication/world-greenhouse-gas-emissions-in-2005> (Retreived on June 2010).

Wuebbles, D., Hayhoe, K., Kotamarthi, R. (2000). “Atmospheric methane in the global environment.” In: Khalil, M. (ed.), *Atmospheric Methane: Its Role in the Global Environment*. Springer-Verlag, New York, NY, 304–341.

CHAPTER 7

Impact of Greenhouse Gas Emissions and Climate Change on Human Development: Perspectives on Measurement

Amitabh Kundu and Lopamudra Ray Saraswati

7.1 Introduction

The serious impact of greenhouse gas (GHG) emissions on climate change, leading to a degradation of the parameters of human development, the growing "gap between scientific evidence and political response" (UNDP 2008) and the failures to design and operationalise a low-carbon climate resilient development strategy at the global level, has underlined the need to monitor the trends in climatic parameters at regional and sub-regional levels. In the absence of an international mechanism to regulate the emissions of GHG and the pattern of economic activities at national level, the regional or bilateral initiatives are being considered as extremely important to work out a roadmap for the future. Such initiatives can be greatly facilitated if a set of temporally and cross-sectionally comparable indicators can be built up and monitored. This underlines an urgent need to formalize a methodology to determine the degree of exposure, sensitivity, mitigation initiatives and adaptation capacity etc. through a set of transparent and robust indicators and put these in public domain.

Given this macro scenario, the present chapter overviews the indices that have been proposed in recent years to measure different aspects of climate change, including the causal factors like greenhouse gas (GHG) emissions and their impact on vulnerability within the framework of human development. It thus addresses the critical issues pertaining to the assessment of the impact of climate linked factors on socio-spatial development and vice versa. The exercise is helpful also in evolving a methodology for environmental accounting and computation of green income, often used as the basis for restructuring growth strategies for mitigating depletion of non-renewable resources and ensuring their use without compromising sustainability of development. The focus here is on conceptual issues underlying the tools of measurement, examination of their implications for the empirical realities of the region and proposing modifications for better capturing the ground situation.

In the second section which follows the present introductory section, an attempt is made to understand the nature and problems of climate change and the impact of the global and regional initiatives. It also overviews the perspectives of the UN Framework Convention on Climatic Change (UNFCCC) and the negotiations around them, along with the findings of select research studies with the objective of developing a mechanism for intervening and monitoring based on a set of well-defined vulnerability indicators. It underlines the urgent need for working out acceptable measures of vulnerability, incorporating the dimensions of exposure, sensitivity, GHG emissions and adaptive capacity at the level of countries/regions. The problems of the developing countries in the context of impact of climate change and adopting the recommendations of the international organizations have been reviewed in the next section. Suitability or otherwise of the commonly used indicators of vulnerability for these countries, whose capability to adapt is low because of their geographical specificities and socio-economic characteristics, is also discussed in the section. A methodological framework has been proposed in the final section along with a perspective for selection of indicators in the context of developing countries within the human development framework. A few modifications or realignments have been proposed in the indices to focus on geographically isolated countries, vulnerable people, occupational categories, socio-religious groups etc., taking the data availability and their reliability into consideration. An attempt is also made here to ensure that the new measures are not totally unconnected with those employed in the global comparisons today.

7.2 Global Concerns and Initiatives for Dealing with the Impact of Climate Change

The international political response to climate change began with some seriousness with the adoption of the UNFCCC in 1992, with 194 countries endorsing it as ‘Parties’. It put forward a framework for action aimed at stabilizing atmospheric concentrations of greenhouse gases. A landmark Protocol was signed in 1997, at the third Conference of the Parties (COP 3) of the UNFCCC in Kyoto. It made the industrialized countries and countries in transition to commit significant emission reduction within a time frame. The thirty-nine developed and transitional countries, agreed to reduce their overall emissions of six greenhouse gases by an average of 5.2% below 1990 levels by 2012. The spirit of the Protocol was apportionment of responsibility on major polluting countries based on historical data and norms of per capita emission. Despite the equity concerns, grievances were expressed that the Protocol did not adequately address the problems of the developing countries, particularly the small island states. Anna Reynolds, Coordinator for the Climate Action Network Australia, argued that it failed to include the “developing Asian countries in the discussion of global warming", despite their being the most vulnerable in the world.

The Protocol nonetheless has been credited for boldly raising a number of complex political, technical and legal issues, arising out of their differing perspectives of the nations, geophysical character, nature and degree of exposure to climatic factors and current levels and future strategies of economic development, that are yet to be resolved. While Australia and Japan have made a strong plea to use carbon sinks to offset their greenhouse gas emissions, India and China have taken an official position that they must be exempt from the conditionalities as their per capita emissions are far below those of developed nations, notwithstanding the significant rise in their figures in recent years. Indonesia, which is the third-biggest carbon emitter in the world after the U.S. and China and experiencing rapid deforestation, too, has reservations in compromising with its high growth perspective.

Happily, the rate of growth in emissions in the post Kyoto Protocol phase has been less than what was noted during several preceding decades. And yet, the incremental emissions in per capita terms are much higher in the developed compared to less developed countries. This has magnified the concern and apprehensions regarding the threat of climatic change. A large number of small island states and low-lying nations want the targets of temperature rise to be fixed at 1.5 degree Celsius by the turn of this century. They have been vocal and want monitoring of certain indicators in relation to this global goal for all countries. Environmental vulnerability of these states is basically due to limited assimilative and carrying capacity in physical terms and fragile ecosystems that reflect the exposure factor. Economic vulnerability, on the other hand, is due to their limited economies of scale, remoteness resulting in high transport costs and dependence on exports of a few commodities. Understandably, they have pleaded inclusion of indicators reflecting their specific vulnerabilities in the context of climate related negotiations. However, if instead the global target is fixed at 2 degrees, as pleaded explicitly or implicitly by the emerging economies, the reference point for constructing such indicators would change significantly.

The developing countries have been emphasizing the need to transfer technology for assisting them in their adaptation strategies by replacing the Kyoto protocol by another, which hopefully is more stringent. United States not signing the Protocol[1], and a few other developed countries revising emission reduction targets downwards, have also been a handicap in pushing this agenda. On the other side, a strong lobby has emerged in recent years, which holds that selective inclusion of countries within this 'regulatory framework' does not convey seriousness of environmental front. It is demanding inclusion of all rapidly industrialising countries that are reporting significant increases in their emission levels, within the framework, irrespective of their current level of emissions.

At the Montreal summit in 2005 (COP 11), parties established the Ad Hoc Working Group under the Kyoto Protocol (AWG-KP), mandating consideration of the Annex I parties' further commitments, at least seven years before the end of the first commitment period. In addition, it was decided to consider long-term cooperation through a series of workshops known as "the Convention Dialogue," which continued until COP 13 which took place in 2007 in Bali. Despite near unanimity on the urgency of effective intervention, problems have been encountered

[1] US President George W. Bush argued that the 5 per cent reductions required by Kyoto would 'wreck the American economy.'

in making the countries adopt a clear and time-bound roadmap for climate resilient development strategy.

Copenhagen summit, (COP 15) and the fifth Conference of the Parties serving as the Meeting of the Parties of the Kyoto Protocol (MOP 5) was held in 2009. EU reducing its emission by about 8 per cent in 2009 below that of 1990 and US announcing before the summit that it can cut down emissions in 2020 by 17 per cent from the level of 2005 and by another 83 per cent by 2050, seemed to suggest the beginning of an era of ending the conservative mindset. Unfortunately, despite these positive signals, the summit failed to operationalise a treaty to supplant or supplement the Kyoto Protocol or even to set a timetable for working out such a treaty. It produced a climate change convention document, signed by one hundred-and-ninety-two countries, which fell short of being “an accord that is legally binding” (Boer 2009). The agreement makes no mention that the developed countries would contribute a fixed percentage of their GDP to the United Nations managed Green Climate Fund. Also, there is no mention of the requirement of an outside auditing of emission reductions or of the United Nations managed Green Climate Fund which is to provide up to $10 billion a year from 2010 through 2012 and up to $100 billion a year by 2020, to help poorer nations adapt to climate impacts and "green" their economies. On the positive side, however, it stipulated that the industrialized nations would commit to certain voluntary emissions targets by 2020. These informal commitments (Maynard 2008) if adhered to would give the world a 50 per cent chance of holding global warming to 2 degrees Celsius by 2100, the level many scientists consider necessary for averting a catastrophe.

Following the non-binding Copenhagen Accord, very small progress was made at the four preparatory rounds of negotiations held during 2010. Understandably, the international expectation from the COP16 summit at Cancun has been low and indeed its outcome has come once again as an agreement and not a binding treaty. It aims at limiting global warming to less than 2 degrees Celsius above pre-industrial levels. It calls on rich countries to reduce their greenhouse gas emissions and at the same time urges the developing countries to plan to reduce their emissions. The limited success of this summit has, however, been in terms of a number of developed and emerging countries outlining what they are prepared to do to curb emissions[2], including China and the US.

The Cancun agreement has also been criticized[3] for not proposing a timetable and a legal frame of emission reduction and not deciding on how to extend the Kyoto

[2] EU, which is currently aiming at cutting emissions by 20% by 2020, was prepared to raise the target to 30% if other rich countries put forward more ambitious targets. One bright spot, however, was that Japan is to stick with its target to cut emissions by 25% by 2020.

[3] Lumumba Di-Aping, chief negotiator for the G77 group of 130 developing countries, said the deal is a suicide pact for less developed countries and is "nothing short of climate change skepticism in action. It locks countries into a cycle of poverty forever.” Disappointed with the accord, Lydia Baker of Save the Children said world leaders had "effectively signed a death warrant for many of the world's poorest children. It is argued that the emerging economies like India, China and Brazil have buckled under pressure. Their position may be strategically in their interest but does not address the concerns of the less developed countries. Further, their flexibility on Reporting band Verification (MRV) would imply accepting an external power to monitor the adaptation strategy.

Protocol. There has been no agreement on how the $100 billion a year for the Green Climate Fund will be raised. The vulnerable African nations and the low-lying islands in Asia, who want "this money to be immediately unblocked," felt that it is “woefully short of action needed.” The agreement is, however, seen by UN agencies as a "step forward" given that international negotiations had stumbled in recent years. Although the countries merely “took note” of the accord, UN believes it to be as good as their “accepting” the document. It is argued that the international community must respect ‘this product’ of the UN process and build on it. The former World Bank chief economist Lord Stern believes that it is a vital to stick, whatever its frustrations. The skeletal outline for global action, emerging out of Copenhagen and Cancun summit while far from ideal, create “the ingredients of an architecture that can respond to the long-term challenges of climate change” (Boer 2009). The UN Secretary-General Ban Ki-moon argues that “it is a real deal. And we will try to have legally binding [language] as soon as possible.” It has also brought in a new forestry deal which is hoped to significantly reduce deforestation in return for cash.

Going by the commitments of the countries at the summit, several analysts believe the Copenhagen and Cancun pledged emissions reduction much more than the Kyoto Protocol. More importantly, discussions are now taking place outside the UNFCCC umbrella, as well. The key message emerging from the summits is that the issue is complicated and that global leaders will have to work not only within the framework of UN negotiations but also more directly and pragmatically going beyond the framework.

The process of negotiations within and outside the UNFCCC framework can lead to meaningful results only if the basic parameters that describe the state of the environment in different countries and their efforts to put in action mitigation and adaptive programs are defined with specificity. Such assessments assume great importance especially because the developed as well as developing countries may not accept monitoring by an international agency as this makes them to compromise with their sovereignty. Building up indicators measuring the level of GHG emission so as to capture the cause and impact of climate change and the remedial measures launched by different countries, using robust and temporally comparable data base, would help the negotiation processes and facilitate drawing up a specific road map for building a climate resilient world system.

It would be dangerous to be complacent with regard to environmental future by relegating the responsibility of saving the world from environmental disaster on to the developed countries, especially because the less developed countries have a greater stake in it. It would be also unrealistic to assume that a protocol similar to Kyoto can be agreed upon with more stringent provisions without a system being in place which enables the developing countries exhibit their efforts at tackling the problem of climate change in a credible fashion. Given the keenness to usher in fiscal and financial reforms at global and national level and set up a mechanism to conduct carbon trading within and across the countries, it would be important to determine quantitatively the differential exposure and impact of climatic change across different countries. Without reliable statistics on these, the environmental discourses cannot rise above emotional appeal and policy exhortations.

The need of the hour is to devise a system of incentives for the countries to go in for environment friendly technologies and restructure growth pattern so that there is less pressure on natural resources. For this, it is important to quantify the impact and implications of changes in climatic parameters, to the extent our technology makes that possible. For putting the environmental concerns within the framework of national or international law and governance, it is imperative that the degrees of vulnerability are determined at the country level without any ambiguity. There are threshold levels for nature's capacity to absorb and assimilate pollution, and hence to abide with the level of greenhouse gas emission. Indeed, any renewable resource must not be viewed as free commodity as it would have non-zero opportunity cost. Unfortunately, despite the increasing awareness among national and international governments, the methodology for assessing the parameters has not been worked out in a manner that can be incorporated into the global decision making.

It would be important to unambiguously determine the parameters of climate change and their impact on the economy, society and system of governance. The levels of exposure of different countries to this problem are different due to their physiographic conditions and growth strategies, and these need to be quantitatively determined. Similarly, effectiveness of the current adaptation and mitigation strategies need to be assessed and the capacity to sustain these must be determined. It would be possible to make a strong case for adoption of a Kyoto-type Protocol or ensuring its compliance by the developed countries if the developing nations can demonstrate that the opportunity of exemption and accessing the adaptation funds are being utilized for restructuring their development strategy to bring down carbon emissions, reflecting the concern for sustainability and meeting the millennium development goals. It would also be important to keep in mind that given the limitations of our existing knowledge system, the best possible efforts to quantify the parameters of climate change might still leave out some of the components. It would still be important to endeavor to develop a transparent and unambiguous system which would have to be updated at regular intervals, as technical knowledge regarding the parameters of costs and benefits advances over time.

7.3 Overview of the Issues and Problems for Developing Countries

It is important to note that the international organizations working on environmental issues have not been able so far to rank the countries in terms of any vulnerability index for the purpose of resource allocation and launching measures of intervention. Construction of any composite index requires some kind of consensus on the judgments regarding selection of indicators, making them scale free and their aggregation. Also, for evaluating the impact of an adaptive/mitigation measure, one would have to assess and aggregate the benefits or costs across regions at different levels of development and over time, requiring specification of a discount factor based on normative judgment. Attempts must be made to do all this within a well-defined human development framework. Importantly, the global vulnerability indices do not adequately consider the special circumstances of the developing countries that make them particularly vulnerable to climate change. Proposing a set of indicators within this framework would involve making normative choices for "selection and aggregation of diverse information."

United Nations Development Programme's Human Development Report entitled "Fighting climate change: Human Solidarity in a Divided World" provides a stark account of the threat posed by global warming to the countries in developing world in terms of breakdown of agricultural systems due to erratic rainfall and more frequent incidence of droughts and floods. The Report shows how 600 million people are likely to be pushed into malnutrition trap while 300 million people in coastal and low-lying areas, would be displaced from their habitation. Confronted with these problems, meeting the Millennium Development Goals (MDG) relating to poverty, reduction in mortality and provision of basic amenities would be much more challenging.

The immediate impacts of climate change in Asia would be on health with increased epidemics of malaria, dengue, and other vector-borne diseases[4]. Besides, the frequency and duration of severe heat waves and humid conditions is likely to increase the mortality and morbidity rates, affecting the urban poor and slum populations. Increased flooding and intensification of tropical cyclones would increase climate-related injuries and deaths. Poor urban air quality in several metro cities in China, India and Indonesia, could contribute to widespread heat stress and smog induced illnesses. Similarly, the health and livelihood vulnerability in coastal cities would deteriorate. Changing patterns of temperature and rainfall would also cause a shift in the distribution of dengue and malaria-carrying mosquitoes, exposing larger segments of population to these.

IPCC4 holds that future climate change would seriously affect melting of glaciers in the Himalayas, sea levels, forest cover and overall biodiversity here, resulting in displacement of population in this region. It predicts that future climate change would seriously enhance the risk of hunger, water scarcity in many of the countries in the region. It predicts that rapid industrialization and urbanisation would compound the pressures on natural resources and adversely affect human health in the region. Given the seriousness of the problems, urgent actions are required both at the level of global institutions as also the national governments for these regions.

Many policy makers and researchers, however, argue that the future is unlikely to be so alarming, given the policy changes and innovations already underway in several rapidly growing middle income countries like China, Brazil, India, and Indonesia, often described as emerging economies. There is growing awareness among these countries regarding the climate related impending problems.

[4] See Martens *et al*. (1999)

Given this, one would expect greater compliance of the emission norms on a voluntary basis. Indeed, the best way of moving forward in this regard would be if there is increasing awareness among the policy makers and the governments in the region adopt low carbon and climate resilient strategies of development without any external pressure.

Cruz et al.[5] have documented the evidence of increases in the intensity and frequency of many extreme weather events including heat waves, tropical cyclones, prolonged dry spells, severe dust storms etc. In the long term, these would lead to a rise in the snowline and disappearance of many glaciers causing serious impacts on the populations relying on the main river system. Many of the developing countries, particularly the island states and those having large coastal areas, forests and mountainous, would also be severely affected[6].

Many of these countries have proposed the extension of the Kyoto treaty beyond 2012 or replacing it by a more effective agreement, binding the industrialised countries to the objective of reducing carbon emissions with a fixed timetable or/and buying of carbon credits from the former. They, individually as also collectively as Group of 77, have also questioned the validity of bringing the less developed countries within a restrictive policy regime. Their argument stems from the premise that as the present problem is the cumulative impact of emissions and even the present emission in per capita terms continues to be low, any equity based principle for target setting will exempt them from any restriction. Further, an immediate adoption of emission targets would be incompatible with meeting the challenge of poverty reduction and other MDG targets in less than the next five years. It is noted that the per capita CO_2 emissions in most of the countries in the region is about one fourth of the world average of 4.0 tons, one fifteenth that of the USA and about tenth of European Union. The argument, therefore, is that it is the group of developed countries that should undertake the cuts and not the ones currently struggling to provide the minimum needs to large sections of their population. The issue of norms of emission for different countries must therefore be determined within the framework of human development. The principle of not imposing the curbs on emissions in less developed countries which ipso facto allows them to increase energy consumption to meet socio-economic needs of their deprived population would have a strong normative appeal which constitutes the premise of the present UN framework.

There is a strong case to propose a “common but differentiated strategy incorporating the principle of equity” which would place greater responsibility on industrialised countries to control emissions. However, the conditionalities would have to be less stringent to be unanimously acceptable, as long as their incremental emissions are within the framework of the MDG targets. Happily, attempts are being made to bring in fiscal reforms for penalizing the polluting industries/countries and

[5] See Cruz et al. (2007)

[6] See Cruz et al. (2007)

giving incentives to less developed countries to adopt cleaner technology. Scholars like Sven Teske (2010) however argue that the future with regard to energy use in developing countries is unlikely to be so alarming, given the policy changes and innovations already underway.

The acceptance of the proposal to activate disbursal from the United Nations Fund by setting up an Adaptation Fund Board, as agreed upon as a result of the last three summits is being seen as a major achievement by the developing countries. Understandably, they see a new market opening up for their rapidly growing carbon credit sector. There are, however, apprehensions that this would allow the donor countries and multilateral agencies like World Bank to supervise utilisation of this money. Many of the developed countries, on the other hand, argue that the concessions or the funds may not be utilized for meeting the professed objectives of implementing adaptation measures or strengthening the capacity to curb future emissions. Efforts are on to resolve these issues and also work out acceptable formulae and procedures for determining the contributions into and disbursal from the fund.

It would be erroneous to believe that there is a consensus on the areas of concern regarding impacts of climate change and measures to articulate these among the countries in this region. The differences in their perspectives stem from their geophysical factors, the nature and degree of exposure to climatic factors and their levels and future strategies of economic development. A large number of smaller countries in Asia and Africa want the targets of temperature rise to be fixed at 1.5 degree Celsius[7] by the turn of this century which was not acceptable to the larger and emerging economies of the region like India and China. The responsibility of failure to deliver a more ambitious deal is being placed on these economies as they blocked any inclusion of detailed targets, fearing that the responsibility for meeting the targets may soon be transferred to them. They resisted institutionalisation of a system of independent verification of emission reductions that the US and other developed countries had demanded. Small island states and low-lying nations who have most to lose from rising seas have been vocal at the Copenhagen and Cancun and wanted to develop indicators for monitoring in relation to this global goal. Fixing the global target at 2 degree would understandably change the reference point for constructing indicators of climatic vulnerability as this would mean dropping the earlier goal of reducing global CO_2 emissions by 80% by 2050.

It would be important to examine the suitability or otherwise of the commonly used indicators across the countries given the wide differences in their development contexts. Much of the production in several less developed countries is based on small producers and labourers (especially in agriculture) whose capability to adapt is low. Also, a single country specific figure would be inappropriate for large countries

[7] President Nasheed of the Maldives, supported by Brown, fought valiantly to save this crucial number. "How can you ask my country to go extinct?" The more industrialised countries in the region however "not only rejected the target for themselves but also did not allow any other country to take on binding targets?" This attempt to weaken the climate regulation regime now is interpreted as an attempt "to avoid the risk of becoming “more ambitious in a few years' time".

as it hides the variation in the levels of vulnerability across sub-national units and their people. Modifications or realignment required to focus on vulnerable people, occupational categories and social groups. Indicators capturing double exposure (O'brien and Leichenko 2000) owing to long term trend in climate change and globalisation, on the poor would be extremely relevant in this context. Further, one has to examine the robustness of the measures in the context of data availability and temporal and cross sectional comparability across countries in the region. The issues of cost effectiveness and of bringing out the indices on a regular basis also need to be probed in.

The specific issues in selecting measures of climatic vulnerability in the context of developing countries may be summarised as follows. These countries vary significantly in terms of their geographical and population size. Consequently, use of any value at national level figure without bringing in how the factor is likely to impact the people would be misleading. Understandably, per capita figures are likely to be more appropriate in capturing the sensitivity factors except the case of those that affect all uniformly. Further, any macro level value without considering the differential impact on different segments of population in different regions or social groups would miss out the ground reality and therefore be inappropriate for large countries.

In view of the importance of small scale production, particularly in agriculture, indicators need to capture the impact on different occupational groups. Indicators can focus on vulnerability if these capture the impact on vulnerable population. In constructing composite indices, considering indicators pertaining to general population would be important. However, those articulating specific conditions of vulnerable population must also be included and given appropriate weight in the schema of composition.

7.4 Proposing a Framework for Measuring Vulnerability, Adaptation and Mitigation Capacity

The less developed countries, vulnerable to climate change, have made a strong case for a system of development assistance, based on their historical and current data on GHG emission, without any environmental compliance, as noted above. For operationalising this, it would be important to unambiguously determine the parameters of climate change and their impact on the economy, society and system of governance. The degree of exposure and natural capacity to absorb the impact vary across countries, due to their physiographic conditions and growth strategy and these need to be quantitatively determined. A number of UN, governmental and non-governmental agencies have taken up the task of building climate change vulnerability indices taking all these factors into consideration. Similarly, effectiveness of the current adaptation and mitigation strategies and the capacity to sustain these need to be quantitatively determined. It would be possible to make a strong case for adoption of a Kyoto-type Protocol or ensuring its compliance by the developed countries if the developing nations can demonstrate that the opportunity of exemption and accessing the adaptation funds are being utilized for restructuring their development strategy to reflect the concern for both, sustainability and millennium development goals. This requires building a transparent and unambiguous system of indicator linked development assistance. This would have to be updated at regular intervals as technical knowledge regarding the parameters of costs and benefits advances over time. The success of the approach would depend on creation of an institution at the apex level which can formalise the methodology of working out the indices, reflecting both the concerns for sustainability and the MDG. An expert body may be established as a part of the institution through intergovernmental negotiations which can build global consensus on the methodology. Apportionment of global or regional green funds can be proposed based on its recommendations.

Climate process drivers or stimuli emanate from the elements of climate change such as the mean climate characteristics and variability, including average temperature, precipitation etc., at global level (Figure 1). The former are affected by the level of human activity at the country level but the impact in per capita terms is unlikely to be high for the developing countries region when compared to the rest of the world. The climatic stimuli at global level, nonetheless, impact on the earth system which has different manifestations and implications across countries. Now, exposure of a country's earth system is the degree to which it is affected, either adversely or beneficially, by the stimuli. The impact of the earth system on the human system will depend on the sensitivity of the latter which is determined by the country's state of socio-economic development, its programs and policies. Climate vulnerability for a country can now be defined as the degree to which it is susceptible to, or unable to cope with the adverse effects of climate change, caused by both earth and human systems, interacting with global and local factors. In other words, it will depend on the exposure of the earth system and sensitivity of the human system and, therefore, can be measured through indicators pertaining to them. The exposure of the earth system could be assessed in terms of rise or fall in average temperature/rainfall, range, variability and frequency of extreme events and the data base for this is fairly robust. The human system may be seen as comprising two separate components, economic structure and social structure for operational purposes, notwithstanding the degree of their interdependence. Economic structure comprises the sectors of production, trading, technology, investment and settlement system. The social structure, on the other hand, is determined by the quantity and quality of population, governance, equity etc. The earth system would affect the economic structure say material wellbeing of the farmers through variability of rainfall, coastal flooding etc. Similarly, it can endanger the health of tribal and slum population in hilly tracts or slum areas due to their extreme sensitivity to climate linked stimuli and thus impact on social structure. Understandably, the economic and social structures are bi-directionally interactive. The impact of the earth system varies not only across countries but also across regions and social groups, depending on their socio-economic characteristics, geographical location etc. determining their sensitivity. The vulnerability index, therefore, must reflect not just the situation at national level but be sensitive to the changes occurring across regions and social groups within the country. It should incorporate the vulnerability parameters of these groups with different weights, reflecting human development concerns. It is extremely important to add that mitigation and adaptation strategies affect the climatic vulnerability of a country in a significant manner and consequently many of the studies included separate indicators to articulate this dimension. In Figure 7.1, these are subsumed within the human system and shown to be affecting earth system only through social and economic structure. However, given the importance of these strategies in modifying climatic parameters, it makes sense to include separate indicators for these. The framework proposed here is thus more oriented to operationalisation and measurement of vulnerability rather than presenting alternative perspectives on the process of climatic change and its impact.

The indicators relating to the earth system for the countries in the region can be built from the existing global database which does not have serious problems of temporal or cross sectional comparability (UNEP UNFCCC). United Nations organizations and other international agencies are using this to bring out reports at regular intervals and consequently there may not be much disagreement on the choice of indicators as well. For human system, it would be important to identify indicators of economic structure and social structure, based on an assessment of the development processes in the region. Choice of indicators and temporal and cross sectional comparability of database are major issues here. Global studies on the combined effect of climate change and CO_2 emissions on, say agriculture through crop production, would have limited validity as the impact varies widely across regions and countries. The less developed countries are located in a climate zone where additional warming would have serious negative effects on economic and social structure, and consequently specific indicators need to be designed to capture that. It would, however, be important to build consensus on the indicators since cross-sectional analyses as well as modeling studies report "hill-shaped response functions between mean temperature and the productivity of major economic sectors" and not a linear relationship (Füssel 2009). The impact on small island countries would be more severe than the others, and use of any global/regional parameter is bound to be misleading. Unfortunately, the studies on vulnerability of coastal zones to sea-level rise, storm surges, coastal protection etc. are severely hampered by the unavailability of data. Studies on earth system, based exclusively on biophysical data to identify regional hotspots can provide only limited inputs in estimating the levels of coastal protection. However, information from the Population Division of United Nations, UNESCAP and World Development Indicators would be useful in proposing a number of indicators. Vulnerability would thus be determined through aggregation of these two sets of indicators. Building some kind of regional consensus on the choice of indicators and method of composition would be extremely important for classifying the countries into categories and determining fair allocations for adaptation assistance coming from international sources. The final decision regarding the selection of appropriate indicators should therefore be made by a Committee set up by UNDP taking the specific suggestions made regarding their selection to reflect the regional specificity.

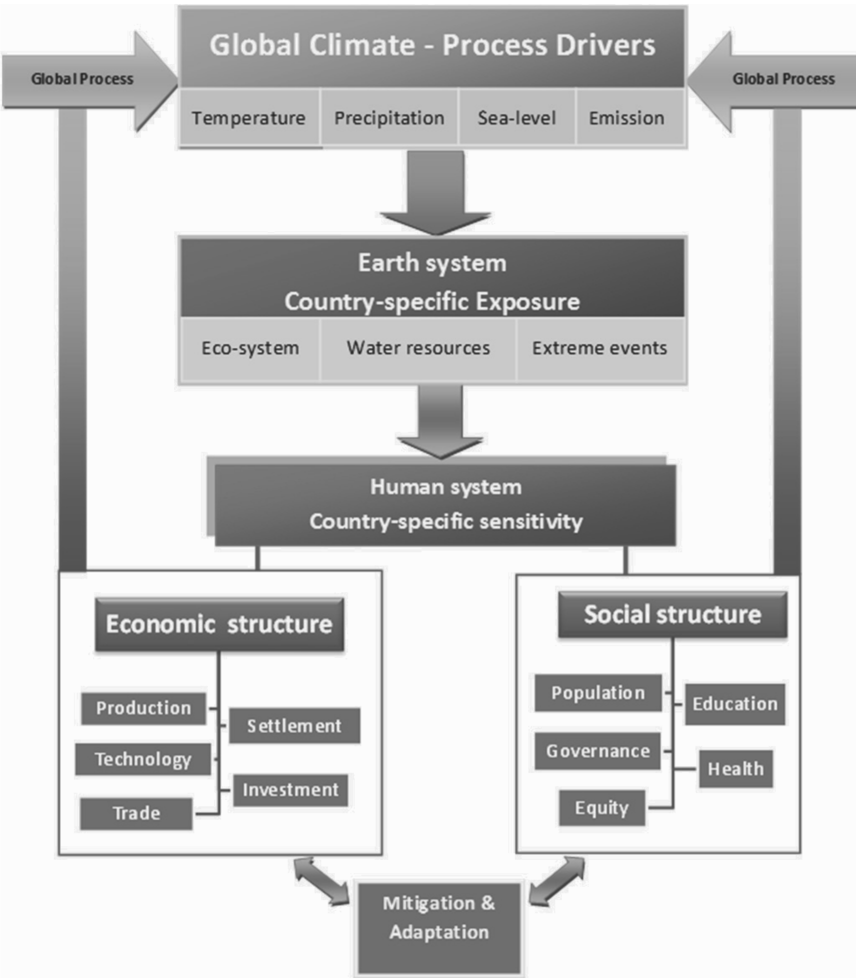

Figure 7.1. Interaction between global system and country sub-systems: A framework for selecting indicators of climatic change vulnerability at country level

Studies attempting construction of summary measures unfortunately, more often than not, tend to hide legitimate political or ethical controversies on conceptual issues. It is important to note that designing vulnerability indices is as much a political as a scientific task. Different interpretations of vulnerability not only produce different rankings of vulnerable regions or systems; they also suggest different strategies for reducing vulnerability. However, instead of identifying vulnerable countries, regions or sectors through political bargaining, attempts must be made to institutionalize the political judgment through a methodology for constructing the indices.

The proposition that the countries that are most vulnerable to climate change should receive priority assistance, irrespective of their scale of adaptation measures, computed within a human development framework, however, has been contested by the lobby of economically developed countries on the ground that this would make the recipient countries complacent with regard to adaptation measures, conflicting with the principle of distributive justice over time. A few scholars have, therefore, defined vulnerability by incorporating indicators pertaining to adaptation/ mitigation strategies as well. It may be argued that separate measures need to be defined for assessing the scale and effectiveness of adaptive/mitigation measures and these must be monitored and reviewed separately. Bringing all these considerations into one concept of vulnerability would blunt the focus in the measures and restrict its usability in policy making. Adaptive and mitigation capacity index, constructed separately, must reflect the ability of the economic and social structure to adjust to climate change, including climate variability and extremes. The indictors must, therefore, capture the technology of production in different sectors, institutional sensitivity to climatic changes, state policies and programs and allocation pattern. A case can be made here to work out a number of disaggregated indices instead of depending on single national level figure. The need for special indicators for special areas like deltas, coastal regions, islands, slums, etc. must be recognised as many of the developing countries have a significant proportion of the global population belonging to these vulnerable categories. The policy perspectives underlying different measures and their usability in monitoring performance of countries or regions and in launching low carbon strategies of development need to be brought into a sharp focus.

Importantly, most of the studies discussed above use 'normalised indicators' for working out composite indices of vulnerability. There is no reason why the method of range equalization should be accepted uncritically for normalising the indicators or making them scale free. This is because, by this, all the indicators are forced to have equal range, implying that the information regarding the differences in inequality in the indicators is lost. In measuring climatic vulnerability, one can argue that exposure factors affect the countries differently depending on the sensitivity and adaptive capacity of the latter. It is possible to argue that the factors that hit hard the more vulnerable countries and create higher inequality in the manifested impact, should be considered more important in measuring vulnerability. In order to retain the differences in the dispersion of the indicators, it would therefore make sense to make them scale free through division by mean so that the coefficients of variation in the indicators are maintained as standard deviations after the scale transformation (See Kundu 2004).

The indicators pertaining to earth system and human system, selected for the purpose of articulating the climatic vulnerability, can be taken as manifestations of the impact of certain key exposure factors or the climate change drivers in different spheres. There is, thus, a possibility of overlapping or duplication of indicators. The strong correlations among the identified indicators can be taken to reflect this overlapping manifestations or the same factor being captured through different indicators. It is well known that the statistical method of Principal Component Analysis gives higher weights to highly correlated indicators. This would compound the problem of overlapping as a few factors may enter the composite index of vulnerability through multiple channels. It is, therefore, proposed that each indicator should get a weight inversely proportional to the sum total of its correlations with other indicators, included in the analysis. Alternately, one can employ the Equal Correlation Method wherein the composite index is correlated equally with all the constituent indicators, instead of being aligned to those that are strongly correlated. The weights can then be obtained by summing up the row values corresponding to each indicator in the inverse of the Correlation Matrix (Kundu 1980). Finally, simple aggregation of the scale free indicators obtained through division by mean, as discussed above, to obtain the aggregative index of vulnerability can also be recommended for its simplicity, transparency and avoiding the problem of indicator overlap.

Expert bodies at the level of the continents like Asia Pacific and Africa need to be established with regional consensus, for determining the degree of climatic vulnerability of the developing countries, based on which apportionment of global green funds can be proposed. It can also monitor how these, enjoying a period of exemption within the UN framework, are accessing adaptation funds and utilizing this opportunity for restructuring their development strategy. For doing this, it would be extremely important to formalise the methodology and work out indicators of depreciation of natural assets and their costs and thereby propose a framework for Green accounting. This would be helpful in assessing the seriousness of the mitigation and adaptation strategies adopted at national and local levels and work out the future course of action. A few among the developed countries are already preparing integrated green income accounts and building temporally comparable indicators on an experimental basis taking into account the depletion, degradation and other harmful impact of socio-economic activities on ecological resources. It is important that at least the rapidly industrialising countries, on their own or through regional institutions, take immediate steps in evolving the methodology for constructing and releasing a set of temporally and cross-sectionally comparable indicators and monitor the information at regular intervals.

7.5 References

Boer, Y. D. (2009). *Press Conference at the conclusion of UNFCC* (COP 15), Copenhagen.

Cruz, R. V., H. Harasawa, M. Lal, S. Wu, Y. Anokhin, B. Punsalmaa, Y. Honda, M. Jafari, C. Li and N. Huu Ninh. (2007). “Asia”. In M. L. Parry, O. F. Canziani, J. P. Palutikof, P. J. van der Linden, and C. E. Hanson (Eds.), *Climate Change 2007: Impacts, Adaptation and Vulnerability. Contribution of Working Group II to the Fourth Assessment Report of the Intergovernmental Panel on Climate Change*. Cambridge University Press. Cambridge, UK.

Füssel, H. M. (2009). "Review and quantitative analysis of indices of climate change exposure, adaptive capacity, sensitivity, and impacts." Background note to the World Development Report 2010, *Potsdam Institute for Climate Impact Research*, Potsdam.

Kundu, A. (1980). "Measurement of Urban Processes–A Study to Regionalisation." *Popular Prakashan*, Bombay.

Kundu, A. (2004). *ICT for Human Development: Towards Building a Composoite Index for Achieving the Millennium Development Goals*. United Nation's Development Programme, New Delhi.

O'Brien, K. L., and Leichenko, R. M. (2000). "Double exposure: Assessing the impacts of climate change within the context of economic globalization". *Global Environmental Change*, 10(3), 221–232.

Teske, S. (2010). *World Energy Revolution: A Sustainable World Energy Outlook.* European Renewable Energy Coulcil and Green Peace International, Amsterdam.

Maynard, T. (2008). "Climate change impact on insurers and how they can help with adaptation and mitigation." *The Geneva papers on Risk and Insurance – Issues and Practices*, Special Issue on Climate Change, 33(1), 140–146.

United Nations Development Programme 2007/08 (UNDP) (2008). *Fighting climate change: Human Solidarity in a Divided World*. *UNDP*, New York.

This page intentionally left blank

PART 2

Modeling and Predicting

CHAPTER 8

Hydrologic Impacts of Climate Change: Quantification of Uncertainties

D. Raje, S. Ghosh and P. P. Mujumdar

Impacts of climate change on hydrology have been widely studied in recent literature. Of large relevance in hydrology is the quantification of uncertainties involved in hydrologic projections. It is also acknowledged that hydrologic analyses and designs using assumptions of stationarity are no longer valid because of non-stationarities introduced by climate change. In this chapter, a broad overview of uncertainty modeling and methodologies for uncertainty quantification in assessment of hydrologic impacts of climate change is provided. Various sources of uncertainties arising in the impact assessment process are presented. Case studies of quantification, combination and propagation of uncertainty in impact assessment are discussed.

8.1 Background: Climate Change Impact Assessment

8.1.1 Introduction

Surface temperature observations show that the global average temperature has increased by about 0.74°C in the past century. This observed rise in temperature since the middle of the 20th century has been attributed to increasing concentrations of greenhouse gases (GHGs) resulting from human activity such as fossil fuel burning and deforestation (IPCC 2007). Anticipated effects of an increase in global temperature are raising sea levels and changes in the amount and pattern of precipitation. Changes in the water cycle will have serious implications for water resources management. Various observed changes in the water cycle include increases in surface specific humidity, increases in heavy precipitation events in many land regions, even in regions where there is a reduction in total precipitation amount and more intense and longer droughts in the tropics and subtropics (IPCC 2007).

8.1.2 Modeling Tools

The most widely used tools for projecting future climate changes are General Circulation Models (GCMs), which are mathematical models based on physical principles including fluid dynamics, thermodynamics and radiative transfer. Simplifications of the actual climate system are necessary in GCMs because of the constraints of available computer power and limitations in knowledge of the climate system. In practice, GCMs are combinations of models for different components of the climate system, with an atmospheric model for air movement, temperature, clouds, and other atmospheric properties; an ocean model for predicting temperature, salt content, and circulation of ocean waters; models for ice cover on land and sea; and a model of heat and moisture transfer from soil and vegetation to the atmosphere. Some models also include treatments of chemical and biological processes (IPCC 2007).

8.1.3 Scenario Evolution

Future GHG emissions are determined by very complex dynamic systems, driven by demographic development, socio-economic development, and technological change. Scenarios are alternative images of how the future might unfold and are an appropriate tool with which to analyze how driving forces may influence future emission outcomes and to assess the associated uncertainties. They assist in climate change analysis, including climate modeling and the assessment of impacts, adaptation, and mitigation. The IPCC in 2000 developed a new set of emissions scenarios in the Special Report on Emission Scenarios (SRES), which provide input to the IPCC Third Assessment Report (TAR) in 2001 and Fourth Assessment Report (AR4) in 2007. The SRES scenarios cover a wide range of the main driving forces of future emissions, from demographic to technological and economic developments. There are 40 different scenarios, each making different assumptions for future GHG pollution, land-use and other driving forces. Assumptions about future technological development as well as the future economic development are thus made for each scenario. Most scenarios include an increase in the consumption of fossil fuels. These emission scenarios are organized into families, which contain scenarios that are similar to each other in some respects. Scenario families contain individual scenarios with common themes. The six families of scenarios discussed in the AR4 of the IPCC (IPCC 2007) are A1FI, A1B, A1T, A2, B1, and B2.

8.2 Downscaling for Hydrologic Needs

8.2.1 Spatio-temporal Scale Issues

The spatial scale on which typical GCMs operate, which is about 2.5^o latitude x 2.5^o longitude (with grid sizes of hundreds of kilometers), is very coarse as compared to that of a hydrologic process, and inadequate for the purpose of hydrologic impact assessment (requiring grid sizes of at most tens of kilometers). GCMs are not able to appropriately model subgrid-scale processes such as cloud formation and convection, and features such as topography (Xu 1999). Therefore, hydrologic variables like precipitation, soil moisture, runoff and evapotranspiration are not accurately simulated by the GCMs. Downscaling is a term used in hydrology, which refers to predicting finer resolution station-scale hydrologic variables such as precipitation or runoff from large scale climatic variables such as mean sea level pressure and wind speed.

8.2.2 Types of Downscaling

Downscaling approaches are broadly classified into two categories: dynamical downscaling and statistical downscaling. Dynamical downscaling uses a nested higher resolution Regional Climate Model (RCM) within a coarser resolution GCM. The RCM uses the GCM to define dynamic atmospheric boundary conditions. Statistical Downscaling (SD) derives a statistical or empirical relationship between the variables simulated by the GCM (predictors) and a point-scale meteorological series (predictand). Accurate estimates are strongly dependent on the quality and the length of the data series used for the calibration (Wilby and Wigley 1997) and on the performance of the regression models in capturing the variability of the observed data (Barrow et al. 1996).

8.2.3 Statistical Downscaling Techniques

Broadly, SD methods can be classified into three categories, namely, regression (transfer function) methods, stochastic weather generators and weather typing schemes. A review of downscaling techniques may be found in Wilby et al. (1998), Prudhomme et al. (2002) and Fowler et al. (2007). Implicitly, use of these methods assumes that (von Storch et al. 2000) the predictors are relevant variables and are realistically modeled by the GCM, they fully represent the climate change signal, and that the downscaling relationship is valid under altered climate conditions. SD methods are preferable in hydrologic impact assessment because they are computationally inexpensive, provide quick results and their domain of application can be easily transferred from one region to another.

Weather Typing Methods. The weather typing approach uses links between large-scale circulation and surface weather. Using weather types for downscaling provides a better conceptual understanding compared to other ‘black box’ techniques. Previous analyses have used Lamb weather types (Jones et al. 1993; Conway and Jones 1998; Lorenzo et al. 2008), counts of weather fronts and air flow indices, which show strong relationships with hydrologic variables such as precipitation. The circulation pattern (CP) classification techniques include subjective and objective methods. The advantage of such methods is the full use of knowledge and experience of meteorologists. Major disadvantages are the inability for results’ reproduction and the limitation of the classification application only to specific geographical regions. The second category of CP-classification methods is based on automated algorithms operating on selecting datasets allowing fast classification, which is necessary especially for climate-change scenarios. The objective-classification methods include k-means clustering (Wilson et al. 1992), fuzzy classification based on subjectively defined rules (Bardossy et al. 1995); principal-component clustering (Goodess and

Palutikof 1998), principal-component analysis coupled with k-means clustering (Bogárdi et al. 1994); screening discriminant analysis (Enke et al. 2005) and neural-network methods (Cawley and Dorling 1996; Cavazos 1999). A detailed comparison of the Lamb subjective and objective classification schemes can be found in Jones et al. (1993). The circulation-surface climate relationship has been widely modeled using four general approaches: (i) Markov Chain models or Hidden Markov models (Hay et al. 1991; Vrac et al. 2007); (ii) regression analysis (Enke et al. 2005) (iii) canonical correlation analysis (Haylock and Goodess 2004); and (iv) sampling from present-day instrumental analogue data (Zorita and von Storch 1999).

Transfer Function Approaches. Transfer functions are regression-based approaches which rely on a direct quantitative relationship between the predictor(s) and the predictand (Karl et al. 1990; Wigley et al. 1990). The methods differ according to the choice of mathematical transfer function, predictor variables or statistical fitting procedure. Various methods used in the recent literature include linear and nonlinear regression (Anandhi et al. 2008; Ghosh and Mujumdar 2008; Ghosh and Mujumdar 2006; Tripathi et al. 2006), artificial neural networks (Crane and Hewitson 1998; Trigo and Palutikof 1999; Dibike and Coulibaly 2005), canonical correlation and principal component analysis or independent component analysis (Benestad and Forland 2000; Tatli et al. 2004).

Weather Generator Techniques. Weather generators (WGs) are statistical models of observed sequences of variables such as daily precipitation, and have been used in a large number of studies on climate change impacts. The standard practice in most weather generators is to treat the occurrence and the amount of precipitation separately (Wilks and Wilby 1999; Srikanthan and McMahon 2001). WGs can be classified as parametric, where data is assumed to follow a specified distribution; and non-parametric or distribution-free WGs. Most parametric weather generators follow the Weather Generation Model (Richardson and Wright 1984), where precipitation occurrence is modeled with a Markov chain, and precipitation amounts follow a given distribution function–generally, the one-parameter exponential distribution, two-parameter gamma distribution or three-parameter mixed exponential distribution. An excellent review of stochastic weather generator models has been presented by Wilks and Wilby (1999). Models based on kernel-based multivariate probability density estimators and K-nearest-neighbour (KNN) bootstrap methods have been used as non-parametric weather generating techniques (e.g., Lall and Sharma 1996; Lall et al. 1996; Rajagopalan and Lall 1999; Buishand and Brandsma 2001). Daily WGs are most common owing to the wide availability of meteorological data at this time-scale and because most impact assessment models are driven by daily data. There are two types of daily WGs, based on the approach to modeling daily precipitation occurrence: the Markov chain approach, where daily precipitation occurrence is modeled as a Markov chain conditioned on the previous days precipitation (eg. Hughes et al. 1999) and the spell-length approach, where a distribution is fitted to wet and dry spell lengths (e.g. Wilks 1999). An approach of using the conditional random field model has been developed by Raje and Mujumdar

(2009) for downscaling daily precipitation and also used for downscaling monthly mean streamflow (Raje and Mujumdar 2010a, b).

8.3 Uncertainty Quantification Methods

Uncertainties in predictions of hydrologic impacts arise from various sources in the climate change predictions including limitations in scientific knowledge (for example, effect of aerosols) which can be classified as GCM uncertainty, randomness, and human actions (such as future GHG emissions) which can be classified as scenario uncertainty. Downscaling of GCM outputs to station-scale hydrologic variables using statistical relationships introduces additional uncertainty. Another source of uncertainty arises in hydrological modeling. These uncertainties accumulate from the various levels and their propagation upto the regional or local level leads to large uncertainty ranges at such scales (Wilby 2005; Rowell 2006; Minville et al. 2008).

8.3.1 Uncertainty in Large Scale Impacts

A number of studies have been conducted to quantify uncertainty in large scale climate change prediction. Recent studies have generally used a comparison or spread of results from various GCMs, scenarios and downscaling methods, perturbation analysis of simplified climate models or expert opinion to quantify uncertainty in climate variables (Katz 2002). Most studies convert emissions scenarios into atmospheric concentrations of GHGs and derive resultant temperature changes using one or more GCMs. Uncertainty in the predictions resulting from the GCMs is estimated by developing probability distributions of key parameters (such as the climate sensitivity, the strength of the terrestrial carbon sink, and oceanic deep-water formation rate), which are then propagated through the GCMs using a Monte Carlo method. Model structural uncertainty is usually assessed by generating and comparing results from multiple model formulations. For computational reasons, many studies use simplified models that emulate the behavior of more complex GCMs (Knutti et al. 2002). Such uncertainty analyses provide a probability distribution for global or regional temperature increase corresponding to each emissions scenario. However, in most studies, subjective judgments are often used for the choice of probability distributions for model parameters (e.g., Morgan and Keith 1995). Recently, Bayesian Monte-Carlo updating approaches have been used to represent uncertainty in key model parameters (New and Hulme 2000; Forest et al. 2002; Tebaldi et al. 2004; Tebaldi et al. 2005). Greene et al. (2006) generated probabilistic regional temperature projections by using a multimodel ensemble of atmosphere-ocean GCMs, using a Bayesian linear model. Some studies have used a 'perturbed physics' ensemble of models by perturbing GCM parameters in turn for modeling physical processes (Allen et al. 2000; Murphy et al. 2004; Stainforth et al. 2005). Many studies use an index or measure of GCM performance with respect to the current climate in order to constrain uncertainty (Allen et al. 2000; Murphy et al. 2004).

8.3.2 Uncertainty in Regional Impacts

A commonly used method of evaluating effects of climate change on flow regime is to use an ensemble of GCMs, scenarios and statistical downscaling / regional climate models to provide inputs to a hydrological model, and examine the range of effects on a statistic of the modeled hydrologic variables (e.g., Prudhomme et al. 2003; Booij et al. 2006; Wilby and Harris 2006; Minville et al. 2008; Buytaert et al. 2009). GCM and scenario uncertainty has been studied in terms of PDFs of a hydrologic drought indicator such as standardized precipitation index (SPI) (Ghosh and Mujumdar 2007), using an imprecise probability approach (Ghosh and Mujumdar 2009) and through a possibilistic approach for streamflow downscaling (Mujumdar and Ghosh 2008). Uncertainty combination has been studied using the Dempster-Shafer theory (Raje and Mujumdar 2010c) and natural variability linkages have been used for constraining uncertainty in regional impacts (Raje and Mujumdar 2010b).

Prudhomme and Davies (2009) examined uncertainties in climate change impact analyses on the river flow regimes in the UK, using either a statistical or dynamical downscaling model for downscaling precipitation from an ensemble of GCMs and scenarios, propagated to river flow through a lumped hydrological model. They showed that uncertainties from downscaling techniques and emission scenarios are of similar magnitude, and generally smaller than GCM uncertainty. They found that for catchments where hydrological modeling uncertainty is smaller than GCM variability for baseline flow, this uncertainty can be ignored for future projections, but it might be significant otherwise. Kay et al. (2009) have compared sources of uncertainty with respect to impact on flood frequency in England. They considered six different sources of uncertainty: future GHG emissions; Global Climate Model (GCM) structure; downscaling from GCMs (including Regional Climate Model structure); hydrological model structure; hydrological model parameters and the internal variability of the climate system (sampled by applying different GCM initial conditions).

Minville et al. (2008) studied the impact of climate change on the hydrology of the Chute-du-Diable watershed in Canada by comparing statistics on current and projected future discharge. They used ten equally weighted climate projections from a combination of five general circulation models (GCMs) and two GHG emission scenarios (GHGES) to define an uncertainty envelope of future hydrologic variables. Figure 8.1 shows probability density functions from the uncertainty analysis of peak discharge, time to occurrence of peak and annual mean discharge for the watershed, for three future time horizons as compared to the control period of 1960–1990. They also found that the largest source of uncertainty in their study came from the choice of a GCM.

Kleinen and Petschel-Held (2007) performed an integrated assessment of changes in flooding probabilities due to climate change using a reduced-form hydrological model for flood prediction and a pattern scaling approach for downscaling. The hydrological model was subjected to a sensitivity analysis with regard to the water balance using different GCMs. Jones et al. (2006) estimated the hydrological sensitivity, measured as the percentage change in mean annual runoff, of two lumped parameter rainfall-runoff models and an empirical model, to climate change using changes in rainfall and potential evaporation.

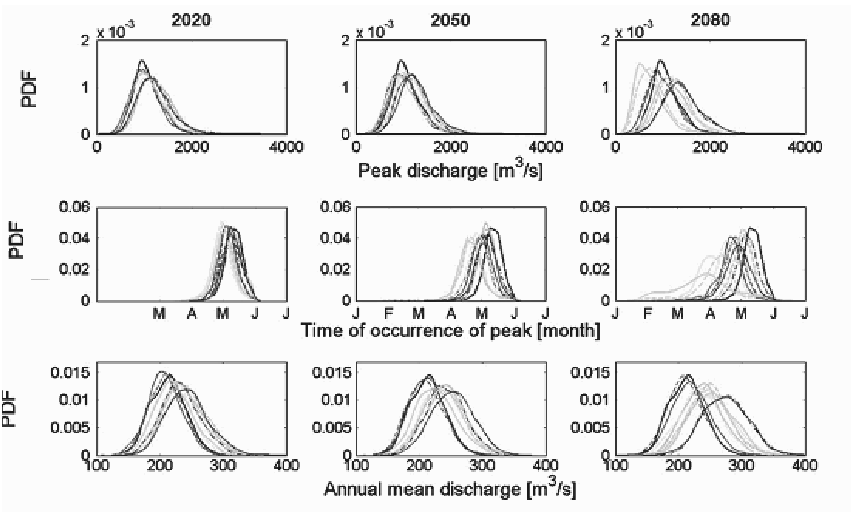

Figure 8.1. Probability density functions of peak discharge (top), time of occurrence of peak (middle) and annual mean discharge (bottom) from the GCM-scenario ensemble for a Nordic watershed for the 2020, 2050 and 2080 time horizons (modified from Minville et al. 2008)

Wilby (2005) studied the relative magnitude of uncertainties in water resource projections arising from the choice of hydrologic model calibration period, model structure, and non-uniqueness of model parameter sets. Using parameter sets of the 100 most skilful model simulations identified by the Monte Carlo sampling, it was found that there is a general increase in the uncertainty bounds of projected river flow changes between the 2020s and 2080s due to equifinality. Figure 8.2 shows projected variations in monthly-mean river flows arising because of equifinality from the study.

Many studies have reported that existing systematic bias in reproducing current climate affects future projections, and must be considered when interpreting results (Prudhomme and Davies 2009). To account for the bias, weights are assigned to different GCMs based on their bias with respect to the observed data and the convergence of simulated changes across models (Giorgi and Mearns 2003). Also, most studies cited above have found that uncertainty due to the driving GCM is by far the largest source of uncertainty in hydrologic impacts (Minville et al. 2008; Kay et al. 2009; Prudhomme and Davies 2009). Some others, however, have found consistent results in hydrologic responses across GCMs, though there are significantly different regional climate responses (Maurer and Duffy 2005). Many studies have also found that understanding current and future natural variability is important in assessing hydrologic impacts of climate change (Prudhomme et al. 2003; Wilby 2005; Kay et al. 2009).

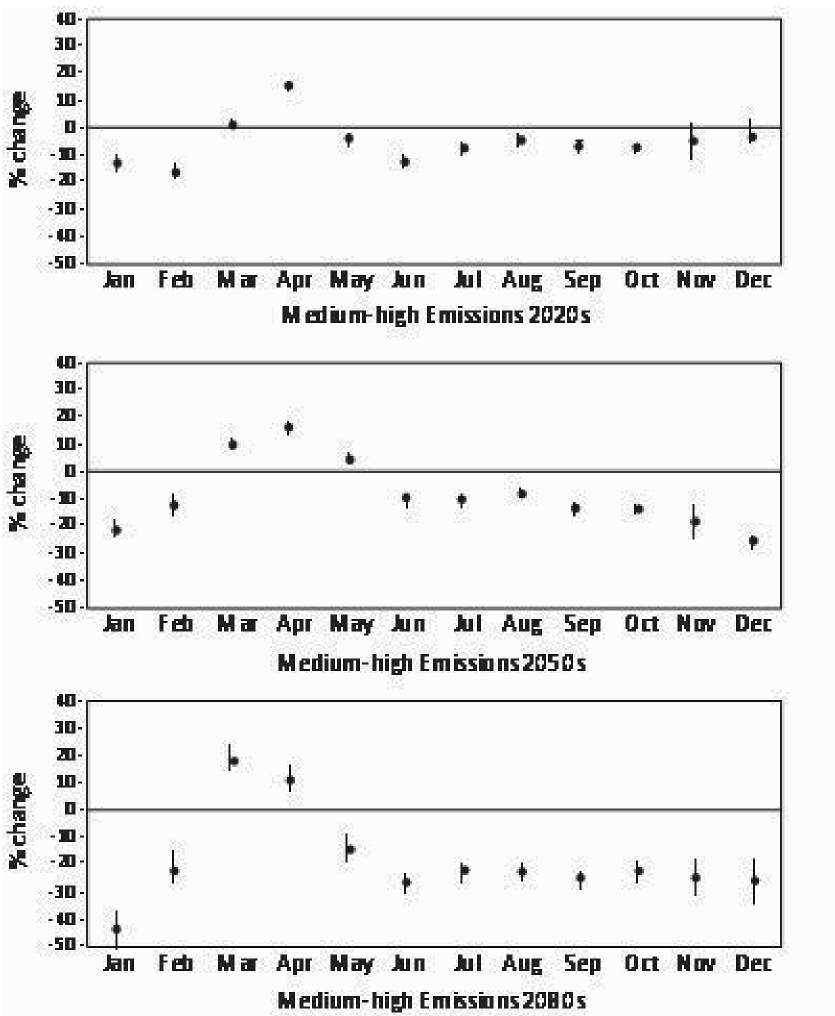

Figure 8.2. Projected changes to monthly mean river flows under medium–high emissions due to non-uniqueness of model parameter sets. Vertical bars show the 95% confidence interval (modified from Wilby et al. 2005)

8.4 GCM and Scenario Uncertainty Modeling

The use of several GCMs and scenarios leads to a wide spread in the downscaled hydrologic projection, especially in years far into the future leading to uncertainties as to which among the several possible predictions should be used in developing responses. Simonovic and Li (2003, 2004) have shown the uncertainty lying in climate change impact studies on flood protection resulting from the selection of GCMs and scenarios. This section describes some recently developed methods for GCM and scenario uncertainty modeling.

8.4.1 Non-parametric Methods for Drought Assessment

In this approach, fuzzy clustering-based downscaling (Ghosh and Mujumdar 2006) is used for modeling future precipitation. Standardized precipitation index (SPI), as originally defined by McKee et al. (1993) is used as a drought index, based on aggregated monthly precipitation as an input variable. Methodologies based on kernel density and orthonormal systems are used to determine the future nonparametric PDF of SPI. Probabilities for different categories of future drought are computed from the estimated PDF. Details of the methodology may be found in Ghosh and Mujumdar (2007). The methodology is applied to the case study of Orissa meteorological subdivision in India to analyze the severity of different degrees of drought in the future, described in the sections below.

8.4.1.1 Fuzzy-clustering based Downscaling

A statistical relationship based on fuzzy clustering and linear regression is developed between MSLP and precipitation, with reanalysis data of MSLP as predictor and observed precipitation as predictand. Gridded MSLP data used in the downscaling are obtained from the National Center for Environmental Prediction/ National Center for Atmospheric Research (NCEP/NCAR) reanalysis project (Kalnay et al. 1996). Monthly average MSLP outputs from 1948 to 2002 were obtained for a region spanning 15^o–25^{o}N in latitude and 80^o–90^{o}E in longitude that encapsulates the study region. Table 8.1 gives a list of GCMs with available scenarios. The outputs of MSLP of GCMs with scenarios, as given in Table 1, are extracted from the IPCC data distribution center for the region covering all the NCEP grid points.

Table 8.1. GCMs used and available scenarios (Ghosh and Mujumdar 2007)

GCM	Scenarios used in study
CCSR/NIES coupled GCM	A1, A2, B1, B2
Coupled global climate model (CGCM2)	IS92a, A2, B2
HadCM3	IS95a, (GHG + ozone + sulphate), A2
ECHAM4/OPYC3	IS92a, A2, B2
CSIRO-MK2	(IS92a + sulphate), IS92a, A1, A2, B1, B2

The downscaling method involves training NCEP data of circulation pattern with observed precipitation and use of the resulting regression relationship in modeling future precipitation from GCM projections. The training involves three steps (Ghosh and Mujumdar 2006): PCA, fuzzy clustering, and linear regression with seasonality terms.

8.4.1.2 Drought Indicator (SPI-12) Projections

McKee et al. (1993) developed the SPI for the purpose of defining and monitoring drought. SPI can be defined by the value of standard normal deviate corresponding to the cumulative distribution function (CDF) value of a precipitation event with a known probability distribution. A common procedure adopted for computing SPI is to fit a gamma distribution to the precipitation data, although the Pearson Type III has also been recommended, and then to transform the data to an equivalent SPI value based on the standard normal distribution (Steinemann 2003). Table 8.2 presents the categories of drought corresponding to their SPI values (McKee et al. 1993; Steinemann 2003).

Table 8.2. Drought categories

Drought category	SPI values
Near normal	0 to -0.99
Mild-to-moderate drought	-1.00 to -1.49
Severe drought	-1.50 to -1.99
Extreme drought	-2.00 or less

The parameters required for estimation of SPI, viz., parameters of gamma distribution and nonzero precipitation probability, are estimated based on the observed annual precipitation. Using these parameters, the future annual precipitation (computed from monthly precipitation), downscaled from GCM output, is converted into SPI-12. The SPI-12 is calculated for all GCMs for available scenarios.

8.4.1.3 Uncertainty Modeling

In this study the SPI-12 values computed with downscaled outputs from GCMs are considered as the realizations of the random variable SPI-12 in each year where there exists a PDF of SPI-12 in each year. The severity of future drought may be studied by estimating the evolution of the PDF of a drought indicator.

Normal Distribution Assumption. Here, no prior information is assumed regarding the future distribution of SPI-12 and, for simplicity, a normal distribution is assumed. The results for each GCM and emission scenario are taken as the set of independent realizations of SPI-12 and this set is used at each time step to establish the probability distribution. The values of the parameters of the normal distribution, i.e., mean and variance, are considered as the sample estimates. The top 4 panels of Figure 8.3 shows the average probabilities of drought events for three time slices, years 2000–2010, 2040–2050, and 2090–2100 using a normal distribution assumption.

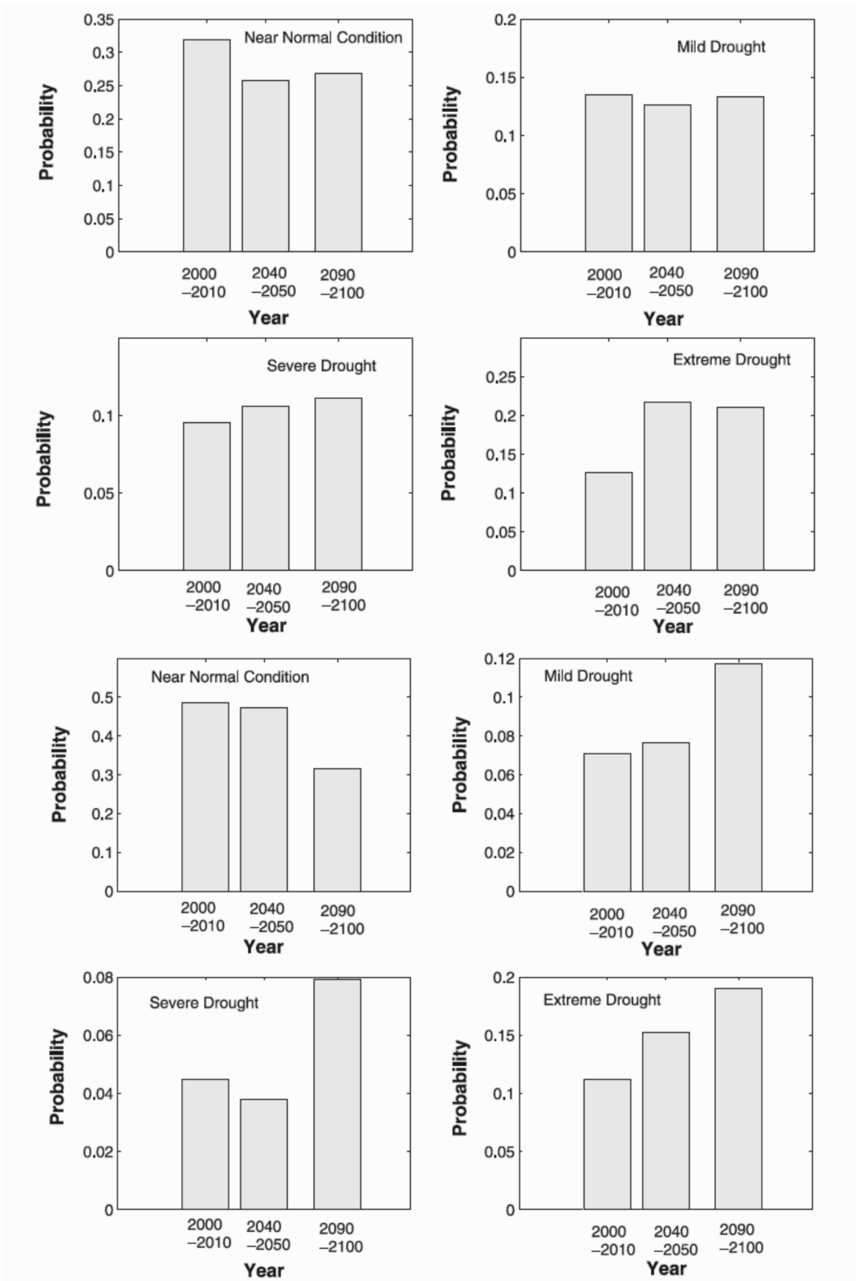

Near Normal Condition
Mild Drought
Severe Drought
Extreme Drought
Near Normal Condition
Mild Drought
Severe Drought
Extreme Drought
Probability
Year
2000 –2010
2040 –2050
2090 –2100

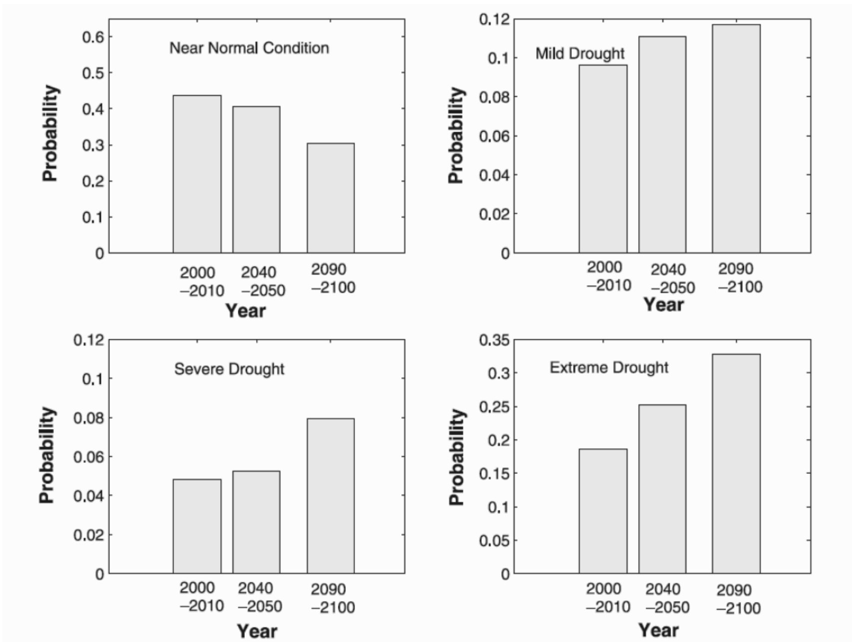

Figure 8.3. Probability of droughts with (top 4) Normal distribution for SPI-12, (middle 4) Kernel density estimation, (bottom 4) Orthonormal series method (Ghosh and Mujumdar 2007)

Considerable variations in the probabilities of near-normal condition and extreme drought are seen from years 2000–2010 to 2040–2050. The probability of near normal condition is reduced, and that of extreme drought is increased significantly in the years 2040–2050. Variations in the probabilities of different droughts are not significant in the later years, 2040–2050 to 2090–2100. This may mean that the assumption of normal distribution does not result in a correct assessment of drought impacts of climate change years farther in the future. A normal probability plot of SPI-12 for three arbitrarily chosen years also shows that SPI-12 values deviate significantly from the normal distribution.

Kernel Density Estimation. Kernel density estimation entails a weighted moving average of the empirical frequency distribution of the data. Most nonparametric density estimators can be expressed as kernel density estimators (Scott 1992; Tarboton et al. 1998). It involves the use of kernel function (K(x)), defined by a function having the following property:

$$\int_{-\infty}^{\infty} K(x)dx = 1 \qquad \text{(Eq. 8.1)}$$

A PDF can therefore be used as a kernel function. A normal kernel (i.e., a Gaussian function with mean 0 and variance 1) is used here. A kernel density estimator ($\hat{f}(x)$) of a PDF at x is defined by:

$$\hat{f}(x) = (nh)^{-1} \sum_{l=1}^{n} K((x - x_l)/h) \qquad \text{(Eq. 8.2)}$$

where n is the number of observations (here number of available GCM outputs), x_l is the l^{th} observation (here SPI-12), and h is the smoothing parameter known as bandwidth, which is used for smoothening the shape of the estimated PDF. Figure 8.3(b) presents the probabilities of drought conditions in the years 2000–2010, 2040–2050, and 2090–2100, as obtained using the kernel density estimation. A significant change is found for the years 2090–2100 from the years 2040–2050 in the probabilities of near-normal condition from kernel density estimation method, which is absent in the plots obtained from the model based on the assumption of normal distribution. The probability of extreme drought has a continuous increasing trend in the middle 4 panels of Figure 8.3, which is not seen in the top 4 panels of Figure 8.3.

Orthonormal Series Method. A PDF from a small sample can be estimated using the orthonormal series method, which is essentially a series of orthonormal functions obtained from the sample. The summation of the series with coefficients results in the desired PDF. For this work, the orthonormal series as the subset of the Fourier series consisting of cosine functions is selected:

$$\phi_o(x) = 1 \text{ and } \phi_j(x) = \sqrt{2}\cos(\pi j x), \quad j = 1,2,3... \qquad \text{(Eq. 8.3)}$$

The bottom 4 panels of Figure 8.3 present the probabilities of drought conditions in the years 2000–2010, 2040–2050, and 2090–2100 as obtained using orthonormal series-based density estimation. The results are by and large similar to those of kernel density estimation except for the probabilities of mild drought. Kernel density estimation procedure projects a sudden increase in the probability of mild drought for the years 2090–2100, whereas such significant change is not observed in the results obtained from orthonormal series method.

From the overall trend in probabilities of all categories of drought, it is seen that the probability of near-normal condition is likely to decrease, and the probabilities of mild, severe, and extreme droughts are likely to increase over time. The Orissa meteorological subdivision is projected to be more drought-prone in the future.

8.4.2 Possibilistic Approach to GCM and Scenario Uncertainty

Dissimilarities between bias-corrected GCM simulations under different scenarios after the year 1990 (end of baseline period) result in different system performance measures which do not validate the assumptions of equi-predictability of

GCMs and equipossibility of scenarios, which are made in the earlier nonparametric analysis. In this section, an uncertainty modeling methodology is described which uses possibility theory for deriving a weighted distribution function of monsoon streamflow (Mujumdar and Ghosh 2008). A downscaling method based on fuzzy clustering and Relevance Vector Machine (RVM) is applied to project monsoon streamflow from three GCMs with two green house gas emission scenarios. Possibility theory is an uncertainty theory essentially used to address partially inconsistent knowledge and linguistic information based on intuition. Unlike probability, possibility is not computed from a frequency resulting from a sample, but is assigned to an event based on intuitive argumentation (Spott 1999). This intuition about the future hydrologic condition is derived here based on the performance of GCMs with associated scenarios in modeling the streamflow of the recent past (1991–2005), when there are signals of climate forcing. Figure 8.4 presents an overview of the possibilistic approach. Application of the possibilistic model is demonstrated with the monsoon streamflow of Mahanadi at Hirakud dam and described in the following sections.

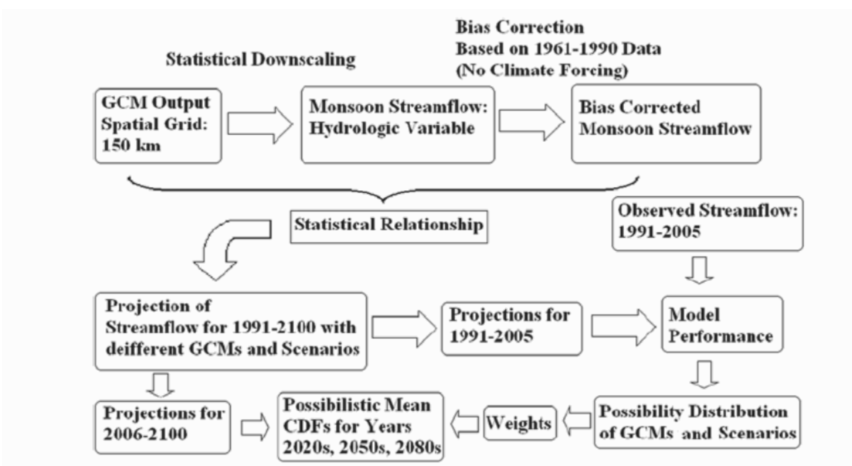

Figure 8.4. Overview of the possibility model (Mujumdar and Ghosh 2008)

8.4.2.1 Downscaling using Relevance Vector Machine

A statistical downscaling model based on PCA, fuzzy clustering and Relevance Vector Machine (RVM) is developed to predict the monsoon streamflow of Mahanadi River at Hirakud reservoir, from GCM projections of large scale climatological data. Surface air temperature at 2 m, Mean Sea Level Pressure (MSLP), geopotential height at a pressure level of 500 hecto Pascal (hPa) and surface specific humidity are considered as the predictors for modeling Mahanadi streamflow in monsoon season. Three GCMs, CCSR/NIES coupled model developed by Center for Climate System Research/National Institute for Environmental Studies (CCSR/NIES), Japan, Hadley Climate Model 3 (HadCM3), developed by Hadley

Centre for Climate Prediction and Research, U.K. and Coupled Global Climate Model 2 (CGCM2), developed by Canadian Center for Climate Modeling and Analysis, Canada with two scenarios, A2 and B2 are used for the purpose. Monthly climate data were obtained from the NCEP/NCAR reanalysis project for 1961 to 1990 for a region spanning 15^{o}N-25^{o}N and 80^{o}E–90^{o}E. Standardization is used prior to downscaling as detailed earlier. PCA is performed on the predictor variables at 25 NCEP grid-points to convert them into a set of uncorrelated variables.

8.4.2.2 Future Stream Flow Projection

For each GCM and scenario, the downscaling model is applied to give a future streamflow projection. Interpolation, PCA and fuzzy clustering are performed in the same way as described earlier. Principal components and cluster membership of GCM output are then used in the developed RVM regression model to project the monsoon streamflow of Mahanadi for the future.

Possibilistic Uncertainty Modeling. Possibility theory, founded by Zadeh (1978), is an uncertain theory devoted to addressing incomplete information, and partially inconsistent knowledge (Dubois 2006). It is related to the theory of fuzzy sets as a fuzzy restriction which acts as an elastic constraint on the values that may be assigned to a variable (Zadeh 1978). More specifically, if F is a fuzzy subset of a universe of discourse Ω = u which is characterized by its membership function μ_F, then a proposition of the form ''X is F'', where X is a variable taking values in Ω, induces a possibility distribution Π_X which equates the possibility of X taking the value u to μ_F (u) - the compatibility of u with F. In this way, X becomes a fuzzy variable which is associated with possibility distribution Π_X in much the same way as a random variable is associated with a probability distribution (Zadeh 1978). If X is a variable in the universe Ω, and it is not possible to estimate X precisely, then the possibility that X can take the value x (i.e., the degree of possibility of X = x) can be mathematically defined as (Spott 1999):

$$\Pi_X(x) : \Omega \rightarrow [0,1] \qquad \text{(Eq. 8.4)}$$

A possibility system (Drakopoulos 1995) is a triple (Ω, ß, Π) where Ω is the set of all possible outcomes, ß is a sigma-algebra on Ω and Π is a real valued function defined for each $A \in$ ß such that:

$$\Pi(\phi) = 0, \quad \Pi(\Omega) = 1, \quad and \quad \Pi(\bigcup_i A_i) = \sup_i(\Pi(A_i)) \qquad \text{(Eq. 8.5)}$$

The operator ''sup'' or supremum refers to maximum. Complete ignorance about climate forcing will lead to assignment of equal possibility (i.e., $\Pi_X(x) = 1 \ \forall x$) to all the GCMs and scenarios or all GCMs and scenarios are equally possible. With time, using the growing evidence from signals of climate forcing it should be relevant to assign a possibility distribution to the GCMs and scenarios based on their performance in the period where climate change is visible. To compute the goodness of fit between the two CDFs derived by the observed and predicted streamflow using Weibull's probability plotting position, the co-efficient (C) used as a performance measure is given by:

$$C = 1 - \frac{\sum_F (Q_{oF} - Q_{pF})^2}{\sum_F (Q_{oF} - \overline{Q}_o)^2} \qquad \text{(Eq. 8.6)}$$

where, Q_{oF} and Q_{pF} are the observed and predicted streamflow (by a GCM under a scenario) corresponding to a CDF value F, and Q_o is the mean observed streamflow. Being a measure of how well a particular scenario simulated by a GCM predicts the observed values during recent past, the coefficient C provides a measure of possibility value. As it is quite reasonable to expect that the CDF generated by a GCM will not perfectly match the observed CDF, a C value of 1 is nearly impossible. According to the properties of possibility distribution there should be at least one scenario simulated by any of the GCMs with a possibility value 1. To satisfy the property, the results obtained from equation (6) for all the three GCMs and associated scenarios, are normalized by dividing the C values with the maximum value of C and the normalized value thus obtained is used as the corresponding possibility value.

The possibility distribution (or more appropriately, possibility mass function) obtained for the GCMs and scenarios (normalized values is presented in Figure 8.5. The difference between the possibility values of two GCMs for a given scenario is higher than that between the possibility values for two scenarios of a given GCM, which denotes that the uncertainty due to selection of GCM is greater than scenario uncertainty.

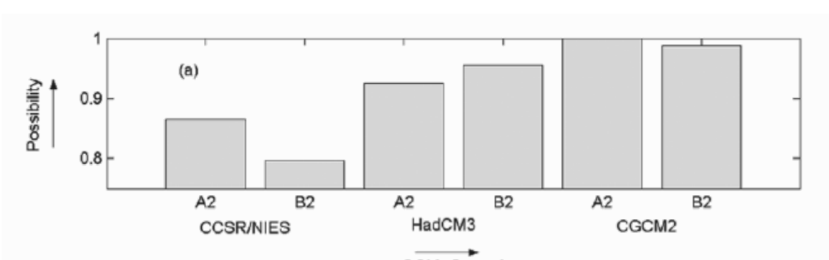

Figure 8.5. Possibility distribution of GCMs and scenarios (Mujumdar and Ghosh 2008)

The possibility values obtained for each GCM and scenario are used as weights to compute the possibilistic mean CDF (F_{pm}) for the time slices 1991–2005, 2020s, 2050s, and 2080s.

$$F_{pm} = \frac{\sum_g \sum_s \Pi(g,s) \times F_{gs}}{\sum_g \sum_s \Pi(g,s)} \qquad \text{(Eq. 8.7)}$$

where $\Pi(g, s)$ and F_{gs} are the possibility and CDF associated with g^{th} GCM and s^{th} scenario. We also calculate the range in predictions from the GCM/scenario combinations to compare with the possibilistic mean CDF as follows. For each of the discrete streamflow values at equal intervals, maximum and minimum CDF values are obtained from the CDFs generated using the projections with three GCMs and two scenarios. The maximum and minimum CDF values are considered as upper and lower bounds of the CDF $([F^+, F^-])$, resulting in an imprecise CDF. The interval between F^+ and F^- is known as the probability box. The upper and lower bounds, possibilistic mean CDF and the most possible CDF (CDF for the GCM/scenario with possibility 1) are presented in Figure 8.6 for years 1991–2005, 2020s, 2050s and 2080s. It is observed that the value of streamflow at which the possibilistic mean CDF reaches the value of 1 for years 2020s, 2050s and 2080s are lower than that of baseline period 1961–1990 and also reduces with time, which shows reduction in probability of occurrence of extreme high flow events in future. Table 8.4 presents the values of streamflow corresponding to possibilistic mean CDF values of 0.25, 0.5, 0.75 and 0.9 for the periods of 2020s, 2050s and 2080s. The results show that the monsoon flow of Mahanadi River is likely to reduce in future. Significant changes are observed in the low flow conditions for the periods 2020s, 2050s and 2080s. For the high flow condition (flow corresponding to the CDF value of 0.95) the change is most significant for the period of 2080s.

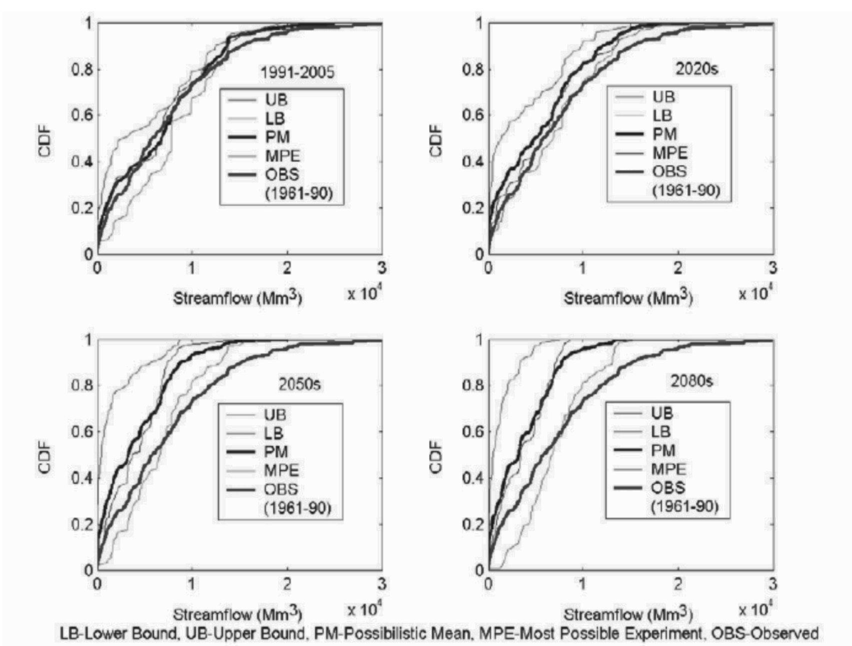

Figure 8.6. Upper bound, lower bound and possibilistic mean CDF (Mujumdar and Ghosh 2008)

8.5 Uncertainty Combination: GCM, Scenario and Downscaling Uncertainty

Assessing regional hydrologic impacts of climate change through downscaling adds another source of uncertainty, through the choice of downscaling method. These uncertainties, which arise from incomplete and unknowable information (New and Hulme 2000), propagate through the climate change impact assessment in an inter-dependent, but not necessarily additive or multiplicative manner.

Table 8.4. Streamflow (in Mm^3) Derived From Possibilistic Mean CDF (Mujumdar and Ghosh 2008)

	1961–1990	2020s		2050s		2080s	
CDF Value	Streamflow	Streamflow	Change[a]	Streamflow	Change[a]	Streamflow	Change[a]
0.25	2063	911	−55.84%	774	−62.48%	791	−61.66%
0.50	6283	4926	−21.60%	3254	−48.21%	3180	−49.39%
0.75	11273	8480	−24.78%	6757	−40.06%	6018	−46.61%
0.90	15430	12170	−21.28%	8800	−27.69%	7788	−36.01%
0.95	18148	13773	−24.11%	11350	−37.46%	9725	−46.41%

[a]Change is measured with respect to the streamflow (Col.2) derived from the CDF of observed flow for the period 1961–1990.

Kay et al. (2009) investigated the uncertainty in the impact of climate change on flood frequency in England, through the use of continuous simulation of river flows. Two ways of assessing the effect of climate variability are explored in their study. The first uses the model-based approach of running an ensemble of climate model integrations started from different initial conditions. The second is to apply a simple and pragmatic resampling of rainfall series to produce a large number of new rainfall series. Monthly resampling involves the formation of new time-series through the random selection of rainfall, month by month, from the original series. Figure 8.7 shows results from this flood frequency analysis which incorporates uncertainty due to natural variability.

8.5.1 Uncertainty Combination Using Dempster-Shafer Evidence Theory

An uncertainty modeling framework is described in this section which combines GCM, scenario and downscaling uncertainty. For this purpose, the study evaluates the use of a generalized uncertainty measure using the Dempster-Shafer evidence theory (Shafer 1976). The Dempster-Shafer (D-S) evidence theory, which can be considered a generalized Bayesian theory (Dempster 1967), is used for representing and combining uncertainty. The D-S theory has in recent years found wide applications in the fields of statistical inference, sensor fusion, expert systems, diagnostics, risk analysis, and decision analysis, due to its versatility in representing and combining different types of evidence obtained from multiple sources.

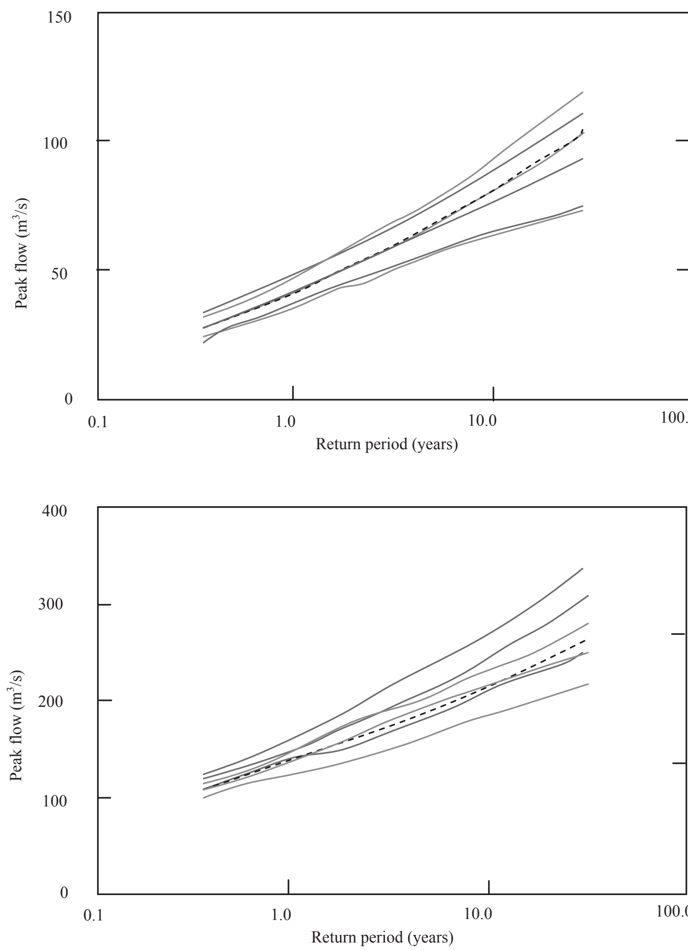

Figure 8.7. Flood frequency uncertainty from natural variability, showing results from resampled baseline (blue) and future (red) rainfall. The median flood frequency curve and the upper and lower 90% bounds are shown for each return period, from 100 resampled series using 3-month blocks (replotted from Kay et al. 2009)

8.5.1.1 D-S Evidence Theory and Uncertainty Combination in D-S Theory

The Dempster-Shafer (D-S) theory or the theory of belief functions is a mathematical theory of evidence which can be interpreted as a generalization of probability theory. The basic Dempster-Shafer's (D-S) theory of evidence was first formulated by Shafer in 1976 (Shafer 1976). D-S theory (Klir and Yuan 1995) can be considered as a variant of probability theory in which the elements of the sample space (to which nonzero probability mass is attributed) are not single points but sets.

Unlike a discrete probability distribution on the real line, where the mass is concentrated at distinct points, the focal elements of a Dempster-Shafer structure may overlap one another. This fundamental difference distinguishes D-S theory from traditional probability theory. The model is hence designed to cope with varying levels of precision regarding the information and no further assumptions are needed to represent the information. The D-S theory also provides methods to represent and combine weights of evidence. Sentz and Ferson (2002) reviewed methods for aggregating multiple Dempster-Shafer structures from different information sources. The D-S theory has found wide applications in the fields of statistical inference, sensor fusion, expert systems, diagnostics, risk analysis, and decision analysis.

The Dempster-Shafer theory represents a problem domain by a set, Θ, of mutually exclusive and exhaustive atomic hypotheses called the Frame of Discernment. For example, the frame of discernment used here based on standardized monsoon streamflow index is: Θ = {extreme drought, severe drought, moderate drought, normal, moderate wet, very wet, extreme wet}. A function $\mathbf{m}: 2^{\Theta} \rightarrow [0,1]$ is called a basic probability assignment (bpa) over Θ if it satisfies $\mathbf{m}(\phi) = 0$ and

$$\sum_{S \subseteq \Theta} \mathbf{m}(S) = 1 \qquad \text{(Eq. 8.8)}$$

m(*S*) represents the strength of evidence in the proposition that *S* represents.

From the basic probability assignment, the upper and lower bounds of an interval can be defined. This interval contains the precise probability of a set of interest (in the classical sense) and is bounded by two nonadditive continuous measures called Belief and Plausibility. A function, $\mathbf{Bel}: 2^{\Theta} \rightarrow [0,1]$ is called a belief function if it satisfies $\mathbf{Bel}(\phi) = 0$, $\mathbf{Bel}(\Theta) = 1$ and for any collection $A_1, A_2, \ldots A_n$ of subsets of Θ,

$$\mathbf{Bel}(A_1 \cup A_2 \cup \ldots \cup A_n) \geq \sum_{i} \mathbf{Bel}(A_i) - \sum_{i_i < i_2} \mathbf{Bel}(A_{i_1} \cap A_{i_2}) + \ldots$$
$$+ (-1)^{k+1} \sum_{i_i < i_2 < \ldots < i_k} \mathbf{Bel}(A_{i_1} \cap A_{i_2} \cap \ldots A_{i_k}) + \ldots + (-1)^{n+1} \sum_{i<j} \mathbf{Bel}(A_1 \cap A_2 \cap \ldots \cap A_n) \qquad \text{(Eq. 8.9)}$$

The lower bound for a set *A*, **Bel**(*A*) is defined as the sum of all the basic probability assignments of the proper subsets (*B*) of the set of interest (*A*) ($B \subseteq A$). Formally, for all sets *A* that are elements of the power set, $A \in 2^{\Theta}$

$$\mathbf{Bel}(A) = \sum_{B \subseteq A} \mathbf{m}(B) \qquad \text{(Eq. 8.10)}$$

A function, $\mathbf{Pl}: 2^{\Theta} \rightarrow [0,1]$ is called a plausibility function satisfying

$$\mathbf{Pl}(A) = \sum_{B \cap A \neq \phi} \mathbf{m}(B) \quad \text{(Eq. 8.11)}$$

The plausibility represents the upper bound for a set A, and is the sum of all the basic probability assignments of the sets (B) that intersect the set of interest (A) ($B \cap A \neq \phi$). The precise probability *P(A)* of an event (in the classical sense) lies within the lower and upper bounds of Belief and Plausibility*,* respectively:

$$\mathbf{Bel}(A) \leq P(A) \leq \mathbf{Pl}(A) \quad \text{(Eq. 8.12)}$$

Combination rules are special types of aggregation methods for data obtained from multiple sources, which may provide different assessments for the same frame of discernment. Various rules of uncertainty combination used in Dempster-Shafer theory are defined below.

Dempster's Rule. Dempster's rule is a generalization of Bayes' rule (Dempster 1967). Dempster's rule combines multiple belief functions through their basic probability assignments (m) as

$$m_{12}(A) = m_1 \oplus m_2(A) = \frac{\sum_{B \cap C = A} m_1(B) m_2(C)}{1 - K} \quad \text{when } A \neq \phi \quad \text{(Eq. 8.13)}$$

$$m_{12}(\phi) = 0 \quad \text{(Eq. 8.14)}$$

where

$$K = \sum_{B \cap C = \phi} m_1(B) m_2(C) \quad \text{(Eq. 8.15)}$$

Multiple sources can be combined sequentially using the above rule, and the order of combination does not affect the final result.

Weighted Dempster's Rule. Weighted Dempster-Shafer allows taking into account the different reliabilities of the sources as (Yu and Frincke 2005):

$$m_{12}(A) = m_1 \oplus m_2(A) = \frac{\sum_{B \cap C = A} m_1(B)^{w_1} m_2(C)^{w_2}}{\sum_{B \cap C \neq \phi} m_1(B)^{w_1} m_2(C)^{w_2}} \quad \text{(Eq. 8.16)}$$

where w_i is the weight assigned to source with bpa m_i. When w_1=w_2=1, this equation reduces to the basic Dempster's rule of combination.

Zhang's Center Combination Rule. Zhang's (1994) rule of combination, introduces a measure of the intersection of two sets *A* and *B* assuming finite sets. This is defined as the ratio of the cardinality of the intersection of two sets divided by the product of the cardinality of the individual sets, denoted with *r*(*B,C*):

$$r(B,C) = \frac{|B \cap C|}{|B||C|} = \frac{|A|}{|B||C|} \qquad \text{(Eq. 8.17)}$$

where $B \cap C = A$. The scaled products of the masses for all pairs whose intersection equals *A* are summed and multiplied by a renormalization factor *k*. A weighted version of Zhang's rule is:

$$m_{12}(A) = k \sum_{B \cap C = A} [\frac{|A|}{|B||C|} m_1(B)^{w_1} m_2(C)^{w_2}] \qquad \text{(Eq. 8.18)}$$

Disjunctive Consensus Rule. Dubois and Prade take a set-theoretic view of a body of evidence to form their disjunctive consensus rule (Dubois and Prade 1992). They define the union of the basic probability assignments $m_1 \cup m_2$ (denoted by $m_\cup(A)$) by extending the set-theoretic union:

$$m_\cup(A) = \sum_{B \cup C = A} m_1(B) m_2(C) \qquad \text{(Eq. 8.19)}$$

A weighted disjunctive consensus rule is:

$$m_\cup(A) = \sum_{B \cup C = A} m_1(B)^{w_1} m_2(C)^{w_2} \qquad \text{(Eq. 8.20)}$$

The union does not generate any conflict and does not reject any of the information asserted by the sources.

Mixing Combination. Mixing (or p-averaging or averaging) is a generalization of averaging for probability distributions (Ferson and Kreinovich 2002) as:

$$m_{12\ldots n}(A) = m_1 \oplus m_2 \oplus \ldots m_n(A) = \frac{\sum_{i=1}^{n} w_i m_i(A)}{\sum_{i=1}^{n} w_i} \qquad \text{(Eq. 8.21)}$$

where m_i's are the bpa's for the belief structures being aggregated and the w_i's are weights assigned according to the reliability of the sources.

8.5.1.2 Case Study Application

A case study for the uncertainty quantification methodology is presented for predicting future streamflow of Mahanadi River at Hirakud reservoir in Orissa. The Mahanadi basin lies in eastern India between 80°-30′E to 86°-50′E longitude and 19°-20′N to 23°-35′N latitude. It drains most of the state of Chhattisgarh, much of Orissa, and portions of Jharkhand and flows east to the Bay of Bengal. There is no major control structure upstream of the Hirakud reservoir and hence the inflow to the dam is considered as unregulated flow. The river is rain-fed with high streamflow during June to September due to monsoon rainfall, with insignificant contribution from groundwater during this season. The monsoon flows are important in Hirakud reservoir to meet the demands during the year. Hence, only monsoon streamflow is modeled here. Monsoon monthly mean inflow data for the Hirakud dam for years 1959–2005 is obtained from the Department of Irrigation, Government of Orissa, India.

Predictors used in the study are 2-m surface air temperature, MSLP, 500 hPa geopotential height and surface specific humidity. Land use is one of the important factors in generating streamflow from rainfall because of the impact of the land cover on the runoff process. In the present study, land use pattern was assumed to remain unchanged in the future. Predictor variable data was obtained from the National Center for Environmental Prediction/National Center for Atmospheric Research (NCEP/NCAR) reanalysis data for years 1948-2008 (Kalnay et al. 1996) for a region spanning 15^o–25^oN and 80^o-90^oE for years 1959–2005. For future monsoon streamflow projections, data from three GCMs for three scenarios (A2, A1B, B1) (following guidelines prescribed by the Intergovernmental Panel for Climate Change Assessment Report 4, IPCC AR4) is extracted for two time slices of years 2045–65 and 2075–95 from the multi-model dataset of the World Climate Research Programme's Coupled Model Intercomparison Project (WRCP CMIP3). The GCMs used are CGCM2 (Meteorological Research Institute), MIROC3.2 medium resolution (Center for Climate System Research), GISS model E20/Russell (NASA). Similarly, predictor variable data (2-m surface air temperature, MSLP, 500 hPa geopotential height and surface specific humidity) output from the three GCMs for two time slices of years 2046–2065 and 2075–2095 for the A2, A1B and B1 scenarios are used to downscale streamflow.

CRF-downscaling Model Projections for Streamflow. CRFs belong to a class of stochastic models called undirected graphical models (Lafferty et al. 2001). CRFs have been applied to a variety of domains, from initial applications in text processing to computer vision, image processing and bioinformatics. Raje and Mujumdar (2009) introduced the CRF model for downscaling to daily precipitation in the Mahanadi basin and provide details of the training and inference methodology. Here, the monsoon mean-monthly streamflow is modeled as a Conditional Random Field (CRF). The conditional distribution of the streamflow sequence at a site, given the monthly atmospheric (large-scale) variable sequence, is modeled as a linear-chain CRF. Let the monthly streamflow sequence at a site be represented by $\mathbf{y}$, and the observed daily atmospheric variable sequence by **x**. Then, we can write the conditional distribution of the streamflow sequence **y** as:

$$p(\mathbf{y} \mid \mathbf{x}) = \frac{1}{Z(\mathbf{x})} \exp\left\{ \sum_{t=1}^{T} \sum_{k=1}^{K} \lambda_k f_k(y_t, y_{t-1}, \mathbf{x}) \right\} \tag{Eq. 8.22}$$

where $\{\lambda_k\}$ is a parameter vector, and $\{f_k(y, y', \mathbf{x})\}_{k=1}^{K}$ is a set of real valued feature functions defined on pairs of consecutive streamflow values and the entire sequence of atmospheric data. Various feature functions used in this model are intercept and transition features, raw observation features, difference features and threshold features. Prior to training, bias removal, normalization and principal component analysis is performed on the raw NCEP data. The CRF-downscaling model is trained using the first few principal components of atmospheric variables (accounting for more than 95% of the variance) and streamflow. Maximum likelihood (Sutton and McCallum 2006) is used for training, by maximizing the log likelihood ($p(\mathbf{y} \mid \mathbf{x}, \lambda)$ as a function of λ). A limited-memory version of BFGS (lBFGS) (Nocedal and Wright 1999) is used for optimization in this model. Using maximum *a posteriori* inference by the Viterbi algorithm (Rabiner 1989), the most likely streamflow sequence is computed for testing. Prediction for a future scenario is made using principal components of atmospheric variable monthly outputs from a GCM to compute the *n* most likely streamflow sequences using *n*-best Viterbi algorithm. In order to keep *n* consistent across predictions for all GCMs and scenarios, *n* is chosen such that

$$\sum_{i=1}^{n} \ln(P_i) > -1000 \quad i.e. \quad \ln(P_1 P_2 \ldots P_n) > -1000 \tag{Eq. 8.23}$$

where P_i is the probability of the i^{th} most likely streamflow sequence. *n* computed in this way will be large if the probability of first few most likely sequences does not decay quickly. Hence, for projections with high downscaling uncertainty, this gives a larger spread in projections and vice versa.

SSFI-4 Projections. Standardized streamflow index (SSFI) is statistically similar to the standardized precipitation index (SPI) introduced by McKee et al. (1993) for meteorological drought analysis. In this study the SSFI is calculated in a similar manner from streamflow. Drought classification based on SSFI values is shown in Table 8.5. The methodology for computing monsoon SSFI-4 is as follows. The observed time series comprising of streamflow for monsoon months (Jun-Sep) for a sufficiently long period (1959-2005) is taken. This is converted to a 4-monthly aggregated streamflow time series. Then, an equi-probability transformation of the aggregated streamflow into a standard normal variable is performed. In this work, a gamma probability distribution is fitted to the aggregated monthly streamflow series. Then, for computing the SSFI-4 for any future projected aggregated streamflow time series, the non-exceedence probability related to such aggregated values is calculated and the corresponding standard normal quantile is defined as the SSFI.

Table 8.5. Drought classification based on SSFI values

Classification	SSFI value
Extreme wet	SSFI ≥ 2
Very wet	1.5 ≤ SSFI < 2
Moderate wet	1 ≤ SSFI < 1.5
Normal	-1 < SSFI < 1
Moderate drought	-1.5 < SSFI ≤ -1
Severe drought	-2 < SSFI ≤ -1.5
Extreme drought	SSFI ≤ -2

Quantifying Uncertainty through Dempster-Shafer Structure. Each scenario-GCM gives a projected range of CDFs for SSFI-4 classifications as *n*-best projections. This range is converted to an equivalent Dempster-Shafer structure (DSS). The frame of discernment for the problem domain used here is based on SSFI-4 classifications as Θ = {extreme drought, severe drought, moderate drought, normal, moderate wet, very wet, extreme wet}. In this work, the following methodology is used to construct a DSS, following Ferson et al. (2002). By extracting minimum and maximum predicted probabilities for each SSFI-4 classification, the left and right bounds of a probability box are constructed. These are step functions from zero to one with the horizontal axis being SSFI-4 classifications. The location of a rectangle along the horizontal axis defines a focal element of the Dempster-Shafer structure. The height of each rectangle is the basic probability mass associated with that interval.

Combining Projections. Each scenario-GCM gives a projected range of future CDFs for SSFI-4 classifications. This projected range is used to construct a Dempster-Shafer structure (DSS) by the basic probability assignment (bpa) and quantification of beliefs on SSFI-4 classifications. The DSSs obtained from all scenarios for a particular GCM are first combined using the mixing combination rule by assigning equal weights to each scenario, to get the bpa for the DSS corresponding to their combination. Application of this rule is equivalent to averaging applied to probability distributions. The bpa for the combination is used to derive the belief and plausibility for each proposition (SSFI-4 classification). These DSSs for each GCM are further combined across GCMs with three different rules viz. weighted Dempster's rule, weighted Zhang's Center Combination rule and weighted Disjunctive Consensus rule with equal weights for each GCM. The belief and plausibility for each SSFI-4 classification is then obtained to represent the final uncertainty.

Figure 8.8 shows the results after combining GCM uncertainty using the weighted Dempster's rule, weighted Zhang's Center Combination rule and weighted Disjunctive Consensus rule with equal weights assigned to GCMs. The difference between plausibility and belief for a given classification shows the associated uncertainty. Since Dempster's rule ignores all conflicting evidence, application of this rule yields the smallest band of uncertainty. Disjunctive Consensus based on the union operation does not ignore any evidence and hence shows the largest uncertainty. Since the Disjunctive Consensus rule is based on the union operation, there is large uncertainty in combination results, where the belief or lower bound on probability of an SSFI classification may be near zero. It is seen that the SSFI-4 projects an increasing probability of drought and decreasing probability of normal and wet conditions in future in Orissa.

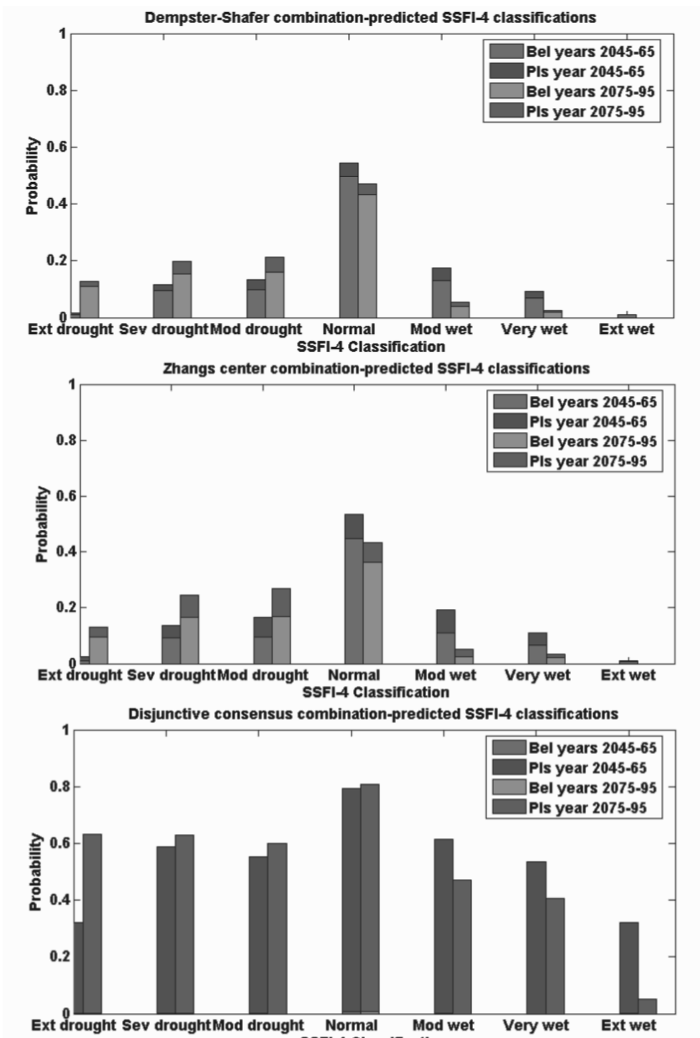

Figure 8.8. Combining uncertainty in terms of belief and plausibility for SSFI-4 classifications for years 2045–65 and 2075–95 using various combination rules (Raje and Mujumdar 2010c)

8.5.2 Non-stationarity in Downscaling: Constraining Uncertainty in Hydrologic Impacts

An extended uncertainty modeling framework is presented in this section, in which, in addition to GCM and scenario uncertainty, uncertainty in the downscaling relationship itself is explored by linkages to changes in frequencies of modes of natural variability (Raje and Mujumdar 2010b). In most studies to date, the nature of the downscaling relationship has been assumed to remain unchanged in a future climate. However, studies show that climate change may manifest in terms of changes in frequencies of occurrence of the modes of natural variability. Earlier studies have found (Arnell 2004; Minville et al. 2008; Prudhomme and Davies 2009) that GCMs contribute the largest uncertainty in modeling regional impacts.

Approaches such as optimal fingerprinting (Allen et al. 2000) and climate prediction index (Murphy et al. 2004) have been proposed to constrain future predictions using a measure of agreement with recent observed changes.

Figure 8.9 shows the predictions of global mean temperature increase with observationally constrained predictions for four scenarios, from a study by Stott et al. (2008). The probabilistic predictions represent the possible range of decadal mean temperatures observed in future relative to the forced temperatures in the 1980–1999 period, and includes an estimate of future natural variability. However, none of the studies have used objective constraints to reduce the uncertainty in regional predictions.

The study presented in this section demonstrates that incorporating changes in projected frequencies of natural regimes, and applying a novel constraint of GCM performance with respect to natural variability, results in a large reduction in uncertainty in regional hydrologic prediction.

8.5.2.1 Identifying Clusters of Natural Variability

Initially, patterns of natural variability simulated by large-scale observed climate variables over the region of interest are identified, for which some subjective judgments regarding the variables and size of area are necessary and can be based on expert knowledge about existing patterns in the region.

Figure 8.10 shows a general methodology for identifying clusters of natural variability and frequencies of each cluster. The climate variable data is deseasonalized by subtracting the long-term monthly mean and detrended by taking deviations from a running mean of a pre-specified timescale. Since this data is high-dimensional, it is subjected to a Principal Component Analysis (PCA) by taking projections onto the first few Principal Components (PCs). A clustering analysis is performed on the projected data to identify clusters of natural variability and to assign cluster memberships to each time point (e.g., month). In this work, k-means clustering has been used to identify clusters.

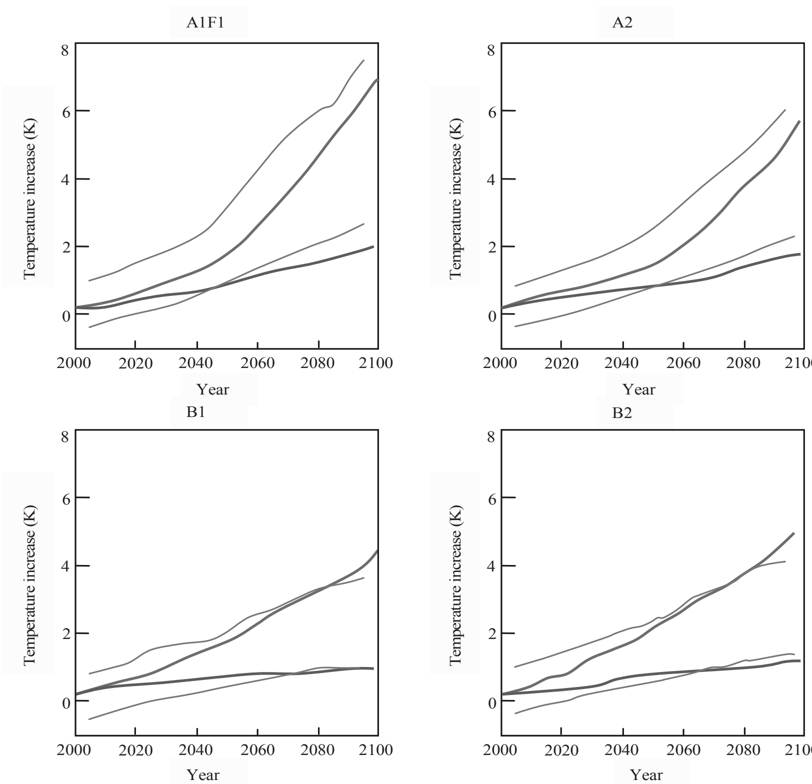

Figure 8.9. Comparison between the observationally constrained probabilistic predictions of future global mean temperature (relative to 1980–1999) following four SRES scenarios and simple climate model predictions assuming no present-day aerosol cooling (blue curve) and strong present-day aerosol cooling (red curve) (redrawn from Stott et al. 2008)

8.5.2.2 Deriving Weights for Clusters

The years 1960-2000 are chosen as the basis for comparison of observed versus GCM-simulated frequencies of clusters. Observed frequencies of each cluster are obtained as the number of months with memberships in a particular cluster, from NCEP data for years 1960–2000. GCM-computed frequencies are also obtained for this period from output variables for the 20C3M scenario or experiment for climate of the 20th century. Similarly GCM-projected frequencies for each cluster for a future time slice are obtained. Then weights for each cluster are computed based on the GCM performance with respect to that cluster for 1960–2000, called ‘frequency scaling’ as well as the GCM-scenario projected future frequency of occurrence of that cluster, called ‘cluster-linking’ as:

$$w_{ijk} = \frac{f_{ijk}}{\sum_i f_{ijk}} \cdot \frac{(f_{i,NCEP})_{1960-2000}}{(f_{i,j})_{1960-2000}}$$

(Eq. 8.26)

where w_{ijk} is the weight for cluster i in GCM j and scenario k, f_{ijk} is the simulated frequency of cluster i in GCM j and scenario k, $(f_{i,NCEP})_{1960\text{-}2000}$ is the observed cluster frequency of cluster i in NCEP data for 1960–2000, and $(f_{i,j})_{1960\text{-}2000}$ is frequency of cluster i simulated by the GCM j for 1960–2000. The weights w_{ijk} can be considered as ‘corrected future relative frequencies of clusters’. Each weight is applied to the output of a downscaling model trained on the associated cluster, in uncertainty combination. Subsequently, while combining scenario projections, weights for each scenario are taken as the sum of weights for each cluster in that scenario. Similarly, weights for a GCM are the sums of weights assigned to scenarios for the GCM.

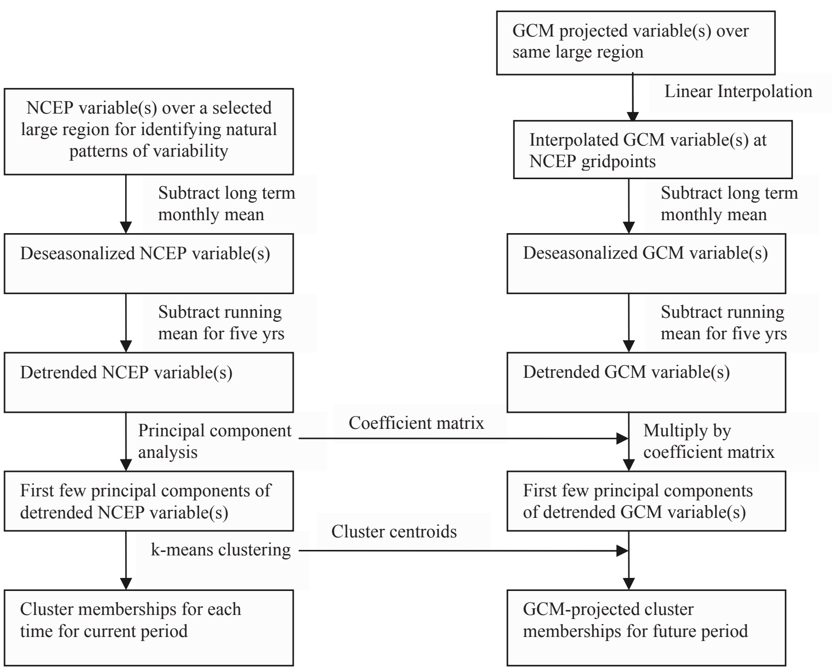

Figure 8.10. Methodology for identifying clusters of natural variability (Raje and Mujumdar 2010b)

8.5.2.3 Case Study Application

The uncertainty quantification methodology is tested for predicting future hydrologic drought from monsoon monthly streamflows of Mahanadi River at Hirakud reservoir in Orissa, India. The case study details are as given in Section 5.1. Monsoon monthly mean inflow data for the Hirakud dam for years 1959-2005 is obtained from the Department of Irrigation, Government of Orissa, India. The intensity of the Asian summer monsoon is linked to a land-sea heating contrast (Meehl 1994). For identifying natural patterns of variability in this region, data for geopotential height at 500 hPa over a large area spanning the Indian subcontinent and Indian Ocean from 15^{o}S to 45^{o}N and 45^{o}E to 120^{o}E is extracted. Use of geopotential height at 500 hPa follows the methodology adopted by Corti et al. (1999) for identifying Northen Hemisphere modes of variability. The data for monsoon monthly-mean 500 hPa geopotential height is taken from the National Center for Environmental Prediction/National Center for Atmospheric Research (NCEP/NCAR) reanalysis project for years 1948-2008 (Kalnay et al. 1996). Predictor variables for downscaling monsoon streamflow are chosen as 2m surface air temperature, mean sea level pressure (MSLP), 500 hPa geopotential height and surface specific humidity. The predictor variable data is also obtained from NCEP/NCAR reanalysis project for a region spanning 15^o–25^{o}N and 80^o–90^{o}E for years 1959-2005. Monsoon monthly mean inflow data for the Hirakud dam for years 1959-2005 is obtained from the Department of Irrigation, Government of Orissa, India.

For future projections of natural cluster frequencies, GCM-projected 500 hPa monsoon monthly geopotential height data is used. Data from the Intergovernmental Panel for Climate Change Assessment Report 4 (IPCC AR4) dataset for three GCMs for three scenarios each (A2, A1B, B1) is extracted for two time slices of years 2045–65 and 2075–95 from the multi-model dataset of the World Climate Research Programme's Coupled Model Intercomparison Project (WRCP CMIP3). The GCMs used are CGCM2 (Meteorological Research Institute, Japan), MIROC3.2 (Center for Climate System Research, Japan) medium resolution version and GISS model E20/Russell (NASA Goddard Institute for Space Studies, USA). Predictors output from the three GCMs for two time slices of years 2046–2065 and 2075–2095 for the A2, A1B and B1 scenarios are used to project future streamflow.

Data for the monsoon monthly-mean geopotential height at 500 hPa field covering a large area spanning the Indian subcontinent and Indian Ocean from 15^{o}S to 45^{o}N and 45^{o}E to 120^{o}E is extracted from NCEP/NCAR output variables for years 1948–2008. First, seasonality is removed from the raw data by subtracting the long-term monthly mean. The data is detrended by subtracting the running mean for five years. A principal component analysis is then performed on the data. The first four principal components contributing more than 70% variance are retained. A k-means clustering is performed on this four dimensional data to identify clusters and assign cluster memberships to each time point or month. Two validity indices, the Dunn's index (Dunn 1974) and the Davies-Bouldin index (Davies and Bouldin 1979) are used to determine the optimum number of clusters. Since the optimal number of clusters corresponds to a minimum Davies-Bouldin index and a maximum Dunn index, the number of clusters were chosen here as five.

8.5.2.4 Uncertainty Combination

The conditional random field (CRF) downscaling model used in the earlier section, is used for downscaling future streamflow. The CRF-downscaling model is trained separately on NCEP data belonging to each cluster for the current period using the first one or two principal components of each predictor and streamflow. This is compared to the CRF model trained on the entire dataset for the current period without clustering. The monsoon 4-monthly standardized streamflow index (SSFI-4) is used for hydrologic drought projections from projected streamflows.

The steps involved in the methodology are as follows:

- Separate downscaling relationships (DSRs), each with a different set of downscaling model parameters, are derived from each natural variability cluster.
- Each of these DSRs is used to project future SSFI-4 from each GCM-scenario combination. Thus each DSR-scenario-GCM gives a projected range of CDFs for SSFI-4 classifications.
- This projected range of CDFs is used to construct a Dempster-Shafer structure (DSS) through a basic probability assignment (bpa) on SSFI-4 classifications.
- The DSSs obtained from each DSR for a particular scenario-GCM combination are first combined using the weighted mixing combination rule, with associated cluster weights for weighting each DSS.
- Projections from scenarios obtained from the previous step are then further combined using the weighted mixing combination rule, with associated scenario weights for weighting each DSS.
- GCM projections obtained from the previous step are finally combined using the weighted rules, viz. Dempster's rule, Zhang's Center Combination rule and Disjunctive Consensus rule, with associated GCM weights for weighting each DSS, to get combined projections with the associated uncertainty.

In order to compare results from cluster-linked projections with unclustered projections, a combination is made across projections for scenarios in the unclustered approach, with equal weightages assigned to each scenario. Figure 8.11 shows results for the unclustered approach versus cluster-linked combination across scenarios, for the current period (1960–2000) as well as future time periods. It is seen that cluster-linked projections have a much smaller spread across GCMs as compared to unclustered projections, implying a smaller uncertainty as measured by the spread of projections for the cluster-linked projection. It can be seen that cluster-linking is able to effectively reduce the spread of GCM projections for the 20th century simulations, while bringing them closer to the observed CDF. However, there are still discrepancies for very wet and extreme wet classifications, where cluster-linked projections are farther from the actual or observed CDF as compared to unclustered projections.

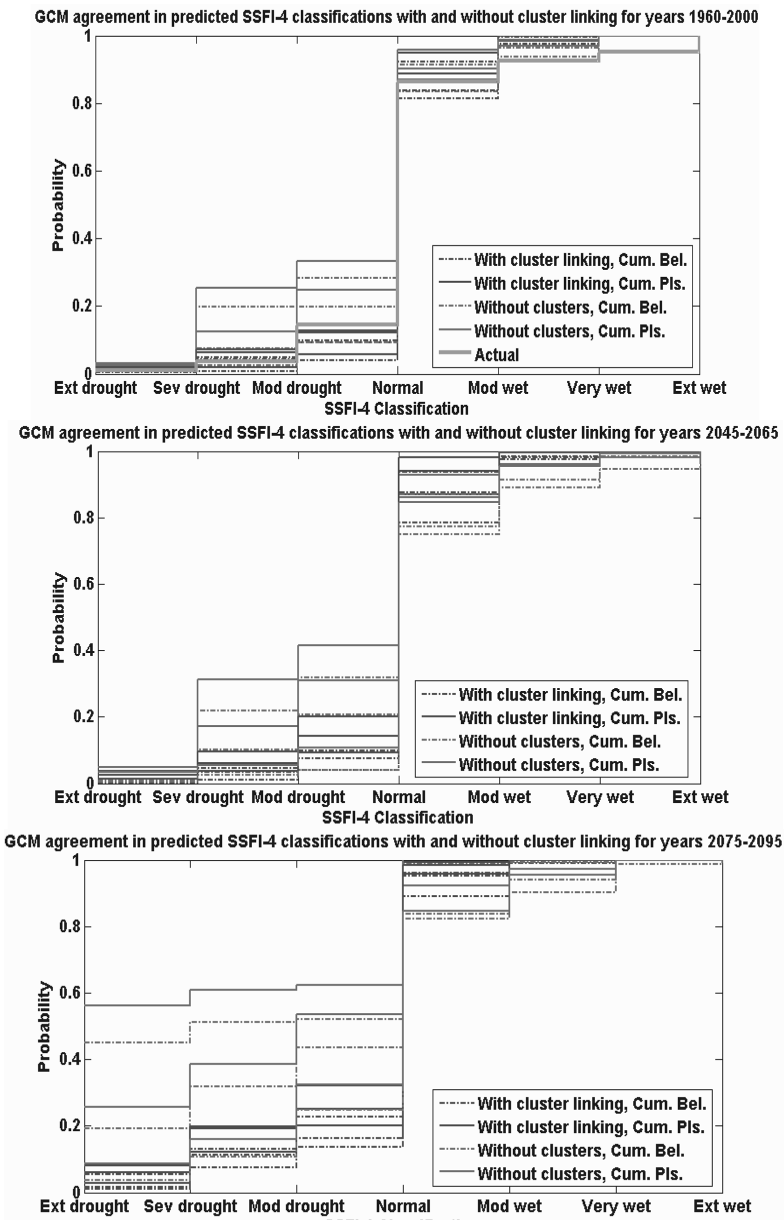

Figure 8.11. Comparison of GCM agreement in projected hydrologic drought classifications after combining scenario uncertainty (Raje and Mujumdar 2010b)

8.6 Summary and Conclusions

Climate change impact on hydrology has been extensively studied using downscaling methods. Despite significant progress made in modeling future climate, large uncertainties still exist in GCMs' parameterization of atmospheric processes and surface interactions, and also in evolution of socio-economic scenarios and GHG emissions. The results of downscaling are subject to various uncertainties which need to be quantified. Several methodologies for uncertainty quantification are discussed in this chapter. There are specific advantages and drawbacks associated with each of the methods. The choice of a suitable uncertainty quantification methodology depends on several factors such as the robustness of application, associated economic costs and also the geographical region, season and other physical factors.

Use of nonparametric PDFs is studied to estimate the probability of occurrence of different categories of droughts under future climate change scenarios. Use of a parametric distribution, such as the normal distribution, does not lead to precise or accurate estimate of such probabilities.

Modeling SPI assuming normal probability distribution should be considered only when the resulting imprecision is modeled. Use of nonparametric PDF by kernel function or orthonormal system also has imprecision associated with the smoothing of kernel estimate and the determination of support of the orthonormal system. Given a suitable index for a hydrologic event, the described methodology may be used to examine the hydrologic implications of GCM simulations for the particular event in the future. A limitation of the method is that it does not consider the uncertainty due to parameterization and the structure of the impact model (GCM) itself, and those due to starting conditions used in GCM simulations and the downscaling techniques. Also, since only a few scenarios and GCMs are used, there is an implicit weighting of the GCMs in this methodology.

For water resources management it is important to understand the effectiveness of the GCMs in modeling climate change and which of the scenarios best represent the present situation under global warming. The possibilistic mean CDF provides a way of incorporating such information in projection of future uncertainty by assigning weights to GCMs and scenarios. Though significant differences between the possibilities assigned to different scenarios may not be observed in the near future, there will be a growing difference between the possibility values assigned to GCMs with passage of time. This growing difference of the possibility values for different GCMs will increase the importance of the possibilistic model with time in future. A limitation of this approach is that uncertainties due to choice of downscaling method are not addressed in the methodology.

The Dempster-Shafer evidence combination framework can handle epistemic as well as aleatory uncertainty, and is well suited to the climate change impact assessment problem. The D-S theory shows good versatility to represent and combine different types of evidence obtained from multiple sources. The evidence combination using Dempster's rule of combination is analogous to Bayes' equation in the Bayesian uncertainty modeling framework. Luo and Caselton (1997) have earlier shown that the Bayesian approach has shortcomings under near-ignorance conditions, primarily due to the restriction placed on Bayesian probability assignments, namely that they can only be made to mutually exclusive point values or intervals. Several factors can influence the choice of a combination rule in practice. In this step, essentially, a projection using multiple information sources (GCMs) with varying reliability is obtained. It should be noted that there are, however, numerous other sources of uncertainty, such as uncertainty in identifying modes, uncertainty in deciding the number of modes, and uncertainty in classifying future circulation pattern to a mode, which are not quantified and included in the final estimated uncertainty. There can also be numerous alternatives for deriving weights for modes of variability, all logical but possibly giving different results, adding yet another source of uncertainty.

Stationarity in the downscaling relationship is a common assumption made by nearly all downscaling methods. The study presented in this chapter shows that a stationary downscaling relationship will either over- or under-predict downscaled hydrologic variable values and associated uncertainty. It is seen that the predicted changes due to cluster-linking and weighting are such that agreement between GCMs is improved for a given scenario. When projections are further combined across scenarios, it is seen that cluster-linked projections have a much smaller spread across GCMs as compared to unclustered projections. It is seen that cluster-linking is able to effectively constrain uncertainty in GCM projections for the current period (1960–2000) and brings them closer to observed streamflow probabilities, with some deficiencies for extreme streamflows or very wet and extreme wet classifications. Previous attempts to constrain predictions of climate change have used recent observed changes in the 'optimal fingerprinting' approach (Allen et al. 2000), climate prediction index (Murphy et al. 2004) or used reliability and convergence criteria (Tebaldi et al. 2004) to weight GCMs. The presented work uses a novel constraint of performance with respect to natural variability using 'frequency scaling'. However, the methodology for identification of natural clusters is based on previous work (Corti et al. 1999; Liang et al. 1996) with some modifications and is subject to further scrutiny. The monsoon standardized streamflow index (SSFI-4) used is assumed to be representative of drought and wet conditions since it depicts water supply availability. Limitations of the CRF-downscaling model include discretization of streamflow, subjectivity in the choice of feature functions and computationally intensive code. Use of multiple downscaling models in the methodology would provide robustness in prediction.

In summary, prediction at regional scales is subject to large uncertainties which must be quantified for informed decision-making. The case studies presented in this chapter indicate an increasing probability of extreme, severe and moderate drought in Orissa, and decreasing probability of normal to wet conditions due to a decrease in monsoon streamflow in the Mahanadi River, as a result of climate change. Generalized uncertainty-based information theories can be explored in order to handle the various types of uncertainty presented in climate and hydrologic modeling problems and their implications for policy needs to be studied.

8.7 References

Allen, M. R., Stott, P. A., Mitchell, J. F. B., Schnur, R., and Delworth, T. L. (2000). "Quantifying the uncertainty in forecasts of anthropogenic climate change." *Nature*, 407(6804), 617–620.

Anandhi, A., Srinivas, V. V., Nanjundiah, R. S., and Kumar, D. N. (2008). "Downscaling precipitation to river basin in India for IPCCSRES scenarios using support vector machine." *International Journal of Climatology*, 28(3), 401–420.

Arnell, N. W. (2004). "Climate change and global water resources: SRES emissions and socio-economic scenarios." *Glob Environ Change,* 14, 31–52.

Bardossy, A., Duckstein, L., and Bogardi, I. (1995). "Fuzzy rule-based classification of atmospheric circulation patterns." *International Journal of Climatology*, 15(10), 1087–1097.

Barrow, E. M., Hulme, M., and Semenov, M. (1996). "Effect of using different methods in the construction of climate change scenarios: examples for Europe." *Climate Research*, 7, 195–211.

Benestad, R. E., and Forland, E. J. (2000). "Local climate scenarios for Norway based on MPI's ECHAM/OPYC3, a new DNMI data analysis, and the common EOF method." *International Scientific Meeting on the Detection and Modelling of Recent Climate Change and its Effects on a Regional Scale*, Tarragona, Spain, 471–481.

Bogárdi, I., Matyasovszky, I., Bárdossy, A., Duckstein, L. (1994). "A hydroclimatological model of areal drought." *J. Hydrol.*, 153, 245–264.

Booij, M. J., Huisjes, M., and Hoekstra, A. Y. (2006). "Uncertainty in climate change impacts on low flows." *5th FRIEND World Conference*, Havana, CUBA, 401–406.

Buishand, T. A., and Brandsma, T. (2001). "Multisite simulation of daily precipitation and temperature in the Rhine basin by nearest-neighbor resampling." *Water Resources Research*, 39(11), 2761–2776.

Buytaert, W., Celleri, R., and Timbe, L. (2009). "Predicting climate change impacts on water resources in the tropical Andes: Effects of GCM uncertainty." *Geophysical Research Letters*, 36, L07406, doi:10.1029/2008GL037048

Cavazos, T. (1999). "Large-scale circulation anomalies conducive to extreme precipitation events and derivation of daily rainfall in northeastern Mexico and southeastern Texas." *Journal of Climate*, 12(5), 1506–1523.

Cawley, G. C., and Dorling, S. R. (1996). "Reproducing a subjective classification scheme for atmospheric circulation patterns over the United Kingdom, using a neural network." In *Proceedings of the International Conference on Artificial Neural Networks (ICANN-96)*, pp. 281–286, Springer, Bochum.

Conway, D., and Jones, P. D. (1998). "The use of weather types and air flow indices for GCM downscaling." *Journal of Hydrology*, 212–213, 348–361.

Corti, S., Molteni, F., and Palmer, T. N. (1999). "Signature of recent climate change in frequencies of natural atmospheric circulation regimes." *Nature*, 398(6730), 799–802.

Crane, R. G., and Hewitson, B. C. (1998). "Doubled CO_2 precipitation changes for the susquehanna basin: Down-scaling from the genesis general circulation model." *International Journal of Climatology*, 18(1), 65–76.

Davies, D. L., and Bouldin, D. W. (1979). "A cluster separation measure." *IEEE Trans. Pattern Anal. Machine Intell.*, 1, 224–227.

Dempster, A. P. (1967). "Upper and Lower Probabilities Induced by a Multivalued Mapping." *The Annals of Statistics*, 28, 325–339.

Dibike, Y. B., and Coulibaly, P. (2005). "Temporal neural networks for downscaling climate variability and extremes." *IEEE International Joint Conference on Neural Networks (IJCNN 2005)*, Montreal, CANADA, 135–144.

Drakopoulos, J. A. (1995). "Probabilities, possibilities, and fuzzy sets." *Fuzzy Sets Systems*, 75(1), 1– 15.

Dubois, D. (2006). "Possibility theory and statistical reasoning." *Comput. Stat. Data Anal.*, 51, 47–69.

Dubois, D. and Prade, H. (1992). "On the combination of evidence in various mathematical frameworks." *Reliability Data Collection and Analysis*. Brussels, ECSC, EEC, EAFC, 213–241.

Dunn, J. (1974). "Well separated clusters and optimal fuzzy partitions." *Journal of Cybernetics*, 4, 95–104.

Enke, W., Schneider, F., and Deutschlander, T. (2005). "A novel scheme to derive optimized circulation pattern classifications for downscaling and forecast purposes." *Theoretical and Applied Climatology*, 82(1–2), 51–63.

Ferson, S., and Kreinovich, V. (2002). *Representation, Propagation, and Aggregation of Uncertainty*. Sandia National Laboratories, Livermore, CA.

Ferson, S., Kreinovich, V., Ginzburg, L., Myers, D. S., and Sentz, K. (2002). *Constructing Probability Boxes and Dempster-Shafer Structures*. Sandia National Laboratories 2002-0835.

Forest, C. E., Stone, P. H., Sokolov, A. P., Allen, M. R., and Webster, M. D. (2002). "Quantifying uncertainties in climate system properties with the use of recent climate observations." *Science*, 295(5552), 113–117.

Fowler, H. J., Blenkinsop, S., and Tebaldi, C. (2007). "Linking climate change modelling to impacts studies: recent advances in downscaling techniques for hydrological modelling." *International Journal of Climatology*, 27(12), 1547–1578.

Ghosh, S., and Mujumdar, P. P. (2006). "Future rainfall scenario over Orissa with GCM projections by statistical downscaling." *Current Science*, 90(3), 396–404.

Ghosh, S., and Mujumdar, P. P. (2007). "Nonparametric methods for modeling GCM and scenario uncertainty in drought assessment." *Water Resources Research*, 43(7).

Ghosh, S., and Mujumdar, P. P. (2008). "Statistical downscaling of GCM simulations to streamflow using relevance vector machine." *Advances in Water Resources*, 31(1), 132–146.

Ghosh, S and Mujumdar, P. P. (2009), “Climate change impact assessment-uncertainty modeling with imprecise probability,” *Journal of Geophysical Research- Atmosphere (AGU)*, 114, D18113, doi:10.1029/2008JD011648

Giorgi, F., and Mearns, L. O. (2003). "Probability of regional climate change based on the Reliability Ensemble Averaging (REA) method." *Geophysical Research Letters*, 30(12), 1629, doi:10.1029/2003GL017130

Goodess, C., and Palutikof, J. (1998). "Development of daily rainfall scenarios for southeast Spain using a circulation-type approach to downscaling." *International Journal of Climatology*, 18(10), 1051–1083.

Greene, A.M., Goddard, L., and Lall, U. (2006). "Probabilistic multimodel regional temperature change projections." *Journal of Climate*, 19 (17), 4326–4343.

Hay, L. E., McCabe, G. J., Wolock, D. M., and Ayers, M. A. (1991). “Simulation of precipitation by weather type analysis.” *Water Resources Research*, 27(4), 493–501.

Haylock, M. R., and Goodess, C. M. (2004). “Interannual variability of European extreme winter rainfall and links with mean large-scale circulation.” *International Journal of Climatology*, 24(6), 759–76.

Hughes, J. P., Guttorp, P., and Charles, S. P. (1999). "A non-homogeneous hidden Markov model for precipitation occurrence." *Journal of the Royal Statistical Society Series C-Applied Statistics*, 48, 15–30.

IPCC (2007). *Climate Change 2007: The Physical Science Basis*. Contribution of Working Group I to the Fourth Assessment Report of the Intergovernmental Panel on Climate Change, edited by Solomon, S., Qin, D., Manning, M., Chen, Z., Marquis, M., Averyt, K.B., Tignor, M., and H.L. Miller, Cambridge University Press, Cambridge, United Kingdom and New York, NY, USA.

Jones, R. N., Chiew, F. H. S., Boughton, W. C., and Zhang, L. (2006). "Estimating the sensitivity of mean annual runoff to climate change using selected hydrological models." *Advances in Water Resources*, 29(10), 1419–1429.

Jones, P. D., Hulme, M., and Briffa, K. R. (1993). “A comparison of Lamb circulation types with an objective classification scheme.” *International Journal of Climatology*, 13(6), 655–63.

Kalnay, E., Kanamitsu, M., Kistler, R., Collins, W., Deaven, D., Gandin, L., Iredell, M., Saha, S., White, G., Woolen, J., Zhu, Y., Chelliah, M., Ebisuzaki, W., Higgins, W., Janowiak, J., Mo, K. C., Ropelewski, C., Wang, J., Leetma, A., Reynolds, R., Jenne, R. and Joseph, D. (1996). "The NCEP/NCAR 40-year reanalysis project." *Bullet. Amer. Meteorol. Soc.*, 77, 437–471.

Karl, T. R., Wang, W. C., Schlesinger, M. E., Knight, R. W., and Portman, D. (1990). "A method of relating general-circulation model simulated climate to the observed local climate .1. Seasonal statistics." *Journal of Climate*, 3(10), 1053–1079.

Katz, R. W. (2002). “Techniques for estimating uncertainty in climate change scenarios and impact studies.” *Climate Research*, 20, 167–185.

Kay, A. L., Davies, H. N., Bell, V. A., and Jones, R. G. (2009). "Comparison of uncertainty sources for climate change impacts: flood frequency in England." *Climatic Change*, 92(1–2), 41–63.

Kleinen, T., and Petschel-Held, G. (2007). "Integrated assessment of changes in flooding probabilities due to climate change." *Climatic Change*, 81(3–4), 283–312.

Klir, G., and Yuan, B. (1995). *Fuzzy Sets and Fuzzy Logic: Theory and Applications.* Prentice Hall, New Jersey.

Knutti, R., Stocker, T. F., Joos, F., and Plattner, G. K. (2002). "Constraints on radiative forcing and future climate change from observations and climate model ensembles." *Nature*, 416(6882), 719–723.

Lafferty, J., McCallum, A., and Pereira, F. (2001). "Conditional random fields: Probabilistic models for segmenting and labeling sequence data." In *Proc. 18th International Conf. on Machine Learning*, edited by C.E. Brodley, and A.P. Danyluk, Morgan Kaufmann, San Francisco, CA, pp. 282–289.

Lall, U., Rajagopalan, B., and Torboton, D. G. (1996). "A nonparametric wet/dry spell model for resampling daily precipitation." *Water Resources Research*, 32(9), 2803–2823.

Lall, U., and Sharma, A. (1996). "A nearest neighbour bootstrap for time series resampling." *Water Resources Research*, 32(3), 679–693.

Liang, X. Z., Wang, W. C., and Dudek, M. P. (1996). "Northern hemispheric interannual teleconnection patterns and their changes due to the greenhouse effect." *Journal of Climate*, 9(2), 465–479.

Lorenzo, M. N., Taboada, J. J, and Gimeno, L. (2008). "Links between circulation weather types and teleconnection patterns and their influence on precipitation patterns in Galicia (NW Spain)." *International Journal of Climatology*, 28(11), 1493–505.

Luo, W. B., and Caselton, B. (1997). "Using Dempster–Shafer Theory to Represent Climate Change Uncertainties." *Journal of Environmental Management*, 49, 73–93.

Maurer, E. P., and Duffy, P. B. (2005). "Uncertainty in projections of streamflow changes due to climate change in California." *Geophysical Research Letters*, 32(3), L03704, doi:10.1029/2004GL021462

McKee, T. B., Doesken, N. J. and Kleist, J. (1993). "The relationship of drought frequency and duration to time scale." In *Proceedings of the Eighth Conference on Applied Climatology*, American Meteorological Society, pp. 179–184.

Minville, M., Brissette, F., and Leconte, R. (2008). "Uncertainty of the impact of climate change on the hydrology of a nordic watershed." *Journal of Hydrology*, 358(1–2), 70–83.

Morgan, M. G., and Keith, D. W. (1995). "Climate-change–Subjective judgements by climate experts." *Environmental Science & Technology*, 29(10), A468–A476.

Mujumdar, P. P., and Ghosh, S. (2008). "Modeling GCM and scenario uncertainty using a possibilistic approach: Application to the Mahanadi River, India." *Water Resources Research*, 44(6).

Murphy, J. M., Sexton, D. M. H., Barnett, D. N., Jones, G. S., Webb, M. J., and Collins, M. (2004). "Quantification of modelling uncertainties in a large ensemble of climate change simulations." *Nature*, 430(7001), 768–772.

New, M., and Hulme, M. (2000). "Representing uncertainty in climate change scenarios: A Monte Carlo approach." *Int. Assessment*, 1, 203– 213.

Nocedal, J., and Wright, S. J. (1999). *Numerical optimization*, Springer-Verlag, New York.
Prudhomme, C., and Davies, H. (2009). "Assessing uncertainties in climate change impact analyses on the river flow regimes in the UK. Part 2: Future climate." *Climatic Change*, 93(1–2), 197–222.
Prudhomme, C., Jakob, D., and Svensson, C. (2003). "Uncertainty and climate change impact on the flood regime of small UK catchments." *Journal of Hydrology*, 277(1–2), 1–23.
Prudhomme, C., Reynard, N., and Crooks, S. (2002). "Downscaling of global climate models for flood frequency analysis: Where are we now?" *Hydrological Processes*, 16(6), 1137–1150.
Rabiner, L. (1989). "A tutorial on hidden Markov models and selected applications in speech recognition." In *Proceedings of the IEEE*, 77(2):257–285.
Rajagopalan, B., and Lall, U. (1999). "A k-nearest-neighbor simulator for daily precipitation and other variables." *Water Resources Research*, 35(10), 3089–3101.
Raje, D., and Mujumdar, P. P. (2009). "A conditional random field based downscaling method for assessment of climate change impact on multisite daily precipitation in the Mahanadi basin." *Water Resources Research*, 45(10), W10404. doi: 10.1029/2008WR007487.
Raje, D., and Mujumdar, P. P. (2010a). "Reservoir performance under uncertainty in hydrologic impacts of climate change." *Advances in Water Resources*, 33, 312–326. doi:10.1016/j.advwatres.2009.12.008.
Raje, D., and Mujumdar, P. P. (2010b). "Constraining uncertainty in regional hydrologic impacts of climate change: Nonstationarity in downscaling." *Water Resources Research*, 46, W07543. doi:10.1029/2009WR008425.
Raje, D., and Mujumdar, P. P. (2010c). "Hydrologic drought prediction under climate change: Uncertainty modeling with Dempster-Shafer and Bayesian approaches." *Advances in Water Resources*. doi:10.1016/j.advwatres.2010.08.001.
Richardson, C.W., and Wright, D. A. (1984). *WGEN: a model for generating daily weather variables. ARS-8*, US Department of Agriculture, Agricultural Research Service, Washington, DC.
Rowell, D. P. (2006). "A demonstration of the uncertainty in projections of UK climate change resulting from regional model formulation." *Climatic Change*, 79(3–4), 243–257.
Scott, D.W. (1992), *Multivariate Density Estimation, Theory, Practice, and Visualization*, John Wiley, Hoboken, N. J.
Sentz, K., and Ferson, S. (2002). *Combination of Evidence in Dempster-Shafer Theory*. Sandia National Laboratories 2002–4015.
Shafer, G. (1976). *A Mathematical Theory of Evidence*. *Princeton University Press*, Princeton.
Simonovic, S. P., and Li, L. (2003). "Methodology for assessment of climate change impacts on large-scale flood protection system." *J. Water Resour. Plan. Manage.*, 129(5), 361– 371.

Simonovic, S. P., and Li, L. (2004). “Sensitivity of the red river basin flood protection system to climate variability and change.” *Water Resour. Manag.*, 18, 89– 110.

Spott, M. (1999). “A theory of possibility distributions.” Fuzzy Sets Systems, 102(2), 135–155.

Srikanthan, R., and McMahon, T. A. (2001). "Stochastic Generation of Annual, Monthly and Daily Climate Data: A Review." *Hydrol. Earth Sys. Sci.*, 5, 643–670.

Stainforth, D. A., Aina, T., Christensen, C., Collins, M., Faull, N., Frame, D. J., Kettleborough, J. A., Knight, S., Martin, A., Murphy, J. M., Piani, C., Sexton, D., Smith, L. A., Spicer, R. A., Thorpe, A. J., and Allen, M. R. (2005). "Uncertainty in predictions of the climate response to rising levels of greenhouse gases." *Nature*, 433(7024), 403–406.

Steinemann, A. (2003). “Drought indicators and triggers: A stochastic approach to evaluation.” *J. Am. Water Resour. Assoc.*, 39(5), 1217– 1233.

Stott, P. A., Huntingford, C., Jones, C. D. and Kettleborough, K. A. (2008). “Observed climate change constrains the likelihood of extreme future global warming.” *Tellus*, 60B, 76–81.

Sutton, C., and McCallum, A. (2006). "An introduction to conditional random fields for relational learning." In *Introduction to Statistical Relational Learning*, edited by L. Getoor, and B. Taskar, MIT Press, Cambridge, MA, pp. 1–35.

Tarboton, D. G., Sharma, A., and Lall, U. (1998). “Disaggregation procedures for stochastic hydrology based on nonparametric density estimation.” *Water Resour. Res.*, 34(1), 107– 119.

Tatli, H., Dalfes, H. N., and Mentes, S. (2004). "A statistical downscaling method for monthly total precipitation over Turkey." *International Journal of Climatology*, 24(2), 161–180.

Tebaldi, C., Mearns, L. O., Nychka, D., and Smith, R. L. (2004). "Regional probabilities of precipitation change: A Bayesian analysis of multimodel simulations." *Geophysical Research Letters*, 31(24), L24213, doi:10.1029/2004GL021276

Tebaldi, C., Smith, R. L., Nychka, D., and Mearns, L. O. (2005). "Quantifying uncertainty in projections of regional climate change: A Bayesian approach to the analysis of multimodel ensembles." *Journal of Climate*, 18(10), 1524–1540.

Trigo, R. M., and Palutikof, J. P. (1999). "Simulation of daily temperatures for climate change scenarios over Portugal: a neural network model approach." *Climate Research*, 13(1), 45–59.

Tripathi, S., Srinivas, V., and Nanjundiah, R. (2006). "Dowinscaling of precipitation for climate change scenarios: A support vector machine approach." *Journal of Hydrology*, 330(3–4), 621–640.

von Storch, H., Langenberg, H., and Feser, F. (2000). "A spectral nudging technique for dynamical downscaling purposes." *Monthly Weather Review*, 128(10), 3664–3673.

Vrac, M., Stein, M., and Hayhoe, K. (2007). "Statistical downscaling of precipitation through nonhomogeneous stochastic weather typing." *Climate Research*, 34(3), 169–184.

Wilks, D. S. (1999). "Multisite downscaling of daily precipitation with a stochastic weather generator." *Climate Research*, 11(2), 125–136.

Wilks, D. S., and Wilby, R. L. (1999). "The weather generation game: a review of stochastic weather models." *Progress in Physical Geography*, 23(3), 329–357.

Wigley, T. M. L., Jones, P. D., Briffa, K. R., and Smith, G. (1990). "Obtaining sub-grid-scale information from coarse-resolution general-circulation model output." *Journal of Geophysical Research-Atmospheres*, 95(D2), 1943–1953.

Wilby, R. L. (2005). "Uncertainty in water resource model parameters used for climate change impact assessment." *Hydrological Processes*, 19(16), 3201–3219.

Wilby, R. L., and Harris, I. (2006). "A framework for assessing uncertainties in climate change impacts: Low-flow scenarios for the River Thames, UK." *Water Resources Research*, 42(2).

Wilby, R. L., and Wigley, T. M. L. (1997). "Downscaling general circulation model output: a review of methods and limitations." *Progress in Physical Geography*, 21, 530–548.

Wilby, R. L., Wigley, T. M. L., Conway, D., Jones, P. D., Hewitson, B. C., Main, J., and Wilks, D. S. (1998). "Statistical downscaling of general circulation model output: A comparison of methods." *Water Resources Research*, 34(11), 2995–3008.

Wilson, L. L., Lettenmaier, D. P., and Skyllingstad, E. (1992). "A hierarchical stochastic model of largescale atmospheric circulation patterns and multiple station daily rainfall." *J. Geophys. Res.*, 97(ND3), 2791–2809.

Xu, C. Y. (1999). "Climate change and hydrologic models: A review of existing gaps and recent research developments." *Water Resources Management*, 13(5), 369–382.

Yager, R. R. (1987). "On the Dempster-Shafer framework and new combination rules." *Information Sciences*, 41, 93–137.

Yu, D., and Frincke, D. (2005). "Alert Confidence Fusion in Intrusion Detection Systems with Extended Dempster-Shafer Theory." In *ACM-SE 43: Proceedings of the 43rd annual southeast regional conference*, 2, 142–147.

Zadeh, L. A. (1978). "Fuzzy sets as a basis for a theory of possibility." *Fuzzy Sets Systems*, 1(1), 3–28.

Zhang, L. (1994). "Representation, independence, and combination of evidence in the Dempster-Shafer theory." In *Advances in the Dempster-Shafer Theory of Evidence*. John Wiley & Sons, Inc., New York, pp. 51–69.

Zorita, E., and von Storch, H. (1999). "The analog method as a simple statistical downscaling technique: comparison with more complicated methods." *Journal of Climate*, 12(8), 2474–89.

CHAPTER 9

Statistical Downscaling of Precipitation and Temperature for a Lake Basin

Manish Kumar Goyal, C. S. P. Ojha, Donald H. Burn, and Rao Y. Surampalli

9.1 Introduction

Impacts of climate change on hydrology have been widely studied recently. It is well known that climate model resolution issues have important implications. Hydrological models are frequently concerned with small, subcatchment-scale processes, whereas atmospheric models deal most proficiently with fluid dynamics at the planetary scale. To overcome possible problems related to the scale mismatch between vegetation and land-surface processes, and the large-scale atmospheric circulation, a powerful tool (e.g., statistical downscaling) is needed, in order to utilize General Circulation Models (GCMs) based outputs to locally observed hydrologic and meteorological variables.

The very basic question to be addressed first is "What is downscaling?" Here, we will define downscaling as the process of making the link between the state of some variable representing a large scale/space and the state of some variable representing a much smaller/regional space. The large-scale variable may, for instance, represent the circulation pattern over a large region whereas the small scale may be the local temperature/precipitation, etc. as measured at one given station. The second important question is: "Why downscaling?" The answer to this question is connected to a specific purpose, such as using General Circulation Models (GCMs) to make an inference about the local/regional climate at a given location. The global mean value of the meteorological variables such as temperature/ precipitation is usually not directly relevant for practical use. The GCMs represent an important tool for studying our climate; however, they do not give a realistic description of the local climate in general. Because of the complex physics of the atmosphere and the short-lived nature of most synoptic systems, a GCM usually may never provide reliable information at the mesoscale. It is therefore, common to downscale the results from the GCMs through either a nested high-resolution regional climate model (RCM) or empirical/statistical downscaling. The GCMs do not give a perfect description of the real climate system as they include "parameterizations" that involve simple statistical models giving an approximate or ad-hoc representation of sub-grid processes.

This chapter introduces the principles of statistical downscaling and different downscaling techniques; it then introduces the site information (Pichola Lake in India) and methods for data extraction; it then uses the extracted data to demonstrate the application/effectiveness and two methods (i.e., linear regression and artificial neural network) as the downscaling tools in projections of different parameters.

9.2 Statistical Downscaling

9.2.1 Definition

The process of inferring information about the small/regional-scale, given the large-scale variables by the means of a statistical model, is referred to as “statistical downscaling” (Benestad 2001; Anandhi et al. 2008; Goyal et al., 2012). Statistical downscaling involves deriving empirical relationships that transform large-scale features of the GCM (Predictors) to regional-scale variables (Predictands) such as precipitation, temperature and stream flow. Predictor sets are typically derived from sea level pressure, geopotential height, wind fields, humidity variables, and temperature variables (Cecilia et al. 2001). Typically, GCMs have a resolution of 150–300 km. Many climate change studies and impacts models require information at scales of 50 km or less, so some method is needed to estimate the smaller-scale information. Statistical downscaling first derives statistical relationships between observed small-scale (often station level) variables and larger (GCM) scale variables, using either analogue methods (circulation typing), regression analysis or soft computing methods such as neural networks (Cannon and Whitefield 2002). Future values of the large scale variables obtained from GCM projections of future climate are then used to drive the statistical relationships and so estimate the smaller-scale details of future climate. Statistical downscaling is a two-step process basically consisting of i) development of statistical relationships between local climate variables (e.g., surface air temperature and precipitation) and large-scale predictors, and ii) application of such relationships to the output of GCM experiments to simulate local climate characteristics (Wilby et al. 2002; Cavazos and Hewitson 2005; Goyal et al., 2010; Goyal and Ojha 2010a).

9.2.2 Assumptions

There are three implicit assumptions involved in statistical downscaling:

(1) The predictors are variables of relevance and are realistically modeled by the host GCM. Prior knowledge of climate model limitations can be advantageous when screening potential predictors.

(2) The empirical relationship is valid also under altered climatic conditions. This needs careful assessment for future climate projection as it is impossible to check with observational data.

(3) The predictors employed fully represent the climate change signal. Some approaches may exclude predictors based on current climate performance that could be important in the future changed climates.

Statistical downscaling is most appropriate for (i) subgrid scales (small islands, point processes, etc.); (ii) complex/heterogeneous environments; (iii) extreme events; (iv) exotic predictands such as tidal surges, air quality, extreme event indices etc.; and (v) transient change/ensembles; it is not appropriate for (i) data-poor regions and (ii) where relationships between predictors and predictands may change.

9.2.3 Methodology

Here are the steps to construct a statistical downscaling model:

(1) **Selection of GCM and choice of the statistical downscaling method:** Several GCMs are in use and one needs to select the GCM based on physical relevance and literature findings. The choice of the statistical method to find a predictor-predictand relationship is to a great extent dependent on statistical properties of the predictand variables.

(2) **Selecting appropriate predictor variables:** In order to choose predictor variables, a profound knowledge of the GCM model and the driving forces of local and regional scale meteorology are necessary. The availability of reanalysis data sets has significantly increased the number and variety of candidate predictors.

(3) **Standardization of data:** Standardization is widely used prior to statistical downscaling method to reduce systematic biases in the mean and variance of GCM predictors relative to observations. The procedure typically involves subtraction of the mean and division by the standard deviation of the predictor for a predefined baseline period.

(4) **Model evaluation using independent data and force downscaling model with GCM predictor variables:** A standard approach to model validation is to use one portion of the available observation records for model calibration and one portion for the validation.

9.3 Statistical Downscaling Techniques

9.3.1 Multiple Linear Regression

Linear regression attempts to model the relationship between two variables by fitting a linear equation to observed data. One variable is considered to be an explanatory variable, and the other is considered to be a dependent variable. For example, a modeler might want to relate the weights of individuals to their heights using a linear regression model.

In statistical methods, the order in which the predictor variables are entered into (or taken out of) the model is determined according to the strength of their correlation with the criterion variable. In direct regression, all available predictor variables are put into the equation at once and they are assessed on the basis of proportion of variances in the criterion variable (Y) they uniquely account for. In Forward selection, the variables are entered into the model one at a time in an order determined by the strength of their correlation with the criterion variable. The effect of adding each is assessed as it is entered, and variables that do not significantly add to the success of the model are excluded. In Backward selection, all the predictor variables are entered into the model. The weakest predictor variable is then removed and the regression re-calculated. If this significantly weakens the model then the predictor variable is re-entered–otherwise it is deleted. This procedure is then repeated until only useful predictor variables remain in the model. Stepwise regression is the most sophisticated of the regression methods. Each variable is entered in sequence and its value assessed. If adding the variable contributes to the model then it is retained, but all other variables in the model are then re-tested to see if they are still contributing to the success of the model. If they no longer contribute significantly they are removed. Thus, this method should ensure that one ends up with the smallest possible set of predictor variables included in one's model (Schoof and Pryor 2001; Goyal and Ojha 2010b; Goyal and Ojha 2011a).

9.3.2 PLS Regression

Partial Least Squares projection to latent structures (PLS) regression is used to describe the relationship between multiple response variables and predictors through the latent variables. PLS regression can analyze data with strongly collinear, noisy, and numerous X-variables, and also simultaneously model several response variables, Y. In general, the PLS approach is particularly useful when one or a set of dependent variables (or time series) need to be predicted by a (very) large set of predictor variables (or time series) that are strongly cross-correlated. This is often the case in empirical downscaling of climate variables.

$$
\begin{aligned}
X &= TP^T + E \\
Y &= TQ^T + F
\end{aligned}
\qquad \text{(Eq. 9.1)}
$$

where X is an n x m matrix of predictors, Y is an n x p matrix of responses, T is an n x l matrix (the *score*, *component* or *factor* matrix), P and Q are, respectively, m x l and p x l *loading* matrices, and matrices E and F are the error terms (Goyal and Ojha 2010c; Goyal and Ojha 2011b).

9.3.3 Artificial Neural Network (ANN)

A neural network is characterized by its architecture that represents the pattern of connection between the nodes, its method of determining the connection weighs and the activation function. A feed forward artificial neural network is one of the most commonly used tools in the modeling of various engineering and science related problems. A feed forward ANN can have many layers. The first layer contains the input variables and is called the input layer. The last layer connects to the output variables and is referred as output layer. Layers between the input and output layers are called hidden layers (Figure 9.1). The processing elements in each layer are called nodes. Each of these nodes connections will have associated weight. All connections are "feed-forward"; i.e. they allow information transfer only from an earlier layer to the next consecutive layers. Nodes within a layer are not interconnected and nodes in nonadjacent layers are not connected.

It should be pointed out that the structures of most current ANNs are extremely simple, and capabilities are quite poor when compared to biological neural networks. Nonetheless since the last few decades, many ANN structures have been proposed and explored. The structures include multi-layer feed forward networks, self-organizing feature maps, Hopfield networks and counter propagation networks. Like any intelligent models, ANN has the capability of learning. For training of ANN, various algorithms are used. These are back propagation algorithms, conjugate gradient algorithms, radial basis function, cascade correlation algorithm. Back propagation is perhaps the most popular algorithm for training ANNs. Out of these, back propagation gradient descent technique using momentum and adaptive learning rate and back propagation gradient descent technique using Levenberg-Marquardt Algorithm are often used (Cannon and Lord 2000; Dibike and Coulibaly 2006; Ojha et al. 2010; Goyal and Ojha 2012c).

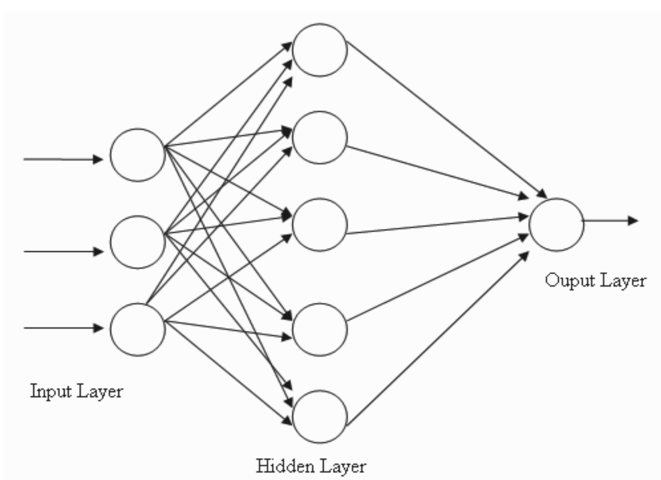

Figure 9.1. Three layer Feed-Forward Neural Network

9.3.4 K Nearest Neighbor

K nearest neighbor (K-NN) is a part of supervised learning that has been used in many applications in the field of data mining, statistical pattern recognition and image processing. Although more sophisticated alternative techniques have been developed since their inception, nearest neighbor methods remain very popular. The fundamental idea of the K-NN algorithm is to find analogs of a feature vector (vector of variables for which analogs are sought) based on similarity criteria in the observed time series.

A nearest neighbor algorithm typically involves selecting a specified number of data vectors similar in characteristics to the vector of interest. Performance of K-NN is dependent largely upon the efficient selection of K-Nearest Neighbors. All the attributes describing an instance do not have same importance in selecting the nearest neighbors. Assuming a sample of points from some underlying distribution may contain several distinct clusters. Therefore, one needs to construct various graphs/shapes on the sample points such that clusters are "identified": that is, the sub-graphs/shape induced by nearest neighbors from the same cluster is connected, while sub-graphs/shape corresponding to different clusters is not connected to each other. These shapes induced by nearest neighbors may be either square/rectangle or triangle/circle. The choice of K-Nearest Neighbors is based on the prescriptive choice of the square-root of all possible candidates. ($K = n^{1/2}$).

Squared Euclidian distance is to be calculated for each of the projected feature vector and the squared Euclidean distances are sorted in ascending order. Finally, a set of K-NN states is selected in which an element of set records the time t associated with closest historical state with the current vector. In this manner, sampling is continued to achieve the similar states and hence corresponding climatic variable state is taken into account for the forecast based on average of all these states (Goyal et al. 2012). Furthermore, one can refer Young (1994), Lall and Sharma (1996), Rajagopalan and Lall (1999), and Dimri et al. (2008) for detailed description of the approach.

9.4 Study Region and Data Extraction

The study area considered is the Pichola Lake catchment in Rajasthan state in India that is situated from 72.5°E to 77.5°E and 22.5°N to 27.5°N as shown in Figure 9.2. The Pichola Lake basin, located in Udaipur district, Rajasthan is one of the major sources for water supply for this arid region. During the past several decades, the stream-flow regime in the catchment has changed considerably, which resulted in water scarcity, low agriculture yield and degradation of the ecosystem in the study area. Regions with arid and semi-arid climates could be sensitive even to small changes in climatic characteristics. Temperature affects the evapotranspiration, evaporation and desertification processes and is also considered as an indicator of environmental degradation and climate change (Linz et al. 1990). Understanding the relationships among the hydrologic regime, climate factors, and anthropogenic effects is important for the sustainable management of water resources in the entire catchment hence this study area was chosen because of afore mentioned reasons.

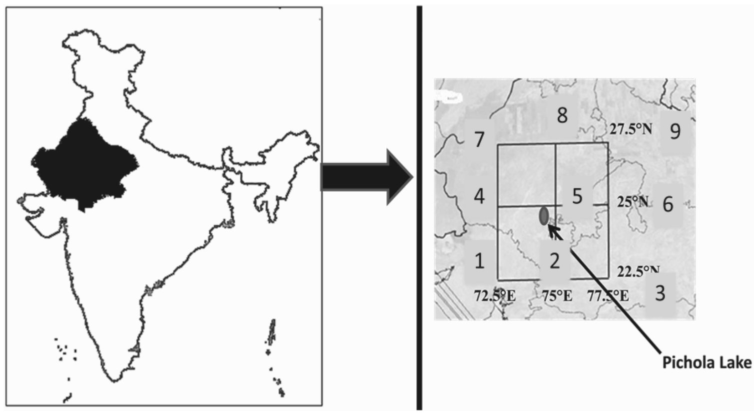

Figure 9.2. Location map of the study region in Rajasthan State of India with NCEP grid

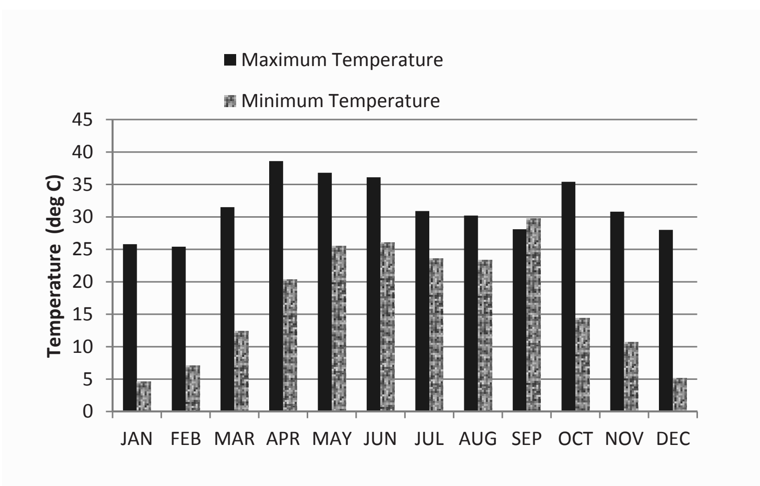

Figure 9.3. Maximum and minimum temperature in the study region for year 2000

The monthly mean atmospheric variables were derived from the reanalysis data set of the National Center for Environmental Prediction (NCEP/NCAR) (hereafter called NCEP) for a period of January 1948 to December 2000 (Kalnay et al. 1996). The data have a horizontal resolution of 2.5° latitude X longitude and seventeen constant pressure levels in vertical. The atmospheric variables are extracted for nine grid points whose latitude ranges from 22.5 to 27.5 °N, and longitude ranges from 72.5 to 77.5 °E at a spatial resolution of 2.5°. The maximum temperature (Tmax), minimum temperature (Tmin) and precipitation are used at monthly time scale from records available for Pichola Lake which is located in Udaipur at 24° 34'N latitude and 73°40'E longitude. The data is available for the period January 1990 to December 2000 (Khobragade 2009). The mean monthly *T*max in the catchment varies from 19°C to 39.5°C and mean annual *Tmax* is 30.6°C. The mean monthly *T*min ranges from 3.4°C to 29.8°C based on decadal (1990–2000) observed value. The observed mean monthly *T*max and *T*min have been shown in Figure 9.3 for various months of year 2000 respectively. The study area receives an average annual precipitation of 597 mm. It has a tropical monsoon climate where most of the precipitation is confined to a few months of the monsoon season. The south–west (summer) monsoon has warm winds blowing from the Indian Ocean causing copious amount of precipitation during June–September months. The observed precipitation has been shown in Figure 9.4 for various months of year 2000. The Canadian Center for Climate Modeling and Analysis (CCCma) (http://www.cccma.bc.ec.gc.ca/) provides GCM data for a number of surface and atmospheric variables for the CGCM3 T47 version which has a horizontal resolution of roughly 3.75° latitude by 3.75° longitude and a vertical resolution of 31 levels. CGCM3 is the third version of the CCCma Coupled Global Climate Model which makes use of a significantly updated atmospheric component AGCM3 and uses the same ocean component as in CGCM2. The data comprise of present-day (20C3M) and future simulations forced by four emission scenarios, namely A1B, A2, B1 and COMMIT.

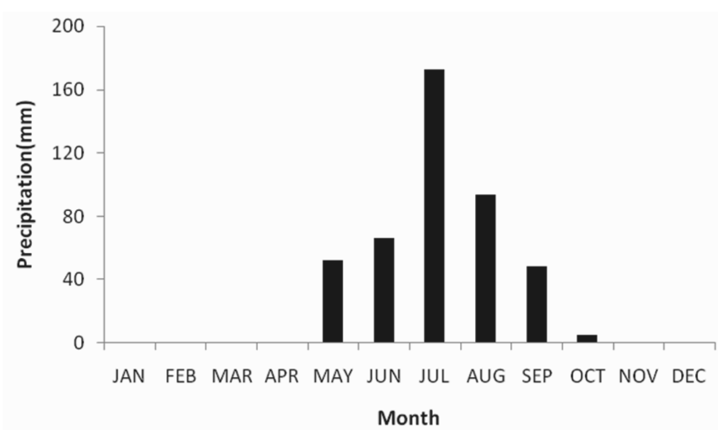

Figure 9.4. Observed precipitation for the study region for year 2000

The nine grid points surrounding the study region as shown in Figure 9.2 are selected as the spatial domain of the predictors to adequately cover the various circulation domains of the predictors considered in this study. The GCM data are re-gridded to a common 2.5° using inverse square interpolation technique (Willmott et al. 1985). The utility of this interpolation algorithm was examined in previous downscaling studies.

9.4.1 Selection of Predictors

The selection of appropriate predictors is one of the most important steps in a downscaling exercise for downscaling predictands. Predictors have to be selected based both on their relevance to the downscaled predictands and their ability to be accurately represented by the GCMs. The most favorable predictors must be strongly correlated with the predictand, be physically sensible, and have the ability to capture the climate change signal (Goyal et al. 2010). The predictors are chosen by the following criteria: (1) they should be skilful in representing large-scale variability that is simulated by the GCMs and are readily available from archives of GCM output and reanalysis data sets; (2) they should strongly correlated with the surface variables of interest/predictands, i.e., they should be statistically significant contributors to the variability in predictands; and (3) they should represent important physical processes in the context of the enhanced greenhouse effect (Ghosh and Mujumdar 2007; Goyal and Ojha 2012d). In this section, the selection of predictors for Pichola Lake basin has been carried out using (i) scatter plots and cross correlations and (ii) VIP scores obtained from PLS regression. The details of these approaches are given below.

9.4.1.1 Application of Scatter Plots and Cross Correlation

Cross-correlations and scatter plots are in use to select predictors to understand the presence of nonlinearity/linearity trends in dependence structure. Cross-correlations and scatter plots between each of the predictor variables in NCEP and GCM datasets are useful to verify if the predictor variables are realistically simulated by the GCM. Cross-correlations are computed, and scatter plots are prepared between the predictor variables in NCEP and GCM datasets. The cross correlations are estimated using three measures of dependence, namely product moment correlation, Spearman's rank correlation and Kendall's tau. Spearman's rank correlation (ρ) is computed using the difference between the ranks of contemporaneous values of predictor and predictand (Di).

Various authors have used large-scale atmospheric variables, viz., air temperature, geo-potential height, zonal (u) and meridional (v) wind velocities, as the predictors for downscaling GCM output to temperature, precipitation and evaporation over an area. For this study, we have used total 9 possible predictor variables, namely, air temperature (at 925,500hPa and 200hPa pressure levels), geo-potential height (at 200hPa and 500hPa pressure levels), zonal (u) and meridional (v) wind velocities (at 925 and 200hPa pressure levels), as the predictors for downscaling GCM output to mean monthly temperature, precipitation and pan evaporation over the lake basin.

The cross-correlations enable verifying the reliability of the simulations of the predictor variables by the GCM, are shown in Tables 9.1, 9.2 and 9.3 for Tmax, Tmin and precipitation, respectively. In general, most of predictor variables are realistically simulated by the GCM where CC was greater than 0.65. It is noted that air temperature at 925hPa (Ta 925) is the most realistically simulated variable with a CC greater than 0.8, while meridional wind at 200hPa (Va 200) is the least correlated variable between NCEP and GCM datasets (CC = -0.17). It is clear from Tables 9.1, 9.2 and 9.3 that air temperature at 925hPa (Ta 925), air temperature at 500 hPa (Ta500), air temperature at 200 hPa (Ta200), meridional wind at 925hPa (Va 925), zonal wind at 925hPa (Ua925), geo-potential height at 200hPa (Zg200) and geo-potential height at 500hPa (Zg500) are better correlated than meridional wind at 200hPa (Va200) and zonal wind at 200hPa (Ua200). The cross-correlations are computed between the predictor variables in NCEP and GCM datasets (Table 9.4).

Scatter plots are prepared between the predictor variables in NCEP and GCM datasets (Figures 9.5 and 9.6). It is to be noted that these figures represent how well the predictors simulated by NCEP and GCM are correlated. Generally, the correlations are not very high due to the differences in the simulations of GCM (e.g. for different runs) and possible errors in NCEP-reanalysis. In addition, the inherent errors due to re-gridding from GCM scale to NCEP scale also contribute to low correlation.

9.4.1.2 VIP Scores by the PLS Regression

The VIP (Variable Importance in the Projection) scores obtained by the PLS regression has been paid an increasing attention as an importance measure of each explanatory variable or predictor. The variable selection procedure under PLS is proposed with an application to downscaling technique for identifying influencing variables to understand the impact of climate change. The VIP scores which are obtained by PLS regression, can be used to select most influential variables or predictors, X. The VIP score can be estimated for *j-th* X-variable by

$$VIP_j = \sqrt{\frac{p}{\sum_{i=1}^{k} R_d(Y,t_i)} \sum_{i=1}^{k} R_d(Y,t_i) w_{ij}^2} \qquad \text{(Eq. 9.2)}$$

where R_d is defined as the mean of the squares of the correlation coefficients (R) between the variables and the component.

$$Rd(X,c) = \frac{1}{p} \sum_{i=1}^{k} R^2(x_j,c) \qquad \text{(Eq. 9.3)}$$

Table 9.1. Cross-correlation computed between probable predictors in NCEP data and observed Tmax (predictands), P, S and K represent Product moment correlation, Spearman's rank correlation and Kendall's tau, respectively

	Va200	**Va925**	**Ta200**	**Ta500**	**Ta925**	**Zg200**	**Zg500**	**Ua925**	**Ua200**
P	0.44	0.67	0.81	0.71	0.88	0.54	0.51	0.53	0.34
S	0.21	0.43	0.67	0.57	0.71	0.40	0.38	0.38	0.29
K	0.37	0.61	0.71	0.59	0.88	0.61	0.54	0.56	0.45

Table 9.2. Cross-correlation computed between probable predictors in NCEP data and observed Tmin (predictands), P, S and K represent Product moment correlation, Spearman's rank correlation and Kendall's tau, respectively

	Va200	**Va925**	**Ta200**	**Ta500**	**Ta925**	**Zg200**	**Zg500**	**Ua925**	**Ua200**
P	0.34	0.62	0.81	0.64	0.78	0.61	0.60	0.72	0.31
S	0.48	0.43	0.63	0.44	0.60	0.59	0.42	0.51	0.42
K	0.28	0.61	0.78	0.58	0.80	0.67	0.54	0.73	0.39

Table 9.3. Cross-correlation computed between probable predictors in NCEP data and observed Precipitation (predictands), P, S and K represent Product moment correlation, Spearman's rank correlation and Kendall's tau, respectively.

	Va200	**Va925**	**Ta200**	**Ta500**	**Ta925**	**Zg200**	**Zg500**	**Ua925**	**Ua200**
P	0.11	0.59	0.31	0.46	0.20	0.41	0.61	0.39	0.18
S	0.18	0.45	0.39	0.61	0.23	0.39	0.45	0.32	0.11
K	0.17	0.63	0.48	0.47	0.34	0.51	0.48	0.45	0.12

Table 9.4. Cross-correlation computed between probable predictors in NCEP and GCM datasets. P, S and K represent product moment correlation, Spearman's rank correlation and Kendall's tau respectively

	Va200	**Va925**	**Ta200**	**Ta500**	**Ta925**	**Zg200**	**Zg500**	**Ua925**	**Ua200**
P	-0.18	0.67	0.66	0.81	0.83	0.81	0.60	0.79	0.23
S	-0.14	0.43	0.46	0.64	0.68	0.64	0.39	0.56	0.57
K	-0.20	0.61	0.68	0.85	0.87	0.85	0.59	0.76	0.73

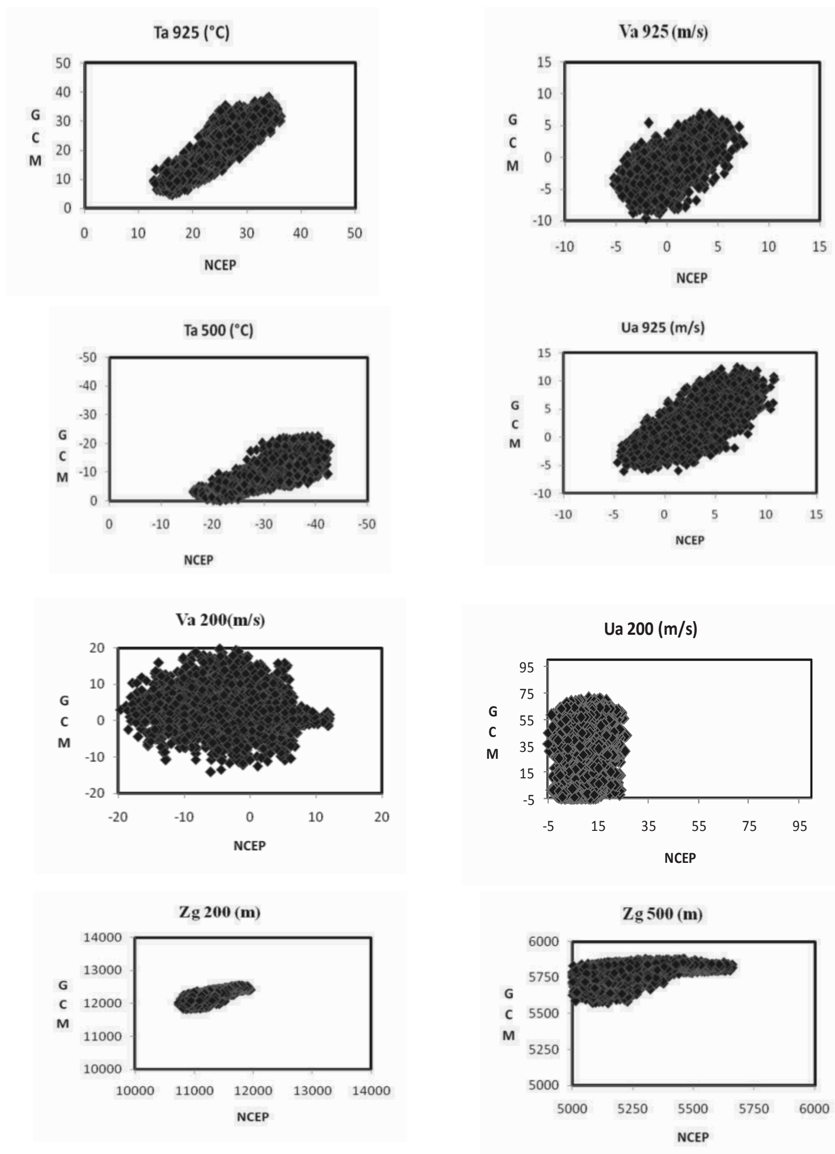

Figure 9.5. Scatter plots prepared to investigate dependence structure between probable predictor variables in NCEP and GCM datasets

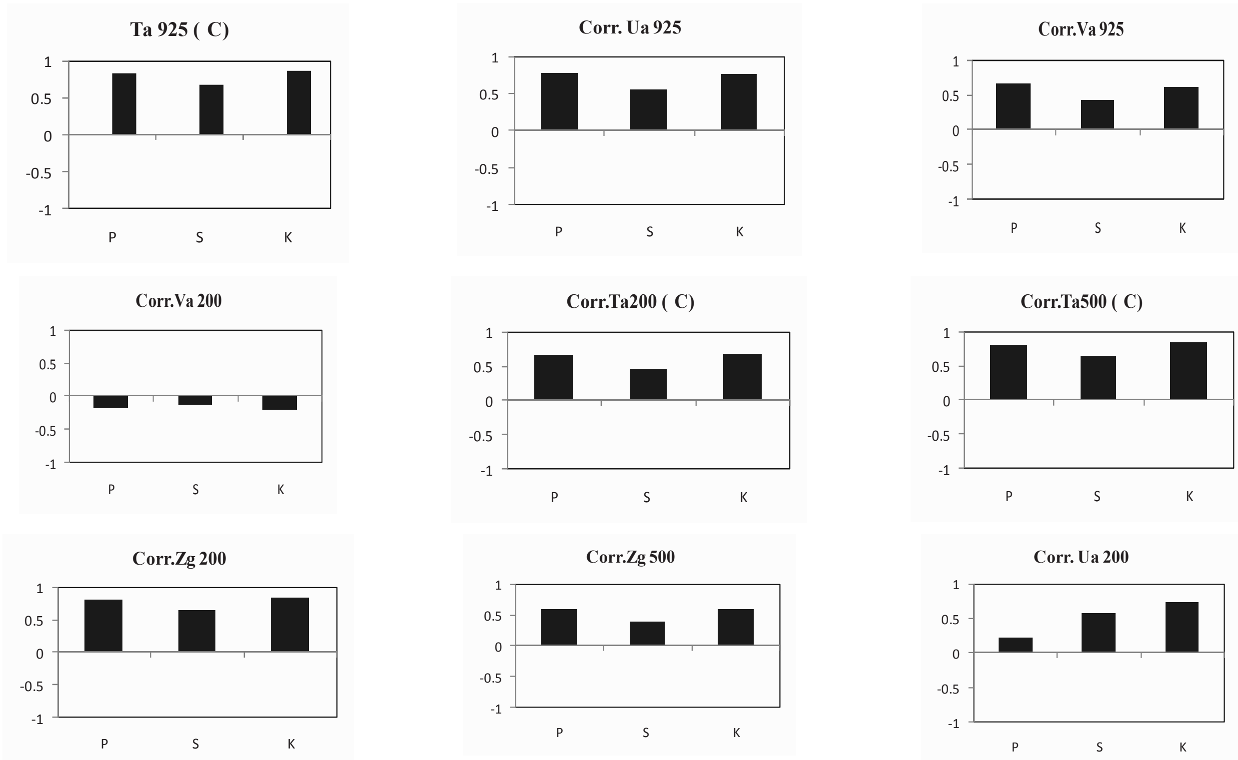

Figure 9.6. Bar plots for cross-correlation computed between probable predictors in NCEP and GCM datasets. P, S and K represent product moment correlation, Spearman's rank correlation and Kendall's tau respectively

Usually the predictor variable whose VIP score is greater than 0.8 and above is considered as an important variable. It can be seen from Figures 9.7, 9.8 and 9.9 that seven predictor variables namely air temperature at 925hPa, 500hPa and 200hPa; zonal wind (925hPa); meridional wind (925hPa); geo-potential height 500hPa and 200hPa have their VIP scores greater than 0.8. Correlation matrices of predictors also yielded the similar results. It is noted that different predictors control different local variables, and mean temperature is most sensitive to surface and near surface atmospheric factors.

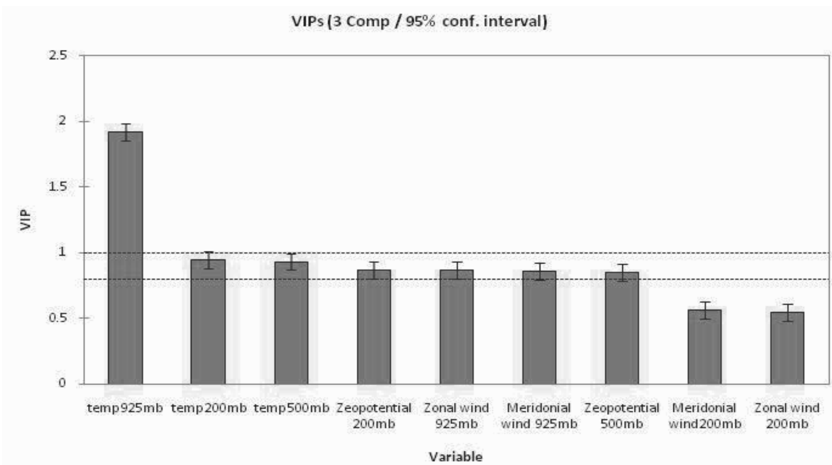

Figure 9.7. VIP of the predictand variable (Tmax) of the two-component PLSR model

9.4.2 Correcting Bias by a Multiplicative Shift

Many GCMs either overestimate or underestimate maximum and minimum temperature as well as precipitation. The correction scheme brings the distributions close to the observed pattern. A simple multiplicative shift is used to correct the bias of the mean monthly GCM simulated variable as follows:

$$X_i^{'} = X_i \frac{\bar{X}_{obs}}{\bar{X}_{GCM}} \qquad \text{(Eq. 9.4)}$$

where $X_i^{'}, X_i$ refers to raw and corrected GCM simulated variable, and $\bar{X}_{GCM}$ and $\bar{X}_{obs}$ are long term mean monthly variable from the GCM and the observations for given month (Ines and Hansen, 2006)

9.5 Evaluation of Linear Regression Methods

9.5.1 Model Development

In this section, various linear regression approaches are used to downscale the mean monthly precipitation for the Pichola lake region. The data of potential predictors is first standardized. Standardization is widely used prior to statistical downscaling to reduce bias (if any) in the mean and the variance of GCM predictors with respect to that of NCEP-reanalysis data. Standardization is done for a baseline period of 1948 to 2000 because it is of sufficient duration to establish a reliable climatology, yet not too long, nor too contemporary to include a strong global change signal. The procedure typically involves subtraction of mean and division by standard deviation of the predictor variable for a predefined baseline period for both NCEP/NCAR and GCM output. A feature vector (standardized predictor) is formed for each month of the record using the data of standardized NCEP predictor variables. However, another way to implement the regression model is that principal components should be extracted first since multi-dimensionality of the predictors may lead to a computationally complicated and large sized model with high multi-collinearity (high correlation between the explanatory variables/regressors). Then, the use of principal component (PCs) as input to a downscaling model helps in making the model more stable and at the same time reduces its computational burden. Here, regression approaches with and without principal components have been used in this analysis.

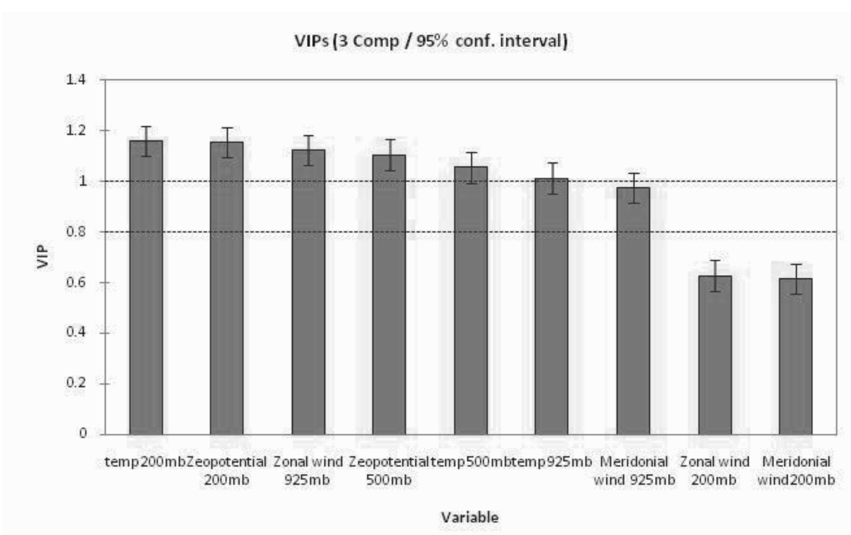

Figure 9.8. VIP of the predictand variable (Tmin) of the two-component PLSR model

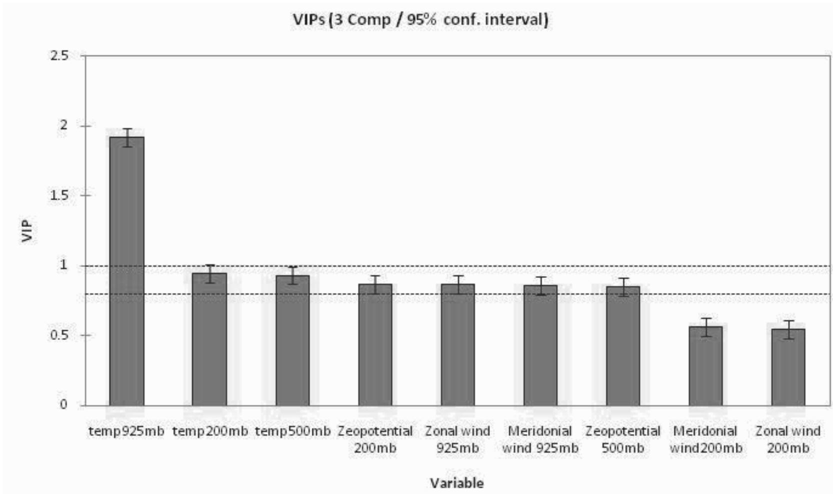

Figure 9.9. VIP of the predictand variable (precipitation) of the three-component PLSR model

To develop downscaling models using regression approaches (see Table 9.5), the feature vectors which are prepared from NCEP record are partitioned into a training set and a validation set. Feature vectors in the training set are used for calibrating the model, and those in the validation set are used for validation. In case of using PCA, it is observed that the four leading principal components (PCs) of the PCA method explained about 97% of the information content (or variability) of the original predictors. Hence, PCs are extracted to form feature vectors from the standardized data of potential predictors. The 11-year mean monthly observed precipitation data series were broken up into a calibration period and a validation period. The models were calibrated on the calibration period of 1990 to 1995 and validation involved the period of 1996 to 2000. Seven predictor variables, namely air temperature (925hPa, 500hPa and 200hPa); zonal wind (925hPa); meridional wind (925hPa); geo-potential height (500hPa and 200hPa) at 9 NCEP grid points with a dimensionality of 63, are used as the standardized data of potential predictors. These feature vectors are provided as input to the various regressions downscaling model.

Table 9.5. Different regression models used for obtaining projections of precipitation

Approach	Stepwise		Forward		Backward		Direct	
	Without PCs	Without PCs	Without PCs	Without PCs	Without PCs	Without PCs	Without PCs	Without PCs
Model	M1	MP1	M2	MP2	M3	MP3	M4	MP4

9.5.2 Training and Validation Results

Results of the different regression models (viz.*M1* to *M4* and *MP1* to *MP4*) as discussed in Table 9.5 are tabulated in Table 9.6. For predictand precipitation, the coefficient of correlation (CC) was in the range of 0.60–0.95; RMSE was in the range of 27.71–58.33; N-S Index was in the range of 0.24–0.90 and MAE was in the range of 0.23–0.72 for regression based models for the training and validation set. It can be observed from Table 9.6 that the performance of direct regression models with and without principal components for mean monthly precipitation are clearly superior to that of forward-, backward- and stepwise-regression-based models in the training data set while the performance of stepwise- and forward-regression-based models for predictand are clearly superior to that of backward- and direct-regression-based models in the validation data set. Results of forward and stepwise regression are quite similar. However, models developed using principal components yielded slightly better results. It can be inferred that model *MP4* using direct regression performed best for predictand precipitation. Now, multiplicative shift is used to correct the bias of GCM of model MP4. The corrected model MP4 performed better than uncorrected in terms of various performance meausres (CC, RMSE and N-S Index), as shown in Table 9.7. It can be inferred that the performance of direct regression models bias corrected (viz. MP4(corrected) performed well.

Table 9.6. Various performance statistics of models using various regression approaches for precipitation

Model	CC		RMSE		N-S Index	
	Training	Validation	Training	Validation	Training	Validation
M1	0.90	0.79	39.37	45.80	0.81	0.53
M2	0.95	0.60	27.77	58.33	0.90	0.24
M3	0.94	0.65	32.03	55.14	0.87	0.32
M4	0.91	0.79	39.33	45.80	0.81	0.53
MP1	0.90	0.80	39.18	44.01	0.80	0.51
MP2	0.94	0.61	27.71	55.34	0.91	0.25
MP3	0.95	0.66	31.03	55.64	0.88	0.35
MP4	0.93	0.81	38.65	44.04	0.82	0.57

Table 9.7. Various performance statistics of model using bias correction for precipitation

Model	CC		RMSE		N-S Index	
	Training	Validation	Training	Validation	Training	Validation
MP4 (corrected)	0.94	0.82	37.71	41.44	0.86	0.62

A comparison of mean monthly observed precipitation with precipitation simulated using forward regression models *MP4 (corrected)* has been shown from Figure 9.10 for the calibration and validation period. Regression coefficients (Aij) for predictor (*precipitation*) corresponding to model *M4* has been shown in Table 9.8 where i ranges from 1 to 7 indicating Ta 925, Ua 925, Va 925, Ta 500, Ta 200, Zg

200 and Zg 500, respectively while j ranges from 1 to 9 representing the location of grid points shown in Figure 9.2.Here the values of coefficient for some variables were in the third and fourth order. Hence, many coefficients are given as 0.00 in above Table 9.8.

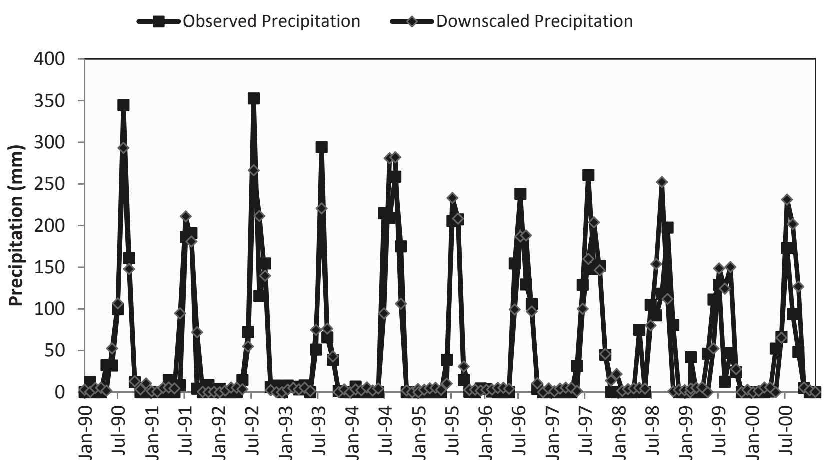

Figure 9.10. Typical results for comparison of the monthly observed Precipitation with Precipitation simulated using direct regression downscaling model *M4(corrected)* for NCEP data

9.5.3 Discussion of Downscaling and Trend Analysis

Once the downscaling models have been calibrated and validated, the next step is to use these models to downscale the scenarios simulated by the GCM. The GCM simulations are run through the calibrated and validated direct regression model *MP4(corrected)* to obtain future simulations of predictand. The predictand patterns are analyzed with box plots for 20-year time slices. Typical results of downscaled predictand obtained from the predictors are presented in Figure 9.11. In part (i) of Figure 9.11, the precipitation downscaled using NCEP and GCM datasets are compared with the observed precipitation for the study region using box plots. The projected precipitation for 2001–2020, 2021–2040, 2041–2060, 2061–2080 and 2081–2100 for the four scenarios A1B, A2, B1 and COMMIT are shown in Figure 9.11 (ii), (iii), (iv) and (v), respectively. From the box plots of downscaled predictand (Figure 9.11), it can be observed that precipitation are projected to increase in the future for A1B, A2 and B1 scenarios.

Table 9.8. Regression coefficients (Aij) for models M4

Model	**Intercept**	**A11**	**A12**	**A13**	**A14**	**A15**	**A16**	**A17**	**A18**	**A19**	**A21**	**A22**	**A23**
M4	-5078.8	-189	168.1	6.9	275.3	-245	-14	-81	28.4	65.6	39.9	-106	68.4
Model	**A24**	**A25**	**A26**	**A27**	**A28**	**A29**	**A31**	**A32**	**A33**	**A34**	**A35**	**A36**	**A37**
M4	-119	189.9	-104	67.0	-102	65.8	94.7	-127.0	61.7	-255.5	359.6	-147.6	136.1
Model	**A38**	**A39**	**A41**	**A42**	**A43**	**A44**	**A45**	**A46**	**A47**	**A48**	**A49**	**A51**	**A52**
M4	-235.6	136.1	-34.6	12.2	0.0	51.1	0.00	0.00	0.00	0.00	-29.84	-21.67	-15.75
Model	**A53**	**A54**	**A55**	**A56**	**A57**	**A58**	**A59**	**A61**	**A62**	**A63**	**A64**	**A65**	**A66**
M4	-4.07	0.00	0.00	0.00	30.58	0.00	0.00	0.59	0.00	-0.11	0.35	0.00	0.00
Model	**A67**	**A68**	**A69**	**A71**	**A72**	**A73**	**A74**	**A75**	**A76**	**A77**	**A78**	**A79**	
M4	0.00	0.00	0.00	1.28	-3.69	1.44	0.00	0.00	0.00	0.00	0.00	0.00	

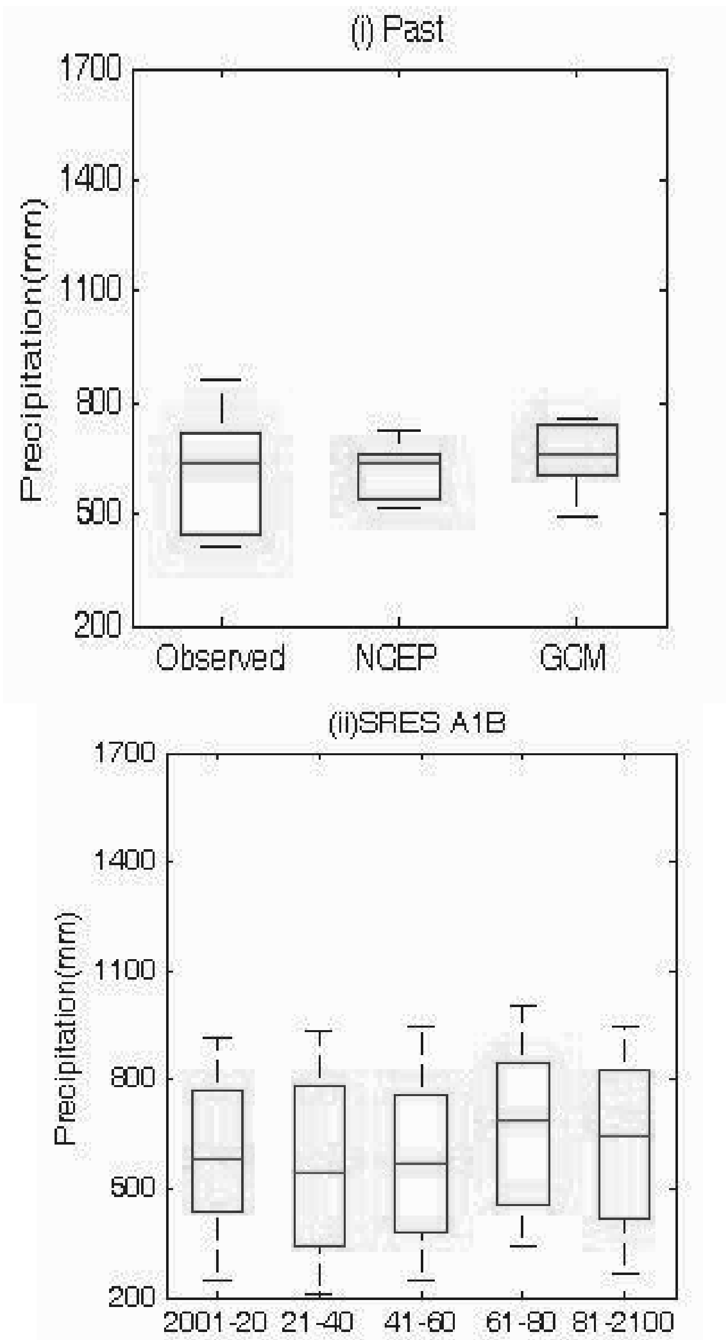
(i) Past
Precipitation(mm)
1700
1400
1100
800
500
200
Observed
NCEP
GCM
(ii)SRES A1B
Precipitation(mm)
1700
1400
1100
800
500
200
2001-20
21-40
41-60
61-80
81-2100

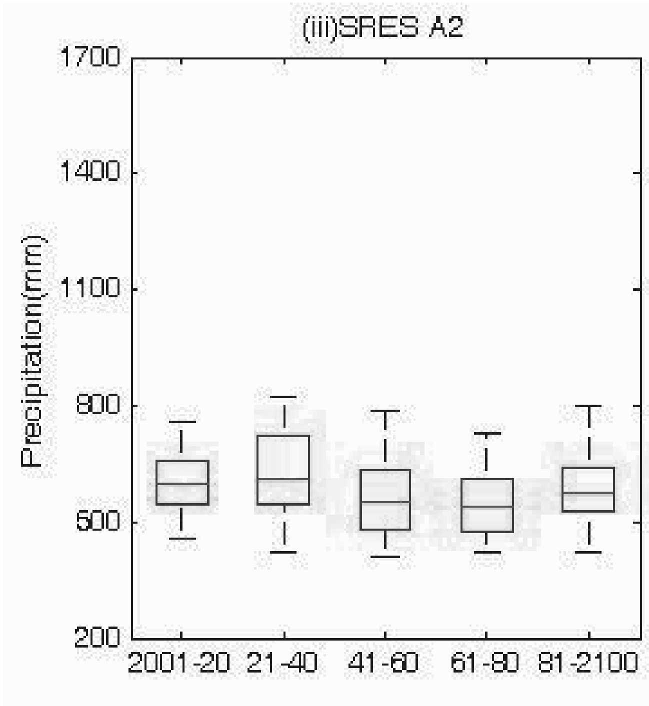
(iii)SRES A2
1700
1400
1100
800
500
200
Precipitation(mm)
2001-20
21-40
41-60
61-80
81-2100

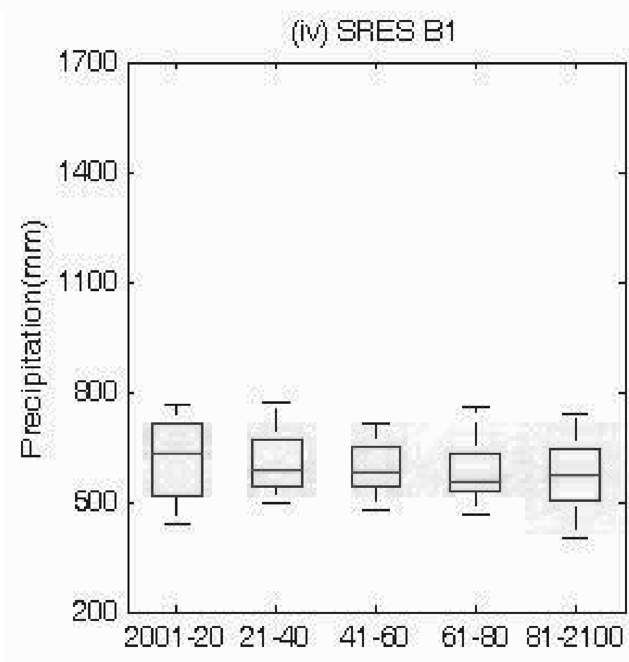
(iv) SRES B1
1700
1400
1100
800
500
200
Precipitation(mm)
2001-20
21-40
41-60
61-80
81-2100

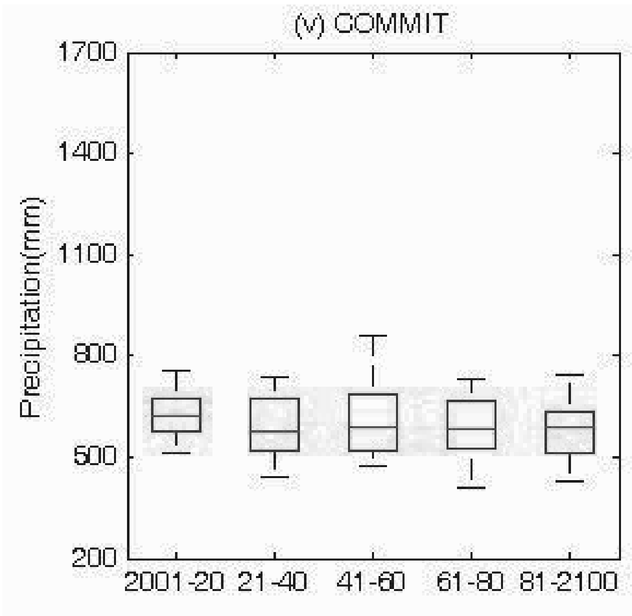

Figure 9.11. Box plots results from the direct regression-based downscaling model MP4 for the predictand Precipitation

Overall, direct regression performed best followed by the backward regression method. Backward regression was followed by forward regression and stepwise regression which yielded the similar results. Direct regression yielded better results for the training data set while forward regression performed better for the validation data set. The results of downscaling models show that precipitation is projected to increase in the future for A2 and A1B scenarios, whereas it is least for B1 and COMMIT scenarios using predictors.

9.6 Evaluation of Artificial Neural Network Methods

9.6.1 Model Development

In this section, ANNs are used to downscale mean monthly maximum (*T*max) and minimum (*T*min) temperature as well as evaporation. Seven predictor variables namely air temperature (925hPa, 500hPa and 200hPa); zonal wind (925hPa); meridional wind (925hPa); geo-potential height 500hPa and 200hPa at 9 NCEP grid points with a dimensionality of 63, are used, as discussed in the earlier section. To develop the ANN downscaling models, the feature vectors (i.e. predictors) which are prepared from NCEP record are partitioned into a training set and a test set. Table 9.9 shows certain details of different ANN downscaling models.

Table 9.9. Different ANN downscaling models used for obtaining projections of predictands (*T*max and *T*min as well as evaporation)

Predictand	Model	Predictand	Model
T_{max}	ANNM1	T_{min}	ANNM7
T_{max}	ANNM2	T_{min}	ANNM8
T_{max}	ANNM3	Evaporation	ANNM9
T_{max}	ANNM4	Evaporation	ANNM10
T_{min}	ANNM5	Evaporation	ANNM11
T_{min}	ANNM6	Evaporation	ANNM12

The architecture of ANN is decided by the trial-and-error procedure. A comprehensive search of ANN architecture is done by varying the number of nodes in the hidden layer. The network is trained using a back-propagation algorithm. Tan-sigmoid activation function has been used in the hidden layer, whereas linear activation function has been used in the output layer. The network error is computed by comparing the network output with the target or the desired output. Mean square error is used as an error function.

9.6.2 Training and Validation Results

Results of the different models (*ANNM1* to *ANNM12*) as discussed in Table 9.9 are tabulated in Table 9.10.

Calibration /Training Results. It is clear from Table 9.10 that model *ANNM4, ANNM8 and ANNM9* performed better than any other model for predictand Tmax, Tmin and evaporation investigated here. It can be observed from Table 9.10 that for predictand Tmax, CC, RMSE and N-S Index were 0.98 0.91 and 0.97, respectively using ANN model ANNM4. For predictand Tmin, values of CC, RMSE, N-S Index and MAE were 0.99, 0.96 and 0.98, respectively. For predictand evaporation using ANNM9, RMSE, N-S Index and MAE were 0.70, 0.94 and 0.77, respectively.

Validation /Testing Results. For predictand Tmax, values of CC, RMSE and N-S Index were 0.96, 1.46 and 0.84, respectively for ANNM4 model. For predictand Tmin, the values of CC, RMSE and N-S index were 0.95, 2.26 and 0.98, respectively for ANNM8 model. For evaporation, the values of CC, RMSE and N-S index were 0.86, 0.91 and 0.73, respectively for ANNM9 model.

Table 9.10. Various performance statistics of ANN models

Model	Hidden nodes	CC		SSE		MSE		RMSE		NMSE		N-S Index		MAE	
		Training	Validation	Training	Validation	Training	Validation	Training	Validation	Training	Validation	Training	Validation	Training	Validation
ANNM1	1	0.98	0.94	59.31	157.58	0.82	2.63	0.91	1.62	0.04	0.13	0.96	0.87	0.83	0.64
ANNM2	3	0.98	0.95	60.12	154.78	0.79	2.45	0.89	1.57	0.05	0.14	0.95	0.86	0.81	0.63
ANNM3	5	0.98	0.94	56.31	159.58	0.81	2.36	0.90	1.54	0.03	0.15	0.96	0.87	0.83	0.62
ANNM4	7	0.98	0.96	57.21	157.47	0.82	2.12	0.91	1.46	0.03	0.13	0.97	0.88	0.84	0.62
ANNM5	1	0.99	0.96	66.21	319.47	0.92	5.32	0.96	2.31	0.02	0.09	0.98	0.91	0.89	0.79
ANNM6	3	0.99	0.95	61.21	321.47	0.91	6.12	0.95	2.47	0.01	0.08	0.97	0.92	0.91	0.80
ANNM7	5	0.99	0.96	59.21	311.25	0.93	5.62	0.96	2.37	0.01	0.07	0.97	0.93	0.90	0.78
ANNM8	7	0.99	0.95	61.19	318.47	0.93	5.12	0.96	2.26	0.02	0.08	0.98	0.93	0.91	0.77
ANNM9	1	0.97	0.96	35.51	39.49	0.49	0.66	0.70	0.81	0.06	0.08	0.94	0.92	0.77	0.74
ANNM10	3	0.98	0.95	20.93	48.73	0.29	0.81	0.54	0.90	0.04	0.10	0.96	0.90	0.83	0.72
ANNM11	5	0.98	0.95	26.72	44.86	0.37	0.75	0.61	0.86	0.05	0.09	0.95	0.91	0.81	0.73
ANNM12	7	0.97	0.95	30.38	50.75	0.42	0.85	0.65	0.92	0.05	0.10	0.95	0.89	0.80	0.72

Now, multiplicative shift is used to correct the bias of GCM of models ANNM4, ANNM8 and ANNM9 corresponding to Tmax, Tmin and evaporation, respectively. All the corrected models performed better than uncorrected in terms of various performance measures, as shown in Table 9.11. It can be inferred that the performance of ANN models bias corrected [viz. ANNM4 (corrected), ANNM8 (corrected) and ANNM9 (corrected)] for predictands (Tmax, Tmin and evaporation, respectively) performed well.

A comparison of mean monthly observed Tmax and Tmin with Tmax and Tmin simulated using ANN models ANNM4 (corrected) and ANNM8 (corrected) have been shown from Figures 9.12 and 9.13, respectively for calibration and validation period. A comparison of mean monthly observed evaporation with evaporation simulated using ANN model ANNM9 (corrected) has been shown in Figure 9.14 for the calibration and validation period.

Table 9.11. Various performance statistics of models using bias correction

Model	CC		RMSE		N-S Index	
	Training	**Validation**	**Training**	**Validation**	**Training**	**Validation**
ANNM4 (corrected)	0.98	0.96	0.91	1.46	0.97	0.88
ANNM8 (corrected)	0.99	0.95	0.96	2.26	0.98	0.93
ANNM9 (corrected)	0.97	0.97	0.70	0.76	0.94	0.93

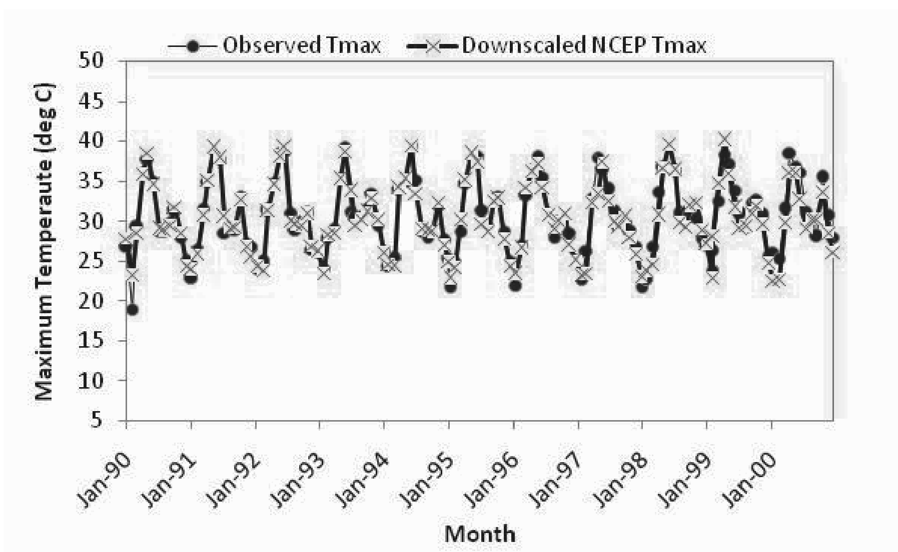

Figure 9.12. Typical results for comparison of the monthly observed *T*max with *T*max simulated using ANN downscaling model ANNM4 (corrected) for NCEP data

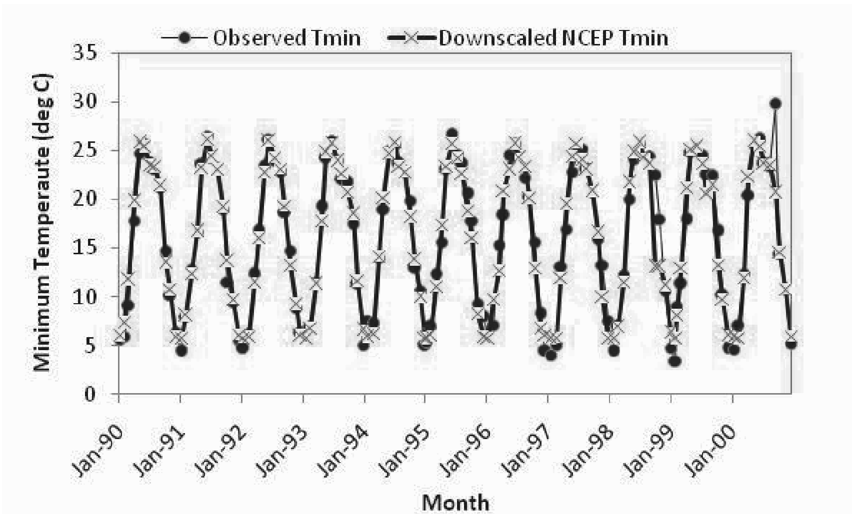

Figure 9.13. Typical results for comparison of the monthly observed *T*min with *T*min simulated using ANN downscaling model ANNM8 (corrected) for NCEP data

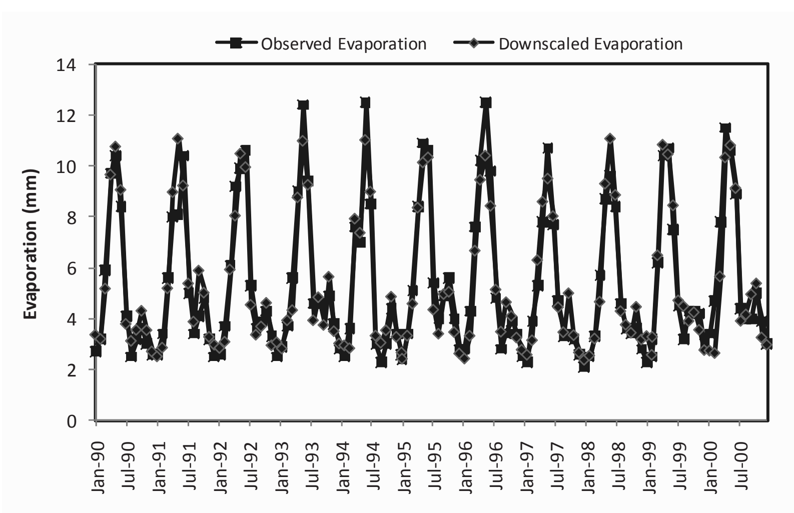

Figure 9.14. Typical results for comparison of the monthly observed *evaporation* with *evaporation* simulated using ANN downscaling model ANNM9 (corrected) for NCEP data

9.6.3 Discussion of Downscaling results and Trend analysis

Once the downscaling models have been calibrated and validated, the next step is to use these models to downscale the scenarios simulated by the GCM. The GCM simulations are run through the calibrated and validated ANN downscaling models (ANNM4 (corrected), ANNM8 (corrected) and ANNM9 (corrected) for Tmax, Tmin and evaporation, respectively) to obtain future simulations of predictand. The predictands (viz. *Tmax* and *Tmin* as well as evaporation) patterns are analyzed with box plots for 20 year time slices. Typical results of downscaled predictands (*T*max and *T*min as well as evaporation) obtained from the predictors are presented in Figures 9.15, 9.16 and 9.17. In part (i) of these Figures, the *T*max and *T*min as well as evaporation downscaled using NCEP and GCM datasets are compared with the observed *T*max and *T*min as well as evaporation for the study region using box plots. The projected precipitation for 2001–2020, 2021–2040, 2041–2060, 2061–2080 and 2081–2100, for the four scenarios A1B, A2, B1 and COMMIT are shown in (ii), (iii), (iv) and (v), respectively, of Figures 9.15, 9.16 and 9.17. From the box plots of downscaled predictands (Figures 9.15, 9.16 and 9.17), it can be observed that *T*max and *T*min are projected to increase in the future for A1B, A2 and B1 scenarios, whereas no trend is discerned with the COMMIT scenario by using predictors.

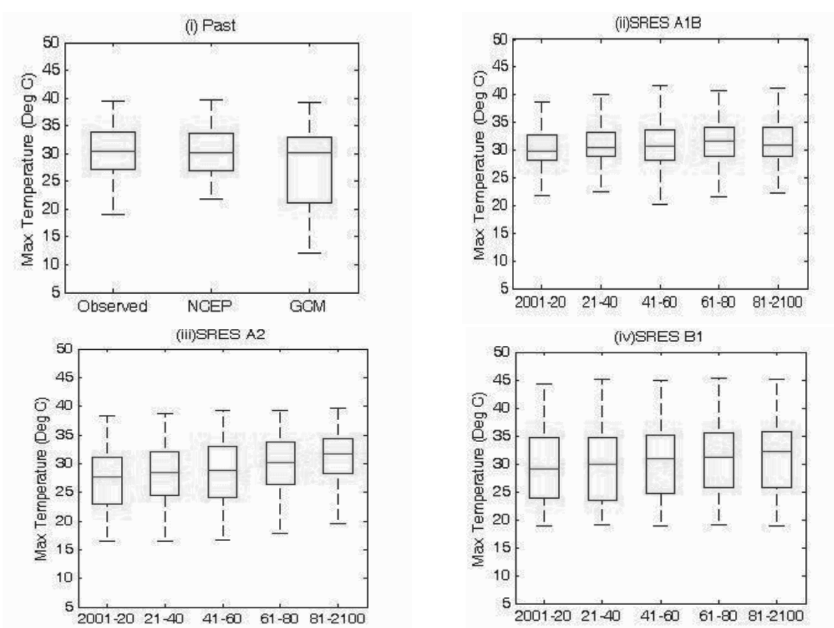

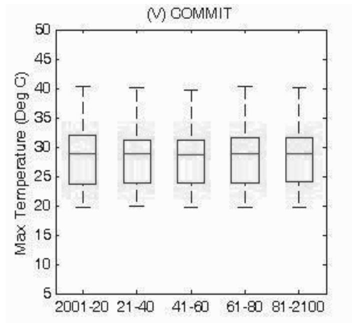

Figure 9.15. Box plots results from the ANN-based downscaling model (ANNM4) for the predictand *T*max

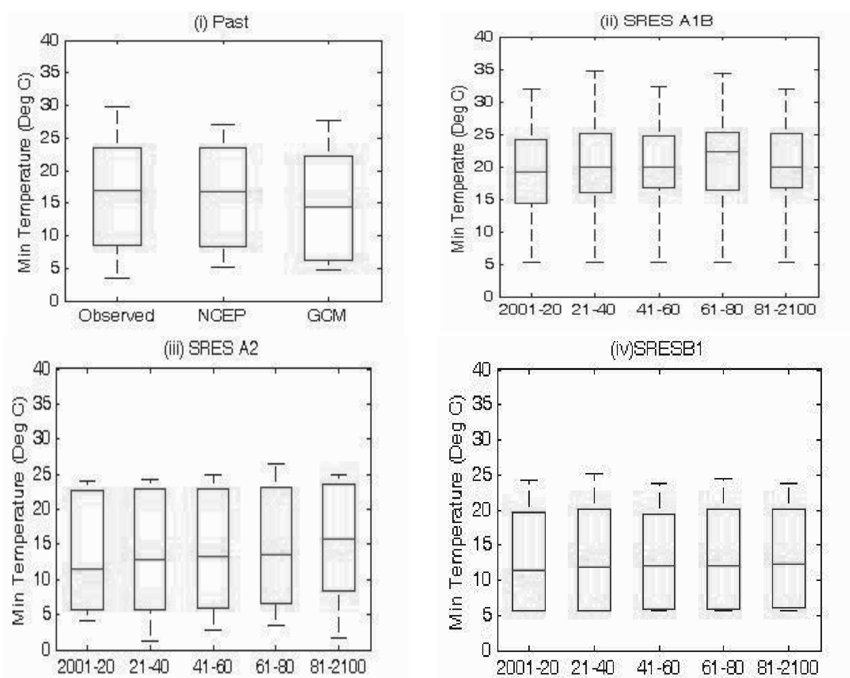

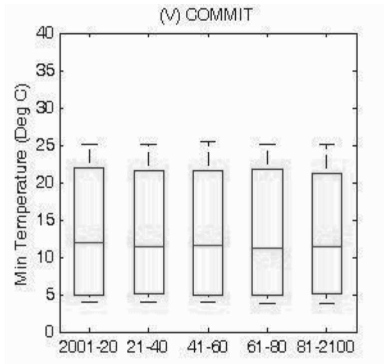

Figure 9.16. Box plots results from the ANN-based downscaling model(ANNM8) for the predictand *T*min

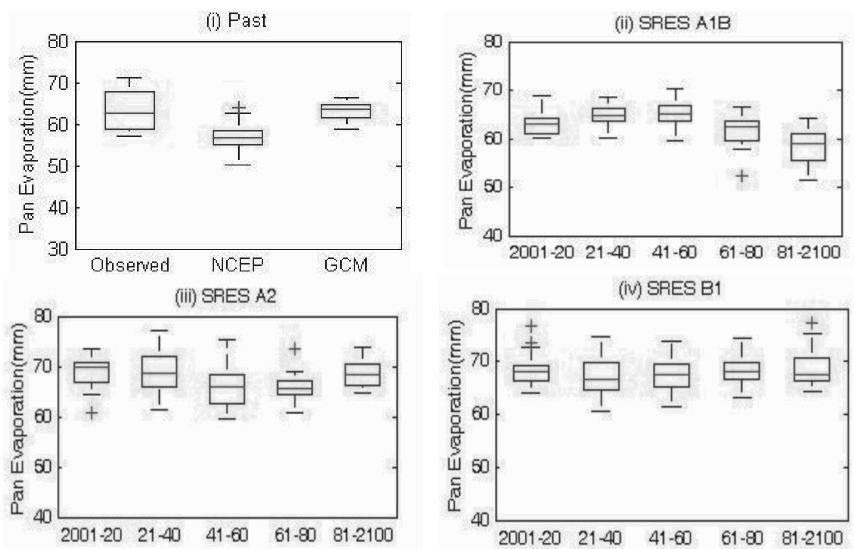

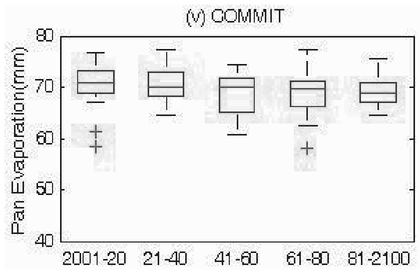

Figure 9.17. Box plots results from the *ANNM9(corrected)* based downscaling model for the predictand pan evaporation

9.7 Conclusions

The downscaling models are developed for obtaining projections of precipitation, maximum and minimum temperatures as well as evaporation (predictands) at the lake-basin scale. The effectiveness of the models is demonstrated through application to the catchment of Pichola Lake in India. The predictands are downscaled from simulations of CGCM3 for four IPCC scenarios, namely SRES A1B, A2, B1 and COMMIT. The results of downscaling models show that precipitation is projected to increase in the future for A2 and A1B scenarios, whereas it is least for B1 and COMMIT scenarios using predictors while Tmax and Tmin are projected to increase in the future for A1B, A2 and B1 scenarios, whereas no trend is discerned with the COMMIT. The projected increase in predictands is high for A2 scenario, whereas it is least for B1 scenario. For pan evaporation, it can be concluded that trend is not obvious for future years since the factors working on pan evaporation are complicated.

However, one should remember that all of the downscaling experiments in this study use the outputs of only one GCM. Previous studies showed that data taken from different GCMs could produce significant results in a given region. Therefore, caution should be exercised in interpreting the outcome of such impact analysis for practical applications.

9.8 References

Anandhi, A., Srinivas, V. V., Nanjundiah, R. S., and Kumar, D. N. (2008). "Downscaling precipitation to river basin for IPCC SRES scenarios using Support Vector Machines." *International J. Climatology*, 28, 401–420.

Ines, A.V.M. and Hansen , J.W. (2006). "Bias correction of daily GCM rainfall for crop simulation studies." *Agricultural & Forest Meteorology*, 138, 44–53.

Benestad, R. E. (2001). "A comparison between two empirical downscaling strategies." *International Journal of Climatology*, 21, 1645–1668.

Cannon, A. J., and Lord E. R. (2000). "Forecasting summertime surface-level ozone concentrations in the Lower Fraser Valley of British Columbia: An ensemble neural network approach." *Journal of the Air and Waste Management Association*, 50, 322–339.

Cannon, A. J., and Whitfield, P. H. (2002). "Downscaling recent streamflow conditions in British Columbia, Canada using ensemble neural network models." *Journal of Hydrology*, 259(1), 136–151.

Cavazos, T., and Hewitson, B. C. (2005). "Performance of NCEP variables in statistical downscaling of daily precipitation." *Climate Research*, 28, 95–107.

Cecilia, H., Deliang C., Christine A., and Jouni R. (2001). "Comparison of climate change scenarios for Sweden based on statistical and dynamical downscaling of monthly precipitation." *Climate Research*, 19, 45–55.

Dibike, Y. B., and Coulibaly, P. (2006). "Temporal neural networks for downscaling climate variability and extremes." *Neural Networks*, 19(2), 135–144.

Dimri, A. P., Joshib, P., and Ganjub, A. (2008). "Precipitation forecast over western Himalayas using k-nearest neighbour method." *Int. J. Climatol*. 28, 1921–1931.

Ghosh, S., and Mujumdar, P. P. (2007). "Nonparametric methods for modeling GCM and scenario uncertainty in drought assessment." *Water Resour. Res.*, 43, W07405, doi:10.1029/2006WR005351.

Goyal, M. K., Ojha, C. S. P., and Burn, D. H. (2010). "An evaluation of decision tree algorithm as a downscaling tool: Application on a Lake Basin for an arid region in India." Tenth conference of Canadian Geophysical Union, *University of Guelph*, Ontario, Canada.

Goyal, M. K., and Ojha, C. S. P. (2010a). "Robust weighted regression as a downscaling tool in temperature projections." *International Journal of Global Warming*, Interscience Publishers, UK, 2(3), 234–251.

Goyal, M. K., and Ojha, C. S. P. (2010b). "Evaluation of various linear regression methods for downscaling of mean monthly precipitation in arid Pichola Watershed." *Natural Resources*, Scientific Research, USA, 1(1), 11–18. DOI: 10.4236/nr.2010.11002.

Goyal, M. K., and Ojha, C. S. P. (2010c). "Application of PLS-regression as downscaling tool for Pichola Lake basin in India." *International Journal of Geosciences*, Scientific Research, USA, 1, 51–57.

Goyal, M. K., Ojha, C. S. P., and Burn Donald H. (2012). "An evaluation of nonparametric statistical downscaling of temperature, precipitation and evaporation for semi-arid region in India." *ASCE-Journal of Hydrologic Engg.*, 17(5) 615-627, DOI: 10.1061/(ASCE)HE.1943-5584.0000479.

Goyal, M. K., and Ojha, C. S. P. (2011a). "Evaluation of linear regression methods as downscaling tool in temperature projections over Pichola Lake Basin in India." *Hydrological Processes*, *John Wiley & Sons*, DOI: 10.1002/hyp.7911, 25 (9), 1453–1465.

Goyal, M. K., and Ojha, C. S. P. (2011b). "PLS regression based pan evaporation and minimum-maximum temperature projections for an arid lake basin in India."

Theoretical and Applied Climatology, Springer Netherlands, 105(3-4):403-415, DOI: 10.1007/s00704-011-0406-z.

Goyal, M. K., and Ojha, C. S. P. (2012d). "Downscaling of surface temperature for lake catchment in arid region in india using linear multiple regression and neural networks." *International Journal of Climatology*, John Wiley & Sons, DOI: 10.1002/joc.2286.

Goyal, M. K., and Ojha, C. S. P. (2012e). "Downscaling of precipitation on a lake basin: evaluation of rule and decision tree induction algorithms." *Hydrology Research*.43 (3), 215–230.

Kalnay, E., Kanamitsu, M., Kistler, R., Collins, W., Deaven, D., Gandin, L., Iredell, M., Saha, S., White, G., Woollen, J., Zhu, Y., Chelliah, M., Ebisuzaki, W., Higgins, W., Janowiak, J., Mo KC, Ropelewski C,,Wang J., Leetmaa A., Reynolds, R., Jenne, R., and Joseph, D. (1996). "The NCEP/NCAR 40-year reanalysis project." *Bulletin Am. Meteorol. Soc.*, 77(3), 437–471.

Khobragade, S. D. (2009). "Studies on evaporation from open water surfaces in tropical climate." Ph.D. Dissertation, Dept of Civil Engg, *Indian Institute of Technology*, Roorkee, India.

Linz, H., Shiklomanov, I., and Mostefakara, K. (1990). "Hydrology and water Likely impact of climate change." Ch. 4 in *IPCC WGII report*, WMO/UNEP Geneva.

Ojha, C. S. P., Goyal, M. K., and Adeloye, A. J. (2010). "Downscaling of precipitation for lake catchment in arid region in india using linear multiple regression and neural networks." *The Open Journal of Hydrology*, Bentham Science Publishers, 4, 122–136.

Lall, U., and Sharma, A. (1996). "A nearest neighbour bootstrap for time series resampling." *Water Resour. Res*. 32(3), 679–693.

Schoof, J. T., and Pryor, S. C. (2001). "Downscaling temperature and precipitation: a comparison of regression-based methods and artificial neural networks." *International Journal of Climatology*, 21, 773–790.

Rajagopalan, B., and Lall, U. (1999). "A k-nearest neighbour simulator for daily precipitation and other variables." *Water Resour. Res*., 35(10), 3089–3101.

Wilby, R. L., Dawson, C. W., and Barrow, E. M. (2002). "SDSM–a decision support tool for the assessment of climate change impacts." *Environmental Modelling & Software*, 17, 147–159.

Willmott, C. J., Rowe C. M., and Philpot W. D. (1985). "Small-scale climate map: a sensitivity analysis of some common assumptions associated with the grid-point interpolation and contouring." *American Cartographer*, 12, 5–16.

Young, K. C. (1994). "A multivariate chain model for simulating climatic parameters with daily data." *J. Appl. Meteorol*., 33(6), 661–671.

CHAPTER 10

Essence of Climate Change on Hydrologic Extremes

R. P. Pandey, Rakesh Kumar, R. D. Singh and C. S. P. Ojha

10.1 Introduction

The climate varies naturally on all time-scales. Variations may occur due to forces such as volcanic eruptions or changes in the Sun's output of energy. They may also be generated by interactions among the different components of the global climate system: the atmosphere, oceans, biosphere, ice cover, and land surface. These internal interactions may cause fairly regular fluctuations, such as the El Niño phenomenon, or apparently random changes in climate.

Since the human settlements and the economic activities on the earth are largely concentrated in mid-latitudinal regions, the impacts of floods and droughts are more apparent in these regions (Karl 1983; Ponce 1995a). Natural variability often produces climate extremes and disasters. On time-scales of days, months, and years, variability in weather and climate can produce heat waves, frosts, flooding, droughts, severe storms, and other extremes. An important question which scientists are trying to answer is whether mankind's interference with the climate system through the enhancement of the natural greenhouse effect will increase the frequency or magnitude of extreme weather events like floods and drought. Given the large natural variability and the obvious rarity of extreme weather events it is hard to ascribe the observed phenomena to the enhanced greenhouse effect or even discern a definite trend in extreme event throughout this century. What can be said with certainty, however, is that any change in climate will affect society mainly through extreme weather events.

Global climate change is one of the key factors that affect the hydrological cycle (IPCC 2007). Any change in temperature affects the atmospheric moisture, precipitation and circulation pattern of the atmosphere, e.g., changes in the rate of evaporation affects the hydrological cycle. Higher temperatures turn some part of snowfall into rainfall; the snowmelt season occurs earlier, consequently the timing and volume of spring flood changes substantially (IPCC 2001). Inconsistency of elements characterizing the processes of hydrologic cycle is responsible for occurrence of hydrologic extremes (Ponce et al. 2000). Here, the hydrologic extremes refer to the circumstances when there is either too much of water that may cause damages (floods), or too less of water that may cause water scarcity in sustaining usual regional activities and the ecosystem (droughts). Regions with higher variability of rainfall and runoff are more vulnerable to floods and droughts (Kundzewicz and Kaczmarek 2000). Floods and drought have always been a major concern of the society. Despite fascinating achievements of science and technology in 20th century, extreme hydrological events continue to hit human heritage and undermine development by breaking continuity. Devastating droughts and floods can be viewed as enemies of sustainable development (Kundzewicz and Kaczmarek 2000). They cause damage to crops and agricultural farms and induce the threats of adversity and famine.

The primary purpose of this Chapter is to present the current level of comprehension on relevance of climate change with floods and droughts in different climatic regions. It is hoped that the Chapter may enhance understanding and ability to cope with adverse impacts of floods and droughts on the society.

10.2 Climate Change and Occurrence of Extreme Events

Definition of Climatic Extremes. Some definitions of climatic extremes choose to separate the nature of the event from its social and economic consequences. A climate extreme, then, is a significant departure from the normal state of the climate, irrespective of its actual impact on life or any other aspect of the Earth's ecology. When a climate extreme has an adverse impact on human welfare, it becomes a climatic disaster. In some parts of the world climatic disasters occur so frequently that they may even be considered as part of the norm. It is being believed that greenhouse gas-induced climate change may possibly alter the frequency, magnitude, and character of both climate extremes and climatic disasters.

Many other researchers have defined climatic extremes or extreme weather events as sufficiently anomalous to cause substantial socio-economic damage. In this second definition, natural and social factors are interpreted together. Thus, it is a socio-economic threshold, which is, for a suitably adapted society, rarely crossed. Rare is defined as the return period of the extreme event being substantially longer than the recovery period of the damage caused. The climatic extremes may be categorized as follows:

- Droughts (due to increased evaporation and reduced precipitation);
- River floods (due to increased precipitation);
- Landslides (due to increased precipitation);
- Storms, cyclones and tornadoes (due to changing heat transport patterns and increased land-ocean temperature differential);
- Ocean and coastal surges and related flooding (due to atmospheric pressure changes and sea level rise); and
- Heat spells and cold snaps.

Signals of Climate Change. The facts of observed climate change and its reported impacts on environment and the society are summarized below (IPCC 2007):

(1) The earth has warmed by 0.74 (0.56 to 0.92) °C during the last 100-years (1906–2005).
(2) Out of the last twelve years during 1995–2006, eleven years were warmest years in the instrumental record of past 25 years.
(3) Average global ocean temperature has increased up to 3000 m depth, and the ocean has been absorbing more than 80% of the heat added to the climate system.
(4) More intense and longer droughts observed over wider areas since the 1970s, in the tropics and subtropics.
(5) The frequency of heavy precipitation events has increased over most land areas.
(6) Significantly increased rainfall has been observed in eastern parts of North and South America, northern Europe and northern and central Asia.
(7) Average Arctic temperatures increased at almost twice the global average rate in the past 100 years.
(8) Cold days, cold nights and frost have become less frequent, while hot days, hot nights, and heat waves have become more frequent.
(9) Mountain glaciers and snow cover have declined on average in both hemispheres.

Other Signals of Adverse Impacts on Society and Environment.

(1) 40% of world population now faces chronic shortage of fresh water for daily needs.
(2) Half of the world's wetlands have been lost.
(3) Contaminated water kills around 2.2 million people every year.
(4) Air pollution has now become major killer accounting for death of 3 million people every year.
(5) Since 1990, 24% of the world's forests have been destroyed. The rate of loss is 90,000 sq. km every year.
(6) Half of the world's grasslands are overgrazed.
(7) 800 wildlife species have become extinct and 11,000 more are threatened.
(8) Almost 75 per cent of the world's marine captures is over fished or fully utilized. In North America, 10 fish species went extinct in the 1990s.
(9) Two-thirds of the world's farm lands suffer from soil degradation.

Occurrence of Extreme Events. Global climate change could well affect the frequency, magnitude and location of extreme events. Any shift in mean climate will almost inevitably result in a change in the frequency of extreme events. In general, more heat waves and fewer frosts could be expected as the mean temperature rises. All India time series of average temperature published by India meteorological department (IMD) is shown in Figure 10.1.

As the average global temperature increases one would expect that the moisture content of the atmosphere to rise, due to increased rates of evaporation from the sea surface. For every 1°C sea surface temperature rise, atmospheric moisture over the oceans increases by 6–8%. Increases in atmospheric moisture may lead to increased precipitation rates in some parts of the world (causing floods and landslides), whilst decreases may be experienced in other parts (leading to droughts) due to changes in energy and moisture transport patterns in the atmosphere. In general, as more energy and moisture is put into the atmosphere, the likelihood of storms, hurricanes and tornadoes increases (Kaczmarek et al. 1997). Computer models which simulate the effects on the global climate of doubling atmospheric carbon dioxide concentrations have revealed some alarming results. A model used by the UK Meteorological Office, for example, has projected that the daily maximum rainfall in North Western Europe will increase by 40%. Consequently, a 1 in 10 year flood becomes a 1 in 3 year flood. Another model predicts that up to 89% of years will be warmer than 1997 in the UK by the 2050s, currently the third warmest year on record. Distribution of number of low, moderate, heavy and very heavy rainfall events are shown in Figure.10.2.

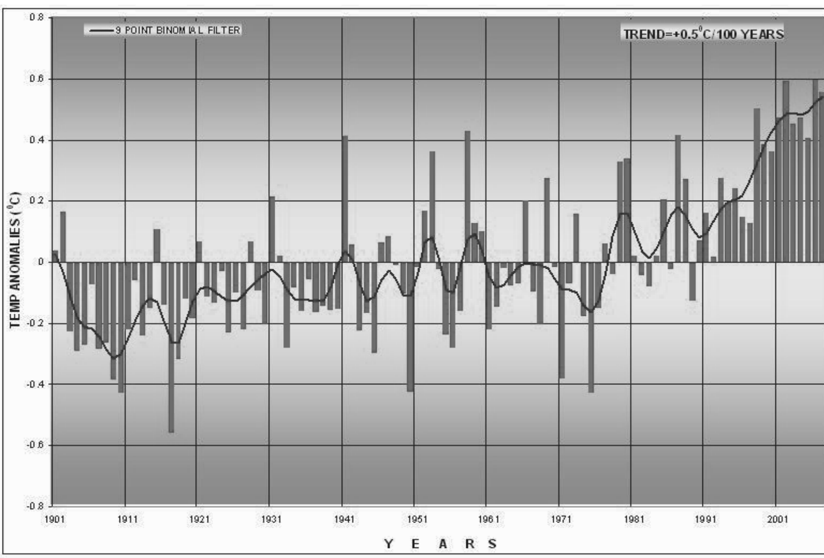

Figure 10.1. Time series all India of average temperature from 1901–2006

The All-India monsoon rainfall does not show any definite trends, however, small pockets of increasing and decreasing trends are observed. West coast, north Andhra Pradesh and north-west India show increasing trend in seasonal rainfall while decreasing trend is observed over east Madhya Pradesh and adjoining areas, north-east India and parts of Gujarat and Kerala (-6 to -8% of normal over 100 years). Some of the significant changes in rainfall pattern observed in India are listed below:

- Frequency of intense rainfall events has increased significantly; and
- Mean annual surface air temperatures show a significant warming of about 0.5^o C/100 year during the last century.

An increase in air temperature would increase potential evapotranspiration, but the magnitude of increase also depends on changes in sunlight, humidity, wind speed, rainfall and vegetation characteristics. Actual evapotranspiration may increase or decrease according to the availability of soil moisture. It is not certain how individual catchment areas will respond to changing evapotranspiration rates and precipitation. It is likely, however, that drier hydrological regimes will be more sensitive to changes in climate. Relatively small changes in temperature and precipitation could cause relatively large changes in run-off. Arid and semi-arid regions will therefore be particularly sensitive to reduced rainfall and to increased evaporation and plant transpiration.

In the developed world, the return period of extreme events may still be substantially greater than the recovery period from the disasters which the events cause. For less adaptable societies in the developing world, however, a shorter *return period* of extreme events may not allow them to fully recover from the effects of one event before the next event strikes.

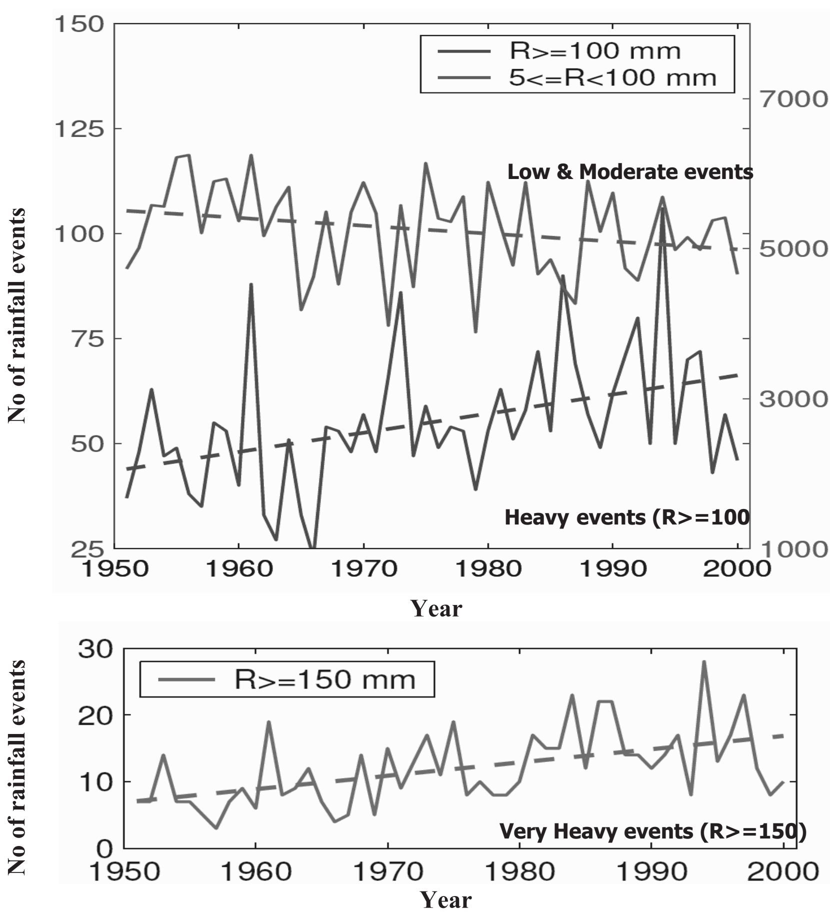

Figure 10.2. Distribution of number of low & moderate, heavy and very heavy rainfall events in India

10.3 Changes in Earth's Climate and Expected Changes in Extreme Events

The extreme events, like heat waves, droughts and floods are expected to change as the earth's climate changes. Instrumental observations over the past 157 years show that temperatures at the surface have risen globally, with important regional variations. For the global average, warming in the last century has occurred in two phases, from the 1910s to the 1940s (0.35°C), and more strongly from the 1970s to the present (0.55°C). An increasing rate of warming has taken place over the last 25 years, and 11 of the 12 warmest years on record have occurred in the past 12 years. Above the surface, global observations since the late 1950s show that the troposphere (up to about 10 km) has warmed at a slightly greater rate than the surface, while the stratosphere (about 10–30 km) has cooled markedly since 1979. This is in accord with physical expectations and most model results. Confirmation of global warming comes from warming of the oceans, rising sea levels, glaciers melting, sea ice retreating in the Arctic and diminished snow cover in the Northern Hemisphere.

The type, frequency and intensity of extreme events are expected to change as Earth's climate changes, and these changes could occur even with relatively small mean climate changes. Changes in some types of extreme events have already been observed, for example, increases in the frequency and intensity of heat waves and heavy precipitation events. In a warmer future climate, there will be an increased risk of more intense, more frequent and longer-lasting heat waves. The European heat wave in 2003 is an example of the type of extreme heat event lasting from several days to over a week that is likely to become more common in a warmer future climate. A related aspect of temperature extremes is that there is likely to be a decrease in the daily (diurnal) temperature range in most regions. It is also likely that a warmer future climate would have fewer frost days (i.e., nights where the temperature dips below freezing). Growing season length is related to number of frost days, and has been projected to increase as climate warms. There is likely to be a decline in the frequency of cold air outbreaks (i.e., periods of extreme cold lasting from several days to over a week) in Northern Hemisphere winter in most areas. Exceptions could occur in areas with the smallest reductions of extreme cold in western North America, the North Atlantic and southern Europe and Asia due to atmospheric circulation changes.

In a warmer future climate, most Atmosphere-Ocean General Circulation Models project increased summer dryness and winter wetness in most parts of the northern middle and high latitudes. Summer dryness indicates a greater risk of drought. Along with the risk of drying, there is an increased chance of intense precipitation and flooding due to the greater water-holding capacity of a warmer atmosphere. This has already been observed and is projected to continue because in a warmer world, precipitation tends to be concentrated into more intense events, with longer periods of little precipitation in between. Therefore, intense and heavy downpours would be interspersed with longer relatively dry periods. Another aspect of these projected changes is that wet extremes are projected to become more severe in many areas where mean precipitation is expected to increase, and dry extremes are projected to become more severe in areas where mean precipitation is projected to decrease.

In concert with the results for increased extremes of intense precipitation, even if the wind strength of storms in a future climate did not change, there would be an increase in extreme rainfall intensity. In particular, over Northern Hemisphere land, an increase in the likelihood of very wet winters is projected over much of central and northern Europe due to the increase in intense precipitation during storm events, suggesting an increased chance of flooding over Europe and other mid-latitude regions due to more intense rainfall and snowfall events producing more runoff. Similar results apply for summer precipitation, with implications for more flooding in the Asian monsoon region and other tropical areas (IPCC 2007).

The increased risk of floods in a number of major river basins in a future warmer climate has been related to an increase in river discharge with an increased risk of future intense storm-related precipitation events and flooding. Some of these changes would be extensions of trends already underway.

There is evidence from modeling studies that future tropical cyclones could become more severe, with greater wind speeds and more intense precipitation. Studies suggest that such changes already be underway; there are indications that the average number of Category 4 and 5 hurricanes per year has increased over the past 30 years. Some modeling studies have projected a decrease in the number of tropical cyclones globally due to the increased stability of the tropical troposphere in a warmer climate, characterized by fewer weak storms and greater numbers of intense storms. A number of modelling studies have also projected a general tendency for more intense but fewer storms outside the tropics, with a tendency towards more extreme wind events and higher ocean waves in several regions in association with those deepened cyclones. Models also project a poleward shift of storm tracks in both hemispheres by several degrees of latitude.

10. 4 Evidences of Increase in Extreme Events

Every region of the world experiences record-breaking climate extremes from time to time. In 1989, for example, the "Big Wet" in eastern Australia brought torrential downpours and the worst flooding in two centuries. The same year also saw an extreme typhoon season in Southeast Asia. The Philippines was hit by three typhoons in October, including Typhoon Elsie with its peak winds of 200 km/hr. More than 1,000 people drowned a month later when southern Thailand was struck by the most powerful storm in fifty years. Many people in England will remember the "Hurricane" of October 1987. Droughts are another devastating type of climate extreme. Early this century, a trend towards increased drought in the North American Midwest culminated in the "Dust Bowl" decade of the "dirty thirties," after which conditions eased. During nine of the years since 1970, annual rainfall over the Sahel zone of northern Africa dropped more than 20% below the average prevailing during this century's first seven decades; those previous 70 years saw only one extreme of this magnitude (Wilhite 2000). Indian subcontinent faced more frequent and severe drought events in last three decades of the last century (i.e., major drought events in 1979, 1987, 1989, 1996, 2002, and 2006) (Pandey et al. 2002; Pandey et al. 2008). Major cyclone events in India have been too frequent in last 50 years of the 20th century as can be seen in Table 10.1 below.

Table 10.1. List of major cyclone events in India

No.	Location	Date/ Area	Documented Damages
1	Bengal	Oct, 1847	75,000 people and 6000 cattle killed. Damage to property.
2	Bengal	October, 1874	80,000 people killed heavy loss to property and communication disrupted.
3	Andhra Pradesh	November, 1946	750 people and 30,000 cattle lost life. Damage to property and roads also reported.
4	Tamil Nadu	December, 1972	80 people and 150 cattle killed and communication disrupted.
5	Bengal	September, 1976	10 people and 40,000 cattle lost life. Damage to property including communication.
6	Andhra Pradesh	November, 1977	8,547 people and 40,000 cattle lost life. Communication disrupted heavy loss to property.
7	Tamil Nadu	May, 1979	700 people and 300,000 cattle lost life. Communication disrupted.
8	Orissa	September, 1985	84 people and 2600 cattle lost life. Land of 4.0 has damaged.
9	Andhra Coast	November, 1987	50 people and 25,800 cattle lost life, 84,000 houses, roads, and other communication disrupted.
10	Orissa	June, 1989	61 people and 27,000 cattle lost life, 145,000 houses, communication disrupted.
11	Andhra Pradesh	May, 1990	928 human lives lost, 14,000 houses damaged.
12	Tamil Nadu	November, 1991	185 people and 540 cattle dead. Property including roads worth 300 crores damaged.
13	Bengal	April, 1993	Over 100 causalities, communication system including road disrupted and damaged.
14	Bengal	November, 1994	More than a thousand houses damaged in 26 villages, damage to lake and fisheries, disrupted all communication.
15	Andhra Coast	October, 1996	1057 causalities, 647,000 houses damaged road network completely damaged.
16	Gujarat	June, 1998	1,261 casualties, 2.57 lakh houses damaged.
17	Orissa	October, 1999	10,086 Casualties, 21.6 Lakh houses damaged.

Frequent reports of record-breaking events suggest that climate extremes are becoming more common. There are few documented scientific evidences indicating greater frequency of climatic extremes at the global level. The Intergovernmental Panel on Climate Change scientific assessment (IPCC 2001) concluded that the higher maximum and minimum temperatures, more hot days and fewer cold days, and more intense precipitation events have been observed in the latter half of the 20th century. Nevertheless, it is still plausible that increased human vulnerability to climate extremes (particularly in developing countries) is transforming extreme events into climatic disasters. This may be because people in many parts of the world are being forced to live in more exposed and marginal areas. In other areas, high-value property is being developed in high-risk zones. This explains, for example, why Hurricane Hugo, which devastated the Caribbean and southern United States in 1989, proved the costliest hurricane in history, with an estimated damages in the order of about $10 billion. Finally, because the communications revolution has made news and information more widely available than ever before, people are much more aware of the occurrence of extreme events and of their impact.

The earth has warmed by 0.74 during the last 100-years (1906–2005). Noticeable changes in climatic attributes could be observes after 1981 and the last decade of 20th century was warmest among all. The average global ocean temperature has increased to 3000 m depth. More intense and longer droughts have been observed over wider areas since the 1970s, in the tropics and subtropics. It is widely recognized that the frequency of severe drought events may increase significantly. Also, the frequency of heavy precipitation events and floods has increased over most land areas. However, current documented evidences still need comprehensive verification to conclude that the extreme events are the first signs of climate change. There is need to develop better understanding on the climate system and the effects of greenhouse gas emissions well enough to conclude that particular events are linked to the problem. Nevertheless, monitoring and studying extreme events, and learning how to predict and cope with them, must be a priority. Of all aspects of climate variability, extreme events are likely to have greatest effect on human well-being in the decades to come. What is most certain, however, is that it is likely to be the poorest and most vulnerable societies in the developing world which will be least able to adapt to any increase in the frequency and magnitude of extreme weather phenomena.

10.5 Flood Frequency Estimation and Impact of Climate Change

Information on flood magnitudes and their frequencies is needed for design of various types of water resources projects/ hydraulic structures such as dams, spillways, road and railway bridges, culverts, urban drainage systems as well as for taking up various non-structural measures such as flood plain zoning, economic evaluation of flood protection projects etc. Since scientific hydrology began in the seventeenth century, one of the most difficult problems facing engineers and hydrologists is how to predict flow in basins with no records. Whenever, rainfall or river flow records are not available at or near the site of interest, it is difficult for hydrologists or engineers to derive reliable design flood estimates, directly. Also, there are situations when river flow records are available for a short period of time for a number of sites for a region. In such a situation, regional flood frequency relationships developed for the region are one of the alternative methods for prediction of design floods, especially for small to medium size catchments. Thus regional flood frequency analysis is a procedure for substitution of space for time.

Considering the importance of prediction in ungauged catchments, the International Association of Hydrological Sciences (IAHS) launched “Prediction of Ungauged Basins (PUBs)” as one of its initiatives and declared the current decade as “Decade of PUBs.” As per the Indian design criteria, frequency based floods find their applications in estimation of design floods for almost all the types of hydraulic structures viz. small size dams, barrages, weirs, road and railway bridges, cross drainage structures, flood control structures etc., excluding large and intermediate size dams. For design of large and intermediate size dams, probable maximum flood and standard project flood are adopted, respectively. Most of the small size catchments are ungauged or sparsely gauged. To overcome the problems of prediction of floods of various return periods for ungauged and sparsely gauged catchments, a robust procedure of regional flood frequency estimation is required to be developed.

10.5.1 L-moments Approach

L-moments are a recent development within statistics (Hosking 1990). In a wide range of hydrologic applications, L-moments provide simple and reasonably efficient estimators of characteristics of hydrologic data and of a distribution's parameters (Stedinger et al. 1992). Like the ordinary product moments, L-moments summarize the characteristics or shapes of theoretical probability distributions and observed samples. Both moment types offer measures of distributional location (mean), scale (variance), skewness (shape), and kurtosis (peakedness).

10.5.2 Probability Weighted Moments and L-Moments

The L-moments are an alternative system of describing the shapes of probability distributions (Hosking and Wallis 1997). They arose as modifications of probability weighted moments (PWMs) of Greenwood et al. (1979). Probability weighted moments are defined as:

$$\beta_r = E\left(x\{F(x)\}^r\right) \qquad \text{(Eq.10.1)}$$

which can be rewritten as:

$$\beta_r = \int_0^1 x(F) F^r \, dF \qquad \text{(Eq.10.2)}$$

where, F = F(x) is the cumulative distribution function (CDF) for x, x(F) is the inverse CDF of x evaluated at the probability F, and r = 0, 1, 2, …, is a nonnegative integer. When r = 0, β_0 is equal to the mean of the distribution $\mu = E[x]$. For any distribution the r^{th} L-moment λ_r is related to the r^{th} PWM (Hosking 1990), through:

$$\lambda_{r+1} = \sum_{k=0}^{r} \beta_k (-1)^{r-k} \binom{r}{k} \binom{r+k}{k}$$ (Eq.10.3)

For example, the first four L-moments are related to the PWMs using:

$$\lambda_1 = \beta_0$$ (Eq.10.4)

$$\lambda_2 = 2\beta_1 - \beta_0$$ (Eq.10.5)

$$\lambda_3 = 6\beta_2 - 6\beta_1 + \beta_0$$ (Eq.10.6)

$$\lambda_4 = 20\beta_3 - 30\beta_2 + 12\beta_1 - \beta_0$$ (Eq.10.7)

Hosking (1990) defined L-moment ratios as:

L-coefficient of variation, L-CV (τ_2) = λ_2 / λ_1 (Eq.10.8)

L-coefficient of skewness, L-skew (τ_3) = λ_3 / λ_2 (Eq.10.9)

L-coefficient of kurtosis, L-kurtosis (τ_4) = λ_4 / λ_2 (Eq.10.10)

10.5.3 Screening of Data Using Discordancy Measure Test

The objective of screening of data is to check that the data are appropriate for performing the regional flood frequency analysis. In this study, screening of the data was performed using the L-moments based Discordancy measure (D_i). Hosking and Wallis (1997) defined the Discordancy measure (D_i) considering if there are N sites in the group.

$$\overline{u} = N^{-1} \sum_{i=1}^{N} u_i$$ (Eq.10.11)

Let $u_i = [t_2^{(i)} \ t_3^{(i)} \ t_4^{(i)}]^T$ be a vector containing the sample L-moment ratios t_2, t_3 and t_4 values for site i, analogous to their regional values termed as τ_2, τ_3, and τ_4, expressed in Eqs. (10.8) to (10.10). T denotes transposition of a vector or matrix. Let be the (unweighted) group average. The matrix of sums of squares and cross products is defined as:

$$A_m = \sum_{i=1}^{N} (u_i - \overline{u})(u_i - \overline{u})^T$$ (Eq.10.12)

The Discordancy measure for site i is defined as:

$$D_i = \frac{1}{3} N (u_i - \bar{u})^T A_m^{-1} (u_i - \bar{u})$$ Eq.10.13

The site i is declared to be discordant, if D_i is greater than the critical value of the Discordancy statistic D_i, given in a tabular form by Hosking and Wallis (1997).

10.5.4 Test of Regional Homogeneity

For testing regional homogeneity, a test statistic H, termed as heterogeneity measure was proposed by Hosking and Wallis (1993). It compares the inter-site variations in sample L-moments for the group of sites with what would be expected of a homogeneous region. The inter-site variation of L-moment ratio is measured as the standard deviation (V) of the at-site L-CV's weighted proportionally to the record length at each site. To establish what would be expected of a homogeneous region, simulations are used. A number of, say 500, data regions are generated based on the regional weighted average statistics using a four parameter distribution e.g. Kappa distribution. The inter-site variation of each generated region is computed and the mean (μ_V) and standard deviation (σ_V) of the computed inter-site variation is obtained. Then, heterogeneity measure H is computed as:

$$H = \frac{V - \mu_V}{\sigma_V}$$ (Eq.10.14)

The criteria for assessing heterogeneity of a region are: if $H < 1$, the region is acceptably homogeneous; if $1 \le H < 2$, the region is possibly heterogeneous; and if $H \ge 2$, the region is definitely heterogeneous.

10.5.5 Identification of Robust Regional Frequency Distribution

The choice of an appropriate frequency distribution for a homogeneous region is made by comparing the moments of the distributions to the average moments statistics from regional data. The best fit distribution is determined by how well the L-skewness and L-kurtosis of the fitted distribution match the regional average L-skewness and L-kurtosis of the observed data (Hosking and Wallis 1997). The goodness-of-fit measure for a distribution, Z_i^{dist} –statistic defined by Hosking and Wallis (1997) is expressed as:

$$Z_i^{dist} = \frac{\left(\bar{\tau}_i^R - \tau_i^{dist}\right)}{\sigma_i^{dist}}$$ (Eq.10.15)

Where, $\bar{\tau}_i^R$ is weighted regional average of L-moment statistic i, τ_i^{dist} and σ_i^{dist} are the simulated regional average and standard deviation of L-moment statistics i, respectively, for a given distribution. The fit is considered to be adequate if $|Z_i^{dist}|$–statistic is sufficiently close to zero, a reasonable criterion being $|Z_i^{dist}|$ –statistic less than 1.64.

10.5.6 A Case Study for Chambal Subzone 1(b)

10.5.6.1 Study Area and Data Availability

The Chambal Subzone 1 (b) lies between 73^0 20' and 79^0 east longitudes and 22^0 30' and 27^0 15' north latitudes. This covers major parts of states of Rajasthan and Madhya Pradesh and a small portion of Uttar Pradesh in India. The Chambal is the principal tributary of the Yamuna and other important rivers of the Subzone are Banas from the left bank and Kali Sindh, Parbati, Kunu and Kunwari from the right bank. The river Chambal rises in the Vindhya range near Mhow in the Indore district of Madhya Pradesh at an elevation of 854 m. The total length of the river from its source to confluence with Yamuna is about 960 km. There are mainly three types of soil, viz. medium black soil, mixed red and black soil, alluvial soil. Other types of soil are red and yellow soil, gray-brown soil, deep-black soil, laterite soil and skeletal soil. The arable land in the Subzone is about 52%, forest cover 23%, grass land scrub 19% and the remaining portions are waste land urban area. Annual maximum peak flood data of 13 Bridge sites lying in the hydrometeorologically homogeneous region (Central Water Commission, 1982) of Chambal Subzone 1 (b) as well as the catchment areas of the Bridge sites were available for the study.

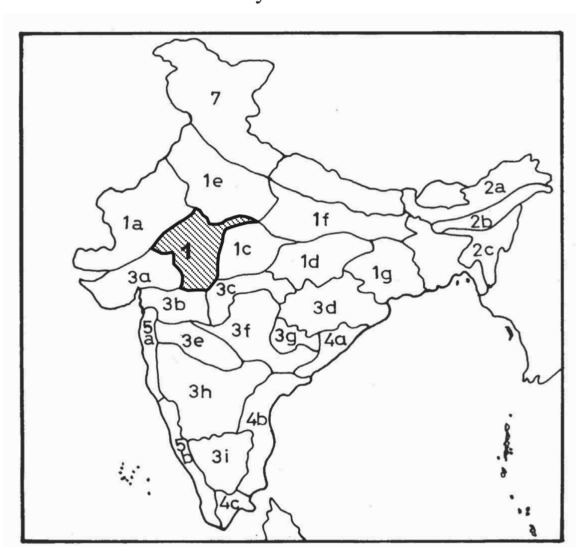

Figure 10.3. Index map showing location of Chambal Subzone 1(b) in India

10.5.6.2 Analysis and Discussion of Results

Regional flood frequency analysis was performed using the various frequency distributions, viz. Extreme value (EV1), Generalized extreme value (GEV), Logistic

(LOS), Generalized logistic (GLO), Normal (NOR), Generalized normal (GNO), Uniform (UNF), Pearson Type-III (PE3), Exponential (EXP), Generalized Pareto (GPA), Kappa (KAP), and five parameter Wakeby (WAK). Screening of the data, testing of regional homogeneity, identification of the regional distribution and development of regional flood frequency relationships are described below.

10.5.6.3 Screening of Data using Discordancy Measure Test

Values of Discordancy statistic (D_i) have been computed in terms of the L-moments for all the 13 gauging sites of the study area. It is observed that the critical D_i value (Hosking and Wallis, 1997) for a group of 13 sites is 2.869 and as per the D_i test the data of all the 13 sites are found to be suitable for regional flood frequency analysis.

10.5.6.4 Test of Regional Homogeneity

Based on the heterogeneity measure, the data sample comprising of 12 gauging sites and is considered as homogeneous. The details of catchment data and statistical parameters for the 12 gauging sites are given in Table 10.2. The D_i values for these 12 sites vary from 0.09 to 2.12. The values of heterogeneity measures computed by carrying out 500 simulations using the Kappa distribution based on the data of 12 sites are given in Table 10.3

Table 10.2. Catchment area, sample statistics, sample size and discordancy measure for 15 gauging sites of Chambal Subzone 1(b)

Stream Gauging Site	Catchment Area (km^2)	Mean Annual Peak Flood (m^3/s)	Sample Size (Years)	L-CV (τ_2)	L-skew (τ_3)	L-kurtosis (τ4)	Discordancy Measure (D_i)
94	2297.330	1549.000	20	0.3816	0.2044	0.1582	0.64
72	662.800	597.520	23	0.5447	0.2907	0.1185	0.57
118	41.000	70.800	10	0.2574	0.1193	0.3110	2.12
1116/3	361.050	339.560	16	0.5308	0.4779	0.3076	1.63
1	44.750	100.078	13	0.5197	0.3285	0.2394	0.95
437	237.140	197.130	10	0.5253	0.2520	-0.0186	1.43
77	26.180	18.820	11	0.6632	0.4965	0.2180	1.56
306	43.770	76.770	31	0.4650	0.2911	0.1820	0.09
35	39.520	184.654	26	0.3348	0.0108	0.0340	1.67
44	109.000	202.680	22	0.4598	0.2517	0.0875	0.64
406	48.090	92.210	24	0.4068	0.1454	0.1263	0.39
519	1500.020	1551.600	25	0.5212	0.2804	0.0749	0.31

Table 10.3. Heterogeneity measures for 12 gauging sites of Chambal Subzone 1(b)

Heterogeneity measures	Values
Standardized test value H	1.65
Standardized test value H(2)	0.91
Standardized test value H(3)	0.08

10.5.6.5 Identification of Robust Regional Frequency Distribution

The L-moment ratio diagram and $|Z_i^{dist}|$ –statistic are used as the best fit criteria for identifying the robust distribution for the study area. Figure 10.4 shows the L-moments ratio diagram for the study area. The Z_i^{dist} –statistic for various three parameter distributions is given in Table 9.4. It is observed that the $|Z_i^{dist}|$ –statistic values are lower than 1.64 for the three distributions viz. PE3, GNO, GPA and GEV distributions. Further, the $|Z_i^{dist}|$ –statistic is found to be the lowest for PE3 distribution i.e. 0.01. Thus, based on the L-moment ratio diagram and $|Z_i^{dist}|$ –statistic criteria, the PE3 distribution is identified as the robust distribution for the study area. The values of regional parameters for the various distributions which have Z^{dist} –statistic value less than 1.64 as well as the five parameter Wakeby distribution are given in Table 10.5.

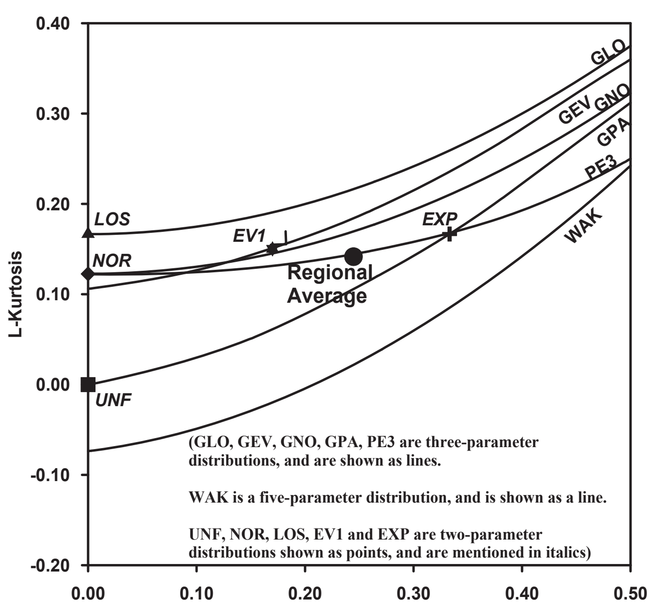

Figure 10.4. L-moment ratio diagram for Chambal Subzone 1(b) for various distributions

The regional parameters of the Wakeby distribution have been included in Table 10.5 because the Wakeby distribution has five parameters, more than most of the common distributions, and it can attain a wider range of distributional shapes than can the common distributions. This makes the Wakeby distribution particularly useful for simulating artificial data for use in studying the robustness, under changes in distributional form of methods of data analysis. It is preferred to use Wakeby distribution for heterogeneous regions.

Table 10.4. Z_i^{dist}–statistic for various distributions Chambal Subzone 1(b)

S. No.	Distribution	Z_i^{dist}–statistic
1	Pearson Type III (PE3)	0.01
2	Generalized Normal (GNO)	0.88
3	Generalized Pareto (GPA)	-1.32
4	Generalized Extreme Value (GEV)	1.37
5	Generalized logistic (GLO)	2.46

Table 10.5. Regional parameters for various distributions of Chambal Subzone 1(b)

Distribution	Parameters of the Distribution				
PE3	$\mu = 1.000$	$\sigma = 0.875$	$\gamma = 1.477$		
GNO	$\xi = 0.801$	$\alpha = 0.734$	$k = -0.509$		
GPA	$\xi = -0.021$	$\alpha = 1.237$	$k = 0.212$		
GEV	$\xi = 0.584$	$\alpha = 0.592$	$k = -0.114$		
WAK	$\xi = -0.074$	$\alpha = 0.990$	$\beta = 1.631$	$\gamma = 0.663$	$\delta = 0.050$

10.5.6.6 Regional Flood Frequency Relationship for Gauged Catchments

The inverse form of the Pearson type-III (PE3) distribution is not explicitly defined. Hosking and Wallis (1997) mention that the PE3 distribution combines Gamma distributions (which have positive skewness), reflected Gamma distributions (which have negative skewness) and the normal distribution (which has zero skewness). The authors parameterize the Pearson type-III distribution by its first three conventional moments, viz. mean μ, the standard deviation σ, and the skewness γ. The relationship between these parameters and those of the Gamma distribution is as follows. Let X be a random variable with a Pearson type-III distribution with parameters μ, σ and γ. If $\gamma > 0$, then $X - \mu + 2\sigma/\gamma$ has a Gamma distribution with parameters $\alpha = 4/\gamma^2$, $\beta = \sigma\gamma/2$. If $\gamma = 0$, then X has normal distribution with mean μ and standard deviation σ. If $\gamma < 0$, then $-X + \mu - 2\sigma/\gamma$ has a Gamma distribution with parameters $\alpha = 4/\gamma^2$, $\beta = |\sigma\gamma/2|$. If $\gamma \neq 0$, let $\alpha = 4/\gamma^2$, $\beta = |\sigma\gamma/2|$, and $\xi = \mu - 2\sigma/\gamma$ and $\Gamma(.)$ is Gamma function. If $\gamma > 0$, then the range of x is $\xi \leq x < \infty$ and the cumulative distribution function is:

$$F(x) = G\left(\alpha, \frac{x-\xi}{\beta}\right) \Big/ \Gamma(\alpha) \qquad (Eq\,10.16a)$$

If $\gamma < 0$, then the range of x is $-\infty < x \leq \xi$ and the cumulative distribution function is:

$$F(x) = 1 - G\left(\alpha, \frac{\xi - x}{\beta}\right) \bigg/ \Gamma(\alpha) \qquad (Eq.10.16b)$$

Floods of various return periods may be computed by multiplying mean annual peak flood of a catchment by the corresponding values of growth factors of robust identified PE3 distribution given in Table 10.6 (Kumar and Chatterjee 2005).

Table 10.6. Values of growth factors ($Q_T/\overline{Q}$) for Chambal Subzone 1(b)

	Return period (Years)						
Distribution	**2**	**10**	**25**	**50**	**100**	**200**	**1000**
	Growth factors						
Pearson Type-III(PE3)	0.793	2.167	2.873	3.392	3.901	4.403	5.059
Generalized normal (GNO)	0.801	2.127	2.874	3.460	4.070	4.709	5.599
Generalized Pareto (GPA),	0.777	2.233	2.865	3.267	3.615	3.915	4.249
Generalized extreme value (GEV)	0.805	2.102	2.869	3.493	4.164	4.888	5.935
Five parameter Wakeby (WAK)	0.805	2.136	2.844	3.395	3.963	4.551	5.360

10.5.6.7 Regional Flood Frequency Relationship for Ungauged Catchments

For ungauged catchments, on-site mean cannot be computed in the absence of the observed flow data. Hence, a relationship between the mean annual peak flood of gauged catchments in the region and their pertinent physiographic and climatic characteristics is needed for estimation of the mean annual peak flood. Figure 10.5 shows a plot of the mean annual peak flood versus catchment area in a log domain for the 12 gauging sites of Chambal Subzone 1(b). The regional relationship developed in the log domain using the least squares approach based on the data of 12 gauging sites is given below.

$$\overline{Q} = 4.105(A)^{0.778} \qquad (Eq.10.17)$$

where, A is the catchment area, in km^2 and $\overline{Q}$ is the mean annual peak flood in m^3/s. For Eq. (10.17), the coefficient of determination, r^2 is 0.975.

For development of regional flood frequency relationship for ungauged catchments, the regional flood frequency relationship developed for gauged catchments is coupled with regional relationship between mean annual peak flood and catchment area, given in Eq. (10.17) and following regional frequency relationship is developed.

$$Q_T = C_T * A^{0.778} \qquad (Eq.10.18)$$

where, Q_T is flood estimate in m^3/s for T year return period, and A is catchment area in km^2 and C_T is a regional coefficient. Values of C_T for some of the commonly used return periods are given in Table 10.7. The above regional flood formula (Eq.10.18) may be used for estimation of floods of desired return periods for ungauged catchments of the Chambal Subzone 1(b).

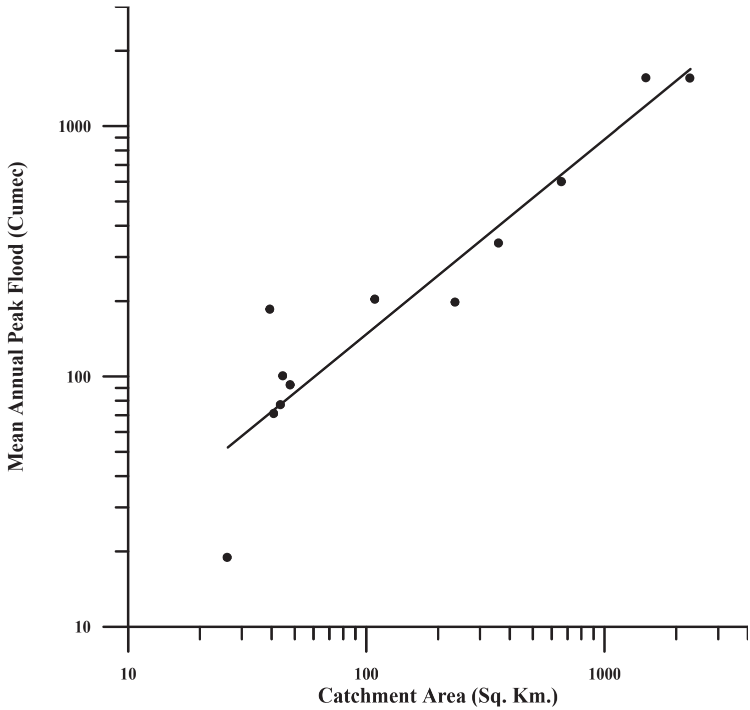

Figure 10.5. Variation of mean annual peak flood with catchment area for various gauging sites of Chambal Subzone 1(b)

Table 10.7. Values of regional coefficient C_T for Chambal Subzone 1(b)

	Return period (Years)						
Distribution	**2**	**10**	**25**	**50**	**100**	**200**	**1000**
	Growth factors						
PE3	3.255	8.896	11.794	13.924	16.014	18.074	22.783

10.6 Impact of Climate Change on Floods of Various Return Periods – A Case Study

For evaluation of impact of climate change on floods of various return periods, data of 98 years of a snow and rain-fed dam have been used. Floods of various return periods have been estimated using the annual maximum peak flood series of 98 years of the study areas employing the L-moments approach. Two scenarios are considered:

- **Scenario-1:** Under Scenario-1 of climate change the highest 20% values of the annual peak flood have been increased by 20%; and

- **Scenario-2:** Under Scenario- of climate change the highest 20% values of the annual peak flood have been increased by 20% and the lowest 20% values of the annual peak flood have been decreased by 20%.

The flood estimates for various return periods for the original series and Scenario-1 and Scenario-2 are given in Table 10.8. The percentage deviations in floods of various return periods for Scenario-1 and Scenario-2 under climate change with respect to the original annual maximum peak foods series are given in Table 10.9. Figures 10.6, 10.7 and 10.8 show comparison of 50, 100 and 1000 years return period floods for the original series and Scenario-1 and Scenario-2 under climate change.

For evaluation of impact of climate change on Probable Maximum Flood (PMF) a case study for a snow and rain-fed catchment of above 5000 km^2 has been carried out by considering the following possible cases of climate change:

(1) Impact of change of sequencing of rainfall;
(2) Impact of increase in peak of the unit hydrograph;
(3) Impact of change of temporal distribution pattern of design storm; and
(4) Impact of change of loss rate.

For estimation of design flood, 1-hour unit hydrograph has been derived using the Clark IUH model. The parameters of Clark IUH model have been estimated as $T_c = 9$ and $R = 12$. The unit hydrograph which is derived based on the principle of linearity, has been applied to convert the excess rainfall hyetograph into direct surface runoff hydrograph. The design loss rate of 1-mm/hour has been adopted for computation of design excess rainfall hyetograph from the design storm values. Based on analysis of the observed flow records, a design base flow of 340 m^3/s has been added with the ordinates of design direct surface runoff hydrograph for estimation of the PMF hydrographs.

Table 10.8. Flood of various return periods for original flood series and Scenario-1 and Scenario-2 under climate change

Return Periods	**20**	**25**	**50**	**100**	**200**	**500**	**1000**	**10000**
Original series	8548	8978	10419	12042	13883	16715	19209	30308
Scenario 1	9950	10603	12896	15657	19000	24543	29803	56911
Scenario 2	10033	10658	12810	15319	18257	22954	27247	47818

Table 10.9. Percentage deviations in floods of various return periods for Scenario-1 and Scenario-2 under climate change

Return Periods	**20**	**25**	**50**	**100**	**200**	**500**	**1000**	**10000**
Scenario 1	16	18	23	30	36	46	55	87
Scenario 2	17	18	22	27	31	37	41	57

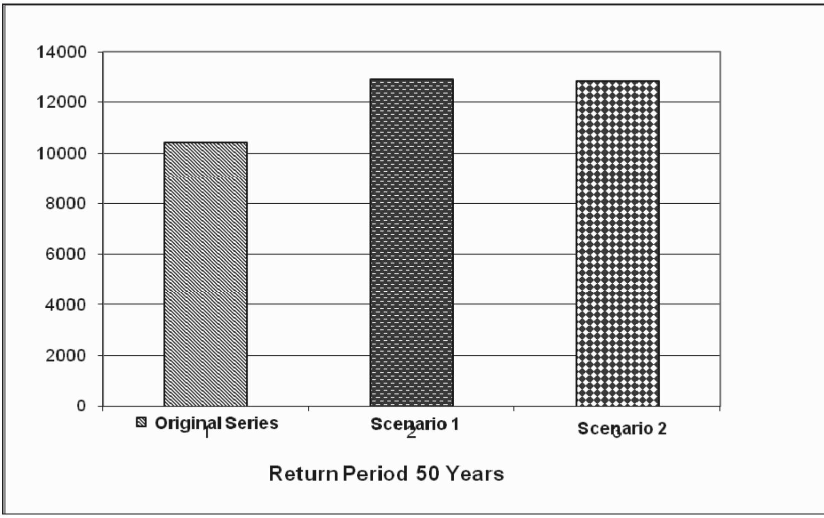

Figure 10.6. Comparison of floods for 50 years return period floods for the original series and Scenario-1 and Scenario-2 under climate change

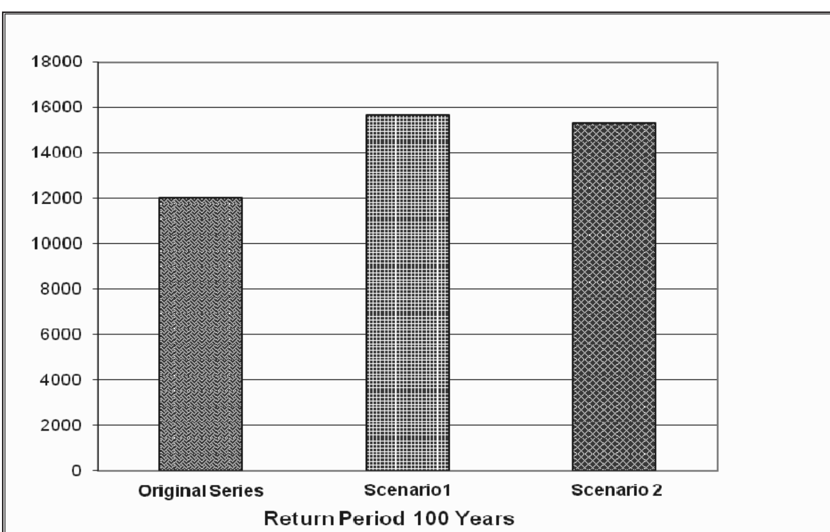

Figure 10.7. Comparison of floods for 100 years return period floods for the original series and Scenario-1 and Scenario-2 under climate change

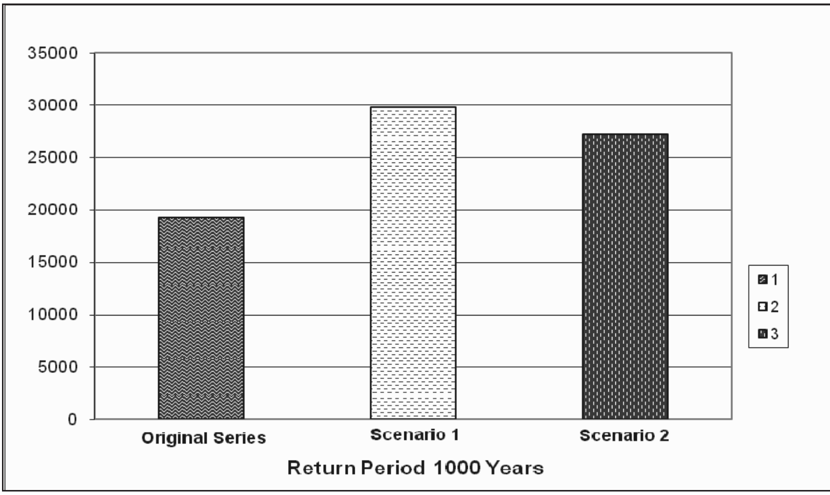

Figure 10.8. Comparison of floods for 1000 years return period floods for the original series and Scenario-1 and Scenario-2 under climate change

10.7 Impact of Climate Change on Probable Maximum Flood –A Case Study

10.7.1 Impact of Change of Sequencing of Rainfall

Due to climate change the rainfall pattern including intensity of rainfall, depth of rainfall, numbers of rain days are likely to be changed. Due to aforementioned changes and other factors the pattern and sequence of rainfall over short duration are likely to change. This aspect has been studied as given below. A comparison of the considered possible changes with reference to the conventional practice of design storm has also been examined. Probable maximum flood has been estimated by converting the 2-days PMP value and its time distribution into 48 hour design storm and convoluting it with the unit hydrograph derived based on the Clark IUH model. The PMFs estimated based on the conventional critical sequencing of the 48-hours design storm approach as well as recent approach of multiple bells design storm approach have been compared. As the multiple bell approach does not provide details of arrangement of 1-hourly excess-rainfall values within the one or two bells per day of the design storm the following four cases of storm patterns have been studied and PMF estimates resulting from these cases are compared for identifying the rational pattern of design storm for optimal design flood estimation.

10.7.2 Impact of Increase in Peak of the Unit Hydrograph

To study the impact of increase in peak of the unit hydrograph on the design flood peak, different unit hydrographs (Figs. 10.9-10.13) have been applied with the design storm of one bell (considered to be reference design storm). It may be observed from Figure 10.13 that for a 50% increase in the peak of unit hydrograph there is an increase of about 25% in the design flood peak. Figure 10.14 shows variation of percentage increase in the peak of the unit hydrograph.

10.7.3 Impact of Change of Temporal Distribution Pattern of Design Storm

The pattern of temporal distribution of design storm also plays a significant role in determining the peak of the design storm hydrograph. Whenever, the problem is referred to IMD, the IMD provides the values of the PMP along with its temporal distribution within bells to be used for design flood estimation as per the recommendations of WMO. Whenever, there is concurrent data of the storm under consideration for design the time distribution of areal rainfall over the catchment is recommended (Central Water Comission 1992). In this study, the sensitivity of the temporal distribution of storm pattern has been conducted by considering two more distribution patterns apart from the storm pattern available for the design storm. The design storm distribution adopted for the reference run as well as the two other distribution patterns considered in the study are shown in Figure 10.15.

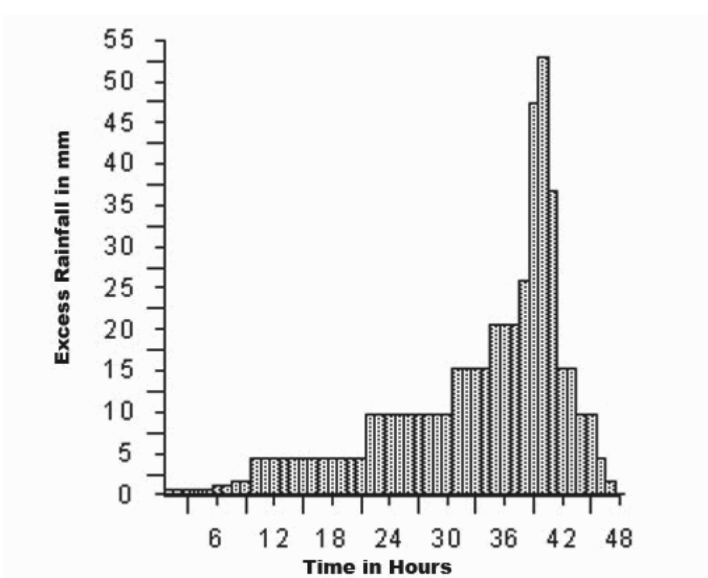

Figure 10.9. Critically sequenced excess rainfall hyetograph as single bell (Case 1) – Reference Run

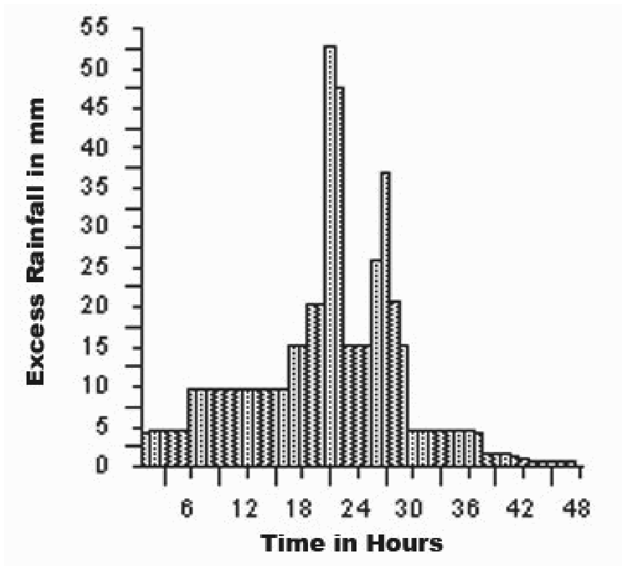

Figure 10.10. Design excess rainfall hyetograph considered as 2 bell (Case 2)

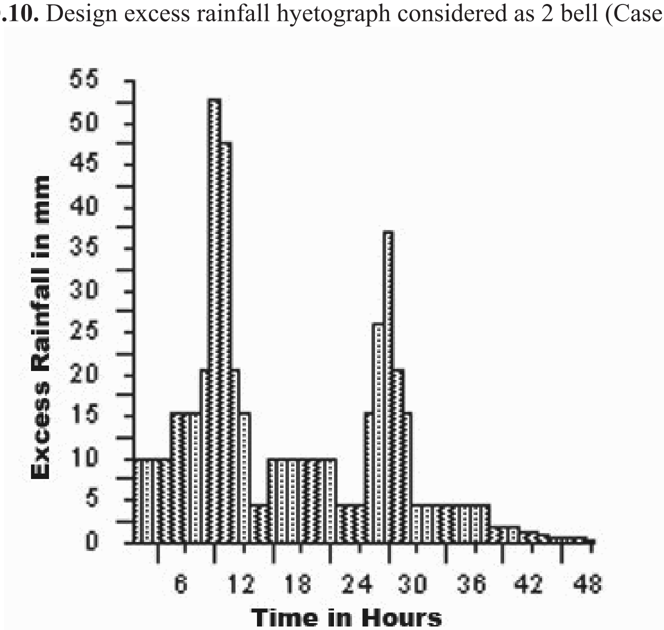

Figure 10.11. Design excess rainfall hyetograph considered as 4 bell (Case 3)

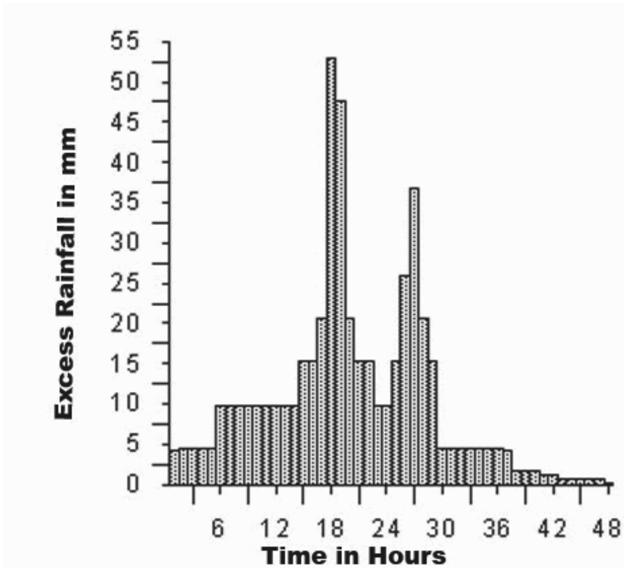

Figure 10.12. Design excess rainfall hyetograph considered as 4 bell (Case 4)

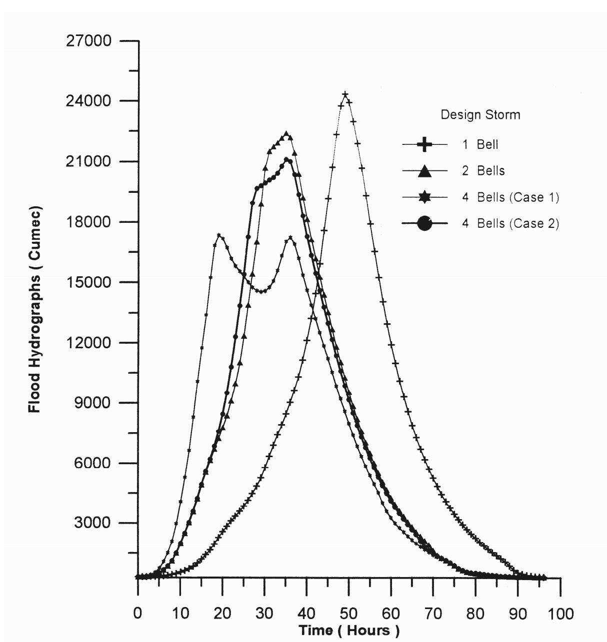

Figure 10.13. Design flood hydrographs for various storm patterns

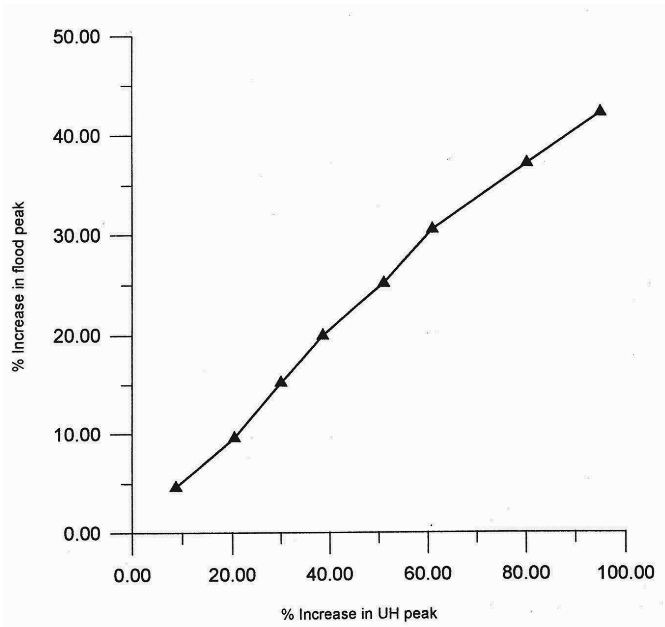

Figure 10.14. Variation of percentage increase in peak of flood hydrograph with percentage increase in peak of UH

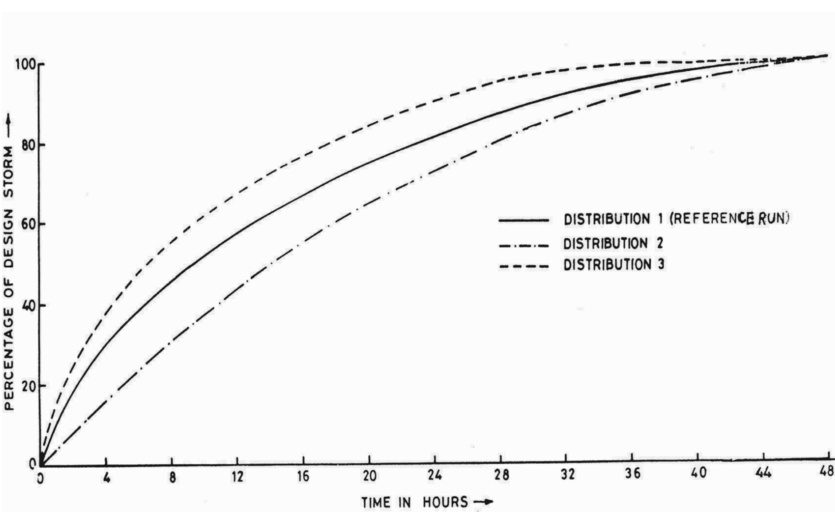

Figure 10.15. Various percentage design storm distribution patterns

The design flood hydrographs of the design storm distributions of the reference run as well as for the two sensitivity runs are shown in Figure 10.16. It is seen from the figure that the design flood peak decreases from 24,359 (reference run/distribution pattern 1) to 20,023 cumec, i.e. by 17.8% for the design storm distribution pattern 2; whereas, for the design storm pattern 3, the peak increases to 27,745 viz. 13.9%. The time to peak does not get effected for the above cases. It shows that the design storm pattern affects the peak of the design flood hydrograph very significantly.

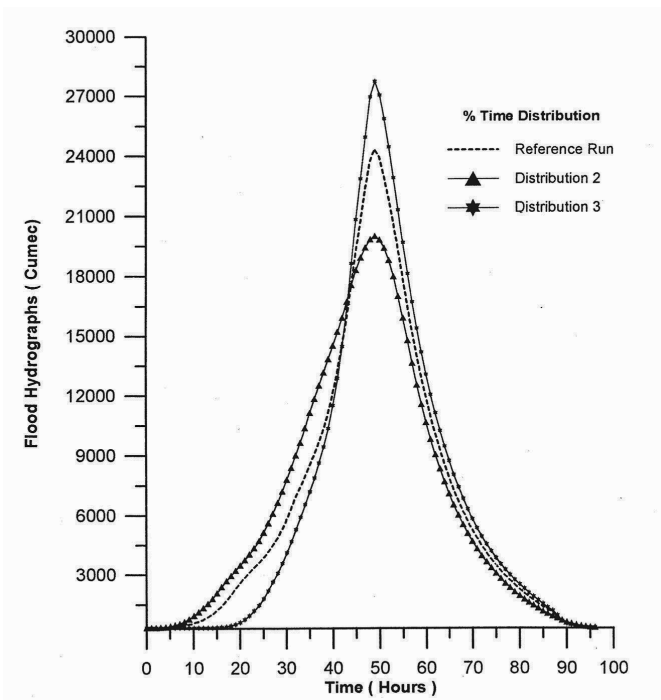

Figure 10.16. Design flood hydrographs for various percentage design storm distribution patterns

10.7.4 Impact of Change of Design Loss Rate

In order to study the sensitivity of the design flood peak to change in loss rate values sensitivity run have been taken up for the uniform loss rates of 0.0, 0.5, 1.0, 1.5, 2.0, 2.5, 3.0, 3.5 and 4.0 mm/hour, considering other design parameters same as for the reference run. Figure 10.17 shows the variation of percentage decrease in peak of the flood hydrograph with increase in loss rate. Variation of peak (Qp) and time to peak (Tp) of the design flood hydrograph with loss rate is shown in Table 10.10. It is seen from Table 10.10 that with an increase in loss rate the peak of the design flood hydrograph decreases. The percentage decrease corresponding to the loss rate of 4 mm/hour (400% increase) is only 15%, with respect to the reference run. It indicates that the design flood hydrograph is not much sensitive to the lost rate.

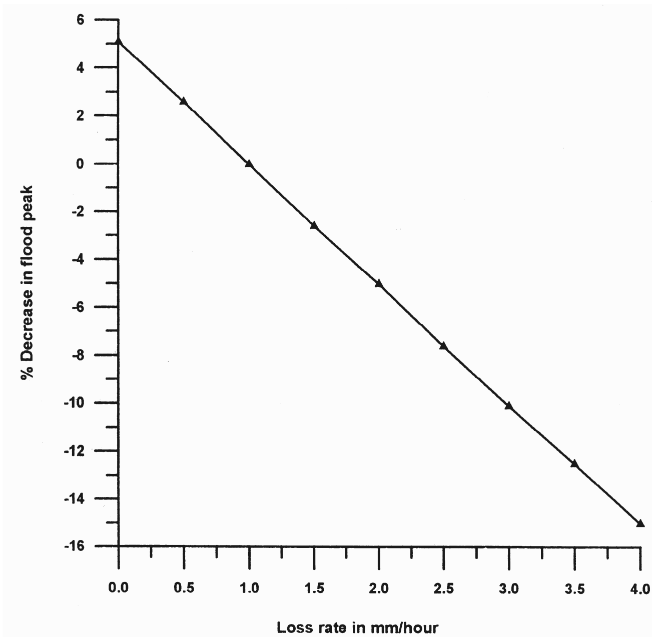

Figure 10.17. Variation of percentage decrease in flood peak with loss rate

Table 10.10. Design flood peak (Q_p) and time to peak (T_p) and the percentage variation with respect to the values of the reference run for various storm patterns

No.	Design storm Patterns	Peak (Q_p) (m^3/s)	Percent deviation in Q_p	Time to Peak (T_p) (Hours)	Percent deviation in T_p
1	1 Bell (Case-1) (Reference run)	24359	Reference run	49	Reference run
2	2 Bells (Case-2)	22407	-8.0	35	-28.6
3	4 Bells (Case-3)	17369	-28.7	19	-61.2
4	4 Bells (Case-4)	21121	-13.3	35	-28.6

10.8 Climate and Drought

The primary purpose of any study on drought is to develop better understanding and ability to cope with adverse impacts of drought on the society. Since the human settlements and the economic activities on the earth are largely concentrated in mid-latitudinal regions, the impacts of droughts in these regions are more apparent (Karl 1983; Ponce 1995a). Classifications of the earth's climate have been proposed by several researchers from time to time, primarily based on plant/vegetation characteristics and temperature. However, the existing classifications do not specify the central tendency of the climate. Droughts are usually defined by relative deficiency of moisture (precipitation, streamflow, water storages etc.) with reference to their central tendency (mean of predefined threshold). Therefore, to characterize droughts in midlaitudinal regions a classification was proposed by Pandey and Ramasastri (2002, 2001) which essentially defines the middle of climatic spectrum and clearly demarcates the climatic spectrum into dry and wet regions. This new classification of the earth's climate was proposed particularly for drought characterization in mid-latitudinal regions.

Droughts are driven by the regional climatic conditions. Therefore, happening and characteristics of droughts are related to regional climatic parameters (Pandey and Ramasastri 2001, 2002; Ponce et al. 2000). The most common climatic elements which govern regional drought characteristics are precipitation and temperature, and hence the evapotranspiration. The other important feature of climate that influence regional drought characteristics is the distribution of rainfall over the year and hence, the length of wet season. Since the long-term records of precipitation, potential evapotranspiration, and length of wet period are usually available in mid-latitudinal regions, defining climatic areas on the basis of these climatic factors may be particularly useful for drought characterization, in mid-latitudinal regions, where impacts of droughts on society are more compelling.

10.8.1 Historical Classification of Earth's Climatic Regions

The initiatives for climatic classification of living cover of the earth were launched by the biologists in the mid-nineteenth century (Thornthwaite 1948). They initially considered plant/vegetation characteristics and natural landscape to describe global climate classes. The monographs of 1866 by Carl Linsser have become the outstanding monument to this phase; his work, concerned with the effects of temperature on phenology, rainfall, and vegetation, leading to dividing the world into climatic zones based on vegetation characteristics. The idea that climate can be classified according to the type of vegetation and physiological response was well established by the year 1875 (Thornthwaite and Hare 1953). Wladimir Köppen of University of Graz, Austria, elevated this notion further into a primacy of place that it has never lost.

Köppen first presented his classification in 1900 with primary division of the earth's surface into five great zones separated by certain critical values of temperature and precipitation. These five climatic zones were described as dry, tropical rainy, temperate rainy, cold snowy forest, and polar climate. The dry climates were defined on the basis of there being an excess of evaporation over precipitation, which was determined from the mean annual temperature and the mean annual rainfall. The tropical rainy climates were demarcated as climates with a mean temperature of the coolest month of at least 18°C. The polar climates and cold snowy forest were defined with a mean temperature of the warmest month of below 10°C and of the coolest month of below -3°C respectively. Remaining climates were defined as temperate rainy. Each of these climatic groups was further divided into sub-divisions based on differences in the seasonal distribution of temperature and precipitation (Köppen 1931; Köppen and

Geiger, 1939).

Köppen used many different formulae to determine this critical rainfall (R), and finally adopted the relationship (Köppen and Geiger 1928) R = 0.44(T-k) to estimate the value of critical rainfall, where T is mean annual temperature, and k is a constant whose value may be determined by the seasonal concentration of rainfall. Stations having rainfall greater than R were thus categorized as humid group and with rainfall less than R as dry group. Simple values of mean temperature for the coldest or warmest month separate them into different climatic classes.

In spite of the wider acceptance of the Köppen's climatic classification, Trewartha (1943) noted that Köppen's classification was criticized from various points of view (Jones 1932; Ackerman 1941; Jones and Weymouth 1997). Rigid boundary criteria often lead to large discrepancies between climatic subdivisions and features of the natural landscape. Some boundaries were chosen largely keeping natural landscape features in mind (for example, "rainforest"), whilst other boundaries were chosen largely keeping human experience of climatic features in mind (for example, "monsoon"). Trewartha (1943) acknowledges the validity of these criticisms when he writes that "climatic boundaries even when precisely defined are neither better nor worse than the human judgment that selected them, nor the wisdom of those selections is always open to debate". Köppen's climatic classification was, however, subjected to frequent change with revision of boundary limits. Such revisions were made by Köppen himself and by other climatologists as well.

Nearly 50 years contribution of various researchers on climatic classification led to believe that the living world can be categorized into different climatic groups like any other variable quantities. Thornthwaite (1948) presented an entirely new climatic classification based fundamentally on balance between incoming and outgoing heat and moisture at the earth's surface. In this world climatic classification, Thornthwaite considered potential evapotranspiration (PE) as key climatic constituent equal in importance to precipitation (P). Using a simple concept of water balance, the potential evapotranspiration was compared with the precipitation and the periods of moisture deficiency (D) and excess (S) were obtained to express relative moistness or aridity of a climate. Finally, an annual/seasonal moisture adequacy index, I_m, was derived from the following relationships (Eqs.10.19 & 10.20).

$$I_m = \frac{100(S-D)}{PE} \quad \text{(Eq.10.19)}$$

If the soil moisture is assumed to be constant, the equation is simplified to:

$$I_m = \frac{100P}{PE} - 1 \quad \text{(Eq.10.20)}$$

Based on I_m, the earth's climatic system was categorized into nine classes (Table 10.11).

Table 10.11. A rational classification of climate by Thornthwaite (1948)

Sl No.	Climate Class	Class code	Moisture adequacy index, I_m
1	Perhumid	A	100 and above
2	Humid	B_4	80 to 99.9
3	Humid	B_3	60 to 79 9
4	Humid	B_2	40 to 59.9
5	Humid	B_1	20 to 39.9
6	Moist subhumid	C_2	0 to 19.9
7	Dry subhumid	C_1	- 19.9 to 0
8	Semiarid	D	- 39.9 to - 20
9	Arid	E	- 60 to - 40

10.8.2 A New Climatic Classification for Characterization of Regional Drought

Existence and distribution of moisture in the atmosphere plays a key role in description of weather and climate of a region. The water vapour content in the atmosphere is maintained largely by evaporation from the ocean, smaller inland water bodies, moist ground and transpiration from plants and vegetation. There are large variations in the vapour pressure with time and location. Several climatic factors combine in complex manner to influence precipitation over the earth. An estimate of annual precipitation averaged over the entire earth surface amounts to about 1000 mm (Trewartha and Horn 1980). However, precipitation is very unevenly distributed over the earth's surface. Among the terrestrial regions, some deserts receive very little rainfall (< 100 mm) while a few places receive even more than 10000 mm of annual rainfall (Critchfield 1983). In fact, two factors chiefly account for meager precipitation of mid-latitude dry regions: (i) they may be situated in deep interiors of the large continent or separated from the ocean by mountain barrier so that precipitable water is meager (Thornthwaite and Hare 1953), and (ii) geographical differences in the intensity and seasonality of precipitation are the other significant features contributing to its inequitable distribution over the terrestrial regions.

For defining climatic classes in respect of drought characterization, the precipitation over the terrestrial regions is of major concern. Considering the distribution of precipitable moisture in the atmosphere (UNESCO 1978) over the terrestrial regions of the earth, Ponce et al. (2000) estimated global terrestrial mean annual precipitation (P_g) equal to 800 mm. Further, Ponce et al. (2000) concluded that the land area with 800 mm of mean annual rainfall (P_g) may have reasonable scope to practically manage and cope with water scarcity and drought condition and hence it was considered that a region receiving about 800 mm mean annual rainfall falls in the middle of the climatic spectrum. Thus, a value of P_g= 800 mm was preferred as a landmark value in the new climatic classification.

Accordingly, the middle of the climatic spectrum was defined as $P_a/P_g = 1$, where, P_a refers to mean annual rainfall at a given place. Thus, regions with $P_a/P_g < 1$ have less than average moisture. On the other hand, regions with $P_a/P_g > 1$ have more than average moisture. Terrestrial mean annual precipitation varies typically in the range 100–6000+ mm (Baumgartner and Reichel 1975). Thus to depict the relationship of regional drought characteristics (duration, severity and frequency) with climatic parameters, the climatic spectrum was divided into eight regions as shown in *column (2)* in Table 10.12 (Pandey and Ramasastri 2002). The climatic spectrum was further characterized using the ratio of mean annual potential evapotranspiration (E_p) to mean annual precipitation and length of wet season as shown in *column (3) & (4)* in Table 10.12 (Ponce et al. 2000; Pandey and Ramasastri 2002). Also, this classification found in close agreement with other existing classifications given by Bull (1991), Dutt (1986), Stern et al. (1999) and Ponce *et al.(*2000).

Table 10.12. Delineation of climatic regions based on Pa/Pg and E_p/P_a ratio

Sl. No.	Climatic regions	P_a/P_g ratio	E_p/P_a ratio	Length of Wet season *(Month approx)*
	(1)	(2)	(3)	(4)
1	Superarid	$P_a/P_g < 1/8$	$E_p/P_a \geq 30$	< one month
2	Hyperarid	$1/8 \leq P_a/P_g < 1/4$	$30 > E_p/P_a \geq 12$	Nearly one
3	Arid	$1/4 \leq P_a/P_g < 1/2$	$12 > E_p/P_a \geq 5$	Nearly two
4	Semiarid	$1/2 \leq P_a/P_g < 1$	$5 > E_p/P_a \geq 2$	Nearly three
5	Subhumid	$1 \leq P_a/P_g < 2$	$2 > E_p/P_a \geq 3/4$	Nearly four
6	Humid	$2 \leq P_a/P_g < 4$	$3/4 > E_p/P_a \geq 3/8$	Nearly six
7	Hyperhumid	$4 \leq P_a/P_g < 8$	$3/8 > E_p/P_a \geq 3/16$	Nearly eight
8	Superhumid	$P_a/P_g \geq 8$	$E_p/P_a < 3/16$	> 10 months

In view of the Indian conditions, the above classification appeared to be completely justified as high rates of evapotranspiration prevail over arid Rajasthan, in western India, with annual rates exceeding 2000 mm and reaching 2500 mm in some parts of Northwest Rajasthan (Abbi 1974). Low rates of evapotranspiration prevail over humid Assam and the Himalayan Bengal, in northeastern India, with annual rates in the range of 1200 to 1500 mm. Over the central parts of India, which are semiarid to subhumid, evapotranspiration rates vary in the range 1400–1800 mm (Rao et al. 1971; Abbi 1974; Ponce 2000).

Mean annual precipitation and potential evapotranspiration data from Australia also support the values chosen in climatic classification. For instance, in hyperarid William Creek (South Australia), precipitation is 127 mm and potential evapotranspiration is more than 2540 mm. In arid Alice Springs (Northern Territory) precipitation is 250 mm and potential evapotranspiration is 2460 mm. In semiarid/subhumid Perth (Western Australia) precipitation is 890 mm and potential evapotranspiration is 1670 mm. In subhumid Sydney (New South Wales) precipitation is 1200 mm, and evapotranspiration exceeds 1220 mm (Kendrew 1961).

Ponce (1995a) and Ponce et al. (2000) considered that the middle of the climatic spectrum had nearly four months of wet season. The length of the wet season is shortest in arid regions (one month) and longest in humid regions (ten months) (Sinha et al.

1987). Accordingly the average length of wet season for different climatic regions has been incorporated as the third parameter in delineation of climatic regions as given in *column (4)* in Table 10.12.

This type of climatic classification may be particularly useful for characterization of drought in mid-climatic regions where the droughts are quite common and their impacts on the society and environment are more significant. The limits of E_p/Pa across the climatic regions are indicative of general trends, and should not be regarded as exact values separating climatic regions. This classification has been utilized in the study for describing the drought characteristics in different climatic regions of India.

10.8.3 Description of Drought Characteristics in Climatic Regions

The most popular perception of drought is as a "meteorological phenomenon," characterized by lack of rainfall compared to the expected amount over a given period of time. A drought exists when rainfall is below 75% of the long-term mean (Glantz 1994), while others might consider it to occur at or below 60 or 50% of normal. In this study a definition suggested by the India Meteorological Department (IMD) has been used, i.e. "for a given time period (seasonal/yearly), if a meteorological station/division receives total rainfall less than 75 percent of its normal, it is considered as a drought" (National Commission on Agriculture 1976).

The objective of study presented in this Chapter is to describe the relationship of average drought, frequency, intensity and duration with the climatic parameters in arid, semiarid and sub-humid climatic regions in India. The climatic parameters are defined in terms of the ratio of mean annual precipitation (P_a) and mean annual potential evapotranspiration (E_p) and mean annual deficit to P_a. The mean annual deficit is defined as (E_p- P_a). It is believed that the relationships characterizing regional drought frequency, duration, and intensity in terms of E_p/P_a and $(E_p - P_a)/P_a$ may provide an appropriate framework for the systematic analysis of droughts and in the planning of management strategies for coping with drought catastrophe in a given region.

A drought year is one with less than average annual precipitation. A drought event is a series of one or more consecutive drought years. Drought frequency (*F*) pertains to the number of years that it would take a drought of a certain intensity to recur; for instance, once in 10 years. The reciprocal of the frequency is the return period or recurrence interval. In common usage, however, frequency and return period are often used interchangeably, for instance, a frequency of 10 years. Since dry periods are generally followed by corresponding wet periods, it follows that the recurrence interval of drought is always greater than the drought duration. The climatic parameters used in this study refer to mean annual precipitation and mean annual potential evapotranspiration. Since the time unit is a year, the minimum duration of a meteorological drought is one year and the minimum drought return period may be two years.

In the present study, the annual rainfall series for 35–106 years for each of the given stations was analysed using percentage annual rainfall departure from normal (PARD) to identify the drought years and the drought events. Using the definition given by IMD, a meteorological drought year is marked as PARD ≤ -25%. Plots of percentage annual rainfall departure from mean were prepared for identification of drought years and the drought events. The sample plots of PARD for Damoh station in Madhya Pradesh is shown in Figure 10.18.

The average drought return period (T) has been obtained as numbers of years of rainfall records analyzed divided by the number of meteorological drought years. The years for which rainfall records were missing at a given station, were not accounted in the analysis while estimating total number of years of records analyzed for a given station.

Drought intensity (I) ascribes to the magnitude to which actual precipitation is lesser than the mean or a predefined threshold value. Drought intensity (I) may be considered independent of the duration (Dracup et al. 1980b; Sharma 1997a, b). In this study, drought intensity (I), for a given place during a drought year with actual rainfall, P_{id}, and with mean annual rainfall, P_a, has been obtained as follows:

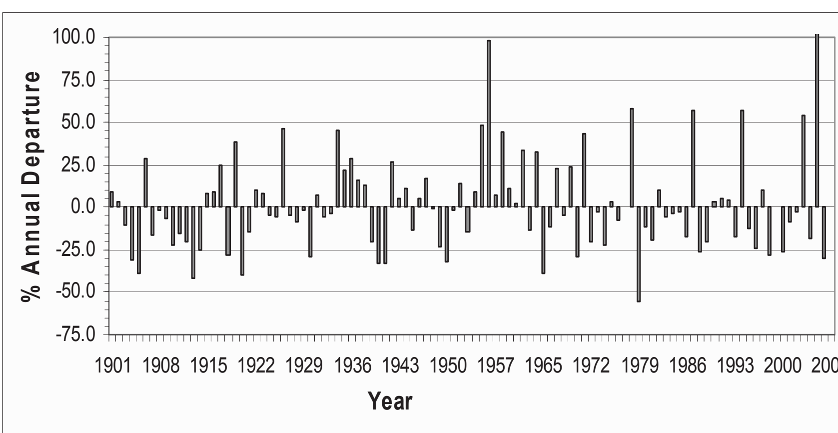

Figure 10.18. Plot of percentage annual rainfall departure from mean for Damoh, Madhya Pradesh

$$I = \frac{p_{id} - p_a}{p_a} \qquad \text{(Eq.10.21)}$$

The precipitation P_{id} in a drought year is always less than P_a at a given place (i.e. $P_{id} < P_a$), and therefore, equation 10.21 estimates the negative values of drought intensity (I). Depending on the magnitude of deficits, Banerji and Chhabra (1963) categorized meteorological drought intensity index, I, in to three classes; Moderate I_m; Severe I_s; and

Extreme I_e. They defined a moderate intensity as -0.25 ≥ I > -0.50, a severe intensity as -0.5 ≥ I > -0.75, and an extreme intensity as I ≤ -0.75. However, it was subsequently realized that this classification of 'I' was very crude and the perception needed further rationalization (National Institute of Hydrology 1990). While studying the applicability of various drought indices in India, Dash (2006) proposed a new classification for I as Mild (CI_{ml}) = -0.25 ≥ I > -0.35; Moderate (CI_m) = -0.35 ≥ I > to -0.45, Severe (CI_s) = -0.45 ≥ I > -0.60, and Extreme (CI_e) I ≤ -0.60. This classification of I has been utilized for further analysis of drought intensity in this study. Out of the total estimated drought events at a given station, over the period of record analyzed, the percent probabilities of occurrence of drought events of different intensity classes were estimated. For the purpose of simplicity in presentation, CI_{ml} and CI_m were combined into a single class, and percent probabilities of occurrence of three major categories (i.e. CI_{ml}-CI_m, CI_s, and CI_e) were computed.

Drought duration (D) may be defined as the period of time when there is a deficiency of precipitation, preceded and followed by periods when there is no deficiency. A meteorological drought can have duration of one or more years. Using the plots of percent annual departure from mean, the number of drought events of different durations (1-, 2-, 3-, 4-, and 5-years) were identified over the period of records analysed for each station. The percent probabilities of occurrence of drought events of different duration out of total events at each station were estimated. The relations of percent probabilities of occurrence of drought events of different durations were thus derived with the E_p/P_a ratio and the ratio of mean annual deficit to mean annual precipitation $\{(E_p - P_a)/P_a\}$.

Regressions have been applied to develop the relationships of the E_p/P_a ratio and the ratio of mean annual deficit to mean annual precipitation $\{(E_p - P_a)/P_a\}$ with (1) the average return period of drought; (2) percent probabilities of occurrence of mild-moderate, severe and extreme intensity droughts; and (3) percentage probabilities of occurrence of droughts of 1-, 2-, 3-, 4-, and 5-years duration. The inferences for drought frequency (F), drought intensity (I) and drought duration (D) have been drawn in relation to the E_p/P_a ratio and $\{(E_p - P_a)/P_a\}$. The results have been compared with the documented experiences in various countries.

Drought severity (S) refers to the accumulated deficit over the period of drought duration. It may be depicted using simple law of multiplication of duration and intensity (i e. S=*I x D*) (Bonacci 1993; Dracup et al. 1980a, b; Sharma 1997b). In other words, if one can predict duration and intensity then the severity can be predicted using simple law of multiplication of duration and intensity.

The annual rainfall records for 110 stations located in different climatic regions of India have been used for establishing relationships between drought characteristics (viz. frequency, intensity and duration) and climatic parameters. To estimate potential evapotranspiration rates, 35 years of daily meteorological data (1965–2002) from various stations were used. Potential evapotranspiration (PET) was estimated using the Penman (1963) method and the results were compared with the data published by the India

Meteorological Department (IMD) (Rao et al. 1971) to assess trustworthiness of the estimates.

Among the 110 selected stations of the country (India), the mean annual rainfall (P_a) ranges from 190 mm at Jaisalmer in Rajasthan to 1628 mm at Madurai in Tamilnadu and the potential evapotranspiration varies from 874 mm in Doda (in J&K) to 2144.6 mm at Jafrabad (in Gujarat). Here, the mid-climatic regions of India are defined as arid, semiarid and subhumid climatic regions. These regions are categorized as the areas which receive mean annual rainfall between 200–400, 400–800 and 800–1600 mm, respectively, and have mean annual potential evapotranspiration/ precipitation ratio (E_p/P_a) as: $5 \leq E_p/P_a < 12$, $2 \leq E_p/P_a < 5$ and $0.75 \leq E_p/P_a < 2$, respectively. These climatic regions have a wet season length of approximately two, three and four months, respectively.

10.8.3.1 Relationship of Drought Frequency with Climatic Parameters

Percentage annual rainfall departures from normal were estimated from long-term annual rainfall series for each of the given stations to identify the drought years and the drought events. The average drought return period for each station was thus computed from the number of years of rainfall records at a given station divided by number of meteorological drought years (i.e. the number of years for which annual rainfall was less than 75% of its mean value). The drought frequency (F) refers to reciprocal of return period (T) (i.e. F = 1/T). Since the ratio of mean annual potential evapotranspiration to mean annual precipitation (E_p/P_a) may never be zero, both power and exponential regression models were applied to relate the E_p/P_a ratio with the average drought frequency (i.e. in terms of return period) (Figure 10.19). The power type regression showed better correlation ($R^2 = 0.68$) than did the logarithmic or exponential type regression. Figure 9.19 shows that the frequency of meteorological droughts has a significant relationship with the Ep/Pa ratio. Average drought frequency (expressed in terms of return period) varies from 2 to 3 years in arid regions (with $12 > E_p/P_a \geq 5$), 3 to 5 years in semiarid regions (with $5 > E_p/P_a \geq 2$), and 5 to 9 years in subhumid regions (with $2 > E_p/P_a \geq 3/4$). In Figure 10.20, the average drought frequency was correlated with the ratio of mean annual deficit to mean annual precipitation. Since the mean annual deficit ($E_p - P_a$) may be zero or less than zero, the relationship between the average drought return period and the ratio of mean annual deficit ($E_p–P_a$) to mean annual precipitation (P_a) was derived using an exponential regression model.

Figure 10.19 reveals that the average return period decreases with increase in the E_p/P_a ratio. In the arid and semiarid regions, it decreases gradually from 2.5 years on an average to 5 years for a long range of E_p/P_a ratio of 2–10. However, in wet sites (sub-humid regions), it increases sharply from 5 years to 9 years for a short range of the E_p/P_a ratio of 0.75–2.0. This may also be seen in Figure 10.20, which clearly indicates that the drought frequency decreases exponentially with the increase of wetness.

In arid regions ($E_p/P_a \geq 5$) the average drought frequency is found to be once in every 2–3 years (Figure 10.19). This indicates that those regions, in which the mean annual potential evapotranspiration is more than five times the amount of mean annual precipitation would experience drought on an average every 2–3 years. In the semiarid regions, the mean annual potential evapotranspiration is two to five times the total amount of mean annual rainfall. In these semiarid areas, where the total annual rainfall is of the order of about half of the local mean annual potential evapotranspiration (i.e. $E_p/P_a \approx 2$), droughts occur once in every 5 years (Figure 10.19). In areas with E_p/P_a ratios between 2.0–3.0 and 3.0–5.0, droughts recur every 4–5 and 3–4 years, respectively (Figure 10.19).

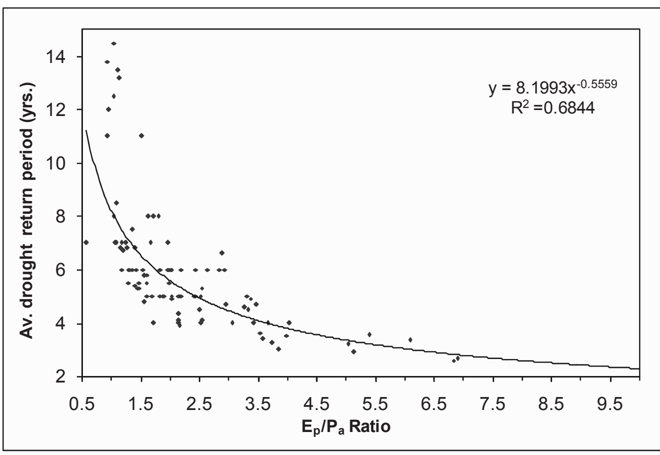

Figure 10.19. Relationship of average drought return period with E_p/P_a ratio

In sub-humid areas ($0.75 \leq E_p/P_a < 2$), the average drought frequency is once in 5–10 years (Figure 10.19). The areas which receive mean annual rainfall nearly equal to their mean annual potential evapotranspiration (i.e. $E_p/P_a \approx 1$) experience drought every 8 years (Figure 10.19). Further, if the area belongs to the further wet side of the climatic spectrum, (i.e. $0.5 \leq E_p/P_a < 1$), the drought frequency is of the order of once in 9–11 years. However, it can also be seen from analysis (Figure 10.19) that a few stations in sub-humid regions, namely, Midnapur and Bankura in West Bengal, Phulbani in Orissa and Belgaum in Karnataka State, whose mean annual rainfall nearly equals the local mean annual potential evapotranspiration, experienced less frequent droughts. The average frequency of drought at these stations was once in every 14, 13, 12 and 11 years, respectively. This typically indicated the possibility of some influence of other physical/regional/morphological factors particularly in respect of the presence of orographic barrier (distance of station from mountains, h_s and from the sea, d_s). It may also be one of the possible reasons restricting the value of correlation coefficient of above relationships to moderately significant (i.e., $R^2 = 0.68$ & 0.59).

In Figure 10.20, the average drought frequency was correlated with the ratio of mean annual deficit to mean annual precipitation ($R^2 \approx 0.56$). Similar to Fig 10.19, Figure 10.20 reveals that the average frequency of drought decreases exponentially with decrease in the ratio of mean annual deficit (E_p–P_a)/mean annual precipitation.

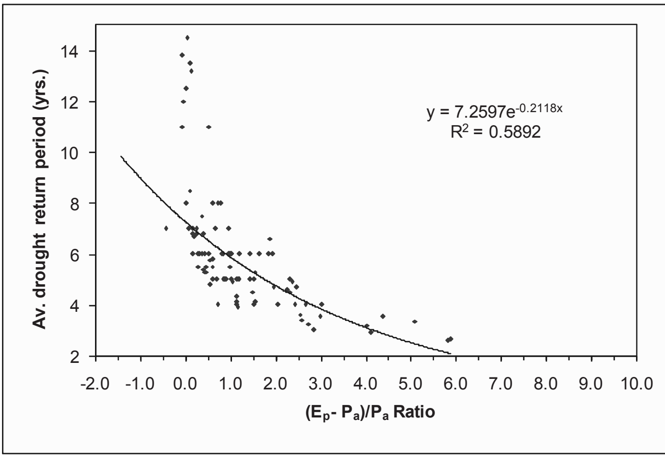

Figure 10.20. Relationship of average drought return period with (E_p–P_a)/P_a ratio

A comparison of the above inferences with drought data and experiences elsewhere (Table 10.13) indicates that the results are rationally comparable. For instance, in Brazil, in Sarido, which belongs to an arid region with $E_p/P_a \approx 5.8$, and in semiarid Caatinga and Saritao, where the E_p/P_a ratio varies from 2.2 to 4.8 (Ponce, 1995a), droughts recur approximately once in every 3 and 5 years, respectively.

However, in sub-humid Agreste and Mata, where the Ep/Pa ratio varies between 1.3 and 2.0 and between 0.7 and 1.1, respectively, the drought conditions occur every 8–12 years on an average (Magalhaes & Magee 1994; Ponce 1995a). For sub-humid climatic regions in the upper midwest United States with mean annual precipitation of about 1500 mm (NOAA 1980), the average return period of drought is reported as approximately 10 years (Klugman, 1978). French (1987) analysed long-term series of annual rainfall for Georgetown in South Australia, where the mean annual rainfall is 475 mm. The records from 1874 to 1985 show 20 drought events, i.e. an average frequency of once in 5.5 years. Swearingen (1994) reported that Morocco, which belongs to the semiarid climatic region (Pa = 400–500 mm), experienced approximately 25 years of drought during the period from 1901 to 1994, i.e. an average drought frequency of once in 3.5 years. Thus, the relationships proposed broadly follow the drought frequency behavior in similar climatic regions in other parts of the world. It is hoped that these relations may be useful for further critical analysis of drought in different climatic regions.

Table 10.13. Summary of some documented drought experiences on drought frequency

Climatic region	Place or location	E_p/P_a	Drought frequency
Arid	1. Kazakhstan in Russia	5.4–6.2 *(Zonn et al. 1994)*	35 severe drought in last 100 yrs. *(Kogan 1997)*
	2. Sarido in Brazil	5.8 *(Ponce 1995a)*	Once in 3 yrs *(Magalhaes and Magee 1994)*
Semi-Arid	1. Ukraine in Russia	2.8 *(Zonn et al.1994)*	Once in 4–5 yrs *(Kogan 1997)*
	2. Caasinga & Saritao in Brazil	3.2–4.8 *(Ponce 1995a)*	Once in 5 yrs *(Magalhaes and Magee 1994)*
	3. Georgetown, in Australia	*3.9 (French 1987)*	Once in 5 years *(French 1987)*
	4. Morocco, Algeria & Tunisia in Africa (NW)	3.8–4.4	Once in 3.5 yrs *(Swearingen 1994)*
Sub-humid	1. Agreste & Mata in Brazil	1.3–2.0 & 0.7–1.1 *(Ponce 1995a)*	Once in 8–12 yrs *(Magalhaes and Magee 1994*; *Ponce,1995a*)
	1. Upper midwest in USA	0.7 –1.2 *(NOAA 1980)*	Once in 10 yrs. *(Klugman 1978)*

10.8.3.2 Relationship of Climatic Parameters with Probability of Occurrence of Meteorological Droughts of Different Intensity

For given drought years, the magnitudes of annual deficits were computed using equation 10.21 to get the intensity of drought in the respective years. Being a percentage, it is purely qualitative and descriptive in nature which is used to express the magnitude (i e. intensity) and severity of drought in terms of rainfall deficiency. Based on the extent of deficit, the droughts of mild, moderate, severe and extreme intensity were identified and their percent probabilities of occurrence estimated. Regressions were applied to exhibit the relationships between the E_p/P_a ratio and probabilities of occurrence of mild-&-moderate, severe and extreme intensity droughts (Figure 10.21). The power type regression showed better correlation ($R^2 = 0.57$) than the logarithmic or exponential type regression. Thus, Figure 10.21 indicates that the intensities of meteorological droughts are evidently related with the E_p/P_a ratio.

Figure 10.21 shows that the probability of occurrence of severe and extreme intensity droughts increases progressively from the sub-humid to arid regions; it however, decreases in the case of mild-moderate intensity drought. For example, an area with the E_p/P_a ratio equal to 1.5 has percent probabilities of occurrence of mild-moderate, severe and extreme intensity droughts as 80%, 18% and 2%, respectively, and for the area with the E_p/P_a ratio as 4.0 these values are 64%, 28% and 7%, respectively. In case of a place in arid region where the E_p/P_a ratio is 7.0 the values are 55%, 35% and 10%, respectively. Thus, the areas located in arid and semiarid climatic regions are likely to suffer relatively more frequent severe and extreme meteorological drought conditions than the areas in sub-humid climatic region. The probability of occurrence of severe droughts is below 18% in the regions with the E_p/P_a ratio less than 1.5. The relationships, shown in Figure 10.21, indicate that the extreme drought events are almost none in the regions with the E_p/P_a ratio less than 1.25. This categorically substantiates that the regions which receive mean annual precipitation in the order of more than 80% of their local mean annual potential evapotranpiration (i.e., $E_p/P_a < 1.25$) are nearly free from the risk of occurrence of extreme drought events. Further, it is also clear from Figure 10.21

that the regions where amount of mean annual rainfall is more than local mean annual potential evapotranpiration (i.e. $E_p/P_a < 1$) the prevalence of severe drought events is rare or negligible. Above discussed pattern of probability of occurrence exhibits that the climatic regions with a lesser E_p/P_a ratio are less vulnerable for intense meteorological droughts. In other words, the climatic regions with less mean annual deficit (E_p-P_a) face less intense droughts, consistent with the work of Lugo and Morris (1982), Gol'tsberg (1972), Gregory (1989), etc. For instance, Magalhaes and Magee (1994) and Ponce (1995a, b) found Agreste (sub-humid) to be affected by drought but not as severely as the Sertao (semiarid) in Brazillian Northeast. Also, the Australian experience shows the droughts to be most serious (i.e., intense) where rainfall ranges between 250 and 750 mm, i.e., in arid and semiarid regions (Kendrew 1961), further supporting the results. Thus, the arid and semiarid climatic regions are more vulnerable to severe and extreme intensity droughts than those of sub-humid climatic regions in India.

10.8.3.3 Relationship of Climatic Parameters with Probability of Occurrence of Meteorological Droughts of Different Duration

Duration of drought is one of the important characteristics, which forms a basis in the planning of strategies to cope with drought for a given region. Drought conditions may continue to prevail for one or more consecutive years. The tendency of drought conditions to prolong for more than one year is termed as drought persistence. For example, an event of drought with duration of two or more years is a persistent drought event. The experiences (reported in literature) show that the droughts have a tendency to last longer in those climatic regions which have greater inter-annual precipitation variability (WMO 1975; Karl 1983; Rasool 1984; Johnson and Kohne 1993). The changes in drought duration across the climatic spectrum point to be regional, rather than local in their nature of persistence (UNESCO-WMO 1985).

In this study, an attempt has been made to relate drought persistence with climatic parameters in the arid, semiarid, and sub-humid climatic regions in India. The drought duration is seen to vary between 1 and 5 years in the different climatic regions. Identified drought events yielded the median duration of a persistent drought as 2 years, and maximum duration of persistent droughts has been 5 years. Relatively, a greater number of persistent drought events are observed in arid and semiarid climatic regions with the E_p/P_a ratio between 3.0 and 10.0. The persistent drought events ($\geq$ 3 yrs. duration) are very few in sub-humid regions.

From the data-spread sheet, it was found that the drought events of 4- and 5-year durations are a few only. Therefore, plots of percent probability of occurrence of droughts for 2- and 3-years duration with the E_p/P_a ratio and $(E_p - P_a)/P_a$ ratio were prepared and presented in Figure 10.22 and 10.23, respectively. The depicted relationships could not lead to significant interpretation as the plots are quite scattered with low values of correlation coefficient. However, it can be expressed that the chances of occurrence of meteorological droughts of more than one year duration are relatively more in arid and semiarid regions.

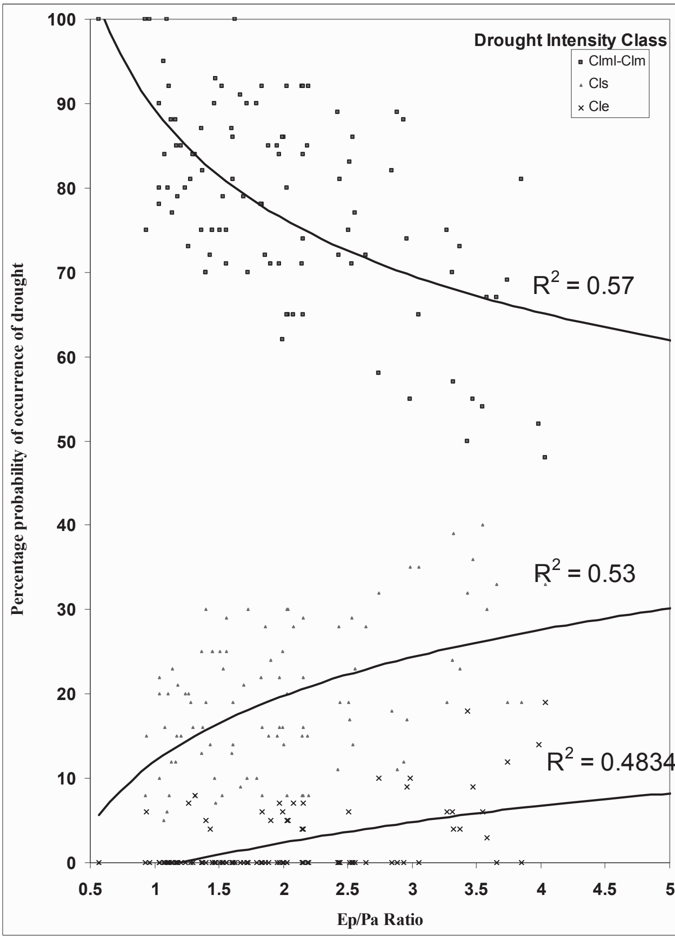

Figure 10.21. Relationship of $(E_p–P_a)/P_a$ ratio with percent probability of occurrence of droughts of different intensity

On examining the spread-sheet of data analyses, it was found that the stations located in the sub humid climatic regions indicate different patterns in respect of drought persistence. However, it was seen that the stations (particularly with the E_p/P_a ratio < 2.0) which are either located close to sea coast (distance < 100 Km from coast) or close to mountain (distance < 100 Km) rarely face persistence drought events of 2 or more than 2 year durations.

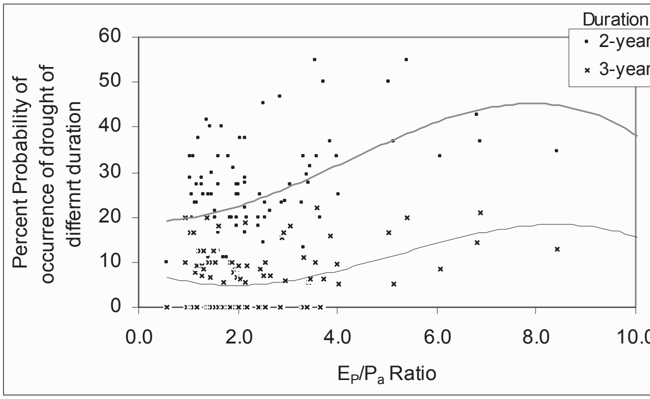

Figure 10.22. Relationship of E_p/P_a ratio with percent probability of occurrence of droughts of 2- and 3-years duration

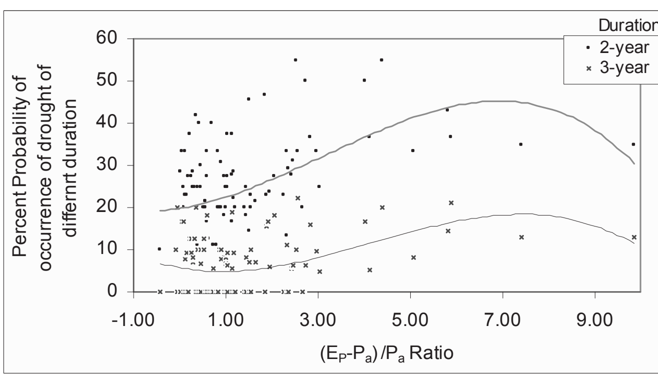

Figure 10.23. Relationship of $(E_p- P_a)/P_a$ ratio with percent probability of occurrence of droughts of 2 and 3 years duration

For the purpose of clarity, the relationship for semiarid and arid regions were derived separately and shown in Figure 10.24. Relatively, a greater probability of occurrence of drought events of two-year duration is found in areas with the E_p/P_a ratio between 4.0 and 6.0. Further, the percent probability of occurrence of persistent drought events of three-year duration is relatively more in areas with the E_p/P_a ratio between 6.0 and 8.0 as compared to the other areas.

Relatively a greater number of persistent drought events are observed in many parts of Rajasthan followed by Gujarat, Karnataka, and Andhra Pradesh. It is also observed that the longest persistent droughts of 5 years duration occurred repeatedly in semiarid and arid climatic regions with the E_p/P_a ratio > 3.0. Few persistent drought events of 5 years duration are also observed in sub-humid climatic regions with the E_p/P_a ratio between 1.20 and 2.0. This broadly supports to the conclusion of Rasool (1984) that

”in semiarid and sub-humid regions, the drought duration can approach as long as 4–5 yrs due to greater inter-annual precipitation variability”. Also, Laird et al. (1996) have documented the evidences of greater drought persistence in the Great Plains of central North America than in any other part of the United States.

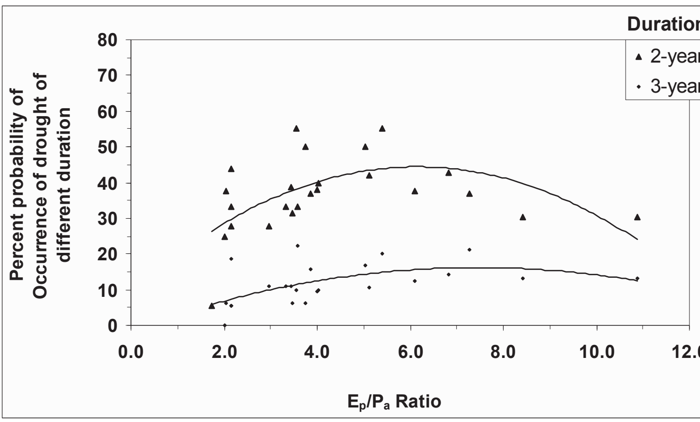

Figure 10.24. Relationship of E_p/P_a ratio with percent probability of occurrence of droughts of 2 and 3 years duration in arid and semi-arid regions

Thus, the above comparison of relationships between drought characteristics and regional climatic parameters (i.e., the E_p/P_a ratio and $(E_p - P_a)/P_a$ ratio), derived using drought data, and experiences documented throughout the world indicate that the results are reasonably acceptable. These relationships can be used as a base for further critical analysis of drought and for planning of drought management strategies for given areas. The work’s strength basically lies in its climatic basis, i.e., its ability to depict regional variability.

10.8.3.4 Influence of Morphological Factors on Drought Characteristics

According to Lana & Burgueno (1998), besides morphological factors orography affects the drought characteristics significantly. In view of this, an attempt was made to assess relevance of drought characteristics with the distance of major orographic barriers (d_h), distance from sea coast (d_s) and elevation of the place from mean sea level (m.s.l.). Multiple regressions were applied to determine significance of these factors in description of frequency, duration, and intensity of meteorological droughts using long-term data for 110 stations. Some influences of elevation could be observed in drought intensity and of distance from sea coast on drought persistence (i.e. duration). However, no specific pattern could be established among them. From the spreadsheet analysis of long-term meteorological drought, it was seen that the stations which are close to the sea, and are situated near some mountains/major hills did not face drought events of severe and extreme intensity (Table 10.14).

Table 10.14. Stations which never faced drought events of severe and extreme intensity

Sl. No.	Station	Ep/Pa	Data length, years	Total No. of drought events	No. of events with duration > 1 yr	No. of events with CI_s & CI_e intensity	Approx. Altitude (w.r.t . msl), m	Distance from sea coast km	Distance from major hill/mountain km
1	Tumkur Karnataka	1.84	77	12	0	0	300	252	150
2	Bangalore Karnataka	1.66	80	11	0	0	1200	280	95
3	Mandya Karnataka	2.0	79	14	0	0	800	195	90
4	Hassan Karnataka	1.62	76	8	1	0	1000	135	50
5	Tirunelveli Tamilnadu	1.96	76	13	1	0	40	52	40
6	Salem Tamilnadu	1.8	78	9	1	0	300	178	12
7	Madurai Tamilnadu	1.03	78	6	0	0	100	98	45
8	Agastheswara Kanyakumari Tamilnadu	1.19	76	9	0	0	30	10	15
9	Belgaum Karnataka	1.10	77	6	1	0	700	90	40
10	Hulsi Maharashtra	0.9	77	9	1	0	1200	114	On hills

It was found from the data that stations which are located at relatively shorter distance from sea and have $P_a \approx E_p$ did not faced persistent droughts of 2 or more consecutive years. Regions with Ep/Pa < 1.2, d_s < 100 km, and d_h < 100 km hardly ever faced persistent droughts or the drought events of severe and extreme intensity. For example, Madurai and Kanyakumai in Tamilnadu (Ep/Pa < 1.2, ds < 100 km and d_h < 100) have respectively experienced 7 and 9 drought events during 1901–2001, but none of them persisted for two or more consecutive years. Further, the stations which are within 100 to 150 km from ocean (100 < d_s < 150) and have close distance (d_h < 100 km) from mountain/major hill seldom faced the drought events of severe and extreme intensity, and also the occurrences of persistent droughts events were very few. Thus, beside the climatic parameters, drought characteristics at a given location are influenced by the distance from sea coast and mountain barrier.

10.9 Summary and Conclusions

Drought and flood has a major impact on human well-being. They affect the environment and the economy we depend on. Drought may, for example, cause losses in crop production, lead to lack of drinking water, hinder waterborne transport, reduce hydropower production and cause forest fires. The impacts are serious and they cause loss of life and especially in developing countries aggravation of poverty and mass migration. Impacts are likely to increase with time as societies' demands for water and environmental services increase.

Floods can also result in huge economic losses due to damage to for example infrastructure, property and agricultural land, and indirect losses in or beyond the flooded areas, such as production losses caused by damaged stock or roads, or the interruption of power generation and navigation. Unfortunately, climate change is expected to intensify the hydrological cycle and both floods and droughts are predicted to become more severe and frequent in the future.

The average drought frequency can be significantly described using dimensionless climatic parameters derived as the ratio of mean annual potential evapotranspiration to mean annual precipitation (E_p/P_a) and the ratio of mean annual deficit to mean annual precipitation ($(E_p - P_a)/P_a$). The frequency and intensity of meteorological droughts have notable relationship with the E_p/P_a ratio. Average drought frequency (i.e. yr^{-1}) is seen to decrease gradually from dry to wet regions, from once in two to three years in the arid regions ($12 > E_p/P_a \geq 5$), three to five years in the semiarid regions ($5 > E_p/P_a \geq 2$) and five to nine years in the sub-humid regions ($2 > E_p/P_a \geq 3/4$). In semiarid to sub-humid regions with the E_p/P_a ratios between 3.5 and 0.5, the drought frequency decreases exponentially with increase in wetness. The relationship obtained between the average drought return period and the ratio of mean annual deficit to mean annual precipitation ($(E_p - P_a)/P_a$) also indicates the drought frequency to increase with increase in mean annual deficit.

The probability of occurrence of a severe or extreme intensity drought increases gradually from wet to dry regions, the case is however reverse for moderate intensity droughts. Thus, it can be concluded that the areas located in arid and semiarid climatic regions are prone to suffer from relatively more intense meteorological droughts than areas in the sub-humid climatic region. The occurrences of severe droughts are much rare in the regions with the E_p/P_a ratio less than 1.2. The extreme drought events are almost unnoticed in the regions with the E_p/P_a ratio less than 1.20. More frequent persistent drought events occur in arid and semi-arid climatic regions compared to other climatic regions. Presence of mountains and ocean in close vicinity influences the drought characteristics in the regions with $P_a \approx E_p$.

The relations presented in this Chapter can be used as a sensible tool for prediction of regional drought characteristics and planning of appropriate drought management strategies for different climatic regions in India. A prerequisite for an adequate assessment and management of the impacts of hydrological hazards, and associated policy-making (pro-active and re-active) is through knowledge on the generation and development of floods and drought. This applies to both current and future conditions, the latter related to climate change adaptation.

10.10 References

Abbi, S. D. S. (1974). "Hydrometeorological studies in India." *Preprints, International Tropical Meteorology Meeting*, American Meteorological Society East African

Metorological Department, *World Meteorological Organization*, January 31–February 7, 1974, Nairobi, Kenya.

Ackerman, E. A. (1941). "The Köppen classification of climates in North America." *Geog. Rev.,* 31, 105–111.

Banerji, S. and Chhabra, B. M. (1963). "Drought conditions in Telangana division (Andhra Pradesh) during the south-west monsoon season." *Indian Journal of Meteorology and Geophysics*, 14(4), 403–415.

Baumgartner, A., and Reichel, E. (1975). "The world water balance." *Mean annual global, continental and maritime precipitation, evaporation, and runoff*. (Editors: Roger G. Barry and Richard J. Chorley) Elsevier, Amsterdam.

Bonacci, O. (1993). "Hydrological identification of drought." *Hydrological Processes*, 7, 249–262.

Bull, W. B. (1991). *Geomorphic response to climatic change*. Oxford University Press, New York.

Central Water Commission, (1982). "Flood Estimation Report for Mahanadi Subzone 3 (d)." *Directorate of Hydrology (Small Catchments)*, New Delhi.

Critchfield, H. J. (1983). "Atmospheric moisture." *General climatology*, Prentice Hall of India Pvt. Ltd., New Delhi, 42–74.

Dash, B. B. (2006). *Objective estimation of drought severity and associated parameters*. Master of Tech. dissertation, Dept. of Water Resources Development and Management, Indian Institute of Technology, Roorkee (India), p. 65.

Dracup, J. A., Lee, K. S., and Paulson, E. G. Jr. (1980a). "On the definition of droughts." *Water Resources Research*, 16(2), 297–302.

Dracup, J. A., Lee K.S. and Paulson E.G. Jr. (1980b). "On the statistical characteristics of drought events." *Water Resources Research*, 16(2), 289–296.

Dutt, D. K. (1986). "Management of ground water under drought conditions." Jal Vigyan Sameeksha, *High Level Technical Committee on Hydrology*, NIH, Roorkee, 111–128.

French, R. J., 1987. "Adaptation and adjustments in drought prone areas: An overview South Australian Study." *Planning for Drought, Toward a Reduction of Societal Vulnerability*, D.A. Wilhite et al., eds., Westview Press, Boulder, Colorado.

Glantz, M. H. (1994). "Drought, desertification and food production." *Drought follows the plow*, M. H. Glantz, (eds.), Cambridge University Press, Cambridge, England, 9–29.

Gol'tsberg, I. A. (1972). "Agroclimatic Atlas of the World." *Hydrometizdat*, 212 p.

IPCC (2001). *Climate Change–2001: The Scientific Basis*. Contribution of Working Group I to the Third Assessment Report of the Intergovernmental Panel on Climate Change–2001 (eds. J.T. Houghton), Published for the Intergovernmental Panel on Climate Change by Cambridge University Press.

IPCC (2007). *Climate Change–2007: Final report on climate change by Intergovernmental Panel*. Published for the Intergovernmental Panel on Climate Change, Cambridge University Press.

Greenwood, J. A., Landwehr, J. M., Matalas, N. C., and Wallis, J. R. (1979). "Probability weighted moments: Definition and relation to parameters of several distributions expressible in inverse form." *Water Resources Research*, 15(5), 1049–1054.

Hosking, J. R. M. (1990). "L-moments: Analysis and estimation of distributions using linear combinations of order statistic." *J. Royal Stat. Soc.,* Series B, 52(2), 105–124.

Hosking, J. R. M. (1991). *Approximations for use in constructing L-moment ratio diagram.* Res. Report RC 16635, IBM Research Division, Yorktown Heights, NY 10598.

Hosking, J. R. M., and Wallis, J. R. (1993). "Some statistics useful in regional frequency analysis." *Water Resources Research*, 29(2), 271–281.

Hosking, J. R. M., and Wallis, J. R. (1997). *Regional frequency analysis-an approach based on L-moments*. Cambridge University Press, New York.

Johnson, W. K., and Kohne, R. W. (1993). "Susceptibility of reservoirs to drought using Palmer Index." *ASCE Journal of Water Resources Planning and Management*, 119(3), 367–387.

Jones, S. B. (1932). "Classifications of North American climates." *Econ. Geog.,* 8, 205–208.

Jones, D., and Weymouth, G. (1997). *An Australian monthly rainfall dataset*. Technical Report 70, *Bur. Meteor.,* Australia. Pp. 19.

Kaczmarek, Z.D., Jurak, and Napioekowski, J. J. (1997). *Impact of climate change on water resources in Poland*. Publication of Institute of Geophysics, Polish Academy of Science, E–1(295), p. 51.

Karl, T. R. (1983). "Some spatial characteristics of drought duration in the United States." *Journal of Climate and Applied Meteorology*, 22(8), 1356–1366.

Kendrew, W. G. (1961). *The climates of the continents. Oxford University Press*, London, England.

Klugman, M. R. (1978). "Drought in the Upper Midwest, 1931–1969." *Journal of Applied Meteorology*, 17(10), 1425–1431.

Kogan, F. N. (1995). "Droughts of the late 1980s in the United States as derived from NOAA polarorbiting satellite data." Bulletin of the American Meteorological Society, 76(5), 655–668.

Kogan, F. N. (1997). "Global drought watch from space." *Journal of the American Meteorological Society*, 78(4), 621–636.

Köppen, W. (1931). *Klimakarte der Erde*. *Grundriss der Klimakunde*, 2nd Ed., Berlin and Leipzig.

Köppen, W. and Geiger R. (1928). *Klimakarte der Erde, Wall-map 150 cm x 200 cm*. *Verlag Justus Perthes*, Gotha.

Köppen, W. and Geiger R. (1939). *Handbuch der Klimatologie*. 5 Vols., Berlin.

Kumar, R., and Chatterjee, C. (2005). "Regional flood frequency analysis using L-moments for North Brahmaputra Region of India." *J. Hydrologic Engineering*, ASCE, 10(1), 1–7.

Kundzewicz, Z. W., and Kaczmarek, Z. ((2000). "Copping with hydrological extremes." *Jour. of Water International,* 15(1), 66–75.

Laird, K. R., Fritz S. C., Maasch K. A., and Cumming B. F. (1996). "Greater drought intensity and frequency before AD 1200 in the Northern Great Plains, USA." *Nature*, 384(12), 552–554.

Lana, X., and Burgueno, A. (1998). “Spatial and temporal characterization of annual extreme droughts in Catalona (North Spain).” *International Journal of Climatology*, 18, 93–110.
Lugo, A. E., and Morris, G. L. (1982). “Los sistemas ecologicos y la humanidad (The ecological systems and humanity).” Organizacion de los Estados Americanos, Monografia No. 32, Washington, D.C. (in Spanish).
L’vovich, M. I. (1979). “World water resources and their future.” *American Geophysical Union,* Translated from the Russian edition, 1974.
Magalhaes, A., and Magee, P. (1994). “The Brazilian Nordeste (Northeast).” In: *Drought Follows the Plow* (ed. by M. H. Glantz), Cambridge University Press, Cambridge, UK., pp.59–76.
Merz, R., and Bloschl, G. (2005). “Flood frequency regionalization–spatial proximity vs. catchment attributes.” *Journal of Hydrology*, 302, 283–306.
National Commission on Agriculture (1976). *Climate and agriculture-Part IV.* Govt. of India, Ministry of Agriculture and Irrigation, New Delhi.
NOAA, (1980). *Climates of the States*. National Oceanic and Atmospheric Administration, Volume 1: Alabama North Dakota, Vol. 2, Ohio Wyoming, Gale Research Co., Detroit, Michigan.
Pandey, R. P. and K. S. Ramasastri (2002), “Incidence of droughts in different climatic regions”. *Hydrological Sciences*, *IAHS*, August especial issue 47(S), S31-S40.
Pandey, R. P. and K. S. Ramasastri (2001), ”Relationship between the common climatic parameters and average drought frequency”. *Hydrological Processes*, 15(6), 1019-1032.
Pandey R. P., Dash, B. B., Mishra, S. K., and Singh, R. (2008). “Study of indices for characterization of drought in KBK Districts in Orissa (INDIA).” *Journal of Hydrological Processes*, 22 (12), 1895–1907.
Penman, H. L. (1963). “Vegetation and hydrology.” Tech. comm. no. 53, *commonwealth Bureau of soils*, Harpenden, Eng., p. 125.
Pilgrim, D. H., and Cordery, I. (1992). “Flood runoff”. In *Handbook of Hydrology*. Mc Graw-Hill, Inc, New York.
Ponce, V. M. (1995a). “Management of droughts and floods in the semiarid Brazilian Northeast-The case for conservation.” *Jour. of Soil and Water Conservation*, 50(5), 422–431.
Ponce, V. M. (1995b). “Hydrologic and environmental impact of the Parana Paraguay waterway on the Pantanal of Mato Grosso, Brazil: A reference study.” San Diego State University, Department of Civil and Environmental Engineering, p. 124.
Ponce, V. M., Pandey R. P., and Sezan E. (2000). “Characterization of drought across climatic spectrum.” *Journal of Hydrologic Engineering*, ASCE, 5(2), 222–224.
Rao, K. N., George C. J., and Ramasastri K. S. (1971). *Potential evapotranspiration over India*. IMD Scientific Report No. 136, Meteorological Office, Pune-5.
Rasool, S. I. (1984). “On dynamics of deserts and climate.” Chapter 7 in: *The Global Climate*, J. T. Houghton, ed., Cambridge University Press, Cambridge, England, 107p.
Sharma, T. C. (1997a). “A drought frequency formula.” *Hydrological sciences Journal*, 42(6), 803–814.

Sharma, T. C. (1997b). “Estimation of drought severity on independent and dependent hydrologic series.” *Water Resources Management*, 11(1), 35–49.

Sinha, S. K., Kailasanathan K., and Vasistha A. K. (1987). “Drought management in India: Steps toward eliminating famines.” *Planning for Drought, Toward a Reduction of Societal Vulnerability*, Chapter 27, *Wilhite*, *D.A.*, and Easterling W.E. eds., *Westview Press*, Boulders Colorado.

Stedinger, J. R., Vogel, R. M., and Foufoula-Georgiou, E. (1992). “Frequency analysis of extreme events.” Chapter 18 in: *Handbook of Hydrology*, D. R. Maidment (ed.), McGraw-Hill, Inc., New York.

Stern, H., de H. G., and Ernst J. (1999). “Objective classification of Australian climates.” 8th Conf. on Aviation, Range and Aerospace Meteorology, Amer. Meteor. Soc., Dallas, Texas, 10–15.

Swearingen, W. (1994). *Northwest Africa. Drought follows the plow*. M. H. Glantz, (eds.), Cambridge University Press, Cambridge, England, 117–134.

Thornthwaite, C. W. (1948). “An approach toward a rational classification of climate.” *The Geographical Review,* 38, 55–94.

Thornthwaite, C.W., and Hare F. K. (1953). “Climatic Classification in Forestry.” *FAO Corporate Document Repository Unasylva*, 9(2), 1–17. Available at <http:// www. fao,org/docrep/x5375e/5375202.htm> (accessed Feb. 2012).

Trewartha, G. T. (1943). *An introduction to weather and climate*. *McGraw-Hill*, p. 545.

Trewartha, G.T., and Horn L. H. (1980). “Atmospheric moisture and precipitation.” *An Introduction to Climate* (5^{th} Ed.). *McGraw Hills Book Company*, New York, pp. 41–232.

UNESCO (1978). *World water balance and water resources of the earth*. Unesco Press, Paris, France.

UNESCO-WMO (1985). *Hydrological aspects of drought*. A contribution to the International Hydrological Programme, M. A. Beran and J. A. Rodier. rapporteurs, Paris, France.

Wilhite D. A. 2000. “Drought as a natural hazard: Concept and definition.” Chapter 1 in *Drought: A Global assessment, Natural Hazards and Disaster Series*, Vol. 1, Wilhite Donalt A (eds.), Routledge Publisher, UK.

WMO (1975). “Drought and agriculture.” Technical Note No. 138, *World Meteorological Organization* No. 392, Geneva, Switzerland.

Zafirakou-Koulouris, A., Vogel, R. M., Craig, S. M., and Habermeier, J. (1998). “L moment diagrams for censored observations.” *Water Resources Research*, 34(5), 1241–1249.

Zonn, I., Glantz M. H., and Rubinstein A. (1994). “The Virgin lands scheme in the former Soviet Union.” in *Drought follows the plow*, M. H. Glantz, (ed.), Cambridge University Press, Cambridge, England, pp.135–150.

CHAPTER 11

Modelling the Impact of Climate Change on Water Systems and Implications for Decision-Makers

Adebayo J. Adeloye, Najmur R. Nawaz and Timothy J. Bellerby

11.1 Introduction

Each year, weather-related disasters cost the global economy tens of billions of dollars, and the damage appears to be increasing. Planners and decision-makers responsible for designing protection measures to guard against the threat of severe floods and droughts appear to be having a difficult time. With record-breaking events occurring more frequently, the planner is rightly concerned about the validity of existing design procedures. Planners across the world have started to incorporate climate change into the design process. However, the lack of consensus among the climate modeling community, especially in regard to future regional precipitation changes makes informed decision-making impossible and is unhelpful to develop and operate robust flood and drought protection facilities and infrastructures.

Since the start of the new millennium, extreme climatic events with severity not witnessed in living memory have brought misery to millions across the world. The well-publicised summer 2010 floods in both China and Pakistan that affected over a hundred million people provide just one example of the scale of destruction brought about by climatic extremes. The current droughts ravaging the Horn of Africa and resulting in numerous deaths among displaced communities and their herds in Somalia and Kenya, and the attendant catastrophic crop failures provide a further example of the impacts of climate change and climate variability.

Many planners now realize that the traditional approach to design protection measures, based on the assumption of stationarity, is no longer valid due to climate change. However, the uncertainty associated with climate change itself means that planners and decision-makers may have little confidence in the published guidance for incorporating climate change into the design process.

Thus, although central to good long-term decision making are reliable climate change projections and decades of climate modeling research has meant that the decision-maker is not short of information to aid the planning process, there are still numerous challenges to be overcome before confidence can be had in the information. These challenges arise from the limits of predictability of climate; the complexity of climate modelling for impacts assessment; and the difficulties caused by climate change prediction uncertainties.

11.2 Limits of Predictability of Climate

Whilst climate scientists tackle with one of the most complex problems, decision-makers and practitioners often fail to realize that the scientists are not in possession of a crystal ball. The underlying tool used as a basis for simulating future climate, the climate model, is far from perfect. Models can provide likely future *projections* but certainly nothing approaching a *prediction*. An example of the difficulties in producing reliable climate forecasts is provided by the infamous seasonal forecast by the UK Meteorological Office climate model for 2009. Forecasts indicated that warmer than average summer ('barbecue summer') and winter were to be expected[1]. In reality, the 2009 British summer was disappointingly wet whilst the 2009/2010 winter turned out to be one of the coldest for decades. Understandably, the UK Met Office has since decided to abandon its long-range seasonal forecasts.

Despite climate model limitations, it would appear that decision-makers are often willing to put blind trust in climate model output, usually in the guise of smooth curves indicating a gradual change in climate. As noted by the eminent environmentalist, James Lovelock, history tells us that climate change does not occur as smoothly as models would suggest. The earth's emergence from the last ice age 14000–15000 years ago, in a series of warm and cold periods, is testimony to the unpredictable way in which eventual warming can take place. Indeed, such unpredictability is being observed currently in the northern hemisphere as it experiences a relatively cool decade of 2000–2010. It is therefore likely that, contrary to climate model simulations, eventual warming of the planet will happen in a series of dips, slides and jumps.

This view is echoed to some extent by the Princeton physicist, Freeman Dyson[2], who argues that "*The (climate) models solve the equations of fluid dynamics and do a very good job of describing the fluid motions of the atmosphere and the oceans. They do a very poor job of describing the clouds, the dust, the chemistry and the biology of fields, farms and forests. They do not begin to describe the real world that we live in*."

11.3 Complexity of Climate Modelling for Impacts Assessment

Climate modelling has made great advances in the last few decades, helped in part by the exponential growth in computing power that has increased by a factor of

[1] http://www.metoffice.gov.uk/corporate/pressoffice/2009/pr20090430.html
[2] http://www.canada.com/nationalpost/news/story.html?id=985641c9-8594-43c2-802d-947d65555e8e

approximately one million between the 1970s and the new millennium (Le Treut et al. 2007). This has enabled advances to be made on a number of fronts including incorporation of an increasing number of processes (see Figure 11.1), increased simulation length and finer spatial and temporal resolutions. The earliest work on climate change was based on atmospheric general circulation models coupled to simple 'slab' ocean models which did not account for ocean dynamics (e.g. Manabe and Wetherald 1975). A typical model in the 1970s divided the world up into boxes 600 km across with five levels to represent all the vertical structure. They were used to predict changes on timescales of months up to a year or so.

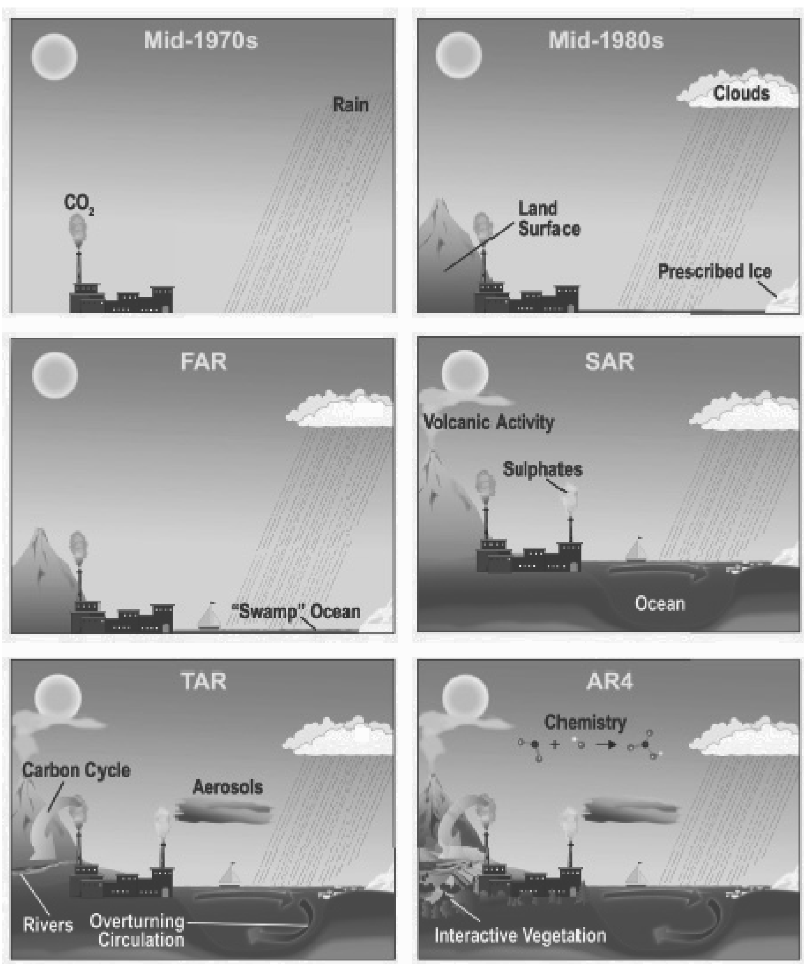

Figure 11.1. Increasing level of climate model complexity since the mid-1970s (source: Le Treut et al. 2007)

Such models were used to analyse changes in the equilibrium climate resulting from a doubling of concentrations of atmospheric CO_2. The climate models of today are much more complex and include fully coupled clouds, oceans, land surfaces and aerosols, etc. Some models such as the UK Hadley Centre HadGEM1 (Martin et al. 2006) are beginning to include detailed chemistry and the carbon cycle. Model resolution is also much improved in the HadGEM1 which uses 135 km boxes with 38 levels in the vertical.

However, model complexity does not necessarily lead to more accurate climate projections. As pointed out by Nof (2008), a theme that is frequently encountered is the sense that the resolution of modern state-of the-art global climate models is so high that—when compared with simple models—their results represent the "absolute truth." This statement has highlighted the fact that although genuine efforts are being done to improve various aspects of numerical modelling of climate, a point often forgotten is that they are still models with their inherent uncertainties and thus cannot substitute for observational data.

Dessai and Hulme (2008) state that national climate scenarios are increasingly being used in long-term strategic planning and decision-making, but their projections have rarely been compared with observations. In their study, the authors evaluated output from four generations of UK climate change scenarios developed between 1991 and 2002 by comparing model temperature and precipitation series with that observed in the UK from 1659 and 1766, respectively. They found that the greatest ambiguity was in summer precipitation simulation which is of concern since it is precipitation which is a significant driver of water systems being considered (e.g. water supply reservoirs).

11.4 Decision-Making under Climate Change Uncertainty

The climate impacts community may conveniently be categorised into two groups; one group is interested in assessing the effects of climate impact uncertainty whilst the other is primarily focused on using the highest resolution output in impacts assessments. The former usually involves use of several different models to produce climate projections for a given time period, whilst the latter often results in use of lengthy climate durations of a single projection for each greenhouse gas emissions scenario. Model resolution has received much coverage in the literature and this has had the effect on planners that an impacts study is somehow invalid without use of a high resolution modelling such as a regional climate model, or some other method to achieve the greater resolution, such as statistical downscaling. Clearly, planners would be best served through a case by case approach; coarse resolution climate model output will be of little use for an impacts assessment in a mountainous catchment, whilst its application in relatively large flat basins with little spatial rainfall variability would be entirely appropriate. Data availability should also dictate the adopted approach. High resolution observational data often needed to accompany high resolution climate modelling, something lacking in many developing countries.

Given some of the above discussion on climate model limitations, decision-makers may be best served by placing greater emphasis on climate model uncertainty than resolution.

Probabilistic climate change scenarios have recently emerged as offering the decision-maker with information to make his or her job easier. The extensive set of scenarios developed by the UK Climate Impacts Programmes (Murphy et al. 2009) is reported to be amongst the first probabilistic scenarios available to decision makers. The basis for such scenarios is the assumption that certain climate models are more reliable than others and therefore there is a greater likelihood of their projections with such models being realised. However, before adopting such scenarios for planning, it is useful to be aware of the rather significant limitation. Confidence established in a particular climate model owing to its success in simulating observed climate may not guarantee its validity under future conditions. As pointed out by Reifen and Toumi (2009), *"there is no evidence of future prediction skill delivered by past performance-based model selection."*

Given some of the limitations of climate models identified above, how then should the planner go about making decisions? A combination of two approaches is one possible solution. The first approach entails a series of what-if scenarios, allowing performance of existing and proposed water systems to be assessed in terms of specified changes in climate. The second approach is based on the application of stochastic hydrology to account for observed trend in data records. This combined, or hybrid approach has the advantage of placing greater emphasis on the observational records. This is appropriate given that the signals of global warming should now begin to manifest themselves in hydrologic records.

In light of the preceding discussion, it is useful to draw up a list of issues that a prudent planner should consider to enable good decision-making:

1. Despite all the uncertainties surrounding future climate, there is general consensus that global warming will lead to an intensification of the hydrological cycle and weather extremes.
2. Climate models are best able to provide an estimate of future average global temperature for a given greenhouse gas emissions scenario.
3. Climate models are very poor at simulating small-scale precipitation.
4. It is impossible for climate models to *forecast* future climate. Time-series plots of future climate are therefore entirely misleading. It is more meaningful if output is presented as 30 year averages for instance.
5. Use of high spatial resolution climate model output might not be suitable under all situations.
6. Probabilistic climate change scenarios have recently emerged as an aid to the decision-maker; however, these should be approached with caution.

In the next sections, two case studies are presented that demonstrate approaches to climate impacts assessment.

11.5 Case Study 1: Climate Change Impact on Reservoir Yield in Yorkshire, UK

11.5.1 Introduction

The reservoirs are located in Yorkshire, northeast England and consist of three direct catchments namely Hebden, Luddenden, and Ogden. Hebden (which comprises three sub-catchments; Gorple, Widdop and Walshaw Dean) is the largest of the catchments with a total area of 26.43 km^2. Luddenden is much smaller with an area of 6.46 km^2, and Ogden is the smallest of the three (5.39 km^2). These catchments are located between 53° 41’ and 53° 50’ northern latitude, and 1° 53’ and 2° 10’ western longitude as shown in Figure 11.2.

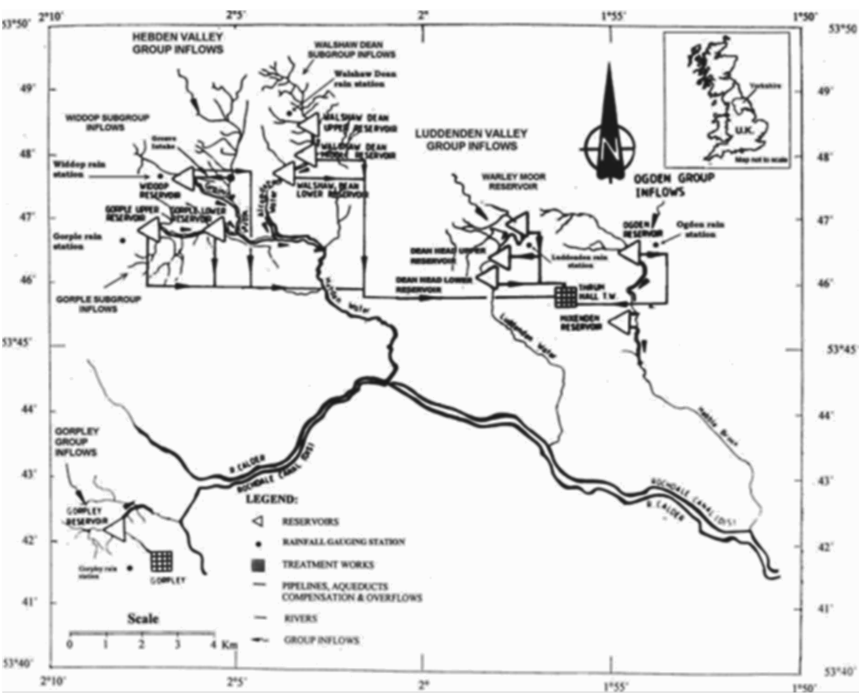

Figure 11.2. The Yorkshire catchments

Although there are 11 inter-linked reservoirs in the system, they were simplified into five stand-alone systems for the purpose of the analysis-Gorple, Widdop, Walshaw Dean, Luddenden, and Ogden–as shown in Figure 11.3. Daily baseline (1961–1990) data of precipitation and runoff were made available by Yorkshire Water Services Ltd (YWS) for the analysis.

11.5.2 Climate Change Scenarios

There are a number of GCMs available for use in climate impacts assessments; the selection of appropriate models will be dictated by the ease of GCM data access and whether the required climatological variables are available.

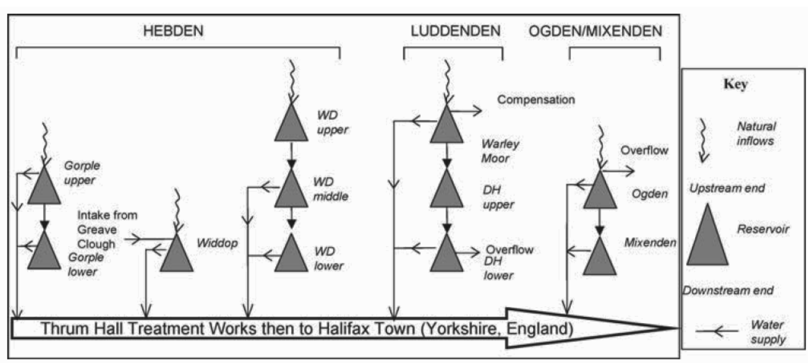

Figure 11.3. Yorkshire catchments schematic

The IPCC recommends several GCMs for impact assessments (Kundzewicz 2007). Given time constraints, for this investigation it was decided to apply the results from three of these:

(i) CGCM1–Canadian first generation coupled general circulation model (Boer et al. 2000);

(ii) CSIRO1 (also known as CSIRO-mk2b)–Australian Commonwealth Scientific and Industrial Research Organisation, first generation atmosphere-ocean coupled GCM (Hirst et al. 2000);

(iii) HadCM3–UK Hadley Centre for Climate Prediction and Research Coupled Model no. 3 (Gordon et al. 2000).

Since GCM output is at a relatively coarse spatial scale, temperature, radiation and precipitation were downscaled to the catchment scale using the linear interpolation approach described by von Storch et al. (1993). The interpolation was carried out on the basis of linear averaging of the inverse of distance between the catchment and the four GCM grid points surrounding it as follows (see also Smith et al. 1992):

$$VAR_D = \frac{\sum^{i}\left(\frac{1}{D_i^s}\right)VAR_i}{\sum\left(\frac{1}{D_i^s}\right)} \qquad \text{(Eq. 11.1)}$$

where VAR_i is the value for the variable (temperature, radiation, precipitation) at grid point i; D_i^s is the distance from the site to the GCM grid point i; and VAR_D is the downscaled variable.

The advantage of the simple approach in equation (1) is that it allows regional climate change scenarios to be defined that would otherwise be difficult or costly to obtain. Besides, other more sophisticated downscaling schemes such as statistical downscaling have been shown to be characterised by huge uncertainties (Wilby and Wigley 1997). It was felt that the use of the simple linear downscaling would remove the extra dimension of uncertainty. .

In general as shown in Table 11.1 which contains the root mean square (rms) error estimates, CSIRO1 appears to be reproducing the observed baseline solar radiation most adequately. Observed temperature is being modeled well by HadCM3 while CGCM1 is performing most adequately in reproducing observed precipitation

Table 11.1. RMS difference between observed and GCM-simulated climatological variables

GCM	**Radiation (w/m^2)**	**Temperature (^oC)**	**Precipitation (mm)**
HadCM3	94	3	140
CSIRO1	59	8	112
CGCM1	153	11	50

Scenarios representative of the climate in the 2020s (2010–39), 2050s (2040–69) and 2080s (2070–99) compared to the baseline (1961–1990) were used. The complete range of climate change scenarios expressed as absolute monthly changes in temperature, net solar radiation and precipitation from the baseline are provided in Tables 11.2–11.4.

Table 11.2. Absolute changes (from baseline) in monthly mean temperature (^oC)

Scenario	**Jan**	**Feb**	**Mar**	**Apr**	**May**	**Jun**	**Jul**	**Aug**	**Sep**	**Oct**	**Nov**	**Dec**
C2	0.3	0.5	0.2	0.3	0.5	0.8	1.1	0.8	0.7	0.9	0.4	0.5
C5	0.6	0.7	0.4	0.5	0.8	1.6	1.9	1.4	1.5	1.4	0.9	0.9
C8	1.4	1.1	1.0	1.1	1.5	2.1	2.6	2.7	2.6	2.3	1.5	1.5
A2	0.4	0.7	0.9	0.8	1.2	1.0	1.0	0.9	0.9	1.3	0.7	0.9
A5	0.7	0.9	1.4	1.5	1.8	1.6	1.7	1.6	1.6	1.8	1.6	1.3
A8	1.2	1.3	1.7	2.0	2.6	2.1	2.3	2.3	2.5	2.4	2.3	1.8
H2	0.7	0.8	0.7	0.7	0.7	0.9	0.9	1.2	0.9	0.9	0.6	0.2
H5	1.9	1.4	1.3	1.2	1.7	1.8	1.8	2.5	2.3	2.0	1.0	1.2
Baseline	*2.7*	*2.6*	*4.3*	*6.5*	*9.9*	*12.9*	*14.6*	*14.3*	*12.3*	*9.4*	*5.4*	*3.6*

C: CGCM1, A: CSIRO1, H: HadCM3, 2: 2010–39, 5: 2040–69, 8: 2070–99

11.5.3 Applying the Scenarios

It is usually straightforward to perturb baseline climate using a 'simple perturbation' approach in which mean monthly climatic change scenarios are applied to scale the baseline climate. However, a limitation of such an approach is that the temporal structure (such as length of dry periods and inter-annual variability) of the perturbed records will be the same as the historic record; only the mean will change. This is certainly not useful for water resources assessment applications where the variability of the runoff and rainfall is more important in determining the outcome than the mean. To overcome this limitation, the Long Ashton Research Station Weather Generator (LARS-WG) (Racsko et al. 1991) was used to generate climate-perturbed data series which does not suffer from this limitation. LARS-WG uses observed daily precipitation, minimum temperature, maximum temperature, and net solar radiation to simulate data. To drive the model, parameters such as the mean and variance of the various processes were estimated based on the baseline data. Additionally, for rainfall, the probability of wet and dry days, and the inter-event duration were also required and these were also obtained from the baseline data. With the parameters determined, the LARS-WG was used to simulate the baseline climate in order to assess its efficacy. Table 11.5 is a comparison of the average monthly precipitation between the observed baseline climate and that simulated by LARS-WG, averaged over the three reservoir catchments–Hebden, Luddenden and Ogden. As table 5 reveals, the performance of the LARS-WG in reproducing the historic rainfall is very satisfactory, with a maximum absolute error of less than 10%.

Table 11.3. Absolute changes (from baseline) in monthly mean net solar radiation (w/m^2)

Scenario	**Jan**	**Feb**	**Mar**	**Apr**	**May**	**Jun**	**Jul**	**Aug**	**Sep**	**Oct**	**Nov**	**Dec**
C2	0.5	-2.3	-10.4	5.8	20.9	1.2	13.4	5.6	3.5	6.4	3.7	0.9
C5	0.4	-2.4	-10.3	1.4	21.7	5.1	-4.9	-7.6	0.1	7.5	3.6	1.6
C8	-0.2	1.3	-6.5	8.2	16.3	18.6	-13.2	-10.1	0.6	5.5	5.3	1.1
A2	1.0	-1.2	-5.0	7.8	13.6	7.7	4.6	-8.9	-6.9	1.3	1.4	-0.6
A5	1.7	3.0	-9.2	-1.2	13.5	27.2	5.7	-3.4	-4.8	-0.9	-0.3	-0.8
A8	-0.1	2.8	-11.9	5.4	-4.5	24.2	-7.3	-3.3	-6.6	2.4	-4.0	-0.6
H2	-2.5	-0.4	-7.7	-5.6	8.3	21.9	8.6	4.1	11.7	3.1	2.8	-1.3
H5	-3.9	0.8	-5.0	7.1	11.4	13.7	22.8	15.0	30.7	6.3	3.3	-2.3
H8	-2.6	-2.6	-0.1	5.8	12.1	15.8	28.9	15.3	31.0	4.1	0.3	-0.5
Baseline	*51.2*	*108.2*	*224.5*	*338.3*	*455.7*	*492.7*	*485.3*	*394.4*	*261.3*	*153.9*	*67.9*	*35.4*

C: CGCM1, A: CSIRO1, H: HadCM3, 2: 2010–39, 5: 2040–69, 8: 2070–99

Table 11.4. Absolute changes in monthly mean precipitation (mm)

Scenario	Jan	Feb	Mar	Apr	May	Jun	Jul	Aug	Sep	Oct	Nov	Dec
C2	-5.0	19.0	33.3	2.1	-20.5	-4.6	-14.9	-6.8	-12.3	-21.1	-7.5	5.5
C5	16.8	21.8	42.2	-2.1	-13.5	-13.9	9.1	8.0	-4.0	-29.2	2.9	10.3
C8	33.2	17.0	46.9	6.9	-8.9	-25.7	11.3	5.5	-1.4	-7.5	-6.5	7.3
A2	-2.0	27.1	28.9	3.3	7.4	7.0	9.1	18.6	16.3	-17.8	6.6	33.4
A5	-14.7	6.5	35.7	17.7	7.4	-5.2	4.8	17.4	12.1	-2.5	14.2	33.5
A8	18.0	7.3	52.7	17.5	30.2	-19.1	11.1	18.0	8.2	7.1	58.0	43.0
H2	11.5	-14.4	1.4	3.3	0.7	-30.0	-26.6	-21.6	-11.9	-7.4	8.6	16.1
H5	37.8	1.8	22.3	-8.6	-20.2	-29.8	-44.8	-59.8	-60.3	5.8	-4.8	50.3
H8	48.1	13.7	10.9	6.0	-9.4	-32.6	-53.2	-55.6	-46.7	12.9	18.6	36.3
Baseline	*136.1*	*98.2*	*112.7*	*93.1*	*83.8*	*85.7*	*83.7*	*113.8*	*115.4*	*130.7*	*137.9*	*146.4*

C: CGCM1, A: CSIRO1, H: HadCM3, 2: 2010–39, 5: 2040–69, 8: 2070–99

With the satisfactory performance of LARS-WG over the historic sequence established, the next step was to use the model to generate future climate data. First, the daily GCM data were used to calculate 2010–39, 2040–69 & 2070–99 changes (from baseline) in precipitation intensity, duration, probability of wet and dry days and temperature means and variances. These changes were then applied to perturb the LARS-WG parameters previously calculated from the observed daily data. The perturbed parameters were then used to generate 30 years of daily data for the three GCMs and the three time slices (2010–39, 2040–69 & 2070–99). A new sequence of daily climatic variables (temperature, radiation and precipitation) representing the future was thus produced.

Table 11.5. Comparison of observed and LARS-WG simulated precipitation

Month	Observed	Simulated	Difference
Jan	129.8	135	-4.0
Feb	95.4	96.4	-1.0
Mar	111.6	110.2	1.3
Apr	88.8	89.8	-1.1
May	84	78.6	6.4
Jun	84.2	83.4	1.0
Jul	79.6	79.8	-0.3
Aug	109	106	2.8
Sep	113	117.2	-3.7
Oct	127	138.2	-8.8
Nov	133.6	133.8	-0.1
Dec	138.4	137.2	0.9

11.5.4 Hydrological Modelling

The hydrologic modelling used the daily water balance model MODHYDROLOG (Chiew and McMahon 1994). MODHYDROLOG is a conceptual daily rainfall-runoff model structured around five moisture stores that are inter-related by catchment processes as shown in Figure 11.4.

A detailed description of MODHYDROLOG is provided by Chiew and McMahon (1994). The model requires daily precipitation and potential evapotranspiration as input and simulates groundwater recharge in addition to runoff. The model that has 19 parameters (see Chiew and McMahon 1994; Reungoat 2000 for details) simulates soil moisture and surface water movement and has been extensively tested in arid and temperate climates and used in a number of climate impacts investigations.

Model calibration with respect to the runoff was carried out using daily data over 1962–1975 with validation based on daily data over the period 1976–1990. Given the schematization of the reservoirs as three parallel systems, model calibration was carried out separately for each of the three lumped reservoir catchments shown in Figure 11.3. In general, it was observed that model performance was excellent during calibration with an R^2 exceeding 0.96 for all three catchments. Performance over validation, though not as good as that over calibration, was generally adequate with R^2 exceeding 0.87.

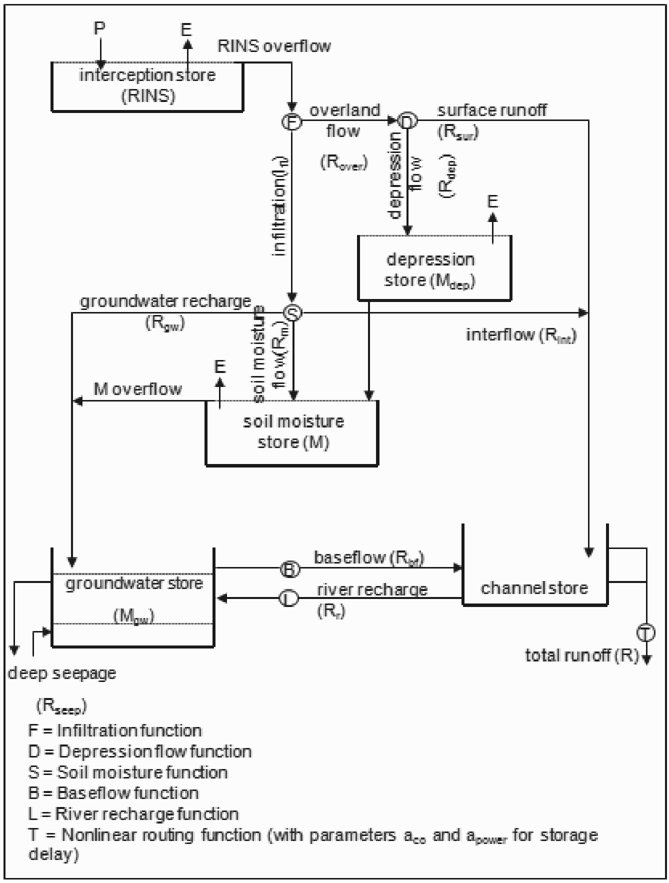

Figure 11.4. MODHYDROLOG model schematic

11.5.5 Monte Carlo Experiments and Runoff Sensitivity to Climate Change

The LARS-WG generated baseline and future climate data were each used to force MODHYDROLOG catchment simulation model to produce the one off baseline and one-off future daily runoff time-series for each of the climate change scenarios. Then, 1000 replicates of the baseline-future pair of monthly runoff were obtained using stochastic runoff generation. The generation of alternative runoff data utilised a parametric, multivariate annual lag-one autoregressive (AR(1)) model. This enabled generation of streamflow simultaneously at a number of sites, taking into account the covariances of the runoff.

Table 11.6 provides a comparison of observed and generated runoff at the Hebden site, which is quite satisfactory. The average changes in runoff, as a consequence of climate change based on the 1000-paired replicates, were then determined. These are presented for nine climate change scenarios in Figure 5, lumped for the reservoir catchments. This is valid given that the reservoir systems are considered as parallel systems. The results indicate that changes in runoff follow a similar pattern to precipitation changes presented earlier (see Table 11.5). For instance, the CSIRO1 scenario predicted increases in precipitation throughout most of the year with the maximum increases expected in March and November. Similarly, the CSIRO1 scenario results in an increase in runoff during most of the year with maximum increases expected in March and November (see Figure 11.5).

Table 11.6. Comparison of observed and generated mean runoff at Hebden site (1961–1990)

Month	Observed runoff (mm)	Generated runoff* (mm)	Percentage difference
Jan	138	153	-11
Feb	101	112	-11
Mar	95	104	-9
Apr	72	71	2
May	44	46	-3
Jun	33	37	-12
Jul	32	34	-8
Aug	52	49	6
Sep	66	66	1
Oct	102	115	-13
Nov	124	127	-3
Dec	142	150	-6

* based on the average of 1000 traces

The scenarios based on the CGCM1 and HadCM3 GCMs are showing a tendency for reduced runoff during the summer. The largest reduction in runoff results from HadCM3 in September during 2040–69 (66% = 38mm) whilst the largest increase of 54% (59mm) is expected under the CSIRO1 in November during 2070–99. Such large reductions will no doubt lead to significant reductions in future reservoir yield, when the storage capacity is fixed.

11.5.6 Climate Change Impacts on Reservoir Yield and its Sampling Uncertainty

Figure 11.6 shows the empirical distribution of the yield changes using all 1000 runoff replicates. The yields were estimated based on the modified sequent peak algorithm introduced by Adeloye et al. (2001); see also McMahon and Adeloye (2005). The *one-off* yield change based on the traditional single records approach is also shown in the figure. What the box plots highlight is the range of likely impacts on yield, which is not captured by the use of a single historic record. It may therefore be misleading to rely too heavily on mean impacts and single record analysis.

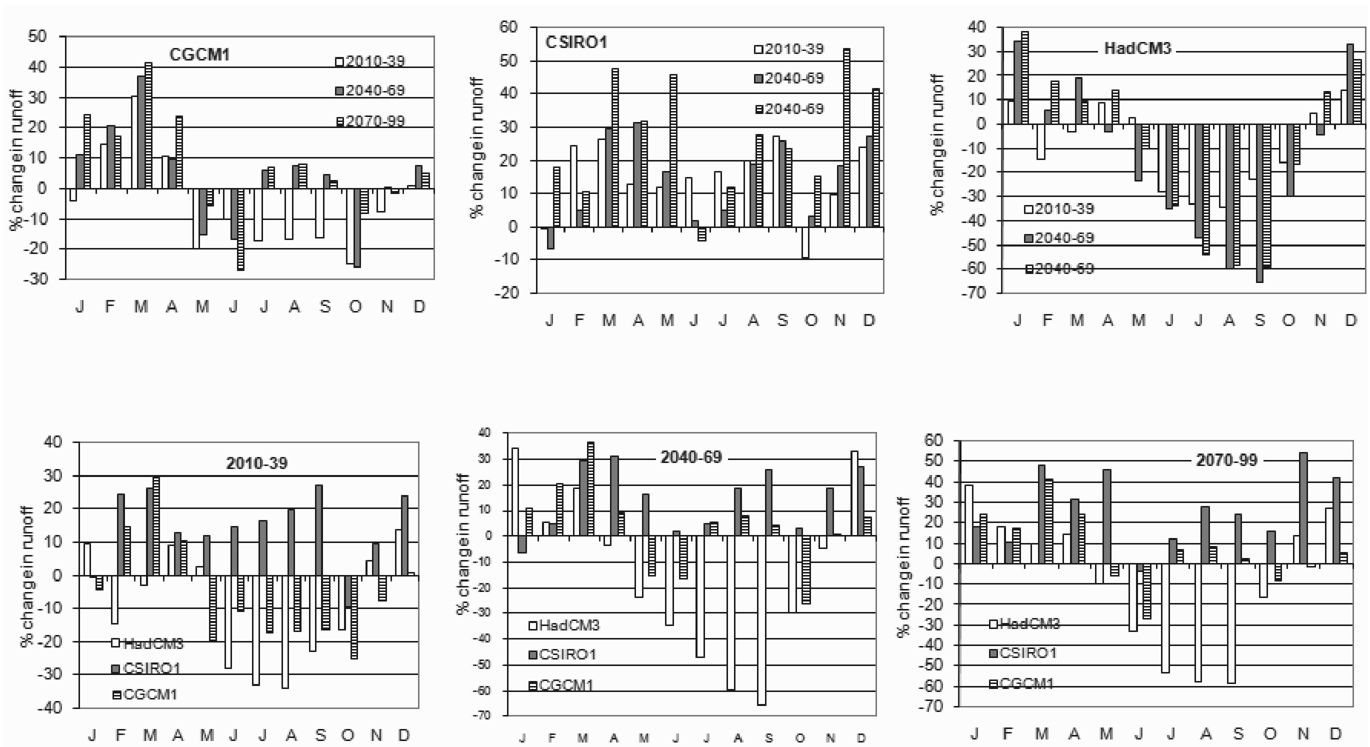

Figure 11.5. Percentage change in mean monthly runoff in Yorkshire (average for all catchments)

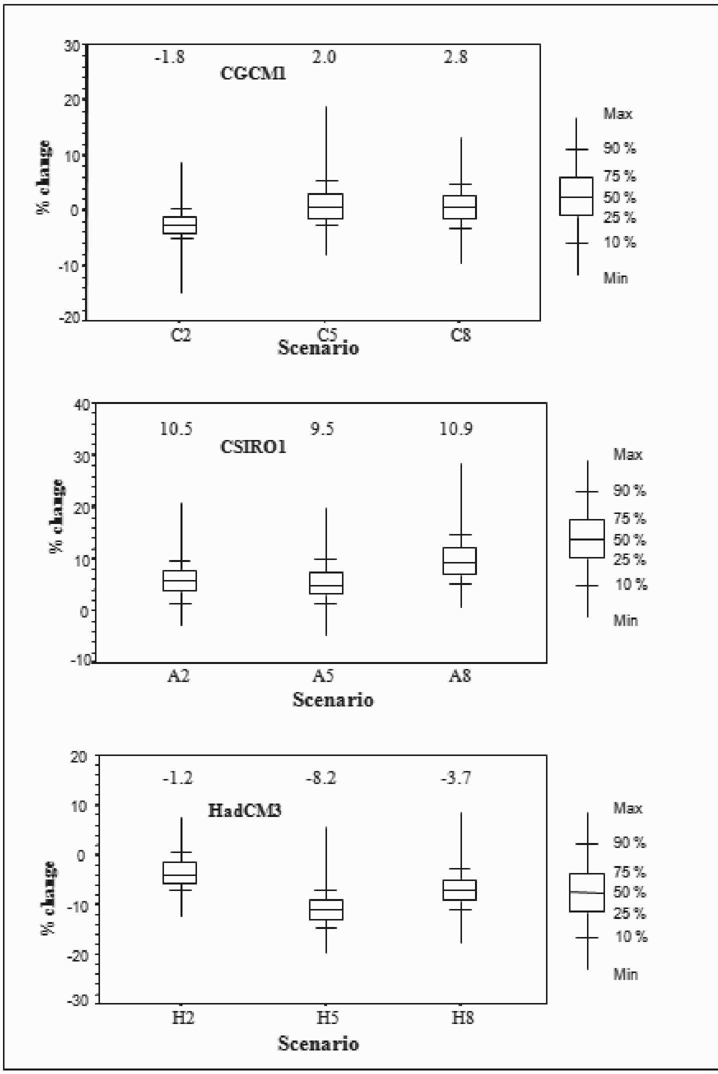

Figure 11.6. Box plots of yield changes for different climate scenarios (storage = 31% of MAF; C = CGCM1; A = CSIRO1; H = HadCM3; 2 = 2010–39; 5 = 2040–69, 8 = 2070–99; numbers above box-plots indicate the 'one-off' yield change)

11.5.7 Implications for Water Managers

Results from the present study have confirmed that mean impacts which have received so much attention from climate impacts studies could be misleading because large variability in this mean is possible, given the usual length of streamflow data records available for water resources planning and operational studies in practice. By being aware of such variability, water managers are better able to plan climate change mitigating measures. Specific impacts are viewed against their associated risks of happening and intervention measures are devised appropriately. In other words, impacts which have very low probability of occurring should concern less than those which have a higher probability.

11.5.8 Summary

This study has used a Monte Carlo approach to characterise the sampling uncertainty of the climate change impacts on hydrology and yields of a water resources system in Yorkshire, England. The results have shown that yield changes can be highly variable and can be much different from mean changes often addressed in traditional, deterministic impact studies. Knowledge of such variability allows more meaningful planning of mitigating measures for climate change impacts because probabilities can be ascribed to different levels of predicted yield changes, enabling resources to be targeted as appropriate.

To gain an idea of what these measures may entail, it would be useful to look at an actual drought episode in Yorkshire in 1995 and its aftermath. Evidence indicated that changing temperature and rainfall trends across Yorkshire were responsible for the severe drought. For example, Holden and Adamson (2002) reported that mean annual temperatures in the uplands of Yorkshire were significantly higher during the 1991–2000 period compared to the 1931–1979 period. Also, total rainfall between April–October 1995 in Yorkshire was the lowest for 200 years (POST 1995).

The immediate response to the drought was to impose hose-pipe bans, issue drought orders, inform the public on saving water, and begin the transfer of water to Yorkshire from other regions.

Water demand and efficiency were a key issue and the public were educated through media and press on the importance of saving water. Discussion began on the possibility of installing more water meters, although this raised all sorts of issues concerning the less affluent. The benefits were clear in that demand would reduce. For example, summer peak demands had been known to fall by up to 30% (POST 1995) if a customer was asked to pay more for higher water-usage. Water-metering also has the advantage that it allows leaking pipes to be detected more easily since there is precise record of the water-balance. There were large reductions in water leakage as a result of pipe rehabilitation carried out over a number of years. Studies were commissioned to re-assess storage reservoir yield in Yorkshire using a similar

Monte Carlo approach described in this study (see Adeloye and Nawaz 1997) and reservoir operational strategies (especially for multiple-reservoirs) were revised. It is remarkable that, although similar water scarcity situations have occurred over the UK in recent times, such measures as recommended by Adeloye and Nawaz (1997) have enhanced the better preparedness of the Yorkshire region to cope with severe droughts similar to those experienced during the hydroclimatological conditions of 1995.

Another evidence, albeit not new, coming out from the study is that climate change water resources impacts are highly uncertain because of differences in GCM projections. The study used three different GCM experiments but while all the three GCMs agreed on the likely change and direction of future temperature in the same catchments, projections of precipitation changes often varied from one GCM to another. This is a major problem for water resources impacts assessment since precipitation often has a much bigger impact on runoff than evaporation. Of the climate change scenarios used in the case study, those based on the HadCM3 GCM indicate drier future conditions whilst wetter conditions are predicted by the CSIRO1 GCM for the same catchments. Consequently, use of scenarios based on different GCMs had led to opposite impacts on the yield of the same water resources system. However, rather than worry about which of these impacts are correct, the impacts should be viewed as the likely range of projections which should all be considered when making plans for accommodating climate change.

11.6 Case Study 2: Climate Change Impact on Blue Nile Flow

11.6.1 Introduction

The Nile Basin (Figure 11.7) drains an area of around 3 million km^2 providing freshwater to millions of people across Africa. The increasing population density of this area will reduce Egypt's flexibility and options for responding to climate change impacts. In addition to increased stresses of a growing population, the water requirements of other large scale users such as Ethiopia and Sudan will also increase. Coupled with the effects of climate change, the country could be faced with an explosive situation.

Investigation was limited to the area upstream of Diem river gauging station (see Figure 11.8) at the Sudanese Ethiopian border (termed the upper Blue Nile Basin), shown in Figure 11.8 which also contains the rainfall measurement stations (see also Table 11.7).

Daily flow values at Diem gauging station were available for the study. The complete record spanning for 1966–2001 was available although only the shorter record coinciding with available daily rainfall data (spanning 1992–2001) was used for model calibrations.

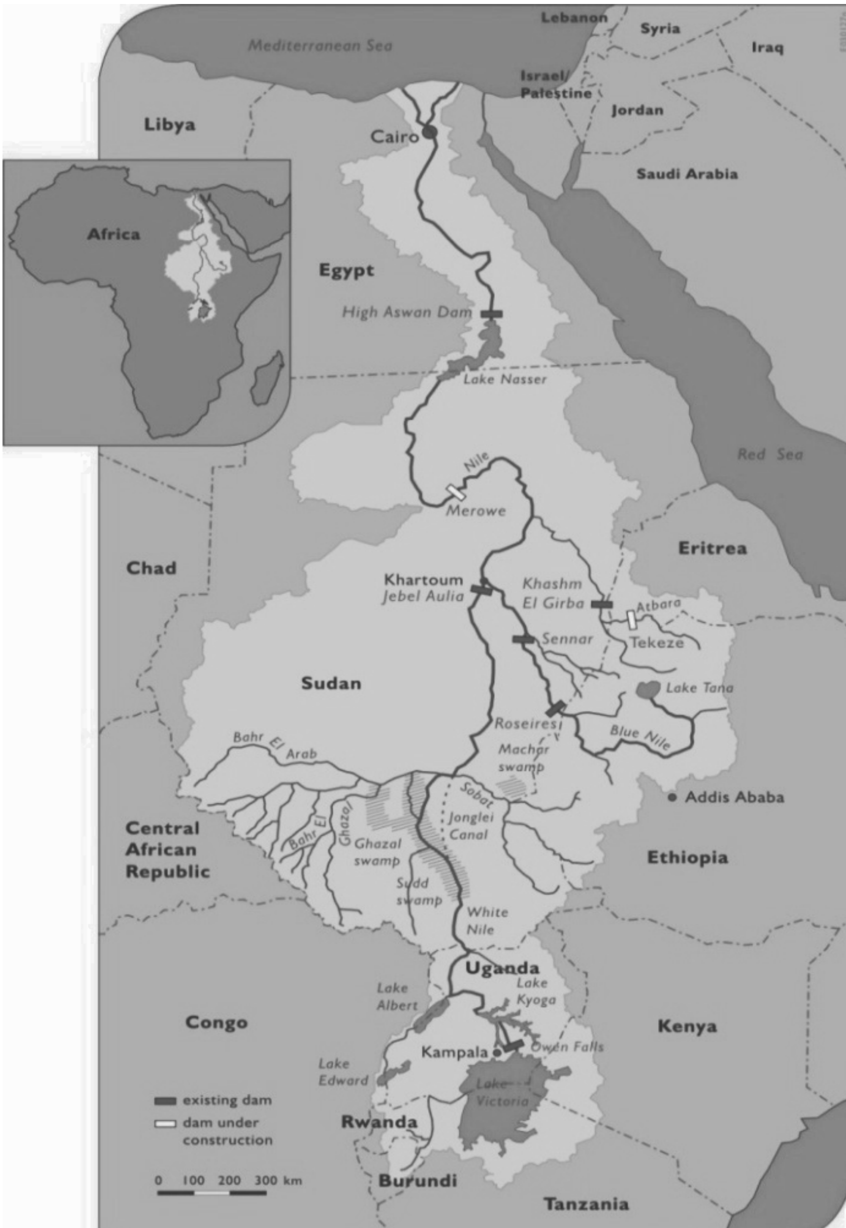

Figure 11.7. The entire Nile basin and the upper Blue Nile sub-Basin

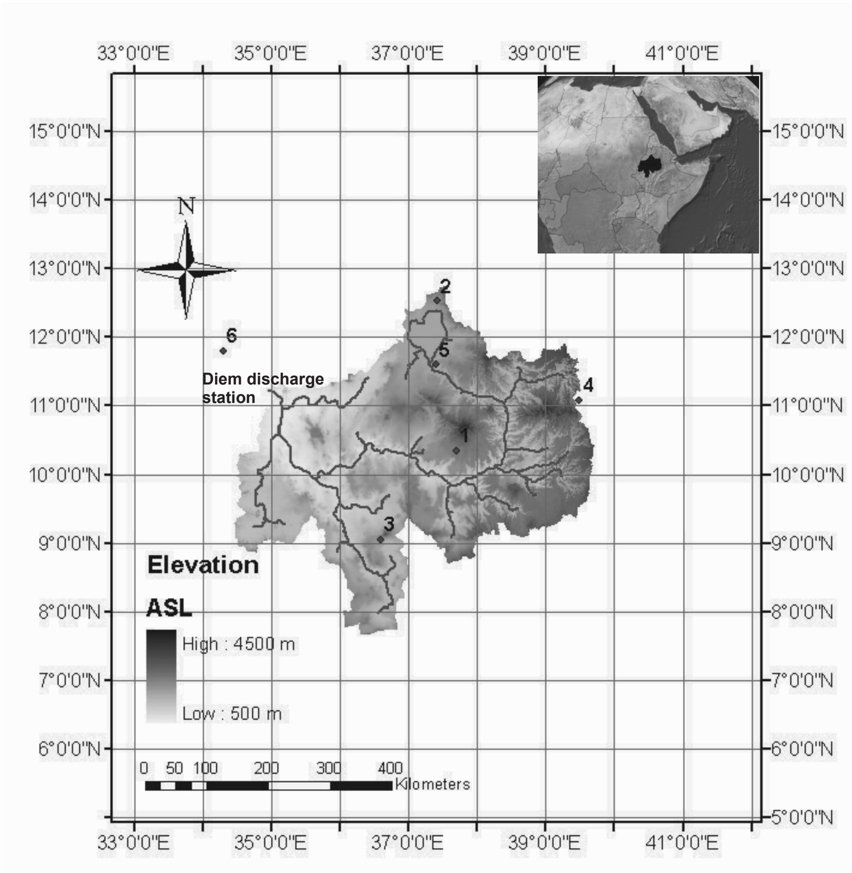

Figure 11.8. The upper Blue Nile Basin and location of rainfall stations and Diem flow gauging station [(1) Debre-Markos; (2) Gonder; (3) Nekemte; (4) Kembolcha; (5) Bahar Dar; (6) Roseires]

Table 11.7. Rainfall station information for upper Blue Nile Basin

Station	WMO ID	Long. (E)	Lat. (N)	Elev. (m)	Annual rainfall (mm)
1) Debre-Markos	63334	37.71	10.35	2440	1328
2) Gonder	63331	37.43	12.53	2270	1176
3) Nekemte	63340	36.60	09.05	1950	2005
4) Kembolcha	63333	39.75	11.08	1903	980
5) Bahar Dar	63332	37.40	11.60	1805	1247
6) Roseires	63330	34.40	11.80	520	541

11.6.2 Climate Change Scenarios

As with the Yorkshire Case Study, it was decided to use climate change scenarios based on three GCMs allowing the effects of GCM uncertainties to be explored: (i) CGCM2 (the Canadian second generation coupled general circulation model), (ii) ECHAM4 (Max Planck Institute for Meteorology, Hamburg) and (iii) HadCM3 (UK Hadley Centre) because they performed better in reproducing the baseline (1992–2001) rainfall data (Nawaz et al. 2010). The CGCM2 had become available at the time of the Nile study and hence was used in place of the first generation used for the UK study.

To explore the effects of future greenhouse gas (GHG) emissions uncertainties, two GHG emissions scenarios for forcing the GCMs were considered; the SRES A2 and B2. The A2, with a high climate sensitivity (4.5^{o}C) assumes higher GHG emissions than the B2 scenario (a medium climate sensitivity of 2.5^{o}C), especially after 2050, when emissions under B2 scenario are expected to stabilise.

The GCMs outputs were downscaled using a statistical downscaling approach (Frias et al. 2006; Tripathi, et al. 2006; Timbal et al. 2008). Table 11.8 illustrates the performance of the downscaled rainfall, which is not dissimilar from the characteristics of most GCMs in simulating rainfall. It can be seen that all three GCMs are under-estimating the rainy season rainfall at all stations except Roseires. Additionally, all three GCMs seem to perform rather poorly at Nekemta and Roseries stations when compared to the other stations. Hulme et al. (2001) provide several reasons for differences between GCM simulated and observed climate in Africa and these include poor model replication of natural climate variability, the absence of dynamic land-cover/atmosphere feedback processes and the absence of any representation of changing atmospheric dust aerosol concentration.

Table 11.8. Comparison of downscaled rainfall and observed rainfall at six stations within the upper Blue Nile Basin (1992–2001)

Rainfall	**Total rainfall during June-Sept. (mm)**				**Percentage difference**		
Station	**Observed**	**HADCM**	**CGCM**	**ECHAM**	**HADCM**	**CGCM2**	**ECHAM**
Debre Markos	924	913	865	833	-1	-6	-10
Gonder	877	805	752	688	-8	-14	-22
Nekemte	1379	1122	1077	1113	-19	-22	-19
Kembolcha	615	590	575	476	-4	-6	-23
Bahar Dar	999	939	876	831	-6	-12	-17
Roseires	383	464	488	500	21	27	30

11.6.3 Hydrological Modelling

A previously calibrated version of the Nile Forecasting System NFS hydrological model (van der Weert 2003; Elshamy 2006) was used in this study. The core of the NFS is a conceptual distributed hydrological model of the Nile basin operating at a daily time-step on a 20 km grid (Schaake et al. 1996) including soil moisture accounting, hillslope and river routing, lakes, wetlands, and man-made reservoirs within the basin. The distributed hydrological model requires gridded precipitation and potential evapotranspiration (PET) data as inputs. Gridded rainfall data were generated using the Turning Bands method (Matheron 1963) coupled with ARIMA time series modeling.

To limit the number of GCM variables required for PET estimation, the Thornthwaite formula (Thornthwaite 1948) was used for estimating the PET. The formula requires temperature and day length as input. Monthly mean baseline and future temperature simulated by all three GCMs was used to obtain PET changes. The percentage changes were then applied to the observed PET dataset which already exist as gridded 20 km estimates in the NFS database. Prior examination of the NFS gridded baseline PET revealed that in general, the PET field is somewhat smoother than the precipitation field; thus, no stochastic modelling of PET downscaling uncertainty was deemed necessary. Additionally, although the use of only GCM temperature is quite restrictive in that changes in rainfall are likely to be accompanied by changes in humidity and cloudiness, thus calling for the use of more complete PET method such as the Penman-Montheith model, it was decided to proceed with the parsimonious Thornthwaite approach since only the relative changes were of interest.

11.6.4 Results–Impacts of Climate Changes

Runoff based on GCM downscaled rainfall (50 sequences) over the baseline period was compared with observations (1992–2001) at Diem gauging station (see Figure 11.8). Because of the importance of rainy season flows to water resources planners, the results will focus on the rainy season (June–September). The downscaled rainfall scenarios for the rainy season until 2100 are presented in Figure 11.9, while Figure 11.10 illustrates the full range of possible changes. Changes are shown for mean daily rainfall during the rainy season. By the 2020s, the CGCM and HadCM3 models indicate a general wetting pattern whilst the ECHAM indicates less rainfall. In general, however, it can be concluded that the HadCM3 and ECHAM models suggest a wetter future whilst the CGCM indicates a drier future. For example, up to 20% increase in mean rainfall and rainfall intensity is likely in the eastern part of the basin by the 2080s according to ECHAM. In contrast, the CGCM indicates rainfall reductions by up to 15%. Results also show that a much wet future is likely over much of the eastern portion of the basin by the 2080s according to ECHAM whilst it is the northern part of the basin that is likely to experience wetter conditions in future according to the HadCM3. Changes are generally more pronounced under the A2 emissions scenario since GHG emissions continue to rise by the 2080s whilst under the B2 scenario, they are stabilised at 2050 levels (IPCC 2000).

Future changes in PET during the rainy season are presented in Figure 11.11 for the SRES A2 GHG emissions scenarios. Since the PET was based on the Thornthwaite model and hence driven largely by temperature, results are indicative of temperature changes. PET is set to rise under all scenarios with the largest increase according to the ECHAM4 model of +15 to +30% (2050s) and up to 90% increase in the northern part of the basin by the 2080s. The CGCM2 model results in more

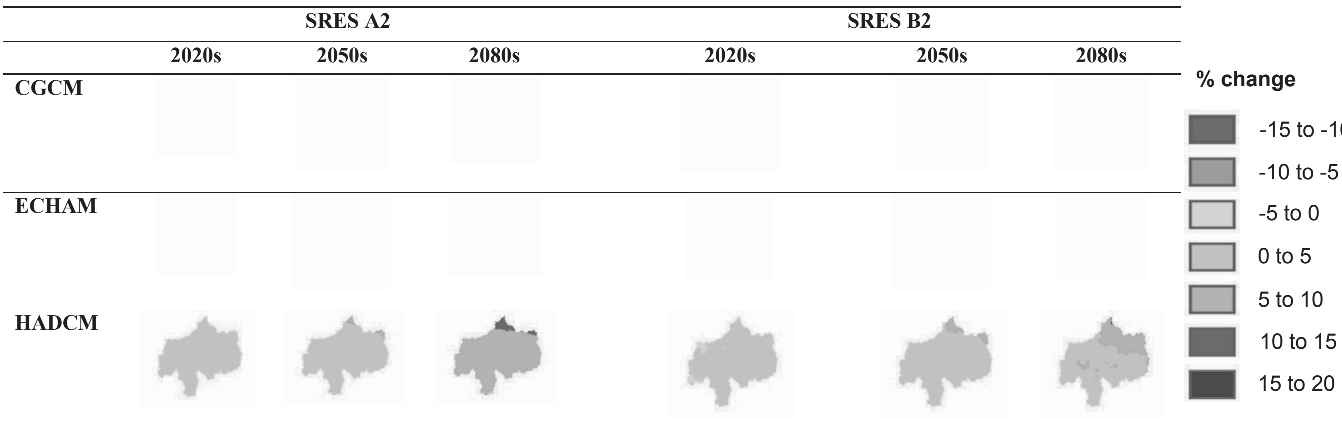

Figure 11.9. Percentage change in mean rainfall over the Blue Nile basin

moderate increases of 0 to +5% (2050s) to +15% to +30% (2080s). Projected HadCM3 increases lie between those estimated by the CGCM2 and ECHAM4.

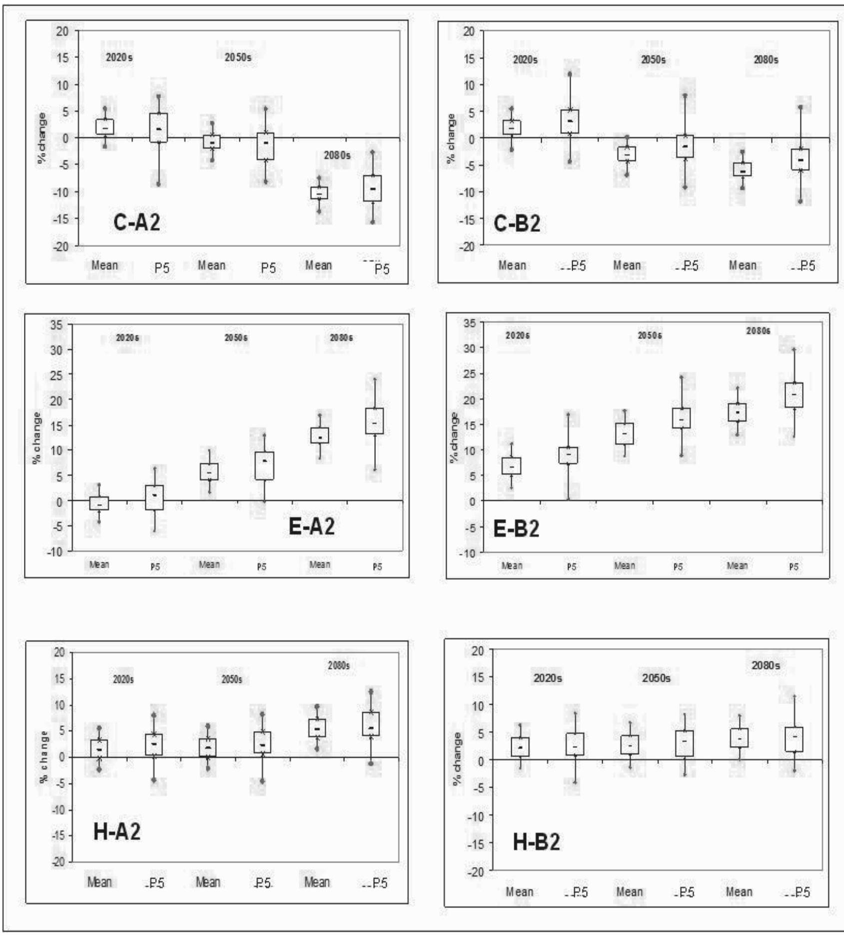

Figure 11.10. Percentage change in Blue Nile basin areal rainfall (from baseline) for A2 and B2 GHG emissions scenarios over wet season (June–September; P5 is the change in areal rainfall exceeded 5% of the time)

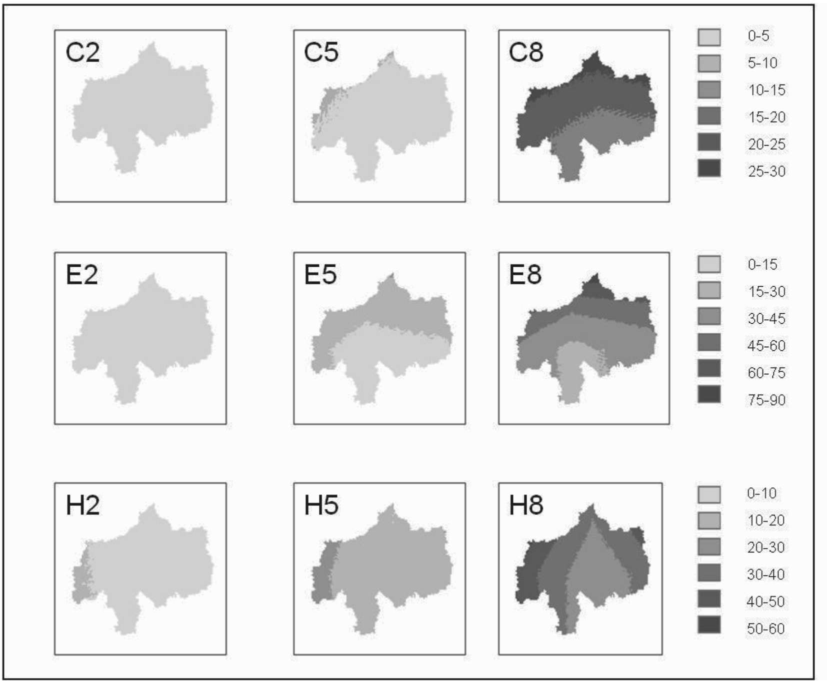

Figure 11.11. Wet season potential evapotranspiration changes (% from baseline) SRES A2

Figure 11.12 shows the future change (percentage from baseline) in flow at Diem station for the rainy season (June–September). Changes are presented in a similar format to rainfall changes presented as box-plots earlier.

By considering only the inter-quartile range in the box plots, it can be concluded that some rather significant changes in flow are likely during all three time-periods, which is in contrast to the moderate rainfall changes. The CGCM2 indicates drier conditions driven by the rainfall scenarios. The marked difference between projected flow reductions under the CGCM2 A2 and B2 scenarios for the 2050s is noteworthy. Results highlight the high sensitivity of flow changes to rainfall changes (see rainfall scenarios in Figures 11.9 & 11.10). Results from HadCM3 suggest that although a wetter future is likely (Figure 11.10), flow is set to decrease, especially by the 2080s. This is because increased PET across the basin (Figure 11.11) leads to flow reduction even though rainfall increases by a small amount. Although future rainfall is likely to generally increase (substantially in some cases) over the future according to the ECHAM4, flow increases are rather modest (and likely to reduce in some cases) because of the PET increases (Figure 11.11).

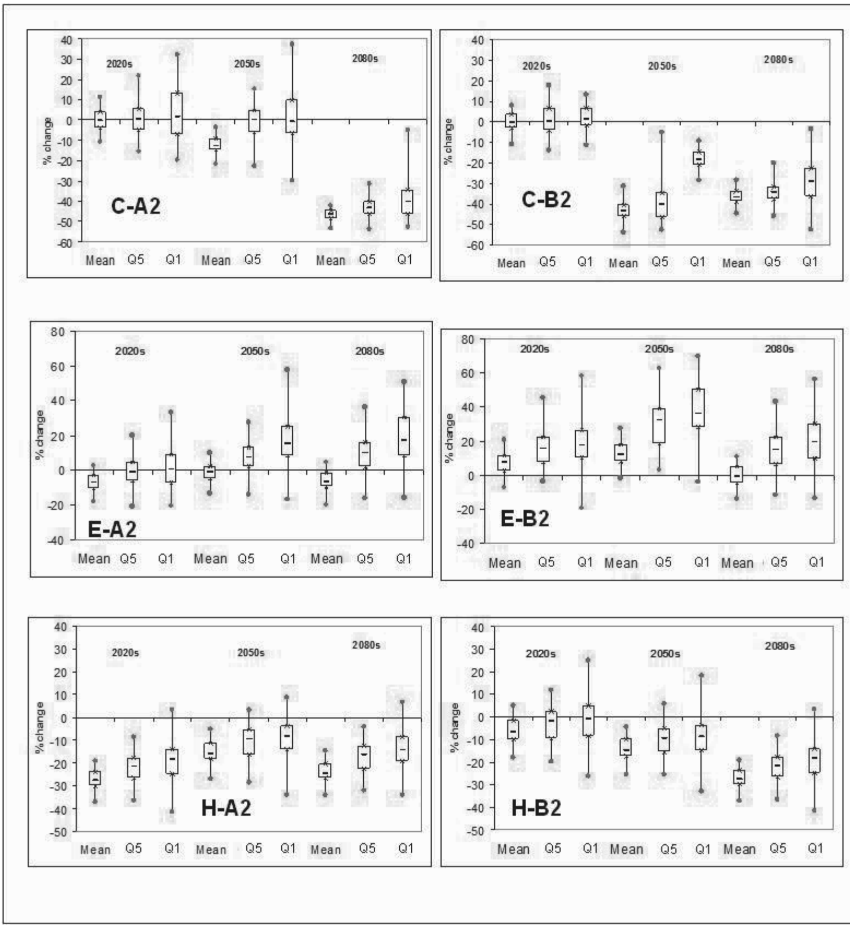

Figure 11.12. Percentage change in discharge (from baseline) of Blue Nile flow (at Diem) for A2 and B2 GHG emissions scenarios over wet season (June–September; Q5 and Q1 is the flow exceeded 5% and 1% of the time, respectively)

11.6.5 Summary and Implications for Water Management in the Nile Basin

It is evident that despite advances in climate modeling over the years, there still appears to be disagreement amongst GCMs in simulating future precipitation for a given region. In the case of the Blue Nile, results reported in this study indicate a drier future according to one GCM whilst two others indicate wetter futures. Better consistency is observed in temperature changes, which leads to more consistent potential evapotranspiration changes and these are expected to be very large by the

2080s. Based on work reviewed by the IPCC (Trenberth et al. 2007), East Africa has experienced an increasingly wetter climate and is likely to become wetter in future according to the majority of climate model simulations. However, it should be noted that the lack of good rain gauge coverage prevents conclusive rainfall trend detection. In time, this should become less of a problem as the availability and accuracy of remotely sensed rainfall data increases. The expectation of wetter futures is consistent with the findings reported in the present study; 13 out of 18 climate change scenarios for three future time periods indicate wetter conditions over the Blue Nile basin.

As expected, future wetter conditions in the basin result in increased average and extreme flows. However, the impact on flow is offset by increasing PET, and in some cases, flow is expected to reduce despite small increases in rainfall. This does require further investigation since a relatively simple approach for PET estimation was adopted that is not able to account for extra cloudiness and humidity associated with increasing rainfall.

Future wetter conditions within the basin could result in severe flood events occurring more frequently and devastating communities, particularly in Khartoum. Something which has been overlooked in this study is the continued impacts of land-use change related to overgrazing, deforestation, and improper farming practices in the Ethiopian highlands. Such practices will inevitably lead to soil erosion, loss of soil fertility and reduced infiltration thus exacerbating the flood problem. Blue Nile basin flood managers therefore need to continue to prepare for such eventualities by adopting a range of measures to minimize loss of life and other flood damage.

Whilst the approach adopted in the current study is only able to inform decision-makers about the *possible* range of impacts, more recent outputs from the climate modelling community may enable the *probable* range of impacts to be determined in future. The UK Climate Impacts Programme (UKCIP) has pioneered this work and recently published the UKCP09 scenarios (Jenkins et al. 2009) which attach likelihood to climate change scenarios.

There are a range of actions that can be taken to minimise the threat from global warming. Efforts must be made at turning *threats* into *opportunities*. A range of possibilities are available including ‘soft’ and ‘hard’ engineering options. The role of dams should not be dismissed; much of the flood devastation in Pakistan during summer 2010 could have been avoided if a planned dam had seen construction. Neighbouring China avoided catastrophe from similar amounts of record rainfall to that observed in Pakistan due to the three gorges dam. There is no reason why both types of options cannot be implemented simultaneously. Afforestation programmes can have a significant impact on downstream flood risk and sediment deposition into rivers and reservoirs.

In summary, it may serve water managers well to learn from the recent financial crisis. Prior to the collapse, leading financial institutes provided economic growth predictions for years ahead. Sophisticated economic models were used as a basis for making such forecasts. The decision makers (i.e. the public) made important decisions on the basis of such information. It would appear too much emphasis was placed on smooth growth curves. Reality turned out to be rather different and the status of the City genius transformed very quickly to the City novice. This provides a good example to water managers on the dangers of placing blind trust in sophisticated climate model output.

11.7 Acknowledgements

We would like to thank Yorkshire Water Services Ltd., UK for providing relevant data for the Yorkshire case study. We also wish to extend our thanks to the British Atmospheric Data Centre (BADC), UK Climate Impacts Programme (UKCIP) and the Climate Research Unit (CRU) at the University of East Anglia, UK for providing hydrometric data.

For the Nile research, we gratefully acknowledge the support of Dr Mohamed Elshamy and Dr Mamdouh Antar of the Nile Forecast Centre, for allowing access to their datasets and use of the NFS. Thanks are also due Dr Mohamed Sayed, Regional Coordinator, Flood Preparedness and Early Warning & Eastern Nile Planning Model Projects, Adis Ababa, Ethiopia and Dr Jaap Kwadijk of Delft Hydraulics.

11.8 References

Adeloye, A. J., and Nawaz, N. R. (1997). *The reliability of storage-yield estimates for some reservoir sites in Yorkshire*. Dept. Civil & Offshore Eng., *Edinburgh*, 66pp.

Adeloye, A. J., Montaseri, M., and Garmann, C. (2001). "Curing the misbehaviour of reservoir capacity statistics by controlling shortfall during failures using the modified sequent algorithm." *Water Resour. Res*. 37(1), 73–82.

Boer, G. J., Flato, G. M., Reader, M. C., and Ramsden, D. (2000). "A transient climate change simulation with greenhouse gas and aerosol forcing: experimental design and comparison with the instrumental record for the 20th century." *Climate Dynamics*, 16, 405–425.

Chiew, F. H. S., and McMahon, T. A. (1994). "Application of the daily rainfall-runoff model MODHYDROLOG to 28 Australian catchments." *J. Hydrol.* 153(1–4), 383–416.

Dessai, S., and Hulme, M. (2008). "How do UK climate scenarios compare with recent observations?" *Atmospheric Science Letters*, 9, 189–195.

Elshamy, M. E. A. M. (2006). *Improvement of the hydrological performance of land surface parameterization: An application to the Nile Basin*. Doctor of Philosophy (PhD) Dissertation, Imperial College, University of London, London.

Frias, M. D., Zorita, E., Fernandez, J., and Rodriguez-Puebla, C. (2006). “Testing statistical downscaling methods in simulated climates.” *Geophy. Res Lett*; 33, L19807.

Gordon, C., Cooper, C., Senior, C. A., Banks, H., Gregory, J. M., Johns, T. C., Mitchell, J. F. B., and Wood, R. A. (2000). “The simulation of SST, sea ice extents and ocean heat transports in a version of the Hadley Centre coupled model without flux adjustments.” *Climate Dynamics*, 16, 147–168.

Hirst, A. C., O' Farrell, S. P., and Gordon, H. B. (2000). “Comparison of a coupled ocean-atmosphere model with and without oceanic eddy-induced advection, 1: Ocean spin-up and control integrations.” *J. Climate*, 13 (1), 139–163.

Holden, J., and Adamson, J. (2002). “The Moor-House long-term upland temperature record–new evidence of recent warming.” *Weather*, 57, 119–126.

Hulme, M., Doherty, R., New, M., and Ngara, T. (2001). “African climatic change: 1900–2100.” *Clim. Res.* 17, 145–168.

IPCC (2000). *IPCC Special Report –Emissions Scenarios*. Summary for Policymakers, Intergovernmental Panel on Climate Change. <http://sres.ciesin.org/index. html> (accessed Jan. 2012).

Jenkins, G. J., Murphy, J. M., and Sexton, D. (2009). *UK Climate Projections: Briefing report.* Met Office Hadley Centre, Exeter, UK.

Kundzewicz, Z. W., Mata, L. J., Arnell, N. W., Döll, P., Kabat, P., Jiménez, B., Miller, K. A., Oki, T., Sen, Z., and Shiklomanov, I. A. (2007). “Freshwater resources and their management.” *Climate Change 2007: Impacts, Adaptation and Vulnerability. Contribution of Working Group II to the Fourth Assessment Report of the Intergovernmental Panel on Climate Change,* M.L. Parry, O.F. Canziani, J.P. Palutikof, P.J. van der Linden and C.E. Hanson, Eds., Cambridge University Press, Cambridge, UK, 173–210.

Le Treut, H., Somerville, R., Cubasch, U., Ding, Y., Mauritzen, C., Mokssit, A., Peterson, T., and Prather, M. (2007). “Historical Overview of Climate Change.” In: *Climate Change 2007: The Physical Science Basis. Contribution of Working Group I to the Fourth Assessment Report of the Intergovernmental Panel on Climate Change* [Solomon, S., D. Qin, M. Manning, Z. Chen, M. Marquis, K.B. Averyt, M. Tignor, and H.L. Miller (eds.)]. Cambridge University Press, Cambridge, United Kingdom and New York, NY, USA.

Manabe, S., and Wetherald, R. T. (1975). “The effects of doubling the CO_2 concentration on the climate of a general circulation model.” *J. Atmos Sci*. 32, 3–15.

McMahon, T. A., and Adeloye, A. J. (2005). *Water Resources Yield*, *Water Resources Publications*, Littleton, Colorado, 234pp.

Martin, G. M., Ringer, M. A., Pope, V. D., Jones, A., Dearden, C., and Hinton, T. J. (2006). “The physical properties of the atmosphere in the new Hadley Centre Global Environmental Model, HadGEM1. Part I: Model description and global climatology.” *J. Climate*, 19, 1274–1301.

Matheron, G. (1963). “Principles of geostatistics.” *Econ Geol*, 58, 1246–1266.

Murphy, J. M., Sexton, D. M. H., Jenkins, G. J., Booth, B. B. B., Brown, C. C., Clark, R. T., Collins, M., Harris, G. R., Kendon, E. J., Betts, R. A., Brown, S. J., Humphrey, K. A., McCarthy, M. P., McDonald, R. E., Stephens, A., Wallace, C., Warren, R., Wilby, R., and Wood, R. A. (2009). *UK Climate Projections Science Report: Climate change projections*. Met Office Hadley Centre, Exeter, UK. 192pp.

Nawaz, N. R., Bellerby, T, Sayed, M. and Elshamy, M. (2010) "Blue Nile runoff sensitivity to climate change." *The Open Hydrology Journal*, *Bentham Open*, 4, 1-15.Nof, D. (2008). "Simple versus complex climate modelling." *EOS Transactions American Geophysical union*, 89(52), 544.

POST (The UK Parliamentary Office of Science and Technology) (1995). *The 1995 Drought.* Technical Report 71.

Racsko, P., Szeidl, L., and Semenov, M. (1991). "A serial approach to local stochastic weather models." *Ecol. Modelling*, 57, 27–41.

Reungoat, A. (2000). *Rainfall-runoff modelling with MODHYDROLOG.* Unpublished MSc Thesis, Heriot-Watt University, Edinburgh, UK.

Reifen, C., and Toumi, R. (2009). "Climate projections: Past performance no guarantee of future skill?" *Geophysical Research Letters*, 36(L13704), 1–5.

Schaake J. C., Koren, V. I., Duan, Q. Y., Mitchell, K., and Chen, F. (1996). "Simple water balance model for estimating runoff at different spatial and temporal scales." *J Geophys Res Atmos,* 101(D3), 7461–7475.

Smith, T. M., Leemans, R., and Shugart, H. H. (1992). "Sensitivity of terrestrial carbon storage to CO_2-induced climate change: comparisons of four scenarios based on general circulation models." *Climatic Change*, 21, 367–384.

Thornthwaite, C. W. (1948). "An approach toward a rational classification of climate." *Geogr. Rev*. 38(1), 55–94.

Timbal B., Hope P., and Charles S. (2008). "Evaluating the consistency between statistically downscaled and global dynamical model climate change projections." *J. Climate*, 23(2), 54–78.

Trenberth, K.E., P.D. Jones, P. Ambenje, R. Bojariu, D. Easterling, A. Klein Tank, D. Parker, F. Rahimzadeh, J.A. Renwick, M. Rusticucci, B. Soden and P. Zhai, (2007). "Observations: Surface and Atmospheric Climate Change." In: *Climate Change 2007: The Physical Science Basis. Contribution of Working Group I to the Fourth Assessment Report of the Intergovernmental Panel on Climate Change* [Solomon, S., D. Qin, M. Manning, Z. Chen, M. Marquis, K.B. Averyt, M. Tignor and H.L. Miller (eds.)]. Cambridge University Press, Cambridge, United Kingdom and New York, NY, USA.

Tripathi. S., Srinivas, V. V., and Nanjundiah, R. S. (2006). "Downscaling of precipitation for climate change scenarios: A support vector machine approach." *J. Hydrol*, 330(4), 621–40.

van der Weert R. (2003). *Performance of the NFS system in simulating water balances, Nile Forecast Center.* Ministry of Water Resources and Irrigation, Egypt.

von Storch, H., Zorita, E., and Cubasch, U. (1993). "Downscaling of global climate change estimates to regional scales: an application to Iberian rainfall in wintertime." *J. Climate,* 6(6), 1161–1171.

Wilby, R. L., and Wigley, T. M. L. (1997). "Downscaling general circulation model output: a review of methods and limitations." *Progress in Physical Geography*, 21(4), 530–548.

CHAPTER 12

Impact of Climate Change on Hydrometeorological Variables in a River Basin in India for IPCC SRES Scenarios

Aavudai Anandhi, V. V. Srinivas, and D. Nagesh Kumar

12.1 Introduction

In the recent years, the new paradigm of abrupt climate change has been well established, and a major global concern is to assess implications of climate change on hydrology of river basins and availability of water, which is considered to be a vulnerable resource. The future climate is unknown and uncertain. Hence to evaluate plausible impacts of climate change on the hydrology of a river basin, it is necessary to develop plausible future projections of hydrometerological processes in the river basin for various climate scenarios. For this purpose, a variety of methods are available. The classical methods use climate variables simulated by General Circulation Models (GCMs) for projected changes in GCM boundary conditions based on emissions scenarios. Among the scenarios available in literature, those that were published in the Special Report on Emissions Scenarios (SRES) (Nakicenovic et al. 2000) are widely used, and are known as SRES scenarios.

The GCMs are among the most advanced tools, which use transient climate simulations to simulate the climatic conditions on earth, several decades into the future. For quantitative climate impact studies in hydrological processes, the various projections of variables output from the GCM simulations are studied. Since GCMs are run at coarse resolutions, the output climate variables from these models cannot be used directly for impact assessment on a local scale. Hence in the past two decades, several downscaling methodologies have been developed to transfer information from the GCM simulated climate variables to local scale.

The remainder of this chapter is structured as follows. First, a brief description of SRES scenarios, downscaling methods and Support Vector Machine (SVM) is provided in section 12.2. The description of Malaprabha river basin in India, which is considered for case study, is provided in section 12.3. Subsequently, the SVM based methodology suggested for downscaling precipitation and temperature in the river basin is presented in section 12.4. Following this, results of downscaling models are presented in section 12.5, and possible consequences on hydrology of the river basin are discussed. Finally, summary and conclusions drawn based on the study and some of the conceptual and philosophical issues concerning the use of downscaling models are provided in section 12.6.

12.2 Background

In this section a general description on the various SRES scenarios, downscaling methods and SVM is provided.

12.2.1 SRES

The SRES scenarios are constructed based on the major driving forces or factors (e.g., human development including economic, demographic, social and technological changes) that are suited for climate impact assessment. These factors play significant role in energy consumption, land use changes and emissions, and represent a diverse range of different development pathways of the world for impact assessment. Hence they are useful for research on sustainable development and impact assessment, serving as inputs for evaluating climatic and environmental consequences of future greenhouse gas emissions and for assessing alternative mitigation strategies. These SRES scenarios were constructed with different ranges for each projection called ‘‘storyline.’’ There are four storylines (A1, A2, B1 and B2), describing the way the world population, land use changes, new technologies, energy resources, economies and political structure may evolve over the next few decades. Thus different world futures are represented in two dimensions, with one dimension representing economic or environmental concerns, and the other representing global or regional development patterns. For each storyline several emission scenarios were constructed, producing four ‘‘scenario families.’’ Ultimately, six SRES marker scenarios were defined: A1 has three marker scenarios (A1B, A1FI and A1T) and the others have one each.

A1 Story-line. This scenario represents very rapid economic growth with increasing globalization, an increase in general wealth, with convergence between regions and reduced differences in regional per capita incomes. Materialist–consumerist values will be predominant, with rapid technological change and low population growth when compared to A2 scenario. Three variants within this family make different assumptions about sources of energy for this rapid growth: fossil intensive (A1FI), non-fossil fuels (A1T), and a balance across all sources (A1B).

A2 Story-line. A2 scenario is represented as a heterogeneous, market-led world, with rapid population growth but less rapid economic growth than A1. The underlying theme is self reliance and preservation of local identities. Economic growth is regionally oriented, and hence both income growth and technological change are regionally diverse. Fertility patterns across regions converge slowly, resulting in high population growth.

B1 Story-line. This scenario represents low population growth as A1, but development takes a much more environmentally sustainable pathway with global-scale cooperation and regulation. Clean and efficient technologies are introduced. The emphasis is on global solutions to achieving economic, social and environmental sustainability.

B2 Story-line. B2 scenario represents population increase at a lower rate than A2, but at a higher rate than A1, with development following environmentally, economically and socially sustainable local oriented pathways.

In SRES, none of the presented scenarios explicitly assumes implementation of the United Nations Framework Convention on Climate Change or the emissions target of the Kyoto Protocol. They exclude even the outlying "surprise" or "disaster" scenarios. It is preferable to consider a range of scenarios for climate impact studies as such an approach better reflects the uncertainties of the possible future climate change. For the case study presented in this chapter, A1B, A2, B1 and COMMIT scenarios were considered. In the COMMIT scenario, the atmospheric carbon-dioxide concentrations are maintained ('Committed') at the same level as in the year 2000.

12.2.2 Methods of Downscaling

The various downscaling methods available in literature can be broadly classified as dynamic downscaling and statistical downscaling (Figure 12.1).

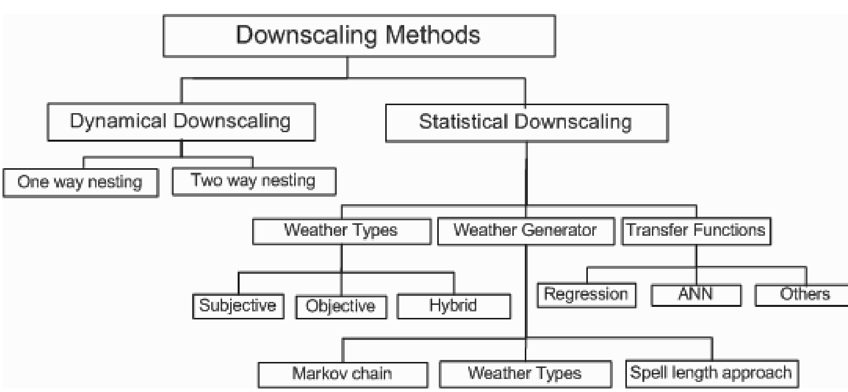

Figure 12.1. Methods of downscaling

In the dynamic downscaling method, a Regional Climate Model (RCM) is embedded into GCM. There are two types of dynamic downscaling based on the types of nesting: one-way nesting and two-way nesting (Wang et al. 2004). One-way nesting consists of driving a limited-area high-resolution RCM with low-resolution data obtained previously by a GCM or by analyses of atmospheric observations. The one-way nesting technique does not allow feedback from the RCM to the driving data. In two-way nesting, the RCM is run simultaneously with the host GCM, and it regularly updates the host GCM in the RCM region. Models of this type are typically developed using different numeric and physical parameterizations. They are not presently in use as they are cumbersome. Benefits similar to ‘‘two-way nesting’’ can be derived from the use of a variable-resolution GCM.

Statistical downscaling involves developing quantitative relationships between large-scale atmospheric variables (predictors) and local surface variables (predictands). There are three types of statistical downscaling namely- weather types, weather generators and transfer functions.

Weather types or weather classification methods group the days into a finite number of discrete weather types or ‘states’ according to their synoptic similarity. These methods in turn are classified as subjective, objective, or hybrid.

In subjective classification methods, the classifications were carried out manually using empirical rules. Some of the most widely known subjective classifications are Grosswetterlagen (Hess and Brezowsky 1969) and British Isles Weather Types (Lamb 1972).

In objective classification methods, a variety of automated techniques developed using computers are used to group the weather types. The most popular objective classification methods are based on correlation based algorithms (Brinkmann 1999), clustering techniques (Huth et al. 1993; Kidson 1994) and Fuzzy rules based approaches (Wetterhall et al. 2005).

The hybrid techniques combine elements of empirical/manual and automated procedures for grouping weather types, thereby avoiding time delay and enabling the production of easily reproducible and interpretable results (Frakes and Yarnal 1997; Anandhi 2010). Some of the hybrid techniques are screening discriminant analysis (Enke and Spekat 1997) and Classification and Regression Trees (CART) (Breiman et al. 1984).

Weather generators are statistical models of observed sequences of weather variables. They can also be regarded as complex random number generators, the output of which resembles daily weather data at a particular location. There are three fundamental types of daily weather generators, based on the approach to modeling the daily precipitation occurrence: the Markov chain approach (Hughes et al. 1999), the spell-length approach (Wilks 1999) and weather types (Conway and Jones 1998). In the Markov chain approach, a random process is constructed which determines a day at a station as rainy or dry, conditional upon the state of the previous day, following given probabilities. If a day is determined as rainy, then the rainfall amount is drawn from yet another probability distribution. In case of the spell-length approach, instead of simulating rainfall occurrences day by day, the models operate by fitting probability distribution to observed relative frequencies of wet and dry spell lengths.

Transfer functions are a conceptually simple means for representing linear and nonlinear relationships between the predictors and predictands. Therefore, a diverse range of statistical downscaling methods using transfer functions have been developed in the recent past. Examples include transfer functions based on linear and nonlinear regression, artificial neural networks, canonical correlation analysis, principal component analysis, Support vector machine (Tripathi et al. 2006; Anandhi et al. 2008; Anandhi et al. 2009) and Relevant vector machine (Ghosh and Mujumdar 2008). Transfer function based downscaling methods are sensitive to the subjective choices made in their design, viz., the type of transfer function used, choice of predictors and how well they are simulated by GCM, type of predictand, calibration period, timescale of downscaling (e.g., annual, seasonal, monthly, or daily), and temporal variation of the relationship between the predictors and predictand. However, transfer function methods have generally not been subjected to careful evaluation as the other downscaling techniques (Winkler et al. 1997; Anandhi et al. 2008; Anandhi et al. 2009). In spite of this, transfer functions are most commonly used for downscaling due to relative ease of their application. Individual downscaling schemes differ according to the choice of mathematical transfer function, predictor variables or statistical fitting procedure (Conway et al. 1996; Schubert and Henderson-Sellers, 1997).

Regression-based downscaling methods rely on the direct quantitative relationship between the local scale climate variable (predictand) and the variables containing the larger scale climate information (predictors) through some form of regression function (Karl et al. 1990; Wigley et al. 1990). The main advantage of the regression-based downscaling methods is the relative ease of their application. However, these models often explain only a fraction of the observed climate variability as they are unable to capture the extremes, especially when the predictand is precipitation (Wilby et al. 2004; Tripathi et al. 2006; Anandhi et al. 2008). Downscaling future extreme hydrologic events using regression based models may be problematic, because these events usually tend to be situated at the margins or beyond the range of the extremes in the calibration data set (Wilby et al. 2002).

Artificial Neural Network (ANN) based downscaling techniques have gained wide recognition owing to their ability to capture nonlinear relationships between predictors and predictand (Tatli et al. 2005). Mathematically, an ANN is often viewed as a universal approximator. The ability to generalize a relationship from given patterns makes it possible for ANNs to solve large-scale complex problems such as pattern recognition, nonlinear modeling and classification. The ANNs have been extensively used in a variety of physical science applications, including hydrology (ASCE Task Committee 2000; Govindaraju and Rao 2000).

Despite a number of advantages, the traditional neural network models have several drawbacks including possibility of getting trapped in local minima and subjectivity in the choice of model architecture (Suykens 2001). (Vapnik 1995; Vapnik 1998) pioneered the development of a novel machine learning algorithm, called support vector machine (SVM), which provides an elegant solution to these problems. The SVM has found wide application in the field of pattern recognition and time series analysis. Introductory material on SVM is available in a number of books (Cortes and Vapnik 1995; Vapnik 1995; Schölkopf et al. 1998; Vapnik 1998; Cristianini and Shawe-Taylor 2000; Haykin 2003; Sastry 2003). Most of the traditional neural network models seek to minimize the training error by implementing the empirical risk minimization principle, whereas the SVMs implement the structural risk minimization principle, which attempts to minimize an upper bound on the generalization error, by striking a right balance between the training error and the capacity of the machine (i.e., the ability of the machine to learn any training set without error). The solution of traditional neural network models may tend to fall into a local optimal solution, whereas global optimum solution is guaranteed in SVM (Haykin 2003). Further, the traditional ANNs have considerable subjectivity in model architecture, whereas for SVMs the learning algorithm automatically decides the model architecture (number of hidden units). Moreover, traditional ANN models do not give much emphasis on generalization performance, while SVMs seek to address this issue in a rigorous theoretical setting. The flexibility of the SVM is provided by the use of kernel functions that implicitly map the data to a higher, possibly infinite, dimensional space. A linear solution, in the higher dimensional feature space, corresponds to a non-linear solution in the original lower dimensional input space. This makes SVM a plausible choice for solving a variety of problems in hydrology, which are non-linear in nature.

12.2.3 Least-Square Support Vector Machine (LS-SVM)

The Least-Square Support Vector Machine (LS-SVM) provides a computational advantage over standard SVM (Suykens 2001). This subsection presents the underlying principle of the LS-SVM and is extracted from Anandhi et al. (2008) and Tripathi et al. (2006).

Consider a finite training sample of *N* patterns $\{(\mathbf{x}_i, y_i), i = 1, \ldots, N\}$, where $\mathbf{x}_i$ representing the "*i*-th" pattern in *n*-dimensional space (i.e., $\mathbf{x}_i = [x_{1i}, \ldots, x_{ni}] \in \Re^n$) constitutes the input to LS-SVM, and $y_i \in \Re$ is the corresponding value of the desired model output. Further, let the learning machine be defined by a set of possible mappings $\mathbf{x} \mapsto f(\mathbf{x}, \mathbf{w})$, where $f(\cdot)$ is a deterministic function which, for a given input pattern $\mathbf{x}$ and adjustable parameters $\mathbf{w}$ ($\mathbf{w} \in \Re^n$), always gives the same output. The training phase of the learning machine involves adjusting the parameter $\mathbf{w}$. These parameters are estimated by minimizing the cost function $\psi_{\mathrm{L}}(\mathbf{w}, e)$.

$$\psi_{\mathrm{L}}(\mathbf{w}, e) = \frac{1}{2}\mathbf{w}^{\mathrm{T}}\mathbf{w} + \frac{1}{2}C\sum_{i=1}^{N} e_i^2$$

subject to the equality constraint

$$y_i - \hat{y}_i = e_i \qquad i = 1,\ldots,N \tag{Eq. 12.1}$$

$$\hat{y}_i = w^T \phi(x) + b \tag{Eq. 12.2}$$

where C is a positive real constant, and $\hat{y}_i$ is the actual model output. The first term of the cost function represents weight decay or model complexity-penalty function. It is used to regularize the weight sizes and to penalize the large weights. This helps in improving the generalization performance (Hush and Horne 1993). The second term of the cost function represents penalty function.

The solution of the optimization problem is obtained by considering the Lagrangian as

$$L(\mathbf{w}, b, \mathbf{e}, \boldsymbol{\alpha}) = \frac{1}{2}\mathbf{w}^{\mathrm{T}}\mathbf{w} + \frac{1}{2}C\sum_{i=1}^{N} e_i^2 - \sum_{i=1}^{N} \alpha_i \{\hat{y}_i + e_i - y_i\} \tag{Eq. 12.3}$$

where α_i are Lagrange multipliers, and b is the bias term defined in eq. 2. The conditions for optimality are given by

$$\begin{cases} \dfrac{\partial L}{\partial \mathbf{w}} = \mathbf{w} - \sum\limits_{i=1}^{N} \alpha_i \phi(\mathbf{x}_i) = 0 \\ \dfrac{\partial L}{\partial b} = \sum\limits_{i=1}^{N} \alpha_i = 0 \\ \dfrac{\partial L}{\partial e_i} = \alpha_i - Ce_i = 0 & i = 1,\ldots,N \\ \dfrac{\partial L}{\partial \alpha_i} = \hat{y}_i + e_i - y_i = 0 & i = 1,..,N \end{cases} \tag{Eq. 12.4}$$

The above conditions of optimality can be expressed as the solution to the following set of linear equations after elimination of **w** and e_i.

$$\begin{bmatrix} 0 & \vec{\mathbf{1}}^{\mathrm{T}} \\ \vec{\mathbf{1}} & \boldsymbol{\Omega} + \mathrm{C}^{-1}\mathbf{I} \end{bmatrix} \begin{bmatrix} b \\ \boldsymbol{\alpha} \end{bmatrix} = \begin{bmatrix} 0 \\ \mathbf{y} \end{bmatrix} \tag{Eq. 12.5}$$

where $\mathbf{y} = \begin{bmatrix} y_1 \\ y_2 \\ \vdots \\ y_N \end{bmatrix}; \vec{\mathbf{1}} = \begin{bmatrix} 1 \\ 1 \\ \vdots \\ 1 \end{bmatrix}_{N\times 1}; \boldsymbol{\alpha} = \begin{bmatrix} \alpha_1 \\ \alpha_2 \\ \vdots \\ \alpha_N \end{bmatrix}; \mathbf{I} = \begin{bmatrix} 1\,0 \ldots 0 \\ 0\,1 \ldots 0 \\ \vdots\;\vdots\;\vdots\;\vdots \\ 0\,0 \ldots 1 \end{bmatrix}_{N\times N}$

In Eq. 12.5, $\boldsymbol{\Omega}$ is obtained from the application of Mercer's theorem.

$$\Omega_{i,j} = K(\mathbf{x}_i, \mathbf{x}_j) = \phi(\mathbf{x}_i)^{\mathrm{T}} \phi(\mathbf{x}_j) \qquad \forall i, j \tag{Eq. 12.6}$$

where $\phi(\cdot)$ represents nonlinear transformation function defined to convert a non-linear problem in the original lower dimensional input space to linear problem in a higher dimensional feature space.

The resulting LS-SVM model for function estimation is:

$$f(\mathbf{x}) = \sum \alpha_i^* K(\mathbf{x}_i, \mathbf{x}) + b^* \tag{Eq. 12.7}$$

where α_i^* and b^* are the solutions to Eq. 12.5 and $K(\mathbf{x}_i, \mathbf{x})$ is the inner product kernel function defined in accordance with Mercer's theorem (Mercer 1909; Courant and Hilbert 1970) and b^* is the bias. There are several choices of kernel functions, including linear, polynomial, sigmoid, splines and Radial basis function (RBF). The linear kernel is a special case of RBF (Keerthi and Lin 2003). Further, the sigmoid kernel behaves like RBF for certain parameters (Lin and Lin 2003). In this study RBF is chosen to map the input data into higher dimensional feature space, which is given by:

$$K(\mathbf{x}_i, \mathbf{x}_j) = \exp\left(-\frac{\left\| \mathbf{x}_i - \mathbf{x}_j \right\|^2}{\sigma} \right) \tag{Eq. 12.8}$$

where, σ is the width of RBF kernel, which can be adjusted to control the expressivity of RBF. The RBF kernels have localized and finite responses across the entire range of predictors.

The advantage with RBF kernel is that it maps the training data non-linearly into a possibly infinite-dimensional space, and thus, it can effectively handle the situations when the relationship between predictors and predictand is nonlinear. Moreover, the RBF is computationally simpler than polynomial kernel, which requires more parameters. It is worth mentioning that developing LS-SVM with RBF kernel involves a judicious selection of RBF kernel width σ and parameter C.

12.3 Study Region and Data Used

The study region is the catchment of Malaprabha River, upstream of Malaprabha reservoir in India. The region covers an area of 2093.46 km^2 situated between 15°30'N and 15°56' N latitudes, and 74°12' E and 75°8' E longitudes. It lies in the extreme western part of the Krishna River basin in India, and includes parts of Belgaum, Bagalkot and Dharwad districts of North Karnataka (Figure 12.2). Analysis of temporal variation of rainfall showed that, in general, the climate of the study region is dry, except in monsoon months (June–September) when warm winds blowing from Indian Ocean cause copious amount of rainfall. Isohyetal map prepared for the region showed considerable variation in spatial distribution of annual rainfall. Heavy rainfall (more than 3000 mm) is recorded at gauging stations in the upstream reaches of the Malaprabha catchment, which forms a part of the western Ghats. In contrast, the average annual rainfall in the reservoir command area (i.e., downstream of the dam) is 576 mm. The average annual rainfall in the basin is 1051 mm. It may be noted that the Malaprabha River originates in a region of high rainfall, and it is the main source of surface water for arid and semi-arid regions downstream of Malaprabha reservoir.

The data adopted for this study consists of monthly mean atmospheric variables simulated by Canadian Center for Climate Modeling and Analysis's (CCCma) third generation Coupled Global Climate Model (CGCM3). The data comprised of the 20th century simulations (20C3M) for the period of 1971–2000, and future simulations forced by four SRES scenarios namely, A1B, A2, B1 and COMMIT for the period of 2001–2100. Reanalyzed data of the monthly mean atmospheric variables prepared by National Centers for Environmental Prediction (NCEP) for the period 1971–2000 were used. The data on observed precipitation were obtained from the Department of Economics and Statistics, Government of Karnataka, India, for the period of 1971–2000. The data on observed temperature were obtained from India Meteorological Department (IMD) for the period of 1978–2000. The details of the data are furnished in Table 12.1. For the sake of analysis, the GCM data were re-gridded to NCEP grid using Grid Analysis and Display System (GrADS) (Doty and Kinter 1993).

12.4 Methodology

The development of a downscaling model begins with the selection of probable predictors, followed by their stratification (which is optional and variable dependant), and training and validation of the model. The developed model is subsequently used to obtain projections of predictand for simulations of GCM.

12.4.1 Selection of Probable Predictors

The selection of appropriate predictors is one of the most important steps in a downscaling exercise (Fowler et al. 2007). The choice of predictors could vary from region to region depending on the characteristics of the large-scale atmospheric circulation and the predictand to be downscaled. Any type of variable can be used as predictor as long as it is reasonable to expect that there exists a relationship between the variable and the predictand. Often, in climate impact studies, only such variables are chosen as predictors that are: (i) reliably simulated by GCMs and are readily available from archives of GCM output and reanalysis data sets; (ii) strongly correlated with the predictand; and (iii) based on previous studies. The number of probable predictors is referred to as m_1 in this chapter.

12.4.2 Stratification of Predictors

For the sake of stratification of predictors, the m_2 climate variables (potential predictors), which are realistically simulated by the GCM, were selected from the m_1

probable predictors, by specifying a threshold value (T_{ng1}) for correlation between the probable predictor variables in NCEP and GCM data sets. For the estimation of correlation, product moment correlation (Pearson 1896), Spearman's rank correlation (Spearman 1904a and b) and Kendall's tau (Kendall 1951) were considered.

Table 12.1 The details of the meteorological data used in the study

Data type	Source of data	Period	Details	Time scale
Observed data of precipitation	Dept. of Economics & Statistics, Government of Karnataka (GOK), India	1971–2000	Data at 11 gauging stations are used to arrive at representative values of precipitation for the basin	Daily
Observed data of temperature	India Meteorological Department (IMD)	1978–2000	Data at 2 gauging stations namely Santhebasthewadi and Gadag	Daily
CGCM3 T/47 data on atmospheric variables	http://www.cccma.bc.ec.gc.ca/cgi-bin/data/cgcm3	1971–2100; baseline: 20C3M (1971–2000); future: SRES A1B, A2, B1 & COMMIT (2001– 2100).	12 grid points for atmospheric variables, with grid spacing ≈ 3.75°. Latitudes range: 9.28°N to 20.41°N. Longitudes range: 71.25°E to 78.75°E	Monthly
NCEP re-analysis data of atmospheric variables	Kalnay et al. (1996)	1971–2000	9 grid points for atmospheric variables, with grid spacing 2.5°. Latitudes range: 12.5°N to 17.5°N. Longitudes range: 72.5°E to 77.5°E	Monthly
NCEP re-analysis data of atmospheric fluxes	Kalnay et al. (1996)	1971–2000	16 grid points for atmospheric fluxes with grid spacing 1.9°. Latitudes range: 12.3°N to 20.0°N longitude range : 71.6°E to 77.5°E	Monthly

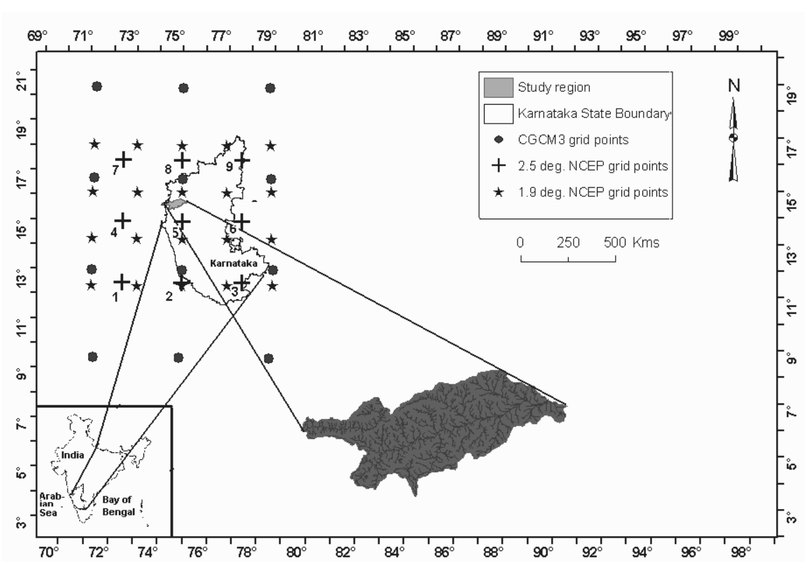

Figure 12.2. Location of the study region in Karnataka State, India. The latitude, longitude and scale of the map refer to Karnataka State. The data extracted at CGCM3 and 1.9° NCEP grid points are re-gridded to the nine 2.5° NCEP grid points. Among the nine grid points 1, 4 and 7 are on Arabian Sea, and the remaining points are on land

Depending on the predictand variable to be downscaled, the stratification of the corresponding potential predictors was carried out in space (land and ocean) or in time (e.g., wet and dry seasons). When precipitation was considered as predictand, the stratification of the predictors was carried out in time domain to form clusters corresponding to wet and dry seasons. When maximum and minimum temperatures were considered as predictands, the stratification of predictors was carried out in space domain. The following part of this subsection outlines finer details on the procedure suggested for stratification of potential predictors in the context of downscaling precipitation and temperature.

Stratification of Predictors for Downscaling Precipitation. The climate of a region can be broadly classified into seasons for analyzing precipitation. The predictor variables for downscaling a predictand could vary from season to season. Further the relationship between the predictor variables and the predictand varies seasonally because of the seasonal variation of the atmospheric circulation (Karl et al. 1990). Hence seasonal stratification has to be performed to select the appropriate predictor variables for each season to facilitate development of a separate downscaling model for each of the seasons. The seasonal stratification can be carried out by defining the seasons as either conventional (fixed) seasons or as ''floating'' seasons. In fixed season stratification, the starting dates and lengths of seasons remain the same for every year. In contrast, in “floating” season stratification, the date of onset and duration of each season is allowed to change from year to year. Past studies have shown that floating seasons are better than the fixed seasons, as they reflect ‘natural’ seasons, especially under altered climate conditions (Winkler et al. 1997). Therefore identification of the floating seasons under altered climate conditions helps to effectively model the relationships between predictor variables and predictands for each season, thereby enhancing the performance of the downscaling model. Hence, for the case study presented in this chapter, the floating method of seasonal stratification is considered to identify dry and wet seasons in a calendar year for both NCEP and GCM data sets. In the floating method of seasonal stratification, the NCEP data are partitioned into two clusters depicting wet and dry seasons by using the K-means clustering method (MacQueen 1967), whereas the GCM data are partitioned into two clusters by using the nearest neighbor rule (Fix and Hodges 1951).

From NCEP data on the m_2 variables, n principal components (PCs), which preserve more than 98% of the variance, are extracted using principal component analysis (PCA). The PCs corresponding to each month are used to form a feature vector for the month. The PCs are also extracted from GCM data, but along the principal directions obtained for the NCEP data. They are used to form feature vectors for GCM data. Each feature vector (representing a month) can be visualized as an object having a specific location in multidimensional space, whose dimensionality is defined by the number of PCs.

The feature vectors of the NCEP data are partitioned into two clusters (depicting wet and dry seasons) using the K-means cluster analysis. The clustering should be such that the feature vectors within each cluster are as close to each other as possible in space, and are as far as possible in space from the feature vectors of the other clusters. The distance between each pair of feature vectors in space is estimated using Euclidian measure. Subsequently, each feature vector of the NCEP data is assigned a label that denotes the cluster (season) to which it belongs. Following this, the feature vectors prepared from GCM data (past and future) are labeled using the nearest neighbor rule to get the past and future projections for the seasons. As per this rule, each feature vector formed using the GCM data is assigned the label of its nearest neighbor from among the feature vectors formed using the NCEP data. To determine the nearest neighbors for this purpose, the distance between each pair of NCEP and GCM feature vectors is computed using Euclidean measure. Comparison of the labels of contemporaneous feature vectors formed from NCEP and GCM past data is useful in checking if the GCM simulations represent the regional climate fairly well, during the past period.

Optimal T_{ng1} is identified as a value for which the wet and dry seasons formed for the study region using NCEP data are well correlated with the possible true seasons for the region. For this analysis, the plausible true wet and dry seasons in the study region are identified using a method based on truncation level (TL). In this method, the dry season is considered as consisting of months for which the estimated Theissen Weighted Precipitation (TWP) values for the region are below the specified TL, whereas the wet season is considered as consisting of months for which the estimated TWP values are above the TL. Herein, two options have been used to specify the TL. In the first option, the TLs are chosen as various percentages of the observed mean monthly precipitation (MMP) (70 to 100% of MMP at intervals of 5%). In the second option, the TL is chosen as the mean monthly value of the actual evapotranspiration in the river basin. The actual evapotranspiration is obtained for Krishna basin from Gosain et al. (2006). The potential predictors corresponding to optimal T_{ng1} are noted.

Stratification of Predictors for Downscaling Surface Temperature. The surface temperature in a region is dominated by local effects such as evaporation, sensible heat flux and vegetation in the region. Therefore the potential predictor variables influencing surface temperature in the study region are stratified based on the location of grid points (land and/or ocean) corresponding to the variables, to assess the impact of their use on downscaled temperature. Out of the nine 2.5° NCEP grid points considered in the study region, six are above land and the remaining three are over sea. As there are no distinct seasons based on temperature, seasonal stratification as in the case of precipitation is not relevant.

12.4.3 SVM Downscaling Model

For downscaling the predictand, the m_1 probable predictors at each of the NCEP grid points will be considered as probable predictors. Thus, there are m_3 (= m_1 × number of NCEP grid points) probable predictor predictors. The potential predictors (m_4) are selected from the m_3 probable predictor variables. For this purpose, the cross-correlations are computed between the probable predictor variables in NCEP and GCM data sets, and the probable predictor variables in NCEP data set and the predictand. A pool of potential predictors is then identified for each season by specifying threshold values for the computed cross-correlations. The threshold value for cross-correlation between variables in NCEP and GCM data sets is denoted hereafter by T_{ng2}, whereas the same between NCEP variables and predictand is depicted as T_{np}. The T_{np} should be reasonably high to ensure choice of appropriate predictors for downscaling the predictand. Similarly, T_{ng2} should also be reasonably high to ensure that the predictor variables used in downscaling are realistically simulated by the GCM in the past, so that the future projections of the predictand obtained using GCM data would be acceptable.

The downscaling model is calibrated to capture the relationship between NCEP data on potential predictors and the predictand. The data on potential predictors is first standardized for each season or location separately for a baseline period. Such standardization is widely used prior to statistical downscaling to reduce systemic bias (if any) in the mean and variance of the predictors in the GCM data, relative to those of the same in the NCEP reanalysis data (Wilby et al. 2004). This step typically involves subtraction of mean and division by the standard deviation of the predictor for the baseline period. The standardized NCEP predictor variables are then processed using PCA to extract such PCs which are orthogonal and which preserve more than 98% of the variance originally present in them. A feature vector is formed for each month using the PCs. The feature vector forms the input to the SVM model, and the contemporaneous value of predictand is its output. The PCs account for most of the variance in the input and also remove the correlations, if any, among the input data. Hence, the use of PCs as input to a downscaling model helps in making the model more stable and at the same time reduces the computational load.

To develop the SVM downscaling model, the feature vectors formed are partitioned into a training set and a testing set. The partitioning was initially carried out using multifold cross-validation procedure, which was adopted from Haykin (2003) in an earlier work (Tripathi et al. 2006). In this procedure, about 70% of the feature vectors are randomly selected for training the model, and the remaining 30% are used for validation. However, in this study the multifold cross-validation procedure is found to be ineffective because the time span considered for analysis is small and there are more extreme events in the past decades than in the recent decade. Therefore, the feature vectors formed from approximately first 70% of the available data are chosen for calibrating the model and the remaining feature vectors are used for validation. The 'normalized mean square error' is used as an index to assess the performance of the model. The training of SVM involves selection of the model parameters σ and C. The width of RBF kernel σ gives an idea about the smoothness of the derived function. Smola et al. (1998), in their attempt to explain the regularization capability of RBF kernel, have shown that a large kernel width acts as a low-pass filter in frequency domain. It attenuates the higher order frequencies, resulting in a smooth function. Alternately, RBF with a small kernel width retains most of the higher order frequencies leading to an approximation of a complex function by the learning machine. In this study, grid search procedure (Gestel et al. 2004) is used to find the optimum range for each of the parameters. Subsequently, the optimum values of the parameters are obtained from within the selected ranges, using the stochastic search technique of genetic algorithm (Haupt and Haupt 2004).

The feature vectors prepared from GCM simulations are processed through the validated SVM downscaling model to obtain future projections of the predictand, for each of the four emission scenarios considered (i.e., SRES A1B, A2, B1 and COMMIT). Subsequently, for each scenario, the projected values of the predictand are chronologically divided into five parts (2001–2020, 2021–2040, 2041–2060, 2061–2080 and 2081–2100) to determine the trend in the projected values of the predictand. The procedure is illustrated in the flowchart in Figure 12.3.

12.5 Results

The results of the downscaled precipitation, maximum and minimum temperatures are discussed in this section.

12.5.1 Predictor Selection

For downscaling precipitation, the predictor variables are screened on the twin basis that monsoon rain is dependent on dynamics through advection of water from the surrounding seas and thermodynamics through effects of moisture and temperature, both of which can modify the local vertical static stability. In a changed climate scenario, both the thermodynamic and dynamic parameters may undergo changes. Therefore in the present study, only such probable predictor variables, which incorporate both the effects, are chosen. Winds during south-west monsoon season advect moisture into the region while temperature and humidity are associated with local thermodynamic stability and hence are useful as predictors. Zonal wind is the response to heating in the monsoon trough in the North India. Meridional wind has more local effects, and together the winds are responsible for convergence of moisture and hence related to precipitation. Temperature affects the moisture holding capacity and the pressure at a location. The pressure gradient affects the circulation which in turn affects the moisture brought into the place and hence the precipitation. Higher precipitable water in the atmosphere means more moisture, which in turn causes statically unstable atmosphere leading to more vigorous overturning, resulting in more precipitation. Lower pressure leads to more winds and so more precipitation. At 925 mb pressure height, the boundary layer (near surface effect) is important. The 850 mb pressure height is the low level response to regional precipitation. The 200 mb pressure level depicts the global scale effects. Temperature at 700 mb and 500 mb represent the heating process of the atmosphere due to monsoonal precipitation which is maximum at mid-troposphere on a constant pressure height. Geopotential height represents the pressure variation, which reflects the flow, based on which the moisture changes. Due to these reasons, fifteen probable predictors are extracted from the NCEP reanalysis and CGCM3 data sets. They are the air temperature at 925 mb

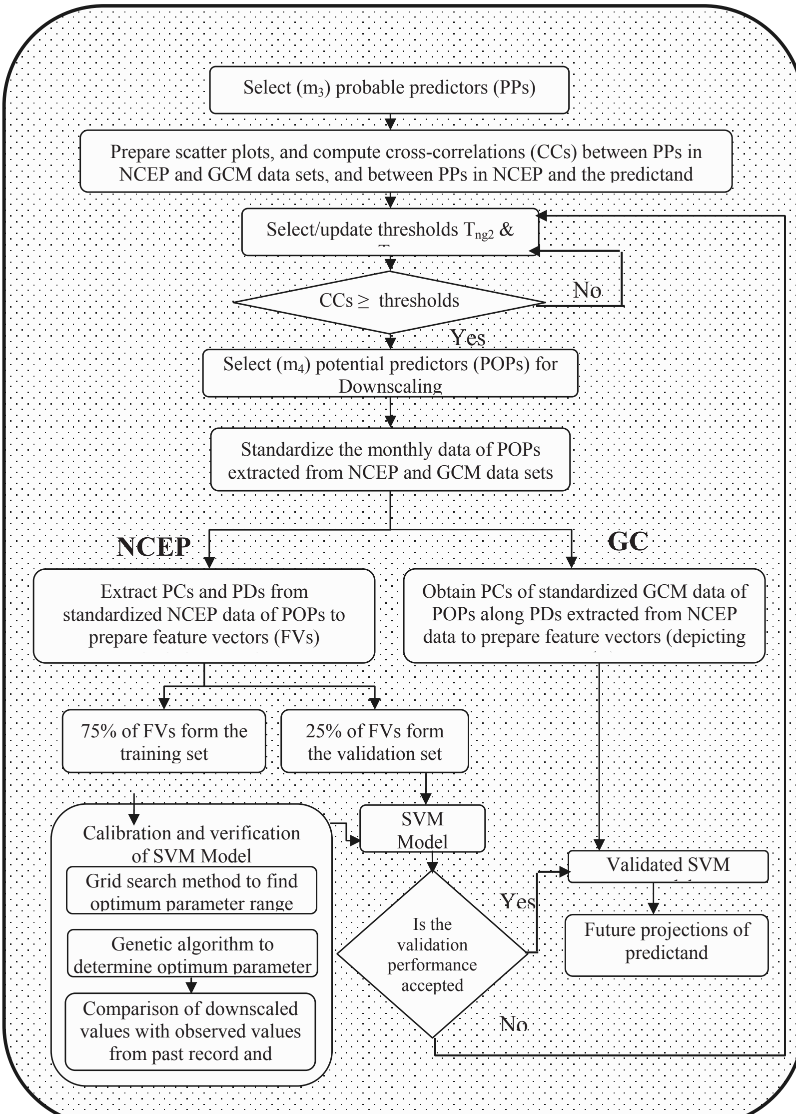

Figure 12.3. Methodology followed for SVM downscaling. PCs and PDs denote principal components and principal directions, respectively. T_{ng2} is the threshold between predictors in NCEP and GCM data sets. T_{np} denotes the threshold between predictors in NCEP data and the predictand

(Ta 925), 700 mb (Ta 700), 500 mb (Ta 500) and 200 mb (Ta 200) pressure levels, geo-potential height at 925 mb (Zg 925), 500 mb (Zg 500) and 200 mb (Zg 200) pressure levels, specific humidity at 925 mb (Hus 925) and 850 mb (Hus 850) pressure levels, zonal (Ua) and meridional wind velocities (Va) at 925 mb (Ua 925, Va 925) and 200 mb (Ua 200, Va 200) pressure levels, precipitable water (prw) and surface pressure (ps).

For downscaling temperature, large scale atmospheric variables, namely air temperature, zonal and meridional wind velocities at 925 mb, which are often used, are considered as predictors. Surface flux variables, namely latent heat, sensible heat, shortwave radiation and longwave radiation fluxes can also be considered for downscaling temperature as they control the temperature of the earth's surface. The incoming solar radiation heats the surface, while latent heat flux, sensible heat flux, and longwave radiation cool the surface. Due to these reasons, seven probable predictors are extracted from the NCEP reanalysis and CGCM3 data sets to downscale temperature. They are air temperature, zonal, and meridional wind velocities at 925 mb, and four fluxes: latent heat (LH), sensible heat (SH), shortwave radiation (SWR), and longwave radiation (LWR).

12.5.2 SVM Downscaling Models

From the selected potential predictors for each season, principal components are extracted to form feature vectors. These feature vectors are provided as input to develop SVM downscaling model following the procedure described in Section 12.4. For obtaining the optimal range of each of the SVM parameters (kernel width σ, and penalty term C), the grid search procedure is used. Typical results of the domain search performed to estimate the optimal ranges of the parameters for wet and dry seasons are shown in Figure 12.4. From this figure, the range of σ and C having the least NMSE (Normalized Mean Square Error) is selected as the optimum parameter range. The NMSE values are indicated in the bar code provided close to the two parts of the figure. Using Genetic algorithm, the optimum parameter is selected from the optimum parameter range. The optimal values of SVM parameters C and σ thus obtained are 550 and 50 for wet season, and 850 and 50 for dry season, respectively. For maximum temperature the optimal values of SVM parameters C and σ are 2050 and 50 while for minimum temperature 1050 and 50 were the optimal values of SVM parameters. The results of downscaling are compared with observed variables and showed in figure 12.5 The details of the downscaled variables were elaborated in Anandhi et al. (2008, 2009).

12.5.3 Projected Future Scenarios

The future projections of three meteorological variables (precipitation, maximum and minimum temperatures) were obtained for each of the four SRES scenarios (A1B, A2, B1 and COMMIT) using the developed SVM downscaling models. The projections were subsequently divided into five 20-year intervals (2001–2020, 2021–2040, 2041–2060, 2061–2080, 2081–2100). The mean monthly values of observed and projected precipitation for the study area were estimated using the Theissen method. For each of the four SRES scenarios, average of the mean monthly values of Theissen weighted precipitation, maximum and minimum temperatures are presented as bar plots, for all the five 20-year intervals in Figures 12.6, 12.7 and 12.8 respectively. These plots facilitate in assessing the projected changes in each meteorological variable across twenty-year intervals over the period of 2001–2100, with respect to the past (20C3M), for each SRES scenario. Secondly, for each of the five 20-year intervals, the average of the mean monthly values of the aforementioned variables are plotted individually, for all the five scenarios (20C3M, SRES A1B, A2, B1 and COMMIT) in Figures 12.9, 12.10 and 12.11 respectively. These plots facilitate comparison of the past and projected mean monthly values of each meteorological variable across SRES scenarios, for each 20-year interval, and thus, help in assessing the changes in the variables across all the months in a year.

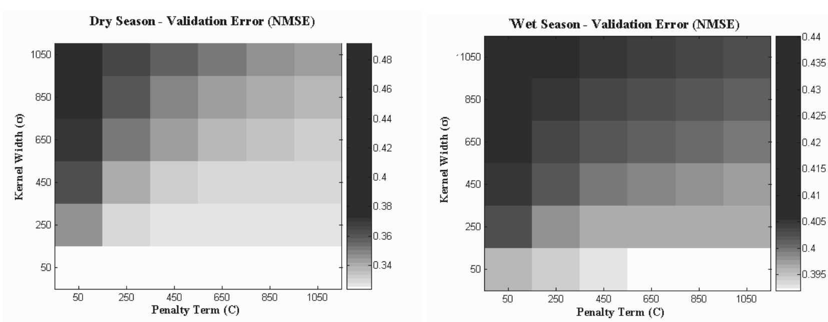

Figure 12.4. Illustration of the domain search performed to estimate optimal values of kernel width (σ) and penalty (C) for the SVM, for dry and wet seasons

From the figures it is observed that precipitation, and maximum and minimum temperatures are projected to increase in future for A1B, A2 and B1 scenarios, whereas no trend is discerned with the COMMIT. The projected increases are high for A2 scenario, whereas they are least for B1 scenario. This is because among the scenarios considered, the scenario A2 has the highest concentration of carbon dioxide (CO_2) equal to 850 ppm, while the same for A1B, B2 and COMMIT scenarios are 720 ppm, 550 ppm and ≈ 370 ppm respectively. Rise in the concentration of CO_2 in atmosphere causes the earth's average temperature to increase, which in turn causes increase in evaporation especially at lower latitudes. The evaporated water would eventually precipitate. In the COMMIT scenario, where the emissions are held the same as in the year 2000, no significant trend in the pattern of projected future precipitation could be discerned.

From a perusal of Figures 12.6, 12.7 and 12.8 it can be observed that, in general, for the meteorological variables, the change from past to future is gradual, and the change is more for A1B scenarios, while it is the least for B1 scenario. In A2 scenario the change is more and different from A1B. In the case of COMMIT no clear pattern change is visible.

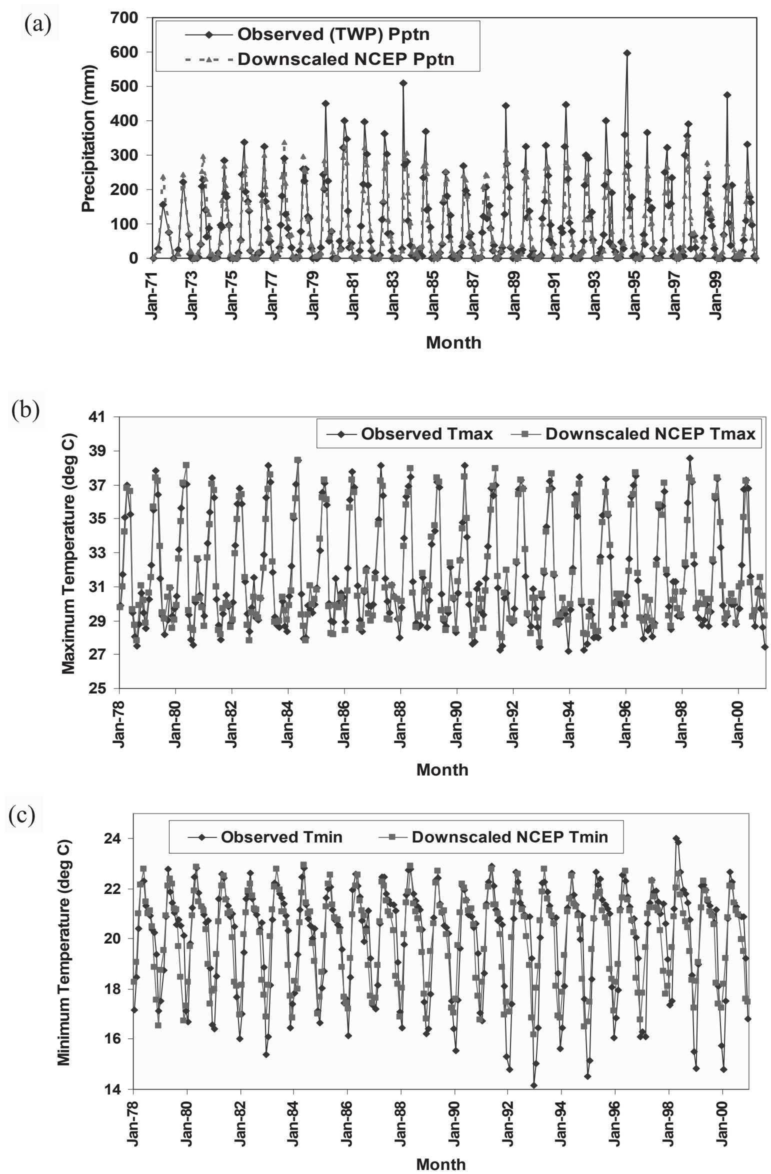

Figure 12.5. Comparison of the monthly observed meteorological variable with the corresponding simulated variable using SVM downscaling model for NCEP data (a) Thiessen weighted precipitation (TWP) (b) maximum temperature (Tmax) (c) minimum temperature (Tmin)

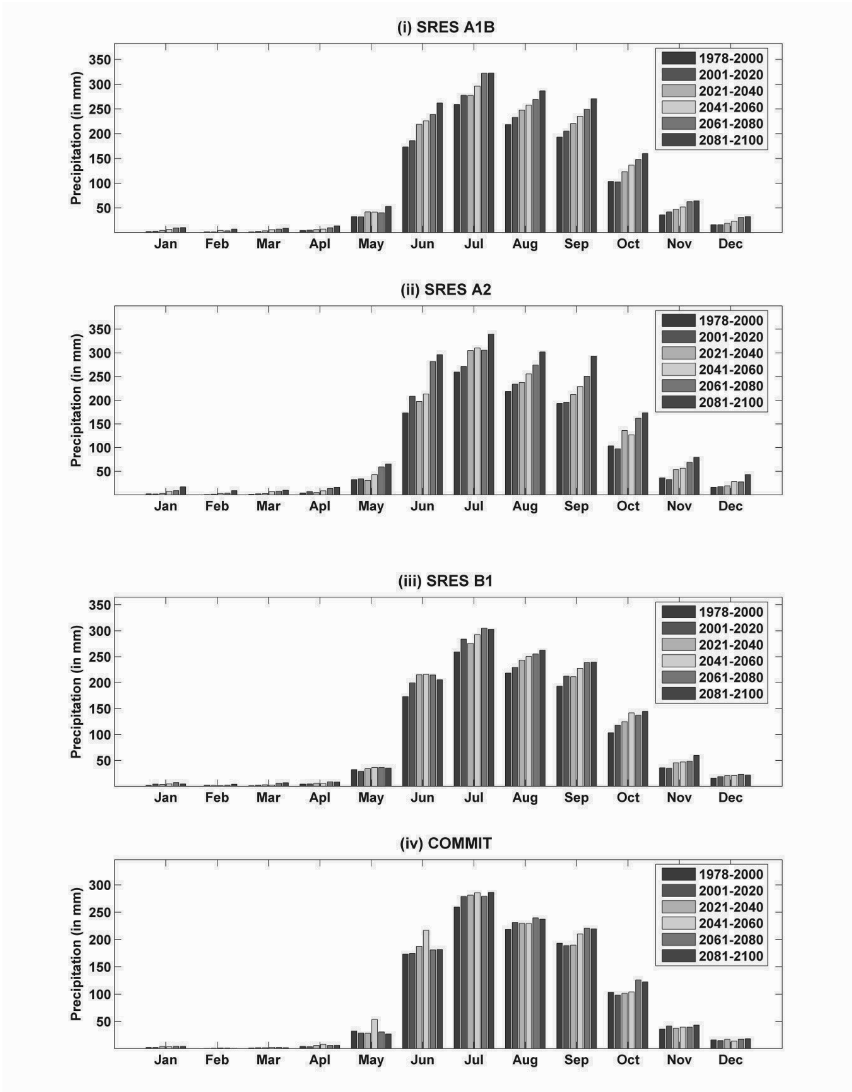

Figure 12.6. Mean monthly precipitation in the study region for the period 1971–2100, for the four scenarios considered

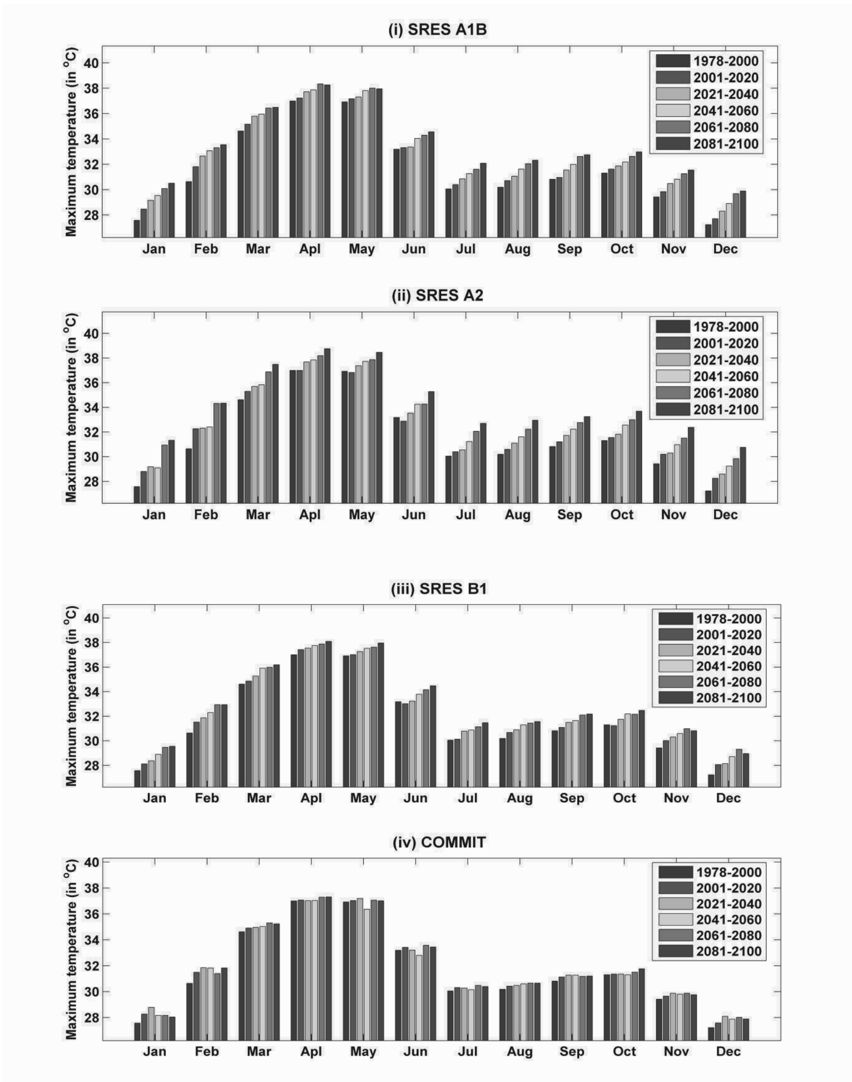

Figure 12.7. Mean monthly maximum temperatures in the study region for the period 1978–2100, for the four scenarios considered

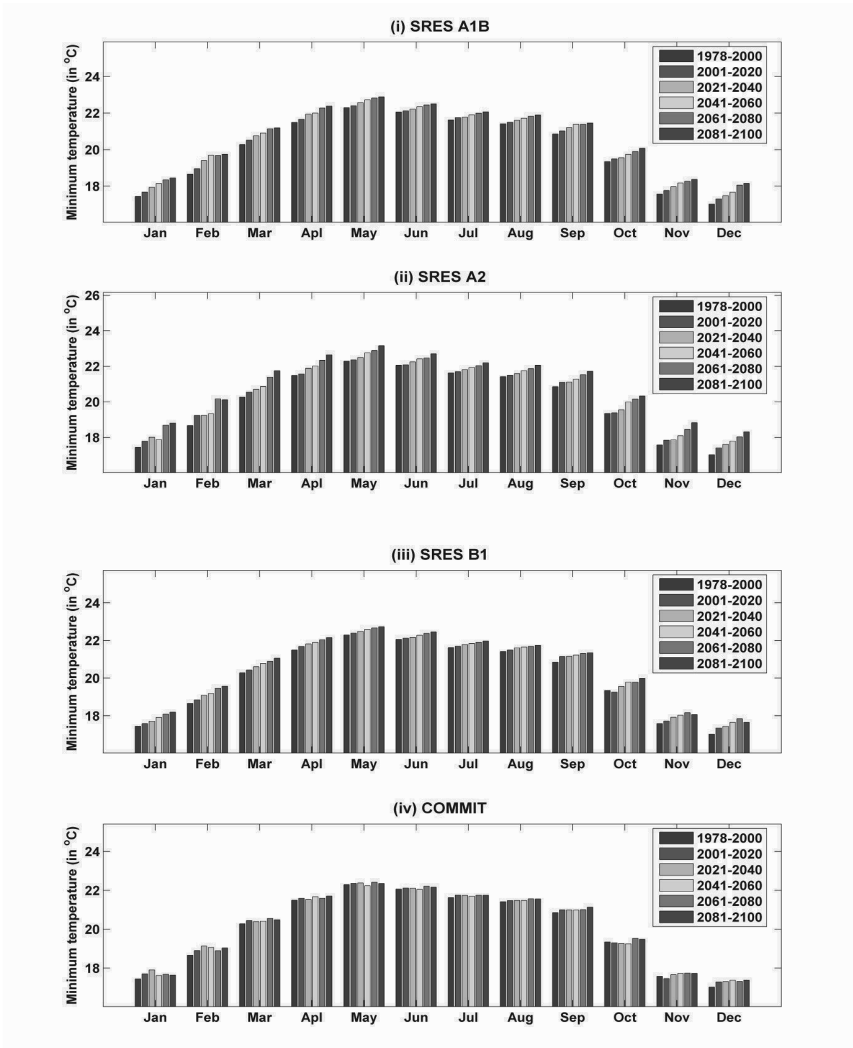

Figure 12.8. Mean monthly minimum temperatures in the study region for the period 1978–2100, for the four scenarios considered

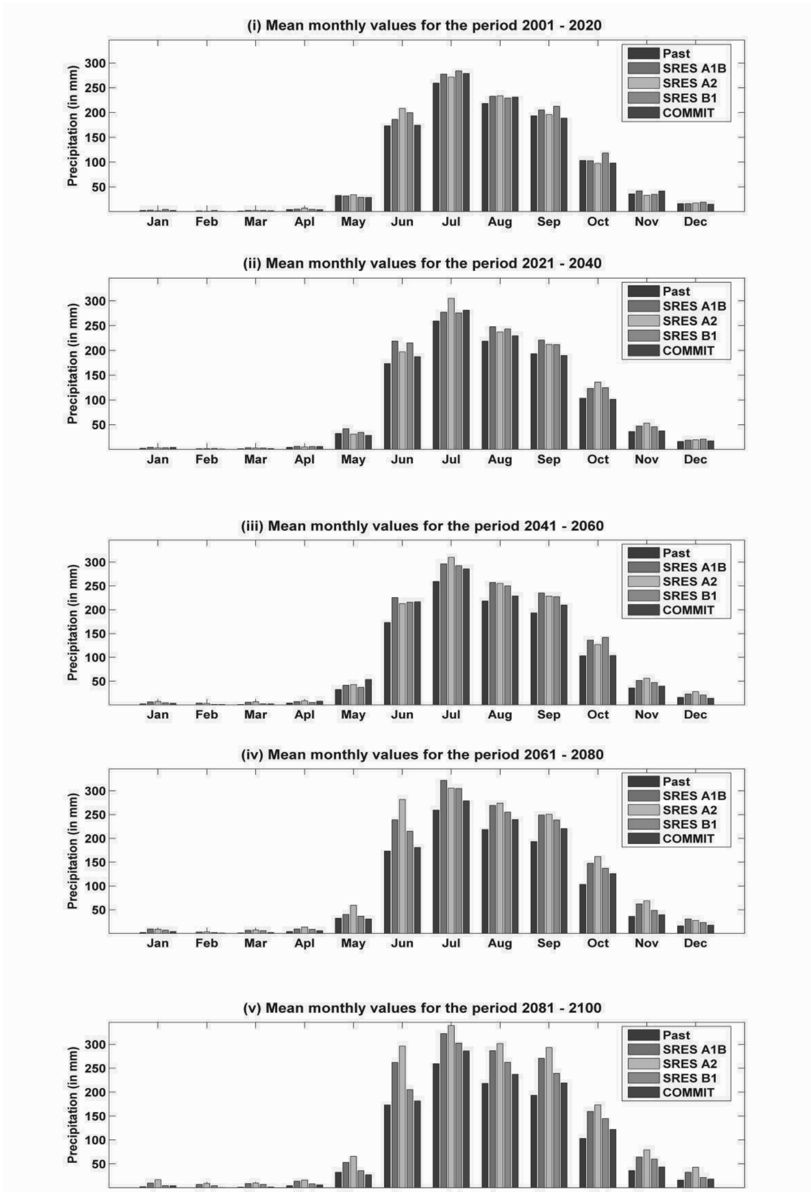

Figure 12.9. Projections obtained for 'mean monthly precipitation' in the study region for the four scenarios are compared with the past (20C3M) value of the statistic, for different future periods

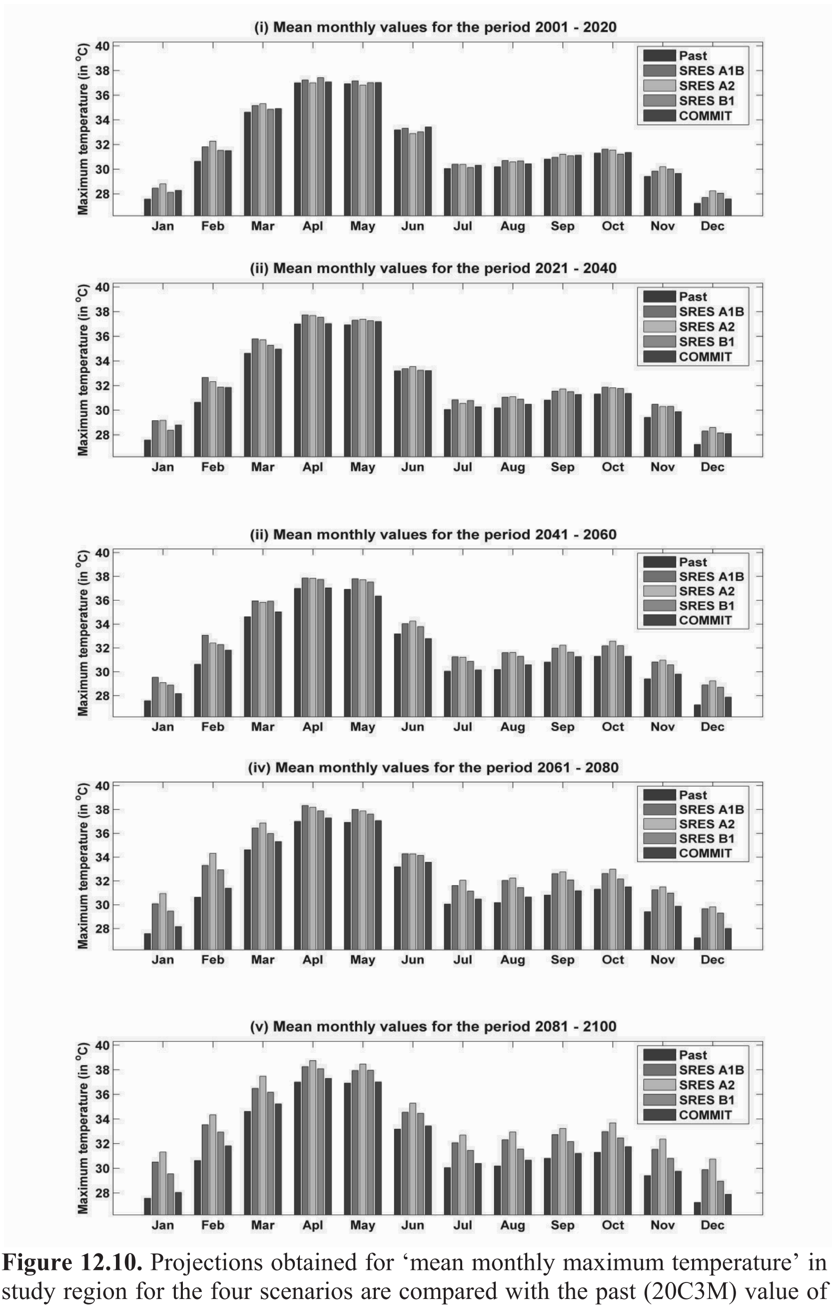

Figure 12.10. Projections obtained for 'mean monthly maximum temperature' in the study region for the four scenarios are compared with the past (20C3M) value of the statistic, for different future periods

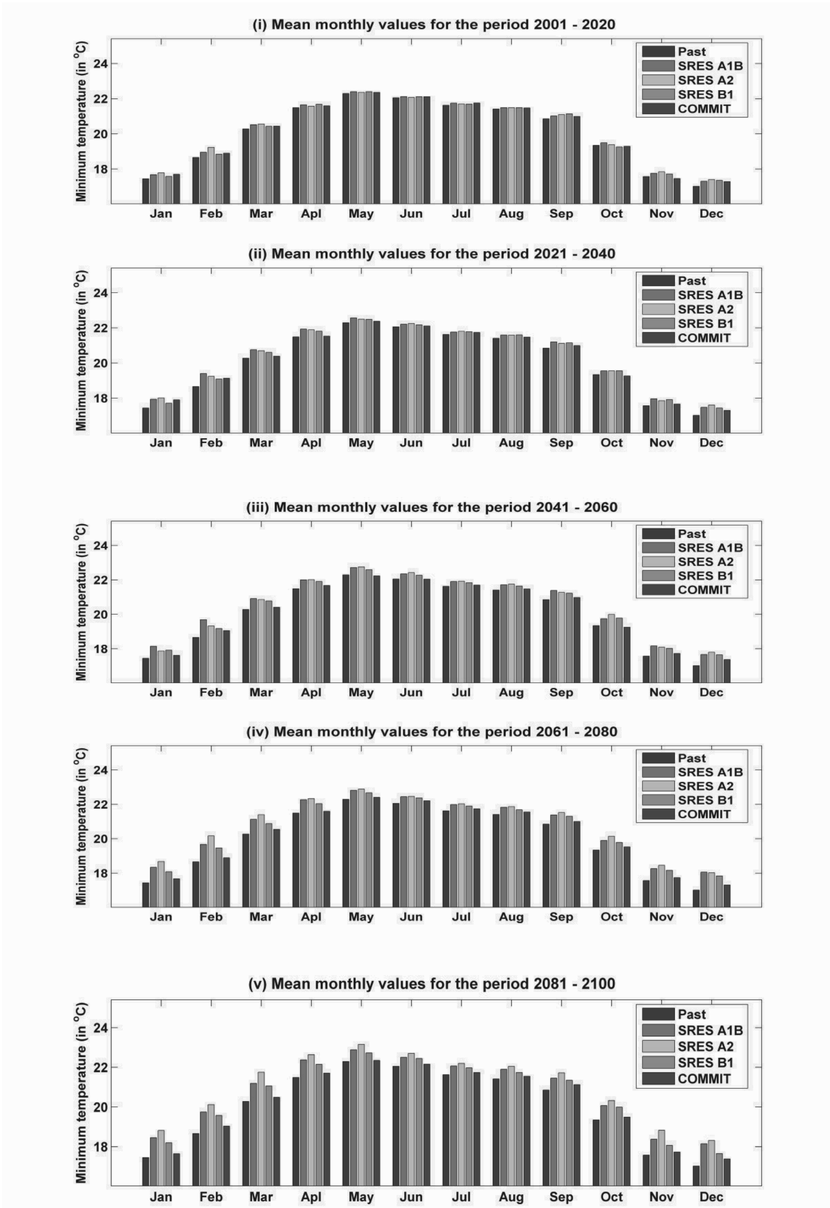

Figure 12.11. Projections obtained for 'mean monthly minimum temperature' in the study region for the four scenarios are compared with the past (20C3M) value of the statistic, for different future periods

From the Figures 12.9, 12.10 and 12.11 it can be inferred that the change in the variables is least in the first 20-year interval (2001–2020) and maximum in the last 20-year interval (2081–2100).

12.5.4 Impacts of Climate Change on Hydrology

The variables–precipitation and temperature play an important role in the hydrology of a river basin and are commonly used for impact studies. Some of the possible impacts of changes in the aforementioned variables are discussed in the following part of this subsection.

In general, changes in climate variables (precipitation and temperature) cause changes in the water balance, by changing the various components of hydrologic cycle such as runoff, evapotranspiration, soil moisture, infiltration and groundwater recharge.

Changes in precipitation and temperatures can affect the magnitude and timing of runoff, which in turn affect the frequency and intensity of hydrologic extremes such as floods and droughts. Changes in precipitation could be in the amount, distribution, intensity and frequency. Most of the precipitation in the region occurs in the monsoonal months (June to October). An increased precipitation amount, intensity and frequency during monsoon period could affect the frequency of floods while a decreased precipitation during the period could affect the frequency of drought. In general, the increase in surface temperatures modify the hydrologic cycle through changes in the volume, intensity, or type of precipitation (rain versus snow), and through shifts in the seasonal timing of stream flow (Regonda et al. 2005). In this region, with no snow cover, changes in temperature may not directly affect the runoff, but will cause changes in precipitation patterns and other climate variables and may also affect the evaporation and hence the runoff of the region. The changes in runoff affect the water resources infrastructure such as reservoirs. Reduced flow will mean less supply and potential economic damages, and increased flow may mean an under-designed reservoir or spillway with potential flood risk.

A change in temperature affects the evaporation, evapotranspiration, and desertification processes and is also considered as an indicator of environmental degradation and climate change. These changes affect soil moisture content. Apart from temperature, the other factors that affect the evaporative demand of the atmosphere include vapor-pressure deficit, wind speed and net radiation. Therefore implications of the change in all these factors on evaporative demand should be carefully analyzed. Increased temperature increases evaporation from the reservoirs and evapotranspiration from plants. Further, increased temperatures can cause warming of reservoir and rivers in the region which in turn will increase evaporation as well as will affect their thermal structure and water quality.

With changes in the various components of the hydrologic cycle, agriculture and the natural ecosystems in the river basins are affected. The growth of biological pests and diseases increases as temperature and relative humidity levels increase with increase in precipitation. Natural ecosystems such as forests, pastures, deserts, mountain regions, lakes, streams, wetlands, coastal systems and oceans may face difficulties in adapting, and it is also possible to lose some of the flora and fauna.

With increase in population, the demand of freshwater for domestic, industrial and agricultural uses definitely increases. This situation makes it prudent to assess the sensitivity of hydrological processes to the potential future changes in climate and population to meet the requirements. Incident solar radiation, relative humidity and wind speed are other variables that are also worth analyzing owing to their significance in effecting hydrological processes.

12.6 Conclusions

The Support Vector Machine (SVM) based models are developed to downscale monthly sequences of hydrometeorological variables (precipitation, maximum and minimum temperatures) in Malaprabha river catchment (upstream of Malaprabha reservoir) of Krishna river basin, India. The large scale atmospheric variables simulated by the third generation coupled Canadian GCM for various IPCC scenarios (SRES A1B, SRES A2, SRES B1 and COMMIT) were used to prepare inputs to the SVM models.

The variables, which include both the thermodynamic and dynamic parameters, and which have a physically meaningful relationship with the precipitation, are chosen as the probable predictors for downscaling precipitation. For downscaling temperatures, large-scale atmospheric variables often used for downscaling maximum and minimum temperatures, and fluxes which control the temperature at the earth's surface are chosen as plausible predictor variables in this study.

Precipitation, maximum and minimum temperatures are projected to increase in future for A1B, A2 and B1 scenarios, whereas no trend is discerned with the COMMIT. The projected increase in predictands is high for A2 scenario and is least for B1 scenario.

The implications of climate change on monthly values of each of the hydrometeorological variables are assessed. The changes in the intensity, frequency of extreme values need to be considered. Further, the uncertainties in the projections to the choice of downscaling methods and GCMs should also be considered to draw reliable conclusions about the possible impacts of climate change in the study region, which would help policy makers for realistic assessment, management and mitigation of natural disasters, and for sustainable development. Investigating these uncertainties is a future scope of the study.

Acknowledgements

This work is partially supported by Dept of Science and Technology, Govt. of India, through AISRF project no. DST/INT/AUS/P-27/2009. Third author acknowledges support from Ministry of Earth Sciences, Govt. of India, through project no. MoES/ATMOS/PP-IX/09.

12.7 References

Anandhi, A. (2010). "Assessing impact of climate change on season length in Karnataka for IPCC Scenarios." *Journal of Earth System Science*, 119(4), 447-460.

Anandhi, A., Srinivas, V. V., Kumar, D. N., and Nanjundiah, R. S. (2009). "Role of Predictors in Downscaling Surface Temperature to River Basin in India for IPCC SRES Scenarios using Support Vector Machine." *International Journal of Climatology*, 29(4), 583–603.

Anandhi, A., Srinivas, V. V., Nanjundiah, R. S., and Kumar, D. N. (2008). "Downscaling Precipitation to River Basin in India for IPCC SRES Scenarios using Support Vector Machine." *International Journal of Climatology*, 28(3), 401–420.

ASCE Task Committee (2000). "ASCE Task Committee, Artificial neural network in hydrology." *Journal of Hydrologic Engineering*, 5(2), 124–144.

Breiman, L., Friedman, J., Ohlsen, R., and Stone, J. (1984). *Classification and Regression Trees*. Wadsworth and Brooks, 358.

Brinkmann, W. (1999). "Application of non-hierarchically clustered circulation components to surface weather conditions: Lake Superior basin winter temperatures." *Theoretical and Applied Climatology*, 63, 41–56.

Conway, D., and Jones, P. D. (1998). "The use of weather types and air flow indices for GCM downscaling." *Journal of Hydrology*, 212-213, 348–361.

Conway, D., Wilby, R., and Jones, P. (1996). "Precipitation and air flow indices over the British Isles." *Climate Research*, 7, 169–183.

Cortes, C., and Vapnik, V. (1995). "Support vector networks." *Machine Learning*, 20, 273–297.

Courant, R., and Hilbert, D. (1970). *Methods of Mathematical Physics*, vols. I and II. *Wiley Interscience*, New York, USA.

Cristianini, N., and Shawe-Taylor, J. (2000). *An Introduction to Support Vector Machines and other kernel-based learning methods*. *Cambridge University Press*, Cambridge.

Doty, B., and Kinter, J. I., (1993). "The Grid Analysis and Display System (GrADS): a desktop tool for earth science visualization." American Geophysical Union 1993 Fall Meeting, San Fransico, CA, 6–10 December, 1993.

Enke, W., and Spekat, A. (1997). "Downscaling climate model outputs into local and regional weather elements by classification and regression." *Climate Research*, 8, 195–207.

Fix, E., and Hodges, J. (1951). *Discriminatory analysis: Nonparametric discrimination: Consistency properties.* In: *USAF School of Aviation Medicine* (Editor). Project 21-49-004.

Fowler, H. J., Blenkinsop, S., and Tebaldi, C. (2007). "Linking climate change modelling to impacts studies: recent advances in downscaling techniques for hydrological modelling." *International Journal of Climatology*, 27(12), 1547–1578.

Frakes, B., and Yarnal, B. (1997). "A procedure for blending manual and correlation-based synoptic classifications." *International Journal of Climatology*, 17, 1381–1396.

Gestel, T., Suykens, J., Baesens, B., Viaene, S., Vanthienen, J., Dedene, G., Moor, B., and Vandewalle, J. (2004). "Benchmarking least squares support vector machine classifiers." *Machine Learning*, 54(1), 5–32.

Ghosh, S., and Mujumdar, P. P. (2008). "Statistical downscaling of GCM simulations to streamflow using relevance vector machine." A*dvances in Water Resources*, 31, 132–146.

Gosain, A., Sandhya, R., and Debajit, B. (2006). "Climate change impact assessment on hydrology of Indian river basins." in special issue on Climate change and India, *Current Science*, 90(3), 346–353.

Govindaraju, R., and Rao, A. (Editors) (2000). *Artificial neural networks in hydrology*. Kluwer Academic Publishers, Holland, 348.

Haupt, R., and Haupt, S. (2004). "Practical Genetic Algorithms." *John Wiley and Sons*, New Jersey, 253.

Haykin, S. (2003). *Neural Networks: A comprehensive foundation*. Fourth Indian Reprint. *Pearson Education*, Singapore.

Hess, P., and Brezowsky, H. (Editors) (1969). "Katalog der Grosswetterlagen Europas." Selbstverlag des Deutschen Wetterdienstes 113(15). Offenbach am Main, Germany, 56.

Hughes, J., Guttorpi, P., and Charles, S. (1999). "A non-homogeneous hidden Markov model for precipitation occurrence." *Applied Statistics*, 48, 15–30.

Hush, D. R., and Horne, B. G. (1993). "Progress in supervised neural networks: What's new since Lippmann?" *IEEE Signal Processing Magazin*e, 10, 8–39.

Huth, R., Nemesova, I., and Klimperova, N. (1993). " Weather categorization based on the average linkage clustering technique: An application to European mid-latitudes." *International Journal of Climatology*, 13, 817–835.

Kalnay, E., Kanamitsu, M., Kistler, R., Collins, W., Deaven, D., Gandin, L., Iredell, M., Saha, S., White, G., Woollen, J., Zhu, Y., Chelliah, M., Ebisuzaki, W., Higgins, W., Janowiak, J., Mo, K. C., Ropelewski, C., Wang, J., Leetmaa, A., Reynolds, R., Jenne, R., and Joseph, D. (1996). "The NCEP/NCAR 40-year reanalysis project." *Bulletin of the American Meteorological Society*, 77(3), 437–471.

Karl, T., Wang, W., Schlesinger, M., Knight, R., and Portman, D. (1990). "A method of relating general circulation model simulated climate to the observed local climate Part I: Seasonal statistics." *Journal of Climate*, 3, 1053–1079.

Keerthi, S. S., and Lin, C.J. (2003). "Asymptotic behaviors of support vector machines with Gaussian kernel." *Neural Computation*, 15(7), 1667–1689.

Kendall, M. G. (1951). *Regression, Structure And Functional Relationship. Part I. Biometrika*, 38, 11–25.

Kidson, J. (1994). "Anautomated procedure for the identification of synoptic types applied to the New Zealand region." *International Journal of Climatology*, 14, 711–721.

Lamb, H., (1972). *British Isles weather types and a register of daily sequence of circulation patterns, 1861–1971. Geophysical Memoir*, 116. HMSO, London.

Lin, H. T., and Lin, C. J. (2003). "A study on sigmoid kernels for SVM and the training of non-PSD kernels by SMO-type methods." Department of Computer Science and Information Engineering, *National Taiwan University*, Taiwan.

MacQueen, J. (Editor) (1967). "Some methods for classification and analysis of multivariate observation." *Proceedings of the fifth Berkeley Symposium on mathematical statistics and probability*. *University of California Press*, Berkeley, 281-297.

Mercer, J. (1909). "Functions of positive and negative type and their connection with the theory of integral equations." P*hilosophical Transactions of the Royal Society*, London, A 209, 415–446.

Nakicenovic, N., Alcamo, J., Davis, G., de Vries, B., Fenhann, J., Gaffin, S., Gregory, K., Grübler, A., Jung, T., Kram, T., La Rovere, E., Michaelis, L., Mori, S., Morita, T., Pepper, W., Pitcher, H., Price, L., Raihi, K., Roehrl, A., Rogner, H., Sankovski, A., Schlesinger, M., Shukla, P., Smith, S., Swart, R., van Rooijen, S., Victor, N., and Dadi, Z. (2000). *IPCC Special Report on Emissions Scenarios*, Cambridge, United Kingdom and New York, NY, USA.

Pearson, K. (1896). "Mathematical contributions to the theory of evolution III regression heredity and Panmixia." *Philosophical Transactions of the Royal Society of London* Series 187, 253–318.

Regonda, S. K., Rajagopalan, B., Clark, M., and Pitlick, J. (2005). "Seasonal cycle shifts in hydroclimatology over the western United States." *Journal of Climate*, 18(2), 372–384.

Sastry, P. (2003). "An Introduction to Support Vector Machines." In *Computing and information sciences: Recent trends*. Narosa Publishing House: New Delhi.

Schölkopf, B., Burges, C., and Smola A., (1998). *Advances in Kernel Methods:* Support Vector Learning. MIT Press, 386.

Schubert, S., and Henderson-Sellers (1997). "A statistical model to downscale local daily temperature extremes from synoptic-scale atmospheric circulation patterns in the Australian region." *Climate Dynamics*, 13, 223–234.

Smola, A., Scholkopf, B., and Muller, K. (1998). "The connection between regularization operators and support vector kernels." *Neural Networks*, 11(4), 637–649.

Spearman, C. (1904a). "'General intelligence' objectively determined and measured." *American Journal of Psychology*, 5, 201–293.

Spearman, C. (1904b). "Proof and measurement of association between two things." *American Journal of Psychology*, 15, 72–101.

Suykens, J. A. K. (2001). "Nonlinear modelling and support vector machines." IEEE Instrumentation and measurement technology conference, Budapest, Hungary, pp. 287–294.

Tatli, H., Dalfes, H., and Mentes, S. (2005). "Surface air temperature variability over Turkey and its connection to large-scale upper air circulation via multivariate techniques." *International Journal of Climatology*, 25, 161–180.

Tripathi, S., Srinivas, V. V., and Nanjundiah, R. S. (2006). "Downscaling of precipitation for climate change scenarios: A support vector machine approach." *Journal of Hydrology*, 330, 621–640.

Vapnik, V. (1995). *The nature of statistical learning theory*. *Springer*, New York.

Vapnik, V. (1998). *Statistical learning theory*. *Wiley*, New York.

Wang, Y., Leung, L. R., McGregor, J. L., Lee, D. K., Wang, W. C., Ding, Y., and Kimura, F. (2004). "Regional climate modeling: progress, challenges, and prospects." *Journal of the Meteorological Society of Japan*, 82, 1599–1628.

Wetterhall, F., Halldin, S., and Xu, C. (2005). "Statistical precipitation downscaling in central Sweden with the analogue method." *Journal of Hydrology*, 306, 136–174.

Wigley, T., Jones, P., Briffa, K., and Smith, G. (1990). "Obtaining subgrid scale information from coarse-resolution general circulation model output." *Journal of Geophysical Research-Atmospheres*, 95, 1943–1953.

Wilby, R. L., Charles, S. P., Zorita, E., Timbal, B., Whetton, P., and Mearns, L.O. (2004). *The guidelines for use of climate scenarios developed from statistical downscaling methods*. Supporting material of the Intergovernmental Panel on Climate Change (IPCC), prepared on behalf of Task Group on Data and Scenario Support for Impacts and Climate Analysis (TGICA). <http://ipccddc.cru.uea.ac.uk/guidelines/StatDown_Guide.pdf)> (accessed Apri 2011).

Wilby, R. L., Dawson, C. W., and Barrow, E. M. (2002). "SDSM–a decision support tool for the assessment of regional climate change impacts." *Environmental Modelling & Software*, 17(2), 147–159.

Wilks, D. S. (1999). "Multi-site downscaling of daily precipitation with a stochastic weather generator." *Climate Research*, 11, 125–136.

Winkler, J., Palutikof, J., Andresen, J., and Goodess, C. (1997). "The simulation of daily temperature time series from GCM output Part II: Sensitivity analysis of an empirical transfer function methodology." *Journal of Climate*, 10(10), 2514–2532.

CHAPTER 13

A New Framework for Modeling Future Hydrologic Extremes: Nested Bias Correction as a Precursor to Stochastic Rainfall Downscaling

Ashish Sharma, Rajeshwar Mehrotra, and Fiona Johnson

13.1 Introduction

General circulation models (GCMs) (also referred to as Global Climate Models) are widely used to simulate the present and future climate under assumed greenhouse gas emission scenarios (e.g., IPCC 2007). In general, a GCM is formulated using principles of conservation of mass, energy and momentum, with presumed changes in future climates being simulated by altering the concentration of greenhouse gases as a function of time, while keeping energy inputs into the system relatively unchanged. While GCMs are known to be able to simulate pressures, temperatures and humidity well, especially at the higher levels in the atmosphere, the uncertainty associated with their simulations increases as one approaches the land surface (Xu 1999). At the land surface, particularly at finer spatial scales, while simulations of pressure and temperature again exhibit greater reliability, the simulation of the hydrologic cycle (rainfall and ensuing flux changes in the surface and subsurface) is often limited in its ability to match the magnitude and variability our observed record displays. Of special concern to water managers is the uncertainty associated with GCM simulations of rainfall over the land surface; this uncertainty reduces when simulations are aggregated over long periods of time or large extents of space, but assumes considerably high proportions at scales corresponding to that of a mid-sized hydrologic catchment.

One of the reasons behind the limited ability of GCMs to simulate accurately on the land surface is the coarse grid resolution at which they are run. As a result, they are incapable of representing local sub-grid-scale features and dynamics that are often required for impact studies, especially at a catchment scale (Charles et al. 2004; IPCC 2007). Consequently, techniques have been developed to transfer the GCM output from coarse spatial scales to local or regional scales by means of downscaling. These downscaling techniques can be classified into two categories: "Dynamical downscaling" that uses regional climate models (RCMs) to simulate finer-scale physical processes (e.g., Giorgi et al. 2001; Mearns et al. 2004; Fowler et al. 2007);

and "Statistical downscaling" that is based on developing statistical relationships between the regional climate and pre-identified large-scale parameters (e.g. Mehrotra and Sharma 2005). A diverse range of statistical downscaling techniques has been developed over the past few years, with most falling into a category where the responses (precipitation) are related to predictors (coarse scale atmospheric and local scale time-lagged variables), or into a category where the responses are related to a discrete or continuous state, which is modelled as a function of atmospheric and local scale predictors (Bartholy et al. 1995; Hewitson and Crane 1996; Hughes et al. 1999; Charles et al. 2004; Mehrotra and Sharma 2005). There are limitations and assumptions involved in both techniques which contribute to the uncertainty of results (see also Yarnal et al. 2001; Fowler et al. 2007). Charles et al. (2004), IPCC (2007) and Fowler et al. (2007) provide good reviews and discussions of various downscaling techniques.

However, as both dynamical and statistical downscaling approaches rely on the raw GCM simulations to provide their boundary conditions or predictor variables, the accuracy of these simulations becomes important. Of special concern are the many biases that are present in GCM simulations of rainfall and many other variables of interest for simulation of the local hydroclimatology. One needs, either, considerable care in selecting the variables used for specifying the downscaling model, or, a procedure that can rectify any of the biases that are apparent, hence allowing the downscaling to proceed.

An added concern with biases in GCM simulations is the representation of low-frequency variability or long-term persistence in rainfall and other atmospheric variables. Incorrect modelling of this variability can lead to a poor simulation of periods of sustained low or high flows, or the “sustained extremes” of most interest in hydrologic design. As will be shown in later sections of this chapter, GCM simulations of rainfall and other atmospheric variables do suffer from a range of biases at the spatio-temporal scales of relevance in hydrology, including biases in the representation of low-frequency or interannual variability. Consequently, we emphasise the need for identifying and correcting these biases before using GCM simulations for downscaling and related applications, and present a recently developed procedure (termed Nested Bias Correction or NBC) (Johnson and Sharma 2012) to correct these biases and ensure the resulting simulations reflect the distributional and dependence attributes associated with the historical record.

While the NBC method is able to impart appropriate distributional and low-frequency variability attributes to the raw GCM data, the post-processed simulations are still limited by the coarse spatial resolution they are available at. The transformation to finer spatial resolutions is achieved using the Modified Markov Model (MMM, Mehrotra and Sharma 2010), a stochastic downscaling model designed to generate rainfall at multiple point locations in a catchment, and impart additional low-frequency variability in the resulting simulations. The MMM results in multiple replicates of the rainfall at multiple locations, allowing a risk-based assessment of any plans proposed to deal with changes to water availability in a future climate. This two-staged procedure (the NBC followed by the MMM) completes our framework for assessing climate change impacts to water resources systems at the catchment scale.

This chapter is presented as follows. The next section outlines the major sources of uncertainties in GCM simulations of variables relevant for hydrology, and illustrates the extent of biases. This is followed by the rationale for the Nested Bias Correction (NBC) procedure that is designed to impart appropriate distributional and persistence attributes across a range of time scales, to produce post-processed GCM simulations that are consistent with the observed record. Next, we present the rationale behind the MMM, that uses the post-processed (bias corrected) GCM outputs as the basis of generating multiple replications of point rainfall across the rain gauge network for the catchment it is applied to. The NBC and the MMM are presented here as two stages of a framework for catchment scale climate change impact assessment, with the intention of generating sequences that are better able to simulate the sustained extremes we consider important for water resources planning and design. We illustrate the utility of the proposed framework using an application of the CSIRO Mk3.0 GCM using three emission scenarios (B1, A1B, A2), using 45 long term rain gauges located in and around Sydney, Australia. We conclude the chapter by summarizing the main issues presented and drawing attention to the many problems still outstanding in the field.

13.2 Uncertainty in GCM Rainfall

GCMs operate at coarse resolutions which make it difficult to simulate processes that fall within the finer spatial scales being modeled. These processes can include local heating or cooling, energy balance over lakes or reservoirs or other extents of water, along with factors leading to local instability in the atmosphere that includes convection and the causation of orographic rainfall. As a result, while GCM simulations exhibit features consistent with observations when aggregated over large extents of space, and over long spans of time, they exhibit considerable mismatch when evaluated at the finer spatio-temporal scales available. This mismatch is amplified even more in the case of some variables, and has recently been quantified using the Variable Convergence Score (VCS) (Johnson and Sharma 2009), presented in Table 13.1 below.

The VCS is derived by comparing simulations of multiple variables for a future setting, the rationale being that if multiple GCMs agree on their projections for the same variable, there is a greater chance that the variable is being simulated accurately. The VCS is estimated by calculating the Coefficient of Variation (CV, or, standard deviation divided by the mean) of average monthly simulations for each GCM, for a given emission scenario and a time window in the future, for each grid cell in the region being assessed. These CVs are then expressed as an empirical cumulative distribution function and the averaged percentile associated with variable calculated. While the VCS metric is simplistic and suffers from the sensitivity to the manner in which the variable is estimated, it offers a clear way in which multiple variables (or time-periods/regions) can be compared. As can be noted from the VSS values in Table 13.1, rainfall exhibits the lowest score across the other atmospheric variables used.

Table 13.1. GCM variable convergence score for a 20-year window centered at 2030 for two SRES CO_2 emission scenarios (Johnson and Sharma 2009a, with permission from AMS)[a]

Variable	SRESA2 (%)	SRESB1 (%)
Temperature	72	82
Wind speed	42	50
Longwave Rad	24	24
Shortwave Rad	68	69
Specific Humidity	53	51
Precipitation	7	7
Precipitable water	53	53
Surface Pressure	97	99

[a] The skill score is ascertained based on the Coefficient of Variation (CV) across 21 model integrations chosen using rankings as per Perkins et al. (2007) using monthly values. A skill score of 100% denotes consistency in future simulations across the GCMs.

The uncertainty in GCM rainfall can also be inferred from the simulation results in Figure 13.1. Figure 13.1(a) shows the observed annual mean rainfall and Figure 13.1(b) the bias in the annual means from the CSIRO Mk3.5 GCM for Australia for 1961 to 2000. We see that over the relatively dry, flat interior of Australia, the model overpredicts the annual rainfall by up to 200% in some locations. In coastal areas, annual average rainfall is underestimated. In Figure 13.1(c) we present a comparison of the ratio of the projected changes in annual average rainfall by 2080 to the bias in the annual average rainfall for the 20th century. Areas shown in light grey are those where the ratio of the change is larger than the bias, medium grey shows areas where the change and bias are of the same order of magnitude. Areas shown in black indicate where the bias is much larger than the projected changes for the SRESA2 scenario.

It is well known that at a finer time scale i.e. daily, there are problems in the GCM simulated rainfall both in occurrence and intensity. Sun et al. (2006) found that GCMs tend to overestimate the number of days with rainfall less than 10 mm, whilst underestimating more intense events, with the errors cancelling each other out to give seasonal totals that can be reasonably realistic, although this is very model dependent (Randall et al. 2007). Other problems related to the modelling of daily rainfalls include preserving observed dry and wet spell lengths (Ines and Hansen 2006) and interannual variability of rainfall which is dependent on regional and global climate teleconnections, along with the nature and extent of this variability changes around the world.

Despite the problems with GCM rainfall simulations, impact assessment studies still require future projections of rainfall for a range of applications. Stochastic and dynamic downscaling both have been used in many studies in an attempt to provide better future rainfall projections. However, both stochastic and dynamic downscaling approaches tend to be highly specialized and are developed for a particular region or to address specific questions. Additionally, their use is impacted by the biases present in the raw GCM simulations, and can be especially misleading if these biases extend to the representation of inter-annual variability, resulting in misrepresentation of the sustained extremes so important for water related applications. In the next section, we present a simple methodology to correct the biases in GCM simulations at multiple time scales. The utility of this procedure is demonstrated by applying the procedure to the GCM derived rainfall and comparing the processed results with observations. In the subsequent section, we further demonstrate the usefulness of the procedure by applying it to GCM derived variables used in a stochastic downscaling and note the improvements.

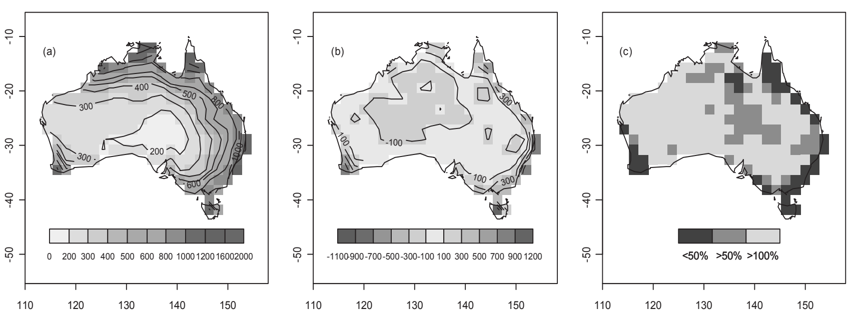

Figure 13.1. Biases in mean annual GCM rainfall outputs. a) Observed mean annual rainfall (mm/yr) for 1901 to 2000; b) mean annual bias (observed – modelled) in mean annual rainfall (mm/yr); and c) ratio of changes projected for SRESA2 for 2061 to 2080 compared to bias for 1901 to 2000

13.3 Nested Bias Correction (NBC)

Given the range of biases in GCM rainfall and other atmospheric variables, it is often necessary that corrective measures be taken to ensure simulations of the future which are of use in catchment scale applications. While such measures range from simply transforming the observed record by multiplicative scaling factors that are derived based on the proportional increases noted in GCM simulations of the future with respect to the current climate (known as scaling approaches, see Chiew et al. 2009), to more complex options that post-process GCM outputs to impart attributes that are notably biased, little has been done to accommodate biases in the representation of low-frequency variability that are so important in water related applications. The commonly used bias-correction procedures aim at reducing systematic biases in the mean and variance of GCM simulations relative to observations (or reanalysis data). The procedure routinely involves first standardising the GCM predictor series by removing the mean and standard deviation and thereafter adding the mean and standard deviation of the reanalysis predictor series for the predefined baseline period (Wilby et al. 2004). While many additional alternatives exist that focus on a range of attributes or time-scales of interest (see Wood et al. 2004; Ines and Hansen 2006; and Fowler et al. 2007 for details and associated references), little is available that can represent sustained extremes such as droughts in rainfall, and similar inter-annual or longer variability in other atmospheric variables. We present next the recently developed Nested Bias Correction (NBC) approach (Johnson and Sharma 2012) that attempts to formulate a simple basis for correcting biases across a range of time scales of interest.

13.3.1 The NBC Approach

The bias correction methods described above primarily focus on correcting for biases at a single time scale i.e. either monthly or daily, thus leading to a poor representation of any longer term attributes of interest. The issue of correctly modelling inter-annual variability in precipitation has been addressed by researchers looking at stochastic rainfall generation models. A nesting of daily generated rainfall sequences at the monthly level was used by Wang and Nathan (2007). Srikanthan and Pegram (2009) described a nested two part model wherein daily, stochastically generated, rainfalls are modified by nesting in monthly and annual data to ensure that the daily, monthly and annual statistics of the observed rainfall are reproduced in the simulations. Recently, Johnson and Sharma (2012) proposed a Nested Bias Correction (NBC) procedure that addresses the missing inter-annual variability by using statistics from the observed rainfall at multiple time scales. This procedure as used by Johnson and Sharma (2012, 2011a) to modify the daily GCM rainfall over Australia is discussed in detail in the following paragraphs.

In the NBC procedure (illustrated in Figure 13.2), daily GCM sequences (of rainfall or other variables), y, are modified by nesting the correction across a range of time-scales (typically daily, monthly and annual). The equation number is used as superscript to define the modified time series at each step. Also, subscript '*mod*' is used for GCM time series related statistics. Step 1 of the approach involves transforming the raw simulations into independent and identically distributed residuals by forming an inverse-autoregressive model. The first step is standardization of the simulations (y_i) for time-step i, using the mean (μ) and standard deviation (σ) of the model simulations for the current climate, as shown in equation 13.1a below.

$$y_i^{1a} = \frac{y_i - \mu_{\mathrm{mod},i}}{\sigma_{\mathrm{mod},i}} \qquad \text{(Eq. 13.1a)}$$

This is followed by the removal of the lag one autocorrelations ($\rho_{mod,i}$), under the assumption that the simulations follow a Markov Order 1 dependence structure, as per equation 13.1b.

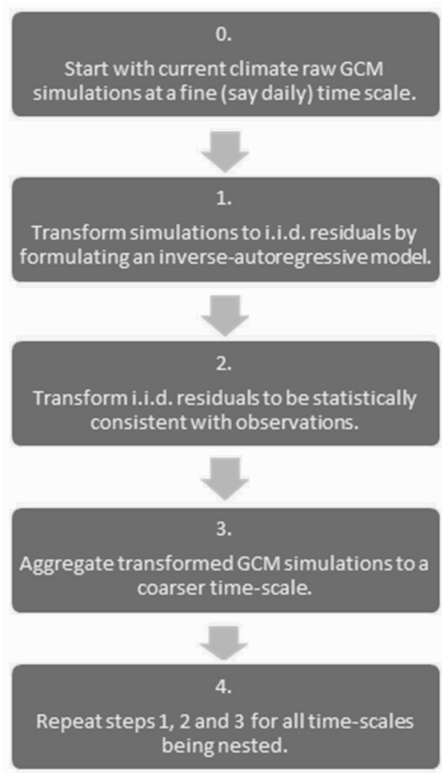

Figure 13.2. Proposed nesting bias correction logic. Note that "i.i.d." refers to independent and identically distributed, and "inverse-autoregressive" to the estimation of residuals after removing sample moments (standardization) and persistence attributes. Note that once the model (in steps 1 and 2) has been formed, it can then be used to transform GCM simulations for any future climate

$$y_i^{1b} = \frac{y_i^{1a} - \rho_{\text{mod},i}\, y_{i-1}^{1a}}{\sqrt{1-\rho_{\text{mod},i}{}^2}} \qquad \text{(Eq. 13.1b)}$$

The resulting residuals are independent and identically distributed (i.i.d.) if underlying assumptions are valid, and can now be transformed to represent the distributional attributes present in the historical record (step 2 in Figure 13.2). This transformation again assumes a Markov order 1 dependence structure, and leads to the following equation:

$$y_i^{2a} = \rho_{obs,i}\, y_{i-1}^{2a} + \sqrt{1-\rho_{obs,i}{}^2}\, y_i^{1b} \qquad \text{(Eq. 13.2a)}$$

$$y_i^{2b} = y_i^{2a}\sigma_{obs,i} + \mu_{obs,i} \qquad \text{(Eq. 13.2b)}$$

The resulting simulations now exhibit the same moments and lag one correlation as the observations, but only at the time scale being modeled. This implies that when aggregated to longer scales (such as monthly or annually, step 3 in Figure 13.2) there is a high possibility that the persistence and moments at those scales will be incorrectly represented. This is addressed by using the nesting procedure described next.

The nesting procedure (step 4 in Figure 13.2) involves repeating steps 1–3 at longer (aggregated) time scales, progressively correcting for biases in distributional and dependence attributes. In applying the approach to raw GCM rainfall simulations, we have limited the nesting to a monthly and annual time scale. Denoting these time scales as (d), (m) and (y), the NBC procedure can be expressed in the following single equation:

$$y_{d,m,y}^{NBC} = y_{d,m,y}\left(\frac{y_{d,m,y}^{2b}}{y_{d,m,y}}\right)\left(\frac{y_{m,y}^{2b}}{y_{m,y}}\right)\left(\frac{y_{y}^{2b}}{y_{y}}\right) \qquad \text{(Eq. 13.3)}$$

The NBC logic in Eq. (13.3) is formulated to ensure similarity of the GCM modeled simulations to the observed (historical) record. Therefore to correct GCM future simulations, the model is simply applied to future raw GCM simulations, with the correction statistics estimated based on the current climate observations. Because the method deals with correctly representing distributional and dependence attributes, future simulations are able to exhibit low-frequency variability even if raw model simulations do not. The post processed simulations are therefore suitable for use in water related applications, something that cannot be said for the raw GCM simulations. An illustration of the methodology using GCM simulated rainfall is presented next.

13.3.2 Application to Rainfall

Annual Rainfall. Comparative results for the nesting bias correction versus simpler approaches that do not nest across time scales are presented in this section. In the results that follow (summarized from Johnson and Sharma 2012), the simplified procedure represents the case where only monthly mean and standard deviations are corrected (termed as Monthly Bias Correction or MBC), whilst the nested algorithm outlined in Section 3.1 is termed as the Nested Bias Correction (NBC). Figure 13.3 shows the bias corrected rainfall using the MBC and NBC methods at the annual scale for the validation period of 1951 to 2000, using gridded rainfall over the 1901–1950 period as the "observed" record, and CSRIO Mk3.5 GCM rainfall in 1901–1950 as the "modeled" rainfall for the calibration period, and in 1951–2000 for the validation period. The number of points in each graph corresponds to one GCM grid cell in Australia. As can be noted from the figure, the NBC procedure offers a better representation of annual level persistence than the non-nested bias correction approach (MBC). This is expected to lead to a better representation of low-frequency variability, which is explored in greater detail next.

Inter-annual Rainfall Variability. The modeling of inter-annual variability can be measured using 2 and 5 year minimum rainfall from the raw and bias corrected simulations. These statistics are standardized by the mean annual rainfall to allow comparisons across Australia and presented in Figure 13.4 for the "validation" period (1951–2000) described above. By correcting the GCM outputs at the annual level for the lag one autocorrelation, the modeling of minimum rainfall totals is improved. This is important for ensuring that drought and flood periods are modelled correctly, particularly if the GCM outputs are being considered for analysis of dam capacities.

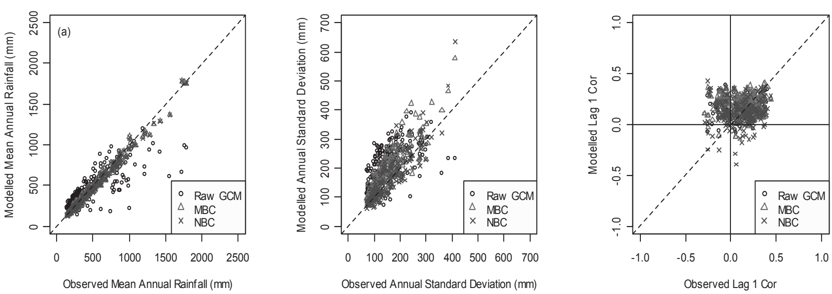

Figure 13.3. Modelled vs. observed statistics of annual rainfall for raw GCM outputs and MBC and NBC bias corrected models for a) annual mean, b) annual standard deviation and c) annual lag one autocorrelation (Johnson and Sharma 2012)

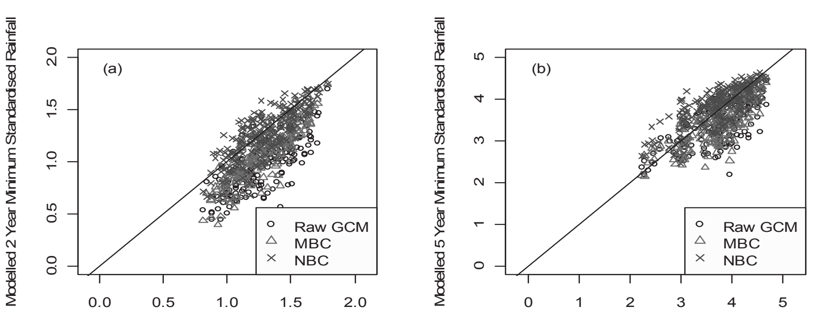

Figure 13.4. a) 2 year and b) 5 year minimum rainfall totals, standardised by mean annual rainfall (Johnson and Sharma 2012)

Drought. The results from an application of the bias corrected outputs for drought analysis using the Standardized Precipitation Index (SPI) are presented here. The SPI was developed to provide a simple calculation of drought (Guttman 1999) A time series of precipitation is fitted to a standard normal distribution and the quantiles of the fitted distribution are used to assess the severity of the drought. Negative values of the index occur during dry periods, with positive values indicating wet conditions. The SPI can be calculated for varying intervals; intervals of 1, 2 and 5 years are assessed and reported in this section.

Two alternative calculations using the SPI are carried out. The first compares the modelling of drought frequencies across Australia from the raw and bias corrected GCM outputs for the validation period of 1951–2000. Figure 13.5 shows scatter plots of the estimated 5th percentile of the SPI at each grid cell compared to the observed data for SPI values calculated for the three time periods. The 5th percentile has previously been defined as severe drought by Burke and Brown (2008).

Both bias correction methods improve the modelling of severe drought. The NBC is found to provide the best estimate of the magnitude of observed severe drought at each location. For both bias correction methods, performance is best when we calculate the SPI at a one year interval and decreases for increasing SPI intervals. This is to be expected as our nesting model only corrects for lag one autocorrelations. We would require a measure of longer term persistence in our model to capture the variations of drought over longer periods.

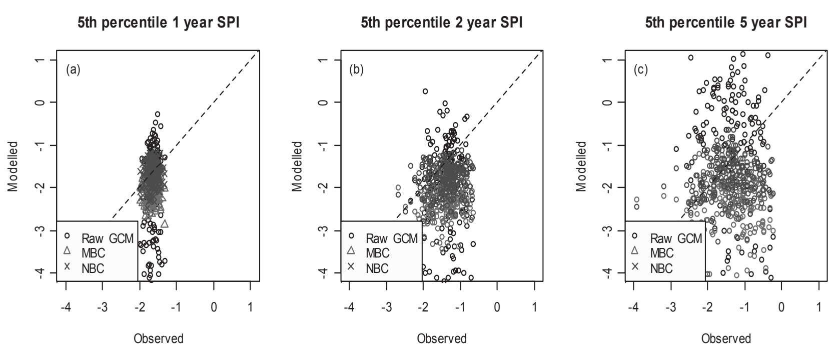

Figure 13.5. Modelled vs. observed 5th percentile SPI values for a) 1 year SPI, b) 2 year SPI and c) 5 year SPI (Johnson and Sharma 2009b)

With confidence that the nested bias correction method can improve the modelling of droughts, we move to assessing the frequency of future severe droughts. To do this, we use the observed 5th percentile SPI value to define a severe drought threshold at each grid cell. We then use the future GCM projections (both raw and bias corrected, using the CSIRO Mk3.5 GCM for the A2 scenario for a window covering 2061-2100) to see how frequently we expect severe droughts to occur in the future (Burke and Brown 2008).The results of this analysis highlight the impact of incorrectly modeling inter-annual variability in GCM outputs. Figure 13.6 shows the predictions of drought frequency for the future across Australia. The mean frequency of severe droughts occurring in the future using the raw GCM outputs is approximately 20% –meaning that in any one year, 20% of the country is likely to be suffering from a severe drought. If the GCM outputs are bias corrected using monthly scaling, then the pattern of severe droughts is quite similar, and the mean occurrence frequency is approximately 18%. On the other hand, using the nesting bias correction technique, severe droughts are less likely to occur than it would seem from the raw GCM outputs. The mean occurrence frequency is 15% in this case, and the differences in the spatial patterns of severe drought frequency, with decreases in occurrence frequency are noted particularly in Western Australia. It is important to note that still increases in the frequency of severe droughts over 90% of the country are found. Readers are referred to Johnson and Sharma (2012, 2011a) for more details and additional results on the analysis presented here.

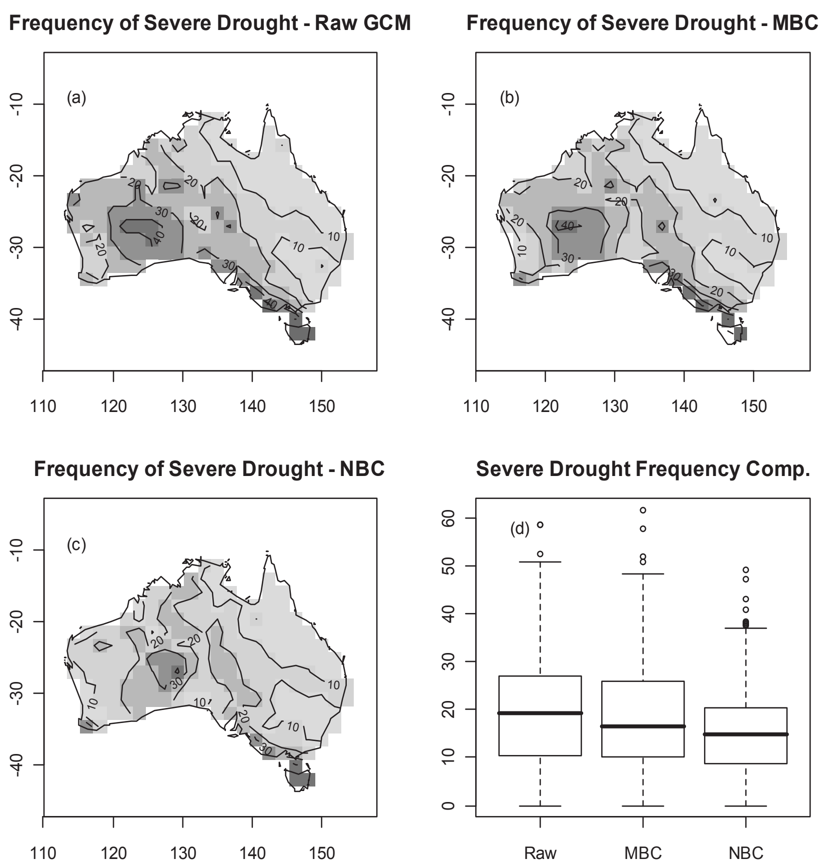

Figure 13.6. Maps of severe drought frequency in 2080 for a) raw GCM, b) monthly and c) nested bias correction. A comparison of the distribution of values for the three cases is shown in d)

13.3.3 Extension to Other Variables

While the previous section outlined the results obtained using GCM simulated rainfall, and illustrated the benefits that stand to be achieved especially in the ability to represent longer-term persistence or low-frequency variability, we must return to the basic argument put forward earlier, that GCM rainfall is obtained at a coarse resolution that limits its applicability to medium sized catchments, and that it suffers from considerably greater variability than many other atmospheric variables. We argue that hydrologic applications will often require rainfall to be simulated at finer spatial resolutions, and propose that one of the better ways forward is to adopt a stochastic downscaling rationale to generate multiple realizations of future point rainfall at as many locations as needed. This argument, however, suffers from the need to use GCM simulated atmospheric predictors (hopefully those that are more consistent across GCMs as measured by the VCS in Table 13.1), which may still be biased in their representation of low-frequency variability. We argue that if these atmospheric predictors misrepresent the inter-annual persistence that exists, their use in downscaling may lead to rainfall sequences that suffer from the same problem. We thus propose that to proceed for downscaling, the first step following selection of the atmospheric predictor variables to be used, must entail the application of the NBC post-processer described above. Use of these post-processed predictors for downscaling the rainfall is likely to enhance the representation of low-frequency variability and drought related characteristics in the simulations attained. This argument is explored in greater detail in the context of the Modified Markov stochastic downscaling Model (MMM) in the following section.

13.4 Modified Markov Stochastic Downscaling Model (MMM)

As mentioned in introduction, downscaling of rainfall to finer- or point-scale resolutions is commonly used for hydrological climate change impact assessment studies. Stochastic downscaling uses an empirically formulated relationship between the response(s) (rainfall) and predictors (past lags of rainfall and selected atmospheric variables), and generates stochastic sequences of the response being studied. This section presents a stochastic downscaling model developed to impart low-frequency variability in the simulated rainfall, using atmospheric predictor variables that have been post-processed using the Nested Bias Correction approach described previously.

13.4.1 Methodology

The general structure of the rainfall downscaling model (MMM–for rainfall occurrences and Kernel Density Estimation (KDE) procedure–for rainfall amounts) is presented in Mehrotra and Sharma (2007b) in a stochastic generation context and is described here in the context of downscaling, following Mehrotra and Sharma (2010).

Rainfall Occurrence Downscaling–MMM. The multi-site stochastic downscaling model presented here simulates rainfall at individual stations independently. The method used to incorporate spatial dependence in such simulations over many point locations involves using uniform random variates that are independent in time, but exhibit a strong dependence across the multiple point locations considered.

In general, the rainfall downscaling problem could be expressed as the conditional simulation of $R_t(k)|\mathbf{Z}_t(k)$ where $\mathbf{Z}_t(k)$ represents a vector of conditioning variables at a location k and at time t, that consists of atmospheric predictor variables, lagged rainfall to assign daily or short term persistence, and derived rainfall indicators selected to impact specific characteristics of interests. For rainfall occurrences, if $\mathbf{Z}_t(k)$ comprises of $R_{t-1}(k)$ alone then formulation reduces to a simple Markov order one model, whereas addition of variables representing longer time scale persistence also, would reduce it to the stochastic rainfall generator presented in Mehrotra and Sharma (2007b).

In the following discussions, we present the parameterization of $R_t(k)|\mathbf{Z}_t(k)$ as a modulation of the Markov order one (or higher) transition probability representation by the impact of non-discrete exogenous predictors. For brevity, site notations are dropped in the subsequent discussions. The parameters (or transition probabilities) of the Markov order one rainfall occurrence process are represented as $P(R_t|R_{t-1})$. Inclusion of non-discrete predictors $\mathbf{X}_t$ in the conditioning vector $\mathbf{Z}_t$ modifies the transition probabilities to $P(R_t|R_{t-1},\mathbf{X}_t)$, which can be expressed as:

$$P(R_t=1|R_{t-1}=i,\mathbf{X}_t)=\frac{P(R_t=1,R_{t-1}=i,\mathbf{X}_t)}{P(R_{t-1}=i,\mathbf{X}_t)}=\frac{f(\mathbf{X}_t|R_t=1,R_{t-1}=i)\times P(R_t=1,R_{t-1}=i)}{f(\mathbf{X}_t|R_{t-1}=i)\times P(R_{t-1}=i)}$$

$$=\frac{P(R_t=1,R_{t-1}=i)}{P(R_{t-1}=i)}\times\frac{f(\mathbf{X}_t|R_t=1,R_{t-1}=i)}{[f(\mathbf{X}_t|R_t=1,R_{t-1}=i)P(R_t=1|R_{t-1}=i)]+[f(\mathbf{X}_t|R_t=0,R_{t-1}=i)P(R_t=0|R_{t-1}=i)]} \quad \text{(Eq. 13.4)}$$

The first term in Eq. 13.4 defines the transition probabilities $P(R_t|R_{t-1})$ of a first order Markov model (representing order one dependence), while the second term signifies the effect of inclusion of predictor set $\mathbf{X}_t$ in the conditioning vector $\mathbf{Z}_t$. If $\mathbf{X}_t$ consists of derived measures (typically linear combinations) of atmospheric variables and/or summation of number of wet days in pre-specified aggregation time periods (as explained later), one could approximate the associated conditional probability density $f(\mathbf{X}_t|R_t=1,R_{t-1}=i)$ using a multivariate normal distribution. Consequently, the conditional probability density $f(\mathbf{X}_t|R_{t-1}=i)$ as specified in (13.4) can be expressed as a mixture of two multivariate normals. This leads to the following simplification:

$$P(R_t|R_{t-1},\mathbf{X}_t)=p_{1i}\frac{\frac{1}{\det(\mathbf{V}_{1,i})^{1/2}}\exp\left\{-\frac{1}{2}(\mathbf{X}_t-\boldsymbol{\mu}_{1,i})\mathbf{V}_{1,i}^{-1}(\mathbf{X}_t-\boldsymbol{\mu}_{1,i})^{\mathrm{T}}\right\}}{\left[\frac{1}{\det(\mathbf{V}_{1,i})^{1/2}}\exp\left\{-\frac{1}{2}(\mathbf{X}_t-\boldsymbol{\mu}_{1,i})\mathbf{V}_{1,i}^{-1}(\mathbf{X}_t-\boldsymbol{\mu}_{1,i})^{\mathrm{T}}\right\}p_{1i}\right]+\left[\frac{1}{\det(\mathbf{V}_{0,i})^{1/2}}\exp\left\{-\frac{1}{2}(\mathbf{X}_t-\boldsymbol{\mu}_{0,i})\mathbf{V}_{0,i}^{-1}(\mathbf{X}_t-\boldsymbol{\mu}_{0,i})^{\mathrm{T}}\right\}p_{0i}\right]} \quad \text{(Eq. 13.5)}$$

where $\mu_{1,i}$ represent the mean vector $E(\mathbf{X} \mid R_t = 1, R_{t-1} = i)$ and $\mathbf{V}_{1,i}$ is the corresponding variance-covariance matrix, and similarly $\mu_{0,i}$ and $\mathbf{V}_{0,i}$ represent, respectively, the mean vector and the variance-covariance matrix of **X** when ($R_{t-1} = i$) and ($R_t = 0$). The parameters p_{1i} represent the baseline transition probabilities of the first order Markov model defined by $P(R_t = 1 | R_{t-1} = i)$ with p_{0i} equaling (1- p_{1i}). The det(.) represents the determinant operation and T represents the transpose operator. While the assumption of a multivariate normal distribution simplifies the specification of the conditional probabilities in Eq. 13.5, this assumption may not be suitable for atmospheric variables that are known to have skewed or other non-Gaussian traits. In such situations, use of some appropriate transformation to convert the data back to normal may be attempted. However, it may be noted that most common data transformation techniques are developed for univariate cases only while data set **X** as described here is multivariate and univariate normal transformation does not necessarily translate into multivariate normal. Alternatively, the conditional multivariate probabilities $f(\mathbf{X}_t | R_t = 1, R_{t-1} = i)$ and $f(\mathbf{X}_t | R_t = 0, R_{t-1} = i)$ of Eq. 13.4 may be estimated using a nonparametric kernel density estimation procedure.

A key predictor for imparting low-frequency variability in rainfall is the aggregated wetness state of the catchment. A vector of aggregated rainfall $\mathbf{X}r_t$ representing the wetness over the recent past can be expressed as (following Sharma and O'Neill 2002; Harrold et al. 2003; Mehrotra and Sharma 2007a, b):

$$\mathbf{X}r_t \in \{ Xr_{j_1,t}, Xr_{j_2,t}, \ldots\ldots, Xr_{j_m,t} \}; \qquad Xr_{j_i,t} = \frac{1}{j_i} \sum_{l=1}^{j_i} R_{t-l} \qquad \text{(Eq. 13.6)}$$

where m is the number of such predictors and $Xr_{j_i,t}$ describes how wet it has been over the preceding j_i days with R_{t-l} representing rainfall occurrence. This aggregated wetness state, by formulation, assumes values between 0 and 1 that are increasingly continuous as the aggregation period j_i increases. Please note that the aggregated wetness state is determined separately for each station.

Rainfall Amount Downscaling–KDE. A nonzero rainfall amount [with a rainy day defined using a threshold of 0.3 mm/day following Harrold et al. (2003) and Mehrotra et al. (2004)] must be simulated for each day at each location that the MMM occurrence downscaling model simulates as wet. Additionally, the downscaled rainfall amount series (for the current climate) should represent accurately the spatial and temporal dependence present in the observed rainfall record. The downscaling of rainfall amount is based on the kernel density procedure. The model downscales the rainfall at individual stations conditional on the selected atmospheric variables as well as the previous days' rainfall. As rainfall amounts are downscaled independently at each location, observed spatial dependence across the stations is not directly reproduced. This is introduced by making of spatially correlated random numbers as described in the next section. The use of rainfall amounts on the previous day as a conditioning variable provides a Markov order one dependence to the downscaled series. Further details on the general structure of the KDE model are as follows:

The conditional distribution of $R_t|\mathbf{Z}_t$ (here R_t represent rainfall amount at time step t at a location) is estimated using the kernel density estimation (KDE) procedure:

$$f(R_t \mid \mathbf{Z}_t) = \sum_{i=1}^{N} \frac{1}{(2\pi\lambda^2 S')^{1/2}} w_i \exp\left(-\frac{(R_t - b_i)^2}{2\lambda^2 S'} \right) \qquad \text{(Eq. 13.7)}$$

where, $f(R_t \mid \mathbf{Z}_t)$ is the estimated conditional multivariate probability density, S' is the conditional variance of the data, specified as:

$$S' = S_{RR} - \mathbf{S}_{ZR}{}^{T} \mathbf{S}_{ZZ}{}^{-1} \mathbf{S}_{ZR} \qquad \text{(Eq. 13.8)}$$

where the covariance of (R_t, $\mathbf{Z}_t$) is written as:

$$Cov(R_t, \mathbf{Z}_t) = \begin{bmatrix} S_{RR} & \mathbf{S}_{ZR}{}^{T} \\ \mathbf{S}_{ZR} & \mathbf{S}_{ZZ} \end{bmatrix} \qquad \text{(Eq. 13.9)}$$

where, w_i is the weight associated with each kernel, representing the contribution that kernel has in forming the conditional probability density:

$$w_i = \frac{\exp\left(-\frac{1}{2\lambda^2} [(\mathbf{Z}_t - \mathbf{Z}_i)\boldsymbol{\psi}]^T [\mathbf{S}_{ZZ}]^{-1} [(\mathbf{Z}_t - \mathbf{Z}_i)\boldsymbol{\psi}] \right)}{\sum_{j=1}^{N} \exp\left(-\frac{1}{2\lambda^2} [(\mathbf{Z}_t - \mathbf{Z}_j)\boldsymbol{\psi}]^T [\mathbf{S}_{ZZ}]^{-1} [(\mathbf{Z}_t - \mathbf{Z}_j)\boldsymbol{\psi}] \right)} \qquad \text{(Eq. 13.10)}$$

where $\boldsymbol{\psi}\ (\equiv \psi_1, \psi_2, \ldots\ldots \psi_m)$ represents a vector of influence weights and is introduced to incorporate the relative influence of each predictor in estimating the conditional probability density, λ is a measure of spread, known as a kernel bandwidth and, b_i is the conditional mean associated with each kernel and is expressed as:

$$b_i = R_i - [\mathbf{S}_{ZR}]^T [\mathbf{S}_{ZZ}]^{-1} [(\mathbf{Z}_t - \mathbf{Z}_i)\boldsymbol{\psi}] \qquad \text{(Eq. 13.11)}$$

A simplistic choice, the Gaussian reference bandwidth (Scott 1992) is considered as the appropriate bandwidth and is optimal if the underlying probability density is Gaussian. However, when modelling variables exhibiting significant skewness, assuming a Gaussian distribution and assuming the variance associated with each kernel (or each observation) to be the same, may not be appropriate. In such situations, varying the bandwidth depending on the associated observation helps characterizing the probability more meaningfully, especially in regions where there may be many observations (requiring a smaller bandwidth) or where there may be few (requiring a larger bandwidth). The local Gamma bandwidth λ_{Z_k} for the k^{th} data point of the individual variables in **Z** series is written as (Mehrotra and Sharma 2007a):

$$\lambda_{Z_k} = \left(\frac{1}{2\sqrt{\pi} f(Z_k) \left[\gamma^2 - \frac{2\gamma(\eta - 1)}{Z_k} + \frac{(\eta - 1)(\eta - 2)}{Z_k^2} \right]^2} \right)^{1/(d+4)} N^{(-1/(d+4))} \qquad \text{(Eq. 13.12)}$$

where $f(Z_k)$ is the Gamma density at Z_k, γ and η, respectively, are the scale and shape parameters of the Gamma distribution for the variable being modelled (resulting in different local bandwidths associated with individual variables in **Z**), N is again the number of observations in **Z** when $(R_t = j\,(0\,or\,1), R_{t-1} = i)$, d is the number of predictor variables and λ_{Z_k} being equivalent to λ of Eqs. 13.7 and 13.10. Further details on the derivation of equation (13.12) are available in Mehrotra and Sharma (2007a) while further discussions related to the kernel density procedure are presented in Sharma and O'Neill (2002) and Mehrotra and Sharma (2007a, b).

The conditional density in Eq. 13.7 can be viewed as a slice of the multivariate density $f(R_t \mid \mathbf{Z}_t)$ across a conditional plane defined by $\mathbf{Z}_t$. This is in effect with the cumulative effect of kernel function (which is analogous to a legitimate, usually symmetrical, probability density function) placed over each observation and scaled so as to ensure that the resulting density integrates to 1.

Modelling Spatial Dependences in Rainfall Occurrence and Amounts. As discussed in the above sections, stochastic downscaling of rainfall occurrences or amounts for a given location proceeds through simulation from the associated conditional probability (or transition probability) distribution independently. The method used to incorporate spatial dependence in such simulations over many point locations involves using uniform random variates that are independent in time, but exhibit a strong dependence across the multiple point locations considered. Denote u_t as a vector of uniform [0, 1] variates of length n_s at time step t, with n_s being the number of stations. The vector u_t $(\equiv u_t(1), u_t(2), \ldots. u_t(n_s))$ is defined such that for locations k and l, $corr[u_t(k), u_{t+1}(l)] = 0$ (or, random numbers are independent across time), but $corr[u_t(k), u_t(l)] \neq 0$ (or, random numbers are correlated across space). As a result, there is spatial dependence between individual elements of the vector u_t, this dependence being introduced to induce observed spatial dependence in the response variables they are used to simulate. More details on this approach are available in Wilks (1998) and Mehrotra et al. (2006). In the algorithm that follows, the correlation matrix consisting of $corr[u_t(k), u_{t+1}(l)]$ is denoted $\boldsymbol{\omega}$.

Stepwise Procedure for Downscaling of Rainfall Occurrences and Amounts. The following describes in brief, a stepwise procedure for downscaling of rainfall occurrences using MMM and amounts using KDE at all stations.

<u>For Rainfall occurrence downscaling:</u>

1. Form correlation matrices $\boldsymbol{\omega}$ for each day of the year before the start of the rainfall downscaling following the procedure outlined in subsection 13.4.1. Note that these correlation matrices are formed assuming unconditional distribution of rainfall occurrences at each station.
2. Identify the number of longer-term predictor variables and atmospheric predictors, m, number of nearest neighbours, K, and length of the moving window, ℓ, needed for the application.

3. Calculate mean, variances and covariances of conditioning variables for each day using the data falling within the moving window. Also calculate daily transition probabilities of the Markov model.
4. Consider a day t.
5. Generate a vector $\mathbf{v}_t$ of n_s normally distributed random numbers with 0 mean and variance $\boldsymbol{\omega}$ and convert them into uniform random numbers using inverse normal transformation $\mathbf{u}_t = \boldsymbol{\Phi}^{-1}[\mathbf{v}_t]$. As mentioned earlier, n_s is the number of stations under consideration in the study
6. Consider a station k.
7. Calculate the values of the longer-term predictors for the day t in the simulated sequence (zt) and form a conditioning vector using longer-term and atmospheric predictors.
8. Ascertain transition probabilities $p01$ and $p11$ from the selected K observations. If previous day was wet, assign critical probability p as $p11$ otherwise assign $p01$. Calculate rainfall occurrence conditional probability using Eq. 13.9.
9. Compare p with the uniform random variate $u_t(k)$ for station k. If $u_t(k)$ is $\leq p$, assign rainfall occurrence, $Ro_t(k)$ for the day t at station k is 1 otherwise zero.
10. Move on to the next station.
11. Repeat steps 6–12 until all the stations are selected.
12. Move to the next date in the simulated sequence.
13. Repeat steps 4–12 until the desired length of simulated sequence is obtained.

For rainfall amount downscaling:

Stochastic simulation of rainfall amounts on wet days using kernel density estimation (KDE) procedure which is based on the following steps:

1. Similar to rainfall occurrence simulation, form correlation matrices $\boldsymbol{\omega}$ for each day of the year before the start of the simulation, following the procedure outlined in subsection 13.4.1. Note that these correlation matrices are formed assuming unconditional distribution of rainfall amounts at each station and considering wet days only.
2. Consider a day t.
3. Find number (n_w) and location of stations being simulated wet by the occurrence model on the day t. Form a sub set of correlation matrix ($\boldsymbol{\omega}_w$) from the correlation matrix $\boldsymbol{\omega}$ extracting correlations of wet stations.
4. Generate a vector $\mathbf{v}_t$ of n_w normally distributed random numbers with 0 mean and variance $\boldsymbol{\omega}_w$ and convert them into uniform random numbers using inverse normal transformation $\mathbf{u}_t = \boldsymbol{\Phi}^{-1}[\mathbf{v}_t]$.
5. Consider a wet station k.
6. Form a moving window of ℓ days centred on the current day t. Form a sub-sample of rainfall amounts $R_i(k)$ from the historical record of the moving window. Also identify all corresponding predictor variables ($R_{i-1}(k)$ values and current day atmospheric predictors) and store them as $\mathbf{X}_i(k)$. Denote total number of observations as N.

7. Rank R(k) series and associated **X**(k) observations from highest to lowest.
8. Calculate variances and covariances of R(k) and **X**(k) series. Also calculate the local bandwidths of these two series at each data point and store.
9. Form a set of predictor variables for the day t (previous day (t-1) simulated rainfall, and current day atmospheric predictors). This forms our conditioning vector.
10. Estimate the weights w_i for the kernel slices that are associated with each data pair [$R_i(k)$, $\mathbf{X}_i(k)$]. These weights represent the contribution that each kernel has in forming the conditional probability density. Transform these weights to cumulative probability P_i using the following:

$$p_i = \frac{w_i}{\sum_{j=1}^{N} w_j} \text{ and}$$

$$P_i = P_{i-1} + p_i \text{ for } i>1 \text{ ; } P_i = p_i \text{ for } i=1 \qquad \text{(Eq. 13.13)}$$

11. Use the cumulative probabilities $u_t(k)$ as defined in step 4, and identify the position i^* such that $P_{i^*-1} < u_t(k) \le P_{i^*}$, thereby selecting an $R_i(k)$ value from R(k) series.
12. Calculate b_i as the conditional mean associated with the kernel $R_i(k)$ using Eq. 13.11.
13. Sample $\hat{R}_t(k)$ as a random variate from the kernel centred on b_i (the conditioned kernel slice being a Gaussian PDF with a mean b_i and a variance equal to $\lambda(Z_i)^2 S'$),

$$\hat{R}_t(k) = b_i + \lambda(Z_i)(\sqrt{S'})W_t \qquad \text{(Eq. 13.14)}$$

where W_t is a random variate from a normal distribution with mean of 0 and variance of 1 and S' is a measure of spread of the conditional density given by Eq. 13.12). As Eq. 13.14 can lead to rainfall amounts that are less than the threshold amount of 0.3 mm, a minimum rainfall amount of 0.3 mm is assigned to such days.
14. Move on to the next wet station of the day t.
15. Repeat steps 6–14 for all wet stations.
16. Move on to the next day.
17. Repeat steps 3–16 for all days of the downscaled occurrence sequences.

13.4.2 Data Used

Continuous record of 43 years (from 1960 to 2002) of daily rainfall at 45 stations around Sydney (Figure 13.7) is used in the analysis. The required observed atmospheric variables for 25 grid points over the study area are extracted from the National Center for Environmental Prediction (NCEP) reanalysis data provided by the NOAA-CIRES Climate Diagnostics Centre, Boulder, Colorado, USA, from their web site at <http://www.cdc.noaa.gov/>. Runs of Commonwealth Scientific and Industrial Research Organization (CSIRO), Australia Mark3 GCM (Gordon et al. 2002) for the three emission scenarios SRES B1, A1B and A2 (IPCC 2007) are used.

GCM datasets of atmospheric variables for the baseline (covering a 43-year period between 1960 and 2002 and representing the current climate) and the future climate by 2070 (2061–2080) periods are considered in the analysis.

13.4.3 Application

The MMM-KDE downscaling framework was used to stochastically downscale rainfall at point locations illustrated in Figure 13.7. The model was tested using GCM simulations for the current climate and applied to simulate rainfall for three emission scenarios for 2070 conditions. Atmospheric predictors for the model were chosen on a seasonal basis using measures of partial dependence. While the results presented here are based on the use of a single GCM, we are confident about their stability across GCMs because the atmospheric variables considered as predictors were restricted to those exhibiting high Variable Convergence Score (VCS, refer Table 13.1).

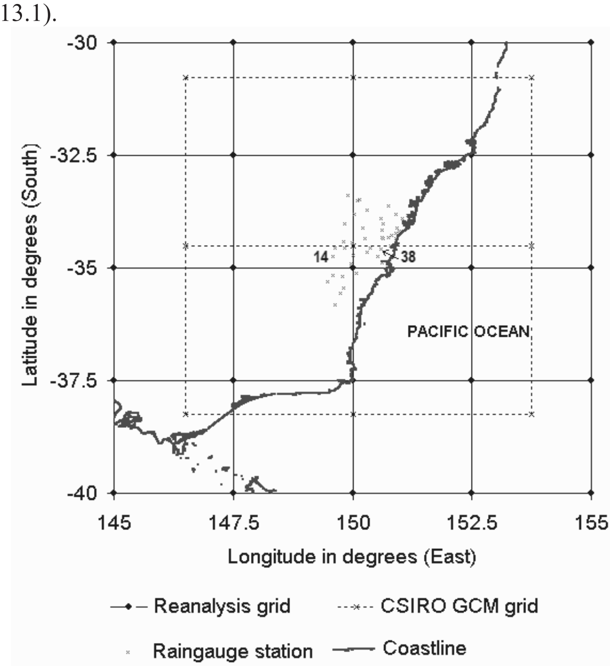

Figure 13.7. Reanalysis and CSIRO GCM data grids and study region (Mehrotra and Sharma 2010)

In all the results that follow, the statistics reported are ascertained by generating 100 realisations of the downscaled rainfall from the model. The individual statistics from these realisations are ranked and 5th, 50th and 95th percentile values are extracted. The best estimate refers to the 50th percentile value (median), while 5th and 95th percentile values are used to form the confidence bands around the median estimate. As all emission scenarios exhibit similar performances for the baseline period (current climate 1960–2002), results of only one emission scenario are presented for the current climate and these are mentioned hereafter as 'GCM current climate'. The model outcomes were assessed on the basis of its ability to reproduce the average conditions and extremes including the low-frequency variability in the downscaled rainfall attributes.

Number of Wet Days and Rainfall Totals–Current Climate. Table 13.2 compares the observed and downscaled (5^{th}, median and 95^{th} percentile estimates) seasonal and annual wet days and rainfall totals over the study region. The model adequately reproduces these rainfall occurrences and amounts attributes over the study area for all seasons and year during calibration (using reanalysis data) and evaluation (using GCM current climate data) stages. The model also captures the observed high and low rainfall regions, for example, more wet days over the inland region in comparison to coastal during winter, more rainfall in the northern part of the region in comparison to the southern on an annual basis, and more rainfall in northern coastal region during summer (results not included).

Table 13.2. Observed and downscaled (5th, Median (50th) and 95th percentile estimates) seasonal and annual wet days and rainfall amount using reanalysis and GCM data for the current climate (Mehrotra and Sharma 2010)

Season	Wet days				Rainfall amount in mm			
	Observed	Simulated percentile estimates			Observed	Simulated percentile estimates		
		5^{th}	Median	95^{th}		5^{th}	Median	95^{th}
Using reanalysis data								
Autumn	28	28	27	26	266	291	273	256
Winter	26	26	26	25	210	230	212	196
Spring	29	29	29	28	230	264	246	235
Summer	30	30	29	28	280	302	285	269
Annual	112	113	111	109	984	1047	1020	989
Using current climate GCM data								
Autumn	28	29	28	27	266	253	238	223
Winter	26	26	25	25	210	209	195	182
Spring	29	29	28	27	230	246	235	222
Summer	30	31	30	29	280	298	284	270
Annual	112	114	111	109	984	981	951	918

Representation of Low Frequency Variability–Current Climate. The year to year persistence or low frequency variability forms an important rainfall characteristic when it is used to assess the likelihood of sustained droughts or flood regimes. Figure 13.8 presents the year to year distribution of area averaged wet days and rainfall amounts obtained using the reanalysis and GCM data sets. The yearly area averaged time series is formed by averaging across the stations individual station values of annual wet days and annual rainfall. Ranking of this area averaged series provides an indication of the over-the-year distribution of annual rainfall or wet days over the study region. In this figure, percentiles of the model simulated values are shown as continuous lines while the observed values are superimposed as circles. The downscaling model successfully reproduces the distribution of observed area averaged annual rainfall occurrences and amounts in the downscaled sequences, using both the reanalysis as well as GCM data. The good fit of the simulated statistic indicates that the downscaling model is capable of reproducing the observed occurrences of dry and wet years successfully over the study region. The model performs equally well at a majority of individual stations (results not included).

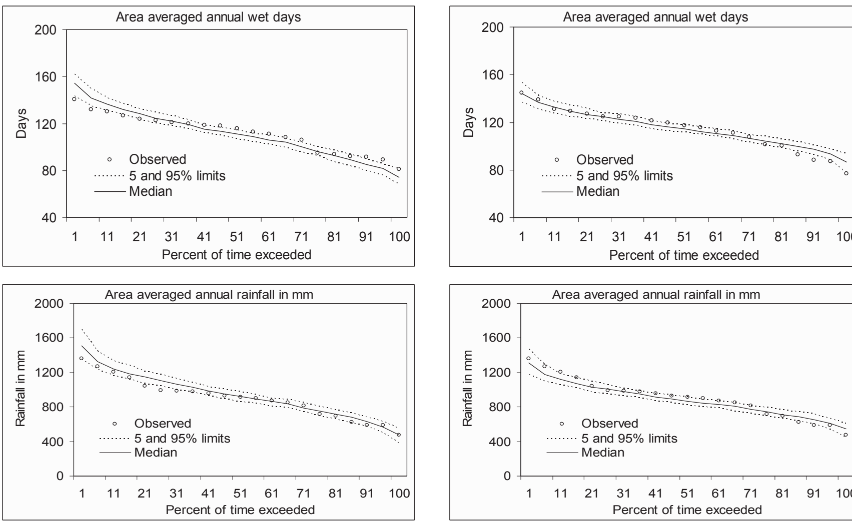

Reanalysis GCM current climate

Figure 13.8. Distribution plots of observed and model simulated area averaged annual wet days and rainfall amount (in mm) for the baseline period using reanalysis and GCM current climate data sets (Mehrotra and Sharma 2010)

Extreme Rainfall Characteristics–Current Climate. Sustained periods of wet and dry spells are important for flood management, water storages and agricultural studies. Here, a wet spell is defined as a continuous sequence of days when daily rainfall is greater than or equal to 0.3 mm and likewise a dry spell represents a sequence of days with daily rainfall being less than 0.3 mm. Rainfall amount in a wet spell represents the total amount of rainfall received during that spell. The top row of Figure 13.9 compares the average annual frequency of occurrence of wet spells of durations 5–7 days and greater than 7 days at individual stations using observed, reanalysis data and GCM data simulated rainfall. The second row presents the plots of average rainfall totals (in mm) in these wet spells (amount per wet spell) and third row shows the average number of dry spells of 9–18 days and more than 18 days in a year. The bottom row shows the plots of average number of days in a year when daily rainfall is greater than 35 mm. The dots refer to the values for individual stations. As shown in these plots, the model adequately reproduces these extreme rainfall attributes at individual station using both reanalysis and GCM data sets simulated rainfall albeit some underestimation of number of wet spells and days with extreme rainfall at many stations for GCM data simulated rainfall.

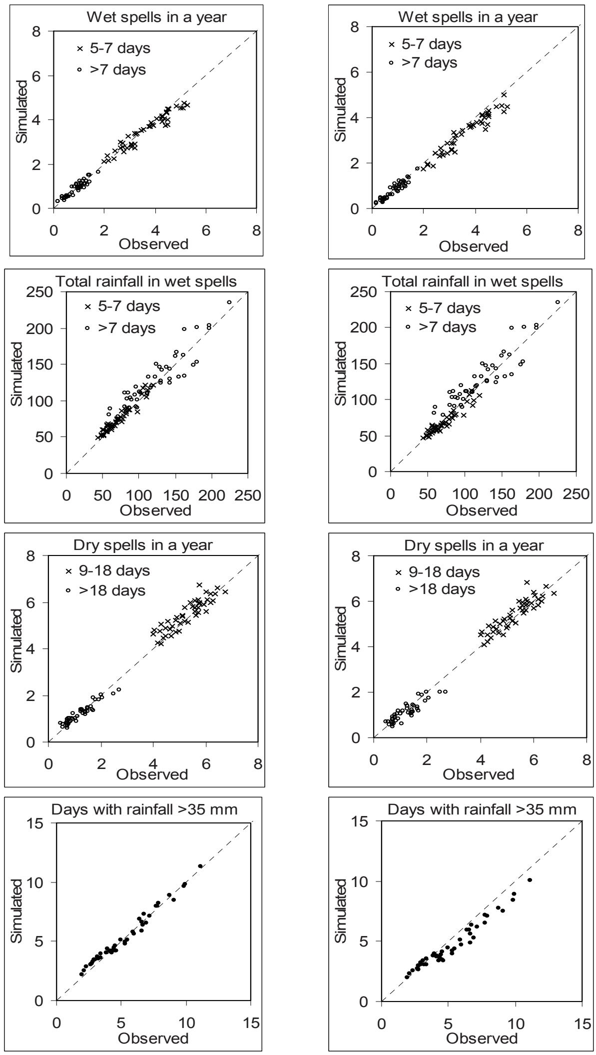

Reanalysis GCM current climate

Figure 13.9. Observed and models simulated (a) number of wet spells of 5–7 and > 7 days in a year, (b) average total rainfall (in mm) in these wet spells, (c) number of dry spells of 9–18 and > 18 days in a year, and (d) number of days with daily rainfall > 35 mm in a year (Mehrotra and Sharma 2010)

Model Results for Year 2070. In the following discussions, a likely range of change, as well as a best estimate of future rainfall statistic over the study region is included. Differences in all statistics are calculated using the median best estimate of rainfall statistics (ranking a particular rainfall statistic derived from 100 realisations and picking up middle value of the ranked series) for future climates and finding the percent change in relation to the current climate. For majority of statistics analysed, climate projections show wide variations across the scenarios and seasons. All emission scenarios are assigned equal weightage in the results below.

<u>Changes in number of wet days and average rainfall.</u> Table 13.3 provides the details on the estimated changes in the number of wet days and rainfall amount on seasonal and annual basis in year 2070. The results show wide variations in the projected wet days and rainfall amount over the study area from season to season and from one scenario to another. On the whole, results project wetter autumn and summer and drier spring and winter conditions over the region in year 2070. Also, wetter conditions along the coastal areas and drier conditions for far inland region are projected (details not included). By 2070, under the B1 scenario, the range of annual wet days change is -1.3 to +4.4% with the best estimate of 1.5% increase while for annual rainfall the change is from +5% to +15.9% with the best estimate of 9.4% increase (Table 13.3). Both A1B and A2 scenarios project slight decreases in annual number of wet days and rainfall amount. Collectively, by 2070 the estimated range of annual wet days change is -8 to +4% with 2% decrease and of annual rainfall as -8 to +16% with 2% increase.

<u>Changes in daily rainfall intensity, wet and dry spells and extreme rainfall.</u> Along with the changes in number of wet days and average rainfall, the statistics of daily rainfall may also change, e.g. rainfall intensity (rainfall amount per wet-day), spells of wet and dry days and the intensity of extreme rainfall. Results of projected changes in per wet day rainfall amount and maximum daily rainfall in 2070 are analysed at seasonal and annual levels. An increase (about 4%) in daily rainfall intensity (rain per wet-day) is estimated with B1 projecting a maximum increase of 7.7%. Number of days with extreme rainfall (greater than 35 mm/day) is likely to increase annually and in all seasons. More specifically, this increase is more pronounced in the north-east part of the study area varying from 25 to 35% while west and south-west part of the region projects a decrease from 0 to 15%. Increased occurrences of short spells of days with intense rain of greater than 35 mm in the future are estimated.

<u>Increased instances of wet spells of 7 days or more are projected more specifically along the coastal areas.</u> Also, increases in autumn and summer and decreases in winter and spring in the frequency of such events are estimated. The rainfall amount in wet spells of 7 days or more is likely to increase in all seasons. Rainfall amount in these spells is likely to increase in autumn and summer and decrease in winter. Increased frequency of occurrences of longer dry spells (of 18 days or more in a year) is also estimated in the future. The increased frequency of longer wet spells with lesser increase in wet spell rainfall, and decreased frequency of

wet spells of 3-4 days with increased wet spell rainfall suggest that the future rainfall regime will have fewer shorter rainfall events with increased intense rainfall.

Influence of low-frequency variability variable on the results. The downscaling approach proposed here provides a time dependent parameter updating procedure and is formulated to reproduce the most part of the observed low frequency variability in the downscaled simulations. To emphasize this point further, we focus on a few rainfall characteristics indicative of the low frequency behavior of rainfall. These include standard deviation of the aggregated wet days at monthly, seasonal and annual levels and frequency of sustained wet and dry spells. We re-run the downscaling model by dropping the 365 days wetness state variable and evaluate these rainfall attributes in the revised downscaled simulations and compare them with the observed and original downscaled results. Table 13.4 compares these results in terms of mean squared error (MSE) measure. MSE of these rainfall attributes is calculated, by computing the median statistic from the 100 realization, calculating squared difference of observed and median statistic at each station and averaging across the stations. The MSE for future climate is calculated only to convey the message that the proposed model provides a realistic representation of low-frequency variability (also referred to as long-term persistence) in the rainfall, leading to simulations that are consistent with observations, making them viable for water planning and design for a future climate. These results indicate that the use of 365 days wetness state variable not only improves the standard deviation of wet days at seasonal and annual time scale but also improves the representation of frequency of dry spells in the downscaled sequences specifically when using GCM dataset.

Finally, in order to evaluate the impact of nested bias correction on the downscaled rainfall, the GCM predictor series is bias corrected using the standard bias correction and nested bias correction procedure. The downscaling model is run using these bias corrected GCM variables and with and without the 365 days wetness state variable; rainfall simulations for the current and future climate (year 2070) are simulated. The impact of bias correction procedure in the downscaled results is evaluated on the basis of reproduction of year-to-year variability in the downscaled rainfall. This is achieved by forming the aggregated wet days and rainfall series at one to seven years aggregation scale, and calculating the standard deviation of the aggregated series. The ratio of simulated and observed standard deviation provides a measure of the capability of the model in simulating the year-to-year variability. For a perfect model the ratio is one. Values > 1 indicate over estimation while values < 1 indicate under estimation of the variability. Briefly, the absolute deviation is calculated for all aggregation levels and for all stations and average computed. Table 13.5 provides the average deviation for rainfall occurrences and amounts obtained using the sum of the combinations of bias correction procedure and 365 days wetness state. The results indicate that, in comparison to the standard bias correction procedure, NBC improves the reproduction of year-to-year variability in the downscaled rainfall. Combination of NBC standardized GCM predictors and previous 365 days wetness state variable yields rainfall simulations that reproduce better the low frequency variability in the downscaled rainfall for current and future climates.

Table 13.3. Percent changes in seasonal and annual number of wet days and rainfall amounts in 2070 (Mehrotra and Sharma 2010)

(a) Percent changes in number of wet days in 2070

		Scenario					
		B1		**A1B**		**A2**	
Season	**Current climate # of wet days**	**Median estimate of # of wet days**	**Percent change in Median, 5th and 95th percentile values**	**Median estimate of # of wet days**	**Percent change in Median, 5th and 95th percentile values**	**Median estimate of # of wet days**	**Percent change in Median, 5th and 95th percentile values**
Autumn	28	32	+13 (+18 to +9)	30	+7 (+12 to +2)	29	+3 (+7 to -2)
Winter	25	23	-11 (-6 to -15)	23	-10 (-6 to -14	23	-9 (-4 to -13)
Spring	28	28	-2 (+3 to -6)	26	-8 (-4 to -13)	26	-7 (-2 to -11)
Summer	30	32	+6 (+11 to +2)	28	-7 (-3 to -12)	31	+3 (+7 to -1)
Annual	111	113	+2 (+4 to -1)	106	-5 (-3 to -8)	109	-3 (0 to -6)

(b) Percent changes in rainfall amount in year 2070

		Scenario					
		B1		**A1B**		**A2**	
Season	**Current climate rainfall amount in mm**	**Median estimate of rainfall in mm**	**Percent change in Median, 5th and 95th percentile values**	**Median estimate of rainfall in mm**	**Percent change in Median, 5th and 95th percentile values**	**Median estimate of rainfall in mm**	**Percent change in Median, 5th and 95th percentile values**
Autumn	238	297	+25 (+41 to +12)	266	+12 (+21 to +3)	242	+2 (+10 to -6)
Winter	195	177	-9 (+3 to -20)	190	-3 (+11 to -12)	178	-9 (+4 to -19)
Spring	235	249	+6 (+17 to -4)	207	-12 (-4 to -19)	221	-6 (+4 to -15)
Summer	284	329	+16 (+25 to +8)	265	-7 (+1 to -14)	314	+11 (+22 to 0)
Annual	951	1040	+9 (+16 to +5)	919	-3 (+1 to -8)	946	-1 (+5 to -6)

Table 13.4. Mean squared error for selected area averaged rainfall attributes in the downscaled simulations obtained using reanalysis (RE) and GCM datasets only and also including the 365 days wetness state variable (L) (Mehrotra and Sharma 2010)

Rainfall attribute		Observed Statistic	Mean square error (MSE)					
			RE	RE+L	GCM	GCM+L	A2 2070	A2 2070+L
Standard deviation of annual wet days		20.49	16.35	0.09	66.23	20.03	33.51	12.38
Standard deviation of monthly wet days		3.41	0.00	0.01	0.14	0.00	0.01	0.03
Standard deviation of seasonal wet days	Autumn	8.38	0.82	0.03	3.97	1.44	3.98	4.20
	Winter	7.91	1.79	0.31	2.94	0.49	0.03	0.28
	Spring	7.66	0.39	0.04	3.37	0.64	1.50	0.20
	Summer	8.09	0.97	0.20	2.31	0.65	5.42	3.54
Number of dry spells of 9–18 days in a year		5.3	5.28	0.13	0.03	0.00	0.02	0.10
Number of dry spells of > 18 days in a year		1.2	1.23	0.00	0.00	0.10	0.01	0.00
Number of wet spells of 5–7 days in a year		3.7	3.65	0.03	0.02	0.31	0.11	0.12
Number of wet spells of > 7 days in a year		0.9	0.87	0.00	0.00	0.07	0.01	0.00

Table 13.5. Average deviation of ratio of observed and simulated standard deviations of one to seven years sums of annual wet days and rainfall amounts (ADR)

Predictor variables	ADR of Rainfall	
	Occurrences	Amounts
Reanalysis atmospheric variables and 365 days wetness state	0.18	0.33
GCM variables bias corrected using daily mean, standard deviation and daily LAG1 correlation – current climate	1.13	0.16
GCM variables bias corrected using daily mean, standard deviation and daily LAG1 correlation and 365 days wetness state variable–current climate	0.53	0.31
GCM variables bias corrected using NBC–current climate	0.31	0.29
GCM variables bias corrected using NBC and 365 days wetness state variable–current climate	0.19	0.22
GCM series bias corrected using daily mean, standard deviation and daily LAG1 correlation–future climate	0.81	0.19
GCM variables bias corrected using daily mean, standard deviation and daily LAG1 correlation and 365 days wetness state variable–future climate	0.35	0.14
GCM series bias corrected using NBC–future climate	0.43	0.17
GCM series bias corrected using NBC and 365 days wetness state variable–future climate	0.18	0.20

13.5 Conclusions

Two approaches for catchment scale climate change impact assessment are presented. The first of the two approaches (Nested Bias Correction or NBC) presents a basis for incorporating low-frequency variability in GCM simulations, and is found to result in better simulations of drought related characteristics in Australia. The second approach (Modified Markov Model and Kernel density Estimation stochastic downscaling Model, or MMM-KDE) presents a rationale for stochastically generating rainfall in future climates with appropriate low-frequency variability as present in the historical data. While both approaches are aimed at the same outcome, the former operates at the GCM scale and hence is limited in the spatial resolution it simulates the variables at, while the latter generates stochastic rainfall sequences at point scale using raw GCM variables that may have low-frequency variability biases present. The combination of these two approaches by removing low-frequency variability bias in the GCM simulated atmospheric variables, and then using the MMM-KDE downscaling model to produce downscaled rainfall, provides better results in terms of the representation of low-frequency variability. While the choice of the GCM to be used is of a lesser concern as predictor variables are to be selected based on their convergence over future climate simulations, readers may use recommendations on GCMs as per Johnson et al. (2011b) which compare the ability of GCMs to simulate low frequency variability in current climate simulations. It is recommended that such an approach, coupled with the VCS and NBC alternatives recommended here be adopted when the intent is to simulate the "sustained extremes" that are of considerable importance in water resources planning and design.

13.6 Acknowledgements

This research was funded by the Australian Research Council and the Sydney Catchment Authority. The rainfall data used in the study was obtained from the Australian Bureau of Meteorology.

13.7 References

Bartholy, J., Bogardi I., and Matyasovszky I. (1995). "Effect of climate change on regional precipitation in lake Balaton watershed." *Theor Appl. Climatol.*, 51, 237–250.

Burke, E. J., and Brown, S. J. (2008). "Evaluating uncertainties in the projection of future drought." *Journal of Hydrometeorology*, 9, 292–299.

Charles, S. P., Bates, B. C., Smith I. N., and Hughes J. P. (2004). "Statistical downscaling of daily precipitation from observed and modelled atmospheric fields." *Hydrol. Process.*, 18, 1373–1394.

Chiew, F. H. S., Teng, J., Vaze, J., Post, D. A., Perraud, J. M., Kirono, D. G. C., and Viney, N. R. (2009). "Estimating climate change impact on runoff across southeast Australia: Method, results and implications of modelling method." *Water Resources Research*, 45, W10414, doi:10.1029/2008WR007338.

Fowler, H. J., Blenkinsop, S., and Tebaldi, C. (2007). "Linking climate change modelling to impacts studies: recent advances in downscaling techniques for hydrological modelling." *International Journal of Climatology*, 27(12), 1547–1578.

Giorgi, F., Hewitson, B., Christensen, J., Hulme, M., Von Storch, H., Whetton, P., Jones, R., Mearns, L., and Fu, C. (2001). "Regional Climate Information: Evaluation and Projections ." Chapter 10 in *Climate Change 2001: The Scientific Basis, Contribution of Working Group I to the Third Assessment Report of the IPCC* [Houghton, J. T., Y. Ding, D. J. Griggs, M. Noguer, P. J. van der Linden, X. Dai, K. Maskell, and C. A. Johnson (eds.)].Cambridge U. Press: Cambridge, pp. 739–768.

Gordon, H. B., and co-authors (2002). "The CSIRO Mk3 Climate System Model (Electronic publication)." Aspendale: CSIRO Atmospheric Research. (CSIRO Atmospheric Research technical paper; no. 60), 130 pp. <http://www.dar.csiro.au/publications/gordon_2002a.pdf>.

Guttman, N. B. (1999). "Accepting the standardized precipitation index: A calculation algorithm." *Journal of the American Water Resources Association*, 35, 311–322.

Harrold, T. I., Sharma, A., and Sheather, S. J. (2003). "A nonparametric model for stochastic generation of daily rainfall occurrence." *Water Resour. Res*., 39(12), 1343, doi:10.1029/2003WR002570.

Hewitson, B. C., and Crane, R. G. (1996). "Climate downscaling: techniques and application." *Clim. Res.*, 7, 85–95.

Hughes, J. P., Guttorp, P., and Charles S. P. (1999). "A non-homogeneous hidden Markov model for precipitation occurrence." *Appl. Stat.,* 48(1), 15-30.

Ines, A. V. M., and Hansen, J. W. (2006). "Bias correction of daily GCM rainfall for crop simulation studies." *Agricultural and Forest Meteorology*, 138(1–4), 44–53.

IPCC (2007). *Climate Change 2007: Synthesis Report. Contribution of Working Groups I, II and III to the Fourth Assessment Report of the Intergovernmental Panel on Climate Change* [Core Writing Team, Pachauri, R.K and Reisinger, A.(eds.)]. IPCC, Geneva, Switzerland, 104 pp.

Johnson, F., and Sharma, A. (2009a). "Measurement of GCM Skill in Predicting Variables Relevant for Hydroclimatological Assessments." *Journal of Climate*, 22, 4373–4382.

Johnson, F. M., and Sharma, a. (2009b). “Assessing Future Droughts in Australia - A Nesting Model to Correct for Long Term Persistence in General Circulation Model Precipitation Simulations.” *18th IMACS Congress MODSIM 09*.

Johnson, F. and A. Sharma (2012). "A nesting model for bias correction of variability at multiple time scales in general circulation model precipitation simulations." *Water Resources Research* 48(W01504): 16.

Johnson, F., and Sharma, A. (2011a). "Accounting for interannual variability–a comparison of options for water resources climate change impact assessments." *Water Resources Research*, 47, W04508, doi:10.1029/2010WR009272.

Johnson, F., Westra, S., Sharma, A., and Pitman, A. (2011b). "GCM skill assessment from an interannual variability perspective." *Journal of Climate*, doi: 10.1175/2011JCLI3732.1.

Mearns, L. O., Giorgi, F., Whetton, P., Pabon, D., Hulme, M., and Lal, M. (2004). *Guidelines for use of climate scenarios developed from regional climate model experiments*. Tech. rep., Data Distribution Centre of the IPCC.

Mehrotra, R., Sharma, A., and Cordery, I., (2004). "Comparison of two approaches for downscaling synoptic atmospheric patterns to multisite precipitation occurrence." *J. Geophys. Res*., 109, D14107, doi:10.1029/ 2004JD004823.

Mehrotra, R., and Sharma, A. (2005). "A nonparametric nonhomogeneous hidden Markov model for downscaling of multi-site daily rainfall occurrences." *J. Geophys. Res*., 110, D16108, doi:10.1029/2004JD005677.

Mehrotra, R., Srikanthan, R., and Sharma, A. (2006). "A comparison of three stochastic multi-site precipitation occurrence generators." *J. Hydrol*., 331, 280–292, doi:10.1016/j.jhydrol.2006.05.016.

Mehrotra, R., and Sharma, A. (2007a). "A semi-parametric model for stochastic generation of multi-site daily rainfall exhibiting low frequency variability." *J. Hydrol*., 335, 180–193, doi:10.1016/ j.jhydrol.2006.11.011.

Mehrotra, R., and Sharma, A. (2007b). "Preserving low-frequency variability in generated daily rainfall sequences." *J. Hydrol*., 345, 102–120, doi:10.1016/j.jhydrol.2007.08.003.

Mehrotra R., and Sharma, A. (2010). "Development and Application of a Multisite Rainfall Stochastic Downscaling Framework for Climate Change Impact Assessment." *Water Resources Research*, 46, W07526, 17, doi:10.1029/2009WR008423.

Perkins, S. E., Pitman, A. J., Holbrook, N. J., and McAneney, J. (2007). "Evaluation of the AR4 Climate Models' Simulated Daily Maximum Temperature, Minimum Temperature, and Precipitation over Australia Using Probability Density Functions." *Journal of Climate*, 20, 4356–4376.

Randall, D. A., and Co-authors (2007). *Climate Models and Their Evaluation. Climate Change 2007: The Physical Science Basis. Contribution of Working Group I to the Fourth Assessment Report of the Intergovernmental Panel on Climate Change*, S. Solomon, and Coauthors, Eds., Cambridge University Press,.

Scott, D. W. (1992). *Multivariate density estimation: Theory, practice and visualization*, John Wiley, New York.

Sharma, A., and O'Neill, R. (2002). "A nonparametric approach for representing interannual dependence in monthly streamflow sequences." *Water Resour. Res*., 38(7), 5.1–5.10.

Srikanthan, R., and Pegram, G. G. S. (2009). "A Nested Multisite Daily Rainfall Stochastic Generation Model." *Journal of Hydrology*, DOI: 10.1016/j.jhydrol. 2009.03.025.

Sun, Y., Solomon, S., Dai, A., and Portmann, R. W. (2006). "How Often Does It Rain?" *Journal of Climate*, 19, 916–934.

Wang, Q. J., and Nathan, R. J. (2007). "A method for coupling daily and monthly time scales in stochastic generation of rainfall series." *Journal of Hydrology*, 346, 122–130.

Wilby, R. L., Charles, S. P., Zorita, E., Timbal, B., Whetton, P., and Mearns, L. O. (2004). *Guidelines for use of climate scenarios developed from statistical downscaling methods.* Tech. rep., Data Distribution Centre of the IPCC.

Wilks, D. S. (1998). "Multisite generalization of a daily stochastic precipitation generation model." *J. Hydrol*., 210, 178–191.

Wood, A. W., Leung, L. R., Sridhar, V., and Lettenmaier, D. P. (2004). "Hydrologic implications of dynamical and statistical approaches to downscaling climate model outputs." *Clim. Change*, 62, 189–216.

Xu, C. Y. (1999). "Climate change and hydrologic models: A review of existing gaps and recent research developments." *Water Resources Management*, 13, 369–382.

Yarnal, B., Comrie A. C., Frakes, B., and Brown, D. P. (2001). “Developments and prospects in synoptic climatology.” *Int. J. Climatol*., 21, 1923–1950.

CHAPTER 14

Statistical Analysis of Hydro-Climatic Variables

R. K. Rai, Alka Upadhyay, C. S. P. Ojha and L. M. Lye

In many instances, a time series is generally not statistically independent but is comprised of patterns of persistence, cycles, trends or some other non-random components. In climatology, identification of the precise nature and extent of non-randomness in the time series of meteorological data is very important and is usually the first step of time series analysis. Statistical evidence of non-randomness in such time series is equated with evidence of bona fide climatic fluctuations and said to be dependent or exhibits persistence of some sort. A climatologic time series may consists either of wholly random variations, of wholly random changes, or both random and non-random components. In a hydrological point of view, dependence in the time series is associated with the hydro-climatic paths followed by moisture from atmosphere to earth through surface and sub-surface route and back to the atmosphere. If a time series is non-random, the time series is further investigated for trends, persistence, periodic fluctuations or combination of these. Therefore, this chapter presents the statistical approach applied for understanding the hydro-climatic time series, in which three components were discussed in detail with application to the hydro-climatic data of the Yamuna River basin of Ganga River system of India. The components are: (a) tests of short and long term dependence; (b) trend analysis; and (c) tests of persistence and periodicity.

14.1 Statistical Methods of Short- and Long-term Dependence

Many types of hydrologic time series exhibit significant serial correlation. That is, the value of the random variable under consideration at one time period is correlated with the values of the random variable at earlier time periods. When the time series shows the persistence for a shorter period then it is referred as short-term dependence. It can be measured through the serial correlation of the time series. The series is said to be completely random (or not dependent) if the serial correlation is zero. However, in practice, this situation never occurs. Therefore, for confidence in the test of short-term dependence, it is necessary to test the time series using alternate statistical tests.

For short term dependence, statistical tests may be divided into two sets, viz., non-parametric and parametric. The non-parametric test accounts for the length and relative sign of the observation in the time series whereas, parametric test is based on the values associated with the series and requires fulfilling strict assumptions of the distribution of the data and therefore, is less robust than the non-parametric test.

14.1.1 Non-Parametric Test

The commonly used non-parametric statistical tests to investigate the short term dependence are described as follows.

Median-Crossing Test (Fisz 1963). In this test $X = 0$ is considered when $x_i < x_{median}$, and X = 1 for $x_i > x_{median}$. If the original sequence of X_s has been generated by a purely random process, then u, the number of times zero is followed by one or one is followed by zero, is approximately normally distributed. Initial value of u is taken as zero (i.e., $u = 0$). If $x_i > x_{median}$ and $x_{i+1} < x_{median}$ or $x_i < x_{median}$ and $x_{i+1} > x_{median}$ then $u = u + 1$. The expected value of u is defined as follows.

$$E(u) = (n-1)/2 \tag{Eq. 14.1}$$

$$Var(u) = (n-1)/4 \tag{Eq. 14.2}$$

where, n is the length of sample, E(u) is the expectation of the series, and Var (u) is the variance. The Z statistic is computed as follows.

$$Z = \frac{u - E(u)}{[Var(u)]^{1/2}} \tag{Eq. 14.3}$$

If $Z < Z_\alpha$ then the null hypothesis is not rejected, otherwise it is rejected and the series is assumed to be non-random. The null hypothesis can be tested on 5% and 10% significance level. The value of Z_α at 5% and 10% significance level is 1.96 and 2.65, respectively.

Turning Point Test. Kendall's turning point test (Kendall and Stuart 1976) is also based on the binary series. If $x_{i-1} < x_i > x_{i+1}$ or $x_{i-1} > x_i < x_{i+1}$ then $x_i = 1$; otherwise $x_i = 0$. The total number of ones u (i.e., initial value of $u = 0$ and if above stated condition is satisfied then $u = u + 1$), is approximately normally distributed. The expected value of u is defined as follows.

$$E(u) = 2(n-2)/3 \tag{Eq. 14.4}$$

$$Var(u) = (16n - 29)/90 \tag{Eq. 14.5}$$

The Z statistic can be computed as follows.

$$Z = \frac{u - E(u)}{[Var(u)]^{1/2}} \tag{Eq. 14.6}$$

If $Z < Z_\alpha$ then the null hypothesis is not rejected otherwise it is rejected and the series is assumed to be non-random.

Rank Difference Test (Meacham 1968). Values are replaced by their relative ranks R_i with the lowest being denoted by rank 1 (R1). The statistic u is calculated by

$$u = \sum_{i=2}^{n} |R_i - R_{i-1}| \qquad \text{(Eq. 14.7)}$$

The expected value of u is estimated by using the following relationship.

$$E(u) = [(n+1)\cdot(n-1)]/3 \qquad \text{(Eq. 14.8)}$$

The variance of u is given by

$$Var(u) = [(n-2)\cdot(n+1)\cdot(4n-7)]/90 \qquad \text{(Eq. 14.9)}$$

The Z statistic is estimated as follows:

$$Z = \frac{u - E(u)}{[Var(u)]^{1/2}} \qquad \text{(Eq. 14.10)}$$

If $Z_\alpha < Z$ then the null hypothesis is rejected and the series is assumed to be non-random.

Cumulative Periodogram Test (Box and Jenkins 1976). The periodogram of a time series is defined as

$$I(f_j) = \frac{2}{n}\left[\left(\sum_{i=1}^{n} x_i \cos 2\pi i f_j\right)^2 + \left(\sum_{i=1}^{n} x_i \sin 2\pi f_j\right)^2\right] \qquad \text{(Eq. 14.11)}$$

where $f_j = j/n$ is the frequency; j = 1, 2,……., (n – 2)/2 for n even; and j = 1, 2,……., (n – 1) for n odd. The normalized cumulative periodogram is obtained from following relation.

$$C(f_j) = \sum_{i=1}^{j} I(f_i)/ns^2 \qquad \text{(Eq. 14.12)}$$

where S^2 is the variance of x_i. For a white-noise series the plot of $C(f_i)$ against f_i would be scattered about a straight line joining points (0, 0) and (0.5, 1). The approximate confidence limit lines for a truly random series are drawn at distances:

$$\pm K_\alpha / [(n-2)/2]^{1/2} \qquad \text{(Eq. 14.13)}$$

where n is even and K_α is 1.63 (99%), 1.36 (95%), 1.22 (90%) or 1.02 (75%).

Wald-Wolfowitz Test (Wald and Wolfowitz 1943). For a sample of size n

$$R = \sum_{i=1}^{n-1} x_i x_{i-1} + x_1 x_n \qquad \text{(Eq. 14.14)}$$

If the elements of the sample are independent then expectation and variance are computed as

$$E(R) = \frac{s_1^{\ 2} - s_2}{n-1} \quad \text{(Eq. 14.15)}$$

$$Var(R) = \frac{s_2^{\ 2} - s_4}{n-1} - \left(\frac{s_1^{\ 2} - s_2}{n-1}\right)^2 + \frac{s_1^{\ 4} - 4s_1^{\ 2}s_2 + 4s_1s_3 + s_2^{\ 2} - 2s_4}{(n-1)\cdot(n-2)} \quad \text{(Eq. 14.16)}$$

where,

$$s_r = x_1^{\ r} + x_2^{\ r} + \cdots\cdots + x_n^{\ r} \quad \text{(Eq. 14.17)}$$

Similarly, the Z-statistic is computed as:

$$Z = \frac{R - E(R)}{[Var(R)]^{1/2}} \quad \text{(Eq. 14.18)}$$

If the mean is subtracted first, $s_1 = 0$, then

$$R \approx N\left\{\frac{-s_2}{n-1}, \left[\frac{s_2^{\ 2} - s_4}{n-1} - \left(\frac{-s_2}{n-1}\right)^2 + \frac{s_2^{\ 2} - 2s_4}{(n-1)\cdot(n-2)}\right]^{1/2}\right\} \quad \text{(Eq. 14.19)}$$

If $Z_\alpha < Z$ then the null hypothesis is rejected and the series is assumed to be non-random.

Rank von Neumann ratio Test (Madansky 1988). Let $r_1, r_2, \cdots, r_n$ denote the ranks associated with the x_i values. The rank Von Nuemann ratio is given by

$$\upsilon = \frac{\sum_{i=2}^{n}(r_i - r_{i-1})^2}{n(n^2-1)/12} \quad \text{(Eq. 14.20)}$$

Critical value of $C = [n^2(n^2-1)/12]\upsilon$ and approximate critical value of υ were given by Madansky (1988). For large n, υ is approximately distributed as $N(2, 4/n)$, although Bartels recommended $20/(5n+7)$ as a better approximation to the variance of υ (Madansky 1988).

Kendall's Rank Correlation Test. If the series is thought to have a random component, Kendall's rank correlation test can be used to test for significance. This measures the 'disarray' in the data; it is particularly effective if the underlying trend is of a linear type. This test is also referred as $\tau-$ test and is based on the proportionate number of subsequent observations which exceeds a particular value. The statistics u is calculated as follows: if $(x_{i+1} > x_i)$ *then* $u = u + 1$, whereas initial value of u is assigned zero (i.e. u = 0). The Z statistic is computed as:

$$Z = \frac{T}{[Var(T)]^{1/2}} \quad \text{(Eq. 14.21)}$$

where, $$T = \frac{4u}{n(n-1)} - 1 \quad \text{(Eq. 14.22)}$$

$$Var(T) = \frac{2(2n+5)}{9n(n-1)} \quad \text{(Eq. 14.23)}$$

If $Z_\alpha < Z$ then the null hypothesis is rejected and the series is assumed to be non-random.

Run Test. In this test, x is replaced by 0 if $x_i < x_{median}$, and x is replaced by 1 if $x_i > x_{median}$. If the original sequence of X_s has been generated by a purely random process, then u, the number of times 0 is followed by 1 or 1 is followed by 0, is approximately normally distributed. The test is worked out using the following steps. Initially $u = 0$. If $x_i > x_{median} > x_{i+1}$ or $x_i < x_{median} < x_{i+1}$ then $u = u + 1$. The expected value of u is defined as follows.

$$E(u) = m + 1 \quad \text{(Eq. 14.24)}$$

where, m is the rank corresponding to the median value. The variance of u is estimated as follows.

$$Var(u) = \frac{m(m-1)}{2m-1} \quad \text{(Eq. 14.25)}$$

The Z statistic can be computed as follows.

$$Z = \frac{u - E(u)}{[Var(u)]^{1/2}} \quad \text{(Eq. 14.26)}$$

If $Z < Z_\alpha$ then the null hypothesis is not rejected otherwise it is rejected (i.e., the series is assumed to non-random).

Spearman's Rho Test. For a sample data set of $\{x_i, i = 1, 2, ..., n\}$, the null hypothesis H_o of S-R test is that all the x_i are independent and identically distributed. The alternative hypothesis is that x_i increases or decreases with i, then non-randomness exists. The Z statistics of S-R test is given as follows:

$$D = 1 - \frac{6\sum_{i=1}^{n}\{R(x_i) - i\}^2}{n(n^2-1)} \quad \text{(Eq. 14.27)}$$

$$Var(D) = 1/(n-1) \quad \text{(Eq. 14.28)}$$

$$Z = \frac{D}{[Var(D)]^{0.5}} \quad \text{(Eq. 14.29)}$$

where, $R(x_i)$ is the rank of i^{th} observation x_i in the sample of size n. The standardized statistics Z follow the standard normal distribution $Z \approx N(0, 1) = 1.96$ at 5%.

14.1.2 Parametric Test

In the above section, non-parametric tests have been described, which uses the scores, rank or sign of the data to perform the analysis. Whereas, parametric tests are often robust which uses the time series statistics such as population mean and standard deviation computed from the sample. In the parametric test of short-term dependence, two tests viz. autocorrelation (Yevjevich 1976) and von Nuemann ratio test (Madansky 1988) has been described.

Autocorrelation Test (Yevjevich 1971). Short-term dependence is usually measured by the magnitude of the low-order autocorrelation coefficients. It is extensively used to determine the linear dependence in the time series. The autocorrelation function, r_k, is estimated from

$$r_k = \frac{\sum_{t=1}^{n-k}(x_t - \bar{x}_t)\cdot(x_{t+k} - \bar{x}_{t+k})}{\left[\sum_{t=1}^{n-k}(x_t - \bar{x}_t)^2 \cdot \sum_{t=1}^{n-k}(x_{t+k} - \bar{x}_{t+k})^2\right]^{1/2}} \quad \text{(Eq. 14.30)}$$

where k is lag, x_t is the observation at time t, and n is sample size. The lag-1 autocorrelation, r_1 is calculated from eq. (14.30) and checked whether or not is significantly different from the expected value as

$$E(r_1) = -1/n \quad \text{(Eq. 14.31)}$$

and,

$$Var(r_1) = (n^3 - 3n^2 + 4)/\left[n^2(n^2 - 1)\right] \quad \text{(Eq. 14.32)}$$

and,

$$Z = r_1 - E(r_1)/\left[Var(r_1)\right]^{0.5} \quad \text{(Eq. 14.33)}$$

where, Z is the normally distributed Z-statistic at α significance level. If $Z < Z_\alpha$ then the null hypothesis is not rejected otherwise it is rejected (i.e., the series is assumed to non-random). The value of Z_α is 1.96 and 2.65 for 5% and 10% significance level.

von Neumann Ratio Test (Madansky 1988). If $x_i, i = 1, 2, ...$ is a time series of hydrologic variable then the V-statistics need to be computed based on the assumption that the series is normally distributed with N (0, 1) and is computed as follows:

$$Z(V) = \frac{V - E(V)}{[Var(V)]^{0.5}} \quad \text{(Eq. 14.34)}$$

with, $$V = \frac{\sum_{i=2}^{n}(x_i - x_{i-1})}{\sum_{i=1}^{n}(x_i - \overline{x})^2} \quad \text{(Eq. 14.35)}$$

$$E(V) = 2 \quad \text{(Eq. 14.36)}$$

$$Var(V) = \frac{4(n-2)}{(n^2-1)} \quad \text{(Eq. 14.37)}$$

14.1.3 Test for Long Term Dependence (Lye and Lin 1994)

The long-term dependence in hydrologic time series is manifested by the fact that the extreme events may persist for a long time. In water resources design long sequence of hydrologic data are required (more than 100 years). In such long records it is expected to have the extreme events. Therefore, the generation of long range dependence effect is of vital importance to the water resources system planning.

In this chapter, long term dependence can be measured by the magnitude of the Hurst coefficient. The Hurst's coefficient *k* is estimated by eq. (14.38).

$$k = \frac{\log(R_n / \sigma_n)}{\log(n/2)} \quad \text{(Eq. 14.38)}$$

where R_n = range of cumulative departure from the mean, σ_n = standard deviation of the sample, n = sample length. If k = 0.5, series is independent (i.e. random in nature) and for greater degree of dependence k > 0.5, but not exceed to unity.

Range Analysis: Computation of R_n **.** The *range*, related to the storage capacity of the reservoir and *run*, the property related to the drought, are the additional characteristics important in water resources studies that may be derived from a time series. The range of cumulative departures from the sample mean is related to the minimum storage capacity required to deliver the sample mean throughout a time period equal to the length of the sample *n.* Range of the cumulative departure from mean R_n can be expressed as follows.

$$R_n = d_n^+ - d_n^- \quad \text{(Eq. 14.39)}$$

In eq. (14.39), d_n^+ is the maximum value of the cumulative departure from mean, and d_n^- is the minimum value of cumulative departure from mean. If z_i $(z_1, z_2, z_3, ...)$ is the flow series with mean of $\overline{z}$, then

$$d_n^+ = \max_{1 \le i \le n} \sum_{i=1}^{n} (z_i - \overline{z}) \qquad \text{(Eq. 14.40)}$$

and

$$d_n^- = \min_{1 \le i \le n} \sum_{i=1}^{n} (z_i - \overline{z}) \qquad \text{(Eq. 14.41)}$$

If z_i is the annual flow and initial storage is d_n^- then a reservoir having capacity R_n will be able to meet the average demand and could be full without overflow at least once and empty at least once.

Rescaled Range. The rescaled range is the range divided by the sample standard deviation σ_n . The rescaled range is defined by eq. (14.42):

$$R_n^* = R_n / \sigma_n \qquad \text{(Eq. 14.42)}$$

It is proportional to $N^{0.5}$ as $N \to \infty$ for models most typically used in hydrology such as AR and the ARMA models. Analysis made by Hurst (1951) using long records of geophysical time series, appears to show that the rescaled range is proportional to n^k with $k \ge 0.5$ (while for models such as those referred above (i.e. eq. 14.38) $k = 0.5$). This apparent discrepancy has been called the “Hurst Phenomenon”. i.e.,

$$R_n^* = f(n) = n^k \qquad \text{(Eq. 14.43)}$$

For random series $R_n^* = f(n) = n^{0.5}$, *i.e.* $k = 0.5$.

Bootstrap Method for Testing the Significance of Hurst’s k. To test the significance of Hurst’s K, the non-parametric bootstrap approach (Efron 1979; 1981; 1982) was applied. The bootstrap samples are generated from the data of the original samples as follows: (i) suppose that the annual flow series $x_1, x_2, ...x_n$ are independent observations. Each x_i has the same probability of occurrence and is equal to $1/n$, where n is the number of observations in the series; (ii) generate a uniform random data i between 1 and *n*, then choose x_i as one point in the bootstrap sample. Repeat this step *n* times to generate a bootstrap sample of the same size *n* as the original sample size; (iii) calculate the Hurst’s *k* for the bootstrap samples; (iv) repeat steps (ii) to (iii) for a large number of times (say, 10000); (v) count the number of times the observed *k* value of sample is exceeded by 10000 bootstrap *k* values; and (vi) calculate the *P* value as follows:

$$P_{\text{value}} = \frac{\text{Number of } k > k_{\text{observed}}}{\text{Number of Bootstrap samples (i.e. 10000)}} \qquad \text{(Eq. 14.44)}$$

If the $P_{value} < \alpha$ (say 0.05) then the series has long term dependence at the specified level (i.e. $\alpha = 5\%$); otherwise, series does not have long term dependence. It is important to note that the null hypothesis of this bootstrap test is that of independence.

14.2 Statistical Methods of Trend Analysis

A steady and regular movement in a time series through which the values are on average either increasing or decreasing is termed a trend. This type of behavior can be local, in which case the nature of the trend is subject to change over short intervals of time, or, on the other hand, it can be visualized as a global trend that is long lasting. If a trend in a hydrologic time series appear it is, in effect, part of a low frequency oscillatory movement induced by climatic factors or through change in land use and catchment characteristics. There are several approaches to detecting the trend in the time series. These approaches can be either parametric or non-parametric. Parametric methods assume that the data are normally distributed and free from outliers. On the other hand, non-parametric methods are free from such assumptions. The most commonly used non-parametric tests for detecting trend in the time series is the Mann-Kendall (MK) test (Mann 1945; Kendall 1955). It is widely used for various climatic variables (Hirsch et al. 1982; Hirsch and Slack 1984; Lettenmaier et al. 1994, Gan 1998; Lins & Slack 1999; Douglas et al. 2000; Burn and Elnur 2002; Yue et al. 2002; Yue and Pilon 2004; Burn et al. 2004; Zhang et al. 2005; Aziz and Burn 2006; Chen et al. 2007; Rai et al. 2010).

This section demonstrates the different techniques of trend analysis for climatic variables. The statistical tests applied for the analysis are the original Mann-Kendall, modified Mann-Kendall (MK), and Mann-Kendall with pre-whitening.

14.2.1 Original Mann-Kendall Test (Mann 1945; Kendall 1955)

The original MK test searches for a trend in a time series without specifying whether the trend is linear or nonlinear (Khaliq et al. 2009). It works on the null hypothesis that data are independent and randomly ordered, i.e. there is no trend or serial correlation structure present in the observations. The Mann-Kendall test for detecting monotonic trends in hydrologic time series is described by Yue et al. (2002). It is based on the test statistics S, which is defined as:

$$S = \sum_{i=1}^{n-1} \sum_{j=i+1}^{n} \operatorname{sgn}(x_j - x_i) \qquad \text{(Eq. 14.45)}$$

where, x_j are the sequential data values, n is the length of the data set and

$$\operatorname{sgn}(t) = \begin{cases} 1, & for\, t > 0 \\ 0, & for\, t = 0 \\ -1, & for\, t < 0 \end{cases} \qquad \text{(Eq. 14.46)}$$

The value of S indicates the direction of trend. A negative (positive) value indicates falling (rising) trend. Mann-Kendall has documented that when $n \geq 8$, the test statistic S is approximately normally distributed with mean and variance as follows:

$$E(S) = 0 \qquad \text{(Eq. 14.47)}$$

$$Var(S) = \frac{n(n-1)(2n+5) - \sum_{i=1}^{m} t_i(t_i-1)(2t_i+5)}{18} \qquad \text{(Eq. 14.48)}$$

where, m is the number of tied groups and t_i is the size of the i^{th} tie group. The standardized test statistics Z is computed as follows.

$$Z_{MK} = \begin{cases} \frac{S-1}{\sqrt{Var(S)}}, & for\ S > 0 \\ 0, & for\ S = 0 \\ \frac{S+1}{\sqrt{Var(S)}}, & for\ S < 0 \end{cases} \qquad \text{(Eq. 14.49)}$$

The standardized Mann-Kendall statistics Z follows the standard normal distribution with zero mean and unit variance. If $|Z| \geq Z_{1-(\alpha/2)}$, the null hypothesis about no trend is rejected at the significance level α (10% in this study).

14.2.2 Mann-Kendall Test for Autocorrelated Data

For the original Mann-Kendall test, the time series must be serially independent. However, in many real situations the observed data are auto-correlated. The autocorrelation in the observed data may cause misinterpretation of the trend test results. Cox and Stuart (1955) stated that “positive serial correlation among the observations would increase the chance of a significant answer, even in the absence of a trend”. A closely related problem that has been studied is the case where seasonality exists in the data (Hirsch et al. 1982). By dividing the observations into separate classes according to the season and then performing the Mann-Kendall trend test on the sum of the statistics from each season, the effect of seasonality can be eliminated. This modification is called the seasonal Mann-Kendall test (Hirsch et al. 1982; Hirsch and Slack 1984). Although the seasonal test eliminates the effect of seasonal dependence, it does not account for the correlation in the series within the season (Hirsch and Slack 1984). The same problem exists when yearly time series is considered for the analysis as it can be significantly auto correlated. Therefore, the original Mann-Kendall test is modified so that it can account for serially dependent data.

Modified Mann-Kendall Test. For the Modified Mann-Kendall’s test, the statistic *S* tends to normality for large *n*, with mean and variance given by:

$$E(S) = 0 \quad \text{(Eq. 14.50)}$$

$$Var(S) = n(n-1)(2n+5)/18 \quad \text{(Eq. 14.51)}$$

where S is given by eq. (14.52):

$$S = a_{ij} = \sum_{i=1}^{n-1} \sum_{j=i+1}^{n} \operatorname{sgn}(x_j - x_i) \quad \text{(Eq. 14.52)}$$

with the same mean and variance as in eqs. (14.50) and (14.51). A modified version of the Mann-Kendall test which is robust in the presence of autocorrelation is based on the modified variance of S given by eq. (14.52).

$$V^*(S) = Var(S) \cdot \frac{n}{n_s^*} = \frac{n(n-1)(2n+5)}{18} \cdot \frac{n}{n_s^*} \quad \text{(Eq. 14.53)}$$

where, n/n_s^* represents a correlation due to the autocorrelation in the data. The n/n_s^* is evaluated using eq. (14.54).

$$\frac{n}{n_s^*} = 1 + \frac{2}{n(n-1)(n-2)} \times \sum_{i=1}^{n-1} (n-i)(n-i-1)(n-i-2)\rho_s(i) \quad \text{(Eq. 14.54)}$$

In eq. (14.54), n is the actual number of the observations and $\rho_s(i)$ is the autocorrelation function of the ranks of the observations. The advantage of using eqs. (14.53) and (14.54) for the evaluation of variance of S is that there is no need of either normalized data or their autocorrelation function. The autocorrelation of ranks of observations $\rho_s(i)$ is related with the parent autocorrelation function and is given as follows (Kendall 1955):

$$\rho(i) = 2 \sin\left(\frac{\pi}{6}\rho_s(i)\right) \quad \text{(Eq. 14.55)}$$

The inverse of eq. (14.55) can therefore be used to evaluate the autocorrelation of the ranks $\rho_s(i)$ that appeared in eq. (14.54) and is given by eq. (14.56).

$$\rho_s(i) = \frac{6}{\pi} \sin^{-1}\left(\frac{\rho(i)}{2}\right) \quad \text{(Eq. 14.56)}$$

The significance of the trends is tested by comparing the standardized test statistics Z.

$$Z = \frac{S}{[V^*(S)]^{0.5}} \quad \text{(Eq. 14.57)}$$

A significant level of $\alpha = 0.1$ for the autocorrelation of the ranks $\rho_s(i)$ was used, which produced the best overall empirical significance level. The serial correlation of the series can be computed as follows:

$$r_k = \frac{Cov(x_t, x_{t+k})}{S_t \cdot S_{t+k}} = \frac{\sum_{t=1}^{n-k} (x_t - \overline{x}_t) \cdot (x_{t+k} - \overline{x}_{t+k})}{\left\{\sum_{t=1}^{n-k} (x_t - \overline{x}_t)^2 . \sum_{t=1}^{n-k} (x_{t+k} - \overline{x}_{t+k})^2\right\}^{1/2}} \quad \text{(Eq. 14.58)}$$

where, $\overline{x}_t$ is the mean of the first $n-k$ values $x_1, x_2, ..., x_{n-k}$, and $\overline{x}_{t+k}$ is the mean of the last $n-k$ values $x_{k+1}, x_{k+2}, ..., x_n$. r_k varies in the range of $-1 \le r_k \le +1$. To test the significance of serial correlation 95 and 99% of probability level, eqs. (14.59) and (14.60) are used respectively (Yevjevich 1971).

$$r_k(95\%) = \frac{-1 \pm 1.965(n-k-1)^{1/2}}{n-k} \quad \text{(Eq. 14.59)}$$

For 99 % of probability level,

$$r_k(99\%) = \frac{-1 \pm 2.326(n-k-1)^{1/2}}{n-k} \quad \text{(Eq. 14.60)}$$

Mann-Kendall Test with Pre-whitening. An alternative approach to perform the trend analysis of time series with the presence of serial correlation using the Mann-Kendall test is to first remove the serial correlation from data and then apply the test. Several approaches have been suggested for removing the serial correlation from a data set prior to applying the test. The pre-whitening approach is most common which involves computation of serial correlation and removing the correlation if the calculated serial correlation is significant at 5% significance level (Burn and Elnur 2002). The pre-whitening is accomplished as follows:

$$X_t' = X_{t+1} - \rho_1 X_t \quad \text{(Eq. 14.61)}$$

where, X_t = original time series with autocorrelation for time interval *t*; X_t' = pre-whitened time series; and ρ_1 = the lag-1 autocorrelation coefficient. This pre-whitened series is then subjected to Mann-Kendall test (i.e. eqs. 14.45 to 14.49) for detecting the trend.

14.3 Statistical Methods of Periodicity

For analyzing the persistence and periodicity in the climatic series over the world, considerable efforts have been made in the past by many investigators. For example, Angell et al. (1966) investigated quasi-biennial oscillation in troposphere zonal winds of the Tropics and sub-tropics; whereas it is also evident in the surface temperature in many parts of the world (Landsberg et al. 1963).

14.3.1 Test of Persistence and Periodicity

To test the persistence and periodicity in the climatological time series, normalized anomaly of the time series is used. A normalized series is obtained as follows:

$$X_{sN(j)} = (X_{s(j)} - \overline{X}_s) / \sigma_s \quad \text{(Eq. 14.62)}$$

where, $X_{sN(j)}$ is the normalized anomaly of the series, X_s is the observed time series for station *s* during j^{th} year, $\overline{X}_s$ and σ_s are the long-term mean and standard deviation of annual/seasonal time series.

14.3.2 Computation of the power spectrum

Periodicity is one of the deterministic components in the time-series. Most of the climatic, atmospheric and hydrological time-series would consist of a combination of stochastic and deterministic components. The power spectrum is a method of analysis that was developed to handle the problem of periodicity in variations of natural events observed in time, such as in climatological and hydrological time series. Power spectrum analysis, also called generalized harmonic analysis, was derived from the principles first developed by Wiener (1930, 1949). It is based on the premise that the time series are not necessarily composed of a finite number of oscillations, each with a discrete wavelength, but rather that they consist of virtually infinite number of small oscillations spanning a continuous distribution of wavelengths. The spectrum therefore, gives the distribution of variations in a time series over a continuous domain of all possible wavelengths.

Procedures for computing the power spectra may vary. Here, in this study, an approach described in WMO (1966), developed by Tukey (1950) and Blackman and Tukey (1958), was employed. A detailed description of this approach can also be found in various textbooks: Blackman and Tukey (1958), Jenkins and Watts (1968) and Julian (1967). It can be summarized through the following steps:

(i) First, all serial correlation coefficients of normalized climatic series are computed for lags from $L = 0$ to *m*, where *m* is the maximum lag considered to be *N/3* in which; *N* is the length of the series. The serial correlation coefficient can be computed using eq. (14.63).

$$r_L = \frac{\sum_{t=1}^{n-L}(x_t - \overline{x}_t)\cdot(x_{t+L} - \overline{x}_{t+L})}{\left[\sum_{t=1}^{n-L}(x_t - \overline{x}_t)^2 \cdot \sum_{t=1}^{n-L}(x_{t+L} - \overline{x}_{t+L})^2\right]^{1/2}} \qquad \text{(Eq. 14.63)}$$

(ii) Using the values of r_L, the 'raw' spectral estimates, $\hat{s}_k$ are computed using the following set of equations:

$$\hat{s}_0 = \frac{1}{2m}(r_0 + r_m) + \frac{1}{m}\sum_{L=1}^{m-1} r_L \qquad \text{(Eq. 14.64)}$$

$$\hat{s}_k = \frac{r_0}{m} + \frac{2}{m}\sum_{L=1}^{m-1} r_L\, Cos(\frac{\pi kL}{m}) + \frac{1}{m} r_m (-1)^k \text{; for } k = 1,2,.......,m-1 \qquad \text{(Eq. 14.65)}$$

$$\hat{s}_m = \frac{1}{2m}[r_0 + (-1)^m r_m] + \frac{1}{m}\sum_{L=1}^{m-1}(-1)^L r_L \quad \text{(Eq. 14.66)}$$

Smallest is the value of k longest will be the wavelength of the spectrum, i.e. shortest wavelength is achieved at $k = m$.

(iii) The raw spectrum $\hat{s}_k$ is then smoothened with a 3-term weighted average. For smoothing, procedure suggested by Hanning was used (WMO 1966).

$$s_0 = (\hat{s}_0 + \hat{s}_1)/2 \quad \text{(Eq. 14.67)}$$

$$s_k = (\hat{s}_{k-1} + 2\hat{s}_k + \hat{s}_{k+1})/4\text{; for } k = 1, 2, \ldots\ldots, m-1 \quad \text{(Eq. 14.68)}$$

$$s_m = (\hat{s}_{m-1} + \hat{s}_m)/4 \quad \text{(Eq. 14.69)}$$

The averaging procedure is performed to derive a constant estimate of the final spectrum in terms of $m+1$ discrete estimates (WMO 1966).

14.3.3 Test for Statistical Significance

The procedure for evaluating the results of power spectrum analysis mention in WMO (1966) is described below:

A 'null' hypothesis continuum is fitted to the computed spectrum. To start with, significance of the lag-1 serial correlation coefficient r_1 of the climatic series is tested by the following equation.

$$(r_1)_t = [-1 \pm t_g\sqrt{N-1}]/(N-1) \quad \text{(Eq. 14.70)}$$

where, $t_g = 1.645$ at 90 percent confidence level. The 'null' hypothesis of the randomness of climatic series against the serial correlation is rejected for the large value of $(r_1)_t$. If r_1 is not significantly different from zero, then series is regarded to be free from persistence. In this case, the appropriate null continuum is 'white noise'. In other words, a horizontal straight line, the value of which is everywhere equal to the average of the values of all the $m+1$ 'raw' spectral estimates (i.e., $\bar{s}$) in the computed spectrum (i.e., $S_k = \bar{s}$), is taken as the most suitable theoretical approach.

On the other hand, if the computed r_1 is positive and statistically significant, serial correlation coefficients for lag-2 and lag-3 are checked to see whether they approximate the exponential relations $r_2 \cong r_1^2$ and $r_3 \cong r_1^3$ (WMO 1966). If these relations are ensured with the computed serial coefficients, the approximate 'null' continuum is assumed as the simple "Markov red noise", whose shape depends on unknown value of the lag-1 serial correlation coefficient for a population ρ. Then the 'null' continuum can be created by following an approximate procedure. By assuming that the sample r_1 is an unbiased estimation of serial correlation coefficient ρ, of the Harmonic number of *k* between *k* = 0 to *m* are assessed:

$$S_k = \bar{s}[(1-r_1^2)/\{1+r_1^2 - 2r_1 Cos(\pi k/m)\}] \quad \text{(Eq. 14.71)}$$

where, $\bar{s}$ is the average of all $m+1$ 'raw' spectral estimates $\hat{s}_k$ in the computed spectrum. The resulting values of S_k can be plotted superposed on the sample spectrum, and a smoothed curve passed through these values to reach the required null continuum. If r_1 is statistically significant but a few serial correlation coefficients for higher lags do not show the required exponential relations with r_1, then doubt arises as to whether the simple Markov-type persistence is the dominant form of non-randomness in series of climatic observations. Nevertheless, WMO (1966) suggested that this procedure could be continued with just as before to compute the red noise continuum for r_1.

At this stage of the power spectrum analysis a first choice of the null continuum is made, and this selected continuum is superposed on the studied spectrum. In this case, it would be possible to make an assessment of the spectrum for its consistency with the chosen continuum. Then, the value of each spectral estimate s_k is compared with the local value of the null continuum. The statistic associated with each spectral estimate is the ratio of the magnitude of the spectral estimate to the local magnitude of the continuum (red noise continuum). Tukey (1950) found that the quantity of this ratio is distributed as Chi-square divided by the degree of freedom. The degree of freedom, ν, of each estimate of a computed spectrum is given as follows.

$$\nu = (2N - m/2)/m \quad \text{(Eq. 14.72)}$$

In eq. (14.72) *N* is the length of series and *m* is the maximum lag. The ratio of any sample spectral estimate s_k to its local value of the red noise continuum is then compared with critical percentage-point levels of χ^2/ν distribution for the proper ν value. This comparison produces the required statistical significance level. The χ^2 value can be obtained from standard statistical books. In a sample spectrum, critical percentage-point levels of the χ^2/ν distribution, e.g. the 0.95 confidence level, is the same for all spectral estimates s_k. The confidence limits are finally derived by multiplying the 'null' continuum (i.e. S_k) with the χ^2/ν. Finally, the cycle is computed using the relation of $P = 2m/L$.

14.4 Application of Methodology

The application of the described methodology for dependence, trend and periodicity is demonstrated using the hydro-climatic data of the Yamuna River basin.

The Yamuna River is a major tributary of the Ganga River system which originates from the Shivalik range of Himalaya which after traversing of 1325 km joins with the River Ganga at Allahabad. In 1325 km of stretch, it faces large hydro-climatic variation, and the catchment of it also has large variation between semi arid to humid with diversified land uses.

14.4.1 Data Used

The variables used in the analysis are categorized into two sets: direct variables and derived variables. The variables are: rainfall (annual, monsoon and non-monsoon rainfall), and few derived variables important for agricultural planning such as: the onset of effective monsoon (OEM), number of rainydays (annual, monsoon and non-monsoon) and the Aridity Index (AI).

For rainfall, one degree grid data of daily rainfall for the period 1951 to 2002 supplied by the India Meteorological Department (IMD) was used. Sixty five rain-grids points falling under the Yamuna basin with 1° buffer were used in the analysis. For seasonal analysis, only two seasons were considered, viz. the monsoon (July to October) and non-monsoon (November to June).

The OEM, an important governing agro-climatic parameter for planning of *kharif* crops was estimated using the Ashokraj (1979) criteria, which uses the daily rainfall and potential evapotranspiration data. The potential evapotranspiration was estimated using the Thornthwaite method (1948). A seven days rainfall spell satisfying the following conditions are terms as OEM. These conditions are (Ashokraj 1979): (i) first day rainfall in the seven days spells should be more than evaporation of that particular day; (ii) a day with-more than 3 mm of rainfall is considered to be a rainy day; (iii) total rainfall during the seven days spell is more than (3× PET + 10) mm; and (iv) at least four out of seven days are rainy days.

The aridity index (AI), an indicator of annual soil moisture deficit was estimated using the procedure of UNEP (1993) as:

$$AI = (R / PET) \times 100\ \% \qquad \text{(Eq.14.73)}$$

where, AI is the aridity index (%), R is the annual rainfall (mm) and PET is the annual potential evapotranspiration (mm). AI values below 100 % shows annual moisture deficit in average climatic conditions.

14.4.2 Analysis of Short- and Long-Term Dependence Test

As stated above, 12 statistical tests (10 non-parametric and 2 parametric tests) for short-term dependence and a single test (i.e. Hurst's coefficient with the boot strap method) for long-term dependence were used. For the long term dependence, Hurst's K and lag-1 serial correlation for all the considered variables has been estimated. A sample table for the OEM is given in Table 14.1, and the summary statistics is presented in Tables 14.2.

Table 14.1. Start of onset of effective monsoon, OEM (days)[a]

ID	Grid Point		Mean	Hurst's K	r_1	ID	Grid Point		Mean	Hurst's K	r_1
	Lat	Long					Lat	Long			
1	21.5N	75.5E	180	0.7	0.049	34	25.5N	81.5E	188	0.68	**0.033**
2	22.5N	74.5E	185	***0.78***	0.068	35	25.5N	82.5E	188	0.549	**-0.137**
3	22.5N	75.5E	178	0.662	-0.028	36	26.5N	73.5E	203	0.625	**0.018**
4	22.5N	76.5E	180	0.61	0.039	37	26.5N	74.5E	198	**0.735**	**0.156**
5	22.5N	77.5E	186	0.665	-0.069	38	26.5N	75.5E	200	**0.744**	**0.187**
6	22.5N	78.5E	177	***0.752***	0.096	39	26.5N	76.5E	195	**0.749**	**0.008**
7	22.5N	79.5E	181	***0.768***	**0.195**	40	26.5N	77.5E	196	***0.767***	**0.09**
8	23.5N	73.5E	194	0.678	0.4	41	26.5N	78.5E	196	**0.74**	**-0.055**
9	23.5N	74.5E	187	***0.796***	0.054	42	26.5N	79.5E	193	***0.787***	**0.112**
10	23.5N	75.5E	186	***0.787***	***0.235***	43	26.5N	80.5E	192	0.691	**-0.064**
11	23.5N	76.5E	187	0.677	-0.145	44	26.5N	81.5E	186	0.631	**-0.203**
12	23.5N	77.5E	182	0.632	***-0.297***	45	27.5N	74.5E	207	0.714	**-0.011**
13	23.5N	78.5E	182	0.632	-0.02	46	27.5N	75.5E	198	0.712	**0.015**
14	23.5N	79.5E	182	0.662	0.056	47	27.5N	76.5E	196	0.687	**-0.056**
15	23.5N	80.5E	181	***0.761***	0.072	48	27.5N	77.5E	201	***0.789***	**0.124**
16	24.5N	72.5E	200	0.647	0.195	49	27.5N	78.5E	196	***0.812***	**-0.053**
17	24.5N	73.5E	191	0.642	-0.101	50	27.5N	79.5E	193	**0.73**	**0.037**
18	24.5N	74.5E	190	***0.862***	***0.315***	51	27.5N	80.5E	190	0.672	**-0.177**
19	24.5N	75.5E	189	***0.824***	***0.372***	52	28.5N	75.5E	203	0.704	**0.057**
20	24.5N	76.5E	191	0.706	-0.099	53	28.5N	76.5E	204	0.678	**-0.161**
21	24.5N	77.5E	189	***0.772***	0.203	54	28.5N	77.5E	194	0.616	**-0.154**
22	24.5N	78.5E	187	***0.761***	0.063	55	28.5N	78.5E	193	***0.832***	**0.277**
23	24.5N	79.5E	188	**0.745**	0.117	56	29.5N	76.5E	205	**0.741**	**-0.147**
24	24.5N	80.5E	188	**0.746**	0.054	57	29.5N	77.5E	190	0.65	**-0.084**
25	24.5N	81.5E	186	**0.748**	0.127	58	29.5N	78.5E	188	0.448	**-0.068**
26	25.5N	73.5E	195	0.621	-0.17	59	30.5N	76.5E	194	0.677	**-0.042**
27	25.5N	74.5E	196	***0.75***	-0.073	60	30.5N	77.5E	184	0.692	**0.094**
28	25.5N	75.5E	196	***0.759***	0.129	61	30.5N	78.5E	173	0.687	**0.13**
29	25.5N	76.5E	191	0.717	0.048	62	31.5N	76.5E	181	0.712	**0.078**
30	25.5N	77.5E	189	0.694	0.041	63	31.5N	77.5E	180	0.664	**0.082**
31	25.5N	78.5E	191	0.727	0.089	64	31.5N	78.5E	197	0.479	**-0.129**
32	25.5N	79.5E	189	0.697	-0.026	65	31.5N	79.5E	186	0.683	**-0.05**
33	**25.5N**	**80.5E**	**192**	**0.734**	**0.142**						

[a] Values bold: dependence at 10% significance level; bold & italic: dependence at 5% significance level. The lower and upper critical limit for r1 are: $r1(l)$ = -0.248 and $r_1(u)$ = 0.208.

Table 14.2. Spatial summary of variables of Yamuna river basin

S. No	Variable	Mean Value			Hurst's K			R_1		
		Spatial mean (mm)	**Range (mm)**	**SD (mm)**	**Spatial mean**	**Range**	**SD**	**Spatial mean**	**Range**	**SD**
1	Annual rainfall	893.3	372.2-1653.5	280.3	0.652	0.436 - 0.887	0.088	0.039	(-0.329) - 0.591	**0.199**
2	Monsoon rainfall	806.8	327.0 - 1568.9	259.7	0.653	0.407 - 0.880	0.097	0.028	(-0.386) - 0.557	**0.220**
3	Non-monsoon rainfall	86.5	19.5 - 479.0	100.1	0.656	0.516 0.767	0.062	0.077	(-0.207) - 0.493	**0.149**
4	Annual rainydays	88	46.0 - 160.0	25	0.678	0.476 - 0.881	0.073	0.105	(-0.118) - 0.456	**0.125**
5	Monsoon rainydays	70	43 - 96	15	0.664	0.519 - 0.821	0.060	0.025	(-0.200) - 0.416	**0.118**
6	Non-monsoon rainydays	17	1 - 72	14	0.695	0.534 - 0.882	0.069	0.132	(-0.194) - 0.547	**0.139**
7	OEM	190	173 - 207	7	0.704	0.448 - 0.862	0.074	0.031	(-0.297) - 0.400	**0.138**
8	**AI**	**38.0**	**14.9 - 74.6**	**12.9**	**0.650**	**0.445 - 0.883**	**0.085**	**0.038**	**(-0.334) - 0.615**	**0.197**

For all the tests, the tests were conducted at 5% and 10% significance levels as these significance levels are quite appropriate for engineering practices (Lye and Lin 1994). The results obtained for these two levels were compared and summarized in Table 14.3 for sample variables. Different tests for independence have been designed for different assumptions and conditions, and do not have equal power to discriminate between the time series (Wall and Englot 1985; Lye and Lin 1994). Sometimes various tests can give different results for the same time series. This can be clearly seen from Table 14.3. Because of this, it is difficult to conclude whether the time series is said to be independent or not. Under such circumstances, similar criteria proposed by Lye and Lin (1994) were applied, i.e., if 4 out of 12 tests failed the test of independence, the series is considered to be dependent (i.e. not-random). Based on all the tests performed, the number of grid stations showing the significant dependence is presented (Table 14.4), and it is clear that no time series has passed all the tests.

Apart from this, it can be clearly seen from Table 14.1, in which only Hurst's K and r1 values are shown along with the means of the variables that there is no exact relationship between Hurst's K and r1. However, most of the time series that showed significant r1 also showed significant long term dependence, which is expected sometimes. To clarify this observation, a comparison of short term and long term dependence tests was made which is presented in Table 14.5. It can be seen from the Table 14.5 that time series of rainfall including rainydays and AI having long term dependence can pass short term dependence tests, but it is not the case for OEM. It is also observed from Table 14.5 that the number of time series having only long term dependence is fewer than the number of time series having both long- and short-term dependence for all the considered variables except for non-monsoon rainfall which seems to reflect the existence of some relationship between the short term and long term dependencies for climatic time series.

Table 14.3. Dependence as a function of test for onset of effective monsoon (OEM) and annual aridity index (AI) series over Yamuna river basin

S. No.	Test	Number of Series (Percentage) Indicating Dependence out of 65 series			
		OEM		AI	
		5%	10%	5%	10%
Short-term dependence: Non-parametric					
1	Median crossing test	3 (4.62)	4 (6.15)	10 (15.38)	15 (23.08)
2	Turning Point	7 (10.77)	12 (18.46)	5 (7.69)	6 (9.23)
3	Rank difference	5 (7.69)	7 (10.77)	13 (20.00)	15 (23.08)
4	Cumulative periodogram	12 (18.46)	16 (24.62)	12 (18.46)	17 (26.15)
5	Wald-Wolfowitz	4 (6.15)	5 (7.69)	11 (16.92)	16 (24.62)
6	Rank Von Neumann	5 (7.69)	7 (10.77)	10 (15.38)	16 (24.62)
7	Kendal rank	26 (40.00)	35 (53.85)	8 (12.31)	10 (15.38)
8	Run test	5 (7.69)	11 (16.92)	11 (16.92)	16 (24.62)
9	Spearman Rho	32 (49.23)	40 (61.54)	8 (12.31)	13 (20.00)
Short-term dependence: Non-parametric					
10	Autocorrelation	4 (6.15)	5 (7.69)	11 (16.92)	16 (24.62)
11	Von Neumann Ratio	5 (7.69)	7 (10.77)	12 (18.46)	16 (24.62)
Long-term dependence: Non-parametric					
12	Hurst's K test	17 (26.15)	27 (41.54)	7 (10.77)	12 (18.46)

Based on the above analysis of short term and long term dependence, following remarks can be made based on the time series data of Yamuna basin:

(i) Most of the time series showing significant r_1 when there is significant long term dependence. This is not unusual as short term dependence can give rise to some long term dependence.

(ii) Most of the time series indicating long term dependence can pass for short term independence also except for OEM.

14.4.3 Analysis of Trend Test

All the three tests were applied to the entire range of considered variables. The sample test results are given in Table 14.6 for OEM. Table 14.6 also includes the values of lag-1 serial correlation along with their lower and upper limits at 95% percent probability level. The results for all the variables are summarized in Table 14.7. The spatial variation of lag-1 serial correlation of the considered climatic series is depicted in Figure 14.1. Figure 14.1 also comprise of spatio-temporal variation of trend in climatic variables except the number of rainydays. The modified Mann-Kendall's Z-statistic was used for depicting the spatio-temporal trend in the climatic series with significance level at 10 percent. To present the, spatio-temporal variation in the trend, the Mann-Kendall's Z-statistic value was spatially interpolated using the Inverse Distance Weighted (IDW) technique in ArcGIS 9x. The interpolated raster surface is based on a weighted average of the location. The value of each cell is influenced mostly by nearby points and less by more distant stations. The IDW method works on the power parameter and a search radius. The power parameter controls the significance of calculated station values on the interpolated values. A high power value gives more emphasis on the nearest points, and the resulting surface will have more detail. In the present analysis, a power of six was fixed with quadrant search radius.

Based on the analysis, it was observed that annual rainfall and monsoon rainfall shows a declining trend whereas rising trend was observed in case of the non-monsoon rainfall. A similar result was also observed in case of rainydays. The number of rainydays and rainfall magnitude during the monsoon is declining. The overall mean Z-statistic for monsoon rainfall and monsoon rainydays was -0.874 and -0.62, respectively. However, trend statistics for annual rainfall pattern and annual rainydays were obtained as -0.832 and -0.362, respectively. It was evident from Figure 14.1 that rainfall is increasing during the non-monsoon period. The average Z - statistic for non-monsoon rainfall and rainydays were +0.209 and +0.258, respectively. The critical limit at 95% confidence level is 1.645. OEM is dependent on the rainfall pattern and potential evapotranspiration, and both the variable has shown a general falling trend in the basin. Therefore, the increasing trend in the OEM was the resulting effect of the rainfall and evapotranspiration patterns. The overall mean Z-statistic for the OEM was +1.81. Similarly, AI is the ratio of annual rainfall and potential evapotranspiration. Overall falling trend in the rainfall pattern in the Yamuna basin has been observed (Figure 14.1). Trend analysis of AI shows the falling trend in the Yamuna basin, which confirms the overall soil moisture deficit in the Yamuna basin. The overall mean Z-statistic value for AI was -0.78. A summary of results for the Yamuna basin is seen in Table 14.7.

Based on the analysis, the following remarks can be made:

(i) The presence of serial correlation in the time series significantly affects the Mann-Kendall's trend analysis.

(ii) The original Mann-Kendall test overestimated the presence of significant trend in the series than the modified Mann-Kendall and Mann-Kendall with Pre-whitening tests. Based on the overall trend results, the original Mann-Kendall test resulted in approximately 37% more significant trend than the modified Mann-Kendall test.

14.4.4 Analysis of Persistence and Periodicity

Persistence Analysis. For climatic variability and changes, the definition of persistence given by WMO (1966) is very common. According to this definition, persistence is a 'tendency for successive values of the series to "remember" their antecedent values, and to be influenced by them.' The value of r_1 has been used to detect the possible persistence in the observed year-to-year variations of normalized anomaly series and to examine its nature and magnitude. The approach proposed by WMO (1966) and Matalas (1967) was widely used later in many studies related to long-term climatic variations (e.g. Rodhe and Virji 1976; Granger 1977; Ogallo 1979;

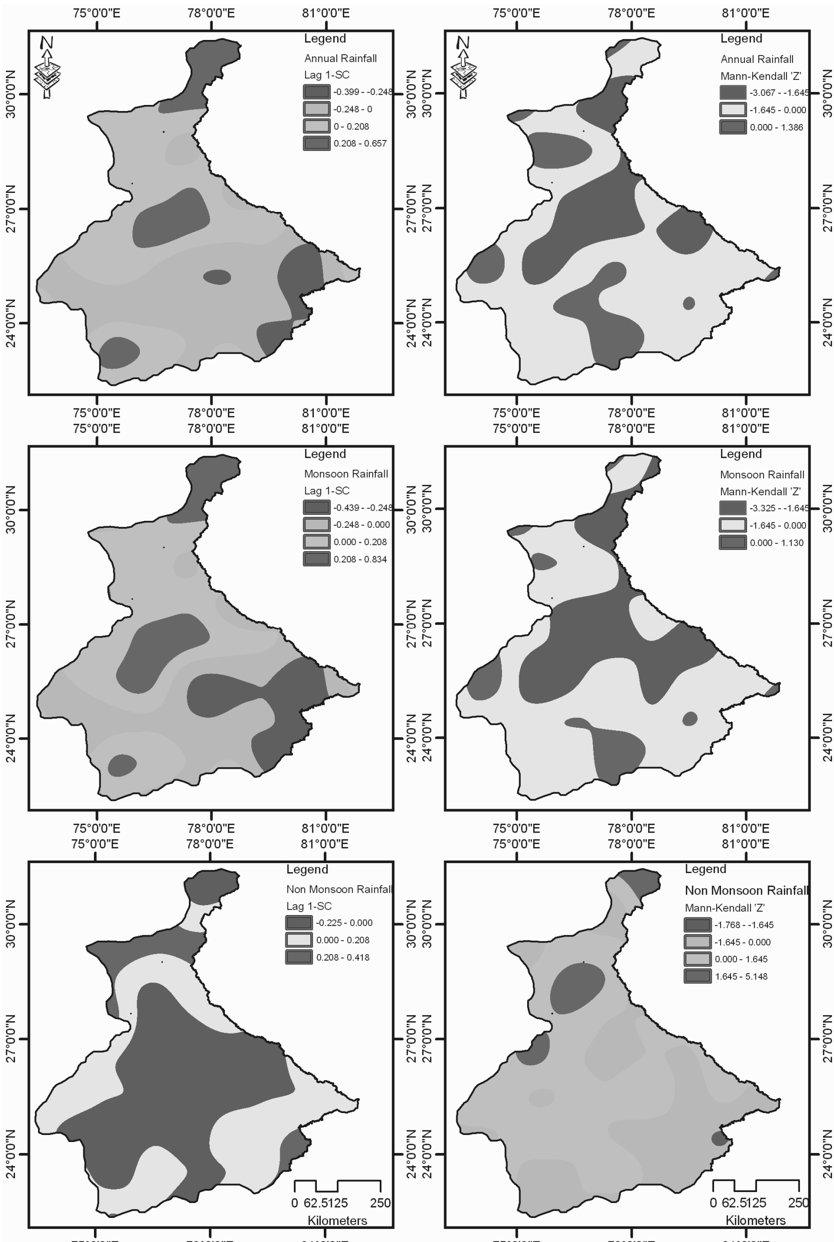

Figure 14.1. Spatial pattern of lag-1 serial correlation coefficient and Mann-Kendall's Z-Statistic

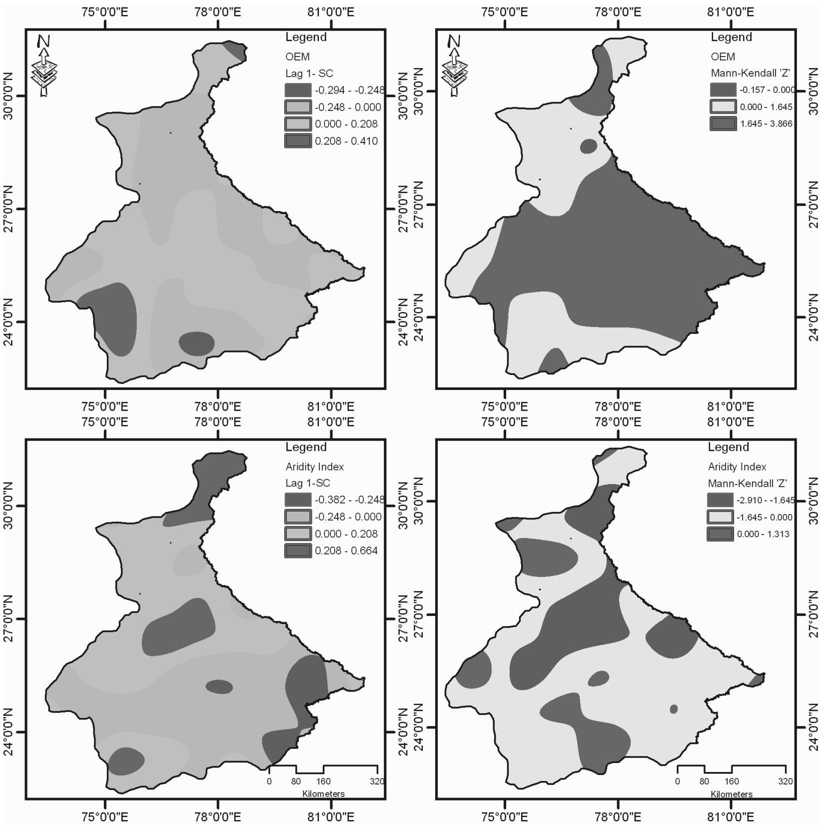

Figure 14.1. (Continued)

Anyadike 1993; Drosdowsky 1993; Nicholson and Palao 1993; Türkeş 1998; 1999; Türkes et al. 2002). Persistence is evident in long series of climatic observations characterized by a positive serial correlation. Significant negative r_1 are very likely to be indicative of high-frequency oscillations, whereas significant positive r_1 is likely to be indicative of low-frequency fluctuations and persistence in climatic series. In the study, serial correlation coefficient for all the lags $L = 0$ to m for all the variables, where $m = N/3$. However, serial correlation coefficients up to lag 3 was assessed. Serial correlation coefficient up to lag-3 is plotted for all the climatic variables except non-monsoon, although all the variables were analyzed. Approximately 15 percent of grid points showed significant positive lag-1 serial correlation coefficient in the annual rainfall series which indicated the presence of persistence. The statistical significance of serial correlation was assessed at 90% significance level. Little positive spatial coherence for the stations characterized by statistically significant lag-1 serial correlation coefficient was identified. A similar spatial variation in the time series was observed in annual and monsoon rainfall, annual rainy days, and AI.

Table 14.4. Number of time series passing the test of dependence out of 65 series

No. of Test Indicating Dependence	Rainfall						Rainydays						OEM		Aridity Index (AI)	
	Annual		Monsoon		Non-monsoon		Annual		Monsoon		Non-monsoon					
	5%	10%	5%	10%	5%	10%	5%	10%	5%	10%	5%	10%	5%	10%	5%	10%
10	0	0	0	0	0	0	0	0	0	0	0	0	0	0	0	0
9	2	3	3	4	0	1	0	2	0	1	1	3	1	0	2	3
8	2	5	4	5	2	1	2	4	1	3	3	9	1	2	2	5
7	4	9	6	10	2	5	4	7	3	4	7	15	3	5	5	8
6	8	11	7	12	7	10	6	10	3	5	11	17	3	5	5	10
5	12	13	11	17	7	11	7	13	3	6	14	21	5	7	11	13
4	**13**	**17**	**13**	**21**	**9**	**13**	**11**	**16**	**3**	**6**	**18**	**28**	**6**	**9**	**11**	**19**
3	13	20	18	27	12	19	13	19	6	10	24	33	9	15	14	20
2	21	28	25	35	18	25	23	30	12	28	31	38	31	37	21	28
1	26	33	28	38	22	28	31	37	21	36	39	48	37	43	28	33
0	39	32	37	27	43	36	34	27	44	29	26	16	28	21	37	32
Hurst's K	**7**	**12**	**10**	**16**	**4**	**7**	**9**	**15**	**5**	**10**	**15**	**21**	**17**	**27**	**7**	**12**

Table 14.5 Comparison of short-term and long-term dependence in the climatic variables

	Rainfall						Rainydays						OEM		Aridity Index (AI)	
	Annual		Monsoon		Non-monsoon		Annual		Monsoon		Non-monsoon					
	5%	10%	5%	10%	5%	10%	5%	10%	5%	10%	5%	10%	5%	10%	5%	10%
Short-term	13	17	13	21	9	13	11	16	3	6	18	28	6	9	11	19
Long-term	7	12	10	16	4	7	9	15	5	10	15	21	17	27	7	12
Only short-term	8	9	7	10	9	12	5	9	1	2	10	13	2	3	7	11
Only long-term	0	0	1	1	3	3	2	4	0	1	0	2	2	1	0	0
Both short & long-term	**5**	**8**	**6**	**11**	**0**	**2**	**6**	**8**	**2**	**4**	**8**	**16**	**4**	**7**	**4**	**8**

Table 14.6. Lag-1 serial correlation and Mann-Kendall's Z statistics of OEM of the Yamuna river basin [r1(l) = -0.248, r1(u) = 0.208]

ID	r_1	Z-MK			ID	r_1	Z-MK		
		Org	Rank	PW			Org	Rank	PW
1	0.099	1.320	1.321	1.321	34	0.020	***2.647***	***2.648***	***2.648***
2	0.084	1.785	1.785	1.785	35	-0.118	1.358	1.359	**1.359**
3	0.050	1.335	1.335	1.335	36	0.042	-1.153	-1.154	**-1.154**
4	0.028	***1.990***	***1.991***	***1.991***	37	0.172	0.569	0.569	**0.569**
5	0.001	0.917	0.918	0.918	38	0.155	***2.559***	***2.559***	***2.559***
6	0.168	***2.354***	***2.356***	***2.356***	39	-0.036	***1.991***	***1.993***	***1.993***
7	**0.234**	**2.110**	**2.111**	1.184	40	0.144	***3.002***	***3.003***	***3.003***
8	0.117	***3.776***	0.056	***3.777***	41	-0.188	***2.606***	***2.607***	***2.607***
9	0.035	***2.678***	***2.679***	***2.679***	42	0.085	***3.502***	***3.507***	***3.507***
10	**0.323**	**2.472**	**2.473**	1.097	43	-0.065	***2.141***	***2.141***	***2.141***
11	-0.136	1.517	1.519	1.519	44	-0.194	0.924	0.924	**0.924**
12	**-0.291**	1.146	0.031	0.963	45	-0.007	0.079	0.079	**0.079**
13	-0.101	1.406	1.407	1.407	46	0.032	1.193	1.193	**1.193**
14	0.014	1.763	1.766	1.766	47	-0.069	0.371	0.372	**0.372**
15	0.037	***2.433***	***2.433***	***2.433***	48	0.003	***3.270***	***3.271***	***3.271***
16	0.074	***1.998***	***1.999***	***1.999***	49	-0.025	***3.341***	***3.343***	***3.343***
17	-0.097	1.240	1.241	1.241	50	0.026	1.808	1.808	**1.808**
18	**0.307**	**3.658**	0.020	**1.965**	51	-0.141	1.011	1.012	**1.012**
19	**0.320**	**2.441**	-0.025	1.515	52	0.046	1.125	1.131	**1.131**
20	-0.043	1.651	1.652	1.652	53	-0.100	0.537	0.537	**0.537**
21	0.019	***3.792***	***3.793***	***3.793***	54	-0.153	0.134	0.134	**0.134**
22	0.051	***3.160***	***3.162***	***3.162***	55	0.194	***4.447***	0.000	***4.448***
23	0.136	***3.106***	***3.108***	***3.108***	56	-0.047	1.047	1.096	**1.096**
24	0.004	***2.782***	***2.786***	***2.786***	57	-0.071	1.936	1.937	**1.937**
25	0.167	2.938	2.939	2.939	58	0.024	0.672	0.673	**0.673**
26	-0.157	0.537	0.538	0.538	59	0.009	1.698	1.699	**1.699**
27	-0.106	1.509	1.509	1.509	60	0.051	***2.156***	***2.157***	***2.157***
28	0.115	***2.566***	***2.566***	***2.566***	61	0.118	0.387	0.387	**0.387**
29	0.030	***2.812***	***2.813***	***2.813***	62	0.158	***2.267***	***2.268***	***2.268***
30	0.030	***2.173***	***2.174***	***2.174***	63	0.115	1.216	1.216	**1.216**
31	0.096	***3.238***	***3.239***	***3.239***	64	-0.056	-0.348	-0.348	**-0.348**
32	-0.104	***3.100***	***3.107***	***3.107***	65	-0.035	0.963	0.963	**0.963**
33	**0.014**	***2.964***	***2.966***	***2.966***					

Table 14.7. Summary of trend analysis based on Modified Mann-Kendall test

S. No	Variable	No. of Series Indicating significant lag-1 serial correlation	No. of Series Indicating Significant			
			Rising Trend	Falling Trend	No Trend	Overall Trend
1	Annual rainfall	16		6 (8)	59 (57)	- ve
2	Monsoon rainfall	18		8 (13)	57 (52)	- ve
3	Non-monsoon rainfall	13	3 (2)		62 (63)	+ ve
4	Annual rainydays	17	4 (2)	7 (11)	54 (52)	- ve
5	Monsoon rainydays	5		5 (6)	60 (59)	- ve
6	Non-monsoon rainydays	22	6 (2)	1 (2)	58 (61)	+ ve
7	OEM	5	29 (30)		36 (35)	+ ve
8	**Aridity Index (AI)**	**17**		**6 (8)**	**59 (57)**	- ve

(Values in the parenthesis are the results from Mann-Kendall with Pre-whitening test).

Detailed tables of the serial correlation coefficients up to lag-3 are estimated. The sample table is presented in Table 14.8. There are very few coherent area with significant negative lag-1 serial coefficient over the basin was observed. Looking into the figures of lag-1 and lag-2 serial correlation pattern, it was indicated that coherent area of significant positive lag-2 serial correlation are greater than that of the lag-1. The lag-2 serial correlation coefficients are mostly positive but insignificant for all the variables except for the non-monsoon rainfall, non-monsoon rainydays and OEM.

Table 14.8. Results of serial correlation and power spectrum for OEM

ID	r_1	r_2	r_3	L	Conf. Level		Cont.	ID	r_1	r_2	r_3	L	Conf. Level		Cont.
					90	95							90	95	
1	0.10	0.06	0.08	4	8.5	0.0	WN	36	0.04	-0.16	0.09				**WN**
2	0.08	-0.07	0.38	10	3.4	3.4	WN	37	0.17	0.08	0.16	1	34.0	0.0	**WN**
3	0.05	-0.03	0.42	1	34.0	0.0	WN					2	17.0	0.0	
				2	17.0	0.0		38	0.16	0.11	0.08	2	17.0	0.0	**WN**
				12	2.8	0.0		39	-0.04	0.14	0.10	14	2.4	0.0	**WN**
				13	2.6	2.6		40	0.14	0.02	0.33	1	34.0	0.0	**WN**
4	0.03	0.06	0.12				WN					9	3.8	0.0	
5	0.00	-0.18	-0.03	7	4.9	4.9	WN	41	-0.19	-0.02	0.22	13	2.6	0.0	**WN**
				8	4.3	4.3						14	2.4	0.0	
6	0.17	0.07	0.06	1	34.0	0.0	WN	42	0.09	0.29	0.29	1	34.0	0.0	**WN**
7	0.23	-0.04	-0.03	6	5.7	0.0	WN					13	2.6	0.0	
				9	3.8	0.0		43	-0.07	-0.13	0.17	9	3.8	3.8	**WN**
8	0.12	-0.09	-0.06				WN					13	0.0	0.0	
9	0.04	0.13	0.34	1	34.0	34.0	WN	44	-0.19	-0.14	-0.02	14	2.4	2.4	**WN**
10	0.32	0.13	0.12	7	4.9	0.0	RN	45	-0.01	-0.01	0.19				**WN**
11	-0.14	-0.05	0.01				WN	46	0.03	-0.08	0.10				**WN**
12	-0.29	0.06	-0.12	15	2.3	0.0	WN	47	-0.07	0.00	-0.04	8	4.3	4.3	**WN**
				16	2.1	2.1						9	3.8	0.0	
				17	2.0	2.0		48	0.00	0.19	0.32	1	34.0	0.0	**WN**
13	-0.10	-0.21	-0.02	9	3.8	0.0	WN					13	2.6	0.0	
				10	3.4	3.4		49	-0.03	0.29	0.19	13	2.6	0.0	**WN**
14	0.01	-0.19	0.17	8	4.3	0.0	WN	50	0.03	-0.10	0.22	9	3.8	3.8	**WN**
				9	3.8	3.8						10	3.4	0.0	
				10	3.4	0.0		51	-0.14	-0.11	0.09	9	3.8	0.0	**WN**
15	0.04	0.03	0.06				WN					13	2.6	0.0	
16	0.07	-0.02	-0.11				WN	52	0.05	0.19	0.17	1	34.0	34.0	**WN**
17	-0.10	-0.15	0.21	10	3.4	0.0	WN					2	17.0	0.0	
				11	3.1	3.1		53	-0.10	-0.02	0.20	11	3.1	0.0	**WN**
				12	2.8	0.0		54	-0.15	-0.19	0.13	6	5.7	0.0	**WN**
18	0.31	0.29	0.30				RN					11	3.1	3.1	
19	0.32	0.04	-0.01	8	4.3	4.3						12	2.8	2.8	

20	-0.04	0.04	0.14	11	3.1	0.0	WN					13	2.6	0.0	
21	0.02	0.04	0.21				WN	55	0.19	0.30	0.07	1	34.0	34.0	**WN**
22	0.05	-0.10	0.35	9	3.8	3.8	WN	56	-0.05	0.06	0.08				**WN**
23	0.14	-0.06	0.24	9	3.8	0.0	WN	57	-0.07	0.33	0.07	2	17.0	0.0	**WN**
24	0.00	-0.13	0.24				WN					15	2.3	2.3	
25	0.17	-0.15	0.18	8	4.3	4.3	WN	58	0.02	0.03	-0.25	4	8.5	8.5	**WN**
				9	3.8	3.8						5	6.8	6.8	
26	-0.16	-0.05	-0.08	10	3.4	0.0	WN	59	0.01	0.13	0.08	13	2.6	0.0	**WN**
27	-0.11	0.03	0.15	13	2.6	2.6	WN	60	0.05	-0.28	-0.04	8	4.3	4.3	**WN**
28	0.12	0.10	0.15				WN					9	3.8	3.8	
29	0.03	0.12	0.14	14	2.4	2.4	WN	61	0.12	0.12	-0.13	2	17.0	0.0	**WN**
30	0.03	0.09	0.10	14	2.4	0.0	WN	62	0.16	-0.03	0.02				**WN**
31	0.10	0.13	0.22				WN	63	0.12	-0.19	-0.08	5	6.8	0.0	
32	-0.10	0.26	0.14	13	2.6	2.6	WN					6	5.7	5.7	**WN**
33	0.01	0.20	0.21	12	2.8	0.0	WN	64	-0.06	-0.19	0.08	8	4.3	0.0	**WN**
				13	2.6	2.6						9	3.8	3.8	
34	0.02	-0.21	0.17	8	4.3	0.0	WN	65	-0.04	-0.14	0.13	9	3.8	0.0	**WN**
				9	3.8	0.0									
35	-0.12	-0.25	0.20	9	3.8	3.8	WN								
				10	3.4	3.4									

WN: white noise, RN: Markov red noise

By analyzing the lag-3 serial correlation coefficients of the climatic variables, it was evident that the percentage coherent area is significantly reduced for all the variables. However, it is increase in case of non-monsoon rainfall, non-monsoon rainydays and OEM. Based on the spatial distribution of lag-1 serial correlation coefficient, it is indicated that a simple Markov type persistence is experienced in the upper Himalayan, central and south-west region of the Yamuna basin.

Periodicity. Significance of the spectral estimates was evaluated at 90 and 95 percent confidence levels of the appropriate null continuum (red or white noise). If a time series has persistence, the spectrum over all the wavelengths and the magnitude of the spectrum has a decreasing trend from long to short wavelengths; and the spectrum is termed as 'red noise'. For the spectrum having necessary exponential relationships among r_1 , r_2 and r_3 for simple Markov type persistence, the appropriate null hypothesis was assumed to be a Markov red noise continuum. A series characterized by an insignificant positive lag-1 serial correlation coefficient or a series that has a significant positive lag-1 serial correlation coefficient but not a simple Markov-type, and any series with negative lag-1 serial correlation coefficient was evaluated as a white noise continuum. For all the variables, power spectrum plots for representative stations in the Yamuna basin are prepared. The sample plot for the OEM is presented in Figure 14.2.

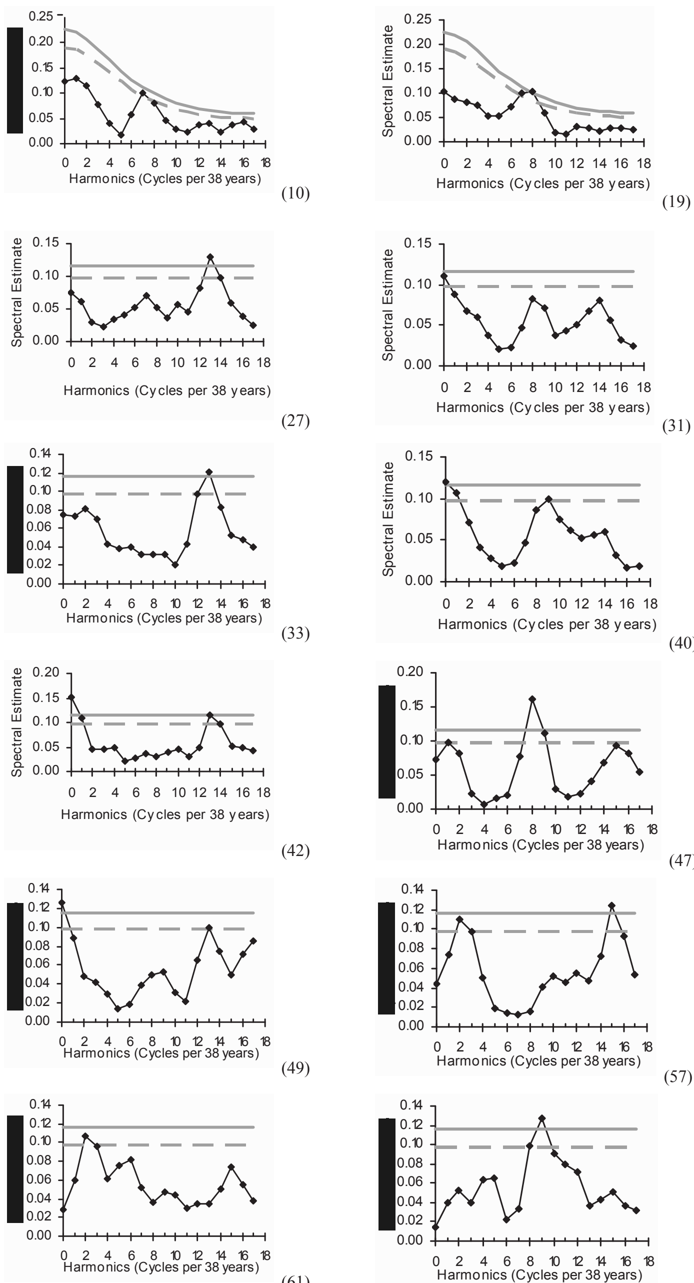

Figure 14.2. Power spectrum plot for OEM (solid line and dashed line represents the 95% and 90% confidence limits, respectively)

To evaluate the power spectrum results, generally periodicity values computed by the equation *P* (= *2 m* / *L*) for all the time series. The periodicity along with their significance level was also computed (for examples refer Table 14.8). Table 14.8 also comprised of the serial correlation coefficients up to lag-3. Based on the Table 14.8, it is evident that the short-term period fluctuation of 2.0 to 4.9 is dominant in the annual and monsoon rainfall, whereas for non-monsoon rainfall medium and long-term period of 5.0 to 34.0 is dominant. This feature of rainfall pattern over the Yamuna basin should be kept in mind while preparing the water resources plan. In case of number of rainydays, the long-period is dominated over the short- periodicity. Results of the power spectrum analysis of OEM and AI are indicated that OEM and AI have dominating short-period fluctuations of 2.0 to 3.0 years, which leads to high probability of meteorological and agricultural drought and will frequently disturbs the planning of *kharif* crops in the Yamuna basin.

Based on the above analysis on periodicity, a good consistency between the lag-1 serial correlation coefficient and results of the power spectrum analysis was remarked. Positive lag-1 serial correlation coefficients gives low frequency fluctuations, whereas negative is an indicator for the high frequency.

14.5 Conclusions

This chapter has demonstrated the various statistical tests for investigating the short-term and long-term dependence, trend analysis, and periodicity in the hydrological time series.

The short term dependence is very important for small water resources projects, which requires less period of hydrologic data. For short-term dependence, 10 tests were used and hypothesis test statistics was performed at 5% and 10% significance level. However, it may be questioned that why so many of tests have been applied. The answer may be that since the analysis is based on the statistics, therefore, to ascertain the short-term dependence or short term persistence in the series, it will be better option to establish through various tests followed by personal judgment. In the analysis, if 4 tests out of 10 have been passed through the test, then the series is said to have persistence.

Similar to the short term dependence, when water resources project is planned based on the longer series (say up to 500 years), then it is required to test the long term dependence or persistence. In this chapter, only non-parametric test (i.e. Hurst coefficient followed by boot-strap sampling of 10000 samples) was successfully demonstrated.

Once the persistence test (i.e. short- and long-term dependence) is over, the series is subjected to the trend analysis. For trend analysis, a well-established Mann-Kendall test has been demonstrated with their limitation. It was appeared in the analysis, that presence of persistence plays a vital role in the trend analysis. It may be established that either modified Mann-Kendall or original Mann-Kendall test with removal of persistence (represented by lag-1 serial correlation) should be used to investigate the trend in hydrologic time series.

In last, methodology for the periodicity in the hydrologic time series has been demonstrated. Again the persistence in the time series has great impact on the periodicity.

14.6 References

Angell, J. K., Korshover, J., and Carpenter, T. H. (1966). "Note concerning the period of the quasi-biennial oscillation." *Monthly Weather Review*, 94, 319–323.

Anyadike, R. N. C. (1993). "Seasonal and annual rainfall variations over Nigeria." *Int. J. Climatol.*, 13, 567–580.

Ashokraj, P. C. (1979). "Onset of effective monsoon and critical dry spell-A computer based forecasting technique." Indian Agricultural Research Institute, ICAR, New Delhi, Bulletin No. 11, India.

Aziz, O. I. A., and Burn, D. H. (2006). "Trends and variability in the hydrological regime of the Mackenzie River Basin." *J. Hydrol.*, 319 (1–4), 282–294.

Blackman, R. B., and Tukey, J. W. (1958). *The measurement of power spectra. Dover Publications*, New York.

Box, G. E. P., and Jenkins, G. M. (1976). *Time Series Analysis: Forecasting and Control.* Holden-Day, San Francisco, CA.

Burn, D. H., and Elnur, M. A. H. (2002). "Detection of hydrologic trends and variability." *J. Hydrol.*, 255, 107–122.

Burn, D. H., Cunderlink, J. M., and Pietroniro, A. (2004). "Hydrological trends and variability in the Liard river basin." *Hydrol. Sci. J.*, 49 (1), 53–67.

Chen, H., Guo, S., Xu, C. Y., and Singh, V. P. (2007). "Historical temporal trends of hydro-climatic variables and runoff response to climate variability and their relevance in water resource management in the Hanjiang basin." *J. Hydrol.*, 344, 171–184.

Cox, D. R., and Stuart, A. (1955). "Some quick tests for trend in location and dispersion." *Biometrika*, (42), 80–95.

Douglas, E. M., Vogel, R. M., and Kroll, C. N. (2000). "Trends in floods and low flows in the United states: Impact of spatial correlation." *J. Hydrol.*, 240 (1–2), 90–105.

Drosdowsky, W. (1993). "An analysis of Australian seasonal rainfall anomalies: 1950–1987. II: Temporal variability and teleconnection patterns." *Int. J. Climatol.*, 13, 111–149.
Efron, B. (1979). "Bootstrap methods: another look at the jackknife." *Ann. Statist.*, 7, 1–26.
Efron, B. (1981). "Nonparametric standard errors and confidence intervals." *Can. J. Statist.*, 9, 139–172.
Efron, B. (1982). "The jackknife, the bootstrap, and other resampling plans." SIAM (Soc. Ind. Appl. Math.) Monogr., 38.
Fisz, M. (1963). *Probability Theory and Mathematical Statistics*. Wiley, New York.
Gan, T. Y. (1998). "Hydroclimatic trends and possible climatic warming in the Canadian Prairies." *Water Resources Research*, 34(11), 3009–3015.
Granger, O. E. (1977). "Secular fluctuations of seasonal precipitation in lowland California." *Mon Weather Rev.*, 105, 386–397.
Hirsch, R. M., and Slack, J. R. (1984). "A nonparametric trend test for seasonal data with serial dependence." *Water Resour. Res.*, 20(6), 727–732.
Hirsch, R. M., Slack, J. R., and Smith, R. A. (1982). "Techniques of trend analysis for monthly water quality data." *Water Resour. Res.*, 18(1), 107–121.
Hurst, H. E. (1951). "Long term storage capacity of reservoirs." *Trans. Am. Soc. Civ. Eng.*, 116, 770–808.
Hurst, H. E. (1956). "Methods of using long-term storage in reservoirs." *Proc. Inst. Civ. Eng.*, 1, 519–543.
Jenkins, G. M., and Watts, D. G. (1968). *Spectral analysis and its applications*. Holden-Day, San Francisco.
Julian, P. R. (1967). "Variance spectrum analysis." *Water Resour. Res.*, 3, 831–845.
Kendall, M., and Stuart, A. (1976). *The Advanced Theory of Statistics*, Vol. 3, Charles Griffin, London.
Kendall, M. G. (1955). *Rank Correlation Methods*. Charles Griffin, London.
Khaliq, M. N., Ouarda, T. B. M. J., Gachon, P., Sushma, L., and St-Hilaire, A. (2009). "Identification of hydrological trends in the presence of serial and cross correlations: A review of selected methods and their application to annual flow regimes of Canadian rivers." *J. Hydrol.*, 368, 117–130.
Landsberg, H. E., Mitchell, J. M. Jr., Crutcher, H. L., and Quinlan, F. T. (1963). "Surface signs of the biennial atmospheric pulse." *Monthly Weather Review*, 91 (10–12), 549–556.
Lettenmaier, D. P., Wood, E. F., and Wallis, J. R. (1994). "Hydro-climatological trends in the continental United States 1948–1988." *J. Clim.*, 7 (4), 586–607.
Lins, H. F., and Slack, J. R. (1999). "Streamflow trends in the United States." *Geophys. Res. Let.*, 26 (2), 227–230.

Lye, L. M., and Lin, Y. (1994). “Long-Term Dependence in Annual Peak Flows of Canadian Rivers.” *Journal of Hydrology*, 160, 89–103.

Madansky, A. (1988). *Prescriptions for Working Statisticians*. *Springer*, New York, 93–118.

Mann, H. B. (1945). “Non-parametric tests against trend.” *Econometrica*, 13, 245–259.

Matalas, N. C. (1967). “Time series analysis.” *Water Resour. Res.*, 3, 817–829.

Meacham, I. (1968). “Correlation in sequential data–three sample indicators.” *Civ. Eng. Trans. Inst. Eng. Aust*., CE10(2), 225–228.

Nicholson, S. E., and Palao, I. M. (1993). “A re-evaluation of rainfall variability in the Sahel. Part I. Characteristics of rainfall fluctuations.” *Int. J. Climatol*., 13, 371–389.

Ogallo, L. (1979). Rainfall variability in Africa. *Mon. Weather Rev*., 107, 1133–1139.

Rai, R. K., Upadhyay, A., and Ojha, C. S. P. (2010). “Temporal variability of climatic parameters of Yamuna River basin: spatial analysis of persistence, trend and periodicity.” *The Open Hydrol. J.*, 4, 184-210.

Rodhe, H., and Virji, H. (1976). “Trends and periodicities in East African rainfall data.” *Mon. Weather Rev.*, 104, 307–315.

Tukey, J.W. (1950). “The sampling theory of power spectrum estimates.” In: *Symposium on applications of autocorrelation analysis to physical problems*. US Office of Naval Research, NAVEXOS-P-735, Washington, DC, p. 47–67.

Türkes¸, M. (1998). “Influence of geopotential heights, cyclone frequency and southern oscillation on rainfall variations in Turkey.” *Int. J. Climatol*., 18, 649–680.

Türkes¸, M. (1999). “Vulnerability of Turkey to desertification with respect to precipitation and aridity conditions.” *Tr. J. Eng. Environ. Sci*., 23, 363–380.

Türkes¸, M., Sümer, U. M., and Kiliç, G. (2002). “Persistence and periodicity in the precipitation series of Turkey and associations with 500 hPa geopotential heights.” *Climatic Research*, 21, 59–81.

UNEP (1993). *World Atlas of Desertification*. United Nations Environment Programme (UNEP), London, 1993.

Wald, A., and Wolfowitz, J. (1943). “An exact test for randomness in the non-parametric case based on serial correlation.” *Ann. Math. Statist*., 14, 378–388.

Wall, D. J., and Englot, M. E. (1985). “Correlation of annual peak flows for Pennsylvania systems.” *Water Resour. Bull*., 21(3), 459–264.

Wiener, N. (1930). “Generalized harmonic analysis.” *Acto Math*, 55, 117–258

Wiener, N. (1949). *Extrapolation, interpolation, and smoothing of stationary time series*. *Wiley and Technology Press*, Cambridge, MA.

WMO (1966). “Climatic change.” WMO Technical Note 79, *World Meteorological Organization*, Geneva.

Yevjevich, V. (1971). *Stochastic Processes in Hydrology*. *Water Resources Publications*, Fort Collins, CO.

Yue, S., and Pilon, P. (2004). "A comparison of the power of the t-test, Mann-Kendall and bootstrap tests for trend detection." *Hydrol. Sci. J.*, 49 (1), 21–37.

Yue, S., Pilon, P., and Cavadias, G. (2002). "Power of the Mann-Kendall and Spearman's rho test for detecting monotonic trends in hydrological series." *J. Hydrol.*, 259, 254–271.

Zhang, Q., Jiang, T., Gemmer, M., and Becker, S. (2005). "Precipitation, temperature and runoff analysis from 1995–2002 in the Yangtze basin, China." *Hydrol. Sci. J.*, 50 (1), 65–80.

CHAPTER 15

Climate Change and Its Impact on Indian Agriculture

B. Venkateswarlu and V. U. M. Rao

15.1 Introduction

Climate change impacts on agriculture are being witnessed all over the world, but countries like India are more vulnerable in view of the high population depending on agriculture and excessive pressure on natural resources. The warming trend in India over the past 100 years (1901 to 2007) was observed to be 0.51^{o}C with accelerated warming of 0.21^{o}C per every10 years since 1970 (Kumar 2009). The projected impacts are likely to further aggravate yield fluctuations of many crops with impact on food security and prices. Cereal productivity is projected to decrease by 10–40% by 2100 and greater loss is expected in *rabi*. There are already evidences of negative impacts on yield of wheat and paddy in parts of India due to increased temperature, increasing water stress and reduction in number of rainy days. Modeling studies project a significant decrease in cereal production by the end of this century (Mujumdar 2008). Climate change impacts are likely to vary in different parts of the country. Parts of western Rajasthan, Southern Gujarat, Madhya Pradesh, Maharashtra, Northern Karnataka, Northern Andhra Pradesh, and Southern Bihar are likely to be more vulnerable in terms of extreme events (Mall et al. 2006a). For every one degree increase in temperature, yields of wheat, soybean, mustard, groundnut and potato are expected to decline by 3–7% (Agarwal 2009). Similarly, rice yields may decline by 6% for every one degree increase in temperature (Saseendran et al. 2000). Water requirement of crops is also likely to go up with projected warming and extreme events are likely to increase. Hence, there is a need to address the whole issue of climate change and its impacts on Indian agriculture in totality so as to cope with it through adaptation and mitigation.

15.2 Trends in Key Weather Parameters

Rainfall is the key variable influencing crop productivity in agricultural crops in general and rainfed crops in particular. Intermittent and prolonged droughts are a major cause of yield reduction in most crops. Long-term data for India indicates that rain fed areas witness 3–4 drought years in every 10-year period. Of these, 2–3 are in moderate and one may be of severe intensity. However, no definite trend is seen on the frequency of droughts as a result of climate change so far. For any R&D and policy initiatives, it is important to know the spatial distribution of drought events in the country. Analysis of number of rainy days based on the IMD grid data from 1957 to 2007 showed declining trends in Chhattisgarh, Madhya Pradesh, and Jammu Kashmir. In Chhattisgarh and Eastern Madhya Pradesh, both rainfall and number of rainy days are declining which is a cause of concern as this is a rain-fed rice production system supporting large tribal population who have poor coping capabilities.

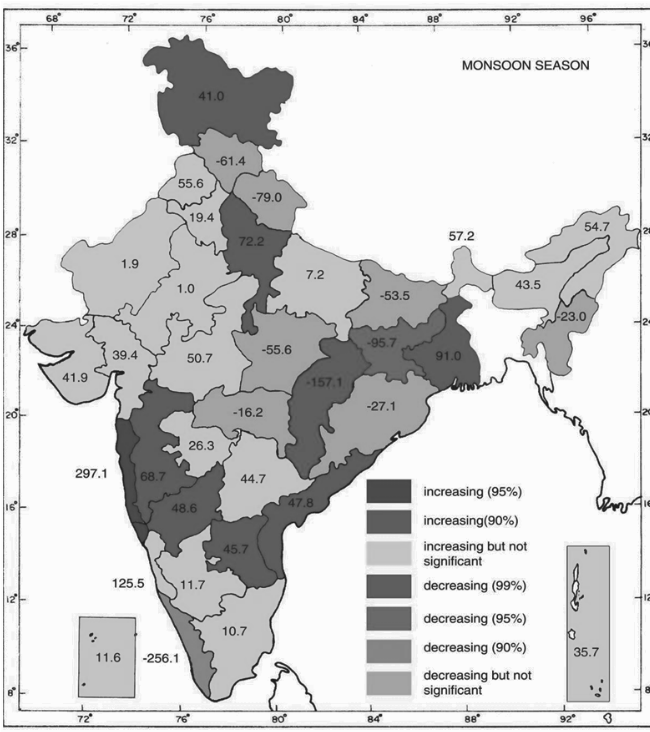

Figure 15.1. Increase/decrease in summer monsoon rainfall (mm) in India during last century (Guhathakurta and Rajeevan 2008)

Guhathakurta and Rajeevan (2008) reported that all India summer monsoon (June to September) rainfall does not show any significant trend during the last century. However, three subdivisions *viz.,* Jharkhand, Chhattisgarh, Kerala show significant decreasing trend and eight subdivisions *viz.,* Gangetic West Bengal, West Uttar Pradesh, Jammu & Kashmir, Konkan & Goa, Madhya Maharashtra, Rayalaseema, Coastal Andhra Pradesh and North Interior Karnataka show significant increasing trends (Figure 15.1).

However, the amount and distribution of rainfall is becoming more erratic which is causing greater incidences of droughts and floods. A study carried out by Goswami (2006) indicated an increase in frequency of heavy rainfall events in last 50 years over Central India (Figure 15.2).

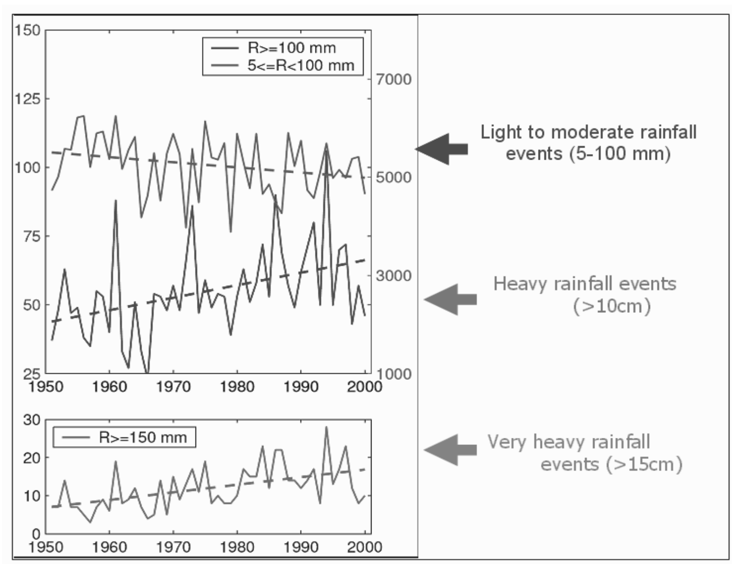

Figure 15.2. Change in intensity of rainfall over Central India in last 50 years

Temperature is another important variable influencing crop production particularly during *rabi* season. A general warming trend has been predicted for India but knowing temporal and spatial distribution of the trend is of equal importance. Lal (2001) reported that annual mean area-averaged surface warming over the Indian sub-continent is likely to range between 3.5 and 5.5 ^{o}C by 2080s (Table 15.1).

Table 15.1. Projected mean temperature changes over the Indian subcontinent

		Temperature change (^{0}C)	
Year	**Season**	**Lowest**	**Highest**
	Annual	1.00	1.41
2020s	Rabi	1.08	1.54
	Kharif	0.87	1.17
	Annual	2.23	2.87
2050s	Rabi	2.54	3.18
	Kharif	1.81	2.37
	Annual	3.53	5.55
2080s	Rabi	4.14	6.31
	Kharif	2.91	4.62

15.3 Role of Greenhouse Gases

The increasing levels of greenhouse gases (GHGs) in the atmosphere have been attributed as a major driving force for rapid climate change. The main GHGs contributing to this phenomenon are CO_2, CH_4 and N_2O. Apart from fossil fuel burning, the frequent volcanic eruptions are also contributing to this increase. India's share in global CO_2 emissions is still very small. The contribution of India to the cumulative global CO_2 emissions from 1980 to 2003 is only 3.11%. Thus, historically and currently India's share in the carbon stock in the atmosphere is relatively very small when compared to the population. India's carbon emissions per person are twentieth of those of the US and a tenth of most Western Europe and Japan (Figure 15.3).

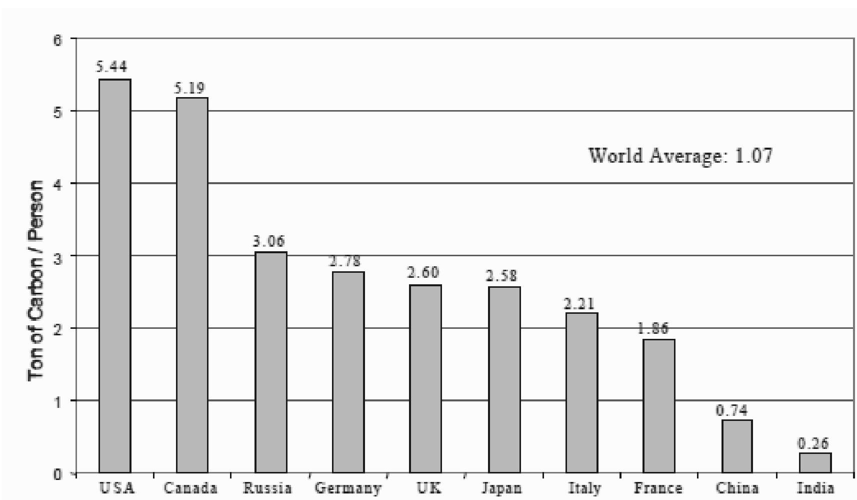

Figure 15.3. Per capita carbon emissions at different countries from energy for the year 2003 (IPCC 2007)

Though the increase in the level of CO_2 is expected to produce some beneficial effects on crop production, it may soon be nullified by associated water and thermal stresses leading to overall deterioration of agro-climatic conditions for food production systems. At the global scale, the historical temperature-yield relationships indicate that warming from 1981 to 2002 is very likely to offset some of the yield gains from technological advances, rising CO_2 and other non-climatic factors (Lobell and Field 2007). The recent GHG inventory released by Indian government has revealed that the Net GHG emissions from India in 2007, including LULUCF, were 1727.71 million tons of CO_2 equivalent (eq) of which CO_2, CH_4, N_2O emissions were 1221.76, 20.56, 0.24 million tons, respectively. GHG emissions from agriculture sector alone constitute about 17% of the net CO_2 eq missions.

15.4 Emission of GHGs from Indian Agriculture

It is also important that role of agricultural activities in increasing the levels of GHGs is often overlooked. Assessment of GHG inventory that identifies and quantifies a country's primary anthropogenic sources and sinks of GHG emission is central to any climate change study. India being a party to the United Nation's Framework Convention on Climate Change (UNFCCC) develops, periodically updates, and makes available to the Conference of Parties, a national inventory of anthropogenic emissions by sources and removals by sinks of all GHGs. Accordingly the inventory of GHG emission by Indian agriculture was developed for the base year 2000 (Table 15.2).

Table 15.2. GHG inventory for Indian agriculture for the year 2000

Source	CH_4 (Tg)	N_2O (Gg)	CO_2 eq. (Tg)
Ruminant	10.1	-	252.0
Rice cultivation	3.5	-	87.3
Manure management	0.1	0.1	2.5
Crop residue	0.2	4.0	4.9
Soil	-	132.3	39.4
Total	14.7	137.3	386.1

Tg = million ton, Gg = thousand ton

In 2000, Indian agriculture contributed 386.1 million ton (Tg) CO_2 eq. The agriculture sector primarily emitted CH_4 (14.7 Tg) and N_2O (137.3 thousand ton, Gg). The sources accounting for emissions in the agriculture sector are enteric fermentation in livestock, manure management, rice cultivation, agricultural soils and burning of agricultural crop residue. The bulk of the GHG emission from the agriculture sector was from enteric fermentation (65%) followed by rice cultivation (23%) and the rest were contributed by manure management, burning of crop residue and application of N fertilizer to soil (Figure 15.4).

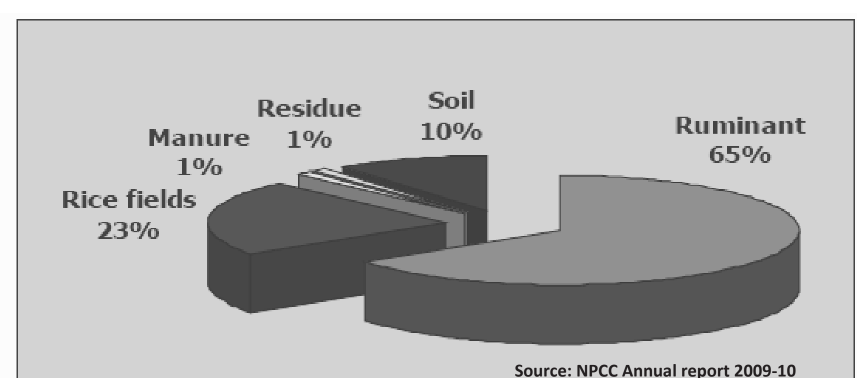

Figure 15.4. Relative contribution of various sources to GHG emission in 2000

15.4.1 Methane Emission

Livestock rearing, an integral part of Indian agriculture is the major contributor of methane. Although the livestock includes cattle, buffaloes, sheep, goat, pigs, horses, mules, donkeys, camels and poultry, the bovines and small ruminants are the most dominant components, and the major source of methane emission. Methane emission due to enteric fermentation in 2000 was estimated to be 10.1 Tg. Buffalo and indigenous cattle, which are the main milk-producing animals in the country, contributed 44 and 42% total methane emission from livestock sector (Figure 15.5). Cross bred cattle emitted 8% and the small ruminants emitted about 7% of methane.

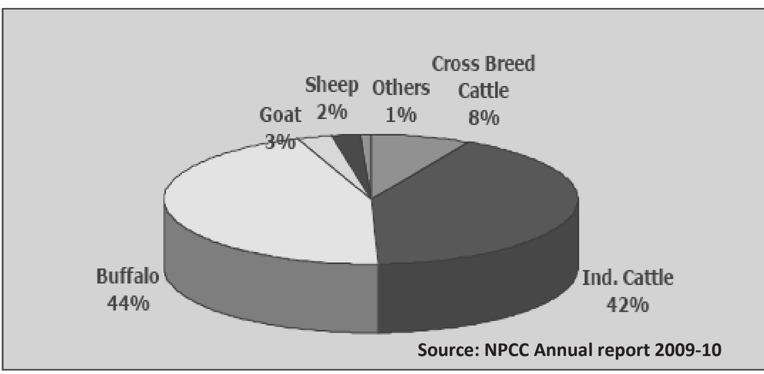

Figure 15.5. Relative contribution of methane emission by different categories of ruminants

In India, rice is cultivated under various management conditions, depending on availability of water (Table 15.3). Methane emission due to rice cultivation was estimated to be 3.5 Tg. Continuously flooded rice emitted maximum methane (1111 Gg) followed by flood prone (827 Gg) and single aerated (598 Gg) rice cultivation.

Table 15.3. Area and methane emission in various rice-ecosystems in India (NPCC 2009)

Ecosystem	Water regime	Area (M ha)	Emission (Gg)
	Continuous flooded	6.85	1111
Irrigated	Single aeration	9.08	598
	Multiple aeration	9.49	175
Rainfed	Drought prone	8.66	570
Flood prone		4.35	827
Deep water		1.37	218
Upland		4.83	0
Total		44.62	3499

15.4.2 N_2O Emission

During 2000, Indian agriculture produced 137.3 Gg of N_2O-N. Nitrogenous fertilizer application contributed 68% of that emission followed by manure and crop residue (Figure 15.6). Because of increased use of N fertilizer, N_2O emission is also increasing over the years (Figure 15.7).

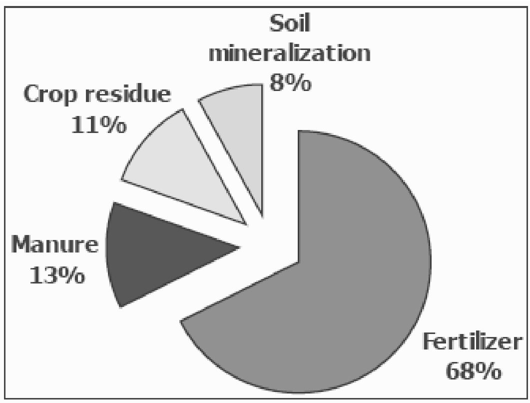

Figure 15.6. Relative contribution of different sources to nitrous oxide emission (NPCC 2009)

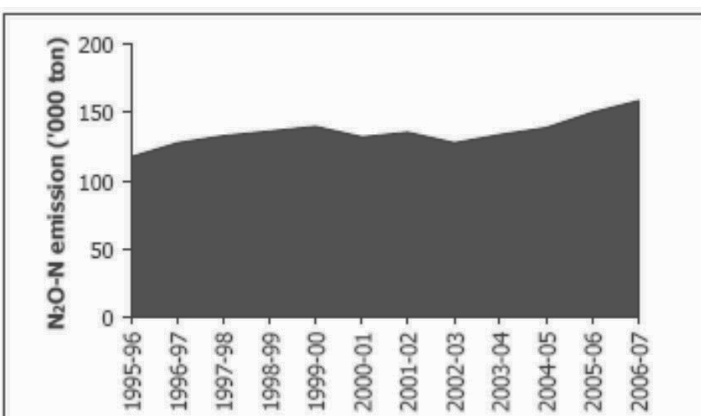

Figure 15.7. Trend in nitrous oxide emission during 1995–2006 (NPCC 2009)

Though the inventory of GHG emission from Indian agriculture is fairly robust but it still suffers from various deficiencies like non-availability of country specific emission factors, lack of adequate monitoring stations and data quality. To capture the diverse soil and climatic conditions, different management practices and socio-economic status of the farmers influencing GHG emission, a robust national exercise is needed. This will not only improve estimates of emission and related impact assessments, but also provides a baseline from which future emission trajectories may be developed to identify and evaluate mitigation strategies.

15.5 Impact of Climate Change on Agriculture

15.5.1 Direct and Indirect Impacts

The impact of climate change on agriculture may accentuate at regional level creating more vulnerability in food security rather than global level as a whole. The potential impact will be shifts in sowing time and length of growing seasons, which may necessitates adjustment in sowing and harvesting windows, change in genetic traits of cultivars and sometimes total adjustment of cropping system itself. Warmer environment coupled with erratic rainfall distribution, results in higher rate of evaporation and depletion of soil moisture. Hence for sustaining the crop productivity efforts should be made to enhance the water and nutrient efficiencies by adopting resilient management practices. Apart from these, experiencing intense extreme events like heat and cold waves, droughts and floods may become norm of the day for farming community (IPCC 2001). Such phenomena will impact agriculture considerably through their direct and indirect effects on crops, livestock, and incidences of pest-disease-weeds, increasing deterioration of soil health and thereby threatening the food security like never before.

The output of the studies so far carried out by Agarwal (2009) have indicated that a marginal 1°C increase in atmospheric temperature along with increase in CO_2 concentration would cause very minimal reduction in wheat production of India if simple adaptation strategies like adjustment of planting date and varieties are adopted uniformly. But in absence of any adaptive mechanism, the yield loss in wheat can go up to 6 million tonnes. A further rise by 5 ^{0}C may cause loss of wheat production up to 27.5 million tonnes. Similarly, rice yields may decline by 6% for every one degree increase in temperature (Saseendran et al. 2000).

In addition to direct effects on crops, climate change is likely to impact natural resources like soil and water. Increased rainfall intensity in some regions would cause more soil erosion leading to land degradation. Water requirement of crops is also likely to go up with projected warming. Extreme events like floods, cyclones, heat wave and cold wave are likely to increase.

The availability of viable pollen, sufficient numbers of germinating pollen grains and successful growth of pollen tube to the ovule are of fundamental importance in grain formation. The Network study on wheat and rice suggested that high temperature around flowering reduced fertility of pollen grains as well as pollen germination on stigma. These effects are more pronounced in *Basmati* rice as well as *Durum* wheat cultivars. A positive finding of the study was that the *Aestivum* wheat cultivars are more or less tolerant to such adverse effects. But differential impact of increasing temperature is observed with respect to grain quality of wheat where it is found that *Aestivum* wheat cultivars are more prone to reduced grain quality due to increasing temperature during the fruit setting stage than *Durum* cultivars. Field experiments using advanced 'Temperature gradient tunnels' with different dates of sowing to study impact of rising temperature on growth and development of different crops revealed that an increase of temperature from 1 to 4 ^{0}C reduced the grain yield of rice (0–49%), potato (5–40%), green gram (13–30%) and soybean (11–36%). However, one of the important pulse, chickpea, registered 7–25% increase in grain yield by an increase in temperature up to 3 ^{0}C, but was reduced by 13% with further 1^{o}C rise in temperature.

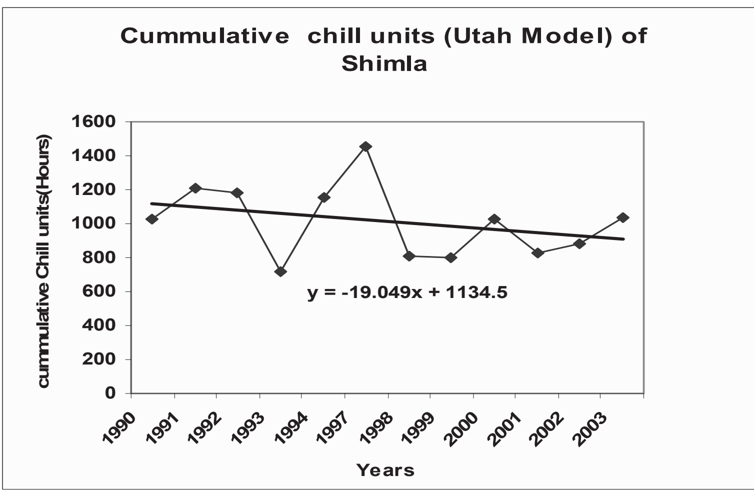

Figure 15.8. Linear trend of cumulative chill units for Apple at Shimla

A significant decrease in average productivity of apples in Kullu and Simla districts of Himachal Pradesh has been reported which is attributed mainly to inadequate chilling required for fruit setting and development (Figure 15.8). Reduction in cumulative chill units of coldest months might have caused shift of the apple belt to higher elevations of Lahaul-Spitti and upper reaches of Kinnaur districts of Himachal Pradesh. In general temperature below 7^{0}C for total 800–1400 hours is taken as chilling requirement of apple; however temperature below 1^{0}C and above 18^{0}C is not desired for chill units accumulation.

The impact of rising temperature and CO_2 are also likely to change insect-pest dynamics. Dilution of critical nutrients in crop foliage may result in increased herbivory of insects. For example, Tobacco caterpillar (*Spodoptera litura*) consumed 39% more castor foliage under elevated CO_2 conditions than ambient environment (Srinivasa Rao et al. 2009b). The advancement of breeding season of major Indian carps as early as March has been reported from West Bengal which is extended from 110 to 120 days due to increase in environmental temperature, which stimulates the endocrine glands of fish and helps in the maturation of the gonads. This brings about a possibility to breed these fishes twice a year at an interval of 30 to 60 days. Besides, the nutrient loss from soil through high rate of mineralization and CO_2 emissions from soil could be accelerated as a result of increase in temperature. Low carbon soils of mainly dryland areas of India are likely to emit more CO_2 compared to high or medium carbon temperate region soils. Simulation of water balance using Global and Regional Climate Models revealed likely increase in annual as well as seasonal stream-flows of many Indian river basins pointing to the need for adoption of more effective runoff and soil loss control measures to sustain crop production across the country.

The Indian Council of Agricultural Research instituted All India Network Project on Climate Change in 2004 to study in detail the possible impact of climate change on major crops, livestock, fisheries, soils and other biotic factors as well as to understand different natural adaptation capabilities of both flora and fauna. The possible interventions to increase the adaptability of crop-livestock systems and mitigation measures to minimize the adverse impacts were studied across length and breadth of different agro-ecosystems of India.

15.5.2 Climate Change Impact Studies through Crop Simulation Modelling

Climate change impacts agricultural crop production/productivity directly through drought and heat stresses and indirectly through land degradation (due to more erosion) and reduced soil and water availability. Studies were carried out to model the impacts on yields under different climate change scenarios for major cereal, pulse, oilseed, horticultural and plantation crop under the network project on climate change.

Crop simulation studies carried out at IARI, New Delhi on the impact of climate change on irrigated *kharif* maize indicated reduction in maize yields by -6.83% in A1b 2030 scenario. This adverse effect on irrigated *kharif* maize production is projected to be even higher in 2080 scenarios ranging from ~-14% in B2 scenario to about -25% in A1b and A2 scenarios (Figure 15.9). The negative impacts are more in states like Bihar, Chhattisgarh, Gujarat, Madhya Pradesh, Karnataka, Orissa, Tamil Nadu and Uttar Pradesh. These negative impacts ranged from about -8 to -20% in these states in A1b 2030 scenario while it ranged from -15 to -43% in A1b 2080 scenario. The impacts are almost similar in A2 2080 scenario but in B2 2080 scenario, impacts are less negative. The response of irrigated maize crop to climate change is more negative than either rice or wheat due to its limited response to higher CO_2, being a C4 crop.

Managing the current variety or improved variety under improved input efficiency and additional fertilizer application are also assessed for adaptation capacity. Results indicate that managing the current variety under improved input efficiency and providing additional nitrogen can reduce the impacts but still leave the irrigated *kharif* maize production vulnerable by -1.82% in A1b 2030 scenario and by -10.6% in B2 2080 scenario. Gains due to this adaptation option are very less in A1b 2080 and A2 2080 scenarios. However, improved variety managed under improved input efficiency with additional nitrogen fertilizer can improve the production by about 24% in A1b 2030 scenario. This adaptation option can almost offset the negative impacts of climate change in A1b 2080 scenario while can improve the yields marginally (3.5%) in A2 2080 scenario and substantially (~14.8%) in B2 2080 scenario.

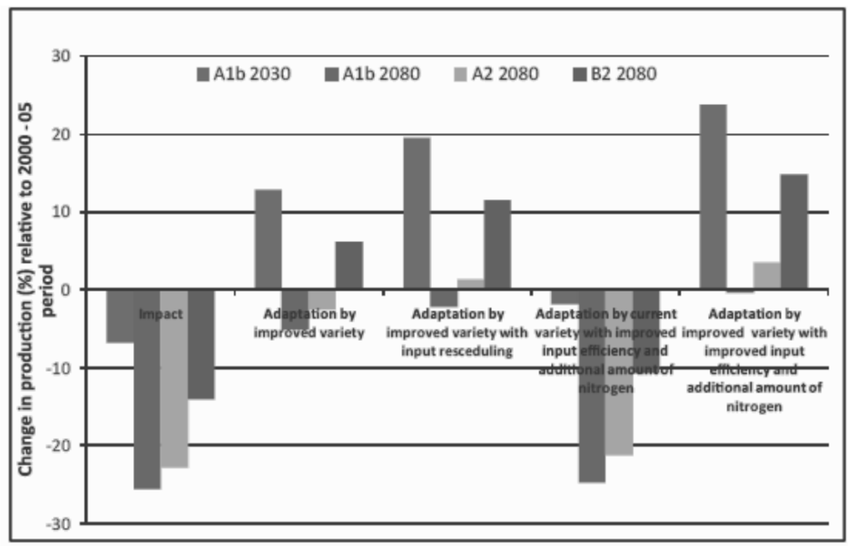

Figure 15.9. Impacts of climate change on irrigated maize during *kharif* season and net vulnerability after adaptation in different scenarios

In a related study by the World Bank South Asia Regional Office (World Bank 2008), using SWAT (a hydrological water resource model which evaluates the effects of climate change on water resources) and EPIC model (an agronomic model which predicts crop yields based on estimated temperature, rainfall and soil moisture), the impacts on sorghum and groundnut were predicted for A2 and B2 scenarios for Anantapur district of Andhra Pradesh and pearl millet for Nashik and Ahmednagar districts of Maharashtra. Groundnut yields in Anantapur district fall by 28% in A2 scenario and 6% by B2. On the other hand, sorghum exhibited greater resilience with a decline of only 4% in A2 and 2% in B2. The impacts are attributed to changes in quantum and distribution of rainfall, higher temperature and elevated CO_2. Similarly, with the rise in temperature and rainfall, the model predicts that the average yields of pearl millet increase significantly in the relatively dry district of Ahmednagar while in Nashik, the increase is moderate. The impact is however negligible in B2. Sorghum yields are also predicted to increase marginally in both the scenarios in these two districts.

Study on effect of elevated temperature and CO_2 on response of coconut seedlings at CPCRI, Kasargod, indicated that providing additional fertilizer dose improved the photosynthetic rate in coconut seedlings grown under elevated CO_2 and temperature regimes (Figure 15.10). This increase in net photosynthetic rate translated into higher seedling vigour as indicated by improved seedling girth at collar in coconut seedlings (Table 15.4).

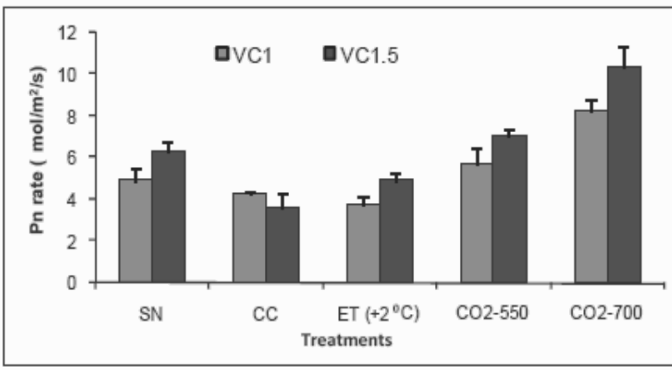

Figure 15.10. Change in Pn rate in coconut seedlings grown in elevated CO_2 and temperature conditions and provided with different nutrient quantities

Table.15.4. Collar girth in coconut seedlings grown in elevated CO_2 and temperature conditions and provided with different nutrient quantities

Nutrient level	Chamber control	Elevated temp. (+2°C)	[CO_2] 550 ppm	[CO_2] 700 ppm
Currently recommended	19.4	22.1	19.9	29.6
50% > currently recommended	26.3	23.4	29.8	40.9

The coconut seedlings were also provided with differential irrigation and results indicate that life-saving irrigation reduced photosynthetic rates in elevated temperature condition. However, in elevated CO_2 conditions photosynthetic rates were higher even in seedlings receiving life-saving irrigation. Reduction in net photosynthetic rates due to delayed irrigation or life-saving irrigation was found to be more under elevated CO_2 conditions (Figure 15.11).

However results from simulation models suggest that climate change could benefit coconut crop. Coconut yields are likely to increase by 4, 10, and 20% by 2020, 2050 and 2080, respectively, in the western coastal areas of Kerala, Maharashtra, Tamil Nadu and Karnataka. But the impact may be negative in east coast areas as they are already facing a much warmer atmospheric thermal regime than western coast.

The analysis of rainfall patterns during the grape growing season for the extracted scenarios with respect to baseline for two major wine grape growing regions viz., Nasik and Bangalore was taken up at Indian Institute of Horticultural

Research, Bangalore. It is observed that in A1B 2050 and 2080 scenarios, there is an average increase in rainfall of 11.11% and 18.98% with respect to baseline average whereas in A2 2080 scenario there is an increase of 81.74% during the fruit maturation period. When rainfall is considered in terms of millimeters during fruit maturity it is low and would not affect fruit quality. Hence, in A1B 2050, 2080 and A2 2080 scenarios there would not be much influence of rainfall on berry quality due to slight increase in rainfall during berry maturation phase, February to April. However only in A2 2080 scenario rainfall during the month of October would increase the incidence of downey mildew disease on leaves and flower clusters.

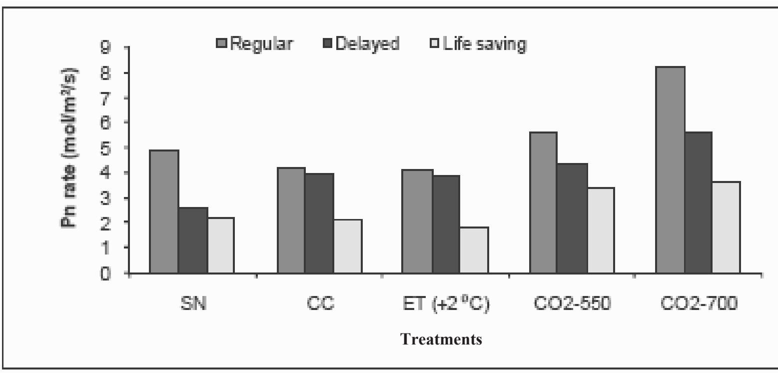

Figure 15.11. Change in Pn rate in coconut seedlings grown in elevated CO_2 and temperature conditions and provided with differential irrigation

Temperature has greater bearing on wine grape quality. Growing season temperatures are a measure of the ripening potential for grape varieties grown in different regions. The extracted monthly data for the scenarios A2 and B2 2080 and A1B 2050 and 2080 was analysed and average growing season temperatures were compared. In 2050 A1B scenario the increase in average temperature for Bangalore and Nasik regions are 2.46 and 2.84 ºC and in B2 2080 scenario 2.48 and 2.61ºC, respectively are expected (Table 15.5). And the temperature increases are expected to be still higher in A2 2080 and A1B 2080 scenarios. The berry skin accumulates large amounts of anthocyanin, fruit juice include sugars, acids, tannins, flavanoids and other chemicals, that are produced as the berries ripen. The proportion of these substances greatly depends on weather and growing season.

Table 15.5. Average increase in temperatures during grape growing season for Bangalore and Nashik regions under different scenarios with respect to baseline

Scenarios	Bangalore			Nasik		
	T max ºC	T min ºC	Average	T max ºC	T min ºC	Average
A1B 2050	2.53	2.39	2.46	2.82	2.85	2.84
A1B 2080	4.45	5.09	4.77	4.25	5.00	4.63
A2 2080	2.41	3.67	3.04	3.37	3.95	3.66
B2 2080	2.33	2.63	2.48	2.40	2.82	2.61

Yield impacts on soybean and groundnut were predicted using INFOCROP model, by VS Bhatia and his group at NRCS, Indore (NPCC 2009), for 2050 and 2100. Simulation results indicate significant increase in crop season temperature and rainfall compared to the base line of 1961–1990. The simulation results indicate a positive impact of future climate (combined change in temperature, rainfall and CO_2 levels) on the productivity of soybean and groundnut (Figure 15.12). As compared to current yields of soybean, 10, 8, 13 and 12% increase in yield was observed by the middle of the century in A1B and by the end of the century in A1B, B2 and A2 scenarios, respectively. In case of groundnut, except for the end of century climate scenario of A1B, which showed a decline of 5% in yield, rest of the scenarios showed 4–7% increase in rainfed yields as compared to the current yield.

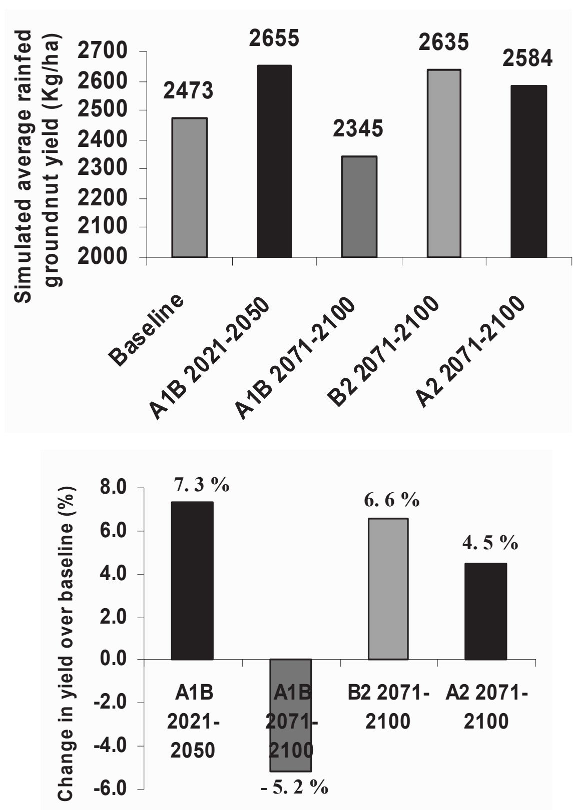

Figure 15.12. Average simulated rainfed groundnut yields under current and future scenarios (top) and projected average change in simulated groundnut yields under future climate scenarios as compared to baseline (bottom) in major crop growing regions of India

However, there was a large spatial variability for magnitude of change in the productivity due to future climate scenarios across major crop growing regions of India. Across the locations, the rainfed yields of soybean and groundnut showed significant positive association with crop season rainfall while association with temperature was poor/non-significant, which indicated that under rainfed conditions, the availability of water will remain a major yield limiting factor.

Simulation studies with INFOCROP-POTATO model using current and future climate scenarios (A1B) were done for impact analysis of climate change and global warming on potato production in India at Central Potato Research institute, Shimla. Potato tuber yield was simulated for all the selected sites without adaptations *i.e*. with recommended date of planting and optimal management practices of seed rate and depth of planting *etc.* for the current and future climates of varying temperature and CO_2 concentrations. Without adaptations the total potato production in India under the impact of climate change and global warming may decline by 2.61 and 15.32 % in the year 2020 and 2050, respectively (Figure 15.13).

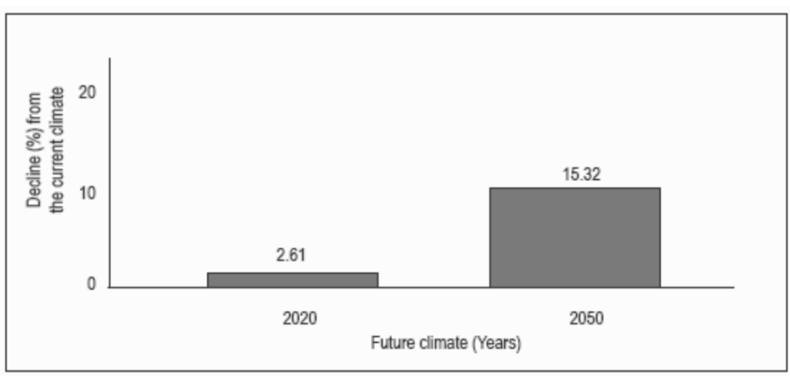

Figure 15.13. Impact of climate change on potato production in India

The impacts on productivity and production varied among different agro-ecological zones. Potato productivity is likely to increase in Punjab, Haryana and Western UP by 7.11 and 3.46 % in the year 2020 and 2050, respectively. In other states productivity is likely to decrease by 0.52 to 16.59 % and 0.69 to 46.51 % in the year 2020 and 2050, respectively (Table 15.6).

15.6 Impacts of Carbon Fertilization

Elevated carbon dioxide level in the lower atmosphere is another important manifestation of climate change. In some crops, higher carbon dioxide levels in the air have a fertilization effect and result in production of more bio-mass and grain yield when water is not limiting and temperatures remain within the tolerance thresholds. In major rainfed crops grown during *kharif* season, it is found that water limitation is a major yield limiting factor than temperature. Therefore, there is a possibility that these crops would benefit from elevated CO_2 coupled with higher rainfall as predicted in most scenarios.

Table 15.6. Impact of climate change without adaptations on potato productivity and production in India under current (2000) and A1B future climate change scenarios

Major States	Mean tuber yield (q/ha)			Production*	
	Years			Change (%) from current	
	2000	2020	2050	2020	2050
UP	210	209	179	-0.52	-14.83
West Bengal	248	237	200	-4.42	-19.45
Bihar	188	184	172	-2.38	-8.62
Jharkhand	145	141	144	-2.51	-0.69
Punjab	211	226	218	+7.11	+3.46
Madhya Pradesh	150	137	124	-8.43	-17.27
Gujarat	226	189	142	-16.59	-37.14
Karnataka	119	97	65	-8.48	-38.92
Maharashtra	100	93	86	-6.58	-13.52
Orissa	129	112	69	-13.47	-46.51
INDIA	183	178	155	-2.61	-15.32

*At constant acreage at current levels

15.6.1 Influence on Growth

Studies at CRIDA, Hyderabad through Open Top Chambers (OTCs) revealed that the response of different rainfed crops varies significantly to elevated CO_2 (CRIDA 2009). In general, the response of C3 crops was found to be higher than C4 crops. The increment in total biomass was 46% in pulses (C3) and 29% in oilseeds at vegetative stage with 600 ppm CO_2, whereas with C4 cereals it was only 15% (Vanaja et al. 2006). Similarly, the response of black gram (*Vigna mungo* L. Hepper) to increased levels of CO_2 (600 ppm) was significantly higher when moisture stress was imposed. This was possible due to greater proportioning of assimilates to the roots than to shoots under stress.

15.6.2 Influence on Flowering

Flowering is a critical milestone in the life cycle of plants, and changes in the timing of flowering may alter processes at the species, community and ecosystem levels. Therefore, flowering response to elevated CO_2 was studied in castor bean, a monoecious plant bearing both male and female flowers on the same spike. The flowering in castor is sensitive to temperature. Our study revealed that elevated CO_2 levels significantly reduced the duration of "days to initiation of flowering" and increased the number of female flowers in the spike (Vanaja et al. 2008) and there by improved the seed yield. However, the mechanisms controlling these responses are not known. Past studies indicate that carbon metabolism exerts partial control on flowering time, and therefore may be involved in elevated CO_2 induced changes in flowering time. More studies are needed on the impacts of climate change drivers on plant development processes.

15.6.3 Influence on Seed Yield

The grain yield of pigeon pea improved from 22.8 g/plant at ambient to 42.4 g/plant at 700 ppm thereby showing an increment of 85.9% with enhanced CO_2. In black gram, the grain yield recorded an increment of 129.3% at elevated CO_2. The pod number per plant in pigeon pea showed an increase of 97.9% over ambient control making it an important yield contributing component. The flower to pod conversion and retention of flowers as well as pods in pulses is moisture, temperature and nutritional stresses there by reduction in sink size which results in reduced grain yield. A significant increase in the harvest index was observed in pulse crops under elevated CO_2 due to improved partitioning efficiency.

15.6.4 Influence on Quality Parameters

The experiments conducted with Open Top Chambers also revealed that there was no significant change in the content and quality of castor bean oil at two elevated CO_2 levels of 550 and 700 ppm. However, the total oil yield was significantly higher owing to higher seed yields (Vanaja et al. 2008). In groundnut an increase of 3.3% oil content was observed at 550 ppm CO_2 level when compared with ambient control and the change in protein content was insignificant. In edible oils, unsaturated fatty acids *viz*., oleic, linoleic and linolenic acids play a vital role for the human nutrition view while in the non-edible oil like castor it is the ricinoleic acid which is responsible for its industrial utility.

15.7 Climate Change Impact on Livestock

India owns 57 % of the world's buffalo population and 16 % of the cattle population. It ranks first in the world in respect of cattle and buffalo population, third in sheep and second in goat population. The sector utilizes crop residues and agricultural by-products for animal feeding that are unfit for human consumption. Livestock sector has registered a compounded growth rate of more than 4.0% during last decade, in spite of the fact that a majority of the animals are reared under sub-optimal conditions by marginal and small holders and milk productivity per animal is low. Increased heat stress associated with rising temperature may, however, cause distress to dairy animals and possibly impact milk production. A rise of 2 to 6°C in temperature is expected to negatively impact growth, puberty and maturation of crossbred cattle and buffaloes. The low producing indigenous cattle are found to have high level of tolerance to these adverse impacts than high yielding crossbred cattle. Therefore, high producing crossbred cows and buffaloes will be affected more by climate change.

Upadhyay et al. (2009) at National Dairy Research Institute, Karnal studied the temperature and humidity induced stress level on Indian livestock. Livestock begin to suffer from mild heat stress when THI reaches higher than 72, moderate heat stress occurs at THI 80 and severe stress is observed after THI reaches 90. In India, huge variation in THI is observed throughout the year (Table 15.7). In most of the agroclimatic zones of India, the average THI are more than 75. More than 85% places in India experiences moderate to high heat stress during April, May and June. THI ranges between 75 and 85 at 2.00 PM at most part of India. The THI increases and exceed 85, i.e., severe stress levels at about 25% places in India during May and June. Even during morning the THI level remains high during these months. On an average THI exceed 75 at 75–80% places in India throughout the year. As can be seen from data, the congenial THI for production *i.e.* 70 is during Jan and Feb at most places in India and only about 10–15 % places have optimum THI for livestock productivity i.e. during summer and hot humid season. Climate change scenario constructed for India revealed that temperature rise of about or more than 4°C is likely to increase uncomfortable days (THI > 80) from existing 40 days (10.9%) to 104 days (28.5%) for Had CM 3-A2 scenario and 89 days for B2 scenario for time slices 2080–2100. The results further indicate that number of stress days with THI > 80 will increase by 160 %.

Table 15.7. Distribution of THI (%) in India at 7:20 and 14:20 hrs

Months	**< 70**		**70–75**		**75–80**		**80–85**		**85–90**	
	7:20 hrs	**14:20 hrs**	**7:20 hrs**	**14:20 hrs**	**7:20 hrs**	**14:20 hrs**	**7:20 hrs**	**14:20 hrs**	**7:20 hrs**	**14:20 hrs**
January	85	58	12	25	3	17	-	-	-	-
February	82	40	12	21	6	39	-	-	-	-
March	59	12	26	16	15	57	-	15	-	-
April	13	11	41	1	34	22	12	65	-	1
May	9	9	8	2	49	11	34	53	-	25
June	9	8	10	5	33	15	48	47	-	25
July	6	8	20	10	45	30	29	49	-	3
August	6	8	20	10	57	37	17	45	-	-
September	8	8	20	8	57	36	15	48	-	-
October	16	10	50	10	34	74	-	6	-	-
November	73	23	14	49	13	48	-	-	-	-
December	83	56	13	30	4	14	-	-	-	-

It is estimated that global warming is likely to result in a loss of 1.6 million tonnes in milk production by 2020 and 15 million tonnes by 2050. Based on temperature-humidity index (THI), the estimated annual loss in milk production at the all-India level by 2020 is valued at Rs. 2661.62 crores at current prices. The economic losses were highest in Uttar Pradesh followed by Tamil Nadu, Rajasthan and West Bengal. Stressful THI with 20h or more daily THI-hrs (THI >84) for several weeks, affect animal responses. Under climate change scenario, increased number of stressful days with a change in maximum and minimum temperature and decline in availability of water will further impact animal productivity and health in Punjab, Rajasthan and Tamil Nadu (Upadhyay et al. 2009).

A rise of 2–6 °C due to global warming (time slices 2040–2069 and 2070–2099) is likely to negatively impact growth, puberty and maturity of crossbreds and buffaloes and time to attain puberty of crossbreds and buffaloes will increase by one to two weeks due to their higher sensitivity to temperature than indigenous cattle. Lactating cows and buffaloes have higher body temperature and are unable to maintain thermal balance. Body temperature of buffaloes and cows producing milk is 1.5–2°C higher than their normal temperature, therefore more efficient cooling devices are required to reduce thermal load of lactating animals as current measures are becoming ineffective (Upadhyay et al. 2009).

15.8 Climate Change Impact on Poultry

The analysis of mortality data from 2004 to 2009 at Project Directorate of Poultry, Hyderabad revealed that the overall mortality was increased with rise in the ambient temperature of broiler, layer and native chickens (Figure 15.14). The mortality started increasing when the temperature reached 32°C and the peak was observed at 38 to 39°C (13.5%). The mortality was highest in broiler type chickens followed by layers and native chicken. The mortality due to heat stress in broiler type birds started appearing at the ambient temperature of 30°C, while in layer and native chicken the heat stress related mortality was observed at the ambient temperature of 31°C. The deaths due to heat stress were 10 times more in broiler type chickens as compared to layer and native type chickens (Figure 15.15). The mortality due to heat stress was negligible in native (Desi type chickens) which may be due to low metabolic rate and natural heat tolerance.

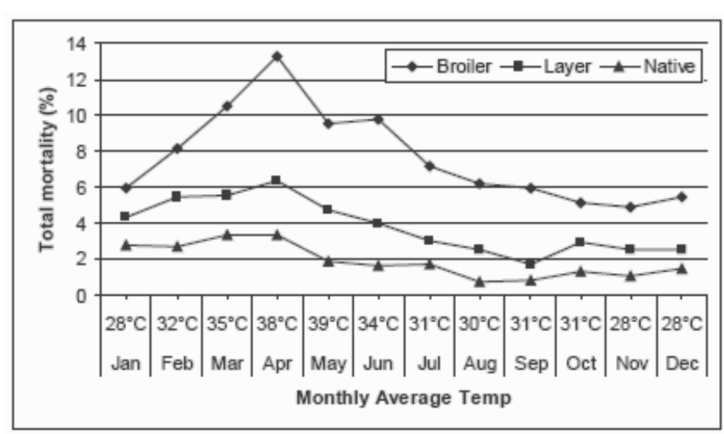

Figure 15.14. Effect ambient temperature on the survivability of meat type (broiler), egg type (layer) and native (desi) chicken

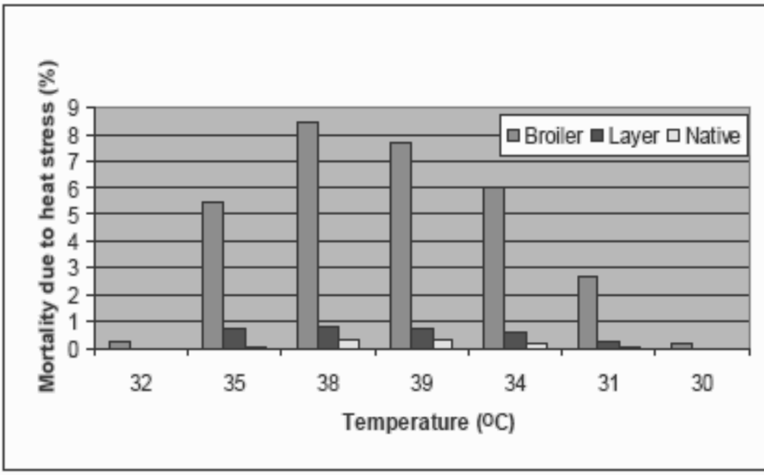

Figure 15.15. Mortality due to heat stress caused by high ambient temperature

Another study was conducted to find the influence of high ambient temperature on feed intake body temperature and respiratory rate in commercial layers for 13 weeks. The consumption which was 108 g/bird-day at 28°C was reduced to 68 g/bird-day at the shed temperature 37.8°C (Figure 15.16).

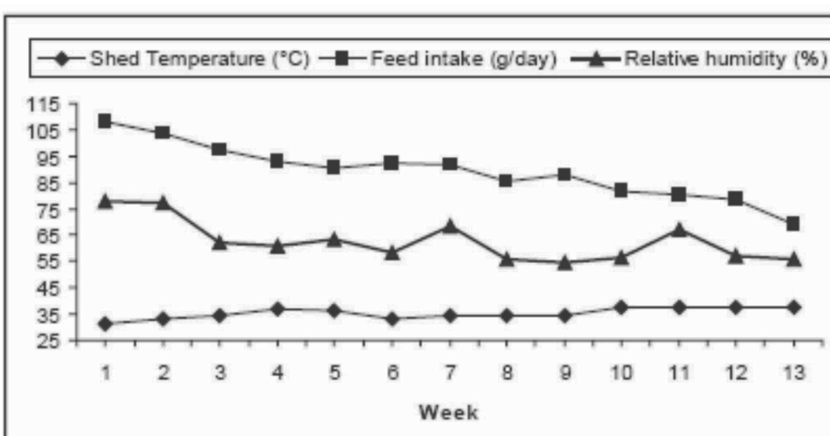

Figure 15.16. Influence of elevated ambient temperature on feed consumption

15.9 Climate Change Impact on Fisheries

15.9.1 Marine fisheries

A rise in temperature as small as 1°C could have important and rapid effect on the mortality of fish and their geographical distributions. Oil sardine fishery did not exist before 1976 in the northern latitudes and along the east coast of India as the resource was not available and sea surface temperature (SST) were not congenial. With warming of sea surface, the oil sardine is able to find temperature to its preference especially in the northern latitudes and eastern longitudes, thereby extending the distributional boundaries and establishing fisheries in larger coastal areas as shown in Figure 15.17 (Vivekanandan et al. 2009a).

The dominant demersal fish, the threadfin breams have responded to increase in SST by shifting the spawning season off Chennai. During past 30 years period, the spawning activity of *Nemipterus japonicus* reduced in summer months and shifted towards cooler months (Figure 15.18a). A similar trend was observed in *Nemipterus* mesoprion too (Figure 15.19b). Analysis of historical data showed that the Indian mackerel is able to adapt to rise in sea surface temperature by extending distribution towards northern latitudes, and by descending to depths (Vivekanandan et al. 2009b).

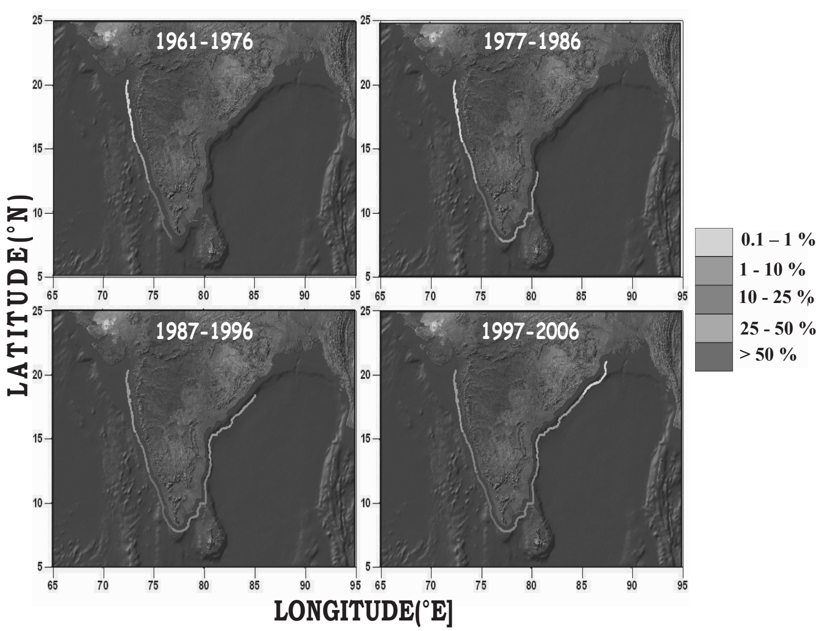

Figure 15.17. Extension of northern boundary of oil sardine (% in colour code indicates the % contribution of oil sardine catch from each 2° grid to the total oil sardine catch along the entire sea coast)

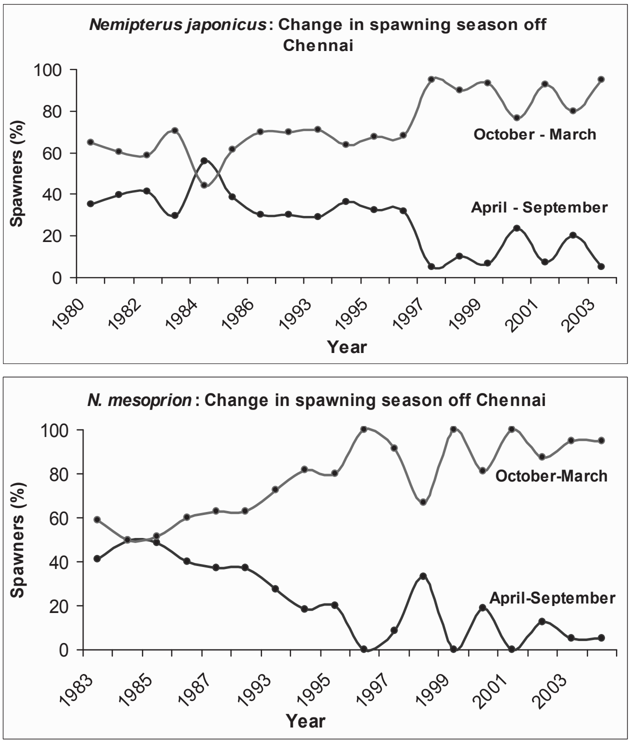

Figure 15.18. Change in spawning season of threadfin breams (N*emipterus japonicus* and *N. Mesoprion)* off Chennai

Central Marine Fisheries Research Institute, Cochin has studied the vulnerability of 75 coastal fishing villages of Maharashtra which are located within 100 m from the high tide line to sea level rise. Among the 75 coastal villages five coastal districts (Thane, Mumbai, Raigad, Ratnagiri and Sindhudurg) of Maharashtra, it was found that 35 villages in Raigad and Ratnagiri districts would be affected due to rise in sea level by 0.3 m (Table 15.8).

15.9.2 Inland Fisheries

In recent years, the phenomenon of Indian Major Carps maturing and spawning as early as March is observed in West Bengal with its breeding season extending from 110–120 days (Pre1980–85) to 160–170 days (2000–2005). Consequently, it has become possible to breed them twice in a year at an interval ranging from 30–60 days. A prime factor influencing this trend is elevated temperature, which stimulates the endocrine glands and help in the maturation of the gonads of Indian major carp. The average minimum and maximum temperature throughout the state has increased in the range of 0.1 to 0.9ºC (Das 2009; NPCC 2009).

Table 15.8. Area (km^2) of coastal fishing villages in Maharashtra likely to be submerged due to sea level rise by 0.3 to 1.0 m

District	No. of villages	Sea level increase by		
		0.3 m	0.6 m	1 m
Thane	8	0.95	1.04	1.45
Mumbai	5	0.12	0.19	0.28
Raigad	19	0.29	0.38	2.03
Ratnagiri	16	0.005	0.05	0.332
Sindhudurg	27	0	0	0.905
Total	75	1.365	1.66	4.997

Recent climatic patterns have brought about hydrological changes in the flow pattern of river Ganga. This has been one major factor resulting in erratic breeding and decline in fish spawn availability. As a result of this, the total average fish landing in the Ganga river system declined from 85.21 tonnes during 1959 to 62.48 tonnes during 2004. In the middle and lower Ganga, 60 genera of phytoplankton were recorded during 1959 which declined to 44 by 1996. During the same period the Zooplankton number diminished from 38 to 26. A number of fish species, which were predominantly only available in the lower and middle Ganga in 1950s, are now recorded from the upper cold-water stretch up to Tehri (Das 2009; NPCC 2009).

15.10 Impact of Climate Change on Crop Water Requirements and Water Resources

Besides hastening crop maturity and reducing crop yields, increased temperatures will also increase crop water requirement. A study carried out by CRIDA (unpublished) on the major crop growing districts in the country for four crops, viz., wheat, maize, sorghum and pearl millet indicated a 2.2 % increase in crop water requirement by 2020 and 5.5 % by 2050 across all the crops/locations. The climate scenarios for 2020 and 2050 were obtained from HadCM3 model outputs using 1960–1990 as base line weather data (Table 15.9).

Next to agriculture and related to agricultural needs, is the water sector. It can be seen from the projections of future water requirements (Figure 15.19) that would result due to climate change that the current level of water availability is fast dwindling and may fail to meet the future water needs. The targets are fast increasing due to increased population demands and poverty eradication needs to be met by 2015, 2030 and 2050. Efficient irrigation and rain water management in rainfed areas will play a key role in minimizing the impacts and in improving agricultural productivity and also protect soil environment (Ramakrishna et al. 2007).

At present, available statistics on water demand shows that the agriculture sector is the largest consumer of water in India using 83% of the available water. The quantity of water used for agriculture has increased progressively through the years as more and more areas were brought under irrigation. Possible impact of climate change on water resources during the next century over India is furnished in Table 15.10. The enhanced surface warming over the Indian subcontinent by the end of the next century would result in an increase in pre-monsoonal and monsoonal rainfall, with no substantial change in winter rainfall over the central plains. This would result in an increase in the monsoonal and annual run-off in the central plains, with no substantial change in winter run-off and increase in evaporation and soil wetness during the monsoon on an annual basis (Mall et. al. 2006b).

Table 15.9. Estimated crop water requirement (mm) of four crops in major growing districts of the country under projected climate change scenario

District (State)	1990	2020	2050	% change over 1990 in	
				2020	2050
			Wheat		
Sirsa (Haryana)	281.8	293.1	301.4	4.0	7.0
Ahmedabad (Gujarat)	523.0	536.8	551.0	2.6	5.4
Ahemedanagar (Mah)	485.8	496.1	509.5	2.1	4.9
Ganganagar (Raj)	278.9	290.3	298.2	4.1	6.9
Hardoi (UP)	475.0	488.2	502.2	2.8	5.7
Kangra (HP)	367.7	380.7	391.2	3.5	6.4
Vidisha (MP)	437.1	446.9	460.4	2.3	5.3
Sangrur(Punjab)	391.1	405.4	416.3	3.7	6.4
			Maize		
Udaipur (Raj)	388.8	392.4	400.9	0.9	3.1
Karimnagar (AP)	424.7	433.4	440.0	2.0	3.6
Jhabua (MP)	424.5	430.6	441.9	1.4	4.1
Begusarai (Bihar)	370.0	374.7	388.9	1.3	5.1
Bahraich (UP)	407.4	412.1	426.5	1.1	4.7
Godhra (Gujarat)	426.3	432.3	444.0	1.4	4.2
Khargaon (MP)	354.3	365.0	381.0	3.0	7.6
Aurangabad (Mah)	413.4	423.1	435.7	2.3	5.4
			Sorghum		
Solapur (Maha)	348.8	373.2	399.9	7.0	14.7
Gulburga (Kar)	387.2	396.9	411.9	2.5	6.4
Khargaon (MP)	350.3	355.1	364.1	1.4	3.9
Mahabubnagar (AP)	383.4	393.7	409.1	2.7	6.7
Ajmer (Raj)	362.9	365.4	375.4	0.7	3.4
Coimbatore (TN)	378.8	387.8	396.9	2.4	4.8
Banda (UP)	326.7	332.5	347.0	1.8	6.2
Surat (Guj)	308.9	314.3	321.7	1.8	4.1
			Pearl Millet		
Barmer (Raj)	337.8	338.6	347.4	0.2	2.8
Nashik (Maha)	284.2	289.9	296.9	2.0	4.5
Agra (UP)	277.5	279.7	289.7	0.8	4.4
Gulburga (Kar)	325.2	333.5	344.0	2.6	5.8
Bhind(MP)	285.8	287.4	298.0	0.6	4.3
Villupuram (TN)	311.4	317.7	333.7	2.0	7.2

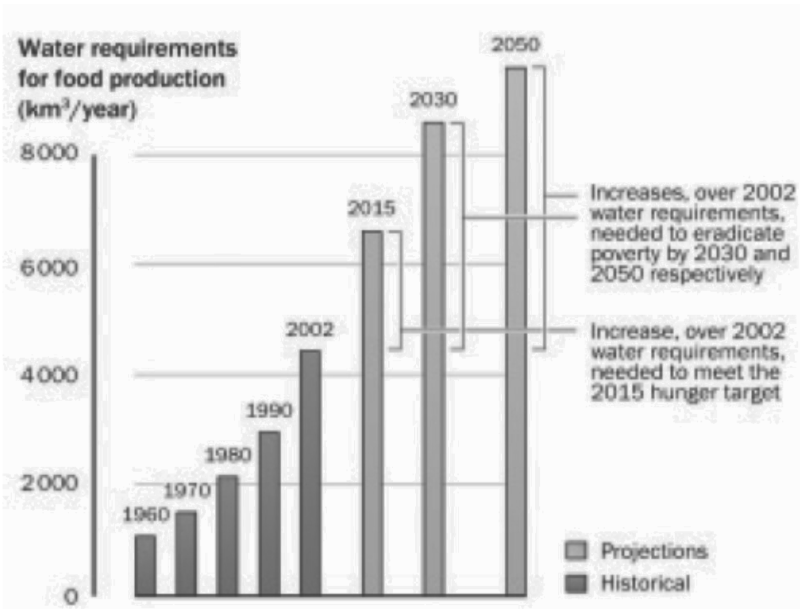

Figure 15.19. Future water requirements for food production

Table 15.10. Impact of climate change on water resources during the next century over India

Region / location	Impact
Indian subcontinent	• Increase in monsoonal and annual run-off in the central plains • No substantial change in winter run-off • Increase in evaporation and soil wetness during monsoon and on an annual basis
Orissa and West Bengal	One metre sea-level rise would inundate 1700 km^2 of prime agricultural land
Indian coastline	One metre sea-level rise on the Indian coastline is likely to affect a total area of 5763 km^2 and put 7.1 million people at risk
All-India	Increases in potential evaporation across India
Central India	Basin located in a comparatively drier region is more sensitive to climatic changes
Kosi Basin	Decrease in discharge on the Kosi River; Decrease in run-off by 2–8%
Southern and Central India	Soil moisture increases marginally by 15–20% during monsoon months
Chenab River	Increase in discharge in the river
River basins of India	General reduction in the quantity of the available run-off, increase in Mahanadi and Brahmini basins
Damodar Basin	Decreased river flow
Rajasthan	Increase in evapotranspiration

15.11 Adaptation and Mitigation Strategies

Successful adaptation to climate change requires long-term investments in strategic research and new policy initiatives that mainstream climate change adaptation into development planning. As a first step, we need to document all the indigenous practices rainfed farmers have been following over time for coping with climate change. Secondly, we need to quantify the adaptation and mitigation potential of the existing best bet practices for different crop and livestock production systems in different agro-ecological regions of the country. Thirdly, a long-term strategic research planning is required to evolve new tools and techniques including crop varieties and management practices that help in adaptation.

More recently during 2010, ICAR has launched the National Initiative on Climate Resilient Agriculture (NICRA) as a comprehensive project covering strategic research, technology demonstration and capacity building. Targeted research on adaptation and mitigation is at nascent stage in India but based on knowledge already generated, some options for adaptation to climate variability induced effects like droughts, high temperatures, floods and sea water inundation can be suggested. These strategies fall into two broad categories viz., (i) crop based and (ii) resource management based.

15.11.1 Crop-based Strategies

Crop based approaches include growing crops and varieties that fit into changed rainfall and seasons, development of varieties with changed duration that can overcome winter the transient effects of change, development of varieties for heat stress, drought and submergence tolerance; evolving varieties which respond positively in terms of growth and yield under high CO_2. In addition, varieties with high fertilizer and radiation use efficiency and also novel crops and varieties that can tolerate coastal salinity and sea water inundation are needed. Intercropping is a time tested practice to cope with climate variability and climate change, if one crop fails due to floods or droughts second crop gives some minimum assured returns for livelihood security. Germplasm of wild relatives and local land races could prove valuable source of climate ready traits. We need to revisit the germplasm collected so far which has tolerance to heat and cold stresses but not made use in the past due to low yield potential. A detailed account of crop based approaches is beyond the scope of this paper. Kumar (2006) provides a succinct account of breeding objectives under climate change in India.

15.11.2 Strategies based on Resource Management

There are large number of options in soil, water and nutrient management technologies which contribute to both adaptation and mitigation. Much of the research done in rainfed agriculture in India relates to conservation of soil and rain water and drought proofing which is an ideal strategy for adaptation to climate change (Venkateswarlu et al. 2009). Important technologies include *in situ* moisture conservation, rainwater harvesting and recycling, efficient use of irrigation water, conservation agriculture, energy efficiency in agriculture and use of poor quality water. Watershed management is now considered an accepted strategy for development of rainfed agriculture. Watershed approach has many elements which help both in adaptation and mitigation. For example, soil and water conservation works, farm ponds, check dams etc. moderate the runoff and minimize floods during high intensity rainfall. The plantation of multi-purpose trees in degraded lands helps in carbon sequestration. The crop and soil management practices can be tailored for both adaptation and mitigation at the landscape level. Some of the most important adaptation and mitigation approaches with high potential are described below:

Rainwater Conservation and Harvesting. These are based on *in-situ* and *ex-situ* conservation of rainwater for recycling to rainfed crops. The arresting of soil loss contributes to reduced carbon losses. Lal (2004) estimates that if water and wind erosion are arrested, it can contribute to 3 to 4.6 Tg year^{-1} of carbon in India. Increased ground water utilization and pumping water from deep tube wells is the largest contributor to GHG emissions in agriculture. If surface storage of rainwater in dug out ponds is encouraged and low lift pumps are used to lift that water for supplemental irrigation, it can reduce dependence on ground water. Sharma et al. (2010) estimated that about 28 m ha of rainfed area in eastern and central states has the maximum potential to generate runoff of 114 billion cubic meters which can be used to provide one supplemental irrigation in about 25 m ha of rain-fed area. For storing such quantum of rainwater about 50 million farm ponds are required. This is one of the most important strategies not only to control runoff and soil loss but also contribute to climate change mitigation. Conjunctive use of surface and ground water is an important strategy to mitigate climate change. Innovative approaches in ground water sharing can also contribute to equitable distribution of water and reduced energy use in pumping.

Soil Carbon Sequestration. Soil carbon sequestration is yet another strategy towards mitigation of climate change. Although, tropical regions have limitation of sequestering carbon in soil due to high temperatures, adoption of appropriate management practices helps in sequestering reasonable quantities of carbon in some cropping systems particularly in high rainfall regions. The potential of cropping systems can be divided in to that of soil carbon sequestration and sequestration in to vegetation. Tree-based systems can sequester substantial quantities of carbon in to biomass in a short period. Total potential of soil C sequestration in India is 39 to 49 Tg year^{-1} (Lal 2004).This is inclusive of the potential of the restoration of degraded soils and ecosystems which is estimated at 7 to 10 TgC year^{-1} (Table 15.11). The potential of adoption of recommended package of practices on agricultural soils 6 to 7 Tg year^{-1}. In addition, there is also a potential of soil inorganic carbon sequestration estimated at 21.8 to 25.6 TgC year^{-1}. Long-term manurial trials conducted in arid regions of Andhra Pradesh (at Anantapur) under rain-fed conditions indicate that the rate of carbon sequestration in groundnut production system varied from 0.08 to 0.45 t ha^{-1} year^{-1} with different nutrient management systems (Srinivasa Rao et al. 2009a). Under semi-arid conditions in Alfisol region of Karnataka, the rate of carbon sequestration was 0.04 to 0.38 t ha^{-1} $year^{-1}$ in finger millet system under diverse management practices. Under *rabi* sorghum production system in Vertisol region of Maharashtra (semi arid) the sequestration rate ranged from 0.1 to 0.29 t ha^{-1} $year^{-1}$ with different integrated management options. In soybean production system in black soils of Madhya Pradesh (semi-arid) the potential rate of carbon sequestration is up to 0.33 t ha^{-1} $year^{-1}$ in top 20 cm soil depth.

Table 15.11. Soil organic carbon sequestration potential through restoration of degraded soils

Degradation process	Area (M ha)	SOC sequestration rate (kg/ha/y)	Total SOC sequestration potential (Tg C/y)
Water erosion	32.8	80–120	2.62–3.94
Wind erosion	10.8	40–60	0.43–0.65
Soil fertility decline	29.4	120–150	3.53–4.41
Waterlogging	3.1	40–60	0.12–0.19
Salinization	4.1	120–150	0.49–0.62
Lowering of water table	0.2	40–60	0.01–0.012
Total			7.20–9.82

Site Specific Nutrient Management. Integrated Nutrient Management and Site-Specific Nutrient Management (SSNM) is another approach with potential to mitigate effects of climate change. Demonstrated benefits of these technologies are; increased rice yields and thereby increased CO_2 net assimilation and 30–40% increase in nitrogen use efficiency. This offers important prospect for decreasing GHG emissions linked with N fertilizer use in rice systems. It is critical to note here that higher CO_2 concentrations in the future will result in temperature stress for many rice production systems, but will also offer a chance to obtain higher yield levels in environments where temperatures are not reaching critical levels. This effect can only be tapped under integrated and site directed nutrient supply, particularly N. Phosphorus (P) deficiency, for example, not only decreases yields, but also triggers high root exudation and increases CH_4 emissions. Judicious fertilizer application, a principal component of SSNM approach, thus has twofold benefit, i.e. reducing GHG emissions; at the same time improving yields under high CO_2 levels. The application of a urease inhibitor, hydroquinone (HQ), and a nitrification inhibitor, dicyandiamide (DCD) together with urea also is an effective technology for reducing N_2O and CH_4 from paddy fields. Very little information is available on the potential of SSNM in reducing GHG emissions in rainfed crops.

Conservation Agriculture (CA). In irrigated areas, zero tillage (ZT) in particular has effectively reduced the demand for water in rice-wheat cropping system of Indo-Gangetic plains and is now considered as a viable option to combat climate change. ZT has some mitigation effect in terms of enhancing soil carbon, reducing energy requirement and improving water and nutrient use efficiency but actual potential has to be quantified from long term experiments. The scope of CA in rainfed agriculture has been reviewed by Singh and Venkateswarlu (2009). While reduced tillage is possible in few production systems in high rainfall regions in eastern and northern India, non-availability of crop residue for surface application is a major constraint, particularly in peninsular and western India where it is mainly used as fodder.

Biomass Energy and Waste Recycling. A large amount of energy is used in cultivation and processing of crops like sugarcane, food grains, vegetables and fruits, which can be recovered by utilizing residues for energy production. This can be a major strategy of climate change mitigation by avoiding burning of fossil fuels and recycling crop residues. The integration of biomass-fuelled gasifiers and coal-fired energy generation would be advantageous in terms of improved flexibility in response to fluctuations in biomass availability with lower investment costs. Waste-to-energy plants offer twin benefits of environmentally sound waste management and disposal, as well as the generation of clean energy.

Livestock production has been an integral part of agriculture in India. Livestock provides an excellent recycling system for most of crop residue. Most by products of cereals, pulses and oilseeds are useful as feed and fodder for livestock while that of other crops like cotton, maize, pigeonpea, castor and sunflower and sugarcane are used as low calorie fuel or burnt to ashes or left in open to decompose over time. Ideally such residue is incorporated into soil to enhance physical properties of the soil and its water holding capacity. Lack of availability of proper chipping and soil incorporation equipment is one of the major reasons for the colossal wastage of agricultural biomass in India. Increased cost of labour and transport is another reason for lack of interest in utilizing the biomass. This is one area where little or no effort has gone in despite availability of opportunities for reasons such as aggregation, transport and investment in residue processing facilities. Many technologies like briquetting, anaerobic digestion vermin-composting and bio-char etc. exist, but they have not been commercially exploited. This area is gradually receiving attention now as a means to producing clean energy by substituting forest biomass for domestic needs. Modest investments in decentralized facilities for anaerobic digestion of agricultural residue through vermin-composting and biogas generation can meet the needs of energy-deficit rural areas and simultaneously contribute to climate change mitigation.

Biomass-based Biogas Production. There is renewed interest in the use of anaerobic digestion processes for efficient management and conversion of cattle dung and other agro industrial wastes (livestock, paper and pulp, brewery and distillery) into clean renewable energy and organic fertilizer source. The biogas captured could not only mitigate the potential local and global pollution but could either be combusted for electricity generation using combined heat and power generator in large to medium enterprises or used for cooking and lighting for small households. A 2 m^3 digester can generate up to 4.93 t CO_2 $year^{-1}$ of certified emission reduction (CER). Animal wastes are generally used as feedstock in biogas plants. But, the availability of these substrates is one of the major problems hindering the successful operation of biogas digesters. Khandelwal (1990) reported that the availability of cattle waste could support only 12–30 million family-size biogas plants against the requirement of 100 million plants. A significant portion of 70–88 million biogas plants can be run with fresh/dry biomass residues. Of the available 1,150 billion tons of biomass, a fifth would be sufficient to meet this demand.

Agroforestry. Agroforestry systems like agri-silvi-culture, silvipasture and agri-horticulture offer both adaptation and mitigation opportunities. Agroforestry systems buffer farmers against climate variability, and reduce atmospheric loads of GHGs. Agroforestry can both sequester carbon and produce a range of economic, environmental, and socioeconomic benefits; the extent of sequestration can be upto 10 t ha^{-1} $year^{-1}$ in short rotation eucalyptus, leucaena plantations (Table 15.12). Agrisilviculture systems with moderate tree density with intercrops have however lower potential.

Table 15.12. Carbon storage (Mg/ha/year) in different Agri silvicultural systems

Location	System	C sequestration (Mg ha^{-1} $year^{-1}$)	Reference
Raipur	Gmelina based system	2.96*	Swami & Puri (2005)
Chandigarh	Leucaena based system	0.87	Mittal & Singh (1989)
Jhansi	Anogeissus based system	1.36	Rai et al. (2002)
Coimbatore	Casuarina based system	1.45	Viswanath et al. (2004)

*Includes soil carbon storage of 0.42 Mg ha^{-1} $year^{-1}$ (up to 60 cm depth)

15.12 Socio Economic and Policy Issues

Apart from the use of technological advances to combat climate change, there has to be sound and supportive policy framework. The frame work should address the issues of redesigning social sector with focus on vulnerable areas/ populations, introduction of new credit instruments with deferred repayment liabilities during extreme weather events, weather insurance as a major vehicle to risk transfer. Governmental initiatives should be undertaken to identify and prioritize adaptation options in key sectors (storm warning systems, water storage and diversion, health planning and infrastructure needs). Focus on integrating national development policies into a sustainable development framework that complements adaptation should accompany technological adaptation methods.

In addition, the role of local institutions in strengthening capacities e.g., SHGs, banks and agricultural credit societies should be promoted. Role of community institutions and private sector in relation to agriculture should be a matter of policy concern. There should be political will to implement economic diversification in terms of risk spreading, diverse livelihood strategies, migrations and financial mechanisms. Policy initiatives in relation to access to banking, micro-credit/insurance services before, during and after a disaster event, access to communication and information services is imperative in the envisaged climate change scenario. Some of the key policy initiatives that are to be considered are: Mainstreaming adaptations by considering impacts in all major development initiatives Facilitate greater adoption of scientific and economic pricing policies, especially for water, land, energy and other natural resources. Consider financial incentives and package for improved land management and explore CDM benefits for mitigation strategies. Establish a "Green Research Fund" for strengthening research on adaption, mitigation and impact assessment (Venkateswarlu and Shanker 2009).

15.13 India's National Action Plan on Climate Change

On June 30, 2008, Prime Minister Manmohan Singh released India's first National Action Plan on climate Change (NAPCC) outlining existing and future policies and programs addressing climate mitigation and adaptation. The plan identifies eight core "National Missions" running through 2017 and directs ministries to submit detailed implementation plans to the Prime Minister's Council on Climate Change by December 2008. Emphasizing the overriding priority of maintaining high economic growth rates to raise living standards, the plan "identifies measures that promote our development objectives while also yielding co-benefits for addressing climate change effectively." It says these national measures would be more successful with assistance from developed countries, and pledges that India's per capita GHG emissions "will at no point exceed that of developed countries even as we pursue our development objectives."

National Solar Mission. This mission aims to promote the development and use of solar energy for power generation and other uses with the ultimate objective of making solar competitive with fossil-based energy options. The plan includes:

- Specific goals for increasing use of solar thermal technologies in urban areas, industry, and commercial establishments.
- A goal of increasing production of photovoltaic to 1000 MW/year.
- A goal of deploying at least 1000 MW of solar thermal power generation.

Other objectives include the establishment of a solar research center, increased international collaboration on technology development, strengthening of domestic manufacturing capacity, and increased government funding and international support.

National Mission for Enhanced Energy Efficiency. Current initiatives are expected to yield savings of 10,000 MW by 2012. Building on the Energy Conservation Act 2001, the plan recommends:

- Mandating specific energy consumption decreases in large energy-consuming industries, with a system for companies to trade energy-savings certificates.
- Energy incentives, including reduced taxes on energy-efficient appliances.
- Financing for public-private partnerships to reduce energy consumption through demand-side management programs in the municipal, buildings and agricultural sectors.

National Mission on Sustainable Habitat. To promote energy efficiency as a core component of urban planning, the plan calls for:

- Extending the existing Energy Conservation Building Code.

- A greater emphasis on urban waste management and recycling, including power production from waste.
- Strengthening the enforcement of automotive fuel economy standards and using pricing measures to encourage the purchase of efficient vehicles.
- Incentives for the use of public transportation.

National Water Mission. With water scarcity projected to worsen as a result of climate change, the plan sets a goal of a 20% improvement in water use efficiency through pricing and other measures.

National Mission for Sustaining the Himalayan Ecosystem. The plan aims to conserve biodiversity, forest cover, and other ecological values in the Himalayan region, where glaciers that are a major source of India's water supply are projected to recede as a result of global warming.

National Mission for a "Green India." Goals include the afforestation of 6 million hectares of degraded forest lands and expanding forest cover from 23% to 33% of India's territory.

National Mission for Sustainable Agriculture. The plan aims to support climate adaptation in agriculture through the development of climate-resilient crops, expansion of weather insurance mechanisms, and agricultural practices.

National Mission on Strategic Knowledge for Climate Change. To gain a better understanding of climate science, impacts and challenges, the plan envisions a new Climate Science Research Fund, improved climate modeling, and increased international collaboration. It also encourages private sector initiatives to develop adaptation and mitigation technologies through venture capital funds.

15.14 Conclusions

Even though climate change in India is now a reality, a more certain assessment of the impacts and vulnerabilities of rainfed agriculture sector and a comprehensive understanding of adaptation options across the full range of warming scenarios and regions would go a long way in preparing the nation for climate change. A multi-pronged strategy of using indigenous coping mechanisms, wider adoption of the existing technologies and or concerted R&D efforts for evolving new technologies are needed for adaptation and mitigation. Policy incentives will play crucial role in adoption of climate ready technologies in rainfed agriculture too as in other sectors. The state agricultural universities and regional research centers will have to play major role in adaptation research which is more region and location specific while national level efforts are required to come up with cost effective mitigation options, new policy initiatives and global cooperation.

15.15 References

Agarwal, P. K. (2009). *Global Climate change and Indian agriculture: Case studies from ICAR network project.* Indian Council of Agricultural Research. 148p.

CRIDA (2009). *Annual Report 2009*. Central Research Institute for Dryland Agriculture, Indian Council of Agricultural Research, New Delhi.

Das, M. K. (2009). "Impact of recent changes in weather on inland fisheries in India." In: *Global Climate Change and Indian Agriculture: Case Studies from the ICAR Network Project* (ed. by Aggarwal, P. K.). ICAR Publication. pp.101–103.

Goswami, B. N. (2006). "Increasing trend of extreme rain events and possibility of extremes of seasonal mean Indian monsoon in a warming world." <http: saarc-sdmc.nic.in/pdf/workshops/Kathmandu/pres16.pdf)> (accessed Jan. 2012).

Guhathakurta, P. and Rajeevan, M. (2008). "Trends in rainfall pattern over India." *International Journal of Climatology,* 28, 1453–1469.

IPCC (2001). *Climate Change 2001: The Scientific Basis*. Contribution of Working Group – I to the Third Assessment Report of the IPCC. [Houghton, J.T., Ding, Y., Griggs, D.J., Noguer, M., van der Linden, P.J., Dai, X., Maskell, K. and Johnson, C.A. (Eds)]. Cambridge University Press, United Kingdom and New York, USA, 94p.

IPCC (2007). *Climate Change 2007, The Physical Science Basis*. Contribution of Working Group – I to the Fourth Assessment Report of the IPCC. [Solomon, S., Quin, D., Manning, M., Chen, Z., Marquis, M., Averut, K.B., Tignor, M. and Miller, H.L. (Eds)]. Cambridge University Press, United Kingdom and New York, USA, 996p.

Khandelwal, K. C. (1990). "Biogas technology development implementation strategies: Indian experience." *Proceedings of the International Conference on Biogas Technology, Implementation Strategies*, Pune, India, 10–15 January 1990.

Kumar, K. (2009). "Impact of climate change on India's monsoon climate and development of high resolution climate change scenarios for India." Presented at MoEF, New Delhi on October 14, 2009. <http: moef.nic.in> (accessed Jan. 2012).

Kumar, S. (2006). "Climate change and crop breeding objectives in the twenty first century." *Current Science,* 90, 1053–1054.

Lal, R. (2001). "Future climate change: Implications for India Summer monsoon and its variability." *Current Science,* 81, 1205–1207.

Lal, R. (2004). "Soil carbon sequestration in India." *Climatic Change,* 65, 277–296.

Lobell, D. B., and Field, C. B. (2007). "Global scale climate-crop yield relationships and the impacts of recent past." *Environmental Research Letter,* 2, 1–7.

Mujumdar, P. P. (2008). "Implications of climate change for sustainable water resources management in India." *Physics and Chemistry of the Earth, Parts A/B/C*, 33, 354–358.

Mall, R. K., Gupta, A., Singh, R., Singh, R.S., and Rathore, L. S. (2006a). "Water resources and climate change: An Indian perspective." *Current Science*, 90 (12), 1610–1626.

Mall, R., Singh, R., Gupta, A., Srinivasan, G., and Rathore, L. (2006b). "Impact of Climate Change on Indian Agriculture: A Review." *Climatic Change,* 78, 445–478.

Mittal, S. P., and Singh, P. (1989). "Intercropping field crops between rows of *Leucaena leucocephala* under rainfed conditions in northern India." *Agroforestry Systems,* 8, 165–172.

NPCC (Network Project on Climate Change) (2009). Annual Report for 2009–10. Central Research Institute for Dryland Agriculture, Hyderabad, pp. 221–227.

Rai, A. K., Solanki, K. R., and Rai, P. (2002). "Performance of *Anogeissus pendula* genotypes under agrisilvicultural system." *Indian Journal Agroforestry,* 4(1), 71 –74.

Ramakrishna,Y. S., Rao, G. G. S. N., Rao, V. U. M., Rao, A. V. M. S., and Rao, K. V. (2007). "Water management- water use in rainfed regions of India." In : *Managing Weather and Climate Risks in Agriculture* (Eds. Sivakumar, M.V.K., and Motha, R.P.), Springer, pp.245–262.

Saseendran, A. S. K., Singh, K. K., Rathore, L. S., Singh, S. V., and Sinha, S. K. (2000). "Effects of climate change on rice production in the tropical humid climate of Kerala, India." *Climate Change,* 44, 495–514.

Singh, A. K., Aggarwal, P. K., Gogoi, A. K., Rao, G. G. S. N., and Ramakrishna, Y. S. (2009). "Global Climate Change and Indian Agriculture: Future priorities." In: *Global Climate Change and Indian Agriculture: Case studies from the ICAR Network Project*. (ed. by Aggarwal, P. K.). ICAR Publication. pp.146–148.

Singh, A. K., and Venkateswarlu, B. (2009). "Conservation agriculture in arid and semi regions: Opportunities and constraints." *Indian Farming* (Special Issue): February, pp.3–8.

Srinivasa Rao, Ch., Ravindra Chary, G., Venkateswarlu, B., Vittal, K. P. R., Prasad, J. V. N. S., Sumanta Kundu, Singh, S. R., Gajanan, G. N., Sharma, R. A., Deshpande, A. N., Patel, J. J., and Balaguravaiah, G. (2009a). *Carbon sequestration strategies under rainfed production systems of India.* Central Research Institute for Dryland Agriculture, Hyderabad. 102p.

Srinivasa Rao, M., Srinivas, K., Vanaja, M., Rao, G. G. S. N., Venkateswarlu, B., and Ramakrishna, Y. S. (2009b). "Host plant (*Ricinus communis* Linn.) mediated effects of elevated CO_2 on growth performance of two insect folivores." *Current Science,* 97(7), 1047–1054.

Swamy , S. L., and Puri S. (2005). "Biomass production and C-sequestration of *Gmelina arborea* in plantation and agroforestry system in India." *Agroforestry systems,* 64(3), 181–195.

Upadhyay R. C., Ashutosh, V. S. Raina and Singh, S. V. (2009). "Impact of climate change on reproductive fu nctions of cattle and buffaloes." In: *Global Climate Change and Indian Agriculture: Case Studies from the ICAR Network Project* (Ed. P.K. Aggarwal). ICAR Publication. pp.107–110.

USDE (2005). "*International Energy Outlook 2005.*" Office of Integrated Analysis and forecasting. US Department of Energy, Energy Information Administration of Government of United States of America, 194p.

Vanaja, M., Jyothi, M., Ratnakumar, P., Vaheera, P., Raghuram reddy, P., Jyothi Lakshmi, N., Yadav, S. K., Maheswari, M., and Venkateswarlu, B. (2008). "Growth and yield responses of castor bean (*Ricinus communis* L.) to two enhanced CO_2 levels." *Plant Soil Environment,* 54(1), 38–46.

Vanaja, M., Vegheera, P., Ratnakumar, P., Jyothi Lakshmi, N., Raghuram Reddy, P., Yadav, S.K., Maheswari, M., and Venkateswarlu, B. (2006). "Evaluation of certain rainfed food and oil seed crops for their response to elevated CO_2 at vegetative stage." *Plant Soil Environment,* 52(4), 164–170.

Venkateswarlu, B., and A. K. Shanker, (2009). "Climate change and agriculture: Adaptation and mitigation strategies." *Indian Journal of Agronomy,* 54(2), 226–230.

Venkateswarlu, B., A K. Shankar., and Gogoi, A. K. (2009). "Climate change adaptation and mitigation in Indian agriculture." *Proceedings of National Seminar on Climate Change Adaptation Strategies in Agriculture and Allied Sectors*. Kerala Agricultural University, Thrissur, December 2008, pp.109–121.

Viswanath, S., Peddappaiah, R. S., Subramoniam, V., Manivachakam, P. and George, M. (2004). "Management of *Casuarina equisetifolia* in wide-row intercropping systems for enhanced productivity." *Indian Journal of Agroforestry,* 6(2), 19–25.

Vivekanandan, E., Hussain Ali, M. and Rajagopalan, M. (2009b). "Impact of rise in seawater temperature on the pawning of threadfin beams." In: *Global Climate Change and Indian Agriculture: Case Studies from the ICAR Network Project* (ed. by P. K. Aggarwal). ICAR Publication. pp.93–96.

Vivekanandan, E., Rajagopalan, M., and Pillai, N. G. K. (2009a). "Recent trends in sea surface temperature and its impact on oil sardine." In: *Global Climate Change and Indian Agriculture: Case Studies from the ICAR Network Project* (ed. by P.K. Aggarwal). ICAR Publication. pp.89–92.

World Bank (2008). *Climate change impacts in drought and flood affected areas: Case studies in India.* Report No.43946-IN, South East Asia Regional Office, New Delhi.

CHAPTER 16

Modeling the Impact of Climate Change on Agriculture and Food Production

C. M. Kao, Y. T. Tu, S. F. Cheng, R. Y. Surampalli, and Tian C. Zhang

16.1 Introduction

The earth is undergoing a warming process, and humanity faces an increasing possibility that extreme natural disasters are on the rise due to climate change and global warming (Saptomo et al. 2009; Yasuhara et al. 2011). The gradually increased temperature caused by the enhanced greenhouse effects has been found to be an important factor significantly affecting the Earth's hydrological cycles and agricultural activities. Climate change resulting from human activity has the potential to substantially alter agricultural systems (IPCC 2001; Parry et al. 2004). Studies emphasized that the adaptation potential to reduce costs or increase gains associated with climate change, suggesting that systems that are slow to adapt are more vulnerable (Rosenzweig and Hillel 1998; Burton and Lim 2005). The relationship between agriculture and climatic change is an important issue because the food production resources are under pressure due to a rapid increase in population (Matthews and Wassmann 2003). Researchers have estimated that a 60% increase in rice production is required by the year 2020 to meet the demands of an increased population (Hossain 1998).

The Fourth Assessment Report (AR4) of the Intergovernmental Panel on Climate Change (ICPP) (IPCC 2001) has warned international communities that the increase in anthropogenic greenhouse gas (GHG) emissions is resulting in a climate change problem. Associated with the expected global temperature rise, precipitation patterns and quantities will change and the frequency and intensity of major natural hazards will also increase (Roudier et al. 2011). However, the production of reliable future agricultural production scenarios remains challenging because of large uncertainties in climate change projections, in the coupling between climate models and crop productive functions, in the response of crops to environmental changes, and in the adaptation of agricultural systems to climate change (Challinor et al. 2007).

To assess the impact of climate change on crop production, it is necessary to define scenarios describing the future evolution of meteorological variables. The simplest way is to define a uniform scenario (for instance +10% in rainfall, +2.5^{o}C in temperature) and to add these changes to the observed climate data of a present time period (Ben Mohamed et al. 2002; Vanduivenbooden et al. 2002; Salack 2006). However, this method relies on assumptions of future climate. It has no real physical basis and does not preserve consistency among climate variables. Thus, a more physics-based approach is the use of global climate models (GCMs) that are able to generate physically consistent sets of climate variables. These models are forced by scenarios of future radiative forcing (e.g., increasing GHG concentrations). Several emissions scenarios, describing different future socio-economic evolutions, have been defined by the IPCC. GCMs can provide different climate projections over the study area, and therefore, the majority of the published papers used several GCMs and/or scenarios (Schlenker and Lobell 2010).

During agricultural activities, climate conditions and meteorological phenomena play important roles in crop production. However, some reactions between meteorological environments and crop production are not positively correlated. Thus, hypotheses are required during the modeling of crop production. Some of the crop production models with meteorological modules have been developed including DSSAT (Jones et al. 2003), CENTURY (Parton 1996), ORYZA2000 (Bannayan et al. 2005), EPIC (Tan and Shibasaki 2003), and DNDC (Li 2000). The Global Assessment of Security (GLASS) model developed for analyzing global change impacts on food and water security also took into account the extreme climate events in the model (Alcamo et al. 2000a, b, 2007). The modeling results indicate that an increase in the annual average temperature of roughly 1–3^{o}C is expected by the 2020s. Depending on the scenario, the climate model estimated that a 3–6^{o}C increase in annual average temperature is expected by the 2070s (Alcamo et al. 2000b, 2007). Moreover, precipitation during the summer crop growing period increases in many countries (Alcamo et al. 2007).

Bannayan et al. (2005) used the ORYZA2000 model for the evaluation of the growth and yield of rice plants in a 3-year field experiment, and their results showed that rice plants were subjected to elevated carbon dioxide (CO_2) with free air CO_2 enrichment (FACE) under varying nitrogen (N) fertilization rates in rice paddies in northern Japan. The results indicated that the model overestimated the increase in peak green leaf area index due to elevated CO_2. However, the modeling results only had a minor overestimation for the enhancement of total plant biomass. The model was successful in simulating the increase in rice yield due to the CO_2 enrichment, but it failed to reproduce the observed interaction with N in the rice yield response to elevated CO_2 (Bannayan et al. 2005).

Tan and Shibasaki (2003) developed a methodology for global estimation of crop productivity. This methodology integrates the Erosion Productivity Impact Calculator (EPIC) model with Geographic Information System (GIS) and the Inference Engine (IE) technique. EPIC was developed to analyze the relationship between soil erosion and agricultural productivity at field level (Tan and Shibasaki 2003). With the integration of GIS, EPIC can be extended to the application of the global or regional level. In this integration, IE was developed to determine possible crop combinations, the optimum starting and ending dates of growth cycle for each crop type and grid cell, to ensure the best possible crop yields for both rain-fed and irrigated conditions. In 2000, a case of global crop productivity estimation was tested with GIS-based EPIC. National averages are computed to be comparable to yields in FAO statistics. The comparison indicated that the GIS-based EPIC was able to simulate crop productivity at global level. In addition, with the global climate change data provided by the IPCC from the first version of the Canadian Global Coupled Model (CGCM1), GIS-based EPIC was run for scenarios of future climate in the year of 2010, 2020, 2030, 2040, and 2050 to predict the effects of global warming on main crop yields (Tan and Shibasaki 2003). Results showed the global warming will be harmful for most of the countries, and an efficient adaptation to alternative climates tends to reduce damages (Tan and Shibasaki 2003). There are many pathways through which climate related factors may impact food safety, including: changes in temperature and precipitation patterns, increased frequency and intensity of extreme weather events, ocean warming and acidification, and changes in the transport pathways of complex contaminants (Tirado et al. 2010).

16.2 Crop Models

To translate climate scenarios into possible agricultural outputs, approaches of statistical modeling and process-based crop modeling are applied, and they aim at estimating crop productivity as a response to climate (Schlenker and Lobell 2010). Empirical crop models are statistical relationships derived from observations, linking crop yields in a given location to local climate variables. Although such relationships are relatively easy to compute, calibrating and validating a robust statistical model requires a long series of data. One advantage is that such relationships can be established directly at a large scale using spatially aggregated climate variables to predict average yields over large areas. In this review, Lobell et al. (2008) and Schlenker and Lobell (2010) indicated that it provides a straightforward assessment of future climate impacts at a scale directly relevant to informing policymakers and stakeholders.

The other approach is process-based crop modeling. These models represent the physiological processes of crop growth and development as a response to climate (Roudier et al. 2011), thus simulating the seasonal crop cycle and its different parts. Because this approach allows the capture of detailed, intraseasonal, and non-linear effects of climate on crops, most climate impact studies use a mechanistic crop model (Roudier et al. 2011). Although many crop models have been developed, not all models have the same physiological approach, nor go into the same level of detail (Roudier et. al. 2011). In particular, the positive effect of higher atmospheric CO_2 concentrations on crop photosynthesis is not taken into account in all crop models (Salack 2006; Tubiello et al. 2007b). In addition, these models usually require numerous parameters and are thus applied at the plot scale where these data are available and can be considered homogeneous. The Ricardian analysis (Mendelsohn et al. 1994) is also used for estimating the impact of climate change on agriculture in West Africa (Kurukulasuriya and Mendelsohn 2007; Molua 2009). This approach focuses on the net income of farming systems instead of focusing on crop yields, and thus, no adaptation strategies are taken.

16.2.1 EPCI Model

The EPIC model uses a daily time step to simulate weather, hydrology, soil erosion, nutrient cycling, tillage, crop management and growth, as well as field-scale costs and returns (Tan and Shibasaki 2003). It uses a general plant growth model with crop specific parameters to simulate the growth of rice, wheat, maize, grain, sorghum, and soybean. In this model, interception of solar radiation is estimated as a function of the crop's leaf area index. The leaf area index is simulated with equations dependent upon heat units, the maximum leaf area index for the crop, a crop parameter that initiates leaf area index decline, and five stress factors (Tan and Shibasaki 2003). Plant growth is constrained by water, nutrient, and temperature stresses. The potential biomass is adjusted daily using the product of the minimum stress factor. The water stress factor is computed by considering supply and demand. The temperature stress factor is computed using a function dependent upon the daily average temperature, the optimal temperature, and the base temperature for the crop. The N and P stress factors are based on the ratio of accumulated plant N and P to the optimal values. The aeration stress factor is estimated as a function of soil water relative to porosity in the root zone (Williams et al. 1990; Tan and Shibasaki 2003).

Perennial crops maintain root systems through frost-induced dormancy and start regrowth when the average daily air temperature exceeds the base temperature specified for the plant. The crop yield is estimated using the harvest index concept. Harvest index increases as a nonlinear function of heat units from zero at the planting stage to the optimal value at maturity. The harvest index may be reduced by high temperature, low solar radiation, or water stress during critical crop stages. Two kinds of standard data sets are developed as EPIC input files. One is basic input file, which includes miscellaneous field information such as climatic data, soil data, and management information. The other consists of parameter files such as crop parameter file, tillage parameter file, pesticide parameter file, and fertilizer parameter file. These parameters for most of the major crops do not need to be modified if there is no specific knowledge or specific application.

16.2.2 ORYZA2000

The ORYZA2000 model simulates growth and development of lowland rice in situations of potential production, water limitation, and N limitation. To simulate all of these production situations, several modules are combined in ORYZA2000: modules for aboveground crop growth, evapotranspiration, N dynamics, and soil-water balance. To ease the linkage between these modules, they are all programmed in the FORTRAN Simulation Environment (FSE) developed by ban Kraalingen (1995). The FSE system was designed to dynamically simulate agroecological growth processes, which require daily weather data. The next sections provide a brief explanation of the FSE system, followed by a summary description of the scientific simulation modules that are included in ORYZA2000, an explanation of a special system to handle weather data in FSE, and a summary of the important utility functions and subroutines used (Matthews and Wassmann 2003).

16.2.3 ORYZA1

The ORYZA1 model (Kropff et al. 1994) was developed to simulate the potential production of rice, and was derived largely from the MACROS module L1D, but also contained elements from the SUCROS model (Spitters et al. 1989), the INTERCOM model (Kropff and Laar 1993), and the GUMCAS cassava model (Matthews and Hunt 1994). It was reasoned that such a model, containing detailed processes at the leaf level, was appropriate, as much of the knowledge of CO_2 and temperature effects on growth processes is available at this level of organization.

16.2.4 SIMRIW

SIMRIW (Simulation Model for Rice/weather Relations) (Horie 1987) was a model based on the underlying physiological processes involved in the growth of the rice crop. It required fewer crop parameters than ORYZA1, all of which could be obtained easily from well defined field experiments. Although SIMRIW predicted only the potential yield that can be expected from a given cultivar under a given climate, actual farmers' yield at a given location or district could also be obtained by multiplying the potential yield by a technological coefficient that characterized the current level of rice cultivation technology at the location. The model had been shown to satisfactorily explain site-to-site variability of rice yields in the USA and Japan based on the respective climates (Horie 1987), and could also explain the yearly variations in yield at various districts in Japan based on the weather (Horie et al. 1992). In combination with the Meash Weather Information System, SIMRIW was being used for growth and yield forecasting of regional rice in some of the prefectures in Japan (Horie et al. 1992).

16.2.5 CERES-Rice

CERES-Rice is a process-based, management-oriented model simulating the growth and development of rice, and has been relatively well tested in a range of environments (Ritchie et al. 1998; Bachelet et al. 1993b). It also has routines describing the main crop components involved in CH_4 dynamics along with routines describing the relevant crop management options such as water management and applications of organic and inorganic fertilizers (Horie 1993).

16.3 Application of Crop Models

16.3.1 Rice Production Simulation

Climate change can affect rice yields due to direct effects of temperature and CO_2 on crop growth and yield (Aggarwal and Mall 2002). The influence of changes in climate on rice production is of particular interest, not only because of its importance as a food source throughout the world, but also because recent intensification of rice production, particularly in the Asian region, itself contributes to global warming through the release of methane (CH_4) into the atmosphere (Matthews and Wassmann 2003). Penning de Vries et al. (1990) used the MACROS crop simulation model (Penning de Vries et al. 1989) and weather data from four contrasting sites (Netherlands, Israel, Philippines, and India) to simulate average grain yield, and its variability. The results indicated that a doubling of the CO_2 level would increase yield by 10–15%, and this would be offset by the effect of the expected accompanying rise in temperatures. These effects were the results of increased photosynthesis at higher CO_2 levels, and a reduced length of the growing season and increased maintenance respiration rates at higher temperatures. They also predicted that yield variability would be higher in cooler climates. The modeling results from Jansen (1990) using MACROS modeling indicated that the crop yields would rise if temperature increases were small, but would decline if temperatures increased more than 0.8^{o}C per decade, with the greatest decline in crop yields occurring between latitude 10 and 35 digrees. Penning de Vries (1993) used MACROS modeling to evaluate the effect of temperature, CO_2, and solar radiation on rice yields in Asia. He found that increased CO_2 levels increased crop yield. However, there was a negative linear relation between temperature and crop yield due to its effect on photosynthesis, respiration, and crop duration, and thus, two factors more-or-less cancelled each other out.

The first attempt to link rice crop models with scenarios predicted by General Circulation Models (GCMs) was by an international team of collaborators, who used the IBSNAT crop models to simulate likely changes in production of different crops under various GCM scenarios (Rosenzweig et al. 1993). They predicted that crop yields were likely to decline in the low-latitude regions, but could increase in the mid- and high-latitudes. At low-latitudes, crops were currently grown nearer their limits of temperature tolerance, so that any warming subjected them to higher stress, whereas in many mid- and high latitude areas, increased warming benefited crops currently limited by cold temperatures and short growing seasons.

The IRRI/EPA project used crop simulation models ORYZA1, SIMRIW, and CERES-Rice to investigate the influence of changes in CO_2 and temperature on rice production at the regional level (Matthews and Wassmann 2003). In this study, the ORYZA1 and SIMRIW models were used to predict changes in regional rice production for different scenarios, respectively. The corresponding changes predicted by two models were different. Although the ranking of the different scenarios were the same for the two crop models, the range of changes from -12.8 to +6.5% makes it clear that any predictions of changes in rice production for the region depend very much on the combination of climate change scenario and the crop model used. The average across both crop models and all three GCM scenarios suggested a -3.4% decline in overall regional rice production (Matthews and Wassmann 2003).

Possible adaptations that may occur are the adjustments of planting dates to take advantage of longer growing seasons in northern climates or to avoid high temperature stress in hotter countries, and the use of varieties more tolerant to higher temperatures in the low-latitude regions. Although potential yields were lower than that under the current climate due to the effect of increased temperatures on spikelet sterility, the wider sowing window allowed the possibility of two rice crops per year. This analysis was extended to estimate the potential effect on China's national rice production brought about by a move from single- to double-cropping (Matthews et al. 1995). Penning de Vries (1993) reasoned that future varieties would likely be selected for tolerance of spikelet fertility to high temperatures. The use of temperature tolerant genotypes could more than offset the detrimental effect of increased temperatures under a changed climate (Defeng and Shaokai 1995).

Masutomi et al. (2009) assessed the impact of climate change on rice production in Asia in comprehensive consideration of the process/parameter uncertainty in GCMs. The results indicated that in the 2020s, the probability of a production decrease value was high for the Special Report on Emissions Scenarios (SRES) because the negative impacts of climate change were larger than the positive effects of CO_2 fertilization in almost all climate scenarios in the near future. This suggests that it will be necessary to take immediate adaptive actions, regardless of the emission scenario, in the near future. In the 2080s, there are large differences in the average change in production (A_{CP}), the standard deviation of the change in production (SD_{CP}), and the probability of a production decrease (P_{PD}) among the SRES scenarios (Masutomi et al. 2009). The scenario with the highest atmospheric CO_2 concentration, A2, showed a notable decrease in production and a high P_{PD} in the 2080s compared with the other scenarios, despite having the largest CO_2 fertilization effect. In addition, A2 had the largest SD_{CP} among the SRES scenarios. On the other hand, the scenario with the lowest atmospheric CO_2 concentration, B1, showed a small decrease in production, and a much smaller SD_{CP} and a much lower P_{PD}, than in the case of A2. These results for the 2080s suggest that a reduction in CO_2 emissions in the long term has great potential not only to mitigate decreases in rice production, but also to reduce the uncertainty in these changes.

Zhang et al. (2010) used the data at 20 experiment stations, in counties and in provinces of China for the period from 1981 to 2005 to assess the responses of rice yields to climate change in China. Their empirical results indicate that rice yields were positively correlated to solar radiation, which primarily drove yield variation. At most stations, yields were positively correlated to temperature and there was no significant negative correlation between them. Their empirical results argue against the often-cited hypothesis of lower yields with higher temperature. They explain this by the positive correlation between temperature and radiation at their stations.

Empirical analysis to yield at a regional scale (20 counties and 22 provinces) indicates a varying climate to yield relationships. In some places, their results showed that yields were positively regressed with temperature when they were also positively regressed with radiation, showing the similar pattern at above experiment stations. But, in others, lower yield with higher temperature was accompanied by positive correlation between yield and rainfall, which did not happen at stations. This could be due to the irrigation water availability, which played a crucial role in determining climatic effects on yield variability at a regional scale in China (Zhang et al. 2010).

16.3.2 Wheat, Potatoes, Maize, and Barley Production Simulation

The IPCC summed up the literature on climate change and agriculture in North Asia, including the Asian part of Russia, by asserting that higher CO_2 levels and longer frost-free periods will increase agricultural productivity (Lal et al. 2001; Alcamo et al. 2007). Sirotenko et al. (1997) used the ‘‘weather-yield’’ model to estimate that changed climatic conditions in agricultural regions would decrease mean grain production in Russia by 15% and fodder production by 3% by the year 2030. They also computed that higher levels of CO_2 in the atmosphere by the 2030s would increase grain and fodder production by 15% and 13%, respectively, and thereby compensate for yield decreases (Sirotenko et al. 1997).

Using a variety of crop models and climate scenarios, researchers have concluded that climate change would increase average agricultural production over most of the territory of Russia because of increasing CO_2 and/or more favorable temperature and precipitation conditions for crop growth. Based on an evaluation of average changes in climate, assessments of climate impacts on water resources have shown an increase rather than a decrease in water availability over most of Russia (Alcamo et al. 2000a, b; Vorosmarty et al. 2000).

Alcamo et al. (2007) used the GAEZ submodel of GLASS to assess the climate change impacts on food production in Russia. The results have shown that an increase in temperature and precipitation will lead to increased production of potatoes and grains in the current marginal agricultural areas of the regions of Far East, Kaliningradskaya, East Siberia, and West Siberia. Results from their study showed that the warmer and drier climate in the South will threaten the potential production of important crops such as wheat, potatoes, maize, and barley. They computed that average potential production of grain in the densely populated and highly productive economic regions would drop by 7–29% in the 2020s and 23–41% in the 2070s. A decrease as large as 40% in the 2020s and 65% in the 2070s is possible for individual administrative regions. Under current climate conditions, food production shortfalls typically occur in the main crop growing regions in about 1–3 years out of every decade, depending on the region. In the 2020s, some regions may have a decreased frequency of shortfalls due to longer and warmer growing seasons. The majority of the main crop growing regions experience more frequent shortfalls in the 2020s because of combined warmer temperatures and declining precipitation. By the 2070s, almost all of the main crop growing regions show large increases in the frequency of shortfalls. Some of these regions will have three times the frequency of shortfalls in the 2070s as compared to current climate conditions (Alcamo et al. 2007). However, the gains largely balance out the losses in Russia. Depending on the scenario, they computed either a 9% loss or a 12% gain in total potential grain production by the 2020s. By the 2070s, only losses are estimated, ranging from 5–12% for net country-wide grain production (Alcamo et al. 2007).

16.3.3 Sugarcane Production Modeling

The GCM model (a sugarcane crop growth model) and a GIS have been combined to assess the spatial and temporal impacts of climate change on cane yield and irrigation needs (Knox et al. 2001). Using selected IPCC SRES scenarios for the 2050s (Nakicenovic et al. 2000), future climate data sets were derived for a reference site using outputs from the HadCM3 model. The net annual irrigation water requirements and crop productivity for the baseline and selected IPCC scenario were then simulated using the CANEGRO model embedded within the DSSAT (Decision Support System for Agrotechnology Transfer) program (Jones et al. 2003). Results from their study have shown with climate change, relatively minor increases in productivity are estimated, principally due to increased radiation levels and higher temperatures (1–6% and 10–29% above the baseline, respectively). This is consistent with Batchelor (1992) who observed trends of increasing growth with increasing temperature. When the CO_2 concentration for the baseline (330 ppmv) was increased to 600 ppmv for the 2050s, there was a noticeable increase in biomass and sucrose yield. This is consistent with IPCC (1996) who reported that a doubling of CO_2 concentration from present levels would increase biomass by 10–30%. The enrichment of CO_2 of the atmosphere increases the rate of photosynthesis, and thus yields, and is expected to reduce water use. In this study, the crop modeling suggests that sucrose yield under the SRES 2050-A2 scenario, with CO_2-fertilisation would be 15% higher than the baseline yield.

16.3.4 Maize Production Modeling

Walker and Schulze (2008) used the CERES-Maize (Jones and Kiniry 1986) model and nine plausible future climate scenarios over a 44-year period to estimate maize yields and soil organic nitrogen loss. A sensitivity analysis of plausible scenarios was performed with incremental increases in temperature by 1, 2 or 3°C, increases/decreases of rainfall by 10% and a doubling of pre-industrial atmospheric CO_2 concentrations to 555 ppmv. Their results show that climatic changes could have major negative effects on the already drier western, and therefore, more vulnerable, areas of the South African Highveld. The Highveld region in South Africa is an important area for its food production for the nation, as 70% of the country's cereal crops and 90% of the commercially grown maize is cultivated there. An increase in temperature increases the variability of yields in the relatively moist Piet Retief area (mean annual precipitation 903 mm), while at the more sub-humid Bothaville, with a mean annual precipitation of only 552 mm, the inter-annual variability remains the same but the mean yield over 44 seasons is reduced by 30% (Walker and Schulze

2008). A simulated increase in temperature coupled with a doubling of CO_2 increases the rate of soil organic nitrogen depletion from the agro-ecosystem (Walker and Schulze 2008).

Abraha and Savage (2006) used CropSyst, a cropping systems simulation model to assess the potential maize grain yield using generated weather data and generated weather data modified by plausible future climate changes. CropSyst is a multi-year and multi-crop simulation model developed to evaluate the effect of cropping systems management on productivity and environment (Stöckle and Nelson 2000; Stöckle et al. 2003). The CropSyst model has been used to simulate the growth and development of several crops such as maize, wheat, barley, soybean, and sorghum in many countries with generally good results (Stöckle 1996). CropSyst has also been used to investigate potential impacts of climate change on crop production (Tubiello et al. 2000; Donatelliv et al. 2003). Maize grain yields simulated using the observed and generated weather data series with different planting dates were compared. The simulated grain yields for the respective planting dates were not statistically different from each other. However, the grain yields simulated using the generated weather data had a significantly smaller variance than the grain yields simulated using the observed weather data series. The generated baseline weather data were modified by synthesized climate projections to create a number of climatic scenarios. The climate changes corresponded to a doubling of CO_2 concentration to 700 ppm without air temperature and water regime changes, and a doubling of CO_2 concentration accompanied by mean daily air temperature and precipitation increases of 2°C and 10%, 2°C and 20%, 4°C and 10%, and 4°C and 20%, respectively. The increase in the daily mean minimum air temperature was taken as three times the increase in daily mean maximum air temperature (Donatelliv et al. 2003). Input crop parameters of radiation use and biomass transpiration efficiencies were modified for maize in the CropSyst model, to account for physiological changes due to increased CO_2 concentration. Under increased CO_2 concentration regimes, maize grain yields are much more affected by changes in mean air temperature than by precipitation. The results indicate that the analysis of the implications of variations in the planting date on maize production may be most useful for site-specific analyses of possible mitigation of the impacts of climate change through alteration of crop management practices (Donatelliv et al. 2003).

Jones and Thornton (2003) used the model CERES-Maize (Ritchie et al. 1998) to simulate the growth, development and yield of the maize crop production in Africa and Latin America to the year 2055. CERES-maize runs with a daily time step and requires daily weather data. It calculates crop and morphological development using temperature, day length, and genetic characteristics. Water and N balance submodels provide feedback that influences the developmental and growth processes (Ritchie et al. 1998). The results indicate an overall reduction of only 10% in maize production to 2055. A 10% decrease in maize yield to 2055 is certainly serious, but it can reasonably be expected that this level of decrease will be compensated by plant breeding and technological interventions in the intervening period, given the history of cereal yield increases since 1950 (Pardey and Beintema 2001).

16.3.5 Soybean Production Modeling

Soybean [*Glycine max* (L.) *Merrill*] ranks first among the oilseeds in the world and has now found a prominent place in India. It has significant growth in area and production in India in the past decade (Paroda 1999). This increasing trend of fast adaptation of the crop by the farmers in India indicates that soybean is going to be the future leading commercial venture in the country. Future climatic change is likely to have a substantial impact on soybean production depending upon the magnitude of variation in CO_2 and the temperature. Increased temperature significantly reduces the grain yield due to accelerated development and decreased time to accumulate grain weight (Seddigh and Joliff 1984a, b; Baker et al. 1989). There have been a few studies in India and elsewhere aimed at understanding the nature and magnitude of gains/losses in yields of soybean crops at different sites under elevated atmospheric CO_2 conditions and associated climate change (Adams et al. 1990; Sinclair and Rawlins 1993; Haskett et al. 1997; Lal et al. 1999).

The CROPGRO-soybean model is provided by Boote et al. (1996). The model uses empirical functions to compute daily canopy gross photosynthesis in response to CO_2 concentration, air temperature, and daily canopy evapotranspiration. Canopy photosynthesis is computed at hourly time steps using leaf-level photosynthesis parameters and hedgerow light interception calculations (Boote and Pickering 1994). Photosynthesis and evapotranspiration algorithms also take into account the changes in daily canopy photosynthesis under elevated CO_2 concentration and temperature conditions (Curry et al. 1990a, b). The model simulates the potential, water, and nutrient limited yields of soybean.

Mall et al. (2004) used CROPGRO model to simulate the impact of climate change on soybean production in India. The projected scenarios for the Indian subcontinent as inferred from three state-of-the-art GCMs have been used in the present study. There was a decrease (ranging between about 10 and 20%) in soybean yield when the effect of the rise in surface air temperature at the time of the doubling of CO_2 concentration was considered. The results obtained on the mitigatory option for reducing the negative impacts of temperature increases indicate that delaying the sowing dates would be favorable for increased soybean yields at all the locations in India. Sowing in the second season would also be able to mitigate the detrimental effects of future increases in surface temperature due to global warming at some locations.

Mera et al. (2006) studied the effect of radiation (R), precipitation (P), and temperature (T) on plant response such as crop yields. The CROPGRO (soybean) and CERES-Maize (maize) models response to individual changes in R and P (25%, 50%, 75%, 150%) and T (±1, ±2°C) with respect to control were studied. For the model setting and the prescribed environmental changes, results from the experiments indicate: (i) precipitation changes were most sensitive and directly affected yield and water loss due to evapotranspiration; (ii) radiation changes had a non-linear effect and were not as prominent as precipitation changes; (iii) temperature had a limited impact and the response was non-linear; and (iv) soybeans and maize responded differently for R, P, and T, with maize being more sensitive (Mera et al. 2006).

16.4 Discussion

Carbon dioxide is one of the main components for plants to conduct the photosynthetic process. The increase in CO_2 concentration should have a positive impact on the crop production. The increased CO_2 concentration would cause the global warming problem. The increase in annual average temperature has a negative impact on the crop production in lower latitude areas. However, an increase in crop production would be observed in mid and higher latitude areas. Thus, different crops have different responses to the global warming. The impact of climate change on agricultural production can be minimized by breeding of specific crop species. If it is assumed that more temperature tolerant varieties would be selected–a reasonable assumption given that genetic variation already exists for this–then regional production is predicted to increase due to the positive influence of increased CO_2 levels on crop growth. Rainfall is also a major determinant of recently observed trends in agricultural production in many regions. Rainfall change does have an impact, even if it is lower than that due to a temperature change. The effects of temperatures and rainfall changes can interplay. For instance, for crops, the combination of high temperatures and abundant rainfall fosters high rates of chemical weathering and leaches clay soils of low inherent fertility

Comparison among different climate change and agricultural impacts studies could be a difficult task. This is due to the fact that these studies used different countries (or regions), scales, crops, scenarios, assumptions, and climate models for the prediction of agricultural yield. Hence combining yield impact studies is a first step in the estimation of sign, magnitude, and uncertainty of climate change impacts, but is not sufficiently precise. The multi-ensembles approach, with varying climate models, emissions scenarios, crop models, and downscaling techniques would enable a move towards a more complete sampling of uncertainty in crop yield projections. Among those parameters, it may be particularly interesting to focus on the differences between crop models and between the downscaling methods.

16.5 References

Abraha, M. G., and Savage, M. J. (2006). "Potential impacts of climate change on the grain yield of maize for the midlands of KwaZulu-Natal, South Africa." *Agriculture, Ecosystems and Environment,* 115, 150–160.

Adams, R. M., Rosenzweig, C., Peart, R. N., Ritchie, J. T., McCarl, D. A., Glyer, J. D., Jones, J. W., Boote, K. J., and Allen, L. H. (1990). "Global climate change and U.S. Agriculture." *Nature*, 345, 219– 224.

Aggarwal, P. K., and Mall, R. K. (2002). "Climate change and rice yields in diverse agro-environments of India. II: Effect of uncertainties in scenarios and crop models on impact assessment." *Clim. Change*, 52, 331–343.

Alcamo, J., Dronin, N., Endejan, M., Golubev, G., and Kirilenk, A. (2007). "A new assessment of climate change impacts on food production shortfalls and water availability in Russia." *Global Environmental Change*, 17, 429–444.

Alcamo, J., Endejan, M., Kaspar, F., and Rosch, T. (2000a). "The GLASS model: a strategy for quantifying global environmental security." *Environmental Science and Policy*, 4 (1), 1–12.

Alcamo, J., Henrichs, T., and Rosch, T. (2000b). *World water in 2025–global modeling scenarios for the World Commission on Water for the 21st century. World Water Series 2*, Center for Environmental Systems Research. University of Kassel, Germany.

Bachelet, D., van Sickle, J., and Gay, C. A. (1993). "The impacts of climate change on rice yield: evaluation of the efficacy of different modelling approaches." In: Penning de Vries, F. W. T., Teng, P. S., and Metselaar, K. (Eds.), *Systems Approaches for Agricultural Development*. *Kluwer Academic Publishers*, Dordrecht, The Netherlands, 145–174.

Baker, J. T., Allen Jr., L. H., Boote, K. J., Jones, P. H., and Jones, J. W. (1989). "Response of soybean to air temperature and carbon dioxide concentration." *Crop. Sci.* 29, 98–105.

Bannayan, M., Kobayashi, K., Kim, H. Y., Lieffering, M., Okada, M., and Miura, S. (2005). "Modeling the interactive effects of atmospheric CO_2 and N on rice growth and yield." *Field Crops Res.*, 93, 237–251.

Batchelor, C. H., 1992. *Water Use and Growth of Drip-irrigated Sugarcan*e. Unpublished Ph.D. Dissertation, University of Reading, UK.

Ben Mohamed, A., Vanduivenbooden, N., and Abdousallam, S. (2002). "Impact of climate change on agricultural production in the Sahe–Part1. Methodological approach and case study for millet in Niger." *Clim. Change,* 54, 327–348.

Boote, K. J., Jones, J. W., Hoogenboom, G., and Pickering, N. B. (1996). "CROPGRO model for grain legumes." In Tsuji, G.Y., Hoogenboom, G., and Thornton, P.K. (Eds.), *International Benchmark Sites Network for Agrotechnology Transfer*. *A system Approach to Research and Decision Making*. Kluwer Academic Publishers, Dordrecht, The Netherlands.

Boote, K. J., and Pickering, N. B. (1994). "Modeling photosynthesis of row canopies." *Hort. Sci.* 29, 1423–1434.

Bouwman, A. F. (1991). "Agronomic aspects of wetland rice cultivation and associated methane emissions." *Biogeochemistry*, 15, 65–88.

Burton I., and Lim, B. (2005). "Achieving adequate adaptation in agriculture." *Clim. Change,* 70, 191–200.

Challinor, A., Wheeler, T., Garforth, C., Craufurd, P., and Kassam, A. (2007). "Assessing the vulnerability of food crop systems in Africa to climate change." *Clim. Change,* 83, 381–399.

Curry, R. B., Peart, R. M., Jones, J. W., Boote, K. J., and Allen, L. H. (1990a). "Simulation as a tool for analyzing crop response to climate change." *Trans. ASAE*, 33, 981–990.

Curry, R. B., Peart, R. M., Jones, J. W., Boote, K. J., and Allen, L. H. (1990b). "Response of crop yield to predicted change in climate and atmospheric CO_2

using simulation." *Trans. ASAE,* 33, 1383– 1390.
Defeng, Z., and Shaokai, M. (1995). "Rice production in China under current and future climates." In: Matthews, R.B., Kropff, M.J., Bachelet, D., and van Laar, H.H. (Eds.), *Modelling the Impact of Climate Change on Rice Production in Asia*. IRRI/CAB International, Wallingford, UK, pp. 217–235.
Donatelli, M., Tubiello, F. N., Peruch, U., and Rosenzweig, C. (2003). "Impacts of climate change and elevated CO_2 on sugar beet production in northern and central Italy." *Ital. J. Agron.,* 6, 133–142.
Haskett, J. D., Pachepsky, Y. A., and Acock, B. (1997). "Increase of CO_2 and climate change effects on IOWA soybean yield simulated using GLYCIM." *Agron. J.,* 89, 167–176.
Horie, T. (1987). "A model for evaluating climatic productivity and water balance of irrigated rice and its application to Southeast Asia." *Southeast Asian Studies*, 25, 62–74.
Horie, T. (1993). "Predicting the effects of climate variation and effect of CO_2 on rice yield in Japan." *J. Agric. Meteorol.* (Tokyo), 48, 567–574
Horie, T., Yajima, M., and Nakagawa, H. (1992). "Yield forecasting." *Agric. Syst.,* 40, 211–236.
Hossain, M. (1998). "Sustaining food security in Asia: economic, social and political aspects." In: Dowling, N.G., Greenfield, S.M., and Fischer, K.S. (Eds.), *Sustainability of Rice in the Global Food System*. Pacific Basin Study Centre and the International Rice Research Institute, Davis, California and Manila, pp. 404.
IPCC (1996). *Climate change 1995. Impacts, adaptations and mitigation of climate change: scientific-technical analyses*. In: Watson, R.T., Zinyowera, M.C., Moss, R.H., and Dokken, D.J. (Eds.), *Contribution of Working Group II to the Second Assessment Report of the Intergovernmental Panel on Climate Change*. Cambridge University Press, Cambridge, UK. 878 pp.
IPCC (2001). *Intergovernmental Panel on Climate Change Working Group 2. Climate Change 2001: Impacts, Adaptation and Vulnerability*. IPCC Working Group 2.
Jansen, D. M. (1990). "Potential rice yields in future weather conditions in different parts of Asia." *Netherlands J. Agric. Sci.,* 38, 661–680.
Jones, C. A., and Kiniry, J. R. (Eds.). (1986). *CERES-Maize: a Simulation Model of Maize Growth and Development.* Texas A&M University Press, College Station, TX, USA.
Jones, J. W., Hoogenboom, G., Portera, C. H., Boote, K. J., Batchelor, W. D., Hunt, L. A., Wilkens, P. W., Singh, U., Gijsman, A. J., and Ritchie, J. T. (2003). "The DSSAT cropping system model." *European Journal of Agronomy*, 18, 235–265.
Jones, P. G., and Thornton, P. K. (2003). "The potential impacts of climate change on maize production in Africa and Latin America in 2055." *Global Environmental Change*, 13, 51–59.
Knox, J. W., Rodriguez Diaz, J. A., Nixon, D. J., and Mkhwanazi, M. (2010). "A preliminary assessment of climate change impacts on sugarcane in Swaziland." *Agricultural Systems*, 103, 63–72.

Kropff, M. J., and Laar, H. H. V. (Eds.), (1993). “Modeling Crop Weed Interactions.” CAB-International, Wallingford, UK, and International Rice Research Institute, Manila, Philippines, 274 pp.

Kropff, M. J., Laar, H. H. V., and Matthews, R. B. (1994). “ORYZA1: an ecophysiological model for irrigated rice production.” *SARP Research Proceedings*, IRRI/AB-DLO, 110 pp.

Lal, M., Harasawa, H., and Murdiyarso, D. (2001). “Asia.” In: Intergovernmental Panel on Climate Change, Climate Change 2001. (Ed.), *Impacts, Adaptation, Vulnerability*, Cambridge University Press, Cambridge, p. 533–590.

Lal, M., Singh, K. K., Srinivasan, G., Rathore, L. S., Naidu, D., and Tripathi, C. N. (1999). “Growth and yield response of soybean in Madhya Pradesh, India to climate variability and change.” *Agric. Forest Meteorol.,* 93, 53–70.

Li, C. S. (2000). “Modeling trace gas emissions from agricultural ecosystems.” *Nutrient Cycling in Agroecosystems,* 58, 259–276.

Mall, R. K., Lal, M., Bhatia, V. S., Rathore, L. S., and Singh, R. (2004). “Mitigating climate change impact on soybean productivity in India: a simulation study.” *Agricultural and Forest Meteorology*, 121, 113–125.

Matthews, R. B., and Hunt, L. A. (1994). “GUMCAS: a model describing the growth of cassava (Manihot esculenta L. Crantz).” *Field Crops Res*., 36, 69–84.

Masutomi, Y., Takahashi, K., Harasawa, H., and Matsuoka, Y. (2009). "Impact assessment of climate change on rice production in Asia in comprehensive consideration of process/parameter uncertainty in general circulation models.” *Agriculture, Ecosystems and Environment*, 131, 281–291.

Matthews, R., and Wassmann, R. (2003). “Modelling the impacts of climate change and methane emission reductions on rice production: a review.” *Europ. J. Agronomy*, 19, 573–598.

Matthews, R. B., Kropff, M. J., Horie, T., and Bachelet, D. (1995). “Simulating the impact of climate change on rice production in Asia and evaluating options for adaptation.” *Agric. Syst.,* 54, 399–425.

Mera, R. J., Niyogi, D., Buol, G. S., Wilkerson, G. G., and Semazzi, F. H. M. (2006). “Potential individual versus simultaneous climate change effects on soybean (C3) and maize (C4) crops: An agrotechnology model based study.” *Global and Planetary Change*, 54, 163–182.

Nakicenovic, N., Alcamo, J., Davis, G., de Vries, B., Fenhann, J., Gaffin, S., Gregory, K., Grubler, A., Jung, T. Y., Kram, T., La Rovere, E. L., Michaelis, L., Mori, S., Morita, T., Pepper, W., Pitcher, H., Price, L., Raihi, K., Roehrl, A., Rogner, H., Sankovski, A., Schlesinger, M., Shukla, P., Smith, S., Swart, R., van Rooijen, S., Victor, N., and Dadi, Z. (2000). *IPCC Special Report on Emissions Scenarios.* Cambridge University Press, Netherlands. p. 175–189.

Pardey, P. G., and Beintema, N. M. (2001). *Slow magic: agricultural R&D a century after Mendel*. Food Policy Report, International Food Policy Research Institute, Washington, DC.

Parton, W. J. (1996). “The CENTURY model.” In Powlson, D.D., Smith, P., and Smith, J. U. (eds.) *Evaluation of Soil Organic Matter Models*. Springer-Verlag, Berlin, 283–291.

Parry, M. L., Rosenzweig, C., Iglesias, A., Livermore, M., and Fischer, G. (2004).

"Effects of climate change on global food production under SRES emissions and socio-economic scenarios." *Global Environ. Change,* 14, 53–67.

Penning de Vries, F. W. T., (1993). "Rice production and climate change." In: Penning de Vries, F.W.T., Teng, P., and Metselaar, K. (Eds.), *Systems Approaches for Agricultural Development*. Kluwer Academic Publishers, Dordrecht, The Netherlands,

Penning de Vries, F. W. T., Jansen, D. M., ten Berge, H. F. M., and Bakema, A. (1989). *Simulation of ecophysiological processes of growth in several annual crops*. Simulation Monographs, Pudoc/International Rice Research Institute, Wageningen, Netherlands, p. 271.

Penning de Vries, F. W. T., van Keulen, H., van Diepen, C. A., Noy, I. G. A. M., and Goudriaan, J. (1990). "Simulated yields of wheat and rice in current weather and in future weather when ambient CO_2 has doubled." Climate and Food Security, International Rice Research Institute, Los Ban˜ os, Philippines, p. 347–358.

Ritchie, J. T. (1998). "Soil water balance and plant water stress." In: Tsuji, G. Y., Hoogenboom, G., and Thornton, P. K. (Eds.), *Understanding Options for Agricultural Production*. *Kluwer Academic Publishers*, Dordrecht, The Netherlands, pp. 41–54.

Ritchie, J. T., Singh, U., Godwin, D. C., and Bowen, W. T. (1998). "Cereal growth, development and yield." In: Tsuji, G. Y., Hoogenboom, G., and Thornton, P. K. (Eds.), *Understanding Options for Agricultural Production. Systems Approaches for Sustainable Agricultural Development*. Kluwer Academic Publishers, Dordrecht, Netherlands, pp. 79–98.

Rosenzweig, C., and Hillel, D. (1998). *Climate Change and the Global Harvest. Oxford University Press*, New York. 324 pp.

Rosenzweig, C., Parry, M. L., Fischer, G., and Frohberg, K. (1993). *Climate Change and World Food Supply*. 3, Environmental Change Unit, University of Oxford.

Roudier, P., Sultan, B., Quirion, P., and Berg, A. (2011). "The impact of future climate change on West African crop yields: What does the recent literature say?." *Global Environ. Change,* 21, 1073–1083.

Salack, S. (2006). "Impacts des changements climatiques sur la production du mil et du sorgho dans les sites pilotes du plateau central, de Tahoua et de Fakara." *CILSS*. Niamey, Niger.

Saptomo, S. K., Setiawan, B. I., and Yuge, K. (2009). "Climate change effects on paddy field thermal environment and evapotranspiration." *Paddy Water Environ.,* 7, 341–347.

Schlenker, W., and Lobell, D. B. (2010). "Robust negative impacts of climate change on African agriculture." *Environ. Res. Lett.,* 5, 1–8.

Seddigh, M., and Joliff, G. D. (1984a). "Effects of night temperature on dry matter partitioning and seed growth of indeterminate field grown soybean." *Crop Sci.,* 24, 704–710.

Seddigh, M., and Joliff, G. D. (1984b). "Night temp. effects on morphology, phenology, yield, and yield components of indeterminate field grown soybean." *Agron. J.,* 76, 824–828.

Sinclair, T. R., and Rawlins, S. L. (1993). “Interseasonal variation in soybean and maize yields under global environmental change.” *Agron. J.,* 85, 406–409.

Sirotenko, O., Abashina, E., and Pavlova, V. (1997). “Sensitivity of the Russian agriculture to changing climate, CO_2, and tropospheric ozone concentrations and soil fertility.” *Climatic Change*, 36, 217–232.

Spitters, C. J. T., Keulen, H. van, and Kraalingen, D. W. G. (1989). “A simple and universal crop growth simulator: SUCROS87.” In: *Simulation and systems management in crop protection*. Rabbinge, R., Ward, S. A., and van Laar, H. H., (eds.). Pudoc, Wageningen, 1989. 147–181.

Stöckle, C. O. (1996). “GIS and simulation technologies for assessing cropping systems management in dry environments.” *Am. J. Alternative Agric.,* 11, 115–120.

Stöckle, C. O., Donatelli, M., and Nelson, R. (2003). “CropSyst, a cropping systems simulation model.” *Eur. J. Agron.,* 18, 289–307.

Stöckle, C. O., and Nelson, R. (2000). *Cropping Systems Simulation Model User’s Manual*. Biological Systems Engineering, Washington State University, Pullman, WA.

Tan, G., and Shibasaki, R. (2003). “Global estimation of crop productivity and the impacts of global warming by GIS and EPIC integration.” *Ecological Modelling*, 168, 257–370.

Tirado, M. C., Clarke, R., Jaykus, L. A., McQuatters-Gollop, A., and Frank, J. M. (2010). “Climate Change and Food Safety: A review.” *Food Research International*, 43, 1745–1765.

Tubiello, F. N., Donatelli, M., Rosenzweig, C., and Stöckle, C. O. (2000). “Effects of climate change and elevated CO_2 on cropping systems: model predictions at two Italian locations.” *Eur. J. Agron.,* 13, 179–189.

Vanduivenbooden, N., Abdousallam, S., and Ben Mohamed, A. (2002). “Impact of climate change on agricultural production in the Sahel–Part 2. Case study for groundnut and cowpea in Niger. ” *Clim. Change,* 54, 349–368.

Vorosmarty, C. J., Green, P., Salisbury, J., and Lammers, R. B. (2000). “Global water resources: vulnerability from climate change and population growth.” *Science*, 289, 284–288.

Walker, N. J., and Schulze, R. E. (2008). “Climate change impacts on agro-ecosystem sustainability across three climate regions in the maize belt of South Africa.” *Agriculture, Ecosystems and Environment*, 124, 114–124.

Williams, J. R., Dyke, P. T., Fuchs, W. W., Benson, V. W., Rice, O. W., and Taylor, E. D. (1990). “EPIC-erosion/productivity impact calculator.” *United State Department of Agriculture,* Technical Bulletin Number 1768.

Yasuhara, K., Komine, H., Yokoki, H., Suzuki, T., Mimura, N., Tamura, M., Chen, G. (2011). “Effects of climate change on coastal disasters: new methodologies and recent results.” *Sustain Sci.*, 6, 219–232.

Zhang, T., Zhua, J., and Wassmann, R. (2010). “Responses of rice yields to recent climate change in China: An empirical assessment based on long-term observations at different spatial scales (1981–2005).” *Agricultural and Forest Meteorology*, 150, 1128–1137.

CHAPTER 17

Diagnosis of Climate and Weather

Koji Nishiyama

17.1 Introduction

For the last decade, there are increasing concerns regarding global warming and associated future climate as well as recent climate change and weather situations that have caused serious damages (e.g., extremely high or low temperature, serious flood, draught with water stress) to human life and ecosystems. Therefore, it is important to diagnose 'past and future' climate changes and weather situations. However, too many meteorological information composing climate and weather situations makes it difficult to extract and interpret significant signals related to serious disasters.

So far, for the extraction of the significant signals, the analysis of the Empirical Orthogonal Function (EOF), which is basically the same as the Principle Component Analysis (PCA) based on linear orthogonal transform among many meteorological variables, has been the most widely used and developed as a conventional method for pattern recognition. For the last decade, unlike the EOF linear analysis, non-linear pattern recognition technique called a self-organizing map (SOM), which is a kind of unsupervised artificial neural networks (ANNs) technique, has also been applied to meteorological studies. The technique is one of useful information tools for classifying visually interpreting high-dimensional complicated climate and weather data.

In such a context, the main topic of this chapter is how to apply the SOM analysis to the diagnosis of climate and weather. The first part of this chapter explains the SOM methodology for identifying high-dimensional complicated weather situations to easily-recognizable patterns, by showing an example of synoptic weather causing heavy rainfall in the Kyushu Islands of Japan, and relates these weather patterns to independent local variable (heavy rainfall frequency) in a specific target area. The second part of this chapter introduces fundamental studies on future climate change caused by global warming, motivated by the Intergovernmental Panel on Climate Change (IPCC), and explains how to apply SOM to the analysis of such future climate change studies.

17.2 Methods for Signal Extraction

EOF and SOM. In the field of climate meteorology, in order to extract globally significant signals related to disasters such as drought, flood, and extremely high temperature, from high-dimensional meteorological variables (e.g., spatial and temporal distribution such as geo-potential height, sea surface temperature, surface pressure), the analysis of the EOF (Preisendorfer 1988) has been the most widely used and developed as a conventional method for pattern recognition. The analysis is basically equivalent to the Principle Component Analysis (PCA), which mathematically determines a new coordinate system consisting of principle components by conducting an orthogonal linear transformation of a set of correlated variables into uncorrelated variables so that variance among variables can be the greatest. Therefore, the EOF analysis has contributed largely to the extraction of a set of globally dominant climate and teleconnection modes with large variance, affecting the past and anticipated climate change. For example, the Pacific Decadal Oscillation (PDO) index (Mantua et al. 1997; Zhang et al. 1997) and Arctic Oscillation (AO) index (Thompson and Wallace 1998) are derived as the leading principal components of monthly SST and 1000 hPa height anomalies north of 20N, respectively. However, there is a shortcoming that the assumption of linearity and orthogonality imposed by EOF, making it difficult to interpret physical meanings of patterns obtained from principal components. There is no guarantee that the EOF patterns have physical meanings, as pointed by Dommenget and Latif (2002). Moreover, even if principal components obtained are mathematically independent from each other, there is no guarantee they are physically independent actually.

On the other hand, unlike the EOF based on the linear constraint, non-linear pattern recognition technique called a SOM, which is a kind of unsupervised artificial neural networks (ANNs) technique in the field of information science, was developed by Kohonen (1995). The SOM provides useful information for helping the interpretation of non-linear complicated features by classifying a set of high-dimensional data into the units (patterns) arranged regularly on a two-dimensional space that can be *easily* and *visually* recognized by '*human eye*' although there is a shortcoming that the number of patterns must be arbitrarily determined in advance. The results obtained by the SOM training show that, in each unit, similar input samples are classified after the SOM training, and the similarities and dissimilarity between the units can be visually recognized by the Euclidean distance between them on the two-dimensional space, as explained in Section 117.3. Moreover, the analysis of the SOM has no cumbersome process equivalent to careful consideration on physical meanings of principal components obtained by the EOF. Owing to such a powerful ability, in the last decade, the SOM has been widely used in many research fields (e.g., various engineering areas, physics, biology, ecological science, medical science, economic science) that require pattern recognition. For example, Nikkilä et al. (2002) applied the SOM to the analysis and visualization of gene expression, and Park et al. (2003) applied it to the recognition of aquatic insect species richness in running water. Since the development of the SOM, it has also been applied to the field of climate and synoptic meteorology, as shown in the next section.

Application of SOM to Meteorology. The SOM methodology available for the analysis of synoptic meteorology is introduced by Hewitson and Crane (2002). The first step of the analyses is to conduct the pattern recognition of high-dimensional synoptic situations (e.g., spatial distribution of geo-potential height, wind, temperature, moisture). The next step is to construct visualized relationships on the two-dimensional SOM space between formed patterns and independent local variables (e.g., extreme high and low temperature, strong wind, heavy rainfall frequency) observed in a specific target area. The final step is to investigate the frequency of synoptic patterns, the frequency of the independent local variable(s) per each synoptic pattern, temporal variability in the frequency per each synoptic pattern, and so on. For example, Hope et al. (2006) investigated temporal variability of synoptic situations and the decrease in precipitation accompanying the decrease in the frequency of troughs in southwest Western Australia. Cavazos (1999) conducted the classification of winter large-scale atmospheric circulation and humidity fields related to extreme rainfall events in northeastern Mexico and southeastern Texas. Nishiyama et al. (2007) extracted synoptic situations related to the occurrence of heavy rainfall in western Japan. Cassano et al. (2006a) extracted synoptic patterns in the western Arctic associated with extreme events at Barrow, Alaska, USA. Crimins (2006) conducted the analysis on synoptic situations related to extreme fire-weather in the southwest United States.

On the other hand, in the analysis of climate, the features of decadal climate change and associated teleconnection patterns were investigated by visualizing spatial climate patterns using the SOM methodology. For example, Johnson et al. (2008) provided the continuum properties of the Northern Hemisphere teleconnection patterns related to climate shift characterized by the North Atlantic Oscillation (NAO). Leloup et al. (2007) demonstrated that the SOM methodology provides the potential ability to classify the ENSO phase and to enhance the understanding of seasonal and decadal variability of ENSO.

The SOM was also applied for evaluating the ability of climate models to reproduce past significant climate modes through inter-comparison among climate models by visualizing the performance of each model. Leloup et al. (2008) assessed the ability of 23 climate models (IPCC-AR4/CMIP3) to reproduce spatial SST variability related to ENSO in the twentieth century. Tennant (2003) assessed the ability of three atmospheric general circulation models (AGCMs) to reproduce daily circulation patterns by comparing these model results with each other. Such analyses are useful for identifying adequate and poor performance of each model.

17.3 Principle of SOM

As shown in Figure. 17.1, the basic structure of SOM consists of two-dimensional arrangement (hereafter named, map) of the units. It takes a hexagonal form, having the same distance between neighboring units. Each unit has a reference vector $m_i(t)$, which is updated through the training process of the SOM. After training, the updated reference vector represents common features among the input data classified into each unit. The reference vector m_i (t) has the same dimension as the input vector x (t). Prior to the SOM training, the reference vector elements are initialized on a random basis, and the input vector elements are normalized to values between 0 and 1 using the maximum and minimum in each element.

The first step is to calculate the Euclidean distance between an input vector $\boldsymbol{x}(t)$ and all the reference vectors $\boldsymbol{m}_i(t)$ and, subsequently, to find the 'winner' unit c with the reference vector closest to the input vector, as shown by Eq. 17.1 and the top panel of Figure 17.1. The 'winner' unit c is called the best matching unit (BMU).

$$c = arg\ \min_i \{\|\boldsymbol{x}(t) - \boldsymbol{m}_i(t)\|\} \qquad \text{(Eq. 17.1)}$$

The next step is to update all the reference vectors against the presentation of the input vector according to Eqs.17.2 and 17.3.

$$\boldsymbol{m}_i(t+1) = \boldsymbol{m}_i(t) + h_{ci}\left(t, \|\boldsymbol{r}_c - \boldsymbol{r}_i\|\right)\left[\boldsymbol{x}(t) - \boldsymbol{m}_i(t)\right] \qquad \text{(Eq. 17.2)}$$

$$h_{ci}\left(t, \|\boldsymbol{r}_c - \boldsymbol{r}_i\|\right) = \alpha(t) \cdot \exp\left(-\frac{\|\boldsymbol{r}_c - \boldsymbol{r}_i\|^2}{2\sigma^2(t)}\right) \qquad \text{(Eq. 17.3)}$$

The modification of the reference vectors is represented by the second term on the right hand in Eq. 17.2 and depends on the neighborhood function $h_{ci}(t, \| \boldsymbol{r}_c - \boldsymbol{r}_i \|)$. This neighborhood function takes a Gaussian form, decreasing with the distance from the BMU, as shown by Eq. 17.3. Therefore, the reference vectors in units closer to the BMU are more strongly modified. Moreover, the neighborhood function decreases with the iteration step t. The rate is governed by a monotonic decrease with the iteration step t according to the decreasing of both the learning-rate $\alpha(t)$ and the width of the neighborhood function $\sigma(t)$ with the iteration step. Consequently, the modification of the reference vectors decreases with the iteration step. To keep the stability of the SOM training, the series of computation procedures from Eqs. 17.1–17.3 needs to be repeated as many times as possible, as shown by Kohonen (1995).

As a result of the SOM training, similar input samples are classified into an identical unit on the map. In other words, each unit on the map can be interpreted as the assembly of similar input samples with a reference vector, which shows representative features among these input samples. Moreover, the neighboring units in the map are similar to each other while distant units are dissimilar on the map, as shown in the bottom panel of Figure 17.1. Therefore, the SOM provides visually recognizable information for interpreting non-linear complicated features.

17.4 Classification of Synoptic Field Patterns Using SOM

The objective of this section is to a) visualize high-dimensionally complicated synoptic fields using the SOM algorithm, and b) extract synoptic field patterns related

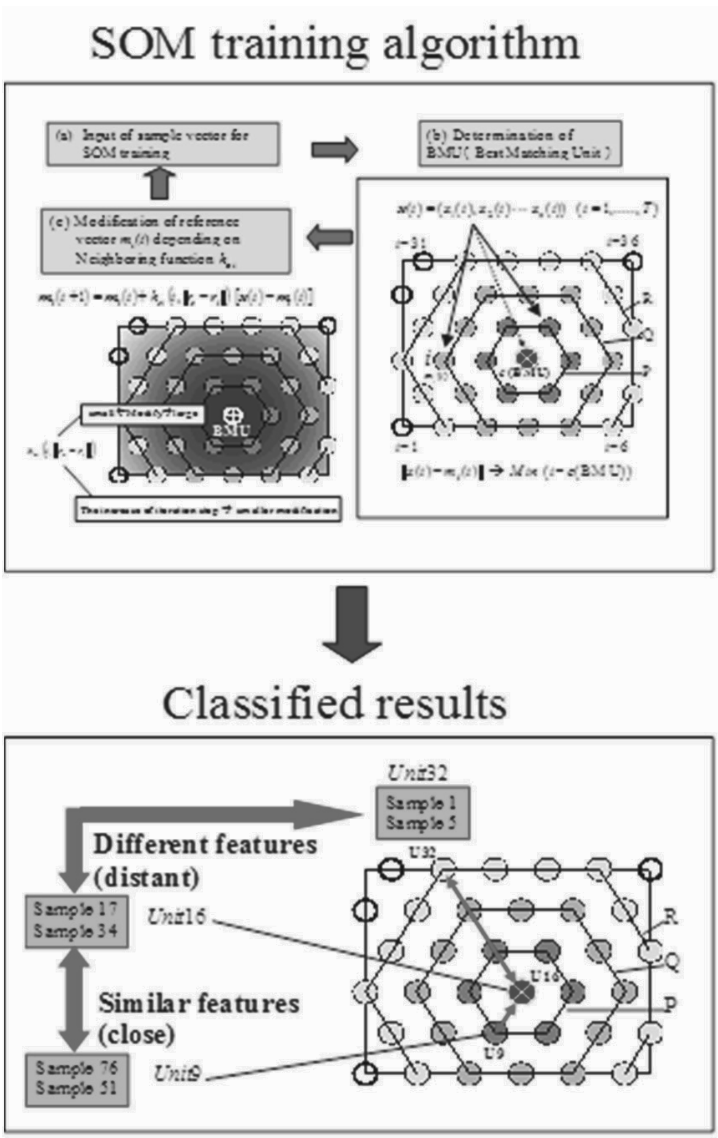

Figure 17.1. Flowchart of the SOM training (top) and the interpretation of classified pattern results on the SOM map (bottom)

to heavy rainfall in western Japan, showing an example of the application of the SOM to meteorology (climate science and weather science). The example of the application is based on Nishiyama et al. (2007), which conducted pattern classification analysis of synoptic fields related to heavy rainfall events during a very short period (3 years) within narrow extent by applying the SOM. However, this section shows the result of the extended version of Nishiyama et al. (2007). The version shows that the target period is extended from 3 years to 30 years for enhancing the performance of the SOM training in a larger target area. Here, a 'synoptic' field corresponds to a scale of few thousands kilometers that can resolve high and low-pressure systems, warm and cold fronts, and typhoon. Simply speaking, the synoptic field is equivalent to a scale of weather chart used for daily weather prediction.

17.4.1 Heavy Rainfall during a Warm Season in Japan

During a warm season in Japan, especially, in June and July, heavy rainfall frequently occurs along a stationary front maintained by the dynamical balance between the Pacific high-pressure system and the northern high-pressure system. The stationary front is basically characterized by a steep gradient of water vapor in lower layers in Japan, as shown by Akiyama (1973). Along the stationary front, the supply of a large amount of warm and humid air enhances atmospheric instability over the Japan islands, causing the repetition of the generation and subsequent dissipation of strong atmospheric instability, as pointed out by Ninomiya (2000). Therefore, many heavy rainfall events have caused flooding and associated serious damages to human life and properties all around Japan, especially in western Japan.

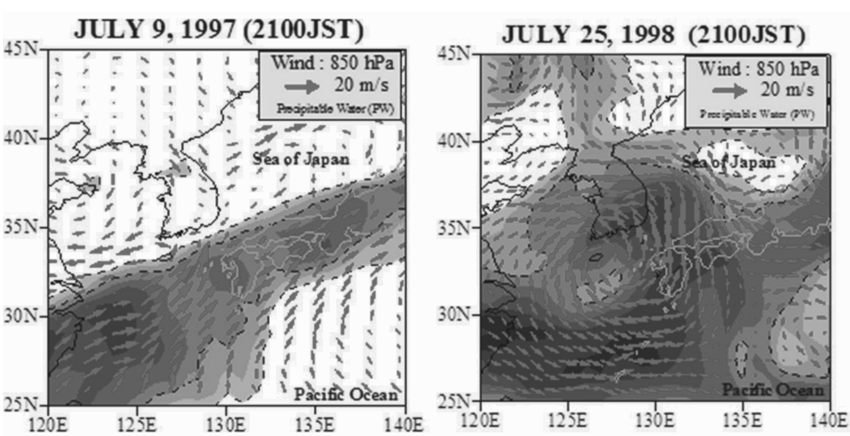

Figure 17.2. Examples of the synoptic fields causing heavy rainfall in Japan. The field is represented by the wind fields at the 850 hPa level and the spatial distribution of PW (Precipitable Water: unit in mm). The PW is depicted per 5 mm from the lower limit of 40 mm

Figure 17.2 shows examples of typical synoptic fields causing heavy rainfall in Japan. The synoptic fields are represented by wind components at the 850 hPa level and precipitable water (PW), which is defined as the total amount (mm in unit) of vertically-accumulated water vapor in the atmosphere. The left panel shows the dominant band-like structure (called as '*moist tongue*': technical term of meteorology) of high PW distributed from the southwest to the northeast (or the west to the east). Moreover, the moist tongue accompanies Low-Level Jet (LLJ), which represents strong northeastward (or eastward) wind in lower layers. The formation of the high PW means that a large amount of water vapor supplied into the high PW area is transported upward by strong convective activity. Therefore, the appearance of the band-like high PW area can be interpreted as the result of the occurrence of strong convective activity causing heavy rainfall. On the other hand, the right panel shows a typhoon that passed through the west of Kyushu. The cyclonic flow originating from the east side of typhoon transported a large amount of water vapor into Kyushu. Therefore, the enhancement of atmospheric instability caused convective activity and associated heavy rainfall. Including the above-mentioned examples, there are many kinds of synoptic field patterns causing heavy rainfall. In this chapter, according to the SOM methodology of the next subsection, too many synoptic fields are classified into recognizable field patterns.

17.4.2 Methodology

This study investigates significant relationships between synoptic field patterns and heavy rainfall features for 30 years (1979–2008) by applying the SOM. The synoptic fields are represented by the spatial distribution of wind components at the 850 hPa level and Precipitable Water (PW) using NCAR-NCEP reanalysis data (4 times per a day). A data sample characterizing the pattern consists of 48 dimensions (16 grid points, 3 variables), as shown in Figure 17.3(a). On the other hand, for detecting heavy rainfall features, this study uses rainfall data recorded in Kyushu located in the west of Japan, as shown in Figure 17.3(b). The rainfall observation system is called as the Automated Meteorological Data Acquisition System (AMeDAS), which has been maintained by the Japan Meteorological Agency (JMA). The observational items of AMeDAS consist of rainfall, temperature, wind, and sun duration, although all items are not observed in each location. However, rainfall only is observed as indispensable item at all the locations. Its resolution is very fine and equivalent to about 17 km, covering all areas in Japan. These data are recorded per 10 minutes and 1 hour.

The outline for the SOM training is shown in Table 17.1. The training uses input samples (*total_num* = 14648) obtained from the outputs (NCAR-NCEP reanalysis data) of 4 times (T = 0, 6, 12, 18 UTC) per day in the warm season (June to September) for 30 years. Here, it should be noted that rainfall data such as heavy rainfall frequency are not used for the SOM training. In other words, rainfall data is treated as a variable independent of synoptic field patterns classified by the SOM. As a result of SOM training, the input samples are classified into the 30 (x-axis) ×30 (y-axis) hexagonal units, in other words, 900 synoptic field patterns. Each unit includes a reference vector and the most similar input samples to it. The reference vector obtained by the SOM training shows a representative feature among the input samples classified in the unit. In addition, all the patterns formed by the SOM training are arbitrarily divided into 25 groups (36 units per group) so that significant features among patterns can be easily understood, as shown in Figure 17.4.

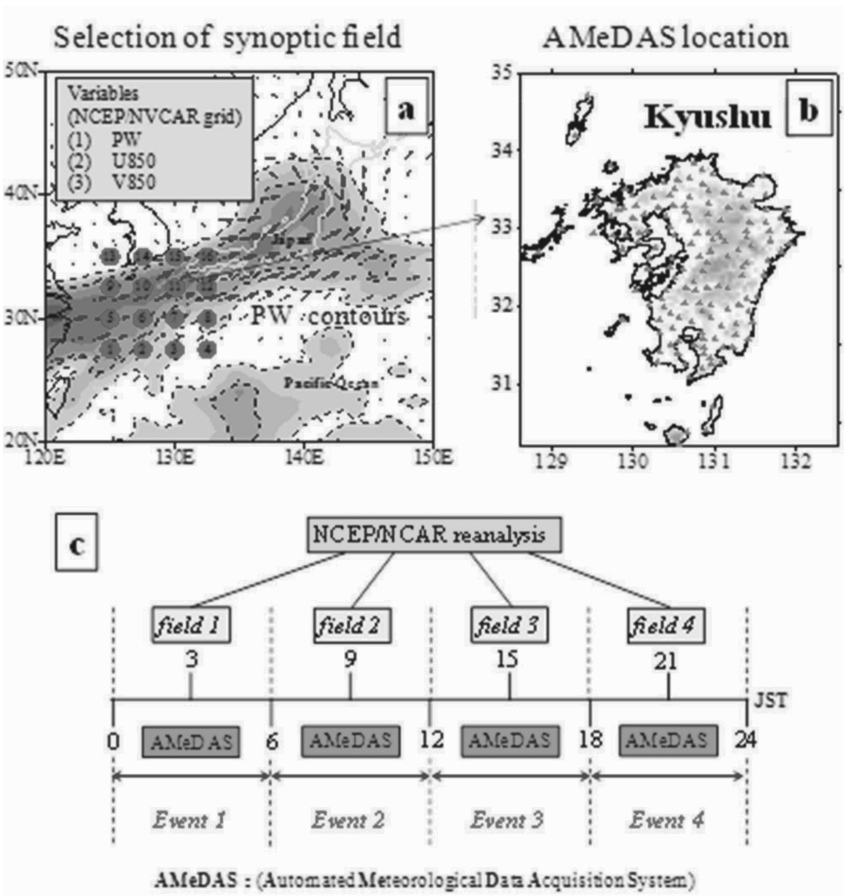

Figure 17.3. (a) NCEP/NCAR Grid space (16 grids) specified for constructing synoptic field patterns using the variables (PW, U850, V850). (b) Target area specified for obtaining AMeDAS rainfall data. (c) Extraction of AMeDAS rainfall data within 6 hours interval centering at 0, 6, 12, 18 UTC to each synoptic field

Here, a set of 14648 samples is used repeatedly for the SOM training. Hereafter, the training of a set of 14648 samples is called '*epoch*'. In this study, both the learning-rate $\alpha(t_e)$ and the width $\sigma(t_e)$ of the neighborhood function are constant during a given epoch (t_e) according to the formula given by Eq. 17.4. The operation is conducted for keeping the performance of the SOM training during an epoch.

Table 17.1. Setting for the SOM training and outcomes after training

DATA	**NCEP /NCAR reanalysis data** **Resolution : grid spacing (LAT, LON) of 2.5 deg, 4 times per a day**
The number of input data samples	**14648 (1979-2008) : Warm season : 4 month (JJAS)**
Variables for input vector	**Precipitable Water (PW), (U, V at 850 hPa)**
Input vector	**48 dimensions** x=(PW$_1$~PW$_{16}$, U$_1$~U$_{16}$, V$_1$~V$_{16}$) 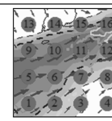
Map size	**30 (x-axis) × 30 (y-axis)** **=900 units, (in other words, 900 patterns)**
Outcomes classified in each unit after SOM training	**(1)Reference vector m$_i$** **(2)Input data closest to the features (m$_i$) of the unit**
Format of reference vector in each unit *i*	m$_i$=(PWm$_1$~PWm$_{16}$, Um$_1$~Um$_{16}$, Vm$_1$~Vm$_{16}$) **Each elements are formed by repetitive SOM training**

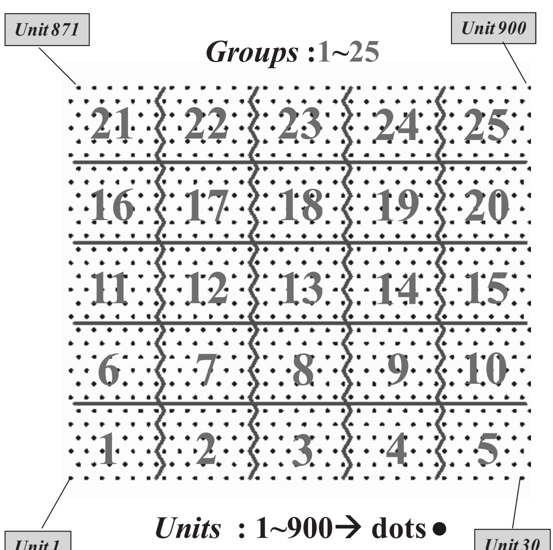

Figure 17.4. The structure of the SOM defined in this study. The SOM consists of 900 units (patterns). In addition, all the units are divided into 25 groups

$$\alpha(t_e) = max\left\{\alpha(0)\frac{T_e - t_e + 1}{T_e},\quad 0.005\right\}$$
$$\sigma(t_e) = max\left\{\sigma(0)\frac{T_e - t_e + 1}{T_e},\quad 1.1\right\} \tag{Eq. 17.4}$$

where, T_e, the total epoch number, is set to 20 (repetition of 20 epochs). t_e is iterative step of epoch. $\alpha(0)$, a value between 0 and 1, is set to 0.2. About half of a map size is widely used as a value of $\sigma(0)$. The value is set to 15 because the map size is given as 30 × 30 in this study.

In this study, to investigate relationships between synoptic field and heavy rainfall, assuming that a synoptic field at T (= 0, 6, 12, 18 UTC) is dominant during 6 hours between T-3 and T+3, heavy rainfall frequency is calculated by summing up AMeDAS hourly rainfalls (≥ 30 mm/h) recorded during 6 hours in the target area (Kyushu), as shown in Figure 17.3(c).

17.4.3 Synoptic Field Patterns Causing Heavy Rainfall

This subsection performs the identification of synoptic field patterns or groups related to the occurrence of heavy rainfall based on the SOM training described in the previous subsection. Figure 17.5 shows the frequency of observed heavy rainfall at the AMeDAS stations (Kyushu) depicted in Figure 17.3(b) in each unit (pattern) on the SOM map. The frequency is defined as the total number of heavy rainfall ≥ 30 mm/h (Figure 17.5(a)) and 50 mm/h (Figure 17.5(b)) observed in all the events classified in each unit. Figure 17.6 shows a histogram of heavy rainfall frequency ≥ 30 mm/h in each group.

From these results, it is found that the dominant heavy rainfall activity is related to the groups (G1 and 3) situated in the lower left of the SOM map, and the groups (G16~19, 21~24) situated in the upper of the map. Therefore, these ten groups are recognized as '*heavy rainfall groups.*' Especially, G21, 22 and 24 among the heavy rainfall groups show the high frequency of heavy rainfall occurrence.

Figure 17.7 shows features of synoptic field patterns of the heavy rainfall groups. The patterns are obtained by averaging all the reference vectors included in each group. The common feature of these ten heavy rainfall groups shows the existence of high PW (≥ 40 mm) area. The differences among these groups can be recognized by wind direction and strength at 850 hPa, the location of high PW area, the existence of a front characterized by a steep gradient of PW, and cyclonic motion of small-scale (meso-scale) low-pressure system or typhoons. Focusing on G21, 22 and 24 showing the top three groups of heavy rainfall frequency, the common features are characterized by high PW distribution and strong wind, the Low Level Jet (LLJ) at 850hPa. G21 shows typical synoptic field pattern in a rainy season in Japan. G22 is similar to G21 in that Kyushu is affected by the dominant area of high PW, accompanying strong LLJ. However, G22 is characterized by eastward LLJ and a steep gradient of PW in the northern area of Kyushu. The steep PW gradient is related to frontal activity. G21 and 24 have common feature of high PW area in Kyushu with dominant northeastward LLJ. However, wind patterns of the synoptic field in G24 are characterized by cyclonic motion in the northwest edge of the target area. The feature implies the passage of the meso-scale low-pressure system formed frequently on a stationary front, or typhoons. Moreover, features of the groups except for the above

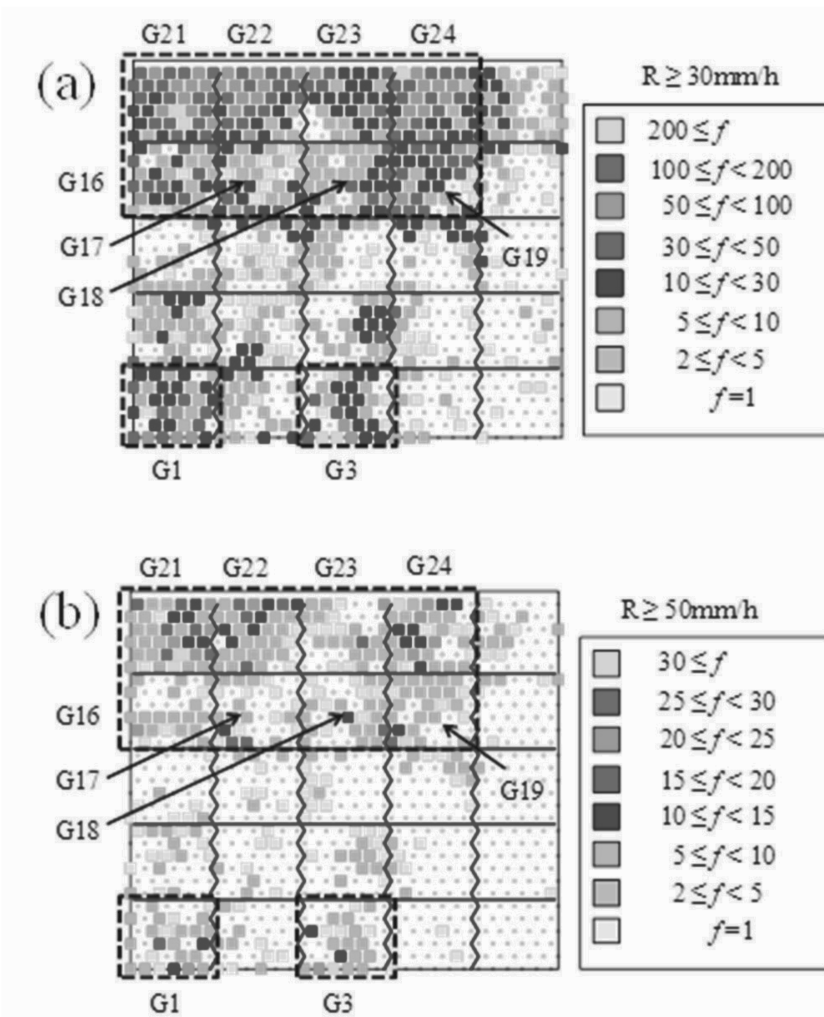

Figure 17.5. Heavy rainfall frequency per each unit (pattern). The top and bottom panels show frequency ≥ (a) 30mm/h and (b) 50mm/h, respectively. The groups enclosed by black frames are defined as *'heavy rainfall groups'* in this study

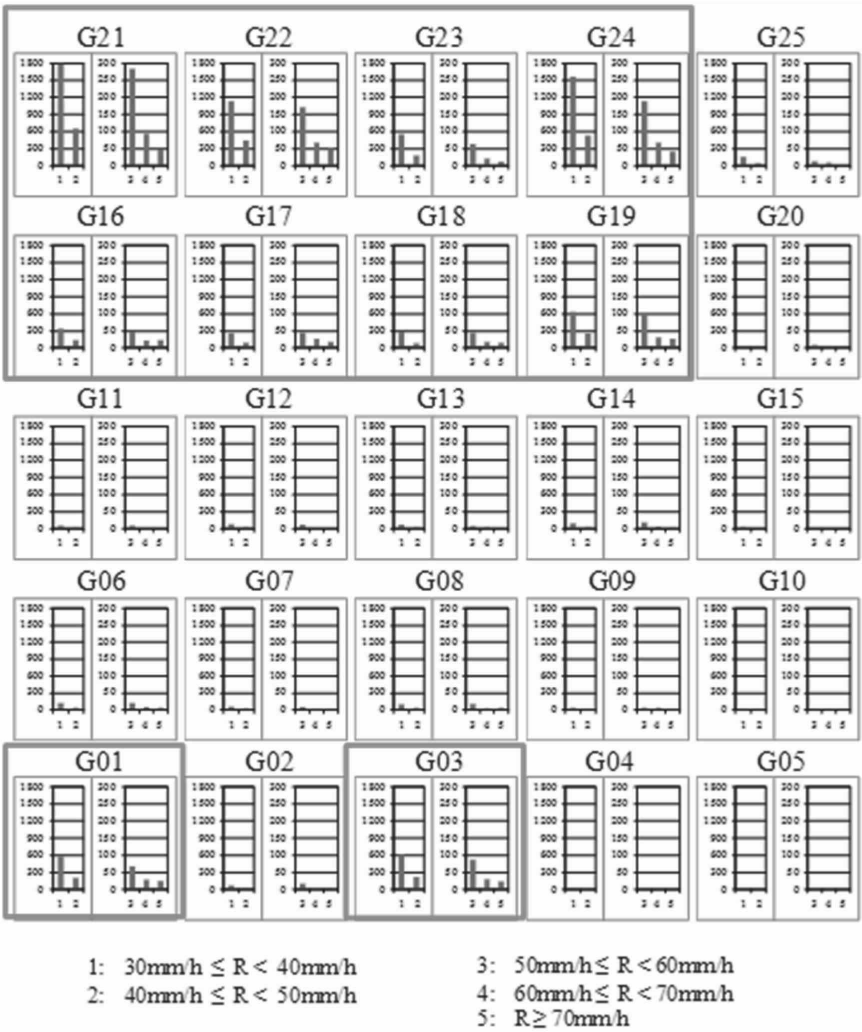

Figure 17.6. Heavy rainfall frequency ≥ 30mm/h in each group. The groups enclosed by green frames are *'heavy rainfall groups'*

top three heavy rainfall groups are shown here. The feature of G16 and 17 shows northward shift in the axis of high PW distributed from the southwest to northeast, accompanying the development of the Pacific high-pressure system. The feature of G19 is basically the same as those of G24, which is characterized by the combination of high PW and cyclonic motion. However, the axis of high PW distributed from the southwest to the northeast in G19 is located in the north of the axis of high PW of in

G24. G18 and 23 have no features excepting the existence of high PW area. On the other hand, heavy rainfall of G1 and 3 are related to cyclonic motion of typhoons. The feature of G1 shows that a typhoon moves northward around the East China Sea situated in the west of Kyushu. The feature of G3 shows the approach of a typhoon towards Kyushu from the south.

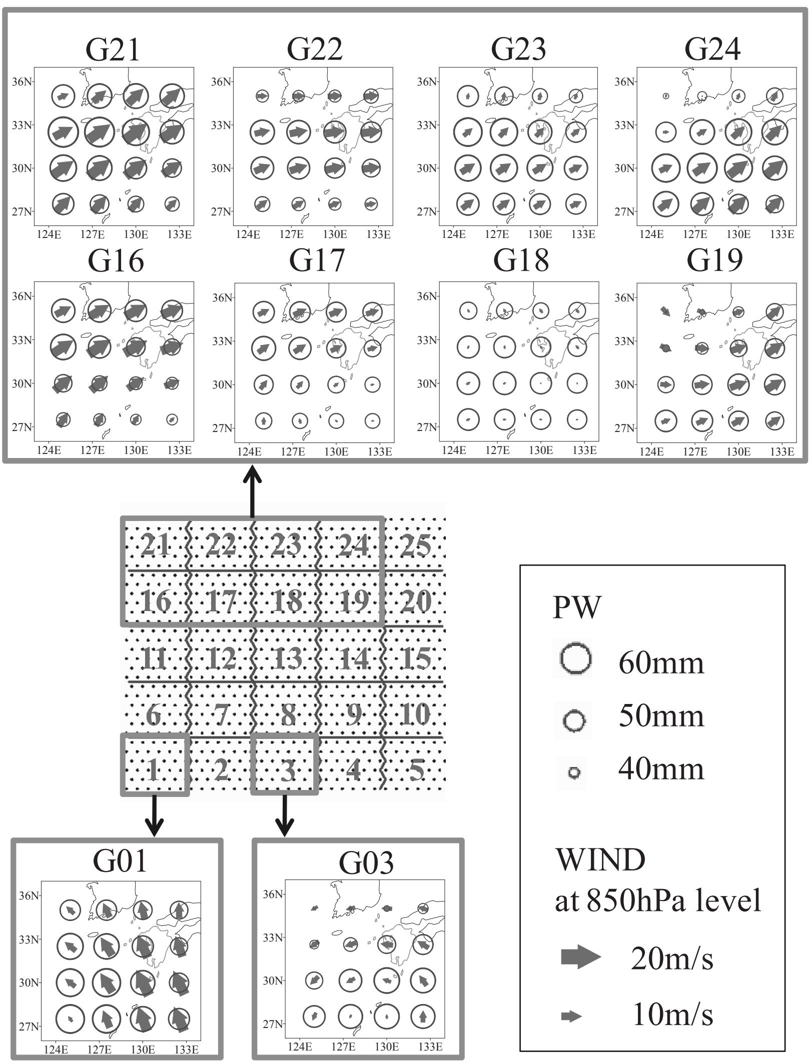

Figure 17.7. Average features of synoptic field patterns included in each group. The groups enclosed by green frames are *'heavy rainfall groups'*

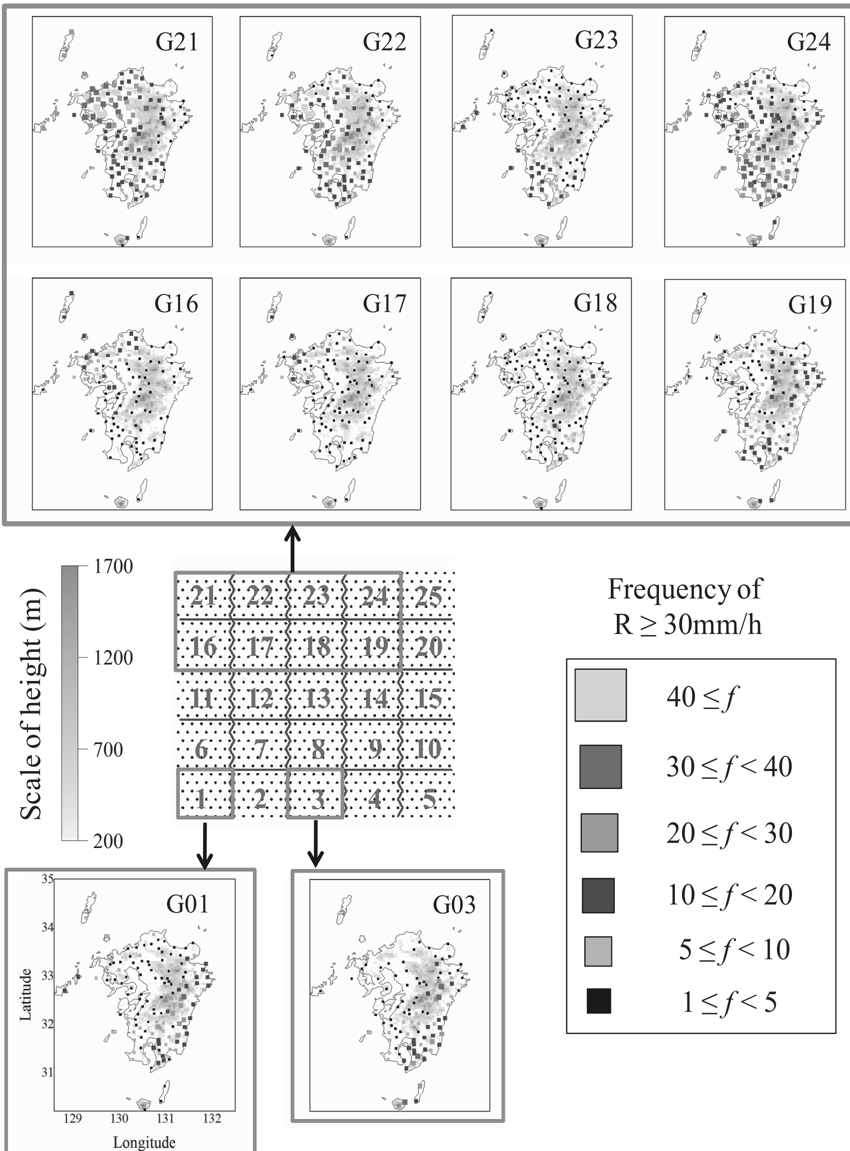

Figure 17.8. Spatial distributions of the frequency ≥ 30 mm/h in Kyushu in heavy rainfall groups enclosed by green frames

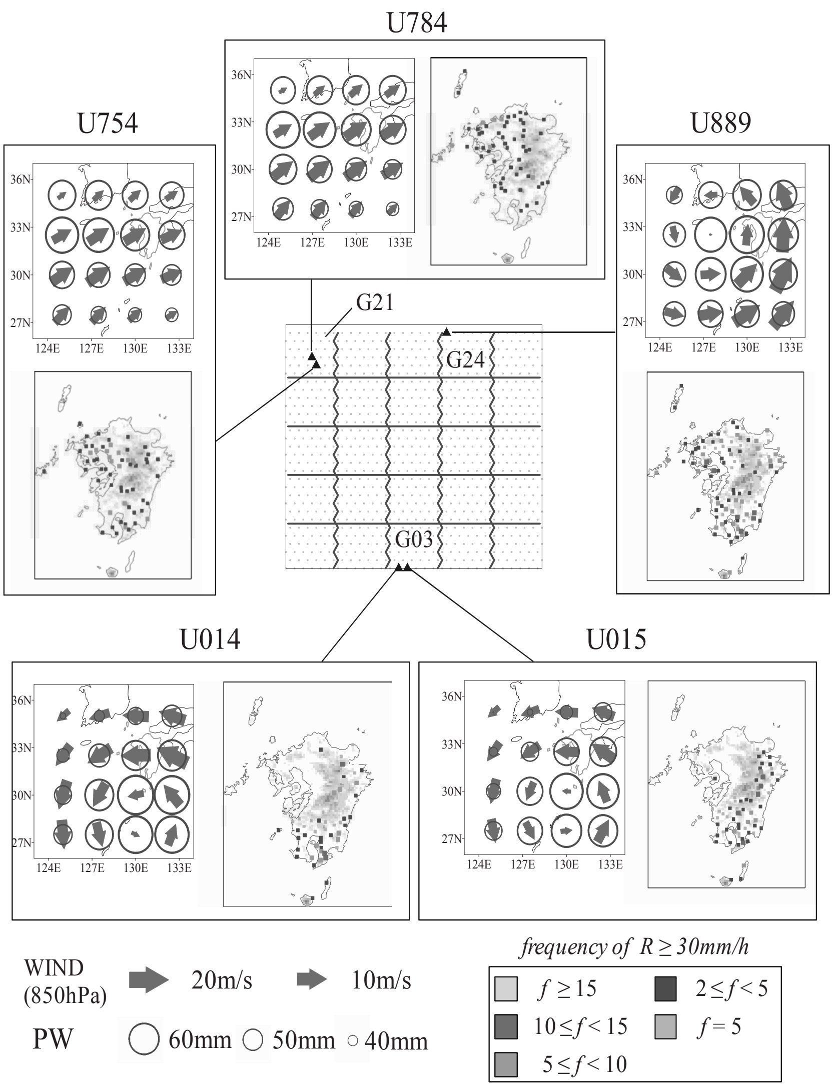

Figure 17.9. Synoptic field patterns and heavy rainfall distributions of the top five units showing remarkably large frequency ≥ 30 mm/h.

Table 17.2. Features of the top five units showing remarkably large heavy rainfall frequency

rank	*unit(pattern)*	*group*	*freq of R≥30mm/h*	*freq1*	*freq2*	*freq3*	*feature*
1	889	24	529	352	116	61	Typhoon
2	14	3	298	218	56	24	Typhoon
3	754	21	250	134	72	44	Moist tongue
4	15	3	223	129	58	36	Typhoon
5	784	21	209	138	51	20	Moist tongue

freq1: $30 \leq R(mm/h) < 40$ *freq2*: $40 \leq R(mm/h) < 50$ *freq3*: $R(mm/h) \geq 50$

In the next, features of spatial distribution of heavy rainfall in each group are shown in Figure 17.8. The synoptic fields characterized by the upper groups (G16~19, G21~24) on the map caused heavy rainfall all over Kyushu. Especially, G21 and G22 show high frequency of heavy rainfall in the western area of Kyushu. G24 shows high frequency in the southern and central area of Kyushu. The occurrence of heavy rainfall caused by these groups basically depends on 1) the axis location of the band-like high PW area, and 2) the wind direction of LLJ or cyclonic wind accompanying the passage of the low-pressure system or a typhoon. The axis of high PW in G21, 22, and 24 show the direction from the southwest to the northeast (or the west to the east) just above Kyushu. In these cases, heavy rainfall occurred all over western Kyushu. The axes of G16 and 17 are similar to G21 and G24 and, however, are located to the northwest of Kyushu. Therefore, the spatial distribution of heavy rainfall is defined to the northwest side of Kyushu. On the other hand, the synoptic fields characterized by the lower left groups (G1 and 3) lead to the formation of heavy rainfall distribution along the eastern side of the Kyushu mountain range. The reason can be basically explained by topographical effect and cyclonic wind enhanced by a typhoon. The central area of Kyushu is characterized by the mountain range of 1000–1800 m height. In these cases, warm and humid air is transported along the eastern slope of the Kyushu mountain range due to strong cyclonic wind (typhoon) from the southeast. Therefore, resultant deep convection leads to the release of atmospheric instability enhanced by the supply of warm and humid air, and the occurrence of heavy rainfall in the eastern slope of Kyushu.

Finally, features of the top five units (patterns) with high frequency of heavy rainfall are shown in Table 17.2. Figure 17.9 shows the location of these units on map and the spatial distribution of heavy rainfall in Kyushu against each unit related to heavy rainfall. Three units (U889, U014, and U015) are related to typhoon activity. On the other hand, the other two units (U754 and U784) are related to the appearance of moist tongue (high PW and strong LLJ). First, features of the former units (U889, U014, and U015) are explained. U889 shows the highest frequency (total number ≥ both 30 mm/h and 50 mm/h) among all the patterns. The typhoons moving northward above the East China Sea are located to the west side of Kyushu. In this case, the supply of warm and humid air into entire area of Kyushu is very dominant. Therefore, heavy rainfall is caused all over Kyushu. U014 and U015 show that a typhoon approaching towards Kyushu is located to the southern area of Kyushu. In this case, warm and humid air (wind direction: southeast) transported by the typhoon is supplied into the eastern slope of the Kyushu mountain range. Therefore, heavy rainfall is caused along the eastern area of Kyushu. On the other hand, these units (U754 and U784) show a typical synoptic field pattern during rainy season in Japan, characterized by high PW and strong LLJ. In these cases, high PW formed by convective activity corresponds to the occurrence of heavy rainfall in the high PW area.

From these results, the SOM application successfully visualized non-linear complicated synoptic field patterns on the two-dimensional map. Moreover, it provided significant information on frequency and spatial distribution of heavy rainfall occurrence. It was found that SOM has a potential ability to find some specific synoptic field patterns showing high frequency of heavy rainfall.

17.5 Diagnosis of Future Climate Change

Future climate change caused by anthropogenic global warming is a major concern in the present day. It is highly significant to evaluate how future climate change will affect the global environment and human life. The features can be obtained from numerically-simulated outputs by a Global Climate Model (GCM). This section introduces fundamental processes for diagnosing future climate change assuming future climate scenarios, and the application of the SOM for evaluating critical issues caused by future climate change.

17.5.1 Global Climate Model (GCM)

For investigating key features obtained from future climate change, the most important point to be carefully treated for the analysis is that any methodology as well as the SOM should not depend on the output from only a GCM. The reason is that there are a wide range of biases between these GCMs because of many differences in physical framework, model structure, resolution, and so on, between these GCMs. Actually, the Program for Climate Model Diagnosis and Intercomparison (PCMDI) was established in 1989 at the Lawrence Livermore National Laboratory (LLNL) and has collected the output from GCMs around the world in order to develop improved methods and tools for the diagnosis and intercomparison of GCMs for past, present, and future climate. In a series of future climate change projects, the Coupled Model Intercomparison Project 3 (CMIP3) contributed to the physical science basis IPCC (2007) in the Fourth Assessment Report (AR4) of the Intergovernmental Panel on Climate Change (IPCC). The archives of CMIP3 consist of the model outputs listed in Table 17.3 of the past, present and future climate, which were collected by PCMDI in 2005 and 2006. The archives can be obtained from <http://www-pcmdi.llnl.gov/ipcc/about_ipcc.php>.

Table 17.3. Modeling groups (ID name) participating in CMIP3

Group	Country	CMIP3 I.D.
Beijing Climate Center	China	BCC-CM1
Bjerknes Centre for Climate Research	Norway	BCCR-BCM2.0
National Center for Atmospheric Research	USA	CCSM3
Canadian Centre for Climate Modelling & Analysis	Canada	CGCM3.1(T47)
Canadian Centre for Climate Modelling & Analysis	Canada	CGCM3.1(T63)
Météo-France / Centre National de Recherches Météorologiques	France	CNRM-CM3
CSIRO Atmospheric Research	Australia	CSIRO-Mk3.0
CSIRO Atmospheric Research	Australia	CSIRO-Mk3.5
Max Planck Institute for Meteorology	Germany	ECHAM5/MPI-OM
Meteorological Institute of the University of Bonn, Meteorological Research Institute of KMA, and Model and Data group.	Germany / Korea	ECHO-G
LASG/ Institute of Atmospheric Physics	China	FGOALS-g1.0
US Dept. of Commerce / NOAA / Geophysical Fluid Dynamics Laboratory	USA	GFDL-CM2.0
US Dept. of Commerce / NOAA / Geophysical Fluid Dynamics Laboratory	USA	GFDL-CM2.1
NASA / Goddard Institute for Space Studies	USA	GISS-AOM
NASA / Goddard Institute for Space Studies	USA	GISS-EH
NASA / Goddard Institute for Space Studies	USA	GISS-ER
Instituto Nazionale di Geofisica e Vulcanologia	Italy	INGV-SXG
Institute for Numerical Mathematics	Russia	INM-CM3.0
Center for Climate System Research (The University of Tokyo), National Institute for Environmental Studies, and Frontier Research Center for Global Change (JAMSTEC)	JAPAN	MIROC3.2(hires)
Center for Climate System Research (The University of Tokyo), National Institute for Environmental Studies, and Frontier Research Center for Global Change (JAMSTEC)	JAPAN	MIROC3.2(medres)
Meteorological Research Institute	Japan	MRI-CGCM2.3.2
National Center for Atmospheric Research	USA	PCM
Hadley Centre for Climate Prediction and Research / Met Office	UK	UKMO-HadCM3
Hadley Centre for Climate Prediction and Research / Met Office	UK	UKMO-HadGEM1

17.5.2 Emission Scenarios of IPCC

Moreover, it should be noted that future features obtained from climate model run largely differ among many emission scenarios specified by IPCC. These scenarios are based on the Special Report on Emissions Scenarios (SRES) suggested by IPCC (2000). The scenarios basically consist of four families according to the assumption of a wide range of future characteristics such as the mode (globalization or localization) of social and economic interaction among regions around the world, economic growth, population change, and technological aspect accompanying long-term specification of the greenhouse gas emission (CO_2, CH_4, etc.). The A1 family shows a world of rapid economic growth with rapid development of new and efficient technologies under the predominant global interaction among regions. The A1 family is divided by the use of energy sources into three groups characterized by predominant use of fossil fuels (A1FI), non-fossil energy sources (A1T), and balanced use of all energy sources (A1B). The A2 family shows a world of locally-oriented economic growth with slow development of technology under the self-reliance and preservation of local identities. The B1 family shows a world of rapid economic growth characterized by service and information economy with clean and resource efficient technologies, directing towards global solutions to economic, social and environmental stability. The B2 family is characterized by intermediate economic growth and slow development of technology, directing towards environmental protection and social equity in each local world.

17.5.3 Study of Future Climate Change

This subsection explains aspects of future precipitation, focusing on the Japan islands situated in the East Asia, as an example of the study of future climate study. In Japan, heavy rainfall often occurs during a rainy season (BAIU) in June and July, as shown in the subsection of 17.4.1, and has caused serious flood disasters. Therefore, future heavy rainfall caused by global warming during the BAIU is a main concern in Japan. Regional climate projections in the world using IPCC Multi Model Dataset (MMD) for A1B scenario were summarized in the physical science basis (IPCC 2007) included in the Fourth Assessment Report (AR4) of the IPCC. In the report, the MMD projections for the A1B scenario showed an increase in precipitation in East Asia. Focusing on future heavy rainfall in the Kyushu Islands situated in the west of Japan, the future projection of the regional climate model with 5 km resolution performed by Kaneda et al. (2005) showed that future climate change in the East Asia has a potential to cause extremely heavy rainfall in Kyushu Islands due to the confluence of two types of MCSs (Mesoscale Convective Systems) from the China continent and the southern of the East China Sea.

17.5.4 Example of SOM Application

The SOM analysis using the archives of CMIP3 is seen in Cassano et al. (2006b), Hope (2006), and Skific et al. (2009). This subsection introduces a part of the results performed by Hope (2006).

Hope et al. (2006) recognized synoptic field patterns that have caused the decrease in precipitation in Southwest Western Australia (SWWA) between 1957 and 2003 using the SOM. In the analysis, all the synoptic fields represented by the distribution of sea surface pressure were classified into twenty types of synoptic field patterns that can be recognized clearly and visually on the SOM map. The results show the decrease in the patterns of low pressure trough in the southern region of SWWA, and the increase in the pattern of high pressure systems above the Australia continent. In other words, the existence of trough brings the transportation of moisture into SWWA and resultant wet condition causing precipitation. On the other hand, dominant high pressure system blocks moisture flow into SWWA and brings resultant dry condition. Therefore, it was found that such synoptic situations contribute to decreasing trend in precipitation in SWWA.

Based on the abovementioned background leading to critical issue of water resources in Australia, Hope (2006) diagnosed field patterns corresponding to future synoptic situations among the past field patterns constructed by Hope et al. (2006), and investigated how these pattern influences future precipitation in SWWA, comparing with past trend of precipitation. Future synoptic situations were based on the simulated results from five different GCMs (CSIRO-Mk3.0, GFDL-CM2.0, GISS-ER, MIROC3.2, MRI3-CGMC2.3.2) selected from the GCMs (Table 17.3) registered in CMIP3, assuming two future emission scenarios (SRES A2 and B1). The A2 is one of the scenarios leading to strong global warming, and has a potential to cause average temperature increase of 3.4 degrees C for 100 years between 2000 and 2100. The CO_2 emission specified in the A2 increases steadily due to slow development of new technologies under locally-oriented economic growth. On the other hand, the B1 has an increase in the CO_2 emission by 2040, and, after this year, it decreases until 2100 by attaining rapid development of clean and resource efficient technologies under globally-oriented economic growth. The predicted average temperature increase of the B1 is 1.8 degrees C.

Based on the aforementioned condition and assumption, as a part of the results of Hope (2006), predicted frequency of trough and high pressure systems in SWWA between 2081 and 2011 are shown by comparing with past frequency between 1948 and 2003. For the A2 scenario, future projection of CSCIRO-Mk3, GFDL-CM2.0 and MIROC (medres) shows the decrease in the frequency of all the patterns relating to pressure trough in the southern region of SWWA as well as the increase in the frequency of some patterns relating to high pressure systems above the Australia continent. The other GCMs did not show such clear features. On the other hand, for the B1 scenario, remarkable signals such as the A1 scenario cannot be clearly seen in any models. Therefore, as long as we focus on the results, the A2 scenario leading to strong global warming may enhance the decrease in trough and the increase in high pressure system and resultant decrease in precipitation in SWWA, compared with the B1 scenario. However, because of many complicated systems included in projected future climate changes, further discussions including the other analyses were conducted in Hope (2006).

As shown here, although future projection of different GCMs under the assumption of different scenarios leads to features of similar and dissimilar climate changes, it is found that SOM is very useful for climate change research because of the simplification of such complicated many features and conversion of them into easily-recognizable patterns for the interpretation of the results.

17.6 Summary

For the last decade, unlike the EOF linear conventional analysis, non-linear pattern recognition technique called a self-organizing map (SOM), which is a kind of unsupervised ANNs technique and provides useful information for visually interpreting high-dimensional complicated climate and weather data, has also been applied to meteorological studies.

The first part of this chapter explained: 1) the pattern recognition of high-dimensional synoptic fields using the SOM; 2) the construction of visualized relationships on the two-dimensional SOM map between formed synoptic field patterns and independent local variable (heavy rainfall frequency in the example) observed in the target local area (Kyushu, western Japan); and 3) the features of heavy rainfall frequency identified per each synoptic field pattern, according to the extended version of Nishiyama et al. (2007). The second part of this chapter introduces fundamental studies on future climate change caused by global warming, motivated by the Intergovernmental Panel on Climate Change (IPCC), and explains how to apply the SOM to the analysis of such future climate change studies.

The results showed that the visualization of high-dimensional synoptic fields on the map helps us understand the similarities and dissimilarities between formed synoptic field patterns by the SOM, and helps us identify synoptic field patterns related to heavy rainfall occurrence in the target local area. Moreover, it was found that the SOM has potential ability to find some specific synoptic field patterns showing high frequency of heavy rainfall. Therefore, we conclude that the SOM technique is an effective tool for classifying complicated non-linear synoptic fields and identifying disastrous heavy rainfall events. Moreover, it was found that the SOM application is also effective for classifying too many future climate information simulated by many GCMs against the forcing of many climate scenarios.

Finally, based on the results obtained in this chapter, some recommended usages of the SOM methodology are given as follows:

(1) The SOM is a useful tool for providing significant information on which synoptic field patterns cause heavy rainfall and associated disaster in the past period. Moreover, we can confirm similar events classified in each pattern.

(2) The further detailed analysis is to compare features between similar events classified into an identical pattern. Through the comparison, the SOM can extract common features on heavy rainfall, disaster, and damages between similar events. Therefore, it can be expected that such information is available for effectively learning in ahead past situation of heavy rainfall and associated disaster in each pattern in preparation for disaster mitigation activities conducted by local governments in Japan. In other words, the analysis enables us to perform the extraction of significant signals related to heavy rainfall and disaster from past enormous information (past records such as disaster mitigation activity as well as weather data) accumulated for many years.

(3) Once the two-dimensional relationships on the map are established by the SOM training, the relationships enable us to diagnose features of a synoptic field simulated by a numerical prediction model for daily weather forecasting. For example, if the predicted synoptic situation is classified into one of the heavy rainfall patterns, the synoptic field can be judged as a warning situation that may cause heavy rainfall and associated disaster. Moreover, by investigating past common features among similar events included in the diagnosed pattern, we can obtain significant clues on what kind of heavy rainfall and disaster will occur. Therefore, the diagnosis process will be useful

for decision-making by weather forecasters or end users engaging in disaster mitigation activities.

(4) If we make a chart of temporal variation in the frequency of heavy rainfall without considering pattern recognition, the variation includes all the synoptic fields recorded for the past period, which would conceal notable signals in the temporal variation. However, the SOM enables us to obtain temporal variation in the frequency of heavy rainfall *in each synoptic field pattern*.

(5) If we consider other target variables and the heavy rainfall frequency, the SOM can also be applied to the classification and diagnosis of climate and synoptic situation related to the target variable(s) and the frequency analysis of each pattern obtained by the SOM training.

(6) If we investigate the influence of future climate change by global warming on the local environment and human life, the use of the SOM is very effective because of high dimensionality included in the information of future climate obtained from the GCM. It is critical to obtain the information on common and different features in all the GCMs used for the projection of future climate by comparing numerically-simulated outputs obtained from these GCMs with each other. The reason is that there are a wide range of biases between these GCMs because of many differences in physical framework, model structure, resolution, and so on, between these GCMs.

17.7 References

Akiyama, T. (1973). "The large-scale aspects of the characteristic features of the Baiu front." *Papers in Meteor and Geophys*, 24, 157–188.

Cassano, E. N., Lynch, A. H., Cassano, J. J., and Koslow, M. R. (2006a). "Classification of synoptic patterns in the western Arctic associated with extreme events at Barrow, Alaska, USA." *Climate Research*, 30, 83–917.

Cassano, J. J., Uotila, P., and Lynch, A. (2006b). "Changes in synoptic weather patterns in the polar regions in the twentieth and twenty-first centuries, Part 1: Arctic." *International Journal of Climatology*, 26, 1027–1049.

Cavazos, T. (1999). "Large-scale circulation anomalies conducive to extreme events and deviation of daily precipitation in northeastern Mexico and southeastern Texas." *Journal of Climate*, 12, 1506–1523.

Crimins, M. A. (2006). "Synoptic climatology of extreme fire-weather conditions across the southwest United States." *Int. J. Climatology*, 26, 1001–1016.

Dommenget, D., and Latif, M. (2002). "A Cautionary Note on the Interpretation of EOFs." *J. Climate*, 15(2), 216–225.

Hewitson, B. C., and Crane, R. G. (2002). "Self-organizing map: applications to synoptic climatology." *Climate Research*, 22, 13–26.Hope, P. K. (2006). "Projected future changes in synoptic systems influencing southwest Western Australia." *Climate Dynamics*, 26, 765–780.

Hope, P. K., Drosdowsky, W., and Nicholls, N. (2006). "Shifts in synoptic systems influencing southwest Western Australia." *Climate Dynamics*, 26, 751–764.

IPCC (2000). *Emissions Scenarios. Summary for Policymakers*. Special Report IPCC Working Group III, 27 pp.

IPCC (2007). *Climate Change 2007: The Physical Science Basis. Contribution of Working Group I to the Fourth Assessment Report of the IPCC. Cambridge University Press*, 996 pp.

Johnson, N. C., Feldstein, S. B., and Tremblay, B. (2008). "The continuum of northern hemisphere teleconnection patterns and a description of the NAO shift with the use of self-organizing map." *Journal of Climate*, 21, 6354–6371.

Kanada, S., Muroi, C., Wakazuki, Y., Yasunaga, K., Hashimoto, A., Kato, T., Kurihara, K., Yoshizaki, M., and Noda, A. (2005). "Structure of mesoscale convective systems during the late Baiu season in the global warming climate simulated by a non-hydrostatic regional model." *Scientific Online Letters on the Atmosphere*, 1, 117–120.

Kohonen T. (1995). "Self-Organizing Maps." *Springer Series in Information Sciences*, 30, 362pp.

Leloup, J. A., Lachkar, Z., Boulanger, J. P., and Thiria, S. (2007). "Detecting decadal changes in ENSO using neural networks." *Climate Dynamics*, 28, 147–162.

Leloup, J. A., Lengaigne, M., and Boulanger, J. P. (2008). "Twentieth century ENSO characteristics in the IPCC database." *Climate Dynamics*, 30, 277–291.

Mantua, N. J., Hare, S. R., Zhang, Y., Wallace, J. M., and Francis, R. C. (1997). "A Pacific interdecadal climate oscillation with impacts on salmon production." *Bulletin of the American Meteorological Society*, 78, 1069–1079.

Nikkilä, J., Trörönen, P., Kasai, S., Venna, J., Castrén, E., and Wong, G. (2002). "Analysis and visualization of gene expression data using Self-Organizing Maps." *Neural Networks*, 15, 953–966.

Ninomiya, K. (2000). "Large- and meso-α-scale characteristics of Meiyu and Baiu front associated with intense rainfalls in 1-10 July 1991." *J. Met. Soc. Japan,* 78, 141–1517.

Nishiyama, K., Endo, S., and Jinno, K. (2007). "Identification of typical synoptic patterns causing heavy rainfall in the rainy season in Japan by a self-organizing map." *Atmospheric Research*, 83, 185–200.

Park, Y. S., Céréghino, R., Compin, A., and Lek, S. (2003). "Application of artificial neural networks for patterning and predicting aquatic insect species richness in running waters." *Ecological Modeling*, 160, 265–280.

Preisendorfer, R. W. (1988) *Principal component analysis in Meteorology and oceanography. Elsevier*, 425.

Skific, N., Francis, J. A., and Cassano, J. J. (2009). "Attribution of projected changes in atmospheric moisture transport on the Arctic: A self-organizing map prospective." *Journal of Climate*, 22, 4135–4153.

Tennant, W. (2003). "An assessment of intraseasonal variability from 13-Yr GCM simulations." *Monthly Weather Review*, 131, 1975–1991.

Thompson, D. W. J., and Wallace, J. M. (1998). "The Arctic Oscillation signature in the wintertime geopotential height and temperature fields." *Geophys. Res. Lett*, 25, 1297–1300.

Zhang, Y., Wallace, J. M., and Battisti, D. S. (1997). "ENSO-like interdecadal variability: 1900–93." *J. Climate*, 10, 1004–1020.

This page intentionally left blank

PART 3

Reducing and Adapting

CHAPTER 18

Adapting to Climate Change: Technologies, Perceptions, Education, and Perspectives

Ioan M. Ciumasu, Mihai Costica, Cristian V. Secu, Bhola R. Gurjar and Chandra S.P. Ojha

Climate change caused by human activity is now recognized as a real phenomenon (IPCC-WGI 2007), and an impressive literature already investigates its impacts on the natural systems and on human lives (IPCC-WGII 2007). During the past 1–2 decades, the central questions on human-driven climate were still related to whether it really happens (i.e. whether it is not a variation around the natural climate tendencies). At the beginning of the 2^{nd} decade of the 21^{st} century, the main scientific and public inquiry shifted to understanding the consequences of this phenomenon and how to deal with it.

While the qualitative and quantitative details of climate changes are not the same for all countries and world regions, it is largely acknowledged that those changes cannot be ignored by policy makers and by human communities (IPCC-WGIII 2007). Given the complexity of the phenomenon, and its variable effects of various scales, dealing with climate changes requires distinct, albeit related, understanding of climate changes and elaboration of appropriate policies at local, national, continental and global scales. This chapter is a limited introduction to this complex issue.

At each geographical scale, there are two ways to respond to climate changes, and they are intimately interrelated. The first way is to try to limit as much as possible the effects of climate changes by addressing the cause of climate changes, namely by acting in the sense of reducing emissions of greenhouse gases. This approach, though, has some important limitations, related to both (i) the capacity of the human communities to coordinate their actions towards a common goal and expected impacts of such actions and (ii) the extent to which such actions can have *ex ante* quantifiable effects. Moreover, even supposing that reducing emissions would be very quickly achieved, a certain amount of climate change is unavoidable and irreversible, because of (i) the natural time lag between the dynamic of the atmospheric concentration of greenhouse gases and the dynamics of the climate, and (ii) many natural processes being governed by thresholds which only allow unidirectional evolutions. Restoring the initial conditions like initial atmospheric concentrations of greenhouse gases will not result in restoring the initial climate. Therefore, the second way to react to climate changes is to mitigate their effects, i.e. developing and applying methods, institutions and instruments to minimize the impact of the given climate changes on humanity.

In other words, the possibility of prevention of human-driven climate changes has already been lost but the possibility of partial prevention of natural disasters still exists (at least in theory), directly depending on the capacity to prevent developments of vulnerability (whenever possible). At most, prevention of excessive climate changes still has a chance, depending on whether and how we can define excessiveness. As a global society, we have lost the train of awareness and prevention of climate changes. We can only try and limit the damages. We still have the chance of awareness and prevention of climate-related disasters.

The impact of climate changes is typically conceived in terms of climate-related extraordinary events with disastrous consequences, like storms (notably hurricanes), floods or droughts. While such events are much more tangible and therefore more effective in establishing the reality and consequences of climate changes the public opinion (and perhaps determinant in the public support for climate-related policies), the science behind natural disasters is not less complex. In addition to being unstoppable once started, wide-scale physical phenomena causing disasters are hard to gauge. It is impossible to measure the size (amount of energy involved) of a climate-related phenomenon; only its effects can be measured–in terms of the damage caused, typically human casualties and monetary costs. These effects are, nevertheless, a resultant of both (i) the strength of a climate-related phenomenon and (ii) vulnerability of the affected human communities to potentially disastrous climate-related phenomena. Therefore, mitigation of climate change goes beyond the issues of scientifically proving climate changes or demonstrating the links between climate changes and the parameters (e.g., frequency and size) of potentially disastrous climate-related phenomena, and aims at diminishing vulnerability in the face of unavoidable climate-related phenomena (Adger et al. 2005).

While mitigation *per se* deals with lowering vulnerability of a community within intervention means of current lifestyles, it consists in anticipatory preparation to deal with immediate aftermath of climate-related events. Mitigation *per se* has therefore considerable limits. Further success in limiting the effects of climate-related events must go deeper into the functioning of the techno-social-economic systems, and generate changes in lifestyles. When such changes become strong enough to insure a new (better) equilibrium, meaning new ways of life that insure lower vulnerability to climate-related events, we talk about a new type of response to climate changes: adaptation.

To sum up, the relation between humanity (the satisfaction of the needs of the current generations) and climate changes exists at three distinct levels, as illustrated in Figure 18.1. The first level is the generation of climate changes of the emissions of greenhouse gases by a lifestyle grounded on the use of fossil energy. The control that is possible at this level is the control of emissions. The second level is reducing the disastrous effects of climate related phenomena, by reducing vulnerability (or "unpreparedness") to climate related phenomena within the current lifestyles and social structures. The third level involves a major leap, from current to a new paradigm and lifestyle, so that mitigation actually becomes adaptation.

The key concept is therefore vulnerability. Further, the very vulnerability of a human community is two-faceted: it goes both directly through physical effects of climate related phenomena on human individuals and social systems, and indirectly – via the capacity of ecosystems to support the human community under discussion. In other words, vulnerability of human communities largely consists in the vulnerability of their support ecosystems.

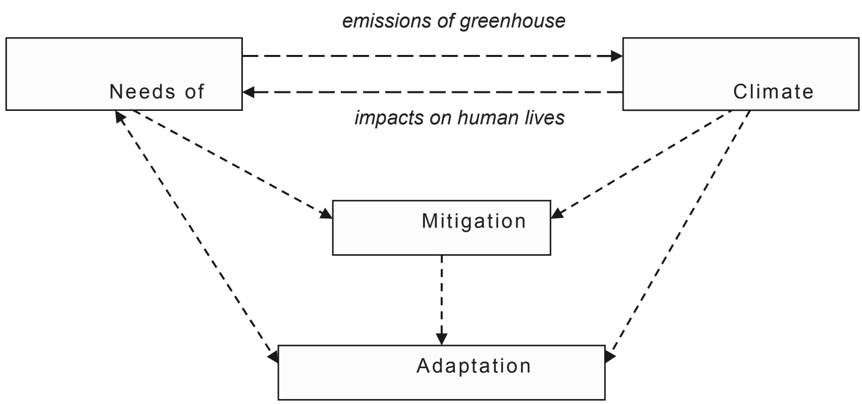

Figure 18.1. Schematic of the roles of mitigation and adaptation in the relation between human actions and climate changes

Various techniques may exist for mitigating climate changes, as described in section 18.1. However, technical solutions largely depend on the social context, as determined by the current perceptions and expectations of the citizens. Section 18.2 discusses these concerns, around the issue of the relation between people and science and the issue of people's lifestyles. The take-home message of this section is that policies and measures towards mitigation and adaptation to climate changes can only succeed as imbedded in a much wider and deeper process of transition to sustainable development. Since such a transition is determined by knowledge and values before being determined by technical approaches, this section reflects the understanding that the main driver of the social processes of mitigation of, and adaptation to climate changes is education. The next section (18.3) details this domain from the perspective of the philosophical and methodological evolution from environmental education to the wider concept of education for sustainable development. The red thread of this educational evolution is that an effective environmental education can only happen if new references and methods are taken into account so as to expand the perspective from that of simply environmental protection to a paradigm that can integrate social and economic aspects. In this sense, education for sustainable development must extend in relation to the science and the social processes related to sustainable development. In doing that it has to deal, along with scientists and decision-makers, with the current challenges and controversies in science and society. The last section of this chapter (18.4) provides a brief introduction to these challenges, and outlines the need to effectively integrate knowledge from various disciplines, as prerequisite for truly informed and coherent decision-making.

18.1 Techniques for Mitigating Climate Change

The typical non-linear behavior of natural systems (where there is no clear cause-effect dynamics but a complex dynamics of various dynamics and unique effects) and the substantial climate changes (as anticipated by the IPCC reports) result in a new climatic situation at global, continental and local scales. The expected new climatic context is not a simple shift in global mean surface temperature (GMST) and precipitations. Instead, complex processes and phenomena will be triggered and the current climates of the Earth will suffer important modifications, some of them will even disappear and new climate states (with not current analog) will appear before the end of the 21st century (e.g., Williams et al. 2007). This illustrates the fact that one can only envisage limited preparation for future climatic situations and that uncertainty will have to be part of the preparation itself. In other words, (i) only limited mitigation and adaptation is possible for humanity, and (ii) living with uncertainty will have to be part of the adaptation to climate changes.

Among the potential solutions that have been proposed for mitigating climate changes, the most attention has been attracted by several techniques, as visible in the scientific literature and in public discussions, belonging to two distinct approaches. The first approach is to address the concentration of carbon dioxide and the other gases that make up the aggregate greenhouse gas (GHG) in the Earth's atmosphere, taking into account the fact that, between 1959 and 2008, only about 43% of the carbon dioxide emitted each year remained in the atmosphere, the rest going to carbon sinks in the oceans and on land (Le Quere et al. 2009). The stabilization of the atmospheric concentration of carbon dioxide can be done by curbing emissions (carbon sources) or by helping the natural uptake of atmospheric carbon dioxide by the oceanic and terrestrial ecosystems (carbon sinks). A related and intensely debated technique consists in the artificial uptake of carbon dioxide from the atmosphere (by technologies based on physico-chemical processes) followed by its injection and trapping in geological deposits.

Those approaches can be seen as part of a recent broad approach in science and business, namely innovation for sustainable development (e.g., Hellstroem 2007), which is a domain under fast development, and which also comprise social and economic aspects, not only technological and ecological. Some of the main directions are being addressed in the next sections of this chapter.

18.1.1 Solar Radiation Management

Due to the slow pace of policy and action for climate mitigation, the concept of solar-radiation management returned to the debates. In principle, this can be achieved by deliberately emitting to the stratosphere aerosols that have the capacity to exert an effect of forcing the balance of solar radiation retained in the atmosphere. The radiative forcing further translates into less solar energy reaching the lower atmosphere and be trapped by the greenhouse effect. Thus, aerosols become climate forcing agents.

Some aerosols are reflectant of the solar radiation and therefore have the effect of cooling the atmosphere, like the sulphate aerosols, while others are absorbant of the solar radiation have the effect of warming the atmosphere, like carbonaceous aerosols resulting from biomass and fossil fuel burning (Penner et al 1998). The overall net effect of aerosols in atmosphere is cooling; which suggests, in theory, that on-purpose pollution of the atmosphere (stratosphere) with certain aerosols can help mitigate global warming. However, the detailed mechanisms are not clear, and the effects are seldom proportional. Many effects are indirect and complex interactions exist among various types of aerosols, between them and the climate, with the ozone and with the water cycle. For example, methane, ozone and aerosols are linked through atmospheric chemistry, so that emissions of a single pollutant can affect the dynamics and concentrations of several others, and often via mechanisms that are poorly understood (Shindell et al. 2009).

To add to the complexity, some aerosols are natural (like the volcanic emissions or the dust from Sahara) and some others are anthropogenic or with an anthropogenic component (like the urban haze caused by urban and industrial pollution; smoke from vegetation fires), others are natural. This may suggest that deliberate human actions may only influence some aerosols. It is nevertheless difficult to make clear distinctions between anthropogenic and natural aerosols, because this requires precise description of the chemical composition based on very detailed and resource demanding *in situ* chemical measurements. Fore example, dust can have a natural part generated by deserts, and an anthropogenic part generated by agriculture. Satellite imagery and computer modeling may attain significant but limited success in estimating the anthropogenic share of aerosols in a given area, based on information on urban, agricultural and forest fire practices and activities. Such measurements modeling may help elucidating some interactions between aerosols, climate and water cycle, but a large amount of uncertainty remains inherent (Ramanathan et al. 2001; Kaufman et al. 2002; Breon 2006; Lenton and Vaughan 2009). The main lesson to retain from the studies on aerosols is not only the intriguing possibility to manipulate solar radiation balance by controlled emissions, but especially the reality that climate change mitigation can only be done effectively in the wider context of air pollution, i.e. beyond the discussion on GHG (Arneth et al. 2009).

In theory, geoengineering methods to attempt to mitigate climate warming would lead, according to the current models, to less extreme temperature and precipitation anomalies when compared with the 'business as usual' scenario of unmitigated climate. Nevertheless, in the situation where atmospheric GHG concentration continues to rise, global temperature and precipitations cannot be stabilized simultaneously. At least as important, not all the regions of the world can be stabilized simultaneously, which leads to the political difficulty of finding global agreement on whether such a technique should be used (Ricke et al. 2010).

A major consequence of this technique, however, will be that the global and local water cycle will be affected, notably with fewer precipitations. This would have important consequences on ecosystems and human societies, since a global water crisis already exist despite wide public ignorance in the developed countries (Duda and El-Ashry 2000) and this water crisis would be severely aggravated. To the negative side of this technique add the side effect of increasing acid depositions (most notably when the aerosols are made up by sulphates), leading to acidification of the oceans, fresh waters and soils (Kravitz 2009). However, the full extent of the consequences of such a biogeochemical disturbance of ecosystems by global acidification is not clear yet, despite considerable efforts in this sense (Menon 2004; Robock 2009). But they are due to be major, since all chemical and biochemical equilibriums in waters, soils and living organisms will be affected.

Because of all these reasons, and because geoengineering is seen in the policy discussions as an unwanted substitute of emission cuts, there is very little support among scientists for such approaches (e.g., Crutzen 2006; Barrett 2008). Given all the risks and uncertainties (some of them are due to the current state of knowledge, but many are due to the intrinsic non-linear behavior of natural systems), it is reasonable to assume that everything should be done to avoid arriving at a necessity to use geoengineering methods. However, we should be aware of these approaches, in order to know the full range of types of approaches that can theoretically be employed, and in order to acknowledge the incredible risks that are posed by using such approaches.

18.1.2 Abatement of Emissions

Emissions of carbon dioxide from fossil fuel have increased significantly and continue to do so, and the anticipated climatic effects have been already discussed extensively in the literature (IPCC-WGI 2007; Manning et al. 2010). However, the abatement of emissions is a very sensitive issue in terms of social acceptability, and thus dependent on regional macroeconomics, local governance and related political decisions, and therefore very tedious and hard to achieve. The detailed dynamics of those decisions has been widely and thoroughly addressed in the literature. What should be retained and stressed for the purpose of this chapter is that GHG abatement is an issue of social and political embeddedness of mitigation measures. Very often in the field of environmental-friendly policies, the limiting factor is not technology, but the social acceptability of those technological solutions.

At a wider international context, a recent reflection of the social and political embededness of climate mitigation measures was failure of the international community to achieve a binding engagement at the United Nations Conference of Climate Change Conference during 7–18 December 2009 in Copenhagen (formally known as The 15th Session of the Conference of the Parties to the United Nations Framework Convention on Climate Change–COP15, and The 5th Session of Meeting of the Parties to the Kyoto Protocol–CMP5). An informal agreement has been achieved, with a document called "the Copenhagen Accord", that climate warming should be kept bellow 2°C, which roughly corresponds to 441 ppm, which further corresponds to cutting emissions with about 25–40% by 2020 as compared to 1990 levels (Hufbauer and Kim 2010; Michaelowa 2010; Ramanathan and Xu 2010; Schnoor 2010). While the political agreement of principle over this goal-limit is to be welcome and strongly supported for the sake of urgent and efficient decision taking towards curbing emissions, two essential aspects need serious attention. First, the scientific basis to establish this 2°C limit is highly debatable in itself, because the non-linear dynamics of the natural systems does not allow any claim that climate warming under this limit is ‘still ok’. In fact, given the complex dynamics of the natural systems (read essentially ecosystems) determined by the existence of thresholds (most of them poorly understood) (e.g., Muradian 2001; Briskie et al. 2006), we know that the more global warming develops at the current fast speed (compared with geological times) the more we approach disaster in the sense of collapse of the natural carrying capacity of the Earth’s ecosystems. But we have no means to know exactly how grave the situation is. In fact, it is perfectly possible that 2°C is already too much. In these circumstances, the agreement over the 2°C limit is rather the result of “trading hopes;” an acknowledgement that getting the global community to agree on limitations below 2°C is probably impossible. The pragmatic logic behind this somehow bizarre political agreement of principle over scientific truth is rather in the domain of efforts to limit the disaster as much as possibly achievable. In this sense, the essential aspect is not to “truly identify” the “correct limit” to work with, but to have emissions curbing as soon as possible, and as deep as possible.

Nevertheless, current national emission targets may not even be able to limit global warming to 2°C (Rogelj et al. 2010). There are many sources of GHG emissions, most of them very difficult to measure and to control/manage. For example, a very important GHG source is municipal solid waste landfills, since they emit considerable amounts of methane, a strong greenhouse gas. Other aspects can be mentioned like uncontrolled forest fires, uncontrolled domestic or industrial uses of fossil fuels, especially in developing countries.

Beside abatement of emissions via limitations of emissions of each country (like the cap-and-trade schemes), another less discussed issue but essential for future policies is the consumption-based accounting and management of emissions. This refers to the amount of emissions of carbon dioxide associated with the consumption of goods and services in each country. Thus, the real impact of a country in terms of generating carbon dioxide emissions is given by the amounts of consumption of goods and services that are produced by generating carbon dioxide emissions. For example, in wealthy countries, the impact of their population in terms of carbon dioxide emissions is increased with more than 30% by consumption of imported goods and services, most notably from China (Davis and Caldeira 2010). In other words, it can be argued that China generates emissions of carbon dioxide on the behalf of the consumers in the rich countries. Such calculations reveal the huge potential for leakages that affect cap-and-trade schemes, and the need for stronger international cooperation in order to effectively design solutions by taking into account global emissions and balances, i.e. true global solutions, not local surrogates. Thus, taking into account international trade, in order to adjust for the separation between production and consumption, can change by up to 60% the carbon dioxide allocations per countries (Peters et al. 2009).

18.1.3 Carbon Trapping in Biomass

In addition to temperature-driven processes, carbon trapping in biomass must take into account the biological and ecological response to elevated carbon dioxide concentrations in the air. Studies on enrichment of free-air carbon dioxide reveal complex processes, and largely a differentiated response in various types of plants/crops. For example, from a physiological perspective, plants belong to three plant functional types (PFT), called C3, C4, and CAM (Crassulacean Acid Metabolism). Most species belong to the first two types, CAM being a peculiar plant physiology adaptation for dessert environments. The difference between them is at the level of physiological pathway (chain of biochemical reactions) behind carbon fixation and biomass production. The C3 pathway is the predominant one in the temperate and cold areas. The C4 pathway starts by the generation molecules with 4 atoms of carbon and allows for higher rates of photosynthesis and a more efficient use of water in comparison to the C3 type, is seen as an adaptation to warmer (and often arid) regions but they have probably appeared as a modification of C_3 type physiology in response to lower concentrations of carbon dioxide in the atmosphere; C_4 plants dominate the tropical environments, and are responsible for about 30% of the global carbon fixation (Slack and Hatch 1966; Ehrleringer et al. 1991; Osborne and Beerling 2006; Osborne and Freckleton 2009). Higher carbon dioxide concentrations appear to favour higher photosynthesis rates, biomass and yield in C_3 species, but not so much in C_4 species; however, whether this physiological difference leads to biomass variations and ecological and biogeographical predominance of one of the two types depends on other factors as well, like temperature, precipitations-humidity, seasonality and nutrients (e.g., Huang et al. 2001, 2006; Kimball et al. 2002; Ward et al. 2008; Kuerschner and Kvacek 2009).

Nevertheless, the capacity of plants to fixate atmospheric carbon into biomass is not only determined by photosynthesis rates changes in relation to carbon dioxide concentrations, but also by the responses of plant respiration. Indeed, the result to take into account is the net balance between plant fixation of carbon dioxide and plant respiration (emission of carbon dioxide). Thus, plants growing in lower carbon dioxide concentration (i.e., 200 ‰ as in Pleistocene times at the end of the last ice age, as compared with 370 ‰ in the current Holocene) have lower respiration rates (Gonzalez-Meler et al. 2009), meaning that higher carbon dioxide concentrations increase rates of both photosynthesis and respiration. Higher temperatures also increase plant respiration. Further, this means that climbing carbon dioxide concentrations and temperatures in the atmosphere will not automatically increase carbon fixation (biomass sink) by plants. Quite remarkably, opposite effects may occur at certain rates of change in environmental factors. Thus, certain studies are concerned about the possibility that, if certain climatic thresholds are crossed, the worlds' forests, especially tropical forests, may actually function as carbon sinks, and become net carbon emitters during the 21st century. Multidisciplinary and integrated studies on forest are essential for understanding of the relation between tropical forest and climate and for designing effective policies related to climate change mitigation and adaptation (Clark 2004, 2007; Bonan 2008).

It is very important that mitigation and adaptation policies acknowledge the full range of consequences of the changes in the rates of carbon dioxide and in the related climate factors. Beyond certain natural thresholds, dramatic changes can occur in the environment to which we are adapted, and so posing existential threats to our own society and even species.

Carbon Trapping in Terrestrial Ecosystems. Forests store about 45% of terrestrial carbon, and they sequester about 1/3 of the human annual emissions of carbon dioxide, in a complex system of interactions and effects which can be studied in terms of the biogeophysical processes (albedo and evapotranspiration), biogeochemical processes (the carbon cycle), and biogeographical processes (land use and vegetation dynamics). But the effect of forests on climates is difficult to understand by simple observations or disciplinary methods (Bonan 2008). Notably, forests and all other vegetation types are in direct relation with soils, which represents a major deposit of carbon in ecosystems, often ignored in the discussions about carbon emissions and mitigation, and thus an important path for future carbon sequestration (Lal 2004).

As described earlier, changes in the atmospheric concentration of carbon dioxide, and changes in temperature or humidity-precipitations can have complex consequences on the biological-physiological processes, like favoring one or another plant functional type in terms of photosynthesis biochemistry. This can easily translate into changes in vegetation types in various biogeographical provinces of the planet (e.g. trees vs. grasses) composition of terrestrial ecosystems, and temperature increases may have stronger impacts than the carbon dioxide concentration (e.g., Flores et al. 2009).

Ecosystem thresholds are not only biologically or biochemical-physiologically determined, but also related to processes and dynamics related to the structure and function of ecosystem. For example, during Miocene, a geological time (23–5 millions years ago) characterized by frequent climatic changes between, the maximum plant diversity in Central Europe does not correlated with changes in the atmospheric concentration of carbon dioxide, but with periods of high climatic stability (Kuerschner and Kvacek 2009). The relation between plant biodiversity and ecosystem productivity and structure is famously complex, but a consensus exists that disturbances large enough to cause major biodiversity loss can trigger cascading effects on losing ecosystem structure and functions. Climate is one of such a disturbance, with the effects being largely determined by the strength and the direction of climate-ecosystem feed-backs, thermal inertia of the oceans (influencing climate on continents) and rates of emissions and climate changes (Serreze et al. 2010); steep changes in the climate parameters (temperature, precipitations, seasonality) can lead to decreasing the capacity ecosystem to fixate atmospheric carbon, with further repercussions on atmospheric carbon dioxide concentrations and climate changes. The series of cascading effects can extend beyond ecosystem, to encompass geophysical phenomena, like it famously happens with the cascading effects of Himalayan glaciers' melting, changes in water amounts and seasonality of the Himalayan rivers, with damaging consequences going further to biodiversity and ecosystem effects and human livelihood (Xu et al. 2010). The risk is therefore, that once certain ecosystem thresholds (say a biodiversity level related to ecosystem stability), a positive feed-back is triggered between ecosystem decay and climate warming, and a point of no-return is passed, when changes cannot be fought back.

Carbon Trapping in Aquatic Ecosystems. Geoengineering methods have been proposed to increase the atmospheric carbon sink in oceans by stimulating biomass production of marine ecosystems. In this sense, probably the most famous hypothesis is that of fertilization of oceans with iron. This idea is based on the acknowledgement that the rate of marine biomass production is limited by the concentration of certain elements in the marine water, most notably iron. This suggests that the rate of the global oceanic biomass production can be significantly increased by simple amendments with iron, i.e. the same way fertilization with various elements is being done in agriculture to increase crop production.

This idea may look simple, but is far from being simple, essentially because of the complexity of the ecosystems, and of the high amount of uncertainty that are inherent to ecosystems. As described in the first section of this chapter, the effects of human interventions into the global biogeochemical cycles are not "mechanical" and the case of fertilization of oceans with iron is no exception. Despite the proliferation of iron fertilization experiments, the efficiency of this approach to sequester atmospheric carbon dioxide remains very uncertain. When included in global models that take into account chlorophyll development and shifts in ecosystem compositions, the results of such local experiments, the expected amount of carbon dioxide trapped by the ocean is several times lower than initially expected by simple extrapolation of local results (Aumont and Bopp 2006). The reason why local results and global results do not coincide pertains to inherent complexity of ecosystems, complexity which increases with increasing scale from local to global. The effect of iron fertilization is not only that of removing iron-limitation of biomass production. Other effects may lead, via complex biological and biogeochemical processes to other types of limitations of biomass production.

Nevertheless, like with the case of aerosols, ocean iron fertilization deserves further investigation, in order to elucidate some aspects that might be useful in the future. A non-negligible aspect is also the relatively low cost of the eventual application of this approach in comparison with other potential climate mitigation solutions. In addition, further studies will hopefully warn us about undesired adverse effects of ocean iron fertilization in the eventuality of emergency-determined policies (Guessow et al. 2010).

18.1.4 Carbon Capture and Geological Storage

Carbon capture and storage (CCS) technologies have become a major path to be explored for future plans to deal with carbon dioxide emissions and climate change (Anderson and Newell 2004).

Carbon dioxide can be injected and stored in aquifers under impermeable layers with a closed dome structure (to prevent lateral migration of the CO_2 plume along the inclination of the impermeable layer). Nevertheless, the amount of such geological situations–with cap rocks as confinement system–is limited, typically far from the sources of CO_2 emissions. Even in the absence of cap rocks, a certain amount of CO_2 can still be trapped via related mechanisms, notably by CO_2 retention in the formation water of the aquifer under the form of solute appeared during CO_2 plume migration through the aquifer–phenomenon called solubility trapping (CO_2 dissolved into water while the CO_2 plume migrates upward to concentrate itself under the impermeable layer) and residual gas in aquifers (Akervoll et al. 2006; Georgescu et al. 2006; Suekane et al. 2009).

Even when such favorable geological conditions exist close to CO_2 sources, this approach is very difficult to apply because of governance issues: it is very hard, usually impossible to convince local communities to accept hosting such a measure at their place. Some companies have tried to gain technological advances by investing in studies on this method. However, a coherent legislation for this does not exist, and technical solutions are for the moment put on the shelf waiting for more favorable social-political context in the future if at all.

Other paths are being under scrutiny so as to identify best geological storage of atmospheric CO_2, notably injection of CO_2 in coal seams, where CO_2 is permanently adsorbed, hence stored if a sealing caprock is present. In this approach CO_2 displaces CH_4, and is so called enhanced coalbed methane recovery–ECBM. This is not yet a mature technology, but significant efforts are being carried out to explore and understand the potential of this approach. The set of CCS technologies by geological means is expected to play a minor role in the next few years, but to gain a significant role within the next two decades (Mazzotti et al. 2009).

18.2 People's Perceptions for Mitigating Climate Change

18.2.1 The relation between Lifestyle and Citizens' Perceptions upon Climate Changes

Current predominant lifestyles are highly carbon-intensive, since we are in an historical technological-economic development cycle that is based on fossil fuels – especially petroleum. The oil cycle can only close via a change in a technological-economic paradigm, generated by a new ground-braking technological development; it is not clear now when and how this change will arrive and in which direction, despite some tempting conclusions invited by exiting developments in ICT and biotechnologies (e.g., Perez 2009; 2010). This means that effective climate policy aiming at forcing limitations in emissions of GHG (mostly carbon dioxide) will demand difficult political-social and individual choices. But acceptability of climate change policies is still quite low in the developed countries (Lorenzoni and Pidgeon 2006), and remains a distant perspective in developing countries due to their primarily economic aspirations. The consequences are that there is a two-way relation between climate changes and GHG emissions.

In a nutshell, lifestyles with respect to climate changes are not so much a matter of individual preferences, but a dynamics of dependence of the socio-economic system of essential technologies. Within those limits, carbon emissions can be reduced at best, but not removed – not until a new technological-economic cycle replaces the current one based on fossil fuel. Therefore the stake of the citizen acceptability of carbon reductions is deeper than just limiting consumption of opting for some more 'environmentally-friendly products'. The later is only marginal, at best secondary. The fundamental stake is to help identify technically feasible and socially acceptable technological paradigms that can open a new, sustainable, technological-economic cycle of development.

18.2.2 Science and Public Perceptions: Towards a Civic Science

With the recent acknowledgement of climate changes by various social actors and by the public in general, environmental sciences have clearly left the cloistered domain of professional peer-reviews and became a subject of public debate along with the overt concerns about climate and other environmental changes (Lubchenco 1998; Mawdsley et al. 2009). In fact, climate change-related sciences, via the International Panel for Climate Changes (IPCC) have championed this convergent dynamics between science in general and the public. Recognition of this central role of climate studies for humanity came from various sectors of the society, like funding agencies, investments in new technologies, and even a recent Nobel Prize for IPCC and public figures promoting climate change mitigation. From within the academic world, there are even calls for a "whole-of-science research agenda" for climate (Heartel and Pearman 2010). Other well-known environmental topics and sciences, notably conservation of biodiversity, have had a less 'spectacular' success to the public, despite similar efforts being made towards raising public awareness and concern.

Climate-related sciences have therefore become champion domains of science-public interaction, in deed promoting a "civic science", where science and society ideally work together, though with specific means, towards common concerns (e.g., Backstrand 2003). While the scientific issues are typically not well understood by the public, given the complexities associated with natural systems and the high level of training required to reach a knowledgeable level, it is not realistic to expect public decisions on climate mitigation and adaptation to be taken mainly on scientific grounds. Instead, a certain minimal understanding of science is necessary to allow relevant public action. Indeed, social dynamics, social capital and capacity of collective action are probably the determinant factor that will allow mitigation and adaptation measures be deliberated, decided and applied (e.g., Adger 2003). The role of science within this dialogue is evolving such that it becomes capable of constant dialogue with the society at large, and science sets its own priorities according to the main social concerns (some determined by communication of scientific realities, like it is precisely the case with climate sciences). This dialogue is set to take place within the wider discussions on environmental changes (other major issues are, e.g., water and soil contamination with persistent and toxic pollutants; depletion of natural resources by overexploitation) and the need for a socio-economic transition towards sustainable development.

Along the process, the place of science in society changes significantly, so that a new paradigm appears to take hold: a new social contract for science and scientist, aiming at sustainable development (Lubchenko 1998). In this sense, in order to gain relevance and to consolidate its important role in society, science is gradually becoming “civic science”: while it retains its quality standards and dynamics, it gains bridges of permanent dialogue with social actors and it becomes more responsive with respect to social issue, and sometimes it takes a driving role.

18.3 Education, Training and Outreach

The capacity of individual and institutional agents to understand climate changes and available decision options in reasonable periods of time is directly determined by their level of education on the matter. Given the current urgent character of climate changes, where it is not about whether climate changes will occur but about how bad its consequences will be, and how effective society can act to develop and apply options for mitigation and adaptation, education of climate change needs to be purpose and priority-driven. While this is already a talk about profound, paradigmatic changes in the education system in many countries, certain issues are very simple, like explaining punctual confusions and misunderstandings (or misrepresentations) that are widespread within the public opinion.

18.3.1 Misunderstanding of Climate Change

One of the most frequent confusion among students and laypersons is between climate changes and other kinds of major environmental concerns. Most typically for poor understanding of climate change issue, many seem to think that climate changes are somehow caused by the hole in the ozone layer. A similar confusion is when acid rain is pointed out to as causing climate changes.

All these confusions appear to be generated by the assumption that there is only one environmental problem, that is, climate change. Subsequently, all other problems of environmental degradation are automatically associated with climate changes, especially if they occur in the atmosphere.

A famous confusion, though subtler and more difficult to combat, is that where many people, even educated persons and high-profile politicians (even when rallying towards environmental protection and sustainable development), attribute perceived increases of hurricane activity with climate changes. While the question whether it is a pure coincidence that hurricane activity and climate changes is a perfectly legitimate one (from both civic and scientific perspectives), questions are not answers. Rhetoric has no scientific relevance or value. The reality is that there is no proven link between climate changes and hurricane activity. This does not mean that it does not exist; simply, we are not allowed to assume that there is a link. We can infer that such a link might exist, and we can pursue this hypothesis as a research goal. This confusion is more dangerous that it might appear at a first inspection, fore several reasons. First, replacing scientific research with assumptions and rhetoric cancels–by simple logic–the 'raison d'être" of science, meaning that skilled politicians can replace "if needed" science voices in the public arena. Second, such assumptions sap the efforts of scientists to communicate to the public some essential (and difficult for the laymen) scientific concepts like scientific proof, scientific uncertainty or non-linear dynamics (thresholds that make difficult–if possible at all–anticipations).

Such confusions must be carefully dealt with, because they have the unhappy potential to compromise urgent and essential efforts towards climate mitigation and adaptation. For example, many essential phenomena are the result of a set of factors, and therefore have no unique cause. Recent perceived changes in hurricanes dynamics, for instance, might be the result of a set of factors where climate plays a minor role. So, even if the climate has a contribution, the short answer will be that climate is not the cause of hurricane changes. From here, there is only one small step towards public opinion falling back into the discussion whether "climate changes even exist after all." Given the importance of acting early, we cannot afford such setbacks. In climate mitigation and adaptation, any delay could translate into a certain amount of irreversible loss (e.g., more human lives lost, more decent livelihood lost, and higher material losses).

18.3.2 A Paradigmatic Change is Necessary in Education

For any citizen, understanding climate changes requires a certain understanding of various domains of natural sciences (meteorology, geography, ecology, chemistry, physics), basic mathematics and statistic. Further, for a minimum understanding of risks related to climate changes and of potential options for mitigation of, and adaptations to, climate changes, any lay person needs to be knowledgeable – at basics – in social and economic issues. In a sense, education must become adapted to the reality that we already live in a knowledge society, where having a limpid delimitation of disciplines and professions does not suffice anymore. Education needs to help citizens becoming capable of understanding complex issues onto which they are being solicited to respond and often to vote on available options or even create those options. Education must aim at preparing the grounds for sustainable development, and thus acknowledge the systemic relations between environment degradation, and social and economic systems (e.g., Giddings *et al.* 2002).

In a sense, the evolution of education follows the evolution of science. Numerous fields of research are recent established disciplines, born from cross-interactions between two or several older disciplines. More and more, an essential skill of a scientist is the capacity to cope with the exponential increase in the number of publications in a field, briefly capacity to integrate knowledge. More and more, in order to be able to carry out relevant research, scientists need more than a core disciplinary expertise: they need acquiring understanding multiple fields and even multiple expertises. In addition, they need to be aware of priorities that may be established outside the academic domain. Nevertheless, borders between domains need not be blurred, but simply increase capacity to do and to optimize "cross-border" communication, problem co-definition, co-analysis of available options and potential actions in all major chapters of mitigation of environmental degradation (e.g., Pohl 2008; Scholz et al. 2009).

To put it briefly, a paradigmatic change in education is necessary in the sense that recent dynamics of (complex) problem-solving-oriented research in science, in the context of the urgency of sustainable development, will need to translate in education for problem-solving-oriented education. Ultimately, effective individual and collective action towards climate change mitigation and adaptation will depend on the capacity to take informed-decision.

18.4 Challenges and Controversies

Even though climate change is already an established reality and a very well-documented phenomenon, and despite the impressive advances in science, the intrinsic mechanisms and dynamics of climate change and the interrelated systems (notably the hydrosphere and the biosphere) are very poorly understood. This is due both (i) to the nature of science, with true interdisciplinary and transdisciplinary studies being at the beginning, and (ii) to the intrinsic complexity of nature, where a given overall climatic effect results from a plethora of factors and direct and indirect effects and multiple interactions. The first consequence of this situation is the serious difficulty in precisely predicting the effects of modifying parameters of one or another factor upon climate, even when the basic mechanisms are known. This uncertainty in understanding climate sensitivity is of paramount importance because it imposes drastic limits in designing policies for climate mitigation (Schwartz 2009). In the same time, this reality reminds the importance of using the precautionary principle of maintaining human interference in natural systems at minimum.

And that is the crux of climate change policies, because they ought to address previous human actions that are now acknowledged to represent climate forcing by human interference in the global biogeochemical cycles. The original problem started with interferences in the global cycle of carbon, the global cycle of water, and that of nitrogen and sulphur (dioxides), and that of other elements. While policies aim to attain predictable outcomes, the difficulty remains that the effects to be obtained do not result from simple "mechanistic": removing the change will not necessarily remove the effects, because the natural systems are too complex and once one or more thresholds have been passed, there is no way back. Therefore, in order to preserve the earth's conditions to which our species is ecologically adapted during millions of years, the most we can hope is to remove the cause, i.e., minimize further forcing upon the global biogeochemical cycles, hope that not too many thresholds have been passed, and then adapt to the changes that are here to stay. The word 'hope' is used here to signal the fact that our knowledge on biochemical cycles (and their thresholds and interferences) is very poor, which means that, in addition to being clearly disturbing the environment of which we depend, our forcing on the global biogeochemical cycles is blindfold. Geoengineering by the mediation of aerosol is therefore confronted with serious uncertainties. All in all, trying to make up for the climate consequences of blind forcing the biochemical cycle of carbon by another blind forcing (radiation forcing by aerososols) looks like the most inappropriate way to go.

Interference in the biogeochemical cycles should be kept to minimum, in order to avoid replacing one global environmental problem with another, especially because we do not fully understand the effects of such methods on the local and planetary systems. Therefore, geoengineering methods should only be considered as last resort, a sort of 'disperate' action, to which we should hope and do everything not to arrive to. If we will arrive to this, we will know already that our environment is fundamentally, drastically and irremediably changed, and that the urgent problem of climate change will only be replaced by other problems not less disturbing for the Earth and ecosystems. If we arrive at the point where we have to decide where to apply geoengineering, we will not choose between having one problem (dramatic climate change) or not. In fact we will be choosing what type of global disaster we want to have. Worse, if we arrive at this point, climate-related disasters will have already started to happen in cascades (following successive breaches of series of natural thresholds); so we will choose between (i) continuing to witness/undergo increasingly frequent and damaging climate disasters and (ii) adding a new type of disaster to the extant ones.

The next challenge follows, as how to adjust our way of development and living, so as to interfere less with the earth's biogeochemical cycles. As 85% of the world's primary energy is supplied by fossil fuels, significant reductions of the emissions and atmospheric concentration of CO_2 and other GHG can be conceived via policies based on current technologies. But stabilizing those concentrations around 450 ppm of CO_2 equivalents (the concentration of CO_2 that would produce the same amount of climate warming as the concentration of all GHG; corresponding to the goal of limiting global warming to 2°C) or even at 750 ppm will require a veritable technological revolution, where carbon would lose its central role (Barrett 2009). Because of risk of leakage, price and other problems of geological carbon trapping, other mitigation means–notably biological carbon trapping–are probably preferable to the geological trapping approach (e.g., Anderson and Newell 2004; Lal 2004). However, it is not clear whether this technique will have other obstacles, more difficult than the technical ones: social acceptability appears to be clearly very low for this type of mitigation option–even if the risk of leakage will be resolved, that may not convince local authorities to accept it (e.g., Schrag 2007). In any case, this debate is far from being finished, and it is a very complex one, involving both scientific and non-scientific aspects, of various domain claims–environmental, social and economic (e.g., Rai et al. 2010).

Another main challenge related to climate change mitigation is the role of cities. While more than half of the world human population lives in urban areas, and cities are the main engines for technological and economic development, cities are both a source of air pollution–hence climate forcing agents–and a source of change for pollution abatement, and climate mitigation and adaptation to climate change. Therefore, urban development and climate change are two inter-related and inter-dependent issues, and their relation has to be accounted for in policies and proposed solutions for coping with climate change (Parrish and Zhu 2009). Within the debates on both mitigation and adaptation to climate changes, yet another main contributing topic is the phenomenon of heat island effect of cities, which exacerbates health problems related to climate changes, and the effects on the local ecology (Grimm et al. 2008). In addition to having specific issues to deal with, cities may prove to weigh even more effectively in the future policy and managerial context of climate mitigation and adaptation to climate changes. Cities are more dynamic than nations and can afford to apply relevant policies even before nations may do it (e.g., Rosenzweig et al. 2010).

The precautionary principle–which states, briefly, that lack of knowledge is no mandate for blind action–need to be a driving principle in mitigation and adaptation. This of course does not prevent testing new options within the limits of what we know are reversible-correctible process. This is especially important when deciding upon global policies of climate mitigation, and particularly when the potential solutions taken into account involve other forcing of the biogeochemical cycles, like with aerosols or ocean iron fertilization (Guessow et al. 2010). Perhaps one of the most telling examples reflecting the importance of the precautionary principle is the situation of the carbon stored in the polar and sub-polar tundra. It is known that Polar Regions act as carbon sink because low temperatures during winter prevent the decay of the litter produced by vegetation during the polar summer. While Polar Regions are among the most affected by climate changes (along with high mountains areas), further warming, after a certain temperature threshold, will trigger a process of decay of the litter accumulated during millennia. Worse, emissions of methane, another GHG, will increase in that situation. The consequence will be that polar areas will cease functioning as carbon sink and will become instead net carbon emitters, accelerating global climate warming (e.g., Oechel et al. 1993).

But probably the overarching debate is between technological optimists, holding that technology got us in, so technology will get us out this unsustainability bottleneck, and technological skeptics, maintaining that technology development will only make things worse because it will continue to have this harmful effect upon the environment–ultimately upon the carrying capacity of the Planet. As human society developed via technological-economical paradigms, technology will definitely be part of the future solutions, though probably unable to provide along any “technological fixes.” The challenge and chance towards sustainability is therefore to become capable of efficient innovation for sustainable development, be it technological, social, managerial, or technological-social-economic. Briefly, the new endeavor of eco-innovation presents itself to us, meaning any innovation, at any level (product design and manufacture and consume, social, economic and managerial, etc.), that will help decoupling prosperity creation from environmental destruction. This aim is bound to be more difficult than "just" innovation, precisely because it will need to integrate constrains related to the finite character of the natural resources, to the non-linear behavior of nature (existence of thresholds), and to systemic perspective of sustainable development.

To conclude, the next technological-economic cycle of development humanity will probably be tailored according to the type and degree of success in achieving eco-innovation: capacity to both mitigate and adapt to environmental impacts of past human activities.

18.5 References

Adger, N. W. (2003). "Social capital, collective action and adaptation to climate change." *Economic Geography,* 79(4), 387–404.

Adger, N. W., Arnell, N. W., and Tompkins, E. L. (2005). "Successful adaptation to climate across scales." *Global Environmental Change*, 15, 77–86.

Akervoll, I., Zweigel, P., and Lindeberg, E. (2006). "CO_2 storage in open, dipping aquifers." In: *Proceedings of the 8th International Conference on Greenhouse Gas Control Technologies*, Elsevier, CD-ROM.

Anderson, A., and Newell, R. (2004). "Prospects for carbon capture and storage technologies." *Annual Review of Environment and Ressources*, 29, 109-142.

Arneth, A., Unger, N., Kulmala, M., Andreae, M. O. (2009). "Clean the air, heat the planet?" *Science*, 326, 672–673.

Aumont, O., and Bopp, L. (2006). "Globalizing results from ocean in situ iron fertilization studies." *Global Biogeochemical Cycles,* 20, GB 2017.

Backstrand, K. (2003). "Civic science for sustainability: reframing the role of experts, policy-makers and citizens in environmental governance." *Global Environmental Politics,* 3, 24–41.

Barrett, S. (2008). "The incredible economics of geoengineering." *Environmental and Resource Economics*, 39, 45–54.

Barrett, S. (2009). "The coming global climate-technology revolution." *Journal of Economic Perspectives*, 23(2), 53–75.

Bonan, G. B. (2008). "Forests and climate change: forcings, feedbacks, and the climate benefits of forests." *Science*, 320, 1444–1449.

Breon, F. M. (2006). "How do aerosols affect cloudiness and climate?" *Science*, 313(5787), 623–624.

Briskie, D. D., Fuehlendorf, S. D., and Smeins, F. E. (2006). "A unified framework for assessment and application of ecological thresholds." *Rangeland Ecology and Management*, 59(3), 225–236.

Clark, D. A. (2004). "Sources or sinks? the responses of tropical forests to current and future climate and atmospheric composition." *Philosophical Transactions of the Royal Society London* B, 359, 477–491.

Clark, D. A. (2007). "Detecting tropical forests' responses to global climatic and atmospheric change: current challenges and a way forward." *Biotropica*, 39(1), 4–19.

Crutzen, P. J. (2006). "Albedo enhancement by stratospheric sulphur injections. A contribution to resolve a policy dilemma?" *Climate Change*, 77, 211–219.

Duda, A. M., and El-Ashry, M. T. (2000). "Addressing the global water and environmental crisis through integrated approaches to the management of land, water and ecological resources." *Water International*, 25(1), 115–126.

Davis, S. J., and Caldeira, K. (2010). "Consumption-based accounting of CO_2 emissions." *Proceedings of the National Academy of Sciences*, 107(12), 5687–5692.

Ehrleringer, J. R., Sage, R. F., Flanagan, L. B., and Pearcy, R. W. (1991). "Climate change and the evolution of C_4 photosynthesis." *Trends in Ecology and Evolution*, 6(3), 95–99.

Flores, O., Gritti, E. S., and Jolly, D. (2009). "Climate and CO_2 modulate the C_3/C_4 balance and $\delta^{13}C$ signal in simulated vegetation." *Clim. Past*, 5, 431–440.

Georgescu, S., Lindeberg, E., and Holt, T. (2006). "Co-injection of CO_2 and water into non-sealed saline aquifers." In: Proceedings of the 8th International Conference on Greenhouse Gas Control Technologies, Elsevier, CD-ROM.

Giddings, B., Hopwood, B., and O'Brian, G. (2002). "Environment, economy and society: fitting them together into sustainable development." *Sustainable Development*, 10, 187–196.

Gonzalez-Meler, M. A., Blanc-Betes, E., Flower, C. E., Ward, J. K., and Gomez-Casanovas, N. (2010). "Plastic and adaptive responses of plant respiration to changes in atmospheric CO_2 concentrations." *Physiologia Plantarum*, 137(4), 473–484.

Grimm, B. N, Faeth, S. H., Golubiewski, N. B., Redman, C. L., Wu, J., Bai, X., and Briggs, J. M. (2008). "Global change and the ecology of cities." *Science*, 319, 756–760.

Guessow, K. Proelss, A., Oschlies, A., Rehdanz, K., and Rickels, W. (2010). "Ocean iron fertilization: Why further research is needed." *Marine Policy*, 34(5), 911–918.

Heartel, C. E. J., and Pearman, G. I. (2010). "Understanding and responding to the climate change issue: Towards a whole-of-science research agenda." *Journal of Managemnt and Organization*, 16, 16–47.

Hellstroem, T. (2007). "Dimensions of environmentally sustainable innovation: The structure of eco-innovation concepts." *Sustainable Development*, 15, 148–159.

Huang, Y, Steet-Perrott, F. A., Metcalfe, S. E., Brenner, M., Moreland, M., Freeman, K. H. (2001)."Climate change as the dominant control on glacial-interglacial variations in C_3 and C_4 plants." *Science*, 293(5535), 1647–1651.

Huang, Y., Shuman, B., Wang, Y., Web III, T., Grimm, E.C., and Jacobson Jr., G. L. (2006). "Climatic and environmental controls on the variation of C_3 and C_4 plant abundances in Central Florida for the past 62,000 years." *Palaeogeography, Palaeoclimatology, Palaeooecology*, 237(2–4), 428–435.

Hufbauer, G. C., and Kim, J. (2010). "After the flop in Copenhagen." *Policy Brief*, 10(4), 1–11.

IPCC-WGI (2007). “Climate Change 2007: The Physical Science Basis.” *Contribution of Working Group I to the Fourth Assessment Report of the Intergovernmental Panel on Climate Change.* Cambridge University Press, Cambridge, UK and New York, NY, USA, 996 pp. Available at <http://www.ipcc.ch/publications_and_data/ar4/wg1/en/contents.html> (accessed Feb. 2012).

IPCC-WGII (2007). “Climate Change 2007: Impacts, Adaptation and Vulnerability.” *Contribution of Working Group II to the Fourth Assessment Report of the Intergovernmental Panel on Climate Change.* Cambridge University Press, Cambridge, UK, 976 pp. Available at <http://www.ipcc.ch/publications_and_data/ar4/wg2/en/contents.html> (accessed at Jan. 2012).

IPCC-WGIII (2007). “Climate Change 2007: Mitigation.” *Contribution of Working Group III to the Fourth Assessment Report of the Inter-governmental Panel on Climate Change*. Cambridge University Press, Cambridge, UK and New York, NY, USA., XXX pp. Available at <http://www.ipcc.ch/publications_ and _data/ar4/wg3/en/contents.html> (accessed Feb. 2012).

Kaufman, Y. J., Tanre, D., and Boucher, O. (2002). "The satellite view of aerosols in the climate system." *Nature*, 419, 215–223.

Kuerschner, W. M, and Kvacek, Z. (2009). "Oligocene-Miocene CO_2 fluctuations, climatic and palaeofloristic trends inferred from fossil plant assemblages in central Europe." *Bulletin of Geosciences*, 84(2), 189–202.

Kimball, B. A., Kobayashi, K., and Bindi, M. (2002). "Responses of agricultural crops to free-air CO_2 enrichment." *Advances in Agronomy,* 77, 293–368.

Kravitz, B., Robock, A., Oman, L., Stenchikov, G., and Marquardt, A. B. (2009). "Sulfuric acid deposition from stratospheric geoengineering with sulfate aerosols." *Journal of Geophysical Research*, 114, D14109.

Lal, R. (2004). "Soil carbon sequestration to mitigate climate change." *Geoderma*, 123, 1–22.

Lenton, T. M., and Vaughan, N. E. (2009). "The radiative forcing potential of different climate geoengineering options." *Atmospheric Chemistry and Physics*, 9, 5539–5561.

Lorenzoni, I., and Pidgeon, N. F. (2006). "Public views on climate change: European and USA perspectives." *Climatic Change*, 77, 73–95.

Le Quere, C., Raupach, M. R., Canadell, J. G., Marland, G., Bopp, L., Ciais, P., Conway, T. J., Doney, S. C., Feely, R. A., Foster, P., Friedlingstein, P., Gurney, K., Houghton, R. A., House, J. I., Huntingford, C., Levy, P. E., Lomas, M. R., Majkut, J., Metzl, N., Ometto, J. P., Peters, G. P., Prentice, I. C., Randerson, J. T., Running, S. W., Sarmiento, J. L., Schuster, U., Sitch, S., Takahashi, T., Viovy, N., van der Werf, G. R., and Woodward, F. I. (2009). "Trends in the sources and sinks of carbon dioxide." *Nature Geosciences*, 2, 831–836.

Lubchenco, J. (1998). "Entering the century of the environment: a new social contract for science." *Science*, 279, 491–497.

Manning, M. R., Edmonds, J., Emori, S., Grubler A., Hibbard, K., Joos, F., Kainuma, M., Keeling, R. F., Kram, T., Manning, A. C., Mainshausen, M., Moss, R., Nakicenovic, N., Riahi, K., Rose, S. K., Smith, S., Swart, R., and van Vuuren, D. P. (2010). "Misrepresentation if the IPCC CO_2 emission scenarios" *Nature Geosciences*, 3, 376–377.

Mawdsley, J. R., O'Malley, R., and Ojima, D. S. (2009). "A review of climate-change adaptation strategies for wildlife management and biodiversity conservation." *Conservation Biology*, 23(5), 1080–1089.

Mazzotti, M., Pini, R., and Storti, G. (2009). "Enhanced coalbed methne recovery." *The Journal of Supercritical Fluids*, 47, 619–627.

Menon, S. (2004). "Current Uncertainties in Assessing Aerosol Effects on Climate." *Annual Review of Environment and Resources*, 29, 1–30

Michaelowa, A. (2010). "Copenhagen and consequences." *Intereconomics*, 45(1), 2–3.

Muradian, R. (2001). "Ecological thresholds: A survey." *Ecological Economics*, 38, 7–24.

Oechel, W. C., Hastings, S. J., Vourltis, G., Jenkins, M., Riechers, J., and Grulke, N. (1993). "Recent change of arctic tundra ecosystems from net carbon dioxide sink to a source." *Nature*, 361, 520–523.

Osborne, C. P., and Beering, D. J. (2006). "Nature's green revolution: the remarkable evolutionary rise of C_4 plants." *Philosophical Transactions of the Royal Society,* B, 361, 173–194.

Osborne, C. P., and Freckleton, R. P. (2009). "Ecological selection pressures for C_4 photosynthesis in the grasses." *Proceedings of the Royal Society* B, 276, 1753–1760.

Parrish, D. D., and Zhu, T. (2009). "Clean air for megacities." *Science*, 326(5953), 674–675.
Penner, J. E., Chuang, C., and Grant, K. (1998). "Climate forcing by carbonaceous and sulphate aerosols." *Climate Dynamics*, 14, 839–851.
Perez, C. (2009). "The double bubble at the turn of the century: Technological roots and structural implications." *Cambridge Journal of Economics*, 33, 779–805.
Perez, C. (2010). "Technological revolutions and techno-economic paradigms." *Cambridge Journal of Economics*, 34, 185–202.
Peters, G. P., Marland, G., Hertwich, E. G., Saikku, L., Rautianen, A., and Kauppi, P. (2009) "Trade, transport, and sinks extend the carbon dioxide responsibility of countries: An editorial essay." *Climatic Change*, 97(3–4), 379–388.
Pohl, C. (2008). "From science to policy through transdisciplinary research." *Environmental Science and Policy*, 11, 46–53.
Rai, V., Victor, D. G., and Thurber, M. C. (2010). "Carbon capture and storage at scale: Lessons from the growth of analogous energy technologies." *Energy Policy*, 38, 4089–4098.
Ramanathan, V. Crutzen, P. J., Kiehl, J. T., and Rosenfeld, D. (2001). "Aerosols, climate, and the hydrological cycle." *Science*, 294, 2119–2124.
Ramanathan, V., and Xu, Y. (2010). "The Copenhagen Accord for limiting global warming: Criteria, constraints, and available avenues." *Proceedings of the National Academy of Sciences*, 107(18), 8055–8062.
Ricke, K. L., Morgan, M. G., and Allen, M. R. (2010). "Regional climate response to solar radiation management." *Nature Geosciences*, 3, 537–541.
Robock, A., Marquardt, A., Kravitz, B., and Stenchikov, G. (2009). "Benefits, risks, and costs of stratospheric geoengineering." *Geophysical Research Letters*, 36, L19703.
Rogelj, J., Nabel, J., Chen, C., Hare, W., Markmann, K., Meinshausen, M., Schaeffer, M., Macey, K., and Hoehne, N. (2010). "Copenhagen Accord pledges are paltry." *Nature*, 464, 1126–1128.
Rosenzweig, C., Solecki, W., Hammer, S. A., and Mehrotra, S. (2010). "Cities lead the way in climate change action." *Nature*, 467(7318), 909–911.
Schnoor, J. L. (2010). "Copenhagen Accord: What if it's broken?" *Environmental Science and Technology*, 44(3), 852–852.
Scholz, R. W, Spoerri, A., and Lang, D. J. (2009). "Problem structuring in transitions: the case of Swiss waste management." *Futures*, 41(3171–181.),
Schrag, D. P. (2007). "Preparing to capture carbon." *Science*, 315(5813), 812–813.
Schwartz, S. E. (2008). "Uncertainty in climate sensitivity: causes, consequences, challenges." *Energy and Environmental Science*, 1, 430–453.
Serezze, M. C. (2010). "Understanding recent climate change." *Conservation Biology*, 24(1), 10–17.
Shindell, D. T., Faluvegi, G., Koch, D. M., Schmidt, G. A., Unger, N., and Bauer, S. E. (2009). "Improved attribution of climate forcing to emissions." *Science*, 326 (5953), 716–718.
Slack, C. R., and Hatch, M. D. (1967). "Comparative studies on the activity of carboxylases and other enzymes in relation to the new pathway of

photosynthetic carbon dioxide fixation in tropical grasses." *The Biochemical Journal*, 103(3), 660–665.

Suekane, T., Nobuso, T., Hirai, S., and Kiyota, M. (2008) "Geological storage of carbon dioxide by residual gas and solubility trapping." *International Journal of Greenhouse Gas Control*, 2(1), 58–64.

Ward, J. K., Myers, D. A., and Thomas, R. B. (2008). "Physiological and growth responses of C_3 and C_4 plants to reduced temperature when grown at low CO_2 of the last ice age." *Journal of Integrative Plant Biology*, 50(11), 1388–1395.

Williams, J. W., Jackson, S. T., and Kutzbach. J. E. (2007). "Projected distributions of novel and disappearing climates by 2100." *Proceedings of the National Academy of Sciences*, 104(14), 5738–5742.

Xu, J., Grumbine, E., Shresta, A., Eriksson, M., Yang, X., Wang, Y., and Wilkes, A. (2010). "The melting Himalayas: Cascading effects of climate change on water, biodiversity, and livelihoods." *Conservation Biology*, 23(3), 520–530.

CHAPTER 19

Enhancing Verdurization for Mitigating Climate Change

C. M. Kao, T. T. Tsai, Y. T. Tu, R. Y. Surampalli, and Tian C. Zhang

19.1 Introduction

The vegetation types, distribution on plant species, and agricultural cropping patterns demonstrate that the climate has very strong control on the growth of plants. Solar radiation, temperature and precipitation values and seasonal patterns are key determinants of plant growth through a variety of direct and indirect mechanisms. Other climatic characteristics such as wind speed and storm frequency are also major influences. There are a rapidly growing number of well-documented instances of change in ecosystems due to climate change (Walther et al. 2002; Lindner et al. 2010; Ogawa-Onishi et al. 2010). In agriculture, there are clear examples of climate change affecting plant growth and cropping potential or performance. Shen et al. (2005) reported that the potential maize-growing zone, defined by temperature limits, has shifted north by 200–300 km over the last century in Alberta, Canada. However, climate change is not just affecting temperate zones. The Intergovernmental Panel on Climate Change (IPCC) also concluded that there is high confidence that regional changes in temperature have had discernible impacts on many physical and biological systems (IPCC 2001a–c). These recent climate changes are likely to accelerate as human activities continue to perturb the climate system, and many reviews have made predictions of serious consequences for ecosystems and for supplies and security.

Plants take carbon from the atmosphere and store it in their biomass and in soils. Thus land use and land management are important tools in mitigating climate change. Furthermore, plant biomass can be used as a bioenergy source, offsetting the use of fossil fuels and reducing carbon emissions (Girardin et al. 2008; Garrett et al. 2009). Avoiding deforestation, increasing plant storage through afforestation and substituting bioenergy for fossil fuels all use the land resources to reduce climate change. Policy makers are currently making decisions, negotiating targets, and agreeing accounting methodologies and rules based around these options. Furthermore, there is a need for integrated scientific information comparing different options, opportunities and consequences.

The main objectives of this chapter are to (1) describe the theories of photosynthesis and its effects on climate change, (2) evaluate the effects of climate changes on the growth of crops and forest vegetation, (3) illustrate the role of forest in carbon sequestration, and (4) describe the climate change mitigation by enhanced verdurization and wetland systems. Thus, the readers could understand the linkages and relationships among climate change, vegetation and how to mitigate the climate change impact through enhanced verdurization.

19.2 Mechanisms of Anthropogenic Climate Change

The totality of the atmosphere, hydrosphere, biosphere, and geosphere and their interactions via physical, biological and chemical processes constitute the climate system. Solar radiation is the major driving force of the global climate conditions (Schurgers et al. 2008). Part of the radiation reaching Earth's surface is scattered or reflected by aerosols, dusts, clouds, and other particles. Thus, the part of the radiation is absorbed causing the Earth to emit thermal radiation and some radiation is reflected back to the atmosphere. There is general consensus among the scientific community that increasing atmospheric levels of the greenhouse gases (GHG) are causing climate change.

The human activities are the main causes of the increase in the concentration of radiatively active gases and added new GHG such as halocarbons and hexafluoride (IPCC 2001d). Together with changes in land cover, this may have contributed to an enhanced greenhouse effect causing global warming and other climatic changes. The recent and future anthropogenic changes to the climate have to be considered in the context of natural climate changes. The Earth's climate results from the complex interaction of many components: the ocean, atmosphere, geosphere, cryosphere, and biosphere (IPCC 1997). Although the climate system is driven by the external solar energy, changes to any of the internal components, and how they interact with each other, as well as variability in the solar radiation received can lead to changes in climatic conditions. Therefore, there are many factors causing the occurrence of climate change that operate on a variety of timescales (IPCC 2001d).

Although most public discussion on climate change currently focuses on fossil fuel combustion, CO_2 emissions and the enhanced greenhouse effect, it must be noted that there are other components of human-induced climate change. Human activity has modified, and continues to modify, the Earth's surface on a very large scale, through deforestation, afforestation, cultivation, mineral extraction, irrigation, drainage, and flooding. The key point of the enhanced greenhouse effect is that human modification of the atmospheric concentration of the key radiation-absorbing gases (CO_2, CH_4, N_2O, and various halocarbons) has resulted in a radiative forcing of the climate system. These gases have been released primarily as a result of industrial, domestic, and agricultural activities and land use changes (Ramanathan and Feng 2009). Direct and indirect determination of CO_2, CH_4, and N_2O in the atmosphere over the past 1000 years show marked and unprecedented increases in concentrations in recent times. Thus, increased atmospheric concentrations of CO_2, CH_4, N_2O and halocarbons are estimated to have placed an additional 2.4 W/m^2 of radiative forcing onto the climate system since 1750 (IPCC 2001a).

To understand effects of temperature on plant growth, more information needs to be obtained than just data on changes to the mean global annual temperature. Investigation results from other studies show that (a) the Post-industrial Warming has affected the mid to high latitudes of the Northern Hemisphere the most, (b) the winter months have warmed more rapidly than summer months, and (c) that night-time temperature are more affected than the day time temperatures (IPCC 2001a; Viner et al. 2006). In addition, there has been a reduction in the frequency of extreme low monthly and seasonal average temperatures across much of the globe and a small increase in the frequency of extreme high temperatures (IPCC 2001a). In addition to the changes in temperature and precipitation, there have been substantial changes in solar irradiance. Stanhill and Cohen (2001) indicated that solar radiation receipt at the surface has varied substantially over decadal timescales, and will change in the future with changes in cloud and aerosol load. The effect of this on plant growth is rarely directly considered.

19.3 Plant Biology and Photosynthesis

There is unprecedented scientific and societal emphasis on assessing future anthropogenic changes in global temperature and subsequent impacts on managed and unmanaged systems. Yet, the principle anthropogenic gas associated with this potential warming, CO_2, is also one of the four abiotic requirements necessary for plant growth (e.g., light, nutrients, water, and CO_2). Any change in the availability of these abiotic parameters, particularly on a global scale, will cause impacts on plant biology and all living systems. Recent data indicate that plants may already be responding to both diurnal and urban-induced differences in atmospheric CO_2. Such studies emphasize that CO_2 may be increased no-uniformly and illustrate the critical need for research that increases our fundamental understanding of how plant biology will respond to changing CO_2 environments (Ziska and Bunce 2006).

Photosynthesis usually occurs within the leaves of plants. Since photosynthesis requires CO_2, water, and sunlight, all of these substances must be obtained by or transported to the leaves. Plants use sunlight to convert water, CO_2, and nutrients into sugars and carbohydrates, which accumulate in their tissues (Nelson 2011). Plants also respire, releasing CO_2. Plants eventually die, releasing their stored carbon to the atmosphere quickly or to the soil where it decomposes slowly and increases soil carbon levels. Carbon dioxide is obtained through tiny pores in plant leaves called stomata. Oxygen is also released through the stomata. Water is obtained by the plant through the roots and delivered to the leaves through vascular plant tissue systems. Sunlight is absorbed by chlorophyll, a green pigment located in plant cell structures called chloroplasts (Nelson 2011). Chloroplasts are the sites of photosynthesis. Chloroplasts contain several structures, each having specific functions (Niu et al. 2008; Nelson 2011): (1) outer and inner membranes: protective coverings that keep chloroplast structures enclosed; (2) stroma: dense fluid within the chloroplast (site of conversion of carbon dioxide to sugar); (3) thylakoid: flattened sac-like membrane structures (site of conversion of light energy to chemical energy); (4) grana: dense layered stacks of thylakoid sacs (sites of conversion of light energy to chemical energy); and (5) chlorophyll: a green pigment within the chloroplast (absorbing light energy).

In summary, photosynthesis is a process in which light energy is converted to chemical energy and used to produce organic compounds. In plants, photosynthesis occurs within the chloroplasts. Photosynthesis consists of two stages, the light reactions and the dark reactions. The light reactions convert light into energy and the dark reactions use the energy and CO_2 to produce sugar (Niu et al. 2008; Nelson 2011). Previous studies have shown that climatic warming may directly stimulate, restrain indirectly through warming-induced water stress, or do not impact photosynthesis of plant species (Apple et al. 2000; Loik et al. 2000; Starr et al. 2000; Pearson and Dawson 2003; Llorens et al. 2004). The inconsistent observations suggest plant photosynthesis in response to climatic warming might be species specific. Differential responses of photosynthesis to rising temperature could change C accumulation, growth, and biomass production of different plant species, which in turn affects their competitive abilities, coverage, and dominance in the community. Therefore, a better understanding of the responses of photosynthesis in different plant species and/or functional types to increased temperature could help predict the potential changes in species composition and ecosystem C cycling under global warming (Niu et al. 2008).

Long-term exposure to changes in temperature can result in plant acclimation. Thermal acclimation of photosynthesis refers to the shift in the photosynthesis-temperature relationship of plants under the altered temperature regime (Bolstad et al. 2003; Yamori et al. 2005). By changing the optimum temperature of photosynthesis, plants can keep efficient photosynthesis at the new growth temperature. Most studies on thermal acclimation of photosynthesis were conducted in the laboratory with constant temperature regimes (Xiong et al. 2000; Bolstad et al. 2003; Yamori et al. 2005). However, there are strong seasonal and diurnal variability in the magnitudes of temperature increase under global warming (IPCC 2007). Therefore, consistent changes in temperature used in the laboratory are obviously unable to simulate the realistic temperature changes under natural conditions (Loik et al. 2000; Llorens et al. 2004).

The influences of increases in CO_2 on gene expression, particularly for photosynthetic regulation of the small subunit of Ribulose-1,5-bisphosphate carboxylase (rubisco), have been examined in a number of studies (Makino et al. 2000; Ziska and Bunce 2006). Genetic regulation is thought to be mediated by increased sugar levels resulting from exposure to future CO_2 concentrations. However, other researchers indicated that high CO_2-induced decline in photosynthetic gene transcripts was due to a temporal shift in leaf ontogeny (Ludewig and

Sonnewald 2000). Changes in gene expression may provide crucial insights into specific mechanisms or cellular systems that may be regulated by changes in atmospheric CO_2, but the mechanistic basis for such changes, whether they involve carbohydrate accumulation or accelerated ontogeny are unclear. Analyses of transcript profiles from microarray experiments, particularly from plants grown from seed in the field over a range of CO_2 values, may be of particular benefit for breeding programs (Ziska and Bunce 2006).

19.4 Impact of Climate Change on Plant Growth and Biodiversity

Environmental and climate conditions play key roles in determining the major functions and distribution of plants. Changes in long-term environmental and climate conditions can cause significant impacts on plant diversity patterns. It is predicted that climate change will remain one of the major drivers of biodiversity patterns in the future (Green et al. 2003; Milad et al. 2011).

There are increased interest and research focus on the phenomenon of recent anthropogenic climate changes. Focus is on identifying the current impacts of climate change on biodiversity, and predicting these effects into the future. Changing climatic variables relevant to the function and distribution of plants include increasing CO_2 concentrations, increasing global temperatures, altered precipitation patterns, and changes in the pattern of extreme weather events (de Chazal and Rounsevell 2009). Because individual plants can only function physiologically, and successfully complete their life cycles under specific environmental conditions, changes to climate are likely to have significant impacts on plants from the level of the individual right through to the level of the ecosystem (de Chazal and Rounsevell 2009).

19.4.1 CO_2 Effects

Increases in atmospheric CO_2 concentration affect how plants photosynthesise, resulting in increases in plant water use efficiency, enhanced photosynthetic capacity and increased growth (Steffen and Canadell 2005). Increased CO_2 has been implicated in ‘vegetation thickening’ which affects plant community structures and function (Gifford and Howden 2001). Depending on environmental conditions, there are differential responses to elevated atmospheric CO_2 between major functional types of plants, or more or less woody species. Increased CO_2 can also lead to increased carbon to nitrogen ratios in the leaves of plants or in other aspects of leaf chemistry, possibly changing herbivore nutrition (Dukes and Mooney 1999).

It has been known that vegetative growth, development, and yield can be enhanced when the atmospheric CO_2 concentration increases. This is the principle in horticultural practice of CO_2 enrichment in greenhouses (Florides and Christodoulides 2009). Where control of CO_2 concentration is employed it is often, for economic reasons, maintained at about 1,000 ppm CO_2 (or approximately three times ambient). However, it is generally found that yield increases with CO_2 until concentrations of several thousand ppm are reached. Thus, it is likely that well-watered and adequately nourished plants will benefit from the increases in global atmospheric CO_2. The global CO_2 concentration is likely to continue to increase until all fossil fuel is used up. Results from Florides and Christodoulides (2009) indicate that the reaction of plants would cause the elevated CO_2 levels, and the air pollutants (e.g., O_3, SO_2 and NO_X) would result in CO_2-enriched and no-enriched plants.

Gifford et al. (1996) outlined a series of interconnected phenomena from simple physiological changes in individual plants to potential changes in species composition, which may occur over various timescales. However, only a small subset of species and physical processes are critical in forming the structure and overall behavior of complex terrestrial ecosystems (Holling et al. 1996). A major difficulty lies in the scaling-up from plant processes to processes that apply to vegetation in an ecosystem (Woodward 2002).

19.4.2 Temperature Effects

Increases in temperature raise the rates of physiological processes such as photosynthesis in plants. Extreme temperatures can be harmful when beyond the physiological limits of plants. In middle and higher latitudes, global warming will extend the length of the potential growing season, allowing earlier planting of crops in the spring, earlier maturation and harvesting, and the possibility of completing two or more cropping cycles during the same season (Florides and Christodoulides 2009). Crop-producing areas may expand pole ward in countries such as Canada and Russia, although yields in higher latitudes will likely be lower due to the less fertile soils that lie there. Many crops have become adapted to the growing-season day lengths of the middle and lower latitudes and may not respond well to the much longer days of the high latitude summers. In warmer, lower latitude regions, increased temperatures may accelerate the rate at which plants release CO_2 in the process of respiration, resulting in less than optimal conditions for net growth. When temperatures exceed the optimal for biological processes, crops often respond negatively with a steep drop in net growth and yield (Florides and Christodoulides 2009). If nighttime temperature minima rise more than do daytime maxima, heat stress during the day may be less severe than otherwise, but increased nighttime respiration may also reduce potential yields. Another important effect of high temperature is accelerated physiological development, resulting in hastened maturation and reduced yield (Green et al. 2003).

On the other hand, the higher air temperatures will also be felt in the soil, where warmer conditions are likely to speed the natural decomposition of organic matter and to increase the rates of other soil processes that affect fertility. Additional application of fertilizer may be needed to counteract these processes and to take advantage of the potential for enhanced crop growth that can result from increased atmospheric CO_2. This can come at the cost of environmental risk, for additional use of chemicals may impact water and air quality (Rosenzweig and Hillel 1995). The continual cycling of plant nutrients such as carbon, nitrogen, phosphorus, potassium, and sulfur in the soil-plant-atmosphere system is also likely to accelerate in warmer conditions, enhancing CO_2 and N_2O greenhouse gas emissions (Green et al. 2003).

19.4.3 Water Effects

Because water supply is an important factor for plant growth, it plays a key role in determining the distribution of plants. Changes in precipitation are predicted to be less consistent than for temperature and more variable between regions, with predictions for some areas to become much wetter, and some much drier. Agriculture of any kind is strongly influenced by the availability of water. Climate change will modify rainfall, evaporation, runoff, and soil moisture storage. Changes in total seasonal precipitation or in its pattern of variability are important. The moisture stress during flowering, pollination, and grain-filling is harmful to most crops (Green et al. 2003). Increased evaporation from soils and accelerated transpiration in the plants themselves will cause moisture stress, and there will be a need to develop crop varieties with greater drought tolerance (Rosenzweig and Hillel 1995; Green et al. 2003).

Water demand for irrigation is projected to rise in a warmer climate, bringing increased competition between agriculture in semiarid regions and urban as well as industrial users. Falling water tables and the resulting increase in the energy needed to pump water will make the practice of irrigation more expensive. Peak irrigation demands are also predicted to rise due to more severe heat waves. Intensified evaporation will increase the hazard of salt accumulation in the soil (Rosenzweig and Hillel 1995; Green et al. 2003).

19.4.4 General Effects

Environmental variables not only act in isolation, but also act in combination with one another, and with other pressures such as habitat degradation and loss or the introduction of exotic species (Mackey 2007). It is suggested that these drivers of biodiversity change will act in synergy with climate change to increase the pressure on species to survive (Mackey 2007).

19.5 Impact of Climate Change on Plant Diseases

Plant growth patterns can be used as an indicator of the impact of climate change on plants (De Wolf and Isard 2007). Change in species distribution and community composition could be preceded by a change in plant growth. Trees and crops are two plant categories whose growth is measured. Plant disease risk is strongly influenced by environmental conditions (De Wolf and Isard 2007). Climate change may have impacts on the occurrence of safety hazards at various stages of the chain, from primary production through to consumption. There are multiple pathways through which climate related factors may impact safety, including: changes in temperature and precipitation patterns, increased frequency and intensity of extreme weather events, and ocean warming and acidification. Climate change may also affect socio-economic aspects related to systems such as agriculture, animal production, global trade, demographics, and human behavior, which all influence safety (Tirado et al. 2010).

A consideration of potential impacts of global climate on plant population structure and dynamics, micro-evolutionary processes, and plant community structure must be a prerequisite to the discussion of climate change impacts on plant diseases (Chakraborty et al. 2000). Potential impacts are relatively easy to determine in monoculture that dominate intensive agricultural systems. Many assessments of potential impact on particular agricultural crops are available (Alcamo et al. 2007). Some integrated studies for regions, countries or the world focus on the security of supply under climate change (Masutomi et al. 2009). Many only consider direct effects of changing mean climate, while some include the physiological effects of increasing CO_2 (Tubiello and Ewert 2002).

19.6 Climate Change Mitigation by Forests

19.6.1 Forest and Carbon Cycle

Carbon sequestration and release vary substantially by forest. Because of the relative similarity of forests, some generalizations are possible. Tropical forests are recognized as terrestrial ecosystems that exert significant influences on regional/global energy and water cycling because they comprise 60% of all global forest areas (FAO 1988, 2001), and are located in regions of high solar radiation and evaporation (Tanaka et al. 2008; Peng et al. 2009). Some tropical forests are relatively dry, open woodlands, but many receive heavy rains and are called moist or humid tropical forests.

Moist tropical forests are important for carbon sequestration, and they usually have very high carbon contents averaging nearly 110 tons per acre (Tanaka et al. 2008). About half of the carbon in moist tropical forests is contained in the vegetation, a higher percentage and a much higher quantity than in any other biome. The remaining carbon is in tropical forest soils. Tropical forest soils have only modest carbon levels, because the dead biomass rapidly decomposes in the warm and humid conditions and the minerals rapidly leach out of tropical forest soils (Tanaka et al. 2008). Temperate forests are areas with high levels of precipitation and humidity. These forests also contain a variety of deciduous trees. Deciduous trees lose their leaves in winter. Temperate forests typically occur in the mid-latitudes-generally to about 50° north and south of the Equator. There are a large variety of temperate forests, including hardwood types, softwood types, lodgepole pine, and a few mixed types. However, within each forest type, temperate forests have much lower tree species diversity than tropical forests (Raymond and Bauer 2001). Temperate forests generally contain less carbon than tropical forests, averaging nearly 70 tons per acre. More than one-third of the carbon is stored in the vegetation, and nearly two-thirds in the soil. Many of these forests are managed to produce commercial wood products, and the management practices used in temperate forests can thus have a significant impact on carbon sequestration (Tanaka et al. 2008).

The Boreal Forests are immense, and they are dominated by conifers-mostly spruce, fir, and larch, with scattered birch and aspen stands. Boreal forests generally contain more carbon than temperate or tropical forests, averaging more than 180 tons per acre. Less than one-sixth of boreal forest carbon is in vegetation (Tanaka et al. 2008); the rest is in boreal forest soils, which is about three times the amount in temperate and tropical forests. Carbon accumulates to high levels in boreal forest soils because of the very slow decomposition rates, owing to the short summers and high acidity of conifer forest soils, both of which inhibit decomposition. The high boreal forest soil carbon level is important for carbon cycling, because many believe that management activities that disturb boreal forest soils can increase their release of carbon (Tanaka et al. 2008).

Forests are a significant part of the global carbon cycle. The ability of forests to store and sequester atmospheric carbon is well known and established (Bolin et al. 2000; Tanaka et al. 2008). Forests represent the largest global terrestrial store of carbon (Bolin et al. 2000). Terrestrial ecosystems are both sources and sinks for carbon. Forests sequester carbon emissions from the atmosphere and store the carbon long term in vegetation and soils. Land use and land use change affect the rate of carbon uptake by forests and the stock of carbon stored in forest sinks. Restoring, expanding, or preserving forest areas can expand or protect global carbon stocks. Forest clearing reduces carbon sequestration and releases stored carbon into the atmosphere (IPCC 2000). Deforestation has produced more than 25% of the carbon emissions from human activity over the last two decades. The largest terrestrial carbon stocks are located in forests in the tropics, where deforestation rates are highest. More than 90% of the carbon released from land use change during the 1980s resulted from deforestation in the tropics (IPCC 2000; Sedjo 2001). Slowing tropical deforestation can significantly reduce global carbon emissions and promote sustainable development (Sheeran 2006).

In forests, many different processes are responsible for carbon transfer including photosynthesis, respiration, and combustion. The net exchange of carbon between a forest and the atmosphere is determined by photosynthesis and respiration by trees, both processes occur above and below ground, and decomposition of soil organic matter. The rate of carbon sequestration is affected by many factors, including tree species, yield class, soil type, management activities such as harvesting and fertilization and previous land use (Sedjo et al. 2001; Byrne and Black 2003; Gorte 2009). When vegetation dies, carbon is released to the atmosphere. For herbaceous plants, the aboveground biomass dies annually and begins to decompose right away, but for woody plants, some of the above-ground biomass continues to store carbon until the plant dies and decomposes. This is the essence of the carbon cycle in forests-net carbon accumulation with vegetative growth, and release of carbon when the vegetation dies. The amount of carbon sequestered in a forest is constantly changing with growth, death, and decomposition of vegetation (Gorte 2009).

Carbon is the organic content of the soil, generally in the partially decomposed vegetation (humus) on the surface and in the upper soil layers, in the organisms that decompose vegetation (decomposers), and in the fine roots. The amount of carbon in soils varies widely, depending on the environment and the history of the site. Soil carbon accumulates as dead vegetation is added to the surface and decomposers respond. Soil carbon is also slowly released to the atmosphere as the vegetation decomposes. Scientific understanding of the rates of soil carbon accumulation and decomposition is currently not sufficient for predicting changes in the amount of carbon sequestered in forest soils (Giardina and Ryan 2002; Gorte 2009).

19.6.2 The Role of Forest in Carbon Sequestration

The process of photosynthesis combines atmospheric carbon dioxide with water, subsequently releasing oxygen into the atmosphere and incorporating the carbons into the plant cells. Forest soils can also capture carbon. Trees, unlike annual plants that die and decompose yearly, are long-lived plants that develop a large biomass, thereby capturing large amounts of carbon over a growth cycle of many decades. A forest ecosystem can capture and retain large volumes of carbon over long periods (Sedjo 2001; Evans et al. 2006; Roulet and Moore 2006; Lemma, et al. 2007). A young forest, when growing rapidly, can sequester relatively large volumes of additional carbon roughly proportional to the forest's growth in biomass. An old forest acts as a reservoir, holding large volumes of carbon even if it is not experiencing net growth. Therefore, a young forest holds less carbon, but it is sequestering additional carbon over time (Gorte 2009).

An old forest may not be capturing any new carbon but can continue to hold large volumes of carbon as biomass over long periods of time. Managed forests offer the opportunity for influencing forest growth rates and providing for full stocking, both of which allow for more carbon sequestration (Sedjo 2001; Karnosky 2003). As forest biomass expands, the amount of carbon contained increases. As the biomass contracts, the forest holds less carbon. Forest disturbance regimes are part of the natural ecological system, with wind, disease, fire and other natural events causing forest destruction and death. These events result in the release of carbon into the atmosphere but also are typically followed by the regrowth of the forest, which begins a new process of carbon buildup in the forest. Carbon release is occasioned by the disturbance and often in the decay and decomposition of dead matter that follows. Most natural forests have provisions for natural regeneration and regrowth, which, once again, captures carbon (Sedjo 2001; Byrne and Black 2003; Karnosky 2003).

Forest management has the potential to increase the terrestrial carbon pool. According to the rules of the Kyoto Protocol and of the United Nations Framework Convention on Climate Change, forestry can generate a sink for GHGs that can contribute to meeting the national commitment to emissions reductions (Jandl et al. 2007). The effects of forest management strategies have been treated in a number of reviews that elaborated on effects of land-use change, rotation length, thinning regimes, harvesting methods, site preparation, nitrogen fertilization, and nitrogen fixers (Berg and McClaugherty 2003). A compilation of forest management activities indicates that few practices are clearly good or bad with respect to carbon sequestration. The verdict on their impact depends on their effect on soil carbon and the degree of stability against disintegration of the stand structure. Optimized forest management with regard to soil carbon sequestration should aim to secure a high productivity of the forest on the input side, and avoid soil disturbances as much as possible on the output side (Berg and McClaugherty 2003).

19.6.3 Case Study in China

Forests are believed to be a major sink for atmospheric CO_2. There are 158.94 million hectares (Mha) of forests in China, which accounts for 16.5% of its land area. These extensive forests may play an important role in the global carbon cycle as well as making a large contribution to China's economic and environmental well-being. Currently there is a trend in China towards increased development in the forests. Thus, accounting for the role and potential of the forests in the global carbon budget is very important (Zhang and Xu 2003; Peng et al. 2009).

Zhang and Xu (2003) indicated that the forests in China annually accumulated 118.1 Mt carbon in growth of trees and 18.4 Mt in forest soils, and release 38.9 Mt, resulting in a net sequestration of 97.6 Mt carbon, corresponding to 16.8% of the national CO_2 emissions in 1990. From 1990 to 2050, soil carbon accumulation was projected to increase slightly while carbon emissions increases by 73, 77, and 84%, and net carbon sequestration increases by -21, 52 and 90% for baseline, trend, and planning scenarios, respectively. Carbon sequestration by China's forests under the planning scenario in 2000, 2010, 2030, and 2050 is approximately 20, 48, 111, and 142% higher than projected by the baseline scenario, and 8, 18, 34, and 26% higher than by the trend scenario, respectively. Over 9 Gt of carbon is projected to accumulate in China's forests from 1990 to 2050 under the planning scenario, and this is 73 and 23% larger than projected for the baseline and trend scenarios, respectively. During the period from 2008 to 2012, Chinese forests are likely to have a net uptake of 667, 565, and 452 Mt C, respectively, for the planning, trend, and baseline scenarios (Zhang and Xu 2003).

19.7 Climate Change Mitigation by Wetland Systems

Wetlands are defined as transitional zones between terrestrial and aquatic systems and periodically support predominant hydrophytes. Wetlands occur in areas where soils are naturally or artificially inundated or saturated by water due to high groundwater or surface water during part or all of the year (Babatunde et al. 2008). Wetlands are common in river deltas and estuaries, floodplains, tidal areas, and are widespread in river beds, depressions, foot slopes, and terraces of undulating landscapes (Babatunde et al. 2008; Zhang et al. 2011). Wetland ecosystems may be discriminated on the basis of hydrology, soils, and vegetation and generally include swamps, marshes, bogs, fens, floodplains and shallow lakes. The importance of wetlands to global biogeochemistry, water balance, wildlife, and human production is much greater than their proportional surface area on the Earth. Wetlands, either constructed or natural, offer a cheaper and low-cost alternative technology for wastewater treatment (Zhang et al. 2011).

Considering the importance of establishing sustainable, climate change proof, technologies for wastewater/stormwater treatment and recovery, the constructed wetlands (CWs), an efficient alternative to conventional wastewater treatment, have been increasingly used to reduce excessive nutrient loading caused by human activities (Vymazal 2005). Pollutant removal in CWs is a function of several physical, chemical, and biological processes, with biological microbial processes driving the removal of organic matter and nitrogen. Constructed wetlands are flexible systems which can be used for single households or entire communities. Also, due to climate change, more and more regions are experiencing droughts or flooding. Hence, water recycling as well as resilient technologies are key aspects to adapt to the effects of climate change (Hoffmann et al. 2011).

Wetlands cover about 6% of the earth's terrestrial area and provide invaluable services and benefits for human populations including the regulation of climate. However, the microbial transformations involved generate several greenhouse gases (GHG) as by-products: CO_2, N_2O, and CH_4, the latter two having a global warming potential (GWP) 296 and 23 times that of CO_2, respectively (IPCC 2001). Researchers reported that wetlands have a key role in controlling the terrestrial carbon cycle as they have the ability to sequester atmospheric carbon into peat (Clair et al. 2002). Though wetlands have acted as sinks since the last glaciation, by incorporation of carbon into accumulating peat and organic matter, they also release carbon back into the atmosphere over time. The main sources of loss are: as CO_2 from plant respiration and aerobic peat decomposition; as CH_4 from the anaerobic decomposition of peat; and as dissolved organic carbon (DOC) from the steeping of soil organic matter in water (Clair et al. 1999).

The relative importance of the carbon losses, especially in response to a changing climate, is poorly known (Moore et al. 1998; Dalva et al. 2001). The main control on a wetland's ability to retain carbon and generate CH_4 and DOC is determined in large part by its ability to remain wet, as peat is maintained under anaerobic conditions. Shifts in seasonal hydrology caused by a changing climate should therefore have measurable impacts on the accumulation or loss of organic carbon from wetland soils. Researchers indicated that it was useful to assess how hydrological changes caused by a changing climate, which could affect the main carbon losses from wetlands in a humid, cool, temperate growing area (Moore et al. 1998; Dalva et al. 2001).

Coastal wetlands and marine ecosystems hold vast stores of carbon. The vegetated wetlands represent 50% of carbon transfer from oceans to sediments. This carbon can remain stored in buried sediments for millennia (Crooks et al. 2011). Loss of coastal wetlands and marine ecosystems such as peatlands, forested tidal wetlands, tidal freshwater wetlands, salt marshes, mangroves and sea grass beds leads to decreased carbon sequestration and can also lead to emissions of large amounts of CO_2 directly to the atmosphere. Large scale emissions from ecosystem degradation and habitat conversion of these wetlands are ongoing, but currently they are not accounted for in national greenhouse gas inventories, nor are these being mitigated to any degree (Crooks et al. 2011).

The current climate policy regime contains few incentives for restoration or disincentives to drain or degrade coastal wetlands. The carbon dioxide emissions from drained coastal wetlands are sufficiently large to warrant inclusion in carbon accounting and emission inventories, and in amendments of national and international policy frameworks to reduce emissions from the loss of these ecosystems. Further work is needed to quantify the magnitude of emissions from near-shore marine ecosystems such as sea grass beds. These systems would slow or reverse ongoing loss of carbon sequestration capacity. Sustainable management of coastal wetlands and marine ecosystems also offer a wide range of co-benefits, including shoreline protection, nutrient cycling, water quality maintenance, flood control, habitat for birds, other wildlife and harvestable resources such as fish, as well as opportunities for recreation. Coastal wetlands and marine ecosystems sequester carbon within standing biomass, but even more within soils. Wetlands in saline environments have the added advantage of emitting negligible quantities of methane, a powerful greenhouse gas, whereas methane production in freshwater systems partially or wholly negates short-term carbon sequestration benefits. However, over multi-century time scales all coastal wetlands are net GHG sinks (Crooks et al. 2011).

Peatlands are areas with a thick organic soil layers (peat), which belong to the wetland systems. Peat-swamps are hotspots for biodiversity and home to many endangered species. Peatland soils have an organic layer of at least 40 cm depth where carbon often has accumulated over a long time due to excess water and suppressed rates of decomposition. However, the present accumulation rate may be lower than the long-term rate. Zicheng et al. (2003) showed large cyclic changes in moisture and carbon accumulation. These soils are characterized by a high water table and an organic layer with a carbon concentration exceeding a minimum value and by a certain minimum depth (Pakarinen 1995). Peatlands with anoxic conditions emit CH_4 (Nilsson et al. 2001; Friborg et al. 2003) while N_2O emissions are insignificant (Martikainen et al. 1993). The most recent results from Sweden and Finland (Minkkinen et al. 2006) suggest also that the cumulative emissions of CO_2 and N_2O are of such a magnitude that they can hardly be compensated by increased uptake in forest biomass. Forest drainage decreases CH_4 emissions but increases N_2O and CO_2 emissions from peat and carbon sequestration in the vegetation. Recent results from Sweden and Finland suggest that the drained forest ecosystems on peatland may be net emitters of GHGs (Jandl et al. 2007).

19.8 Summary

There are clear evidences that forests and wetland systems are able to respond to climate change via changes of phenology and distribution patterns, with species tending to move towards cooler areas. More far reaching changes in plant community composition have been recognized, and they are likely to become increasingly obvious in the future. To date, it is very clear that the responses to temperature are at a global scale, but in the long term, local changes in extreme events may be more important than the global trend in temperatures. Furthermore, soil carbon sequestration and release vary substantially by forest and wetland systems. The potential of the soil carbon sequestration is finite in magnitude and duration. Researchers believe that it is only a short-term strategy to mitigate anthropogenic enrichment of atmospheric CO_2. Developing alternatives to fossil fuels become the long-term strategies. The soil carbon sequestration is able to mitigate CO_2 emission and buy us time during which alternatives to fossil fuel are developed and implemented. Thus, soil carbon sequestration becomes a bridge to the future.

19.9 References

Alcamo, J., Dronin, N., Endejan, M., Golubev, G., and Kirilenko, A. (2007). “A new assessment of climate change impacts on production shortfalls and water availability in Russia.” *Global Environmental Change*, 17, 429–444.

Apple, M. E., Olszyk, D. M., Ormrod, D. P., Lewis, J., Southworth, D., and Tingey, D. T. (2000). “Morphology and stomatal function of Douglas fir needles exposed to climate change: elevated CO_2 and temperature.” *Int. J. Plant Sci.*, 161, 127–132.

Babatunde, A. O., Zhao, Y. Q., O'Neill, M., and O'Sullivan B. (2008). “Constructed wetlands for environmental pollution control: a review of developments, research and practice in Ireland.” *Environment International*, 34, 116–126.

Berg, B., and McClaugherty, C. (2003). *Plant Litter: Decomposition, Humus Formation, Carbon Sequestration. Springer*, Berlin, New York.

Bolin, B., Sukumar, R., Ciais, P., Cramer, W., Jarvis, P., Kheshgi, H., Nobre, C., Semenov, S., and Steffen, W. (2000). “Global perspective.” Ch. 1 in: Special Report on *Land Use, Land-Use Change and Forestry*. R.T. Watson, I.R. Noble, B. Bolin, N.H. Ravindranath, D.J. Verardo and D.J. Dokken (Eds.), Cambridge University Press, Cambridge, UK, pp 23–51.

Bolstad, P. V., Reich, P., and Lee, T. (2003). “Rapid temperature acclimation of leaf respiration rates in *Quercus alba* and *Quercus rubra*.” *Tree Physiol*, 23, 969–976.

Bowes, G. (1993). “Facing the inevitable. Plants and increasing atmospheric CO_2.” *Annu. Rev. Plant Physiol. Plant Mol. Biol.*, 44, 309–332.

Byrne, K. A., and Black, K. (2003). “Carbon Sequestration in Irish Forests.” *COFORD Connects Environment*, No. 3.

Chakraborty, S., Tiedemann, A. V., and Teng, P. S. (2000). “Climate change: Potential impact on plant diseases.” *Environmental Pollution*, 108, 317–326.

Clair, T. A., Ehrman, J. M., and Higuchi, K. (1999). “Changes in freshwater carbon exports from Canadian terrestrial basins to lakes and estuaries under a 2xCO_2 atmospheric scenario.” *Global Biogeochem. Cycles*, 13, 1091–1097.

Clair, T. A., Arp, P., Moore, T. R., Dalva, M., and Meng, F. R. (2002). “Gaseous carbon dioxide and methane, as well as dissolved organic carbon losses from a small temperate wetland under a changing climate.” *Environmental Pollution*, 116, S143–S148.

Crooks, S., Herr, D., Tamelander, J., Laffoley, D., and Vandever, J. (2011). *Mitigating Climate Change through Restoration and Management of Coastal Wetlands and Near-shore Marine Ecosystems–Challenges and Opportunities. Environment Department of the World Bank*, Washington, DC.

Dalva, M., Moore, T., Arp, R. P., and Clair, T. A. (2001). “Methane and soil and plant community respiration from wetlands, Kejimkujik National Park, Nova Scotia: Measurement, predictions, and climatic change.” *J. Geophys. Res*., 106, 2962–2995.

De Chazal, J., and Rounsevell, M. D. A. (2009). “Land-use and climate change within assessments of biodiversity change: A review.” *Global Environmental Change*, 19, 306–315.

De Wolf, E. D., and Isard, S. A. (2007). “Disease cycle approach to plant disease prediction.” *Annu. Rev. Phytopathol.,* 45, 203–220.

Dukes, J. S., and Mooney, H. A. (1999). “Does global change increase the success of biological invaders?” I, 14(4), 135–139.

Evans, C. D., Chapman, P. J., Clark, J. M., Monteith, D. T., and Cresser, M. S. (2006). “Alternative explanations for rising dissolved organic carbon export from organic soils.” *Global Change Biology*, 12, 2044–2053.

Florides, G. A., and Christodoulides, P. (2009). “Global warming and carbon dioxide through sciences.” *Environment International*, 35, 390–401.

Friborg, T., Soegaard, H., Christensen, T. R., Lloyd, C. R., and Panikov, N. S. (2003). “Siberian wetlands: Where a sink is a source.” *Geophysical Research Letters*, 21, 2129–2132.

Garrett, K. A., Nita, M., De Wolf, E. D., Gomez, L., and Sparks, A. H. (2009). *Plant Pathogens as Indicators of Climate Change, Climate Change: Observed Impacts on Planet Earth.* Department of Plant Pathology, *Kansas State University*, Manhattan, Kansas.

Giardina, C. P., and Ryan, M.G. (2002). “Total belowground carbon allocation in a fast-growing Eucalyptus plantation estimated using a carbon balance approach.” *Ecosystems*, 5, 487–499.

Gifford, R. M., Barrett, D. J., Lutze, F. L., and Samarakoon, A. B. (1996). “Agriculture and global change: scaling direct carbon dioxide impacts and feedbacks through time.” In: Walker, B., and Steffen, W. (Eds.), *Global Change and Terrestrial Ecosystems*. Cambridge University Press, Cambridge.

Gifford, R. M., and Howden, M. (2001). “Vegetation thickening in an ecological perspective: significance to national greenhouse gas inventories.” *Environmental Science & Policy*, 4, 59–72.

Girardin, M. P., Raulier, F., Bernier, P. Y., and Tardif, J. C. (2008). “Response of tree growth to a changing climate in boreal central Canada: A comparison of empirical, process-based, and hybrid modelling approaches." *Ecological modeling*, 213, 209–228.

Gorte, R. W. (2009). "Carbon Sequestration in Forests." *Congressional Research Service*, Washington, DC.

Green, R. E., Harley, M., Miles, L., Scharlemann, J., Watkinson, A., and Watts, O. (2003). "Global Climate Change and Biodiversity." *University of East Anglia*, Norwich, UK.

Hoffmann, H., Platzer, I. C., Winker, I. M., and von Muench, E. (2011). *Technology review of constructed wetlands–subsurface flow constructed wetlands for greywater and domestic wastewater treatment. Deutsche Gesellschaft für Internationale Zusammenarbeit (GIZ) GmbH Eschborn*, Germany.

Holling, C. S., Peterson, G., Marples, P., Sendzimir, F., Redford, K., Gunderson, L., and Lambert, D. (1996). "Self-organization in ecosystems: lumpy geometrics, periodicities and morphologies." In: Walker, B., and Steffen, W. (Eds.), *Global Change and Terrestrial Ecosystems,* Cambridge University Press, Cambridge.

IPCC (Intergovernmental Panel on Climate Change) (1997). *An introduction to Simple Climate Models Used in the IPCC Second Assessment Report*. Houghton, J. T., Filho, L. G. M., Griggs, D. J., Maskell, K. (Eds.), IPPC Secretariat.

IPCC (2000). *Land Use, Land Use Change and Forestry: A Special Report of the IPCC.* Cambridge University Press, New York.

IPCC (2001). *Climate Change 2001: The Scientific Basis*. Contribution of Working Group I to the Third Assessment Report of the Intergovernmental Panel on Climate Change. *Cambridge University Press*, Cambridge.

IPCC (2001a). *Climate Change 2001: The Scientific Basis*. (eds J. T. Houghton, Y. Ding, D. J. Griggs, M. Noguer, P. J., van der Linden, X. Dai, K. Maskell, and C. A. Johnson), 881 pp. Cambridge University Press, Cambridge, UK.

IPCC (2001b). *Climate Change 2001: Impacts, Adaptation, and Vulnerability*. (eds J. J. McCarthy, O. F. Canziani, N. A. Leary, D. J. Dokken, and K. S. White), 1032 pp. Cambridge University Press, Cambridge, UK.

IPCC (2001c). *Climate Change 2001: Mitigation*. (eds B. Metz, O. Davidson, R. Swart, and J. Pan), 752 pp. Cambridge University Press, Cambridge, UK.

IPCC (2001d). *The Climate System: an Overview Report of the IPCC.* Cambridge University Press, New York.

IPCC (2007). *Climate Change 2007: the Physical Science Basis: Summary for Policymakers*. IPCC WGI Fourth Assessment Report.

Jandl, R., Vesterdal, L., Olsson, M., Bens, O., Badeck, F., and Rock, J. (2007). "Carbon sequestration and forest management." CAB Reviews: Perspectives in Agriculture, *Veterinary Science, Nutrition and Natural Resources,* 2, No. 017.

Karnosky, D. F. (2003). "Impacts of elevated atmospheric CO_2 on forest trees and forest ecosystems: knowledge gaps." *Environment International*, 29, 161–169.

Lawlor, D. W., and Keys, A. J. (1993). "Understanding photosynthetic adaptation to changing climate." In: L. Fowden, T.A. Mansfield, and J. Stoddart (Eds.), *Plant Adaptation to Environmental Stress*, Chapman & Hall, London, UK, , pp. 85–106.

Lemma, B., Kleja, D. B., Olsson, M., and Nilsson I. (2007). "Factors controlling soil organic carbon sequestration under exotic tree plantations: A case study using the CO2Fix model in southwestern Ethiopia." *Forest Ecology and Management*, 252, 124–131.

Lindner, M., Maroschek, M., Netherer, S., Kremer, A., Barbati, A., Garcia-Gonzalo, J., Seidl, R., Delzon, S., Corona, P., Kolström, M., Lexer, M. J., and Marchetti, M., (2010). "Climate change impacts, adaptive capacity, and vulnerability of European forest ecosystems." *Forest Ecology and Management*, 259, 698–709.

Llorens, L., Penuelas, J., Beier, C., Emmett, B., Estiarte, M., and Tietema, A. (2004). "Effects of an experimental increase of temperature and drought on the photosynthetic performance of two ericaceous shrubs species along a north-south European gradient." *Ecosystems*, 7, 613–624.

Loik, M. E., Redar, S. P., and Harte, J. (2000). "Photosynthetic responses to a climate warming manipulation for contrasting meadow species in the Rocky Mountains Colorado, USA." *Funct. Ecol*. 14, 166–175.

Ludewig, F., and Sonnewald, U. (2000). "High CO_2-mediation down-regulation of photosynthetic gene transcripts is caused by accelerated leaf senescence rather than sugar accumulation." *FEBS Lett*., 479, 19–24.

Luo, Y., Wan, S., Hui, D., and Wallace, L. L. (2001). "Acclimatization of soil respiration to warming in a tall grass prairie." *Nature,* 413, 622–625.

Mackey, B. (2007). "Climate change, connectivity and biodiversity conservation." In: Taylor M., and Figgis, P. (eds.), *Protected Areas: Buffering nature against climate change*. *Proceedings of a WWF and IUCN World Commission on Protected Areas symposium*, Canberra, 18–19 June 2007. Sydney: WWF-Australia. pp. 90–96.

Makino, A., Nakano, H., Mae, T., Shimade, T., and Yamamoto, N. (2000). "Photosynthesis, plant growth and N allocation in transgenic rice plants with decreased rubisco under CO_2 enrichment." *J. Exp. Bot.*, 50, 383–389.

Martikainen, P., Nykanen, H., Crill, P., and Silvola, J. (1993). "Effect of a lowered water table on nitrous oxide fluxes from northern peatlands." *Nature*, 366, 51–53.

Masutomi, Y., Takahashi, K., Harasawa, H., and Matsuoka, Y. (2009). "Impact assessment of climate change on rice production in Asia in comprehensive consideration of process/parameter uncertainty in general circulation models." *Agriculture, Ecosystems and Environment*, 131, 281–291.

Milad, M., Schaich, H., Burgi, M., and Konold, W. (2011). "Climate change and nature conservation in Central European forests: a review of consequences, concepts and challenges." *Forest Ecology and Management*, 261, 829–843.

Minkkinen, K., Laine, J., Shurpali, N., Mkiranta, P., Alm, J., and Penttila, T. (2006). "Heterotrophic soil respiration in forestry-drained peatlands." *Boreal Environment Research*, 11, 1–12.

Nelson, N. (2011). "Photosystems and global effects of oxygenic photosynthesis." *Biochimica et Biophysica Acta (BBA)–Bioenergetics*, 1807, 856–863.

Nilsson, M., Mikkela, C., Sundh, I., Granberg, G., Svensson, B. H., and Ranneby, B. (2001). "Methane emissions from Swedish mires: National and regional budgets and dependency on mire vegetation." *Journal of Geophysical Research*, 106,

20847–20860.
Niu, S., Li, Z., Xia, J., Han, Y., Wu, M., and Wan, S. (2008). "Climatic warming changes plant photosynthesis and its temperature dependence in a temperate steppe of northern China." *Environmental and Experimental Botany*, 63, 91–101.
Ogawa-Onishi, Y., Berry, P. M., and Tanaka, N. (2010). "Assessing the potential impacts of climate change and their conservation implications in Japan: a case study of conifers." *Biological Conservation*, 143, 1728–1736.
Pakarinen, P. (1995). "Classification of boreal mires in Finland and Scandinavia: A review." *Vegetation*, 118, 29–38.
Pearson, R. G., and Dawson, T. P., (2003). "Predicting the impacts of climate change on the distribution of species: Are bioclimate envelope models useful?" *Global Ecol. Biogeogr.,* 12, 361–371.
Peng, C., Zhou, X., Zhao, S., Wang, X., Zhu, B., Piao, S., and Fang, J. (2009). "Quantifying the response of forest carbon balance to future climate change in northeastern china: model validation and prediction." *Global and Planetary Change*, 66, 179–194.
Ramanathan, V., and Feng, Y. (2009). "Air pollution, greenhouse gases and climate change: global and regional perspectives." *Atmospheric Environment*, 43, 37–50.
Rasineni, G. K., Guha, A., and Reddy, A. R. (2011). "Responses of gmelina arborea, a tropical deciduous tree species, to elevated atmospheric CO_2: Growth, biomass productivity and carbon sequestration efficacy." *Plant Science*, 181, 428–438.
Raymond, P. A., and Bauer, J. E. (2001). "Riverine export of aged terrestrial organic matter to the North Atlantic Ocean." *Nature*, 409, 497–500.
Rosenzweig, C., and Hillel, D. (1995). "Potential Impacts of Climate Change on Agriculture and Food Supply." *Consequences*, 1(2), 23–32.
Roulet, N., and Moore, T. R. (2006). "Browning the waters." *Nature*, 444, 283–284.
Schurgers, G., Mikolajewicz, U., Gröger, M., Maier-Reimer, E., Vizcaíno, M., and Winguth, A. (2008). "Long-term effects of biogeophysical and biogeochemical interactions between terrestrial biosphere and climate under anthropogenic climate change." *Global and Planetary Change*, 64, 26–37.
Sedjo, R. A. (2001). "Forest carbon sequestration: some issues for forest investments." *Resources for the Future*, Washington, DC.
Sheeran, K. A. (2006). "Forest conservation in the Philippines: A cost-effective approach to mitigating climate change?" *Ecological Economics*, 58, 338–349.
Shen, S. S. P., Yin, H., Cannon, K., Howard, A., Chetner, S., and Karl, T. R. (2005). "Temporal and spatial changes of the agroclimate in Alberta, Canada from 1901 to 2002." *J. Appl. Meteorol.*, 44, 1090–1105.
Stanhill, G., and Cohen, S. (2001). "Global dimming: a review of the evidence for a widespread and significant reduction in global radiation with discussion of its probable causes and possible agricultural consequences." *Agricultural and Forest Meteorology*, 107 (4), 255–278.
Starr, G., Oberbauer, S. F., and Pop, E. W. (2000). "Effects of lengthened growing season and soil warming on the phenology and physiology of Polygonum

bistorta." *Global Change Biol.*, 6, 357–369.

Steffen, W., and Canadell, P. (2005). *Carbon Dioxide Fertilisation and Climate Change Policy.* Department of Environment and Heritage, *Australian Greenhouse Office*, Canberra, 33 pp.

Tanaka, N., Kume, T., Yoshifuji, N., Tanaka, K., Takizawa, H., Shiraki, K., Tantasirin C., Tangtham, N., and Suzuki M. (2008). "A review of evapotranspiration estimates from tropical forests in Thailand and adjacent regions." *Agricultural and forest meteorology*, 148, 807–819.

Tirado, M. C., Clarke, R., Jaykus, L. A., McQuatters-Gollop, A., and Frank, J. M. (2010). "Climate change and food safety: A review." *Food Research International*, 43, 1745–1765.

Tubiello, F. N., and Ewert, F. (2002). "Simulating the effects of elevated CO_2 on crops: approaches and applications for climate change." *Europ. J. Agronomy*, 18, 57–74.

Vesterdal, L., and Raulund-Rasmussen, K. (1998). "Forest floor chemistry under seven tree species along a soil fertility gradient." *Canadian Journal of Forest Research*, 28, 1636–1647.

Viner, D., Morison, J. I. L., and Wallace, C. (2006). *Recent and future climate change and their implications for plant growth, plant growth and climate change*, Edited by James I. L. Morison and Michael D. Morecroft, *Blackwell Publishing Ltd*, Oxford OX4 2DQ, UK.

Vymazal, J. (2005). *Natural and Constructed Wetlands: Nutrients, Metals and Management*. Backhuys Publishers, Leiden.

Walther, G. R., Post, E., Convey, P., Menzel, A., Parmesan, C., Beebee, T. J. C., Fromentin, J. M., Hoegh Guldberg, O., and Bairlein, F. (2002). "Ecological responses to recent climate change." *Nature*, 416, 289–395.

Woodward, F. (2002). "Potential impacts of global elevated CO_2 concentrations on plants." *Current Opinion in Plant Biology*, 5, 207–211.

Xiong, F. S., Mueller, E. C., and Da, T. A. (2000). "Photosynthetic and respiratory acclimation and growth response of Antarctic cascular plants to contrasting temperature regimes." *Am. J. Bot.*, 87, 700–710.

Yamori, W., Noguchi, K., and Terashima, I. (2005). "Temperature acclimation of photosynthesis in spinach leaves: analyses of photosynthetic components and temperature dependences of photosynthetic partial reactions." *Plant Cell Environ.*, 28, 536–547.

Zhang, X. Q., and Xu, D. (2003). "Potential carbon sequestration in China's forests." *Environmental Science & Policy*, 6, 421–432.

Zhang, H., Cui, B., Hong, J., and Zhang, K. (2011). "Synergism of natural and constructed wetlands in Beijing, China." *Ecological Engineering*, 37, 128–138.

Zicheng, Y., Campbell, I. D., Campbell, C., Vitt, D. H., Bond, G. C., and Apps, M. J., (2003). "Carbon sequestration in western Canadian peat highly sensitive to Holocene wet-dry climate cycles at millennial timescales." *The Holocene*, 13, 801–808.

CHAPTER 20

Carbon Capture and Storage for Mitigating Climate Changes

Tian C. Zhang and Rao Y. Surampalli

20.1 Introduction

Currently, three options are being explored to stabilize atmospheric levels of greenhouse gases (GHGs) and global temperatures without severely and negatively impacting standards of living: a) increasing energy efficiency, b) switching to less carbon-intensive sources of energy, and c) carbon capture, storage and sequestration (CCS) (White et al. 2003). While all three options must be used in concert, this chapter focuses on CCS because the CCS option is very compatible with the large energy production and delivery infrastructure now in place (MIT 2012). For the foreseeable future, fossil fuels will continue to be the world's most reliable and lowest-cost form of energy (USDOS 2010). Global energy models suggest that with current global coal use patterns, it will not be possible to stabilize atmospheric GHG concentrations at acceptable levels. Therefore, it is necessary to make major reductions in GHG emissions. The EU, for example, wants to set a target of halving carbon emissions by 2050 in order to keep the rise in global temperature below 2°C. If the temperature increases more than this, it may trigger runaway climate change, i.e., temperatures could easily rise another 2°C, which would be a catastrophe to all living beings. Therefore, to mitigate climate changes, we must aggressively pursue CCS from fossil fuel power plants, other industries, and places where CCS technology can be used.

It should be noted that cutting emissions of other gases (e.g., methane, nitrous oxide, man-made chemicals) could slow changes in climate, leading to some rapid changes for the better. However, the climate-related benefits of reductions in non-CO_2 GHGs have limits. Even if all human-related, non-CO_2 GHG emissions could be eliminated today, it would not be enough to stabilize the warming influence from all GHGs over the next 40 years (Montzka et al. 2011). Therefore, in this chapter, we will focus on CCS. Here, we define the term CCS (= Carbon Capture, Storage, and Sequestration) as any technologies/methods that are to a) capture, transport, and store carbon (CO_2), b) monitor, verify, and account the status/progress of the CCS technologies employed, and c) advance development/uptake of low-carbon technologies and/or promote beneficial reuse of CO_2. Although CCS issues have been addressed/reviewed since the early 1990s (e.g., Riemer et al. 1993; USDOE 1999; Herzog 2001; Anderson and Newell 2003; IPCC 2005; IEA 2009; Lackner and Brennan 2009; CCCSRP 2010; ITF 2010), still there is a need to review CCS technologies because new information is now being generated at a faster pace.

In this chapter, the concept of CCS is introduced with a focus on technologies for CO_2 capture, long-term storage, monitoring, and beneficial reuse of CO_2. Major issues (e.g., concerns, constrains, and major barriers) and future perspectives are discussed. Understanding the technologies and issues would better prepare us for future actions.

20.2 Background

To provide the background for CCS, this section describes and discusses issues related to: a) carbon cycle, b) sources of CO_2 and targeted CO_2 sources for CCS and c) historical evaluation of CCS.

Carbon Cycle. The carbon cycle is the biogeochemical cycle by which carbon is exchanged among the biosphere, pedosphere (the soil-containing earth surface), geosphere, hydrosphere, and atmosphere of the Earth. Carbon moves from: a) atmosphere (as CO_2) to plants (via photosynthesis) or the oceans/other water bodies (via absorption processes), b) plants (or other animals) to animals via food chains, c) died plants/animals to the ground (e.g., fossil fuels formed in millions and millions of years), and d) living things (via respiration) and/or fossil fuels (upon being burned) to the atmosphere. When humans burn fossil fuels for energy, most of the carbon quickly enters the atmosphere as CO_2. Each year, 5.5 billion tons of carbon is released by burning fossil fuels; 3.3 billion tons enter the atmosphere and most of the rest is absorbed by the oceans. CO_2 and other GHGs trap heat in the atmosphere to keep the Earth warm and livable for living beings. However, there is about 30% more carbon dioxide in the air today (due to human fossil burning activities) than there was about 150 years ago, which is causing our planet to become warmer (Johnson 2010).

Sources of CO_2 and Targeted CO_2 Sources for CCS. CO_2, CH_4, nitrous oxide and three groups of fluorinated gases (sulfur hexafluoride, HFCs, and PFCs) are the major GHGs and the subject of the Kyoto Protocol. All GHGs are released from either point or non-point sources (IPCC 2005). Several points need to be discussed below:

- People define point and non-point sources in different ways. As shown in Table 20.1, our point sources include both concentrated major point sources (e.g., from major industries) and mobile/distributed point sources, which were lumped by some researchers (e.g., Oda and Maksyutv 2012) as non-point sources.

- GHG emissions and the contribution from different sources are different in different countries and locations. For example, WRI (2009) reported US GHG emission and sinks for 2006; contributions to the total gross emissions (7054 million metric tons of CO_2 equivalent) are 34% for electric power industry, 28% for transportation, 19% for (other industry), 8% for agriculture, 6% for commercial, and 5% for residential and others; the forest sink is 884, and thus, the net emission is 6170. These numbers are different from what are shown in Table 20.1 because of different databases used.
- Although weak and widespread, the strengths of mobile/distributed point sources may be well correlated with the local human activities, the local population, and living standards. Therefore, mobile/distributed point sources can be estimated by population statistics and activity intensity.
- While estimates vary, the contribution of non-point sources to GHG emissions is relatively large (about 1/3 of the global GHG emissions). For example, the contribution to GHG emissions by food chain is 18% in UK, and 31% in EU (EU 2006). Thus, we should also target non-point sources for CCS.
- Aside from purely human-produced synthetic halocarbons (e.g., CFCs, tetrafluoromethane), GHG emissions are from both natural and anthropogenic sources. The contribution of natural sources can be estimated by subtracting the preindustrial level from the current level. For example, since 1750, CO_2 has increased 113 ppm, methane 1045 ppb, nitrous oxide 44 ppb, and CFC-12 533 ppt, respectively (IPPC 2007).
- In the future, it is desirable to perform CCS from the atmosphere once other major sources are controlled by CCS.

Table 20.1. Sources of CO_2 and targeted sources for CCS[a]

Source	Description
Concentrated point sources: • Fossil fuel power plants • Oil refineries • Industrial process plants • Other heavy industrial sources	• Contributing 43%[b] of global GHG emission • Large sources are targeted for CCS • New technology (e.g., membrane) and pipeline systems for CO_2 transport may make CCS viable also for small, localized emissions, particularly where smaller sources are clustered in a limited area
Mobile/distributed point sources: • Transportation • Resident/comm. HVAC	• Contributing 22%[b] of global GHG emission • Not targeted for CCS because it is significantly less practical than simply changing to a renewable or zero emission fuel.
Non-point Sources • Agriculture/land use • Wetland/waste/volcanoes	• Contributing 35%[b] of global GHG emission • Not targeted for CCS but it is desirable • In the future, CCS from atmosphere may be a viable option

[a] References: Zero (2012); WRI (2012); USEPA (2012). [b] 43% = power (24%) + industry (14%) and other energy related (5%); 22 = transportation (14%) + buildings (8%); and 35% = Land use (18%) + agriculture (14%) + waste (3%) + others (3%). Details can be found in IPCC (2005).

Historical Evolution of CCS Technologies. In general, CCS processes include three major steps: a) capturing carbon (or CO_2) from different sources; b) transporting to a storage site; and c) injecting into a geological formation for CO_2

storage (USDOS 2010). It should be noted that we define CCS in a much broader way (see above), including all technologies/methods that promote carbon sequestration in natural environments, monitor the status/progress of the CCS technologies employed, and advance development/uptake of lower carbon technologies and/or promote beneficial use of carbon (e.g., reuse). Therefore, the boundary of the CCS technologies addressed in this chapter is broader.

CCS technologies themselves are not new. In the 1940s, chemical solvents (e.g., monoethanolamine (MEA)-based solvents) were developed to remove acid gases (e.g., CO_2 and H_2S) from impure natural gas to boost the heating value of natural gas. The same or similar solvents were used to recover CO_2 from their flue gases for application in the foods-processing and chemicals industries by power plants. On the other hand, the feasibility of capturing CO_2 from ambient air was evaluated in the 1940s (Tepe and Dodge 1943; Spector and Dodge 1946). The first patent for CO_2EOR technology (CO_2 enhanced oil recovery) was granted to Whorton, Brownscombe, and Dyes of the Atlantic Refining Company 4 in 1952. In 1964, a field test was conducted at the Mead Strawn Field to inject CO_2 for oil recovery. In 1972, the first commercial CO_2 EOR was initiated by Chevron at SACROC Unit, Texas. Today, petroleum industry operates CO_2 EOR projects in 74 fields and produces 245,000 barrels of incremental oil a day (about 5% of the total US production), and injects over 2.14 BCF of CO_2 per day (Meyer 2012). In the 1970s, two post-combustion commercial amine capture processes were developed, one by Kerr-McGee (using 20% MEA solution) and another by Dow Chemical (using 30% MEA). In 1989, the Massachusetts Institute of Technology (MIT) initiated the Carbon Capture and Sequestration Technologies Program. During that time, there were only a handful of research groups working in CCS (Herzog 2011). Also around that time, Zaslavsky (2006) proposed the concept of the "energy tower."

In 1991, the Norwegian government instituted a tax on CO_2 emission, which triggered the start-up of the Sleipner Project. The First International Conference on Carbon Dioxide Removal (ICCDR-1) was held in Amsterdam with > 250 attendees from 23 countries. Since 1996, Statoil has been using CCS at the Sleipner oil and gas field (located in the North Sea) to compress and then pump CO_2 into a 200-m-thick sandstone layer that lies ~1000 m below the seabed. The Sleipner Project demonstrates the commercial application of CCS, which can be viewed as one of the most significant milestones in evolution of CCS technology (Herzog 2003). In 1997, the Dakota Gasification Company (DGC) agreed to send all of the waste gas (96% CO_2) from its Great Plains Synfuels Plant through a pipeline to the Weyburn oil field (330 km away), Canada; in 2000, EnCana began to inject CO_2 into 37 injection wells to help the oil to flow toward 145 active producer wells. In 2000, Brown proposed replacing water with supercritical CO_2, which is being evolved into CO_2-based geothermal energy (CO_2GE) technology (Randolph and Saar 2011). CO_2GE is up to 5 times more efficient than water geothermal because CO_2 is a more efficient working fluid in natural than hydrofractured reservoirs. Nowadays, a variety of alternative methods (e.g., amine solvents, physical solvents, cryogenic, oxygen methods) are used to separate CO_2 from gas mixtures during the production of hydrogen for petroleum refining, ammonia production, and other industries. All of these capture technologies are considered relatively mature (Plasynski, et al. 2009). Other major milestones about CCS can be found in Wikipedia (2010).

There is considerable interest in improving CCS technology, particularly CO_2 capture processes. Currently, a wide range of options have been evaluated, such as aqueous ammonia, metal organic frameworks (MOFs), ionic liquids (ILs), membranes (e.g., polybenzimidiazole, ion transport membrane, oxygen transport, enzymatic mambranes), solid regenerable sorbents, ceramic auto-thermal recovery, hydrates, chemical-looping, mineral formation, and biological processes. As the knowledge and understanding of CCS technologies grow, some of these emerging CCS processes are anticipated to be commercialized in 5–10 years, others in > 20 years (Figueroa et al. 2008; Herzog et al. 2009).

20.3 CCS Technologies

20.3.1 Carbon Capture Technologies

There are many carbon capture technologies. These technologies can be categorized as a) physical/chemical and biological technologies and b) technologies for carbon capture from concentrated point sources and mobile/distributed point- or non-point sources. In general, on-site capture is the most viable approach for large sources and initially offers the most cost-effective avenue to sequestration. For mobile/distributed sources like cars, on-board capture at affordable cost would not be feasible, but are still needed. On the basis of category b), we will present these technologies as follows.

Concentrated Point-Source CO_2 Capture. All the current commercially available processes for CO_2 capture are similar in concept (i.e., a two-vessel process with liquid, solid or liquid-impregnated solid sorbents). In the first vessel, the CO_2-containing gas contacts a lean solvent (e.g., MEA-based), and the CO_2 is absorbed there. The CO_2-rich solvent is regenerated in the second vessel and then returned to the first vessel. Solvents used in these processes can be broadly grouped into two categories: physical solvents and chemical solvents (Table 20.2). CO_2 can also be captured with solid sorbents; detailed information about these sorbents can be found in different reports (e.g., Choi et al. 2009).

Greenleaf and SenGupta (2009) proposed to use ion-exchange fibers (containing F–COOH) to remove water hardness (Ca and Ma) and sequester CO_2 without requiring any chemicals for regeneration or without the production of residuals (sludge):

$$2\text{F-COOH} + 2\text{Ca(HCO}_3) \Leftrightarrow (\text{F-COO})_2\text{Ca} + 2\text{H}_2\text{CO}_3 \qquad \text{(Eq. 20.1)}$$

$$2\text{F-COOH} + 2\text{Mg}(\text{HCO}_3) \Leftrightarrow (\text{F-COO})_2\text{Mg} + 2\text{H}_2\text{CO}_3 \quad \text{(Eq. 20.2)}$$

$$(\text{F-COO})_2\text{Ca} + 2\text{CO}_2(g) + 2\text{H}_2\text{O} \Leftrightarrow 2\text{F-COOH} + \text{Ca}^{2+} + 2\text{HCO}_3 \quad \text{(Eq. 20.3)}$$

Table 20.2. Physical/chemical technologies for CO_2 capture[a]

Capture processes for concentrated [1)–3)] or mobile/diffused point- or non-point [4)] sources:

1) **Post-combustion:** CO_2 is removed after combustion of the fossil fuel as in power plants. The technology is well understood and is used in other industrial applications.
- Would reduce energy efficiency by 10–40%.
- The thermodynamic driving force for capture CO_2 is low.
- Compatible with the power plants, flexible, and a leading candidate for gas-fired power plants

2) **Pre-combustion:** The CO_2 is recovered from some process stream before the fuel is burned.
- Widely applied in fertilizer, chemical, gaseous fuel plants.
- The partial pressure of CO2 is much higher than in a typical flue gas, and a cheaper CO2 capture process can be used as a result.
- In the US, only two IGCC plants are in operation in the power industry and both were built as demonstration plants.
- The ultimate commercial success of IGCC to provide coal-fired electricity remains uncertain.

3) **Oxy-combustion:** The fuel is burned in oxygen, resulting in an almost pure CO_2 stream that can be transported. The oxy-fuel plant can eliminate all air pollutants (i.e., zero emission).
- May add ~7¢/kWh to the production cost of electricity.
- The need for a cryogenic oxygen plant and flue gas recycle is costly. Chemical looping combustion method (using a metal oxide as a solid oxygen carrier) is a promising emerging technology.

4) **CO_2 capture from mobile/distributed point- or non-point sources:** Work is still in its infancy. Capture costs are higher than from point sources. May be feasible for carbon capture from distributed sources such as automobiles and aircraft. Examples:
- An anionic exchange resin as a solid sorbent that absorbs CO_2 when dry and releases it when wet.
- Ion-exchange fibers to sequester CO_2 into an aqueous Ca or Mg alkalinity while concurrently softening hard water.
- The "Air Capture" system captures ~ 80% of CO_2 from the air.

General processes used for CO_2 capture: absorption processes with liquid, solid or liquid-impreganted solid sorbents:
- **Physical sorbents:** Selexol (a mixture of dimethyl ethers of polyethylene glycol); Rectisol (chilled methanol) and propylene carbonate (Fluor process); and Purisol.
- **Chemical sorbents:** Amines (monoethanol, diethanol, and methyl diethanol amine); NaOH/ $Ca(OH)_2$/NH_3/ion exchange resins/ion exchange fibers

R&D pathways: (1) Mature technology under consideration for CO_2 capture:
- **Scrubbing:**
  - Improved amines: Piperazine (PZ) + MEA or PZ + methyldiethanolamine (MDEA)
  - Aqueous Ammonia (e.g., chilled ammonia process, CAP), resulting in energy savings.
- **Sorption:**
  - Organic materials (e.g., polymers)/minerals and inorganic materials [ceramics with alkaline or alkaline earth elements, silica, alumina, calcium, lithium zirconate, layered double hydroxides, zeolites (5A, 13X, MCM-41), activated carbon, clay]/organic-inorganic hybrids.
  - Amine-doped/Potassium salt-doped sorbents.
- **Membranes:**
  - Enzyme-based membrane systems (using carbonic anhydrase)/PBI, ITM membranes
  - Using porous membranes as platforms for absorption and stripping
  - Two-stage clathrate hydrate/membrane process for capturing CO_2 and H_2.

R&D pathways: (2) Emerging and new concepts under consideration for CO_2 capture:
- Solid sorbents
  - Metal-organic frameworks, MOFs (e.g., zeolitic imidazolate frameworks, ZIFs).
  - Functionalized fibrous matrices
  - Novel liquid sorbents (e.g., CO_2 hydrates, liquid crystals, ionic liquids)

[a]Major references: Herzog (1999); VGB (2004); Choi et al. (2009); Greenleaf and SenGupta (2009); Lackner and Brennan (2009); and Plasynski et al. (2009).

CO_2 is permanently sequestered in the aqueous phase as calcium or magnesium alkalinity; no additional chemicals or salts are present in the regeneration solution. The process is not energy intensive, and CO_2 does not need to be compressed to excessive pressures (150 psi) for efficient use. The use of raw flue gas (17% CO_2) is feasible with the rate of sequestration governed only by the partial pressure of CO_2. The energy balance for a typical electric utility shows that up to 1%

of carbon dioxide emitted during combustion would be sequestered in the softening process.

The major component of flue gas is nitrogen, which enters originally with the air feed. If there were no nitrogen, CO_2 capture from flue gas would be greatly simplified. Therefore, for existing coal-fired combustion plants, there are two main options for CO_2 capture: removal of nitrogen from a) flue gases or b) from air before combustion to obtain a gas stream ready for transport or geo-sequestration. Therefore, there are three major options in CO_2 capture, i.e., post-, pro-, and oxy-combustion capture (Fig. 20.1).

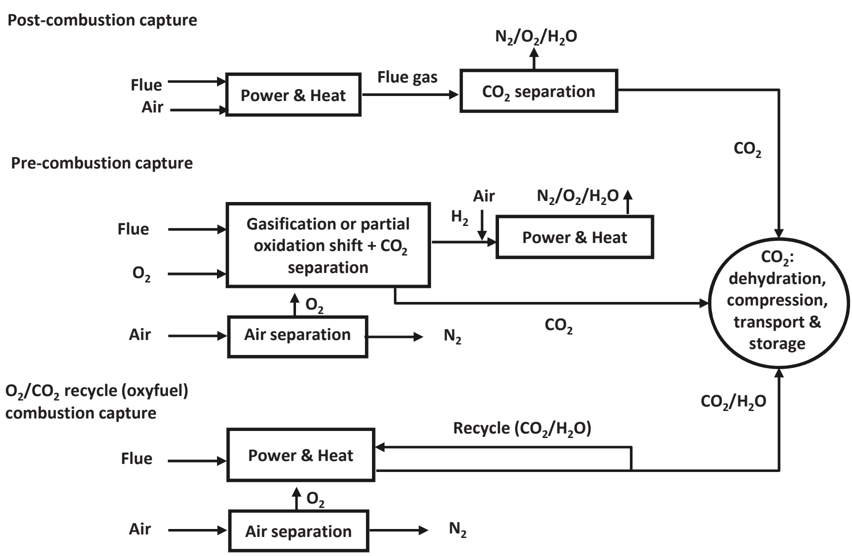

Figure 20.1. Overview of CO_2 capture from power plants (adapted from VGB 2004)

Currently, power plants burn their fuel and generate a flue gas at atmospheric pressure with a CO_2 concentration < 15% and the CO_2 partial pressure < 0.15 atm (Plasynski et al. 2009). Thus, the thermodynamic driving force for capturing CO_2 from flue gas is low. Furthermore, the flue gas approaches in use today require clean-up of the NOx and SO_2 prior to CO_2 separation, which creates a significant technical challenge for the development of cost-effective post-combustion CO_2 capture processes. The post-combustion CO_2 capture system will reduce the plant's overall thermal efficiency by 24%, about one-third (8%) is due to compression, with the rest (16%) attributable to separation (Herzog et al. 2009). Nevertheless, post-combustion technologies are widely used currently for CO_2 capture in power plants because they can be retrofitted to the existing power plants and they constitute, by far, the largest source of CO_2 emissions appropriate for CCS (Herzog et al. 2009). In the past, the amount of CO_2 captured was between a few hundred tons and over a thousand tons of CO_2 a day. However, for combating climate change, the scale of post-combustion CO_2-capture facilities is significantly large since a 500MWcoal-fired plant produces about 10,000 tons/day of CO_2. To improve CO_2 capture, current research and development (R&D) focus on several pathways (Table 20.2). Details of post-combustion capture and their improvement can be found in Choi et al. (2009), Herzog et al. (2009), and Plasynski et al. (2009).

On the other hand, pre- and oxy-combustion processes were developed with the thinking of obtaining much more concentrated CO_2 before its capture or storage. The concept of the pre-combustion capture is to increase the concentration and pressure of the CO_2 containing stream so that the size and cost of the capture facilities can be reduced. Integrated coal gasification combined cycle (IGCC) plants (i.e., the hydrogen route) are an example of the pre-combustion option. Coal is gasified to form syngas of CO and H_2. The gas then undergoes the water-gas shift, where the CO is reacted with steam to form CO_2 and H_2. H_2 is sent to a gas turbine combined cycle; and the CO_2 is then removed (e.g., via a physical solvent process like Selexsol) with much less energy as capture takes place from the high pressure syngas as opposed to the atmospheric pressure flue gas. A similar process is available for natural gas, where the syngas is formed by steam reforming of methane. The hydrogen route opens up opportunities for "polygeneration" of products besides electricity and CO_2. For example, instead of sending hydrogen to a turbine, it can be used to fuel a "hydrogen economy". In addition, syngas is an excellent feedstock for many chemical processes (Herzog 1999). However, the pre-combustion capture is not an option at the pulverized coal (PC) power plants that comprise most of the existing capacity.

An oxyfuel plant that is fed pure O_2 and coal does not need a flue stack; it is sometimes referred to as "zero emission" cycles, because by design they have no gaseous exhaust. Zero emission plants can capture CO_2 and all air pollutants (e.g., NO_x, SO_2, and particulate matter). The technique is promising, but the initial air separation step (such as a cryogenic air separation unit, ASU) demands a lot of energy. Various process options are being considered to make oxy-combustion more economically attractive, such as the use of a) a circulating fluidized bed (CFB) with a reduced requirement for recycled flue gas and easier temperature control, b) an oxygen ion transport membrane to replace the ASU, c) ceramic autothermal recovery (CAR) (Plasynski et al. 2009).

Mobile/Distributed Point- or Non-Point-Source CO_2 Capture. Capturing CO_2 directly from the air could a) offset emissions from distributed sources; b) provide a constant supply of carbon-based liquid fuel; c) balance out a significant fraction of the world's CO_2 emissions; d) operate at the site of disposal and thus eliminating the need to transport CO_2 over long distance; and e) help assure the long-term viability of storage sites (Lackner and Brennan 2009). In addition, it may have several advantages, such as freedom of location, economy of scale, and negative emissions even though it is more difficult and more expensive.

In atmospheric air, CO_2 concentration is ~ 0.04% (about 390 ppm), much smaller than the CO_2 concentration (5–15%) coming out from flue stacks. This makes CO_2 capture from mobile/distributed point-sources and non-point-sources costly and difficult. However, CO_2 is still a reactive sour gas, and thus, can be absorbed by highly selective sorbents, which makes it possible to reduce the partial pressure of CO_2 in air (~40 Pa) to a small fraction of one Pascal. Considering that we do not need to extract all the CO_2 out of the air, it is possible to design sorbent-based air capture systems that scales its energy cost with the amount of CO_2 capture, instead of with the volume of air processes (Stolarooff 2006; Lackner and Brennan 2009). Stolarooff (2006) reviewed the existing alternative routes to air capture, including: a) organic carbon production; b) metal-carbonate production; c) capture with a regenerated sorbent; and d) metal hydroxide sorbents. In this chapter, we classify the methods based on CO_2 capture from mobile/distributed point sources and non-point sources.

As indicated in Table 20.3, methods 1) to 4) are for CO_2 capture from non-point sources; they are biologically related, and in many cases, are called biosequestration (i.e., the capture and storage of the atmospheric GHG CO_2 by biological processes). Trees and other photosynthesizing organisms perform CO_2 capture routinely. Cutting down forests may contribute ~20% of the overall GHGs entering the atmosphere (IPCC 2012). Therefore, the Kyoto Protocol requires mandatory land use, land use change and forestry (LULUCF) accounting for afforestation (no forest for last 50 years), reforestation (no forest on Dec. 31, 1989), and deforestation. While it looks like that method 1) in Table 20.3 has big potential to capture a large fraction of anthropogenic CO_2 emissions, they all have limitations and constrains. For example, biomass is limited by the land available and by the secondary impacts of agriculture. As a base line, trees over an acre will only sequester between 2 to 8 tons of CO_2 each year. Corn, on the other hand, at 150 bushels an acre is taking out more CO_2 than trees do, plus that corn can be used to make biofuels. Therefore, one of the current research focuses is to genetically improve crops for CO_2 capture and biofuel production. One example is to increase the Earth's proportion of C4 carbon fixation photosynthetic plants because these plants account for ~30% of terrestrial carbon fixation even though they only represent about 5% of Earth's plant biomass (Osborne and Beerling 2006). Wheat, barley, soybeans, potatoes and rice (all C3 staple food crops) can be genetically engineered with the photosynthetic apparatus of C4 plants, i.e., modifying C3 crops' ribulose-1,5-bisphosphate carboxylase/oxygenase (Rubisco) genes (Beerling 2008).

Algae are nature's CO_2 scrubbers and they fix > 65 Gt of carbon every year, which is equal to the output of about 65000, 500-MW power generation plants. Algae inhale CO_2 at rates that a few months of algae growth can equal decades of tree growth. Algae such as *Dunaliella salina* are high value commercial cosmetics and food supplements. Recently, algae become more and more popular due to the fact that the yields of bio-diesel from algae are one order of magnitude higher than those for traditional oilseeds; algae can even produce bio-hydrogen. Everything can be used in the algae: after death it can be digested into bio-gas (methane, carbon dioxide, and the fertilizer needed to grow more algae).

Algae can be cultivated in open ponds or closed bioreactor systems. It has been proposed to use watershed nutrients, animal waste, sewage waste, or flue gases to cultivate algae next to power-plant flue stacks for CO_2 capture with marginal lands. However, the available marginal lands may not be enough to solve the problem. For example, a 50-MW 50% base-load natural gas-fired electrical generation plant operating 18 h/day over a 240-day season would produce 216 million kWh/season, releasing 30.3 million kg-C/season of fossil-fuel CO_2. An algal process designed to capture 70% of the flue-gas CO_2 would require an area of 880 ha of high-rate algal ponds operating at a productivity of 20 g VS/m^2-day, which would produce 42.4 million kg algal dry wt/season (Brune et al. 2009). If 100% of the algal biomass were harvested and used for replacing biogas methane usage, soybean feed replacement, and biodiesel production, the gross GHG reduction would be about 36%, the net parasitic energy cost to harvest and process the algal biomass would be about 10% of plant total energy output, resulting in a new GHG reduction of 26% (Brune et al. 2009).

Another suggestion is to utilize the "Jelly Pump" for CO_2 storage. For example, *thaliacean* (appearing similar to jellyfish) are one-third carbon by weight, while jellyfish, by comparison, are 10% carbon, and single-celled algae around 20%. The high carbon content explains why *thaliaceans* are so dense and why they sink so quickly after they die. *Thaliaceans* gather around the world in feeding swarms, billions strong, feasting on algae, and can sink almost twice as much carbon as algae do (Hoffman 2009). However, no detailed information is available on how to use this mechanism to store more CO_2.

Accordingly, another proposal is to seed pulverized iron over the ocean to germinate a plankton bloom. While small-scale tests are not successful, large-scale tests may overshoot the goal and drive CO_2 to levels too low. For each iron atom added to the water, between 10,000 and 100,000 carbon atoms are sunk (Wikipedia 2012). Therefore, further studies are needed to get accurate information on the biological activity that a bloom causes and to measure how much carbon will be displaced.

Method 3) represents an emerging commercial sector that combines carbon sequestration and energy production. For biochar sequestration to work on a much larger scale, an important factor is combining low-temperature pyrolysis with simultaneous capture of the exhaust gases and converting them to energy as heat, electricity, biofuel or hydrogen; emissions reductions of using pyrolysis processes for bioenergy production can be 12–84% greater if biochar is placed into the soil instead of being burned to offset fossil-fuel use (Wikipedia 2011). Thus, biochar sequestration offers the chance to turn bioenergy into a carbon-negative industry.

Table 20.3. Methods for mobile/distributed point or non-point source CO_2 capture[a]

Methods	**Description**
Alternatives for non-point source CO_2 capture:	
1) Trees/organisms	• Capture CO_2 via photosynthesis (e.g., reforestation or avoiding deforestation); cost range 0.03-8\$/t-CO_2; one-time reduction, i.e., once the forest mature, no capture; release CO_2 when decomposed • Develop dedicated biofuel and biosequestration crops (e.g., switchgrass); enhance photosynthetic efficiency by modifying Rubisco genes in plants to increase enzyme activities; choose crops that produce large numbers of phytoliths (microscopic spherical shells of silicon) to store carbon for thousand years.
2) Ocean flora	• Adding key nutrients to a limited area of ocean to culture plankton/algae for capturing CO_2. • Utilize biological/microbial carbon pump (e.g., jelly pump) for CO_2 storage. • Problems/concerns: a) large-scale tests done but with limited success; b) limited by the area of suitable ocean surface; c) may have problems to alter the ocean's chemistry; and d) mechanisms not fully known.
3) Biomass-fueled power plant, bio-oil and biochar	• Growing biomass to capture CO_2 and later captured from the flue gas. Cost range = 41\$/t-CO_2 • By pyrolyzing biomass, about 50% of its carbon becomes charcoal, which can persist in the soil for centuries. Placing biochar in soils also improves water quality, increases soil fertility, raises agricultural productivity and reduce pressure on old growth forests • pyrolysis can be cost-effective for a combination of sequestration and energy production when the cost of a CO_2 ton reaches \$37 (in 2010, it is \$16.82/ton on the European. Climate Exchange).
4) Sustainable practices, e.g., • Soils/grasslands • peat bogs	• Farming practices (e.g., no-till, residue mulching, cover cropping, crop rotation) and conversion to pastureland with good grazing management would enhance carbon sequestration in soil. • Peat bogs inter ~25% of the carbon stored in land plants and soils. However, flooded forests, peat bogs, and biochar amended soils can be CO_2 sources.
Alternatives for mobile/distributed point source CO_2 capture:	
5) Solid sorbents • Organics/polymers • Inorganics/minerals • Org. and inorganic hybrids • Liquid-impregnated clay	• Steel slag & waste concrete: a) Rich in Ca & Mg oxides, readily react w/ CO_2 to form solid carbonates; Cost range = 2–8\$/t-CO_2. The annual US production can capture < 1% of US emissions; b) examples of cementitious materials are cement (CSA Type 10, Type 30), fly ash, ground granulated blast furnace slag, electric arc furnace slag, and hydrated lime. • Ceramics (containing alkaline or alkaline earth elements): a) trap CO_2 via a chemical reaction (absorption) with the respective carbonate being produced (e.g.., CaO); b) absorb CO_2 in a wide temp. range (300–400°C up to 800°C). • Layered double hydroxides (LDHs): a) in general, they are $[M^{II}_{1-x}M^{III}_x(OH)_2]^{x+}(A^{n-})_{x/n}\cdot mH_2O$, where M^{II} and M^{III} stand for divalent and trivalent cations occupying octahedral sites within the hydroxyl layers, $x = M^{III}/(M^{II}+M^{III})$ and takes values in the range of 0.20 to 0.50, and A^{n-} is an exchangeable interlayer anion. One example is Mg-Al-CO_3 known as hydrotalcitelike, has been widely studied; b) Another form is $[Ca_2Al(OH)_6]_2CO_3\cdot mH_2O$, a hydrocalumite-like compound having sevenfold-coordinated Ca. • Limestone, dolomite, CaO/$Ca_{12}Al_{14}O_{33}$, etc. • Liquid-impregnated clay is capable of capturing CO_2 at lower temperature (30–60°C), and can be regenerated at 80–100°C.
6) liquid sorbents (synthetic trees) • NaOH/$Ca(OH)_2$ • NH_3 • Ion exchange resin/fibers	• NaOH has lower vapor pressure to prevent water loss as compared with $Ca(OH)_2$ scheme; 7–20 \$/t-CO_2 for NaOH scheme; 20 \$/t-CO_2 for $Ca(OH)_2$ scheme; the energy requirement of a packed tower contactor similar to the ones used to capture CO_2 from power plant flue gas would be 6–12 times the energy produced when the fossil fuel was initially burned; the water lost by evaporation is a concern. • With NH_3 as sorbent, the "energy tower" can be used to capture CO_2 and generate green power. The process has many advantages, i.e., it will promote the use of NH_3 as fuel and NH_3 fertilizer industry. • Using ion exchange resins/fibers as sorbents may simplify the sorbent regeneration cycle.

[a]Major references: Osborne and Beerling (2006); Stolarooff (2006); Beerling (2008); Choi et al. (2009); Greenleaf and SenGupta (2009); Lackner and Brennan (2009); Liu et al. (2009); Plasynski et al. (2009); Pfeiffer et al. (2011); and de Richter (2012).

Method 4) is very important, and sometimes, these conservation practices are called regenerative agriculture. Currently, worldwide overgrazing is substantially reducing grassland's performance as carbon sinks. It was suggested that, if practiced on the planet's 3.5 billion tillable acres, regenerative agriculture [e.g., method 4) in Table 20.3] could sequester up to 40% of current CO_2 emissions. The U.S. CO_2 emissions from fossil fuel combustion were ~6170 million metric tons in 2006 (EWR 2009). If a 2,000 (lb/ac)/year sequestration rate was achieved on all 434,000,000 acres (1,760,000 km^2) of cropland in the US, about one quarter of the country's total fossil fuel emissions would be sequestered per year (Wikipedia 2012).

Both Methods 5) and 6) depend on the use of reusable sorbents that can be regenerated via a swing of temperature, pressure or chemical reactions. Preliminary systems analysis indicates that CO_2 removal utilizing the solid sorbent [Method 5)] can be more economical than the liquid-amine process [Method 6)] as the regeneration of the solid sorbent requires less energy; the estimated regeneration energy for the solid sorbent is 1,821 KJ/kg CO_2 as compared to 4,648 KJ/kg CO_2 with the liquid-amine process (Siriwardane and Robinson 2009). An ideal sorbent would be inexpensive, abundant, and non-toxic, and have a binding energy with CO_2 > 20 kJ/mol that is required to pull it from the atmosphere (Stolaroff 2006). Lackner and Brennan (2009) stated that a binding energy with CO_2 > 15 kJ/mol is required for flue gas scrubbing processes, and the energy required for recovering CO_2 from a sorbent for air capture or flue gas scrubbing is similar; therefore, the cost of efficient implementations are likely to be similar.

The carbonation of calcium-carrying materials forms thermodynamically stable calcium carbonates (Young et al. 1974):

$$3CaO \cdot SiO_2 + 3CO_2 + xH_2O \rightarrow SiO_2 \cdot xH_2O + 3CaCO_3 \quad \text{(Eq. 20.4)}$$

$$2CaO \cdot SiO_2 + 2CO_2 + xH_2O \rightarrow SiO_2 \cdot xH_2O + 2CaCO_3 \quad \text{(Eq. 20.5)}$$

$$Ca(OH)_2 + CO_2 + H_2O \rightarrow CaCO_3 + 2H_2O \quad \text{(Eq. 20.6)}$$

The theoretical maximum CO_2 uptake is a function of the chemical composition of the sorbent (Steinour 1959):

$$CO_2\ (\%) = 0.785(CaO - 0.7SO_3) + 1.091MgO + 1.420Na_2O + 0.935K_2O \quad \text{(Eq. 20.7)}$$

The maximum CO_2 uptake for a portland cement of typical composition of 63% CaO is ~50% (Monkman and Shao 2006). Thus, if a 100% degree of carbonation is assumed, the sequestration potential of cement would be 0.5 t CO_2/t cement. The annual US production of steel slag and waste concrete can capture < 1% of US GHG emissions (Stolaroff 2006).

Currently, research on using solid reusable sorbents [e.g., Table 20.2 and Method 5) of Table 20.3] to capture and recover CO_2 from different sources is a focal point. Although many solid sorbents are available, it is a challenge to use them for CO_2 capture from distributed/mobile sources because these sources usually do not generate a large quantity of CO_2. One of the major changes is to regenerate sorbents in a cost effective way. For example, CaO or K_2CO_3 can capture CO_2 via the reactions below:

$$CaO(s) + CO_2(g) \Leftrightarrow CaCO_3(s) \qquad \text{(Eq. 20.8)}$$

$$K_2CaO_3(s) + CO_2(g) + H_2O \Leftrightarrow 2KHCO_3(s) + \text{Heat} \qquad \text{(Eq. 20.9)}$$

However, the standard circulating fluidized bed (CFB) systems are difficult to use for CO_2 capture from distributed/mobile sources because several reactors still are needed to transfer solids (often in a much smaller volume) for sorbent generation. In addition, Ca-or K-based sorbents often show a rapid falloff in reversibility for the reactions shown in Eqs. 8 and 9 due to sintering effects associated with the calcination process (Lu et al. 2009). Pfeiffer et al. (2011) reported that $[Ca_2Al(OH)_6]_2CO_3 \cdot mH_2O$ (called CaAl-550) has better properties (efficiency and thermal stability) as a CO_2 sorbent than CaO due to the aluminum presence as $Ca_{12}Al^{14}O_{33}$. However, all these solid sorbents need to be operated at a relatively high temperature range. Liquid-impregnated clay, among others is capable of capturing CO_2 at a lower temperature (30–60^{o}C), and can be regenerated at 80–100^{o}C (Siriwardane and Robinson 2009), which is more useful for capturing CO_2 from mobile and distributed sources.

In the early 1940s, capturing CO_2 from ambient air with absorbents has been explored (Tepe and Dodge 1943; Spector and Dodge 1946). Large scale scrubbing of CO_2 from ambient air for climate mitigation was first suggested by Lackner in the late 1990's (Lackner et al. 1999). In wet scrubbing techniques, a contact reactor, as a point of contention, allows CO_2 to be sorbed into the sorbent solution (e.g., NaOH, $Ca(OH)_2$, NH3, ion exchange resin, etc.) to create an aqueous solution (e.g., NaOH + Na_2CO_3). In the regeneration cycle, a concentrated, pressurized stream of CO_2 is created, along with the regeneration of the sorbent for its reuse. This two-step process is used in almost all of the industrial air capture devices (known as "synthetic trees") currently. For both flue stack scrubbing and air capture, the most expensive processes are the regeneration cycle, which makes the cost of capturing CO_2 from ambient air slightly higher than those incurred during the conventional capture in flue stacks (Lackner and Brennan 2009).

Currently, research and development (R&D) is mainly focused on two directions, i.e., improvement of the contactor and the regeneration cycle. Large convective tower, packed scrubbing towers, and "energy towers" have been proposed/tested as a contactor or theoretically analyzed (Lackner et al. 1999; Baciocchi et al. 2006; Zaslavsky 2006; Zeman 2007; Mahmoudkhani et al. 2009; de Richter 2012). Zeman (2007) estimated a total energy requirement of 380 kJ/mol of CO_2 for the capture and chemical recovery (using a modified lime cycle as the recovery process). Mahmoudkhani et al. (2009) reduced fluid pumping work by 90% in the packed tower by intermittent operation of the contactor with a 5% duty cycle. In the regeneration cycle, the carbonate solution goes through a crystallizer and becomes solid carbonate, which then goes through a kiln reactor to become CaO, NaO, or KO with pure CO_2 being released (CE 2012). Mahmoudkhani et al. (2009) reported a novel process for removing carbonate ions from alkaline solutions based on titanate compounds and compared it to the traditional lime cycle for the caustic recovery. The titanate process reduces the high-grade heat requirement by ~50%. The results support process design of the titanate cycle. The carbonate solution can also be regenerated via a membrane process (a process under research) and the hydroxyl solution can be reused. The membrane process is an electrodialysis process, and the electricity used is substantial (CE 2012).

Lackner (2009) proposed using an anionic exchange resin (Marathon A), that absorbs carbon dioxide when dry and releases it when exposed to moisture, as a solid sorbent to capture CO_2 directly from ambient air. The ion exchange resin is composed of a polystyrene backbone with quaternary amine ligands attached to the polymer. These quaternary amine groups carry a permanent positive charge. The positive ions fixed to the polymer backbone never release a proton (as NH_4^+ would). Thus, the resin is more akin to a solidified sodium salt brine than to an ammonia solution, and it readily absorbs CO_2 diluted in the air at a rate of 10–500 μ mol/m^2-s (similar to NaOH solution). Then, a water vapor of 45 °C is sufficient to drive most of the CO_2 off the resin and have it revert to absorb CO_2. Global Research Technologies, LLC has demonstrated the efficacy of the air extraction device. It is estimated that a cost of \$200/ton of CO_2 is needed for a prototype device with early (1990s) design and a cost of \$30/ton of CO_2 (≈ \$0.25/gallon of gasoline) could be achieved in the near-future (Lackner and Brennan 2009).

Carbon Engineering (Alberta, Canada) developed an "Air Capture" system to capturing CO_2 directly from air (Mahmoudkhani et al. 2009). The system draws air and then sends it to a contactor (similar to a trickling tower) for wet scrubbing–the CO_2 in air is absorbed by the hydroxyl solution and becomes carbonate solution. The system requires an energy source, and produces a stream of pure CO_2 as its principal output. The system enables cost-effective industrial scale applications for CO_2 capture from mobile/ distributed emissions sources. A similar concept is to build an "energy tower" for CO_2 capture; a cooling tower with a diameter of 300 m and a height of 800 m would capture 6,8000,000 tC/year and generate 1130 GWh electricity (at 3–5 cts/kWh). Both NaOH and NH_3 can be used as absorbents, but ammonia is more suitable for CO_2 capture because ammonia (a strong base) can be produced from neutral air and water ($N_2 + 3H_2O \rightarrow 2NH_3$) with renewable energy. Ammonia can be stored and transported in $MgCl_2$, e.g., in the form of $Mg(NH_3)_6Cl_2$ and then released at 300°C (ammonia fuel cell) to be used as carbon free energy (Elmøe et al. 2006; de Richter 2012). Ammonia can also be used as a fuel with N_2 and H_2O being the only combustion products ($4NH_3 + 3O_2 \rightarrow 2N_2 + 6H_2O$), a zero-emission combustion. In addition, ammonia is a major technology for emission control of NO_x (Fulks et al. 2009). In energy towers fed with NH_3, the CO_2 is captured via the reaction $2NH_3 + CO_2 \rightarrow\rightarrow (NH_3)_2CO_3$, and $(NH_3)_2CO_3$ can be used to make urea ($H_2N\text{-}CO\text{-}NH_2$). Urea is a fertilizer and is currently produced on a scale of 100,000,000 tons/year worldwide. Therefore, using NH_3 would have many more advantages as compared to NaOH. According to de Richter (2012), only 1600 energy towers worldwide are needed to soak up the 22 billion tons of CO_2 produced annually with green electricity being produced and carbon free fuel (NH_3 or H_2 economy) being produced, together with many other advantages. Details are needed about life-cycle assessment of the feasibility of the system.

20.3.2 Transport of CO_2

After capture, CO_2 will be transported via pipeline to suitable storage sites or locations where CO_2 will be used. Usually, CO_2 in the pipeline is at a very high pressure (e.g., ~150 bars), which makes it a supercritical fluid (i.e., the vapor (gas) phase becomes as dense as the liquid phase but flows easily like gases). In addition, CO_2 can be transported with a conveyor belt system or ship for other applications.

Currently, most of the pipelines are built for transport CO_2 to oil production fields for EOR purposes. For example, at Weyburn, the CO_2 is a purchased by-product from the Dakota Gasification Company's synthetic fuels plant in Beulah, North Dakota; the CO_2 (95%) is transported through a 320-km pipeline at a rate of about 5,000 tonnes/day. Only a few of the pipelines are used in several pilot projects to test the long-term storage of CO_2 in different geologic formations. In the future, a massive pipeline network will be needed if large-scale CCS implementation occurs, which will raise several issues, such as a) regulatory classification of CO_2 itself (commodity or pollutant), b) economic regulation, c) utility cost recovery, d) pipeline right-of-ways, e) pipeline safety, f) environmental impact. Optimization of pipeline network in concert with sophisticated CCS (e.g., zero-emission power generation plants), CO_2 inventory (what, where, when), renewable energy technologies, and CO_2 reuse technologies is needed and will be very challenging.

20.3.3 Long-Term Storage of CO_2

As shown in Table 20.4 (Cuff and Goudie 2008), the major long-term storage (sequestration) technologies included: a) geological, b) mineral, and c) ocean storage.

Geological Storage. Currently, geological storage may be the most popular option. The total worldwide CO_2 storage capacity is ≥ 2000 – 10,000 Gt (IPCC 2005; Plasynski et al. 2009; Lin 2010), which is enough to store emissions at the current emission rate of about 28 Gt per year. Table 20.5 shows examples of commercial geological storage deployment. There are a dozen of small- or pilot-scale demonstration projects in the world. At Weyburn site, ~18 million tons CO_2 have been injected between 2000 and 2010 (July); ultimately 20 million tons of CO_2 are expected to be stored. The EOR is expected to enable an additional 130 million barrels of oil to be produced and extend the life of Weyburn field by 25 years. Current cost is about \$20/ton of CO_2 (MIT 2012). Many industrial applications have injected large volumes of CO_2 underground. EOR operations in many parts of the US have been initiated with individual injection values as large as 3 MMt/year (810,000 t C) and cumulative injections of anthropogenic CO_2 of about 10 MM t CO_2/y (2.7 MM t C) (Cuff and Goudie 2008). It should be pointed out that, in many EOR projects, there is almost no monitoring beyond that required for CO_2-flood operations (Cuff and Goudie 2008), which is a concern of the technology because pressure connection can induce fluid flows over very long distances. Shukla et al. (2011) used a two-dimensional (2D) axisymmetric numerical model to predict the displacement of an ideal CO_2 reservoir with 30 years of injection and 70 years of monitoring phase; they found an induced vertical displacement of less than 3 mm at the caprock-reservoir interface at the end of the 100-year period. Therefore, the injection of supercritical CO_2 does not cause any significant disturbance to the stress field and stability of the geological formations in the reservoir if the reservoir has a nearly intact caprock (free of any major faults or fractures).

Table 20.4. CO_2 storage Technologies[a]

Geological storage options and worldwide CO_2 storage capacity (C in Gt CO_2):
- Saline formations contain brine in their pore volumes, commonly with salinities > 10,000 ppm. C > 1000.
- Declining oil and gas fields have some combination of water and hydrocarbons in their pores. Examples include enhanced oil or gas recovery. C = 675–900.
- Unminable coalbeds (= CO_2 enhanced coalbed methane, CO_2-ECBM). C = 3–200.

Concerns and needs:
- Little is known about saline aquifers compared to oil fields; as the salinity of the water increases, less CO_2 can be dissolved into the solution. Larger uncertainty about the saline aquifers exists if the site appraisal study is limited.
- Liquid CO_2 is nearly incompressible with a density of ~1000 kg/m^3; overpressuring and acidification of the reservoir may cause a) changes in the pore/mineral volume, d) saline brines (or water) moving into freshwater aquifers or uplift; old oil wells may provide leak opportunities.
- In CO_2-ECBM, the key reservoir screening criteria include laterally continuous and permeable coal seams, concentrated seam geometry, minimal faulting and reservoir compartmentalization, of which there is not much known.
- New technologies are needed to ensure CO2 stays in place forever.
- Need thorough site appraisal studies to reduce harmful effects.

Mineral storage options:
- Natural silicate minerals can be used in artificial processes that mimic the natural weathering process; alkaline industrial wastes can also be considered. It is a permanent storage option, and has minimal monitoring requirements.
- Magnesium and calcium silicate deposits are sufficient to fix the CO_2 that could be produced from the combustion of all fossil fuels resources. To fix a tonne of CO_2 requires about 1.6 to 3.7 tonnes of rock.

Concerns and needs:
- The kinetics of natural mineral carbonation is slow. To speed up the process, solid reactants and additives are needed.
- The resulting carbonated solids must be stored at environmental suitable locations.
- Needs: a) to reduce cost and energy requirement; b) to integrate/optimize power generation, mining, carbonation reaction, carbonates' disposal, transport of materials, and energy in a site-specific manner; and c) demonstration plants/projects.

Ocean storage options (capacity > 40000 Gt in water column but (66–100) x10^6 Gt if marine sediments considered):
- CO_2 dispersal in a very dilute form at depths of 1000–2000 m, a most promising option in the short-term. The cost of capturing the CO_2 + transporting it 500 km + storing it = ~ $70/tonne CO_2.
- Injecting CO_2 directly into the sea at > 3000 m to for a lake of liquid CO_2 on the seabed.
- Formation of a sinking plume (e.g., bicarbonate) to carry most of the CO_2 into deeper water.
- Release of carbonate minerals to accelerate carbonate neutralization.

Concerns and needs:
- Concerns: a) unknown impact on ecosystems (e.g., ocean acidification, wildlife, oxygen supply); b) difficult to certify the dissolution, leakage and location of CO_2; c) unknown impact on microbial carbon pump and biological carbon pump.
- Needs: a) making reliable predications of the technical feasibility and storage times; b) understand how to predict and minimize any environmental impact; and c) making reliable cost estimates and assess the net benefit.

[a]Major references: Stevens and Spector (1998); IEA (2004); IPCC (2005); Schiller (2007); Cuff and Goudie (2008); Hoffman (2009); Plasynski et al. (2009); Lin (2010); MIT (2012); and Reeves (2012).

Table 20.5. Three large-scale CO_2 injection projects (Wikipedia 2010, 2011, 2012)

Site/start date	Geo-formation	Reservoir type	Permeability	Seal type
Sleipner, Norway, 1996	Offshore saline	Deep-water sandstone	Very high	Thick shale
Weyburn, Canada, 2000	Onshore EOR	Ramp carbonate	Moderate	Evaporate
In Salah, Algeria, 2004	Krechba Carboniferous Fm.	Fluvial/tidal sandstone	Low	Thick shale

Storage of CO_2 in deep saline formations does not produce value-added by-products, but it has other advantages, such as: a) its carbon storage capacity is large, making them a viable long-term solution. For example, in the US, such capacity is > 12,000 billion tonnes of CO_2; b) most existing large CO_2 point sources are within easy access to a saline formation injection point, and therefore it is compatible with near-zero carbon emissions; c) a significant baseline of information and experience exists. For example, information generated by the oil industry on injecting brines from the recovered oil into saline reservoirs can be used (DOE 2012). In addition, coupled reactive transport models for heat and density driven flow in CO2 storage in saline aquifers have been proposed and evaluated (Li 2011).

Coal has the capacity to hold considerably more CO_2 than either CH_4 or N_2 in the adsorbed state (in an approximate ratio of 4:2:1). Operational practices for CO_2-ECBM recovery are still in its infancy. Field experiments in San Juan Basin, USA indicated that the process is technically and economically feasible. To date, over 2 Bcf of CO_2 has been sequestered. Enhancement of gas production can be as high as 150% over conventional pressure-depletion methods. Dewatering of the reservoir is also improved. ECBM development may be profitable in the San Juan basin at wellhead gas prices above $1.75/Mcf, adding as much as 13 Tcf of additional methane resource potential within this mature basin (Stevens and Spector 1998). The RECOPOL (Reduction of CO_2 emission by means of CO_2 storage in coal seams in the Silesian Coal Basin of Poland) project indicates that injection in coal seams is not trivial as coal is swelling, causing the reduction of permeability, which may be the reason why the gas production rate was lower than expected (even though gas production is enhanced). Relative low permeability limits injectivity to be probably < 100 ton/d-vertical well, which requires a large number of wells for injection (Lin 2010).

The world is rich in coal-bed methane (CBM) resources; the gas content of some of the coal basins has been confirmed. These coal basins have significant CO_2-ECBM potential. In the U.S., CO_2-ECBM can be used in many places, such as the Texas Gulf Coast, Northern Appalachia and Illinois/Indiana (Reeves 2012). Coal basins in Australia, Russia, China, India, Indonesia and other countries also have large CO_2-ECBM potential. Results from research held in 29 sites for potential CBM and ECBM in China have determined that CO_2 storage potential is about 143Gt in the countries coal bed. This could sequester CO_2 emissions for an estimated 50 years based on China's CO_2 emission levels in 2000. Simultaneously, the production of methane from ECBM has been estimated to reach 3.4 and 3.8 Tm^3 respectively, which equates to 218 years of production at China's 2002 production rates (Hongguan et al. 2007). Actually, the total worldwide potential for CO_2-ECBM is estimated at approximately 68 Tcf, with about 7.1 billion metric tons of associated CO_2 sequestration potential. If viewed purely as a non-commercial CO_2 sequestration technology, the worldwide sequestration potential of deep coal seams may be 20–50 times greater (Stevens and Spector 1998). In addition, ECBM techniques may be applied to tap remaining gas in coal after production in a secondary production phase.

Mineral Storage. In recent years, carbonation of magnesium- and calcium-based silicates has emerged as a potential option for CO_2 storage. The major metal oxides of Earth's Crust include: SiO_2 (59.71%), Al_2O_3 (15.41%), CaO (4.90%), MgO (4.36%), Na_2O (3.55%), FeO (3.52%), Fe_2O_3 (2.63%). In mineral sequestration process, CO_2 exothermically reacts with available metal oxides to form stable carbonates ($CaCO_3$, $MgCO_3$, Na_2CO_3, $FeCO_3$, K_2CO_3, and $FeCO_3$). Theoretically, up to 22% of the earthen mineral mass is able to form carbonates. The process occurs naturally over many years. For example, silicate mineral weathering is a combination of dissolution of calcium silicate minerals and carbonate precipitation, and the nest reaction is the formation of limestone and silica (SiO_2) (IPCC 2005):

$$CaSiO_3 + 2H_2O + 2CO_2 \rightarrow Ca^{2+} + 2HCO_3^- + SiO_2 + H_2O \quad \text{(Eq. 20.10)}$$

$$Ca^{2+} + 2HCO_3^- \rightarrow CaCO_3 + H_2O + CO_2 \quad \text{(Eq. 20.11)}$$

$$CaSiO_3 + CO_2 \rightarrow CaCO_3 + SiO_2 \quad \text{(Eq. 20.12)}$$

Similarly, CO_2 can react with other earthen oxides and be sequestrated as carbonates:

$$Ca(OH)_2 + 2CO_2 \rightarrow Ca(HCO_3)_2 \quad \text{(Eq. 20.13)}$$

$$Mg(OH)_2 + 2CO_2 \rightarrow Mg(HCO_3)_2 \quad \text{(Eq. 20.14)}$$

$$CaCO_2 + CO_2 + H_2O \rightarrow Ca(HCO_3)_2 \quad \text{(Eq. 20.15)}$$

$$CaO + 2CO_2 + H_2O \rightarrow Ca(HCO_3)_2 \quad \text{(Eq. 20.16)}$$

$$MgO + 2CO_2 + H_2O \rightarrow Mg(HCO_3)_2 \quad \text{(Eq. 20.17)}$$

Serpentine $Mg_3Si_2O_5(OH)_4$ and Olivine Mg_2SiO_4 are the most abundant Mg-silicates. It has been proposed to use them for CO_2 storage (IPCC 2007):

$$Mg_3Si_2O_5(OH)_4 + 3CO_2 \rightarrow 3MgCO_3 + 2SiO_2 + 2H_2O, \ \Delta H = -89 \text{ kJ/mol} \quad \text{(Eq. 20.18)}$$

$$Mg_2SiO_4 + 2CO_2 \rightarrow 2MgCO_3 + SiO_2, \ \Delta H = -64 \text{ kJ/mol} \quad \text{(Eq. 20.19)}$$

The basic steps include: a) mining (and later mine reclamation); b) mineral pretreatment; c) CO_2 transport and pre-processing; d) carbonation reaction; and e) product handling and disposal. However, the direct fixation of carbon dioxide on solid unrefined material particles is too slow to be used. To speed up the process, several schemes have been proposed and tested for the mineral carbonation process (Table 20.6). All these schemes are energy intensive and costly. For example, the cost of using natural silicate olivine to store CO_2 is \$50–100/tCO_2 stored, which is 30–50% energy penalty on the power plant. Adding 10–40% energy penalty in the capture plant, a full CCS system with mineral carbonation may need 60–180% more energy than a power plant with equivalent output without CCS (IPCC 2005).

Ocean Storage. There are four basic ways to store CO_2 in the ocean (see Table 20.4). Currently, major conclusions about these options are based on modeling. CO_2 injected at a depth of 3000 m is a better option because the efficiency of CO_2 retention will be between 48–82% after 500 years, substantially more efficient than the other options (IEA 2004). This is because at the depth of 3000 m, the CO_2 may be denser than the surrounding pore fluids and thus, be gravitationally trapped there. As a result, deep-ocean, sub-seafloor storage appears to offer a particularly safe location to store CO_2. It should be pointed out that, the four options do not consider the contributions by marine organisms via biological carbon pumps, mainly because these pumps are thought to be a slow solution. However, more and more results indicate that our understanding of these topics is very limited, and future breakthrough is possible once the knowledge gap is filled. Some related information is briefly discussed below.

Table 20.6 CO_2 mineral carbonation processes (Schiller 2007).

Direction Carbonation	Indirection Carbonation	Indirection Carbonation (cont'd)
• Gas phase–one step	• HC extraction	• pH swing
• Aqueous–one step	• Acetic acid	• Caustic soda (NaOH)—three step
o Simple	• Molten salt	• Dual alkali
o Additive enhanced	• Gas phase–two step	• Precipitated calcium carbonate (PCC)
• Molten salt	• NH_4–salt extraction	• Alkaline brine

On average, the ocean absorbs 2% more carbon than they emit each year, forming an important sink in the overall carbon cycle. CO_2 is absorbed by the ocean as per the reactions below (IPCC 2005):

$$CO_2\ (g) + H_2O \leftrightarrow H_2CO_3\ (aq) \leftrightarrow HCO_3^- + H^+ \leftrightarrow CO_3^{2-} + 2H^+ \quad \text{(Eq. 20.20)}$$

Once in the ocean, CO_2 is transported and/or transformed in two major mechanisms:

a) Physical pump. Cold water holds more CO_2 than warm water. Because cold water is denser than warm water, this cold, CO_2-rich water is pumped down by vertical mixing to lower depths. Total dissolved inorganic carbon (DIC) is the sum of carbon contained in H_2CO_3, HCO_3^-, and CO_3^{2-}, but majorly in the form of HCO_3^-. The net results of adding CO_2 to sea water is the generation of H^+ (i.e., lowering pH) and decreases the concentration of CO_3^{2-}.

b) Biological carbon pump (BCP) forcing CO_2 going through the food chain. This is a process whereby CO_2 in the upper ocean is fixed by primary producers and transported to the deep ocean as sinking biogenic particles or as dissolved organic matter. The fate of most of this exported material is remineralization to CO_2, which accumulates in deep waters until it is eventually ventilated again at the sea surface. However, a proportion of the fixed carbon is not mineralized but is instead stored for millennia as recalcitrant dissolved organic matter.

The consequence of pathways a) and b) are that ocean surface waters are super-saturated with respect to $CaCO_3$, allowing the growth of corals and other organisms that produce shells or skeletons of carbonate minerals. In contrast, the deepest ocean waters have lower pH and lower CO_3^{2-} concentrations, and are thus undersaturated with respect to $CaCO_3$. The net effect of pathway b) is that a large amount of carbon is suspended in the water column as dissolved organic carbon (DOC). For example, green, photosynthesizing plankton converts as much as 60 gigatons of carbon per year into organic carbon–roughly the same amount fixed by land plants and almost 10 times the amount emitted by human activity. Even though most of DOC is only stored for a short period of time, marine organisms are capable to convert immense amounts of bioavailable organic carbon into difficult-to-digest forms known as *refractory* DOC; this organisms driven conversion has been named the "jelly pump" (Hoffman 2009) and the microbial carbon pump (MCP) (Jiao et al. 2010). Once transformed into "inedible" forms, these DOCs may settle in undersaturated regions of the deep oceans and remain out of circulation for thousands of years, effectively sequestering the carbon by removing it from the ocean food chain (Hoffman 2010). As shown in Table 20.7, there is a tremendous amount of CO_2 storage capacity in marine sediments and sedimentary rocks. However, what is the contribution due to the inedible forms of DOCs or carbonate compounds that are formed by biological pumps and the related mechanisms are not fully understood yet, rending more studies about the real contribution of these mechanisms to CO_2 storage.

Table 20.7. Capacity of different CO_2 sink (adapted from Hoffman 2009)

Sink	Amount (Gt)	Sink	Amount (Gt)
Atmosphere	578 (as of 1700) 766 (as of 1999)	Marine sediments & sedimentary rocks	60,000,000–100,000,000
Ocean	38,000–40,000	Soil organic matter	1,500–1,600
Terrestrial plants	540–610	Fossil fuel deposits	4,000

20.3.4 Monitoring and Life Cycle Risk Management of CCS

CCS involves 4 major systems: a) capture and compression; b) transportation; c) injection; and d) geological storage reservoir. Each system can leak CO_2 and thus, should be treated as a source for emissions. In this section, however, we will focus on monitoring, verification and accounting (MVA) of CO_2 storage in geological storage reservoirs due to complexity of the system and the related issues. Comprehensive information can be found in NETL (2009).

Leakage, MVA and Life Cycle Risk Management (LCRM) of CCS. For well-selected, designed and managed geological storage sites, IPCC estimates that risks are comparable to those associated with current hydrocarbon activity. Nevertheless, leakage in geological formations is possible, such as leakage a) through poor quality or aging injection well completions, b) through abandoned wells, c) due to inadequate caprock characterization; and d) due to inconsistent or inadequate monitoring. Table 20.8 shows potential risks associated with large-scale injection of CO_2. For example, in January 2011, Weyburn was reported to leak CO_2 at the surface of a pond on a farm around the injection site (MIT 2012). The CO_2 with concentrations > 5–10% of the air volume is lethal. Therefore, there are serious safety concerns here. Mineral storage is not regarded as having any risks of leakage. However, carbonic acid formed due to the CO_2 storage or mineral processing can release heavy metals from storage sites or minerals, requiring monitoring of the seepage of heavy metals and groundwater contamination. It is very difficult to account for ocean storage as CO_2 mixes throughout the ocean. The IPCC estimates 85%

of the sequestered carbon dioxide would be retained after 500 years for depths 3000 m, indicating that the option may still be questionable. In addition, hydrate formation (due to the reaction between liquid CO_2 and water) in deep ocean CO_2 storage would provide sufficient energy to transport CO_2-laden fluid to locations far away from the storage site (Anderson 2003).

MVA of injected CO_2 over the long term are formidable due to harsh environmental conditions and complicated processes involved, combined with the deep location and size of the storage sites. For example, the flux of CO_2 leaving a reservoir is extremely difficult to determine because they might be much smaller than the biological respiration rate and photosynthetic uptake rate of the ground cover. In general, MVA aims at (NETL 2009):

- Site performance assessment. This is to a) image and measure CO_2 in the reservoir (e.g., to make sure the CO_2 is effectively and permanently trapped in the deep rock formations), b) show if the site is currently preforming as expected, c) estimate inventory and predicate long-term site behaviors (e.g., enable site closure), and d) evaluate the interactions of CO2 with formation solids and fluids for improved understanding of storage processes, model calibration, future expansion, design improvement;
- Regulatory compliance. This is to a) monitor the outer envelope of the storage complex for emissions accounting, b) collect information for regulatory compliance and carbon credit trading, and c) provide a technical basis to assist in legal dispute resulting from any impact of CCS; and
- Health, safety, and environmental (HSE) impact assessment. This is to a) detect potentially hazardous leakage and accumulations at or near surface, b) identify possible problems and impact on HSE, and c) collect information for designing remediation plans.

Briefly, the time course of the LCRM of CCS includes:

Development and quality CCS technology → Propose site → Prepare site → operate site → close site → post closure liability.

The LCRM can be classified as three phases:

- Pre-operation phase (about 1–2 years), including technology development, site selection, site characterization, and field design;
- Operation phase (about 10–50 years), including site construction, site preparation, injection, and monitoring; and
- Post-injection phase (about 100–1000 years), including site retirement program, and long-term monitoring (operation, seismic verification, HSE impact).

Risk assessment will be a key ongoing activity that will drive the future activities of the project. Moreover, contingency plants with mitigation strategies need to be established. At each project decision point, the risk assessment needs to be reviewed, and the decision to proceed to the next phase will depend on the ability of the project partners to manage the assessed risks.

Table 20.8. Potential risks associated with large-scale injection of CO_2[a]

Phase	Associated risks	Qualification and mitigation strategy
Pre-operation	• Problems with licensing/permitting. • Poor conditions of the existing well bores. • Lower-than-expected injection rates.	• Revise injection rates, well members, and zonal isolation. • Test all wells located in the injection site and the vicinity for integrity and establish good conditions. • Determine new injection rates or add new wells/pools.
Operation	• Vertical CO_2 migration with significant rates. • Activation of the pre-existing faults/fractures. • Substantial damage to the formation/caprock. • Failure of the well bores. • Lower-than-expected injection rates. • Damage to adjacent fields/producing horizons.	• The monitoring program will allow for early warning regarding all associated risks and for the injection program to be reconfigured upon receiving of such warnings. • If wellbore failure, recomplete or shut it off. • Include additional wells/pools in the injection program.
Post-injection	• Leakage through pre-existing faults/or fractures. • Leakage through the wellbores.	• Decrease formation pressure and treat with cement. • Test periodically all wells in the injection site. In case of leakage, wells will be recompleted and/or plugged.

[a] Adapted from NETL (2009).

Current Methods for MVA and Future Needs. MVA of CO_2 sequestration in different geological formations for CO_2 storage is very challenging because for each setting, there are so many different layers that need monitoring, often, with different methods. For example, for on-shore storage systems (e.g., a CO_2-EOR system), monitoring and measurement are needed in a) CO_2 plume, b) primary seal, c) saline formation, d) secondary seal, e) groundwater aquifer, f) vadose zone, g) terrestrial ecosystem, and g) atmosphere, while for an off-shore storage system, it would need in a)–d), e) seabed sediments, f) water column and aquatic ecosystem, and g) atmosphere. Currently, available monitoring methods include (NETL 2009):

- Atmospheric monitoring tools: such as CO_2 detectors, eddy covariance, advanced leak detection system, laser systems and LIDAR, tracers and isotopes (Campbell et al. 2009).
- Near-surface monitoring tools: such as ecosystem stress monitoring, tracers, groundwater monitoring, thermal hyperspectral imaging, synthetic aperture radar, color infrared transparency films, tiltmeter, flux accumulation chamber, induced polarization, spontaneous (self) potential, soil and vadose zone gas monitoring, shallow 2-D seismic.
- Subsurface monitoring: such as multi-component 3-D surface seismic time-lapse survey, vertical seismic profile, magnetotelluric sounding, electromagnetic resistivity, electromagnetic induction tomography, injection well logging (wireline logging), annulus pressure monitoring, pulsed neutron capture, electrical resistance tomography, acoustic logging, 2-D seismic survey, time-lapse gravity, density logging, optical logging. Cement bond long, Gamma ray logging, microseismic survey, crosswell seismic survey, aqueous geochemistry, resistivity log.

The criteria of judging which methods are suitable for different settings are a) simple and cost effective (regarding explaining and implementing the method), b) defensible (sufficiently stringent to ensure that the method is of good QA/QC–quality assurance and quality control), and c) verifiable (the value obtained by the method can be assigned with confidence and certainty).

Currently, many problems exist, such as detection limits and precision levels of different methods have not been completely established; strategies for different locations have not been fully established. The procedures for detecting, locating and then quantifying leakage have not been developed. Sensitivity analysis of different methods is still in their infancy. Current underground storage accounting is at best qualitative. For example, seismic data can show where CO_2 exists qualitatively but not quantitatively. Similarly, it is difficult to use chemical samples to verify storage, since CO_2 can take on many different forms and will mingle with carbon resources that were at the site prior to injection (Lankner and Brennan 2009). Several methods have been proposed to improve accounting of stored carbon, such as using C-14 as a tracer for a) monitoring fluxes from geologic sequestration (Bachelor et al. 2008), b) facilitating measurement via sampling (Landcar and Brennan 2009), c) optical techniques with path lengths of ~1 km, and d) computer simulation and model development. In the future, improvement is needed for a) direct emission measurements from existing CO_2-EOR projects, b) controlled release experiments for demonstrating the ability to detect, locate and quantify emissions in various settings, c) best practices and procedures that can be used to respond to any detected changes, d) approaches to distinguish natural ecosystem fluxes, and other anthropogenic emissions from geological storage reservoir emissions, and e) improve detection of small secondary accumulations of CO_2.

20.3.5 Beneficial Uses of CO_2

Carbon dioxide is rather inert and non-reactive. This inertness is the reason why CO_2 has broad industrial and technical applications. Efforts for CO_2 beneficial uses focus on pathways and novel approaches that can use captured CO_2 for value-added products (e.g., chemicals, cements, or plastics) or beneficial activities so that a portion of the CO_2 capture cost can be offset. Usually, LCA must be considered for processes or concepts to ensure that additional CO_2 is not produced, and extra energy not consumed, due to CO_2 reuse processes.

While the concept is relatively new and less well-known compared to other CCS technologies, many different pathways/reuse technologies have been explored (Figure 20.2). In these processes/technologies, CO_2 is either being used a) as a substrate for boosting production (e.g., algae cultivation) or an additive for enhancing the processes (extraction of alumina from bauxite residue), b) as a feedstock for synthesizing stable product (e.g., for urea yielding boosting, polymer processing, liquid fuel production), c) for integration into pre-existing products (e.g., in concrete curing, carbonate mineralization), or d) as a working fluid for enhancing other activities (e.g., EOR, ECBM, EGS). Details of these technologies are described in PB and GCCSI (2011).

The global CO_2 reuse market currently amounts to ~80 million tonnes/year, of which ~50 million tonnes per year are used for EOR at a price of \$15–19/tonne. Potentially, the global supply of anthropogenic CO_2 is ~500 million tonnes of low-cost (< \$20/tonne) high concentration CO_2; at a much higher cost (\$50–100/tonne), around 18,000 million tonnes per year could also be captured for CO_2 reuse (PB and GCCSI 2011). Advances of CO_2 reuse technologies depends on future carbon restrictions and prices and their interaction with other CCS technologies.

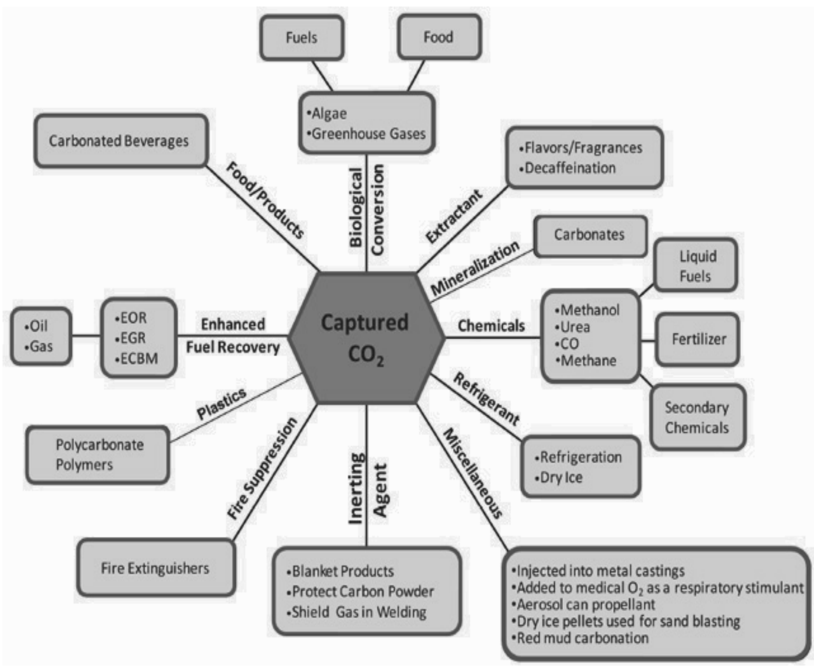

Figure 20.2. Schematic diagram of beneficial uses of CO_2 (Damiani et al. 2012)

20.4 Concerns, Constrains and Future Perspectives

Concerns. Major public concerns about CCS include: a) limitations of CCS for power plants, b) cost of CCS, c) mandating CO_2 emission reductions at power plants, d) regulating the long-term storage of CO_2, and e) concerns related to HSE. One limitation of CCS is its energy penalty. Wide-scale application of CCS would reduce CO_2 emissions from flue stacks of coal power plants by 85–90% with an increase in resource consumption by one third. Completing the cycle of carbon capture and storage may double the US industrial electricity price (i.e., from 6 to 12 ¢/kWh) or increase the typical retail residential electricity price by ~50% (Charles

2009; IPCC 2005). There is a need to invest over \$2.5–3 trillion for CCS deployment from 2010 to 2050, which is about 6% of the overall investment needed to achieve a 50% reduction in GHG emissions by 2050 (IEA 2009). Because CCS is expensive, regulatory frameworks should help in establishing and promulgating best practices and allowing regulated utilities to make investments in capture technologies (Landcar and Brennan 2009). In addition, government should be more involved in clarifying legislation barriers and in the management of safe and permanent carbon storage.

Constrains. The pros and cons of CCS have been discussed recently (IDEA 2012). The opponents of CCS believe that CCS has several constrains, such as:

a) CCS efficacy: CCS delays inevitable transition to clean energy; CCS distracts attention and resources form clean energy; CCS is not feasible; CCS will take far too long to implement for climate change.

b) Risks involved: The potential problems associated with CCS are not fully understood. Leakage of CO_2 from CCS facilities is a risk and a burden of taxpayers and our children.

c) Economics: The estimated costs for CO_2 transportation (\$1–3/t-100 km) and sequestration (\$4–8/t-CO_2) are small compared to that for CO_2 capture (\$35–55/t CO_2 capture) (Li et al. 2009). In general, CCS is less cost-effective than renewable energy; CCS raises costs and energy prices, and requires significant water (e.g., power plants with CCS technology needs 90% more freshwater than those without CCS); without a price on carbon, CCS will not fly.

Obviously, constrains a) and c) are related to the regulatory and legal frameworks for GHG emission limits and carbon price. A concrete carbon price would be vital for stable framework for investment in low-carbon technologies such as CCS. Establishment of new regulations (e.g., GHG emission limits) and related permitting pathway for CCS technologies and projects is important. With GHG emission limits imposed, CCS systems will be competitive with other large-scale mitigation options, such as nuclear power and renewable energy technologies (ITF 2010). Constrain b) is related to CCS technologies. It seems that considerable research is needed in the future for a) clearing the uncertainty with long term predictions about submarine or underground storage security, b) developing technologies that can prevent CO_2 leakage from the storage, and c) minimizing possible HSH impacts.

Future Perspectives. We anticipate that future trends/needs will focus on overcoming the following major barriers related to large-scale deployment of CCS:

1) Technical: While technology currently exists for safe and effective CCS, it is imperative to improve CCS technologies to lower the cost and to reuse CO_2 in a beneficial way:
   a) promote government support to establish framework for CCS deployment;
   b) foster the success of CCS projects (including commercial-scale demonstrations);

c) conduct cutting-edge research to establish CCS
   i. technologies and the related fundamentals (e.g., long-term strategies for CO_2 source clusters and CO_2 pipeline networks, mapping CO_2 storage potential of deep saline formations, value-added CO_2 reuse pathways).
   ii. standards and consistent requirements to ensure the safe and effective operation of CCS, MVA and reporting.
d) support international collaboration to facilitate the global deployment of CCS.

2) Regulatory: Governments (state and federal) must work together to:
   a) establish comprehensive climate change legislation (e.g., GHG emission limits, carbon credit trading/carbon price);
   b) provide legal and regulatory clarity, authority and support for safe and effective CCS deployment (e.g., clarify agencies for issuing CCS permits, clarifying the right to use geological formation for CO_2 storage, preventing significant environmental impacts in CCS projects, regulating the safety and operation of CCS projects); and
   c) address key legal issues and uncertainties related to CCS implementation (e.g., improve long-term liability and stewardship framework; establish procedures for aggregating and adjudicating the use of and compensation for pore space for CCS projects; development of an international MVA protocol for CO_2 storage and allowance of transboundary CO_2 transfer).
3) Financial: To put specific frameworks and policies in place to support large-scale CCS deployment, governments need to
   a) share burdens and benefits of CCS equally among the taxpayers;
   b) spread widely cost allocation mechanisms for CCS projects;
   c) establish the commercial market at economically viable prices for CCS technologies; and
   d) increase funding for CCS demonstration projects to an average annual level of \$3.5–4 billion from 2010 to 2020 and provide \$1.5–2.5 billion per year from 2010 to 2020.
4) Social barriers. It is important to
   a) expand government education and engagement efforts (e.g., develop well-thought-out and well-funded public outreach programs to educate the public about the risks and benefits of CCS technologies; provide enhanced funding for outreach programs);
   b) provide transparent information about planned CCS projects in a timely manner to increase public understanding of CCS benefits and risks (e.g., develop regulations to require public consultation at and participation in planned CCS projects; create toolkits defining common principles and strategies for public engagement and make them available to the public); and
   c) Formalize the existing international network of CCS public education and engagement professionals.

20.5 Summary

In this chapter, we define CCS as any technologies/methods that can a) capture, transport, and store carbon (CO_2), b) monitor, verify and account the status/progress of the CCS technologies employed, and c) advance development/uptake of low-carbon technologies and/or promote beneficial reuse of CO_2. CCS can play a central role in the mitigation of GHG emissions (ITF 2010). The estimated costs for CO_2 transportation (\$1–3/t-100 km) and sequestration (\$4–8/t-CO_2) are small compared to that for CO_2 capture (\$35–55/t CO_2 capture) (Li et al. 2009). Currently, CCS technologies are available for large-scale applications, but much more improvements, particularly in CO_2 capture are needed. Currently, there's a huge gap between what can technically do and what we are doing. High costs, inadequate economic drivers, remaining uncertainties in the regulatory and legal frameworks for CCS deployment, and uncertainties regarding public acceptance are barriers to large-scale applications of CCS technologies in the world (CCCSRP 2010). It is imperative to overcome the technical, regulatory, financial and social barriers.

20.6 References

Anderson, G. K. (2003). "Enthalpy of dissociation and hydration number of carbon dioxide hydrate from the Clapeyron equation." *J. Chem. Thermodyn.,* 35(7), 1171–1183.

Anderson, S., and Newell, R. (2003). "Prospects for Carbon Capture and Storage Technologies." Discussion Paper published by Resources for the Future, Washington, DC. Available at <http://rff.org/rff/Documents/RFF-DP-02-68.pdf> (accessed Feb. 2012).

Bachelor, P. P., McIntyre, J. I., Amonette, J. E., Hayes, J. C., Milbrath, B. D., Saripalli, P. (2008). "Potential method for measurement of CO_2 leakage from underground sequestration fields using radioactive tracers." *J. Radioanal. Nucl. Chem*., 277(1), 85–89.

Baciocchi, R., Storti, G., and Mazzotti, M. (2006). "Process design and energy requirement for the capture of carbon dioxide from air." *Chemical Engineering and Processing*, 45, 1047–1058.

Beerling, D. (2008). *The Emerald Planet: How Plants Changed Earth's History.* Oxford Univ. Press. pp.194–195.

Brune, D. E., Lundquist, T. J., and Benemann, J. R. (2009). "Microalgal biomass for greenhouse gas reductions: Potential for replacement of fossil fuels and animal feeds." *J. Environ. Eng*., 135(11), 1136–1144.

Campbell, J. E., Fox, J. F., Davis, C. M., Rowe, H. D., and Thompson, N. (2009). "Carbon and nitrogen isotopic measurements from southern Appalachian soils: Assessing soil carbon sequestration under climate and land-use variation." *J. Environ. Eng*., 135(6), 439–448.

CCCSRP (California Carbon Capture and Storage Review Panel) (2010). *Findings and Recommendations by the California Carbon Capture and Storage Review Panel.* CCCSRP, Dec. 2010. Available at <www.climatechange.ca.gov/carbon_capture_review_panel/.../2011-01-14...> (accessed Feb. 2012).

Charles, D. (2009). "Stimulus gives DOE billions for carbon-capture project." *Science*, 323(5918), 1158.

Choi, S., Drese, J. H., Jones, C. W. (2009). "Adsorbent materials for carbon dioxide capture from large anthropogenic point sources." *ChemSuschem*, 2, 796–854.

Cuff, D. J., and Goudie, A. (eds.) (2008). *The Oxford Companion to Global Change*. Oxford Univ. Press, Oxford, N.Y., 2008.

Damiani, D., Litynski, J. T., Mcllvried, H. G., Vikara, D. M., and Srivastava, R. D. (2011). "The US Department of Energy's R&D program to reduce greenhouse gas emissions through beneficial uses of carbon dioxide." *Greenhouse Gases Sci. Technol.,* 1, 1–11.

de Richter, R. (2012). "Optimizing geoengineering schemes for CO_2 capture from Air." PPT slides Available at <http://data.tour-solaire.fr/optimized-Cabon-Capture%20RKR% 20final.pps> (accessed Feb. 2012).

DOE (U.S. Department of Energy) (2012). "Carbon Storage Research." Available at http://www.fossil.energy.gov/programs/sequestration/geologic/ (accessed Feb. 2012).

Elmøe, T. D., Sørensen, R. Z., Quaade, U., Christensen, C. H., Nørskov, J. K., and Johannessen, T. (2006). "A high-density ammonia storage/delivery system based on $Mg(NH_3)_6Cl_2$ for SCE-DeNOx in vehicles." *Chemical Eng. Sci*., 61, 2618–2625.

Figueroa, J. D., Fout, T., Plasynski, S., McIlvried, H., and Srivastava, R. D. (2008). "Advances in CO_2 capture technology–the U.S. Department of Energy's carbon sequestration program." *Intl. J. Greenhouse Gas Control,* 2, 9–20.

Fowles, M. (2007). "Black carbon sequestration as an alternative to bio-energy". *Biomass and Bioenergy*, 31, 426–32.

Fulks, G., Fisher, G. B., Rahmoeller, K., Wu, M.-C., D'Herde, E., and Tan, J. (2009). "A review of solid materials as alternative ammonia sources for lean NO_x reduction with SCR." SAE International, available at <http://delphi.com/pdf/techpapers/ 2009-01-0907.pdf> (accessed Feb. 2012).

Greenleaf, J. E., and SenGupta, A. K. (2006). "Flue Gas Carbon Dioxide Sequestration during Water Softening with Ion-Exchange Fibers." J. Environ. Eng., 135(6), 386–396.

Herzog, H.. J. (1999). "An introduction to CO_2 separation and capture technologies." Available at <http://sequestration.mit.edu/pdf/introduction_to_capture.pdf> (accessed Oct. 2011).

Herzog, H. J. (2001). "What future for carbon capture and sequestration?" *Environ. Sci. Technol*., 35(7), 148A–153A.

Herzog, H. J., Meldon, J., and Hatton, A. (2009). *Advance Post-Combustion CO_2 Capture.* Technical Report prepared for the Clean Air Task Force. <http://web.mit.edu/mitei/docs/reports/herzog-meldon-hatton.pdf> (accessed Feb. 2012).

Hoffman, D. L. (2009). “New Jelly pump rewrites carbon cycle.” Available at <http://theresilientearth.com/?q=content/> (accessed Feb. 2012).

Hoffman, D. L. (2010). “Ocean CO_2 storage revised.” Available at <http://www.theresilientearth.com/?q=content/> (accessed Feb. 2012).

Hongguan, Y., Guangzhu, Z., Weitang, F., and Jianping, Y. (2007). “Predicted CO_2 enhanced coal-bed methane recovery and CO_2 sequestration in China.’ *International Journal of Coal Geology*, 71(2–3), 345–357.

IDEA (International Debate Education Association) (2012). “Is carbon capture good technology and investment?” Available at <http://debatepedia.idebate.org/en/index.php/Debate:_Carbon_capture_and_storage> (accessed Feb. 2012).

IEA (International Energy Agency) (2004). *Modelling of ocean storage of CO_2–the GOSAC study.* Report #: PH4/37, Dec., 2004, IEA Greenhouse Gas R&D Program.

IEA (International Energy Agency) (2009). *Technology Roadmap: Carbon Capture and Storage.* An IEA report, Available at <http://www.iea.org/papers/2009/CCS_ Roadmap.pdf> (accessed Feb. 2012).

IPCC (Intergovernmental Panel on Climate Change) (2005). *IPCC Special Report on Carbon Dioxide Capture and Storage.* IPCC Working Group III. Cambridge Univ. Press, Dec., 19, 2005, 431 pp.

IPCC (2007). *Climate Change 2007: Synthesis Report.* The Fourth Assessment Report (AR4). Contribution of Working Groups I, II and III to the Fourth Assessment Report of IPCC. ISBN 92-9169-122-4.

IPCC (2012). The IPCC website <http://www.ipcc.ch/> (accessed Feb. 2012).

ITF (Interagency Task Force) (2010). *Report of the Interagency Task Force on Carbon Capture and Storage.*

Jiao, N., Herndl, G. J., Hansell, D. A., Benner, R., Kattner, G., Wilhelm, S. W., Kirchman, D. L., Weinbauer, M. G., Luo, T., Chen, F., and Azam, F. (2010). “Microbial production of recalcitrant dissolved organic matter: long-term carbon storage in the global ocean.” *Nature Reviews Microbiology*, 8, 593–599.

Johnson, R. (2010). “The carbon cycle.” Available at <http://www.windows2universe.org> (accessed Feb. 2012).

Lackner, K. S., Grimes, P., and Ziock, H. J. (1999). “Capturing carbon dioxide from air.” 24th Annual Technical Conference on Coal Utilization: Clearwater, FL.

Lackner, K. S. (2009). “Carbon dioxide capture from ambient air.” In: Blum, K., Keilhacker, M., Platt, U., and Roether, W. (eds.) *The physics perspective on energy supply and climate change–a critical assessment*. Eur. Phys. J. Special Topics, Springer Verlag, Bad Honnef, 2009.

Lackner, K. S., and Brennan, S. (2009). “Envisioning carbon capture and storage: expanded possibilities due to air capture, leakage insurance, and C-14 monitoring.” *Climatic Change*, 96, 357–378.

Li, Q. (2011). “Coupled reactive transport model for heat and density driven flow in co2 storage in saline aquifers.” *J. Hazardous, Toxic, and Radioactive Waste*, 15(4), 251–258.

Li, Z.-S., Fang, F., and Cai, N.-S. (2009). “CO_2 capture from flue gases using three ca-based sorbents in a fluidized bed reactor.” *J. Environ. Eng*., 135(6), 418–425.

Lin, W. (2010). *Gas Sorption and the Consequent Volumetric and Permeability Change of Coal*. Dissertation, Stanford Univ., March 2010.

Lu, D. Y., Hughes, R. W., Anthony, E. J., and Manovic, V. (2009). “Sintering and reactivity of $CaCO_3$-based sorbents for in situ co2 capture in fluidized beds under realistic calcination conditions.” *J. Environ. Eng*., 135(6), 404–410.

Mahmoudkhani, M., Keidel, K. R., Ferreira, J. C., Keith, D. W., and Cherry, R. S. (2009). “Low energy packed tower and caustic recovery for direct capture of CO2 from air.” *Energy Procedia 1*. (2009) 1535–1542.

Meyer, J. P. (2012). *Summary of Carbon Dioxide Enhanced Oil Recovery (CO_2EOR) Injection Well Technology*. Background Report prepared for the American Petroleum Institute. Available at <http://www.gwpc.org/e-library/documents/co2/API%20CO2%20Report.pdf> (accessed Feb. 2012).

MIT (2012). “About the MIT CC&ST Program: Technology overview.” Available <http://sequestration.mit.edu/> (accessed Feb. 2012).

Montzka, S. A., Dlugokencky, E. J., and Bulter, J. H. (2011). “Non-CO_2 greenhouse gases and climate change.” *Nature*, 476(7358), 43–50.

NETL (National Energy Technology Laboratory) (2009). *Monitoring, verification, and accounting of CO_2 stored in deep geological formations*. DOE NETL-311/081508, Jan. 2009.

NETL (National Energy Technology Laboratory) (2009). “Carbon sequestration: CO_2 utilization focus area.” Available at <http://www.netl.doe.gov/technologies/carbon_seq/corerd/co2utilization.html> (accessed Feb. 2012).

Osborne, C. P., and Beerling, D. J. (2006). “Nature’s green revolution: the remarkable evolutionary rise of C4 plants.” *Philos. Trans. R. Soc. Lond., D, Biol. Sci.*, 361(1465) 173–194.

PB (Parsons Brinkderhoff) and GCCSI (Global CCS Institute) (2011). *Accelerating the uptake of CCS: Industrial use of captured carbon dioxide*. A technical report written by Parsons Brinckerhoff in collaboration with the Global CCS Institute, March 2011, 260 pp.

Pfeiffer, H., Ávalos-Rendón, T., Lima, E., and Valente, J. S. (2011). “Thermochemical and cyclability analyses of the CO_2 absorption process on a Ca/Al layered double hydroxide.” *J. Environ. Eng*., 137(11), 1058–1065.

Plasynski, S. I., Litynski, J. T., McIlvried, H. G. and Srivastava, R. D. (2009). “Progress and New Developments in Carbon Capture and Storage.” *Critical Reviews in Plant Sciences*, 28(3), 123–138.

Randolph, J. B., and Saar, M. O. (2011). “Combining geothermal energy capture with geologic carbon dioxide sequestrations.” *Geophysical Research Letter*, 38, L10401, 7 pp.

Reeves, S. (2012). “Geological sequestration of CO_2 in deep, unmineable coalbeds: An integrated research and commercial-scale field demonstration project.” Available at <http://www.netl.doe.gov/publications/proceedings/01/carbon_seq/3a1.pdf> (accessed Feb. 2012).

Riemer, P., Audus, P., and Smith, A. (1993). *Carbon Dioxide Capture from Power Stations.* Cheltenham, United Kingdom: International Energy Agency Greenhouse Gas R&D Program.

Schiller, C. (2007). “Feasibility study of carbon dioxide mineral sequestrations.” European Talent Award for Innovative Energy Systems 2007. Available at <http://www.efpe.org/DownloadThesis.asp?file=3&thesis=18> (accessed Feb. 2012).

Shukla, R., Ranjith, P. G., Choi, S. K., and Haque, A. (2011). “Study of caprock integrity in geosequestration of carbon dioxide.” *International J. Geomechanics*, 11(4), 294–301.

Siriwardane, R., and Robinson, C. (2009). “Liquid-impregnated clay solid sorbents for CO_2 removal from postcombustion gas streams.” *J. Environ. Eng.,* 135(6), 378–385.

Spector, N. A., and Dodge, B. F. (1946). “Removal of carbon dioxide from atmospheric air.” *Trans. Am. Inst. Chem. Eng.*, 42, 827–848.

Stevens, S. H., and Spector, D. (1998). “Enhanced coalbed methane recovery using CO_2 injection: worldwide resource and CO_2 sequestration potential.” *Proceedings of SPR International Oil and Gas Conference and Exhibition in China*, 2–6 November 1998, Beijing, China, 489 pp, published by Society of Petroleum Engineers. ISBN: 978-1-55563-377-6.

Steinour, H. H. (1959). “Some effects of carbon dioxide on mortars and concrete: A discussion.” *J. Am. Concr. Inst.*, 4, 905–907.

Stolaroff, J. K. (2006). *Capturing CO_2 from ambient air: a feasibility assessment*. Ph.D. dissertation, Carnegie Mellon University.

Tepe, J.B., and Dodge, B.F. (1943). “Absorption of carbon dioxide by sodium hydroxide solutions in a packed column.” *Trans. Am. Inst. Chem. Eng.*, 39, 255–276.

USDOE (U.S. Department of Energy.) (1999). *Carbon Sequestration Research and Development.* Washington, DC: Office of Science and Office of Fossil Energy.

USDOS (United States Department of State) (2010). *U.S. Climate Action Report 2010.* 5th ed., Washington: Global Publishing Services, January 2010.

USEPA (U.S. Environmental Protection Agency) (2012). “Climate change–Greenhouse Gas Emission.” Available at http://epa.gov (accessed Feb. 2012).

VGB (2004) *CO_2 Capture and Storage - VGB Report on the State of the Art.* VGB PowerTech e.V., Essen/Germany, August 2004. Available at http://www.vgb.org /en/CO2cace.html. (accessed Oct. 2010).

White, C. M., Strazisar, B. R., Granite, E. J., Hoffman, J. S., and Pennline, H. W. (2003). “Separation and capture of CO_2 from large stationary sources and sequestration in geological formatons: Coalbeds and deep saline aquifers.” *J. Air & Waste Manag. Asso*., 53(6), 645–715.

Wikipedia (2010). “Carbon capture and storage (timeline).” Available at <http://en.wikipedia.org/wiki/Carbon_capture_and_storage_timeline> (accessed May 2010).

Wikipedia (2011). “Biochar.” Available at <http://en.wikipedia.org/wiki/Biochar> (accessed Oct. 2011).

Wikipedia (2012). "Carbon sink." Available at <http://en.wikipedia.org/wiki/Carbon_sink> (accessed Feb. 2012).
WRI (World Resources Institute) (2012). Available at <http://www.wri.org> (accessed Feb. 2012).
Zaslavsky, D. (2006). "Energy towers." *Physicaplus* (Online Magazine of the Israel Physical Society), Issue # 7, 2006. Available at <http://physicaplus.org.il/zope/home/en/1124811264/1137833043_en> (accessed Oct. 2011).
Zeman, F. (2007). "Energy and material balance of CO_2 capture from ambient air." *Environ. Sci. Technol.*, 41, 7558–7563.
Zero (2012). "Stationary point sources of CO_2." Available at <http://www.zero.no/ccs/capture/sources-of-co2> (accessed Feb. 2012).

CHAPTER 21

Estimation and Reduction of GHG Emissions in Wastewater/Sludge Treatment and Management

Xiaolei Zhang, Song Yan, R. D. Tyagi, A. Ramakrishnan, Rao Y. Surampalli, and Tian C. Zhang

21.1 Introduction

Global warming has grabbed growing attention since the 1970's (Broecker 1975; Mann and Jones 2003; Rosso and Stenstrom 2008). It is considered that greenhouse gas (GHG) emissions play a significant role in global warming. Over the last several decades since the 1800s, anthropogenic activities in agriculture, industry, and transportation have resulted in a huge increase of GHG concentration, particularly CO_2, CH_4, and N_2O, in the atmosphere, by ~30, 145 and 15% (El-Fadel and Massoud 2001). There is an increasing concern that methane levels have more than doubled since pre-industrial times, showing a consistent increase from 0.7–1.7 ppm_v (1994 levels) at a current estimated annual growth rate of 0.008 ppm_v (Pipatti et al. 1996; Augenbraum et al. 1999; IEA 1999). Wastewater treatment plants are recognized as one of the great contributors of GHG emissions (Sahely et al. 2006; Bani Shahabadi et al. 2010). The GHG emissions of wastewater treatment plants are from two sources; one is considered as direct emissions due to the production of CO_2, CH_4, and N_2O during the processes, and the other is called indirect emissions caused by the utilization of electricity, fossil fuels, and materials (such as chemicals). The CO_2 emission from the biological treatment process due to organic matter conversion is not counted towards GHG emission, because it will be finally sequenced to the system by photosynthesis and finally reenters the treatment. Therefore, GHG emissions produced in wastewater treatment plants result from CH_4 and N_2O discharges during treatment processes as well as CO_2 emission due to energy consumption.

Methane is considered as the most important GHG emitted from the wastewater treatment plant as it contributes 5% of the total global methane emission (El-Fadel and Massoud 2001). Treatment of both industrial and domestic wastewater is aimed at removing soluble organic matter, suspended solids, pathogenic organisms, and chemical contaminants. Specifically, methane is produced when soluble organic matter of wastewater and their residual solids (sludge) are handled by biological processes under anaerobic conditions. In addition, during collection and treatment, wastewater with soluble organic matter may be accidentally or deliberately managed under anaerobic conditions. Therefore, it is understandable that the organic load is the key factor in methane emission from the process (El-Fadel and Massoud 2001). Generally, the methane producing potential of wastewater can be determined in terms of biochemical oxygen demand (BOD) or chemical oxygen demand (COD) (IPCC 1997). Nitrous oxide could also be emitted during wastewater treatment when produced wastewater has significant nitrogen (urea, ammonia, and proteins) loading, ultimately leading to nitrification and denitrification processes responsible for the emission. Most of the nitrogen sources are first converted into nitrate through nitrification; further, the nitrate will be degraded to nitrogen gas (N_2) via a denitrification process which occurs under anoxic conditions. Nitrous oxide can be formed as an intermediate product of both processes (Equation 21.1 and 21.2), still denitrification is the major contributor for the emissions (Ritchie and Nicholas 1972; Maag and Vinther 1996; Wunderlin et al. 2012).

$$NH_4^+ + NO_2^- \rightarrow N_2O \quad \text{(Eq. 21.1)}$$

$$NO_3^- \rightarrow NO_2^- \rightarrow NO + N_2O \rightarrow N_2\,(g) \quad \text{(Eq. 21.2)}$$

In this chapter, GHG emissions in wastewater treatment plants (including both wastewater and sludge treatment processes) are estimated; the strategies of the emission reduction are discussed; and a case study assessing the impacts of changes in treatment technology on energy production and GHG emissions is presented.

21.2 GHG Emissions during Wastewater Treatment

21.2.1 Estimation of GHG Emission

21.2.1.1 Domestic Wastewater Emission Estimates

Methane emission from domestic wastewater in the US is estimated using the default methodology from IPCC (IPCC 1997; IPCC 2000), which is determined by the total population and a per capita wastewater BOD production rate. The estimation is based on the following three assumptions:

(1) wastewater BOD_5 produced per day per capita is 0.065 kg;
(2) 16.25 kg out of 100 kg BOD_5 is going to anaerobic degradation; and
(3) the emission factor of BOD_5 is 0.6 kg CH_4/kg $BOD_5$and

Accordingly, methane emission from domestic wastewater treatment can be expressed as Eq. 21.3:

$$\text{Methane emissions (kg/d)} = \text{N (person)} \times 0.065\ (\text{kg } BOD_5/\text{d/person}) \times 16.25\% \times 0.6\ (\text{kg } CH_4/\text{kg } BOD_5) \quad \text{(Eq. 21.3)}$$

where N = the total population covered by the wastewater treatment plant.

21.2.1.2 Industrial Wastewater Emission Estimates

The estimation of methane emission from industrial wastewater is more complicated than domestic wastewater as there is a determination of the anaerobic degradation fraction (0–100%), which normally has to be decided by expert judgement. Generally, only the industry which produces wastewater with a large amount of organic matter would count for the methane emission. It has been reported that methane is produced mainly from several major industries, including meat, poultry, pulp and paper, vegetables, fruits, and juices. The methane emission from these types of industrial wastewater is estimated below.

Meat and Poultry Industry. Wastewater produced from meat and poultry industry is normally treated by anaerobic lagoons followed by screening, fat trapping, and air floating. According to an estimation of the U.S. Environmental Protection Agency (U.S. EPA), the anaerobic degradation fraction of the treatment is 77% (U.S. EPA 1997). It is reported that per ton of product produced would generate 13 m^3wastewater and per cube meter wastewater contains 4.1 kg COD; therefore, the total methane emission can be calculated based on Equation 21.4:

$$\text{Methane emission (kg/d)} = \text{M (ton)} \times 13\ (\text{m}^3) \times 4.1\ (\text{kg COD/m}^3) \times 77\% \qquad \text{(Eq. 21.4)}$$

where M = product production rate (ton/d).

Pulp and Paper Industry. Typical treatment for pulp and paper industrial wastewater includes solid removal via sequential processes, including neutralization, screening, sedimentation, and flotation/hydrocycloning, followed by soluble organic matter removal via biological treatment, also known as secondary treatment (Pokhrel and Viraraghavan 2004; Soloman et al. 2009; Stoica et al. 2009; Buyukkamaci and Koken 2010). According to the EPA report, around 42% of the total soluble organic matter enters secondary treatment, and out of this only 25 % is treated under anaerobic conditions. In per ton product generated, 85 m^3 wastewater is generated with a BOD_5 load of 0.4 kg/m^3 in the wastewater (Worldbank 1999). The BOD_5 contribution to methane emission is 0.6 kg CH_4/kg BOD_5. Relying on the data, the methane emission can be described as (Eq. 21.5):

$$\text{Methane emission (kg/d)} = \text{M (ton)} \times 85\ (\text{m}^3) \times 0.4\ (\text{kg BOD}_5/\text{m}^3) \times 0.6\ (\text{kg CH}_4/\text{kg BOD}_5) \times 42\% \times 25\% \qquad \text{(Eq. 21.5)}$$

where M = product production rate (ton/d).

Fruits, Vegetables and Juice Processing Industry. Screening, coagulation/ sedimentation and aerobic biological treatment are the general processes used for treating fruits, vegetables, and juice processing industry wastewater (Artés and Allende 2005; Arvanitoyannis and Varzakas 2008). Normally, aerobic treatment is applied for the wastewater treatment; hence there is just a small portion of the soluble organic matter that would be subject to anaerobic treatment. However, an anaerobic zone could be formed with the occurrence of large seasonal organic loading. Therefore, generally a 5% soluble organic matter out of the total is estimated to be degraded under anaerobic conditions (Scheehle and Doorn 2003). It is assumed that per ton of product produced generates 5.6 m^3 wastewater, and per cube meter wastewater contains 5 kg COD. The estimation can be calculated with Equation 21.6:

$$\text{Methane emission (kg/d)} = M\ (\text{ton}) \times 5.6\ (m^3) \times 5\ (\text{kg COD}/m^3) \times 5\% \qquad \text{(Eq. 21.6)}$$

where M = product production rate (ton/d).

Analogous to methane emission estimation, nitrous oxide emission from domestic wastewater could also be estimated by the nitrous oxide production per person per year. It can be simply described as Equation 21.7. The emission factor is obtained by the basic factor (3.2 g N_2O/person/year for domestic wastewater) multiplying a co-factor r (industry nitrogen discharge to the wastewater treatment plant), also called emission co-factor with an estimated value of 1.25 (Czepiel et al. 1995).

$$\text{Nitrous emission (kg/year)} = N\ (\text{person}) \times 3.2\ (\text{g } N_2O/\text{person/year}) \times r \qquad \text{(Eq. 21.7)}$$

where N = the total population covered by the wastewater treatment plant; r = emission co-factor.

According to Equations 21.4–21.7, the GHG emissions can be directly estimated by the sum of the methane and nitrous emissions from the domestic and industrial wastewater treatment in the area. However, the estimated emission greatly depends on the area and is not governed by the treating percentage and the degree of area wastewater, even though modification has been gradually introduced into the calculation (Préndez and Lara-González 2008); the method seems to be quite debatable. In fact, the method can only be used for a rough and fast estimation. For accurate estimation, the emission should be estimated from each stage of the treatment process. For example, in a general treatment, there are screening, primary settling, biological treatment, secondary settling, etc.; thus, the methane emission should be the sum of the emission of each process.

21.2.1.3 Estimation of the Treatment Process Emissions

It is well known that domestic and industrial wastewaters have significantly different characteristics, because most of the industrial wastewaters have very low organic loading which is the cause of GHG emissions with the exception of the food industry wastewater. Therefore, generally industrial wastewaters are not integrated with domestic wastewaters for treatment but treated inside the industries separately, and then discharged into the sewerage system or water bodies.

The sewerage wastewater is normally treated via screening, primary settling, biological processing, and secondary settling (Fig. 21.1). As mentioned earlier, the organic loading plays a major role of GHGs emission from wastewater treatment as it directly leads to the methane and nitrous oxide emission. Among all the processes (Fig. 21.1), bioreactor is the emission generator, while others contribute GHG emissions due to the energy or chemical consumption. Therefore, the total emission can be described with Equation 21.8.

GHG emissions = GHG emission from biological treatment +
CO_2 from material (energy and chemicals) consumption (Eq. 21.8)

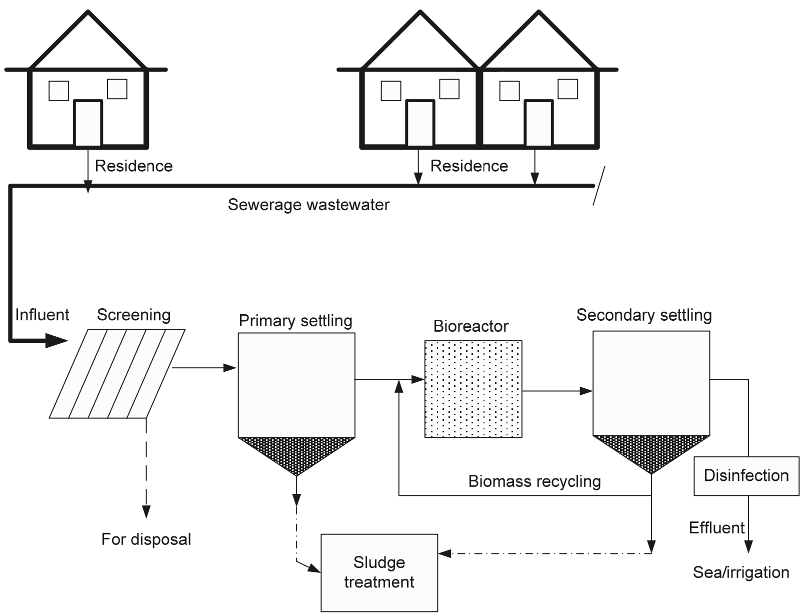

Figure 21.1. A typical wastewater treatment process

Under normal circumstances, CO_2 emission during biological treatment is not considered, as its emission involved a short life cycle (i.e., emission → sequestration → emission → sequestration →…). Therefore, GHG emissions from biological wastewater treatment will be predominantly from methane and nitrous oxide, which are generated under anaerobic conditions. Hence, the type of biological treatment becomes a critical factor for GHG emissions. Aerobic, anaerobic, and anoxic are three basic categories of biological treatment, and generally, the three types of treatment operate together in a wastewater treatment plant (Abdul-Talib et al. 2002; Chan et al. 2009; Kassab et al. 2010). Aerobic biological treatment involves contacting wastewater with microorganisms, which act as catalysts to biodegrade organics and other contaminants such as ammonia, in the presence of oxygen. Carbon dioxide, water, and excess biomass (sludge) are the final products of the treatment; thus it can be considered that no GHG emissions occur in the process. Anaerobic (an oxygen free system) and anoxic (an oxygen deficient but nitrite/nitrate rich system) treatments complete the biodegradation of organics and other contaminants using the microorganisms that have the ability to use the combined oxygen (e.g., SO_4^{2-}, NO_2^-, NO_3^-, CO_2) or organic compounds (e.g., via the fermentation processes) for oxidation. The resulting products are methane, denitrogen gas, nitrous oxide, and excess biomass (sludge). Hence, it is clear that GHG emissions from wastewater treatment are due to the employment of anaerobic and anoxic treatments; however there is biomass decay in the aerobic system which would contribute to ammonia generation (Eq. 21.9). This should be counted as it can be converted into nitrous oxide in the denitrification process.

$$C_5H_2O_2N + 5O_2 \rightarrow 5CO_2 + 2H_2O + NH_3 \qquad \text{(Eq. 21.9)}$$

where $C_5H_2O_2N$ = the element composition of biomass (Bridle Consulting 2007; Snip 2010).

In the anaerobic process, the methane emission can be estimated if the organic material composition is known, and the general reaction can be expressed as Equation 21.10. In Equation 21.10, $C_nH_aO_b$ represents the organic material composition. However, the composition is unknown as wastewater is a complex mixture. Instead of using Equation 21.10 to obtain methane production, COD loading can be used for the estimation. It is reported that for each kg COD, 0.23 kg methane is generated (Angelidaki and Sanders 2004); therefore, the methane emission can be calculated by multiplying the influent COD with 0.23. Nitrous oxide emission from the anaerobic condition can be estimated with Equation 21.11.

$$C_nH_aO_b + (n - a/4 - b/2)\,H_2O \rightarrow$$
$$(n/2 - a/8 + b/4)\,CO_2 + (n/2 + a/8 - b/4)\,CH_4 \qquad \text{(Eq. 21.10)}$$

$$N_2O \text{ emission} = Q \times C_{TN} \times R_{N2O} \qquad \text{(Eq. 21.11)}$$

where Q = influent of anaerobic reactor (m^3/d); C_{TN} = total nitrogen concentration in the influent of the anaerobic reactor (kg N/m^3); R_{N2O} = the conversion factor of N in the feed to N_2O (kg N_2O/kg N feed), and the factor has to be measured for each anaerobic process of wastewater treatment.

Besides the direct emission (emission from the generation of GHGs during the treatment), there are emissions from the utilization of materials. During the treatment, chemicals such as lime, polymers, and chlorine, are employed to aid the particle removal or disinfect the effluent of secondary treatment in case the additional requirement for the effluent (e.g., irrigation) needs to be satisfied. The GHG emission from the usage of chemicals can be determined based on the amount consumed (Equation 21.12). Apart from chemicals, energy (power) utilization of the treatment is another important contributor of the GHG emission. The emission depends on the power generation sources, which mainly include coal, hydro, nuclear, heavy fuel oil, and natural gas as the source decides the conversion factor of the emission. Equation 21.13 can be used to calculate the emission from the utilization of power in the treatment plant.

$$CO_2 \text{ emission (kg/d)} = Q \times D \times r_{che} \qquad \text{(Eq. 21.12)}$$

where Q = influent of the chemical addition reactor (m^3/d); D = chemical addition ratio (kg chemical/m^3); r_{che} = CO_2 emission ratio of the chemical production (kg CO_2/kg chemical production).

$$CO_2 \text{ emission (kg/d)} = P \times f \qquad \text{(Eq. 21.13)}$$

where P = the total power used in the treatment plant (kW/d); f = conversion factor of power generation (kg CO_2/kW).

Based on the above discussion, the GHG emissions from wastewater treatment can be estimated according to the treatment processes (aerobic, anaerobic, or anoxic) (Equation 21.14).

$$\begin{array}{c}\text{GHG} \\ \text{emissions} \\ \text{(kg } CO_2\text{/d)}\end{array} = \begin{array}{l} 21 \times CH_4 \text{ production (kg/d)} + \\ 310 \times N_2O \text{ production (kg/d)} + \\ CO_2 \text{ emission of chemical utilization (kg/d)} + \\ CO_2 \text{ emission of power consumption (kg/d)} \end{array} \qquad \text{(Eq. 21.14)}$$

where 21 and 310 are global warming potential (GWP) of methane and nitrous oxide, respectively (U.S. EPA 2003).

21.2.2 Management and Reduction of GHG Emissions

21.2.2.1 Emission Reduction by Process Selection

The section on the estimation of GHG emission during wastewater treatment gives us an insight into the sources of GHG emission during the process. It is therefore implied that the strategies of GHG emission control can be selected accordingly. In most domestic wastewater treatment plants, the aerobic process is adopted for organic matter removal, while in industrial wastewater treatment, the anaerobic process is more frequently applied (Cakir and Stenstrom 2005; Bani Shahabadi et al. 2009; Chan et al. 2009; Soloman et al. 2009). Compared to aerobic treatment, the anaerobic process generates more GHG emissions due to the fact that methane is the major end product of organic conversion and contributes to 21 times GWP (Cakir and Stenstrom 2005; Kassab et al. 2010). Therefore, using the aerobic process instead of the anaerobic one would reduce the GHG emissions. However, be aware that the methane emission from the anaerobic process can be used for heating (or power generation), which would compensate the GHG emission from power production. It is reported that the anaerobic process could reduce the GHG emission by 60% (1.0 kg CO_2/kg COD removal for the anaerobic and 2.4 kg CO_2/kg COD removal for the aerobic) as compared to the aerobic process when the produced methane of the anaerobic process was used for electricity generation (Keller and Hartley 2003). Another study also reported a similar result (Bani Shahabadi et al. 2009). Hence, it is advisable to conduct comparisons under practical conditions. The methane emission in the anaerobic process is due to methanogenesis. In the aerobic process, normally, a high aeration rate is given in order to prevent oxygen limitation, which would enhance the stripping of GHG. The anoxic process does not encounter such problems, which suggests that it could be a better option to reduce the GHG emission from wastewater treatment. Some researchers have reported that the anoxic process emits the lowest methane as compared to aerobic and anaerobic processes (1.33, 015, 2.93 g/m^2-d for the aerobic, anoxic, and anaerobic process) (Wang et al. 2011).

21.2.2.2 Emission Reduction by Operational Process Controls

Dissolved Oxygen (DO) Concentration. Methane emission is due to the organic matter degradation under anaerobic conditions. It is well known that all methanogens are strict anaerobic microbes (Bitton 2005), so the general idea is to maintain a high DO in the process to minimize methane emission. However, as mentioned earlier the high aeration rate would also lead to higher emission due to stripping (normally there is dissolved methane in the wastewater generated during collection and storage). In addition, it would also increase the energy demand, which contributes to GHG emissions as well.

Wastewater with a high nitrogen load has a high potential of nitrous oxide emission. It has been reported that there are mainly three ways of nitrous oxide production, i.e., nitrification, denitrification, and chemical reaction (for example, the reaction between nitrite and hydroxylamine forms NO and N_2O) (Van Cleemput 1998; Wunderlin et al. 2012). Among them, denitrification is the main emission source. In wastewater water treatment processes, it is found that the activated sludge unit is the leading emission compartment as compared to other units, such as grit tank, primary settling tank, and secondary settling tank (Czepiel et al. 1995; Kampschreur et al. 2008b). In the nitrification process, low oxygen concentration would result in local oxygen limitation, which leads to nitrous production (Tallec et al. 2006; Kampschreur et al. 2008a). However, for increasing oxygen concentration, aeration is normally applied, which leads to a surge in the stripping of N_2O, and hence increases its emission. Oxygen presence during denitrification can inhibit the denitrification enzyme synthesis and activity, and it is known that nitrous oxide reductase is very sensitive to oxygen, which means even a trace amount of oxygen present in the denitrification process would cause nitrous oxide reductase inhibition, which would lead to high nitrous oxide emission. Therefore, DO concentration is critical for GHG emission control. In the nitrification process, low oxygen concentrations should be prevented, and in the denitrification process, oxygen free conditions should be maintained.

Solids Retention Time (SRT). It is well known that biomass respiration increases with an increase in SRT. Additionally, the high SRT would also enhance the methanogenesis and finally cause high methane emission. In order to prevent the large emission, SRT should be carefully designed and controlled. A recent study has shown that high SRTs results in high methane emission (Corominas et al. 2010).

Nitrite and Nitrate Concentration. Nitrite has great effect on nitrous oxide production in both nitrification and denitrification processes as high nitrite concentration in the nitrification process would enhance denitrification and thus cause N_2O emission; in the denitrification process, the high nitrite concentration results in a low denitrification rate, which would cause N_2O accumulation instead of reduction to nitrogen gas (Schulthess et al. 1995; Colliver and Stephenson 2000). Moreover, it has been revealed that the high amount of nitrite can inhibit the methanogenic process due to the toxicity of nitrite to the methanogenic bacteria, and thus, results in reduced methane production (Mohanakrishnan et al. 2008; Banihani et al. 2009; Jiang et al. 2010). A similar trend (inhibition on the methanogenic process) has been reported for high nitrate concentrations in the process (Banihani et al. 2009). Some researchers pointed out that nitrate was a better electron acceptor than nitrous oxide (Park et al. 2000), which suggests that the nitrate would compete for electrons with nitrous oxide. It would result in the cut off for nitrous oxide to enhance further reduction to nitrogen gas, and finally increase nitrous oxide emission. Thus, in order to control N_2O emission, nitrite accumulation should be avoided by increasing SRT and supplying enough oxygen to accomplish nitrite oxidation. In addition, nitrogen-rich wastewater can be mixed with nitrogen deficient wastewater to control nitrate and nitrite concentrations in the process.

C/N Ratio. C/N is reported to be related to nitrous oxide emission (Hanaki et al. 1992; Itokawa et al. 2001), and the low C/N ratio provides high nitrous oxide production; it could be due to the enrichment of aerobically denitrificans, which is associated with N_2O emission and nitrite accumulation (Van Niel et al. 1993). When the C/N ratio is low in the treatment process, an extra carbon source such as methanol should be added to adjust the ratio. It is a costly measure and also causes more GHG emission due to the chemical utilization. On the other hand, a high C/N ratio would cause large production of biomass (sludge), which would increase the sludge digestion load and further increase methane emission (Corominas et al. 2010). Compared to nitrous oxide emission under high DO condition, methane emission in sludge management is a greater concern for GHG emissions. Therefore, it is necessary to avoid the low or high C/N ratio during treatment. It can be accomplished by mixing wastewater of the high C/N ratio with wastewater of the low C/N ratio, thus reducing GHG emissions.

pH. It is reported that the optimal pH for methanogenic bacterial growth is 7–7.2, and methane production may decrease when pH is lower than 6.3 or higher than 7.8 (Gerardi 2006). There are also studies on the investigation of the relationship between nitrous oxide emission and pH; these studies reported the maximum and minimum emission of nitrous oxide to be occurring at pH 8.5 and 6, respectively

(Hynes and Knowles 1984; Hanaki et al. 1992). Therefore, it indicates that controlling pH would manipulate GHG emission during the process. A recent study revealed that in fact pH had minor effect on the emission because pH of the wastewater in biological tanks is well regulated (i.e. adjusted before entering to the biological tanks) (Wang et al. 2011).

21.2.2.3 Other Strategies

Two studies revealed that the treatment plant scale has an effect on GHG emission. The emission decreases with an increase in the scale that could be attributed to the efficient utilization of the power and other materials (Bani Shahabadi et al. 2009; Xie and wang 2011). For wastewater treatment plants with similar loading of influent at 10,000 m^3/day and 500 000 m^3/day, GHG emissions were about 5 and 3.8 kg CO_2/ kg COD, respectively. In addition, it has been observed that higher COD loading rates showed lower GHG emissions, which could be related to an increase in the efficiency of operating equipment (the equipment operating efficiency increases with the increase of organic loading) (Xie and wang 2011). The rapid change in processing conditions also showed impacts on GHG emissions. The sudden increase in the loading of nitrogen and organics in the influent would lead to an increase in nitrous oxide emission, presumably due to the fact that denitrifying bacteria requires time to react (metabolism) to the change and cause an increase in nitrous oxide emission.

21.3 GHG Emissions during Sludge Management

Wastewater treatment sludge is generated in both the primary (primary sludge) and secondary (secondary sludge) sedimentation tanks. Primary sludge is unsolved wastewater contaminate. The composition of the sludge depends on the wastewater characteristics; it mainly contains organic matter such as faeces, vegetables, fruits, textiles, and paper. Secondary sludge is generated from biological processes, and is a mixture of living or dead microorganisms and organic or minerals adsorbed on the microorganisms. In most of the treatment plants, primary and secondary sludge are treated together. Sludge management includes sludge treatment (stabilization) and disposal. The GHG emissions during sludge management are from the GHGs produced during the stabilization and the GHG emission due to the utilization of fuels that are used for transportation.

21.3.1 GHG Emissions during Sludge Treatment and Disposal

Sludge treatment is aimed at reducing the sludge volume and organic content, as well as killing the pathogens and eliminating other toxins in the sludge. The most common treatments are aerobic or anaerobic digestion, incineration, and composting. The disposal methods are landfilling (after digestion) and land application (after composting).

21.3.1.1GHG Emissions during Sludge Digestion followed by Landfilling

Aerobic Digestion. It is a process that introduces oxygen to the digester. Under aerobic conditions, bacteria can rapidly consume organic materials and produce carbon dioxide and water as final products. As there is no methane and nitrous oxide formation during the process, it is considered that the major GHG emissions is due to energy consumption. The GHG emissions can be estimated according to the energy utilization.

Anaerobic Digestion. It is employed worldwide as the oldest and the most applied technology for sludge stabilization before final disposal (Kim et al. 2011). The digestion occurs in the absence of oxygen and proceeds through a series of metabolic interactions among microrganisms. There are mainly four steps of the digestion: hydrolysis, acidogenesis, acetogenesis, and methanogenesis (Fig. 21.2). The hydrolysis step breaks down the complex materials such as polymeric matters into soluble molecules such as sugar and amino acid by hydrolytic enzymes. It is also the rate controlling step of the whole digestion process. The simple materials will be then converted to volatile fatty acids (VFAs) through acidogenesis. During the acetogenesis process, the VFAs will be further degraded to hydrogen gas, carbon dioxide, and acetic acid. At last, methane is produced under methanogenesis. Normally, the temperature in anaerobic digestion is maintained between 30 to 70°C.

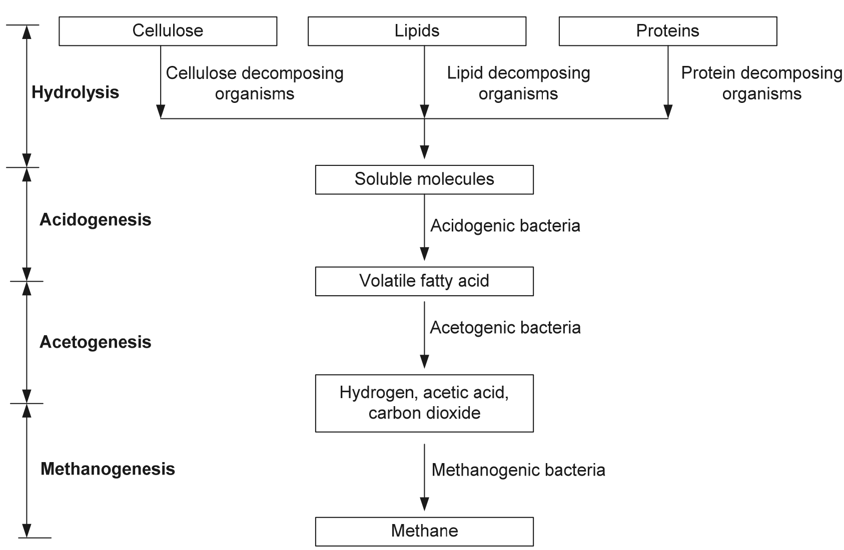

Figure 21.2. The degradation steps of the anaerobic digestion process

From Fig. 21.2, it can be seen that methane and carbon dioxide are produced, while as aforementioned the carbon dioxide production belongs to the short carbon cycle which would not count for GHG emission. Methane emission is determined by the sludge amount as well as the volatile suspended solid (Johansson et al. 2004) fraction in the sludge (SYLVIS 2009; Snip 2010). Sludge production from primary and secondary treatment is expressed in Equation 21.15. The total sludge is the sum of primary and secondary sludge.

$$\text{Primary sludge production (kg/day)} = Q_{in} \times TSS \times R_{TSS} \qquad \text{(Eq. 21.15.1)}$$
$$\text{Secondary sludge production (kg/day)} = f \times BOD_5 - Q_{out} \times TSS_{rem} \qquad \text{(Eq. 21.15.2)}$$

where Q_{in} and Q_{out} represent the daily influent and effluent flow of the wastewater treatment plant (m^3/d), respectively; TSS and TSS_{rem} are the total suspended solid in the influent (kg/m^3) and total suspended solid that is removed in the primary sedimentation tank; f is the conversion factor of BOD_5 to biomass, which is normally 0.5 (kg biomass/kg BOD_5); BOD_5 is the BOD_5 load of the secondary treatment.

In anaerobic digestion, not all of the sludge can be degraded to biogas (mixture of methane and carbon dioxide), and only the volatile suspended solid would be converted to it. The degraded sludge is the product of total sludge and the biodegradable VSS fraction, which is determined by the wastewater characteristics. It is reported that the biogas production is proportional to the concentration of sludge degraded, which implies that 1 kg of sludge degraded will generate 1 kg of biogas (Snip 2010). It is known that the general fraction of methane in biogas generated from sludge anaerobic digestion is around 60 to 75% (Sosnowski 2003; El-Mashad and Zhang 2010). Therefore, methane emission from sludge anaerobic digestion can be described as follows (Equation 21. 16).

$$\text{Methane emission (kg methane/day)} = S \times f_{bVS} \times 1 \times 0.675 \qquad \text{(Eq. 21. 16)}$$

where S = total sludge production per day (kg sludge/day); f_{bVS} = biodegraded volatile solid fraction in the total volatile solid; 1 = biogas production (kg biogas/kg sludge degraded); 0.675 = the average faction of methane in biogas generated from digestion.

Methane emission can be roughly calculated based on Equation 21. 16. Apart from the direct GHG emission (methane production), there is also GHG emission due to the energy consumption that is utilized for heating the digester in order to regulate the temperature between 30 to 65 °C which maintains the digestion process. The GHG emission from the energy utilization is dependent on the region as well as the season. The GHG emissions would be high in the cold region and winter season due to the high energy requirement; on the contrary, the GHG emissions would be low in the warm/hot region and summer season because the temperature requirements can be met under these conditions.

After digestion, sludge thickening and dewatering are performed to further reduce sludge volume. During the thickening, generally chemicals such as polymers are added at an average rate of 5 kg/ton dry solid (SYLVIS 2009). Therefore according to the dry solid production, GHG emission from the usage of chemicals can be estimated. Mechanical devices such as the rotary drum and belt filter press are mostly applied for sludge dewatering. The energy consumption would vary according to the applied method, and thus, GHG emissions can be calculated. The total GHG emission in the thickening and dewatering section can be expressed as Equation 21. 17.

$$\text{GHG emission (kg } CO_2\text{/d)} = 5 \times S_{total} \times r_{che} + P \times f \qquad \text{(Eq. 21.17)}$$

where S_{total} = total dry solid after the sludge thickening (ton/day); 5 = polymer addition per ton dry sludge production (kg polymer/ton dry sludge); r_{che} = ratio of CO_2 emission to chemical production (kg CO_2/ kg chemical production); P = the total power used in the treatment plant (kW/d); f = conversion factor of power generation (kg CO_2/ kW).

After dewatering, landfilling is one of the most popular options of residual sludge disposal (Monni et al. 2006; Lou and Nair 2009; Chalvatzaki and Lazaridis 2010). GHG emission from landfill is highly dependent on the type of solids disposed of. GHG emission from a landfill is comparable to an anaerobic process, as anaerobic microorganisms convert organic matter to methane and nitrous oxide. The methane emission from a landfill can be estimated according to the fraction of volatile organic carbon in the solid (Chalvatzaki and Lazaridis 2010; Park 2011). Transportation of the waste to the landfill site contributes to additional GHG emissions due to the utilization of fuels. The GHG emission from transportation can be estimated according to the type of fuel and vehicle used and the distance between the landfill site and wastewater treatment plants. When there is collection of methane from landfill and utilization for energy replacement, the methane production should be counted as a credit. Hence, the GHG emissions in landfilling operation are shown in Equation 21. 18.

$$\text{GHG emissions} = \begin{array}{l}\text{GHG (methane and nitrous oxide) production in landfilling } + \\ \text{GHG emission from the consumption of fuels for transportation } - \\ \text{GHG credit taken from the methane replacement to other energy} \\ \text{(such as electricity)}\end{array} \qquad \text{(Eq. 21.18)}$$

21.3.1.2 GHG Emissions in Sludge Composting and Land Application

Sludge composting is another sludge management strategy (Amlinger et al. 2008). It is a process to breakdown the organic materials into more stable substances through the aerobic or anaerobic process. The process is performed after sludge thickening and dewatering and before land application. The GHG emission in sludge thickening and dewatering processes can be estimated with Equation 21.17. Aerobic composting generates heat and carbon dioxide, while anaerobic one produces methane as well as heat. Compared to anaerobic composting, aerobic composting methods decompose material faster and more efficiently. The GHG emissions during composting are governed by the composting type (aerobic or anaerobic). While energy consumption accounts for GHG emissions in aerobic composting, methane and nitrous oxide emissions contribute to GHG emission from anaerobic composting.

It is known that the residue from composting is normally used as a slow release fertilizer which indicates that the compost application to the agricultural land would reduce the inorganic fertilizer addition. Accordingly, the GHG emission in composting can be considerably reduced due to the replacement of fertilizer applications in agriculture. Similar to landfilling, transportation of the sludge from the wastewater treatment site to the composting site and transportation of the compost to land application also generate GHG emission due to the fuel utilization. The total GHG emission can be estimated according to Equation 21. 19.

GHG emissions = GHG emission in sludge thickening and dewatering processes +
GHG (methane and nitrous oxide) production during composting +
GHG emission from energy consumption in the process (aeration & heating) +
GHG emission from the consumption of fuels for transportation –
GHG credit taken from fertilizer production (Eq. 21.19)

21.3.1.3 GHG Emissions in Sludge Incineration

Incineration is considered as the simplest sludge management method (Wall et al. 1984; Bogner et al. 2008); however, incineration is chosen only when sludge is not possible for utilization (agriculture application) and has no economic feasibility. Incineration is a process in which dewatered sludge will be ignited at 420–500°C in the presence of oxygen (the complete combustion of organic matter requires even higher temperature, normally being 760–820°C). During incineration, organic materials are converted into carbon dioxide, water vapor and ash. During incineration, a great amount of heat is generated which can be substituted for other fuels to aid steam production. The recovery of heat from the waste can be credited for GHG emissions during incineration. In addition, incineration can be performed inside the wastewater treatment plant which avoids the otherwise necessary GHG emission due to the energy consumption in transportation. Based on the discussion, the GHG emission in incineration can be summarized in Equation 21.20.

GHG emissions = GHG emission in sludge thickening and dewatering (Eq. 21. 17) +
GHG (methane and nitrous oxide) production in incineration +
GHG emission from the consumption of energy for heating +
GHG emission from the consumption of fuels for transportation (if the location of incineration site and wastewater treatment are different) –
GHG credit taken from the heat recovery from the process (Eq. 21.20)

21.3.2 Management and Reduction GHG Emissions during Sludge Treatment and Disposal

As mentioned above, sludge treatment and disposal mainly include sludge digestion followed by landfilling, composting with other agents such as wood chips and then application to land as a soil conditioner or fertilizer, and incineration. In terms of GHG emissions, incineration would be a good alternative of sludge management comparing the other two (composting and digestion with landfilling) due to the large heat recovery (Report 2005). The selection of specific treatment and disposal methods has to be determined according to the real situation. For example, incineration has the risk of air toxic emissions when the sludge contains the hazardous substances such as heavy metals, and will not be a suitable option; hence generally only large municipalities consider this process. Similarly for composting, the C/N ratio of the sludge should be around 20 to 30. If the C/N ratio is too low composting will demand a large addition of organic carbon which would not be favorable. Additionally, most sludge composts are too low in nutrient value, which makes them unattractive to farmers. Compared to other options, sludge digestion along with landfilling is the method that is applied globally and is the most efficient GHG emission reduction approach with the methane collection from landfill and utilization for energy generation. Thus, reduction of GHG emissions in digestion is much more realistic and useful.

21.3.2.1 GHG Emission Reduction by Selection on Digestion Processes

Comparing the three sludge treatment technologies including aerobic, anaerobic digestion, and composting, anaerobic digestion could mitigate GHG emissions due to the low energy requirement and the credit from the utilization of produced methane (Yasui et al. 2005b; Barber 2009). Mesophilic (30–38°C) and thermophilic (50–70°C) anaerobic digestion are the two basic sludge treatment technologies; the former is more widely used compared to the latter due to the lower energy requirements and higher stability of the process (Gavala et al. 2003; Skiadas et al. 2005). On the other hand, it was pointed out that thermophilic anaerobic digestion could accelerate biochemical reactions, increase microbial growth rates, and enhance interspecies hydrogen transfer leading to an increased methanogenic potential at a low retention time (Zábranská et al. 2000; Nosrati et al. 2011). From the standpoint of GHG emission, the mesophilic process has a lower organic degradation rate than the thermophilic process which suggests that the latter produces more methane than the former in a given time. The methane (in the form of biogas) generated from sludge digestion is usually captured and used for heating or cogeneration of electricity. The use of methane for substituting other modes of energy consumption would indirectly reduce the GHG emission. Furthermore, the higher degradation of sludge (high percentage degradation of organic matter) would reduce the methane production in the final disposal step such as landfill, in which the produced methane is normally not collected. However, on the other hand, the thermophilic digestion requires more energy input which would cause higher GHG emission than mesophilic digestion. Therefore, the total GHG emission in the two processes should be estimated according to the practical condition (sludge characteristics and the local energy production method) and then compared to select the process that emits less GHG.

21.3.2.2 GHG Emission Reduction by Sludge Pre-treatment

Pre-treatment of the sludge before entering the anaerobic digestion tank(s) has been widely studied. The pre-treatment method mainly includes thermal, chemical, mechanical, and biological processes (Muller 2001b; Skiadas et al. 2005; Yasui et al. 2006; Nges and Liu 2009). As mentioned earlier, hydrolysis, which is the first step of anaerobic degradation, is the rate limiting step. Therefore, enhancing hydrolysis would highly improve the anaerobic digestion process, and the pre-treatment focuses on accomplishing this. Once hydrolysis is enhanced, methane yield during anaerobic digestion will be increased. It is known that methane can be collected and used for heating or power generation which would reduce the otherwise necessary GHG emission from power generation using other sources. Moreover, as anaerobic digestion with pre-treatment converts more organic matter in the sludge to methane than that without pre-treatment, it will reduce the amount of organic matter degradation in landfill with no methane collection. Therefore, the pre-treatment with high methane yield would be a preferred process to reduced GHG emission in sludge treatment.

Thermal pre-Treatment. Considerable studies have been carried out on thermal pre-treatment to increase the disintegration and solubilisation of sludge solids and to improve the sludge digestion rate (Stuckey and McCarty 1984; Pinnekamp 1989; Li and Noike 1992; Gavala et al. 2003; Park et al. 2005).These studies showed that the optimum methane yield (70 to 80% higher methane production than anaerobic digestion which has no thermal pre-treatment) occurred at 170–180°C. However, it is known that high temperature processes would increase the energy consumption which results in high GHG emissions. In order to reduce the energy utilization, some researchers have studied the mild temperature (60–100°C) pre-treatment for enhancing the methane production (Wang et al. 1997; Gavala et al. 2003; Appels et al. 2010). It was found that methane yield increased around 50% in comparison to sole anaerobic digestion.

Chemical pre-Treatment. Chemical pre-treatment is to introduce chemicals to the sludge to aid the hydrolysis of complex organic matter to simple substrates that may be easily utilized to form methane in anaerobic sludge digestion. It is pointed out that alkali pre-treatment has the ability to enhance the biodegradation of complex organic materials, such as lignocellulosic materials (Hoon 2004). Other studies found similar results (Chen et al. 2004; López Torres and Espinosa Lloréns 2008). Some researchers have used alkali pre-treatment to investigate methane production in anaerobic digestion, and it was found that the methane yield increased 183% in digestion with alkali pre-treatment than without the pre-treatment (Lin et al. 1997; Lin et al. 2009). However, there is a concern on the GHG emission in chemical production and transportation, while it has been reported that there is a benefit of GHG emission reduction compared to methane production as the emission due to the utilization of chemicals are minor.

Apart from alkali pre-treatment, ozonation has also been performed to enhance methane emission (Weemaes et al. 2000; Goel et al. 2003; Yasui et al. 2003; Yasui et al. 2005a). It is a process in which some fraction of sludge in the digestion tank will be fed to an ozoniser for breaking down the complex organic matter and then revert it to the digestion tank after removing residual ozone and oxygen. The ozone input is normally set at 18 to 30 kg ozone/day, and the fraction sent to the ozoniser depends on the organic material content in the sludge. It is reported that employment of ozonation could increase the methane yield 1.30 times higher than the control (without ozonation) (Yasui et al. 2006). It is apparent that any pre-treatment addition would cause GHG emission, and certainly ozonation would also lead to an increase in GHG emission of the whole process. Therefore, the adoption of the ozonation in anaerobic sludge digestion should be evaluated by comparing the GHG emission of the energy usage and methane yield to compensate GHG emission to generate the energy.

Mechanical pre-Treatment. Mechanical pre-treatment focuses on the improvement of sludge solubility through the rupture of cell membrane of microorganisms in order to accelerate the availability of the usable substrates (Choi et al. 1997). In addition, the other important function of mechanical treatment is to increase protease activity, as hydrolysis of proteins is the rate-limiting step in the digestion (Maa and Hsu 1996). Several mechanical devices including rotor-stator shear devices, dynoMills, lysate-thickening centrifuges, and jetting and colliding, have been employed in pre-treatment (Muller 2001a; Muller et al. 2003; Basu et al. 2004; Muller et al. 2004). These pre-treatments showed great improvement on volatile solids removal (complex matter breakdown) which was from ~2–35% without treatment to ~13–50% with treatment. Certainly, the addition of mechanical treatment would increase GHG emission due to energy consumption. Evaluation of GHG emission from the digestion with or without mechanical pre-treatment should be carried out before applying the pre-treatment according to the practical situation.

Biological pre-Treatment. The above pre-treatment technologies yielded benefit of enhancing methane production in sludge anaerobic digestion. However, chemical treatments are based on strong acidic or basic conditions and the aggressive reaction conditions that often impose special material requirements. While mechanical pre-treatment is complicated and expensive, thermal pre-treatment consumes a substantial amount of energy with the risk of the toxic compound formation (Chiu et al. 1997; Delgenes et al. 2002; Nges and Liu 2009). Biological pre-treatment is to provide one or more stages of anaerobic treatment before sludge digestion; in fact it can also be called multi-stage digestion. The previous anaerobic step increases endogenous enzyme secretion and hence enhances the hydrolysis. Nges and Liu (2009) reported an improved methane production and higher volatile solids reduction with the 25–50°C pre-biological treatment than the control (without pre-treatment). Another study has reported a similar finding (Kim et al. 2011). Biological pre-treatment could be a suitable process to enhance sludge anaerobic degradability with no increase in GHG emission from the energy or chemical utilization. However, the capital cost could be higher due to the demand of the extra anaerobic chambers.

Other pre-Treatment. Ultrasonic pre-treatment is a relatively new technology that offers the benefit of reducing sludge quantity, breaking down complex organic matter into soluble substrate, and preventing sludge bulking by destroying filamentous microorganisms (Tiehm et al. 2001; Dewil et al. 2006). It is found that the soluble COD of the sludge significantly increased with the increase in specific energy input, and 30% of the insoluble COD was converted to soluble COD with an energy input of 30000 kJ/kg dry sludge (Dewil et al. 2006). Microwave irradiation has also been utilized to pretreat the sludge. Reports reveal that microwave irradiation can cause ions to accelerate and collide with other molecules to change the protein structure of microorganisms, and accelerate cell lysis (Tsai 1986; Banik et al. 2003). Some researchers found that microwave pre-treatment increased 80% higher methane production than control (Park et al. 2004). In addition to the increased energy input (leading to higher GHG emission), ultrasonic and microwave pre-treatment enhanced methane production. Hence, these methods should be carefully evaluated in terms of GHG emission with and without the pre-treatment.

Thermo-chemical treatment is a combination of thermal and chemical pre-treatment methods (Sawayama et al. 1996; Tanaka et al. 1997; Penaud et al. 1999). It is reported that the thermo-chemical treatment could further increase complex organic material (such as lignocellulosic materials) biodegradability compared to sole chemical (alkali addition) or thermal pre-treatment. It is pointed out that the increase in the biodegradability is due to protein hydrolysis facilitated by pH variation and could be accomplished by heating. A report showed that the application of thermo-chemical pre-treatment along with the addition of sodium hydroxide (26 g/L at 140 °C) enhanced COD solublilization over 30% (52% of total COD for ambient to 85% of total COD for 140 °C) (Penaud et al. 1999). Compared to direct digestion (without pre-treatment), the process requires lesser chemical and energy inputs and, hence, has lower GHG emissions. The application of thermo-chemical treatment needs to be carefully evaluated in order to reduce GHG emissions.

21.4 Key Strategies for Mitigation of GHG Emissions from Wastewater Treatment/Management

Five key strategies are indicated below, which the wastewater treatment plants could adopt to reduce GHG emissions (Georges et al. 2009), thereby mitigating the potential carbon impact of the process.

- *Source Control*: In most of the situations, extensive carbon savings may be accomplished through the control, at the source of priority pollutants of concern, thus avoiding the need for additional wastewater treatment.
- *Least Carbon End-of-pipe/Process Addition:* This strategy emphasizes the employment of least-carbon treatment solutions, recognizing the fact that an increase in emissions is inevitable. End-of-pipe treatment technologies have the capacity to enhance the carbon content of the waste as well as increase the operational needs for energy. Hence, it is advisable to implement significant changes in the conventional approach to wastewater treatment to reduce significant carbon emissions.
- *Greater Operational Efficiencies:* This strategy minimizes the higher energy demand through better design approaches and focuses on optimization of sewage or any combined wastewater treatment systems. Adoption of this strategy enhances the operational efficiency of the system and reduces GHG emissions
- *Redesigning Existing Treatment Processes:* This strategy aims to convert conventional wastewater treatment processes to lower energy alternatives.

Redesigning the process has dual advantages of reducing the concentration of pollutants in the effluent as well as reduced carbon emissions.

- *Renewable Energy Generation:* This strategy aims at on-site energy generation, or generation within the wastewater treatment facility, thereby reducing transportation costs.

21.5 Case Study: Assessment of Impacts of Changing Wastewater Treatment Technologies on GHG Emissions and Energy Balance

This case study evaluates the historic data on organic waste and wastewater treatment during the period of 1970–2020 to assess the impact of treatment of on energy production, nutrient recycling and GHG emissions (Poulsen and Hansen 2009). It is a classic example of a scenario in which significant environmental and economic benefits may be attained if energy in the wastewater is efficiently extracted and utilized. Aalborg Municipality, located in North Denmark, has changed its waste treatment strategy significantly during 1970–2005 from landfilling in an unlined landfill to a combined technology including controlled landfilling in a protected landfill coupled with anaerobic digestion, composting and incineration with energy production. These changes in treatment technology has resulted in a significant transformation of waste and wastewater treatment systems in Aalborg processing from being net energy consumers and net GHG emitters to net energy producers and net GHG emission savers. It has also resulted in significant environmental benefits, as the system has progressed from an annual net GHG emission of 200 kg CO_2-eq. per capita in 1970 to a net saving of 170 kg CO_2-eq. per capita in 2005 for urban organic waste management.

21.5.1 Transformation of Water and Wastewater Treatment Systems in Aalborg Municipality, Denmark

During 1970–2005, significant changes in the waste and wastewater treatment systems have been made in Aalborg (Poulsen and Hansen, 2009). In 1970, there was no treatment of wastewater (it was discharged to the ocean), and hence no sludge was generated. Food, yard waste and other organic waste were collected and deposed of in an unlined landfill with soil cover over deposited waste daily. There was no methane collection at the landfill.

In 1980, there was a construction of an aeration tank at the wastewater treatment plant which resulted in biological removal of organic matter from the wastewater. Sludge produced was dewatered using filter press and was deposited at a sludge deposit pit. Food, yard waste and other organic waste were incinerated in a rotary oven incinerator without energy generation, with the ash being disposed of in the landfill.

By 1990, there was an expansion of the wastewater treatment plant with a set of mesophilic (37°C) anaerobic digesters for extraction of biogas from the sludge. Biogas was ultimately converted to electricity and heat by employing a gas engine-generator. Digested sludge was dewatered in a filter press and transported for agricultural use as fertilizer. Yard and park waste were segregated and composted in open windrows. The compost generated was utilized as soil amendment and fertilizer on agricultural and urban soils. The left out waste was incinerated in the rotary oven incinerator with extraction of energy as heat and utilized for district heating. Ash, the byproduct of incineration, is employed for road construction.

During 1990–2005, the wastewater treatment process was further expanded with extra process tanks for nitrogen and phosphorus removal; anaerobic digesters were modified to operate under thermophilic conditions (53°C), and the digested sludge was dewatered in a centrifuge and dried using a fluidized bed drying facility that was operated on biogas obtained from digesters and natural gas. The drying facility was conveniently located in one of the wastewater treatment plants and had access to 30% of biogas produced from the sludge. The remaining 70% of the sludge was transported to a drying facility, and the dried sludge was ultimately heated for heat and power production at a commercial combined heat-power generation plant. The remaining solid waste incineration process was also modified to encourage heat and electricity production by installation of a steam turbine generator system at the incinerator site.

In 2020 additional arrangements will be made through which the incinerator will be operating with condensation of water vapor present in flue gases for enhanced heat recovery. Source separation of household food waste and subsequent treatment by anaerobic digestion together with sewage sludge will be set up by 2020. Additionally, sludge will be thermally pretreated prior to digestion to enhance biogas production. Furthermore, the digested, dewatered sludge and food waste will be incinerated separately to avoid contamination; the phosphorus extracted from ash will be utilized as fertilizer.

21.5.2. Economic and Environmental Benefits of Improved Technology

Transformation of waste and wastewater treatment plants in Aalborg Municipality had significant economic and environmental benefits. There was a net increase in heat and electricity production by each of wastewater treatment plants since 1970.

In 1970 and 1980, the electricity consumption was modest, which could be attributed to the sewer transport and wastewater treatment. In 1990, a net energy output was realized in the form of heat produced by waste incineration. Relatively little electricity consumption was associated with water transport and treatment as well as the operation of the incineration plant. In 2005, both net electricity and net heat productions are positive. About 9% and 33% of energy contained in the waste is converted to heat and electricity, respectively. This improvement could be linked to the implementation of a combined heat and power production unit at the waste incineration plant, to substitute the previous plant that produced only heat. In 2020, an estimated electricity and heat production of 19% and 49% of the total energy content in the waste will be realized. The main reason for improved electricity balance could be attributed to the production of biogas from food waste with concomitant electricity production in a gas engine at the wastewater plant. The main reason for improved heat balance could be related to the adoption of flue gas water vapor condensation at the incineration plant. Mainly, incineration and biogas production have huge impacts on the heat and electricity production, while other processes contribute less to it.

The net GHG balances per capita for the five waste and wastewater treatment plants in terms of CO_2 equivalents emitted or saved annually showed that there is a significant improvement in GHG emissions as a function of time. During 1970–2005, the waste and wastewater (http://www.positivehealth.com/article/ thought-field-therapy/chemical-fragrances-effects-on-the-autonomic-nervous-system) treatment system in Aalborg transformed into one from being a net emitter of CO_2 (about 200 kg CO_2-eq (capita- year)$^{-1}$) to a net saver of CO_2 emissions (170 kg CO_2-eq (capita-year)$^{-1}$). Further improvements in waste and wastewater treatment expected for 2020 could save as much as 340 kg CO_2-eq (capita-year)$^{-1}$, thus significantly reducing the carbon foot print of the average citizen (Poulsen and Hansen, 2009)

21.6 Future Perspectives

Reducing GHG emissions is one of the key challenges of the current generation. Wastewater treatment and sludge management are great contributors of the GHG emissions that attract growing attention. It is clear that GHG emissions increase with the increase on wastewater production. Industry, agriculture, and residential water usage are three major sources of wastewater production. It is well known that industries keep expanding all over the world; agriculture is becoming more and more modern with an increasing water consumption pattern and consequently produces more wastewater than before; and the global population is steadily growing. It implies that global GHG emissions contributed from wastewater treatment and sludge management would increase significantly, and it is reported that the average increase is around 5% per year (RTI Report 2010). As the production of wastewater is difficult to control due to economic considerations, measures of GHG emission reduction from wastewater treatment and sludge management should be maintained. To do so, comparison of the GHG emissions in the treatment processes (aerobic or anaerobic) as a function of the region/location, climate, wastewater characteristics (organic and nitrogen loading), and power generation sources should be performed first, and suitable processes that emit lower GHG should be chosen. Additionally, before selecting sludge management methods, comparison of GHG emissions from different types of management options (digestion and landfilling, composting and land application, and incineration) should be conducted. It is easy to understand that the most efficient way to reduce GHG emission can be accomplished by changing our habits (driving cars instead of walking, wasting water in washing, using a large amount of detergent, chasing high tech products, etc.) and paying attention to our actions. By adjusting our behavior and daily activities, we can reduce GHG emissions greatly and find a permanent solution to the problem before it passes on to future generations.

21.7 Conclusions

Preventing and reducing GHG emissions in wastewater and sludge treatment and management becomes significantly essential. There are many possible ways to fulfill the mission. The most simple and efficient one is to minimize wastewater production. Due to the development of industry and agriculture, a large amount of water is required, which results in a large amount of wastewater production, and certainly brings more GHG emissions due to the treatment of the wastewater as well as sludge treatment and management. The other way to reduce the GHG emission is to select suitable treatment processes in wastewater treatment. Aerobic treatment produces only carbon dioxide which is considered as a short life GHG, and usually doesn't count for GHG emission from wastewater and sludge treatment as it will be sequenced by plants and stored in the plants. Anaerobic treatment produces methane and nitrous oxide which are high GWP GHGs. Therefore, employing aerobic instead of anaerobic treatment would reduce GHG emissions. However, the emissions due to the consumption of power in aerobic treatment should be counted and compared with the GHG emission from the anaerobic process, and then make the final decision on which process should be used to minimize GHG emissions. Additionally, redesigning existing treatment plants would also result in transformation of them to low energy alternatives. Sludge treatment and disposal also greatly contribute to GHG emissions. Incineration and composting followed by land application needs to be carried out after a careful evaluation of air toxicants present in the wastewater as well as the nutrient value of the compost. Digestion (aerobic or anaerobic) followed by landfilling is the most common method of sludge management and is also the most efficient way of GHG emission reduction due to the possibility of methane collection from landfill. Incineration and biogas production seem to have huge impacts on electricity and heat production, thus contributing a balance of energy generation and GHG emissions. The adoption of key strategies for reducing GHG emissions in wastewater treatment could significantly reduce the average carbon footprint of citizens and prevent adverse climate change before it affects future generations.

21.8 Acknowledgement

Sincere thanks are due to the Natural Sciences and Engineering Research Council of Canada (Grant A 4984, Canada Research Chair) for their financial support. The views and opinions expressed in this paper are those of the authors.

21.9 References

Abdul-Talib, S., Hvitved-Jacobsen, T., Vollertsen, J., and Ujang, Z. (2002). “Anoxic transformations of wastewater organic matter in sewers--process kinetics, model concept and wastewater treatment potential.” *Water Science and Technology*, 45, 53–60.

Amlinger, F., Peyr, S., and Cuhls, C. (2008). “Green house gas emissions from composting and mechanical biological treatment.” *Waste Management & Research*, 26, 47–60.

Angelidaki, I., and Sanders, W. T. M. (2004). “Assessment of the anaerobic biodegradability of macropollutants.” *Reviews in Environmental Science & Biotechnology*, 3, 117–129.

Appels, L., Degrève, J., Van der Bruggen, B., Van Impe, J., and Dewil, R. (2010). “Influence of low temperature thermal pre-treatment on sludge solubilisation, heavy metal release and anaerobic digestion.” *Bioresource Technology*, 101, 5743–5748.

Artés, F., and Allende, A. (2005). "26 - Minimal fresh processing of vegetables, fruits and juices." In *Emerging Technologies for Food Processing*, 677–716 (Ed. S. Da-Wen). London: Academic Press.

Arvanitoyannis, I. S., and Varzakas, T. H. (2008). "Fruit/Fruit juice waste management: treatment methods and potential uses of treated waste." Chapter 9 In *Waste Management for the Food Industries*, 569–628 (Ed. Arvanitoyannis, I.S.). Amsterdam: Academic Press.

Augenbraum, H., Matthews, E., and Sharma, D. (1999). "The global methane emission cycle." Available at <icp.giss.nasagov/research/methane.html> (accessed June 2012).

Bani Shahabadi, M., Yerushalmi, L., and Haghighat, F. (2009). “Impact of process design on greenhouse gas (GHG) generation by wastewater treatment plants.” *Water Research*, 43, 2679–2687.

Bani Shahabadi, M., Yerushalmi, L., and Haghighat, F. (2010). “Estimation of greenhouse gas generation in wastewater treatment plants – Model development and application.” *Chemosphere*, 78, 1085–1092.

Banihani, Q., Sierra-Alvarez, R., and Field, J. (2009). “Nitrate and nitrite inhibition of methanogenesis during denitrification in granular biofilms and digested domestic sludges.” *Biodegradation*, 20, 801–812.

Banik, S., Bandyopadhyay, S., and Ganguly, S. (2003). “Bioeffects of microwave - A brief review.” *Bioresource Technology*, 87, 155–159.

Barber, W. P. F. (2009). “Influence of anaerobic digestion on the carbon footprint of various sewage sludge treatment options.” *Water and Environment Journal*, 23, 170–179.

Basu, S., M. , Abu-Orf, M., Laquidara, O., Boe, G., Sanchez, G., Law, C., Muller, D., and Novak, J. T. (2004). “High rate anaerobic digestion with mechanical shear- A case study at the Caldwell, ID WWTP.” *Water Environment Federation 77th Annual Technical Exhibition and Conference, New Orleans, LA, Water Environment Federation*.

Bitton, G. (2005). *Wastewater microbiology.* 3rd ed. Wiley-Liss, New York.

Bogner, J., Pipatti, R., Hashimoto, S., Diaz, C., Mareckova, K., Diaz, L., Kjeldsen, P., Monni, S., Faaij, A., Qingxian Gao, Tianzhu Zhang, Mohammed Abdelrafie Ahmed, Sutamihardja, R. T. M., and Gregory, R. (2008). "Mitigation of global greenhouse gas emissions from waste: conclusions and strategies from the Intergovernmental Panel on Climate Change (IPCC) Fourth Assessment Report. Working Group III (Mitigation)." *Waste Management & Research*, 26, 11–32.

Bridle Consulting (2007). "Development of a process model to predict GHG emissinos from the water corporation metropolitan WWTPs." *Agriculture, Ecosystems and Environment*, 136, 292–300.

Broecker, W. S. (1975). "Are we on the brink of a pronounced global warming?" *Science*, 189, 460–463.

Buyukkamaci, N., and Koken, E. (2010). "Economic evaluation of alternative wastewater treatment plant options for pulp and paper industry." *Science of The Total Environment*, 408, 6070–6078.

Cakir, F. Y., and Stenstrom, M. K. (2005). "Greenhouse gas production: A comparison between aerobic and anaerobic wastewater treatment technology." *Water Research*, 39, 4197–4203.

Chalvatzaki, E., and Lazaridis, M. (2010). "Estimation of greenhouse gas emisison from landfill: application to the Akrotiri landfill site." *Global NEST Journal*, 12, 108–116.

Chan, Y. J., Chong, M. F., Law, C. L., and Hassell, D. G. (2009). "A review on anaerobic–aerobic treatment of industrial and municipal wastewater." *Chemical Engineering Journal*, 155, 1–18.

Chen, Y., Chen, Y.-S., and Gu, G. (2004). "Influence of pretreating activated sludge with acid and surfactant prior to conventional conditioning on filtration dewatering." *Chemical Engineering Journal*, 99, 137–143.

Chiu, Y., Chang, C., Lin, J., and Huang, S. (1997). "Alkaline and ultrasonic pretreatment of sludge before anaerobic digestion." *Water Science and Technology*, 36, 155–162.

Choi, H. B., Hwang, K. Y., and Shin, E. B. (1997). "Effects onanaerobic digestion of sewage sludge pretreatment." *Water Science and Technology*, 35, 200–207.

Colliver, B. B., and Stephenson, T. (2000). "Production of nitrogen oxide and dinitrogen oxide by autotrophic nitrifiers." *Biotechnology Advances*, 18, 219–232.

Corominas, L. l., Flores-Alsina, X., Snip, L., and Vanrolleghem, P. A. (2010). "Minimising overall greenhouse gas emissions from wastewater treatment plants by implementing automatic control." Available at <http://biomath.ugent.be/~peter/ftp/pvr912.pdf> (accessed Dec. 2011).

Czepiel, P., Crill, P., and Harriss, R. (1995). "Nitrous oxide emissions from municipal wastewater treatment." *Environmental Science & Technology*, 29, 2352–2356.

Delgenes, J., Penaud, V., Torrijos, M., and Molletta, R. (2002). "Investigation of the change in anaerobic biodegradability and toxicity of an industrial biomass induced by thermo chemical pre-treatment." *Water Science and Technology*, 41, 137–144.

Dewil, R., Baeyens, J., and Goutvrind, R. (2006). "Ultrasonic treatment of waste activated sludge." *Environmental Progress*, 25, 121–128.

El-Fadel, M., and Massoud, M. (2001). "Methane emissions from wastewater management." *Environmental Pollution*, 114, 177–185.

El-Mashad, H. M., and Zhang, R. (2010). "Biogas production from co-digestion of dairy manure and food waste." *Bioresource Technology*, 101, 4021–4028.

Gavala, H. N., Yenal, U., Skiadas, I. V., Westermann, P., and Ahring, B. K. (2003). "Mesophilic and thermophilic anaerobic digestion of primary and secondary sludge: Effect of pre-treatment at elevated temperature." *Water Research*, 37, 4561–4572.

Georges, K., Thornton, A., and Sadler, R. (2009). *Transforming Wastewater treatment to Reduce Carbon Emissions*. Environmental Agency Report: SC070010/R2, Available at: <http://publications.environment-agency.gov.uk /PDF/SCHO 1209 BRNZ-E-E.pdf> (accessed June 2012).

Gerardi, M. H. (2006). *Wastewater Bacteria.* John Wiley & Sons, Inc., New York.

Goel, R., Komatsu, K., Yasui, H., and Harada, T. (2003). "Process performance and change in sludge characteristics during anaerobic digestion of sewage sludge with ozonation." *Water Science and Technology*, 49, 105–114.

Hanaki, K., Hong, Z., and Matsuo, T. (1992). "Production of nitrous oxide gas during denitrification of wastewater." *Water Science and Technology*, 26, 1027–1036.

Hoon, K. S. (2004). *Lime pretreatment and enzymatic hydrolysis of corn stover*. Ph.D. Dissertation. University of Texas A & M.

http://www.positivehealth.com/article/thought-field-therapy/chemical-fragrances-effects-on-the-autonomic-nervous-system.

Hynes, R. K., and Knowles, R. (1984). "Production of nitrous oxide by *Nitrosomonas europaea*: effects of acetylene, pH, and oxygen." *Canadian Journal of Microbiology*, 30, 1397–1404.

IEA (International Energy Agency) (1999). "Greenhouse gas and climate change." Available at <http://www.ieagreen.org.uk/ghgs.htm> (accessed June 2012).

IPCC (1997). *Revised 1996 IPCC guidelines for national greenhouse gas inventories. IPCC, Paris.*

IPCC (2000). *Good practice guidance and uncertainly management in national greenhouse gas inventories*. Intergovernmental Panel on Climate Change, National Greenhouse Gas Inventories Programme. Montreal, IPCC/Doc. 10 (1.IV.2000). May 2000.

Itokawa, H., Hanaki, K., and Matsuo, T. (2001). "Nitrous oxide production in high-loading biological nitrogen removal process under low COD/N ratio condition." *Water Research*, 35, 657–664.

Jiang, G., Gutierrez, O., Sharma, K. R., and Yuan, Z. (2010). "Effects of nitrite concentration and exposure time on sulfide and methane production in sewer systems." *Water Research*, 44, 4241–4251.

Johansson, A. E., Gustavsson, A. M., Öquist, M. G., and Svensson, B. H. (2004). "Methane emissions from a constructed wetland treating wastewater–seasonal and spatial distribution and dependence on edaphic factors." *Water Research*, 38, 3960–3970.

Kampschreur, M. J., Tan, N. C. G., Kleerebezem, R., Picioreanu, C., Jetten, M. S. M., and van Loosdrecht, M. C. M. (2008a). "Effect of dynamic process conditions on nitrogen oxides emission from a nitrifying culture." *Environmental Science & Technology*, 42, 429–435.

Kampschreur, M. J., van der Star, W. R. L., Wielders, H. A., Mulder, J. W., Jetten, M. S. M., and van Loosdrecht, M. C. M. (2008b). "Dynamics of nitric oxide and nitrous oxide emission during full-scale reject water treatment." *Water Research*, 42, 812–826.

Kassab, G., Halalsheh, M., Klapwijk, A., Fayyad, M., and van Lier, J. B. (2010). "Sequential anaerobic–aerobic treatment for domestic wastewater–A review." *Bioresource Technology*, 101, 3299–3310.

Keller, J., and Hartley, K. (2003). "Greenhouse gas production in wastewater treatment: Process selection is the major factor." *Water Science and Technology*, 47, 43–48.

Kim, J., Novak, J. T., and Higgins, M. J. (2011). "Multistaged anaerobic sludge digestion processes." *Environmental Engineering*, 137, 746–751.

López Torres, M., and Espinosa Lloréns, M. d. C. (2008). "Effect of alkaline pretreatment on anaerobic digestion of solid wastes." *Waste Management*, 28, 2229–2234.

Li, Y.-Y., and Noike, T. (1992). "Upgrading of anaerobic digestion of waste activated sludge bythermal pretreatment." *Water Science and Technology*, 26, 857–866.

Lin, J.-G., Chang, C.-N., and Chang, S.-C. (1997). "Enhancement of anaerobic digestion of waste activated sludge by alkaline solubilization." *Bioresource Technology*, 62, 85–90.

Lin, Y., Wang, D., Wu, S., and Wang, C. (2009). "Alkali pretreatment enhances biogas production in the anaerobic digestion of pulp and paper sludge." *Journal of Hazardous Materials*, 170, 366–373.

Lou, X. F., and Nair, J. (2009). "The impact of landfilling and composting on greenhouse gas emissions - A review." *Bioresource Technology*, 100, 3792–3798.

Maa, Y.-F., and Hsu, C. C. (1996). "Effect of Shear on Proteins." *Biotechnology Bioengineering*, 51, 458–465.

Maag, M., and Vinther, F. P. (1996). "Nitrous oxide emission by nitrification and denitrification in different soil types and at different soil moisture contents and temperatures." *Applied Soil Ecology*, 4, 5–14.

Mann, M. E., and Jones, P. D. (2003). "Global surface temperatures over the past two millennia." *Geophysical Research Letters*, 30, 15–18.

Mohanakrishnan, J., Gutierrez, O., Meyer, R. L., and Yuan, Z. (2008). "Nitrite effectively inhibits sulfide and methane production in a laboratory scale sewer reactor." *Water Research*, 42, 3961–3971.

Monni, S., Pipatti, R., Lehtilä, A., Savolainen, I., and Syri, S. (2006). "Global climate change mitigation scenarios for solid waste management." *Espoo, Technical Research Centre of Finland. VTT Publications*, 603, 51–55.

Muller, C. D. (2001a). *High-intensity shear as a wet sludge disintegration technology and a mechanism for floc structure analysis*. M.S. Thesis, Virginia Polytechnic Institute and State University. pp. 76.

Muller, J. (2001b). “Prospects and problems of sludge pretreatment processes.” *Water Science and Technology*, 44, 121-128.

Muller, C. D., Abu-Orf, M., and Novak, J. T. (2003). “The effect of mechanical shear on mesophilic anaerobic digestion.” *Proceedings of the Water Environment Federation*, 2003, 558–578.

Muller, C. D., Verma, N., Higgins, M. J., and Novak, J. T. (2004). “The role of shear in the generation of nuisance odors from dewatered biosolids.” WEFTEX 2004: Session 21 through Session 30, pp. 376–388(13).

Nges, I. A., and Liu, J. (2009). “Effects of anaerobic pre-treatment on the degradation of dewatered-sewage sludge.” *Renewable Energy*, 34, 1795–1800.

Nosrati, M., Amani, T., and Sreekrishnan, T. R. (2011). “Thermophilic anaerobic digestion of waste activated sludge versus mesophilic anaerobic digestion.” *International Conference on Advances in Biotechnology and Pharmaceutical Sciences, Bangkok Dec., 2011*, 226–229.

Park, B., Ahn, J.-H., Kim, J., and Hwang, S. (2004). “Use of microwave pretreatment for enhanced anaerobiosis of secondary sludge.” *Water Science and Technology*, 50, 17–23.

Park, C.-J. (2011). “The study on the estimation of greenhouse gas emission from landfill facilities.” 2nd International Conference on Environmental Science and Technology, 2011, Singapore, 6, 118–190.

Park, C., Lee, C., Kim, S., Chen, Y., and Chase, H. A. (2005). “Upgrading of anaerobic digestion by incorporating two different hydrolysis processes.” *Journal of Bioscience and Bioengineering*, 100, 164–167.

Park, K. Y., Inamori, Y., Mizuochi, M., and Ahn, K. H. (2000). “Emission and control of nitrous oxide from a biological wastewater treatment system with intermittent aeration.” *Journal of Bioscience and Bioengineering*, 90, 247–252.

Penaud, V., Delgen-s, J. P., and Moletta, R. (1999). “Thermo-chemical pretreatment of a microbial biomass: Influence of sodium hydroxide addition on solubilization and anaerobic biodegrability.” *Enzyme Microbiological Technology*, 25, 258–263.

Pinnekamp, J. (1989). “Effects of thermal pretreatment of sewage sludge on anaerobic digestion.” *Water Science and Technology*, 21, 97–108.

Pipatti, R., Savolainnen, I., and Sinsalo, J. (1996) “Greenhouse impacts of anthropogenic CH_4 and N_2O emissions in Finland.” *Environmental Management*, 20 (2), 219–233.

Pokhrel, D., and Viraraghavan, T. (2004). “Treatment of pulp and paper mill wastewater—A review.” *Science of The Total Environment*, 333, 37–58.

Poulsen, T.G., and Hansen, J.A. (2009). "Assessing the impacts of changes in treatment technology on energy and green house gas balances for organic waste and wastewater treatment using historical data." *Waste Management and Research*, 27, 861–870.

Préndez, M., and Lara-González, S. (2008). "Application of strategies for sanitation management in wastewater treatment plants in order to control/reduce greenhouse gas emissions." *Journal of Environmental Management*, 88, 658–664.

Report (2005). "Determination of the impact of waste management activities on greenhouse gas emissions: 2005 update final report, ICF consulting." *Environment Canada and Natural Resources Canada, October 31, 2005*.

Ritchie, G. A. F., and Nicholas, D. J. D. (1972). "Identification of the sources of nitrous oxide produced by oxidative and reductive processes in *Nitrosomonas europaea*." *Biochemstry*, 126, 1181-1191.

Rosso, D., and Stenstrom, M. K. (2008). "The carbon-sequestration potential of municipal wastewater treatment." *Chemosphere*, 70, 1468–1475.

RTI Report (2010). *Greenhouse gas emissions estimation methodologies for biogenic emissions from selected source categories: solid waste disposal wastewater treatment ethanol fermentation.* Submitted to U.S. Environmental Protection Agency Sector Policies and Programs Division Measurement Policy Group by RTI International 3040 Cornwallis Road Research Triangle Park on Dec. 14th 2010.

Sahely, H. R., MacLean, H. L., Monteith, H. D., and Bagley, D. M. (2006). "Comparison of on-site and upstream greenhouse gas emissions from Canadian municipal wastewater treatment facilities." *Journal of Environmental Engineering and Science*, 5, 405–415.

Sawayama, S., Inoue, S., Tsnkahara, K., and Ogi, T. (1996). "Thermochemical liquidization of anaerobically digested and dewatered sludge and anaerobic retreatment." *Bioresource Technology*, 55, 141–144.

Scheehle, E. A., and Doorn, M. R. J. (2003). "Improvements to the U.S. wastewater methane and nitrous oide emssions etimates." Available at <http://www.epa.gov/ttnchie1/conference/ei12/green/scheehle.pdf> (accessed Jan. 2012).

Schulthess, R. V., Kuehni, M., and Gujer, W. (1995). "Release of nitric and nitrous oxides from denitrifying activated sludge." *Water Research*, 29, 215–226.

Skiadas, I., Gavala, H., Lu, J., and Ahring, B. (2005). "Thermal pre-treatment of primary and secondary sludge at 70 degrees C prior to anaerobic digestion." *Water Science and Technology*, 52, 161–166.

Snip, L. J. P. (2010). *Quantifying the greenhouse gas emissions of waste water treatment plants.* M.S Thesis of Wageningen University, Department of Environmental Science, April 2010.

Soloman, P. A., Ahmed Basha, C., Velan, M., Balasubramanian, N., and Marimuthu, P. (2009). "Augmentation of biodegradability of pulp and paper industry wastewater by electrochemical pre-treatment and optimization by RSM." *Separation and Purification Technology*, 69, 109–117.

Sosnowski, P. (2003). "Anaerobic co-digestion of sewage sludge and organic fraction of municipal solid wastes." *Advances in Environmental Research*, 7, 609–616.

Stoica, A., Sandberg, M., and Holby, O. (2009). "Energy use and recovery strategies within wastewater treatment and sludge handling at pulp and paper mills." *Bioresource Technology*, 100, 3497–3505.

Stuckey, D. C., and McCarty, P. L. (1984). "The effect of thermal pretreatment on the anaerobic biodegradability and toxicity of waste activated sludge." *Water Research*, 18, 1343–1353.

SYLVIS (2009). "The Biosolids Emissions Assessment Model (BEAM): a method for determining greenhouse gas emissions from Canadian biosolids management practices." *Executive Summary for Canadian Council of Ministers of the Enviroment*.

Tallec, G., Garnier, J., Billen, G., and Gousailles, M. (2006). "Nitrous oxide emissions from secondary activated sludge in nitrifying conditions of urban wastewater treatment plants: effect of oxygenation level." *Water Research*, 40, 2972–2980.

Tanaka, S., Kobayashi, T., Kamiyama, K. L., and Bildan, M. L. N. S. (1997). "Effects of thermochemical pretreatment on the anaerobic digestion of waste activated sludge." *Water Science and Technology*, 35, 209–215.

Tsai, T. S. (1986). "A microwave method for the extraction of cellular ATP." *Biochem Biophys Methods*, 13, 343–345.

U.S. EPA (1997). *Estimate of global greenhouse gas emissions from industrial and domestic wastewater treatment.* United States Environmental Protection Agency, Office of Policy Planning and Evaluation, EPA-600/R-97-091, Washington, DC, September 1997.

U.S. EPA (2003). *International analysis of methane and nitrous oxide abatement opportunities: Report to energy modeling forum, working group 21*. Available at <http://www.epa.gov/climatechange/economics/pdfs/methodologych4.pdf> (accessed Dec. 2011).

Van Cleemput, O. (1998). "Subsoils: chemo- and biological denitrification, N_2O and N_2 emissions." *Nutrient Cycling in Agroecosystems*, 52, 187–194.

Van Niel, E. W. J., Arts, P. A. M., Wesselink, B. J., Robertson, L. A., and Kuenen, J. G. (1993). "Competition between heterotrophic and autotrophic nitrifiers for ammonia in chemostat cultures." *FEMS Microbiology Ecology*, 102, 109–118.

Wall, H., Waltz, E., and Verdouw, A. (1984). "Fuel in sewage sludge incineration." *Waste Management & Research*, 2, 205–225.

Wang, J., Zhang, J., Xie, H., Qi, P., Ren, Y., and Hu, Z. (2011). "Methane emissions from a full-scale A/A/O wastewater treatment plant." *Bioresource Technology*, 102, 5479–5485.

Wang, Q., Noguchi, C., Hara, Y., Sharon, C., Kakimoto, K., and Kato, Y. (1997). "Studies on anaerobic digestion mechanism: influence of pretreatment temperature on biodegradation of waste activated sludge." *Environmental Technology*, 18, 999–1008.

Weemaes, M., Grootaerd, H., Simoens, F., and Verstraete, W. (2000). "Anaerobic digestion of ozonized biosolids." *Water Research*, 8, 2330–2336.

Worldbank (1999). *Pollution Prevention and Abatement Handbook 1998, Toward Cleaner Production.* The International Bank for Reconstruction and Development/The WORLDBANK. 1818 H Street, N.W. Washington, DC. 20433, USA.

Wunderlin, P., Mohn, J., Joss, A., Emmenegger, L., and Siegrist, H. (2012). "Mechanisms of N_2O production in biological wastewater treatment under nitrifying and denitrifying conditions." *Water Research*, 46, 1027–1037.

Xie, T., and wang, C. (2011). "Impact of different factors on greenhouse gas generation by wastewater treatment plants in China." *Water Resource and Environmental Protection, 2011 International Symposium on 20-22 May 2011*, 1448–1451.

Yasui, H., Goel, R., Fukase, T., Matsuhashi, R., Wakayama, M., Sakai, Y., and Noike, T. (2003). "Bioleaderw, a novel activated sludge process minimizing excess sludge production." *In Proc. IWA Leading Edge Conference, Noordwijk/Amsterdam, The Netherlands.*

Yasui, H., Komatsu, K., Goel, R., Li, Y.Y., and Noike, T. (2005a). "Full-scale application of anaerobic digestion process with partial ozonation of digested sludge." *Water Science and Technology*, 52, 245–252.

Yasui, H., Komatsu, K., Goel, R., Matsuhashi, R., Ohashi, A., and Harada, H. (2005b). "Minimization of greenhouse gas emission by application of anaerobic digestion process with biogas utilization." *Water Science and Technology*, 52, 545–552.

Yasui, H., Matsuhashi, R., Noike, T., and Harada, H. (2006). "Anaerobic digestion with partial ozonation minimises greenhouse gas emission from sludge treatment and disposal." *Water Science and Technology*, 53, 255–263.

Zábranská, I., Štěpová, J., Wachtl, R., Jeníček, P., and Dohányos, M. (2000). "The activity of anaerobic biomass in thermophilic and mesophilic digesters at different loading rates." *Water Science and Technology*, 42, 49–56.

CHAPTER 22

Mitigation/Reduction of GHG Emissions in Solid/Hazardous Waste Management

J. Patrick A. Hettiaratchi and Uriel Mancebo del Castillo Sternenfels

The greenhouse gas (GHG) emissions associated with the solid waste sector includes emissions from the collection, treatment and disposal of wastes. Among all GHG emission sources related to solid waste, by far, the largest source is waste disposal, and therefore this chapter deals with the emission and mitigation of GHGs from solid waste disposal. Among the various methods at minimizing waste-related GHG emissions, the most cost-effective and the most promising method is the most recent introduction, the application of methanotrophic processes to naturally attenuate and assimilate methane escaping from closed landfills. This chapter first provides a brief review of the literature related to landfill methane generation, migration and methods available to quantify biogas generation within landfills. Second, a short description of innovative landfill technologies available to minimize GHG escape is provided concentrating primarily on landfill bioreactor technology. Third, a detailed description of soil methanotrophy and the technologies that utilize methanotrophy to mitigate GHG emissions from landfills is provided.

22.1 Introduction

The GHG emissions associated with the solid waste sector includes emissions from the collection, treatment and disposal of wastes. The waste-collection-related GHG emissions are non-point sourced whereas waste treatment and disposal constitute point source emissions. Among all GHG emission sources related to solid waste, by far, the largest source is waste disposal, and therefore this chapter deals with the emission and mitigation of GHGs from land disposal of solid waste.

Much of the solid waste disposed of on land is either biomass or biomass based. Carbon dioxide (CO_2) emissions attributable to such wastes are not included in national or international greenhouse gas inventory totals. It is assumed that there are no net emissions if the biomass associated with the waste is sustainably harvested. For example, CO_2 generated from the decomposition of food wastes would be consumed by the next year's crop. On the other hand, methane emissions from anaerobic decomposition of wastes are included in GHG inventories. Considering these facts, the focus of this chapter is on methane (CH_4) emissions from land disposal of waste materials and methods available to mitigate such emissions.

CH_4 is the most abundant oxygen-free C-containing constituent of the atmosphere and is present globally in the troposphere at a concentration of 1–2 ppm. Alternatively, CH_4 sources can be divided into anthropogenic and natural. The anthropogenic sources include paddy fields, livestock, engineered anaerobic processes (anaerobic digesters, landfills), oil and gas industry, some biomass burning, and fossil fuel combustion. Natural CH_4 is emitted from sources such as wetlands, oceans, forests, fire, termites and geological sources (Atkinson 2000; IPCC 2007).

CH_4 is a major by-product of anaerobic degradation of organic materials. Large amounts of CH_4 are emitted to the atmosphere through fugitive emissions from both natural and anthropogenic sources. Landfill gas (LFG) generated from anaerobic degradation of waste in land disposal sites consists of CH_4 (55–60%) and CO_2 (40–45%) and trace concentrations of other gases (Tchobanoglous et al. 1993; Tchobanoglous and Kreith 2002). CH_4 emissions from landfills are estimated at 35–73 Tg/year and represent 30%, 24% and 25% of the anthropogenic emissions of CH_4 into the atmosphere in Europe, the United States and Canada, respectively (Nozhevnikova et al. 2003; Nikiema et al. 2007). Further discussion of CH_4 generation and migration is provided in the following sections.

There are microorganisms that have evolved and developed the capacity of grow aerobically on CH_4 as a sole carbon and energy source. These organisms are known as methanotrophs and play an important role in recycling CH_4 into organic compounds and make it available as CO_2 to autotrophs (Large 1983). Nevertheless, the main sink for atmospheric CH_4 is reaction with hydroxyl radical (OH). This radical is the key reactive species in the trophosphere; it is produced photochemically in the atmosphere and reacts with all kind of organic compounds (Cullis and Hirschler 1989; Atkinson 2000). The oxidation of CH_4 in the presence of OH radicals is undertaken through a number of photochemical reactions (Hanson & Hanson 1996; Atkinson 2000). The processes associated with the CH_4 cycle is shown in Figure 22.1.

The energy content of CH_4 is 55,525 kJ/kg at 25°C and 1atm. Consequently, CH_4 has been regarded as a bioenergy source that has proved its potential on large scale industrial and even on municipal applications for electricity generation and as fuel for vehicles (Khanal 2008). However, sometimes it is not economically or technically feasible to collect and use CH_4 streams as alternative energy source; as a result, CH_4 is released into the atmosphere. This situation is counterproductive as the global warming potential (GWP) of CH_4 is 25 times more than that of CO_2 on a 100-year time horizon. On a 20-year time horizon, the GWP of CH_4 is estimated to be about 72. Additionally, increasing release rates of CH_4 into the atmosphere will decrease OH radical concentrations. This effect will allow an increase of the lifetime of CH_4 in the atmosphere by as much as 20% by the year 2050 (Atkinson 2000; IPCC 2007).

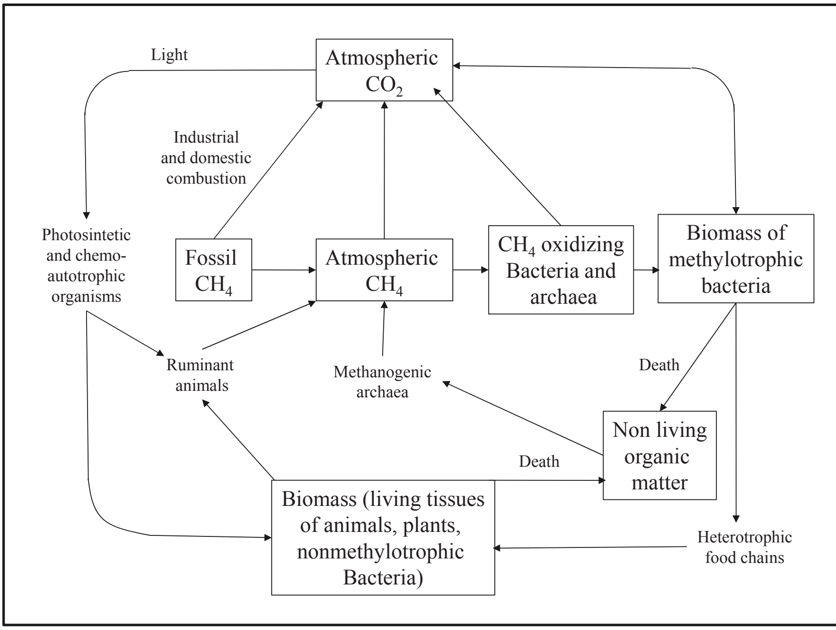

Figure 22.1. The CH_4 cycle (adapted from Large 1983)

There is increasing interest in the development of cost-effective and reliable alternatives for treatment of CH_4 gas from sources where its use is not technically or economically feasible. The options for the treatment of gaseous streams for CH_4 such as incineration or catalytic oxidation can be expensive and complex (Huber-Humer et al. 2009). As mentioned earlier, methanotrophs are microorganisms that have the capacity to grow aerobically on CH_4 and to oxidise it into CO_2 and water (Large 1983; IPCC 2007). Additionally, the development of novel approaches for waste management, such as landfill bioreactors, have become a promising alternative to optimize production, collection, and extraction of CH_4, which in turn, allow the minimization of uncontrolled emissions of LFG into the atmosphere. Further details of these processes are included in following sections.

22.2 Production and Emission of CH_4 at Land Disposal Sites

The production of landfill gas (LFG) is thought to occur in five sequential phases as illustrated in Table 22.1 and Tchobanoglous et al. (1993).

The Scholl Canyon model is the most commonly used model for determining LFG generation rates. This method assumes that the lag growth phase is negligible and that CH_4 generation peaks immediately following first order kinetics (EPA 2005). The derivation of this model is described with the following equations:

Table 22.1. Phases of LFG generation (adapted from Tchobanoglous et al. 1993)

Phase	Description
I–initial adjustment	In this phase, biodegradable components in waste undergo microbial decomposition as they are placed in a landfill. As certain amount of air is trapped within the landfill, this biological decomposition occurs under aerobic conditions.
II–transition	Once oxygen is depleted, anaerobic conditions begin to develop. High presence of organic acids and CO_2 levels within the landfill.
III–acid phase	It is developed the hydrolysis of higher molecular compounds into compounds suitable for use by anaerobic microorganisms. Fermentation and anaerobic oxidation processes produce high amounts of intermediary products like organic acids and VFAs.
IV–methanogenic phase	Acetotrophic and hydrogenotrophic methanogenic processes convert intermediary products into CH_4 and CO_2.
V–maturation phase	This phase occurs after the readily available organic material has been converted to CH_4 and CO_2. As moisture continues to migrate through the waste, portions of biodegradable material that were previously unavailable will undergo through the anaerobic degradation process. The LFG production in this phase diminishes significantly.

$$-\frac{dL}{dt} = kL \quad \text{(Eq. 22.1)}$$

where: L= volume of CH_4 remaining to be produced after time t; and k= gas production constant. Integrating Equation 22.1 gives:

$$L = L_0 e^{-kt} \quad \text{(Eq. 22.2)}$$

$$V = L_0 - L = L_0\left(1 - e^{-kt}\right) \quad \text{(Eq. 22.3)}$$

where: L_0= volume of CH_4 remaining to be produced at t=0; ultimate CH_4 generation potential; and V= cumulative CH_4 volume produced prior to time t. From Equation 22.3

$$\frac{dV}{dt} = -\frac{dL}{dt} = kL = kL_0 e^{-kt} \quad \text{(Eq. 22.4)}$$

where: kL_0= peak generation rate which occurs at time zero in units of volume per time. The total generation rate is the summation of the generation rates of the sub masses:

$$Q = kL = kL_0 \sum_{i=1}^{n} M_i e^{-kt_i} \quad \text{(Eq. 22.5)}$$

where: Q= total CH_4 production rate; and M_i= Sub mass landfilled in period i.

At CH_4 concentrations in LFG below 30–40% and production rates lower than 50 m^3h^{-1}, the use of LFG in power generation becomes technically and economically infeasible. Flaring is an option when CH_4 concentrations are higher than 20– 25% v/v and LFG flow rates are low (Huber-Humer et al. 2008). However, low temperature flaring produces toxic substances (Cherubini et al. 2009).

22.3 Control of CH_4 Emissions at Waste Disposal Sites

The control of fugitive emissions of CH_4 into the atmosphere from organic waste disposal sites can be achieved either by preventive or remedial approaches. Preventive schemes can be deployed by developing new holistic waste management systems allowing the maximization of CH_4 recovery rates and the minimization of fugitive emissions as part of the design criteria. A remedial or "end of pipe" approach should be considered in existing sites because redesign is not technically and economically feasible. In this case, gas extraction for energy recovery could be practiced as long as the quantity of LFG is sufficient to enable economical implementation of a gas to energy facility. However, at small and/or old landfills, sufficient gas volumes are not generated to warrant the implementation of gas recovery and utilization for energy production. In such cases, the use of biological methane oxidation methods could be a cost-effective and reliable alternative for the control and treatment of uncontrolled CH_4 emissions.

22.3.1 The Landfill Bioreactor as an Effective Emission Control Approach

Recently, the "landfill bioreactor" concept has received significant attention from waste management professionals. A landfill bioreactor is a waste cell that uses enhanced microbiological processes to transform and stabilize the readily and moderately decomposable organic waste constituents within 5 to 10 years of bioreactor process implementation. The landfill bioreactor significantly increases the extent of organic waste decomposition, conversion rates and process effectiveness over what would otherwise occur within the landfill (Pacey et al. 1999). The landfill bioreactor provides control and process optimization, primarily through the addition of leachate or other liquid amendments, the addition of sewage sludge or other amendments, temperature control, and nutrient supplementation (Reinhart et al. 2002). Beyond that, bioreactor landfill operation may involve the addition of air. Based on waste biodegradation mechanisms, different kinds of "bioreactor landfills" including anaerobic bioreactors, aerobic bioreactors, and aerobic-anaerobic (hybrid) bioreactors have been constructed and operated worldwide. The landfill bioreactor concept was first introduced as a solution to the leachate management problem. However, there are three other advantages to employing anaerobic landfill bioreactor technology compared to conventional sanitary landfills: (1) rapid recovery of air space, (2) accelerated waste stabilization and avoidance of long-term monitoring and maintenance, and (3) potential benefits from increased methane generation. In the case of aerobic landfill bioreactors, the major advantages are: (1) significant increase in the biodegradation rate of waste over anaerobic processes, (2) a reduction in the volume of leachate, and (3) significantly reduced methane generation and "anaerobic" odors. A comprehensive discussion of anaerobic and aerobic landfill bioreactor technology is provided in Elagroudy et al. (2009).

22.3.2 Application of Methanotrophic Processes as a Remedial Approach

In traditional sanitary landfills, the primary role of a final cover is to minimize infiltration of precipitation falling on the landfill surface. A secondary role is to trap the generated gas within the waste matrix, which in turn, reduces the emission of LFG into the atmosphere. This is achieved by using a barrier layer, which can be a thick compacted clay layer or a plastic liner (e.g. low density polyethylene or poly-vinyl chloride). Another, less well-known, role could be to attenuate and control the escape of methane across the final cover using a naturally occurring process known as methanotrophy, or biological oxidation of CH_4 to CO_2 by naturally occurring methanotrophic bacteria.

Earlier research and numerous reports have documented the CH_4 biological removal in landfills cover soils. It has been concluded that biological CH_4 oxidation in engineered systems is possible by providing optimum conditions for methanotrophic bacteria growth. This has prompted research activity related to the development of feasible and cost-effective technologies for CH_4 removal. As a result, there have been developments related to biological CH_4 removal systems.

A second application of methanotrophy deals with the LFG extracted, either using active or passive methods, from relatively small landfills. When the gas volume is low, the conventional practice is to burn the gas off using flares. But, a better and environmental benign approach is to treat such gas using a methane biofilter, or MBF. The MBF technology can also be used at later stages of landfill gas to energy project when the leachate quality and quantity decreases substantially.

22.3.2.1 Biochemistry of Methanotrophic Processes

CH_4 is one of the most abundant organic compounds on this planet, and this is reflected by the abundance of methanotrophic bacteria in the environment. Although there have been a few descriptions of facultative methanotrophs, nearly all aerobic methane utilizing bacteria are obligate methanotrophs and all of them are Gram-negative bacteria (Anthony 1982; Dunfield 2009). Depending on the guanine and cytosine content of their DNA, intracellular membrane arrangement, carbon assimilation pathway, and phospholipid fatty acids composition, methanotrophic bacteria were previously divided into three groups, Type I, Type II, and Type X (Dunfield 2009). Type I methanotrophs were characterized as those having bundles of disc-shaped vesicles while Type II methanotrophs were those having a system of peripheral membranes. Regarding the predominant fatty acids in their membranes, saturated phospholipid fatty acids with 16 carbon atoms (16:0) were associated with Type I methanotrophs while those with 18 carbons in length (18:0) were associated with Type II strains. According to this classification, those methanotrophs utilizing the ribulose monophosphate (RuMP) pathway for carbon assimilation were considered as Type I, and those utilizing the serine pathway were classified as Type II. All Type II methanotrophs were considered to fix molecular nitrogen due to nitrogenase activity. Type X methanotrophs were defined as a subset of type I methanotrophs and had characteristics of both types. Type X strains were observed to grow at thermophilic temperatures, fix atmospheric nitrogen, and in some cases, to use the serine pathway for carbon assimilation. Recent discoveries of new species have shown that these generalizations are not universal. As a result, terms Type I and Type II are now generally used as synonyms for *Gamaproteobacteria* and *Alphaproteobacteria* respectively (Hanson and Hanson 1996; Bodelier et al. 2009; Semrau et al. 2010).

A defining characteristic associated with methanotrophs is the use of enzyme CH_4 monooxygenases (MMOs) to catalyze the oxidation of CH_4 to methanol (CH_3OH). These enzymes utilize two electrons to split the di-oxygen bonds. One of these atoms is reduced to form H_2O, and the other is incorporated into CH_4 to form CH_3OH (Hanson and Hanson 1996; Bull et al. 2000). Most known methanotrophs are capable of forming a particulate or membrane-bound MMO (pMMO) when growing in the presence of copper. Cytoplasmic soluble MMO (sMMO) has been observed to be formed by some methanotrophs. The sMMO has a broader substrate specificity than the pMMO; it can oxidise a wide range of non-growth substrates such as alkanes, alkenes and aromatic compounds. Methanotrophs forming only pMMO appear to have a higher affinity for methane than those producing sMMO (Hanson and Hanson 1996; Murrell et al. 2000; Wilshusen et al. 2004a).

During the oxidation of CH_4 to CO_2, the oxidation number of carbon increases from -4 to +4 with a release of energy (exothermic reaction). This oxidation reaction is defined by Equation 22.7.

$$CH_4 + 2O_2 \longrightarrow CO_2 + 2H_2O \qquad \text{(Eq. 22.7)}$$

The free energy (ΔG°) available from this reaction is -632 kJ/ mol of CH_4. The heat of combustion released (ΔH°) if the H_2O vapour formed is condensed to form liquid water is -890.51 kJ/ mol of CH_4 (gross heat); ΔH° is -802.51 kJ/ mol of CH_4 if the water remains as vapour or gas (Wilshusen 2002).

During the methanotrophic processes, only two C_1 oxidation products are converted into cell material via assimilatory pathways, namely formaldehyde

(HCOH) and CO_2. However, there are two carbon assimilation pathways occurring during methanotrophic metabolism, the serine pathway and the RuMP pathway (Figure 22.2). In the serine pathway, two moles of HCOH and one mole of CO_2 are utilized to form a three carbon intermediate of central metabolism, in which all cellular carbon is assimilated at the oxidation level of HCOH. In the RuMP pathway, three moles of HCOH are used to form three carbon intermediate of central metabolism. The RuMP pathway is more efficient in terms of energy consumption than the serine pathway, which has higher ATP requirements; therefore, the molar yield values (g of cell dry weight/mol of substrate utilized) are higher for bacteria utilizing C_1 compounds via RuMP pathway than the ones observed for bacteria assimilating carbon utilizing the serine pathway. Hilger and Humer (2003) suggested equations 22.8 and 22.9 for CH_4 oxidation through serine and RuMP pathways, respectively.

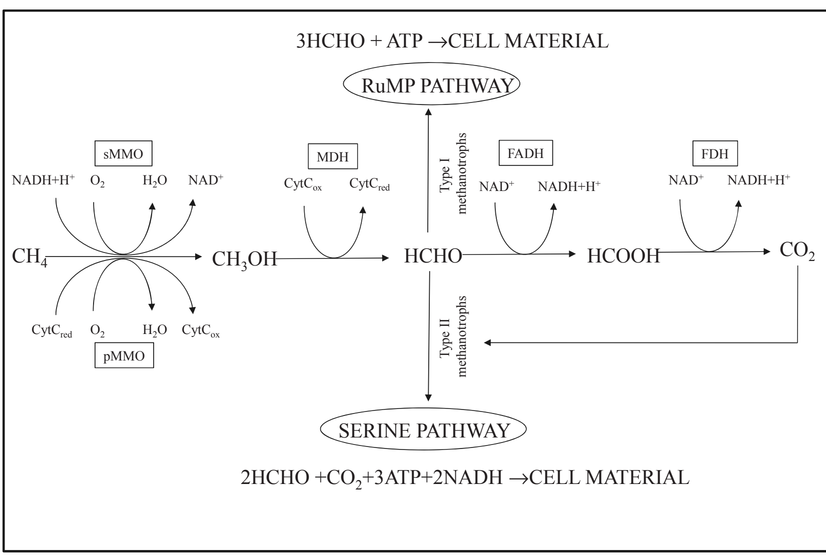

Figure 22.2. Pathways for CH_4 oxidation and carbon assimilation/dissimilation (Adapted from Large 1983)

$$CH_4 + 1.5O_2 + 0.118NH_4^+ \longrightarrow 0.118(C_4H_8O_2N) + 0.529CO_2 + 1.71H_2O + 0.118H^+ \quad \text{(Eq. 22.8)}$$

$$CH_4 + 1.57_2 + 0.102NH_4^+ \longrightarrow 0.102(C_4H_8O_2N) + 0.593CO_2 + 1.75H_2O + 0.102H^+ \quad \text{(Eq. 22.9)}$$

Biological CH_4 oxidation rates in soils can be described by Michaelis-Menten kinetics. Research has shown that there are methanotrophic systems with high CH_4

affinity (low K_m) and low oxidation rates (low V_{max}) which are likely to inhabit natural soils layers located near to the surface with low CH_4/O_2 concentration ratios. There are also methanotrophic systems with low CH_4 affinity (high K_m) and high oxidation rates (high V_{max}). This kind of methanotrophic condition is common in environments with high CH_4/O_2 concentration ratios, which can be found in landfill cover soils (Bender and Conrad 1993).

22.3.2.2 Factors Affecting Methanotrophic Processes

Methanotrophic processes are controlled by a number of factors such as CH_4 and O_2 concentrations, nutrients availability, pH, temperature, and the availability of carbon sources and water. CH_4 and O_2 are key parameters influencing the presence of methanotrophic systems with high or low CH_4 affinity. Methanotrophs are strictly aerobic microorganisms. From laboratory experiments, it has been observed that CH_4 oxidation rates are insensitive to O_2 mixing ratios greater than 1 to 3%, decreasing significantly at lower levels (Bender and Conrad 1993; Czespiel et al. 1995). It has been also indicated that O_2 concentrations ranging from 0.45 to 20% could support maximum CH_4 oxidation rates (Ren et al. 1997; Wilshusen et al. 2004a). Amaral and Knowles (1995) found that Type I methanotrophs are likely to inhabit zones with low CH_4/O_2 ratios, whereas Type II appear to outcompete Type I methanotrophs in zones with high CH_4/O_2 ratios. The ability of methanotrophs with a serine pathway to fix atmospheric nitrogen (N) under inorganic N limiting conditions is given by the nitrogenase activity, which is inhibited at O_2 concentrations higher than 4–6.27% (Graham et al. 1993).

Methanotrophic bacterial strains capable of growth from 0˚C to 72˚C have been identified. The optimum temperature for methanotrophic activity ranges from 25 ˚C to 35˚C; however, it has been suggested that Type I methanotrophs dominate at low temperatures. Methanotropic bacteria have been reported to thrive in a wide pH range of 1 to 10. However, there are reports of methanotrophic bacteria growing at pH values below 1 (Gebert et al. 2003; Dunfield et al. 2007; Scheutz et al. 2009). Water availability is an important factor affecting the growth of microorganisms in natural environments. When an organism grows in a medium with a low moisture content, it must overcome energy to obtain water and utilize it for their metabolism; thus, the rate of metabolic activity decreases with decreasing water availability. As mentioned before, obligated methanotrophs are Gram-negative bacteria. Highest metabolic rates for this kind of bacteria have been reported to occur in a water activity (a_w) range of 0.97 to 0.995 equivalent to a matric pressure (ψ) between -300 and -10 kPa (Bohn and Bohn 1999).

All methanotrophs are able to use ammonia nitrogen (NH_3) as N source; most use nitrite (NO_2^-) and nitrate (NO_3^-). All those with a serine pathway (and some with the RuMP-pathway) have nitrogenase activity and are able to fix atmospheric nitrogen. However, inorganic N might stimulate or inhibit CH_4 oxidation. It has been demonstrated that high NH_3 concentrations tend to inhibit CH_4 oxidation as ammonium (NH_4^+) acts as competitive inhibitor towards MMO enzymes (Large

1983). Nitrate nitrogen (NO_3-N) has proven to be inhibitory through osmotic effects only at high concentrations. This condition is generally found when large populations of ammonia oxidizing bacteria are in place (Bodelier and Laanbroek 2004). For every mole of assimilated carbon, methanotrophic bacteria require 0.25 mole of N. In environments in which the CH_4/N molar ratio is higher than 10 (assuming 40% assimilation of every CH_4 mole consumed), limitation of inorganic N may occur. This situation leads to the reduction of the bacterial growth rate. This condition cannot be avoided by atmospheric N fixation as this process is energetically less favourable than inorganic N consumption (Anthony 1982).

The particle size and distribution of the growing media is an important parameter influencing methanotrophic processes. Small particle sizes provide large specific surface areas but also create resistance to gas flow. Large sizes favour gaseous flow but reduce the number of potential sites for microbial activity. Boeckx et al. (1997) observed that coarse textured soils have higher CH_4 oxidising capacity than fine textured soils, which can even produce CH_4. Wilshusen et al. (2004a) found that homogenous compost mixed on a regular basis could achieve and maintain high CH_4 oxidation efficiencies. Texture and compaction determine the pore size distribution, which in turn, is a factor influencing moisture retention and gas transport (Gebert et al. 2010).

Besides NH_4^+, methanotrophic processes can be inhibited by other substances due to competition with CH_4 for MMO binding sites (reversible) or due to enzyme toxication (irreversible binding). Some of these substances are diflouromethane, dichloromethane, methyl fluoride, acetylene, ethylene, methanethiol, carbon disulfide, hydrochlorofluorocarbons as well as some pesticides like lenacil, oxadixyl, atrazine and dimethenamid (Scheutz et al. 2009).

Biologically stable environments with limited additional carbon sources availability for other heterotrophic microorganisms to grow allow methanotrophic bacteria low competition conditions for available O_2 and nutrients. In contrast, high additional carbon source availability allows the development of heterotrophic organisms capable of outcompete methanotrophic bacteria for available nutrients and O_2. This situation leads to lower methanotrophic bacteria metabolic rates (Chandrakanthi and Hettiaratchi 2005; Hurtado 2009; Hettiarachchi et al. 2011).

22.3.2.3 Biological CH_4 Removal in Methane Biofilters

Biofiltration is a biological air pollution control technology that has been proven to be effective for the odour control and for the removal of volatile organic compounds (VOCs) and other compounds produced by stationary sources (Morgan-Sagastume and Noyola 2006; Maestre et al. 2007; Rodrigues et al. 2010). These processes have been developed considering the benefits obtained from the capacity that some bacteria, fungi and yeast have to degrade pollutants into non-toxic compounds like CO_2 and water. The principles governing biofiltration are similar to those of common biofilm processes; first, the substrate goes through a gas/liquid interface from the pore to the biofilm, which is supported by a solid particle, then the substrate diffuses through the biofilm to a consortium of microorganisms. These microorganisms, in the presence of nutrients, obtain energy from the oxidation of the substrate, and in some specific cases they co-metabolize some compounds via nonspecific enzymes (Warren and Raymond 1997; Devinny et al. 1999; Delhomenie and Heitz 2005).

There is some basic terminology related to the design and operation of biofiltration systems. Surface or volumetric loading and mass loading rates are used to characterize the amount of contaminant potentially treated. Surface loading (Equation 22.10) is defined as the volume of gas per unit area of filter material per unit time. The volumetric loading rate (Equation 22.11) is defined as the volume of gas per unit volume of filter material per unit time (Devinny et al. 1999).

$$\text{Surface loading} = \frac{Q}{A} \qquad \text{(Eq. 22.10)}$$

$$\text{Volumetric loading} = \frac{Q}{V_f} \qquad \text{(Eq. 22.11)}$$

where A is the filter's horizontal area, Q is the flow rate and V_f is the filter bed volume. As defined in Equations 22.12 and 22.13, the mass loading rate is the mass of the contaminant entering the biofilter per unit area or volume of filter material per unit time. The mass loading along the bed will decline as contaminant is removed.

$$\text{Mass loading (surface)} = \frac{Q * C_{in}}{A} \qquad \text{(Eq. 22.12)}$$

$$\text{Mass loading (volumetric)} = \frac{Q * C_{in}}{V_f} \qquad \text{(Eq. 22.13)}$$

where C_{in} is the concentration in the biofilter inlet point. InMBFs, the CH_4 oxidation efficiency (η) is defined by Equation 22.14. This parameter is sensitive to changes in the inlet flow rate of contaminant.

$$\eta(\%) = \frac{(C_{in} * Q_{in}) - (C_{out} * Q_{out})}{C_{in} * Q_{in}} \qquad \text{(Eq. 22.14)}$$

where Q_{in} and Q_{out} are the flow rates in the inlet and in the outlet, respectively. Empty bed residence time (EBRT) is a term also known as empty bed contact time or empty bed retention time (Devinny et al. 1999). This term is defined as the empty bed filter volume divided by the air or gas inlet flow rate (Equation 22.15).

$$\text{EBRT} = \frac{V_f}{Q_{in}} \qquad \text{(Eq. 22.15)}$$

As the filtering medium occupies an important fraction of the biofilter total volume, it is important to consider that EBRT overestimates the actual treatment time. The true residence time (τ) is obtained by considering the filtering medium porosity (ϕ) as defined in Equation 22.16.

$$\tau = \frac{V_f \phi}{Q_{in}} \qquad \text{(Eq. 22.16)}$$

A simple methane biofilter involves the use of a self-contained suitable granular material as the filtering medium diverting CH_4 rich gas using a pipe network with a continuous active or passive inlet flow. As presented in Table 22.2, this technology can accomplish high CH_4 removal rates.

Table 22.2. CH_4 removal rates in biofiltration systems

Source	**Filter material**	**Moisture content (%w/dw)**	**CH_4 inlet ($g\ m^{-2}\ day^{-1}$)**	**CH_4 oxidation rate ($g\ m^{-2}\ day^{-1}$)**
Sly et al. (1993)	Glas tubes	Water trickling system	2249	586
Stein and Hettiaratchi (2001)	Soil	9.4–316	310	9.3–171
Streese and Stegmann (2003)	Compost/peat/wood fibre mix	85.2	1809	341
Wilshusen et al. (2004b)	Compost: leaf	124	NA	400
	Compost: municipal waste	123		270
	Woodchips	123		270
Melse and Van der Werf (2005)	Compost/perlite mix	NA	614	377
Haubrich and Widmman (2006)	Compost	30	592	592
Philopoulos et al. (2009)	Compost	45	134	134
	Compost-Sand-Perlite	18		

NA: not available

Most of the studies reported in Table 22.2 have been conducted using packed columns with the objective of evaluate the long term performance of filters. The results of Stein and Hettiaratchi (2001), Streese and Stegmann (2003), Wilshusen et al. (2004b) as well as Melse and van der Werf (2005) show maximum CH_4 removal followed by a decreasing removal in all cases. This declining trend could be associated with exopolymeric substance production (EPS) and to the methanotrophic biofilm growth and decay process itself. Methanotrophic bacteria are known for their propensity to produce EPS, which is linked to either metabolic wasting mechanisms, or to stress responses to environmental conditions like starvation, temperature, and oxygen and water availability, or both (Costerton 1995). The EPS excretion has been related both to high oxygen concentrations and to the lack of either oxygen or nitrogen. It also has been suggested that the production of EPS is a mechanism to prevent the accumulation of formaldehyde under nitrogen limited conditions (Linton et al. 1986; Chiemchaisri et al. 2001). EPS formation is considered limiting gas diffusion into active methanotrophic biofilms leading to decreasing CH_4 oxidation rates.

In attached growth methanotrophic processes, the microorganisms form biofilms, and CH_4 and oxygen diffuse through the methanotrophic biofilm layer. As microorganisms proliferate and the biofilm thickness increases, oxygen and CH_4 are consumed before they can penetrate the full depth. Bacteria in the deeper layer enter into a decay process and, consequently, lose their ability to cling to the growth media surface. The release of soluble organic carbon and nutrients associated with the decay process and the EPS production could be assumed to be a factor boosting the growth of heterotrophic bacteria. The bacterial growth increases competition for available nutrients and oxygen. This condition and the gas transfer limitations generated by the production of EPS are assumed to contribute to the decrease in CH_4 removal rates.

According to Streese and Stegmann (2003) a methane biofilter may require an area of 2848 m^2 with a volume of 940 m^3 to remove 90% of CH_4 from a LFG stream with a flow rate of 9600 m^3d^{-1} (2.5 v/v CH_4). Gebert et al. (2004) concluded that for a passively vented biofilter having the same CH_4 load would require approximately 1920 m^2 considering 1 m for the filtering bed height. Melse and van der Werf (2005) estimated a volume of 47 m^3 for a filter to treat 39600 g CH_4 d^{-1} with 75% efficiency. Haubrich and Widmann (2006) concluded that a filter with a volume of 230 m^3 and an area of 219 m^2 is enough to remove 96% of the CH_4 from a gas stream equivalent to 144 000 g CH_4 h^{-1}.

The properties of the packing materials are key factors influencing a biofilter performance. The following criteria outline the desirable characteristics (Delhoménie and Heitz 2005):

- Presence and availability of intrinsic nutrients
- High specific surface area for biofilm attachment, sorption capacity and gas/biofilm exchange
- A high porosity to maintain a homogeneous distribution of gases and high retention times
- Structural integrity and low bulk density to avoid medium compaction and to reduce pressure drop
- Good moisture retention to avoid medium desiccation and to maintain microbiological activity. However it is important to consider that excess water will fill biofilter void spaces and will slow the substrate, O_2 and CO_2 transfer through the biofilm.

A number of different filtering media like peat, soil, compost, activated carbon, perlite and synthetic materials have been used either in laboratory scale experiments or in the field (Devinny et al. 1999; Delhoménie and Heitz 2005). A summary of important properties for some common filtering materials is included in Devinny et al. (1999, p. 46). Since compost exhibits most of the characteristics required for a filtering medium, it has been used in a number of research and pilot studies (Wilshusen et al. 2004b; Philopoulos et al. 2009).

Wilshusen et al. (2004b) investigated the CH_4 oxidation potential of four different types of compost, i.e., municipal leaf compost (co-composted with manure from a local zoo), commercial garden store compost, un-screened composted wood chips and unscreened composted solid waste. The leaf compost exhibited the highest CH_4 oxidation rates while the commercial compost and the compost derived from waste showed low oxidation potential.

Although compost shows most of the characteristics required for a filter medium, it is a biologically unstable material that tends to break down and compact over time. The changes to diffusion properties of the filter bed due to compaction can lead to the inhibition of biological oxidation of CH_4 and its related co-metabolic processes. To prevent oxygen and substrate transfer limitations due compaction process and to enhance the filtering medium permeability and water retention characteristics, some research has been undertaken employing bulking materials like perlite, woodchips and vermiculite in order to provide compost better structural stability characteristics (Delhoménie and Heitz 2005; Philopoulos et al. 2009).

22.3.2.4 Mass Transfer Processes in Methane Biocaps and Methane Biofilters

Mass transfer in MBFs results from several processes: diffusion, dispersion, advection, biological reactions and sorption processes. Several empirical and process-based models have been developed for simulating CH_4 biological oxidation in porous media.

Czespiel et al. (1996) developed an empirical CH_4 oxidation model to determine the average CH_4 oxidation during one year in landfill cover soils. The input data for this model were surface CH_4 flux, the underlying soil-gas CH_4 mixing ratio, and soil physical parameters such as temperature, moisture content, and bulk density. The oxidation rates were predicted by estimating V_{max} at different depths considering CH_4 mixing ratio values at 7.5 cm-depth, and the temperature and moisture of the soil. Hilger et al. (1999) proposed a one-dimension steady-state model that combined gas diffusion and methanotrophic activity through the filer medium matrix. This model was also applied to predict the process performance considering a thick EPS layer coating the base biofilm, and poor gas transfer conditions. The transport mechanism of each gas in the soil gas mixture was modeled by using the Stefan-Maxwell equation. A steady-state model for biological oxidation and migration of CH_4 in soils was proposed by Stein et al. (2001). This model considers that the transport of gases in soil is mainly governed by diffusion and, to a lesser extent, advection. CH_4 removal was considered to be described by double Monod reaction kinetics. The relative diffusion coefficient determination involved the use of the Millington-Quirk model, as described by Jin and Jury (1996). Perera et al. (2002)

formulated an advective-dispersive-reactive mathematical model for the estimation of source strength of LFG. This model considers LFG flow and CH_4 removal through layered soils. The relative diffusion coefficient was obtained using the empirical equation proposed by Troeh et al. (1982). The biological oxidation rate of CH_4 is modeled considering double Monod kinetics, and the stoichiometric ratios considered in this model for O_2 consumption and CO_2 production were 1.7 for O_2:CH_4, and 0.7 for CO_2:CH_4.

Perera et al. (2004) developed a pseudo 3-D model for the assessment of spatial variability of methane emissions from landfills. The approach involved the use of Geographic Information System (GIS), a geostatistical technique, and a 1-D numerical model to determine the source strength of LFG. This was done by complementing the numerical model developed previously by Perera et al. (2002) with a 2-D geostatistical technique to describe the spatial distribution of LFG. The GIS was used to store and analyze spatially varied data, generate the input data for the 1-D model, execute it and, store its numerical outputs in a database. With the information stored in the database, the source strength was determined based on spatial variations.

Hettiarachchi et al. (2007) presented a comprehensive 3-D mathematical model capable of predicting the CH_4 oxidation capacity of MBFs based on gas and moisture transport, and heat transfer. The gas transfer component involved an advective-dispersive-reactive model. This model considered double Monod kinetics and two correction factors to account for the effects of temperature and moisture content. The heat transfer process was modeled by considering the equation for the conservation of energy. The moisture transport through the filter medium was described with the Richard´s equation for flow of water in the unsaturated zone. The modified Penman equation proposed by Wilson (1990) was used to calculate the evaporative flux from the surface of the biofilter. A water balance was proposed to estimate the water infiltration rate.

22.4 Conclusions

Although all aspects of waste management, including collection, processing, treatment and disposal, produce greenhouse gases (GHGs), the source of primary concern is landfill disposal. Land disposal of solid wastes is a key source of anthropogenic methane emissions in both developed and developing countries. Although the other problems with waste disposal practice, namely aesthetic issues and ground/surface water contamination with leachate, have received considerable attention from practitioners and regulators, emission of GHGs has been largely ignored until recently. The current attempts at minimizing waste related GHG emissions concentrate on several fronts; the application of waste minimization methods (such as 3Rs) to divert waste from landfills, waste treatment using biological methods (composting to recover a soil conditioner and anaerobic digestion to recover biogas) and physical methods (incineration and gasification), the application of advanced landfilling methods to recover biogas (anaerobic bioreactor) and resources and space (aerobic landfill bioreactor and mining), the application of methanotrophic processes to naturally attenuate and assimilate methane escaping from closed landfills. The application of methanotrophic processes such as landfill biocaps and methane biofilters as technologies to control GHG emissions is relatively new. The extensive research undertaken in recent years by various research groups has provided sufficient information to apply these technologies widely. Because of their relatively cost effective and simplistic nature, these technologies can be applied in both developed and developing country situations.

22.5 References

Adams, B., L., Besnard, F., Bogner, J., and Hilger, H. (2011). "Bio-tarp alternative to daily cover prototypes for methane oxidation atop open landfill cells." Waste Management, 31, 1065–1073.

Amaral, J., A., and Knowles, R. (1995). "Growth of methanotrophs in methane and oxygen counter gradients." FEMS Microbiology Letters 126, 215–220.

Anthony, C. (1982). The Biochemistry of Methylotrophs. Academic Press, USA.

Atkinson, R. (2000). "Atmospheric chemistry of VOCs and NOx." Atmospheric Environment, 34(12–14), 2063–2101.

Banar, M., Cokaygil, Z., and Ozkan, A. (2009). "Life cycle assessment of solid waste management options for Eskisehir, Turkey." Waste Management, 29, 54–62.

Bender M., and Conrad R. (1993). "Kinetics of methane oxidation in oxic soils." Chemosphere, 26, 687–696.

Bodelier, P. L. E., and Laanbroek, H. J. (2004). "Nitrogen as a regulatory factor of methane oxidation in soils and sediments." FEMS Microbiology, 47(3), 265–277.

Bodelier, P. L. E., Gillisen, M., H., Hordijk, K., Damste, J., Rijpstra, W., Geenevasen, J., and Dunfield, P. (2009). "A reanalysis of phospholipid fatty acids as ecological biomarkers for methanotrophic bacteria." International Society for Microbiology Ecology Journal, 3, 606–617.

Boeckx, P., and Van Cleemput, O. (1996). "Methane oxidation in a neutral landfill cover soil: Influence of moisture content, temperature, and nitrogen-turnover." Journal of Environmental Quality, 25 (1), 178–183.

Boeckx, P., van Cleemput, O., and Villaralvo, I. (1997). "Methane oxidation in soils with different textures and land use." Nutrient Cycling in Agroecosystems, 49 (1–3), 91–95.

Bogner, J. E. (1992). "Anaerobic burial of refuse in landfills: Increased atmospheric methane and implications for increased carbon storage." Ecologic Bulletins, 42, 98–108

Bogner, J. E., Spokas, K. A., and Burton, A. E. (1997). "Kinetics of methane oxidation in a landfill cover soil: Temporal variations, a whole-landfill oxidation experiment, and modeling of net CH4 emissions." Environmental Science and Technology, 31(9), 2504–2514.

Bohn, H. L., and Bohn, K. H. (1999). "Moisture in biofilters." Environmental Progress, 18(3), 156–161.

Bull, I., D., Parekh, N., R., Hall, G., H., Ineson, P., and Evershed, R., P. (2000). "Detection and classification of atmospheric methane oxidizing bacteria in soil." Nature, 405, 175–178.

Burnley, S. (2001). "The impact of the European Landfill Directive on waste management in the United Kingdom." Resources, Conservation and Recycling, 32, 349–358.

Chandrakanthi, M., and Hettiaratchi, J. P. A. (2005). "Performance of field-scale methanotrophic biofilters (mbfs) used to control point-source methane emissions: A numerical modeling approach." Cossu, R., and Stegmann, R, editors. SARDINIA 2005: Proceedings of the 10th International Waste Management and Landfill Symposium; 2005 Oct 3–7; Cagliari, Italy. Italy: Environmental Sanitary Engineering Centre, pp. 343–344.

Chen, T., T., and Othmer, D., F. (1962). "New generalized equation for gas diffusion coefficient." Journal of Chemical Engineering Data, 7(1), 37–41.

Cherubini, F., Bargigli, S., and Ulgiati, S. (2009). "Life cycle assessment (LCA) of waste management strategies: Landfilling, sorting plant and incineration." Energy, 34, 2116 – 2123.

Chiemchaisri, W., Wu, J., S., and Visvanathan, C. (2001). "Methanotrophic production of extracellular polysaccharide in landfill cover soils." Water Science and Technology, 43(6), 151–158.

Costerton, J., W., Lewandowski, Z., Caldwell, D., E., Korber, D., and Lappin-Scott, H., M. (1995). "Microbial biofilms." Annual Review of Microbiology, 49, 711–745.

Cullis, C., F., and Hirschler, M., M. (1989). "Man's emissions of carbon monoxide and hydrocarbons into the atmosphere." Atmospheric Environment, 23(6), 1195–1203.

Czespiel, P., M., Crill, P., M., and Harriss, R., C. (1995). "Environmental factors influencing the variability of methane oxidation in temperate zone soils." Journal of Geophysical Research, 100, 9359–9364.

Czespiel, P., M., Mosher, B., Crill., P., M.,, and Harriss, R., C. (1996). "Quantifying the effect of oxidation on landfill methane emissions." Journal of Geophysical Research, 101(11), 721–729.

Delhomenie, M. C., Bibeau, L., and Heitz, M. (2002). "A study of the impact of particle size and adsorption phenomena in a compost-based biological filter." Chemical Engineering Science, 57(24), 4999–5010.

Delhomenie, M. C., and Heitz, M. (2005). "Biofiltration of air: A review." Critical Reviews in Biotechnology, 25, 53–72.

Devinny, J., S., Deshusses, M., A., and Webster, T., S. (1999). Biofiltration for Air Pollutants. Lewis Publishers, USA.

Dunfield, P., Yuryev, A., Senin, P., Smirnova, A., Stott, M., Hou, S., Ly, B., Saw, J., Ren, Y., Wang, J., Mountain, B., Crowe, M., Weatherby, T., Bodelier, P., Liesack, W., Feng, L., Wang, L., and Alam, M. (2007). "Methane oxidation by an extremely acidophilic bacterium of the phylum Verrucomicrobia." Nature, 450, 879–883.

Dunfield, P. (2009). “Methanotrophy in extreme environments.” In: Encyclopedia of Life Sciences (ELS). John Wiley & Sons.
Elagroudy, S. A., Warith, M.A., and Hettiaratchi, J. P. A. (2009). “Biogas Recovery from Landfill.” In Energy Recovery.” Editors: E. DuBois., and A. M. Nova, Publishers ISBN: 978-1-60741-065-2, pp. 1–67.
Emery, A., Davies, A., Griffiths, A., and Williams, K. (2007). “Environmental and economic modelling: A case study of municipal solid waste management scenarios in Wales.” Resources, Conservation and Recycling, 49, 244–263.
Environmental Protection Agency (US-EPA), Air Pollution Prevention and Control Division , 2005. First-Order Kinetic Gas Generation Model Parameters for Wet Landfills. EPA-600/R-05/072. USA.
Gebert, J., Groengroeft, A., and Miehlich, G. (2003). “Kinetics of microbial landfill methane oxidation in biofilters.” Waste Management, 23, 609–619.
Gebert, J., Groengroeft, A., Schloter, M., and Gattinger, A. (2004). “Community structure in a methanotroph biofilter as revealed by phospholipid fatty acid analysis.” FEMS Microbiology Letters, 240(1), 61–68.
Gebert, J., Groengroeft, A., and Pfeiffer, E. (2010). “Relevance of soil physical properties for the microbial oxidation of methane in landfill covers.” Soil Biology and Biochemistry, Article in press.
Graham, D., W., Jayesh, A., Ch., Hanson, R., S., and Arnold, R., G. (1993). “Factors affecting competition between type I and type II methanotrophs in two-organism, continuous-flow reactors.” Microbial Ecology, 25(1), 1–17.
Gujer, W., and Zehnder, J., B. (1983). “Conversion processes in anaerobic digestion.” Water Science & Technology, 15(8–9), 127–167.
Hanson, R., and Hanson, T. (1996). “Methanotrohic bacteria.” Microbiological Reviews, 60(2), 439–471.
Haubrichs, R., and Widmann, R. (2006). “Evaluation of aerated biofilter systems for microbial methane oxidation of poor landfill gas.” Waste Management, 26, 408–416.
Hettiarachchi, V. C., Hettiaratchi, J. P. A., and Mehrotra, (2007). “Comprehensive one-dimensional mathematical model for heat, gas, and moisture transport in methane biofilters.” Practice Periodical of Hazardous, Toxic, and Radioactive Waste Management, 11(4), 225–233.
Hettiarachchi, V. C., Hettiaratchi, J. P. A., Mehrotra, A. K., and Kumar, S. (2011). “Field-scale operation of methane biofiltration systems to mitigate point source methane emissions.” Environmental Pollution, 159(6), 1715–1720.
Hilger, H. A., Liehr, S. K., and Barlaz, M., A. (1999). “Exopolysaccharide control of methane oxidation in landfill cover soil.” Journal of Environmental Engineering, 125, 1113–1123.
Hilger, H. A., Cranford D., F., and Barlaz, M., A. (2000). “Methane oxidation and microbial exopolymer production in landfill cover soil.” Soil Biology and Biochemistry, 32, 457–467.
Hilger, H., A., and Humer, M. (2003). “Biotic landfill cover treatments for mitigating methane emissions.” Environmental Monitoring and Assessment, 84(1–2), 71–84.

Huber-Humer, M., Gebert, J., and Hilger, H. (2008). "Biotic systems to mitigate landfill methane emissions." Waste Management & Reseach, 26(1), 33–46.

Huber-Humer, M., Röder, S., and Lechner, P. (2009). "Approaches to assess biocover performance on landfills." Waste Management, 29(7), 2092–2104.

Humer M., and Lechner P. (2001). "Microbial oxidation for the reduction of landfill gas emissions." Journal of Solid Waste Technology and Management, 27(3&4), 146–151.

Hurtado, O. (2009). Thin Biocovers for Methane Emission Mitigation. Ph.D. dissertation, Department of Civil Engineering, University of Calgary, Calgary, Alberta, Canada.

IPCC (2007). Climate Change (2007). The Physical Science Basis. Solomon, S., Qin, D., Manning, M., Chen, Z., Marquis, M., Averyt, K. B., Tignor, M., and Miller, H. L., editors. Contribution of Working Group I to the 4th Assessment Report of the IPCC. UK and USA. IPCC.

Isaaks, E. H., and Srivastava, R. M. (1989). An Introduction to Applied Geostatistics. Oxford University Press, New York. USA.

Jin, Y., and Jury, W. A. (1996). "Characterizing the dependency of gas diffusion coefficient on soil properties." Journal of The American Soil Science Society, 60, 66–71.

Khanal, S. K. (2008). Anaerobic biotechnology for bioenergy production. Wiley-Blackwell, USA.

Large, P. J. (1983). Methylotrophy and Methanogenesis. Aspects of Microbiology 8. American Society for Microbiology. Van Nostrand Reinhold, Wokingham, UK.

Linton, J. D., Watts, P. D., Austin, R. M.,. Haugh, D. E., and Niekus, H. G. D. (1986). "The energetics and kinetics of extracellular polysaccharide production from methanol by micro-organisms possessing different pathwas of C1 assimilation." Journal of General Microbiology, 132, 779–788.

Livingston, G. P., and Hutchinson, G. L. (1995). "Enclosure-based measurement of trace gas exchange: applications and sources of error." In Biogenic trace gases: measuring emissions from soil and water. Edited by P. A. Matson, and R. C. Harris, pp. 14–51.

Maestre, J. P., Gamisans, X., Gabriel, D., and Lafuente, J. (2007). "Fungal biofilters for toluene biofiltration: Evalualtion of the performance with four packing materials under different operating conditions." Chemosphere, 67, 684–692.

Marrero, T. R., and Mason, E. A. (1972). "Gas diffusion coefficients." Journal of Physical and Chemical Reference Data, 1, 3–118.

Matthias, A. D., Yarger, D. N., and Weinbeck, R. S. (1978). "A numerical evaluation of chamber methods for determining gas fluxes." Geophysical Research Letters, 5(9), 765–768.

McBean, E. A. (2007). "Performance results from the Tucumán solid waste bioreactor." Waste management, 27(12), 1783–1791.

Melse, R., W., and van der Werf, A. (2005). "Biofiltration for mitigation of methane emission from animal husbandry." Environmental Science and Technology, 39, 5460–5468.

Moldrup, P., Olesen, T., Gamst, J., Schønning, P., Yamaguchi, T., and Rolston, D. E. (2000a). "Predicting the gas diffusion coefficient in repacked soil: water-induced linear reduction model." Soil Science Society of America Journal, 64, 1588–1594.

Moldrup, P., Olesen, T., Schønning, P., Yamaguchi, T., and Rolston, D. E. (2000b). "Predicting the gas diffusion coefficient in undisturbed soil from soil water characteristics." Soil Science Society of America Journal, 64, 94–100.

Morgan-Sagastume, J. M., and Noyola R. A. (2006). "Hydrogen sulfide removal by compost biofiltration: Effect of mixing the filter media on operational factors." Bioresource Technology, 97(13), 1546–1553.

Murrel, J., C., McDonald, I. R., and Gilbert, B. (2000). "Regulation of expression of methane monooxygenases." Trends in Microbiology, 8(5), 221–225.

Nikiema, J., Brzenzinski, R., and Heitz, M. (2007). "Elimination of methane generated from landfills by biofiltration: A review." Rev Environ Sci Biotechnol, 6, 61–284.

Nozhevnikova, A., Glagolev, M., Nekrasova, J., Einola, J., and Rintala, J. (2003). "The analysis of methods for measurement of methane oxidation in landfills." *Water Science and Technology*, 48(4), 45–52.Pacey, J. P., Ramin Yazdani, D. Reinhart, R. Morck, D. Augenstein, (1999) "The Bioreactor Landfill: An Innovation in Solid Waste Management."SWANA, Silver Springs, Maryland.

Perera, L. A. K., Achari, G., and Hettiaratchi, J. P. A. (2002). "Determination of source strength of landfill gas: A numerical approach." *Journal of Environmental Engineering*, 128, 461–471.

Perera, L. A. K., Achari, G., and Hettiaratchi, J. P. A. (2004). "An assessment of the spatial variability of greenhouse gas emissions from landfills: A GIS based statistical-numerical approach." *Journal of Environmental Informatics*, 4 (1), 11–27.

Philopoulos, A., Ruck, J., McCartney, D., and Felske, C. (2009). "A laboratory comparison of compost and sand-compost-perlite as methane-oxidizing biofilter media." *Waste Management & Research*, 27, 138–146.

Pohland, F. G. (1992). "Anaerobic treatment: Fundamental concepts, applications and new horizons." In: *Design of Anaerobic Processes for the Treatment of Industrial and Municipal Wastes*, Technomic Publ. Co., Inc., Lancaster, PA, 1–40.

Reinhart, D. R., and Townsend, T. G. (1998). *Landfill bioreactor design and operation. Lewis Publisher*, New York.

Ren, T., Amaral, A., J., and Knowles, R. (1997). "The response of methane consumption by pure cultures of methanotrophic bacteria to oxygen." *Canadian Journal of Microbiology*, 43(10), 925–928.

Rodrigues, J. L., Takano, L., Rissato, M. H., Foresti, E., and Silva E. L. (2010). "Performance evaluation of packing materials in the removal of hydrogen sulphide in gas-phase biofilters: Polyurethane foam, sugarcane bagasse and coconut fibre." *Chemical Engineering Journal*, 158, 441–450.

Scheutz, Ch., Kjeldsen P., Bogner J., E., De Visscher A., Gebert J., Hilger H., A., Huber-Humer, M., and Spokas, K. (2009). "Microbial methane oxidation processes and technologies for mitigation of landfill gas emissions." *Waste Management & Research*, 27, 409–455.

Semrau, J., DiSpirito, A., and Yoon, S. (2010). "Methanotrophs and copper." *FEMS Microbiological Review*, 34, 496–531.

Sly, L. I., Bryant, L. Y., Cox, J. M., and Anderson, J. M. (1993). "Development of a biofilter for the removal of methane from coal mine ventilation atmospheres." *Journal of Applied Microbiology and Biotechnology*, 39, 400–404.

Spokas, K., A., and Bogner, J., E. (2011). "Limits and dynamics of methane oxidation in landfill cover soils." *Waste Management*, 31, 823–832.

Stein, V., B., and Hettiaratchi, J., P., A. (2001). "Methane oxidation in three Alberta soils: Influences of soil, parameters and methane oxidation." *Environmental Technology*, 22, 101–111.

Stein, V., B., Hettiaratchi, J., P., A., and Achari, G. (2001). "Numerical model for biological oxidation and migration of methane in soils." *Practice Periodical of Hazardous, Toxic, and Radioactive Waste Management*, 5(4), 225–234.

Streese J., and Stegman, R. (2003). "Microbial oxidation of CH_4 from old landfills in biofilters." *Waste Management*, 23, 573–580.

Tchobanoglous, G., Theisen, H., and Vigil, S. A. (1993). *Integrated solid waste management engineering*. McGraw-Hill, USA.

Tchobanoglous G., and Kreith, F. (2002). *Handbook of Solid Waste Management.* McGraw-Hill, USA.

Thorstenson, D. C., and Pollock, D. W. (1989). "Gas transport in unsaturated zones: Multicomponent systems and adequacy of Fick´s laws." *Water Resources Research*, 25, 477–507.

Troeh, F. R., Jabro, J. D., and Kirkham, D. (1982). "Gaseous diffusion equations for porous materials." *Geoderma*, 27, 239–253.

Warith, M. A., Smolkin, P. A. and Caldwel, J. G. (2001). "Effect of leachate recirculation on enhancement of biological degradation of solid waste: Case study." *Practice periodical of hazardous, toxic, and radioactive waste management*, 5(1), 40–46.

Warren, J., S., and Raymond, C. L. (1997). "Biofiltration: Fundamentals, design and operations principles, and applications." *Journal of Environmental Engineering*, 123, 538–546.

Wilshusen, J. H. (2002). *An Investigation of the Role of Oxygen and Nitrogen in Methane Oxidation and the Formation of Exopolymeric Substances (EPS) in Biofilters*. M.S. thesis, Department of Civil Engineering, University of Calgary, Calgary, Alberta, Canada.

Wilshusen, J. H., Hettiaratchi J. P. A., De Visscher, A., and Saint-Fort, R. (2004a). "Methane oxidation and formation of EPS in compost: Effect of oxygen concentration." *Environmental Pollution*, 129(2), 305–314.

Wilshusen, J. H., Hettiaratchi, J. P. A., and Stein, V. (2004b). "Long-term behavior of passively aerated compost methanotrophic biofilter columns." *Waste Management*, 277, 643–563.

Wilson, G. W. (1990). *Soil evaporation flux for geotechnical engineering problems*. Ph.D. dissertation, University of Saskatchewan, Saskatchewan, Sask., Canada.

CHAPTER 23

Recycling for Mitigating Climate Change

A. Chandran, S. K. Brar, M. Verma, R. D. Tyagi, and R.Y. Surampalli

23.1 Introduction

As one of the major global problems, climate change is a serious threat for the Earth and requires immediate real solutions for the further existence of the human kind. Climate change is a change in the statistical distribution of weather over periods of time which ranges from decades to millions of years. Some use the term "climate change" to refer to "all forms of climatic inconstancy, regardless of their statistical nature (or physical causes)" (Mitchell et al. 1966). Later, the Intergovernmental Panel on Climate Change (IPCC) defines climate change broadly as "any change in climate over time whether due to natural variability or as a result of human activity." United Nation's Framework Convention on Climate Change (UNFCCC) defines climate change as "a change of climate that is attributed directly or indirectly to human activity that alters the composition of the global atmosphere, and that is in addition to natural climate variability over comparable time periods" (Bärring 1993; Pielke 2004). Generally, global climate change is attributed directly or indirectly to human activities that alter the global atmospheric composition, added to natural climate variability observed in comparable periods of time.

Climate change is a long-term shift in the climate of a specific location, region or planet, and this shift is measured by changes in features associated with weather, such as temperature, wind patterns and precipitation. Climate change occurs when the climate of a specific area or planet is altered between two different periods of time. It has been reported by IPCC that the temperature of the earth's surface has risen approximately 0.6°C over the last century.

Mitigating climate change requires action on many fronts, in all sectors of the economy. We must reduce the generation of greenhouse gases that contribute to climate change. These reductions must come from changes in our living style and systems that extract, transport and manufacture materials and products for export. Among the various ways available to help achieve these reductions is the improvement of our waste management systems, particularly the enhancement of recovering materials for manufacturing through recycling collection and processing. Significant reductions in energy consumption are realized when goods are manufactured from secondary, versus primary materials. Thus, recycling post-consumer goods is a necessary component of our legislative framework being designed to address climate change.

The present chapter starts with an introduction to the causes and impact of climate changes and its mitigation strategies mainly by implementing waste management systems; it then presents a detailed discussion on how to use recycling as a mitigation strategy to combat climate change.

23.2. Causes and Impact of Climatic Changes and Its Mitigation Strategies

Climatic changes have been speeded up due to uncontrolled human activities. The causes of climatic changes should be identified first for the better understanding of climate change. The causes of climate change can be divided into two categories, mainly human and natural causes. The earth climate is influenced and changed through many natural causes like ocean currents, volcanic eruptions, earth's orbital changes, solar variations, etc. (IPCC 2007).

Anthropogenic factors are human activities that change the environment. The effect of human influence on the climate is direct and unambiguous in some cases and in other instances it is less clear. The increase in global average temperatures over the past several decades mainly is due to the anthropogenic activities. The anthropogenic factors affecting the climate are mainly variation in the CO_2 level and other greenhouse gases (GHGs), land use, ozone depletion, agriculture, deforestation, etc. The annual emissions of GHGs by different sectors of anthropogenic activities are shown in Figure 23.1 (IPCC 2007).

Global warming and other climatic changes affect many different facets of life on earth. Climatic change has impact across the sectors. The impact of climatic change on the developing and less developed countries are excessively high compared to developed countries due to many reasons, such as geographical location, high dependence of people on natural resources that are highly sensitivity to climate change, low adaptive capacity due to fewer amounts of resources available to them. The effects of climate change may be physical, ecological, social or economical. Major impact of climate changes include sea level rise, decreased snow cover in the northern hemisphere, effects on humans, animals, and agriculture (IPCC 2007).

Climate change mitigation can be defined as an action to decrease the intensity of radiative force in order to reduce the potential effects of global warming (IPCC, 2007). Mitigation is distinguished from adaptation to global warming, which involves acting to tolerate the effects of global warming. Most often, climate change mitigation scenarios involve reductions in the concentrations of GHGs, either by reducing their sources (Molina et al. 2009) or by increasing their sinks. Climate mitigation is any action taken to permanently eliminate or reduce the long-term risk and hazards of climate change to human life, property. The IPCC defines mitigation as: "An anthropogenic intervention to reduce the sources or enhance the sinks of greenhouse gases."

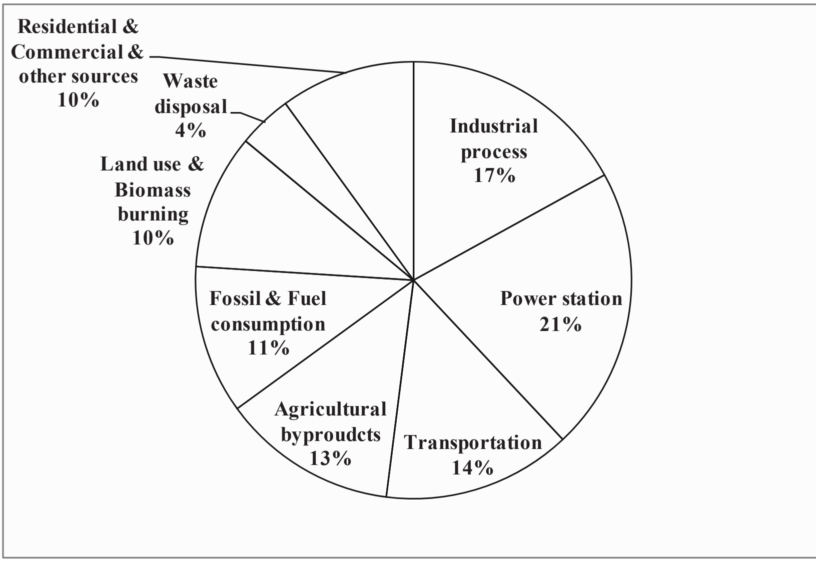

Figure 23.1. Annual GHG emissions by different sectors in 2004

Adaptation and mitigation are the two important factors in climate change. The IPCC defined adaptation as adjustment in natural or human systems in response to actual or expected climatic stimuli or their effects, which moderate harm or exploits beneficial opportunities. Mitchell and Tanner (2007) defined adaptation as an understanding of how individuals, groups and natural systems can prepare for and respond to changes in climate or their environment. Mitigation tackles the causes of climate change whereas adaptation tackles the effects of the phenomenon. The potential to adjust in order to minimize negative impact and maximize any benefits from changes in climate is known as adaptive capacity. Various types of adaptation can be distinguished, including anticipatory and reactive adaptation, private and public adaptation, and autonomous and planned adaptation. A successful adaptation can reduce vulnerability by building on and strengthening existing coping strategies. Adaptation is an active adjustment in response to new stimuli. The idea that less mitigation means greater climatic change and consequently requiring more adaptation is the basis for the urgency surrounding reductions in GHGs. Climate mitigation and adaptation should be viewed as a combined set of actions in an overall strategy to reduce GHG emissions.

23.2.1 Mitigation Options

Most mitigation options can be described broadly into two categories: technical and policy. These options have varying costs, economic impacts, and implementation requirements. Mitigations options generally fall into the short- and long-term options and are given below.

(1) Short-term:
- Improved energy efficiency;
- Utilization of cleaner energy resources and technologies;
- Improved forest management;
- Phasing out of CFCs under Montreal Protocol; and
- Improved livestock waste management, altered use and formulation of fertilizers, and other changes to agricultural land use, while maintaining food security.

(2) Long term:
- Accelerated and coordinated research programs;
- Development of new technologies;
- Review planning in relevant fields;
- Encourage beneficial behavioural and structural changes; and
- Expand global observation and monitoring.

The short-term options have development implications and can assist countries to achieve stabilization of GHG emissions without major sacrifices. In adapting these options, some countries have adopted the following measures:

(1) In the energy sector:
- Shift to low carbon fuels - greater use of renewable energy sources, use of gas fired combined cycles, more use of natural gas as opposed to coal, greater use of biomass;
- Efficiency programs on energy supply and use;
- Reduction of leaks from gas plants; and
- Controlling transport related emissions.

(2) In the land use sector:
- Reduction of emissions by change in agricultural systems;
- Maintaining and expanding sinks by protecting forest and practicing agro-forestry and other plantation exercises; and
- Changing cattle feed to reduce CH_4 emitted and utilizing CH_4 produced.

23.2.2 Mitigation Strategies

Climate change involves complex interactions between climatic, environmental, economic, political, institutional, social, and technological processes. It cannot be addressed or comprehended in isolation of broader societal goals (such as equity or sustainable development), or other existing or probable future sources of stress. In the United Nations Framework Convention on Climate Change (UNFCCC), three conditions are made explicit when working towards the goal of GHG stabilization in the atmosphere:

(1) That it should take place within a time-frame sufficient to allow ecosystems to adapt naturally to climate change;
(2) That food production is not threatened; and
(3) That economic development should proceed in a sustainable manner.

23.2.3 Mitigation of Post-consumer Emissions by Waste Management

Post-consumer waste is a small contributor to global GHG emissions (< 5%), but the waste sector can positively contribute to climate mitigation to 2030 at low cost and promote sustainable development. Proper waste management is one of the important approaches for mitigation of post consumer emissions. The mitigation of GHG emissions from waste relies on multiple technologies whose application depends on local, regional and national drivers for both waste management and GHG mitigation. Existing waste management practices can provide effective mitigation of GHG emissions from this sector: a wide range of mature, environmentally effective technologies are commercially available to mitigate emissions and provide co-benefits for improved public health and safety, soil protection and pollution prevention, and local energy supply. These technologies include a) land filling with landfill gas recovery (to reduce CH_4 emissions), b) post-consumer recycling, c) composting of selected waste fractions (to avoid GHG generation), and d) processes that reduce GHG generation compared to land filling, e.g., i) thermal processes including incineration and industrial co-combustion, ii) mechanical biological treatment with land filling of residuals, and iii) anaerobic digestion.

A flow diagram of an integrated solid waste management system is represented in Figure 23.2. The waste management processes employed in most of the countries so far are given below:
(1) **Landfill and Open-dumping Sites**: Landfill and dumping in open sites are common practices for disposal of wastes. Generally, wastes are dumped in swamp lands and in low lying areas. Approximately 60–80% of the wastes are disposed in this manner in many countries (Ngoc and Schnitzer 2009). This method has become one of the major sources of environmental pollution as the capacity of landfill is surpassed due to lack of environmental planning as well as due to lack of space following increased pressure on land.
(2) **Incineration**: Incineration is another method of waste treatment in most of the countries. The operating efficiency depends on the characteristics and composition of the waste. These methods need high financial start up and operating capital requirements.
(3) **Composting**: Composting is a biological treatment in which microorganisms decompose and stabilize organic material. Composting is a low-technology approach for waste reduction. Composting of organic waste leads into highly nutritive organic manure. However, this method has limitation due to its high operational and maintenance costs and low cost of organic manure compared to the commercial fertilizers.
(4) **Recycling or Recovery**: Recycling of the solid wastes has been carried out in many developed countries. Approximately 44% of solid wastes are recycled

in the developed countries, ~12% in the developing countries, and 8–11% in other low income countries (Ngoc and Schnitzer 2009). Wastes used for recycling are mainly composed of plastic, paper, glass, rubber, ferrous used for the further production of new products. Waste minimization and recycling provide important indirect climate mitigation to 2030 benefits through the conservation of energy and materials.

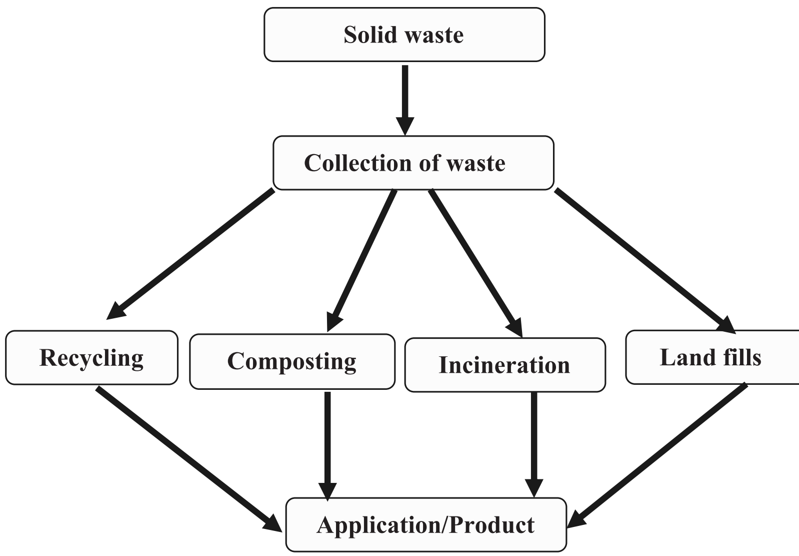

Figure 23.2. Flow diagram of an integrated solid waste management system

Waste generation is closely linked to population, urbanization and affluence. Waste-generation rates can be correlated to gross domestic product (GDP) per capita, energy consumption per capita, and private final consumption per capita (Bogner and Matthews 2003). In developed countries seeking to reduce waste generation, the current goal is to decouple waste generation from economic driving forces, such as GDP (EEA 2005). In most developed and developing countries with increasing population, prosperity and urbanization, it remains a major challenge for municipalities to collect, recycle, treat and dispose of increasing quantities of solid waste and wastewater.

Most technologies for waste management are mature and have been successfully implemented for decades in many countries. Nevertheless, there is significant potential for accelerating both the direct reduction of GHG emissions from waste as well as extended implications for indirect reductions within other sectors. Life-cycle assessment (LCA) can be an important tool for consideration of both the direct and indirect impacts of waste management technologies and policies (Thorneloe et al. 2005; WRAP 2006). Landfill CH_4 recovery and optimized wastewater treatment can directly reduce GHG emissions. GHG generation can be largely avoided through controlled aerobic composting and thermal processes, such as incineration for waste-to-energy. Moreover, waste prevention, minimization, material recovery, recycling and re-use represent a growing potential for indirect reduction of GHG emissions through decreased waste generation, lower raw material consumption, reduced energy demand and fossil fuel avoidance. Recent studies (Smith et al. 2001; WRAP 2006) have begun to comprehensively quantify the significant benefits of recycling for indirect reductions of GHG emissions from the waste sector. Current estimates indicate that global post-consumer waste generation totals approximately 900–1250 Mt/year (Bogner and Matthews 2003). Per capita solid waste generation rates range from < 0.1 t/capita-year in low-income countries to > 0.8 t/capita-year in high-income industrialized countries (Berneche-Perez et al. 2001). The carbon flows through major waste management systems are shown in Figure 23.3. The percentages of waste recycled, composted, incinerated or land filled can differ greatly among municipalities as a result of local economics, national policies, regulatory restrictions, public perceptions and infrastructure requirements.

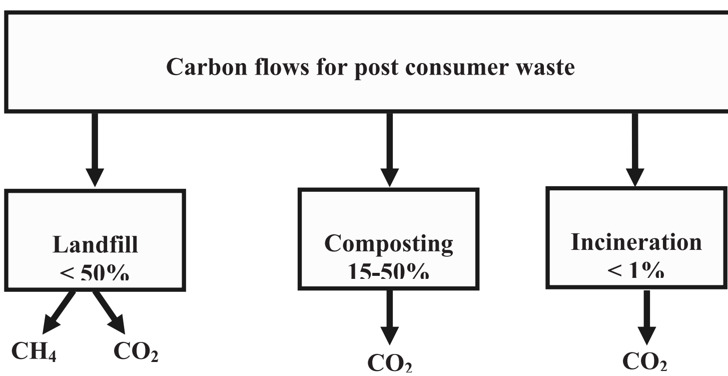

Figure 23.3. Carbon flows through major waste management systems

Wastes and waste management affect the release of GHGs in mainly five major ways: 1) landfill emission of methane; 2) reductions in fossil fuel use by substituting energy recovery from waste combustion; 3) reduction in energy consumption and process gas releases in extractive and manufacturing industries, as a result of recycling; 4) carbon sequestration in forests, caused by decreased demand for virgin paper; and (5) energy used in the transport of waste for disposal or recycling.

23.3 Recycling as Climate Mitigation Strategy

Recycling can be defined as the collection of materials during production or at the end of a product's life time for reuse in the manufacturing process. The treatment during recycling includes simple melting of glass and metal, breaking apart and reconstitution of paper or other fibres such as textiles or carpets, depolymerisation of plastics and synthetic fibres to monomers. Manufacturing products from recycled materials is less energy intensive and associated with less GHG emissions than making virgin materials. The U.S. Environmental Protection Agency (USEPA) analysis reported lower GHG emissions over the product life cycle from recycling than from virgin production and disposal of paper, metals, glass and plastics (USEPA 1999, 2003, 2005).

Recycling reduces pollution, saves energy and reduces GHG emission. Recycling reduces GHG emissions mainly by two ways. First, recycling keeps materials out of the landfill, since landfill produces one of the most dangerous GHGs, methane. Secondly, recycling reduces GHG emissions by reducing the need to continually mine and refine virgin resources for product production. A recent California Department of Conservation report found that using recycled aluminum from soda cans requires only 5 to 8 % of the energy required to produce primary aluminum, which results in a 95% reduction of GHG emissions as compared to primary production (California Department of Conservation, 2008). Utilizing recycled plastic saves 70% of the energy otherwise needed for production, and utilizing recycled glass saves 30% of the energy otherwise needed for production.

Recycling reduces GHG emissions through lower energy demand for production (avoided fossil fuel) and by substitution of recycled feedstock for virgin materials. Quantifying the GHG-reduction benefits of waste minimization, recycling and re-use requires the application of LCA tools (Smith et al. 2001). Efficient use of materials also reduces waste. Material efficiency can be defined as a reduction in primary materials for a particular purpose, such as packaging or construction, with no negative impact on existing human activities. At several stages in the life cycle of a product, material efficiency can be increased by more efficient design, material substitution, product recycling, material recycling and quality cascading. Both material recycling and quality cascading occur in many countries at large scale for metals recovery (steel, aluminum) and recycling of paper, plastics and wood. All these measures lead to indirect energy savings, reductions in GHG emissions, and avoidance of GHG generation. This is especially true for products resulting from energy-intensive production processes, such as metals, glass, plastic and paper (Tuhkanen et al. 2001). The magnitude of avoided GHG-emissions benefits from recycling is highly dependent on the specific materials involved, the recovery rates for those materials, the local options for managing materials, and (for energy offsets) the specific fossil fuel avoided (Smith et al. 2001). All developed countries have implemented comprehensive national, regional or local recycling programmes. Smith et al. (2001) thoroughly addressed the GHG-emission benefits from recycling across the EU, and Pimenteira et al. (2004) quantified GHG emission reductions from recycling in Brazil.

Recycling has an important effect in mitigation of climate change by different ways as described below:

(1) **Reduced energy use:** Recycling reduces air pollutant which is major cause of fog by reducing the amount of energy used for the production of new

products. According to the USEPA, paper and plastics recycling saved approximately 700 trillion British thermal units of energy in 200, equivalent to about 5.5 billion gallons of gasoline.

(2) **GHG emissions:** The USEPA estimates that in 2008, recycling paper and plastics reduced emissions of carbon dioxide (CO_2), the primary GHG, by approximately 98 million metric tons, which is equivalent to the GHG emissions from about 18 million cars.

(3) **Carbon Sequestration:** Paper recycling reduces the need to produce paper from trees, which in turn has a big impact on the green house gas emissions and climate change, thus significantly reducing this impact.

(4) Methane gas: Landfill releases methane gas which is a significant contributor to climate change. Recycling reduces the amount of materials sent to landfills which in turn reduces the production of methane.

(5) Incineration: Incineration produces lot of air pollutants. Recycling reduces the requirements of incineration of trash.

Benefits of recycling due to GHG emission reduction are calculated as the difference of GHG emissions between manufacturing from recycled or unhandled virgin material only. New methods of physical, chemical or biological treatment have been employed for recycling. Paper, textiles, plastics and organic wastes are some of the major wastes contributing to the emission of GHGs. In this context, the mitigation of GHG emission by recycling of these wastes is discussed below.

23.3.1 Recycling of Paper Waste

Paper recycling reuses a renewable resource that sequesters carbon and helps reduce GHG emissions. GHG reductions results from avoided methane emissions and reduced energy required for a number of paper products. One ton of recycled paper saves 3,700 pounds of lumber and 24,000 gallons of water. It was reported that one ton of recycled paper uses 64% less energy, 50% less water, and 74% less air pollution, saves 17 trees and creates 5 times more jobs than one ton of paper products from virgin wood pulp (Colorado university report). Recycling 1 ton of paper saves 17 trees, 2 barrels of oil, 4100 kilowatts of energy, 3.2 cubic yards of landfill space and 60 pounds of air pollution (Colorado university report).

In the GHG perspective, paper waste has more complex life cycle than the other inorganic materials. The waste management of paper can affect forest carbon stocks, landfill CH_4 emissions, and landfill carbon stocks. Recycling of paper waste would reduce the rate of pulpwood harvesting, thereby affecting the mass of carbon stored in forests. Land filling has two countervailing effects–the anaerobic situation results in CH_4 emissions, but it also results in long-term storage of that portion of the disposed carbon that does not readily degrade. The GHG emission factors for the various waste management options in Canada for paper waste products are shown in Table 23.1 (EC and NRC 2005).

The recycling of paper wastes includes mainly different steps, such as collection and separation of paper wastes from other recyclables, repulping through mixing with heated water, deinking in alkaline solution, cleaning, screening, washing, removal of contaminants by the centrifugal cleaning system, sheet formation and drying (using the same process as was used in virgin production), and finally rolling/final processing (USEPA 2005). Recycling paper waste gives emission benefits through the recovery of raw materials (e.g., in this case, pulp), which reduces the need for virgin (or primary) production of those materials. Forest carbon storage is the major driver for overall GHG emission benefits.

Table 23.1. GHG emissions (in tonnes eCO_2/tonne) from waste management options for newsprint, fine paper, cardboard, and other paper

Material type	Net Recycling Emissions	Net Anaerobic Digestion Emissions	Net Combustion Emissions	Net Land filling Emissions (NLE– National Average)
Newsprint	2.75	0.49	0.05	1.22
Fine paper	3.20	0.34	0.04	1.18
Cardboard	3.26	0.32	0.04	0.29
Other paper	3.27	0.23	0.04	0.71

The GHG emission impacts of recycling newsprint, fine paper, cardboard, and other paper are presented in Table 23.2 (EC and NRC 2005). The effects of recycling on forest carbon storage comprise a significant component of the net GHG emission factor.

Table 23.2. Recycling emissions (in tonnes eCO_2/tonne) for newsprint, fine paper, cardboard, and other paper

	A	B	C	D	E
Material type	Process energy	Transportation energy	Process non-energy	Forest carbon sink	Net Emission (= A + B + C + D)
Newsprint	0.28	0.01	0.00	2.45	2.75
Fine paper	0.36	0.00	0.00	2.84	3.20
Cardboard	0.20	0.01	0.00	3.04	3.26
Other paper	0.24	0.01	0.00	3.02	3.27

23.3.2 Recycling of Plastics

Plastic is a significant fraction of solid waste and often consists of packaging waste and discarded tools and goods. Around 11% by weight of waste form households may be plastic waste (Delgado et al. 2007). Polythene and polypropylene are important polymers and polyethylene terephthalate and polystyrene are also present (Delgado et al. 2007). Recovered plastic waste can be used for material recycling or energy utilization (Figure 23.4).

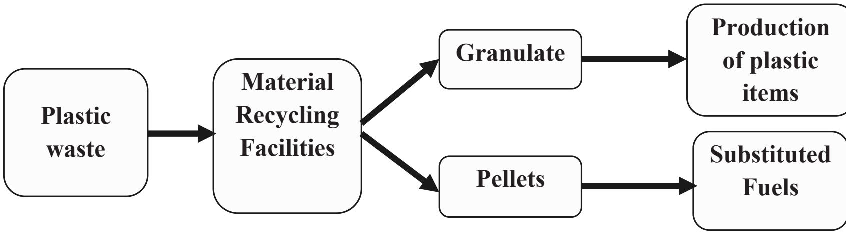

Figure 23.4. Flow diagram outlining plastic waste recycling and downstream options for substitutions

Energy utilization may involve the use of the plastic waste as fuel in industrial process or as solid fuels for energy production in facilities, such as power plant. Plastic recycling are mainly of two types: recycling of plastic into high quality plastics products which require clean and single type of plastics. Thus, the recycled plastics can substitute virgin plastics also. In another case, recycling of plastics with contaminated and mix of different plastics wastes can be done and this type of plastics can be used for products, such as fences, garden furniture and pallets etc. Plastic waste is also used as substitutes for fuels, such as coal, oil, natural gas, etc., depending on the energy technology in which the plastic is used as fuel (Fruergaard et al. 2009). Recycling of plastic waste into new plastic products (material utilization) and the use of plastic waste as fuel (energy utilization) are the most important options for the plastic waste utilization (Delgado et al. 2007).

Material recycling facilities (MRF) for granule production uses mainly high quality, source-separated plastic waste. This will reduce the amount of organic waste and dirty plastics in the output. Generally, the recovered and collected materials received in the receiving area are transported to a manual sorting area and then to the processing area. The mechanical treatment involves screening, magnets, eddy current, washing and drying followed by granulation. Further air-classifiers, near infra-red spectroscopic identification and sorting of the plastics may be involved in the process. Granulates are packed and stored for further processing and use. Residues from the sorting process are incinerated and waste water treated.

MRF for fuel pellet generally receives mixed plastics with higher content of contaminants. Contaminants, such as paper, cardboard and organic matter may not significantly affect the fuel quality. It is important to remove metals, strings and eventually also PVC to avoid higher levels of chlorine in the pellet. Contaminants, such as glass can be removed easily manually or by gravity separation. The final mix is pelletized and they can be then stored.

High quality granulates containing single plastic type (High-density polyethylene (HDPE), Polypropylene (PP) or Polyethylene terephthalate (PET)) can be directly used for the production of plastics similar to virgin plastic granulates. Minor remaining impurities on the melt from granulates can be sieved prior to extruding or casting the material. Plastic pellets which are used as fuel for industrial purpose or power plants are generally fed in directly to the combustion unit. The amount of plastic pellets used the amount of alternative fuels saved can be calculated by their respective energy contents. Usually the pellets have an energy content of about 30–40 GJ per tonne and substitute fossil fuels, such as coal, oil, diesel, natural gas, etc.

Recycling HDPE, PET, and other plastics provides emission benefits through the recovery of raw materials that reduce the need for virgin (or primary) production of those materials. The GHG emission impacts of recycling HDPE, PET, and other plastics in Canadian scenario are presented in the Table.23.3 (EC and NRC 2005).

Table 23.3. Recycling emissions (in tonnes eCO_2/tonne) for HDPE, PET, and other plastic

	A	**B**	**C**	**D**
Material type	**Process energy**	**Transportation energy**	**Process non-energy**	**Net Emission (= A + B + C)**
HDPE	2.26	0.02	0.00	2.27
PET	3.61	0.02	0.00	3.63
Other plastics	1.76	0.01	0.00	1.80

The direct emissions from management of plastic wastes are related to the process of turning plastics into a product. Material recycling for substitution of virgin/primary plastics requires different plastic types to be collected separately to obtain a secondary product of a suitable quality. Material loss is mainly due to contaminants in the waste stream. The magnitude of the material loss depends on the purity of the collected plastic material. Schmidt and Stromberg (2006) reported a material loss of 3% for collected PET bottles in Switzerland; 7.6% loss for LDPE film and PP bottles in Denmark was reported by Frees (2002). One tonne of plastic wastes collected can be a substitute of 720 kg virgin plastic with a material loss of 10% and material quality loss of 20% (Astrup et al. 2009). Table 23.4 shows some examples data input for the reprocessing of plastic wastes by different processing methods.

Plastic wastes can be converted into solid recovered fuel (SRF) or refuse-derived fuel (RDF) and used as fuel industrial processes. Plastic wastes are assumed to be a mixture of plastics with an overall lower heating value of 30-40 MJ /kg and a carbon content of 70–80% per weight (Brandrup 1995; Shonfield 2008). The processing of plastic wastes for energy utilization requires a range of unit operations to produce a high-quality energy product with a high-energy content, low chlorine content to avoid corrosion, and low contents of foreign objects in order to enhance the quality of the by-products (ashes etc.) from the combustion process. The chlorine content should be below 1% for use in cement kilns. So, PVC content of plastic wastes should be below 40–60% of the total weight. It was reported that 10% of the plastic waste in cement could be PVC (Shonfield 2008). Combustion of 1 tonne of plastic waste leads to emissions of 2567 to 3117 kg CO_2 (fossil), assuming complete oxidation of carbon, all carbon being of fossil origin and a carbon content of 70 to 85% (w/w) in the plastic waste. One tonne of plastic wastes with a lower heating value (LHV) of 30–40 MJ/kg may substitute 1230 to 1640 kg hard coal (assuming a LHV of 24.4 MJ/kg hard coal). It has been reported that recycling of plastic waste for substitution of virgin plastics is the preferred option compared to energy utilization in terms of GHG emission and global warming perspective (Astrup et al. 2009).

Table 23.4. Examples of data for reprocessing of plastic wastes

	Unit	Reprocessing of 1 tonne HD-PE boxes to granulate (Frees 2002)	Production of 1 tonne virgin HD-PE granulate (Boustead 2005)	Production of 1 tonne of wood lumber (kiln-dried) (Sathre 2007)
Electricity	kWh	330	681	64
Natural gas	Nm^3	24	136	0
(fuel) Natural	Nm^3	0	565	0
gas (feedstock)	L	0.6	214	17
Oil (fuel)	L	0	928	0
Oil (feedstock)	GJ	0	0	1.5

23.3.3 Recycling of Textile Wastes

Even though quite a large amount of textiles are recycled, the processing of the recovered textiles into new products is relatively minor. The use of recovered textiles reduces the amount disposed off in landfills. It also reduces the use of virgin raw materials and thereby decreases the use of natural resources (e.g. water, energy, chemicals). Textile reprocessing can be roughly divided into three categories: sorting and reuse of good quality textiles, industry and machine cleaning cloth (wipers) production and mechanical defibring (e.g. non-woven fabric products, papers or raw material for yarns). Textile waste reprocessing into cleaning cloths is quite a simple process. Textiles can also be used as a raw material for utility articles. The textiles which are not suitable for second hand clothing are pre-sorted according to the color and type of fabric and are used as a raw material for new products. The end product of the reprocessing plant consists of reprocessed fibres of cotton, wool and acrylic, which is mainly, used in automotive industry for the production of acoustic insulation materials.

Despite the fact that the amount of textile waste is considerable and that a relatively large amount of this is recycled, the reprocessing of textiles into new products is only done to a minor degree. Recycled textiles can be also used for the production of oil sorbent mats. Recovered textiles for producing various non-woven products are mainly for the needs of industry, building and construction, gardening and upholstery. The products for industry include oil adsorption rug (mats), floor protection carpets and wiping cloths for handling and preventing spills of hazardous liquids. Building materials and felting as well wadding for upholsterers are also produced. Gardening products include irrigation mats for growing seeds, seedlings and flowers. About 70 % of the recovered textile waste used in oil absorbent mats is biogenic (wool, cotton, viscose) and the remaining 30% is synthetic fibre (polyester) (Saha 2006). The combustion of biogenic fibre does not produce fossil GHG emissions compared to synthetic fibre. Studies concerning the emissions and energy consumption of textile recycling are very limited. McDougall et al. (2001) presents two relatively old studies concerning textile recycling conducted by Lowe (1981) and Ogilvie (1992). The studies indicated that the energy consumption of producing a woven product from virgin wool was approximately double compared to producing the product from recycled material. In a recent study by Woolridge et al. (2006) the energy consumption of reuse and recycling using donated clothing in UK was compared with the energy consumption of purchasing new clothing made from virgin materials. A recent study by Korhonen and Dahlbo (2007) showed that, for every ton of virgin cotton displaced by second hand clothing, about 65 MWh is saved, and for every ton of polyester, around 90 MWh is saved.

23.3.4 Recycling of Organic Waste

The main forms of organic waste are household food waste, agricultural waste as well as human and animal waste. In industrialized countries, the amount of organic wastes produced is increasing dramatically each year. Most of the organic wastes are used for landfills sites and is often the most hazardous waste. The organic waste component of landfill is broken down by micro-organisms to form a liquid 'leachate' which contains bacteria, rotting matter and may be chemical contaminants from the landfill. Digestion of organic matter in landfills also generates methane, which is a harmful GHG, in large quantity. In developing countries, there is a different approach to dealing with organic waste. The economies of most developing countries dictates that materials and resources must be used to their full potential, and this has propagated a culture of reuse, repair and recycling. There are a variety of ways of using organic waste and three main ways of using organic waste are for soil improvement, for animal raising and to provide a source of energy (Figure 23.5). Recently, there is an increasing trend to use organic wastes mainly agricultural waste for value-addition by growing microorganisms to produce enzymes, single cell protein, amino acids, lipids, carbohydrates and organic acids by different fermentation technologies.

Anthropogenic GHG emissions from agriculture contribute 7% of total carbon equivalent emissions, releasing about 28% of methane emissions and almost 70% of nitrous oxide based on report by the USEPA inventory. Agriculture has substantial potential for offsetting emissions by serving as a sink augmenting the GHG absorption, particularly CO_2, through changes in tillage or land use including conversion of cropland to grassland or forest. Agriculture can also reduce GHG emissions by increasing production of biomass commodities, which can serve either as feedstock for electricity generating power plants or as blend/substitute for fossil fuel based gasoline. Biofuels mitigate GHG emissions because their usage spares fossil fuel use. The net emission savings from biomass amount to approximately 95% of the emissions from extraction and combustion of an equivalent amount of fossil fuels (Kline et al. 1998; Mann and Spath. 1997).

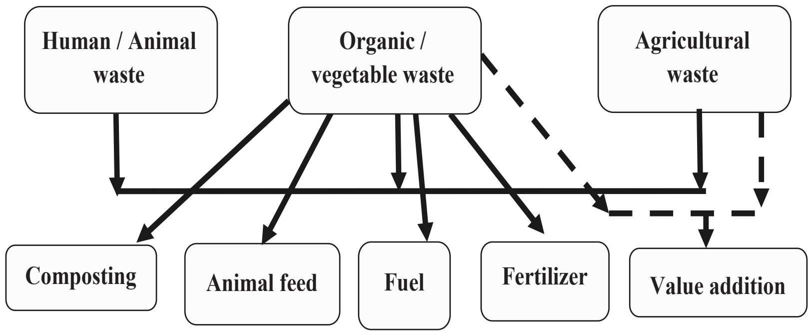

Figure 23.5. Processes and recycling of organic waste

The carbon dioxide emission estimates from burning the three major world crop residues and municipal solid wastes are 10.56 B tons and 414 M tons, respectively or approximately 27% of manmade GHG emission. If these biodegradable solid wastes are composted under controlled conditions with sufficient aeration, the carbon dioxide emission from the agricultural solid wastes is only 5.51 B tons and only 216 M tons from the municipal solid wastes or a total decrease of 5.248 B tons. Relating this decrease to the total man-made carbon dioxide emission of 40 B tons, this translates to ~13% of the total emission (Bogner et al. 2008).

23.4 Conclusion and Future Work

The threat of global climate problem is growing day by day and due to the nature of the problem, actions through regional and international mechanisms are required. However, these actions must be carried within a sustainable and equitable development framework. The importance of local control and management within a politically committed environment cannot be over-emphasized in ensuring sustainable development. Waste recycling is a growing field of activity. Recycling can reduce the use of virgin raw materials and energy, and thus also GHG emissions. By processing waste plastics into plastic profile, emissions can be reduced in situations where the waste plastic is recycled instead of being combusted and the discarded plastic profile is disposed off on landfill sites. When textile wastes are used to replace virgin plastic products, the GHG emissions can be substantially reduced. Recycling is one of the elements of sustainable development. However, there are challenges to increasing material recycling, such as market demand of the recycled products, and process for achieving high quality recycled materials.

23.6 Acknowledgements

The authors are sincerely thankful to the Natural Sciences and Engineering Research Council of Canada (Discovery Grant 355254, Canada Research Chair), FQRNT (ENC 125216), MAPAQ (No. 809051) and Inde Initiative 2010 (Ministère de l'Éducation, du Loisir et du Sport) for financial support. The views or opinions expressed in this article are those of the authors.

23.7 References

Astrup, T., Møller, J., and Fruergaard, T. (2009). "Incineration and co-combustion of waste: accounting of greenhouse gases and global warming contributions". *Waste Manage. Res.,* 27(8), 789–799.

Bärring, L. (1993). "Climate - change or variation?" *Climatic Change,* 25, 1-13.

Berneche-Perez, G., S. C., Salvadro, G. A. María, D. V Artruro and S. S. M. Elena. (2001). "Solid waste characterisation studies in the Guadalajara metropolitan zone, Mexico." *Waste Manage. Res.* 19(5), 413–424.

Bogner, J., and Matthews, E. (2003). "Global methane emission from landfills: new methodology and annual estimates 1980–1996." *Global Biogeochem Cycles,* 17(2), 1065–1083.

Bogner, J., Pipatti, R., Hashimoto, S., Diaz, C., Mareckova, K., Diaz, L., Kjeldsen, P., Monni. S, Faaij, A, Gao, X, Zhang, T, Ahmed, M.A, Sutamihardja, R. T. M, and Gregory, R. (2008). "Mitigation of global greenhouse gas emissions from waste. conclusions and strategies from the Intergovernmental Panel on Climate Change (IPCC) Fourth Assessment Report. Working Group III (Mitigation)." *Waste Manag. Res.*, 26(1), 11–32.

Brandrup, J. (1995). "Preparation of feedstock for petrochemical recycling–requirements imposed on plastics waste". In: *Recycling and Recovery of Plastics*. Hanser Publishers, Munich; Vienna; New York, 393–412.

California Department of Conservation (2008). Recycle. Available at <http://www.wastemanagementsd. com/env/recycle> (accessed June 2011).

Colarado university report. Recycling facts. Available at <http://ecenter.colorado.edu/recycling/education-a-outreach/recycling-facts> (Aceesed on June 2011).

Delgado, C., Barruetabeña, L., Salas, O., and Wolf, O. (2007). *Assessment of the Environmental Advantages and Drawbacks of Existing and Emerging Polymers Recovery Processes.* Institute for Prospective Technological Studies, Joint Research Centre, European Commission.

EC and NRC (2005). *Determination of the Impact of Waste Management Activities on Greenhouse Gas Emissions: 2005. Update Final Report*. Environment Canada and Natural Resources Canada.

Frees, N. (2002). *Miljømæssige fordele og ulemper ved genvinding af plast (Environmental advantages and disadvantages of plastic recycling, in Danish).* Danish Environmental Protection Agency, Copenhagen, Denmark.

Fruergaard, T., Ekvall, T., and Astrup, T. (2009). “Energy use and recovery in waste management and implications for accounting of greenhouse gases and global warming contributions.” *Waste Manage Res*, 27, 724–737.

IPCC (2007). *Climate Change 2007: The Physical Science Basis. Contribution of Working Group I to the Fourth Assessment Report of the Intergovernmental Panel on Climate Change*. Solomon, S., D. Qin, M. Manning, Z. Chen, M. Marquis, K. B. Averyt, M. Tignor, and H. L. Miller (eds.). *Cambridge University Press*, Cambridge

Kaseva, M. E., Mbuligwe, S. E., and Kasenga, G. (2002). “Recycling inorganic domestic solid wastes: results from a pilot study in Dares Salaam City, Tanzania.” *Resour.Conserv. Recycl*, 35(4), 243–257.

Kline. D., Hargrove, T., and Vanderlan, C. (1998). *Treatment of Biomass Fuels in Carbon Emissions Trading Systems*. Center for Clean Air Policy's Greenhouse Gas Emissions Trading, Braintrust, Washington.

Korhonen, M., and Dahlbo (2007). *Reducing Greenhouse Gas Emissions by Recycling Plastics and Textiles into Products*. *Finnish Environment Institute Research Department*, Finland.

Lowe, J. (1981). *Energy Usage and Potential Savings in the Woollen Industry*. Wool Industry Research Association, Leeds, UK.

Mann, M. K., and Spath, P. L. (1997). *Life Cycle Assessment of a Biomass Gasification Combined-Cycle Power System*. National Renewable Energy Laboratory, Golden, CO.

McDougall, F., White, P., Franke, M., and Hindle, P. (2001). *Integrated Solid Waste Management: a Life Cycle Inventory*, 2nd Ed. *Blackwell Science Ltd*, UK.

Mitchell, J. M. Jr., Dzerdzeevskii, B., Flohn, H., Hofmeyr, W. L., Lamb, H. H., Rao, K. N., and Wallén, C. C. (1966). “Climatic Change. WMO Technical Note No 79.” *World Meteorological Organization*, Geneva.

Mitchell, T., and Tanner, T. M. (2007). “Embedding Climate Change Adaptation in Development Processes. In Focus: Issue 02.” Institute of Development Studies, *University of Sussex*, UK.

Molina, M., Zaelke, D., Sarmac, K. M., Andersen, S. O., Ramanathane, V., and Kaniaruf, D. (2009). "Tipping elements in earth systems special feature: Reducing abrupt climate change risk using the Montreal Protocol and other regulatory actions to complement cuts in CO_2 emissions." *Procee. Nat. Academy of Sci*, 106(49), 20616–20621.

Ngoc, U. N., and Schnitzer, H. (2009). “Sustainable solutions for solid waste management in Southeast Asian countries.” *Waste Manag.,* 29(6), 1982–1995.

Ogilvie, S. M. (1992). *A Review of the Environmental Impact of Recycling*. Report LR 911 (MR) Warren Spring Laboratories, Stevenage, UK.

Pielke, R. Jr. (2004). “What is climate change?” *Issues in Science and Technology* 20(4), 31–34.

Pimenteira, C. A. P., Pereira, A. S., Oliveira, L. B., Rosa, L. P., Reis, M. M., and Henriques, R. M. (2004). “Energy conservation and CO_2 emission reductions due to recycling in Brazil.” *Waste Management*, 24(9), 889–897.

Saha. R. (2006). "Genanvendelse i LCA – systemudvidelse (Recycling in LCA – system expansion, in Danish), Miljønyt Nr. 81." *Danish Environmental Protection Agency*, Copenhagen, Denmark.

Shonfield, P. (2008). *LCA of Management Options for Mixed Waste Plastics*. Final report. The Waste and Resources Action Programme (WRAP), Banbury, Oxon, UK.

Smith, A., Brown, K., Ogilvie, S., Rushton, K., and Bates, J. (2001). *Waste Management Options and Climate Change*. *DG Environment*, AEA Technology, European Commission.

Thorneloe, S., Weitz, K., and Jambeck, J. (2005). "Moving from solid waste disposal to materials management in the United States." *In: Proc. Of the Sardinia '05, International Solid and Hazardous Waste Symposium.* CISA, University of Cagliari, Sardinia.

Tuhkanen, S., Pipatti, R., Sipilä, K., and Mäkinen, T. (2001). "The effect of new solid waste treatment systems on greenhouse gas emissions." *Fifth International Conference on Greenhouse Gas Control Technologies (GHGT-5)*, CSIRO Publishing, Collingwood, 1236–1241.

USEPA (1999). *National Source Reduction Characterization Report for Municipal Solid Waste in the United States*. EPA 530R-99-034, *Office of Solid Waste and Emergency Response*, Washington, DC.

USEPA (2003). *International Analysis of Methane and Nitrous Oxide Abatement Opportunities. Report to Energy Modeling Forum, Working Group 21. US Environmental Protection Agency*, Washington, DC.

USEPA (2005). *Municipal Solid Waste Generation, Recycling and Disposal in the United States: Facts and Figures for 2003. US Environmental Protection Agency*, Washington, DC.

Weitz, K., Thorneloe, S., Nishtala, S., Yarkosky, S., and Zannes, M. (2002). "The impact of municipal solid waste management on greenhouse gas emissions in the United States." *J. Air. Waste Manag. Assoc.*, 52, 1000–1011.

Woolridge, A. C., Ward, G. D, Phillips, P. S. Collins, M., and Gandy, S. (2006). "Life cycle assessment for reuse/recycling of donated waste textiles compared to use of virgin material: An UK energy saving perspective." *Resour. Conserv. Recycl*, 46, 94–103.

WRAP (2006). *Environmental benefits of recycling, an international review of life cycle comparisons for key materials in the UK recycling sector.* Waste and Resources Action Program, *WRAP*, Banbury, Oxfordshire, UK.

CHAPTER 24

Green Energy Application for Mitigating Climate Change

Gurpreet S. Dhillon, Mausam Verma, Surinder Kaur, Satinder K. Brar, R. D. Tyagi, and Rao Y. Surampalli

24.1 Introduction

The increase in population with simultaneous industrial growth has put immense pressure on Earth's resources, in particular, the energy sources. The world energy scenario depicts a picture of concern. The adverse effects on the environment caused by the production and consumption of energy have resulted in severe environmental impacts across the globe. The supply of energy is expected to remain adequate in coming years. However, imbalance of energy consumption is prevalent around the world. Energy consumption is high in most developed countries. On the other hand, the developing countries need to consume more energy to ensure economic growth. According to estimates, energy consumption in developing countries is only one-tenth of that in the developed countries as demonstrated in Figure 24.1. Major sources of anthropogenic carbon-dioxide (CO_2) and other greenhouse gases (GHGs) emissions are closely related to the use of energy in transportation, residential and commercial buildings, industrial processes, and associated infrastructure. Improving energy efficiency and reducing GHGs emissions intensity in these economic sectors through a variety of technical advances and process changes present large opportunities to decrease overall GHGs emissions. Four types of technical advancement can bring about these changes, namely, efficiency, infrastructure, and equipment; transition technologies (e.g. high-efficiency natural-gas-fired power plants); enabling technologies (e.g. modernized electricity grid); and finding alternatives to industrial processes, feed stocks, and materials.

Current global energy supplies are dominated by the use of fossil fuels–coal, petroleum products, and natural gas–that emit CO_2 when burned. A transition to a low-carbon future would likely require the availability of multiple energy supply technology options characterized by low, near net-zero, or zero CO_2 emissions. Many such energy supply technologies are available today or are under development. The major sources of energy in the world are oil, coal, natural gas, hydro energy, nuclear energy, and renewable combustible wastes. Combustible wastes include animal products, biomass and industrial wastes. These energy sources can be divided as renewable and non-renewable resources as illustrated in Figure 24.2. Meanwhile, mitigating climate change and achieving stabilization of GHG atmospheric concentrations–the objective of the United Nations Framework Convention on Climate Change (UNFCCC)–will require higher reduction of GHGs, including energy-related carbon dioxide (CO_2) emissions. Renewable energy sources currently meet approximately 14% of global energy demand (Pimentel et al. 2002; Sims et al. 2007), and these resources are destined to play an even greater role in future energy provision (International Energy Agency 2008). These technologies provide a key component of efforts to mitigate climate change (Pimentel et al. 2002; Milford 2007), and they can also contribute to the security of energy supply and environmental protection measures encompassing climate change (Dresselhaus and Thomas 2001; IEA 2007).

In the given context, this chapter discusses the use of different green energy technologies to combat growing GHGs emissions.

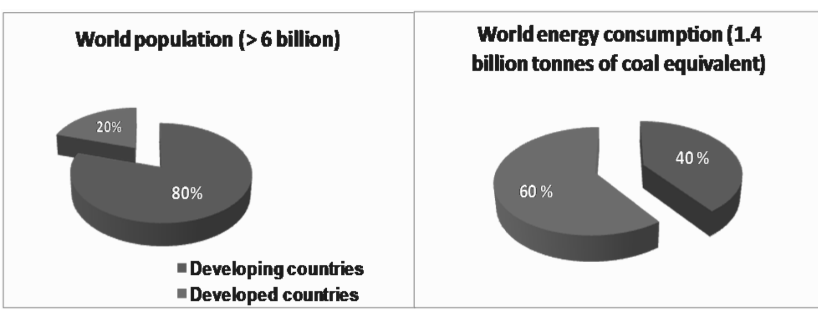

Figure 24.1. Comparison of energy consumption and population in the world

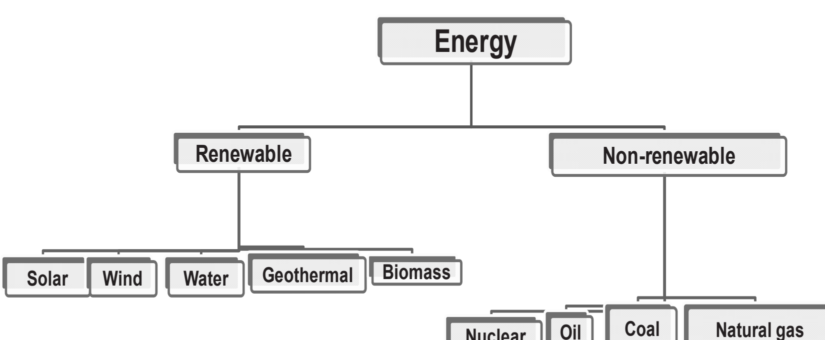

Figure 24.2. Different renewable and non-renewable forms of energy

24.2 Climate Change Mitigation Initiatives

Rapidly increasing concentration of GHGs in the atmosphere, rising land and sea temperatures and amplified frequency and magnitude of extreme events cause enormous risks to all forms of life, various economic activities, fresh water availability and affect the sustainability of agriculture and food security of billions of people around the globe. Moreover, everyday growing concerns regarding the decline in the non-renewable energy sources and the deterioration of the environment are the main concerns needed to be addressed immediately. In the last 140 years, there were about 20% reductions in the area under forests worldwide releasing about 120 giga tons (GT) CO_2 to the atmosphere.

Changing climatic conditions have adverse effects on all forms of life. Irregular rainfall patterns and occurrence of natural calamities, such as floods and droughts could lead to loss of life and property, crop failures, food insecurity, starvation, mass migration, and negative national economic growth. About 80% of the variability in agricultural production is due to the inconsistency in weather conditions. Harsh weather events resulting in natural disasters impact the socio-economic development of many nations. According to an estimate, financial losses in 2005 due to natural disasters are more than $200 billion (WMO 2012).

Climate change is generally considered to be one of the greatest challenges to modern human civilization that has profound socio-economic and environmental impacts. It is necessary to develop strategies that include adaptation, mitigation, technological development and research to combat climate change. According to IPCC (2007), mitigation is defined as the technological change and substitution that reduces resource inputs and emissions per unit of output. Although several social, economic and technological policies would produce an emission reduction, with respect to climate change, mitigation means implementing policies to reduce GHGs emissions and enhance sinks.

The environmental and economic threat posed by possible climate change is commonly referred to as the "greenhouse effect." The major greenhouse gas is carbon dioxide, and the major source of anthropogenic CO_2 is combustion of fossil fuels (Watson et al. 1996). Due to the potential adverse impacts, the world community has adopted the Framework Convention on Climate Change. The Inter-governmental Panel on Climate Change (IPCC) [based in Geneva, Switzerland] is established to provide the decision-makers and others interested in climate change with an objective source of information about climate change. IPCC is a scientific intergovernmental body set up by the World Meteorological Organization (WMO) and by the United Nations Environment Programme (UNEP). Various climate change mitigation initiates are presented in Table 24.1.

24.3 Emerging Developments in Renewables

It is a known fact that the supply of the conventional energy sources, such as fuels, coal, oil, natural gas, uranium and fuel wood is limited and insufficient to sustain rapid rates of development. Non-renewable fossil fuels, such as coal, petroleum and natural gas provide more than 85% of the energy used worldwide (Youngquist 2000). For their basic requirements, modern society is highly dependent on fossil fuels for energy in many parts of the world. The energy crisis has imposed implication for the entire infrastructure of modern society.

Table 24.1. International activities on climate change mitigation initiatives (adapted from Herzog et al. 1997; UNEP 2000; Ramanathan and Xu 2010)

Year	Initiatives
September, 1987	The Montreal protocol. The objective is to reduce the worldwide production, consumption and emissions of ozone depleting substances (ODS) and chlorofluorocarbons (CFCs). Amendments were made later in London 1990, Copenhagen 1992, Vienna 1995, Montreal 1997, Beijing 1999
December, 1990	The Intergovernmental Negotiating Committee (INC) created by the United Nations. Negotiations begin on a climate treaty
June, 1992	The Framework Convention on Climate Change (FCCC) adopted by 143 countries in Rio at the “Earth Summit”. Among its provisions is a goal to stabilize GHGs at their 1990 levels by the year 2000
March, 1994	The FCCC comes into force 90 days after its ratification by 50 countries, including the United States
March, 1995	The first Conference of the Parties (COP-1) to the FCCC held in Berlin. The Climate Technology Initiative (CTI) is adopted. One of its provisions is to “assess the feasibility of developing longer-term technologies to capture, remove or dispose of greenhouse gases and strengthen relevant basic and applied research”
February, 1996	CTI Task Force 7 formed to accelerate international collaboration for R&D in the field of medium- and long-term technologies relating to greenhouse gas capture and disposal
June, 1996	The Intergovernmental Panel on Climate Change (IPCC) *Second Assessment Report* states that “the balance of evidence suggests a discernible human influence on global climate”
July, 1996	COP-2 held in Switzerland. US Under Secretary of State Timothy Wirth states that the US will press for an “agreement that sets out a realistic, verifiable, and binding medium-term emissions target”
December, 1997	The Kyoto protocol Japan. International agreement linked to the United Nations Framework Convention on Climate change (UNFCCC) signed by 180 countries. Entered into force on February, 2005. This protocol commits 38 industrialized nations and European community for reducing their GHGs emissions, particularly CO_2, CH_4, N_2O, SF6, HFC and PFCs levels to 5.2% lower than 1990 levels in 5 years (from 2008–2012)
November, 2001	COP 7. The detailed rules for the implementation of Kyoto protocol were adopted in Marrakesh and are also called *‘‘Marrakesh Accords’’*
February, 2005	The Kyoto protocol, which aims to curb the air pollution blamed for global warming, has come into force 7 years after it was agreed
October, 2009	Underwater meeting of Maldives cabinet to call for global action on climate change
December, 2009	Climate change summit, Copenhagen, Denmark. COP15-discuss the things that can be done across the globe to slowdown or reverse the effects of climate change. More than 100 countries have adopted global average warming limit to2°C or below as a guiding principal for mitigation efforts to reduce climate change risks

Non-renewable resources originate from two natural processes: (1) photosynthesis, which occurred millions of years ago, followed by the fossilization of the plant and animal life that resulted from this natural process; and (2) the formation of Earth itself. The first process gave rise to the fossil fuels, such as coal, oil, and natural gas. The second process resulted in the formation of fuels for nuclear energy, such as uranium for fission and lighter elements for fusion. These non-renewable fuels represent irreplaceable energy that must be invested wisely (Vesterby 2001). Finally, two aspects are vital to any evaluation of non-renewable energy resources, i.e., availability and demand. Both aspects are therefore critical for the evaluation of non-renewable energy reserves (Goldemberg 2004). From the last few centuries, population explosion, economic development and industrial revolution have curtailed these two important parameters. Consumption/demand of these energy sources is all time high, resulting in apparent worldwide shortage of the natural energy sources which mandates to look for alternative renewable energy sources. Various types of energy sources are depicted in Figure 24.3.

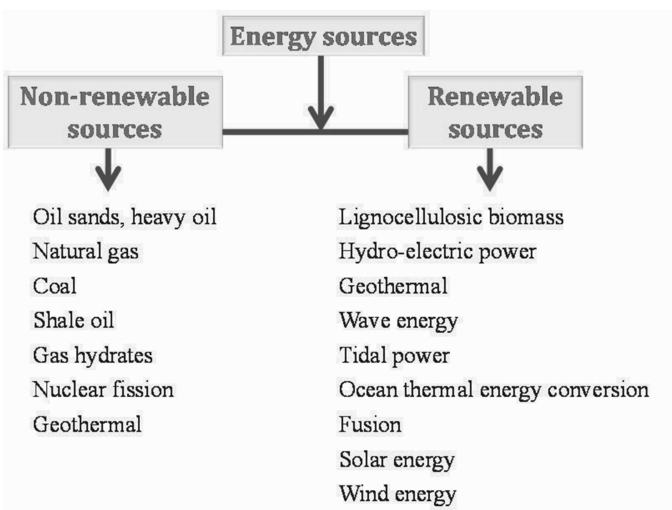

Figure 24.3. Different sources of energy (modified from Youngquist 2000)

24.3.1 Wind Energy

Rapid growth of wind power since the 1990s has led to notable market shares in some electricity markets. Wind power is undergoing the fastest rate of growth of any form of electricity generation in the world. The resource potential is large; with many countries having wind regimes that could serve as a significant energy source. Grid-connected wind capacity is undergoing the fastest rate of growth of any form of electricity generation, achieving global annual growth rates on the order of 20–30%. Capacity has been doubling every three years for the last decade. The World Energy Council has stated that it is doubtful whether any other energy technology is growing, or has grown, at such a rate. Global installed capacity was 40 GW in 2003 (GWEC 2005). According to industry associations, the global wind power capacity was 47.3 GW in 2004 (GWEC 2005).

Wind power is increasingly being viewed as a mainstream electricity supply technology. Its attractiveness as an electricity supply source has cultivated ambitious targets for wind power in many countries around the world. Its benefits include: (1) very low lifetime emissions of harmful gases, particularly CO_2; (2) significant economically exploitable resource potential; (3) no cost uncertainties from fuel supply price fluctuations; (4) increased diversity and security of supply; (5) modular and rapid installation; and (6) opportunities for industrial, economic and rural development. Estimates of the global wind resource potential are large and geographically broad and specific. The total technically recoverable resource is estimated to be 53,000 Terawatt hours (TWh). To put this into context, in 2002 world electricity generation was 16,054 TWh. The IEA's 2008 World Energy Outlook estimated that by 2020 global electricity demand will be 25,578 TWh (de Vries 2008). Europe's electricity generation is projected to increase at an average annual rate of 1.8 per cent between 2000 and 2010, 1.3 per cent in the decade 2010–2020, and 0.8 per cent in the decade up to 2030. The European Commission's baseline scenario assumes an increase in electricity demand of 33 per cent between 2005 and 2030 (4,408 TWh). Taking into account, the fact that if EU electricity demand develops as projected by the European Commission, wind power contribution of EU electricity consumption will reach 5% in 2010, 11.7 per cent in 2020 and 21.2 per cent in 2030 (Table 24.2). An important characteristic of the energy content of wind is that it increases with wind speed to the third power. For example, Clausen et al. (2007) reported that a wind speed of 3 m/s produced 16W/m^2 of wind power whereas a wind speed of 12 m/s can produce 1305 W/m^2 wind power. Thus, relatively small changes to the wind speed can have very large effects on wind power generation. Areas with increasing wind speeds will benefit from an increased wind power potential, whereas areas with decreasing wind speed would have less wind power potential.

Table 24.2. Wind power's share of European Union electricity demand

	2000	2007	2010	2020	2030
Wind power production (TWh)	23	119	177	277	935
Reference electricity demand (TWh)	2,577	3,243	3,568	4,078	4,408
Wind energy share (reference) (%)	0.9 (0.2% in 1995)	3.7	5.0	11.7	21.2

Source: EWEA (2007–09)

Wind energy is market-ready in that the technology is mature, and the price of power is broadly competitive to other types of new generation, depending on the location (Blanco 2009). In terms of energy and carbon balance, about 3–7 months of turbine operation are required to recover the energy spent in the full life cycle of the turbine (including removal and disposal), and the technology can avoid CO_2 emissions ranging from 391 to 828 g CO_2/kWh (Fig. 24.4 and EWEA 2009). Atmospheric icing also influences the life of wind turbines. Climate change, by facilitating the melting of ice, raises the efficiency of wind turbines in those areas characterized by icing problems in wind turbines.

Despite the unprecedented rise in wind energy and its power, in some European countries, onshore development sites are almost saturated paving way for the possible offshore development. However, offshore technologies are less well proven than onshore wind: and more so, the marine environment is more challenging, and it requires large fixed investments to develop the infrastructure–civil engineering, ships, platforms, installation technologies and transmission lines.

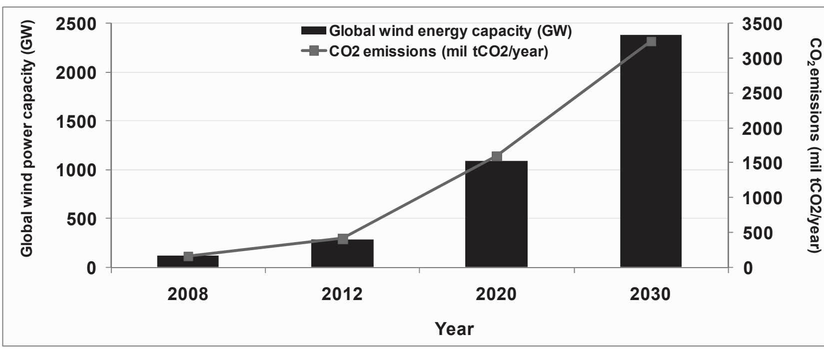

Figure 24.4. Carbon dioxide emissions saved by wind energy deployment from 2008–2030 (modified from data obtained from Sawyer and Zervo, 2009)

There are several challenges in application of wind energy technology:

- Grid integration concerns have come to the fore in recent years as wind power penetration levels have increased in a number of countries as an issue that may impede the widespread deployment of wind power systems. Two of the important challenges to wind power future prospects are the problems of intermittency and grid reliability. Introducing wind generation can increase the regulation burden and need for reserves, due to its natural intermittency. The impact of the wind plant variability may range from negligible to significant depending on the level of penetration and intermittency of the wind resource.
- The conventional management of transmission and distribution operation is challenged by electricity market restructuring, security of supply concerns and the integration of newer generation technologies, such as wind power. Infrastructure replacement and upgrading is an opportunity to re-examine design and operation parameters including integrating wind power generation as a key part of the overall network strategy.
- Offshore wind development presents a lower level of technological maturity and higher risks than onshore wind power developments. Offshore turbines are expected to be in the multi-megawatt range for development in the near term thereby bringing larger amounts of intermittent resources into the

generation mix and increasing the need to find near-term solutions to the integration challenges.

- Transmission availability can be a barrier to wind power development. Favourable wind locations are often in areas distant from existing transmission–offshore areas in Europe and rural areas of North America. Building new transmission lines can be difficult due to planning barriers, land use rights and costs. Market barriers as well as administrative and installation costs can be combated by internationally accepted standards for power performance, safety, noise and other environment-related conditions.
- Market barriers, as well as administrative and installation costs can be combated by internationally accepted standards for power performance, safety, noise and other environment-related conditions.

Further to the challenges, the energy policies of a country also play an important role in the successful progress of an energy resource. Saidur et al. (2010) have reviewed the wind energy policies around the world. They found that that Feed-In-Tariff, Renewable Portfolio Standard, incentives, pricing law and Quota system are the most useful energy policies practiced by many countries around the world. Most policies with the aim of promoting renewables (e.g., Feed-In-Tariff, Renewable Portfolio Standard) do not explicitly address sitting issues, which for wind energy are currently approached as the intersection of wind resource, land control, and transmission factors. Lewis (2010) proposed the use of location marginal price (LMP), the location and time specific cost of electricity on the wholesale market, to signal locations where generation can address electricity system insufficiency.

Wind power is one of the least expensive renewable energy sources; it has become increasingly cost-competitive with fossil-fuelled electricity generation, and it would be even more lucrative with a price on carbon and thus seek a bright future in the coming period.

24.3.2 Biomass Power: Cogeneration and Gasifiers

Biomass can be used in its solid form or gasified for heating applications or electricity generation, or it can be converted into liquid or gaseous fuels. Biomass conversion refers to the process of converting biomass feed stocks into energy that will then be used to generate electricity and/or heat. These technologies include anaerobic digesters for animal waste or wastewater, and three types of direct-fired boiler systems that have been used for decades for converting woody biomass: fixed bed boilers, fluidized bed boilers, and co-firing applications. Additionally, an emerging class of biomass conversion technologies is becoming available that converts woody biomass feed stocks to useable fuel through gasification processes. These technologies, called fixed bed gasifiers and fluidized bed gasifiers, are becoming commercialized and are currently in limited use producing syngas for power and heat.

Biomass is any organic matter, typically plant-based matter that is available on a renewable or recurring basis. Biomass resources include forest and mill residues, agricultural crops and wastes, wood and wood wastes, animal wastes, livestock operation residues, aquatic plants, fast-growing trees and plants, and municipal and industrial wastes. Biomass can be used in its solid form or gasified for heating applications or electricity generation, or it can be converted into liquid or gaseous fuels (Seal 1992; Dai and Ren 2005). The use of biomass to produce heat and power can be environmentally beneficial because biomass is a renewable resource and its combustion does not contribute additional GHGs to the atmosphere.

In almost all cases, the production of electricity from biomass resources is preferentially economical when the resulting waste heat is captured and used for important thermal energy—known as combined heat and power (CHP). These energy alternatives are provided in Figure 24.5. The lowest cost forms of biomass for generating electricity are residues. Residues are the organic byproducts of food, fiber, and forest production, such as sawdust, rice husks, wheat straw, corn stalks, and bagasse (the residue remaining after juice has been extracted from sugar cane). Wood is the most commonly used biomass fuel for heat and power. Economical sources of wood fuels are wood residues from manufacturing, discarded wood products diverted from landfills, and non-hazardous wood debris from construction and demolition activities. Generating energy with these materials can recoup the energy value in the material and avoid the environmental and monetary costs of disposal or open burning (Thornley et al. 2009).

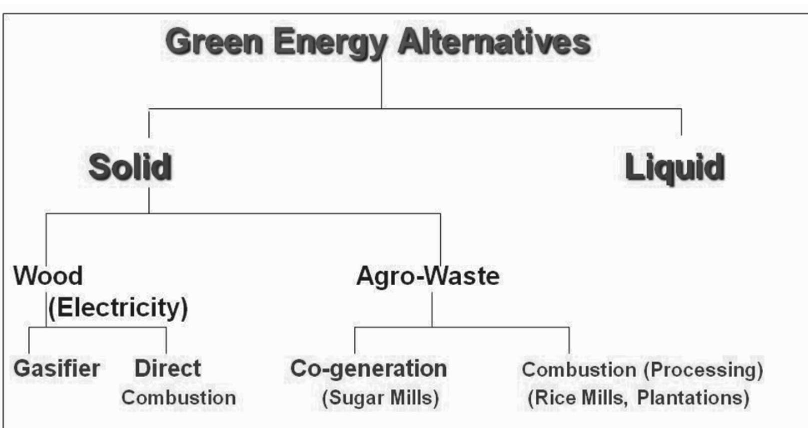

Figure 24.5. Schematic of biomass as green energy alternatives

Cogeneration or combined heat and power (CHP) generation involves the utilization of a single fuel to produce more than one form of energy, in succession. Steam and electricity can be cogenerated, thereby significantly increasing the overall efficiency of fuel utilization in process industries as depicted in Figure 24.6. Capacity of cogeneration projects can range from a few kilowatts to several megawatts of electricity generation along with simultaneous production of heat ranging from less than a hundred kWth (kilowatts thermal) to many MWth (megawatts thermal). Cogeneration requires heat and electricity in a favorable ratio, which is ideally present in the sugar industry. Generally, the cogeneration plants have high conversion energies; nevertheless they lose in terms of high capital costs.

The present global status of cogeneration is that abundant resources and favorable policies are enabling bio-power to expand in Northern Europe (mostly co-generation from wood residues), in the United States and in countries producing sugar cane bagasse (e.g. Brazil).

24.3.3 Small Hydro Power (SHP)

Small scale hydro power is distinct from traditional hydro power based on its generation capacity which is 30MW or less, per site. Such small capacities give them an edge over the conventional larger hydropower systems by protecting the riverine systems and hence the environment (Grimm 2002). The Department of Energy (USDOE 2004) prepared a database for the potential of small hydropower in the US, and they identified nearly 500,000 viable small scale hydropower sites, capable of providing more than 100,000 MW of power. There are two advantages in setting up small hydropower stations: 1) hydroelectricity being hundred years' old– is a mature technology, unlike most other renewables; and 2) there are already competitive companies that produce turbines and other equipment necessary to develop most small scale hydropower potential, and, this equipment is sturdy and reliable, with turbine life spans lasting many decades.

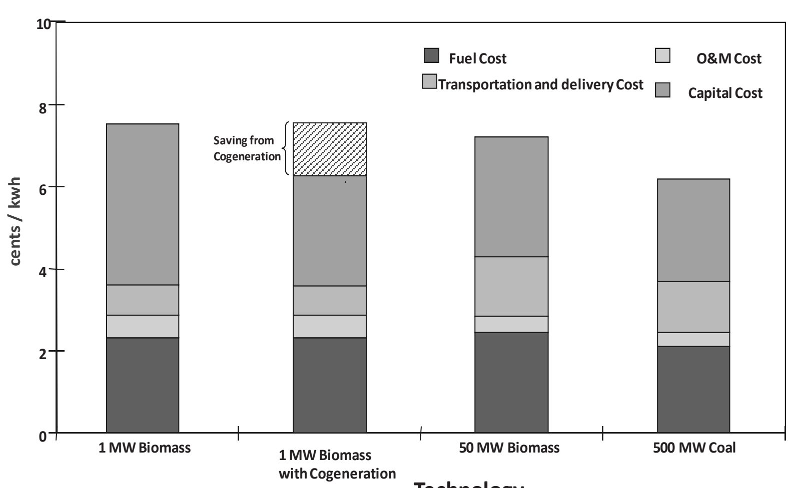

Figure 24.6. Electricity deliverable cost by employing biomass as green energy alternative (USEPA 1995, 2005, 2006; Perlack et al. 2005)

Hydropower is a clean source of energy, as it burns no fuel and does not produce GHGs emissions, other pollutants, or wastes associated with fossil fuels or nuclear power. However, hydropower does cause indirect GHGs emissions, mainly during the construction and flooding of the reservoirs. This may be due to decomposition of a fraction of the flooded biomass (forests, peat lands, and other soil types) and an increase in the aquatic wildlife and vegetation in the reservoir (Hydro Quebec 2009). Hydropower's GHG emissions factor (4 to 18 grams CO_2 equivalent per kilowatt-hour) is 36 to 167 times lower than the emissions produced by electricity generation from fossil fuels. Run-of-the-river systems produce less GHG emissions (5 to 10 g CO_2 equivalent per kilowatt-hour) due to absence of reservoirs (Gapnon and van de Vate 1997, 2002; Meier 2002; Tremblay et al. 2002). Compared to other renewables, on a lifecycle basis, hydropower releases fewer GHG emissions than electricity generation from biomass and solar and about the same as emissions from wind, nuclear, and geothermal plants (Meier 2002).

Emerging trends, driven by more sophisticated energy markets, volatile energy prices, climate change, and increased attention to water management and regional integration, are changing the value proposition of hydropower in development.

24.3.4 Solar Photovoltaics and Thermal

Photovoltaic is simply the direct conversion of light into electricity at the atomic level. Some substances are capable of exhibiting a characteristic known as the photoelectric effect that causes them to absorb light photons and releases electrons. The free electrons are finally captured, resulting in electric current which can be utilized as electricity as represented in Figure 24.7. Solar cells are made of the same kinds of semiconductor materials, such as silicon, used in the microelectronics industry. For solar cells, a thin semiconductor wafer is specially treated to form an electric field, anode on one side and cathode on the other.

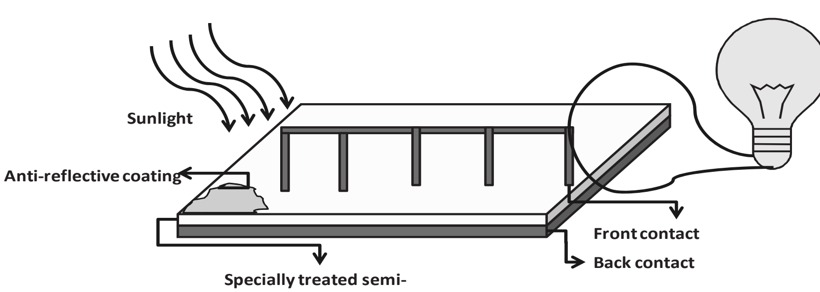

Figure 24.7. Schematic of a typical photovoltaic cell

Existing commercial solar cell converts solar energy into electricity with a relatively low efficiency (< 20%) so that in the event, more than 80% of the absorbed energy is dumped to the environment after electric energy conversion. Some researchers have investigated the possibility of developing hybrid photovoltaic (PV) and thermal (PV/T) collectors (Bergene and Bjerke 1993; Bergene and Lovik 1995; Fujisawa and Tani 1997). The PV/T collector generates electric power and simultaneously produces hot water. The overall efficiency thus increases. The solar photovoltaic and solar thermal methods encompass various pros and cons as illustrated in Table 24.3. The biggest challenge for solar thermal is the amount of space required for efficient production of energy; in fact it's the space that gets a consistent amount of direct sunlight. Solar thermal power plants typically require 1/4 to 1 square mile or more of land. In the present situation, solar photovoltaic and solar thermal systems are current solar electricity supreme, but more improvements are needed to compete with the cost of the lowest-cost fossil fuels in a legislative climate without subsidies or carbon taxes.

Table 24.3. Pros and cons of solar photovoltaic and solar thermal systems

Solar photovoltaic systems	
Pros	**Cons**
It produces clean, green electricity for several decades.	Greater capital investment & longer payoff (10+ years)
The electricity produced by the system can offset 60% or more of a household's energy needs, depending on energy use and system size and orientation.	Average efficiency for solar panels remains under 20%
Peak production coincides with peak energy needs in the summer. Solar panel systems can power demanding appliances like refrigerators and air conditioning without stressing the grid.	Expensive raw materials translate to higher equipment costs
Solar panels can protect & extend the life of roofs or even be integrated directly into a building for a more aesthetic appearance.	More roof space required
Solar thermal systems	
Pros	**Cons**
Up to 70% efficient in collecting heat energy from the sun; less roof space required.	Less effective in the winter
Reduces electricity and gas bills by using the sun to warm water and spaces.	Peak performance in summer coincides with least need for heating
Lower capital investment and shorter payback period (3-5 years).	Less versatile than solar photovoltaic
Dependable, less complex technology already used extensively in Asia & Europe	

24.3.5 Energy from Wastes

Population explosion and the consumption habits of modern lifestyles of consumer are causing huge worldwide waste management problems. Waste feedstock comprise municipal solid waste (MSW); construction and demolition (C&D) debris; agricultural wastes, such as crop silage and livestock manure; industrial waste from coal mining; agro-industrial wastes and their by-products. Solid waste generated at domestic level is the single largest component of all wastes generated. Approximately 300-600 grams of solid waste is generated per person per day (Gujarat Energy Development Agency 2003). Ultimately, municipalities face the problems of urban waste collection, processing/treatment and disposal of voluminous solid wastes in most of the countries. These organic solid wastes rich in nutrients are susceptible to microbial degradation which enhances the spread of infectious diseases. Many developed nations are facing the problem of safe disposal of wastes. Owing to their rich organic contents, the solid wastes can be a good resource to harvest microorganisms for value-added products and energy. Research is in progress to develop new pragmatic ways to recycle wastes by generating energy, such as electricity from landfill wastes.

The municipal solid waste has four fates: recycling, composting, landfilling and waste-to-energy via incineration. According to the US Environmental protection agency (EPA), the municipal waste comprises total waste excluding industrial waste, agriculture waste and sewage sludge. It includes durable goods, non-durable goods, containers and packaging, food wastes, yard wastes and miscellaneous inorganic wastes from residential, commercial, institutional and industrial sources, such as home appliances, newspapers, clothing, food scrapes, kitchen leftovers, boxes, office and classroom paper, wood pallets, rubber tires and cafeteria wastes, among others (U.S. Energy Information Administration 2008).

Today, a new generation of waste-to-energy technologies are emerging, such as: thermal technology which holds the potential to create renewable energy from both inorganic and organic wastes; physical technologies which process waste to make it more useful as fuel; biological technologies in which organic waste is digested by microorganisms to yield fuel as described in Figure 24.8. Advanced waste-to-energy technologies can be used to produce biogas (methane and carbon dioxide), syngas (hydrogen and carbon monoxide), biofuels (bioethanol and biodiesel) and pure hydrogen. These fuels can then be potentially converted to electricity. Different types of routes can be followed for the production of different renewable energy resources.

Physical. This is a mechanical process in which waste is converted to forms which are more suitable for use as fuel, producing refuse-derived fuel (RDF) or solid recovered fuel (SRF). RDF is a fuel produced by either shredding solid waste, such as municipal solid waste, construction and demolition (C&D) debris, or sludge or treating it with high-pressure steam in an autoclave at 121°C. RDF comprises largely of organic materials taken from solid waste streams, such as plastics or biodegradable waste. The municipal waste is first processed in order to remove non-combustible materials, such as glass, metals, and other materials, many of which can then be recycled. Sterilization kills viruses and other potential pathogens, and it also causes plastics to soften and flatten, paper and other fibrous material to disintegrate. Autoclaving reduces the volume of the waste by up to 60%, and the residual material can then be compressed into pellets or bricks and sold as solid fuel. Burning RDF is more clean and efficient than incinerating MSW or other solid waste directly; however the process augments the costs (The Cleantech Report 2007).

Thermal. Thermal waste-to-energy technologies use heat or combustion to treat wastes. Methods employed in the thermal technology are: 1) combustion; 2) pyrolysis; 3) thermal gasification; and 4) plasma-arc gasification.

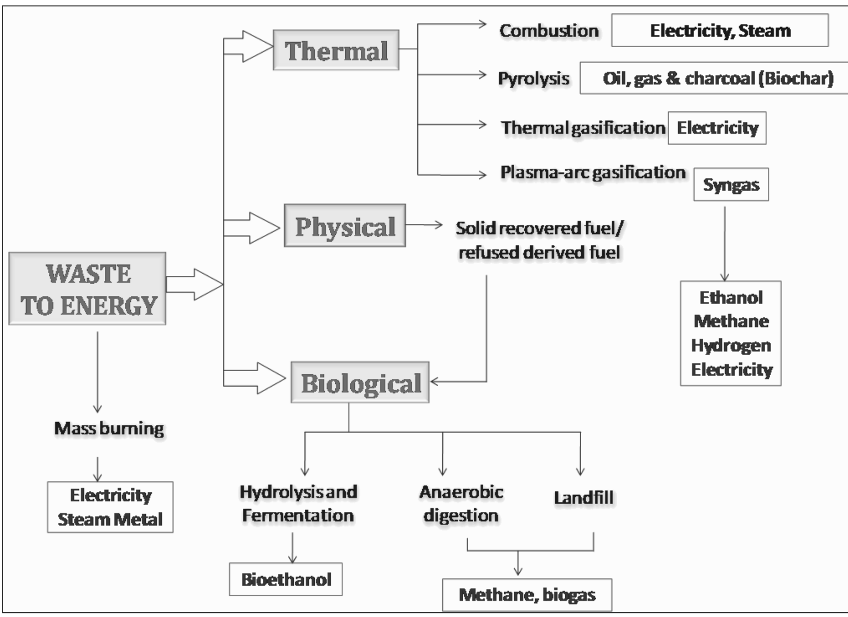

Figure 24.8. Different routes of transformation of waste to energy (modified from The Cleantech Report, 2007)

Combustion. Municipal waste can be directly combusted in waste-to-energy incinerators as a fuel with minimal processing, in a process called "mass burn." Heat produced during the combustion process is used to turn water into steam, which is then applied to power a steam-turbine generator to produce electricity. Advanced next generation waste incinerators also incorporate air-pollution control systems, although ash or other pollutants captured in this process must still be disposed of (The Cleantech Report 2007; Energy Technology Bulletin, 2012). In this context, still there is a need to develop such control systems which can help to eliminate or alleviate the effects of these pollutants in the environment.

Pyrolysis. In this process, heat is used to break down organic materials in the absence of oxygen, producing a mixture of combustible gases, such as methane, complex hydrocarbons, hydrogen, and carbon monoxide and liquids, and solid residues (Belgiorno et al. 2003). Waste-film plastic can be converted to synthetic diesel fuel using low-temperature pyrolysis. "Biochar" a kind of charcoal is a valuable by-product of pyrolysis which can be used as a fertilizer and it can also be used to absorb CO_2 and other emissions from coal dependent power plants (The Cleantech Report 2007).

Thermal Gasification. As compared to pyrolysis, thermal gasification of waste takes place in the presence of limited amounts of oxygen. The gas generated by either of these processes can be used in boilers to provide heat, or it can be cleaned up and used in combustion turbine generators. While incineration converts the input waste into energy onsite, pyrolysis and thermal gasification allow the production of fuel that can be transported. In addition, the gases, oils and solid char from pyrolysis and gasification can also be purified and used as a feedstock for chemical production and for other applications (Belgiorno et al. 2003; The Cleantech Report 2007).

Plasma-Arc Gasification. This technology uses a plasma-arc torch to produce temperatures as high as 13,000°F. The extreme heat breaks down wastes, forming syngas (hydrogen and carbon monoxide) and a rock-like solid by-product called slag, which can be used in construction or road asphalt. The syngas produced can be converted into a variety of marketable fuels, such as ethanol, methane, and hydrogen or it can be used to generate electricity directly. Plasma converters could consume nearly any type of waste, including concrete, steel, and toxic chemicals, but the technology requires large energy inputs (The Cleantech Report 2007).

Biological. Recently, biological waste-to-energy technologies are gaining momentum in relation to green technologies. In biological method, microbes or other organisms are used to produce fuels from waste. Various biological methods are employed for hydrolysis of waste to produce energy, such as: 1) landfilling; 2) biogas plants; and 3) fermentation.

Landfill. It is still the principal method of disposal of municipal solid waste and construction and demolition(C&D) debris in the U.S. and many other countries. Landfill wastes, if left undisturbed produce considerable amounts of gaseous by-products, consisting mainly of carbon dioxide and methane. The landfill gas (biogas) is produced by the anaerobic digestion of organic matter. A consortium of microbes exists in the environment and these microbes individually secrete enzymes needed for anaerobic digestion. Different bacterial populations are involved in this process, which degrade organic compounds to produce a valuable high energy mixture of gases, such as methane and carbon dioxide (Lastella et al. 2002), as presented in Figure 24.9. Apart from treating the wastewater and energy generation, anaerobic digestion of biodegradable waste also results in the reduction of greenhouse gas emissions. It would not only substitute the use of fossil fuels but would also use methane generated from the waste (Kansal et al. 1998). Some other advantages of anaerobic degradation include: low energy requirement, low nutrient requirement, a high efficiency in reducing COD (chemical oxygen demand) in soluble and insoluble forms and no chemical handling (Forday and Greenfield 1983; Massé and Masse 2000). This method of waste treatment is therefore practical and economical.

Carbon dioxide and methane are both GHGs that increase the risk of climate change when they are released unchecked into the atmosphere, but methane is also a useful source of energy and therefore worth collecting as a biogas. Landfill gas can be captured via a collection system, which usually comprises of a series of wells drilled into the landfill and connected by a plastic piping system. The crude biogas can be burned directly in a boiler as a heat-energy source or can be cleaned by removing water vapor and sulfur dioxide and can be used directly in internal-combustion engines, or for electricity generation via gas turbines or fuel cells.

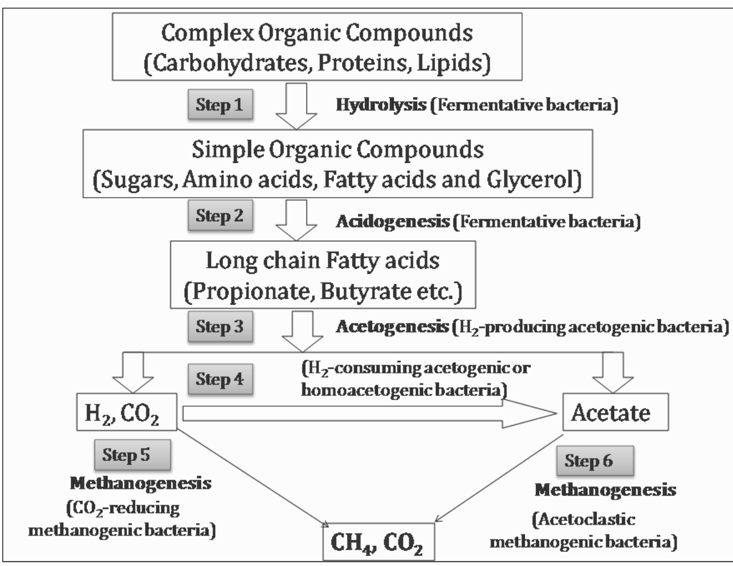

Figure 24.9. Metabolic steps and microbial groups involved in anaerobic digestion (modified from Novaes 1986)

Among all the potential methods of waste management, anaerobic digestion offers promising energy savings and is more stable process for medium and high strength organic effluents. Highly efficient waste-to-energy (WTE) plants based on anaerobic digestion of biomass harvest the untapped renewable energy potential of organic wastes by converting the biodegradable fraction of wastes into high calorific gases, such as biogas. The methane produced from biogas plants can be used to treat wastewater and for generation of electricity, industrial and domestic heating purposes (Zafar 2008).

Anaerobic digestion of wastes not only decreases GHGs emissions but also reduces dependence on fossil fuels for energy needs. Recently, with increasing use of anaerobic process for treating various natural resources, the anaerobic waste treatment plants would become more economically competitive. It offers several advantages over other methods of waste treatment which can be categorized into three groups: 1) environmental; 2) energy; and 3) economic benefits as presented in Table 24.4.

Biogas Plants. Biogas can be produced by anaerobic digestion either naturally (landfill gas) or in a controlled environment, such as a biogas plant. Food-processing waste or other agricultural wastes, such as manure can be used as feedstock in biogas plants. The process starts with the placement of waste and various types of bacteria into an airtight container called a digester. Advanced anaerobic digester systems can produce biogas with pure methane content up to 95%. The biogas can then be either used directly to run boilers or cleaned and supplied as natural gas. Biogas plants can either transfer electrical energy to the main utility grid or they can also generate power for use on-site in applications, such as lighting, processing plants, ethanol plants, and greenhouses (The Cleantech Report 2007). Nowadays, biogas plants have been deployed in India, Israel and Australia among other countries.

Table 24.4. Benefits of anaerobic digestion

Environmental benefits	Energy benefits	Economic benefits
• Capable to accommodate relatively high organic loads • Elimination of toxic (Malodorous) compounds • Reduction of pathogens • Deactivation of weed seeds • Reduced dependence on inorganic fertilizers by capturing and reuse of nutrients • Production of sanitized compost • Reduction in GHGs emissions in the atmosphere • Promotion of carbon sequestration • Beneficial use of recycled water • Protection of groundwater and surface water resources • Improved social approval	• Net energy-producing process • Biogas produced via this process represents high-quality renewable fuel • Surplus energy in the form of electricity and heat is also produced • Reduces reliance on energy imports and renewable fuels • Biogas is a potential source of electricity, heat and transportation fuel	• Transforms waste problems into new profitable energy sources • Adds value to negative value feedstock • Anaerobic digestion is a potential source of income, such as from sale of organic fertilizer, carbon credits and sale of power • A biomass-to-biogas conversion technique reduces water use • Reduces dependence on energy imports • Anaerobic digestion plants helps to increase self-reliance • Anaerobic digestion helps to minimize time needed for transporting, handling and processing wastes

Substrates for Anaerobic Digestion Plants. An array of feedstock is available as a substrate for anaerobic processes, such as various solid and liquid wastes, including municipal secondary waste, fruit industry waste and their by-products, breweries, sugar mills, distilleries, food-processing industries, tanneries, paper and pulp industries, among others. Among all the industrial sectors, food industries alone contribute 40% of the total organic pollution. Agro-based industries including food industries contribute 65–70% of the total industrial wastewater in terms of organic load (Zafar 2008).

Fermentation. Fermentation uses yeast to generate liquid ethanol from biomass waste. Different biomass based waste substrates are available for bioethanol production, such as paddy, wheat and maize straw, sorghum and sunflower stalks, fruit and vegetable residues, agro-industrial wastes and their by-products, sugar industry by-products, such as bagasse, molasses which represents lignocellulosic wastes. Lignocellulose represents the second most abundant biopolymer on Earth. Bioethanol production from lignocellulosics holds a key to solving world's energy problems.

Due to limited availability of molasses and alternative uses of molasses and starchy materials, agricultural biomass which is available in abundance has the potential for conversion into ethanol for use as biofuel. The conversion of lignocellulosics to bioethanol holds great promise as these residues can be enzymatically sachharified to hexose and pentose sugars after certain pre-treatments required for making the residues amenable for enzymatic action. However, commercial cellulosic ethanol is not all that simple as it appears; it requires different biochemical, microbiological, biotechnological and chemical approaches in conjunction for pilot scale feasible ethanol production from agricultural biomass.

With diminishing fossil fuel based oil supplies, the world is facing a major energy risk which needs to be solved by virtue of alternative energy sources. In the last decades, bioethanol has received considerable interest in the transportation sector because of its efficacy as an octane booster, fuel additive and clean fuel (Banerjee et al. 2010). Bioethanol based vehicles holds key for reducing reliance on fossil fuels. Moreover, due to clean burning nature of bioethanol, it would also help to alleviate GHGs emission in the atmosphere.

The generation and disposal of organic wastes without proper treatment alleviates the risks of human health concerns and environmental pollution which jeopardizes the lives of flora and fauna, including humans. Degradation of wastes leads to uncontrolled release of GHGs into the atmosphere. Various conventional methods, such as aeration is energy intensive, expensive and generates a large quantity of biological sludge. Various advanced strategies could be employed for the sustainable utilization of organic wastes to produce energy which would also lessen our dependence on fossil fuels which are on the verge of depletion.

24.3.6 Geothermal

Geothermal energy is the heat energy that occurs naturally in the earth core. In nature, geothermal heat is released up in the form of volcanoes, hot springs and geysers. This heat is produced from radioactive decay beneath the earth's surface. It is concentrated in certain locations, and is close enough to surface waters to be brought to the surface for many different purposes (http://iceland.ednet.ns.ca/schedule.html). For the last few centuries, humans have used naturally occurring hot water springs for many applications. In recent years, geothermal energy has been used to produce electricity and to provide heat for homes and industries. Geothermal energy is considered as a versatile and reliable source of heat and electricity which does not emit GHGs associated with the combustion of fossil fuels. Unfortunately, the finest geothermal resources are concentrated in areas of volcanic activity and are not widely distributed. Geothermal energy is used on a significant scale in some countries, such as California in the US, Iceland, Italy, New Zealand and Japan (USDOE 2009). Geothermal energy represents 0.2–3% of the world's total electric power shared between industrialized and developing countries. These figures indicate that geothermal energy plays a minor role in the world energy scene. However, with their currently limited electrical consumption but good geothermal prospects, the developing countries could achieve relatively significant contribution to their total electric energy from that of geothermal origin, increasing at the moment from 3 to 19% (Barbier 1986). The total potential of the world geothermal energy is equivalent of 40,000 GW while the total world energy demand is only 15,000 GW (World Geothermal Congress (2010). Currently, the worldwide capacity of geothermal power plants is over 9000 MW. The energy cost of geothermal energy power plants is comparable to wind energy. Studies showed that it is feasible to increase the capacity in the US alone to at least 100,000 MW, requiring an investment of up to $1 billion (Post 2004).

24.3.7 Ocean Energy

Energy from the ocean can be harvested in various ways. Different sources for electrical power generation from the oceans include tidal power, wave power, ocean thermal energy conversion, ocean currents, ocean winds and salinity gradients (Seymour 1992; Vattenfall research and development magazine 2009). Among these, the three well-developed technologies comprise: 1) tidal power in which mechanical energy can be derived from the tides; 2) wave power; and 3) ocean thermal energy conversion (OTEC), i.e., thermal energy from the sun's heat.

Ocean mechanical energy, such as derived from tides and wave power is quite different from ocean thermal energy. Tides are driven mainly by the gravitational pull of the moon, and waves are driven primarily by the winds. As a result, tides and waves are irregular sources of energy, while ocean thermal energy is rather invariable. Moreover, the electricity conversion of both tidal and wave energy usually involves mechanical devices which is different from thermal energy. The advantages and disadvantages of the different ocean energy sources are depicted in Table 24.5.

Wave Energy. Wave power has enormous potential for generating electricity from a global prospective. According to Vattenfall research and development magazine (2009), the wave energy is estimated to be the next renewable technology to be commercialized within next 10–15 years. Vattenfall is Europe's 5th largest generator of electricity and the largest generator of heat. The wave power has the large theoretical potential in the order of several thousands of TWh compared to the total electricity consumption in Europe. Wave energy conversion takes advantage of the ocean waves caused primarily by interaction of winds with the ocean surface. For wave energy conversion, there are three basic systems: 1) channel systems that guide the waves into reservoirs; 2) float systems that impel hydraulic pumps; and 3) oscillating water column systems that use the waves to compress air within a container. The mechanical power created from these systems either directly activates a generator or transfers it to a working fluid, water, or air, which then drives a turbine/generator.

A wave energy converter may be placed in various possible locations and conditions in the ocean. It may be floating or submerged completely in the sea offshore or it may be located on the shore or on the sea bed in relatively shallow water. A converter on the sea bed may be completely submerged, it may extend above the sea surface, or it may be a converter system placed on an offshore platform. Apart from wave-powered navigation buoys, however, most of the prototypes have been located at or near the shore (Natgerman 1995). The impact of wave power at deep ocean sites is three to eight times in comparison to wave power at adjacent coastal sites. However, the cost of electricity transmission from deep ocean sites is very high. According to the European Union, among the different converters capable of exploiting wave power, the most advanced is the Pelamis Wave Energy Converter, a type of "undulating sea serpent" developed by Ocean Power Delivery (Shaw 1982).

Still many gaps in this technology remain to be filled, including cost reduction, efficiency and reliability improvements, identification of suitable sites, interconnection with the utility grid, better understanding of the impacts of the technology on marine life and the shoreline. Demonstration of the ability of the equipment to survive the salinity and pressure environments of the ocean as well as weather effects on the life of the facility is also crucial.

Tidal Energy. Another potential form of ocean energy is called tidal energy. The use of tidal energy dates back to the 11th century, when small dams were built along ocean estuaries and small streams. The tidal water behind these dams was used to turn water wheels to mill grains. A barrage/dam is normally required to convert tidal energy into electricity by forcing the water through turbines and activating a generator. When tides come into the shore, they can be trapped in reservoirs behind dams. Later, the water behind the dam can be let out to a regular hydroelectric power plant (The California energy commission 2009).

Relatively large increases in tides i.e. at least 16 feet distance between low tides to high tides is required for the tidal energy to work efficiently. There are only a few places where this tide change occurs around the earth. Some power plants are already operating based on this strategy. According to the European Union, 90% of today's worldwide ocean energy production is represented by a single site ‘‘the La Rance Tidal Power Plant’’ having capacity of 240 MW, which was commissioned in 1966. This power plant installation has remained unique in the world and has only been reproduced at much smaller capacities in Canada (20 MW), China (5 MW) and Russia (0.4 MW) (The California energy commission 2009).

Table 24.5. Comparison of ocean energy technologies

Technology	Advantages	Disadvantages
Wave Energy	• Significant resource. • Converters can be placed offshore at sea level reducing visual impact of device and increasing public acceptability • Wave energy is not synchronised with wind energy, which could possibly lead to reduced reserve power requirements • No impact on bird migration	• The technology is currently in developmental phase with no commercial systems currently available with demonstrated reliability. The technology lacks demonstration experience. • Wave converters must be capable of surviving extreme weather • loading which may add to the cost of the design • Maintenance costs may be high. • Disturbance or destruction of marine life (including changes in the distribution and types of marine life near the shore) • Possible threat to navigation from collisions due to the low profile of the wave energy devices above the water, making them undetectable either by direct sighting or by radar. • Interference of mooring and anchorage lines with commercial and sport-fishing • Degradation of scenic ocean front views from wave energy devices located near or on the shore, and from onshore overhead electric transmission lines • Irregular and oscillating low-frequency energy
Tidal Energy	• Outputs are predictable and regular, reducing the scale and cost of reserve power • No impact on bird migration.	• The technology is currently in a developmental phase with no commercial systems currently available with demonstrated reliability. The technology lacks demonstration experience • May be water depth limited to 20-40m • Growth of marine life on structures may impact on performance. • Turbines must be lifted out of the water in order to service components. This must occur in regions of high current velocity which may create access and maintenance issues. • High current velocities can occur in estuaries and bays which are used for leisure activities. This may impact on public acceptance. • Unknown environmental impacts associated with extraction of tidal energy.
Solar energy	• Solar Energy is clean, renewable and sustainable, helping to protect our environment • It does not pollute our air by releasing carbon dioxide, nitrogen oxide and sulphur dioxide into the atmosphere like many traditional forms of electrical generation does • Solar Energy does not contribute to global warming, acid rain or smog • It actively contributes to the decrease of harmful greenhouse gas emissions • Solar Energy does not contribute to the cost and problems of the recovery and transportation of fuel or the storage of radioactive waste as it not using any fuel, • Solar Energy systems are virtually maintenance free and will last for decades	• The initial cost is the main disadvantage of installing a solar energy system, largely because of the high cost of the semi-conducting materials • The cost of solar energy is also high compared to non-renewable utility-supplied electricity. As energy shortages are becoming more common, solar energy is becoming more price-competitive • Solar panels require quite a large area for installation to achieve a good level of efficiency • The efficiency of the system also relies on the location of the sun, although this problem can be overcome with the installation of certain components • The production of solar energy is influenced by the presence of clouds or pollution in the air • Similarly, no solar energy will be produced during night time although a battery backup system and/or net metering will solve this problem

Source: Modified from Ocean Energy in Ireland (Oct. 2005); The California energy commission (2009).

This project was abandoned for many years due to its very high initial investment costs as well as the strong local impact that result from it. However, the present economic situation has encouraged South Korea to build a 260 MW dam closing off Sihwa Lake, which is set to be commissioned in 2009. Many advanced techniques, such as hydro turbines are being developed today to harness ocean currents (http://ec.europa.eu/energy/atlas/html/wave.html).

Ocean Thermal Energy Conversion (OTEC). Oceans represent more than 70% of Earth's surface, making them the world's largest solar energy absorbers. The Sun's heat warms the surface water more than the deep ocean water, and this temperature difference creates thermal energy. Small portion of the heat trapped in the ocean could power the world. Thermal energy derived from oceans is used for many applications, including electricity generation. There are mainly three types of electricity conversion systems: closed-cycle, open-cycle and hybrid. Closed-cycle systems utilize the ocean's warm surface water to vaporize a 'working fluid', which has a low-boiling point, such as ammonia. The vapour then expands and turns a turbine. The turbine then activates a generator to produce electricity. Open-cycle systems actually boil the seawater by functioning at low pressures. The steam produced then passes through a turbine/generator. However, hybrid systems work on the combined principle of both closed-cycle and open-cycle systems (http://www.energy.ca.gov/oceanenergy).

The use of the concept of temperature of water to produce energy actually dates back to 1881 when a French Engineer by the name of Jacques D'Arsonval first thought of OTEC. Power plants can be built that use the difference in temperature to produce energy. A difference of at least 38^{o}F is required between the warmer surface water and the colder deep ocean water. The utilization of this type of energy source is called Ocean Thermal Energy Conversion (OTEC). The cold ocean water can also be used to cool buildings leaving desalinated water as a by-product. The system was demonstrated in Hawaii at the Open Cycle Ocean Thermal Energy Conversion (OC-OTEC) system located at the Natural Energy Laboratory of Hawaii Authority (NELHA) at Keahole Point on the Big Island of Hawaii.

24.4 International Bodies Involved in Promoting Ocean Energy

24.4.1 The European Commission

The European Commission has been promoting wave-related activities in a number of areas over a considerable length of time. It has promoted collaboration between leading organizations and institutes, via the formation of a Thematic Network (www.waveenergy. net) and a Coordinated Action (www.ca-oe.net). The main objective is to strengthen the development of the markets and technology for ocean energy in the European Union; act as the central network for information exchange and EU financial resources to its members and the promoting of the ocean energy sector by acting as a single EU voice (www.eu-oea.com/). It has made direct contributions towards developing particular technologies, such as shoreline Oscillating Water Column (OWCs) at Pico in the Azores, the Wave Dragon (www.wavedragon.com), the Sea wave Slot-Cone Generator (SSG) (www.waveenergy.no) and the SEEWEC (a multinational project to build a device containing an array of wave energy floats, www.seewec.org/). Presently, the European Commission is considering supporting several other wave devices as well as the European Ocean Energy Association, both within and outside Europe (World Energy Council 2007).

24.4.2 The International Energy Agency (IEA)

The International Energy Agency is an intergovernmental organization which acts as energy policy advisor to 28 member countries in their effort to ensure reliable, affordable and clean energy for their citizens. IEA was founded during the oil crisis of 1973-74, to co-ordinate measures in times of oil supply emergencies. With the change of energy markets, IEAs mandate has broadened to incorporate the "3 E's" of balanced energy policy making: energy security, economic development and environmental protection. Current objectives focus on climate change policies, market reform, energy technology collaboration and outreach to the rest of the world, especially key consumers and producers of energy like China, India, Russia and the OPEC countries. In 2001, IEA formed an Implementing Agreement on Ocean Energy (www.iea-oceans.org), which is the IEA's mechanism for providing a framework for international collaboration in energy technology R&D, demonstration and information exchange. IEA has grown from the original three member countries (Denmark, Portugal and the UK) to nine (Belgium, Canada, the European Commission, Ireland, Japan, USA), with several other countries having been invited to join, including Brazil, France, Germany, Italy, Mexico and Norway. The increasing number of IEA member countries will reflect on how ocean energy is increasingly seen as viable and important future energy source. The implementing agreement has so far completed two important activities: 1) Review, Exchange and Dissemination of Information on Ocean Energy Systems; and 2) Development of Recommended Practices for Testing and Evaluating Ocean Energy System (http://www.iea.org).

24.4.3 The European Marine Energy Centre (EMEC)

The European Marine Energy Centre has been established in the Orkney Islands with support from a various organizations, such as Scottish and UK government bodies and the European Commission. It provides four test sites in 50 m water depth for wave energy devices, each with its own subsea cable, as well as a monitoring station and other facilities (www.emec.org.uk). The Centre has hosted a number of wave energy devices (as well as tidal current devices at a nearby site) and is proving crucial guidelines and support in establishing wave energy as a reliable energy source, such as allowing developers to demonstrate their technologies in real sea conditions, and coordinating activities around performance measurement and design standards (World Energy Council 2007).

24.5 Conclusions

The electricity sector is a major source of the carbon dioxide emissions that contribute to global climate change. Although climate change may not be the prime motivation behind the use of green technologies, the use of renewable or alternative energy can certainly deliver significant GHG emissions reductions. Switching a substantial fraction of world's electricity generating capacity from fossil fuels to renewable technologies, such as geothermal, biomass, or wind-powered turbines would help to reduce carbon emissions from this sector. Further, the entry of wastes into this sector is a recent and ensuing trend. Waste-to-energy technologies can address two sets of environmental issues: a) land use and pollution from landfills; and b) the well-known environmental peril of day-by-day depleting fossil fuels by replacing it with renewable fuel. Thus, development of green fuels is an important step towards reduction of GHGs emissions and mitigates climate change.

24.6 Acknowledgements

The authors are sincerely thankful to the Natural Sciences and Engineering Research Council of Canada (Discovery Grant 355254), FQRNT (ENC 125216) and MAPAQ (No. 809051) for financial support. The views or opinions expressed in this chapter are those of the authors.

24.7 References

Barbier, E. (1987). ''Geothermal energy in the world energy scenario.'' *Geothermics* 15(5–6), 807–819.

Banerjee, S., Mudliar, S., Sen, R., Giri, B., Satpute, D., Chakrabarti, T., and Pandey, R. A. (2010). ''Commercializing lignocellulosic bioethanol: Technology bottlenecks and possible remedies.'' *Biofuels BioproductsBiorefeneries*, 4(1), 77–93.

Belgiorno, V., de Geo, G., Rocca, C. D., and Napoli, R. M. A. (2003). ''Energy from gasification of solid wastes." *Waste management*, 23(1), 1–15.

Bergene, T., and Bjerke, B. (1993). ''Thermodynamic considerations concerning the efficiency and possible utilization of combined quantum/thermal solar energy converters.'' *Proceedings ISES Solar World Congress*, Budapest. 4, 25–30.

Bergene, T., and Lovik, O. (1995). ''Model calculations on a flat-plate solar heat collector with integrated solar cells.'' *Solar Energy*, 55(6), 453–462.

Blanco M. I. (2009). ''The economics of wind energy.'' *Renewable and Sustainable Energy Reviews*, 13, 1372–82.

Clausen, N-E., Per L., Rebecca B., Hannele H., Timo L., and Sara C. P. (2007). Wind power. In: Jes, F. (Ed.), *Impacts of Climate Change on Renewable Energy Sources, their Role in the Nordic Energy System*. ISBN 978-92-893-1465-7, Nordic Co., June 22, 2007, 192 p.

Dai Y., and Ren, D. (2005). ‘‘Review the status and effects of renewable energy of China in term of the energy issues faced by China during the national economy development.’’ *Renewable Energy*, 2, 4–8.

de Vries, E. (2008). ‘‘40,000 MW by 2020: Building offshore wind in Europe.’’ *Renewable Energy World*, 36–47.

Dresselhaus, M. S., and Thomas, I. L. (2001). ‘‘Alternative energy technologies.’’ *Nature,* 414(6861), 332–37.

Energy Technology Bulletin (2012). *Naval Facilities Engineering Service Center, Port Hueneme, California Waste-To-Energy Projects*, 1–8. <http://www.arch.hku.hk/research/beer/waste.pdf> (accessed Dec. 2011).

EWEA (European Wind Energy Association) (2007-09). *Contribution of wind power to electricity generation and generation capacity in the EU-27*. <http://www.wind-energy-the-facts.org/en/scenarios-and-targets/chapter-3-contribution-of-wind-power-to-electricity-generation-and-generation-capacity-in-the-eu-27/> (accessed Dec. 2011).

EWEA (2009). *Wind energy. The facts. A guide to the technology, economics and future ofwind power*. London: Earthscan. 568.

Forday, W., and Greenfield, P. F. (1983). ‘‘Anaerobic digestion.’’ *Effluent and Water treatment Journal*, 23, 405–413.

Fujisawa, T., and Tani, T. (1997). ‘‘Binary utilization of solar energy with photovoltaic-thermal hybrid collector.’’ In: ISES 1997 *Solar World Congress*, Aug. 24–28, Taejon, Korea.

Gapnon, L. and Van de Vate, J. F. (1997). ‘‘Greenhouse gas emissions from hydropower: The state of research in 1996.’’ *Energy Policy*, 25(1), 7–18.

Global Wind Energy Council (GWEC) (2005). “Global Wind Power Continues Expansion: Pace of Installation Needs to Accelerate to Combat Climate Change,” press release. Brussels: 4 March 2005.

Goldemberg, J., Johansson, T., Reddy, A., and Williams, R. (2004). ‘‘A global clean cooking fuel initiative.’’ *Energy for Sustainable Development,* 8(3), 5–12.

Grimm, L. T. (2002). *Certifying Hydropower for ‘‘Green.’’ Energy Markets: The Development, Implementation, and Future of the Low Impact Hydropower Certification Program.* Low Impact Hydropower Institute, Portland, Maine.

Gujarat Energy Development Agency (GEDA) (2003). “Waste to energy.” GEDA, Gujarat India. <http://www.geda.org.in/bio/biomass_energywaste.html> accessed Feb. 2012).

GWEC (Global Wind Energy Council) (2005). This report uses installed wind power capacity and electricity generation data from IEA statistics (IEA 2004a), except where indicated.

Herzog, H., Drake, E., and Adams, E. (1997). *CO_2 Capture, Reuse, and Storage Technologies for Mitigating Global Climate Change*. A White Paper Final Report, DOE Order No. DE-AF22-96PC01257.

Hydro Quebec, (2009). ‘‘Greenhouse Gas Emissions and Hydroelectric Reservoirs.’’ <http://www.hydroquebec.com/sustainable-development/documentation/ges.html> (accessed Dec. 2011).

IEA (International Energy Agency) (2007). *IEA energy security and climate policy: assessing interactions.* Paris, France: International Energy Agency, OECD. Available at <www.iea.org.> (accessed Dec. 2011).

IEA (2008). *World energy outlook: 2008.* OECD/IEA. p. 578.

Kansal, A., Rajeshwari, M. B., Balakrishnan, M., Lata, K., and Kishore, V. V. N. (1998). ''Anaerobic digestion technologies for energy recovery from industrial wastewater- a study in Indian context.'' *TERI Information Monitor on Environmental Science*, 32(2), 67–75.

Lastella, G., Testa, C., Cornacchia, G., Notornicola, M., Voltasio, F., and Sharma, V. K. (2002). ''Anaerobic digestion of semi-solid organic waste: biogas production and its purification.'' *Energy Conversion Management,* 43(1), 63–75.

Lewis, G. McD. (2010). ''Estimating the value of wind energy using electricity locational marginal price.'' *Energy Policy*, 38 (7), 3221–231.

Massé, D. I., and Masse L. (2000). ''Characterization of wastewater from hog slaughterhouses in Eastern Canada and evaluation of their in-plant wastewater treatment systems.'' *Canadian Agricultural Engineering*, 42(3), 139–146.

Meier, P. J. (2002). ''Life-Cycle Assessment of Electricity Generation Systems and Applications for Climate Change Policy Analysis.'' Ph.D. Dissertation, University of Wisconsin, Madison <http://fti.neep.wisc.edu/pdf/fdm1181.pdf> (accessed Feb. 2012).

Milford, E. (2007). ''American dream? Tackling climate change in the US.'' *Renewable Energy World*. 36–47.

Natgerman, G. (1995). "Wave Power," in *Encyclopedia of Energy Technology and the Environment*, John Wiley & Sons.

Niels-Erik, C., Lundsager, P., Barthelmie, R., Holttinen, H., Laakso, T., and Pryor, S. C. (2007). ''Windpower." In: Jes, F. (ed.), *Impacts of Climate Change on Renewable Energy Sources, their role in the Nordic Energy System*. ISBN 978-92-893-1465-7. *Nordic publishers*, pp. 1–192.

Novaes, R. F. V. (1986). ''Microbiology of anaerobic digestion.'' *Water Science and Technology*, 18(12), 1–14.

Ocean Energy in Ireland (Oct. 2005). An ocean strategy for Ireland submitted to the department of communications, Marine and Natural Resources.1–44.

Perlack R. D., Wright L. L., Turhollow A. F., Graham R. L., Stokes B. J., and Erbach D. C. (2005). Biomass as Feedstock for a Bioenergy and Bioproducts Industry: The Technical Feasibility of a Billion-Ton Annual Supply. U.S. Department of Agriculture, 1–78.

Pimentel D., Herz M., Glickstein M., Zimmerman M., Allen R., Becker K., Evans J., Hussain B., Sarsfeld R., Grosfeld A., Seidel T.(2002). ''Renewable energy: current and potential issues.'' *Bioscience*. 52(12), 1111–120.

Post, J. (2004). ''Green Energy Options in Caribbean Hospitality Venues.'' <http://www.economicallysound.com/green_energy_options_in_caribbean_hospitality_venues.html> (accessed Feb. 2012).

Ramanathan, V., and Xu, Y. (2010). ''The Copenhagen Accord for limiting global warming: Criteria, constraints, and available avenues.'' *Proceedings of the National Academy of Sciences*, 107(18), 8055–8062.

Saidur, R., Islam, M. R., Rahim, N. A., and Solangi, K. H. (2010). ''A review on global wind energy policy.'' *Renewable and Sustainable Energy Reviews,* 14(7), 1744–1762.

Sawyer, S., Zervo, A. (2009). Report on Global Wind Energy. ''General Global Wind Energy Council. '' 68 pp.

Seal, K. S. (1992). ''Animal wastes as a source of biomass production.'' *Outlook on Agriculture*, 21, 91–97.

Seymour R. J. (1992). ''Ocean Energy Recovery: the State of the Art.'' *American Society of Civil Engineers*. 1-313.

Shaw Ronald (1982). *Wave Energy: A Design Challenge.* Ellis Horwood Limited, England.

Sims R. E. H., Schock R.N., Adegbululgbe A., Fenhann J., Konstantinaviciute I., Moomaw W., Nimir H.B., Schlamadinger B.,Torres-Martínez J., Turner C., Uchiyama Y., Vuori S. J. V., Wamukonya N., Zhang X, (2007). ''Energy supply. 2007." In: Metz B, editors. *Climate change: mitigation.* Contribution of Working Group III to the fourth assessment report of the intergovernmental panel on climate change. Cambridge, United Kingdom and New York, NY, USA: Cambridge University Press. 1–72.

The california energy commission. (2009). ''Ocean Energy.'' <http://www.energy.ca.gov/oceanenergy/index.html> (accessed Jan 2012).

The Cleantech Report, (2007). ''Waste to Energy: 187.'' <www.luxresearchinc.com> (accessed Jan. 2012).

Thornley, P., Upham, P., Huang, Y., Rezvani, S., Brammer, J., and Rogers, J. (2009). "Integrated assessment of bioelectricity technology options.'' *Energy Policy,* 37, 890–903.

Tremblay, A., Varfalvy, L., Roehm, C., and Garneau, M. (2002). ''The Issue of Greenhouse Gases from Hydroelectric Reservoirs: From Boreal to Tropical Regions.'' Table1, p. 3. Available at <http://www.un.org/esa/sustdev/sdissues/energy/op/hydro_tremblaypaper.pdf> (accessed Dec. 2011).

UNEP (United Nations Environment Programme) (2000). "The Vienna Convention for the Protection of the Ozone Layer and the Montreal Protocol on Substances that Deplete the Ozone Layer." ISBN: 92-807-1888-6.

US Department of Energy (USDOE) (2004). *Idaho National Engineering and Environmental Laboratory, Water energy resources of the United States with emphasis on low head/low power resources*. DOE-ID-11111.

US Department of Energy (USDOE) (2009). *Exploring Ways to Use Geothermal Energy*. <http://www.energysavers.gov> (accessed Feb. 2012).

U.S. Environmental Protection Agency (1995). *AP 42*, Fifth Edition, Volume I, Chapter 2: Solid Waste Disposal, <www.epa.gov/ttn/chief/ap42/ch02/index.html> (accessed Jan. 2011).

U.S. Environmental Protection Agency (2005). ''Municipal Solid Waste Generation, Recycling, and Disposal in the United States.'' Office of Solid Waste, Facts and Figures for 2003. <www.epa.gov/epaoswer/non-hw/muncpl/pubs/ msw05 rpt.pdf> (accessed Jan. 2012).

U.S. Environmental Protection Agency (2006). *Market Opportunities for Biogas Recovery Systems: A Guide to Identifying Candidates for On-Farm and*

Centralized Systems. EPA-430-8-06-004, <www.epa.gov/agstar/pdf/biogas%20recovery%20systems_screenres.pdf> (accessed Dec. 2011).

U.S. Energy Information Administration (2008). ‘‘Municipal solidwaste, 2006.’’ <www.eia.doe.gov> (accessed Jan. 2012).

van de Vate, J. F. (2002). ‘‘Full-energy-chain greenhouse-gas emissions: a comparison between nuclear power, hydropower, solar power and wind power.’’ *International Journal of Risk Assessment and Management,* 3(1), 59–74.

Vattenfall research and development magazine (2009). ‘‘Theme: Ocean energy.’’ *R & D Magazine.* 1, 1–16.

Vesterby, M., and Krupa, S. (2001). ‘‘Major Uses of Land in the United States, 1997.’’ *Washington (DC): Resource Economics Division, Economic Research Service, USDA*. Statistical Bulletin No. 973., Oct. 20, 2002. <www.ers.usda.gov/publications/sb973/> (accessed Dec. 2011).

Watson, R. T., Zinyowera, M. C., and Moss, R. H. (1996). *Climate Change 1995–Impacts, Adaptations and Mitigation of Climate Change*.’’ Scientific-Technical Analyses, Contribution of WorkingGroup II to the Second Assessment Report of the Intergovernmental Panel on Climate Change, Cambridge University Press (1996).

World Energy Council. (2007). Survey of Energy Resources. 1–15.

WMO (the World Meteorological Organization) (2012). <http://www.wamis.org> (accessed Feb. 2012).

World Geothermal Congress. (2010). http://www.jakartaupdates.com/233-04/geothermal-alone-could-solve-the-entire-world-energy-problems

Youngquist, W. L. (2000). ‘‘Alternative Energy Sources.’’ <http://www.hubbertpeak.com/youngquist/altenergy.html> (accessed Jan 2012).

Zafar, S. (2008). ‘‘Anaerobic digestion of biomass.’’ <http://www.alternative-energy-news.info/anaerobic-digestion-biomass> (accessed Feb. 2012).

CHAPTER 25

Greenhouse Gases Emissions from Natural Systems: Mechanisms and Control Strategies

Xiaolei Zhang, Song Yan, R. D. Tyagi, Rao Y. Surampalli, and Tian C. Zhang

25.1 Introduction

Greenhouse gas (GHG) is emitted from human activities and natural systems. The former is counted as the major source of the emission (around 70% of total emissions); however, the latter also pronounce a great amount of emission, which is around 4800 $TgCO_2$ equivalent per year (U.S. EPA 2010). The GHG emissions from natural systems majorly include the emissions from wetlands, oceans, freshwater bodies, permafrost, termites, ruminant animals, geologic settings, and wildfire, and among all, wetlands are majorly responsible (Song et al. 2008; Danevčič et al. 2010).

Wetlands are divided into peat wetlands, also called peat lands, and non-peat wetlands (Wilson et al. 2001; Blain et al. 2006). GHGs emitted from wetlands are mainly in the form of methane rather than carbon dioxide and nitrous oxide. Reports have shown that wetlands are one of the primary sources of atmospheric methane, which accounts for 3900 $TgCO_2$ equivalent per year (> 81% of total natural system GHG emissions) (Zhuang et al. 2009; U.S. EPA 2010). The GHG emissions are due to the degradation of organic materials under the anoxic condition. Strategies that are to cut off methane production or diffusion to the atmosphere should be developed for controlling the emissions from wetlands and peat lands. It is known that methane production is due to the domination of methanogenic microorganisms in the system; therefore, it would mitigate methane emission by promoting the growth of methanotrophs and other microbial communities to diminish the growth of methanogens. When the production occurs, capturing and storing it before it enters into the atmosphere would also be a method (Bourrelly et al. 2005; Chathoth et al. 2010).

Compared to wetlands, other natural systems (oceans, freshwater bodies, permafrost, termites, ruminant animals, geologic settings, and wildfire) contribute a small fraction of the GHG emissions from all natural systems (< 20% of total). The emission from oceans and freshwater are not well understood; however, it may be linked with two important factors: a) the result of anaerobic digestion of fish and zooplankton and b) the result of methanogenic microorganism activities in the sediments (Levitt 2011). Billions of tonnes of methane are locked on the Arctic soil, while as permafrost melts, there is a great risk of methane seeping. In fact, it is a vicious circle because as methane emission increases, thawing of permafrost would be enhanced, which would result in more methane emission (Laurion et al. 2010). Termites is considered as the second largest methane emission natural sources (the first largest is wetlands and peat lands). Methane is produced in their normal digestion process, and the production amount varies according to the species and regions. Ruminant animals such as cattle, sheep, and wild animals are methane emission sources as well. The emission is mainly from the digestion, and highly depending in the population of animals. Geothermal-volcanic systems and hydrocarbon-generation processes in sedimentary basins are two major sources of GHG geologic emissions. These emissions have always been neglected or paid little attentions before year of 2000, while over the last ten years studies have been done to confirm that geological GHG emission significantly contributes to the global GHG emission (Etiope and Klusman 2002; Etiope 2009). Wildfires, also called natural forest fires, also causes GHG emission including carbon dioxide and methane, because of incomplete combustion of organic material.

In this chapter, the mechanisms of GHG emissions from natural systems including wetlands, oceans, freshwater, etc., are described; the strategies to control GHG emissions are discussed.

25.2 GHG Emissions from Wetlands

Wetlands (peat and non-peat), a variety of shallow pools of water, are mainly distinguished by microorganisms, plants, and animals that adapt to life under saturated conditions. They are found in almost all climatic zones, occupying 5% of the earth's land area (Adhikari et al. 2009; Lai 2009). They have many valuable functions: they are natural filters to clean water that passes through them; they reduce flood and drought by adsorbing and recharging water accordingly; they trap pollutants to prevent the contamination in steams, reservoirs, and groundwater; and they provide protection and food for wildlife species. Wetlands provide profound benefits for our environment; however, there are also disadvantages. The most remarkable one is GHG emissions due to the great concern of global warming. In this section, GHG emissions from wetlands are discussed.

25.2.1 Mechanisms

GHG emissions from wetlands include two steps, the first one is the production, and the other one is escaping to the atmosphere. The GHG (CO_2, CH_4, and N_2O) production from wetlands is mainly due to microorganism and aqua animal activities (Figs. 25.1 and 25.2) (Dinsmore et al. 2009; Danevčič et al. 2010). Compared to CO_2 and N_2O, methane is the major source of GHG emissions from wetlands. The production of methane is mainly due to methanogenesis. Usually, it is at an anoxic condition in the sediment zone of wetlands. When methanogenesis occurs, methane is produced along with carbon dioxide (Equation 25.1). Thereafter, it enters the atmosphere via aerenchyma of vascular plants (90% of total methane production), ebullition (7% of total methane production) when the pore-water is supersaturated with methane, and diffusion along a concentration gradient (2% of total methane production) (Chanton 2005). Around 1% of the total methane production will be transferred to carbon dioxide by oxidation and methanotrophic bacteria. A variety of factors such as wetland plant productivity, microbial CH_4 oxidation, water table height, and temperature affect rates of wetland CH_4 production and release (Dinsmore et al. 2009; Danevčič et al. 2010). As mentioned earlier, around 90% of methane escape into the atmosphere via aerenchyma of the plants; hence the plants productivity has a profound effect on methane emission from wetland. In addition, it was reported that plants also influent the microorganism variety through altering substrate availability, competing for nutrients, and creating microenvironments of aerobic conditions (King and Reeburgh 2002; Bardgett et al. 2003; Saarnio et al. 2004). Reports revealed that methane emission from wetland relied on plants species as each species had its unique physical trait which influents the gaseous transport pathway and below ground oxidation levels and microbial metabolism (Strom et al. 2005; Kao-Kniffin et al. 2010). Studies also showed that the emission strongly depends on the temperature and water table level (Huttunen et al. 2003; Watanabe et al. 2009). The temperature effect on methane emission can be understood as temperature impacts the metabolic rate of methane production or consumption by bacteria, while the water table level effect is mainly because of the enhancement of high water table level on anaerobic CH_4 production (Huttunen et al. 2003).

$$CH_3COOH \rightarrow CO_2 + CH_4 \qquad \text{(Eq. 25.1)}$$

Carbon dioxide is another contributor of GHG emissions from wetlands (Fig. 25.1). As stated, one part of the emission of carbon dioxide is from methane conversion. In addition, carbon dioxide is generated during methanogenesis (Equation 25.1). Aqua animals such as fish also cause carbon dioxide emissions. However, generally the GHG emissions from carbon dioxide can be omitted because the emitted carbon dioxide from wetlands is less than the carbon dioxide uptaken by plants (Danevčič et al. 2010).

Nitrous oxide is the most potent GHG as it accounts 300 times more effective than carbon dioxide at retaining atmosphere energy. The emission of N_2O from wetlands is due to the denitrification process which normally takes place in waterlogged soils with abundantly available carbon and nitrogen (Hashidoko et al. 2008; Danevčič et al. 2010). Nitrate enters wetlands in excessive amount due to human activities such as farming, which leads to a high rate of denitrification (Equation 25.2) in which the intermediate product, N_2O is produced and escapes into the atmosphere (Fig. 25.2).

$$NO_3^- \rightarrow NO_2^- \rightarrow NO + N_2O \rightarrow N_2\ (g) \qquad \text{(Eq. 25.2)}$$

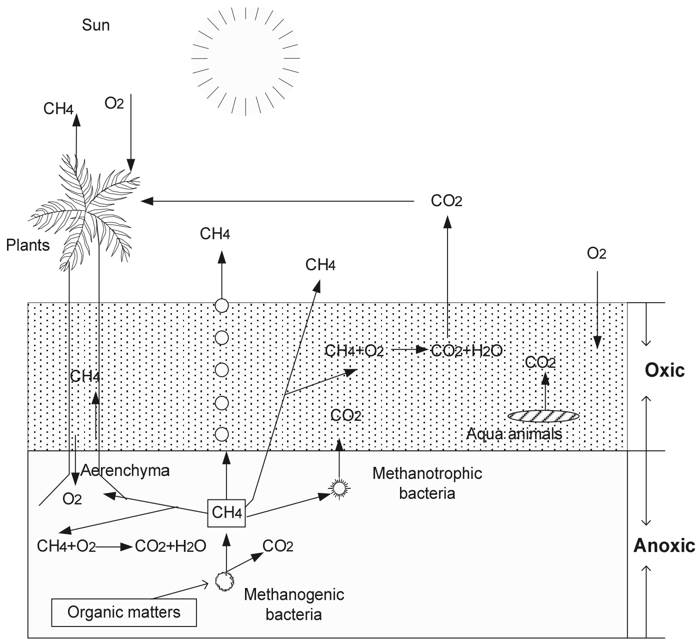

Figure 25.1. Methane and carbon dioxide emissions from wetlands

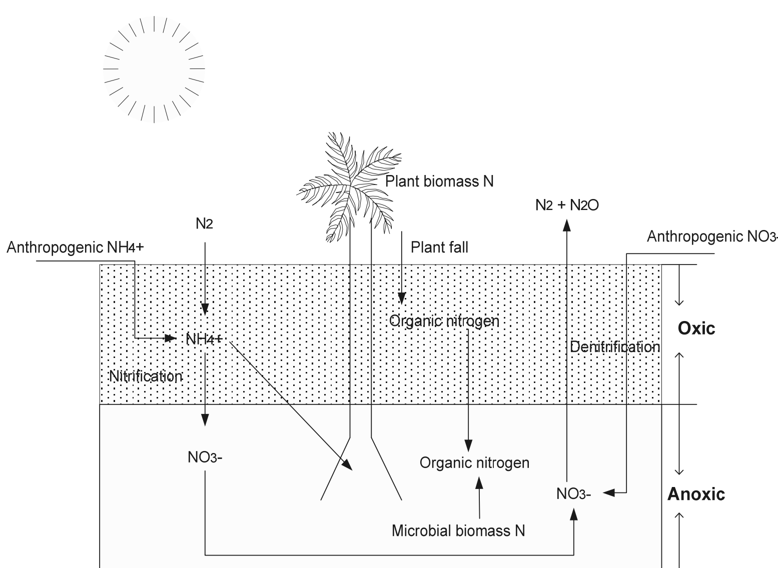

Figure 25.2. Nitrous oxide emission from wetlands

Apart from dinitrification, N_2O also can be produced during the nitrification process. There are two pathways of nitrous oxide production in the nitrification process (Smith 1982; Webster and Hopkins 1996): one is that nitrifying bacteria will produce nitrous oxide from dissimilatory reduction of NO_3^- under the limited oxygen supply condition; the other is that nitrous oxide can also be produced by nitrifying bacteria during NH_4^+ oxidizing to NO_2^-. There are also other processes that would result in nitrous production such as dissimilatory NO_3^- reduction to NH_4^+, fungal denitrification, and NO_3^- assimilation (Bleakley and Tiedje 1982; Smith 1983; Schoun et al. 1992).

25.2.2 Control Strategies

As mentioned above, the GHG emissions from wetlands mainly refer to methane and nitrous oxide emission since a very small amount of the emission is contributed by carbon dioxide, and most of the emitted carbon dioxide is considered to be captured by the wetland plants again. The control of methane and nitrous oxide emissions are discussed below.

Methane Emission Control. Reducing the emissions of GHGs is very important due to their effect on global warming. As the biggest contributor of GHG emissions from wetlands, methane can be controlled by three ways.

Biogeochemical processes, especially the availability of inorganic electron acceptors, might have important consequences for C cycling in wetlands. It has been suggested, based on field studies and laboratory assays, that CH_4 production and emissions in peatlands can be suppressed under high atmospheric deposition levels of sulfate (Watson and Nedwell 1998). In consideration of competitive suppression hypothesis, since methanogens is the cause of methane emission, promoting the growth of methanotrophs, iron oxidizing bacteria and other microbial communities to diminish the growth of methanogens would be a method to control the emission. The biological system of wetlands is complicated. Many other types of microorganisms exist in the system as well as methanogens. In sulfate-rich marine and brackish environments, sulfate-reducing bacteria effectively outcompete methanogens, and CH_4 production is observed as being low in such environments (Watson and Nedwell 1998; Gauci and Chapman 2006). In contrast, methanogenesis is considered to be the dominant anaerobic carbon oxidation process in sulfate-poor, organic matter-rich freshwater sediments. Thus, the addition of sulfate rich wastewater from nearby industries would control the methane production from wetland.

Fe-reducing bacteria are stronger bacteria than any sulfate reducing bacteria and methanogenic bacteria because it was found that Fe-reducing bacteria can outcompete both sulfate-reducing and methanogenic bacteria for organic substrates (Jerman et al. 2009). Numerous studies have indicated that microbial Fe oxide reduction plays an important role in governing the production and release of methane from iron-rich natural and agricultural wetland soils (Roden and Wetzel 2003; Laanbroek 2010; Wang 2011). Available evidence suggests that dissimilatory Fe-reducing bacteria can successfully outcompete methanogenic bacteria for acetate and H_2 (both major intermediates in the anaerobic decomposition of organic carbon to methane in anaerobic environments); therefore, in order to suppress methane production, the growth of Fe-reducing bacteria should be enhanced. A substantial number of microorganisms capable of conserving energy to support growth via Fe reduction are known (Weber et al. 2006), and the final product is carbon dioxide. Even though, carbon dioxide is a GHG as well, it has less effect on global warming; therefore, it can be considered as a way of GHG emission control. The largest known group of Fe reduction microorganisms is the *Geobacteracea* family in the delta subclass of the *Proteobacteria* (Caccavo et al. 1992; Qiu et al. 2008). All of the organisms within this family are capable of conserving energy to support growth from Fe reduction. Additionally, *Geothrix fermentans*, *Geovibrioferrireducens*, and *Ferribacter limneticum* are also capable of completely oxidizing multi-carbon organic acids to carbon dioxide (Caccavo et al. 1996; de Duve 1998; Coates et al. 1999). Adjusting the wetland microorganism community would enhance GHG emission control.

Zeolite is known as an important technological material such as adsorption, catalysis, and ion-exchange (Cavenati et al. 2004; Liu et al. 2004). Zeolites consisted of alumino-silicates are the materials with a negatively-charged crystalline structure and with abundant micropores or cavities, thus they are considered to be a potential mediator for reducing methane emissions. Zeolite has been found to be able to aid methane hydrate formation in aqueous solution (Zang et al. 2009); the formed methane hydrate (positive charge) would be stabilized by zeolite (negative charge), which reduces the amount of methane emission. Methane hydrate is an ice-like nonstoichiometric compound formed when methane reacts with water at high pressures and/or low temperatures, and the hydrate is stable under standard conditions (Sloan and Koh 2007). Researchers pointed out that zeolites could enhance the formation of methane hydrate (Zang et al. 2009). Therefore, there is a possibility that methane hydrate would be formed under standard conditions (20 ºC, 1atm) by using zeolites. On the other hand, studies reported that zeolites could activate methane conversion into carbon dioxide through oxidation (Hui et al. 2005). The oxidation can be described in a few steps. Oxygen molecules are first adsorbed on the ions sites which can be alkali ions, alkaline earth metal ions, transition metal ions, or hydrogen ions. Dissociations of the adsorbed oxygen to form atomic oxygen then occurs. Methane molecules are then adsorbed onto the atomic oxygen. Finally, reactions between the adsorbed methane and the atomic oxygen proceed to form carbon dioxide and water. Additionally, zeolite is also reported to be a great adsorbent for methane adsorption (Kamarudin et al. 2003; Kamarudin et al. 2004; Tedesco et al. 2010). The adsorbed methane would steadily exist in the zeolite framework, and it would be possible to recover the methane as fuel after certain treatments (e.g., chemical reaction or condition adjustments) (Slyudkin 2004).

Various types of zeolites including zeolite A, synthesized zeolite, zeolite rice husk based zeolite, Na-X zeolite, metal modified zeolite, etc., have been studied in methane emission control (Rimmer and Mcintosh 1974; Kamarudin et al. 2003;

Kamarudin et al. 2004; Hui and Chao 2008; Zang et al. 2009). Among them, zeolite A has been reported to be rather efficient in reducing methane emission (Al-Baghli and Loughlin 2005). In addition, metal(s)-ion-exchange zeolites also showed encouraging performance in methane emission reduction (Kamarudin et al. 2003). Furthermore, zeolites derived from wastes are promising materials in methane emission reduction, which not only controls methane pollution but also recycles wastes (Kamarudin et al. 2003). Therefore, the addition of zeolite onto the surface of wetlands would be a method of methane emission control via the principles of methane adsorption and conversion.

As mentioned before, plant species, water table level, and temperature have great effect on methane emission from wetland. Temperature is not a controllable parameter in real situations because wetlands are naturally-existing systems. Many wetland plants have aerenchymous tissue that allows oxygen transportation from the atmosphere to the root zone. Similarly, methane is transported through the aerenchyma into the atmosphere when it is produced in the sediment (Chanton 2005). Plants that are responsible for methane emission include *Nymphaea*, *Nuphar*, *Calla, Peltandra, Sagittaria*, *Cladium, Glyceria, Scirpus, Eleocharis, Eriophorum, Carex, Scheuchzeria, Phragmites*, and *Typha* (Schimel 1995; Yavitt and Knapp 1995; Shannon et al. 1996; Greenup et al. 2000; Chanton 2005). In addition, methane emission through pneumatophores and prop roots has also been observed as well as through aerenchyma of Alder trees (Pulliam 1992; Kreuzwieser et al. 2003; Purvaja et al. 2004). Hence, preventing these plants growth in the wetlands would control the methane emission to some extent. Water table level control is also a strategy of methane emission control as it affects sediment oxygen levels which impacts microorganism domination. High water levels are favorable for methanogenic bacteria growth because of the suitable anaerobic condition (Huttunen et al. 2003); therefore, keeping a low water table level in wetlandd would control methane emissions.

Nitrous Oxide Emission Control. Compared to CH_4 and CO_2, nitrous oxide is the strongest GHG. It is reported that its atmospheric concentration is gradually increasing, approximately 0.25% per year (IPCC 2001). The root of the emission is a large amount of nitrogen in different forms (e.g., organic nitrogen, NH_4-N, NO_2-N and NO_3-N) being discharged to the wetlands, where, via nitrification and denitrification processes, nitrous oxide is formed and emitted from the wetlands into the atmosphere. To solve the emission problem, the first and effective way is to avoid the nitrogen source entering the wetlands. As the main nitrogen source is from agriculture, it would reduce the emission by building efficient blocks between farming and wetlands. However, it normally requires a huge effort and cost on construction/management.

Apart from nitrate, amino acids also take up a great portion of total nitrogen used in agriculture, and are a preferred N source for plants of wetlands of subantarctic herbfield, subtropical coral cay, subtropical rainforest, and wetlands (Schmidt and Stewart 1999; Bardgett et al. 2003); however, they are much less taken up by crop plants (around 6% of the total addition); as a result, the remaining amino acids are rapidly mineralized into nitrate and ammonium by microorganism in the soil (Owen and Jones 2001). Therefore, nitrogen in wetlands mainly includes nitrate and some ammonium. Wetlands have been considered as a natural filter to control nitrate pollution with up to 90% efficiency (Cooper 1990; William J 1992).

As nitrous oxide production is an intermediate in denitrification and a by-product of nitrification, researchers often manipulate the three conditions for nitrous oxide emission control, that is, a) medium-high soil water content; b) high organic carbon availability; and c) pH in wetlands. For example, researchers studied the emission control by reducing water inflow in the rainy season (May to October) and recharging the water back to the wetlands in the dry season (other months but May to October) at Cerrig-yr-Wyn, Plynlimon, mid-Wales, U.K.; they observed that the annual emission decreased more than 95% from 40 mg/m^2 to less than 2 mg/m^2 (Freeman et al. 1997). It is attributed to the soil water content that affects denitrification in the sediment. Too low or too high soil water content would enhance the denitrification process, and thus increased the nitrous oxide emission. Huge reductions of carbon dioxide and nitrous oxide emissions have also been attained by rewetting drained peatlands (Dowrick et al. 1999; Trumper et al. 2009).

On the other hand, control of organic carbon in wetlands is important. Some plants such as *Phalarisarundinacea L.*, *Loliumperenne*, and *Coixlacryma-jobi* are capable of storing nitrogen in their biomass (Bernard and Lauve 1995; Ge et al. 2007); therefore, planting these types of plants would increase nitrogen removal from wetlands. However, the plants only take up the nitrogen inside their bodies, if the plant residue cannot be harvested in a timely manner and taken away from the wetlands, the nitrogen will go back to the wetlands and again becomes a problem. Hence, additional measures should be taken when using plants to control nitrous oxide emission from wetlands. Normally, to reduce the organic carbon in wetlands, it is necessary to remove the plant biomass. Studies have shown that periodical harvest of biomass would greatly reduce nitrous oxide emission from around 30 mg/m^{2}to 6 mg/m^2 (Tiemann and Billings 2008). In addition, to reduce the biomass, productivity would also control the organic carbon concentration in the wetlands. Tiemann and Billings (2008) successfully reduced plant residue by manipulating the C/N ratio with the addition of fertilizers.

Controlling the pH of the wetland system would also reduce the nitrous oxide emission because low pH (< 6) could inhibit the denitrification process (Freeman et al. 1997). Adjusting the pH by adding acidic industrial wastewater to wetlands would be an alternative method of N_2O emission control. In addition, using adsorbents that are able to fix nitrogen inside their structure would also control nitrous oxide emission. Zeolites have physical and chemical properties that are able to attract odors and toxins and trap them safely and effectively in its crystalline structure. It was found that zeolite could bind with ammonium-nitrogen to become slow releasing fertilizers (Luo et al. 2011; Tan et al. 2011). Adding zeolites to the surface of wetlands would reduce nitrous oxide emission, and the absorbed ammonium-nitrogen can be gradually extracted by the plants for growth. Therefore, when the zeolite is saturated with ammonium-nitrogen, they should be removed from the wetlands and applied to the agricultural land as fertilizers.

25.3 GHG Emissions from Oceans and Freshwaters

25.3.1 Mechanisms

One part of the carbon dioxide production from oceans and freshwater systems are from the aquatics, and normally it would be used by phytoplankton to form organic carbon or converted into carbonates before it reaches the atmosphere. Therefore, the emission of carbon dioxide from oceans and freshwaters can be neglected. The other part of the carbon dioxide is produced due to the dissolution of marine $CaCO_3$ sediments (Equation 25.3).

$$CaCO_3 + H_2O \rightarrow Ca(OH)_2 + CO_2 \qquad \text{(Eq. 25.3)}$$

Methane emission from oceans and freshwaters is mainly due to the organic degradation in the sediment. The organic matters are the biomass of dead plankton organisms. In the deep ocean where oxygen concentration is very low (nearly zero), the biomass is decomposed by anaerobic microorganisms such as methanogens; therefore, methane is produced. The mechanism of methane emission from oceans and freshwaters are similar to that from wetlands. In addition, fossil natural gas may leak from seabed due to the migration of the gas within earth's crust; yet it is normally a small quantity and generally negligible (Prather 2001). Moreover, it is also reported that gas hydrate is a contributor of methane production. Gas hydrate, also called methane hydrate or methane ice, is an ice-like nonstoichiometric compound formed when methane reacts with water at high pressures and/or low temperatures, and normally is stable (Sloan and Koh 2007). There is a large amount of methane hydrate accumulates in the ocean sediment, while it is normally stable in the condition (Kvenvolden 1988). When methane ice is melted due to certain earth activities such as an earthquake and plate motion, the gas will escape from the sediment and diffuse to the seawater column. Some of the produced methane will be dissolved into the seawater and the rest will enter into the atmosphere.

No report on nitrous oxide emission from oceans has been reported which is because nitrogen entering oceans from freshwaters is very stable, and does not contribute to the life processes to form nitrate and ammonium (Anthoni 2006). In freshwaters nitrous oxide emission is similar as that from wetlands (Fig. 25.2).

25.3.2 Control Strategies

Carbon Dioxide Emission Control. Compared to carbon dioxide emission, it is more important to understand carbon dioxide sinking in the oceans and freshwaters. Oceans and freshwater bodies are capable of adsorbing carbon dioxide through converting it to HCO_3^- and CO_3^{2-}, which would mitigate global warming pressure. On average, the ocean absorbs 2% more carbon than they emit each year, forming an important sink in the overall carbon cycle. The net results of adding CO_2 to sea water is the generation of H^+ (i.e., lowering pH) and decreases the concentration of CO_3^{2-}, gradually causing seawater and/or freshwater to become more acidic. For example, the ocean pH ocean pH decreases by 0.1 units since preindustrial times and is expected to fall another 0.3–0.4 units by 2100 (The Royal Society 2005; Canadell et al. 2007; Fabry et al. 2008). CO_2-induced acidification is also affecting lower salinity estuaries and temperate coastal ecosystems. Some examples of unexpected impacts on marine eco-systems due to ocean acidification are described as follows:

- Produce irreversible ecological regime shifts in marine eco-systems (e.g., reduction of the availability of carbonate ions for calcifying species and massive reduction in coral reef habitats and their associated biodiversity);
- Affect development, metabolic and the behavioral processes of marine species in general or during a critical life history stage (e.g., loss of larval olfactory ability in marine organisms, the impaired ability of larvae to sense predators);
- Affecting the symbiotic relationship among different organisms (e.g., coral reefs, dinoflagellates) and the productivity of their association;
- Endanger a wide range of ocean life, wipe out species, and disrupt the food web and impact tourism and any other human activities that rely on or are associated with the sea.

On the other hand, CO_2 in the upper ocean is fixed by primary producers, that is, CO_2 is forced, by the biological carbon pump mechanism, going through the food chain. For example, green, photosynthesizing plankton converts as much as 60 gigatons of carbon per year into organic carbon roughly the same amount fixed by land plants and almost 10 times the amount emitted by human activity (Hoffman 2009). Furthermore, marine organisms are capable of converting immense amounts of bioavailable organic carbon into difficult-to-digest forms known as *refractory* dissolved organic matter. Once transformed into "inedible" forms, these dissolved organic carbons may settle in undersaturated regions of the deep oceans and remain out of circulation for thousands of years, effectively sequestering the carbon by removing it from the ocean food chain (Hoffman 2010). Ultimately, the fate of most of this exported material is remineralization to CO_2, which accumulates in deep waters until it is eventually ventilated again at the sea surface. However, a proportion of the fixed carbon is not mineralized; instead it is stored for millennia as recalcitrant dissolved organic matter (Jiao et al. 2010). More and more results indicate that our understanding of these topics is very limited, and future breakthrough is possible once the knowledge gap is filled.

Methane and Nitrous Oxide Emissions Control. Methane emission are due to the decomposition of plankton biomass, and normally the control methods used in wetlands are not practical in oceans, which covers around 70% of the total earth surface area. Therefore, so far, there is no effective measure for methane emission control in oceans. While it is different to control methane and nitrous oxide emissions in freshwaters, the freshwater system is similar as wetlands. Thus, the strategies for their emission control from wetlands are applicable for freshwaters. In addition, there is no concern on nitrous oxide emission from oceans as it is not produced. While we should pay attention to nitrous oxide emission from freshwater, the control methods can adopt from wetland GHG emission control.

25.4 GHG Emissions from Permafrost

25.4.1 Mechanisms

Global warming is leading to the accelerated thawing of permafrost and the mobilization of soil organic carbon pools that has been accumulated for thousands of years in arctic regions. The soil organic carbon in permafrost accounts for 13–15% of the global soil organic carbon. Permafrost melt leads to the formation of ponds and lakes, which are usually surrounded by peaty soil. Peaty soil shows great similarity as wetlands and other freshwater bodies. Thawing of permafrost showed a large amount of emissions of GHG mainly including carbon dioxide and methane (Walter et al. 2007; Schuur et al. 2008). The emission mechanism of methane is similar to its emission from wetlands and freshwaters, in which methane is produced from anaerobic sediment via photochemical and microbial transformation (Equation 25.4). Apart from the portion that is oxidized in oxygen rich water column and consumed by methanotrophs, the remaining produced methane escapes into the atmosphere mainly through bubbling as plants are limited in the regions. Carbon dioxide is mainly produced from benthic respiration, pelagic respiration, and the photolysis of dissolved organic matters (Jonsson et al. 2001; Jonsson et al. 2008). It is reported that the emissions of methane and carbon dioxide vary according to the physical condition of the water column such as temperature, oxygen content, and water level (Laurion et al. 2010).

$$CO_2 + H_2 \rightarrow CH_4$$

$$\text{Acetate} \rightarrow CH_4 + CO_2 \qquad \text{(Eq. 25.4)}$$

25.4.2 Control Strategies

As methane and carbon dioxide are two major GHG emission contributors of permafrost, their emission control methods are addressed here.

Studies found that environmental parameters showed great effects on methane emission, such as soil temperature, wind speed, water table level, and availability of organic carbon to methanogens (Sachs et al. 2008; Wille et al. 2008). Soil temperature would affect the microorganism community distribution, which would impact methane and carbon dioxide production. However, it is difficult to artificially control the temperature, and thus, it is not possible to reduce the emissions through the temperature control method. Wind speed impacts the surface turbulence and thus, the gas exchange between water surface and the atmosphere (MacIntyre et al. 1995).

Additionally, turbulence would change the concentration gradient of carbon dioxide and methane between the soil layer and water layer (Hargreaves et al. 2001). Based on studies, high turbulence could enhance GHG emissions. Therefore, to control GHG emissions, measures should be taken to maintain clam conditions on the surface of the water. For example, building a fence on the side of the ponds and lakes that has the most frequent wind blowing in the year. The GHG emissions also depend on the water table level as it determines the oxygen concentration in the water or sediment. Proper water table levels would inhibit GHG emissions and the principle is similar to that described in the wetland part.

It is known that ponds and lakes derived from permafrost thawing are rich in organic carbon, which can be utilized by methanogens to produce methane. The organic carbon has been sequenced in the sediment over the years, and the process is continually going on due to the plants biomass falling to the system. The organic carbon that was deposited long time ago in the sediment cannot be controlled. It was reported that recently fixed organic carbon is the main substrate of methanogetic microorganism (King and Reeburgh 2002). It is known that plants have an effect on methane emission, mainly because of three reasons: plants can introduce oxygen into anaerobic zone which would inhibit methanogetic bacteria growth and oxidize the surrounding methane; plant aerenchymes could transfer methane produced in the soil layer to the atmosphere by passing through the aerobic zone in which some of the methane can be oxidized; plants can also provide labile organic carbon sources that would be utilized by microorganisms to produce methane. To control the emission of methane from permafrost areas, the growth of vascular plants should be limited as they enhance methane emission (O'Connor 2009). Compared to the old leaves of the plants, the young ones showed less methane emission due to the undeveloped cuticula (Morrissey et al. 1993; Schimel 1995); thus controlling the age of plants by periodical removal of plants leaves would reduce the methane emission. Some researchers reported that root density displayed important effects on methane emission, and high density gave low methane emission (King et al. 1998). This is due to the stomata effect. Stomata are known to enhance methane emission; more stomata lead to low density, while less stomata result in high density. In addition, recently fixed organic matters are more favorable to methane production microorganisms; therefore, avoiding plants biomass entering the system would control methane emission, which can be accomplished by periodical removal of the dead plants.

As mentioned earlier, methane has bigger potential on global warming than carbon dioxide; hence to convert methane to carbon dioxide would reduce the GHG emissions from permafrost. Normally, the ponds and lakes formed by thawing permafrost are small in area, and it is possible to set flexible covers above for methane collection. Thereafter, the gas can be utilized as fuel (with the final product being carbon dioxide), and hence, the GHG emissions are reduced.

The emission of methane could induce global warming, and the global warming would result in thawing of the permafrost which would lead to GHG emissions. The vicious cycle requires the control of GHG emissions. It is known that the utilization of fossil fuels causes the major GHG emissions; hence the control of the utilization amount of fossil fuel should be regulated. In addition, employing substitute fuel, such as biofuel instead of the usage of fossil fuel, would reduce GHG emissions to some extent.

25.5 Geologic GHG Emissions

25.5.1 Mechanisms

Geological gas emission mainly refers to as fossil natural gas leakage from land surface and carbon dioxide seepage by geothermal and volcanic manifestations. The emission was given only minor consideration due to the lack of technologies in the measurement of the gas emissions before 2000. Over the last 10 years, attention has been given to the geological emission because of the awareness on the emission sources such as geothermal and volcanic systems (Milkov et al. 2003; Etiope et al. 2004). There are several ways for geological GHG production. The most familiar one is the organic matter decomposition by methanogetic bacteria. It is also found that methane and carbon dioxide are produced due to the inorganic reaction (Equation 25.5) or thermal breakdown of the organic matters (Equation 25.6) (Etiope and Klusman 2002; Etiope et al. 2007; Fiebig et al. 2009). Magma degassing is a way of geological GHG emission as well.

$$CO + H_2 \rightarrow CH_4 + H_2O \quad \text{(Eq. 25.5.1)}$$

$$CO + H_2O \rightarrow CO_2 + H_2 \quad \text{(Eq. 25.5.2)}$$

$$CO_3^{2-} \rightarrow CO_2 \quad \text{(Eq. 25.5.3)}$$

$$\text{Organic carbon} \rightarrow CH_4 + H_2O \quad \text{(Eq. 25.6)}$$

The GHG emission from soil (faults and fracture rocks) is called micro seepage, while the emission from volcanoes is considered as macro seepage. Compared to macro seepage, micro seepage is taking the major responsibility of GHG geological emission even though its emission is slow (Etiope et al. 2007). There are several factors, including temperature, pressure, mechanical stresses, rock porosity, permeability of porous rocks, and inorganic reactions would affect geological GHG emissions (Etiope and Martinelli 2002). The relationship between the factors and the emission is shown in Equation 25.7 according to Poisseuille's law (Etiope and Martinelli 2002).

$$Q = \frac{\pi R^4 \Delta P}{8 \mu L} \quad \text{(Eq. 25.7)}$$

where Q is the gas emission (m^3/s); R is radius of the pore (m); L is the depth of the gas production site to the soil surface (m); P is the pressure difference of the L depth ($kg/m \cdot s^2$); μ is the dynamic viscosity of the methane of carbon dioxide gases ($kg/m \cdot s$). From equation 25.7, it can be seen that pressure difference is a gas movement force. In addition, it is known that concentration gradients are always the driving force of material movement, which means that gas concentration gradients are also responsible for gas emissions. The pressure-forced gas emission is advection, and the concentration-gradient-forced gas emission is diffusion. Normally gas emissions are the result of a combination of the two forces (Fig. 25.4). In the place where capillaries or small-pored rocks are dominating, diffusion plays the major role of the GHG emission; while in the place where large-pored or fractured media is abundant, advection acts as the main role of the GHG emissions. The GHG emission through these two mechanisms normally refers to as the emission that occurs from less than10 m depth (Mogro-Campero and Fleischer 1977). It is known that a large amount of GHGs (methane and carbon dioxide) buried in the deep layer (even more than 100 m). The gases produced in the deep soil layer would gather into a micro flow geogas. When they meet groundwater, a bubble stream would be formed and spread into groundwater; then, they would flow with the groundwater and would escape into the atmosphere when the chance is caught (Fig. 25.4).

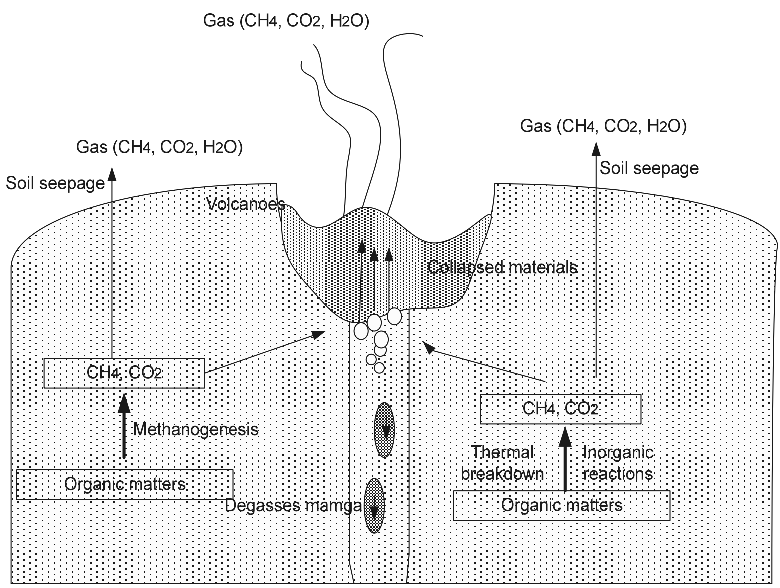

Figure 25.3. Geological gas emission

25.5.2 Control Strategies

As mentioned before, geological GHG emissions are methane and carbon dioxide emissions. Emissions from volcanoes (macro seepage) are not controllable as it is a natural phenomenon, while the emissions due to micro seepage can be reduced to some extent. GHG emissions from soil surface are from faults and fractures which are normally caused due to fossil fuel digging such as coal milling, natural gas exploitation, and oil exploitation. The large amount of fossil fuel consumption is leading to an over-exploitation, which results in surface collapses and frequent earthquakes (Anthoni 2001; Nyre 2011). When these natural disasters occur, GHGs trapped underground escape from the deep layer of the earth from faults and fractures. Yet, once the emissions take place, there is no practical and efficient way to control it. Hence, in order to control the emissions, it should be prevented on the extensive exploitation of fossil fuel. Avoiding the waste on the fossil fuel utilization should be a way of GHG emission control. The waste of fossil fuel expresses in the wide use of high technologies, depending heavily on the automobiles, extensive oil fuel lose during exploitation due to the undeveloped techniques, rapid population increasing, high living requirements, and shortage of education of fossil fuel crisis. Therefore, measures should be taken to control the waste on fossil fuel.

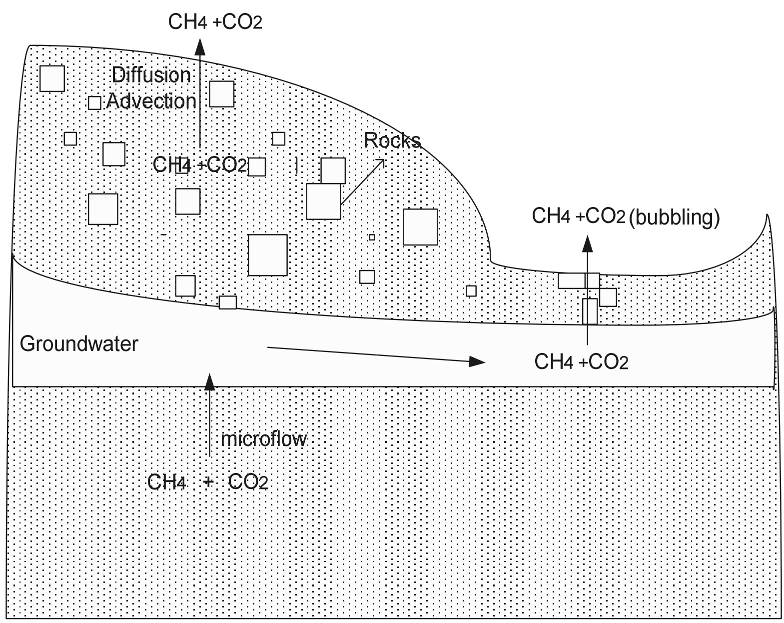

Figure 25.4. Gas emission from soil surface

25.6 GHG Emissions from Other Natural Systems

25.6.1 GHG Emissions from Termites

Tropical grasslands and forests are favorable regions of termite inhabitation, while surely they also live in other ecological regions. GHG emissions from termites display in the methane production during food digestion by symbiotic microorganisms (methanogens) in the gut. The emission amount from termites varies according to the termite species; the total emission amount is around 15 Tg per year (ZimmermanI et al. 1982; Gomati et al. 2011). In a wide range, termites are divided into lower termites, including rhinotermitidae, serritermitidae, hodotermitidae, kalotermitidae, termopsidae, mastotermitidae, and higher termites including termitinae, nasutitermitinae, macrotermitina, apicotermitinae (Ohkuma et al. 2001; Moriya 2008; Gomati et al. 2011). GHG emissions from termites depend on the microorganisms that exist in their guts. The microorganisms include aerobes such as *Bacillus cereus* and *Serratiamarcescens* (Thayer 1976), facultative anaerobes such as *Clostridium termitidis* and *Cellulomonas* sp. (Saxena et al. 1993; Baumann and Moran 1997), N_2 fixing bacteria such as *Citrobacterfreundii* and *E. agglomerans* (French et al. 1976; Golichenkov et al. 2006), CO_2 reducing acetogenic bacteria such as *Acetonemalongum*and *Sporomusatermitida* (Breznak et al. 1988; Kane and Breznak 1991), methanogenic bacteria such as *M. curvatus* and *M. arboriphilicus* (Yang et al. 1985; Leadbetter and Breznak 1996), protozoa such as *Trichomitopsistermosidis* and *Trichonymphssphareica* (Yamin 1980).

Termites take wood and soil as food, and methane and carbon dioxide are produced during breaking down the complex carbon to obtain nutrients for their growth. The detail process is that the complex carbons such as cellulose (polymers) will be broken down into simple compounds (monomers) by protozoa; thereafter, the monomers will be converted into two-group products acetate (the energy source of termite), and hydrogen and carbon dioxide during fermentation in the gut; Some of the hydrogen and carbon dioxide will be utilized to form acetate by homoacetogens or acetogenic bacteria, and some will be utilized to produce methane by methanogens, and the rest will escape into the atmosphere; while the acetate will be oxidized into carbon dioxide which will enter the atmosphere through termites breathing. The whole process is shown in Fig. 25.5.

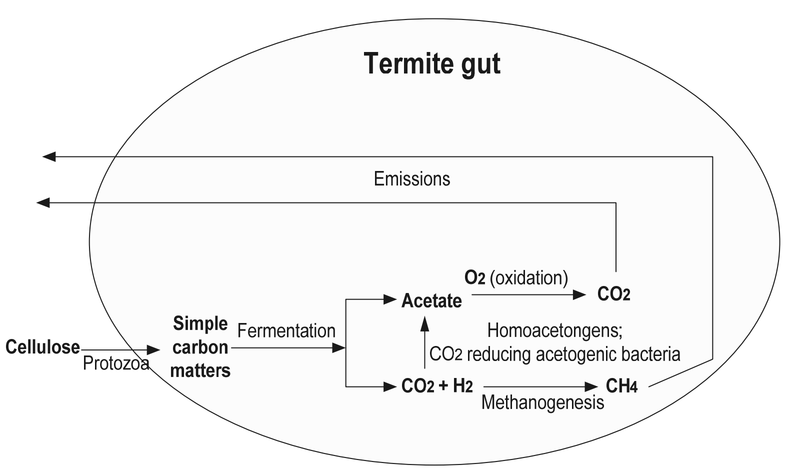

Figure 25.5. GHG emissions from termites

It is known that carbon dioxide will be captured by plants such as trees and again taken as food by termites. Therefore, it can be considered as a balanced cycle which will not contribute to GHG emission from termites. Methane production is impacted by environmental conditions such as lights, humidity, temperature, oxygen concentration, and carbon dioxide concentration. (ZimmermanI et al. 1982; Gomati et al. 2011). Dark, humid, high temperature and carbon dioxide concentration are preferred by termites. Studies showed that increasing temperature by 5 °C could increase up to 110% of methane emission (Fraser et al. 1986). It was also found the condition of high carbon dioxide concentrations enhances methane emission (Seiler et al. 1984). Oxygen concentration would affect the anaerobic condition in the gut and hence influence the methane production as methane-producing bacteria are strict anaerobic microorganisms.

The methane emission from termites is determined by the microbial community in their guts, and generally it depends on the type of species. It is known that they naturally inhibit in tropical regions, which are not controlled by humans. Therefore, there is no efficient and practical method for controlling methane emission from termites.

25.6.2 GHG Emissions from Ruminant Animals

Ruminants, including cows, goats, sheep, and some wild animals, have stomachs with four compartments, namely the reticulum, rumen, omasum and abomasum. Each of the compartments has its special functions: the reticulum located next to heart is the pathway to the other three compartments and catches metals and hardware; the rumen is used for storage, soaking, physical mixing and breakdown, and fermentation of the food [i.e., converting fibrous feeds into volatile fatty acids (VFAs) by microorganisms, mainly anaerobes with little aerobes]; omasum is the part that plays a role to reduce the particle size and adsorb some water; and abomasum is considered as the true stomach as it secretes enzymes for further digestion. Rumen is the compartment, in which methane and carbon dioxide are produced as a by-product of the digestion process by methanogens (Fig. 25.6). Starch or celluloses that were taken as food will first be decomposed to simple sugars (glucose) in the presence of enzymes such as amylase and cellulase, and then glucose will further be converted into pyruvic acid, thereafter pyruvic acid is utilized as substrate to produce VFAs including acetic and butyric acids. In the process that VFAs are produced, methane or carbon dioxide will be produced as well, and discharged into the atmosphere as waste gas. It is reported that GHG emission from ruminant animals counts for more than 13% of the total national GHG emissions in Australia (Hegarty 2007).

GHG emissions from wild animals such as bison and buffalos are not controllable as they are living in the wild fields; while, several strategies have been reported to mitigate GHG emissions from livestock (cow, sheep). The most direct way to control this is to manipulate rumen micro floral populations, and the emissions can be reduced by decreasing the number of ruminant animals. However, the same or higher animal productivity should be maintained when the population is controlled as the requirement in animal products (such as meat and milk) is increasing annually. Genetic selection can be employed for the emission control as well. Two genotypes of dairy cows including New Zealand Freisian (pasture diets) and Holsteins (high concentrated diets) have been studied to compare methane productivity, and the result showed that Holsteins produced around 10% less methane than New Zealand Freisian (Robertson et al. 2002). Even though limited research has been done to further study the point, there is a trend that high concentrated diets give lower methane emission than pasture diets; yet it can be predicted that the raising cost would be increased as well. Therefore, this control method should be evaluated according to the reality. Additionally, forage species selection and pasture forage quality are found to impact GHG emissions from pasture ruminants (Johnson et al. 1997; Olson 1997; Benchaar and Greathead 2011). Forage that contains legumes and has high dry matter digestibility would reduce methane production and further reduce methane emission. The control on rumen bacterial population by manipulating food additives would also be an alternative of GHG emission control. Reports showed that methane emission was reduced by 25% when monensin is used as a supplement (van Nevel and Demeyer 1995), and Jonson et al. (1997) obtained similar results. An addition of fat in the diet has shown the reduction on methane production because the unsaturated fatty acid can be used as electron acceptors instead of hydrogen. An addition of canola oil to the diet of cattle reduced more than 30% of methane compared to the normal diet (without canola oil addition) and sunflower seed addition provided similar conclusions (Mathison 1997; Kreuzer and Hindrichsen 2006; Benchaar and Greathead 2011).

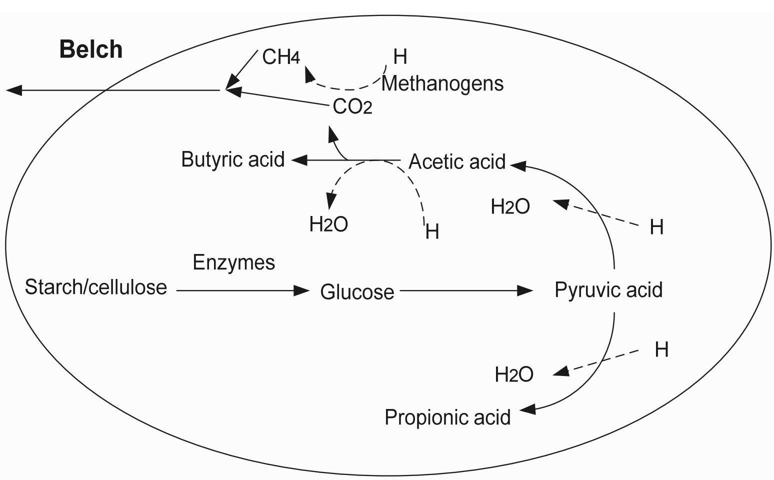

Figure 25.6. GHG emission from ruminant animals

25.6.3 GHG Emissions from Wildfires

GHG emissions from wildfires are getting growing attention as it could emit an average GHG emission of 65 tons of carbon dioxide per acre (50 to 60 trees) during the combustion; however, there is also GHG emission during the gradual decomposition of the remaining biomass. Normally, GHG emissions from the decomposition of the remaining biomass is larger than combustion due to the fact that 3.67 times the carbon content of biomass is released as CO_2 during decomposition (Bonnicksen 2008).

Reducing the number and severity of wildfires is the most efficient way of GHG emission control from wildfires. Wildfire mainly results from lightning and native people activities, and is not avoidable for the former cause but can be prevented when enough carefulness is given during human activities (Bonnicksen 2000; Bonnicksen 2007). In addition, rapid reaction in putting out the fire before it gets out of control would reduce the GHG emissions. As mentioned earlier, the decomposition of the remaining biomass after wildfires contributes more GHG emissions than combustion; therefore, it would reduce GHG emission if the remaining biomass is collected and burned completely into carbon dioxide. After wildfires, when the dead trees have values to produce wood products such as furniture, they can be utilized to manufacture the products to store the carbon content and hence reduce GHG emissions. In addition, replanting the forest is an indirect way of GHG emission control from wildfires. Planting trees would capture carbon dioxide from the atmosphere which can balance the GHG emitted in the wildfires even though it is a slow process.

25.7 Summary

Increasing GHG emissions is threatening in our environment. Global warming is considered as one of the most critical consequences of GHG emissions. Human activities have also caught the most attention in GHG emission; however, in recent years, natural system GHG emission also is getting increasing concern due to the awareness of the large amount of GHG emission (30% of the total global GHG emissions).

Natural systems that cause GHG emissions include wetlands, oceans and freshwaters, permafrost, termites, ruminant animals, geologic emissions, and wildfires. Wetlands are the biggest GHG emission contributor followed by oceans and freshwaters, permafrost, and geologic emissions; termites, ruminant animals, and wildfires give a very small amount of emissions. Methane, carbon dioxide, and nitrous oxides are considered as GHGs. There are several ways for GHGs to be emitted from the natural systems. The most common one is microorganism activities (methanogenesis, denitrification). Inorganic reaction is also responsible for the emissions (thermal breakdown, combustion, carbonate decomposing).

Many strategies have been reported to mitigate GHG emissions from each natural system; however, most of them are not efficient and realistic as the GHG emissions from these systems are natural processes and most of the systems cover huge areas.

25.8 Acknowledgements

Sincere thanks are to the Natural Sciences and Engineering Research Council of Canada (Grant A 4984, and Canada Research Chair) for their financial support. The views and opinions expressed in this chapter are those of the authors.

25.9 References

Adhikari, S., Bajracharaya, R., and Sitaula, B. (2009). "A review of carbon dynamics and sequestration in wetlands." *Journal of Wetlands Ecology*, 2, 42–46.

Al-Baghli, N. A., and Loughlin, K. F. (2005). "Adsorption of methane, ethane, and ethylene on titanosilicate ETS-10 zeolite." *Journal of Chemical & Engineering Data*, 50, 843–848.

Anthoni, J. F. (2001). "Seafriends: Summary of threats to the environment." Avaiable at <www.seafriends.org.nz/issues/threats.htm> (accessed Dec. 2011).

Anthoni, J. F. (2006). "The chemical composition of seawater." Available at <http://www.seafriends.org.nz/oceano/seawater.htm> (accessed Dec. 2011).

Bardgett, R. D., Streeter, T. C., and Roland, B. (2003). "Soil microbes compete effectively with plants for organic-nitrogen inputs to temperate grasslands." *Ecology*, 84, 1277–1287.

Baumann, P., and Moran, N. A. (1997). "Non-cultivable microorganisms from symbiotic associations of insects and other hosts." *Antonie van Leeuwenhoek*, 72, 39–48.

Benchaar, C., and Greathead, H. (2011). "Essential oils and opportunities to mitigate enteric methane emissions from ruminants." *Animal Feed Science and Technology*, 166, 338–355.

Bernard, J. M., and Lauve, T. E. (1995). "A comparison of growth and nutrient uptake in *Phalaris aruninacea L*. growing in a wetland and a constructed bed receiving landfill leachate." *Wetlands*, 15, 176–182.

Blain, D., Row, C., Alm, J., Byrne, K., and Parish, F. (2006). "Wetland." *IPCC Guidelines for National Greenhouse Gas Inventories*, 4, 1–24.

Bleakley, B. H., and Tiedje, J. M. (1982). "Nitrous oxide production by organisms other than nitrifiers or denitrifiers." *Applied and Environmental Microbiology*, 44, 1342–1348.

Bonnicksen, T. M. (2000). *America's ancient forests: from the ice age to the age of discovery*. John Wiley & Sons, Inc., New York., 594.

Bonnicksen, T. M. (2007). *Protecting communities and saving forests: solving the wildfire crisis through restoration forestry.* The Forest Foundation. Auburn, California., 48.

Bonnicksen, T. M. (2008). *Greenhouse gas emissions from four California wildfires: opportunities to prevent and reverse environmental and climate impacts*. Report of Forest Carbon and Emissions Model Prepared for The Forest Foundation 853 Lincoln Way, Suite 208 Auburn, CA 95603.

Bourrelly, S., Llewellyn, P. L., Serre, C., Millange, F., Loiseau, T., and Férey, G. (2005). "Different adsorption behaviors of methane and carbon dioxide in the isotypic nanoporous metal terephthalates MIL-53 and MIL-47." *Journal of the American Chemical Society*, 127, 13519–13521.

Breznak, J. A., Switzer, J. M., and Seitz, H. J. (1988). "*Sporumusa termitida* sp. nov., an H_2 / CO_2 utilizing acetogen isolated from termites." *Archives of Microbiology*, 150, 282–288.

Caccavo, F., Blakemore, R. P., and Lovley, D. R. (1992). "A hydrogen-oxidizing, Fe(III)-reducing microorganism from the Great Bay Estuary, New Hampshire." *Applied and Environmental Microbiology*, 58, 3211–3216.

Caccavo, J., F., Coates, J. D., Rossello-Mora, R. A., Ludwig, W., Schleifer, K. H., Lovley, D. R., and McInerney, M. J. (1996). "Geovibrio ferrireducens, a phylogenetically distinct dissimilatory Fe(III)-reducing bacterium." *Archives of Microbiology*, 165, 370–376.

Canadell, J. G., Quéré, C. L., Raupach, M. R., Fielde, C. B., Buitenhuis, E. T., Ciais, P., Conway, T. J., Gillett, N. P., Houghton, R. A., and Marland, G. (2007). "Contributions to accelerating atmospheric CO_2 growth from economic activity, carbon intensity and efficiency of natural sinks." *Proceedings of the National Academy of Sciences*, 104, 18866–18870.

Cavenati, S., Grande, C. A., and Rodrigues, A. E. (2004). "Adsorption equilibrium of methane, carbon dioxide, and nitrogen on zeolite 13X at high pressures." *Journal of Chemical & Engineering Data*, 49, 1095–1101.

Chanton, J. P. (2005). "The effect of gas transport on the isotope signature of methane in wetlands." *Organic Geochemistry*, 36, 753–768.

Chathoth, S. M., Mamontov, E., Melnichenko, Y. B., and Zamponi, M. (2010). "Diffusion and adsorption of methane confined in nano-porous carbon aerogel: A combined quasi-elastic and small-angle neutron scattering study." *Microporous and Mesoporous Materials*, 132, 148–153.

Coates, J. D., Ellis, D. J., and Lovley, D. R. (1999). "Geothrix fermentans gen. novo sp. nov., an acetate-oxidizing Fe(lII) reducer capable of growth via fermentation." *International Journal of Systematic Bacteriology*, 49, 1615–1622.

Cooper, A. B. (1990). "Nitrate depletion in the riparian zone and stream channel of a small headwater catchment." *Hydrobiologia*, 202, 13–26.

Danevčič, T., Mandic-Mulec, I., Stres, B., Stopar, D., and Hacin, J. (2010). "Emissions of CO_2, CH_4 and N_2O from southern European peatlands." *Soil Biology and Biochemistry*, 42, 1437–1446.

de Duve, C. (1998). "Clues from present-day biology: the thioester world." *In A. Brack (ed.), The Molecular Origins of Life. Cambridge University Press, Cambridge, United Kingdom*, 219–236.

Dinsmore, K. J., Skiba, U. M., Billett, M. F., Rees, R. M., and Drewer, J. (2009). "Spatial and temporal variability in CH_4 and N_2O fluxes from a Scottish ombrotrophic peatland: Implications for modelling and up-scaling." *Soil Biology and Biochemistry*, 41, 1315–1323.

Dowrick, D. J., Hughes, S., Freeman, C., Lock, M. A., Reynolds, B., and Hudson, J. A. (1999). "Nitrous oxide emissions from a gully mire in mid-Wales, UK, under simulated summer drought." *Biogeochemistry*, 44, 151–162.

Etiope, G. (2009). "Natural emissions of methane from geological seepage in Europe." *Atmospheric Environment*, 43, 1430–1443.

Etiope, G., Feyzullayev, A., Baciu, C. L., and Milkov, A. V. (2004). "Methane emission from mud volcanoes in eastern Azerbaijan." *Geology*, 32, 465–468.

Etiope, G., Fridriksson, T., Italiano, F., Winiwarter, W., and Theloke, J. (2007). "Natural emissions of methane from geothermal and volcanic sources in Europe." *Journal of Volcanology and Geothermal Research*, 165, 76–86.

Etiope, G., and Klusman, R. W. (2002). "Geologic emissions of methane to the atmosphere." *Chemosphere*, 49, 777–789.

Etiope, G., and Martinelli, G. (2002). "Migration of carrier and trace gases in the geosphere: an overview." *Physics of the Earth and Planetary Interiors*, 129, 185–204.

Fabry, V. J., Seibel, B. A., Feely, R. A., and Orr, J. C. (2008). "Impacts of ocean acidification on marine fauna and ecosystem processes." *ICES Journal of Marine Science: Journal du Conseil*, 65, 414–432.

Fiebig, J., Woodland, A. B., D'Alessandro, W., and Püttmann, W. (2009). "Excess methane in continental hydrothermal emissions is abiogenic." *Geology*, 37, 495–498.

Fraser, P. J., Rasmussen, R. A., Creffield, J. W., French, J. R., and Khalil, M. A. K. (1986). "Termites and global methane–another assessment." *Journal of Atmospheric Chemistry*, 4, 295–310.

Freeman, C., Lock, M. A., Hughes, S., Reynolds, B., and Hudson, J. A. (1997). "Nitrous oxide emissions and the use of wetlands for water quality amelioration." *Environmental Science & Technology*, 31, 2438–2440.

French, J. R. J., Turner, G. L., and Bradbury, J. F. (1976). "Nitrogen fixation by bacteria from the hindgut of termites." *Journal of General Microbiology*, 95, 202–206.

Gauci, V., and Chapman, S. J. (2006). "Simultaneous inhibition of CH_4 efflux and stimulation of sulphate reduction in peat subject to simulated acid rain." *Soil Biology and Biochemistry*, 38, 3506–3510.

Ge, Y., Li, S. P., Niu, X. Y., Yue, C. L., Xu, Q. S., and Chang, J. (2007). "Sustainable growth and nutrient uptake of plants in a subtropical constructed wetland in southeast China." *Fresenius Environmental Bulletin*, 16, 1023–1029.

Golichenkov, M., Kostina, N., Ul'yanova, T., Kuznetsova, T., and Umarov, M. (2006). "Diazotrophs in the digestive tract of termite *Neotermes castaneus*." *Biology Bulletin*, 33, 508–512.

Gomati, V., Ramasamy, K., Kumar, K., Sivaramaiah, N., and Mula, R. V. R. (2011). "Greenhouse gas emission from termite ecosystem." *African Journal of Environmental Science and Technology*, 5, 56–65.

Greenup, A. L., Bradford, M. A., McNamara, N. P., Ineson, P., and Lee, J. A. (2000). "The role of *Eriophorum vaginatum* in CH_4 flux from an ombrotrophic peatland." *Plant and Soil*, 227, 265–272.

Hargreaves, K. J., Fowler, D., Pitcairn, C. E. R., and Aurela, M. (2001). "Annual methane emission from Finnish mires estimated from eddy covariance campaign measurements." *Theoretical and Applied Climatology*, 70, 203–213.

Hashidoko, Y., Takakai, F., Toma, Y., Darung, U., Melling, L., Tahara, S., and Hatano, R. (2008). "Emergence and behaviors of acid-tolerant *Janthinobacterium sp*. that evolves N_2O from deforested tropical peatland." *Soil Biology and Biochemistry*, 40, 116–125.

Hegarty, R. (2007). *Greenhouse gas emissions from the Australian livestock sector; Australian Greenhouse Office*. Available at <http://www.landlearnnsw.org.au/sustainability/climate-change/agriculture/livestock/methane> (accessed Feb. 2012).

Hoffman, D. L. (2009). "New Jelly pump rewrites carbon cycle." Available at <http://theresilientearth.com/?q=content/> (accessed Feb. 2012).

Hoffman, D. L. (2010). "Ocean CO_2 storage revised." Available at <http://www.theresilientearth.com/?q=content/> (accessed Feb. 2012).

Hui, K. S., and Chao, C. Y. (2008). "Methane emissions abatement by multi-ion-exchanged zeolite A prepared from both commercial-grade zeolite and coal fly ash." *Environmental science technology*, 42, 7392–7397.

Hui, K. S., Chao, C. Y. H., and Kot, S. C. (2005). "Removal of mixed heavy metal ions in wastewater by zeolite 4A and residual products from recycled coal fly ash." *Journal of Hazardous Materials*, 127, 89–101.

Huttunen, J. T., Nykänen, H., Turunen, J., and Martikainen, P. J. (2003). "Methane emissions from natural peatlands in the northern boreal zone in Finland, Fennoscandia." *Atmospheric Environment*, 37, 147–151.

IPCC (2001). *Climate change 2001: The scientific basis*. Contribution of Working Group I to the Third Assessment Report of the Intergovernmental Panel on Climate Change (Houghton, J.T. et al. (eds)). Cambridge University Press, Cambridge, UK, 944.

Jerman, V., Metje, M., Mandi´c-Mulec, I., and Frenzel, P. (2009). "Wetland restoration and methanogenesis: the activity of microbial populations and competition for substrates at different temperatures." *Biogeosciences Discuss*, 6, 2357–2386.

Jiao, N., Herndl, G. J., Hansell, D. A., Benner, R., Kattner, G., Wilhelm, S. W., Kirchman, D. L., Weinbauer, M. G., Luo, T., Chen, F., and Azam, F. (2010). "Microbial production of recalcitrant dissolved organic matter: long-term carbon storage in the global ocean." *Nature Reviews Microbiology*, 8, 593–599.

Johnson, K. A., Westberg, H. H., Lamb, B. K., and Kincaid, R. L. (1997). "Quantifying methane emissions from ruminant livestock and examination of methane reductions strategies." *Ruminant Livestock Efficiency Program Annual Conference Proceedings, EPA USDA*.

Jonsson, A., Åberg, J., Lindroth, A., and Jansson, M. (2008). "Gas transfer rate and CO_2 flux between an unproductive lake and the atmosphere in northern Sweden." *Journal of Geophysical Research*, 113, 1–13.

Jonsson, A., Meili, M., Bergström, A.-K., and Jansson, M. (2001). "Whole-Lake mineralization of allochthonous and autochthonous organic carbon in a large humic lake (Örträsket, N. Sweden)." *Limnology and Oceanography*, 46, 1691–1700.

Kamarudin, K. S. N., Mah, L. M., and Yuan, C. Y. (2004). "Rich husk based zeolite as methane adsorbent." Paper presented at "18th Symposium of Malaysian Chemical Engineers", Universiti Teknologi Petronas, Tronoh, Perak, 13-14 December 2004.

Kamarudin, K. S. N., Mat, H., and Hamdan, H. (2003). "Structural synthesis and modification of zeolite as methane adsorbent." Poster presentation at 'Annual Fundamental Science Seminar 2003, Puteri Pan Pacific, Johor Bahru, 20-21 May 2003.

Kane, M. D., and Breznak, J. A. (1991). "*Acetonema longum* gen.nov.sp.nov., an acetogenic bacterium from the termite, *Pterotermes occidentis*." *Archives of Microbiology*, 156, 91–98.

Kao-Kniffin, J., Freyre, D. S., and Balser, T. C. (2010). "Methane dynamics across wetland plant species." *Aquatic Botany*, 93, 107–113.

King, J. Y., and Reeburgh, W. S. (2002). "A pulse-labeling experiment to determine the contribution of recent plant photosynthates to net methane emission in arctic wet sedge tundra." *Soil Biology and Biochemistry*, 34, 173–180.

King, J. Y., Reeburgh, W. S., and Regli, S. K. (1998). "Methane emission and transport by arctic sedges in Alaska: Results of a vegetation removal experiment." *Journal of Geophysical Research*, 103, 29083–29092.

Kreuzer, M., and Hindrichsen, I. K. (2006). "Methane mitigation in ruminants by dietary means: The role of their methane emission from manure." *International Congress Series*, 1293, 199–208.

Kreuzwieser, J., Buchholz, J., and Rennenberg, H. (2003). "Emission of methane and nitrous oxide by Australian Mangrove Ecosystems." *Plant Biology*, 5, 423–431.

Kvenvolden, K. A. (1988). "Methane hydrate and global climate." *Global Biogeochemical Cycles*, 2, 221–229.

Laanbroek, H. J. (2010). "Methane emission from natural wetlands: interplay between emergent macrophytes and soil microbial processes. A mini-review." *Annals of Botany*, 105, 141–153.

Lai, D. Y. F. (2009). "Methane dynamics in northern peatlands: A review." *Pedosphere*, 19, 409–421.

Laurion, I., Vincent, W. F., MacIntyre, S., Retamal, L., Dupont, C., Francus, P., and Pienitz, R. (2010). "Variability in greenhouse gas emissions from permafrost thaw ponds." *Limnology and Oceanography*, 55, 115–133.

Leadbetter, J. R., and Breznak, J. A. (1996). "Physiological ecology of *Methanobrevibacter cuticularis* sp. nov. and *Methanobrevibacter curvatus* sp. nov., isolated from the hind gut of the termite *Reticulitermes flavipes*." *Applied Environmental Microbiology*, 62, 3620–3631.

Levitt, T. (2011). "Freshwater lakes and rivers contributing to climate change." Avaiable at <http://www.theecologist.org/News/news_round_up/724888/freshwater_lakes_and_rivers_contributing_to_climate_change.html> (accessed Feb. 2012).

Liu, H., Li, Y., Shen, W., Bao, X., and Xu, Y. (2004). "Methane dehydroaromatization over Mo/HZSM-5 catalysts in the absence of oxygen: effects of silanation in HZSM-5 zeolite." *Catalysis Today*, 93–95, 65–73.

Luo, X.-p., Lai, H., Li, J.-c., and Yan, Q. (2011).Experimental study on different modified zeolite's absorption of NH_4-N. In *Electric Technology and Civil Engineering (ICETCE), 2011 International Conference on*, 4150–4154.

MacIntyre, S., Wanninkhof, R., and Chanton, J. P. (1995). "Trace gas exchange across the air-water interface in freshwater and coastal marine environments." *In Biogenic Trace Gases: Measuring Emissions from Soil and Water, ed. by P. Matson and R. Harriss*, 52–97.

Mathison, G. W. (1997). "Effect of canola oil on methane production in steers." *Canidian Journal of Animal Science*, 77, 545–546.

Milkov, A. V., Sassen, R., Apanasovich, T. V., and Dadashev, F. G. (2003). "Global gas flux from mud volcanoes: A significant source of fossil methane in the atmosphere and the ocean." *Geophysical Research Letters*, 30, 17–20.

Mogro-Campero, A., and Fleischer, R. L. (1977). "Subterrestrial fluid convection: A hypothesis for long-distance migration of radon within the earth." *Earth and Planetary Science Letters*, 34, 321–325.

Moriya, O. (2008). "Symbioses of flagellates and prokaryotes in the gut of lower termites." *Trends in Microbiology*, 16, 345–352.

Morrissey, L. A., Zobel, D. B., and Livingston, G. P. (1993). "Significance of stomatal control on methane release from Carex-dominated wetlands." *Chemosphere*, 26, 339–355.

Nyre, L. (2011). "The effects of destroying the natural environment." Avaiable at <http://www.ehow.com/info_8255141_effects-destroying-natural-environment.html> (accessed Feb. 2012).

O'Connor, I. (2009). "The influence of plants on CH_4- emission from permafrost soils." Term Paper in Master Studies of Environmental Sciences Major in Biogeochemistry and Pollutant Dynamics ETH Zürich, 1–16.

Ohkuma, M., Maeda, Y., Johjima, T., and Kudo, T. (2001). "Lignin degradation and roles of white rot fungi : Study on an efficient symbiotic system in fungus-growing termites and its application to bioremediation." *Microbiology*, 42, 39–42.

Olson, K. (1997). "Reducing methane emissions from beef cow herds in range based management systems." *Ruminant Livestock Efficiency Program Annual Conference Proceedings,* EPA USDA, 1997.

Owen, A. G., and Jones, D. L. (2001). "Competition for amino acids between wheat roots and rhizosphere microorganisms and the role of amino acids in plant N acquisition." *Soil Biology and Biochemistry*, 33, 651–657.

Prather, M. (Ed) (2001). *Atmospheric chemistry and greenhouse gases, in climate change 2001: the scientific basis.* Cambridge: Cambridge University Press, Cambridge, UK.

Pulliam, W. M. (1992). "Methane emissions from cypress knees in a southeastern floodplain swamp." *Oecologia*, 91, 126–128.

Purvaja, R., Ramesh, R., and Frenzel, P. (2004). "Plant-mediated methane emission from an Indian mangrove." *Global Change Biology*, 10, 1825–1834.

Qiu, Y.-L., Hanada, S., Ohashi, A., Harada, H., Kamagata, Y., and Sekiguchi, Y. (2008). "Syntrophorhabdus aromaticivorans gen. nov., sp. nov., the first cultured anaerobe capable of degrading phenol to acetate in obligate syntrophic associations with a hydrogenotrophic methanogen." *Applied and Environmental Microbiology*, 74, 2051–2058.

Rimmer, D. L., and Mcintosh, R. (1974). "Sorption of water, ammonia, ethyl chloride, and methane on Na-X zeolite and associated framework distortion." *Canidian Journal of Chemistry*, 52, 3699–3706.

Robertson, L. J., Waghorn, G. C., North, P., and Zealand, N. (2002). "Dairy industry perspectives on methane emissions and production from cattle fed pasture or total mixed rations in New Zealand." *Proceedings of the New Zealand Society of Animal Production*, 62, 213–218.

Roden, E. E., and Wetzel, R. G. (2003). "Competition between Fe(III)-reducing and methanogenic bacteria for acetate in iron-rich freshwater sediments." *Microbial Ecology*, 45, 252–258.

Saarnio, S., Wittenmayer, L., and Merbach, W. (2004). "Rhizospheric exudation of *Eriophorum vaginatum L*. Potential link to methanogenesis." *Plant and Soil*, 267, 343–355.

Sachs, T., Wille, C., Boike, J., and Kutzbach, L. (2008). "Environmental controls on ecosystem-scale CH_4 emission from polygonal tundra in the Lena River Delta, Siberia." *Journal of Geophysical Research*, 113, 3096–3110.

Saxena, S., Bahadur, J., and Varma, A. (1993). "Cellulose and hemicellulose degrading bacteria from termite gut and mound soils of India." *Indian Journal of Microbiology*, 33, 55–60.

Schimel, J. P. (1995). "Plant transport and methane production as controls on methane flux from arctic wet meadow tundra." *Biogeochemistry*, 28, 183–200.

Schmidt, S., and Stewart, G. R. (1999). "Glycine metabolism by plant roots and its occurrence in Australian plant communities." *Functional Plant Biology*, 26, 253–264.

Schoun, H., Kim, D., Uchiyama, H., and Sugiyama, J. (1992). "Denitrification by fungi." *FEMS Microbiol Lett*, 94, 277–282.

Schuur, E. A. G., Bockheim, J., Canadell, J. G., Euskirchen, E., Field, C. B., Goryachkin, S. V., Hagemann, S., Kuhry, P., Lafleur, P. M., Lee, H., Mazhitova, G., Nelson, F. E., Rinke, A., Romanovsky, V. E., Shiklomanov, N., Tarnocai, C., Venevsky, S., Jason, G. V., and Zimov, S. A. (2008). "Vulnerability of permafrost carbon to climate change: Implications for the global carbon cycle." *BioScience*, 58, 701–714.

Seiler, W., Conrad, R., and Scharffe, D. (1984). "Field studies of methane emission from termite nests into the atmosphere and measurements of methane uptake by tropical soils." *Journal of Atmospheric Chemistry*, 1, 171–186.

Shannon, R. D., White, J. R., Lawson, J. E., and Gilmour, B. S. (1996). “Methane efflux from emergent vegetation in peatlands.” *Journal of Ecology*, 84, 239–246.

Sloan, E. D., and Koh, C. A. (2007). "Hydrate formation and dissociation processes." In *Clathrate Hydrates of Natural Gases,* 3rd ed., 113–187: CRC Press.

Slyudkin, M. O. (2004). “Experimental synthesis of ammonia and methane bearing natrolite zeolites.” *Herald of the Department of Earth Sciences RAS*, 1, 1–2.

Smith, M. S. (1982). “Dissimilatory reduction of NO_2^- to NH_4^+ and N_2O by a soil *Citrobacter* sp.” *Applied and Environmental Microbiology*, 43, 854–860.

Smith, M. S. (1983). “Nitrous oxide production by *Escherichia coli* is correlated with nitrate reductase activity.” *Applied and Environmental Microbiology*, 45, 1545–1547.

Song, C., Zhang, J., Wang, Y., Wang, Y., and Zhao, Z. (2008). “Emission of CO_2, CH_4 and N_2O from freshwater marsh in northeast of China.” *Journal of Environmental Management*, 88, 428–436.

Strom, L., Mastepanov, M., and Christensen, T. R. (2005). “Species-specific effects of vascular plants on carbon turnover and methane emissions from wetlands.” *Biogeochemistry*, 75, 65–82.

Tan, W., Wang, Q., Wang, Y., and Pan, Z. (2011).Adsorption of nitrogen and phosphorus on natural zeolite and its influencing factors. In *2011 Third International Conference on Measuring Technology and Mechatronics Automation,* Jan. 6-7, 2011, 347–350 Shanghai, China.

Tedesco, C., Erra, L., Brunelli, M., Cipolletti, V., Gaeta, C., Fitch, A. N., Atwood, J. L., and Neri, P. (2010). “Methane adsorption in a supramolecular organic zeolite.” *Chemistry – A European Journal*, 16, 2371–2374.

Thayer, D. W. (1976). “Facultative Wood-digesting Bacteria from the Hind-gut of the Termite *Reticulitermes hesperus*.” *Journal of General Microbiology*, 95, 287–296.

The Royal Society (2005). “Ocean acidification due to increasing atmospheric carbon dioxide.” Avaiable at <http://royalsociety.org/policy/publications/2005/ocean-acidification/> (accessed Jan. 2012).

Tiemann, L. K., and Billings, S. A. (2008). “Carbon controls on nitrous oxide production with changes in substrate availability in a north American grassland.” *Soil Science*, 173, 332–341.

Trumper, K., Bertzky, M., Dickson, B., van der Heijden, G., Jenkins, M., and Manning, P. (2009). *The natural fix? The role of ecosystems in climate mitigation.* Report of A UNEP rapid response assessment. United Nations Environment Programme, NEPWCMC, Cambridge, UK, <http://www.unep.org/pdf/BioseqRRA_scr.pdf> (accessed on Feb. 2012).

U.S. EPA (2010). “Methane and nitrous oxide emissions from natural sources.” Available at <http://www.epa.gov/nitrousoxide/sources.html> (accessed on Feb. 2012).

van Nevel, C. J., and Demeyer, D. I. (1995).Feed additives and other interventions for decreasing methane emissions. In *Biotechnology in Animal Feeds and Animal Feeding*, 329–349 (Eds. Wallance, R. J. and Chesson, A). VCH, Weinheim.

Walter, K. M., Edwards, M. E., Grosse, G., Zimov, S. A., and Chapin, F. S. (2007). "Thermokarst lakes as a source of atmospheric CH_4 during the last deglaciation." *Science*, 318, 633–636.

Wang, J. (2011). "Ecology of neutrophilic iron-oxidizing bacteria in wetland soils." *Thesis presented to Utrecht University, Science Faculty, Netherlands*, 1–213.

Watanabe, A., Purwanto, B. H., Ando, H., Kakuda, K.-I., and Jong, F.-S. (2009). "Methane and CO_2 fluxes from an Indonesian peatland used for sago palm (*Metroxylon sagu* Rottb.) cultivation: Effects of fertilizer and groundwater level management." *Agriculture, Ecosystems & Environment*, 134, 14–18.

Watson, A., and Nedwell, D. B. (1998). "Methane production and emission from peat: The influence of anions (sulphate, nitrate) from acid rain." *Atmospheric Environment*, 32, 3239–3245.

Weber, K. A., Achenbach, L. A., and Coates, J. D. (2006). "Microorganisms pumping iron: anaerobic microbial iron oxidation and reduction." *Nat Rev Micro*, 4, 752–764.

Webster, F. A., and Hopkins, D. W. (1996). "Contributions from different microbial processes to emission from soil under different moisture regimes." *Biology and Fertility of Soils*, 22, 331–335.

Wille, C., Kutzbach, L., Sachs, T., Wagner, D., and Pfeiffer, E.-M. (2008). "Methane emission from Siberian arctic polygonal tundra: Eddy covariance measurements and modeling." *Global Change Biology*, 14, 1395–1408.

William J, M. (1992). "Landscape design and the role of created, restored, and natural riparian wetlands in controlling nonpoint source pollution." *Ecological Engineering*, 1, 27–47.

Wilson, S., Griffiths, M., and Anielski, M. (2001). "The Alberta GPI Accounts: wetlands and peatlands." The Pembina Institute, Drayton Valley, AB.

Yamin, M. A. (1980). "Cellulose metabolism by the termite *Flagellate Trichomitopsis* termopsidis." *Applied and Environmental Microbiology*, 39, 859–863.

Yang, J., Bordeaux, F., and Smith, P. (1985). "Isolation of methanogenic bacteria from termites." *Abstract of the 85th Annual Meeting of the American Society for Microbiology*. Washinton., D.C1-83, 160.

Yavitt, J. B., and Knapp, A. K. (1995). "Methane emission to the atmosphere through emergent cattail (*Typha latifolia L.*) plants." *Tellus B*, 47, 521–534.

Zang, X., Du, J., Liang, D., Fan, S., and Tang, C. (2009). "Influence of A-type zeolite on methane hydrate formation." *Chinese Journal of Chemical Engineering*, 17, 854–859.

Zhuang, Q., Melack, J. M., Zimov, S., Walter, K. M., Butenhoff, C. L., and Khalil, M. A. K. (2009). "Global methane emissions from wetlands , rice paddies , and lakes." *System*, 90, 3–5.

Zimmerman, P. R., Greenberg, J. P., Wandiga, S. O., and Crutzen, P. J. (1982). "Termites: A potentially large source of atmospheric methane, carbon dioxide, and molecular hydrogen." *Science*, 218, 563–565.

Index

Page numbers followed by *e*, *f*, and *t* indicate equations, figures, and tables, respectively.